ALUMINA

SCIENCE *and* TECHNOLOGY HANDBOOK

CHEMICALS

L.D. HART, EDITOR
ESTHER LENSE, ASSOCIATE EDITOR

The American Ceramic Society, Inc.
Westerville, Ohio

On the cover: Hundreds of different alumina chemicals are produced and made commercially available in large tonnages to every industrialized country in the world. (Photo courtesy of Alcoa. Used with permission.)

Library of Congress Cataloging-in-Publication Data

Alumina chemicals : science and technology handbook /
LeRoy D. Hart, editor.
p. cm.
ISBN 0-916094-33-2
1. Aluminum oxide. 2. Aluminum hydroxide.
I. Hart, LeRoy D.
TP245.A4A36 1990
661'.067--dc20 90-219
CIP

ISBN O-916094-33-2

Printed in the United States of America

2 3 4 5-95

This book is dedicated to an unknown author who wrote,
''Do not follow where the path may lead.
Go instead where there is no path and leave a trail. ''

CONTENTS

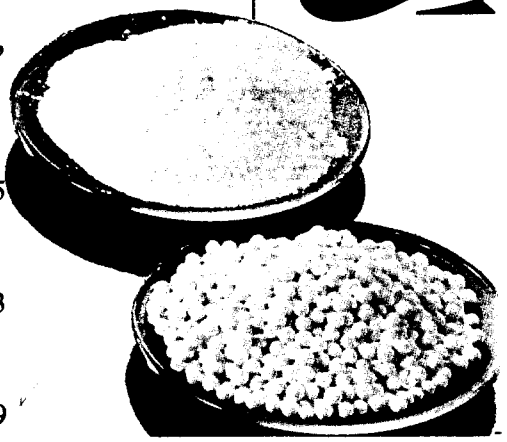

Section IV. State of the Art Assessments in Applications Utilizing Alumina Chemicals

Section VII. Glossary

Preface

Publication of this book was undertaken to provide a comprehensive reference for in-depth information on the science and technology of a remarkable family of products known as alumina chemicals. These low-cost, versatile materials are produced commercially in large quantities for use in a wide variety of end products which serve many of the daily needs of people throughout the world.

A second objective was to have world-renowned scientists and engineers, with expertise in the aluminas, contribute chapters that reflect the knowledge, experience, and future expectations acquired in working with these materials. Many of the contributors have spent most of their careers developing an understanding of alumina chemicals. Their insights add an invaluable dimension to the information presented.

It should be pointed out here that most of the world's major producers of alumina chemicals were extended written invitations and urged verbally to participate in this project. Two Japanese and two U.S. firms elected to contribute manuscripts. While we would have preferred having input from a greater number of producers, we are grateful to those who did respond with important contributions. We also acknowledge with thanks the outstanding support given the authors by their employers. Thirty-four industrial firms, government agencies, universities, and other organizations are represented by the 57 authors contributing to this book.

This book is organized into seven sections comprising a total of 50 chapters. Subjects covered by the 57 authors include fundamental properties of the basic alumina products, current commercial products and production processes, state of the art assessments on applications, industrial hygiene considerations, and the long-range future of alumina chemicals. Each chapter is a "standalone" treatise complete with selected references pertaining to the specific subject.

A project of this magnitude requires input and assistance from many people. I wish to acknowledge and thank each and every one of those individuals involved in the publication for their contributions. I especially wish to thank my colleagues from around the world—the authors—for writing the chapters comprising this book. In most cases, these busy people sacrificed large blocks of their own leisure time to prepare the manuscripts.

The authors and I thank the American Ceramic Society for publishing this book. We also express our gratitude to Alcoa for its generous support of this project. My special thanks are conveyed to Ann Burchick of Alcoa for her administrative assistance; Barney Henderson and Jim Arnold of Alcoa for design and production of the award plaque for authors and for photographs used in the book; Esther Lense and Pam Achter of the American Ceramic Society for their significant contributions as Associate Editor and Managing Editors of the book; and finally, Dr. William Smothers, distinguished Editor of the American Ceramic Society, for his encouragement, guidance, and assistance.

LeRoy D. Hart
Little Rock, Arkansas

SECTION 1

Introduction

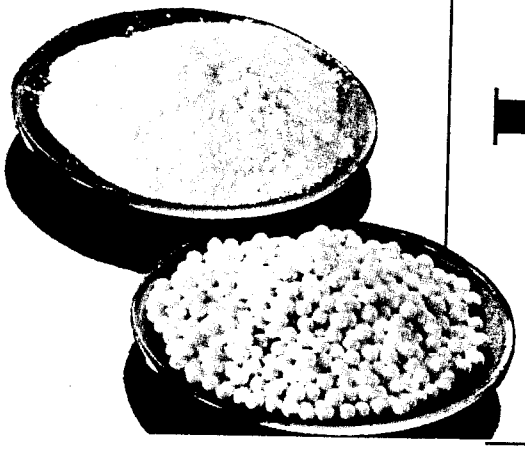

History of Alumina Chemicals

L. D. Hart
Hart Associates
12 Shawbridge Lane
Little Rock, AR 72212

This first chapter traces significant historical events which took place during the 7000-year time span in which man has known, produced, and used naturally occurring and synthetic compounds of aluminum. Today's modern alumina chemicals industry is less than 100 years old but, in that relatively short time, has become a global enterprise in which a wide variety of products with a broad range of properties and applications are produced and sold. These remarkable products serve many of the daily needs of people all over the world. Ongoing research and development on new products and applications ensure a bright future for alumina chemicals.

Today's worldwide alumina chemicals industry had its beginnings in the modern aluminum industry founded by Charles Martin Hall in the United States and Paul Heroult in France in 1886. The impending need for large quantities of pure alumina to produce aluminum metal by the Hall-Heroult process inspired Dr. Karl Joseph Bayer to develop a low-cost method for extracting alumina from bauxite. The Bayer process not only enhanced the feasibility of the Hall-Heroult process, but also attracted a strong interest in nonaluminum uses for Bayer products. Thus, early in its life, the parent aluminum industry produced and nurtured an offspring, the alumina chemicals industry.

A comprehensive review of historical events in both industries would be quite protracted and, hence, will not be undertaken here. For those interested, the literature contains a wealth of historical information.[1-9] Moreover, several of the contributors to this book have covered important historical events in their specific areas of expertise. It seemed advisable, therefore, to confine this chapter to a brief outline of significant historical occurrences that contributed most to the development and growth of the alumina chemicals business.

Naturally occurring compounds of aluminum have been known and used by man for many centuries. Archeological digs in northern Iraq indicate that primitive pottery was first made from clays containing aluminum silicates around 5300 B.C. There is also evidence that the Egyptians and Babylonians used native alums in vegetable dyes and medicines as early as 2000 B.C.

The Romans used the word "alumen" for materials with a styptic or astringent taste. Impure forms of both alum and aluminum sulfate, occurring in nearby volcanic regions, were probably among the compounds included by this term. The English word "alumina" is derived indirectly from alumen.

The first known reference to an aluminum compound was made by Herodotus, who mentioned alumen as early as 425 B.C. Pliny provided descriptions of alum and its use as a mordant for dyes in about 80 B.C.

In 1786, de Marveau named the oxide of aluminum "aluminae," which translated into English becomes alumina. The metal was named by Sir Humphry Davy, who coined the word "aluminum" and later "aluminium" during the years 1808 to 1812. In 1875, the French chemist Le Chatelier prepared pure alumina by thermal decomposition of aluminum salts and by sintering bauxite with soda.

Berthier discovered bauxite near the small village of Les Baux in southern France in 1821. Small-scale mining operations were begun there in 1859.

During the golden age of scientific discovery in the 18th and 19th centuries, many investigators experimented on a variety of processes for producing aluminum metal. Intensive efforts by famous scientists such as Davy, Oersted, Wöhler, Bunsen, and Deville contributed significantly to a better understanding of aluminum and its compounds but, in retrospect, failed to bring forth an economically viable commercial process for producing the elusive metal in large quantities.

A breakthrough in the quest for a cost-effective production process for aluminum occurred in 1886. Charles Martin Hall in the United States and Paul Heroult in France filed similar patents on their independent discoveries of a process for the electrolytic extraction of aluminum from alumina dissolved in cryolite. Two years later, in late November of 1888, the world's first commercial aluminum ingot was poured in the Smallman Street Plant of the Pittsburgh Reduction Company (renamed Aluminum Company of America in 1907) using metal produced by the Hall process. During the period 1891 to 1903, smelting and fabricating plants were built by the new firm at New Kensington, Pennsylvania, and smelting plants were constructed at Niagara Falls and Massena, New York.

Another significant advance in the commercial production of aluminum was contributed by Dr. Karl Josef Bayer, a widely traveled Austrian, who devel-

oped the Bayer process for extracting alumina from bauxite. Bayer was granted German patents on two important steps in his extraction process. In 1887, he discovered and received a patent on his finding that aluminum hydroxide could be precipitated from sodium aluminate solution using aluminum hydroxide seed, vigorous agitation, and cooling of the solution. In 1892, he patented his second and perhaps more important discovery that aluminum hydroxide in bauxite could be selectively dissolved in sodium hydroxide by pressure digestion in an autoclave.

The value of the Bayer process for alumina production was quickly recognized throughout Europe and in the United States. Construction of the first Bayer alumina plant was begun in 1895 at Gardanne, France under the direction of Paul Heroult and Dr. Bayer. During the next 10 years, additional Bayer plants were constructed in Ireland, France, Russia, England, Germany, Italy, and the United States.

The first commercial Bayer alumina plant in the United States was constructed by the Pittsburgh Reduction Company at East St. Louis, Illinois in 1902–1903. Figure 1 is a photograph of the plant.

Operations were started at East St. Louis in May 1903 using Arkansas bauxite as feedstock. The company purchased its own bauxite and began mining operations in Arkansas in 1899. Thus, early in its history, the Pittsburgh Reduction Company became the world's first fully integrated aluminum producer by establishing bauxite mining, alumina refining, and aluminum smelting and fabricating operations at various locations in the United States.

The Bayer process is capable of producing huge quantities of high-purity aluminum hydroxide and aluminum oxides at relatively low cost. This fact created opportunities early on for marketing profitable Bayer plant products outside the aluminum industry. With a reliable source of high-purity, low-cost alumina available in large volumes, potential customers and operators of the Bayer plants in Europe and the United States became interested in and began working cooperatively on applications for these new products.

Alcoa's first sale of alumina for a nonaluminum use was in 1910, some 24 years after the aluminum industry was founded. The product was calcined alumina, which was used by the customer as a feedstock for producing white fused alumina abrasives. This is considered the beginning of Alcoa's alumina chemicals business.

Aluminum hydroxide was first sold as a feedstock for alum manufacture in 1914. From 1916 to 1920, processes were developed and commercialized for the production and sale of dry sodium aluminate for water treatment, ground calcined aluminas for metal polishing compounds, and red mud as an additive for portland cement manufacture. Similar activities were undoubtedly taking place at the same time in Europe.

In 1919, Alcoa's management selected Dr. Francis C. Frary as the first director of the company's newly established Research Bureau. After several name changes over the years, the Research and Development organization today is known as Alcoa Laboratories.

In 1923, Dr. Frary established a branch of the laboratories at the East St. Louis plant to conduct research and development work on alumina, fluorides, and chemical processes, products, and applications. People in this organization, in consort with associates in other divisions of the laboratories, made hundreds of contributions to the science and technology of alumina products and the growing alumina chemicals business. In the mid-1970s, the East St. Louis R & D facilities were moved to Alcoa Technical Center in Pennsylvania (Fig. 2).

A prime reason for success in these endeavors was the close working relationships established with customers in developing and commercializing new

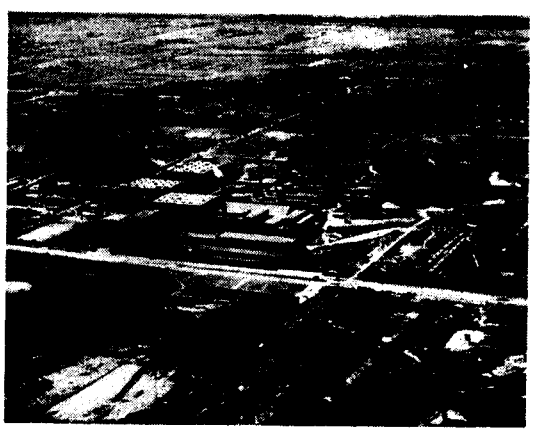

Fig. 1. Alcoa's East St. Louis, Illinois alumina refining plant began operations in 1903 and was the first site for a chemicals development laboratory in 1944. In the late 1950s and early 1960s, chemicals manufacturing was moved to Arkansas operations. Photo courtesy of Alcoa.

Fig. 2. Alcoa Technical Center near Pittsburgh is located on a 2300 acre tract and employs more than 1000 scientists, engineers, and technicians. Photo courtesy of Alcoa.

products and applications. Not only did Alcoa's people work in customers' laboratories and plants on new developments, but customers worked in Alcoa facilities to help perfect products needed for new applications. By sharing resources in this manner, development time was greatly reduced and the quality of results achieved was enhanced.

In the six decades of research and development work on alumina chemicals, numerous new processes, equipment, plants, products, and applications were introduced and commercialized. Included in the list of the most important products are the activated aluminas, calcined aluminas, low-soda calcined aluminas, gel-type activated aluminas, hydral, tabular aluminas, gallium, calcium aluminate cements, reactive aluminas, ultrahigh-purity aluminas, beta and zeta aluminas, a wide range of aluminum hydroxides, and various types of spinels.

In addition to developing processes and equipment to produce the foregoing chemical products, laboratories people also developed the Alcoa combination process for extracting alumina from low-grade bauxites, processes for producing aluminum fluoride from fluorspar and fluosilicic acid and the Alcoa flash-fluid calciner, to name a few of the truly outstanding developments. These technologies were used to build and operate alumina and chemicals plants around the world. Figures 3–5 are examples of these plants operating in various countries.

Today, the alumina chemicals industry has become a global enterprise in which most of the world's major aluminum firms participate. Current world production capacity for alumina is almost 40 million tonnes annually. Approximately 92% of this is for smelting to aluminum metal. The remaining 8% is converted to alumina chemicals products. More detailed information on production of alumina chemicals is given in the chapter entitled "World Production and Economics of Alumina Chemicals."

Today, a wide variety of alumina chemical products with a broad range of properties is available on the world market from numerous suppliers. These products are used in many commercial applications involving thousands of end products used daily by people all over the world. Products containing alumina chemicals in one form or another include toothpaste, carpet backing, plastics, paper, paint, industrial ceramics, electronic substrates, electrical insulators, antiperspirants, antacids, refractories, flame retardants, smoke suppressants, synthetic marble, fine china, optical glass, catalysts, abrasives, polishing compounds, desiccants, selective adsorbents, and many others. Some of these products are shown in Fig. 6.

The future of the alumina chemicals industry remains bright. Raw materials are plentiful, processes are constantly being improved to keep costs low and quality high, and funding for research and development of new products and applications has been generous. The long-range future technology of alumina

Fig. 3. Alcoa's Arkansas Oprations, a few miles south of Little Rock, is the world's largest integrated alumina chemicals facility. It has been in operation since 1952. Photo courtesy of Alcoa.

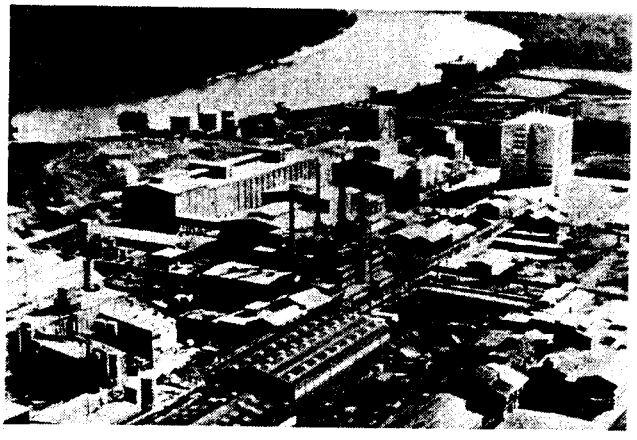

Fig. 4. In 1982, Alcoa purchased this alumina chemical manufacturing facility from Giulini Chemie in West Germany. It is located at Ludwigshafen on the Rhine River, south of Frankfurt. Photo courtesy of Alcoa.

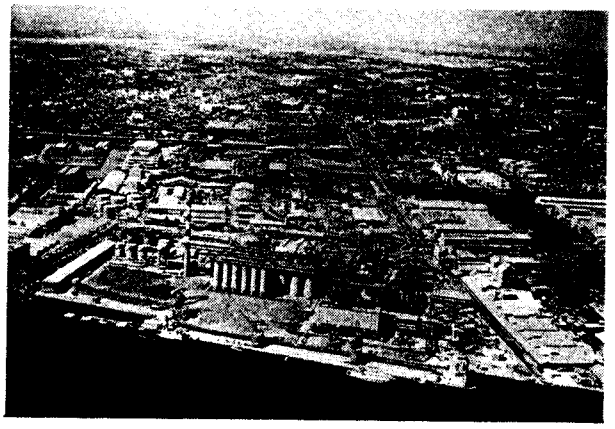

Fig. 5. Yokohama Works of Showa Aluminum Industries KK. Photo courtesy of Showa Aluminum Industries KK.

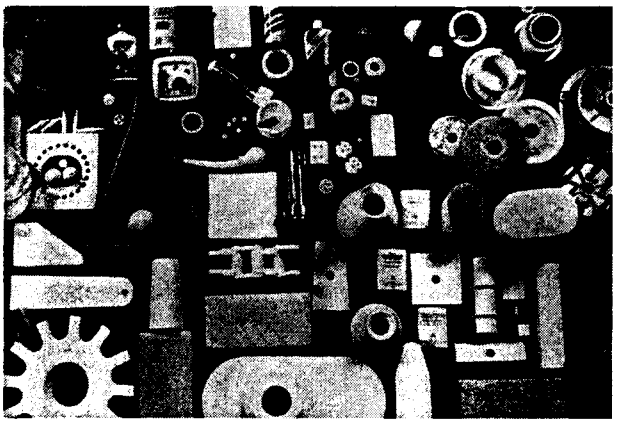

Fig. 6. Some end products made from alumina chemicals. Photo courtesy of Alcoa.

chemicals is discussed in Section VI of this book, including the role of future alumina chemical products as viewed by world authorities.

References

[1]J. D. Edwards, F. C. Frary, and Z. Jeffries, The Aluminum Industry—Aluminum and Its Production. McGraw-Hill, New York, 1930.

[2]W. H. Gitzen, Alumina As A Ceramic Material. The American Ceramic Society, Columbus, OH, 1970.

[3]K. Wefers and G. M. Bell, "Oxides and Hydroxides of Aluminum," Tech. Paper No. 19, Aluminum Co. of America, Alcoa Center, PA, 1972.

[4]G. MacZura, K. P. Goodboy, and J. J. Koenig, "Aluminum Oxide (Alumina)"; in Kirk-Othmer Encyclopedia of Chemical Technology, Vol. 2, 3rd ed. Wiley & Sons, New York, 1978.

[5]L. K. Hudson, Alumina Production. The Aluminum Company of America, Alcoa Center, PA, 1982.

[6]H. Ginsberg and K. Wefers, Aluminum and Magnesium. Alcoa Laboratories, Alcoa Center, PA, 1982; internal publication.

[7]C. Misra, Industrial Alumina Chemicals. The American Chemical Society, Washington, DC, 1986.

[8]K. Wefers and C. Misra, Oxides and Hydroxides of Aluminum. Alcoa Laboratories, Alcoa Center, PA, 1987.

[9]G. D. Smith, From Monopoly to Competition. Cambridge University Press, NY, 1988.

World Production and Economics of Alumina Chemicals

Luke H. Baumgardner
Bureau of Mines
Division of Nonferrous Metals
2401 E Street, NW
Washington, DC 20241

World specialty-alumina production during the period 1975 to 1986 is reviewed and illustrated graphically. Processing steps from crude bauxite to alumina end products are depicted in a flowchart and producer price quotes in February 1987 are listed.

Aluminum oxide, in various forms, is intimately involved in our daily lives and yet most of us are unaware of its presence or widespread uses. It is present in toothpaste, porcelain bathtubs, spark plugs, and tires, in the catalytic converters of our cars, in the condensers and microchips of our TV sets, and in the paper of books and magazines. Figure 1 traces aluminum oxide from its origin at the bauxite mine through various processing stages to a wide variety of end uses.

Product names and grades of the specialty aluminas differ from company to company and from country

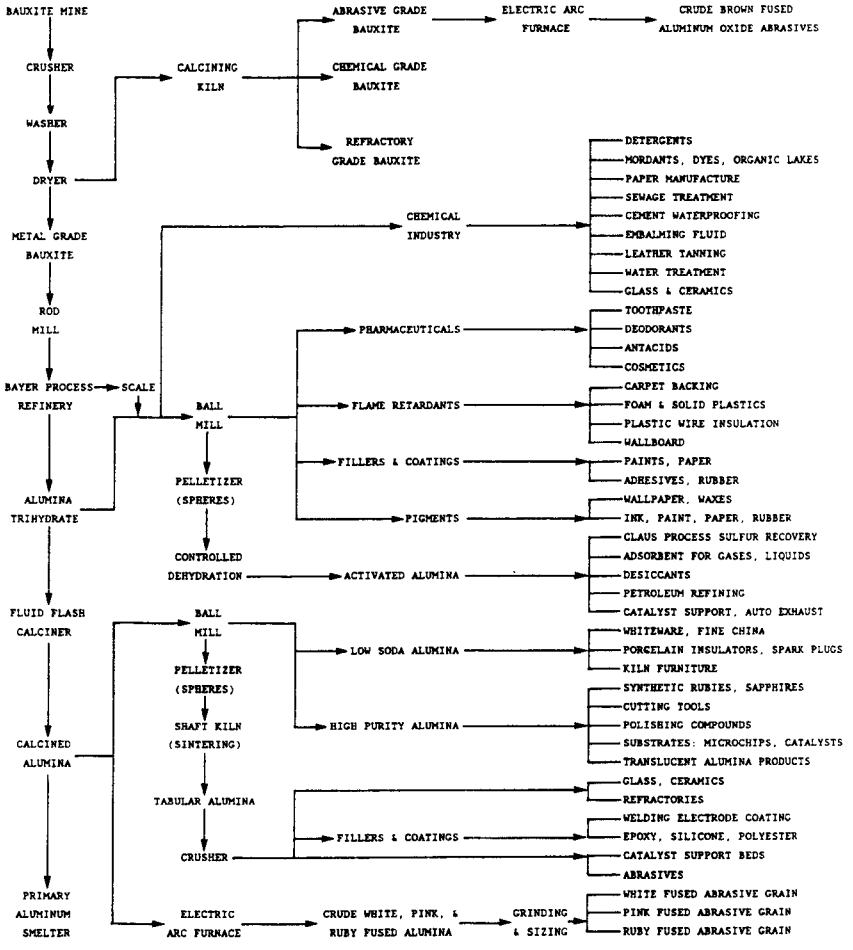

Fig. 1. Specialty alumina production flowchart.

Table I. Alumina Production—Metal and Specialty Grades
(Thousand metric tons as calcined alumina equivalent)

	Africa		North America		Latin America		East Asia		South Asia		Europe		Oceania		Total	
Year	Metal	Other	Metal	Other	Metal	Other	Metal	Other	Metal	Other	Metal	Other	Metal	Other	Metal	Other
1975	639		5583	670	3903	63	1490	355	337		3335	611	5107		20394	1699
1976	562		5628	777	3217	66	1332	377	466	1	3352	666	6219		20776	1887
1977	562		6328	838	3783	98	1677	418	535	20	3560	694	6673		23118	2068
1978	622		6357	863	3899	105	1375	444	555	1	3470	691	6764		23042	2104
1979	656		6419	925	3890	112	1327	551	568	1	3434	766	7386		23680	2355
1980	708		7261	833	4499	97	1749	549	613	36	3700	808	7254		25784	2323
1981	679		6358	814	4392	102	1156	488	607	13	4182	770	7087		24461	2187
1982	578		4676	589	3406	76	706	537	569		3697	767	6629		20261	1969
1983	564		4404	669	4101	69	797	550	531	1	3582	769	7305		21284	2058
1984	550		5013	737	4494	110	844	628	642	2	4400	835	8800		24743	2312
1985	577		3913	647	4426	135	679	637	672	12	3961	907	8804		23032	2338
1986	571		3390	682	5225	164	368	582	683	23	4185	872	9307		23729	2323

Source: International Primary Aluminium Institute (1975 through 1986) (see text for definition of areas).

to country, and available world data are not consistently defined or reported. Accordingly, there is little or no basis for aggregating production, price, and trade data for individual specialty aluminas on a world basis.

World Alumina Supply

World alumina output is reported on a quarterly basis by the International Primary Aluminium Institute (IPAI).[1] The IPAI data are based on reports from 50 worldwide member companies and nonmember official correspondents. The data do not include Yugoslavia and the centrally planned economy countries of China, Czechoslovakia, the German Democratic Republic, Hungary, Poland, Romania, and the U.S.S.R. During 1975 to 1986, not all of the IPAI geographic areas produced alumina for nonmetallurgical or specialty uses. In fact, six countries located in Europe, East Asia, and North America accounted for 92% of the total 2.32 million metric tons of the specialty alumina production reported to IPAI in 1986 (Table I).

Output of the specialty grades in 1975 to 1986 ranged from 1 699 000 metric tons in 1975 to a high of 2 355 000 tons in 1979. The average rate of growth from 1975 to 1986 was 2.9% per year. Alumina production for making aluminum metal generally comprises over 90% of the total alumina produced and has grown at an average rate of 1.4% per year during the same period. The principal producers in Europe include the Federal Republic of Germany, France, and the United Kingdom. Japan is the only alumina producer in the East Asia area, and Canada and the United States represent the industry in North America.

In recent years, the United States has accounted for about 85% of the specialty alumina produced in North America. North American production of specialty alumina has declined from a peak of 925 000 tons in 1979 (Fig. 2). During this period, the number of Bayer plants operating in the United States has been reduced from nine to four, and domestic capacity has declined about 37%. Although specialty alumina production in Japan showed a gradual growth from 1975 through 1985, a decline of nearly 9% in 1986 appears to reflect the progressive permanent closing of that country's primary aluminum smelters and the Bayer plants that supply them.[2] As additional smelters are shut down, further reductions in alumina capacity are expected to continue. Only in the European area has specialty-alumina production shown positive, although at times erratic, growth.

Prices

Different forms and grades of aluminum oxide may be chemically identical, yet command a wide range of prices determined by soda (Na_2O) content, particle size and grading, degree of calcination, crystal form, and grain surface area. There is such a wide

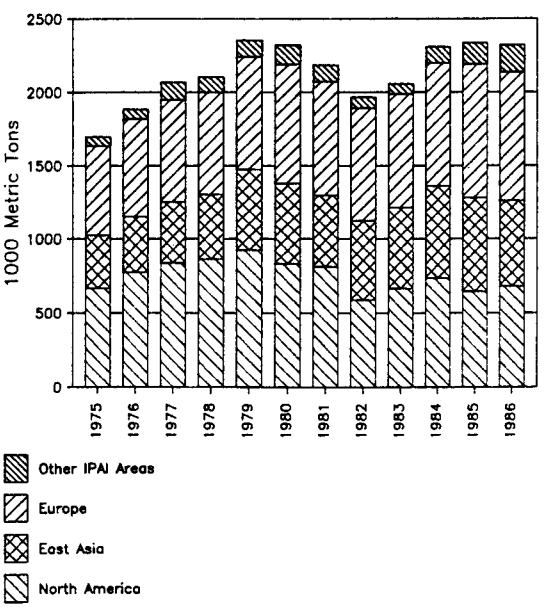

Fig. 2. Specialty alumina production (calcined alumina equivalent).

diversity of specialty-alumina products offered by North American producers that an identical product offered by all producers cannot be defined for most products. A sampling of prices for general alumina product categories, as quoted in February 1987 by representatives of Alcan Aluminium Corporation, the Aluminum Company of America, Kaiser Aluminum & Chemical Corporation, and Reynolds Metals Company, is listed below. Not all of the listed products were available from all of the companies. Unless otherwise indicated, the quotes are for metric tons of bagged alumina in truckload quantities.

Calcined alumina, low to medium soda, ground or unground .....$408–$551
Calcined alumina, very low soda, ground or superground .....$1210–$19
Tabular alumina, crushed, ungraded .....$575–$6
Tabular alumina, crushed, graded .....$650–$7
Tabular alumina, ground, −325 mesh .....$705–$9
Alumina trihydrate, standard Bayer, unground, bulk .....$210–$24
Activated alumina, granular, unground ...$900–$11

References

[1]International Primary Aluminium Institute. Statistical Summaries. Quarterly and Annual Alumina Production, 1975–198 IPAI, New Zealand House, Haymarket, London, U.K.

[2]"Alumina Refiners Cultivate Other Fields Than Aluminiu Smelting," *Jpn. Met. J.* **17** [6] 7–8 (1987).

[3]G. MacZura, T. J. Carbone, and L. D. Hart, "Alumina," *Am Ceram. Soc. Bull.*, Annual Ceramic Mineral Resources Review, 6 [5] 753–54 (1987). (General reference.)

SECTION II

Fundamental Properties *of* Alumina Chemicals

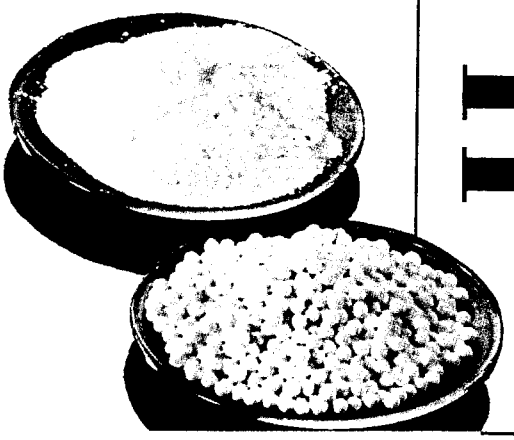

Nomenclature, Preparation, and Properties of Aluminum Oxides, Oxide Hydroxides, and Trihydroxides

K. Wefers

Alcoa Technical Center
Alcoa Center, PA 15069

Methods of preparation and mineralogical, structural, and other physical properties of aluminum oxides, oxide hydroxides, and trihydroxides are reviewed in this chapter. Phase relations in the system alumina-water under equilibrium and nonequilibrium conditions are discussed and recommendations are given with regard to an unambiguous, scientifically correct nomenclature.

Aluminum, oxygen, and hydrogen form three crystalline compounds: Al_2O_3, AlOOH, and $Al(OH)_3$. Pure, stoichiometrically defined aluminum oxide occurs in the crystalline modification corundum, α-Al_2O_3. Two crystalline forms of AlOOH exist: diaspore, α-AlOOH, and boehmite, γ-AlOOH. Bayerite, α-$Al(OH)_3$; gibbsite, γ-$Al(OH)_3$; and nordstrandite are the three trihydroxides.

Gibbsite, diaspore, and corundum have been known as minerals since the early years of the last century. Bayerite and boehmite were first synthesized in the 1920s, nordstrandite in 1956. Their natural occurrence was verified after these compounds had been described in the literature.[1]

Although the crystal structures of five of the aluminum minerals were determined in the 1930s, the nomenclature defining the compounds and the formula prefixes designating structural modifications are still used inconsistently, particularly in the nonscientific literature. The structures of the aluminum oxides and hydroxides are based on aluminum ions surrounded in six-fold coordination by oxygen and/or hydroxyl ions. These coordination octahedra are arrayed in either hexagonal or cubic packing sequence. Consistent with internationally accepted crystallographic nomenclature, the prefix α should be used to designate the hexagonally packed structures; for example, corundum, diaspore, and bayerite. For the cubically packed gibbsite and boehmite the prefix γ should be used. As the structures do not contain molecular water, the terms "trihydrate" or "monohydrate" should be avoided.

A comparison of nomenclatures from Ref. 1 is given in Table I.

Table I. Comparison of Nomenclatures

Mineral Name	Chemical Composition	Accepted Crystallographic Designation	Alcoa (1930)
Gibbsite Hydrargillite	Aluminum trihydroxide	γ-$Al(OH)_3$	Alpha alumina trihydrate
Bayerite	Aluminum trihydroxide	α-$Al(OH)_3$	Beta alumina trihydrate
Nordstrandite	Aluminum trihydroxide	$Al(OH)_3$	
Boehmite	Aluminum oxide hydroxide	γ-AlOOH	Alpha alumina monohydrate
Diaspore	Aluminum oxide hydroxide	α-AlOOH	Beta alumina monohydrate
Corundum	Aluminum oxide	α-Al_2O_3	Alpha alumina

Synthesis and Properties

Bayerite

Bayerite can be prepared in several ways. After depassivating the surface by amalgamation, Schmäh [2] immersed aluminum in pure water at room temperature. Neutralization of aluminum salt solutions by ammonium hydroxide at temperatures below 325 K, followed by aging at pH 8 to 9, is another method. Autoprecipitation at room temperature of supersaturated sodium aluminate solutions[3] or neutralization by CO_2 of sodium aluminate solutions[4] also lead to the formation of bayerite; so does the hydrolysis of aluminum alkoxide solutions at temperatures below 310 K.[5]

Bayerite is composed of layers of $Al(OH)_6$ octahedra which are stacked in an *AB-AB* sequence, that is, an approximately hexagonal close packing. The layers are linked by hydrogen bonds. The structure can be considered a distorted brucite type. However,

only two out of three interstitial cation sites are occupied by Al ions. Slight distortion of the octahedra lowers the symmetry to monoclinic, according to Rothbauer et al.[6] and Zigan et al.[7] Mineralogical properties are listed in Table II, lattice parameters in Table III. Bayerite generally forms spindle- or hourglass-shaped somatoids rarely more than a few micrometers in length (Fig. 1). Single crystals have not been observed to date. Bayerite is produced commercially as a precursor for catalysts, substrates, or adsorbants which require an aluminum oxide with low sodium content.

Gibbsite

While bayerite is rarely found in nature, gibbsite occurs in huge quantities in bauxites, tropical soils, and clays. Industrial production of gibbsite is on the order of 30 million tons per year, the Bayer process[8] being the predominant commercial process. In this procedure, bauxites containing 40 to 70% of the aluminum minerals gibbsite, boehmite, or diaspore plus iron, titanium, and silicate minerals, are digested with sodium hydroxide solutions at 400 to 550 K. Aluminum minerals are selectively leached according to:

$$Al(OH)_3 + NaOH \leftrightarrows Al(OH)_4^- + Na^+ \quad (1)$$

$$AlOOH + H_2O + NaOH \leftrightarrows Al(OH)_4^- + Na^+ \quad (2)$$

Reversal at temperatures between 325 and 340 K of reaction (1) leads to the precipitation of gibbsite. An aggregate of gibbsite crystals formed in the Bayer process is shown in Fig. 2. By far the largest amount of commercial gibbsite is thermally decomposed to metallurgical alumina, which is electrolytically reduced to aluminum by the Hall-Heroult process.[8] Other uses, among them preparation of ceramic aluminas, catalysts, catalyst supports, and adsorbents, are described in Sections III and IV of this book (see Index).

As in the structure of bayerite, double layers of hydroxyl ions, octahedrally coordinated with aluminum ions, are the basic elements of the gibbsite lattice. Hydroxyl ions of adjacent layers are located opposite each other, as shown in Fig. 3. The cubic packaging

Table II. Mineralogical Properties of Oxides and Hydroxides

Phase	Index of Refraction n_D				Cleavage	Brittleness	Mohs Hardness	Luster
	α	β	γ	Average				
Gibbsite	1.568	1.568	1.587	.....	(001) Perfect	Tough	2-1/2 to 3-1/2	Pearly Vitreous
Bayerite	.....	.....	.....	1.583	.....	.....	.....	.....
Boehmite	1.649	1.659	1.665	.....	(010)	.....	3-1/2 to 4	.....
Diaspore	1.702	1.722	1.750	.....	(010) Perfect	Brittle	6-1/2 to 7	Brilliant Pearly
	ε	ω	Average					
Corundum	1.760	1.768	.....		None	Tough when compact	9	Pearly Adamantine

Table III. Structural Properties

Phase	Formula	Crystal System	Space Group	Molecules Per Unit Cell	Unit Axis Length, nm a	b	c	Angle	Density g/cm³
Gibbsite	$Al(OH)_3$	Monoclinic	C_{2h}^5	4	0.8684	0.5078	0.9136	94° 34′	2.42
Gibbsite	$Al(OH)_3$	Triclinic	–	16	1.733	1.008	0.973	94° 10′ 92° 08′ 90° 0′	–
Bayerite	$Al(OH)_3$	Monoclinic	C_{2h}^5	2	0.5062	0.8671	0.4713	90° 27′	2.53
Nordstrandite	$Al(OH)_3$	Triclinic	C_1^1	2	0.5114	0.5082	0.5127	70° 16′ 74° 0′ 56° 26′	–
Boehmite	AlOOH	Orthonombic	D_{2h}^{17}	2	0.2868	0.1223	0.3692	–	3.01
Diaspore	AlOOH	Orthorhombic	D_{2h}^{16}	2	0.4396	0.9426	0.2844	–	3.44
Tohdite	$5Al_2O_3 \cdot H_2O$	Hexagonal	C_{6v}^4	1	0.5576	–	0.8768	–	3.72
Corundum	Al_2O_3	Hexagonal (Rhombohedral)	D_{3d}^6 ($R\bar{3}C$)	2	0.4759	–	1.2992	–	3.98[5]

Fig. 1. Transmission electron micrograph of bayerite somatoid (× 75 000).

sequence in the direction normal to the layers is *AB-BA-AB-BA*. Gibbsite is monoclinic; a triclinic gibbsite showing displacement of the hydroxyl double layers relative to each other in two directions was described by Saalfeld.[9] Pauling[10] proposed the concept of the gibbsite structure in 1930. It was confirmed a few years later by Megaw[11] and subsequently refined by several researchers.[1]

Mineralogical and structural data of gibbsite are summarized in Tables II and III.

Nordstrandite

In 1956, Van Nordstrand and coworkers[12] published the X-ray diffraction data of an aluminum trihydroxide which differed from those of bayerite and gibbsite. They proposed the name bayerite II for this form because of the similarity of its structure and morphology with that of bayerite. The new trihydroxide was later named nordstrandite. Several other authors confirmed the existence of the new form.[1] The most recent structure determinations were published in 1968 by Saalfeld and Jarchow[13] and in 1970 by Bosmans.[14] The structure can be described as an

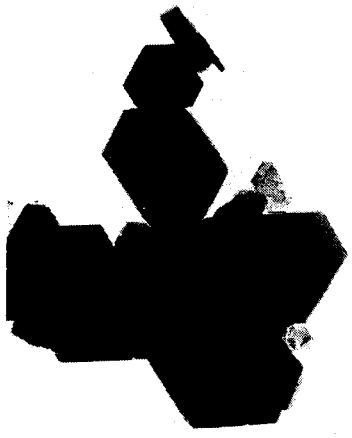

Fig. 2. Transmission electron micrograph of aggregate of gibbsite crystals (× 150 000).

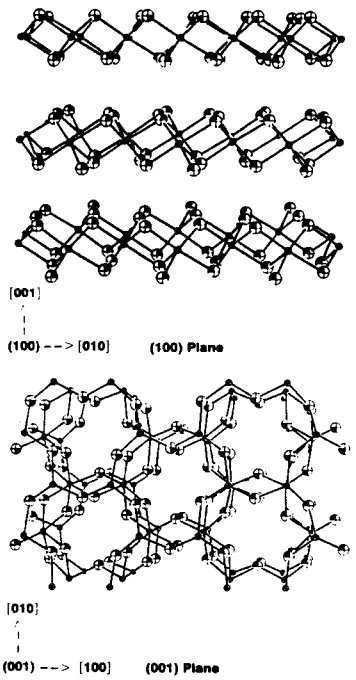

Fig. 3. Structure of gibbsite.

alternate stacking of *AB-AB* and *AB-BA* layers, or an intermediate structure between the bayerite and gibbsite lattice (Table II).

Nordstrandite was found in tropical soils in West Sarawak[15] and on Guam.[16] According to Hauschild,[17] very pure nordstrandite can be prepared by reacting aluminum, aluminum hydroxide gels, or hydrolyzable aluminum compounds with aqueous solutions of alkylenediamines. Other preparative methods have been reported.[1]

Diaspore

This mineral is a major constituent of Mesozoic and older bauxites of the Mediterranean type, but also occurs in alumina-rich metamorphic shales and in certain high-alumina clays.[18,19] The first hydrothermal synthesis of diaspore was published by Laubengayer and Weiss in 1943.[20] No commercial production of diaspore has been reported to date. Use of diaspore bauxites for alumina production has been almost abandoned due to the abundance of gibbsite bauxites, which can be processed under considerably milder conditions.

Deflandre[21] and Takane[22] first determined the structure of diaspore in the early 1930s. Several refinements were published later.[1] Diaspore is orthorhombic. The basic elements of the structure are AlOOH double chains, which are arranged in an approximately hexagonal close packing. A model of the diaspore lattice is shown in Fig. 4. Figure 5 illustrates the acicular crystal habit of hydrothermally grown α-AlOOH. Mineralogical and structural data of diaspore are summarized in Tables II and III.

Boehmite

This modification of AlOOH is the predominant aluminum mineral in many bauxites of Tertiary and Upper Cretaceous age, but is also abundant in geologically younger bauxites.[18,19] Boehmite can be synthesized easily by treating aluminum trihydroxides or aluminum metal hydrothermally at temperatures above 375 K. Formation of boehmite by a solid state reaction occurs on heating of coarse gibbsite particles in air to about 380 to 575 K.[1]

Double chains of AlOOH are also the building blocks of the boehmite structure. These chains form double layers which are arrayed in a cubic stacking sequence, as shown in Fig. 4. Boehmite crystallizes in the orthorhombic system. Lath-shaped crystals are frequently observed (Fig. 6), but other habits can occur, depending on the conditions of preparation.

Boehmite is an industrially important precursor for activated aluminas used in the manufacture of catalysts and adsorbents. Tables II and III list mineralogical and structural properties of boehmite.

Tohdite

An aluminum oxide hydroxide of the composition $5Al_2O_3 \cdot H_2O$ was first described in 1951 by Houben.[23] Torkar and Krischner[24] and Yamaguchi and Okumija[25] confirmed the existence of such a compound. It was named tohdite by Yamaguchi.

Tohdite has hexagonal symmetry, although its structure is of the spinel type. The lattice does not contain molecular water; infrared analysis indicates the presence of hydroxyl ions. Tohdite possibly represents a hydrogen spinel.

Structural data are given in Table III. No commercial use of tohdite has been reported so far.

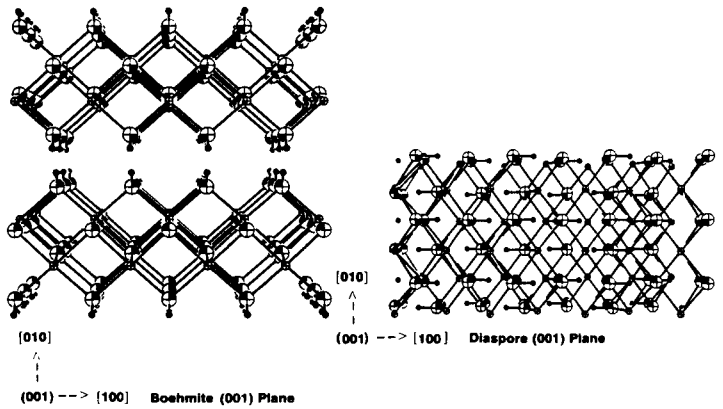

Fig. 4. Structure of diaspore and boehmite.

Corundum

Corundum, α-Al_2O_3, is the only thermodynamically stable form of aluminum oxide. It is a common mineral in igneous and metamorphic rocks; large, clear specimens have been used as gemstones for many centuries.

Fig. 5. Scanning electron micrograph of diaspore crystals (× 500).

Fig. 6. Transmission electron micrograph of boehmite crystals (× 42 000).

Corundum is one of the most important ceramic raw materials, as will be shown in the following chapters. Up to the 1960s, metallurgical alumina used in the Hall-Heroult process contained high amounts of α-Al_2O_3. In today's practice, lower calcination temperatures are used to obtain a product which is only partially transformed to the stable oxide.[1,17]

Corundum is very hard, its hardness exceeded only by that of diamond and a few synthetic compounds having the diamond structure (see Table II). Alpha Al_2O_3 crystallizes in the hexagonal-rhombohedral system (Fig. 7). Its structure was first investigated by Bragg and Bragg[26] and by Pauling and Hendricks.[27] The lattice represents a hexagonal closest packing of oxygen ions. Each Al ion is octahedrally coordinated by six oxygens. A model of the structure is shown in Fig. 8; Table III lists structure data.

Thermal, mechanical, and dielectric properties of corundum are summarized at the end of this chapter in tables taken from Ref. 1. This reference also provides information on electrical, optical, magnetic, and surface properties of aluminum oxide, as well as X-ray diffraction and infrared spectra of oxides and hydroxides. Another source of information is a thorough review of property data and processing of aluminum oxide published in 1984 by Dörre and Hübner. [28]

Fig. 7. Scanning electron micrograph of corundum crystals (× 1000).

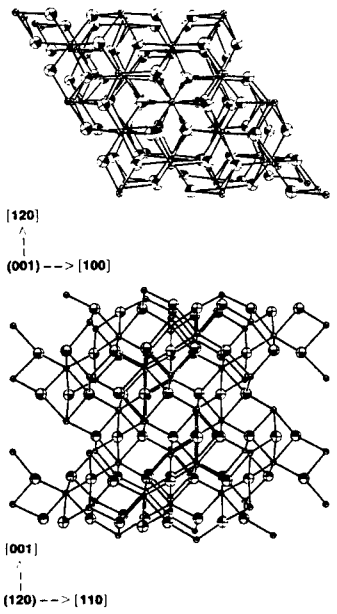

Fig. 8. Structure of corundum.

The System Al_2O_3-H_2O

Solubility

Aluminum oxide is soluble in both acidic and alkaline solutions. The solubility is extremely low in solutions of an intermediate pH between 4.5 and 8.5. At room temperature, a minimum of less then 10^{-7} mol/L occurs at pH 6. Below pH 4 and above pH 9, the solubility increases sharply, resulting in a solubility versus pH curve which is shaped almost like the letter U.

The solubility of Al_2O_3 in strongly alkaline solutions has attracted much interest due to its importance for the Bayer process.[1] The near-neutral to mildly acidic range of pH has been investigated primarily by geologists studying the behavior of aluminum in natural waters. Although general agreement has not yet been reached in the literature, it appears that at pH < 4 the hydrated Al^{3+} ion is the predominant solute species. Above pH 8 and at temperatures below ≈400 K, the $Al(OH)_4^-$ ion prevails. An AlO_2^- species occurs with higher temperatures and increasing alkali concentration, that is, lower activity of water in the solution. Polymeric complex ions are assumed to develop in the pH range between 4 and 8. Hem and Roberson[29] proposed that the aluminum ion is coordinated by six water molecules. The small aluminum ion strongly polarizes the water molecule, leading to deprotonation as the pH increases above 4 to 5. The resulting $Al(OH)(H_2O)_5^{2+}$ complexion can form dimeric or polymeric complexes by further loss of water molecules and deprotonation. The polymeric complexes can assume a hexagonal ring structure, the precursor of crystalline $Al(OH)_3$. Chainlike polymers develop at higher temperatures and lower pH values.

As indicated by the steep slope of the solubility curve, small changes in the pH value can drastically alter the solubility and lead to rapid precipitation of aluminum hydroxide. Such precipitates are often X-ray-indifferent gels; they consist of a poorly ordered solid phase and molecular water occupying capillary interstices. These gels can be dehydrated to form solids having surface areas of several hundred square meters per gram. Left under solutions, the gels "age" to crystalline $Al(OH)_3$ or AlOOH, depending on pH and temperature (see the chapter on colloidal properties of aluminum oxides).

Phase Relations

The phase diagram Al_2O_3-H_2O is shown in Fig. 9. Table IV lists thermodynamic data of aluminum oxides and hydroxides. The phase diagram represents the data of Kennedy[30] and Neuhaus and Heide.[31] The results of hydrothermal experiments by these authors were confirmed by thermodynamic calculations of Fyfe and Hollander,[32] who determined that the transformation temperature for the reaction

$$2\alpha\text{-AlOOH} \rightleftarrows \alpha\text{-}Al_2O_3 + H_2O$$

is 640 ± 7 K at the vapor pressure of the saturated solution.

Wefers[33] extrapolated solubility data for the system Na_2O-Al_2O_3-H_2O and found that the transformation

$$\alpha\text{-}Al(OH)_3 \rightleftarrows \alpha\text{-AlOOH} + H_2O$$

takes place at ≈373 K in pure water.

The stability relationships of the trihydroxides and oxide hydroxides have been a controversial subject in the literature. Gibbsite is by far the most abundant of the trihydroxides. Gelatinous hydroxide precipitates aged under alkali hydroxide solutions first develop into crystalline bayerite, which then transforms to gibbsite. On the other hand, synthesis of aluminum trihydroxide from pure aluminum and pure water always leads to bayerite. This trihydroxide also has the higher density and the higher structural symmetry. The enthalpy and Gibbs free energy of formation data in Table IV indicate that gibbsite is the stable form of $Al(OH)_3$. The differences between the values

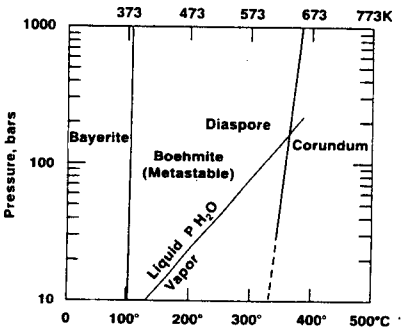

Fig. 9. Phase diagram of Al_2O_3-H_2O.

Table IV. Thermodynamic Data

Substance	MW	State	298.15K (25°C) and 0.1 MPa (1 bar) Molar Vol. cm^3/mol	ΔH_f° kJ/mol	ΔG_f° kJ/mol	S° J/mol · K	C_p J/mol · K
$Al(OH)_3$ gibbsite	78.004	Cryst.	31.956	−1293.2	−1155.0	68.44	91.7
$Al(OH)_3$ bayerite	78.004	Cryst.	30.832	−1288.2	−1153.0	-	-
AlOOH boehmite	59.989	Cryst.	19.55	−990.4	−915.9	48.43	65.6
AlOOH diaspore	59.989	Cryst.	17.76	−999.8	−921.0	35.33	53.3
α-Al_2O_3 corundum	101.961	Cryst.	25.575	−1675.3	−1582.3	50.92	79.0
ρ-Al_2O_3	-	-	-	−1657	-	-	-
γ-Al_2O_3	-	-	-	−1657	-	-	-
κ-Al_2O_3	-	-	-	−1662	-	-	-
δ-Al_2O_3	-	-	-	−1666.5	-	-	-
AlO	42.981	Gas	-	67	41	218.4	30.9
Al_2O	69.962	Gas	-	−145	−173	252	52.0
Al_2O_2	85.962	Gas	-	−395	−400	281	67.2

Sources: (1) NBS Tables of Chemical Thermodynamic Properties Vol. 11, 1982, Supplement No. 2.
(2) JANAF Thermochemical Tables, 1978 Supplement, and Third Edition, 1985
(3) Geological Survey Bulletin 1452, Reprinted with Corrections, 1979.
(4) Kuyunko et al. (1983)

for gibbsite and bayerite are, however, very small. It is rather difficult to prepare a phase-pure bayerite of high crystalline order, whereas well-crystallized gibbsite is obtained easily. The thermodynamic data may, therefore, not accurately reflect the true stability relationship. Several authors claimed that the gibbsite structure is stabilized by alkali ions, and that this trihydroxide has no phase field in the system Al_2O_3-H_2O.[1]

Reliable thermodynamic data have not yet been published for nordstrandite.

Boehmite, γ-AlOOH, crystallizes spontaneously at 373 to 575 K. In the absence of seed crystals, a minimum temperature of 575 K at a pressure of more than 200 bar is needed to induce the formation of diaspore. Transformation of boehmite to diaspore has been observed by many workers; the reverse reaction has never been reported.[1,31] The thermodynamic data in Table IV clearly show that diaspore is the stable phase; newer calculations by Gout and Dandurand[34] suggest, however, that boehmite may have a phase field in the system.

Thermal Decomposition of Aluminum Trihydroxides and Oxide Hydroxides

The phase reactions illustrated in Fig. 9 change drastically when aluminum trihydroxides and oxide hydroxides are heated at ambient pressure and at low vapor pressure of water. Calcination of gibbsite in rotary kilns or fluidized bed furnaces is the commercial process for producing more than 10 million tons of metallurgical and ceramic aluminas each year. Temperatures of 1400 to 1500 K are needed to fully convert gibbsite to anhydrous aluminum oxide, a temperature 800 K higher than that of the $2AlOOH \rightarrow Al_2O_3 + H_2O$ phase transformation in the closed system Al_2O_3-H_2O.

While the fully dehydroxylated product of calcination is α-Al_2O_3, corundum, materials having unique properties are obtained at calcination temperatures lower than about 1200 K. As early as 1879 it was discovered that gibbsite heated to less than 1000 K developed into an effective desiccant.[35] Partially dehydroxylated aluminum hydroxides not only adsorb water but also many organic molecules, inorganic anions, and hydrated cations. They have a large internal porosity, high specific surface area, and show catalytic activity. These properties were reorganized and systematically investigated in the 1930s to 1970s. Excellent review papers were published by Lippens and Steggerda,[36] Oberlander,[37] and Knözinger and Ratnasamy.[38]

The scientific understanding of the relationships between structure and technical properties of the partially calcined hydroxides developed concurrently with a rapidly expanding commercial use of these materials. In 1931, Achenbach[39] and, soon after, Damerell[40] reported that gibbsite crystals retained their original crystal habit after thermal conversion to corundum. As the dehydroxylation leads to a loss of 33% of mass and an increase in density from 2.42 and 3.98 g/cm^3, a large internal porosity develops (Fig. 10).

Long-range crystalline order is almost obliterated in the initial stage of thermal decomposition. Gradual reordering takes place with increasing temperature. Stumpf et al.[41] showed in 1950 that, during reordering, a number of transition forms develop which are reproducible within a certain temperature range. The structures of the forms occurring in a given temperature range are determined by the structure of the starting material; they are different for gibbsite, bayerite, boehmite, or diaspore.

Figure 11 displays the sequence of transition forms which occur during the thermal decomposition

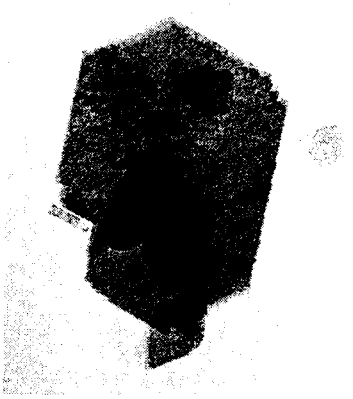

Fig. 10. Transmission electron micrograph of pore system in decomposed gibbsite crystal (× 430 000).

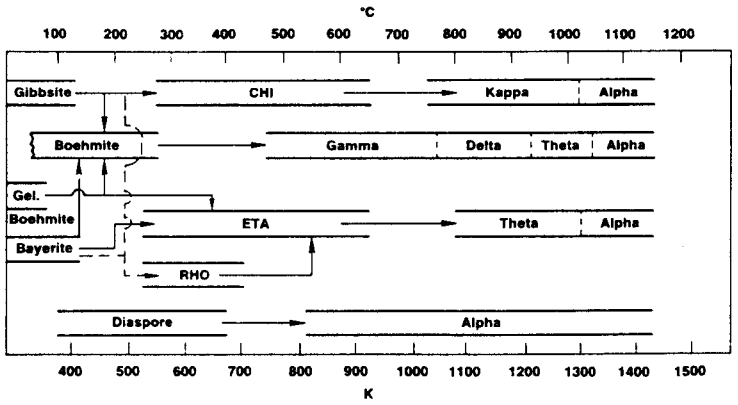

Fig. 11. Sequence of transition aluminas.

of trihydroxides and oxide hydroxides. Structure data are listed in Table V.

No defined structural intermediate develops in the transformation diaspore → corundum. Because of the similarity of the diaspore and corundum lattices, the conversion requires relatively small rearrangements. Epitaxial growth of corundum on diaspore lowers the nucleation energy.

The transformation sequence of gibbsite and bayerite is affected by particle size and partial pressure of water in the heating atmosphere. About 28% of mass is lost between 400 and 650 K. The transition forms chi and eta, respectively, develop. In coarse particles from which the water of dehydroxylation cannot evaporate rapidly, boehmite is formed as a result of local hydrothermal conditions.[42] This boehmite then decomposes according to the sequence outlined in Fig. 11. If, on the other hand, dehydroxylation takes place in vacuum or in rapidly moving air of a temperature above 1000 K, an amorphous form (rho alumina) is obtained.

Boehmite decomposes between 650 and 850 K to form gamma alumina. The term gamma alumina is frequently used to designate any of the poorly ordered transition forms which occur first in the decomposition sequence, that is, chi, eta, rho, and gamma.

The porous texture of the transition aluminas consolidates with increasing temperature. Concurrent with the formation of layer domains of continuous solid, structural reordering progresses via the intermediate stages shown in Fig. 11, until the hexagonally close-packed structure of corundum is obtained.

The sequence of transformation is not reversible. Moreover, the transition aluminas contain varying amounts of hydroxyl ions and are stoichiometrically not well defined. They cannot, therefore, be considered true polymorphs of Al_2O_3 and the schematic diagram of Fig. 11 should not be mistaken for a phase diagram. We prefer to classify the transition aluminas as thermodynamically unstable, but reproducible states of structural reordering.

Surface properties, catalytic activity, and adsorption behavior of transition aluminas are discussed in other chapters of this book (see Index).

Table V. Structural Properties of Transition Aluminas

Form	Crystal System	Space Group	Molecules per Unit Cell	Unit Axis Length, nm a	b	c	Angle	Density g cm
Gamma	Tetragonal	.....	.....	.562	.780	....	.....	3.2[a]
Delta	Orthorhombic	.....	12	.425	1.275	1.021	.....	3.2[a]
	Tetragonal	.....	.....	.790	....	2.34	.....	.....
Eta	Cubic (Spinel)	O_h^7	10	.790	....	....	.....	2.5–3.6
Theta	Monoclinic	C_{2h}^3	4	1.124	.572	1.174	103° 20'	3.56
Chi	Cubic	.....	10	.795	....	....	.....	3.0[a]
	Hexagonal	.....	.....	.556	....	1.344	.....	.....
	Hexagonal	.....	.....	.557	....	8.64	.....	.....
Kappa	Hexagonal	.....	28	9.71	....	.1786	.....	3.1-3.3
	Hexagonal	.....	.....	9.70	....	.1786	.....	.....
	Hexagonal	.....	.....	1.678	....	.1786	.....	.....
Iota	Orthorhombic	.....	4	.773	.778	.292	.....	3.71[a]
	Orthorhombic	D_{2h}^{17} or	3	.759	.767	.287	.....	3.0

[a]Estimated

Aluminum Suboxides

The literature on suboxides of aluminum was reviewed by Mackenzie,[43] Gitlesen et al.,[44] and Yanagida and Kröger.[45] There is general agreement that no solid suboxides exist. Al_2O and AlO have been observed in the gas phase. Ho and Burns[46] claim to have observed AlO_2 and Al_2O_2 in addition to the other suboxides. Data on suboxides have been incorporated in Table IV.

Acknowledgment

All micrographs and tables are courtesy of Aluminum Company of America.

Appendix: Thermal, Dielectric, and Mechanical Properties of Corundum

Table VI. Selected Thermal Properties of α-Al_2O_3 at Various Temperatures

Temperature		Heat Capacity		Thermal Conductivity		Linear Thermal Expansion Coefficient, α	Thermal Diffusivity
K	°C	cal/g·°C	J/g·K	cal/cm·s·°C	J/cm·s·K	$1.^{\circ}K \times 10^{-6}$	cm^2/s
100	−173	0.03	0.126	1.075	4.5	0.6	-
200	−73	0.12	0.502	0.196	0.82	3.3	-
298	25	0.18	0.753	0.110	0.46	5.5	0.075
400	127	0.22	0.920	0.0773	0.324	7.1	0.058
500	227	0.25	1.046	0.0579	0.242	7.5	0.039
600	327	0.26	1.088	0.0451	0.189	7.9	0.030
800	527	0.28	1.172	0.0310	0.130	8.5	0.022
1000	727	0.29	1.216	0.0251	0.105	9.1	0.017
1200	927	0.296	1.238	-	-	9.6	0.013
1400	1127	0.298	1.247	-	-	10.1	0.012
1600	1327	0.30	1.255	-	-	10.5	0.011

Table VII. Dielectric Properties of Corundum

Temperature	Frequency	Dielectric Constant		Dielectric Loss Tangent (Dissipation Factor)		Dielectric[3] Constant	Dielectric Loss Tangent (Dissipation Factor)
		Sapphire[1]		Sapphire[3]			
°C/K	Cycles/sec	⊥ Optic Axis	∥ Optic Axis	⊥ Optic Axis	∥ Optic Axis	Sintered Alumina (99.9% Al_2O_3)	
25/298	10^2	9.34	11.55		0.000012	10.5	0.00086
	10^3	9.34	11.55			10.5	0.00031
	10^4	9.34	11.55			10.5	0.00011
	10^5	9.34	11.55			10.5	
	8.5×10^6	9.34	11.55	0.00003	0.000086	9.6	0.00049 (0.00026)[2]
50/323	10^2	9.36	11.58	0.00001	0.000018	10.6	0.0015
	10^3	9.36	11.58			10.6	0.00056
	10^4	9.36	11.58			10.6	0.00019
	10^5	9.36	11.58			10.6	0.0001
	8.5×10^6	9.36	11.58	0.000032	0.00009	9.7	0.0005 (0.00027)
100/373	10^2	9.41	11.68	0.0002	0.000036	10.7	0.008
	10^3	9.41	11.68		0.00001	10.7	0.002
	10^4	9.41	11.68			10.7	0.00059
	10^5	9.41	11.68			10.7	0.00029
	8.5×10^6	9.41	11.68	0.000036	0.000096	9.7	0.00053 (0.00028)
200/473	10^2	9.53	11.87	0.00012	0.00017	12.0	0.20
	10^3	9.53	11.87	0.000036	0.000034	10.8	0.033
	10^4	9.53	11.87	0.000012	0.00001	10.8	0.0067
	10^5	9.53	11.87			10.8	0.0018
	8.5×10^6	9.53	11.87	0.000047	0.00011	9.8	0.00062 (0.0003)
300/573	10^2	9.65	12.09	0.00062	0.00066	21.6	1.4
	10^3	9.65	12.09	0.00023	0.00015	12.8	0.33
	10^4	9.65	12.09	0.000078	0.00005	11.2	0.06
	10^5	9.65	12.09	0.000037		11.1	0.012
	8.5×10^6	9.65	12.09	0.000062	0.00013	9.9	0.00075 (0.00034)
400/673	10^2	9.82	12.35	0.0033	0.003	100	1.03
	10^3	9.79	12.3	0.001	0.0009	21.5	1.17
	10^4	9.78	12.3	0.00036	0.0003	13.1	0.30
	10^5	9.78	12.3	0.00018		11.5	0.062
	8.5×10^6	9.78	12.3	0.00008	0.00014	10.0	0.001 (0.00039)
500/773	10^2	10.02	12.7	0.026	0.015	25*	0.83
	10^3	9.95	12.55	0.005	0.0035	99	1.10
	10^4	9.92	12.55	0.0012	0.0017	19.0	0.90
	10^5	9.92	12.55	0.00056	0.0011	13	0.24
	8.5×10^6	9.92	12.55	0.000093	0.00015	10.1	0.0016 (0.00048)
600/873	10^2	10.55	13.15	0.21	0.16		
	10^3	10.17	12.83	0.032	0.021		
	10^4	10.07	12.83	0.0054	0.0036		
	10^5	10.07	12.83	0.0011	0.0017		
	8.5×10^6	10.07	12.83	0.00013	0.00017	10.2	0.003 (0.00062)
700/973	10^2		13.15				
	10^3	10.26	13.15				
	10^4	10.26	13.15				
	8.5×10^6	10.26	13.15	0.00021	0.00019	10.3	0.0069 (0.00093)
800/1073	8.5×10^6	10.40	13.50	0.00043	0.00021		

① Data from MIT Technical Report 126: von Hippel (1953, 1959)

② Values in parentheses were obtained from a different sample of sintered alumina.

③ All measurements of sintered alumina at 8.5×10^6 were made with electric field perpendicular to the direction of processing. At other frequencies the field was parallel.

Table VIII. Mechanical Properties of Corundum

Property	25° C Unless Otherwise Noted: Conditions	Values, psi	Alumina
Plastic Constants	C_{11}	72.0.10⁶	Corundum
	C_{12}	23.7.10⁶	Corundum
	C_{13}	16.1.10⁶	Corundum
	C_{11}	−3.4.10⁶	Corundum
	C_{31}	72.2.10⁶	Corundum
	C_{11}	21.4.10⁶	Corundum
Plastic Compliances	S_{11}	2.35.10⁻⁶cm²·dyn⁻¹	Corundum
	S_{12}	−0.72.10⁻⁶cm²·dyn⁻¹	Corundum
	S_{11}	−0.37.10⁻⁶cm²·dyn⁻¹	Corundum
	S_{11}	0.49.10⁻⁶cm²·dyn⁻¹	Corundum
	S_{11}	2.17.10⁻⁶cm²·dyn⁻¹	Corundum
	S_{11}	6.94.10⁻⁶cm²·dyn⁻¹	Corundum
Modulus of Elasticity	25°C	52.6.10⁶	Sapphire
	500°C	48.1.10⁶	Sapphire
	1000°C	43.5.10⁶	Sapphire
	1200°C	41.9.10⁶	Sapphire
	25°C	59.3.10⁶	Polycrystalline
	500°C	57.3.10⁶	Polycrystalline
	1000°C	54.9.10⁶	Polycrystalline
	1200°C	53.6.10⁶	Polycrystalline
Bending Strength	Plates	44,300-115,600[2]	Corundum
		24,000-36,000	RAE Sintered[7]
	1000°C	16,000-22,000	Sapphire
	25°C	37,000(1)28,000[2]	Sapphire
	1000°C	43,000(1)32,000[2]	Sapphire
	Plane[1] 24° / Direction[3] 25°	43,000-131,000	Sapphire
	Plane[1] 45° / Direction[3] 40°	94,000-155,000	Sapphire
	Plane[1] 51° / Direction[3] 55°	17,000-50,000(540°C)	Sapphire
Modulus of Rigidity	25°C	23.3(Reuss).24.1(Voigt)	Sapphire
	25°C	23.3	hot pressed
	25°C	23.9	zero porosity cold pressed zero porosity
Poisson's Ratio	25°C	0.257[4]	cold pressed zero porosity
	25-1000°C	0.32[4]	Sintered
	1400°C	0.45[4]	Sintered
Volume Change[5]		0.00355[6]	Sapphire
Impact Strength		43,000	Sintered
Strength	800°C	27,000	Sintered
	1000°C	24,000	Sintered
	1150°C	16,000	Sintered
	1300°C	11,000	Sintered
	1500°C	3,400	Sintered

Property	25° C Unless Otherwise Noted: Conditions: Temp.	Tension, psi	Duration, hr	Values, psi	Alumina
Strain	1300°C	....	....	Observable	Sintered
	1000°C	7,200	402	$10 \cdot 10^{-2}$%	RAE
	1000°C	20,000	769	$1 \cdot 10^{-2}$%	sintered ① RAE sintered ②
	1000°C	15,100	77	0.49%	Sapphire
	1000°C	12,000	431	1.52%	Sapphire
	1100°C	17,100	95	.08%	Sapphire
	1100°C	13,100	431	2.06%	Sapphire
	1200°C	12,100	53	0.7%	Sapphire
	1300°C	7,250	3	2.34%	Sapphire
	1300°C	8,620	44	32%	Sapphire
Compressive Strength	25°C			443,000 to 495,000	Sapphire
	25°C			50,(XX)	Polycrystalline
	400°C			213,000	Polycrystalline
	1000°C			128,000	Polycrystalline
	1600°C			7,100	Polycrystalline
Tensile Strength	....			21,000	Polycrystalline
	20°C			37,400	Polycrystalline
	800°C			19,500	Polycrystalline
	80°C			33,900	Polycrystalline
	1300°C			11,600	Polycrystalline
	1300°C			6,400	Polycrystalline
	1400°C			7,300	Polycrystalline
	1400°C			4,200	Polycrystalline
	1460°C			1,500	Polycrystalline
	1500°C			0	Polycrystalline
	45° to c-axis				
	30°C			71,000	Sapphire
	300°C			52,5600	Sapphire
	800°C			52,500	Sapphire
	1100°C			88,000	Sapphire
	30° to c-axis			100,000	Sapphire
	45° to c-axis			78,000	Sapphire
	60° to c-axis			65,000	Sapphire
	75° to c-axis			94,000	Sapphire

① Optic axis length of test piece. Bent in plane of optic axis
② Optic axis length of test piece. Bent to plane of optic axis
③ Four-point loading. Angle between rod axis and slip
④ 10 000 kg cm² (142 200 psi)
⑤ Heating to 1770 to 2170 K followed by slow cooling increased strength
⑥ No units
⑦ Specific gravity 3.48–3.82
⑧ Specific gravity 3.61
⑨ Specific gravity 3.78
⑩ Crushing

References

[1]K. Wefers and C. Misra, "Oxides and Hydroxides of Aluminum," Alcoa Tech. Paper No. 19, rev., Pittsburgh, 1987.

[2]H. Schmäh, "Simple Preparation of Bayerite, "*Z. Naturforschg.*, **1**, 322–24 (1946).

[3]J. W. Newsome et al., "Alumina Properties," Alcoa Tech. Paper No. 10, rev., Pittsburgh, 1960.

[4]R. Fricke and B. Wüllhorst, "Energy Differences of Different Modifications of Hydroxides," *Z. Anorg. Allg. Chem.*, **205**, 127–44 (1932).

[5]R. Fricke and K. Jockers, "Hydroxides and Oxide Hydrates," *Z. Anorg. Allg. Chem.*, **262**, 3–14 (1950).

[6]R. Rothbauer, F. Zigan, and H. O'Daniel, "Refinement of the Structure of Bayerite." *Z. Kristallogr.*, **125**, 317–31 (1967).

[7]F. Zigan, W. Joswig, and N. Burger, "The Hydrogen Position n Bayerite, $Al(OH)_3$. "*Z. Kristallogr.*, **148**, 255–73 (1978).

[8]L. K. Hudson, C. Misra, and K. Wefers, "Aluminum Oxide"; pp. 557–94 in Ullmann's Encyclopedia of Industrial Chemistry, Vol. A1. VCh Publishers, Weinheim, 1986.

[9]H. Saalfeld, "Strukturen des Hydrargillits, "*N. Jb. Mineral. Abh.*, **95**, 1–87 (1960).

[10]L. Pauling, "The Structure of the Micas and Related Minerals, "*Proc. Nat. Acad. Sci.*, **16**, 123–28 (1930).

[11]H. D. Megaw, "The Crystal Structure of Hydrargillite," *Z. Kristallogr.*, **A87**, p 185–204 (1934).

[12]R. A. Van Nordstrand, "A New Alumina Trihydrate," *Nature (London)*, **177**, 713–14 (1956).

[13]H. Saalfeld and O. Jarchow, "Crystal Structure of Nordstrandite," *N. Jb. Mineral, Abh.*, **109**, 185–91 (1968).

[14]H. J. Bosmans, "Unit Cell and Crystal Structure of Nordstrandite, "*Acta Crystallogr., Sect. B*, **26**, 649–52 (1970).

[15]J. R. D. Wall, E. G. Wolfenden, E. H. Beard, and T. Deans, "Nordstrandite in Soil from West Sarawak, Borneo," *Nature (London)*, **196**, 264–65 (1962).

[16]J. C. Hathaway and S. O. Schlanger, "Nordstrandite from Guam," *Nature (London)*, **196**, 265–66 (1962).

[17]U. Hauschild, "Nordstrandite, υ-$Al(OH)_3$," *Z. Anorg. Allgem. Chem.*, **324**, 15–30 (1963).

[18]H. Ginsberg and K. Wefers, Aluminium and Magnesium. F. Enke Verlag, Stuttgart, 1971.

[19]I. Valeton, Bauxites. Elsevier, Amsterdam, 1972.

[20]A. W. Laubengayer and R. S. Weiss, "A Hydrothermal Study of Equilibrium in the System Alumina-Water," *J. Am. Chem. Soc.*, **65**, 247–50 (1943).

[21]M. Deflandre, "Crystal Structure of Diaspore," *Bull. Soc. Fr. Mineral.*, **55**, 140–65 (1932).

[22]K. Takane, "Crystal Structure of Diaspore," *Proc. Imp. Acad. Japan*, **9**, 113–17 (1933).

[23]G. M. M. Houben, "Preparation and Properties of Active Aluminas"; Ph.D. Thesis, Technical University, Delft, 1951.

[24]K. Torkar and H. Krischner, "Studies of Aluminum Hydroxide and Oxide, V," *Monatsh. Chem.*, **91**, 757–63 (1960).

[25]G. Yamaguchi and M. Okumiya, "Refinement of the Structure of Tohdite," *Bull. Chem. Soc. Japan*, **42**, 2247–49 (1969).

[26]W. H. Bragg and W. L. Bragg; p. 169 in X-rays and Crystal Structure. Bell and Sons, London, 1916.

[27]L. Pauling and S. B. Hendricks, "The Crystal Structure of Hematite and Corundum," *J. Am. Chem. Soc.*, **47**, 781–90 (1925).

[28]E. Dörre and H. Hübner, Alumina: Processing, Properties and Application. Springer Verlag, New York, 1984.

[29]J. D. Hem and C. E. Roberson, U.S. Geol. Survey Water Supply Paper, 1827-A, 1967.

[30]G. C. Kennedy, "Phase Relations in the System Al_2O_3-H_2O," *Am. J. Sci.*, **257**, 563–73 (1959).

[31]A. Neuhaus and H. Heide, "Hydrothermal Investigations in the System Al_2O_3-H_2O," *Ber. Deutseh, Keram. Ges.*, **42**, 167–84 (1965).

[32]W. S. Fyfe and M. A. Hollander, "Equilibrium Dehydration of Diaspore," *Am. J. Sci.*, **262**, 709–12 (1964).

[33]K. Wefers, "The System Na_2O-Al_2O_3-H_2O," *Erzmetall*, **21**, 423–31 (1967).

[34]R. Gout and J. L. Dandurand, "Phase Equilibria in the System Al_2O_3-H_2O," *Trans. ISCOBA*, **13**, [18] 117–26 (1983).

[35]C. F. Cross, "Rehydration of Metallic Oxides," *J. Chem. Soc.*, **35**, 796–99 (1879).

[36]B. C. Lippens and J. J. Steggerda; pp. 171–209 in Physical and Chemical Aspects of Adsorbents and Catalysts. Edited by B. G. Linsen. Academic Press, London, 1970.

[37]R. K. Oberlander, "Aluminas for Catalysts"; pp. 63–112 in Applications of Industrial Catalysts, Vol. 3. Academic Press, London, 1984.

[38]H. Knözinger and P. Ratnasamy, "Catalytic Aluminas, Surface Models," *Catal. Rev.-Sci. Eng.*, **17**, 31–69 (1978).

[39]H. Achenbach, "Thermal Decomposition of Synthetic Hydrargillite," *Chem. Erde*, **6**, 307–56 (1931).

[40]V. R. Damerell, F. Hovorka, and W. E. White, "Surface Chemistry of Hydrates," *J. Phys. Chem.*, **36**, 1255–67 (1932).

[41]H. C. Stumpf, A. S. Russell, J. W. Newsome, and C. M. Tucker, "Thermal Transformation of Aluminas," *Ind. Eng. Chem.*, **42**, 1398–1403 (1950).

[42]J. H. DeBoer and G. M. M. Houben, "Binding of Water in Aluminum Oxide"; pp. 237–44 in Proceedings of an International Symposium on Reactivity in Solids, Part I, 1952.

[43]K. J. D. Mackenzie, "Oxides of Aluminum Other Than Al_2O_3", *J. Br. Ceram. Soc.*, **5** [2] 183–93 (1968).

[44]G. Gitlesen, O. Herstadt, and V. Motzfeld; pp. 180–96 in Selected Topics in High Temperature Chemistry, Oslo, 1966.

[45]H. Yanagida and F. A. Kröger, "The System Al-O," *J. Am. Ceram. Soc.*, **51** [12] 700–706 (1968).

[46]P. Ho and R. P. Burns, "A Mass Spectrometric Study of the Aluminum Dioxide Molecule," *High Temp. Sci.*, **12**, 31–39 (1980).

[47]A. von Hippel, Table of Dielectric Materials, Vol. IV, Tech. Rep. 57, January 1953 and Vol. VI, Tech. Rep. 126, June 1959, MIT Lab for Insulation Research.

[48]N. S. Kuyunko, S. D. Malinin, and I. L. Khodakovskii, "Thermodynamic Data of Aluminas," *Geokhimiya*, **3**, 419–28 (1983).

Mechanical Properties of Alumina

Richard C. Bradt
University of Nevada-Reno
Reno, NV 89557-0047

William D. Scott
University of Washington
Seattle, WA 98195

Because aluminum oxide is widely used as a structural material over a broad temperature range, its mechanical properties have been extensively investigated and are well documented. This chapter focuses on the important fundamental mechanical properties of aluminum oxide. Subjects addressed herein include elastic behavior, fracture, plastic deformation, and creep.

Since the 1970 publication of Gitzen's[1] classic entitled "Alumina as a Ceramic Material," there have been three additional meritorious publications which contain substantial mechanical property sections. They include Belyaev's[2] "Ruby and Sapphire," Dorre and Hubner's[3] "Alumina," and Kingery's[4] "Structure and Properties of MgO and Al_2O_3 Ceramics." These four in total do not address every aspect of the mechanical behavior of Al_2O_3, so that this article should not be expected to be totally comprehensive either; rather the fundamental aspects of the mechanical behavior are addressed, including the elastic behavior, fracture, plastic deformation, and creep. Each is treated in a manner which focuses on the fundamental aspects rather than simply summarizing the general literature.

Elastic Properties

The single-crystal elastic constants of a crystalline solid such as Al_2O_3, which is usually referred to as sapphire in the single-crystal form, are the most direct measurements of the bonding within the structure. As such, they provide very fundamental data for calculating a wide variety of physical and chemical properties. For that reason, the room-temperature single-crystal compliances (C_{ij}) and stiffnesses (S_{ij}) are initially considered. As with the elastic constants of other common crystals, a number of different researchers have measured the elastic constants of Al_2O_3; they are summarized in Table I. The format in that table is to list first the C_{ij}, then the S_{ij} immediately beneath. As the trigonal structure of single-crystal Al_2O_3 has six independent single-crystal elastic constants, they are listed in the usual subscript order, namely: 11, 12, 13, 14, 33, and 44. The listed C_{ij} are the coefficients of 10^{11} cm^2/dyne, while the S_{ij} are 10^{-12} cm^2/dyne. As these single-crystal measurements are quite difficult to complete, it is not surprising that some of the researchers are in moderate disagreement. It is significant, however, that the four studies since 1960 report virtually the same single-crystal elastic constants.

Simply listing the single-crystal elastic constants, such as in Table I, does not yield an adequate description for the degree of elastic anisotropy which exists in the Al_2O_3 crystal structure. To appreciate that anisotropy, it is convenient to consider the Young's modulus in the crystallographic directions of the $a(1/S_{11})$ and $c(1/S_{33})$ axes. Using Tefft's[9] results, $E\langle\bar{1}2\bar{1}0\rangle$ is 430 GPa, while $E\langle 0001\rangle$ is 465 GPa. However, a minimum in Young's modulus occurs at an intermediate orientation when calculated. The polar plot of Fig. 1 shows the variation on the $(10\bar{1}0)$ and the intermediate minimum of only 380 GPa. Whereas many other single

Table I. Room-Temperature Single-Crystal Elastic Constants of Al_2O_3

Ref.		11	12	13	14	33	44
5 (1956) Hearmon	C	4.66	1.27	1.17	0.94	5.06	2.35
	S	0.28	−0.09	−0.04	−0.15	0.22	0.55
6 (1958) Mayer and Hiedemann	C	4.96	1.35	1.17	−0.23	5.02	0.41
	S	0.24	−0.06	−0.04	0.17	0.22	2.63
7 (1960) Wachtman, Tefft, Lam, and Stinchfield	C	4.97	1.63	1.11	−0.24	4.98	1.47
	S	0.24	−0.07	−0.04	0.05	0.22	0.69
8 (1963) Bernstein	C	4.90	1.65	1.13	−0.23	4.90	1.45
	S	0.24	−0.07	−0.04	0.05	0.22	0.70
9 (1966) Tefft	C	4.97	1.64	1.12	−0.24	4.99	1.47
	S	0.24	−0.07	−0.04	0.05	0.22	0.69
10 (1967) Gieske and Barsch	C	4.98	1.63	1.17	−0.23	5.02	1.47
	S	0.24	−0.07	−0.04	0.05	0.22	0.69

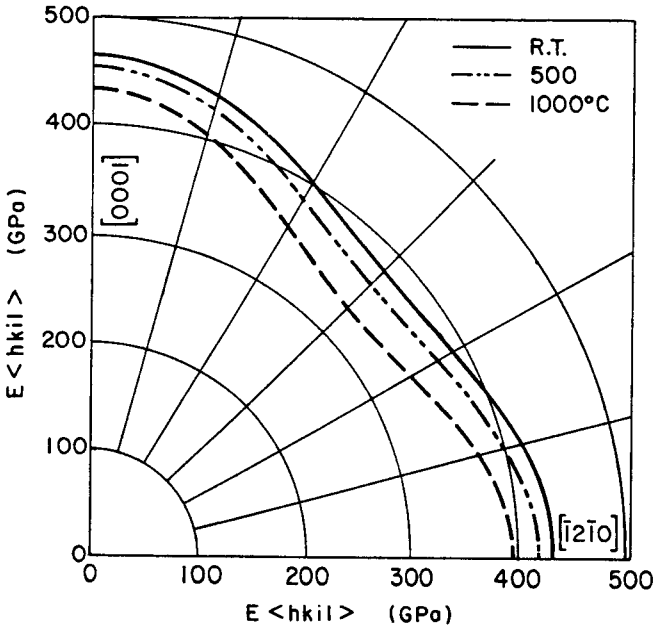

Fig. 1. Elastic modulus of Al_2O_3, $E\langle hkil\rangle$, as a function of orientation on the $(10\bar{1}0)$.

crystals are quite elastically anisotropic, Al_2O_3 is not very much so.

Figure 1 also illustrates the temperature dependence of the Young's moduli, calculated from the single-crystal elastic constants after Tefft.[9] The anisotropy remains about the same; however, the decrease in E with increasing T is not very well revealed. Figure 2 illustrates the temperature dependencies of the

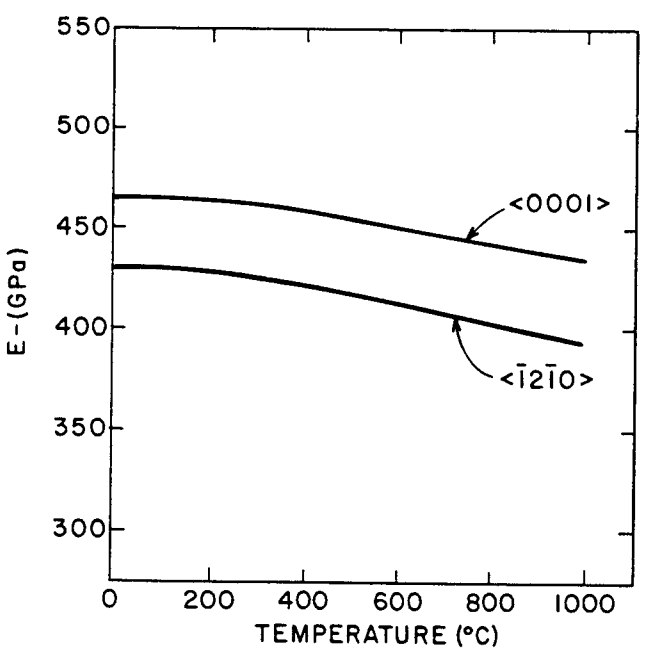

Fig. 2. Elastic modulus, $E\langle hkil\rangle$, of Al_2O_3 as a function of temperature.

$E\langle 0001\rangle$ and $E\langle \bar{1}2\bar{1}0\rangle$ as calculated from the S_{ij} measured at high temperatures by Tefft.[9] It is evident that the decrease is quite minimal and nearly linear from room temperature through about 800°C.

From the individual single-crystal elastic constants it is also possible to estimate the technical elastic moduli E, G, K, and ν for a fully dense, isotropic, polycrystalline Al_2O_3 ceramic body by applying any one of the numerous averaging schemes. That of Hill, which is simply the average of the Voigt and Reuss bounds, is summarized in Table II for room temperature. It is evident that all four of the recent studies are in relatively good agreement in this instance. Particularly important is the Poisson's ratio of only 0.23, a value well below the one-third value sometimes assigned to "all" crystalline solids and often incorrectly applied to Al_2O_3 ceramics.

As Al_2O_3 ceramic bodies are frequently processed in a manner to introduce a preferred grain orientation or crystal texture within their structures, it must be noted that E and G values both higher and lower than those calculated in Table II may be expected in those ceramic bodies. Furthermore, if the structure contains oriented porosity, more anisotropy of a complex nature can be expected.

The presence of porosity is well documented to reduce the elastic moduli of ceramics. In a review article, Rice[11] summarized porosity effects on the elastic moduli of ceramics in general. Dorre and Hubner[3] specifically addressed Al_2O_3 ceramic bodies. Various equations have been demonstrated to adequately describe the effects of porosity on the Young's modulus of some aluminas, including the second-order equation and the usual exponential one. However, when G, K, and ν are also considered, the agreement of experimental data and the fit of equations is less consistent and not wholly satisfactory. Whereas a compilation of equations and constants may seem in order, the disparities between the different experimental results illustrate that the elastic moduli/porosity trends are in fact ceramic-body specific. Thus, rather than compile a list of inapplicable constants, the need to experimentally measure the actual values of porous Al_2O_3 ceramic bodies is emphasized.

Fracture

The fracture of alumina can be addressed progressively, starting with the cleavage of single crystals through the fracture of polycrystalline alumina ceram-

Table II. Calculated Room-Temperature Polycrystalline Elastic Moduli as the Hill Average

Ref.	E^*	G^*	ν	K^*
[7] (1960)	402	163	0.22	251
[8] (1963)	396	159	0.23	250
[9] (1966)	403	163	0.23	252
[10] (1967)	403	163	0.23	254

*In GPa.

ics. That scheme is followed by extending the concept of single-crystal cleavage to the toughness of increasingly larger grain sizes of polycrystalline alumina, including the *R*-curve behavior and the work of fracture. Slow crack growth is considered, again from both the single-crystal and polycrystalline ceramic viewpoints and finally brief attention is given to creep fracture. The conventional strength approach is not given very significant emphasis in this review for little is known about the flaw sizes in most instances.

The fracture or cleavage of single crystals of alumina as corundum, or in the sapphire or ruby forms, has been subjected to intense study by numerous mineralogists, ceramists, and other academic and industrial scientists. It has direct commercial application in the crushing of single-crystal grains of alumina abrasives, the wear and polishing of crystals, the performance of jewel bearings, the failure of vapor arc lamp envelopes, the cracking of microcircuit substrates, and the design and failure of metal-matrix composites using single-crystal alumina whiskers for reinforcement. Of course, the fine grinding or milling of alumina powders for subsequent consolidation into polycrystalline ceramic bodies also depends directly on the cleavage of individual crystallites once the original grain and powders are sufficiently reduced in size.

Studies of the fracture or cleavage of single-crystal alumina can be conveniently grouped into four categories. They include (i) mineralogical investigations such as those of Shappel,[12] Winchell,[13] and Yamaguchi et al.[14]; (ii) conventional strength studies such as those of Wachtman and Maxwell,[15] Brenner,[16] and more recently Noda[17]; (iii) the fracture mechanics studies of Wiederhorn,[18] Wieland,[19] Smith and Pletka,[20] and Iwasa and Bradt[21]; and (iv) a number of different types of general observational efforts including those of Palmour et al.,[22] Mallinder and Proctor,[23] and Anderson.[24] All of this research must necessarily achieve consistency. However, it is the mineralogical and the fracture mechanics investigations that will receive the most attention in this review.

There are numerous statements in the literature concerning the conchoidal fracture of alumina, similar to that often accepted to occur for glasses and single-crystal quartz. However, whenever fracture traces for single crystals of alumina are closely examined, such as was done by Yamaguchi et al.,[14] it is apparent that a number of distinct crystallographic planes do preferentially cleave as the bonds across some planes are broken more readily than others. At room temperature, no crystal plane of alumina cleaves more easily than the rhombohedral *r* plane, the $(\bar{1}012)$. Partings, which are planarlike quasi-cleavage fractures that approximately parallel individual crystal planes, but are not usually accepted as true cleavage, have been reported to occur near to the (0001), $(10\bar{1}0)$, $(11\bar{2}0)$, $(10\bar{1}1)$, $(11\bar{2}3)$, and $(11\bar{2}6)$ planes. It must be concluded that crack propagation in single-crystal alumina can and does readily occur as cleavage on specific crystallographic planes.

The studies have concluded that the rhombohedral $(\bar{1}012)$ plane is the preferred room-temperature cleavage plane; those of Shappel,[12] Wiederhorn,[18] and Iwasa et al.,[21,25] also agree that the basal or *C* plane, the (0001), is very difficult to cleave at room temperature. Shappel assigned an ease-of-cleavability index of 12.4 to the $(\bar{1}012)$ but only 9.5 to the (0001), while Wiederhorn measured a surface energy of 6 J/m^2 for the $(\bar{1}012)$ and estimated that of the (0001) to be >40 J/m^2. Iwasa et al. reported K_{Ic} values of 2.38 ± 0.14 MPa • m$^{1/2}$ and 4.54 ± 0.33 MPa • m$^{1/2}$ for the $(\bar{1}012)$ and (0001), respectively. Several other reports related to the difficulty of basal-plane cleavage at room temperature are noteworthy. For double cantilever beam specimens, Wiederhorn reports that he was not able to propagate a basal plane crack the full thickness of the specimen web. He attributed this difficulty to a lack of charge neutrality on the basal plane. Noda[17] and Becher[26] also confirm similar difficulties with room-temperature basal plane cleavage in their strength studies. Becher's calculations yielded a discontinuity that could not be explained for fracture on the (0001). The fundamental reason for the lack of basal plane cleavage at room temperature is not understood. However, the reason for the ease of cleavage on the $(\bar{1}012)$ rhombohedral plane can be attributed to the extensive array of vacant cation lattice sites that are parallel to that crystal plane.

Table III lists the room-temperature fracture toughnesses after Iwasa and Bradt[21] for the four previously mentioned planes, along with the Shappel[12] ease-of-cleavability index estimates and the fracture surface energies reported by Wiederhorn.[18] It is evident from these values that the rhombohedral plane, $(\bar{1}012)$, is the preferred crystallographic plane for cleavage at room temperature and that the basal plane, (0001), is much more difficult to fracture. Although these results are the most comprehensive, a number of other fracture reports generally confirm these observations. Stofel and Conrad[27] observed numerous rhombohedral cleavage fractures in bend tests of 0° sapphire rods, while Wieland[19] observed that the $(\bar{1}012)$ plane cleaved much more easily than the $(10\bar{1}0)$ plane. Smith and Pletka[20] examined the microindentation toughnesses of the $(10\bar{1}0)$ and $(11\bar{2}0)$ planes and reported that crack extension on the $(10\bar{1}0)$ is more difficult than on the $(11\bar{2}0)$ plane, also in general agreement with Table III.

Kirchner and Gruver,[28] in examining slow crack growth in polycrystalline aluminas, assigned approximate K_{Ic} values to various crystallographic planes of the corundum structure. Their values agree in principle with the order expressed in Table III. In addition, they also estimated a K_{Ic} of 4.3 MPa • m$^{1/2}$ for the $(11\bar{2}6)$ plane, which might be expected to be a rather difficult plane to cleave. Noda[17] made extensive strength measurements on polished single-crystal spec-

Table III. Cleavage Planes of Single-Crystal Alumina at Room Temperature

Plane	Shappel Cleavability (Ref. 12)	γ_f (J/m^2) (Ref. 18)	K_{Ic}(MPa • m$^{1/2}$) (Ref. 21)
c (0001)	9.5	>40	4.54 ± 0.32
m (10$\bar{1}$0)	10.2	7.3	3.14 ± 0.30
r ($\bar{1}$012)	12.4	6.0	2.38 ± 0.14
a (11$\bar{2}$0)	9.2		2.43 ± 0.26

imens of various orientations, including different angles of tension on all four of the planes listed in Table III. He concluded that the ($\bar{1}$012) plane was indeed the dominant room-temperature cleavage plane for sapphire. For single-crystal alumina, it must be concluded that the rhombohedral ($\bar{1}$012) plane, is the preferred cleavage plane at room temperature and that the basal plane, the (0001) plane, is one of the most difficult crystal planes to cleave at room temperature.

In spite of the aforementioned difficulties with achieving room-temperature basal plane cleavage, there are a number of reliable, well-documented reports of extensive basal plane cleavage. Becher[26] shows an excellent micrograph of a flat (0001) region on a room-temperature fracture, while Firestone and Heuer[29] show a similar (0001) region in an 1800°C fracture originating during creep of 0° crystals. Abdel-Latif et al.[30] also describe extensive flat fracture mirror regions of basal plane cleavage for c-axis sapphire crystals tested in tension and Brenner[16] also reports smooth basal plane fractures. However, one of the most outstanding reports of basal plane cleavage is that of Anderson[24] for sapphire vapor arc lamp envelopes. Anderson frequently observed that (0001) basal plane cleavage of the single-crystal envelopes occurred at ≈1100°C. Castaing[31] also reported that well-defined basal plane cleavage of sapphire occurs at high pressures, which is approximately equivalent to a high-temperature observation. Thus, (0001) basal plane cleavage does occur in single-crystal alumina and it apparently occurs more easily at high temperatures. The statement of Wiederhorn et al.[32] that cleavage "planes preferred at low temperatures might not be preferred at high temperatures" is certainly applicable to the rhombohedral plane cleavage of Al_2O_3.

The effects of temperature on the fracture toughnesses of the (10$\bar{1}$2), (0001), (10$\bar{1}$0), and (11$\bar{2}$0) planes were measured by Iwasa and Bradt[21] to 1400°C in air. Figure 3 illustrates the composite temperature trends of the cleavage planes measured by Iwasa and Bradt. All of those orientations exhibited a distinct decrease of K_{Ic} with increasing temperature at lower temperatures, while the ($\bar{1}$012) and (0001) also exhibited increases of K_{Ic} above about 800° to 1000°C, indicative of the brittle-to-ductile transition, but without macroscopically noticeable plastic flow. Wiederhorn et al.[32] also studied the effect of temperature on the K_{Ic} of the (10$\bar{1}$0) plane and observed that it decreased from about 2.5 to 1.8 MPa • m$^{1/2}$ between room temperature and 600°C. Wieland[19] compared the (10$\bar{1}$0) plane and the

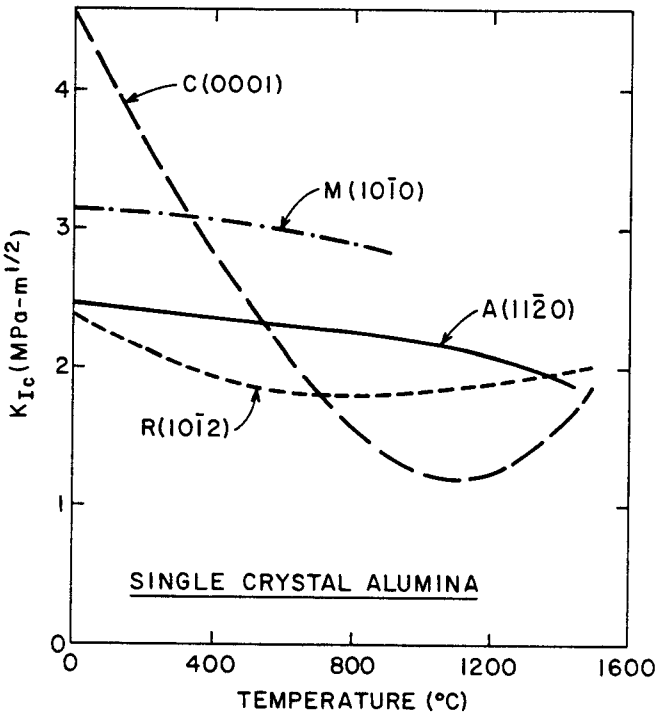

Fig. 3. Fracture toughnesses of the single-crystal planes from room temperature through 1400°C.

($\bar{1}$012) plane, but not in direct K_{Ic} form. He reported "toughness" decreases with increasing temperature for both, with the ($\bar{1}$012) plane toughness perhaps decreasing slightly more rapidly. Both Iwasa and Bradt and Wiederhorn et al. reported a difficulty with high-temperature crack propagation for that plane. Prior to considering the implications of Fig. 3, it is appropriate to address the low-temperature fracture toughness decreases of the cleavage planes.

If the cleavage of single-crystal alumina is considered to be elastic in the low-temperature region, which appears to be a reasonable assumption since dislocation plastic flow processes should be expected to increase K_{Ic} with increasing temperature, then the slope of dK_{Ic}/dT can be estimated. Iwasa and Bradt[21] have shown that:

$$\frac{dK_{Ic}}{dT} = K_{Ic}\left(\frac{1}{E}\frac{dE}{dT} - \frac{1}{2}\alpha\right) \qquad (1)$$

Values for (dK_{Ic}/dT) can be readily calculated from the temperature dependence of the elastic constants after Tefft[9] and the directional coefficients of thermal ex-

pansion after Wachtman et al.[33] The results of these elastic calculations yield negative (dK_{Ic}/dT) slopes with values of 10^{-3} to 10^{-4} (MPa • $m^{1/2}$/°C), in reasonable agreement with the measurements of Wiederhorn et al.[32] and Wieland.[19] The ($\bar{1}012$) plane measurements of Iwasa and Bradt are described quite well by the simple elastic model; however, those for the (0001) plane are not. The failure of this simple elastic model for the (0001) basal plane cleavage is surprising and in this single instance is not understood. Fractographic evidence and other research results support the rapid toughness decrease which is observed experimentally for the (0001) as opposed to the more gradually predicted theoretical elastic calculations.

The limited observations of room-temperature (0001) fracture surfaces reveal that, after the crack has initiated from the original flaw, it tends to seek the lower toughness planes rapidly, so that the fracture surface is just a recurring series of the characteristic stairlike or checkerboard pattern of ($\bar{1}012$) plane cleavage. However, the basal plane (0001) cleavage in the vicinity of 1000°C is a smooth, almost perfectly planar surface without any evidence of the numerous multiple cleavage steps.[21,24] These fracture-surface observations and the toughness measurements reported in Fig. 3 indicate that the basal plane, the (0001), is actually the preferred cleavage plane of single-crystal alumina at high temperatures. Figure 3 clearly illustrates that above about 700°C the basal plane or (0001) rather than the rhombohedral ($\bar{1}012$) is the preferred cleavage plane of alumina. The form of K_{Ic} versus temperature for the (0001) basal plane very strongly suggests that, above about 1700°C, the rhombohedral plane, ($\bar{1}012$), or perhaps even the ($11\bar{2}0$) *A* plane may become the preferred cleavage plane. The rapid K_{Ic} increase for the (0001) basal *C* plane above about 1100°C probably occurs from dislocation plastic flow processes in the crack-tip region, as suggested by Wachtman and Maxwell[15] and by Wiederhorn et al.[32]

The transition from rhombohedral to basal plane cleavage explains Anderson's[24] extensive and frequent observations of basal plane cleavage at about 1100°C. Anderson observed frequent and extensive basal cleavage in the vapor arc lamp envelopes fractured at 1100°C, because the (0001) basal plane is indeed the preferred cleavage plane of single-crystal alumina at that temperature. Figure 3 also explains Firestone and Heuer's[29] observation of only a partial basal cleavage at 1800°C, similar to room-temperature fractures initiating on the basal plane. It is apparent why Firestone and Heuer's observation of a rapid change from a flat basal plane cleavage fracture to cleavage steps of another crystallographic variety at 1800°C is very similar to the fracture surfaces observed by Wachtman and Maxwell[15] and Abdel-Latif et al.[30] for room-temperature fractures. All three papers contain very similar micrographs of the fracture surfaces. Projection of the K_{Ic} versus T curves of Fig. 3 suggests that above about 1700°C the (0001) basal plane is no longer expected to be the preferred cleavage plane, but rather the ($11\bar{2}0$) or ($\bar{1}012$) would have a lower toughness. Thus, for fracture at 1800°C, a propagating crack might be expected to reorient and seek one of the low-toughness planes rather than the (0001), if it initiates on the (0001). The 1800°C fracture pattern would be expected to closely resemble that for a room-temperature basal (0001) plane fracture. That type of behavior is exactly what Firestone and Heuer observed.

It is natural that the temperature dependence of the toughness should influence the strength. Since Jackman and Roberts[34] first reported a minimum for the bend strengths of alumina single crystals with increasing temperature, there have been numerous other studies of that phenomenon, including those of Charles and Shaw,[35] Heuer and Roberts,[36] Davies,[37] Bayer and Cooper,[38] and most recently Shahinian.[39] The latter was a tensile strength study that definitively substantiated the strength minimum which has been observed to occur between 400° and 900°C, the exact temperature depending on the growth process of the crystals, their purity, orientation, surface conditioning, and annealing, as well as the particular test parameters. The basis for this strength minimum with increasing temperature has not been determined with certainty. It has been attributed to different phenomena, including the relief of residual strains developed during the original crystal growth, alteration of the surface condition or surface structure of the test specimens, the role of twinning in crack nucleation, various stress corrosion processes (although Brenner[16] suggests that they are not a factor), and the onset of limited ductility in the form of dislocation processes in the vicinity of stress concentrations. This latter mechanism has been applied to describe the lower temperature weakening by dislocation plastic flow nucleation of cracks and also the high-temperature strengthening by a crack-tip blunting process. Certainly each of the aforementioned processes can be envisioned as a potential contributor to one aspect or another of the strength minimum. The composite fracture toughness results depicted in Fig. 3 can equally well explain the strength minimum with increasing temperature.

The strength of a material is related to the fracture toughness, K_{Ic}, and the flaw size, c, through the Griffith equation:

$$\sigma_f = K_{Ic} Y c^{-1/2} \tag{2}$$

where σ_f is the strength and Y is a flaw geometry parameter. During stressing, fracture can be expected to occur for the most serious situation, that of the largest flaw and lowest toughness. The combined form of the fracture toughness values for the ($\bar{1}012$) and the (0001) planes in Fig. 3 clearly suggests a strength minimum, the exact temperature of which is determined by the critical flaw size relative to the ($\bar{1}012$) or

(0001) planes and perhaps the residual stresses at the flaw tips as well. A strength minimum can readily occur if the lower temperature strength decrease is initially dominated by the toughness decrease on the $(\bar{1}012)$ plane which eventually transfers control to the (0001) toughness, as it assumes a major role in determining the minimum as well as the subsequent increase at the higher temperatures. Since various flaw configurations relative to the $(\bar{1}012)$ and (0001) planes are highly probable, as discussed by Becher,[26] the gradual nature of the often-observed strength minimum is easily visualized as being influenced by the toughness minimum which occurs in the temperature regime of interest.

It may seem like a simple transition to the grain-size effect on toughness for polycrystalline alumina ceramics, having just addressed the toughness for the individual cleavage planes in the alumina crystal structure. An averaging scheme of planar cleavages to estimate a polycrystalline toughness analogous to that which is applied for single-crystal elastic stiffnesses or compliances to arrive at a polycrystalline Young's modulus might be envisioned. However, it has recently become apparent that even though it is possible to apply the toughness concept through the Griffith equation to the strength of polycrystalline alumina ceramics, determination of the correct value for the fracture toughness, or K_{Ic}, to utilize is not a routine exercise.

Since the original study of the grain-size effect on the fracture toughness of polycrystalline alumina by Gutshall and Gross,[40] which reported that the toughness increased with increasing grain size over the grain-size range from about 10 to 50 μm, there have been numerous published reports of the toughness for different polycrystalline alumina ceramics. Included are the excellent studies of Evans and Tappin,[41] Simpson,[42] Rice et al.,[43] and Mussler et al.[44] Although other publications no doubt number in the hundreds, they will not all be referenced, nor even summarized in tabular form in this review for reasons which will become apparent. It will suffice to note that summaries of toughness versus grain size for Al_2O_3 have been for the most part somewhat puzzling and confusing.

The overall trend of the "toughness," whether it is expressed as a critical stress intensity, the fracture toughness, K_{Ic}, or as a fracture surface energy derived from the K_{Ic} value, usually through

$$K_{Ic}^2 = \frac{2E\gamma}{(1 - \nu^2)} \tag{3}$$

or even as the total work of fracture is approximate in general form. It is that the fracture resistance of polycrystalline alumina increases with increasing grain size to a maximum for a grain size somewhere between 50 and 100 μm, then appears to decrease at still larger grain sizes. Hayashi et al.[45] recently summarized this behavior by graphically depicting that trend and its variation with temperature as well as grain size. The general diagram of fracture surface energy versus grain size and temperature which Hayashi et al. constructed is reproduced in Fig. 4. The fracture resistance parameter which they have chosen to present is the least ambiguous quantity, the total work of fracture.

It was previously noted that several different parameters have been utilized to characterize the fracture resistance of polycrystalline alumina. A real problem is that the methods often measure different factors relative to the fracture or crack-growth resistance. The two extremes are the use of K_{Ic} (or a fracture surface energy derived from K_{Ic}) and the total work of fracture. The fracture toughness K_{Ic} is a stress intensity which is characteristic of the initiation and catastrophic propagation of a crack,[46] often measured in a strength-like test. The total work of fracture relates to the quasi-static stable propagation of a crack completely through a test specimen.[47,48] The transition between the two is the R-curve behavior of the ceramic. R-curve behavior characterizes the change of crack-growth resistance with increasing crack length.[45] In the case of polycrystalline alumina ceramics, the research studies of several groups[49–51] have been particularly instrumental in elucidating the R-curve behavior of polycrystalline alumina ceramics.

In the past two decades there have been numerous efforts to specify the fracture surface energies or fracture toughnesses of polycrystalline alumina ceramics (and other ceramics) as those specific fracture resistance parameters vary with grain size. The typical grain-size range that is usually achieved in normal ceramic processing is 10 to 30 μm. The results which are consistently achieved when the K_{Ic} values are examined is that the fracture toughness is within the range of about 3 to 6 MPa • $m^{1/2}$, which converts to fracture surface energies of about 10 to 35 J/m^2. However, when the individual toughness values for similar grain sizes from different measurement tech-

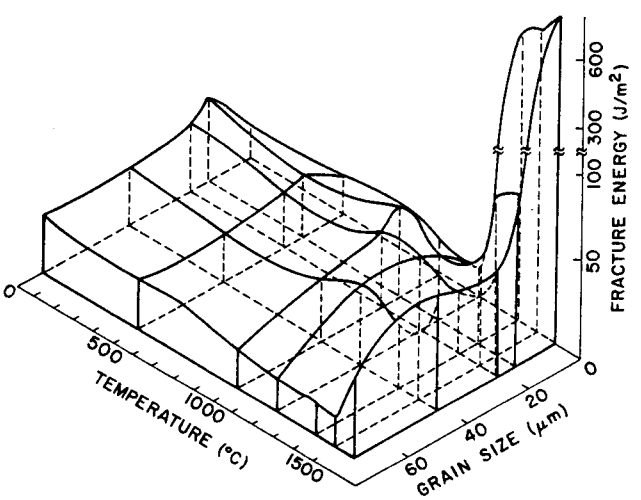

Fig. 4. Work of fracture vs grain size and temperature.

niques or different investigators are examined, it is frequently observed that different experimental results are reported and that the statistical confidence intervals of the individual measurements are unusually large. As previously noted, tabular summaries of these toughness results are somewhat puzzling and have at times appeared to be contradictory. The reason for this is a combination of factors related to the *R*-curve effects that are present in the different experimental techniques and specimen sizes.

One experimental concern has always been the sharpness of the crack, for which sawed notches with finite radii of curvature at the artificial "crack" tip yield artificially high K_{Ic} values. However, even for very sharp cracks, measurement of a K_{Ic} value for polycrystalline alumina is imprecise because of the increasing or rising *R*-curve behavior of large-grained polycrystalline alumina ceramics. Essentially, the crack-growth resistance depends on the crack length, especially for real cracks, as demonstrated by Hubner and Jillek,[49] in their comparison of large sawed artificial cracks and slowly grown real cracks. Large, slowly grown real cracks have a greater resistance to further extension than artificial sawed cracks of the same length. Furthermore, longer real cracks are more crack-growth-resistant than short ones. Figure 5 illustrates a typical comparison of the two types of cracks for a large grain-size alumina.

In addition to the crack-length effect of the rising *R*-curve behavior, it is now apparent that there is also a grain-size effect, although it is not fully understood at this time.[52] As there undoubtedly exist specimen size and type effects, too, it is not possible to present a general set or series of *R*-curves for all alumina ceramics of different grain sizes, but rather it is appropriate to present the trends illustrated in Fig. 6. Larger average alumina grain sizes appear to yield

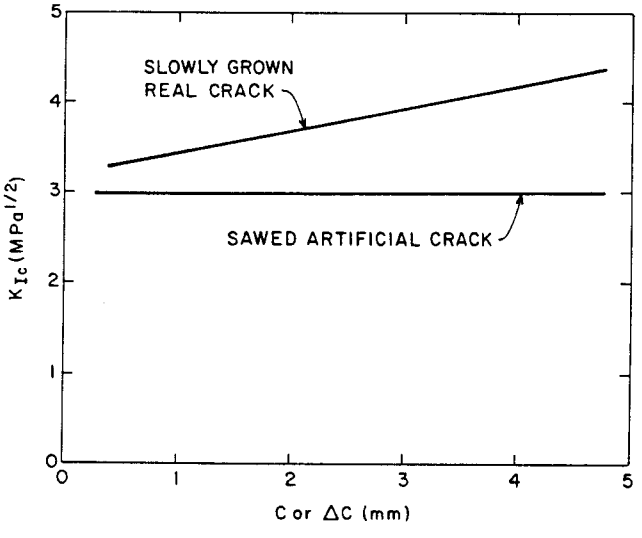

Fig. 5. Typical toughness vs crack length (*c*) or extension (Δc) for a 25 μm average grain size alumina.

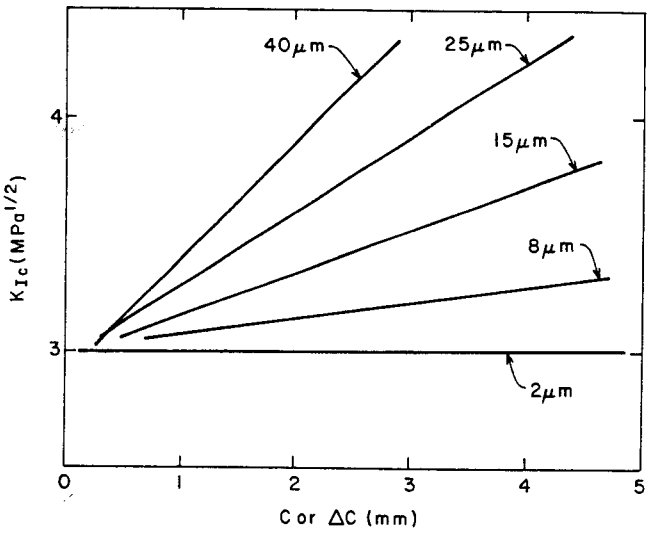

Fig. 6. Typical *R*-curves for different grain size polycrystalline aluminas.

more steeply increasing or rising *R*-curves, that is, larger ($dK_{Ic}/d\Delta C$) values. Very fine grain-size alumina ceramics (<2 to 3 μm) exhibit flat *R*-curves, that is, the crack-growth resistance is not a function of the crack length.

There are at least four other significant observations regarding the presence of increasing or rising *R*-curves in polycrystalline alumina ceramics that need to be considered. Those are that *R*-curves which are determined by different test specimens (i.e., DCB, DT, and SENB) do not yield the same *R* versus Δc or K_{IR} versus Δc results,[53] that rising *R*-curves from flexural or bend specimens for different (a/W) values have different slopes and do not superimpose when normalized,[50] that surface cracks and bulk or long cracks seem to yield different *R*-curves,[54] and finally that *R*-curve textural effects are present in oriented polycrystalline aluminas.[55] It is apparent from the consideration of these in total that the *R*-curve behavior of polycrystalline alumina is not an intrinsic material property or characteristic, but rather relates to a number of different variables, including specimen and test conditions, as described by Sakai and Bradt.[56] There does not exist a unique *R*-curve that characterizes all alumina ceramics!

It is now further appropriate to consider the effect of the grain size of a polycrystalline alumina ceramic on its fracture toughness, K_{Ic}, or fracture surface energy, an issue which was previously avoided. The point is simply that there is no meaningful K_{Ic}-to-grain size relationship, nor even a single *R*-curve descriptive of the fracture behavior of a polycrystalline alumina. The critical stress intensity value, K_{Ic}, where a specimen or object fails catastrophically depends on the critical flaw character, the object's geometry, and its loading conditions, as well as its previous history of slow or subcritical crack extension. It thus is not a

meaningful exercise to describe or to present a unique grain size-fracture toughness relationship for polycrystalline alumina ceramics, for in fact no such relationship exists.

It is necessary to address the microstructural cause or reason for the *R*-curve behavior of polycrystalline alumina, as the cause and mechanism are well known, although not completely understood at the present. Knehans and Steinbrech[57] proved that the mechanism of increasing *R*-curve behavior occurs in the following wake region of an advancing crack, not in the frontal process zone ahead of the crack. They did this through notching experiments of extended natural cracks that removed the following wake region and returned the crack resistance to its original $\Delta c = 0$ level, independent of the amount of stable extension. That the "toughening" should occur behind the crack is not surprising as it is the crack length which provides for a cumulative toughening mechanism as the crack extends, not the region in front of the advancing crack.

The mechanisms which occur in the following wake region behind an advancing crack remain a point of speculation. However, it is clear that for a high elastic modulus, nominally brittle material such as alumina, the crack opening displacement is very small, depending on assumptions, less than 0.1 μm. This allows for various forms of direct and indirect interaction between the newly formed fracture surfaces as a crack extends. Swain[58] proposed that the thermal expansion anisotropy results in crack bridging that maintains ligaments intact after the primary crack front has passed. Lawn and coworkers[59,60] present micrographs of similar events in the following wake region of an alumina, confirming the presence of crack bridging effects. They also proposed a model based on those observations. There seems to be no doubt that there remains some form of direct coherence or attractive forces between the newly formed crack surfaces in polycrystalline alumina ceramics and that it is those interactions which are responsible for the rising *R*-curve behavior. The presence in the following wake region of intact, unfractured ligaments, grain interlocking processes, and even the wedging of individual separated grains have also been observed. Others are also likely to be discovered as the importance of the rising *R*-curve phenomenon has only recently been appreciated and seems to be entering a period of intensive research during the 1990s.

It is possible to present a general form of the expected rising *R*-curve behavior of a large grain-size polycrystalline alumina ceramic from synthesis of published results, although most experimental measurements are not comprehensive. Figure 7 illustrates what is believed to be the general form, although linear regions such as depicted in Figs. 5 and 6 are commonly obtained experimentally. It is evident that there is a lower limit of the crack-growth resistance, which is characteristic of a small critical flaw. With stable crack

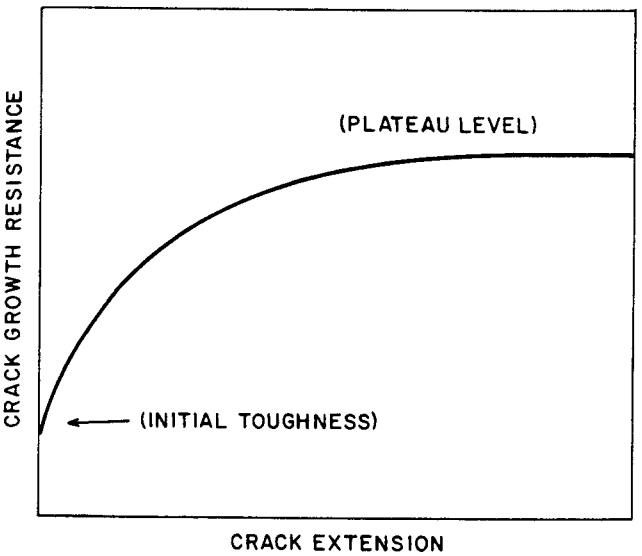

Fig. 7. Schematic of rising *R*-curve for a polycrystalline alumina.

extension, the toughening mechanisms in the following wake region of the crack become active and the crack-growth resistance increases, a rising *R*-curve. These toughening phenomena eventually saturate as the extent of the following wake region achieves a steady state size and the crack-growth resistance reaches a plateau level. It may be expected that the initial toughness, the extent of the increasing region, and the plateau level are all microstructurally dependent and are also subject to the previously noted specimen and test parameter influences. Careful measurements of the fracture toughness, K_{Ic}, or the fracture surface energy could yield correct experimental values at any location on the curve in Fig. 7. As noted earlier, these are between 3 and 6 MPa • $m^{1/2}$, but are not uniquely associated with a specific grain size. It must be reemphasized that there does not exist a unique fracture toughness or fracture surface energy-to-grain size relationship for polycrystalline alumina ceramics.

In Fig. 4, the fracture surface energy versus grain size and temperatures diagram of Hayashi et al.[45] was presented. It is probably not truly unique either; however, the values of their diagram were determined by the total work-of-fracture method and thus may be expected to closely approximate the plateau level expressed in Fig. 7 for the different grain sizes and test temperatures. It should be accepted only as a general trend; yet, since it is the total work-of-fracture and representative of the plateau crack-growth resistance, it is unquestionably the best depiction of the ubiquitous toughness/grain-size relationship.

Closely related to the stable crack extension that is a necessary component of *R*-curve development is the phenomenon of slow crack growth. Although it is obvious that the two phenomena, namely rising *R*-curves and slow crack growth, are related, the com-

plete association of the two has not been well defined. The general relationship appears to be one of more steeply rising R-curves, yielding greater resistance to slow crack growth. There are only two substantial studies directly addressing the microstructural or grain-size effect on the slow crack growth of polycrystalline alumina ceramics, that of Gesing and Bradt[61] and that of Becher and Ferber.[62] Both address the problem on the basis of the N value in the empirical slow crack growth equation:

$$V = AK_I^N$$

Gesing and Bradt measured slow crack growth for a variety of grain sizes of different polycrystalline alumina ceramics and then developed a model based on microcracking in a frontal process zone. An inverse relationship between the grain size and the N value was experimentally observed and also explained by that model; Fig. 8 depicts their experimental observations. Becher and Ferber developed a more general model of stress-induced frontal zone microcracking that is based on the thermal expansion anisotropy and also yields an inverse grain size-to-N value relationship. Obviously, since it is now appreciated that the toughening effects are in the following wake region, rather than the frontal process zone, new modeling is in order.

It is also appropriate to consider where the slow crack growth behavior of single crystal alumina fits into Fig. 8. Only Wiederhorn[63] has measured the slow crack growth on an individual plane of single-crystal alumina. The N value which he observed was intermediate to the extremes for very fine and very coarse grain sizes, again illustrating that the fracture behavior of alumina ceramics is not easily related to the single-crystal cleavage characteristics in a direct manner.

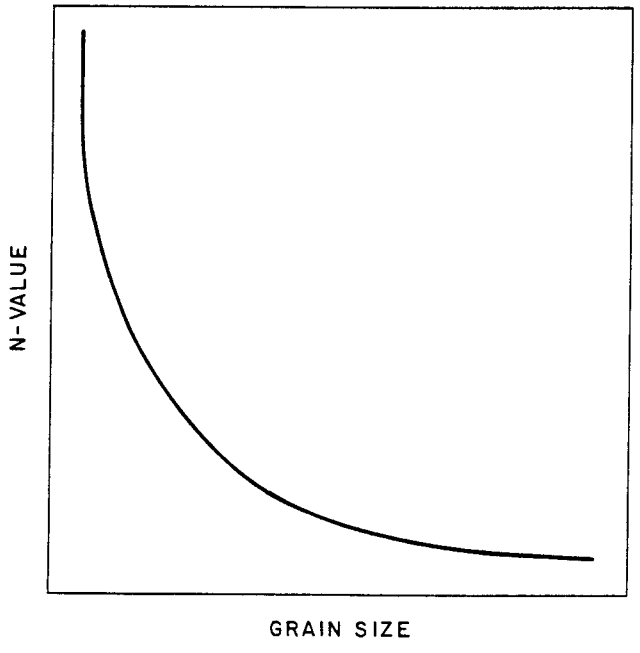

Fig. 8. Slow crack growth N value and grain size relation for polycrystalline alumina.

Coincident with the presence of slow crack growth is the concept of a fatigue limit or stress intensity threshold, K_{th}, below which no slow crack growth occurs. That concept has long been debated for glasses. For alumina, it was suggested originally by Hasselman et al.[64] and more recently revived in principle by Cook[65] that the fatigue limit, K_{th}, may be directly related to the thermodynamic surface free energy, γ_0, through Eq. (3), by simply replacing K_{Ic} and γ with their alternate forms. That concept appears to be applicable to single-crystal cleavage, but also appears to be confronted with the uncertainties of rising R-curve behavior for polycrystalline alumina ceramics. It is possible, perhaps, to argue that the zero crack extension value in Fig. 7 could be utilized for that estimate, although convincing experimental evidence is absent.

The high-temperature fracture of alumina in single-crystal form was previously addressed, while the "fast" fracture of polycrystalline alumina ceramics at high temperatures is confronted by all of the problems just considered at low temperatures, with the added problem that virtually no reliable experimental results exist. High-temperature failure after some creep, or time-dependent deformation constitute other considerations and merit discussion although the detailed processes are far from understood and the proposed models need substantial refinement. The reason for this is that research in this area has only recently become focused, coincident with intensifying concerns regarding the long-term structural application of ceramics at high temperatures.

Because of the recent development of the high-temperature creep fracture models,[66–75] they will not be individually considered, but rather summarized in a general sense. Very broadly, fracture after long-term high-temperature exposure under stress is a multiple-stage process of void and/or crack nucleation followed by the coalescence of these defects into cracks which form a critical flaw at the fracture initiation site.

The initiation of individual internal defects generally occurs preferentially at processing inhomogenities, or naturally at grain boundaries and triple points in sound polycrystalline alumina ceramics.[68,71–74] These individual defects then grow and coalesce to form larger "cracklike" defects.[69,71,75] Some of these larger defects are blunted or arrested,[69] while others continue to grow to larger sizes until one reaches a critical condition. It is obvious that a number of stages are necessary in the modeling and understanding of this failure process. Actually predicting the failure time appears to be a formidable challenge.

Plastic Deformation and Creep of Alumina

Permanent plastic deformation in alumina has been observed over a wide temperature range under a variety of loading conditions. Deformation processes include both dislocation glide and time-dependent creep. These processes are related and often are operating at the same time. For example, dislocation motion is strongly time-dependent, as shown by very large strain-rate effects. Diffusional creep in some cases is controlled by dislocation climb and in some cases by bulk or grain-boundary diffusion. Furthermore, there are special deformation modes such as twinning and grain-boundary sliding which do not fit clearly into either category.

In the following discussion, we will divide the subject into two areas: (1) deformation which is rapid or clearly dominated by dislocation glide, and (2) creep or slow deformation which is mainly diffusion-controlled.

Dislocation Glide

Any discussion of dislocations in alumina must start with the classic paper by Kronberg,[76] which described the crystal structure of alumina and predicted the Burgers vectors of several glide dislocations.

There is some confusion and inconsistency in the literature regarding structural nomenclature for α-alumina. Alpha alumina has a hexagonal (trigonal)/rhombohedral crystal structure and has been described using either a morphological or structural unit cell. Kronberg[76] and Snow and Heuer[77] have discussed the relationship between these various choices. Much of the older literature used the morphological unit cell. The structural unit cell, which is twice the height and rotated 180° relative to the morphological unit cell, is preferable for interpretation of diffraction effects in transmission electron microscopy. The structural unit cell and the hexagonal 4-index Miller-Bravais notation has now been adopted as the common convention to describe the crystal geometry of α-Al_2O_3.[78] Fortunée [79] has summarized the crystallographic specifications for Al_2O_3, as shown in Table IV.

Figures 9 and 10 show two views of the Al_2O_3 crystal lattice with possible dislocation Burgers vectors indicated. Snow and Heuer[77] and Heuer and Castaing[78] have published detailed reviews of the dislocation slip systems for alumina.

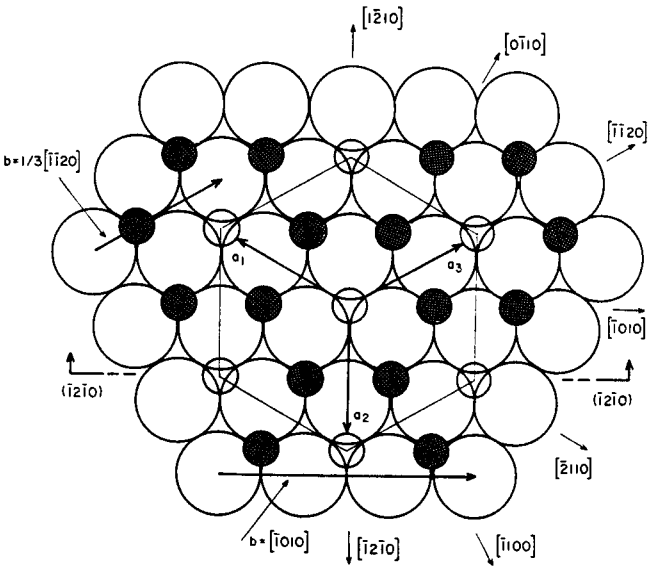

Fig. 9. Basal plane projection of the arrangement of oxygen (large circles), aluminum (small shaded circles), and empty octahedral sites (small open circles) in alpha alumina. The basal plane and prismatic plane Burgers vectors are shown. After Ref. 76.

Basal slip {0001} 1/3 ⟨$\bar{1}$$\bar{1}$20⟩ (Burgers vector 0.475 nm) is the easiest to activate and was the first deformation system identified. Wachtman and Maxwell[80] deformed single crystals in bending and reported the creep/yield behavior for basal slip. Kronberg[81] measured the dynamic mechanical properties of thin single-crystal rods in tension. He found yielding and flow behavior analogous to that for metals, but shifted to much higher temperatures and at slower strain rates, as shown in Fig. 11. Conrad et al.[82] extended this work to tension and compression; Fig. 12 shows a summary of upper yield point data.

Lagerlof et al.[83] reviewed the relationships between dislocation structures and the stress-strain curve for deformation on the basal plane. The screw seg-

Table IV. Formal Crystallographic Specifications for Alpha Al_2O_3*

Space Group: R_3C (No. 167)
Unit Cell Rhombohedral-Hexagonal

Hexagonal	Rhombohedral
A = 0.47592 nm	a = 0.51288 nm
C = 1.29921 nm	α = 55.287°
n = 6	n = 2

Atomic Positions (Rhombohedral Coordinates)

Al: WWW; 1/2 − W 1/2 − W 1/2 − W;
$\bar{W}\bar{W}\bar{W}$; W + 1/2 W + 1/2 W + 1/2

O: UŪO; 1/2 − U U + 1/2 1/2;
OUŪ; U + 1/2 1/2 1/2 − U
ŪOU; 1/2 1/2 − U 1/2 + U

U = 0.303 ± 0.003
W = 0.1050 ± 0.0010

*After Refs. 76 and 79.

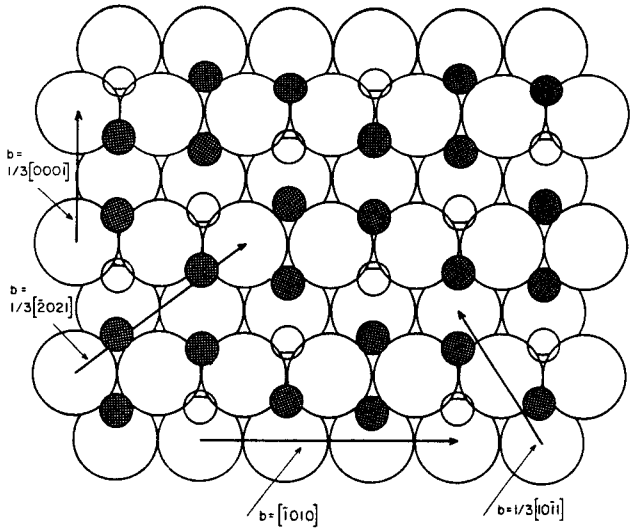

Fig. 10. Section of the unit cell on the $\{\bar{1}2\bar{1}0\}$ plane viewed from the $+a_2$ axis in the $\{1\bar{2}10\}$ direction, as indicated in Fig. 1. The section is through the center of the aluminum atoms and oxygen atoms in front of the section plane are removed. Several possible Burgers vectors are shown.

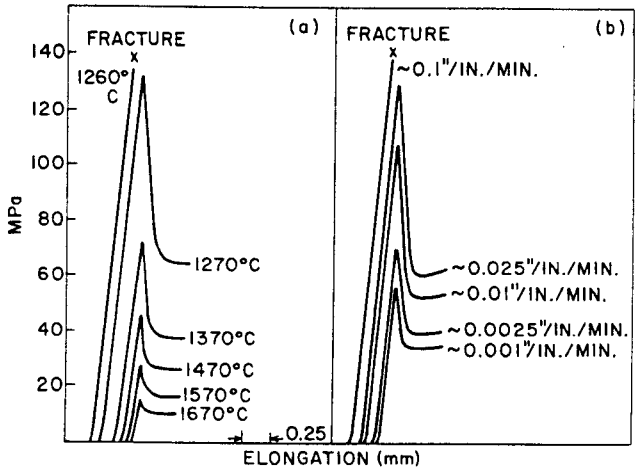

Fig. 11. Effect of strain rate on the yield stress of single-crystal alumina in tension. The crystals were oriented for slip on the basal plane. After Ref. 81.

ments of 1/3 $\langle\bar{1}\bar{1}20\rangle$ dislocations are apparently more mobile, move rapidly out of the crystal, and leave the slowly moving edge segments behind. Pletka et al.[84–86] showed that two edge dislocations of opposite sign on closely spaced parallel glide planes are trapped through elastic interaction to form an edge dipole. The edge-trapped 1/3 $\langle\bar{1}\bar{1}20\rangle$ dislocations dissociate by self-climb according to the following reaction:

$$1/3\ \langle\bar{1}\bar{1}20\rangle \rightarrow 1/3\ \langle\bar{1}010\rangle + 1/3\ \langle 0\bar{1}10\rangle$$

The edge dipoles can also break up into elongated loops by cross slip or into small loops through diffusion. The net result is that basal slip leaves behind a variety of immobile dislocation debris which impedes

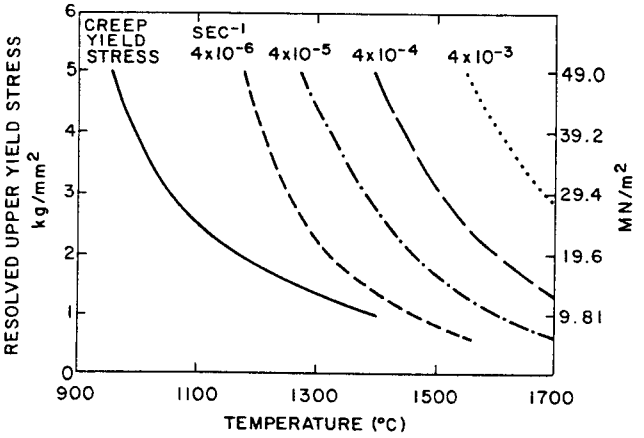

Fig. 12. Summary of the effects of temperature and strain rate on the upper yield stress of sapphire in tension. (After Refs. 80, 81, and 82.)

further dislocation motion and leads to strong work hardening. Lagerlof et al.[83] give a quantitative analysis of this process as a function of strain, strain rate, and temperature.

The second most common slip system is on the prism plane $(\bar{1}2\bar{1}0)$ in the $\langle\bar{1}010\rangle$ direction. The Burgers vector for this dislocation is relatively large, 0.822 nm, and the dislocation might be expected to decompose with a 33% reduction in energy by the following reaction[78]:

$$[\bar{1}010] \rightarrow 1/3[\bar{1}\bar{1}20] + 1/3[\bar{2}110]$$

However, this does not appear to happen, as perfect $\langle\bar{1}010\rangle$ dislocations have been observed.[87]

Scheuplein and Gibbs[88] produced prismatic slip by bending single-crystal rods around a small radius and evaluating the resulting dislocation structure by chemical dislocation etch pit formation.

Castaing et al.[89,90] used compression loading with confining pressure to extend the deformation temperature downward. They were able to produce basal slip as low as 600°C and prismatic slip to as low as 200°C under these conditions. Figure 13 summarizes these results over the temperature range 200° to 1800°C. For three strain rates, 4×10^{-6}, 4×10^{-5}, and 4×10^{-4} • s^{-1}, the critical resolved shear stress can be represented by the equation

$$\ln \tau = -6.15T/T_m + 0.625 \ln \dot{\gamma} + 9.813$$

where τ is in MPa, T_m = 2320 K, and $\dot{\gamma}$ is the shear strain rate per second.

The high-temperature data are in good agreement with results from other workers using four-point bending[91] and tensile testing of *a*-axis filaments.[92]

Castaing et al.[89] showed an interesting comparison of critical resolved shear stress for basal and prismatic slip (Fig. 14). Prismatic slip, which is much more difficult at high temperatures, has a CRSS equal

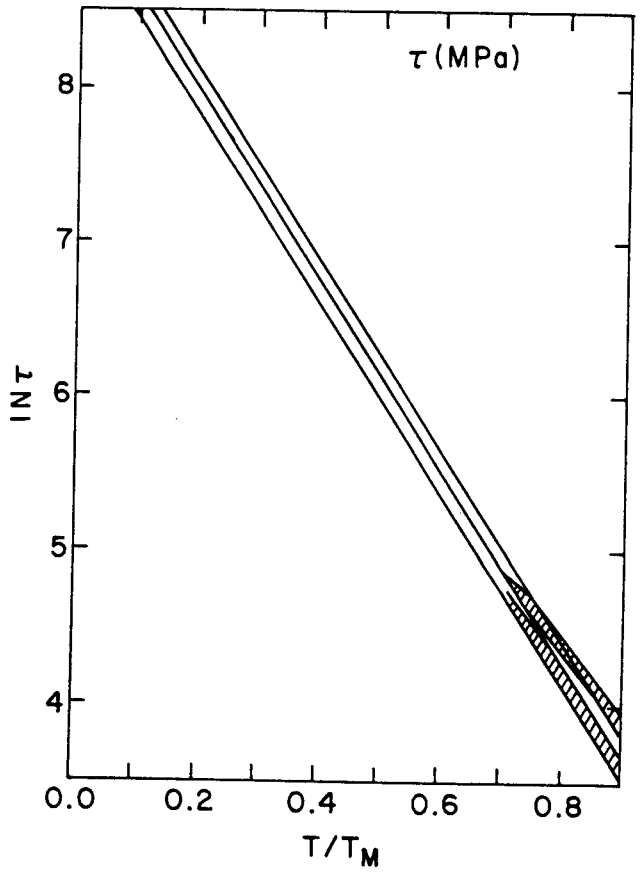

Fig. 13. Prismatic slip in alumina. Variation of the log of the critical resolved shear stress, τ, with reduced temperature (T_m = 2320 K). Low-temperature data, T/T_m = 0.2–0.5, are from tests at high confining pressure (Ref. 90). High-temperature data, T/T_m = 0.7–0.9 are from tests at atmospheric pressure (Ref. 117). After Castaing et al. (Ref. 90).

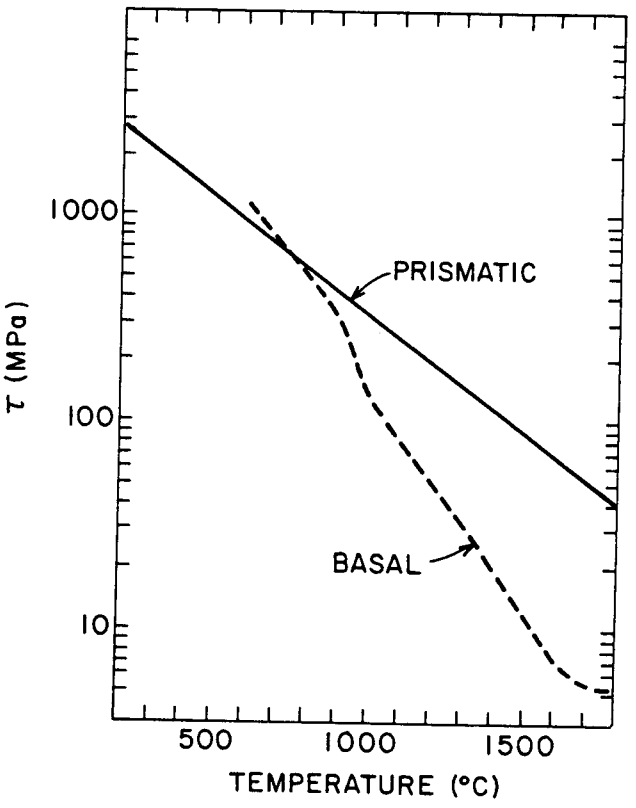

Fig. 14. Critical resolved shear stress vs temperature for basal and prismatic slip. At $T > 1100$°C, data were obtained at atmospheric pressure. At $T < 950$°C, they were obtained under 1500 MPa confining pressure (Ref. 90).

to or slightly less than that for basal slip at lower temperatures.

The two types of slip systems discussed above are insufficient to provide the five independent slip systems necessary for general polycrystalline deformation (Von Mises or Taylor-Von Mises criterion). One additional slip system shown in Fig. 10 has a Burgers vector of 0.512 nm in the 1/3 $\langle 10\bar{1}1 \rangle$ direction. The prism plane, $\{\bar{1}2\bar{1}0\}$, is a possible slip plane, but this system has not been observed. Furthermore, Groves and Kelly[93,94] have shown that basal plus prism plane deformation can provide only four independent slip systems.

Slip systems with planes inclined to the c-axis are called pyramidal systems. Dislocation with a 1/3 $\langle 10\bar{1}1 \rangle$ are also possible on the $\{\bar{1}012\}$ rhombohedral plane and the $\{\bar{1}011\}$ pyramidal plane. Cadoz and Pellissier[95] measured a CRSS of 156 and 70 MPa for these two systems at 1700°C. Several other authors have reported deformation on nonbasal, nonprismatic systems by tensile or compressive deformation of c-axis crystals.[96–100] Pyramidal or rhombohedral slip systems are necessary for general deformation of polycrystalline alumina, but are activated only at higher stresses and temperatures. Therefore, general unconfined deformation of polycrystalline alumina is probably impossible under ordinary engineering loads at high temperatures. The limited plastic deformation which occurs can be expected to lead to crack initiation and apparent brittle failure in polycrystalline bodies subjected to rapid loading.

The details of dislocation behavior in alumina are analogous to dislocation behavior in ductile metals. Dislocation reactions by combination or dissociation into partials, the generation of stacking faults by glide and climb, and the breakup of dislocation dipoles into loops by diffusion have all been observed in alumina. These processes have a pronounced influence on the dynamics of glide deformation. In a recent review, Heuer and Castaing[78] discussed dislocations in alumina; and Bretheau et al.[101] have considered the general question of dislocations in oxides.

Synthetic ruby, a solid solution of Cr in α-Al_2O_3, provided the first evidence of solid solution hardening in alumina. Wachtman and Maxwell[80] observed an increased creep yield stress with 0.5 cation percent Cr

at 1200° and 1300°C. Chang[102] showed that the stress required to maintain a steady state creep rate at 1500°C increased 2.5 to 3 times with the addition of 1.34 cation percent Cr. Pletka et al.[85] carried out constant strain rate tests in compression at 1400° to 1700°C in specimens oriented for basal slip. The CRSS as a function of temperature and Cr^{3+} concentration is shown in Fig. 15. The hardening rate ($d\tau/dc$) was about $\mu/30$ where μ is the shear modulus. Alumina doped with Ti^{3+} showed a lower CRSS than for Cr^{3+} under similar conditions. The hardening rate was also lower, about $\mu/12$.

Pletka et al.[85] presented detailed models for these hardening effects and concluded that ionic size and modulus interaction account for the hardening by isovalent impurities, Cr^{3+} and Ti^{3+}.

When in solution, Ti^{4+}, exhibited a much stronger hardening effect, increasing the flow stress curve by a factor of two over similar Ti^{3+} doping. The hardening rate was nearly a factor of 10 greater, $\mu/1.2$ and $\mu/2$ at 1520° and 1600°C, respectively.

The Ti^{4+} ions are more effective hardeners through the formation of charge-compensating defect complexes which provide strong elastic interactions with dislocation strain fields. Detailed analysis of impurity-dislocation interactions were presented by Lagerlof et al.[83]

Creep

As pointed out in the previous section, glide mechanisms in single crystals are, under practical loading conditions, inadequate to allow the general deformation of a polycrystalline body. However, with a few exceptions, it is the high-temperature mechanical properties of polycrystalline bodies which are of the most practical interest. Slow, time-dependent deformation of polycrystalline bodies is commonly observed. Cannon and Langdon[103] summarize 44 investigations on the creep of polycrystalline alumina.

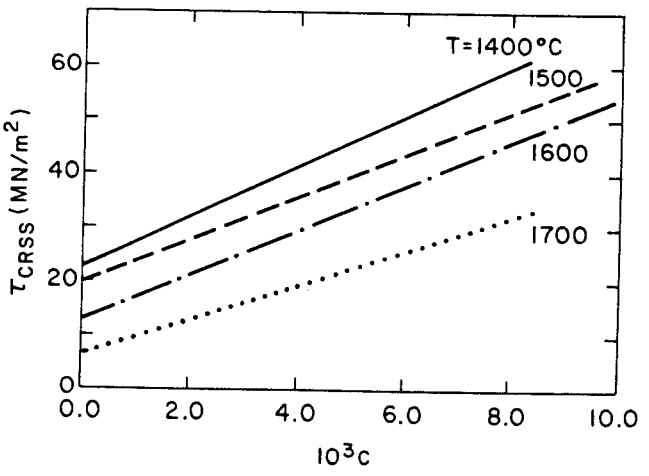

Fig. 15. CRSS vs temperature for Cr^{3+}-doped Al_2O_3 single crystals at various temperatures and strain rates. Solid line, $\epsilon = 1.3 \times 10^{-4} \cdot s^{-1}$. Dashed line, $\epsilon = 2.6 \times 10^{-5} \cdot s^{-1}$. After Ref. 85.

Chokshi and Porter[104] presented the following general equation, which shows the important parameters for steady state creep deformation.

$$\dot{\epsilon} = AGb/kTD_0 \exp[-Q/RT] (b/d)^p(\sigma/G)^n$$

where $\dot{\epsilon}$ is the strain rate, A a dimensionless constant, G the shear modulus, and b the Burgers vector, which, as shown earlier, varies with the operating slip system. The term $D_0 \exp[-Q/RT]$ contains the frequency factor, D_0, and the activation energy, Q, for the appropriate diffusion process. The actual diffusion process dominating at a particular time depends in turn on the stress and grain size.

The grain size, d, enters explicitly as an inverse factor in the third term, and p is called the inverse grain-size exponent. The stress, σ, normalized by G is the last term and this is raised to a stress exponent, n. The general approach is to compare experimentally determined values on Q, n, and p to theoretically predicted values to identify the particular mechanism dominating the creep deformation.

Cannon and Langdon[103] list 29 measurements for n, of which 23 are between 1 and 2 and 6 have upper values of 2.5 to 2.6. The grain-size dependence has been measured less often, with eight values between 2 and 3, two between 1.7 and 1.9, and four at 1 or below. Activation energies ranged from 90 to 1170 kJ/mol but, eliminating the extreme values, the range narrows to 400 to 800 kJ/mol. Thus a single quantitative expression for creep deformation of alumina is still not available and the variables of temperature, stress, grain size, purity, and deformation history must all be considered.

Heuer et al.[105] published a deformation map for MgO-doped Al_2O_3 at 1500°C (Fig. 16). This map shows the relationship of various deformation processes to the variables of grain size and stress. At the highest stress, pyramidal glide, plus basal and prismatic glide, provide five independent slip systems necessary for general deformation. At low stresses and small grain size, grain-boundary sliding or interface-controlled diffusional creep dominate. Other diffusional creep processes depend on both grain size and stress. In general, as grain size decreases and stress increases, the diffusional creep is controlled sequentially by interstitial oxygen, grain-boundary oxygen, interstitial aluminum, and grain-boundary aluminum.

In Part 2 of their recent review on the creep of ceramics, Cannon and Langdon[106] conclude that the enhanced role of diffusional creep in ceramics ($n = 1$) originates in the stable fine grain-size structure which is maintained at higher stresses and strain rates. Furthermore, diffusional creep is important because of enhanced movement of one of the ionic species along grain boundaries.

From results on creep of 0°-oriented alumina single crystals, these authors conclude that a stress

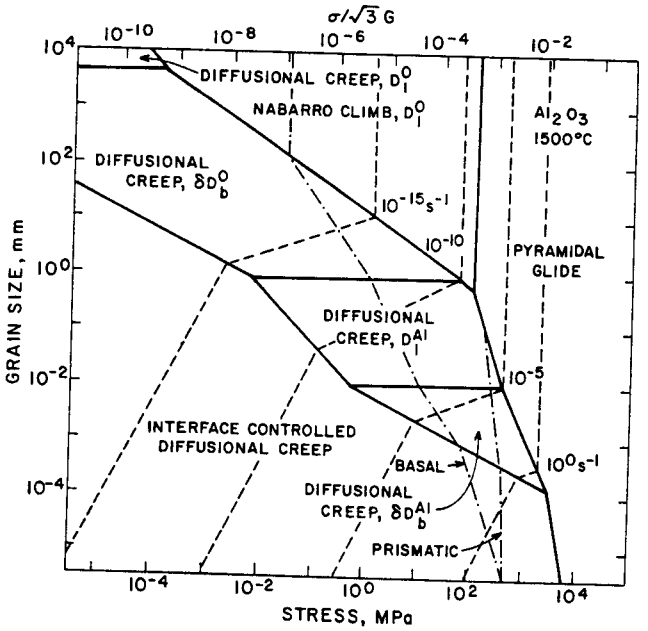

Fig. 16. Deformation map for MgO-doped Al_2O_3 at 1500°C, after Ref. 105. See Ref. 105 for complete list of the original references for the mechanical properties test data.

exponent of $n = 3$ corresponds to creep resulting from climb of dislocations from Bardeen-Herring sources, when only a limited number of slip systems are available or in other conditions where crystallographic slip is restricted. The stress exponent $n = 5$ is associated with fully ductile behavior.

Because of the highly anisotropic nature of glide deformation in alumina, unaccommodated grain-boundary sliding and cavitation at triple-point junctions tends to occur unless it is relieved by diffusion processes. Page et al.[107] showed that cavities are nucleated at triple points and at closely spaced ledges on grain boundaries. Nucleation was continuous during a creep experiment, but at a decreasing rate with time. Although the nucleation rate was not sensitive to the applied stress, there was a threshold stress above which nucleated cavities continued to grow. Below this stress, cavity nucleation was observed, but sustained growth was not. Heuer et al.[105] concluded that, in the absence of very high stresses, important contributions from diffusional deformation mechanisms are required for polycrystalline deformation.

Carry and Mocellin[108] studied compressive forming processes for fine grain-sized (<6 μm) alumina under conditions where superplastic deformation would be expected. True strains of 26 to 27% were obtained in compression at 1500°C. Deformation forming of a thin alumina disk into a dome shape was carried out at two load levels. At low loads (biaxial outer fiber tensile stress of 10 to 13 MPa), the microstructure remained dense without grain-boundary cavities or fractures. However, when the initial load was raised to produce a stress of 100 to 130 MPa, strain rates were produced which were too rapid for microstructural accommodation and extreme grain-boundary cavitation was observed. They concluded that the low-stress deformation was by processes analogous to superplastic deformation in metals.

Twinning

A third distinct mode of plastic deformation in alumina is mechanical twinning. Two twinning modes have been identified: basal[76] and rhombohedral.[109,110] Small basal deformation twins have been observed under hardness indents[111] and under abraded surfaces.[112] Rhombohedral twinning can be much more extensive and has been observed in a variety of mechanical testing conditions.[109,110,113–115] Single crystals of Al_2O_3 oriented to produce maximum shear on one of three equivalent rhombohedral twin planes and tested in compression will experience massive twin deformation at only 12.6 MPa RSS. This value was constant over a temperature range 900 to 1517 K (627° to 1244°C) and is also consistent with earlier high-temperature results up to 1873 K (1600°C).[82]

It has been shown[110,115] that intersections of two rhombohedral twins invariably initiate fracture. This mode of deformation may be an important source of crack initiation.[116]

However, the nucleation mechanism for rhombohedral twins remains unknown. Surface grinding damage seems to be a likely source, and carefully polished crystals can withstand compressive stresses 10 to 100 times greater than 12.6 MPa without spontaneously nucleating twins.

In summary, aluminum oxide exhibits all the plastic deformation mechanisms commonly exhibited by metals, but generally shifted to higher temperatures and lower strain rates. The same fundamentals of dislocation motion, creep deformation, and twin deformation apply to this material and must be considered in attempting engineering applications under conditions of mechanical stress at high temperature.

References

[1]W. H. Gitzen, Alumina as a Ceramic Material. The American Ceramic Society, Columbus, OH, 1970.

[2]L. M. Belyaev, Ruby and Sapphire. Amerind, Ltd., New Delhi, India, 1974

[3]E. Dorre and H. Hubner, Alumina. Springer-Verlag, Berlin, Germany, 1984.

[4]W. D. Kingery, Structure and Properties of MgO and Al_2O_3 Ceramics. The American Ceramic Society, Columbus, OH, 1984.

[5]R. F. S. Hearmon, "The Elastic Constants of Anisotropic Materials II," *Advan. Phys.*, 5, 323–82 (1956).

[6]W. G. Mayer and E. A. Hiedemann, "Optical Methods for the Ultrasonic Determination of the Elastic Constants of Sapphire," *J. Acoust. Soc. Am.*, 30, 756–60 (1958). Correction: *J. Acoust. Soc. Am.*, 32, 1699–1700 (1960).

[7]J. B. Wachtman, Jr., W. E. Tefft, D. G. Lam, Jr., and R. P. Stinchfield, "Elastic Constants of Synthetic Single Crystal Corundum at Room Temperature, *J. Res. Natl. Bur. Stand.*, 64A, 213–28 (1960).

[8]B. T. Bernstein, "Elastic Constants of Synthetic Sapphire at 270°C," *J. Appl. Phys.*, **34**, 169–72 (1963).

[9]W. D. Tefft, "Elastic Constants of Synthetic Single Crystal Corundum," *J. Res. Natl. Bur. Stand.*, **70A**, 277–80 (1966).

[10]J. H. Gieske and G. R. Barsch, "Pressure Dependence of the Elastic Constants of Single Crystalline Aluminum Oxide," *Phys. Status Solidi*, **29**, 121–31 (1967).

[11]R. W. Rice, "Microstructural Dependence of Mechanical Behavior of Ceramics," pp. 199–381 in Treatise on Materials Science. Edited by R. K. MacCrone. Academic Press, New York, 1977.

[12]M. D. Shappel, "Cleavage of Ionic Minerals," *Am. Mineral.*, **21** [2] 75–102 (1936).

[13]H. Winchell, "Orientation of Synthetic Corundum for Jewel Bearings," *Am. Mineral*, **29** [11–12] 399–414 (1944).

[14]G. Yamaguchi, Y. Kubo, and H. Ogawa, "Fracture in Thin-Sectioned Corundum Crystals," *Bull. Chem. Soc. Jpn.*, **39** [2] 287–99 (1966).

[15]J. B. Wachtman and L. H. Maxwell, "Plastic Deformation of Ceramic—Oxide Single Crystals," *J. Am. Ceram. Soc.*, **37** [7] 291–95 (1954).

[16]S. S. Brenner, "Mechanical Behavior of Sapphire Whiskers at Elevated Temperatures," *J.A.P.*, **11** [1] 33–39 (1962).

[17]K. Noda, "Fracture Properties of Sapphire Single Crystals"; M. S. Thesis (Y. Namba, supervisor) Osaka University, 1979.

[18]S. M. Wiederhorn, "Fracture of Sapphire," *J. Am. Ceram. Soc.*, **52** [9] 485–91 (1969).

[19]G. Wieland, "Investigations on the Temperature Dependence of Dislocation Morphology During Fracture of Sapphire"; Dip. Thesis (H. Hubner, supervisor), University of Erlangen-Nurnberg, 1976.

[20]S. S. Smith and B. J. Pletka, "Indentation Fracture of Polycrystalline Alumina"; pp. 189–210 in Fracture Mechanics of Ceramics, Vol. 6. Edited by R. C. Bradt et al. Plenum, New York, 1983.

[21]M. Iwasa and R. C. Bradt, "The Fracture Toughness of Single Crystal Alumina"; pp. 767–79 in Structure and Properties of MgO and Al_2O_3 Ceramics. The American Ceramic Society, Columbus, OH. 1984.

[22]H. Palmour III, D. R. Johnson, C. S. Kim, and C. E. Zimmer, "Fractographic and Thermal Analyses of Shocked Alumina," ONR Tech. Rpt. 69–5, Contract N00014–68–A–0187, August, 1971.

[23]F. P. Mallinder and B. A. Proctor, "Preparation of High-Strength Sapphire Crystals," *Proc. Br. Ceram. Soc.*, **6**, 9–16 (1966).

[24]N. C. Anderson, "Basal Plane Cleavage Cracking of Synthetic Sapphire Arc Lamp Envelopes," *J. Am. Ceram. Soc.*, **62** [1–2] 108–109 (1979).

[25]M. Iwasa, T. Ueno, and R. C. Bradt, "Fracture Toughness of Quartz and Sapphire Crystal at Room Temperature," *J. Jpn. Soc. Mater. Sci.*, **20** [33] 1001–1004 (1981).

[26]P. F. Becher, "Fracture Strength Anisotropy of Sapphire, *J. Am. Ceram. Soc.*, **59** [1–2] 59–61 (1976).

[27]E. Stofel and H. Conrad, "Fracture and Twinning in Sapphire," *Trans. AIME*, **227** [5] 1053–60 (1963).

[28]H. P. Kirchner and R. M. Gruver, "Fractographic Criteria for Subcritical Crack Growth Boundaries in 95% Al_2O_3," *J. Am. Ceram. Soc.*, **63** [3–4] 169–74 (1980).

[29]R. F. Firestone and A. H. Heuer, "Creep Deformation of 0° Sapphire," *J. Am. Ceram. Soc.*, **59** [1–2] 24–29 (1976).

[30]A. I. A. Abdel-Latif, R. E. Tressler, and R. C. Bradt, "Fracture Mirror Formation in Single Crystal Alumina"; pp. 933–39 in Fracture 1977. Vol. 3. Proc. ICF-4, Waterloo, Canada.

[31]J. Castaing; personal communication, 1983.

[32]S. M. Wiederhorn, B. J. Hockey, and D. E. Roberts, "Effects of Temperature on the Fracture of Sapphire," *Philos. Mag.*, **28**, 783–96 (1973).

[33]J. B. Wachtman, T. G. Scuderi, and G. W. Cleek, "Linear Thermal Expansion of Aluminum Oxide and Thorium Oxide from 100 to 1100 K," *J. Am. Ceram. Soc.*, **45** [7] 319–23 (1962).

[34]E. A. Jackman and J. P. Roberts, "On the Strength of Polycrystalline and Single Crystal Corundum," *Trans. Br. Ceram. Soc.*, **54**, 389–98 (1955).

[35]R. J. Charles and R. R. Shaw, "Delayed Failure of Polycrystalline and Single Crystal Alumina," General Electric Report No. 62–RL–308M, 1962.

[36]A. H. Heuer and J. P. Roberts, "The Influence of Annealing on the Strength of Corundum Crystals," *Proc. Br. Ceram. Soc.*, **6**, 17–27 (1966).

[37]L. M. Davies, "The Effect of Heat Treatment on the Tensile Strength of Sapphire," *Proc. Br. Ceram. Soc.*, **6**, 29–35 (1966).

[38]P. B. Bayer and R. E. Cooper, "Tensile Strength of Sapphire Whiskers at Elevated Temperatures," *J. Mater. Sci.*, **4** [1] 15–20 (1969).

[39]P. Shahinian, "High Temperature Strength of Sapphire Filament," *J. Am. Ceram. Soc.*, **54** [1] 67–68 (1971).

[40]P. L. Gutshall and G. E. Gross, "Observations on Mechanisms of Fracture in Polycrystalline Alumina," *Eng. Fract. Mech.*, **1** [3] 463–71 (1969).

[41]A. G. Evans and G. Tappin, "Effects of Microstructure on the Stress to Propagate Inherent Flaws," *Proc. Br. Ceram. Soc.*, **20**, 275–97 (1972).

[42]L. A. Simpson, "Effect of Microstructure on the Measurement of the Fracture Energy of Alumina," *J. Am. Ceram. Soc.*, **56** [1] 7–11 (1973).

[43]R. W. Rice, S. W. Freiman, and P. F. Becher, "Grain Size Dependence of the Fracture Energy in Ceramics, I and II," *J. Am. Ceram. Soc.*, **64** [8] 345–54 (1981).

[44]B. Mussler, M. V. Swain, and N. Claussen, "Dependence of Fracture Toughness of Alumina on Grain Size and Test Technique," *J. Am. Ceram. Soc.*, **65** [11] 566–71 (1982).

[45]K. Hayashi, Y. Tatewaki, S. Ozaki, and T. Nishikawa, "Grain Size Dependence of Fracture Energy in Polycrystalline Alumina," *J. Jpn. Ceram. Soc.*, **96** [5] 532–38 (1988).

[46]D. Brock, Elementary Engineering Fracture Mechanics, Ch. 7. Nordhoff, Leyden, The Netherlands, 1974.

[47]J. Nakayama, "Bending Method for Direct Measurement of Fracture Surface Energy of Brittle Materials," *Jpn. J. Appl. Phys.*, **3** [7] 422–23 (1964).

[48]H. G. Tattersall and G. Tappin, "Work of Fracture and Its Measurement in Metals Ceramics and Other Materials," *J. Mater. Sci.*, **1** [3] 296–301 (1966).

[49]H. Hubner and W. Jillek, "Subcritical Crack Extension and Crack Resistance in Polycrystalline Alumina," *J. Mater. Sci.*, **12**, 117–25 (1977).

[50]R. Steinbreck, R. Knehans, and W. Schaarwachter, "Increase in the Crack Resistance During Slow Crack Growth in Al_2O_3 Bend Specimens," *J. Mater. Sci. Lett.*, **18**, 265–70 (1983).

[51]H. Wieninger, K. Kromp, and R. F. Pabst, "Crack Resistance Curves of Alumina at High Temperatures," *J. Mater. Sci.*, **22**, 1352–58 (1987).

[52]R. Knechans and R. Steinbrech, "Effect of Grain Size on the Crack Resistance Curves of Al_2O_3 Bend Specimens," *Sci. Ceram.*, **12**, 613–19 (1983).

[53]F. Feueler, R. Knechans, and R. Steinbrech, "Testing Methods and Crack Resistance Behavior of Alumina," *J. Phys., Coll. C1 Suppl.*, **2** [47] C1-617–C-621 (1986).

[54]R. W. Steinbrech and O. Schmenkel, "Crack-Resistance Curves of Surface Cracks in Alumina," *J. Am. Ceram. Soc.*, **71** [5] C-271–C-273 (1988).

[55]J. A. Salem, J. L. Shannon, Jr., and R. C. Bradt, "The Effect of Texture on the Crack Growth Resistance of Polycrystalline Alumina," *J. Am. Ceram. Soc.*, **72** [1] 20–27 (1989).

[56]M. Sakai and R. C. Bradt, "The Crack Growth Resistance of Non-Phase Transforming Ceramics," *Nip. Seram. Ky. Gak. Ron.*, **96** [8] 801–09 (1988).

[57]R. Knehans and R. Steinbrech, "Memory Effect of Crack Resistance During Slow Crack Growth in Notched Alumina Specimens," *J. Mater. Sci. Lett.*, **1** [8] 327–29 (1982).

[58]M. V. Swain, "*R*-Curve Behavior in a Polycrystalline Alumina Material," *J. Mater. Sci. Lett.*, **5**, 1313–15 (1986).

[59]P. L. Swanson, C. J. Fairbanks, B. R. Lawn, Y. W. Mai, and B. J. Hockey, "Crack Interface Grain Bridging as a Fracture Resistance Mechanism in Ceramic, I," *J. Am. Ceram. Soc.*, **70** [41] 279–89 (1987).

[60]Y. W. Mai and B. R. Lawn, "Crack Interface Grain Bridging as a Fracture Resistance Mechanism in Ceramics, II," *J. Am. Ceram. Soc.*, **70** [41] 289–94 (1987).

[61]A. J. Gesing and R. C. Bradt, "A Microcracking Model for the Effect of Grain Size on Slow Crack of Polycrystalline Alumina"; pp. 569–90 in Fracture Mechanics of Ceramics, Vol. V. Edited by R. C. Bradt et al., Plenum, New York, 1983.

[62]P. F. Becher and M. K. Ferber, "Grain Size Dependence of the Slow-Crack Growth Behavior in Non-Cubic Ceramics," *Acta Metall.*, **33** [7] 1217–21 (1985).

[63]S. M. Wiederhorn, "Fracture of Ceramics"; pp. 217–41 in Mechanical and Thermal Properties of Ceramics. NBS Publ. 303. Edited by J. B. Wachtman, Jr., National Bureau of Standards, Washington, DC, 1969.

[64]D. P. H. Hasselman, D. A. Krohn, R. C. Bradt, and J. A. Coppola, "The Griffith Criterion and the Reversible and Irreversible Fracture of Brittle Materials"; pp. 749–58 in Fracture Mechanics of Ceramic, Vol. II. Edited by R. C. Bradt et al. Plenum, New York, 1973.

[65]R. F. Cook, "Crack Propagation Thresholds: A Measure of Surface Energy," *J. Mater. Res.*, **1** [6] 852-60 (1986).

[66]J. R. Portner, W. R. Blumenthal, and A. G. Evans, "Creep Fracture in Ceramic Polycrystals — Creep Cavitation Effects in Polycrystalline Alumina," *Acta Metall.*, **29** [4] 1899–1906 (1981).

[67]C. H. Hsueh and A. G. Evans, "Creep Fracture in Ceramic Polycrystals — Effects of Inhomogeneity on Creep Rupture," *Acta Metall.*, **29**, 1907–17 (1981).

[68]B. J. Dagleish, S. M. Johnson, and A. G. Evans, "High-Temperature Failure of Polycrystalline Alumina: I, Crack Nucleation," *J. Am. Ceram. Soc.*, **67** [11] 741–50 (1984).

[69]W. Blumenthal and A. G. Evans, "High-Temperature Failure of Polycrystalline Alumina: Creep Crack Growth and Blunting," *J. Am. Ceram. Soc.*, **67** [11] 751–59 (1984).

[70]S. M. Johnson, B. J. Dagleish, and A. G. Evans, "High-Temperature Failure of Polycrystalline Alumina: Failure Times," *J. Am. Ceram. Soc.*, **67** [11] 751–63 (1984).

[71]T. Okada and G. Sines, "Prediction of Delayed Failure from Crack Coalescence — Alumina"; pp. 297–310 in Fracture Mechanics of Ceramics, Vol. VII. Edited by R. C. Bradt et al. Plenum, New York, 1986.

[72]A. G. Robertson and D. S. Wilkinson, "Damage Accumulation in Hot Pressed Alumina During Flexural Creep and Anneals in Air"; pp. 311–26 in Fracture Mechanics of Ceramics, Vol. VII. Edited by R. C. Bradt et al. Plenum, New York, 1986.

[73]J. Lankford, K. S. Chan, and R. A. Page, "Creep Cavitation Behavior in Polycrystalline Ceramics"; pp. 327–47 in Fracture Mechanics of Ceramics, Vol. VII. Edited by R. C. Bradt et al. Plenum, New York, 1986.

[74]A. H. Chokshi and J. R. Porter, "Cavity Development During Creep Deformation in Alumina with a Bimodal Grain Size," *J. Am. Ceram. Soc.*, **70** [3] 197–202 (1987).

[75]A. Venkateswaran, K. Y. Donaldson, and D. P. H. Hasselman, "Role of Intergranular Damage–Induced Decrease in Young's Modulus in the Nonlinear Deformation and Fracture of an Alumina at Elevated Temperatures," *J. Am. Ceram. Soc.*, **71** [7] 565–76 (1988).

[76]M. L. Kronberg, "Plastic Deformation of Single Crystals of Sapphire: Basal Slip and Twinning," *Acta Metall.*, **5** [9] 507–24 (1957).

[77]J. D. Snow and A. H. Heuer, "Slip Systems in Al_2O_3," *J. Am. Ceram. Soc.*, **56** [3] 153–57 (1973).

[78]A. H. Heuer and J. Castaing, "Dislocations in Alpha Al_2O_3"; pp. 238–57 in Structure and Properties of MgO and Al_2O_3 Ceramics. Edited by W. D. Kingery. The American Ceramic Society, Columbus, OH, 1985.

[79]R. Fortuneé, "Grain Boundary Structures in Al $_2O_3$," M. S. Thesis, Case Western Reserve University, Cleveland, OH, 1981.

[80]J. B. J. Wachtman and L. H. Maxwell, "Plastic Deformation of Ceramic-Oxide Single Crystals, II," *J. Am. Ceram. Soc.*, **40** [11] 377–85 (1957).

[81]M. L. Kronberg, "Dynamical Flow Properties of Single Crystals of Sapphire, I," *J. Am. Ceram. Soc.*, **45** [6] 274–79 (1962).

[82]H. Conrad, G. Stone, and K. Janowski, "Yielding and Flow of Sapphire (Alpha Al_2O_3 Crystals) in Tension and Compression," *Trans. Met. Soc. AIME*, **233**, 889–97 (1965).

[83]K. P. D. Lagerlof, B. J. Pletka, T. E. Mitchell and A. H. Heuer, "Deformation and Diffusion in Sapphire (alpha-Al_2O_3)," *Rad. Eff.* **74**, 87–107 (1983).

[84]B. J. Pletka, T. E. Mitchell and A. H. Heuer, "Dislocation Substructure in Doped Sapphire (alpha-Al_2O_3) Deformed by Basal Slip," *Acta Metall.*, **30**, 491–98 (1974).

[85]B. J. Pletka, A. H. Heuer and T. E. Mitchell, "Work-Hardening in Sapphire," *Acta Metall.*, **25**, 25–33 (1977).

[86]B. J. Pletka, T. E. Mitchell and A. H. Heuer, "Dislocation Substructures in Doped Sapphire (alpha-Al_2O_3) Deformed by Basal Slip," *Acta Metall.*, **30**, 147–56 (1982).

[87]J. Cadoz, D. M. M. Hokim and J. P. Rivere, "Observations of Prismatic Slip Dislocations in Alumina Single Crystals," *Rev. Phys. Appl.*, **12** [3] 473–81 (1977).

[88]R. Scheuplein and P. Gibbs, "Surface Structure in Corundum: I, Etching of Dislocations," *J. Am. Ceram. Soc.*, **43** [9] 458–72 (1960).

[89]J. Castaing, J. Cadoz and S. H. Kirby, "Deformation of Al_2O_3 Single Crystals Between 25 and 1800°C: Basal and Prismatic Slip," *J. Phys. Coll. C3, Suppl. no. 6*, **42**, 43–47 (1981).

[90]J. Castaing, J. Cadoz and S. H. Kirby, "Prismatic Slip of Al_2O_3 Single Crystals Below 1000°C in Compression Under Hydrostatic Pressure," *J. Am. Ceram. Soc.*, **64** [9] 504–11 (1981).

[91]D. J. Gooch and G. W. Groves, "Prismatic Slip in Sapphire," *J. Am. Ceram. Soc.*, **55** [2] 105 (1972).

[92]D. M. Kotchick and R. E. Tressler, "Deformation Behavior of Sapphire via the Prismatic Slip System," *J. Am. Ceram. Soc.*, **63** [7] 429–34 (1980).

[93]G. W. Broves and A. Kelly, "Independent Slip Systems in Crystals," *Philos. Mag.*, **8** [3] 877–87 (1963).

[94]G. W. Groves and A. Kelly, "Change of Shape Due to Dislocation Climb," *Philos. Mag.*, **19** [16] 977–86 (1969).

[95]J. Cadoz and P. Pellissier, "Influence of Three-Fold Symmetry on Pyramidal Slip of Alumina Single Crystal," *Scripta Metall.*, **10**, 597–600 (1976).

[96]P. D. Bayer and R. E. Cooper, "A New Slip System in Sapphire," *J. Mater. Sci.*, **2**, 301–302 (1967).

[97]R. E. Tressler and D. J. Barber, "Yielding and Flow in *C*-Axis Sapphire Filaments," *J. Am. Ceram. Soc.*, **57** [1] 13–19 (1974).

[98]R. F. Firestone and A. H. Heuer, "Creep Deformation of 0° Sapphire," *J. Am. Ceram. Soc.*, **59** [1] 24–29 (1976).

[99]D. J. Gooch and G. W. Groves, "Non-basal Slip in Sapphire," *Philos Mag.*, **28** [3] 623–37 (1973).

[100]P. F. Becher, "Deformation Substructure in Polycrystalline Alumina," *J. Mater. Sci.*, **6**, 275–80 (1971).

[101]T. Bretheau, J. Castaing, J. Rabier, and P. Veyssiere, "Dislocation Motion and High Temperature Plasticity of Binary and Ternary Oxides," *Adv. Phys.*, **28** [6] 829–1014 (1979).

[102]R. Chang, "Creep of Al_2O_3 Single Crystals," *J. Appl. Phys.*, **31**, 484–89 (1960).

[103]W. R. Cannon and T. G. Langdon, "Review: Creep of Ceramics, Part 1, Mechanical Characteristics," *J. Mater. Sci.*, **18**, 1–51 (1983).

[104]A. H. Chokshi and J. R. Porter, "High Temperature Mechanical Properties of Single Phase Alumina," *J. Mater. Sci.*, **21** 705–10 (1986).

[105]A. H. Heuer, N. J. Tighe and R. M. Cannon, "Plastic Deformation of Fine-Grained Alumina (Al_2O_3): II, Basal Slip and Nonaccommodated Grain-Boundary Sliding," *J. Am. Ceram. Soc.*, **63** [1] 53–58 (1980).

[106]W. R. Cannon and T. G. Langdon, "Creep of Ceramics, Part 2, An Examination of Flow Mechanisms," *J. Mater. Sci.*, **23**, 1–20 (1988a).

[107]R. A. Page, J. Lankford, K. S. Chan, K. Hardman-Rhyne and S. Spooner, "Creep Cavitation in Liquid-Phase-Sintered Alumina," *J. Am. Ceram. Soc.*, **70** [3] 137–45 (1987).
[108]C. Carry and A. Morcellin, "Superplastic Forming of Alumina," *Proc. Br. Ceram. Soc.*, **33**, 101–15 (1983).
[109]A. H. Heuer, "Deformation Twinning in Corundum," *Philos. Mag.*, **13**, 379–93 (1966).
[110]W. D. Scott and K. K. Orr, "Rhombohedral Twinning in Alumina," *J. Am. Ceram. Soc.*, **66** [1] 27–32 (1983).
[111]B. J. Hockey, "Plastic Deformation of Aluminum Oxide by Indentation and Abrasion," *J. Am. Ceram. Soc.*, **59** [4] 233–31 (1971).
[112]P. F. Becher, "Abrasive Deformation of Sapphire," *J. Am Ceram. Soc.*, **59** [3–4] 143–45 (1976).
[113]E. Stofel and H. Conrad, "Fracture and Twinning i Sapphire," *Trans. Met. Soc. AIME*, **227**, 1053–60 (1963).
[114]H. Conrad and S. E. Janowski, "Additional Observation on Twinning in Sapphire During Compression," *Trans. Met. Soc AIME*, **233**, 255–56 (1965).
[115]R. L. Bertolotti and W. D. Scott, "Compressive Creep o Al_2O_3 Single Crystals," *J. Am. Ceram. Soc.*, **54** [6] 286–91 (1971)
[116]J. Lankford, "Compressive Strength and Microplasticity i Polycrystalline Alumina," *J. Mater. Sci.*, **12**, 791–96 (1977).
[117]J. Cadoz, J. Castaing, and J. Philbert, "Prismatic Slip i Al_2O_3 by Compression Tests," *Ref. Phys. Appl.*, **16**, 135–44 (1981)

Colloidal Properties of Alumina

Alan Bleier

Oak Ridge National Laboratory
Metals and Ceramics Division
P.O. Box 2008
Oak Ridge, TN 37831-6068

Colloidal alumina is the starting material for many alumina-based ceramics. This chapter describes its unique physical and chemical properties by emphasizing pertinent and representative research focused on particulates and by identifying the impact of colloidal alumina on current and future alumina-containing materials.

Colloidal alumina exists in a finely divided state, often dispersed. It typically has a high surface area-to-volume ratio, characteristic of matter in the submicrometer-size range to just above atomic dimensions (that is, 5 nm). Alumina in this range exhibits physicochemical properties that differ from those of both the constituent atoms or molecules and the macroscopic material, although similarities do exist. Differences between the surface atoms and those in the interior of colloidal alumina lead ultimately to unique character and behavior of the finely divided material, specifics of which can be rather diverse but which nearly always influence the processing and properties of alumina-based components.

It is important to recognize that colloidal properties of alumina and their manifestations in ceramic applications may be either desirable or undesirable and that this evaluation depends on the uses for which the ultimate pieces are being considered. The ability to characterize and control the formation, destruction, or stability of colloidal alumina is consequently a critical and widespread technological problem. Moreover, since colloidal alumina is encountered in various nonceramic industries (for example, mineral beneficiation, paint and pigment, dental, metals, chromatography, food, and health),[1] a rich literature and a corresponding expertise exist to augment ceramic experience and to improve our understanding of finely divided alumina as a material and its role in determining the behavior of fabricated ceramic components.

This chapter (*a*) outlines representative research and concepts appearing primarily since Gitzen's review[1d] in 1970, (*b*) identifies earlier research on colloidal properties of alumina, not covered by Gitzen, that is particularly important for current and future alumina-based ceramics, and (*c*) attempts to identify the long-range impact of research on colloidal alumina in producing new types of ceramic systems. It is not a comprehensive survey of detailed studies but, rather, it offers an informed treatment regarding the surface-chemical character and the corresponding colloidal behavior of alumina.

General Properties of Colloidal Alumina

Dimensions

Most colloidal alumina has dimensions within the size range stated in the previous section. Unique properties of the high-surface-area portion of the material may be evident if only two dimensions, as in fibrillar particulates and whiskers,[2,3] or even one dimension, such as in the laminar structures of certain clays, are in the submicrometer range. Moreover, the overall character of a dispersed alumina system may be dominated by the high-surface-area portion of particulates, even if only one or two dimensions lie within the colloidal range. A particularly striking example is the non-Newtonian rheology of concentrated alumina slurries, whether these are aqueous or nonaqueous.

To describe the colloidal and surface character of highly dispersed systems that do not exhibit a particularly high surface-area-to-volume ratio, a dispersion factor can be used, as defined by van Hardevald and Hartog.[4] This quantity is the ratio of the number of surface atoms to the total number of atoms in the particle. Representative values for 10-, 100-, and 1000-nm alumina particles are, respectively, on the order of 0.04, 0.004, and 0.0004. These values are based on the assumption that the alumina is the alpha phase, that a molecule of Al_2O_3 can be considered spherical with a diameter of 0.43 nm, and that its density is 3.98 $g \cdot cm^{-3}$.[5]

Since three-dimensional colloidal alumina is common, it is useful to compare the effect of particle size on the average root-mean-square displacement, $\langle x^2 \rangle^{1/2}$, derived from Brownian translational diffusion to the distance over which particles will settle, δh, in aqueous and nonaqueous media. Table I contains this comparison for spherical alumina particles in water, toluene, and *n*-propanol, in sufficiently dilute suspensions so that simple Stokes-Einstein treatments apply.[6] The conditions of temperature and time are respectively chosen as 20°C and 1 hour. Dashed lines indicate arbitrary but realistic boundaries between which alumina particles may be considered colloidal since the

Table I. Effect of Particle Size of Alumina and Solvent Properties* on the Ratio of the Root-Mean-Square Displacement ($\langle x^2 \rangle^{1/2}$) Due to Brownian Translational Diffusion† to the Sedimentation Distance (δh) after 1 hour in Three Common Solvents at 20°C

		Water	Toluene	*n*-Propanol	
Radius (nm)	Density ($g \cdot cm^{-3}$) Viscosity (cP)	0.9982 1.002	0.8669 0.590	0.8035 2.256	Multiplier
0.1 (ions)		1.7	1.3	2.4	$\times 10^{7}$
0.3		9.5	7.3	13	$\times 10^{5}$
1 (solvent)		5.3	4.1	7.5	$\times 10^{4}$
3		3.0	2.3	4.2	$\times 10^{3}$
10		1.7	1.3	2.4	$\times 10^{2}$
32		9.5	7.3	13	$\times 10^{1}$
100		5.3	4.1	7.5	$\times 10^{-1}$
316		3.0	2.3	4.2	$\times 10^{-2}$
1000		1.7	1.3	2.4	$\times 10^{-3}$
3162		9.5	7.3	13	$\times 10^{-5}$
10000		5.3	4.1	7.5	$\times 10^{-6}$

*Ref. 7.
†Ref. 8.

effect of translational diffusion and sedimentation is on the order of 1%, relative to each other.

Behavior

Physical properties and associated phenomena often play an important role in determining the overall processing character of alumina and, therefore ultimately, the microstructure of fabricated components.[7] Examples of such properties include diffusion, Brownian motion, electrophoresis, rheology, and optical and electrical properties.[6] However, the relative importance of these types of physical behavior is often derived from and sometimes dominated by the chemical reactivity and adsorption character at the surface of colloidal alumina.

Combinations of physical and chemical behavior may even determine the most feasible options for specific industrial processes and the ultimate control of product characteristics. An illustration of such an impact is the need to pump or otherwise handle fluid suspensions of alumina that contain high concentrations of solids, exceeding 10 to 20% *v/v*.[7] Practical industrial routes to meeting this need require the ability to predict and control suspension rheology, in particular thixotropy and dilatancy.[8] Sometimes gelation of alumina suspensions manifests itself rheologically and can be affected by various soluble electrolytes, as was demonstrated by Gann.[9] These and related phenomena[10] depend ultimately on the specific interactions among alumina particles, dispersing medium, and solute additives such as salts, surfactants, and soluble polymers.

Monitoring Techniques

Bleier[3] recently discussed many techniques that are available for investigating and monitoring the nature and behavior of colloidal particulates; most are applicable to alumina, the various liquid media in which it is typically dispersed, and general ceramic technology. The purpose for which information is sought, that is, for either fundamental knowledge or technological use, must be considered when deciding the appropriate and most reasonable monitoring methods for alumina-containing materials. Obviously, the more complex a system is chemically or regarding its particulate heterogeneities, the more likely it will require a combination of techniques to describe uniquely and completely the changes in slurry behavior.

As an example, consider the doctor blade processes and chemical system described by Shanefield and coworkers[11] for the fabrication of alumina substrates. They are complex and include mixtures of nonaqueous solvents, aluminum and magnesium oxides, menhaden fish oil, polymeric binder, and plasticizers. In an attempt to understand part of such a complicated system, Tormey et al.[12] studied the adsorption of the dispersant, menhaden fish oil,[13] onto α-Al_2O_3 under controlled conditions in toluene and compared the behavior of that adsorption process to that of glycerol trioleate, a synthetic oil comprised of triglycerides with a single constituent fatty acid, oleic acid. These researchers determined that the two dispersants impart steric stability[14] and especially influence the wetting of alumina, a significant factor in determining the ultimate viability of using toluene as the dispersing medium for alumina.

Tormey[15] attempted to understand the relationships among wetting of powder, dispersibility and colloidal stability of alumina in toluene, adsorption of dispersant, and the final microstructure in tape-cast alumina using this relatively simple model system. She ultimately resorted to many techniques and methods, including FTIR spectroscopy, analysis of adsorption

isotherms, sedimentation studies, surface tension measurements, ESCA, thermal analyses, electron microscopy, and theoretical models of colloid stability. Such a broad approach is becoming increasingly necessary for alumina-based ceramics, as demands on consistently reliable fabrication and predictable performance of the components become more stringent.

Physical and Chemical Properties of Colloidal Alumina

Formation

Methods of producing aluminum oxide have been known for a long time.[16,17] Among the early techniques are hydrolysis of aluminum salts and peptization of hydrous alumina. The first documentation of the colloidal properties of alumina accompanies that of its synthesis. As early as in the 1800s, Gay Lussac[16] and later Crum[16] examined the behavior of hydrolyzed aluminum acetate solutions at high temperature, the effect of prolonged aging, and the solubility of the material produced. Graham[16] examined the peptization of gelatinous alumina, which at cold temperatures tends to generate small, highly hydrous primary particles with reactivity and adsorption capacity higher than those of the more granular and denser particulates formed during prolonged aging at high temperature.[17] Thus, understanding the state of hydration and changes induced in it by temperature and components of the generating solution clearly underpin the fundamental challenge of preparing alumina with predictable properties. As demonstrated later in this section, this understanding and the corresponding preparations of alumina are reemerging as a critical area of study for technical alumina ceramics.

Weiser[17] discussed the early syntheses of alumina hydrates and the techniques by which their formation and structure can be determined. For instance, Weiser and Milligan[18] used physicochemical techniques such as potentiometric titration and diffraction of X rays and electrons to investigate the roles of the anion and free acid in the original aluminum salt and the solution pH on the stoichiometry and physical nature of aluminum hydrous oxides. Most of the colloidal alumina formed in these preparations appears to be either a mono- or a trihydrate form, and finds applications in glassy systems. Other levels of hydration, documented in the 1950s and 1960s and recently reviewed by Lippens and Steggerda,[19] include the more common forms of alumina and hydrous aluminum oxides.

Most alumina is currently prepared using various aluminum hydroxides as precursors[1,2b] and, consequently, the removal of water, the nucleation and growth of crystallites, and the accompanying surface-chemical character and colloidal manifestations are noteworthy. The precipitation of aluminum oxides by neutralization of soluble aluminum salts can yield a gelatinous product, pseudoboehmite. As an example, Rubin and Hayden[20] showed that aluminum hydroxide, freshly precipitated from acidic or mildly ac aqueous solutions, is amorphous. However, u X-ray diffraction analysis, they were able to de pseudoboehmite in material precipitated in mildly sic solutions (pH ≈ 8) and mixtures of pseudoboehr and bayerite in the product derived from solution aluminum nitrate at sufficiently high pH (that is, ab pH 9). Hsu[21] examined in detail the formation pseudoboehmite and bayerite when added electroly are present.

Preparations based on solutions of aluminum sa aluminates of Group I elements, and aluminum alk ides usually yield amorphous, gelatinous material the thermodynamically stable product under a w variety of conditions. This material is hydrophilic a exhibits colloidal and surface properties that depe critically on the residual degree of surface hydrat following the calcination stages of treatment.[1c,22] F garding kinetic considerations, Smith[23] establish that freshly prepared $Al(OH)_3$ is an amorphous so which, on proper aging, transforms to well-defin crystalline structures. Similarly, Hem and Robersor found that gibbsite crystals can be detected if dilu aqueous solutions of aluminum salts are aged for days. In an extensive study dealing with the effect aging on the formation of aqueous aluminum hydro ide complexes, Smith and Hem[25] found that polyn clear solute species are stable up to nearly one day the pH range 4.4 to 4.6 and, at longer times, conve slowly to submicroscopic crystalline particles $Al(OH)_3$.

One of the most exciting recent developments i the preparation of aluminum hydroxide and alumir has been the introduction of monosized alumina pr cursors with uniform and controllable morphology For instance, Brace and Matijević [26] prepared mon dispersed, spherical hydrous aluminum oxide sols wit particle-size distributions in the submicrometer range These colloidal particles were produced by aging aque ous solutions of $Al_2(SO_4)_3$ at 98°C. This researcl revealed that the "equilibrium" growth medium, whicl was slightly acidic, requires sulfate species to produc well-defined, model hydrous oxide particles havin modal diameters in the ranges 0.4 to 0.5 and 0.7 to 0.8 μm, and that the ultimate size of particles depends, ir part, on the initial concentration of the starting Al salt. The originally produced particles contained an appre ciable amount of sulfate but this contaminant could be exchanged for hydroxide species, in much the same manner as the one described by Gordon et al.,[27] converting the basic aluminum sulfate to hydrous aluminum oxide. This conversion was accompanied by a decrease in the modal diameter and, possibly, by a slight narrowing of the size distribution. Similar hydrous oxide and uniform, but nonspherical, particles of boehmite were synthesized by Scott and Matijević [28] in a study using aluminum chloride and aluminum perchlorate as reagents.

In related research on the preparation of monodispersed hydrous aluminum oxide sols, Catone and Matijević [29] used aluminum sec-butoxide as a starting material, demonstrating that polar organic media could also be used to synthesize model spherical particulates of alumina precursors. These sols, similar to the ones produced by Brace and Matijević, [26] also have a narrow size distribution. Interestingly, the surface character of the material prepared by Catone and Matijević, particularly that reflected in electrokinetic measurements, resembles the aluminum hydroxide derived from aqueous media by Dezelić et al. [30] Finally, Ingebrethsen and Matijević [31] extended the work with aluminum sec-butoxide and successfully synthesized amorphous, spherical aluminum hydrous oxide with a narrow size distribution by reacting the alkoxide with water vapor after the former reagent had been converted to a liquid aerosol. This novel technique of producing solid aerosols of the hydrous oxide, which exhibit a narrow size distribution with modal diameters (in this case, between 0.2 and 0.6 μm) and which can be calcined to δ-Al_2O_3 at 700°C while retaining the spherical shape,[31] has potential in becoming important for future ceramics. The process is especially germane to technical ceramic applications, the continuous processing and preparation of complex alumina powders, and composite particulates.

Thus, it is seen that in recent years the preparation of uniform hydrous aluminum oxide particles has received considerable attention, particularly by Matijević and coworkers. Recently, [32] he reviewed the various techniques by which this material and related uniform hydrous metal oxides can be synthesized. The role of anions in the synthesis medium is critical to the nucleation of such materials. However, anions may be either physically entrapped as counterions or chemically bound as constituents of the solid but can usually be removed prior to calcination. Additionally, the studies cited here were designed to identify the science and the art by which alumina and its hydrous oxide precursors can be derived and, in some cases, the specific aspects requiring modification for industrial production.

These and related Al-containing precipitates have also been used by other investigators as precursors to alumina, sometimes in attempts to extend the work just summarized, to prepare well-characterized alumina in forms and quantities that would be commercially attractive. Specifically, Cornilsen and Reed[33] studied various basic aluminum salts as potential precursors, whereas Sacks et al.[34] and Blendell et al.[35] restricted studies to those in which spherical basic aluminum sulfate was the specific starting material for conversion to alumina.

Characterization

The proper characterization of colloidal alumina depends, of course, on the technological and scientific purposes for which the information is sought, since the complete characterization would be an enormous task.[3] Among the physical properties to be considered for this colloidal material are (*a*) size, shape, and morphology of primary particles; (*b*) surface area; (*c*) number and size distribution of pores; (*d*) degree of crystallinity and polycrystallinity; (*e*) concentration of defects; (*f*) nature of internal and surface stresses; and (*g*) state of agglomeration. The chemical properties required for complete characterization are chemical and phase composition, including data on the purity of alumina and the nature and quantity of adsorbed surface films or impurities. Items (*a*) to (*f*) are, in principle, applicable to any colloidal material and, therefore, are not described in detail here. Although the specific details required for the alumina may either preclude or, contrastingly, favor a particular characterization technique, as described by Bleier,[3] such a discussion is outside the scope of this chapter.

Item (*g*), state of agglomeration, and the chemical properties of colloidal alumina are, on the other hand, of paramount importance and require being addressed here. Nearly all colloidal alumina systems undergo agglomeration to some extent and this phenomenon affects their physical behavior. Moreover, the chemical structure of the solid-liquid interface is often ultimately responsible for the unique properties of concentrated alumina suspensions that are used to fabricate technical ceramics. These properties have been extensively studied in recent years and are addressed in the next section.

State of Agglomeration

Agglomeration of colloidal alumina occurs via coagulation or flocculation and leads to a distribution of aggregate sizes. Thus, either the rate or the extent of agglomeration is of practical concern whenever the use of colloidal alumina is considered. The most desired method of evaluating the kinetic and equilibrated aspects of agglomeration is ultramicroscopy but, unfortunately, this technique is often impractical owing to technical intricacies and the time required.[36] However, being the only direct and widely available method to observe colloidal suspensions in situ, it will probably be more commonly used when fundamental information on aggregate size distribution is sought. Of course, indirect methods such as neutron scattering and light scattering, together with related models of suspension structure[37] and procedures derived from freeze drying and etching techniques,[38] are closely related to ultramicroscopy in their attempt to examine the structure of suspensions. These techniques have great potential if measurements in situ are required, although apparently they have not yet been systematically applied to alumina systems.

Other methods of qualitatively and quantitatively characterizing aspects of agglomeration have certainly been developed and are quite suitable for colloidal alumina. These methods are based on the principles of sedimentation, rheology, and electrical and thermal

conductivity. They tend to be somewhat empirical, qualitative, and restricted to a specific colloidal system, particularly when additives are present. Often, these limitations are not due to restrictions inherent to the techniques but arise simply from the complexity of relating the status of a given suspension to fundamental properties that can be independently evaluated and used to predict behavior in previously unexamined cases. For instance, the effect of agglomeration on the viscosity of an alumina suspension is a very complicated phenomenon. Taken separately, agglomeration and viscosity can be treated with varying degrees of sophistication and detail.[3,8,14,39–42] Systematic application to alumina systems seems to have been quite limited, notably owing to the unavailability of the model particulates of alumina discussed earlier and to the general lack of recognition of the role that initial powder characteristics play in the processing of alumina-based ceramics.

Nonetheless, it is possible to establish some correlations among transitions in the state of agglomeration, microstructure of fabricated pieces, and physical properties for alumina-based components. For example, in addressing the role of polyacrylic acid on processing behavior in well-characterized alumina and alumina-zirconia composites, Bleier and Westmoreland[43] recently showed, using a variety of techniques, that the state of agglomeration of alumina relates directly to surface charge of α-Al_2O_3, rheology of concentrated slurries, density of both prefired and sintered components, and distribution of zirconia in an alumina matrix.

Figure 1 demonstrates some of the comparisons that can be made among processing properties and density of the fabricated component.[43] The structure

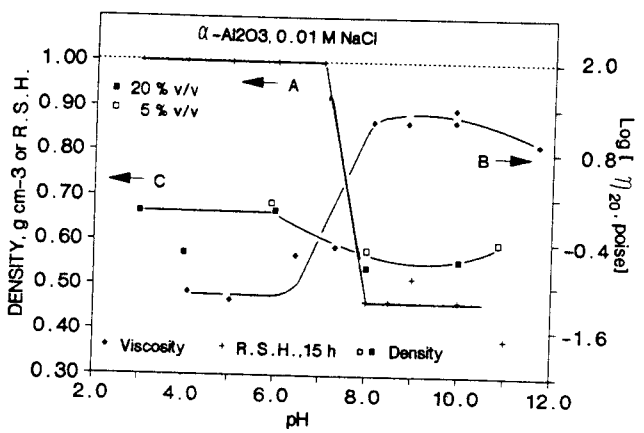

Fig. 1. Comparison of (A) relative sedimentation height (R.S.H.) after 15 h, (B) logarithm of viscosity when shear rate is 20 s^{-1}, and (C) prefired density of pressure-cast pellets for the pH range 2 to 12. Initial concentrations of α-Al_2O_3 (0.5 μm) are (A) 5, (B) 20, and (C) 5 or 20% *v/v*. High values of R.S.H. and density are desirable, whereas low values of viscosity are deemed best. Conditions leading to transitions in the state of agglomeration agree well for the techniques examined (Ref. 43.).

of clusters, produced via agglomeration when surface charge is low, whether or not polyacrylic acid is present, clearly affects the subsequent, important stages of processing: handling of slurries (rheology), microstructure in the prefired state (density), and microstructure after exposure to comparatively mild heat treatment. Ultimate mechanical properties[44] are, in turn, influenced by the initial state of agglomeration. Research by Baik et al.[45] and Bleier[46] demonstrated that appropriate models of colloidal behavior, based ultimately on the surface charge density of alumina[39,47] and particle size, adequately predict the transition between desirable and undesirable final microstructures obtained by sintering pressure-cast pellets of α-Al_2O_3 at 1370°C for 1 hour. These investigations relate fundamental colloidal models to prefired and sintered densities and to the optimum conditions for processing $Al_2O_3 - ZrO_2$ composites without additives. Heterocoagulation,[39,48] involving the secondary minimum[49] that characterizes the interaction between particles of α-Al_2O_3 and *m*-ZrO_2, was deemed of paramount importance for achieving uniform microstructures over the initial pH range 3 to 11 for this alumina-containing composite. Direct and indirect effects on mechanical properties of Al_2O_3-ZrO_2 composites are also anticipated, since physical properties often derive from microstructural features.

Related to this work on colloidal alumina is the research of Cesarano et al.[50], Aksay and Schilling[51], and Sacks and Tseng.[52] Cesarano and co-workers used the concept of a stability map in studies on the processing of alumina in the presence of sodium poly(methacrylate). This research demonstrated the viability of correlating transitions in the state of agglomeration in single component slurries with variations in the consolidated state, in much the same manner as that just described for Al_2O_3-ZrO_2 composites. Aksay and Schilling identified the existence of a relationship among processing conditions and the casting rate of α-Al_2O_3. This study shows that the casting rate of α-Al_2O_3 depends, in part, on the magnitude of colloidal forces as inferred from calculations and measurements of zeta potential in the pH range 1 to 11. When zeta potential was high (≈55 mV), low casting rates were observed but with desirable microstructural and density features. Conversely, low values of zeta potential (≈17 mV) led to high casting rates and undesirably high porosity. Interestingly, Han et al.[53] inferred from microscopic and porosimetric data gathered on α-Al_2O_3 that low casting rates can lead to differential sedimentation when bimodal submicrometer particle size distributions are used. This behavior segregates particles during consolidation and generates enclosed pores that remain after sintering. Finally, Sacks and Tseng demonstrated that the state of agglomeration in aqueous milling of alumina and in the presence of citrate species governs grinding efficiency and that citrate species adsorb onto Al_2O_3, thereby

indirectly affecting comminution by altering the state of agglomeration of alumina.

Contrasting these aqueous studies, those of Tormey and coworkers[12,15] examined in detail requirements for the successful processing of well-characterized alumina in low-dielectric, nonaqueous media. The roles of adsorption and steric stabilization[14] were identified. Most importantly, however, their work on nonaqueous processing using model suspensions demonstrates the validity of systematic studies to relate fundamental properties of colloidal alumina and additives to the state of agglomeration. The latter, in turn, constitutes precursory structures in the slurry that, unless intentionally removed, usually generate remnant, unwanted microstructural features and physical properties.

Sacks et al.[54] also studied nonaqueous alumina suspensions. Specifically, they examined the milling and general behavior of α-Al_2O_3 in methanol and methyl isobutyl ketone and applied the classical theory of colloidal stability.[36,39] This work demonstrates methods and fundamental principles by which zeta potential may be correlated with milling time and rheological properties in sufficiently dielectric nonaqueous media. For instance, high values of zeta potential (25 mV in methanol) apparently promoted good dispersion of particulate fragments produced during milling, thus facilitating breakdown of α-Al_2O_3. A similar effect was observed when nonionic polymer provided steric stability, although no direct or indirect data on steric stability were given.

Summary

Colloidal alumina is technologically and scientifically important. Its unique properties, which ultimately derive from its finely divided state, are generally understood. However, the specific chemical aspects that determine the physical form and crystallinity of synthesized colloidal alumina need to be better defined, although much is already known and promising routes to the controlled, industrial preparation of colloidal alumina with *predictable* properties are being identified. Chemical effects on the state of agglomeration, whether in milling, preparation of ceramic suspensions, or final consolidation during fabrication of components, are emerging and their importance in the manufacture of alumina-based ceramics is increasingly appreciated.

Engineering and scientific research on colloidal alumina needs considerably more attention before this material can be understood and exploited most fully. Specifically, well-designed studies that directly examine the colloidal state of alumina for its own merits, that identify fundamental principles by which this material behaves, and that extend these principles to heretofore unchallenged applications, including prediction of fired microstructures and related physical properties, are required.

Recognition of the interdisciplinary nature of colloidal processing schemes for alumina ceramics is a necessary first development that has occurred since Gitzen's review[1d] and is apparently widespread. Nonetheless, much of the ceramic community that deals with colloidal alumina has not accepted the primary responsibility to develop a detailed understanding of its properties, particularly regarding concentrated suspensions. Without this commitment, principal developments are most likely to emerge only slowly and from basic scientific studies in nonceramic industries and disciplines, for example, with minerals and chemicals. These developments will probably lack the features that ensure immediate acceptance for ceramic products and will therefore remain largely unexamined, unless the alumina industry critically and actively participates in the quest to understand and control the colloidal particulates it encounters. Happily, we find that the process has begun.

Acknowledgment

This review was prepared under contract with the Basic Energy Sciences Program, Division of Materials Sciences, U.S. Department of Energy, Contract No. DE-AC05-840R21400 with Martin Marietta Energy Systems, Inc. The author gratefully thanks F. C. Stooksbury for patience and help in preparing this chapter and C. E. Bamberger for useful comments on editing it.

References

[1(a)]Page 46 in The Merck Index, 8th ed. Edited by P. G. Stecher. Merck, Rahway, NJ, 1968.

[(b)]Industrial Minerals and Rocks, 4th ed. Edited by S. J. Lefond. American Institute of Mineralogical, Metallurgical, Petrological Engineering, New York, 1975; 1360 pp.

[(c)]G. MacZura, "Aluminum Oxide (Alumina)"; pp. 79–80 in Kirk-Othmer Concise Encyclopedia of Chemical Technology. Edited by M. Grayson and D. Eckroth. Wiley & Sons, New York, 1985.

[(d)]"Colloidal Properties of Alumina"; pp. 111–15 in Alumina As a Ceramic Material. Edited by W. H. Gitzen. The American Ceramic Society, Columbus, OH, 1970.

[2(a)]R. W. Hertzberg; pp. 46, 236 in Deformation and Fracture Mechanics of Engineering Materials, 2nd ed. Wiley & Sons, New York, 1983.

[(b)]I. J. McColm; pp. 129, 257–72 in Ceramic Science for Materials Technologists. Blackie and Son, Glasgow, 1983.

[3]A. Bleier, "Colloid Chemistry"; pp. 725–31 in Encyclopedia of Materials Science and Engineering. Edited by M. B. Bever. Pergamon, Oxford, 1986.

[4]R. van Hardeveld and F. Hartog, "Statistics of Surface Atoms and Surface Sites on Metal Crystals," *Surf. Sci.*, **15** [2] 189–230 (1969).

[5(a)]Engineering Property Data on Selected Ceramics, Vol. III, Single Oxides, Report No. MCIC-HB-07-Vol. III. Battelle Laboratories, Columbus, OH, 1981; 251 pp.

[(b)]CRC Handbook of Chemistry and Physics, 66th ed. Edited by R. C. Weast. CRC, Boca Raton, FL, 1985; pp. B-69, C-(446, 518), F-(4, 5, 41, 42).

[6(a)]A. Einstein, Investigations on the Theory of the Brownian Movement. Edited by R. Furth. Dover, New York, 1956; 122 pp.

[(b)]R. D. Vold and M. J. Vold, "The Characterization of Particles in Lyophobic Sols"; pp. 181–221 in Colloid and Interface Chemistry. Addison-Wesley, Reading, MA, 1983.

[c]P. A. Hiemenz, "Sedimentation and Diffusion and Their Equilibrium"; pp. 59–114 in Principles of Colloid and Surface Chemistry, 2d ed. Marcel Dekker, New York, 1986.

[7]R. E. Cowen, "Slip Casting"; pp. 154–71 in Treatise on Materials Science and Technology, Ceramic Fabrication Processes, Vol. 9. Edited by F. F. Y. Wang. Academic Press, New York, 1976.

[8]J. W. Goodwin, "The Rheology of Dispersions"; pp. 246–93 in Colloid Science, Vol. 2. Edited by D. H. Everett. The Chemical Society, London, 1975.

[9]J. A. Gann, "The Velocity of Coagulation of Aluminum Hydroxide Solution," *Kolloidchem. Beihefte*, **8**, 63–138 (1916).

[10]S. G. Lawrence, "Assessment of the State of Dispersion"; pp. 363–94 in Dispersion of Powders in Liquids, 3d ed. Edited by G. D. Parfitt. Applied Science, London, 1981.

[11a]D. J. Shanefield, and R. E. Mistler, "Manufacturing Process for Fine-Grain Alumina Substrates," *Am. Ceram. Soc. Bull.*, **52** [4] 375 (1973).

[b]D. J. Shanefield and R. E. Mistler, "Fine Grained Alumina Substrates. I. Manufacturing Process," *Am. Ceram. Soc. Bull.*, **53** [5] 416–20 (1973).

[c]D. J. Shanefield, P. T. Morzenti, and R. E. Mistler, "Fine Grained Alumina Substrates: II, Properties," *Am. Ceram. Soc. Bull.*, **53** [8] 564–68 (1974).

[12]E. S. Tormey, L. M. Robinson, W. R. Cannon, A. Bleier, and H. K. Bowen, "Adsorption of Dispersants from Nonaqueous Solutions"; pp. 121–36 in Surfaces and Interfaces in Ceramic and Ceramic-Metal Systems, Materials Science Research, Vol. 14. Edited by J. A. Pask and A. G. Evans. Plenum, New York, 1981.

[13a]M. E. Stansby, "Development of Fish Oil Industry in the United States," *J. Am. Oil Chem. Soc.*, **55**, 238–43 (1978).

[b]M. E. Stansby, "Marine Derived Fatty Acids or Fish Oils as Raw Material for Fatty Acids Manufacture," *J. Am. Oil Chem. Soc.*, **56** [11] 793A–796A (1979).

[14]D. H. Napper, Polymeric Stabilization of Colloidal Dispersions. Academic Press, London, 1983; 428 pp.

[15]E. S. Tormey, "The Adsorption of Glyceryl Esters at the Alumina/Toluene Interface"; Ph. D. Thesis, Massachusetts Institute of Technology, Cambridge, 1982; 349 pp.

[16]Cited in Ref. 17:

[a]Gay Lussac, *Ann. Chim. Phys.*, **74** [1] 193 (1810).

[b]Crum, *Liebig's Ann. Chem.*, **89**, 168 (1854).

[c]Graham, *Philos. Mag.*, **23** [4] 290 (1862).

[d]Graham, *Liebig's Ann. Chem.*, **121**, 41 (1862).

[17]H. B. Weiser, "The Hydrous Oxides of Aluminum, Gallium, Indium, and Thallium", in

[a]The Hydrous Oxides. 1st ed. McGraw-Hill New York, 1926, pp. 103–33.

[b]Inorganic Colloid Chemistry, Vol. II. Wiley & Sons, New York, 1935, pp. 90–124.

[18a]H. B. Weiser and W. O. Milligan, "The Constitution of Inorganic Gels"; pp. 227–46 in Advances in Colloid Science Vol. I. Edited by E. O. Kraemer. Interscience, New York, 1942.

[b]H. B. Weiser and W. O. Milligan, "X-Ray Studies on the Hydrous Oxides. VI. Alumina Hydrate," *Phys. Chem.*, **38**, 1175–82 (1934).

[c]H. B. Weiser and W. O. Milligan, "The Constitution of Colloidal Systems of the Hydrous Oxides," *Chem. Rev.*, **25**, 1–30 (1939).

[19]B. C. Lippens and J. J. Steggerda, "Active Alumina"; pp. 171–211 in Physical and Chemical Adsorbents and Catalysts. Edited by B. G. Linsen. Academic Press, London, 1970.

[20]A. J. Rubin and P. L. Hayden, "Studies on the Hydrolysis and Precipitation of Aluminum (III)," Ohio State University, Columbus, OH, U.S. Dept. of Interior Project Report No. 364X, April 1973.

[21]P. H. Hsu, "Effects of Salts on the Formation of Bayerite Versus Pseudo-Boehmite," *Soil Sci.*, **103** [2] 101–10 (1967).

[22a]C. Misra, Industrial Alumina Chemicals, ACS Mono-graph No. 184, The American Chemical Society, Washington, 1986; 165 pp.

[b]W. Baumgart, A. C. Dunham, and G. C. Amstutz (eds) Process Mineralogy of Ceramic Materials. Elsevier, New York. 1984; pp. 107–12.

[c]E. Dorre and H. Huber, Alumina. Springer-Verlag, Berlin. 1984; 329 pp.

[23]R. W. Smith, "Relations Among Equilibrium and Nonequilibrium Aqueous Species of Aluminum Hydroxy Complexes," *Adv. Chem. Ser.*, **106**, 250–79 (1971).

[24]J. D. Hem and C. E. Roberson, U.S. Geol. Survey Water-Supply Paper 1827-A. U.S. Gov't. Printing Office, Washington, DC. 1967.

[25]R. W. Smith and J. D. Hem, U.S. Geol. Survey Water-Supply Paper 1827-D. U.S. Gov't. Printing Office, Washington, DC. 1972.

[26a]R. Brace and E. Matijević, "Aluminum Hydrous Oxide Sols. I. Spherical Particles of Narrow Size Distribution," *J. Inorg. Nucl. Chem.*, **35**, 3691–3705 (1973);

[b]E. Matijević, "Preparation and Characterization of Monodispersed Metal Hydrous Oxide Sols," *Progr. Colloid Polymer Sci.*, **61**, 24–35 (1976).

[27]L. Gordon, M. L. Salutsky, and H. H. Willard; p. 6 in Precipitation from Homogeneous Solutions. Wiley & Sons, New York, 1959.

[28]W. B. Scott and E. Matijević, "Aluminum Hydrous Oxide Sols. III. Preparation of Uniform Particles by Hydrolysis of Aluminum Chloride and Aluminum Perchlorate," *J. Colloid Interface Sci.*, **66**, 447–54 (1978).

[29]D. L. Catone and E. Matijević, "Aluminum Hydrous Oxide Sols. II. Preparation of Uniform Spherical Particles by Hydrolysis of Aluminum Sec-Butoxide," *J. Colloid Interface Sci.*, **48** [2] 291–301 (1974).

[30]N. Dezelić, H. Bilinski, and R. H. H. Wolf, "Precipitation and Hydrolysis of Metallic Ions, IV. Solubility of Aluminum Hydroxide in Aqueous Solution," *J. Inorg. Nucl. Chem.*, **33** [3] 791–98 (1971).

[31]B. J. Ingebrethsen and E. Matijević, "Preparation of Uniform Colloidal Dispersions by Chemical Reactions in Aerosols-2. Spherical Particles of Aluminum Hydrous Oxide," *J. Aerosol Sci.*, **11**, 271–80 (1980).

[32a]E. Matijević, "Monodispersed Metal (Hydrous) Oxides - A Fascinating Field of Colloid Science," *Acc. Chem. Res.*, **14**, 22–29 (1981).

[b]E. Matijević, "Production of Monodispersed Colloidal Particles," *Ann. Rev. Mater. Sci.*, **15**, 483–516 (1985).

[33]B. C. Cornilsen and J. S. Reed, "Homogeneous Precipitation of Basic Aluminum Salts as Precursors for Alumina," *Am. Ceram. Soc. Bull.*, **58** [12] 1199 (1979).

[34]M. D. Sacks, T.-N. Tseng, and S. Y. Lee, "Thermal Decomposition of Spherical Hydrated Basic Aluminum Sulfate," *Am. Ceram. Soc. Bull.*, **63** [2] 301–309 (1984).

[35]J. E. Blendell, H. K. Bowen, and R. L. Coble, "High Purity Alumina by Controlled Precipitation from Aluminum Sulfate Solutions," *Am. Ceram. Soc. Bull.*, **63** [6] 797–802 (1984).

[36a]H. R. Kruyt, "General Properties of Colloid Systems"; pp. 15–53 in Colloid Science, Vol. I. Edited by H. R. Kruyt. Elsevier, Amsterdam, 1952.

[b]P. Stenius, "Svedberg's Early Studies in Colloid Chemistry"; pp. 17–21 in Physical Chemistry of Colloids and Macromolecules. Edited by B. Ranby. Blackwell Scientific, Oxford, 1987.

[37a]R. H. Ottewill, "Small Angle Neutron Scattering"; pp. 143–63 in Colloidal Dispersions. Edited by J. W. Goodwin. The Royal Society of Chemistry, London, 1982.

[b]C. S. Hirtzel and R. Rajagopalan, Colloidal Phenomena. Noyes, Park Ridge, NJ, 1985; 318 pp.

[38a]R. F. Stewart and D. Sutton, "Characterization of Colloidal Suspensions for Ceramic Processing," *Mater. Res. Soc. Symp. Proc.*, **32**, 281–86 (1984).

[b]R. F. Stewart and D. Sutton, "Control of Structure in Particulate Solids Suspensions"; pp. 111–28 in Solid-Liquid Separation. Edited by J. Gregory. Ellis Horwood, Ltd., Chichester, England, 1984.

[c]R. F. Stewart and D. Sutton, "Morphology and Properties of Particle/Polymer Suspensions"; pp. 455–60 in Science of Ceramic Chemical Processing. Edited by L. L. Hench and D. R. Ulrich. Wiley & Sons, New York, 1986.

[39(a)]P. A. Hiemenz, Principles of Colloid and Surface Chemistry, 2d ed. Marcel Dekker, New York, 1986; 815 pp.

[b]R. D. Vold and M. J. Vold, Colloid and Interface Chemistry. Addison-Wesley, Reading, MA, 1983; 694 pp.

[c]H. Sonntag and K. Strenge, Coagulation and Stability of Disperse Systems. Halsted, New York, 1972; 139 pp.

[d]G. D. Parfitt (ed), Dispersion of Powders in Liquids, 3d ed. Applied Science, London, 1981; 518 pp.

[e]A. Bleier, Mixed Colloidal Dispersions; Ph.D. Thesis, Clarkson University, Potsdam, NY, 1976; 272 pp.

[40(a)]I. M. Krieger, "Rheology of Polymer Colloids"; pp. 219–46 in Polymer Colloids. Edited by R. Buscall, T. Corner, and J. F. Stageman. Elsevier Applied Science, London, 1985.

[b]I. M. Krieger, "Rheology of Monodisperse Latices," *Adv. Colloid Interface Sci.*, **3** [2] 111–36 (1972).

[41(a)]B. A. Firth, "Flow Properties of Coagulated Colloidal Suspensions. II. Experimental Properties of the Flow Curve Parameters," J. Colloid Interface Sci., **57** [2] 257–65 (1976).

[b]T. G. M. Van den Ven and R. J. Hunter, "Viscoelastic Properties of Coagulated Sols," *J. Colloid Interface Sci.*, **68** [1] 135–43 (1979).

[c]R. J. Hunter and J. Frayne, "Couette Flow Behavior of Coagulated Colloidal Suspensions. IV. Effect of Viscosity of the Suspension Medium," *J. Colloid Interface Sci.*, **71** [1] 30–38 (1979).

[d]R. J. Hunter and J. Frayne, "Flow Behavior of Coagulated Colloidal Sols. V. Dynamics of Floc Growth Under Shear," *J. Colloid Interface Sci.*, **76** [1] 107–15 (1980).

[42]M. A. Janney, "Plasticity of Ceramic Particulate Systems"; Ph. D. Thesis, University of Florida, Gainesville, 1982; 154 pp.

[43]A. Bleier and C. G. Westmoreland, "Effects of Adsorption of Polyacrylic Acid on the Stability of α-Al_2O_3, *m*-ZrO_2, and Their Binary Suspension Systems"; pp. 217–36 in Interfacial Phenomena in Biotechnology and Materials Processing. Elsevier, Edited by B. Moudgil and Y. A. Attia, Amsterdam, 1988.

[44(a)]A. H. Heuer, F. F. Lange, M. V. Swain, and A. G. Evans, "Transformation Toughening: An Overview," *J. Am. Ceram. Soc.*, **69** [3] i–iv (1986).

[b]R. A. Cutler, J. J. Hansen, A. V. Virkar, D. K. Shetty, and R. C. Winterton, "Strength Improvement in Transformation Toughened Ceramics Using Compressive Residual Surface Stresses," *Mater. Res. Soc. Symp. Proc.*, **78**, 155–63 (1987).

[45]S. Baik, A. Bleier, and P. F. Becher, "Preparation of Al_2O_3-ZrO_2 Composites by Adjustment of Surface Chemical Behavior," *Mater. Res. Soc. Symp. Proc.*, **73**, 791–800 (1986).

[46]A. Bleier, "Heterocoagulation Involving the Secondary Minimum: The Al_2O_3-ZrO_2 System"; in Abstracts of the 61st Colloid and Surface Science Symposium. The American Chemical Society, Ann Arbor, MI, June 1987, Paper No. 64.

[47(a)]W. Hasz, "Surface Reactions and Electrical Double Layer Properties of Ceramic Oxides, in Aqueous Solution"; M. S. Thesis, Massachusetts Institute of Technology, Cambridge, 1983, 165 pp.

[b]W. C. Hasz and A. Bleier, "Surface Reactivity of Silica and Alumina Ceramic Powders"; pp. 189–201 in Advances in Materials Characterization II, Materials Science Research, Vol. 19. Edited by R. L. Snyder, R. A. Condrate, Sr., and P. F. Johnson. Plenum, New York, 1985.

[48(a)]A. Bleier and E. Matijević, "Heterocoagulation. I. Interactions of Monodispersed Chromium Hydroxide with Polyvinyl Chloride Latex," *J. Colloid Interface Sci.*, **55** [3] 510–24 (1976).

[b]A. Bleier and E. Matijević, "Stability of Mixed Colloidal Dispersions"; pp. 81–98 in Chemistry of Waste Water Technology. Edited by A. J. Rubin. Ann Arbor Science Press, Ann Arbor, MI, 1978.

[49]H. S. Chung and R. Hogg, "Stability Criteria for Fine-Particle Dispersions," *Colloids Surf.*, **15**, 119–35 (1985).

[50(a)]J. Cesarano III, I. A. Aksay, and A. Bleier, "Stability of α-Al_2O_3 Suspensions with Poly(methacrylic acid) Polyelectrolyte," *J. Am. Ceram. Soc.*,**71** [4] 250–55 (1988).

[b]J. Cesarano III and I. A. Aksay, "Processing of Highly Concentrated Aqueous α-Alumina Suspensions Stabilized with Polyelectrolytes," *J. Am. Ceram. Soc.*, **71** [12] 1062–67 (1988).

[51]I. A. Aksay and C. H. Schilling, "Colloid Tritration Route to Uniform Microstructures"; pp. 439–47 in Ultrastructure Processing of Ceramics, Glasses and Composites. Edited by L. L. Hench and D. R. Ulrich. Wiley & Sons, New York, 1948.

[52]M. D. Sacks and T-Y. Tseng, "Role of Sodium Citrate in Aqueous Milling of Aluminum Oxide," *J. Am. Ceram. Soc.*, **66** [4] 242–47 (1983).

[53]C. Han, I. A. Aksay, and O. J. Whittemore, "Characterization of Microstructural Evolution by Mercury Porosimetry"; pp. 339–347 in Advances in Materials Characterization II, Materials Science Research, Vol. 19, Edited by R. L. Snyder, R. A. Condrate, Sr., and P. F. Johnson. Plenum, New York, 1985.

[54(a)]M. D. Sacks and D. S. Khadilkar, "Milling and Suspension Behavior of Al_2O_3 in Methanol and Methyl Isobutyl Ketone," *J. Am. Ceram. Soc.*, **66** [7] 488–94 (1983).

[b]M. D. Sacks, "Rheological Science"; pp. 522–38 in Science of Ceramic Chemical Processing. Edited by L. L. Hench and D. L. Ulrich. Wiley & Sons, New York, 1986.

[c]M. D. Sacks and M. I. Alam, "Nonaqueous Suspension Properties of Al_2O_3 and Silicate Glass Powders," *Mater. Res. Soc. Symp. Proc.*, **32**, 313–19 (1984).

Phase Equilibria of Alumina

Lawrence P. Cook

Ceramics Division
National Institute of Standards and Technology
Gaithersburg, MD 20899

In the system Al-O, α-alumina (corundum) is stable over a broad temperature range relative to the other alumina polymorphs. It melts at 2054°C, and at this temperature the total vapor pressure of alumina is $\approx 10^{-1}$ Pa. Corundum is stable at very high isostatic pressures and there are no known high-pressure modifications. Continuous solid solutions of corundum with Cr_2O_3 can be made, and extensive, but partial solid solutions occur with Fe_2O_3 and Ga_2O_3. Additional solid solutions can be postulated from crystal chemical considerations, but data are lacking. Alumina reacts with most other oxides to form one or more intermediate binary compounds; the resulting aluminates include members of the spinel, beta alumina, perovskite, tridymite, and garnet structural families. The corundum liquidus varies appreciably among binary oxide systems. In general, the measured liquidus is at a lower temperature (higher solubility of corundum) than the ideal solution liquidus, possibly indicating the formation of aluminate complexes in the melt. A few of the systems with Group IV oxides have liquidi at higher temperatures than the ideal, perhaps due to association of the additive oxide. Relatively few systems of alumina with nonoxides have been studied. Alumina-boride phase diagrams are not available, and only a few diagrams of alumina with carbides (Al_4C_3) and nitrides (AlN, Si_3N_4) are known. The formation of aluminum oxynitride and oxycarbide phases is well documented. From thermodynamic data, alumina is unstable in contact with many metals in Groups IA and IIA. However, on the basis of available data, it is compatible with Si, Fe, the noble metals, and possibly others. Alumina is also thermodynamically compatible with several molten alkali halides. Alumina in contact with gaseous fluorine is unstable; to a lesser degree the same is true with chlorine and hydrogen sulfide at very high temperatures.

Introduction

Useful properties such as chemical inertness, hardness, electrical resistivity, and high-temperature strength have made α-alumina (corundum) the material of choice for diverse applications ranging from biological implants to abrasives, insulators, and refractories. As a naturally occurring oxide component, alumina is abundant, comprising about 15 wt% (10 mol%) of the earth's crust. Consequently, it is not surprising that numerous alumina-containing phase diagrams have been published, as indicated in Fig. 1. Phase diagrams with alumina as a component form the basis of many processes and materials, and a short list of some technologically important alumina systems is given in Table I.

There are more than 250 published alumina-containing phase diagrams, including a large number of ternary and higher order systems. It is not possible in this review to present and discuss each phase diagram individually. For particular systems of interest, the reader is referred to Ref. 1. Similarly, no attempt will be made to give an in-depth discussion of the principles of phase equilibria, for which the reader is referred to any of numerous textbooks on the subject (e.g., Ref. 2). Rather, the present paper briefly reviews the main features of alumina phase equilibria by treating primarily binary examples drawn from the literature. Emphasis is on the alumina-saturated portions of such systems, in which α-alumina occurs as a phase. In particular, several major types of alumina phase equilibria can be differentiated. Binary equilib-

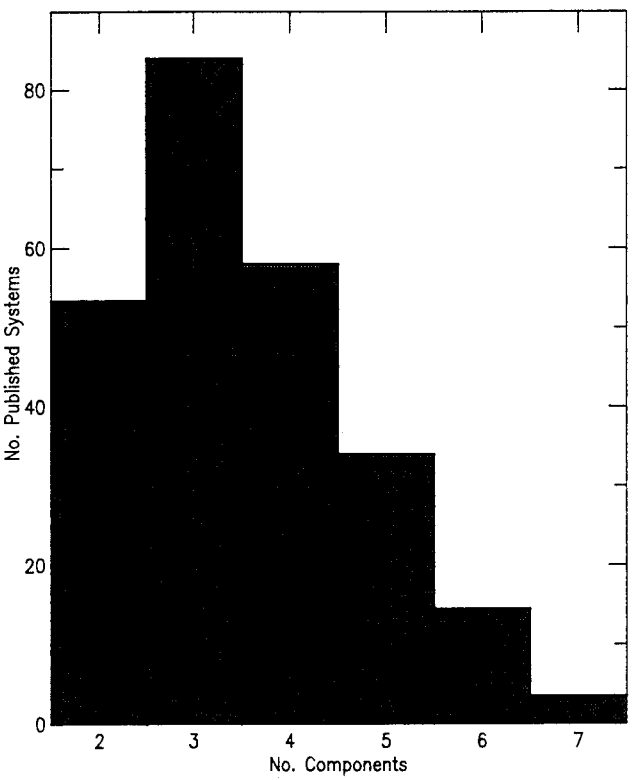

Fig. 1. Published phase diagrams of alumina-containing systems (Ref. 1).

Table I. Selected Applications of Alumina Phase Diagrams

System	Application
Al_2O_3-Na_2O	Beta alumina solid electrolytes
Al_2O_3-CaO	High-alumina cements
Al_2O_3-Y_2O_3	YAG laser materials
Al_2O_3-SiO_2	Mullite ($3Al_2O_3 \cdot SiO_2$) refractories
Al_2O_3-Na_3AlF_6	Aluminum production by molten salt electrolysis
Al_2O_3-Li_2O-SiO_2	Low thermal expansion β-spodumene and β-eucryptite ($Li_2O \cdot Al_2O_3 \cdot 4SiO_2$ and $Li_2O \cdot Al_2O_3 \cdot 2SiO_2$) glass-ceramics
Al_2O_3-MgO-SiO_2	Low thermal expansion β-cordierite ($2MgO \cdot 2Al_2O_3 \cdot 5SiO_2$) glass-ceramics
Al_2O_3-CaO-FeO_x-SiO_2	Refractory/slag interactions in iron- and steelmaking
Al_2O_3-SiO_2-AlN-Si_3N_4	Sialon bonding agents for cutting tools, refractories

ria with other oxides are the most extensively studied, and can be divided into: (*a*) oxide solid solutions in corundum, (*b*) oxide compound formation, and (*c*) oxide melting and dissolution. Interactions with other classes of materials, such as carbides, nitrides, and borides; metals; salts; and water and corrosive gases—also of great technological importance—are each treated separately.

Stability of Al_2O_3 in the System Al–O

The reaction of aluminum metal with oxygen to form alumina, though hindered kinetically by formation of a dense product layer, is accompanied by a substantial reduction in Gibbs energy. The thermodynamic stability of Al_2O_3 relative to its constituent elements is compared to that of other important oxides in Table II, where it can be seen that, in terms of free energies per atom of metal oxidized, alumina is near the top of the list. This high degree of thermodynamic stabilization is in part responsible for many of the useful properties of alumina.

Several structures have been reported for Al_2O_3 (Table III), yet there appears to be no firm evidence that any of the others are thermodynamically stable relative to α-Al_2O_3. Many of these structures are derived from a cubic close-packed lattice, whereas corundum is hexagonally close-packed. Kinetic data presented by Wilson and McConnell[10] show that the transformation sequence with time among the alumina polymorphs at 750° to 1250°C is:

$$\gamma \rightarrow \delta \rightarrow \theta \rightarrow \alpha \qquad (1)$$

Perhaps the greatest uncertainty concerns the stability of ϵ-Al_2O_3, which has been observed above 1930°C by high-temperature X-ray[7]; the ϵ phase may contain ZrO_2, however. Other phases, such as η-Al_2O_3 and

Table II. Comparison of Al_2O_3 Gibbs Energy of Formation with Other Oxides
(kJ • mol^{-1}/metal atom at 25°C)

ZrO_2	−1039.724
TiO_2	− 889.406
SiO_2	− 856.443
Al_2O_3	− 791.138
CaO	− 603.501
B_2O_3	− 596.40
BeO	− 573.209
MgO	− 568.945
BaO	− 520.382
CO_2	− 394.389
Fe_2O_3	− 371.76
Li_2O	− 281.05
FeO	− 251.429
Na_2O	− 189.55
PbO	− 189.28
K_2O	− 161.05
H_2O	− 118.57

Data taken from Ref. 3.

Table III. Reported Al_2O_3 Polymorphs*

Polymorph	Crystal System	Space Group	Unit Cell (nm)	Primary Reference
α (corundum)	Hexagonal	$R\bar{3}c$	a = 0.4758 c = 1.2991	5
δ	Tetragonal		a = 0.7943 c = 2.350	6
ϵ	Hexagonal		a = 0.7849 c = 1.6183	7
γ	Cubic		a = 0.7924	8
κ′	Hexagonal	$P6_3mc$	a = 0.5544 c = 0.9024	9
Θ	Monoclinic	$C2/m$	a = 0.5620 b = 0.2906 c = 1.1790 β = 10.379	10
χ	Hexagonal		a = 0.557 c = 0.864	11

*Ref. 4.

ι-Al_2O_3 have not been included in Table III because their reported syntheses involve the presence of alkalies, silica, or other impurities,[4] or because their published X-ray powder patterns are not indexed. As indicated in Table IV, α-Al_2O_3 is the thermodynamically stable polymorph relative to δ, γ, and κ at all temperatures up to the melting point. These polymorphs are therefore to be regarded as metastable, achieving true stability relative to corundum only to the extent that they can incorporate other oxides or elements into their structure. For example, the "beta aluminas," which at one time were considered to be true polymorphs of Al_2O_3, are now known to contain

Table IV. Relative Stability of Al_2O_3 Polymorphs ($kJ \cdot mol^{-1}$)

Temp. (K)	α-Al_2O_3	δ-Al_2O_3	γ-Al_2O_3	κ-Al_2O_3
298.15	−1582.275	−1572.974	−1563.850	−1569.663
1000	−1361.437	−1353.447	−1346.370	−1351.782
2000	−1034.096	−1031.160	−1028.802	−1030.989

Data taken from Ref. 3.

essential alkalies, and owe their phase diagram fields of stability to that fact.

Alpha alumina varies little in stoichiometry with regard to aluminum and oxygen. A phase diagram for the system Al-Al_2O_3 is shown in Fig. 2. There are no phases richer in oxygen than Al_2O_3. Alumina melts congruently, and its melting point has been studied by Schneider.[13] After a review of the literature values and comparison with his own experimental results, Schneider suggests a value for the melting temperature of 2054° ± 6°C.

Because it is a densely packed structure, α-alumina is stable under conditions of very high isostatic pressure as well; for this reason it is possible to use the fluorescence of synthetic ruby as a measurement of pressure in diamond-cell phase equilibrium experiments. On the basis of this type of use, α-alumina is stable to at least 200 GPa at room temperature and 100 GPa at 1500°C.[14] There are no known high-pressure modifications. The effect of pressure on the melting point has not been studied.

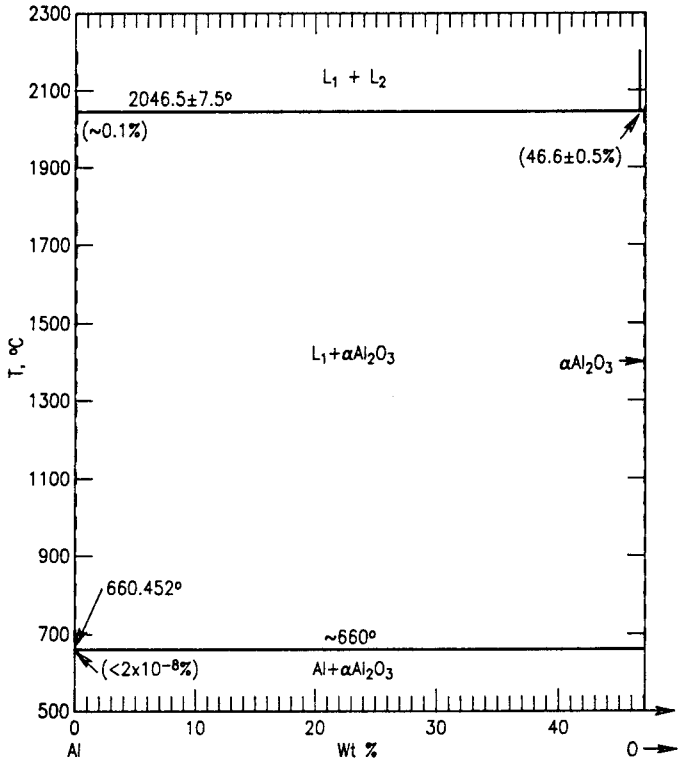

Fig. 2. Phase diagram of the system Al-Al_2O_3 (Ref. 12).

The vapor pressure of Al_2O_3 at high temperatures was measured by Ho and Burns[15] using mass spectrometry. Results are summarized in Table V, where it can be seen that the dominant vapor species are Al, O, and AlO. At 2000°C the total vapor pressure is about 10^{-1} Pa.

Corundum-Based Solid Solutions

The corundum structure is based on a hexagonally close-packed arrangement of oxygens (Fig. 3), in which two-thirds of the octahedral sites are filled with aluminum. In the known systems with corundum where extensive solid solution occurs, the mechanism is apparently substitutional. If we apply the "15% rule,"[17] for replacement of octahedral Al to occur, the radius of the substituting ion should be approximately within the range 0.045 to 0.061 nm (0.45 to 0.61 Å). Table VI lists ionic radii for various octahedrally coordinated ions as a function of valence. On the basis of liberal application of the "15% rule," several substitutions would appear to be reasonable.

Note that, if charge-compensated coupled substitution is permitted, the following types of solid solution might be postulated: (1) $X^{3+} \rightarrow Al^{3+}$, (2) $X^{2+}Y^{4+} \rightarrow Al^{3+}Al^{3}$, and (3) $X^{1+}Y^{5+} \rightarrow Al^{3+}Al^{3+}$. Of the three, the first would be the most favored, since there is no gross disturbance of local charge distribution in the lattice. By similar reasoning, occurrence of type (3) substitution in corundum would be the least likely. However, ilmenite ($FeTiO_3$) and lithium niobate ($LiNbO_3$) have structures similar to corundum in which the altervalent ions are highly ordered, so it is not unreasonable to postulate some degree of substitution according to mechanisms (2) and (3).

From Table VI, a list of substitutional possibilities could be drawn up strictly on the basis of size considerations, yet it should be noted that certain of these would not be practical. For example, substitution of Co^{3+}, Ni^{3+}, and Mn^{3+} to form type (1) solid solutions is not likely due to the instability of these cations at high temperature, compared to their more reduced forms. Similarly, type (2) solid solutions involving octahedral Ge^{4+} (e.g., $Mg^{2+}Ge^{4+}$) are not likely at atmospheric pressure as Ge prefers four-fold (tetrahedral) coordination.

In natural corundum, substitutions of up to a few molecular percent are reported primarily for Cr^{3+} (ruby) and Fe^{3+}.[18] Therefore it is not surprising that the phase diagrams for Cr_2O_3-Al_2O_3 and Fe_2O_3-Al_2O_3 have among the most extensive solid solutions. Referring to Fig. 4(*a*), the system Cr_2O_3-Al_2O_3 shows a continuous solid solution at the solidus. At lower temperatures, a miscibility gap exists at 0.1 GPa (1 Kbar) between Cr_2O_3 (eskolaite) and corundum solid solutions (Fig. 4(*b*)). In the system Fe_2O_3-Al_2O_3, the solubility in corundum is not continuous, presumably due to the impossibility of maintaining the iron in the plus three state at the high temperatures required for miscibility. As Fig. 5 indicates, "Fe_2O_3" solubility is a

Table V. Partial Pressures of Vapor Species over Al_2O_3

T (K)	O (10^{-2} Pa)	Al (10^{-2} Pa)	AlO (10^{-2} Pa)	Al_2O (10^{-3} Pa)	Al_2O_2 (10^{-5} Pa)	AlO_2 (10^{-6} Pa)	Al_2O_3 (10^{-7} Pa)
2318	7.82	6.71	1.50	2.47	2.65	2.24	< 1
2290	5.02	4.52	0.99	1.51	1.53	1.39	
2263	3.63	3.08	0.68	0.88	1.18	1.13	
2213	1.72	1.48	0.33	0.33	0.60	0.43	

Data taken from Ref. 15.

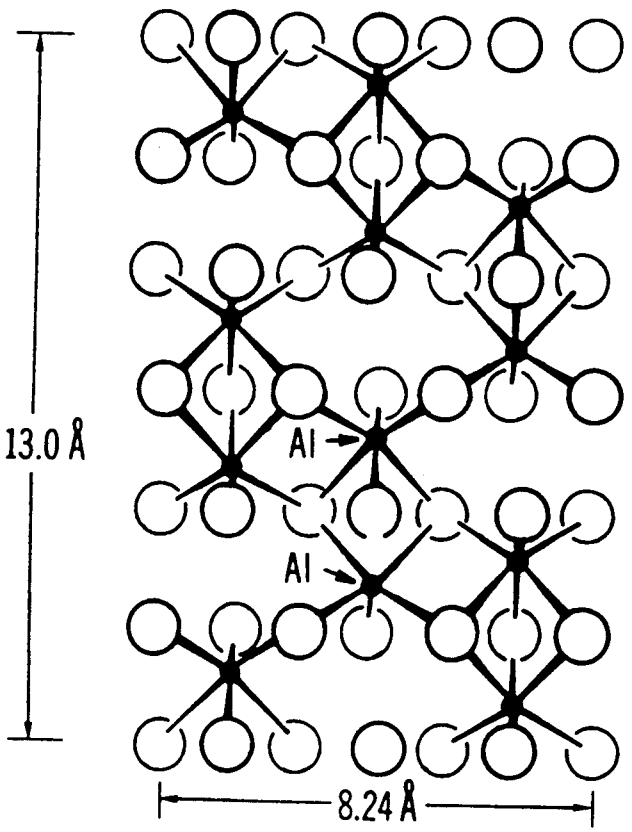

Fig. 3. Structure of corundum, projected on $(2\bar{1}\bar{1}0)$, after Ref. 16.

function of the oxygen partial pressure, as well as temperature. The phase diagram for Ga_2O_3-Al_2O_3 is the third of the type (1) possibilities which shows extensive solid solution (up to 25 mol%) in the corundum structure (Fig. 6). Beta Ga_2O_3 is isostructural with θ-Al_2O_3, and consequently a continuous solid solution with corundum is not possible. At temperatures below 800°C, corundum solid solutions are apparently replaced by $GaAlO_3$ solid solutions. The phase α-Ga_2O_3, though not having a stability field on the diagram, does have the corundum structure, and earlier work[23] noted that a complete solid solution series based on the corundum structure can be formed metastably. Phase diagrams for alumina with V_2O_3, Rh_2O_3, and Ti_2O_3, all of which have the corundum structure, are not available. No solution of Sc_2O_3 in corundum is indicated in the phase diagram for that system (Fig. 7), although an intermediate solid solution is reported, whose structure has apparently not been determined. Up to about 10 mol% Y_2O_3 is reported in solution in Al_2O_3, according to Fig. 8.

The most likely type (2) substitutions would involve Ti^{4+}, since this is the preferred oxidation state of titanium at high temperatures and since its radius 0.058 nm (0.58 Å) is close to that of Al^{3+}. Thus, likely possibilities would be $Fe^{2+}Ti^{4+}$ or $Mg^{2+}Ti^{4+} \rightarrow Al^{3+}Al^{3+}$. The published phase diagram for the system MgO-TiO_2-Al_2O_3[26] shows no solid solution in Al_2O_3, however, in spite of extensive solid solutions based on this mechanism in the neighboring compounds Al_2TiO_5 and $MgAl_2O_4$.

Candidates for type (3) solid solution must rely on Li^{1+} (0.074 nm (0.74 Å)), as all of the other monovalent ions are much larger. Possibilities include $Li^{1+}V^{5+}$, $Li^{1+}Nb^{5+}$, and $Li^{1+}Ta^{5+}$. As noted above, $LiNbO_3$ has an ordered variation of the corundum structure, and so at least a small amount of solid solution might be expected; however no data are available.

Several solid solutions of minor extent are reported for systems in which a substitutional mechanism is not clear. A published phase diagram for the system ZrO_2-Al_2O_3 shows a small amount (≈1%) of solid solution in corundum (Fig. 9). This appears to require vacancies on the aluminum sites, unless high-temperature reduction of the zirconia has occurred. Another unusual substitution which has been reported occurs during the high-temperature reaction of Al_2O_3 with MgO under reducing conditions. Colin et al.[28] reported a field of Mg-spinel solid solution extending nearly all the way to Al_2O_3 at high temperature, with a somewhat more limited field based on a tetragonal spinel-like phase at lower temperatures. Burdese et al.[29] found experimental evidence for solution of up to nearly 10 mol% niobium (treated as Nb_2O_5) in corundum at 1640°C; it appears likely that the niobium is actually entering as Nb_2O_3.

Oxide Compound Formation

In the solid state phase equilibria of alumina, formation of compounds with other oxides is widespread, much more so than the formation of solid solutions discussed above. To a first approximation, the tendency of other oxides to form compounds with alumina should be related to the extent to which the

Table VI. Ionic Radii (nm) for Cations in Octahedral Coordination*

	Monovalent	Divalent	Trivalent	4-Valent	5-Valent	6-Valent	7-Valent
0.010			N(0.016)	C(0.017)	N(0.014)		
0.020			B(0.023)				Cl(0.027)
0.030		Be(0.035)		S(0.037)	P(0.035)	S(0.030)	Br(0.039)
0.040			P(0.044)	Si(0.040)		Se(0.042)	Mn
0.050			Al(0.053)	Se(0.050)	As(0.050)	Cr(0.052)	I(0.050)
				Mn(0.054)	Re(0.052)		
			Co(0.055)	Ge(0.054)	Cr(0.052)	Te(0.056)	
			Ni(0.058)	Cr(0.055)	V(0.054)	Re(0.057)	Re(0.057)
				V(0.059)		W(0.058)	
0.060				Ti(0.061)	Sb(0.061)	Mo(0.060)	
			Fe(0.060)	Rh(0.062)	Mo(0.063)		
			Cr(0.062)	Pd(0.062)	Nb(0.064)		
			Ga(0.062)	Ru(0.062)	Ta(0.064)		
			Mn(0.062)	Ir(0.063)			
			V(0.064)	Re(0.063)			
			Mo(0.067)	Os(0.063)			
			Rh(0.067)	Pt(0.063)			
			Ta(0.067)	Mo(0.065)			
			Ti(0.067)	W(0.065)			
			Ru(0.068)	Ta(0.066)			
		Fe(0.069)		Nb(0.069)			
				Sn(0.069)			
0.070	Li(0.074)	Co(0.070)					
		Ni(0.070)	Nb(0.070)	Hf(0.071)			
		Nb(0.071)	Sc(0.073)	Zr(0.072)	Bi(0.074)		
		Mg(0.072)	Pd(0.076)	Tb(0.076)	U(0.076)	U(0.075)	
		Mn(0.073)	Sb(0.076)	Pb(0.076)			
		Cu(0.073)	In(0.079)	Pr(0.078)			
		Zn(0.075)					
		V(0.079)					
0.080		Pt(0.080)	Lu(0.085)	Te(0.080)			
		Ti(0.086)	Yb(0.086)	Ce(0.080)			
		Pd(0.086)	Tm(0.087)				
			Tl(0.088)				
		Ag(0.089)	Y(0.089)		Pa(0.089)		
			Ho(0.089)				
0.090			Dy(0.091)				
			Tb(0.092)				
			Gd(0.094)				
		Sn(0.093)	Eu(0.095)				
	Cu(0.096)	Cd(0.095)	Sm(0.096)	Pa(0.098)	I(0.095)		
0.100	Na(0.102)	Ca(0.100)	Nd(0.100)	Th(0.100)			
		Hg(0.102)	Pr(0.101)	U(0.101)			
			Bi(0.102)				
			Ce(0.103)				
			U(0.106)				
			La(0.106)				
0.110	Ag(0.115)	Sr(0.116)	Pa(0.113)				
		Eu(0.117)					
		Pb(0.118)					

Table VI. Continued

	Monovalent	Divalent	Trivalent	4-Valent	5-Valent	6-Valent	7-Valent
0.120							
0.130							
	Au(0.137) K(0.138)	Ba(0.136)					
0.140							
	Rb(0.149)						
0.150							
	Tl(0.150)						
0.160							
	Cs(0.170)						
0.170							

*After Ref. 16.

ionic radius and valence of the oxide cations differ from 0.053 nm (0.53 Å) and +3, respectively.[30] Available data on aluminate compounds are summarized in Table VII. In the case of the aluminates, large differences in ionic size apparently have a greater effect in promoting compound formation than do differences in charge. Referring to Table VII, the large alkaline earth cations form the largest numbers of compounds with alumina: BaO, SrO, and CaO each have at least seven aluminates. Similarly, the trivalent lanthanides, also larger ions, each form at least three compounds with Al_2O_3. The ions Mo^{6+}, W^{6+}, and Re^{7+} have radii closer to that of Al^{3+}; yet the oxides MoO_3, WO_3, and Re_2O_7, in spite of the high valences compared to alumina, have only one reported aluminate each.

Structurally, the aluminates are diverse. At least five major structure types are represented (Table VIII): perovskites, spinels, beta aluminas, stuffed silica derivatives, and garnets. The perovskite aluminates may be regarded structurally as comprised of a cubic

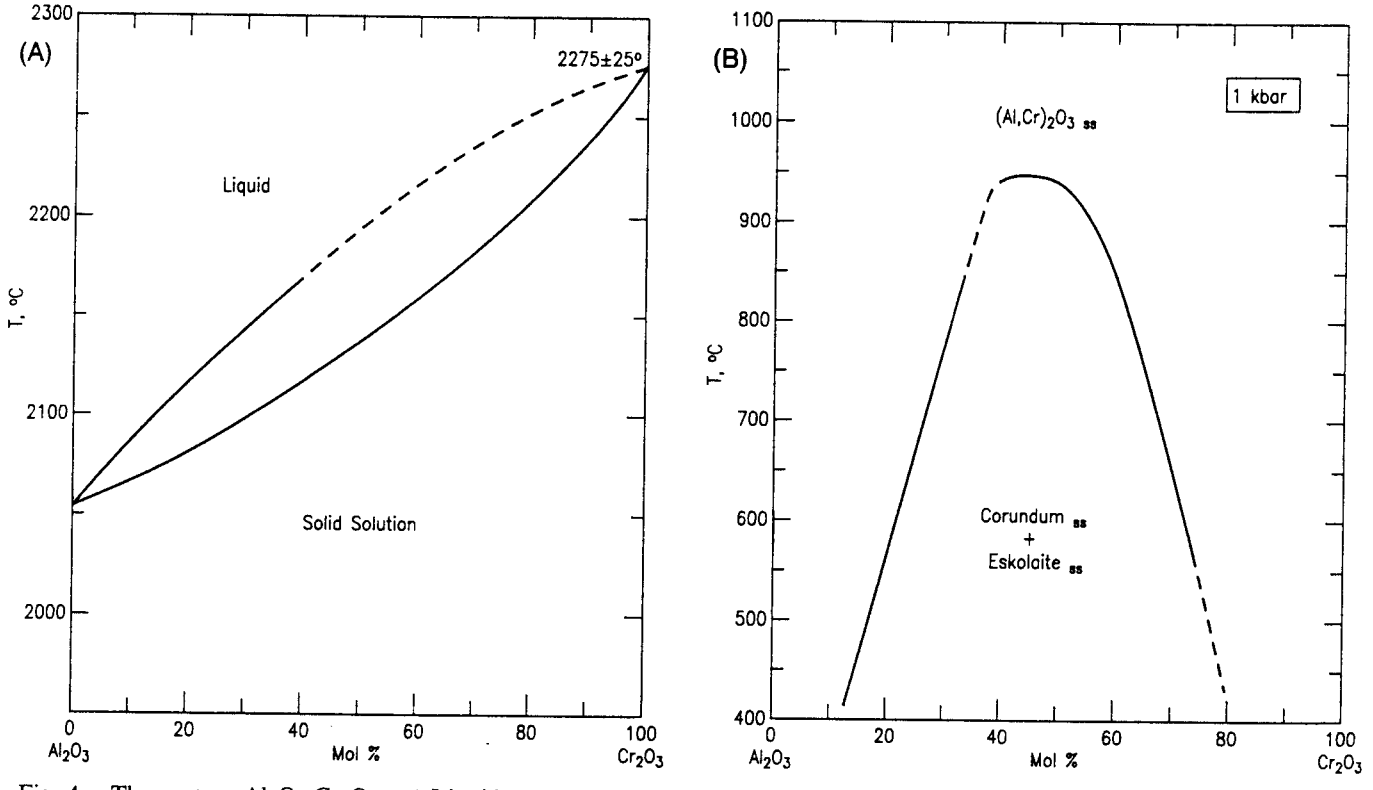

Fig. 4. The system Al_2O_3-Cr_2O_3. (*a*) Liquidus and solidus showing continuous solid solution (Ref. 19); (*b*) subsolidus miscibility gap at 0.1 GPa (1 kbar) (Ref. 20).

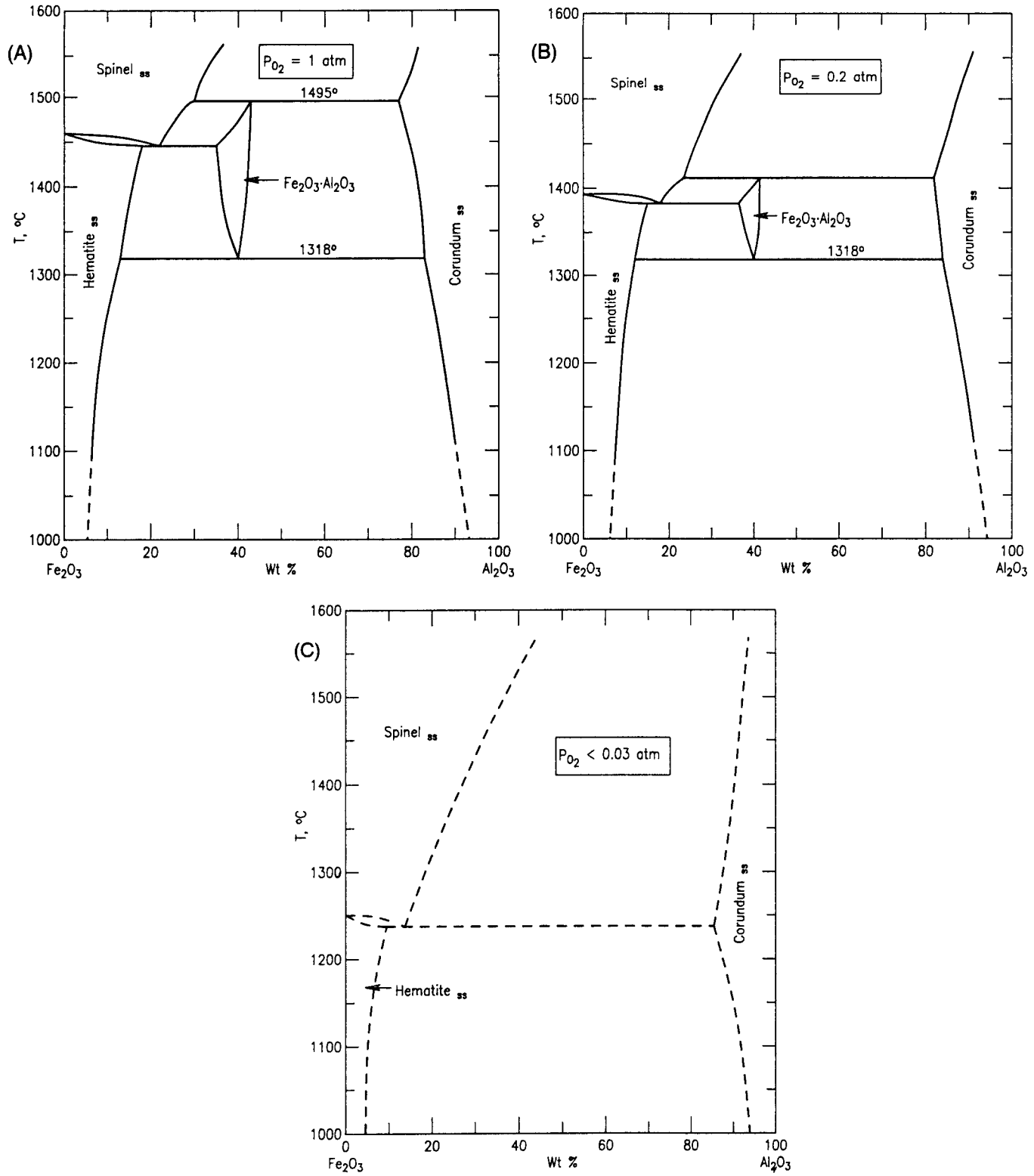

Fig. 5. The system "Fe_2O_3"-Al_2O_3 at three oxygen pressures (Ref. 21).

close-packed array of oxygens with one-fourth of the oxygens replaced by large trivalent cations such as La^{3+}. The smaller aluminum ions then occupy octahedrally coordinated sites not adjacent to the other cations (Fig. 10).

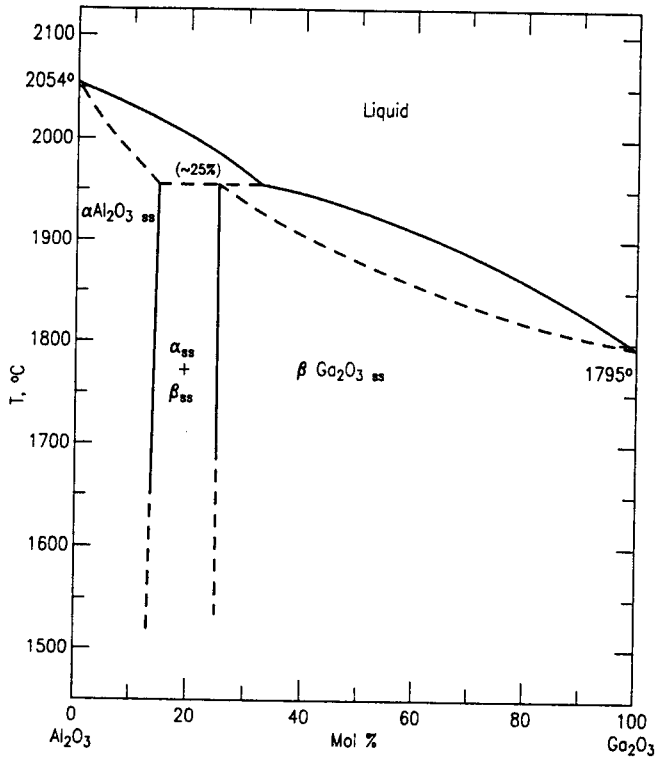

Fig. 6. The system Al_2O_3 Ga_2O_3 (Ref. 22).

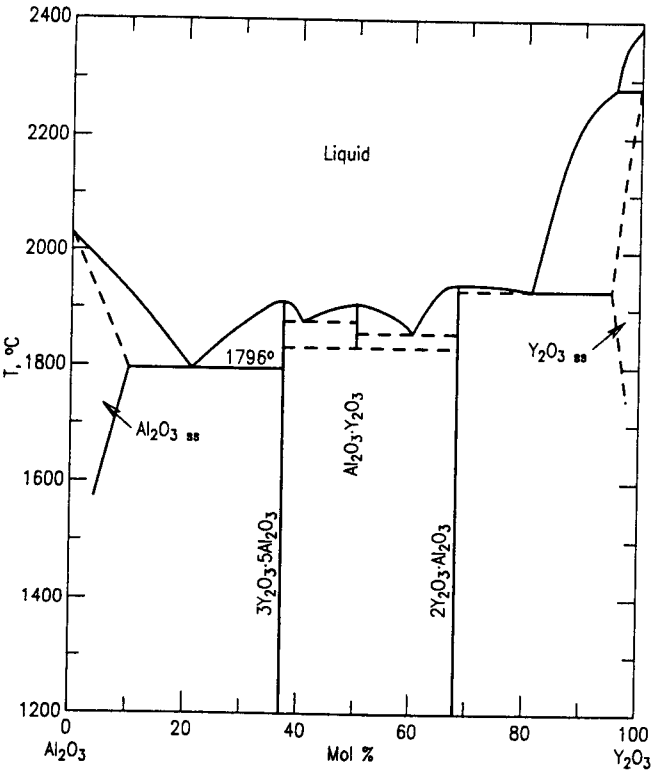

Fig. 8. The system Al_2O_3-Y_2O_3 (Ref. 25).

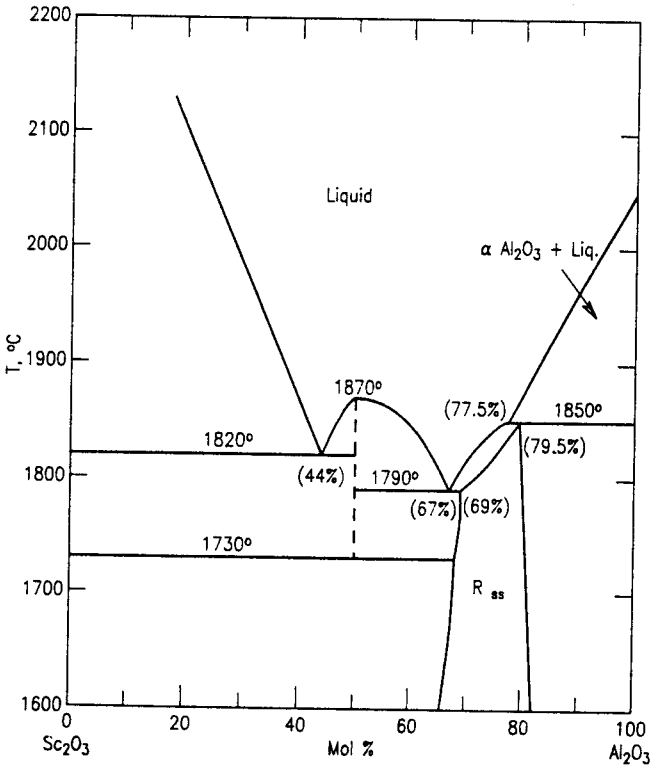

Fig. 7. The system Sc_2O_3-Al_2O_3 (Ref. 24).

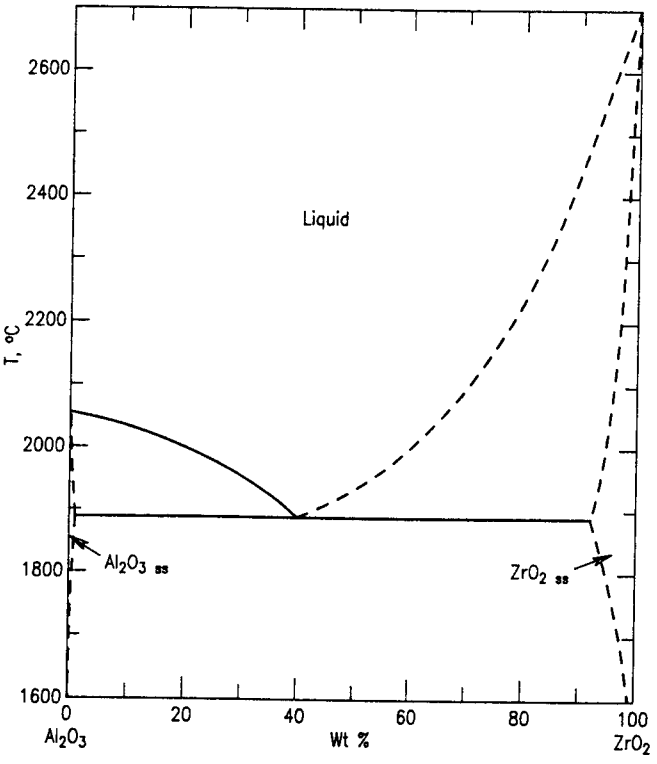

Fig. 9. The system Al_2O_3-ZrO_2 (Ref. 27).

Table VII. Stoichiometry of Reported Aluminate Compounds*

Atomic Number	Element	Oxide	Compounds with Published X-Ray Powder Patterns
1	H	H_2O	$H_2O \cdot Al_2O_3$, $H_2O \cdot 4Al_2O_3$, $H_2O \cdot 5Al_2O_3$, $3H_2O \cdot Al_2O_3$
3	Li	Li_2O	$Li_2O \cdot Al_2O_3$, $5Li_2O \cdot Al_2O_3$, $Li_2O \cdot 5Al_2O_3$
4	Be	BeO	$BeO \cdot Al_2O_3$
5	B	B_2O_3	$2B_2O_3 \cdot 9Al_2O_3$, $B_2O_3 \cdot 2Al_2O_3$, $B_2O_3 \cdot Al_2O_3$, $2B_2O_3 \cdot 3Al_2O_3$, $B_2O_3 \cdot 4Al_2O_3$, $4B_2O_3 \cdot 3Al_2O_3$, $B_2O_3 \cdot 5Al_2O_3$
11	Na	Na_2O	$Na_2O \cdot 5Al_2O_3$, $Na_2O \cdot 7Al_2O_3$, $Na_2O \cdot 11\ Al_2O_3$, $Na_2O \cdot Al_2O_3$, $5Na_2O \cdot Al_2O_3$
12	Mg	MgO	$MgO \cdot Al_2O_3$, $MgO \cdot 13Al_2O_3$
14	Si	SiO_2	$Al_2O_3 \cdot SiO_2$, $3Al_2O_3 \cdot 2SiO_2$
15	P	P_2O_5	$Al_2O_3 \cdot P_2O_5$, $Al_2O_3 \cdot 3P_2O_5$
16	S	SO_3	$Al_2O_3 \cdot 3SO_3$
19	K	K_2O	$K_2O \cdot 5Al_2O_3$, $K_2O \cdot 11Al_2O_3$, $3K_2O \cdot Al_2O_3$, $K_2O \cdot Al_2O_3$
20	Ca	CaO	$CaO \cdot 2Al_2O_3$, $3CaO \cdot 5Al_2O_3$, $5CaO \cdot 3Al_2O_3$, $3CaO \cdot Al_2O_3$, $12CaO \cdot 7Al_2O_3$, $CaO \cdot 6Al_2O_3$, $2CaO \cdot Al_2O_3$, $CaO \cdot Al_2O_3$
21	Sc	Sc_2O_3	$(Al,Sc)_2O_3$, $Sc_2O_3 \cdot Al_2O_3$
22	Ti	TiO_2	$Al_2O_3 \cdot TiO_2$
23	V	V_2O_5	$Al_2O_3 \cdot V_2O_5$
		V_2O_3	$Al_2O_3 \cdot V_2O_3$
25	Mn	MnO	$MnO \cdot Al_2O_3$
26	Fe	FeO	$FeO \cdot Al_2O_3$
		Fe_2O_3	$Fe_2O_3 \cdot Al_2O_3$
27	Co	CoO	$CoO \cdot Al_2O_3$
28	Ni	NiO	$NiO \cdot 16Al_2O_3$, $2NiO \cdot 9Al_2O_3$, $NiO \cdot Al_2O_3$, $NiO \cdot 13Al_2O_3$
29	Cu	Cu_2O	$Cu_2O \cdot Al_2O_3$ $CuO \cdot Al_2O_3$
		CuO	
30	Zn	ZnO	$4ZnO \cdot 11Al_2O_3$, $ZnO \cdot 99Al_2O_3$, $3ZnO \cdot 47Al_2O_3$, $ZnO \cdot Al_2O_3$
31	Ga	Ga_2O_3	$Ga_2O_3 \cdot Al_2O_3$
32	Ge	GeO_2	$GeO_2 \cdot Al_2O_3$, $2GeO_2 \cdot 3Al_2O_3$, $2GeO_2 \cdot Al_2O_3$
33	As	As_2O_5	$As_2O_5 \cdot Al_2O_3$
34	Se	SeO_3	$3SeO_3 \cdot Al_2O_3$
37	Rb	Rb_2O	$Rb_2O \cdot 11Al_2O_3$
38	Sr	SrO	$SrO \cdot 2Al_2O_3$, $SrO \cdot Al_2O_3$, $5SrO \cdot Al_2O_3$, $4SrO \cdot Al_2O_3$, $3SrO \cdot Al_2O_3$, $3SrO \cdot 16Al_2O_3$, $SrO \cdot 6Al_2O_3$
39	Y	Y_2O_3	$Y_2O_3 \cdot Al_2O_3$, $2Y_2O_3 \cdot Al_2O_3$
41	Nb	Nb_2O_5	$49Nb_2O_5 \cdot Al_2O_3$, $9Nb_2O_5 \cdot Al_2O_3$, $25Nb_2O_5 \cdot Al_2O_3$
42	Mo	MoO_3	$3MoO_3 \cdot Al_2O_3$
47	Ag	Ag_2O	$Ag_2O \cdot Al_2O_3$
48	Cd	CdO	$CdO \cdot Al_2O_3$, $CdO \cdot 2Al_2O_3$, $CdO \cdot 6Al_2O_3$
51	Sb	Sb_2O_5	$Sb_2O_5 \cdot Al_2O_3$
55	Cs	Cs_2O	$Cs_2O \cdot Al_2O_3$, $Cs_2O \cdot 11Al_2O_3$
56	Ba	BaO	$10BaO \cdot Al_2O_3$, $8BaO \cdot Al_2O_3$, $7BaO \cdot Al_2O_3$, $5BaO \cdot Al_2O_3$, $4BaO \cdot Al_2O_3$, $3BaO \cdot Al_2O_3$, $BaO \cdot Al_2O_3$, $BaO \cdot 6Al_2O_3$
57	La	La_2O_3	$La_2O_3 \cdot 11Al_2O_3$, $La_2O_3 \cdot Al_2O_3$
58	Ce	Ce_2O_3	$Ce_2O_3 \cdot Al_2O_3$
59	Pr	Pr_2O_3	$Pr_2O_3 \cdot Al_2O_3$
60	Nd	Nd_2O_3	$2Nd_2O_3 \cdot Al_2O_3$, $Nd_2O_3 \cdot Al_2O_3$
62	Sm	Sm_2O_3	$Sm_2O_3 \cdot Al_2O_3$, $2Sm_2O_3 \cdot Al_2O_3$
63	Eu	Eu_2O_3	$Eu_2O_3 \cdot 12Al_2O_3$, $2Eu_2O_3 \cdot Al_2O_3$, $Eu_2O_3 \cdot Al_2O_3$
64	Gd	Gd_2O_3	$2Gd_2O_3 \cdot Al_2O_3$, $Gd_2O_3 \cdot Al_2O_3$, $3Gd_2O_3 \cdot 5Al_2O_3$
65	Tb	Tb_2O_3	$Tb_2O_3 \cdot Al_2O_3$, $3Tb_2O_3 \cdot 5Al_2O_3$
66	Dy	Dy_2O_3	$2Dy_2O_3 \cdot Al_2O_3$, $3Dy_2O_3 \cdot 5Al_2O_3$, $Dy_2O_3 \cdot Al_2O_3$
67	Ho	Ho_2O_3	$2Ho_2O_3 \cdot Al_2O_3$, $3Ho_2O_3 \cdot 5Al_2O_3$, $Ho_2O_3 \cdot Al_2O_3$
68	Er	Er_2O_3	$2Er_2O_3 \cdot Al_2O_3$, $3Er_2O_3 \cdot 5Al_2O_3$, $Er_2O_3 \cdot Al_2O_3$
69	Tm	Tm_2O_3	$Tm_2O_3 \cdot Al_2O_3$, $3Tm_2O_3 \cdot 5Al_2O_3$
70	Yb	Yb_2O_3	$2Yb_2O_3 \cdot Al_2O_3$, $3Yb_2O_3 \cdot 5Al_2O_3$, $Yb_2O_3 \cdot Al_2O_3$
71	Lu	Lu_2O_3	$Lu_2O_3 \cdot Al_2O_3$, $3Lu_2O_3 \cdot 5Al_2O_3$
73	Ta	Ta_2O_5	$Ta_2O_5 \cdot Al_2O_3$
74	W	W_2O_3	$Al_2O_3 \cdot W_2O_3$
		W_2O_5	$Al_2O_3 \cdot W_2O_5$
		WO_3	$Al_2O_3 \cdot 3WO_3$
75	Re	Re_2O_7	$3Re_2O_7 \cdot Al_2O_3$
80	Hg	HgO	$HgO \cdot Al_2O_3$
81	Tl	Tl_2O	$Tl_2O \cdot Al_2O_3$
82	Pb	PbO	$2PbO \cdot Al_2O_3$, $PbO \cdot Al_2O_3$, $PbO \cdot 6Al_2O_3$
83	Bi	Bi_2O_3	$12Bi_2O_3 \cdot Al_2O_3$, $Bi_2O_3 \cdot Al_2O_3$, $Bi_2O_3 \cdot 2Al_2O_3$

*After Ref. 4.

Similarly, the aluminate spinels can also be treated as a cubic close-packed array of oxygens, but with some occupancy of both octahedrally and tetrahedrally coordinated sites. Generally, the Al^{3+} ions occupy one-half of the octahedral sites, and the divalent cations such as Mg^{2+} occupy one-quarter of the tetrahedral sites. An idealized structure is shown in Fig. 11. An exception to the general pattern in aluminate spinels is $LiAl_5O_8$, in which aluminums occupy both tetrahedral and octahedral sites, with lithiums in part of the remaining available octahedral sites.

Table VIII. Some Common Aluminate Structures

Structure Type	General Formula	Compounds
Perovskite	$M^{3+}AlO_3$	$CeAlO_3$, $LaAlO_3$ $SmAlO_3$, $YAlO_3$, $EuAlO_3$, $GdAlO_3$
Spinel	$M^{2+}Al_2O_4$	$NiAl_2O_4$, $MgAl_2O_4$ $MnAl_2O_4$, $FeAl_2O_4$, $ZnAl_2O_4$, $CdAl_2O_4$, $CoAl_2O_4$, $CuAl_2O_4$ $LiAl_5O_8$
Beta alumina	$M^{1+}Al_{11}O_{17}$ or $M^{2+}Al_{12}O_{19}$	$CsAl_{11}O_{17}$, $KAl_{11}O_{17}$ $NaAl_{11}O_{17}$, $RbAl_{11}O_{17}$, $BaAl_{12}O_{19}$, $CaAl_{12}O_{19}$, $SrAl_{12}O_{19}$
Stuffed silica	$M^{1+}AlO_2$ or $M^{2+}Al_2O_4$	$CaAl_2O_4$
Garnet	$M_3^{VIII}M_2^{VI}M_3^{IV}O_{12}$	$Y_3Al_5O_{12}$, $Y_4Al_4O_{12}$

Data taken primarily from Ref. 31.

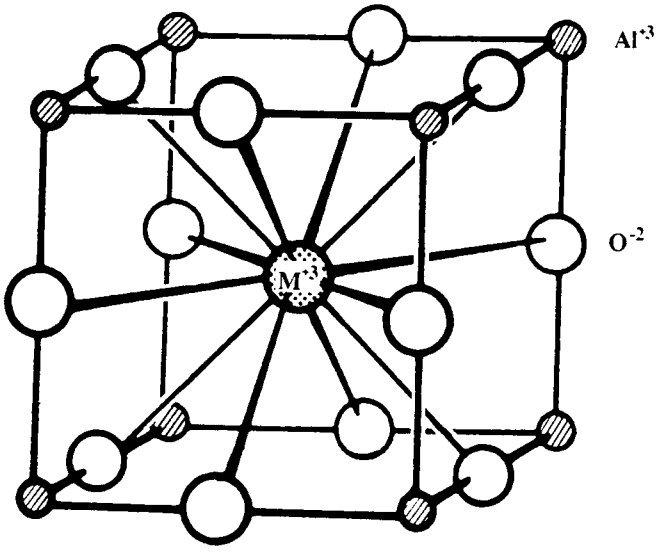

Fig. 10. Idealized aluminate perovskite structure (Ref. 32).

The beta aluminas are structurally related to the spinels in that they are comprised of cubic close-packed layers of oxygen with aluminum in selected octahedral sites. The difference arises in that, while the spinel structure is maintained in blocks four oxygen layers thick, these blocks are joined by layers of close-packed oxygens on either side in which only one-fourth of the oxygens are actually present and which contain the larger alkali ions (see Fig. 12). In Table VIII, members of the $M^{2+}Al_{12}O_{19}$ group (magnetoplumbite structure) have been included with beta alumina since they are closely related. Stacking polytypes based on these structures can also occur, leading to slightly different aluminate stoichiometries.

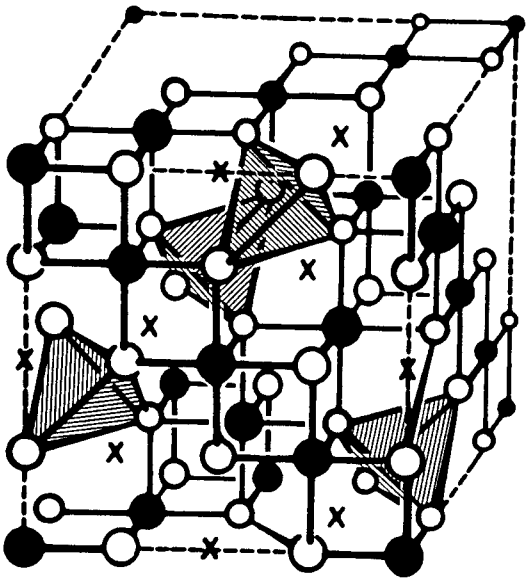

Fig. 11. Aluminate spinel structure (Ref. 33). Shading indicates MO_4 tetrahedra. Open circles indicate oxygen, solid circles are aluminum, and x's are octahedral vacancies.

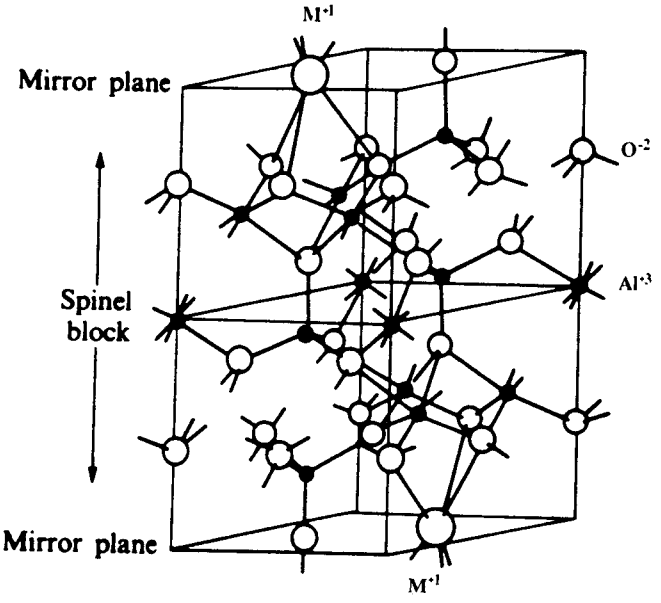

Fig. 12. Beta alumina structure (Ref. 32).

It is noteworthy that, while $MgAl_2O_4$ crystallizes with the classic spinel structure, $CaAl_2O_4$ has the tridymite structure, and may be regarded as an ion-"stuffed" silica derivative. Conclusive data are not available for other 1:1 alkaline earth and alkali aluminates, but it is likely that many of them fall into the latter group also. To form this structure, the aluminum ions are tetrahedrally coordinated by oxygens, and the resulting tetrahedra are linked to form layers of six-membered rings (Fig. 13) which are then stacked to form a continuous three-dimensional framework in

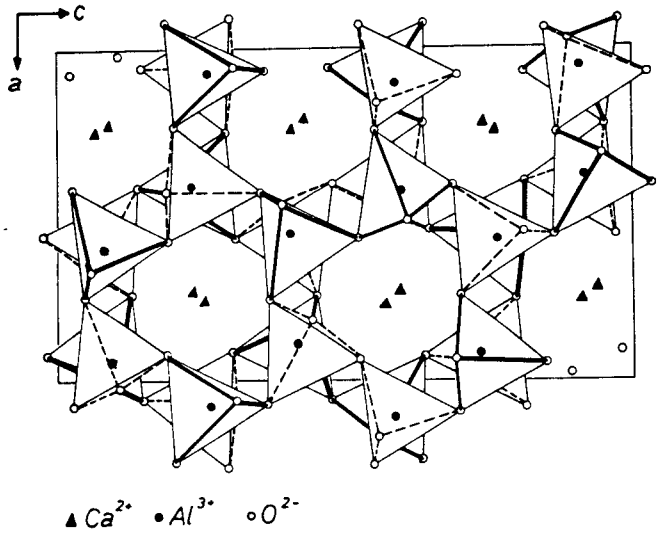

Fig. 13. Aluminate stuffed silica derivative (tridymite) structure, as illustrated by $CaAl_2O_4$ (Ref. 34).

which all the oxygens are shared. The large cations occupy cages formed by the rings.

The aluminate garnets contain both tetrahedrally and octahedrally coordinated aluminum; they can be represented by the general formula $M_3^{VIII}M_2^{VI}M_3^{IV}O_{12}$, where the Roman numerals refer to coordination numbers of the cation sites. The garnet structure can be thought of as built of independent $M^{IV}O_4$ tetrahedra linked to $M^{VI}O_6$ octahedra, with the large M^{VIII} ions in the interstices (Fig. 14). The best-known

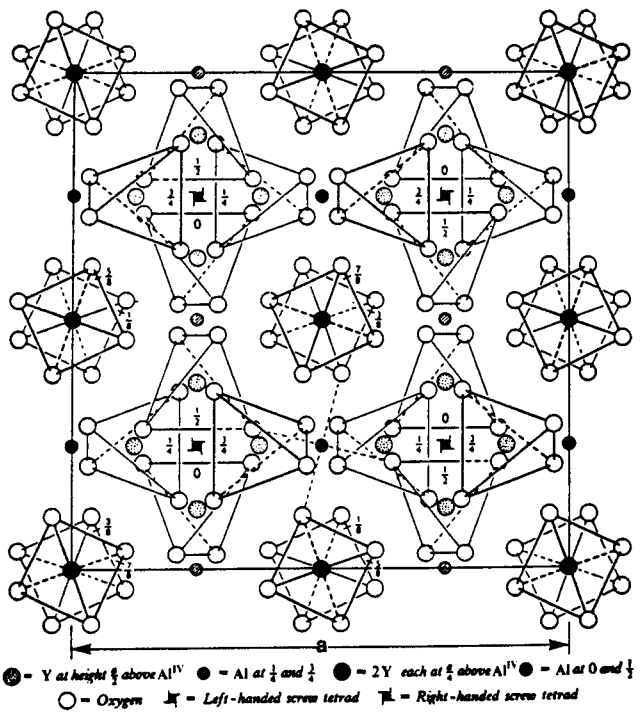

Fig. 14. Garnet structure, projected on (001) (Ref. 18).

aluminate garnets include those based on yttrium, such as $Y_3Al_2^{VI}Al_3^{IV}O_{12}$ or $Y_3Al_5O_{12}$, of great interest for its optical properties. Many substitutions based on this structure are possible. If yttrium occupies one-half the M^{VI} sites, then $Y_3(YAl)^{IV}Al_3^{IV}O_{12}$ or $Y_4Al_4O_{12}$ results. Referring to Table VI, substitution of numerous other elements for octahedral aluminum in M^{VI} sites seems reasonable, with possible charge compensation involving M^{VIII}. The possibilities of substitution for tetrahedral aluminum in M^{IV} are somewhat more limited, as indicated in Table IX. Naturally occurring garnets contain primarily Si^{4+} in M^{IV}; however, various other substitutional schemes could be proposed involving the ions in Table IX. Most of them would require appropriate charge-coupled substitution on either M^{VIII} or M^{VI} sites, or both, with the additional requirement for reasonable high-temperature stability.

Oxide Depression of Melting Point

The extent to which corundum dissolves in oxide melts (i.e., the corundum liquidus) varies appreciably, depending on the oxide involved. Due to the high temperatures, experimental study of the corundum liquidus is difficult, often leading to uncertainty in this area of the phase diagram. Available liquidus data are summarized in Figs. 15 to 20, where the dissolving oxides are chemically grouped, for comparison, according to the periodic table.

Alumina is amphoteric in aqueous solution, and there is evidence that a similar behavior prevails in oxide melts as well. Under some conditions Al_2O_3 may be expected to behave as a network former, functioning in a manner similar to silica, in which polymerized melts are formed. Alumina enters liquid and solid silicate framework structures primarily with alkali (or alkaline earth) charge compensation, for example, as

$$[M^{1+}Al^{3+}O_4]^{4-} \text{ for tetrahedral } [Si^{4+}O_4]^{4-}$$

In other oxide melts, the aluminum may be present in octahedral coordination, or alternatively may be regarded as having the role of the network modifier ion, Al^{3+}. The actual structure of oxide melts is an area of active research, especially with regard to aluminum.

The ideal solution approximation, while it provides only an estimate of the liquidus under assumed conditions, can be used for comparison with experimentally determined corundum liquidi; an ideal solution curve is included in Figs. 15 to 20. This curve is readily calculated from thermodynamic data as follows[3]:

$$\ln X_{Al_2O_3} = (-\Delta H^{fusion}_{Al_2O_3}/R)\,[(T_m - T)/T_mT] \qquad (2)$$

where $X_{Al_2O_3}$ is the mole fraction of alumina in the melt, $\Delta H^{fusion}_{Al_2O_3}$ the enthalpy of fusion of alumina, R the molar gas constant, T_m the melting point of alumina, and T the liquidus temperature. The enthalpy of fusion is taken as 111.1 kJ/mol[2] and the melting point as 2054°C[13]; it is assumed in this calculation that there is no solid solution in corundum. The degree to which

Table IX. Ionic Radii (nm) for Cations in Tetrahedral Coordination*

	Monovalent	Divalent	Trivalent	4-Valent	5-Valent	6-Valent	7-Valent
0.010							
0.020			B(0.012)	C(0.015)	P(0.017)	S(0.012)	
		Be(0.027)		Si(0.026)		Mn(0.027)	Cl(0.020)
0.030						Se(0.029)	Mn(0.026)
			Al(0.039)		Nb(0.32)	Cr(0.030)	
					As(0.034)		
					Cr(0.035)		
0.040					V(0.036)		
		Mg(0.049)	Ga(0.047)	Ge(0.040)		W(0.040)	Re(0.040)
0.050			Fe(0.049)	Cr(0.044)		Mo(0.042)	
	Li(0.059)						
0.060				Ti(0.054)†			
		Zn(0.060)	Ag(0.065)				
		Cu(0.062)					
		Fe(0.063)					
		Pd(0.064)					
0.070							
			Au(0.070)				
			Sb(0.077)				
0.080							
		Cd(0.084)					
0.090							
	Na(0.099)	Pb(0.094)					
		Hg(0.096)					
0.100							
	Ag(0.102)						
0.110							

*After Ref. 16
†Estimated

a liquidus differs from the ideal curve may be determined by several factors, but it is possible in the simplest treatment to differentiate between those likely to cause a flattening of the liquidus (i.e., less solution of corundum in the melt), and those which cause a steepening (more extensive solution).

The general effect of variations in corundum/melt interaction can be seen from examination of Table X, which gives ideal solution calculations for several component choices for a fixed bulk composition with 95 mol% Al_2O_3 and 5 mol% of a hypothetical Group I oxide, M_2O. If the ideal solution curve which treats the components as actual species is taken as a reference (2033°), then it can be seen from Table X that the following situations result in a raising of the liquidus temperature: (1) association of the additive oxide and (2) formation of additive-rich binary complexes. These interactions increase the effective concentration of Al_2O_3 in the melt, thereby requiring less alumina to achieve saturation at a given temperature. The other interactions in Table X decrease the effective concentration of corundum in the melt, thus leading to steeper liquidi and increased corundum solubility. These liquidus-lowering interactions are: (1) dissociation of the additive oxide and (2) formation of equimolar or alumina-rich binary complexes.

Referring to Figs. 15–20, it can be seen that most of the experimental liquidus curves lie at lower temperatures than the calculated ideal solution liquidus. On the basis of the preceding discussion, this may indicate formation of intermediate binary species in the melt. However, within the range 0 to 5 mol% of additive oxide, the ideal solution curve apparently provides a reasonable approximation to the liquidus for oxides of Group I (Fig. 15), Group IV with the exception of GeO_2 (Fig. 18), and Group V (Fig. 19). The alkaline earths (Fig. 16), rare earths (Fig. 17), and transition metals (Fig. 20) show the greatest deviation from ideality. The oxide liquidus which falls closest to the ideal curve over the range 0 to 50 mol% is Bi_2O_3. Certain of the Group IV liquidi in Fig. 19 fall entirely above the ideal curve. This is consistent with a decrease in corundum solubility due to association of the additive oxide; such polymerization is well known for silica.

Table XI gives the temperatures, solid phases, and melt compositions at the corundum-saturated, minimum melting point for the binary oxide systems of

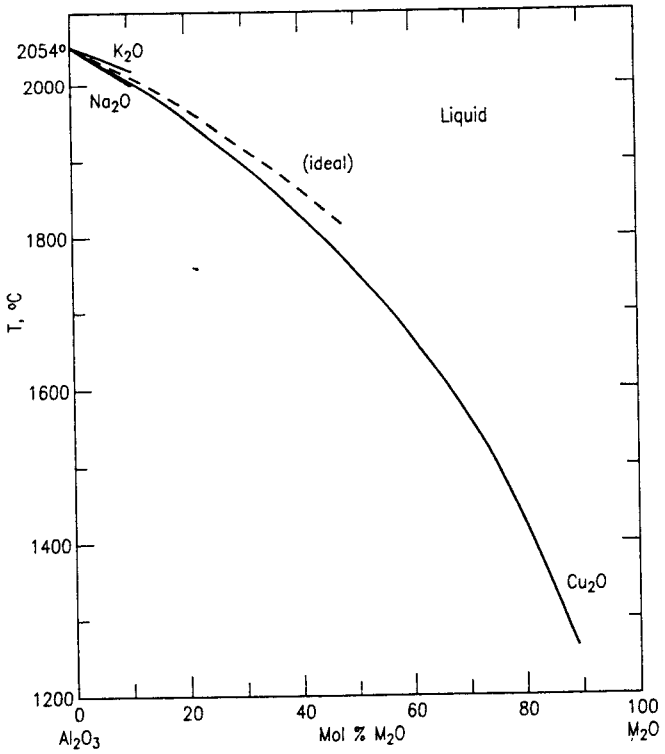

Fig. 15. Corundum liquidus for Group I oxides (Ref. 1).

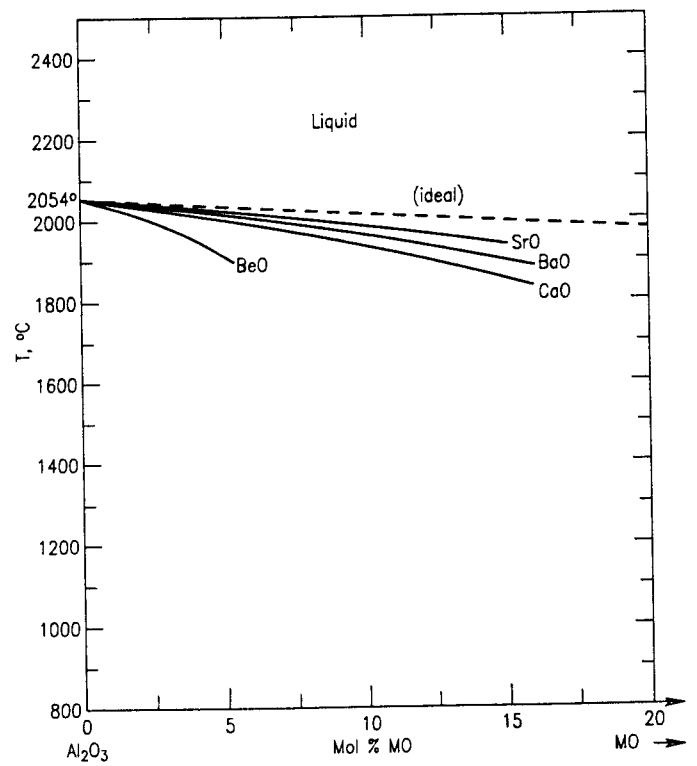

Fig. 17. Corundum liquidus for rare earth oxides (Ref. 1).

Fig. 16. Corundum liquidus for alkaline earth oxides (Ref. 1).

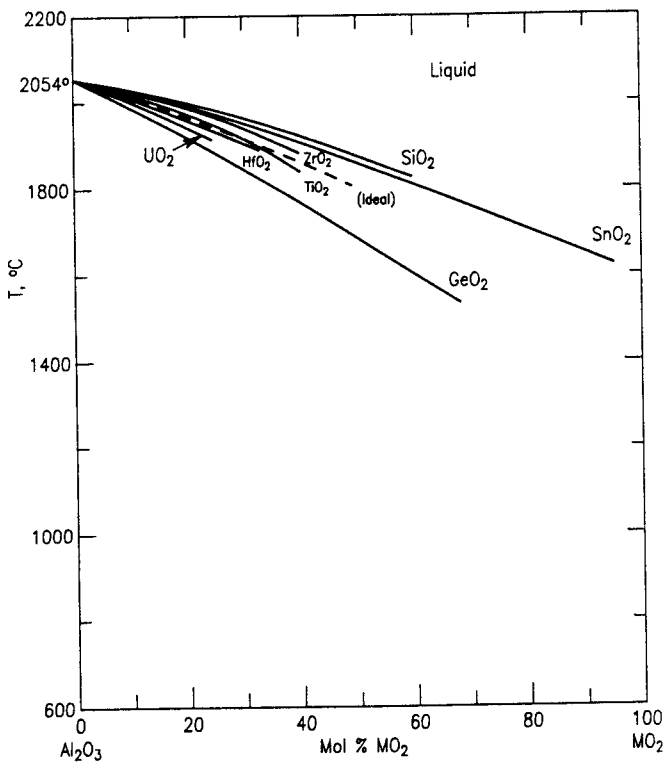

Fig. 18. Corundum liquidus for Group IV oxides and UO_2 (Ref. 1).

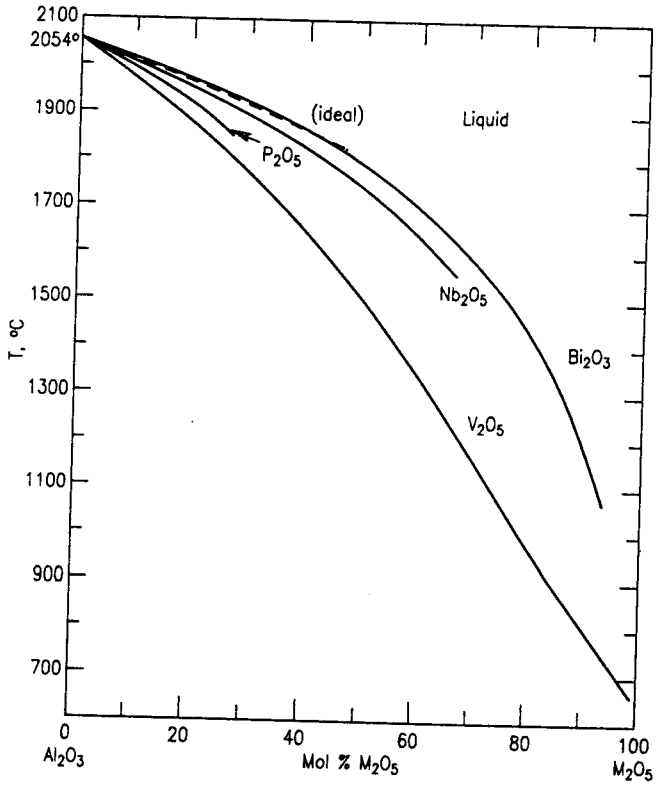

Fig. 19. Corundum liquidus for Group V oxides (Ref. 1).

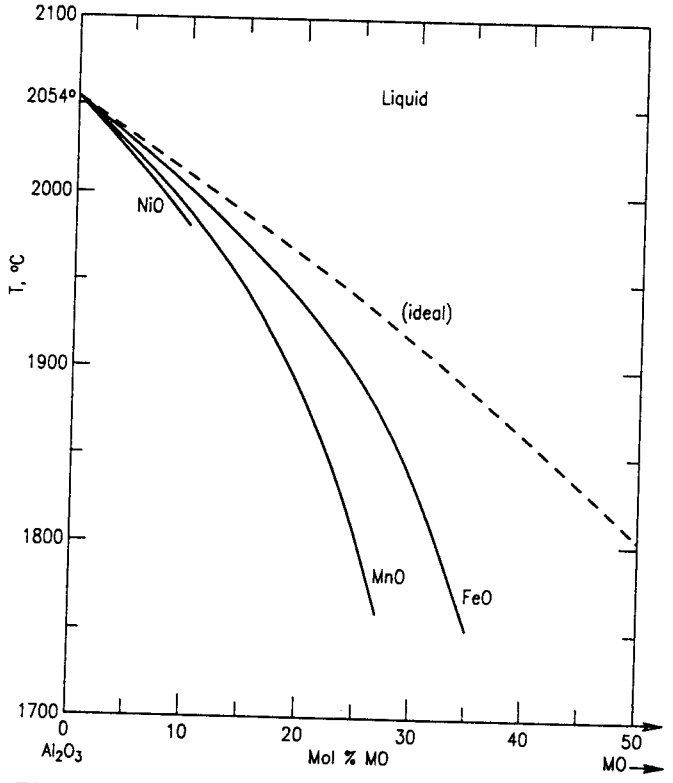

Fig. 20. Corundum liquidus for first-row transition metal oxides (Ref. 1).

Table X. Effect of Melt Chemistry on Ideally Calculated Corundum Liquidus for Bulk Composition $(Al_2O_3)_{95}(M_2O)_5$

Type of Melt Interaction	Mixing Units	Calculated Liquidus Temperature (°C)
None	Al_2O_3, M_2O	2033
Association of additive oxide	Al_2O_3, M_4O_2	2043
Dissociation of additive oxide	Al_2O_3, $MO_{0.5}$	2014
Formation of equimolar binary complex	Al_2O_3, $MAlO_2$	2012
Formation of additive-rich binary complex	Al_2O_3, M_3AlO_3	2040
Formation of alumina-rich binary complex	Al_2O_3, MAl_3O_5	2007

Figs. 15 to 20. With the exception of Cu_2O, V_2O_5, Bi_2O_3, B_2O_3, and WO_3, the minimum melting temperature of corundum-saturated compositions in these systems is above 1500°C.

Carbide, Nitride, and Boride Phase Diagrams

Phase diagrams with carbides, nitrides, and borides are of interest because of the potential of alumina coatings for, or composites with, those materials. Data on alumina-boride phase equilibria are lacking, but at least three carbide and nitride phase diagrams have been published (Figs. 21 to 23).

The Al_2O_3-Al_4C_3 phase diagram was originally studied by Foster et al.,[38] who reported the intermediate oxycarbide phases Al_4O_4C and Al_2OC. Fugishige et al.[39] published a revised X-ray powder diffraction pattern for Al_2OC, which is isostructural with AlN (wurtzite type). A more recent phase equilibrium study by Larrere et al.[35] demonstrated the low-temperature instability of Al_2OC, as indicated in Fig. 21. These authors also note the presence of a metastable Al_2O_3-Al_2OC eutectic, which becomes important in the absence of formation of Al_4O_4C.

In the nitride systems, high-temperature decomposition of nitride phases limits experimental investigation, and so in Figs. 22 and 23 the calculative methods of Kaufmann[36] have been especially useful in estimating the highest temperature parts of the liquidus (metastable). Both the Al_2O_3-AlN and Al_2O_3-Si_3N_4 systems form joins within the technologically important Si-Al-O-N reciprocal ternary. An aluminum oxynitride spinel phase occurs on the join AlN-Al_2O_3; the composition is indicated as $3Al_2O_3 \cdot AlN$ in Fig. 22. However, McCauley and Corbin [37] give experimental data showing considerable solid solution centered at 35.7 mol% AlN. The join Si_3N_4-Al_2O_3 (Fig. 23) shows no intermediate compounds.

Table XI. Binary Corundum Minimum Melting Equilibria*

Oxide Additive	Melting	Temperature (°C)	Liquid Composition (mol%M_xO_y)	Corundum-Saturated Solid
Na_2O	Peritectic	2005	10	Na-beta alumina
K_2O	Peritectic	≈2020	≈10	K-beta alumina
Cu_2O	Peritectic	1260	90	$CuAlO_2$
BeO	Eutectic	1890	5	$BeAl_6O_{10}$
CaO	Peritectic	1830	16	$CaAl_{12}O_{19}$
SrO	Peritectic	≈1930	≈15	$SrAl_{12}O_{19}$
BaO	Eutectic	1875	16	$BaAl_{12}O_{19}$
Sc_2O_3	Peritectic	1850	22	$Sc_{0.40}Al_{1.60}O_3$
Y_2O_3	Eutectic	1790	21	$Y_3Al_5O_{12}$
La_2O_3	Peritectic	1848	9	$LaAl_{11}O_{18}$
Pr_2O_3	Peritectic	1855	12	$PrAl_{11}O_{18}$
Nd_2O_3	Peritectic	1795	18	$NdAl_{11}O_{18}$
Eu_2O_3	Peritectic	1800	12	$EuAl_{11}O_{18}$
Gd_2O_3	Eutectic	1760	23	$GdAlO_3$
Ho_2O_3	Eutectic	1780	19	$Ho_3Al_5O_{12}$
Er_2O_3	Eutectic	1810	19	$Er_3Al_5O_{12}$
Yb_2O_3	Eutectic	1750	50	$Yb_3Al_5O_{12}$
TiO_2	Eutectic	1840	40	Al_2TiO_5
ZrO_2	Eutectic	1885	40	ZrO_2
HfO_2	Eutectic	1890	33	HfO_2
SiO_2	Peritectic	1825	60	$Al_6Si_2O_{13}$
GeO_2	Peritectic	1534	68	$Al_6Ge_2O_{13}$
SnO_2	Eutectic	1620	95	SnO_2
UO_2	Eutectic	1915	25	UO_2
V_2O_5	Eutectic	660	99	V_2O_5
Nb_2O_5	Peritectic	1560	67	$AlNbO_4$
P_2O_5	Eutectic	1850	27	Al_3PO_7
Bi_2O_3	Peritectic	1070	93	$Bi_2Al_4O_9$
MnO	Eutectic	1770	≈27	$MnAl_2O_4$
FeO	Eutectic	1750	35	$FeAl_2O_4$
NiO	Eutectic	≈1980	≈10	$NiAl_2O_4$
B_2O_3	Peritectic	≈1440	≈88	$Al_{18}B_4O_{33}$
WO_3	Eutectic	≈1230	≈65	(?)

*From Ref. 1.

Reaction with Metals

With the exception of Fig. 2, phase diagrams of alumina with metals are not available; many such systems are probably not binary. From Table VII, it can be seen that most of the metals form aluminates, pointing to the likelihood of many of these metals being unstable in contact with alumina. For a metal to react with alumina in the absence of oxygen and form an aluminate, the governing thermodynamic requirement is that ΔG_R (Gibbs energy change) for the reaction:

$$(a)M + (b)Al_2O_3 \rightarrow (c)M_xAl_yO_z + (d)Al \qquad (3)$$

be negative. Thermodynamic data are available for the following aluminate-producing reactions[2,40]

(i) $2Li + 1.33Al_2O_3 \rightarrow 2LiAlO_2 + 0.67Al$

(ii) $Be + 3.33Al_2O_3 \rightarrow BeAl_6O_{10} + 0.67Al$

(iii) $2Na + 1.33Al_2O_3 \rightarrow 2NaAlO_2 + 0.67Al$

(iv) $Mg + 1.33Al_2O_3 \rightarrow MgAl_2O_4 + 0.67Al$

(v) $2Si + 4.33Al_2O_3 \rightarrow Al_6Si_2O_{13} + 2.67Al$

(vi) $Fe + 1.33Al_2O_3 \rightarrow FeAl_2O_4 + 0.67Al$

ΔG_R for reactions (i), (ii), and (iv) is negative from room temperature to 2000 K, indicating instability of alumina in the presence of Li, Be, and Mg. ΔG_R for reaction (iii) is negative in the low-temperature part of this range and positive at higher temperatures; however, thermodynamic data for Na-beta alumina are not available, and the formation of this phase could potentially make alumina unstable at higher temperatures in the presence of metallic Na. This apparently does not happen, given the well-known usage of transparent alumina in high-pressure sodium vapor lamps. ΔG_R for reactions (v) and (vi) is positive at all temperatures, suggesting the stability of alumina in contact with Si,

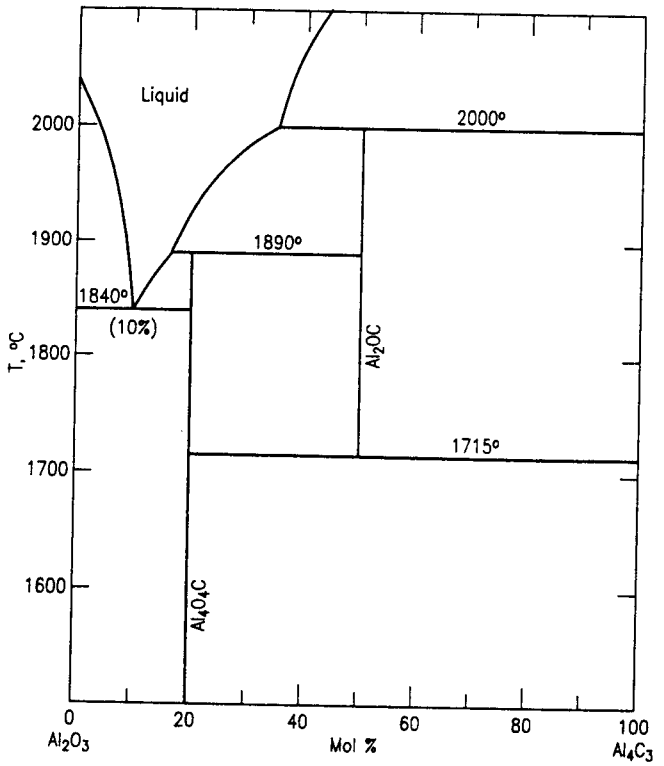

Fig. 21. The system Al_2O_3-Al_4C_3 (Ref. 35).

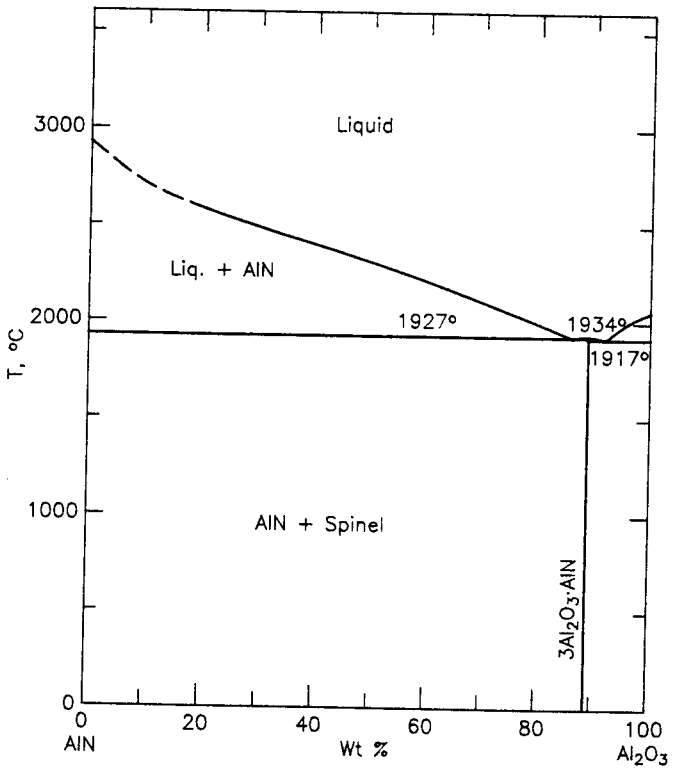

Fig. 22. The system AlN-Al_2O_3. Dashed lines indicate metastability relative to decomposition of AlN into Al and N_2 at 0.1 MPa above 2577°C (Ref. 36). According to Ref. 37, the intermediate solid has a compositional range centered near $2Al_2O_3$ • AlN and melts incongruently at ~ 2050°C.

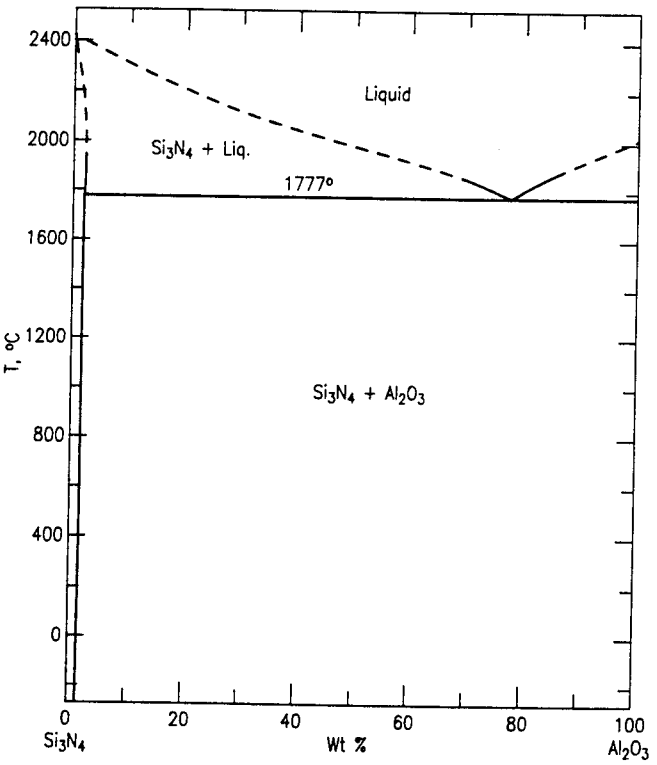

Fig. 23. The system Si_3N_4-Al_2O_3. Dashed lines indicate metastability relative to decomposition of Si_3N_4 into Si and N_2 at 0.1 MPa above 1856°C (Ref. 36).

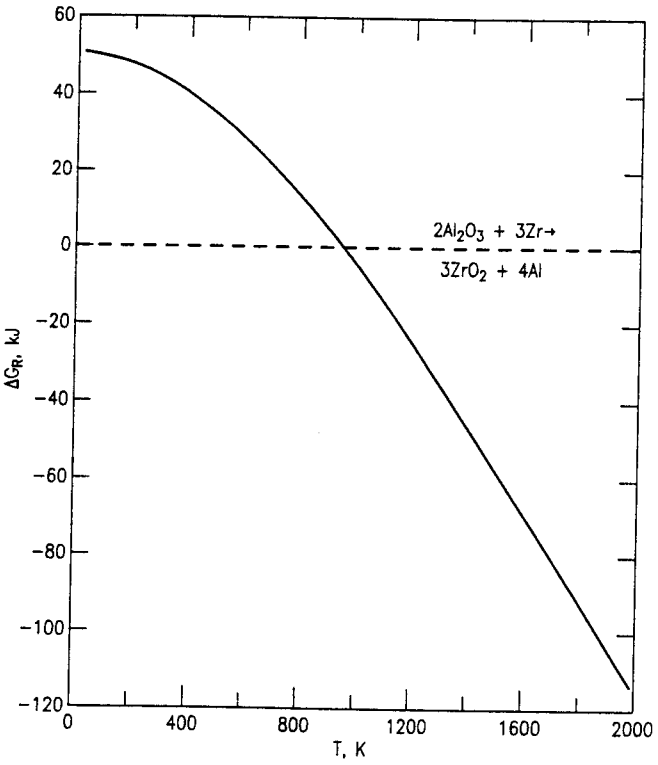

Fig. 24. Calculated ΔG_R for reaction of zirconium metal with alumina as a function of temperature (data from Ref. 3).

and with Fe under reducing conditions; hence the widespread application of high-alumina refractories in the iron and steel industry.

For metals with no aluminate thermodynamic data, if ΔG_R is negative for reactions of the type:

$$(a)\mathrm{M} + (b)\mathrm{Al_2O_3} \rightarrow (c)\mathrm{M}_x\mathrm{O}_y + (d)\mathrm{Al} \qquad (4)$$

then it follows that alumina is not stable in contact with the metal. However, if ΔG_R is positive, this does not necessarily indicate alumina stability, unless there are no aluminates formed, since ΔG_R for the aluminate reaction may be negative. Using this criterion, it can be shown that alumina is thermodynamically unstable in contact with Ba, Ca, Sr, and P; and possibly stable at higher temperatures in contact with Zr (see Fig. 24). Thermodynamically calculated stabilities or instabilities of several metal/alumina pairs are summarized in Table XII.

No data are available for oxides of Pt, Pd, Ir, Rh, and Au, and such oxides are relatively unstable at high temperature. All of these metals (Rh is usually alloyed with Pt) are used in contact with Al_2O_3 at high temperatures, apparently with negligible reaction. Similarly, crucibles of Mo are routinely used for the growth of single-crystal sapphire from the melt in vacuum or inert atmospheres, and tungsten was the material used to support Al_2O_3 during melting-point experiments.[13]

Interaction with Salts and Oxide Fluxes

Molten salts and fluxes (including oxygen-containing anions) are used in a variety of high-temperature applications, including electrolysis, ion exchange, crystal growth, and dissolution studies. The chemical interactions with these salt mixtures influence the extent to which alumina refractories can be used in such applications. The majority of low-melting salts fall into two principal categories: oxyradicals and halides.

Among the salts with oxygen-containing anions, the borates, vanadates, molybdates, and tungstates are mainly used. The carbonates, sulfates, nitrates, and hydroxides tend to decompose when heated and can be extremely reactive toward container materials. Figures 25 and 26 summarize some possible reactions between alumina and alkali carbonates and sulfates, respectively. While such calculations do not give any kinetic predictions, they do suggest the instability of alumina in contact with molten alkali carbonates. As indicated by the atmospheric CO_2 isobar in Fig. 25, if there were no kinetic limitations, the decomposition of alumina could begin as low as 500 to 750 K, depending on the salt, or possibly lower, if stabilities of the beta aluminas (Na or K) are taken into account. Alumina in contact with alkali sulfates (Fig. 26) is somewhat more stable.

Information necessary to evaluate the behavior of alumina in contact with borate fluxes is lacking, with the exception of lithium borate. The subsolidus Li_2O-B_2O_3-Al_2O_3 phase diagram is shown in Fig. 27, where it can be seen that the solid state compatibilities greatly restrict the stability of alumina. It can be expected that this behavior would carry over into the liquidus region; that is, lithium borate melts would dissolve a substantial amount of Al_2O_3, not reaching saturation until compositions are close to the Al_2O_3 corner. Again, however, it is important to note that the attainment of equilibrium may be kinetically hindered, especially at low temperatures.

No data are available for the behavior of alumina in contact with molybdate and tungstate fluxes. How-

Table XII. Thermodynamically Calculated Metal/Alumina Interactions (298 to 2000 K)

Metal	Postulated Reaction Product	Alumina-Metal Interaction
Li	$LiAlO_2$	Unstable
Be	$BeAl_6O_{10}$	Unstable
Na	$NaAlO_2$	Unstable/stable
Mg	$MgAlO_2$	Unstable
Si	$Al_6Si_2O_{13}$	Stable
P	P_2O_5	Unstable
Ca	CaO	Unstable
Fe	$FeAl_2O_4$	Stable
Sr	SrO	Unstable
Zr	ZrO_2	Stable/unstable
Ba	BaO	Unstable

Data for calculation taken from Ref. 3.

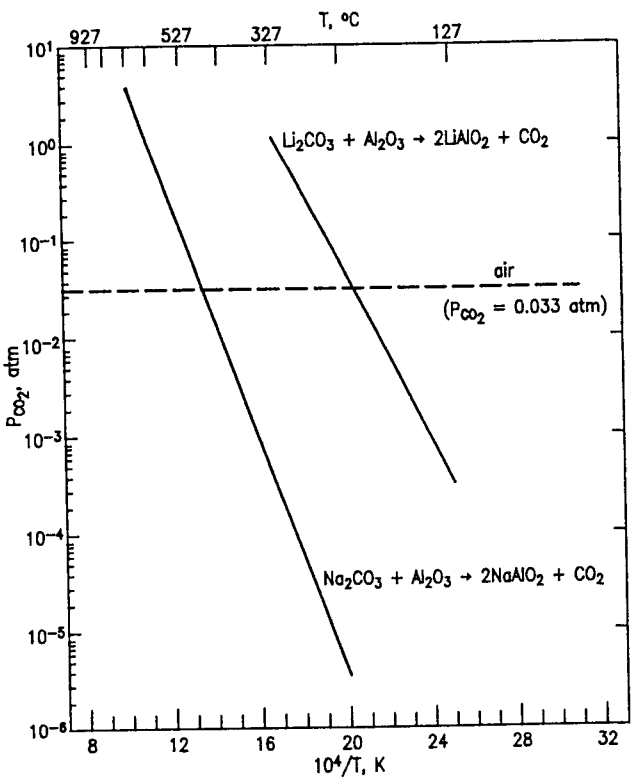

Fig. 25. Thermal decomposition of alkali carbonates in contact with alumina (Ref. 3).

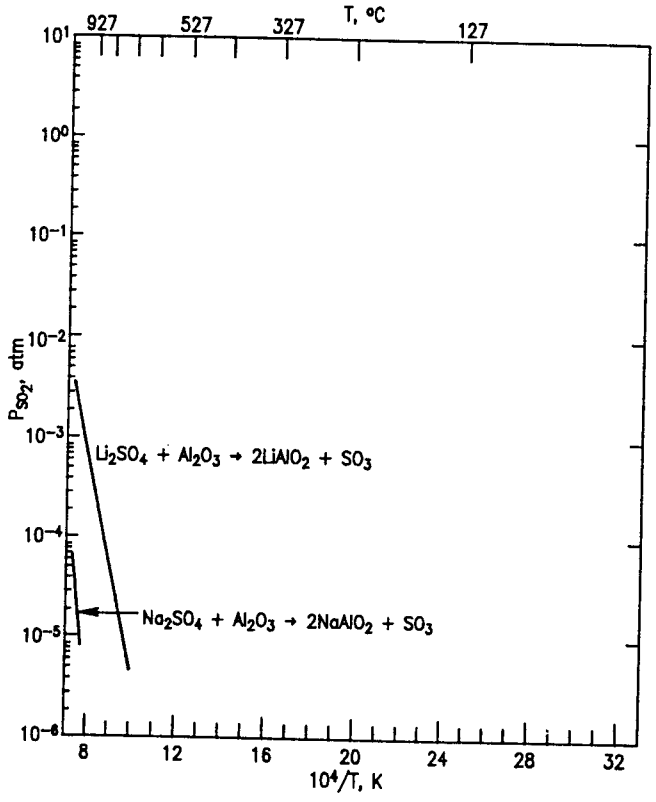

Fig. 26. Thermal decomposition of alkali sulfates in contact with alumina (Ref. 3).

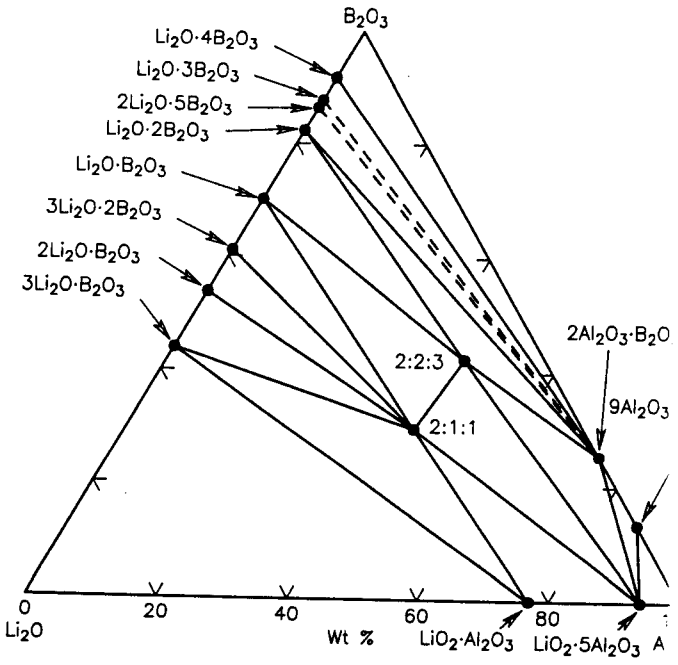

Fig. 27. Subsolidus compatibilities in the system Li_2O-Al_2O_3-B_2O_3 (Ref. 41).

ever, the alkali vanadate-alumina systems have been investigated, as shown in Fig. 28 (*a*) to (*c*). A significant feature of these phase diagrams is the relatively low amount of Al_2O_3 which dissolves in MVO_3 melts, less than 3 mol% up to 1000°C.

A few phase diagrams are available for alumina-halide systems. Figure 29 shows the diagram for CaF_2-Al_2O_3, and the system NaF-Al_2O_3 is shown in Fig. 30. Both these diagrams are nonbinary due to formation of aluminates. By contrast, systems of alumina with lithium and sodium cryolite are binary, as shown in Figs. 31 and 32, which indicate the stability and limited solubility of alumina in cryolite melts at the eutectic.

Thermodynamic data can be used to partially compensate for the lack of halide-alumina phase diagrams of certain systems. Calculation of reactions of the type:

$$4Al_2O_3 + 6MX \rightarrow 6MAlO_2 + 2AlX_3 \qquad (5)$$

(M = Li, Na; X = F, Cl, Br, I)

suggest that alumina is stable in contact with molten alkali halides. Similar calculations indicate stability in contact with magnesium halides.

Vapor-Phase Reactions

While, in principle, reaction of alumina with water vapor or aqueous fluids is important at low temperatures and high water pressures where the aluminum hydroxides are stable, in actuality the kinetics of this reaction are sluggish. A *P-T* phase diagram for the system Al_2O_3-H_2O is given in Fig. 33. Stable phases include bayerite ($Al(OH)_3$) and diaspore (AlOOH); above about 400°C, only corundum appears on the equilibrium diagram. The gibbsite form of $Al(OH)_3$ is not included on the diagram because its apparent stability relative to bayerite is thought to be due to the presence of alkalies.[47] The boehmite form of AlOOH is considered to be metastable with respect to diaspore.[47,48]

The interaction of corundum with gases such as CO_2 and N_2 is negligible, and hence alumina is stable in air to its melting point. Under certain conditions of actual service, however, reactions with halogens and sulfur-containing gases become important. Using a computer code,[49] concentrations of various gas species produced by equilibration of corundum with F_2, Cl_2, and H_2S have been calculated as shown in Figs. 34 through 36, respectively. These curves were calculated by allowing a mixture of Al_2O_3 and the respective gas (diluted with argon) to come to equilibration at the appropriate temperature, while maintaining a total pressure of 0.1 MPa.

On the basis of thermodynamic calculations with presently available data, reaction with fluorine is likely to be extensive, as the curves in Fig. 34 show. The predominant aluminum-containing species should be $AlOF_2$, followed by AlF_3, and, at higher temperatures, by AlOF and AlF_2. The calculated $AlOF_2$ pressure may be unrealistically high and needs experimental verification. Under actual experimental conditions at

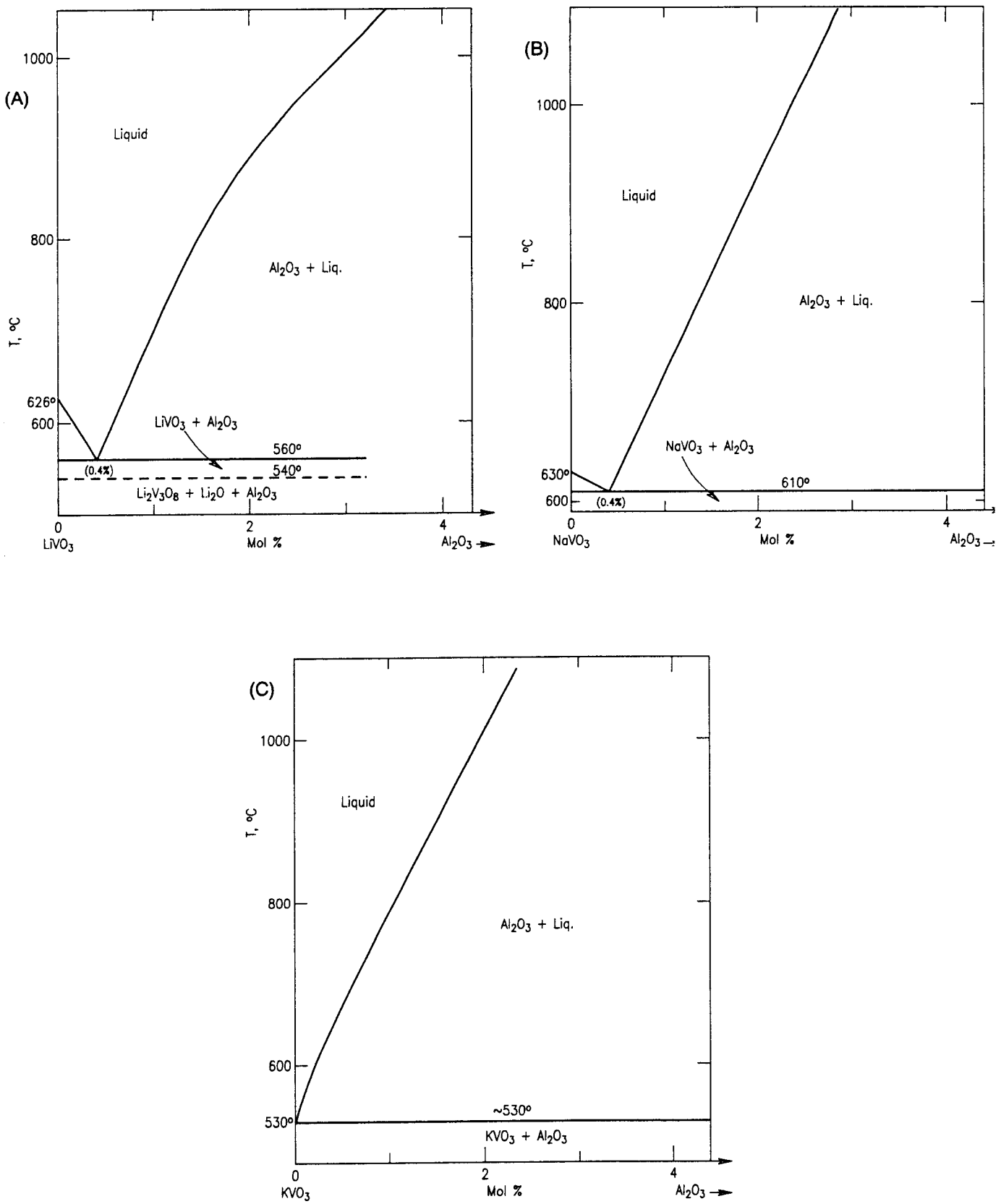

Fig. 28. Alkali vanadate systems. (*a*) The system $LiVO_3$-Al_2O_3; (*b*) the system $NaVO_3$-Al_2O_3; (*c*) the system KVO_3-Al_2O_3. (After Ref. 42.)

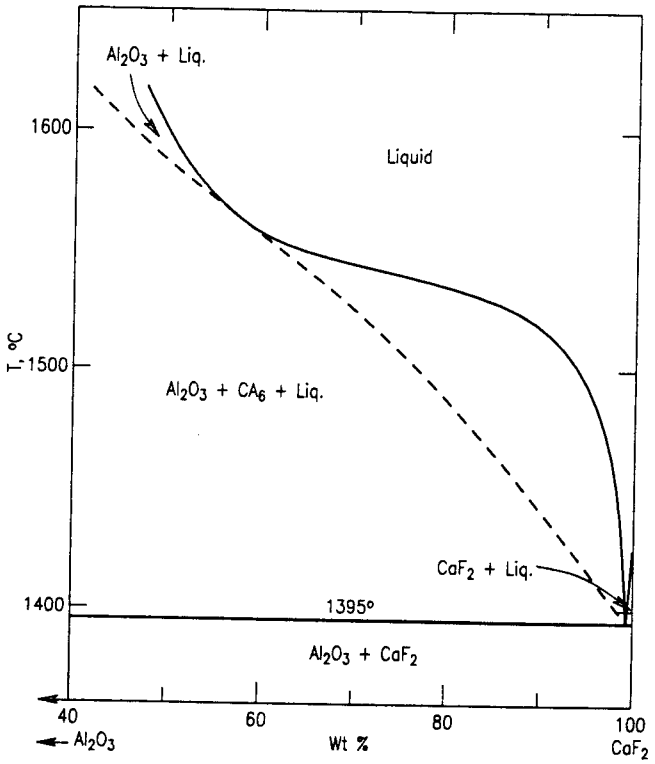

Fig. 29. The system Al_2O_3-CaF_2 (Ref. 43). (CA_6 = $CaAl_{12}O_{19}$.)

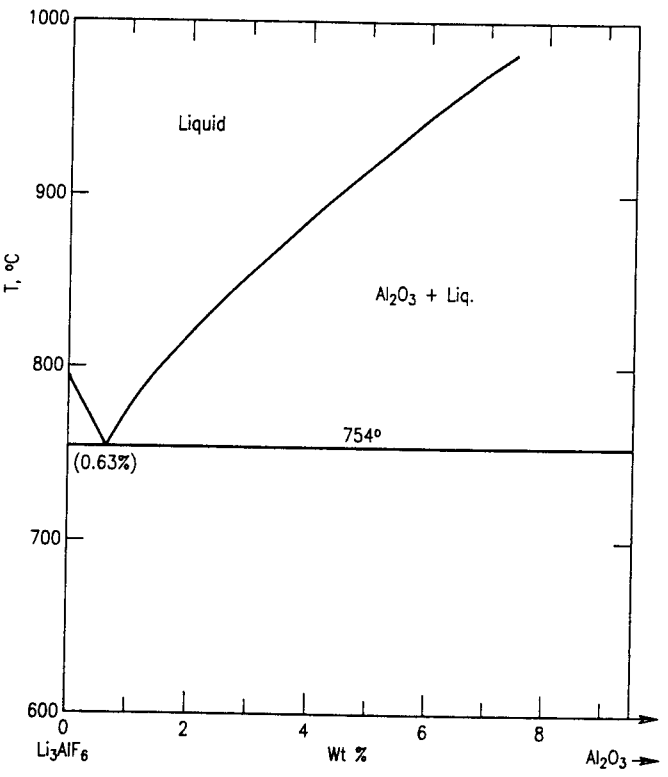

Fig. 31. The system Li_3AlF_6-Al_2O_3 (Ref. 45).

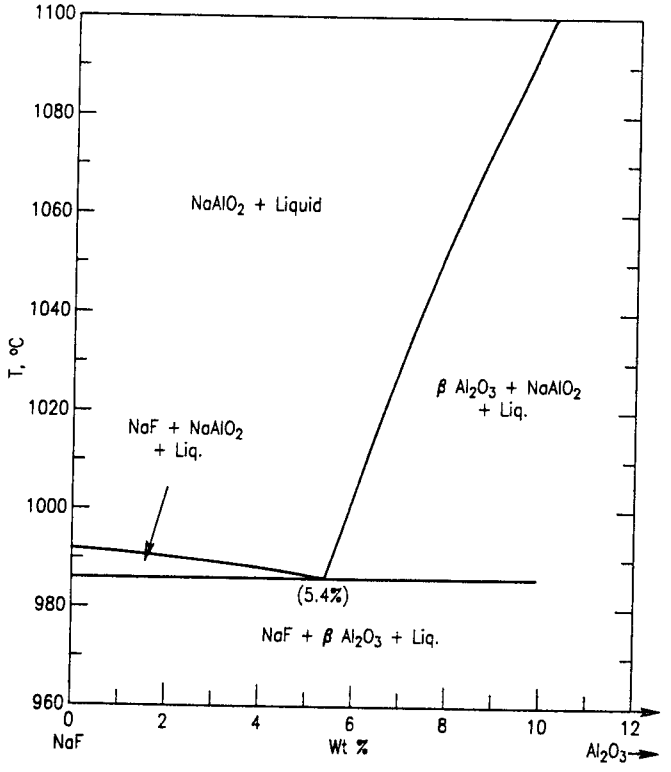

Fig. 30. The system NaF-Al_2O_3 (Ref. 44).

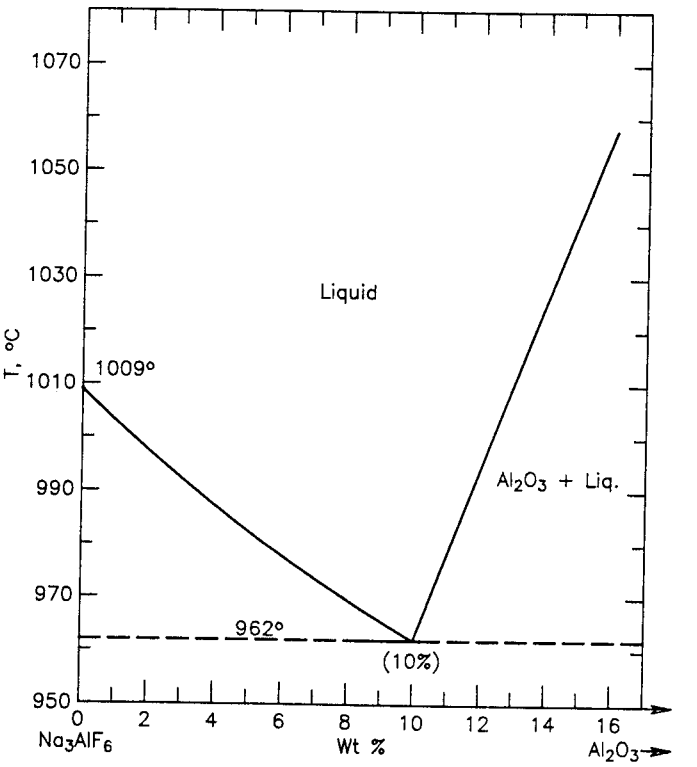

Fig. 32. The system Na_3AlF_6-Al_2O_3 (Ref. 46).

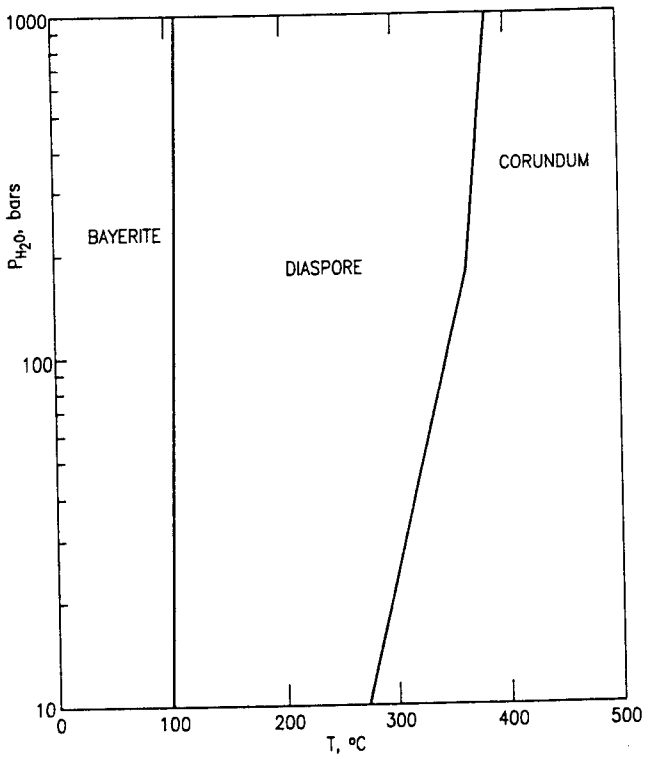

Fig. 33. *P-T* phase diagram for the system Al_2O_3-H_2O (after Refs. 47 and 48).

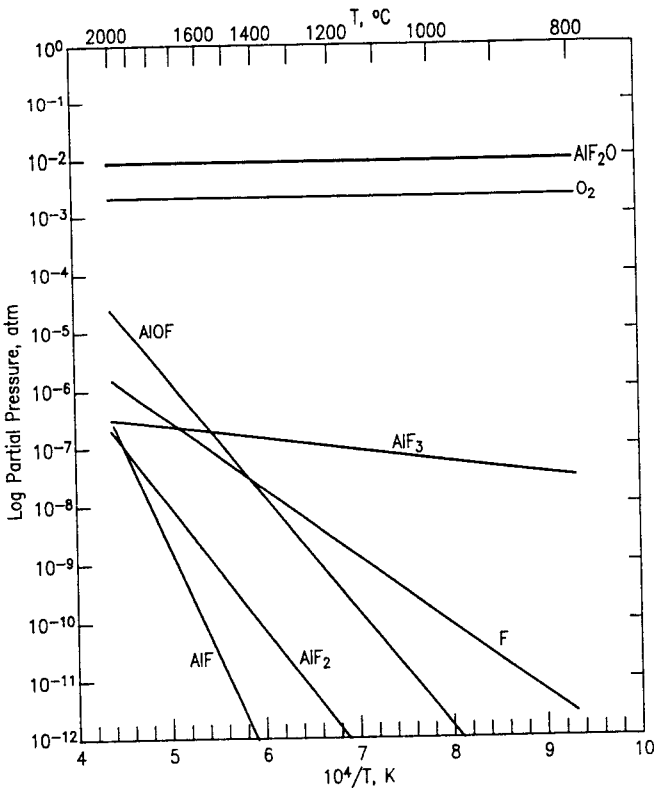

Fig. 34. Calculated partial pressures of species in 1% fluorine-containing gas (99% Ar) in equilibrium with alumina at 0.1 MPa total pressure.

800°C, a thin passivating layer of AlF_3 may form on the surface of the alumina, impeding further reaction.[50] Undoubtedly this becomes less effective at higher temperatures, as the AlF_3 vaporizes. The reaction of chlorine with alumina (Fig. 35), though not predicted to be as extensive, becomes significant at higher temperatures as the partial pressures of $AlCl_2$, and to a lesser degree, $AlCl_2$ and AlOCl, increase. Reaction with H_2S (Fig. 36) should yield primarily AlS as the aluminum-containing species. While pressures are 2 to 3 orders of magnitude below the calculated pressures of aluminum halide species, H_2S reaction with corundum and transport of Al as AlS could possibly become significant in H_2S-containing atmospheres above 1600°C.

Conclusions

Useful thermochemical properties of α-alumina (corundum) include: high melting point, low vapor pressure, high pressure stability, and stability relative to other structural modifications. The formation of solid solutions of corundum with certain oxides, including Cr_2O_3, Fe_2O_3, Ga_2O_3, and others makes possible the modification of physical and chemical properties. Corundum is compatible with many aluminate compounds, including representatives of such technologically important materials as spinels, garnets, and perovskites.

The solubility of corundum in binary oxide melts varies widely, but is usually greater than the ideal solution model predictions; the structural mechanisms of solubility need further study. There is a general lack of phase diagrams of alumina with nonoxide materials, perhaps an additional area for investigation. However, it should be noted that interaction with these materials (including salts) is likely to be nonbinary, as in fact all alumina-nonoxide joins represent a diagonal section within a larger ternary reciprocal system. For information on the behavior of alumina in contact with metals and reactive gases, it has been necessary to rely on thermodynamic calculations. The results of such calculations, as well as the known phase diagrams, indicate the overall direction of equilibrium but do not provide the kinetics data of various reaction paths, for which the reader is referred to the extensive literature on the durability of alumina under conditions of actual service.

Acknowledgments

David Bonnell and Ernest Plante assisted with the computer calculations of corundum/gas equilibria. Michael Rodtang helped with the preparation of the illustrations. The author is indebted to Sammuel Schneider for stimulating interest in alumina phase

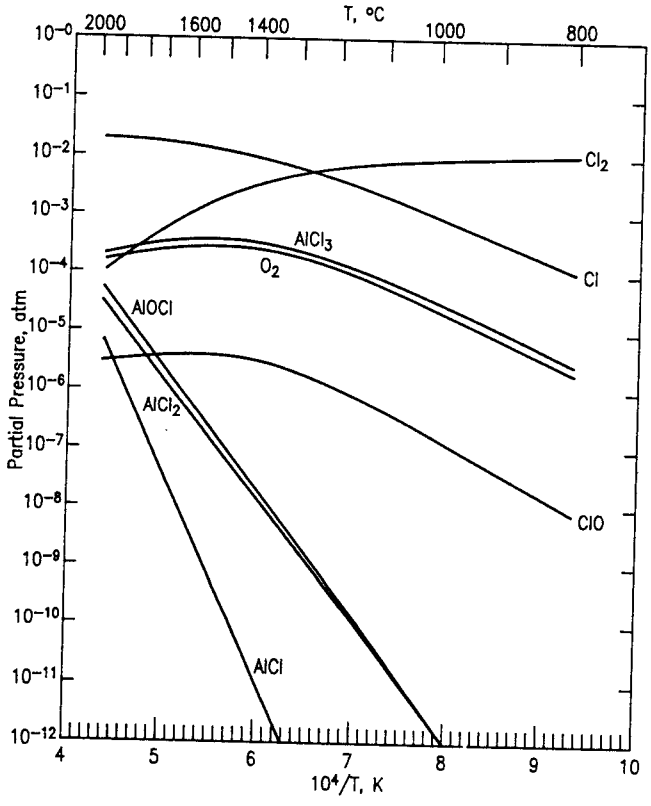

Fig. 35. Calculated partial pressures of species in 1% chlorine-containing gas (99% Ar) in equilibrium with alumina at 0.1 MPa total pressure.

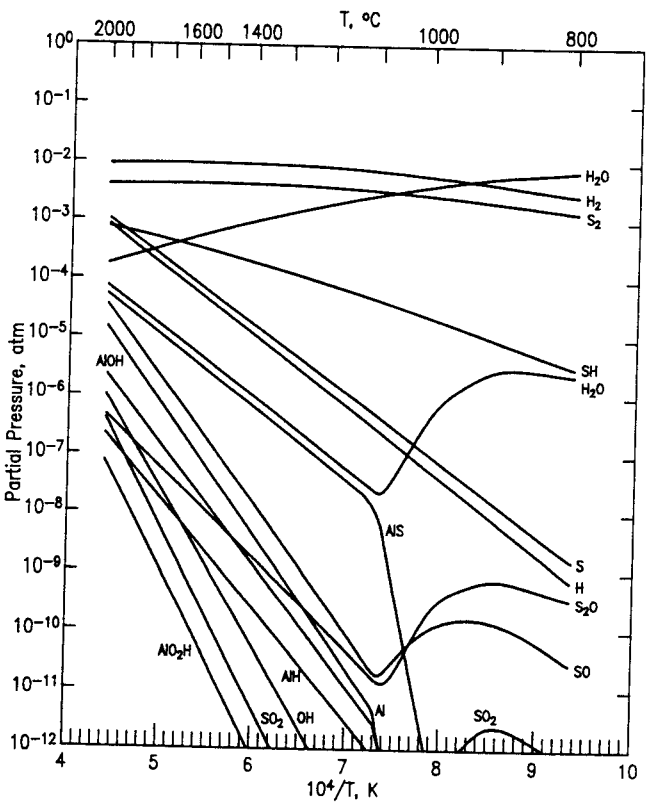

Fig. 36. Calculated partial pressures of species in 1% H_2S-containing gas (99% Ar) in equilibrium with alumina at 0.1 MPa total pressure.

equilibria, to Robert Roth for valuable discussions, and to Lee Hart for his encouragement in preparing this review.

References

[1]Phase Diagrams for Ceramists, Vols. I-VI. The American Ceramic Society, Columbus, 1964–1987.

[2]C. G. Bergeron and S. H. Risbud; pp. 53-57 in Introduction to Phase Equilibria in Ceramics. The American Ceramic Society, Columbus, OH, 1984.

[3]M. W. Chase, Jr., C. A. Davies, J. R. Downey, Jr., D. J. Frurip, R. A. McDonald, and A. N. Syverud. JANAF Thermochemical Tables, 3d ed., Parts I and II. The American Chemical Society and American Institute of Physics, New York, 1986.

[4]International Centre for Diffraction Data, Powder Diffraction, Swarthmore, PA, 1987.

[5]H. E. Swanson, M. I. Cook, T. Isaacs, and E. H. Evans, "Standard X-ray Diffraction Powder Patterns," National Bureau of Standards, Circ. 539, **9**, 3 (1960).

[6]B. C. Lippens and J. H. de Boer, "Study of Phase Transformations During Calcination of Aluminum Hydroxides by Selected Area Electron Diffraction," *Acta Crystallogr.*, **17** [10] 1312–21 (1964).

[7]G. Cevales, "Phase Equilibrium Diagram of Al_2O_3-ZrO_2 and Examination of a New Phase 99% Al_2O_3-1% ZrO_2 (ϵ-Al_2O_3)" (in German), *Ber. Deutsch Keram. Ges.*, **45** [5] 216–19 (1968).

[8]H. P. Rooksby; p. 264 in X-ray Identification and Crystal Structure of Clay Minerals. The Mineralogical Society, London, 1951.

[9]M. Okumiya and G. Yamaguchi, "The Crystal Structure of κ-Al_2O_3, The New Intermediate Phase," *Bull. Chem. Soc. Jpn.*, **44** [6] 1567–70 (1971).

[10]S. J. Wilson and J. D. C. McConnell, "A Kinetic Study of The System δ-AlOOH/Al_2O_3," *J. Solid State Chem.*, **34** [3] 315–22 (1980).

[11]G. W. Brindley and J. O. Choe, "The Reaction Series, Gibbsite → Chi Alumina → Kappa Alumina → Corundum," *Am. Mineral.*, **46** [7–8] 771–85 (1961).

[12]H. A. Wriedt, "The Al-O (Aluminum-Oxygen) System," *Bull. Alloy Phase Diagrams*, **6** [6] 548–53 (1985).

[13]S. J. Schneider, "Cooperative Determination of the Melting Point of Al_2O_3," *Pure Appl. Chem.*, **21** [1] 117–22 (1970).

[14]H-K. Mao; personal communication, Geophysical Laboratory, Washington, DC, 1987.

[15]P. Ho and R. P. Burns, "A Mass Spectrometric Study of the AlO_2 Molecule," *High Temp. Sci.*, **12** [1] 31–39 (1980).

[16]F. D. Bloss, Introduction to Crystallography and Crystal Chemistry. Holt, Rinehart and Winston, New York, 1971.

[17]R. C. Evans; p. 201 in Introduction to Crystal Chemistry. University Press, Cambridge, 1964.

[18]W. A. Deer, R. A. Howie, and J. Zussman, Introduction to The Rock-Forming Minerals. Wiley, New York, 1966.

[19]E. N. Bunting, "Phase Equilibria in the System Cr_2O_3-Al_2O_3," *Bur. Stand. J. Res.*, **6** [6] 947–49 (1931).

[20]D. M. Roy and R. E. Barks, "Sub-solidus Phase Equilibria in Al_2O_3-Cr_2O_3," *Nature (London)*, **235** [58] 118–19 (1972).

[21]A Muan, "On the Stability of the Phase $Fe_2O_3 \cdot Al_2O_3$," *Am. J. Sci.*, **256** [6] 413–22 (1958).

[22]M. Mizuno, T. Yamada, and T. Noguchi, *Yogyo-Kyokai-Shi*, **83** [4] 175–77 (1975).

[23]V. G. Hill, R. Roy, and E. F. Osborn, "The System Alumina-Gallia-Water," *J. Am. Ceram. Soc.*, **35** [6] 135–42 (1952).

[24]N. A. Toropov and V. A. Vasil'eva, "Phase Relations in the System Scandium Oxide-Aluminum Oxide," *Dokl. Akad. Nauk. SSSR*, **152** [6] 1379–82 (1963).

[25]T. Noguchi and M. Mizuno, *Kogyo Kogaku Zasshi*, **70** [6] 839 (1967).

[26]A. S. Berezhnoi and N. V. Gul'ko, "The System $MgO-Al_2O_3$" (in Russian), *Ukrain. Khim. Zhur.*, **21** [2] 158–66 (1955).

[27]A. M. Alper; p. 339 in Science of Ceramics, Vol. 3. Edited by G. H. Stewart. Academic Press, London, 1967.

[28]F. Colin, "Phases Formed by Reduction of Certain Mixed Oxides $mA_2O_3 \cdot MO$" (in French), *Rev. Int. Hautes Temp. Refract.*, **5** [4] 267–83 (1968).

[29]A. Burdese, M. L. Borlera, and P. Rolando, "Systems Between Niobium Oxide and Oxides of Aluminum and Chrome," *Atti Accad. Sci. Torino, Cl, Sci. Fis., Mat. Nat.*, **99**, 1079–87 (1964–1965).

[30]R. E. Newnham, Ch. 1 in Phase Diagrams: Materials Science and Technology, Vol. 1. Edited by A. M. Alper. Academic Press, New York, 1978.

[31]J. D. H. Donnay, H. M. Ondik, and A. D. Mighell, Crystal Data Determinative Tables, Vols. 2 and 4, National Bureau of Standards and International Centre for Diffraction Data, Swarthmore, PA, 1973 and 1978.

[32]A. F. Wells, Structural Inorganic Chemistry. Clarendon Press, Oxford, 1984.

[33]C. N. R. Rao; p. 31 in Solid State Chemistry. Marcel Dekker, New York, 1974.

[34]W. Horkner and Hk. Muller-Buschbaum, "On the Crystal Structure of $CaAl_2O_4$" (in German), *J. Inorg. Nucl. Chem.*, **38** [5] 983–84 (1976).

[35]Y. Larrere, B. Willer, J. M. Lihrmann, and M. Daire, "Stable and Metastable Phase Equilibrium Diagrams in the Al_2O_3-Al_4O_3 Binary System" (in French), *Rev. Int. Hautes Temp. Refract.*, **21** [1] 3–18 (1984).

[36]L. Kaufmann, "Calculation of Quasi binary and Quasi ternary Oxynitride Systems-III, *CALPHAD*, **3** [4] 275–91 (1979).

[37]J. W. McCauley and N. D. Corbin, *J. Am. Ceram. Soc.*, **62** [9–10] 476–479 (1979).

[38]L. M. Foster, G. Long, and M. S. Hunter, "Reactions Between Aluminum Oxide and Carbon. The Al_2O_3-Al_4C_3 Phase Diagram," *J. Am. Ceram. Soc.*, **39** [1] 1–11 (1956).

[39]M. Fujishige et al. *J. Nat. Chem. Labor Ind.*, **77**, 325 (1982).

[40]I. Barin and O. Knacke; p. 306 in Thermochemical Properties of Inorganic Substances. Berlin, Springer-Verlag, 1973.

[41]K. H. Kim and F. A. Hummel, "Studies in Lithium Oxide Systems: XII, Li_2O-B_2O_3-Al_2O_3," *J. Am. Ceram. Soc.*, **45** [10] 487–89 (1962).

[42]L. A. Klinkova and E. A. Ukshe, "Solution of Corundum in Fused Vanadates," *Zh. Neorg. Khim.*, **20** [2] 481–84 (1975); *Russ. J. Inorg. Chem. (Engl. Transl.)* **20** [2] 266–68 (1975).

[43]A. K. Chatterjee and G. I. Zhmoidin, "The Phase Equilibrium Diagram of the System CaO-Al_2O_3-CaF_2," *J. Mater. Sci.*, **7** [1] 93–97 (1972).

[44]P. A. Foster, Jr., "The System Sodium Fluoride-Alumina Investigated by Quenching Methods," *J. Am. Ceram. Soc.*, **45** [4] 145–48 (1962).

[45]R. T. Cassidy and J. J. Brown, Jr., "Phase Equilibria in the System LiF-AlF_3-Na_3AlF_6-Al_2O_3," *J. Am. Ceram. Soc.*, **62** [11–12] 547–51 (1979).

[46]D. A. Chin and E. A. Hollingshead, "Liquidus Curves for Aluminum Cell Electrolyte," *J. Electrochem. Soc.*, **113** [7] 736–39 (1966).

[47]K. Wefers and G. M. Bell, "Oxides and Hydroxides of Aluminum," Technical paper No. 19, E. St. Louis, Il., Alcoa Research Laboratories, 1972; 51 pp.

[48]H. Haas, "Diaspore-Corundum Equilibrium Determined by Epitaxis of Diaspore on Corundum," *Am. Mineral.*, **57** [9–10] 1375–85 (1972).

[49]S. Gordon and B. J. McBride, "Computer Program for Calculation of Complex Chemical Equilibrium Compositions, Rocket Performance, Incident and Reflected Shocks, and Chapman-Jonguet Detonations," NASA SP-273, U.S. Gov't Printing Office, Washington, DC, 1971.

[50]L. P. Cook, E. R. Plante, D. W. Bonnell, and J. W. Hastie, "Reaction of Liquid Aluminum with Gaseous ClO_3F," *High Temp. Sci.* (in press).

SECTION III

Current Commercial Production Processes, Products *and* Applications

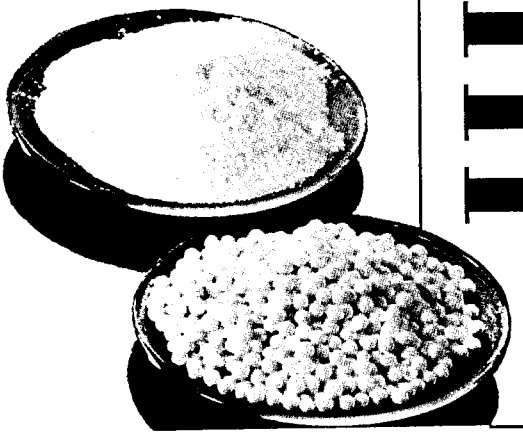

Production Processes, Properties, and Applications for Aluminum-Containing Hydroxides

Larry L. Musselman
AMAX Technical Center
Apollo, PA 15613

Aluminum hydroxides are truly some of the world's most versatile chemicals. In addition to aluminum manufacture, they are used directly or indirectly in almost every major industry, from ceramics and refractories to plastics and pharmaceuticals. Aluminum hydroxides touch our lives every day, from the carpet on which we walk to the pastes we use to brush our teeth. As an introduction to later more in-depth applications chapters, this section discusses the various forms, production methods, properties, commercial aspects, and a few selected applications of aluminum hydroxides.

Although aluminum has been touted as the most abundant metal and the third most abundant element on earth, only a fraction of the aluminum-containing materials are currently used for aluminum hydroxide production. The term aluminum hydroxide based on the chemical formula $Al(OH)_3$, is technically most correct; however, the terms alumina trihydrate (ATH) and hydrated alumina based on the description $Al_2O_3 \cdot 3H_2O$ have been used more historically. All three terms are used interchangeably in the literature.

Although aluminum can be extracted from other sources such as anorthosite, alunite, shales, and clays, virtually all alumina is produced from hydrated alumina ores (bauxites) using variations of classic Bayer-process technology.

Fine particle size, precipitated aluminum trihydrates; higher purity hydrates; and extremely white hydroxide grades are part of a larger family of alumina products which include smelting-grade aluminas for reduction to aluminum metal, Bayer-ground hydrated alumina, and other high-volume commodity aluminas. While being part of these larger streams of products will keep overall costs down long-term, the fine, submicron, high-purity, and white trihydrates are truly high-technology products processed specifically to fit their major market uses. Target properties for these grades are dictated by the end-application property and processing requirements. For this reason the controls on chemical and physical properties of these and other premium chemical-grade alumina trihydrates are much tighter than for metallurgical aluminas, which somewhat limits sources and availability. However, plants to produce these types of products are located in the high-growth industrial centers of the world and the long-term strategy of some of the largest suppliers of alumina chemicals has been to increase capacities for these higher value aluminum hydroxide materials.

In this section, product forms, methods of production, properties, commercial aspects, some data on volumes, and selected applications of aluminum hydroxides will be reviewed.

Forms of Aluminum Hydroxides

Aluminum hydroxide occurs in its naturally most abundant α-trihydrate[1] form (gibbsite)* or as a monohydrate (diaspore or boehmite) in bauxite. The Bayer process† depends on the solubility of alumina at specific concentrations of caustic and temperature. Since trihydrates are much more soluble than monohydrates in sodium hydroxide under pressure, some form of trihydrate is more often extracted from bauxite and then precipitated to obtain the alumina value. The portion of this process unique to each alumina supplier is the commercial extraction, precipitation, and final processing parameters used to obtain a specific purity and morphology of alumina trihydrate.[2,3]

Other important crystalline forms of aluminum-containing hydroxides include bayerite, nordstrandite/diaspore, boehmite, and dawsonite. There are also many forms of aluminum hydroxide gels. These are mainly amorphous or at least partially X-ray-indifferent materials. The most important of these which shows some crystallinity is probably pseudoboehmite. Preparation and processing details for these gels are covered in later chapters. Comparison of the crystalline forms of the aluminum hydroxides is given in Table I from Ref. 4.‡

Bayerite or β-aluminum hydroxide is generally produced commercially by reacting CO_2 with sodium aluminate liquor at ambient temperature or precipitation on bayerite seed from a supersaturated aluminate liquor. An alternate route which can be used is the aging of hydroxide gels.[5] The product obtained is

*Sometimes called hydrargillite, although this was orginally the name given to a mineral later found to be aluminum phosphate (Ref. 2).
†Details given under the section "Methods to Produce Aluminum Hydroxide."
‡References in this table may be obtained from Alcoa.

Table I. Comparison of Nomenclatures Presently Used

	Symposium[a]	ALCOA[b]	Haber	Wesser and Milligan	Other
Aluminum Trihydroxides	Gibbsite or Hydrargillite	Alpha Alumina Trihydrate	Gamma Series	Gamma Alumina Trihydrate	Aluminum Hydroxide Orthoaluminic Acid
	Bayerite	Beta Alumina Trihydrate		Alpha Alumina Trihydrate	Aluminum Hydroxide Bauxite Dihydrate[g]
	Nordstrandite				Randomite[d] Bayerite II[e]
Aluminum Oxide Hydroxides	Boehmite	Alpha Alumina Monohydrate		Gamma Alumina Monohydrate	Pseudoboehmite[f]
		Beta Alumina Monohydrate	Alpha Series	Alpha Alumina Monohydrate	Meta-aluminic Acid
	Diaspore	Alpha Alumina		Alpha Alumina	
	Corundum				

U.S.A	Germany	England		France
Alcoa[c]	Symposium[a]	Day and Hill; Rooksby	Thibon	Pechiney[h]
gamma	gamma	delta	gamma	rho
delta	delta	delta + theta		gamma
			delta	delta
eta	eta	gamma	eta	eta
theta		theta	theta	theta
chi	chi	chi + gamma	chi	chi +gamma
kappa	kappa	kappa +theta	kappa	kappa +delta
iota				

[a]Edwards, et al., Stumpf et al
[b]Discovery
[c]Ginsberg, Hottig, Strunk-Lichtenberg
[d]Teter, Gring, and Keith, U.S. Patent 2,838,373
[e]Bohm
[f]Papee, Tertian and Biais
[g]Tertian and Papee

Reproduced courtesy of Aluminum Company of America.

rarely much better than 90% bayerite. The balance is composed of combinations of partially crystalline materials, gibbsite, and boehmite. The type of equipment used can be the same as described below for Bayer production of gibbsite. However, concentrations, temperature, gas flow rate, mixing conditions, and seeding parameters are all critical to obtain the desired product. Typical Bayer hydroxide clarification, filtering, washing, drying, and packaging techniques are used.

Nordstrandite is not commercially produced, although production processes have been disclosed by Kelly et al.[6] and Hauschild.[7] First discovered by Van Nordstrand et al.,[8] commercial use has probably not occurred because of the similarity to a combination of the structures and properties of gibbsite and bayerite but requiring more complicated production processes. For example, one production technique describing starting materials of aluminum-containing compounds like hydroxide gels with aqueous diamines is discussed by Hauschild.[9] Aluminum chloride or aluminum nitrate can also be reacted with ammonium hydroxide to form nordstrandite by gradual conversion of the gel formed to trihydrate by aging at a pH slightly above neutral.

Doyleite is a recently reported[10,11] form of aluminum hydroxide which will not be discussed in detail because no production techniques have been developed. This material occurs naturally in Canada. The structure appears to be between that of normal gibbsite Bayer hydroxide and nordstrandite.

Diaspore is another crystalline form not commercially produced, probably because of the high temperature and pressure conditions required for its formation, although the conditions for production have been well documented.[12–17] While naturally occurring in some North American shales and clays, the largest concentrations of diaspore are found in Chinese and Russian bauxites. Lesser concentrations have been found in various deposits of some of the geologically older bauxites, depending on the pressure, temperature, and other chemicals in the ore.[18]

Boehmite or aluminum oxide hydroxide[§] can be produced by neutralization of aluminate solutions at around 200°C. Techniques for growing crystals above 100°C from aluminum metal are also available.[4] Generally, higher temperatures and higher pH increase the rate of crystallization.[19] However, specific crys-tal structures can be obtained by precipitation under more acidic conditions.[20] Boehmite can also be formed by rapid heating of gibbsite in air up to 300°C.

Another method to convert gibbsite to boehmite is by heating under water to over 100°C. This latter technique can create a structure that contains 1 to 2% excess water in the crystal lattice. A more thorough description of large-scale production processes is given in later chapters covering activated aluminas.

Dawsonite and the other crystalline aluminum carbonate hydroxides are chemically different from the simple aluminum hydroxides we have discussed to this point but the final mechanical steps in their processing are quite similar. Dawsonite can be produced as a fiber or powdery crystalline material by a number of related processes. The best known is the hydrothermal reaction[21] of sodium aluminate, sodium hydroxide, and sodium carbonate in solution. A typical set of reaction conditions might be 180°C for four hours at two atmospheres or 200°C for one hour. After cooling and precipitation, hot-water washing is used during filtration to reduce soluble carbonates. The resulting material can be fine particulate or acicular crystals, depending on the chemistry of the process streams and the control used. The applications for this type of crystal look quite promising, although more testing is needed to identify particle-size ranges not under the cloud of being possible carcinogens, as has been shown for other fibrous materials.

Lower temperature and pressure reactions can also produce forms of dawsonite but they are generally amorphous materials with limited apparent usefulness. In addition, dawsonite has been found in nature in very limited quantities.[22]

The other useful types of aluminum-containing carbonate hydroxides have also been located in small deposits in places such as Scandinavia. Preparation of crystalline forms of these types of materials is fairly simple.[23] Generally carbonate-containing, well mixed, ambient temperature aqueous solutions of the desired metal (usually magnesium and aluminum) salts will produce uniform crystals under auto generated pressure as the temperature is raised. Normal precipitation, filtering, washing, and drying equipment as described below can be used.

[§]Diaspore and boehmite are referred to in the literature as alumina monohydrates, alumina monohydroxides, or aluminum oxide hydroxide, although the latter are technically more correct.

Methods to Produce Aluminum Hydroxide

Of the primary processes for hydroxide production, the most important by far is the Bayer process, which we have described as producing primarily gibbsite crystals. Although invented almost 100 years ago, it continues to be the most economical technology for aluminum hydroxide manufacture and is still used for well over 95% of the total alumina produced in the world today. Although the growth rate for other uses is increasing rapidly, traditionally around 90% of the aluminum hydroxide generated annually from bauxite in the Bayer process has been calcined to alumina (aluminum oxide) for the production of aluminum metal. However, an increasing number of smaller aluminum hydroxide refineries are being converted solely to the production of alumina chemicals. A schematic of a refinery of this type is shown in Fig. 1.

Today there are alumina plants in over 25 countries. Present world production of alumina exceeds 30 million metric tons per year. World capacity is over 35 million metric tons annually. Some of the newer alumina plants have annual capacities of 2 million metric tons each. This is approximately five times the capacity of the original U.S. plant built in East St. Louis, Missouri.

Bauxite is the prime raw material for alumina production. The largest bauxite reserves are located in Australia, Europe, Jamaica, Malaysia, South America, West Africa, and the United States. Smaller reserves can be found in the U.S.S.R. and other countries. The main bauxite inorganic contaminants that survive processing and are trapped during precipitation of ATH are silica, iron, and soda. Organic contaminants, usually present in very low percentages, are generally some form of humic acid. The level and type of contaminants are very dependent on the bauxite source and final processing technique used.

In normal Bayer processing, the aluminum hydroxide in the bauxite is digested and solubilized as sodium aluminate, according to the reaction:

$$\underset{\text{aluminum hydroxide}}{2Al(OH)_3} + \underset{\text{sodium hydroxide}}{2NaOH} \rightarrow \underset{\text{sodium aluminate}}{2NaAlO_2} + \underset{\text{water}}{4H_2O} \quad (1)$$

The output of this extraction process is separated by dilution and cooling into a clear, filtered sodium aluminate liquor and an insoluble residue called red mud. This solid residue, containing sodium aluminum silicate, iron oxide, titania, etc., is generally washed and discarded; however, one major U.S. supplier has the capability to either use this waste material or bauxite in a sinter operation or to redigest a commodity hydroxide and take advantage of other proprietary concepts to further process the extractable alumina into extremely white, high-purity hydrated products.

The Bayer sodium aluminate liquor described above forms crystalline aluminum hydroxide after further cooling with seeding and uniform agitation. By using specific types of aluminous seed, other additives, and closely controlled processing conditions, technology has been developed and commercial facilities are in place to precipitate a range of products with median particle diameter crystals from 150 to 0.3 μm. The particle-size medians, distributions, and purities have been refined specifically to optimize their effects on processing and final properties of the end applications.

Figure 1 not only shows the basic steps in the process of making Bayer alumina in the upper portion

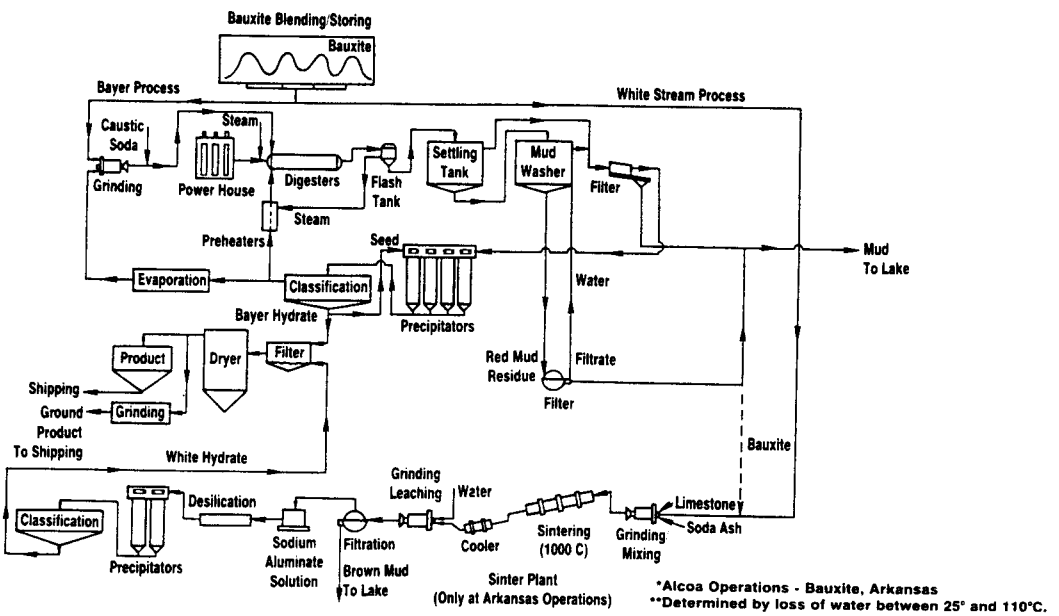

Fig. 1. Combination-process flow diagram of bauxite ore to hydrated alumina.

of the flow sheet, but in the lower section a simplified flow diagram for the sinter process[¶] is also shown. In the sinter system the bauxite or red mud residue is mixed with crude calcium carbonate, sodium carbonate, and other additives, then reacted in kilns to produce sodium aluminate and dicalcium silicates. The silicates and other residue are removed and the sodium aluminate dissolved and taken through steps similar to normal Bayer processing to precipitate a very white alumina trihydrate with unique properties for polymer and other additive applications that ranges in median particle size from 80 to 0.3 μm in diameter.

Alumina trihydrate is generally shipped as a dry powder with nominally 0.4% moisture** in 50- and 100-lb bags, semibulk bags, and boxes, as well as bulk trucks and railroad cars. Generally, the finest grades must be shipped in bags, although one major supplier specially processes a 1-μm median particle-size grade for bulk shipment and easier handling.

Each step shown in Fig. 1[24] can be carried out in a number of ways from an equipment standpoint. The processing begins with bauxite mining and preparation. This usually includes blending and grinding (perhaps starting with large chunk roll crushers or hammermills and finishing with fine grinding rod mills or ball mills). The grinding can also be done in process liquor, followed by digestion.

Digestion begins a cyclic process, shown in Fig. 2, that allows the spent liquor to be reused over and over again with continual adjustment and cleanup. Reactors for digestion can be low-carbon steel or nickel-plated, either in horizontal or vertical configurations. They are usually under constant agitation in series with each successive unit, using higher and higher temperature steam heating under pressure. Operation can be batch or continuous with flows on the order of 12 000 L/min. An example of a continuous tube digester system is shown in Fig. 3.[25]

The digester slurry effluent is decreased in temperature by flashing off steam to remove water and heat the digester in the flow stream, as Figs. 2 and 3 show. The number of flashing stages required is determined by the design digestion temperature. Slurry heating and other heat-transfer requirements are handled with both contact and indirect heat exchangers, depending on plant designer preferences. In either case, similar fouling problems develop over time and slow deposition of desilication products must be removed by dilute acid washing or other cleaning mechanisms. Direct steam injection is used in some cases with less fouling but more dilution.

Settling or clarification takes place in standard weir-type classifiers, generally with some type of scraping mechanism on the bottom or through the use of liquid-solids cyclones. Basically, the concept is to wash the process solution from the solids. While an appreciable amount of the solids are coarse sandy particles, many are finer than 10 μm and can require flocculants to keep the solution, going over the weir, clean. In many cases, countercurrent washing thickeners are used in series to remove as many solids as possible without loss of valuable salts or autoprecipitation of alumina. In the filtration step, less solution is needed if vacuum drum washing filters are used before final polish filtration reduces solids to 0.5 mg/L or less.

Continuing with the flow chart concept of Fig. 2, aluminum hydroxide is precipitated by cooling to between 60° and 75°C for normal coarse Bayer grades by flashing, as discussed previously. This is followed by maintaining a strict time, temperature, and concentration balance in large-diameter (generally about one-

¶This is the portion of the process that can be replaced by a red mud feed or a commercially available hydrated alumina feed to a redigest/impurity removal system, depending on the feed costs and process economics, which change with time and location.

**The moisture level is a function of the particle size, surface area, and relative humidity. It is still most accurately determined by overnight drying at 110°C. Since these materials are slightly hydroscopic, care must be taken to protect from wet or high-humidity conditions until the hydrates are incorporated into the final application. This is expecially important for the finest grades of ATH.

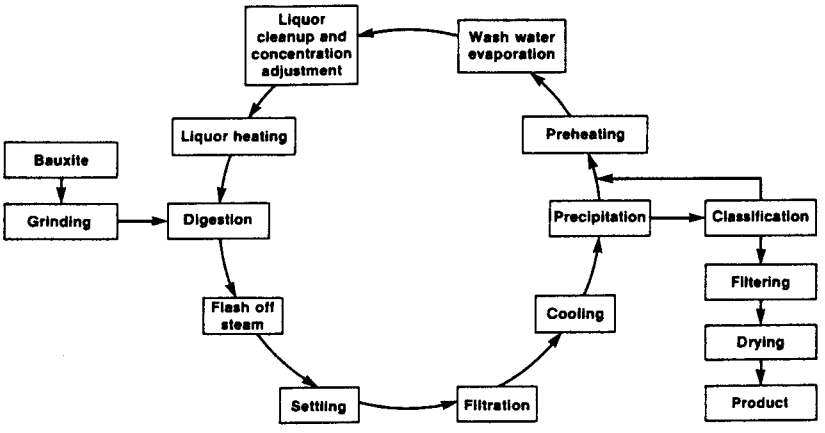

Fig. 2. Recycling of Bayer liquor.

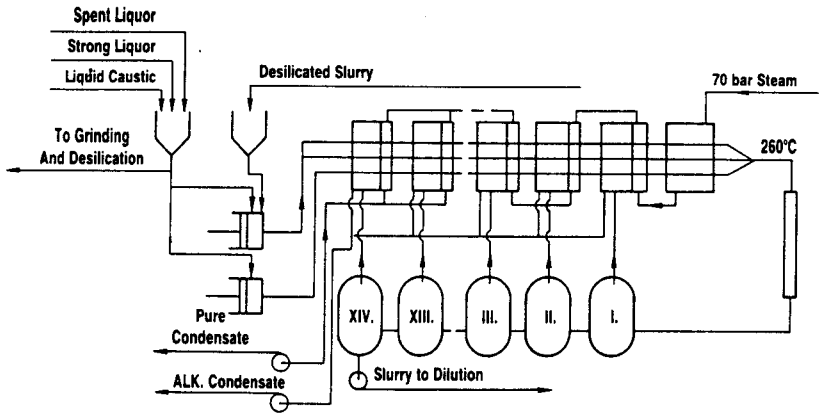

Fig. 3. Tube digester flow sheet (Ref. 25). (Used by permission.)

third the height) cylindrical tanks with seeding to maintain good liquid/solid interfaces for crystallization. All the sciences of crystal nucleation, agglomeration, and growth are involved. While the concepts are similar from plant to plant, solution impurities from the bauxite, chemical additives, cooling mechanism, agitation mechanism, temperature control, concentration control, seed properties, aging time and environmental conditions, etc., can all affect the type of product precipitated in each plant. Because control of these variables is difficult and input changes are not immediately manifested in the output, properties of the finished product cycle somewhat. Most of the time this variation is damped out by large surge volumes in a particular plant; however, average final properties vary from plant to plant and in-depth testing is necessary before arbitrarily switching from one manufacturer to another in critical applications.

After precipitation, the solids again must be separated from the liquor. This is accomplished by the typical chemical processing types of equipment already described. From thickeners to cyclones for classification, from vacuum rotary drum filters to two-stage pressure/squeeze filters for the wash/dewatering steps, and from tunnel dryers to fluid bed dryers for the complete removal of moisture, each plant's particular combination of process equipment along with the bauxite source gives identifiable characteristics to the aluminas produced. For the finest products, spray drying and mild flash drying have also been shown to be effective if proper handling techniques are used.

Other non-Bayer primary aluminum hydroxide processing techniques begin with lower alumina value feedstocks like kaolin clays, fly ash, anorthosite, alunite, etc. as mentioned, but generally the processing costs are at least 50% greater than for the Bayer process. Because of the amphoteric nature of aluminum hydroxide shown in Fig. 4,[4] either low-pH or high-pH processing can be used.

High-pH or alkaline processing can be accomplished by sintering alumina-containing ores with lime/soda-containing compounds at temperatures from

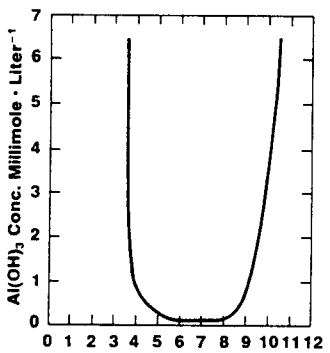

Fig. 4. Solubility of $Al(OH)_3$ as a function of pH (Ref. 4).

1010° to 1399°C, followed by several impurity-removal steps, including leaching and precipitation of silica-containing compounds, followed by carbonation to form $Al(OH)_3$. A typical flow chart is shown in Fig. 5.[26]

Low-pH or acid processes are generally lower in temperature although some begin by roasting clays up to 1000°C. Sulfuric acid, HNO_3, and HCl methods have all been formally operated. The HCl type of processes seem most viable. Many steps, like sedimentation, digestion, crystallization filtration, etc., use equipment and techniques similar to that described for Bayer production. Combination-acid processes[27] have been developed that eliminate clay roasting steps altogether.

In acid-type processing, generally a hydrated aluminum salt is removed from solution, then decomposed to give up the alumina value and allow water and acid to be recycled. Hydrochloric acid advantages[28] include inexpensive reagents, milder processing conditions, ease of salt recovery, less water recycling, and ease of combination with other acid processes. A major disadvantage is equipment corrosion problems that increase with temperature. An example of an acid process is shown in Fig. 6.[26]

Secondary processes to produce particular aluminum hydroxide products are generally mechanical alterations of the gibbsite crystal size, shape, particle

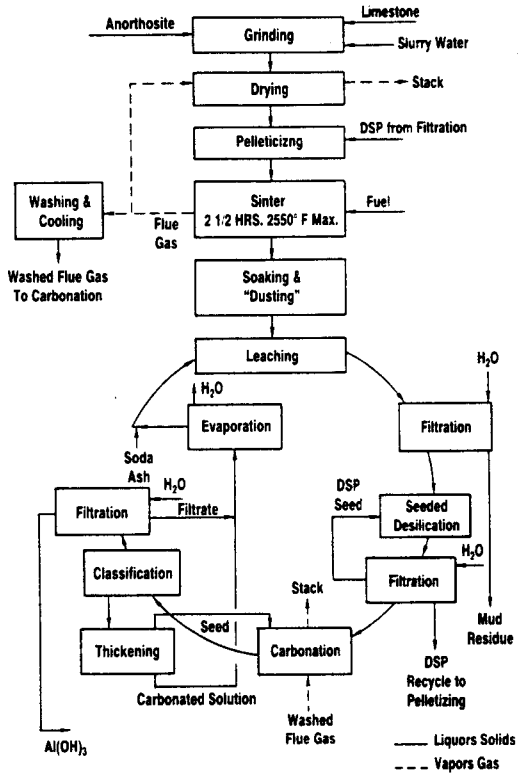

Fig. 5. Alumina from anorthosite via lime sinter (Ref. 26). (Used by permission.)

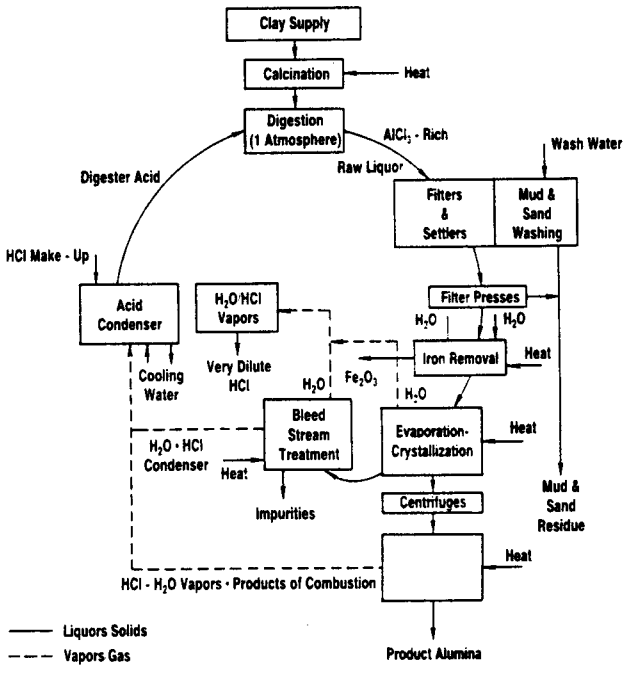

Fig. 6. Alumina from clay via HCl extraction. Evaporative crystallization (Ref. 26). (Used by permission.)

distribution, or surface chemistry. Wet or dry grinding and classification are widely used and surface treatment with compatible chemicals continues to be the fastest growing secondary processing technique, especially for the large range of polymer applications.

One of the earliest pieces of equipment used for high-volume dry grinding and classification of aluminum hydroxides still in use today for additive manufacture is the conical ball mill shown in Fig. 7.[29] This type of ball-mill grinder is generally fed 40- to 110-μm spherical crystals and is used to produce a very uniform series of broad particle-size distribution products from 3 to 30 μm in median particle size. Control is generally good enough to produce separate products at roughly 2-μm median intervals along this entire range. The material is fed into the large end of the mill, as shown in the figure, and is continually mixed with spherical steel or ceramic grinding media which generally range from 1.3 to 3.8 cm (0.5 to 1.5 in.) in diameter. The impact of the gibbsite crystals with each other and the media continually reduces the particle size. The mill and classifier speeds, feed flow rate, media size, and air-flow settings determine the size of the product. When the product reaches the predetermined size, it is swept out of the grinding area by the air current through a whizzer-type classifier which sends any entrained oversize back to the feed.

Many other grinding mill styles including hammer mills, roller mills, vibratory mills, and air-impact (fluid-energy) mills are used with various degrees of success for individual applications. The major limitations to the conical ball mill and these other grinding mills are the characteristic particle-size distributions and surface effects produced by each type of mill. While technology is available to precipitate products over the 3- to 30-μm median range, it has been implemented only where sufficient dollar return is available because of the uniqueness of precipitated products. Most primary suppliers precipitate products with medians above 50 μm; however, since particle-size distributions can best be controlled by precipitation, a few major suppliers produce very unique distributions below this size for specific critical applications.

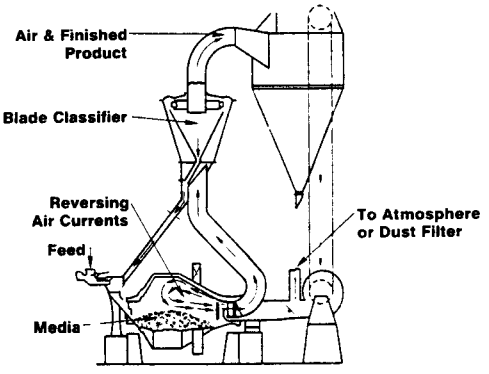

Fig. 7. Conical ball mill (Ref. 29).

To better control particle-size distributions mechanically, several types of external classification units are being used singly and in combination with various return loops to improve efficiency. Classifier performance[30] has to be evaluated individually on the particular feed, product, and plant conditions prevailing. However, the information available on individual units is voluminous.[31-45] All of the referenced classification techniques are usable to some degree for particular applications for the coarser two-thirds of the particle-size median range if the feed has a broad-enough distribution. The difficulties with mechanical separation increase as the requirements for the main product to be classified become finer and narrower in particle-size distribution.

For the lower end of the 3- to 30-μm median particle-size distribution range, classifiers with external fan and cyclone product collection capability with unique sealing and rotary blade designs are required.[46] A unit schematic typical of those which have successfully separated aluminum hydroxides in this particle-size range is shown in Fig. 8. As the median particle-size requirements go below 2 μm, precipitated products return as the only way to obtain narrow distribution products; however, much grinding and classification research has been completed in this area and some broad-distribution, 1- to 2-μm ground products are available.

Of the types of equipment used for below 2-μm median hydroxide grinding with various degrees of success, the most predominant include fluid energy[47] and small-media, wet or dry mills[48,49] with multiple external high-speed classifiers and recycle loops. A simple example of a fluid-energy air-impact mill is shown in Figs. 9 and 10. Because of the inherent classification due to centrifugal forces caused by the rotational motion of the air and particles, allowing only the fines to exit through the center, this type of fluid-energy system can be used without secondary classification. Figures 11 and 12 show possible configurations for a dry, small-media mill with external classification.

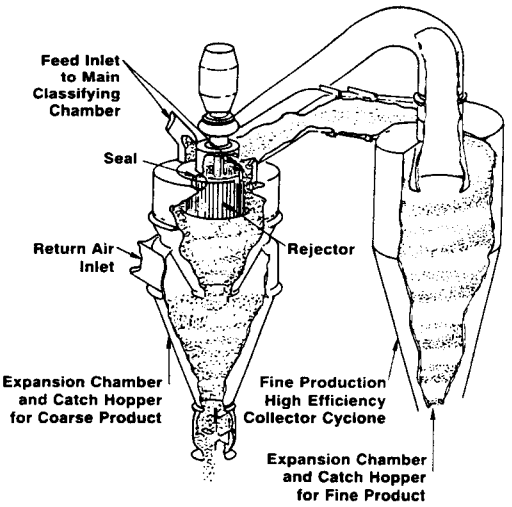

Fig. 8. Air classifier.

Figure 13 shows the type of classifier necessary to separate products that are 3-μm median and finer. Compared with Fig. 8, more rejector blades are needed, along with higher speed operation. All of the problems mentioned with coarser products are encountered, as well as more blade loading and mechanical operation difficulties. Systems of this type have usually required modification after installation, depending on feed, final product split, and local plant environments and capabilities.

Hydraulic classification, although it can be done, is usually characterized by lower classification efficiency. More research is needed in both wet and dry grinding and classification in the superfine particle-size ranges with aluminum hydroxide. While there are significant applications for less than 2-μm, broad-distribution, ground aluminum hydroxide, until the

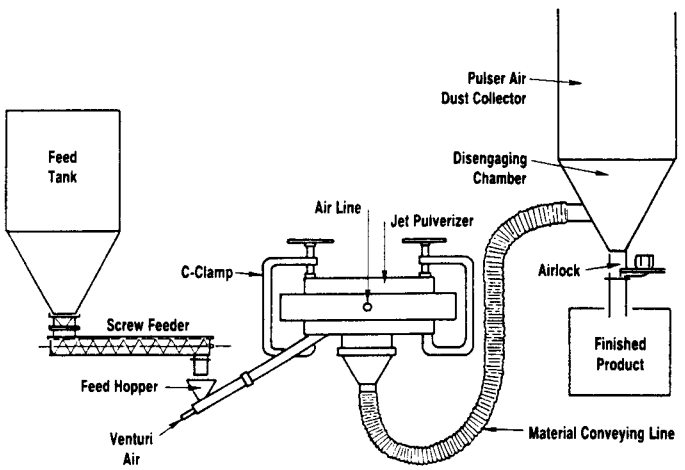

Fig. 9. Fluid-energy mill schematic.

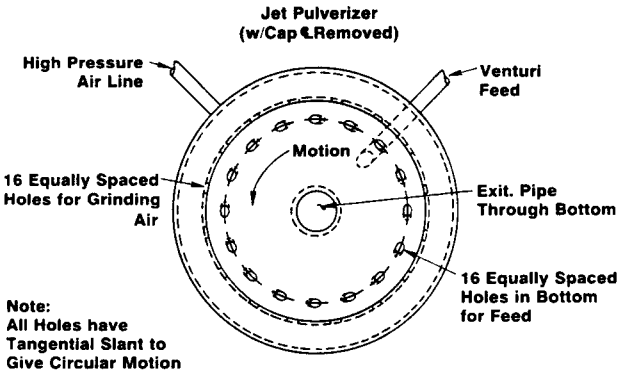

Fig. 10. Fluid-energy mill material and air flow.

state-of-the-art is advanced significantly, the bulk of the critical applications will remain with the unique, fine, precipitated grades.

Surface treatment of aluminum hydroxides for additive applications is growing rapidly due to a wide variety of application system improvements.[50] Although a few commercial surface treatments can be applied in a simple ribbon blender or V-blender type of system, most require intensive mixing-solvent dilution and a minimum temperature to optimize the chemical or physical interaction with the aluminum hydroxide surface. Typical batch process systems include high-speed mixers like Welex (vertical)[††] or Littleford (horizontal)[‡‡] systems. Continuous operations require Littleford or pin mill modifications to control holding time for optimized liquid/solid contact. Some success has been attained with technology based on in-line injection into turbulent areas in pneumatic flow systems.

While some surface treatments have been successfully completed in situ while incorporating the aluminum hydroxide in the application, the best results in most cases have been obtained by pretreatment of the surfaces. Although a wide range of surface-

[††]Welex Inc., Blue Bell, PA.
[‡‡]Littleford Bros., Inc., Florence, KY.

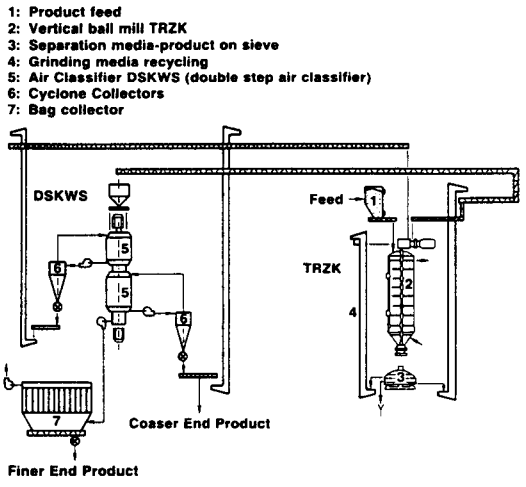

Fig. 12. Small-media grinding system with a prototype double-step classifier system.

treatment types are available and more are being developed each year, generally only one treatment or combination of treatments is usually optimum for each system. Care must be taken to ensure surface-treatment chemical compatibility with other ingredients in the system. For example, the base polymer, processing aids, alloying compounds, etc. must all be tested with the treatment for optimum results in a polymer application.[51,52]

As with grinding and classification, the process technology of hydroxide surface treatment continues to need much more research effort. More sophisticated treatment techniques and routine chemical detection techniques must be developed to ensure adequate quality control. Research to date shows that much less treatment chemical is needed than is normally mixed with the aluminum hydroxide for monolayer coverage; however, many of the individual par-ticles still remain untreated using state-of-the-art equipment.[53] Research also needs to continue into better surface-treatment chemicals. Combination materials[54] and new interactive chemicals[55] have a great potential for use.

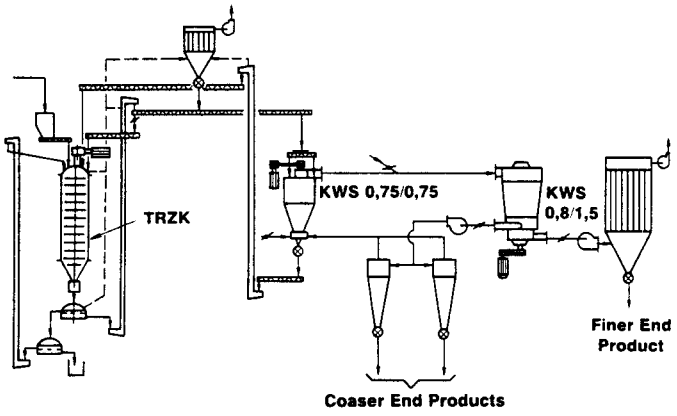

Fig. 11. Flow sheet of a small-media dry grinding and air classification system.

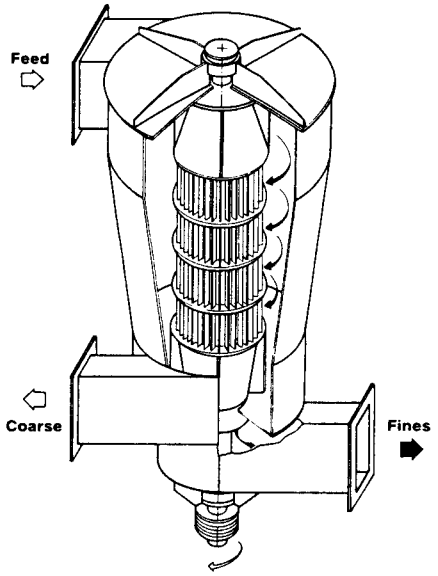

Fig. 13. Air classifier KWS 8/1.5.

Properties of Aluminum Hydroxide

Depending on the final processing techniques, the physical and chemical properties of aluminum hydroxide can be varied tremendously. While all the properties of hydroxide are important, particle size is probably one of the most important when considering use across the extremely wide range of applications. Although there are 12 to 15 particle-size measurement techniques in use today for aluminum hydroxides, and this continues to be an evolving technology, currently two stand out as being most useful over the size ranges discussed. For the coarse end of the range (30 to 150 μm) the most widely used technique is laser-beam light scattering by the particles as measured by a commercial process instrument[§§] (Fig. 14). For the finer end of the range (0.3 to 30 μm) a sedimentation technique using an X-ray detector in a commercial laboratory instrument[¶¶] has performed satisfactorily (Fig. 15).

The type of information that can be extracted from these instruments is shown in Fig. 16. The median particle size is the most repeated number and it is found for each product by following the 50% line to the product curve horizontally from the *Y* axis and dropping vertically to read the particle-size diameter on the *X* axis. The next most important piece of information from this type of analysis is the particle-size distribution. Broad distributions like C-130 (Fig. 16) start at the coarser end of the chart (indicating that some particles are near 50 μm) and go all the way to the fine end, indicating that some particles are near 2 μm. On the other hand, a narrow (or sharp) distribution product like H-705 has an almost vertical curve, indicating that most particles are right around the median of 0.5 μm.

[§§]Microtrac, Leeds & Northrup, North Wales, PA.
[¶¶]Sedigraph, Micromeritics Instrument Corp., Norcross, GA

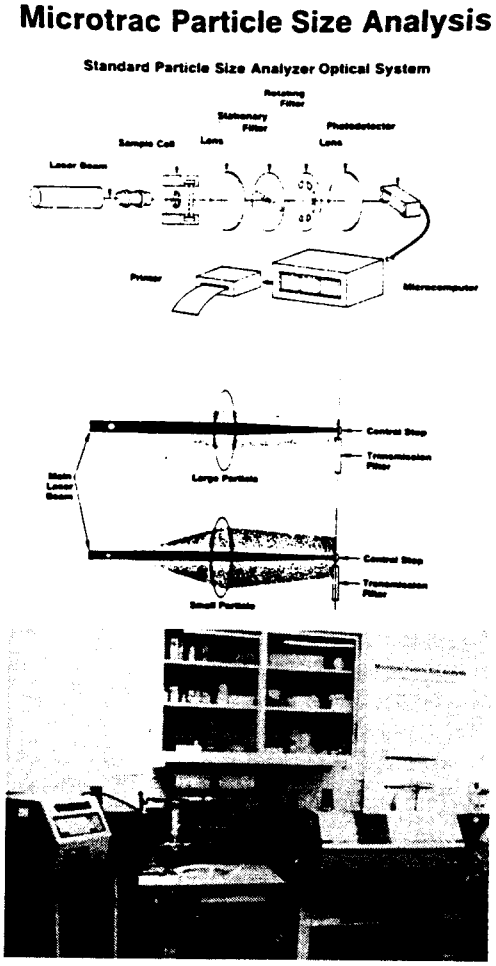

Fig. 14. Leeds & Northrup Microtrac.

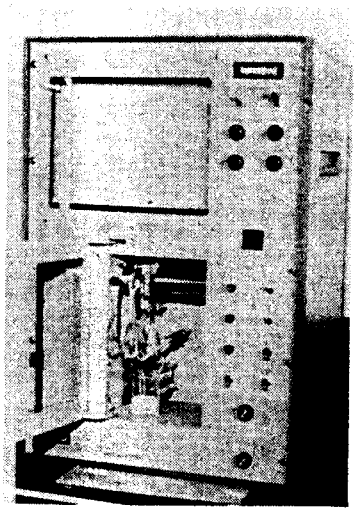

Fig. 15. Micromeritics sedigraph.

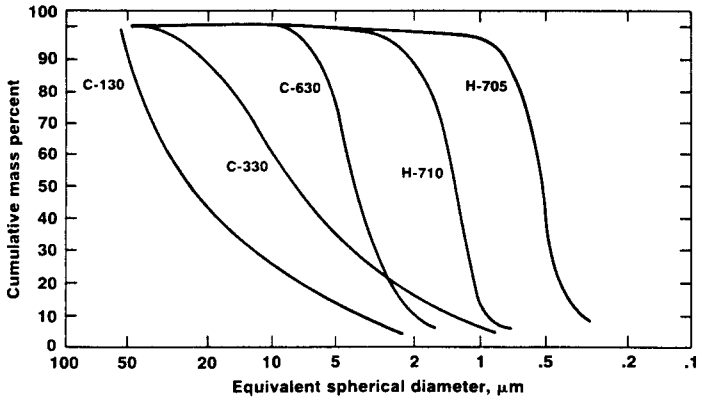

Fig. 16. Sedigraph analysis of several grades of aluminum hydroxide.

This sharp distribution of monosized particles (individual crystals in the case of precipitated products) can be clearly seen in the photomicrographs of C-30, a coarse precipitate using an × 100 magnification (Fig. 17) and H-710, a fine precipitated product (in Fig. 18 at × 5000 magnification). The broader particle-size distribution- (Fig. 16, C-130, C-330) type products are represented by Fig. 19, a ground Bayer-type hydrate. Note the irregular chips and pieces of all sizes and shapes that occur during primary crystal grinding.

Particle-size median, distribution, and particle shape are extremely important in the application of these products since they can severely affect processing properties and final physical properties of the system in which they are used. This is especially true in polymer parts, paper products, dentifrice products, adhesives, and fine polishing products. Details on these effects will be covered in the section on applications.

Chemical and physical properties of examples of the coarse grades of aluminum hydroxides are shown in Table II. Key differences to note can be seen by comparing the C-30 (Bayer) and C-31 (white aluminum hydroxide) columns. The main inorganic impurity differences are in silica (SiO_2), iron (Fe_2O_3), and soda (Na_2O). Other minor impurities may include zinc, calcium, gallium, titanium, manganese, and magne-

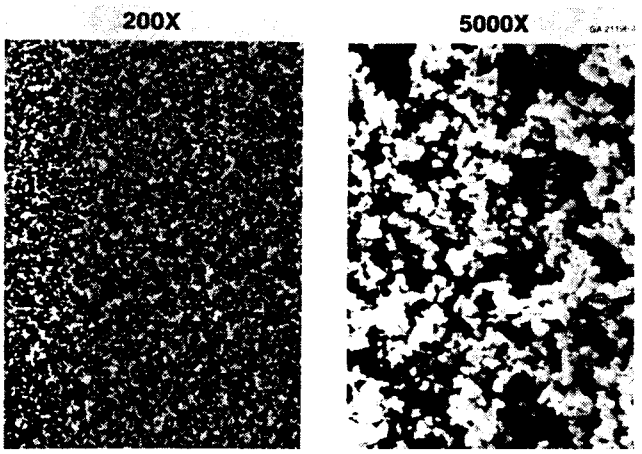

Fig. 18. H-710 fine precipitated aluminum hydroxide.

Fig. 17. C-30 coarse precipitated aluminum hydroxide.

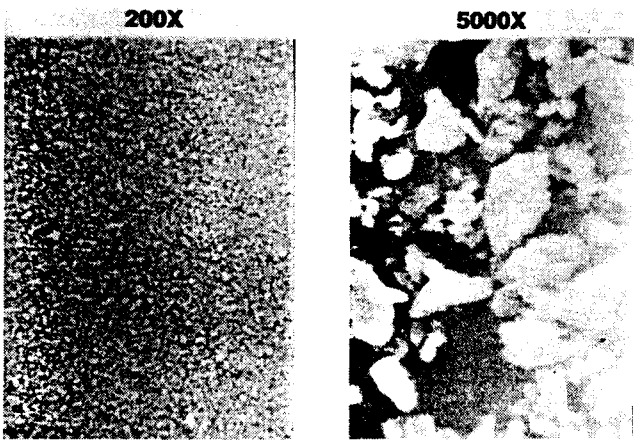

Fig. 19. SB-732. A typical ground Bayer aluminum hydroxide.

Table II. Chemical and Physical Properties of Coarse Hydroxides

Typical Properties	C-30		C-31	C-31 Coarse	C-37
Al_2O_3 (%)	65.0 (64.5 min)		65.0 (64.5 min.)	65.0 (64.5 min)	64.2
SiO_2 (%)	0.015 (0.04 max)		0.01 (0.02 max)	0.01 (0.02 max)	0.07
Fe_2O_3 (%)	0.015 (0.04 max)		0.004 (0.005 max)	0.004 (0.008 max)	0.004
Na_2O (% total)	0.3 (0.4 max)		0.15 (0.2 max)	0.2 (0.35 max)	0.5
LOI 110-1100 C (%)	34.5		34.5	34.5	34.5
Moisture (% at 110C)	0.1 (0.4 max)		0.04 (0.1 max)	0.04 (0.1 max)	0.2
Bulk density, loose, g cm^3	1.2 - 1.4		1.0 - 1.1	1.1 - 1.3	080 - 1.0
Bulk density, packed, g cm^3	1.5 - 1.7		1.2 - 1.4	1.4 - 1.6	1.0 - 1.1
Specific gravity	2.42		2.42	2.42	2.53
Mohs' hardness	2.5 - 3.5		2.5 - 3.5	2.5 - 3.5	2.5 - 3.5
Surface area, m^2 g	0.1		0.15	0.1	0.2
Refractive index	1.57		1.57	1.57	1.58
Color	off-white		white	white	off-white
Particle size analysis* (cumulative)	Bauxite	Pt. Comfort			
% on 100 mesh	0 - 5	0 - 10	0 - 1	0 - 10	6 - 12
% on 200 mesh	35 - 75	60 - 80	2 - 15 (max)	35 - 85	30 - 60
% on 325 mesh	80 - 96	94 - 98	25 - 70	80 - 98	75 - 95
% through 325 mesh	4 - 20	2 - 6	30 - 75	2 - 20	5 - 25

*Tyler Standard Screen Series

Table III. Physical Properties of Fine Precipitated Aluminum Hydroxides

Typical Chemical Analysis	Hydral 705	Hydral 710	Hydral 710B	Hydral PGA	Hydral PGA-B	Lubral 710
Al_2O_3 (%)	64.1	64.1	64.7	64.7	64.7	64.0
SiO_2 (%)	0.04	0.04	0.07	0.04	0.07	0.04
Fe_2O_3 (%)	0.01	0.01	0.02	0.01	0.02	0.01
Na_2O (% Total)	0.60	0.45	0.45	0.45	0.45	0.45
Na_2O (% Soluble)	0.22	0.10	0.10	0.10	0.10	0.10
Moisture (% at 110°C)	0.3 - 1.0	0.3 - 1.0	0.3 - 1.0	0.3 - 1.0	0.3 - 1.0	0.3 - 1.0
Lubral Content (%)						1.0
Typical Physical Analysis						
Bulk density, loose, g/cm^3	0.08 - 0.14	0.13 - 0.22	0.13 - 0.22	0.35	0.35	0.13 - 0.2
Bulk density, packed, g cm^3	0.09 - 0.20	0.26 - 0.45	0.26 - 0.45	0.70	0.70	0.23 - 0.4
Specific gravity	2.42	2.42	2.42	2.42	2.42	2.42
Surface area, m^2/g*	12 - 15	6 - 8	6 - 8	6 - 8	6 - 8	6 - 8
Mohs' hardness	2.5 - 3.5	2.5 - 3.5	2.5 - 3.5	2.5 - 3.5	2.5 - 3.5	2.5 - 3.5
Refractive index	1.57	1.57	1.57	1.57	1.57	1.57
Color	white	white	near white	white	near white	near white
GE brightness	94+	94+	90+	94+	90+	90+
Particle size analysis (cumulative						
% on 325 mesh	0.18 (max)	0.15 (max)	0.15 (max)	0.15 (max)	0.15 (max)	0.15 (max)
% less than 3 μm**	100	90	90			90
% less than 1 μm	90	50	50			50
% less than 0.5 μm	50	10	10			10

*Surface area measured by Brunauer-Emmett-Teller method of nitrogen adsorption
**As determined by electron microscope on a weight basis

sium. Organics are also extremely low-level. Although generally described in terms of grams per liter found in liquor, they can also be measured with very sophisticated chromatographic techniques after extraction from the solid hydroxide crystals. Almost always classified as some form of humic acid, the only standard analytical, relatively quick technique used with repeatability for detection has been percent carbon analysis. For white hydroxides the carbon generally ranges from 0.00% measurable to 0.01%, and for Bayer hydroxides from 0.01 to 0.1 wt%.

Table III shows the chemical and physical properties of the fine, precipitated aluminum hydroxides. Both Tables II and III show surface area values. For the particle-size range listed (0.5 to 80 μm), the surface area ranges from 15 to 0.10 m^2/g. Surface area can be a very useful tool to complement particle size in efforts to determine effects in polymer systems and other hydroxide additive applications. If a 0.5-μm product, for example, with what appeared to be a normal particle-size distribution had a repeatable surface area of 20 m^2/g (rather than the typical 15 m^2/g), one could expect some ultrafine particles, not easily measured by sedigraph, to be present. This could create high apparent viscosities or other problems related to dispersion in a polymer system. Surface area, on the other hand, is only a one data point result and should not be used independently with hydroxides to draw conclusions.

Another important property to note from Table III is the packed bulk density range from 0.09 to 0.7 g/cm^3. At the low end these materials cannot be handled in bulk. One supplier has developed a product that is loosely agglomerated and, while strong enough to hold together during shipping and handling, will break down easily into individual crystals when mixed into most polymer, paper, or adhesive applications. Figure 20 shows the appearance of these loose agglomerates at low and high magnification. This can be compared with the same product as individual crystals in Fig. 18.

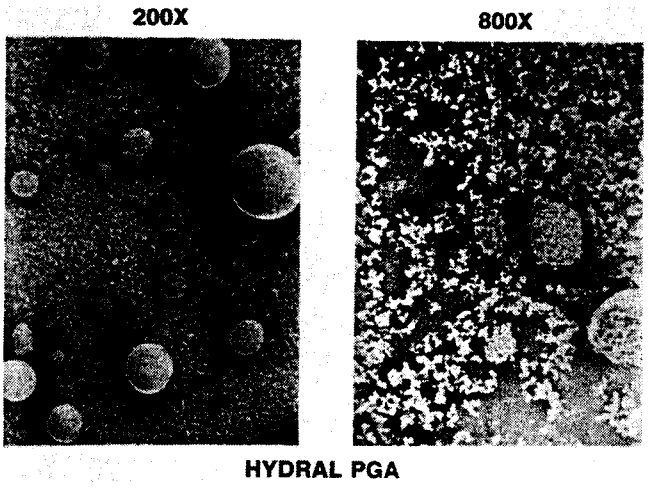

Fig. 20. Loose agglomerates of fine hydroxide crystals formed by spray drying.

Aluminum hydroxide is very different than anhydrous alumina, Al_2O_3, which can be abrasive (Mohs hardness 9, density 3.98 g/cm^3). Alumina trihydrate is

nonabrasive, more like calcium carbonate with a Mohs hardness of 2.3 to 3.5 and a density of 2.42 g/cm^3. Alumina trihydrate has a refractive index of 1.58, which is similar to that of several polymer resins, allowing it to be used with other pigments for a unique in-depth onyx or synthetic marble look.[56] Also important to pigmenting is the color or whiteness of the aluminum hydroxide.

Whiteness in terms of brightness can be controlled over the range of ≈50 to 100% GE brightness as measured by TAPPI Standard T-452. Color is a complex variable tied to many steps in processing but, at a given particle size, shape, and texture, assuming no tramp contamination, color can be correlated to the type of trace impurities found in the crystal structure.

Figure 21 shows how whiteness can be related to five primary colors in the spectrum: black, red to green, and yellow to blue. Generally, Bayer aluminum hydroxides would be in the positive L, b, and a axes. The goal for white aluminum hydroxides is high positive L with near-zero a and b. Currently, the whitest color and highest purity commercial ATH products come from non-Bayer processes. Ultrafine white grades are bright enough to be used alone or as pigments to displace up to 21% TiO_2 in some applications.

As we discussed in the processing section, aluminum hydroxides are insoluble in water and essentially inert between pH 3.5 and 10.5. The isoelectric point is 9.2, and although chemically stable at this pH, the particles may tend to flocculate. Generally, ATH is also considered to be nontoxic and FDA safe for food-packaging applications.

A very important property of aluminum hydroxides that will be covered in much greater depth in the applications section is the ability to create arc and track resistance in a polymer system. Research has shown that, as high voltage creates heat and electrical breakdown of polymer insulators due to salt, dirt or other carbonaceous materials build up on the surface.

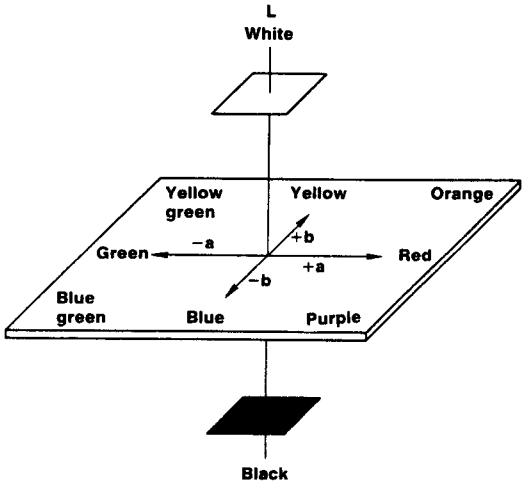

Fig. 21. Color space in terms of L, a, and b values.

Aluminum hydroxide first acts as a heat sink, then gives up oxygen which reacts with carbon to inhibit electrical tracking and insulator breakdown.

Fire Retardant/Smoke Suppressant Properties

While the concept of 34.6% chemically combined water in a dry powder that is stable to processing temperatures of many systems has already been shown, it should be noted that ATH is also unreactive to the curing chemistry of many polymer systems such as unsaturated polyester cross-linking, rubber vulcanization, polyurethane foam curing, or polyolefin copolymer cross-linking.[24] However, on heating to higher temperatures, the heat capacity of aluminum hydroxide keeps organic systems cooler longer. The heat capacity is 1.18 J/kg (0.282 cal/g) at 20°C and varies with temperature according to Eq. (2)

$$C = 0.2694 + 6.43 \times 10^{-4}\, T(°C) \qquad (2)$$

Above 220° to 230°C the hydrate (hydroxyl groups) begins to decompose endothermically. The considerable absorption of heat by this sacrificial decomposition of ATH makes less heat available for decomposing a polymer system into the low-molecular-weight fuel gases that support combustion. The by-products of decomposition are simply anhydrous alumina and water[24]

$$2Al(OH)_3 \rightarrow Al_2O_3 + 3H_2O \qquad (3)$$

The measured enthalpy (heat of dehydroxylation) has been shown to be 1172 J/kg (280 cal/g).[57] Graphically, this phenomenon is shown in Fig. 22 by comparative thermal gravimetric analysis (TGA) for weight loss and differential thermal analysis (DTA) to show the point of maximum weight loss and heat absorption with temperature for a coarsely ground hydrate. Figure 23, which shows a similar heat absorption analysis with ATH and heat release without ATH in a typical polymer system,[24] is a clear example of the transformation of an exothermic, fire-propagating system to an endothermic, fire-retarding system. Here the thermal analysis is compared using differential scanning colorimetry.

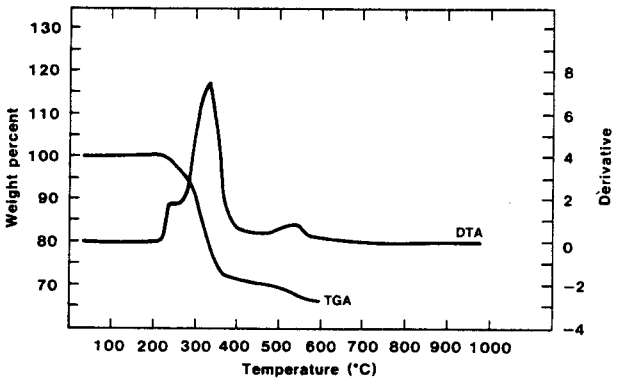

Fig. 22. Thermogravimetric analyses (20°C/min) for coarsely ground ATH.

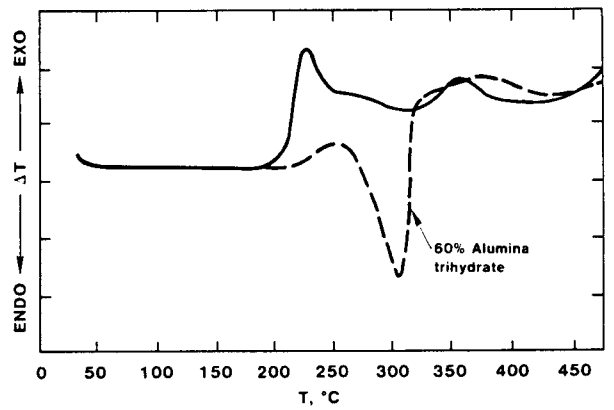

Fig. 23. DSC of GP polyester resin alone and filled with 60% ATH (Ref. 24).

Thermal analysis is used further in Figs. 24 and 25 to show some of the unique advantages of superfine precipitated alumina trihydrates as fire retardants. Figure 24 shows a slightly higher temperature starting point and a much smoother hydrothermal transformation and decomposition for the superfine precipitated hydrate than the coarsely ground hydrate shown in Fig. 22. In practice, this allows short-term higher temperature processing with superfine precipitates than the coarser materials. Figure 25 shows that more heat-absorbing capacity is available at the major endothermic peak because, substantially, all of the trihydrate decomposes at this temperature. Coarser materials have a more pronounced two-step decomposition with a second endotherm between 500° and 600°C. This is shown by the second small peak in the top curve in Fig. 22. Combining these two concepts leads to the conclusion that, while all aluminum hydroxides have tremendous value as fire retardants, the superfine (less than 1 μm) precipitated products can not only be processed at slightly higher temperatures, but also are more efficient when decomposition due to a fire situation does take place.

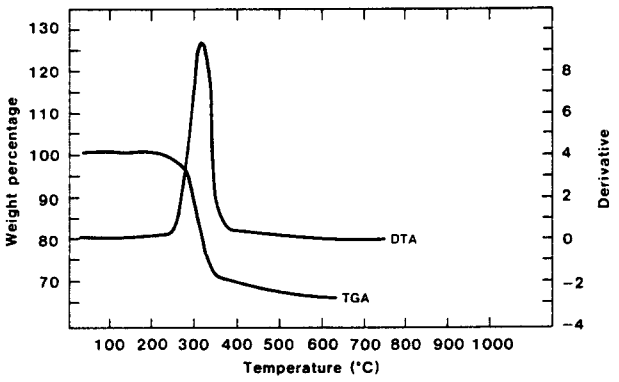

Fig. 24. Thermogravimetric analysis (20°C/min) for Hydral 710 precipitated ATH.

Commercial Products Available

Commercial aluminum hydroxides are available in North America from several primary and secondary producers. The principal suppliers are listed below.

Supplier	Supplier Type	Hydrate Type
Alcan Aluminum Corp. 111 W. 50th Street New York, NY 10020 Tel. (212) 582-2070	Primary	Bayer
Aluchem One Landy Lane Reading, OH 45215 Tel. (513) 733-8519	Secondary	Bayer
Aluminum Company of America P.O. Box 300 Bauxite, AR 72011 Tel. (800) 643-8771	Primary	Bayer white
AMAX Climax Polymer Additives Group AMAX Center Greenwich, CT 06836 Tel. (203) 629-6214	Primary and Secondary	Bayer white
Kaiser Chemicals Division of Kaiser Aluminum and Chemical Corp. P.O. Box 1031 Baton Rouge, LA 70821 Tel. (504) 293-9761	Primary	Bayer
Reynolds Chemicals Division Reynolds Metals Co. Richmond, VA 23261	Primary	Bayer
Solem Industries Inc. 5824-D Peachtree Norcross, GA 30092 Tel. (404) 441-1301	Secondary	Bayer white

The secondary suppliers start with the primary coarse grades, then grind, classify, and surface-modify to meet specific end application requirements. Each of the principal secondary suppliers and other smaller aluminum hydroxide processors usually have specific niche markets they service.

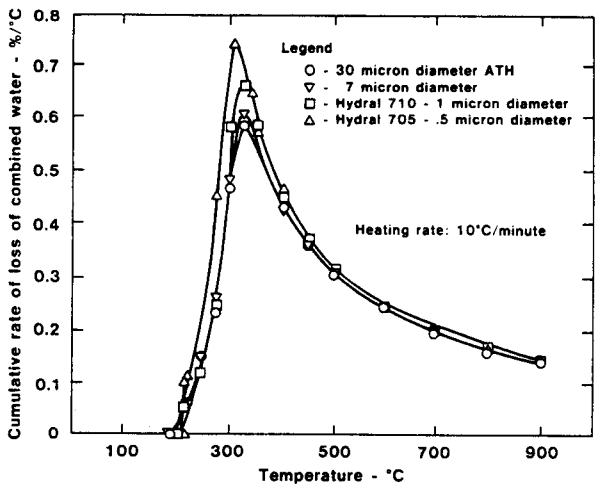

Fig. 25. Cumulative rate of loss of combined water vs temperature from TGA data.

Small quantity volumes and applications service are also provided by distributors. The largest volume distributor of these materials on the West Coast is

Schoofs Incorporated
1675 School Street
Moraga, CA 94556
Tel. (413) 376-7311

and on the East Coast is

Whittaker, Clark & Daniels Inc.
1000 Coolidge Street
South Plainfield, NJ 07080
Tel. (201) 561-6100

Applications

Although the wide range of additive uses for aluminum hydroxides will be covered in more detail in a later section, the principal additive applications are listed here for reference. They include carpet, paper, pharmaceuticals, cosmetics, adhesives, polishes, glass, dentifrices, and polymers. Polymer uses include plastic products, rubber products, coatings and paints for fire retardance, smoke suppression, toxicity reduction, impact resistance, uv weathering resistance, color, arc and track resistance, processing improvements including polymer crystal growth optimization, esthetic appearance improvements, etc. in specific applications. The other major uses include aluminum hydroxides as feedstocks to a wide range of aluminum chemicals from aluminum sulfate for water treatment to aluminum hexachlorohydrate for antiperspirants. They are also the feedstocks for producing most alumina-based ceramics, refractories, and adsorbent/desiccant materials. The major direct chemical applications are as the base reactant[58] for sodium aluminate, zeolites, alum, aluminum fluoride, and titanium dioxide manufacture.

Since the other feedstock applications will also be covered elsewhere, only the five largest direct chemical applications will be mentioned here in slightly more detail. The largest seller of true white pigments is titanium dioxide. This is because of its unequaled whitening and opaquing hiding power. Initially used primarily in exterior paints, enamels, and lacquers, then in paper manufacture, now the fastest growing TiO_2 use is in finished goods in the plastics industry, followed by the rubber, wall and floor covering, leather, and textile industries.

The flowchart covering the two basic titanium dioxide manufacturing processes is shown in Fig. 26. Both processes are still used to produce the more than 5.6 billion pounds of TiO_2 that is consumed annually worldwide. Although prices have faltered recently, both prices and demand are again on the rise, a phenomenon that has allowed the price to more than triple in the last 25 years. The use of aluminum hydroxide in titanium dioxide manufacture is primarily for the production of TiO_2 treating chemicals.

For example, in the chloride process, aluminum trichloride is added in proprietary steps to help produce the rutile form of titanium dioxide and adjust the crystal size. Both the sulfuric acid and chloride-process TiO_2 forms require posttreatments to be stable to uv and other photo/chemical forms of degradation. Alumina compound coatings, generally in the range of 2 to 5 wt%, are used. In special cases where extreme durability is required, 7 to 10 wt% is used. Without these coatings, degrading TiO_2 gives off species that

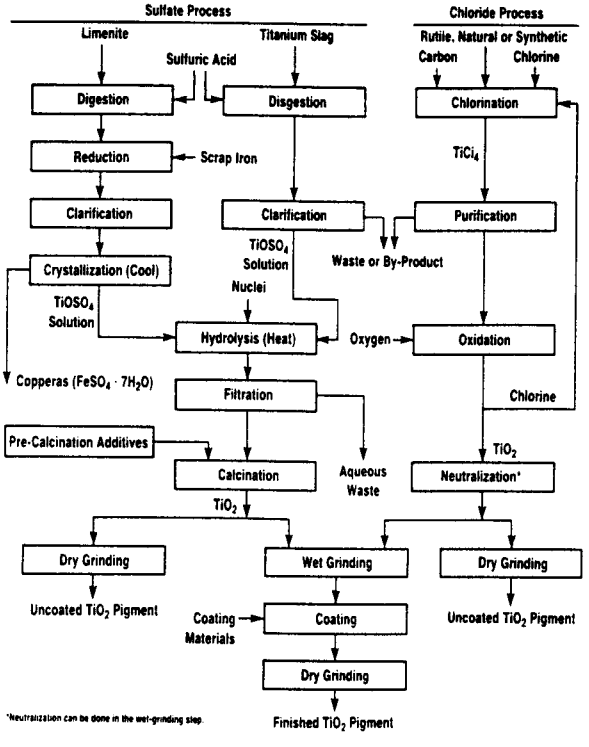

Fig. 26. Titanium dioxide manufacturing processes.

oxidize organics (degrade polymers) in paints, rubbers, and plastics. Other benefits of alumina coating of TiO_2 are better flow in polymer systems, more chalking resistance, better general weathering, and better dispersion. Most treating processes are also proprietary but, generally, after wet grinding, processing is used that causes a thin crust of alumina, silica, or a combination of photochemical stable minerals to be formed on the TiO_2 surface.

Sodium aluminate is produced by the simple reaction of aluminum hydroxide with clean caustic solution to make chemical feedstock for papermaking, water-treatment chemicals, and other applications. The most difficult parameters to overcome are solution stability and color. The high loadings of dissolved solids, usually in the range of 30% or more, require special handling of solutions so fragile that trace impurities can destabilize the liquor and cause cloudiness and viscosity increases that are unacceptable in the marketplace.

High-purity and consistent-quality aluminum hydroxide grades have helped this industry grow, but sometimes special surfactant technology[59] is required. The longer the shelf life needed, the more difficult this problem becomes. One attempt to get around this problem was with the manufacture of dry solid sodium aluminate. However, this product often has solubility difficulties because it tends to clump with moisture, creating handling problems and larger agglomerates that do not dissolve readily. The best results seem to be obtained with reactive and nonreacting stabilizing and clarifying agents in the highly concentrated sodium aluminate liquor.

The third major industrial chemical use for aluminum hydroxide is the alum industry. Primarily prepared industrially today by the reaction of aluminum hydroxide and sulfuric acid in water, alum production has been around as long as the early Egyptian pyramids. Although a true alum is a double sulfate of aluminum, the terms *alum* or *papermaker's alum* are generally used to cover all forms of aluminum sulfates.

The Egyptians used alum as a mordant and in medical preparations. The Romans used it for fireproofing equipment and fortresses. Today, it is used as a sizing agent or precipitant in the paper industry and as coagulating agents in water purification or flocculation agents in other liquid purification systems. However, there are still many pharmaceutical uses such as a mild astringent and antiseptic for the skin. Other uses of alum include the preparation of insoluble complexes in dyes, pigment extenders in printing inks, fire extinguisher CO_2-producing agents, paper-coating reactants, for the purification of glycerin from soap, and to recover fats and oils in meat-packing solutions by flocculation.

The largest application, more than half of alum usage, is as the primary chemical coagulant to clarify municipal and industrial water supplies. The producers for these applications are changing slowly. Originally, they were large stable chemical companies; now, more and more individual entrepreneur facilities are being opened close to the large and mid-sized paper plants and municipal water-treatment plants.

Normally, alum is produced in two grades—an industrial grade which uses Bayer aluminum hydroxide and a low-iron grade which requires white, stream aluminum hydroxide. The industrial production procedure generally is to disperse the aluminum hydroxide in water in large conical reactors, then add roughly 60° Baume sulfuric acid. Addition times, temperatures, and final concentrations are proprietary to individual manufacturers, but in many cases a 35.5° to 36.5° Baume solution is decanted at ambient temperature. Typical conditions might be 107° to 124°C, 1- to 1.5-hour reaction time at pH 1.8 to 4, and 0.4 to 0.5% excess alumina. The reaction can be represented as:

$$2Al(OH)_3 + 3H_2SO_4 + 8H_2O \rightarrow Al_2(SO_4)_3 + 14H_20 \quad (4)$$

In some cases, a solid alum is required and for these applications the water is evaporated until the alumina content is increased to about 17 wt%. The problems with dry alum are: it is usually more expensive, measurements cannot be controlled as accurately, because of packaging considerations it requires more space to store than liquid alum, more labor is necessary to load and unload, and dissolving operations are needed with dry alum.

The largest industrial chemicals use of aluminum hydroxide has been in zeolite production. Zeolites are hydrated silicates of aluminum which are based on either sodium or calcium. Materials formed using aluminum hydroxide as a reactant are normally described as synthetic zeolites. They can range in form from gritty, sandlike, and porous to gelatinous, but are all extremely versatile materials. Zeolite-based materials are so versatile that it would be difficult to list all the possible applications in detail.

Some of the major primary application uses are as ion-exchange resins, catalysts, water softeners, detergent builders, and sorption agents. These concepts in turn are used in cracking and reforming for improved petroleum products, in hydrocarbon conversion (for example, *p*-xylene production for the manufacture of terephthalic acid for polyester production), and in an unbelievably fast-growing series of catalytic and sorptive gas, liquid and solid selective chemical cleanup, scavenging and antipollution devices. One of the earliest uses of zeolite industrially was in ion exchange for the removal of ammonia from liquids by passing the liquids through clays.

Synthetic zeolites are often described as porous, crystalline alumina silicates with a regular structure. Some examples are shown in Fig. 27. Many of the problems associated with high-purity aluminum hydroxide manufacture are also found in zeolite production. Gel formation, scale buildup, chemical impurity concentration in recycling streams, liquor color, and

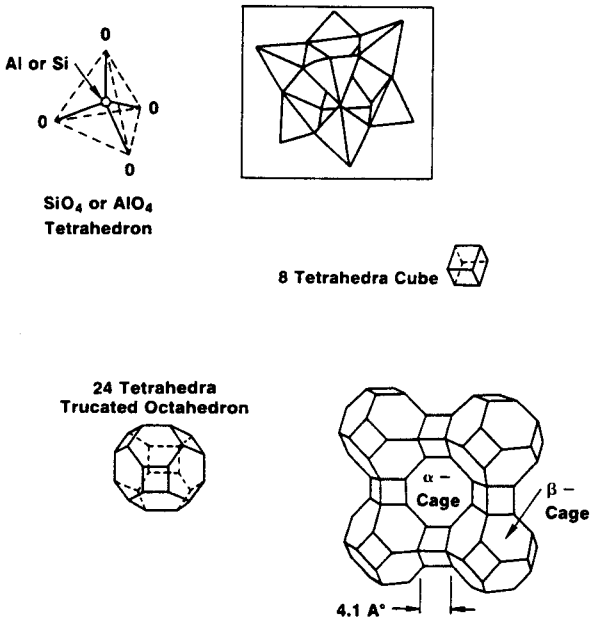

Fig. 27. Zeolite A crystal structure.

quality affect zeolite color, quality, etc. This should not be surprising since zeolite-producing liquors start with the reaction of sodium silicate liquor and sodium aluminate (Bayer-type) liquor.

An example of a crude continuous reactor system flow diagram for the production of crystalline zeolite A is shown in Fig. 28.[60] Before the process shown in Fig. 28 was developed (late 1960s), most of the processes for producing synthetic crystalline zeolites were batch-type processes. Some are still in use today. The

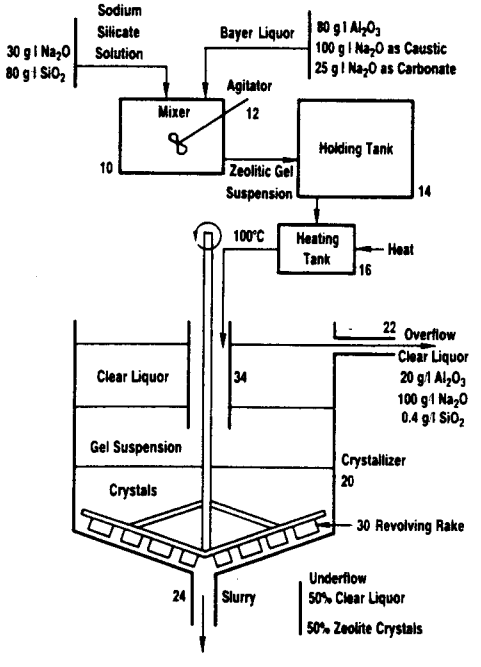

Fig. 28. Production of crystalline zeolites (Ref. 60).

concept was to obtain molecular sieves for applications of the types described above with the highest possible sorptive unit volume capacity by the elimination of inert gel diluent. This type of invention was followed in the 1970s and to this day by a host of process and product improvements.[61–77]

Aluminum fluoride (AlF_3), made from aluminum hydroxide, is an important chemical because of its use as a component of the fused cryolite ($AlF_3 \cdot 3LaF$) solvent for electrolyte reduction of alumina to aluminum in the Hall process.[78] There are two processes available for aluminum fluoride production. The older, known as the dry process, involves reacting aluminum hydroxide with HF gas, generally in a multiple-stage fluid bed reactor. The following reaction takes place at temperatures above 500°C.

$$Al(OH)_3 + 3HF \rightarrow AlF_3 + 3H_2O \quad (5)$$

The resulting product is ≈92% AlF_3 with 0.3% SiO_2. The HF gas is produced by reacting fluorspar (CaF_2) with sulfuric acid (H_2SO_4) at a high temperature.

A second process for producing higher purity AlF_3 than is obtained with the dry process involves wet reaction of $Al(OH)_3$ and fluosilicic acid (H_2SiF_6), a by-product of the phosphate fertilizer industry. The aqueous reaction is as follows:

$$Al(OH)_3 + H_2SiF_6 \rightarrow 2AlF_3 + SiO_2 + 4H_2O \quad (6)$$

Heating and/or agitating the unstable AlF_3 solution precipitates $AlF_3 \cdot 3H_2O$. This product is then calcined to remove the water of crystallization. The resulting product is 96% AlF_3, with only 0.07% SiO_2.

Although the principal use of aluminum fluoride is for smelting of aluminum, there are many other uses. Some of the better-known applications include use as a flux in brazing, and for removing magnesium in the refining of aluminum scrap. In the ceramic industry, aluminum fluoride is used in body compositions and glazes and for specialty refractories, as well as a constituent in fine glass compositions and for manufacture of aluminum silicates.

Current and Projected Usage Trends

Estimated domestic U.S. consumption of ATH sold as aluminum hydroxide was almost 900 million pounds in 1986, with a 45/55% split between the additive/chemical applications. Projections[79] have portions of the additive applications sector requiring as much as 553 million pounds by the early 1990s.

World usage of alumina sold as aluminum hydroxide plus that used as an ATH feedstock to the refractories and ceramic industries has been estimated at over 7 billion pounds, with roughly one-half of the estimate sold as aluminum hydroxide.[80] While most markets show some growth, the polymer, additive chemical adsorption unit, and fire-retardent markets have the largest rate of growth projections for materials sold as hydroxides.

References

[1]J. D. Edwards; pp. 166–68 in The Aluminum Industry. McGraw-Hill, New York, 1930.

[2]L. K. Hudson, Alumina Production. Alcoa Research Laboratories, Alcoa Center, PA, 1982.

[3]L. K. Hudson, C. Misra, and K. Wefers, Aluminum Oxide. Ullmans Encyclopedia of Industrial Chemistry, Vol A1, 1985.

[4]K. Wefers and G. M. Bell, Technical Paper 19, Aluminum Company of America, 1972.

[5]G. MacZura et al., Aluminum Compounds. Kirk Othmer Encyclopedia of Chemical Technology, Vol. 2, 3d ed. Wiley & Sons, 1978.

[6]A. C. Kelly et al., U.S. Pat. No. 3 623 837, Kaiser Aluminum & Chemical, 1971.

[7]U. Hauschild, U.S. Pat. No. 3 222 130, Kai Chemical, 1965.

[8]R. A. Van Nordstrand et al., *Nature (London)*, **177**, 713 (1956).

[9]U. Hauschild, *Anorg. Allg. Chem.*, **324**, 15–20 (1963).

[10]C. Y. Chuo, J. Baker, P. S. Sabina, and A. C. Roberts, *Can. Mineral.*, **23**, 21 (1985).

[11]K. Wefers and C. Misra, Oxides and Hydroxides of Aluminum. Alcoa, 1987.

[12]R. Ray and E. F. Osborn, *Am. Mineral*, **39**, 853–85 (1954).

[13]A. W. Laubengayer and R. S. Weiss, *J. Am. Chem. Soc.*, **65**, 247–50 (1943).

[14]G. Ervin and E. F. Osborn, *J. Geol.*, **59**, 381–94 (1951).

[15]K. Wefers and E. Gau, *Mettallhuettenwesen*, **20**, 13-9, 71–75 (1967).

[16]G. C. Kenedy, *Am. J. Sci.*, **257**, 563–73 (1959).

[17]A. Neuhaus and H. Heide, *Ber. Dtsch. Keram. Ges.*, **42**, 167–84 (1965).

[18]I. Valeton, Bauxites. Elsevier, New York, 1972.

[19]H. Ginsberg and M. Koster, *Anorg. Allg. Chem.*, **271**, 41–48 (1952).

[20]J. Bugosh, U.S. Pat. No. 2 915 475, December 1, 1959.

[21]Bureau of Mines Report RI-7664.

[22]Dana's Mineralogy, 7th ed., Vol. II. 276, 1944.

[23]S. Mizata, *Clay Mineral.*, **28**, 50–56 (1980).

[24]L. L. Musselman and T. L. Levendusky, "Precipitated Alumina Trihydrate for Polymers," SPE 1984 RETEC, Georgia Institute of Technology, October 22, 1984.

[25]F. Orbon, G. Sigmond, P. Seklosi, K. Solymar, and J. Steiner, "Advances in Bayer Process Design," *J. Geol. Soc. Jamacia*, Bauxite Symposium No. IV, June 22, 1980.

[26]K. B. Bengston et al. and Kaiser Aluminum Corp., *Trav. Com. Int. Etude Bauxites, Alumina Alum.*, **16**, 109–32 (1981).

[27]K. B. Bengston, *Light Metal*, 217–82 (1979).

[28]H. W. St. Clair, D. A. Elhers, Wm. Mahan, R. C. Merritt, M. R. Howcroft, and M. Hayashi, Bulletin 577, U.S. Bureau of Mines, 1959.

[29]"Hardinge Mills for Dry Grinding," Bulletin 17-C, Hardinger Co., York, PA, 1976.

[30]"Particle Size Classifiers]—]A Guide to Performance Evaluation," AIChE Equipment Testing Procedure, 1980.

[31]"Comminution and Energy Consumption," National Materials Advisory Board, NMAP-364, PB 81–225708, National Technical Information Service, Springfield, VA. 128–50, May 1981.

[32]P. N. Cheremisinoff and R. A. Young; pp. 246–315 in Air Pollution Control and Design Handbook, Part 2. Marcel Dekker, New York, 1980.

[33]R. S. C. Rogers, "Coal Materials Handling: Classifier Evaluation," Quarter Progress Report, DOE/MC/14266–73, Kennedy-Van Saun Co., Danville, PA, 1973.

[34]"Model 8020 RDC Rotary Drum Classifier, Form 15231," Iowa Manufacturing Corp., Cedar Rapids, IA (1979).

[35]"GE Classifiers," attachment to "International Environmental Services," Bulletin S258R1/1282/7–5M, General Electric Co., Lebanon, PA, 1977.

[36]"Grit Separator," Data Sheet D-1347, Sturtevant, Inc., Boston, MA, December 1980.

[37]"Production and Laboratory Equipment," Catalog No. 018, 11/73–LP–10M, Alpine American Corp., Natick, MA, 1973.

[38]"Acucut Laboratory Classifier," Bulletin 9810–4, Donaldson Co., Majac Division, Minneapolis, MN, undated.

[39]"Centri-Sonic Classifier," Bulletin G–8D, CE Bauer, Springfield, OH, 1971.

[40]"Air Separators," Bulletin AS–B–083, Sturtevant, Inc., Boston, MA, 1983.

[41]"Cyclone Air Classifier," Bulletin 3–440e, HDK Industrieanlagen Humboldt Wedag, Cologne, Germany, 1976.

[42]"TURBOPOL Turbo Separator," Bulletin 1269E (2.5981FM), Polysius, AG, Beckum, Germany.

[43]"Majac Jet Pulverizers and Air Classifiers," Bulletin 2000–1, Donaldson Co., Majac Division, Minneapolis, MN, 1973.

[44]T. Misakav, T. Furukawa, and E. Onuma, "Air Classifier," U.S. Pat. No. 4 296 864, Onoda Cement Co., Tokyo, Japan, October 27, 1981.

[45]R. R. Saverse and H. T. Jones, "Particle Classifier," U.S. Pat. No. 4 551 241, November 5, 1985.

[46]Progressive Industries, "Microsizer," U.S. Pat. No. 4 257 880. [47]B. Mohanty and K. S. Narasimhan, "Fluid Energy Grinding," Regional Research Laboratory, Bhubaneswar (India), January 28, 1982.

[48]J. Kriens, "Fine Mineral Processing Technology," 85e Congress Annual, Winnipeg, April 17, 1983.

[49]F. Matter, "Fine Media to Grind Process Minerals," SME-AIME Annual Meeting, Atlanta, GA, March 6, 1983.

[50]L. L. Musselman and T. L. Levendusky, "Surface Treatment of Alumina Trihydrate for a Better Resin System," *Modern Plastics*, February 1983.

[51]T. Z. Keating, "Aluminum Trihydrate," *Plastics Compounding*, 7 23, (1986).

[52]L. L. Musselman and T. L. Levendusky, "Alumina Trihydrate as a Flame Retardant and Smoke Suppressant Additive in the Development of a Commercial Flame Retardant Polypropylene," SPE 38th Annual Technical Conference, Chicago, IL, May 2, 1983.

[53]L. L. Musselman and T. L. Levendusky, "Surface Modified Alumina," Society of the Plastics Industry 40th Annual Conference, January 28, 1985.

[54]L. L. Musselman and T. L. Levendusky, "Combination of Surface Modifiers for Powdered Inorganic Additives," U.S. Patent pending, Serial No. 783 863.

[55]"Ucarsil FR Organosilicon Chemicals for Flame-Retardant Polyolefin Applications," Bulletin SC–415B, Union Carbide Corp., Danbury, CT, 1987.

[56]L. L. Musselman and T. J. Austin, "New Chemical Products Enhance Appearance and Performance of Cultured Marble," Alcoa Publication F–35–14682, February 1987.

[57]G. V. Jackson and P. Jones, "The Heat of Dehydration of Alumina Trihydrate," *Fire Mater.*, **2** [1] 37–38 (1978).

[58]C. Misra, "Industrial Alumina Chemicals," ACS Homograph, 184, 1986.

[59]W. O. Layer and S. A. Khan, "Stable Aqueous Alkali Metal Aluminate Solutions," U.S. Pat. No. 4 252 735, February 24, 1981.

[60]W. Hirsh, "Production of Crystalline Zeolites," U.S. Pat. No. 3 425 800, February 4, 1969.

[61]B. E. Leach, U.S. Pat. No. 4 078 042, March 7, 1978.

[62]F. R. Kettinger, J. A. Landone, and R. H. Pierce, U.S. Pat. No. 4 150 100, April 17, 1979.

[63]L. D. Rollman, U.S. Pat. No. 4 107 195, August 15, 1978.

[64]L. D. Rollman, U.S. Pat. No. 4 139 600, February 13, 1979.

[65]L. D. Rollman, U.S. Pat. No. 4 146 589, March 27, 1979.

[66]C. J. Plank, E. J. Rosanski, and M. K. Rubin, U.S. Pat. No. 4 076 842, February 28, 1978.

[67]C. J. Plank, E. J. Rosanski, and M. K. Rubin, U.S. Pat. No. 4 021 447, May 3, 1977.

[68]C. J. Plank, E. J. Rosanski, and M. K. Rubin, U.S. Pat. No. 4 046 859, September 6, 1977.

[69]C. J. Plank, E. J. Rosanski, and M. K. Rubin, U.S. Pat. No. 4 175 114, November 20, 1979.

[70]C. J. Plank, E. J. Rosanski, and M. K. Rubin, U.S. Pat. No. 4 151 189, April 24, 1979.

[71]F. G. Dwyer and A. B. Schwartz, U.S. Pat. No. 4 091 007, May 23, 1978.
[72]D. E. W. Vangran, G. C. Edwards, and M. G. Barrett, U.S. Pat. No. 4 178 352, December 11, 1979.
[73]D. E. W. Vangran, U.S. Pat. No. 4 091 079, May 23, 1978.
[74]C. H. Elliot, U.S. Pat. No. 4 164 551, August 14, 1979.
[75]T. V. Whitram, U.S. Pat. No. 4 016 246, April 16, 1977.
[76]G. T. Kerr and A. W. Chester, U.S. Pat. No. 4 093 560, June 6, 1978.
[77]R. W. Grose and E. M. Flanigen, U.S. Pat. No. 4 129 686, November 7, 1978.
[78]L. D. Hart, unpublished consultation, July 30, 1987.
[79]BBC Study, Fire and Smoke Retardant Chemicals, 1985.
[80]G. MacZura, T. J. Carbone, and L. D. Hart, "Alumina Annual Ceramic Mineral Resource Review," *Am. Ceram. Soc. Bull.*, **66** [5] 753–54 (1987).

Production Processes, Properties, and Applications for Activated and Catalytic Aluminas

K. P. Goodboy and J. C. Downing
Aluminum Company of America
Pittsburgh, PA 15219

This paper is a broad overview of the major production processes of activated aluminas. The applications, by dollars, are approximately equally divided between hydrocarbon adsorption and catalysis. Since dehydration, selective adsorption, and Claus catalysis are major applications of activated alumina, only reference is made, since complete chapters on these topics appear in this book.

The thermal dehydroxylation (250° to 1150°C) of aluminum hydroxides results in the formation of activated alumina. The phrase "activated alumina" was a registered trademark of Alcoa, in reference to F-1 and H-151. Today the phrase applies to any alumina crystal morphology that is porous in structure and produced by thermal dehydration, which removes most of the water that is chemically attached as hydroxyls. Although these aluminas are primarily known as "activated," they are sometimes referred to as "active alumina."

Activated aluminas are being used increasingly in adsorption and catalysis where their large surface area, pore structure, and unique surface chemistry play essential roles. Activated aluminas are produced from aluminum hydroxides by controlled heating to eliminate most of the water of constitution. Their crystal structure is chi, eta, gamma, and rho alumina in the low-temperature range (250° to 900°C) and delta, kappa, and theta alumina in the high-temperature range (900° to 1150°C). These two thermal ranges produce aluminas which are collectively known as transition aluminas. Historically, activated aluminas were referred to as simply gamma alumina, which caused much confusion in the technical literature. Today the whole transition series is correctly called activated alumina. X-ray diffraction (XRD) cannot distinguish between gamma and eta aluminas when both are present; therefore, the phases are often written as gamma/eta alumina.

Figure 1 illustrates how the surface area, loss on ignition, and density of gibbsite (starting alumina phase) vary with increasing temperature. Figure 2 gives the corresponding phases in the thermal decomposition sequence of aluminum hydroxides. Figure 3 is a related phase diagram showing water of constitution with thermal dehydration of aluminas. Structural properties of the transition aluminas are given in Table I. Annual combined North American production capacity for activated alumina and monohydrates is estimated at 300 million pounds. Much of the monohydrate capacity is used captively to produce hydrotreating and other types of catalysts. Current activated alumina selling prices range from $0.40 to $3.00/lb, with the bulk of the activated alumina products ranging from $0.40 to $1.25/lb.

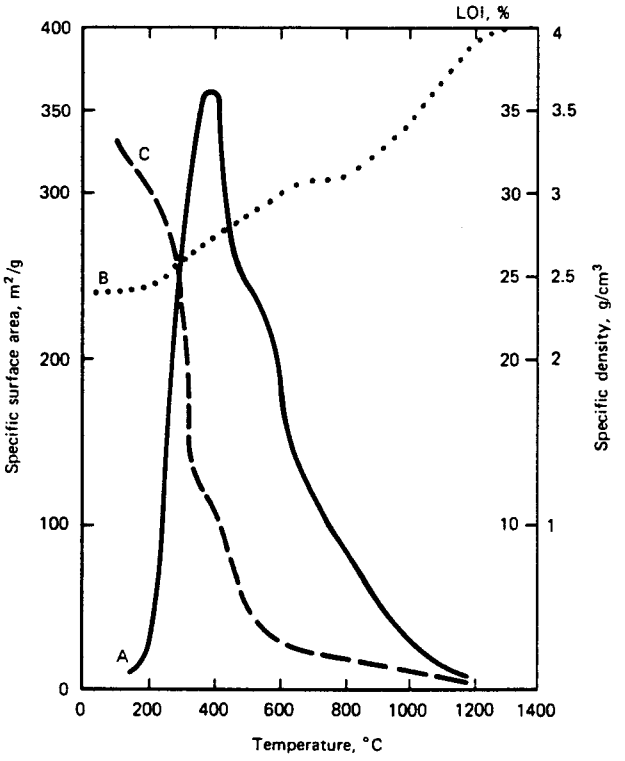

Fig. 1. (A) specific surface area. (B) specific density, and (C) loss on ignition of $Al(OH)_3$ with increasing temperature (Ref. 1). (Used by permission.)

Production Processes—Granular Products

Scale Type

The oldest commercial form of activated alumina, produced in millions of pounds per year and still

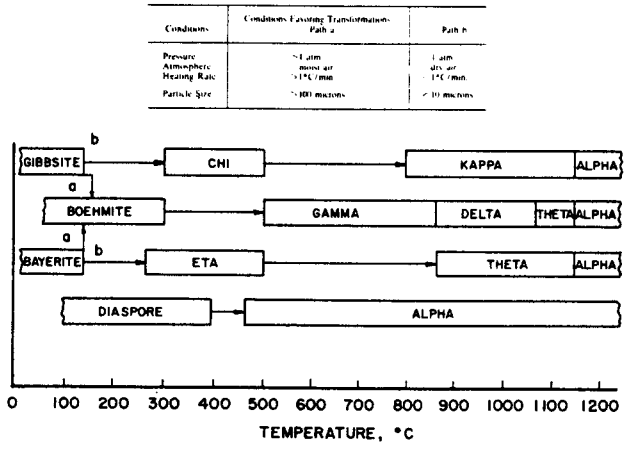

Fig. 2. Decomposition sequence of aluminum hydroxides. Enclosed area indicates range of occurrence; open area indicates range of transition.

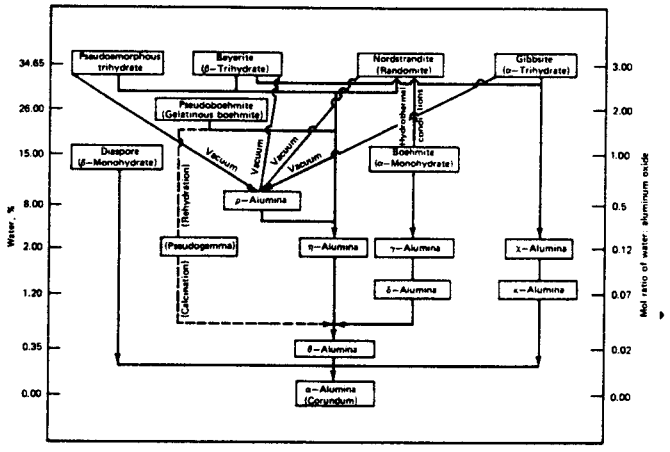

Fig. 3. Thermal degradation of aluminas (Ref. 2).

produced today, is made from Bayer alpha trihydrate.[3] This product, Alcoa F-1, first introduced in 1932, started the history of modern activated alumina. When producing metal-grade alumina from sodium aluminate solutions via the Bayer process, a small amount of gibbsite is deposited on the walls of certain precipitation vessels, where it forms a scale up to 1.5 m thick. This scale is removed periodically from the vessel walls and then crushed, washed, activated, crushed, and sieved to the desired particle size. It is activated by heating to about 400°C in a current of air or other gases, which sweep away the steam formed during activation. Commercial sizes range from 6.4 mm (¼ in.) to 0.074 mm (200 mesh).

X-ray diffraction analysis of F-1 shows a pattern of gamma/eta alumina with minor amounts of boehmite and chi alumina. F-1 loses approximately 6 wt%, as water, from 250° to 1200°C and contains about 0.9 wt% Na_2O, as well as a few hundred ppmw SiO_2 and Fe_2O_3. F-1 has a surface area of 250 m^2/g, with a broad pore-size distribution up to 100 000 nm (1 000 000 Å) in diameter. Pore-size distributions for activated aluminas are normally measured with 414 MPa (60 000 psia) mercury porosimeters, which can measure pores from 3 to approximately 177 000 nm (30 to 1 770 000 Å) in diameter. Figures 4 and 5 illustrate the broad pore distribution of F-1.

Activated Bauxite Type

Activated bauxites are produced in a crushing process similar to that for F-1. The major difference is that this bauxite is selectively mined for its high alumina content and hardness and is processed as mined. Activated bauxites are obtained by thermal activation of bauxite containing alumina in the form of gibbsite. The total oxide content of these bauxites, other than alumina (i.e., primarily SiO_2, Fe_2O_3, and TiO_2), varies from 10 wt% for the softest quality up to 25 to 30 wt% for the hardest. Surface areas vary from 175 to 240 m^2/g. Commercial sizes range from 6.4 mm (¼ in.) to 0.177 mm (80 mesh).

Synthetic Type

A granular product similar to F-1 has been produced by compacting gibbsite by mechanical pressure in a roll compactor. The product from the compactor is broken up and sieved to the required size fractions. Undersized material is recycled. The granular product is then activated in a rotary calciner at 400° to 600°C. The surface area of this product is 150 to 240 m^2/g and the total pore volume (TPV) is 0.35 cm^3/g. These lower values for surface area and TPV are due to its high density, i.e., 0.95 g/cm^3 (59 lbs/ft^3).

Production Processes—Spherical and Extruded Products

Crystalline Type

Another type of activated alumina is obtained by very rapid activation of gibbsite at 400° to 800°C.[4] During this process, the formation of boehmite and its decomposition products is greatly reduced as compared to slower activation. The outcome is essentially an amorphous (rho) alumina with a very weak pattern of gamma/eta alumina. Spheres and other shapes of varying size can be obtained by using water for agglomeration and for further rehydration of this alumina. When rehydrated, the pore volume and hardness of the particles are established. The last stage in manufacture consists of reactivation by exposure to gases at approximately 400°C. The final product shows a loss on ignition from 250° to 1200°C of 2 to 6 wt% and a surface area of 250 to 375 m^2/g.[5,6] Figures 4 and 6 illustrate the smaller pores and crystals of this type of alumina as compared to the scale type.

Table I. Structural Properties of Transition Aluminas*

Form	Crystal System	Space Group	Molecule per Unit Cell	Unit axis length (nm)			Angle	Density, g/m³
				a	*b*	*c*		
γ	Tetragonal			0.562	0.780			3.2
δ	Orthorhombic		12	0.425	1.275	1.021		3.2
	Tetragonal			0.796		2.34		
η	Cubic (spinel)	O^7_h	10	0.790				2.5–3.6
θ	Monoclinic	C^3_{2h}	4	1.124	0.572	1.174	103°20′	3.56
χ	Cubic		10	0.795				3.0
	Hexagonal			0.556		1.344		
	Hexagonal			0.557		0.864		
κ	Hexagonal		28	0.971		1.786		3.1–3.3
	Hexagonal			0.970		1.786		
	Hexagonal			1.678		1.786		
ι	Orthorhombic		4	0.773	0.778	0.292		3.71
	Orthorhombic	D^9_{2h} or C^8_{2v}	3	0.759	0.767	0.287		3.0

*Ref. 1 (used by permission).

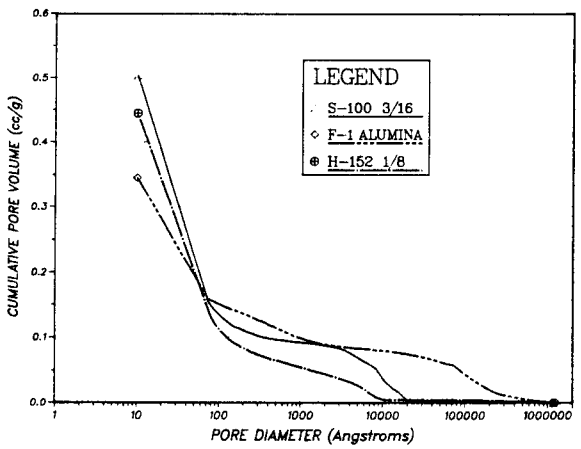

Fig. 4. Pore-volume distributions for activated aluminas.

Fig. 5. Scanning electron micrograph of pore distribution of F-1 (× 5000).

Gel Type from $NaAlO_2$

Alumina gels also serve as starting products for the manufacture of activated aluminas. These gels are generally prepared from solutions of $Al_2(SO_4)_3$ and NH_3, or from $NaAlO_2$ and an acid, or from $NaAlO_2$ and $Al_2(SO_4)_3$ and produce corresponding by-product salts. The precipitate, after being filtered and washed, is thoroughly drained to form a cake which embodies 8 to 20 wt% Al_2O_3. Via XRD, the crystal structure of the alumina at this point is pseudoboehmite.[7] This cake may be dried directly and broken up, or it can be extruded in the form of cylinders. An alternative is to reslurry and spray-dry the washed cake, producing spherical-type particles. The activated powder may be agglomerated into spheres, pressed into pellets, or extruded. The gels are activated under the same conditions as the aforementioned products and usually have an XRD pattern of broad, diffuse bands of gamma alumina. Some of the gels include a small percentage of SiO_2, others up to 2 to 3 wt% sulfate. Although gels of varying textures can be prepared, those that are used as adsorbents have very small pores; surface areas are 300 to 600 m^2/g.[7] Figure 7 illustrates the small pores and crystals of a spherical activated alumina gel. The ability to modify the pore volume distribution of pseudoboehmites with acids and other chemicals makes these aluminas favorites for catalyst manufacture.

Gel Type from Al Metal

Ziegler chemistry is used to produce linear alcohols; a coproduct of this process is alumina. In the Ziegler process, aluminum metal is reacted with ethylene and hydrogen to produce aluminum triethyl. Additional ethylene is added to polymerize each branch of aluminum triethyl, forming aluminum alkyls. When

Fig. 6. Scanning electron micrograph of crystalline-type alumina (× 3000).

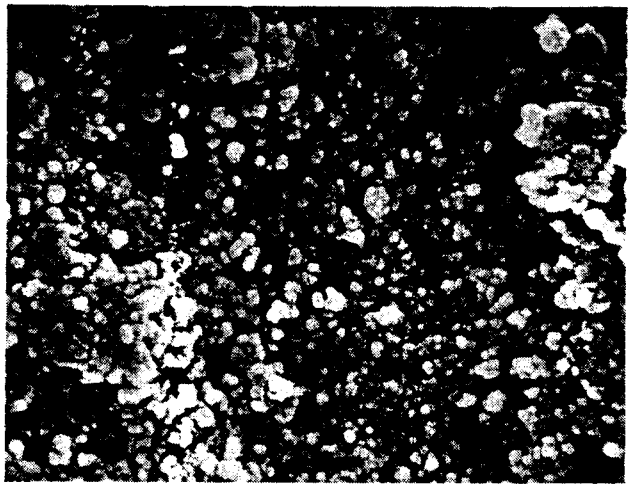

Fig. 7. Scanning electron micrograph of a spherical activated alumina gel (× 10 000).

polymerization has reached the extent desired, the alkyls are partially oxidized to form alkoxides.

The alkoxides are then hydrolyzed, with high-purity water, to form linear alcohols and aluminum hydroxide. The alumina is continuously withdrawn from the reactor and production parameters are controlled in regard to pH, temperature, and residence time to produce a pseudoboehmite of relatively high purity. Two stages of purification are used to remove the residual alcohol. The alumina is then spray dried to final characteristics. A common type is known in the United States as Catapal.* These aluminas are relatively pure and contain carbon and titania as the major impurities. Catapal can be mixed with other aluminas and extruded as a hydrotreating catalyst substrate.

Typical Properties of Activated and Monohydrated Aluminas

Table II illustrates the properties of various formed (granular or spherical) activated aluminas produced by the preceding processes. The crystalline- and gel-type aluminas are the most commonly produced activated aluminas today.

Catalyst substrate spheres (CSS), produced by Alcoa, illustrate the broad range of physical and chemical properties that can be produced in activated aluminas. For example, the Na_2O content can be varied from 0.30 to as low as 0.03 wt%. The total pore volume can range anywhere from 0.5 to 1.5 cm^3/g, with surface areas from 350 down to 25 m^2/g. Sphere sizes can be specified as small as 6.4 to 1.5 mm (¼ to 1/16 in.). Pore-size distribution can also be varied greatly. Thus the process engineer has a great many variables to contend with when designing a catalyst substrate or selective adsorbent.[8] In addition to the above spheres, users can choose from a variety of feedstock powders that are usually extruded as formed products. Table II lists a few of these aluminas as examples.

Table III shows the wide variety of powders that are commercially available. The CP powders can be tailored in particle-size distributions from 1 to 100 μm in diameter. These powders are rehydratable and form strong hydroxyl bonds on contact with water. The

*Vista Chemical Corp., Houston, TX.

Table II. Typical Properties of Granular and Spherical Activated Aluminas

	F-200 1.6 mm	F-1 1.8 mm	CSS-25 3.2 mm	CSS-350 4.8 mm	SRU 12.7 mm
Al_2O_3	93.1	92.0	99.1	95.1	95.1
SiO_2	0.02	0.09	0.02	0.02	0.02
Fe_2O_3	0.02	0.08	0.02	0.02	0.02
Na_2O	0.30	0.90	0.09	0.30	0.30
LOI (250°–1200°C)	6.5	6.5	0.5	4.5	6.0
Form	sph	gran	sph	sph	sph
kg/m^3	769	881	481	721	801
SA, m^2/g	375	250	25	340	250
TPV, cm^3/g	0.50	0.40	1.0	0.55	0.45

Table III. Typical Properties of Powdered Aluminas*

	CP-2	CP-100	CTG SG	Monal-HP	Monal-300
Al_2O_3	93.0	92.0	97.2	79.99	79.9
SiO_2	0.02	0.01	0.02	0.004	0.02
Fe_2O_3	0.01	0.01	0.01	0.004	0.02
Na_2O	0.40	0.40	0.20	0.001	0.04
LOI (250°–1200°C)	6.5	7.5	2.5	20.0	20.0
kg/m^3	432	1025	721	593	593
SA, m^2/g	325†	250†	125	350	300
<90%, μm	7.0	140.0	9.0	85	85
<50%, μm	2.0	92.0	2.0	65‡	65‡
<10%, μm	0.5	45.0	0.3	45	45

*Refs. 9 and 10.
†On rehydration/activation.
‡Spray dried.

rehydration reaction is highly exothermic. The purity can also be varied. The CTG powders, on the other hand, are not rehydratable and can be varied in properties, much like CP powders. The CTG SG has excellent thermal stability and makes an excellent wash-coat alumina.

Monal HP is a very-high-purity pseudoboehmite alumina that can be used in precious metal catalyst manufacture. Monal-300, a pseudoboehmite, can be used as a wash-coat alumina with excellent thermal stability or it can be extruded and used as a catalyst substrate.

Activated Alumina Adsorption Applications

Desiccant

The first major use for activated alumina was as a desiccant (in 1932).[11] Since another chapter in this book is dedicated to this topic, further discussion is deferred.

Selective Adsorbent

Modern uses of activated alumina and its modifications are being used increasingly for selective adsorption applications in petrochemicals and water treatment.[11] Again, since another chapter in this book is dedicated to this topic further discussion is deferred.

Activated Alumina Catalytic Applications

The surfaces of activated aluminas contain oxide, aluminum, and hydroxyl ions. These three ions in tandum have many logistical combinations that lead to a variety of catalytic sites. Peri[12–14] used a classical statistical method to illustrate the different surface sites. More recently, Fourier transform infrared spectrometry (FTIR) has confirmed the work that Peri conducted and has given even further insight into the surface chemistry of activated alumina. With the use of FTIR and gravimetric studies, there are at least five well-identified hydroxyls on activated alumina. This complex surface chemistry, along with thermal stability, bestows on activated alumina its major role in the world of catalysis. When this complex chemistry is combined with the interaction of impregnated metals, it is obvious that many books could and have been written on catalysis. With the advent of modern electronics and instrumentation, man's insight into the world of catalysis and the role that aluminas play has probably never been greater than it has in the last five years.

Claus and Promoted Claus

Activated alumina has essentially replaced activated bauxite in this application. Claus catalysis is a large, worldwide application of activated alumina. Again, since another chapter in this book is dedicated to this topic, further discussion is deferred.

Hydrotreating

These catalysts are used primarily with H_2 to remove organically contained sulfur, nitrogen and oxygen in petroleum feedstocks. Shuit and Gates[15] wrote an excellent review on the chemistry and engineering of hydrodesulfurization. Metallic impurities can also be removed with these catalysts and, as the quality of crude oil in the world decreases with time, this application will see increased emphasis. By the end of the decade, over 100 million pounds per year of alumina is expected to be used in this application. The exact time when hydrotreating catalysts will reach this level of annual consumption has eluded forecasters for years, since world economics and politics greatly influence the world availability of light crude. Nevertheless, it is just a matter of time until hydrotreating and Claus catalysts play an even larger role in catalysis. Monohydrated aluminas are the primary aluminas used to produce extrudates, which later are impregnated with Co, Mo, Ni, W, and combinations of these metals; Co/Mo and Ni/Mo are still the primary catalysts used. Spheres have had some increased use in this application, but extrudates are still the primary support. The alumina acts as an interacting support in this application.

Bulk MoO_3 can be reduced to metal with H_2 at 500°C, but when it is impregnated on activated alumina, the reduction proceeds only to MoO_2.[16,17] The fact

that MoO_3 cannot be totally reduced on activated alumina indicates that there is a strong interaction between the compounds. In fact, Mo accelerates the conversion of activated alumina to theta and alpha aluminas at temperatures as low as 755°C. Normally this phase conversion in unimpregnated alumina does not start until 900°C. Thus, it can be seen that both MoO_3 and activated alumina affect the properties of the other compound and thus derive their enhanced catalytic properties.

Reforming

With the advent of mandatory phase-out of lead as an additive in gasoline, catalytic reforming has become increasingly important. The purpose of the catalyst is to increase the octane number of gasoline. Approximately 5 million pounds per year of high-purity alumina are consumed in this application.

Hydrocracking

Alumina is used in this application as a bonding agent for zeolites. This process, which performs cracking and hydrotreating simultaneously, uses about 2 million pounds per year.

Pollution Control

By far one of the largest uses of alumina in catalysis is in auto exhaust catalysis. At its peak, 40 million pounds per year of low-density spheres were used, with monoliths second in utilization for this application. Today the situation has totally reversed, with spheres amounting to only 10 million pounds per year. The main application today is in truck engines. A significant amount of alumina is also used in the wash coats of the monoliths.

Chemical

The three best-known uses for alumina as a catalyst substrate for chemical reactions are for ethylene oxide, oxychlorination, and isomerization. Millions of pounds per year of alumina are used in these applications. It is impossible to estimate the consumption of alumina in chemical catalysis, because most of these applications are proprietary. The most frequently published of these reactions is the isomerization of olefins.[18–24] The isomerization of butene has been investigated from 0° to 300°C with a variety of aluminas, activated under a variety of conditions.[25,26] The conclusions drawn are that alumina surface chemistry is very complicated, with an abundance of different surface sites, pore distributions, and crystal shapes. Therefore, it is probably safe to say that, even though man has learned much about the surface of alumina with the advent of modern instrumentation, there is still much more to learn with just nacent alumina, much less when it is impregnated.

References

[1]K. Wefers and G. M. Bell, "Oxides and Hydroxides of Aluminum," Technical Paper No. 19, Aluminum Company of America, Pittsburgh, PA, 1972.

[2]H. E. Osment and R. L. Jones, U.S. Pat. No. 3 226 191, December 28, 1965 (to Kaiser Aluminum and Chemical Corporation).

[3]J. B. Barnitt, U.S. Pat. No. 1 868 869, July 26, 1932 (to Aluminum Company of America).

[4]M. L. Pingard, Fr. Pat. No. 1 077 163, March 25, 1953 (to Pechiney).

[5]Alcoa Product Data F-200 CHE 946, August 1985.

[6]Alcoa Product Data S-100 CHE 942, August 1984.

[7]K. P. Goodboy, U.S. Pat. No. 4 157 382, June 5, 1979 (to Aluminum Company of America).

[8]Alcoa Product Data CSS-350 to CSS-50 Catalyst Substrate Spheres CHE 981, September 1985.

[9]Alcoa Product Data Activated Aluminas CP Series CHE 945, April 1985.

[10]Alcoa Product Data Monal HP and HP+2, July 1986.

[11]K. P. Goodboy and H. L. Fleming, "Trends in Adsorption with Aluminas," *Chem. Eng. Prog.* (November 1984).

[12]J. B. Peri, *J. Phys. Chem.*, **69** [1] 220 (1965).

[13]J. B. Peri, *J. Phys. Chem.*, **69** [1] 231 (1965).

[14]J. B. Peri, *J. Phys. Chem.*, **69** [1] 211 (1965).

[15]G. C. A. Schuit and B. C. Gates, *AIChE J.*, **19** [3] 417 (1973).

[16]P. Ratnasamy, R. P. Mehrotra, and A. V. Ramaswamy, *J. Catal.*, **32**, 63 (1974).

[17]A. Cimino and B. A. De Angelis, *J. Catal.*, **36**, 11 (1975).

[18]G. Greco Jr., F. Alfani, and F. Gioia, *J. Catal.*, **30**, 155 (1973).

[19]R. M. Levy, D. J. Bauer, and J. F. Roth, *Ind. Eng. Cem. Prod. Res. Dev.*, **7**, 217 (1968).

[20]H. R. Gerberich, J. G. Larson, and W. K. Hall, *J. Catal.*, **4**, 523 (1965).

[21]H. R. Gerberich and W. K. Hall, *J. Catal.*, **5**, 99 (1966).

[22]J. W. Hightower and W. K. Hall, *J. Phys. Chem.*, **71**, 1014 (1967).

[23]J. W. Hightower and W. K. Hall, *J. Am. Chem. Soc.*, **89**, 778 (1967).

[24]J. W. Hightower and W. K. Hall, *Chem. Eng. Prog. Symp. Ser.*, **63** [73] 122 (1967).

[25]G. Perot, M. Guisnet, and R. Maurel, *J. Catal.*, **41**, 14 (1976).

[26]A. Ghorbel, C. Hoang-Van, and S. J. Teichner, *J. Catal.*, **30**, 298 (1973).

[27]A. Ghorbel, C. Hoang-Van, and S. J. Teichner, *J. Catal.*, **33**, 123 (1974).

Production Processes, Properties, and Applications for Calcined and High-Purity Aluminas

T.J. Carbone
Aluminum Company of America
Bauxite, AR 72011

Calcined aluminas are categorized into three main groups based on soda content and total impurities. While normal- and low-soda, thermally reactive calcined aluminas are produced from the Bayer process, high-purity aluminas are predominately obtained by decomposing aluminum-based salts. Calcination normally is done in rotary kilns or stationary calciners. Some agglomerated aluminas are milled to obtain particles that are equal in size to the ultimate crystals of the alumina. Supergrinding results in aluminas exhibiting enhanced sintering characteristics. Calcined aluminas are used in a wide variety of applications, including abrasives, polishing, electronic and mechanical ceramics, glass, whitewares, and refractories. Future developments in alumina production will include greater emphasis on consistency, more uniform and finer crystal size, removal of alpha-emitting particles, and reduced impurities.

This chapter describes production processes, properties, and applications for a variety of calcined aluminas. Calcined aluminas can be divided into three main categories based on chemistry.[1–14] The categorization is determined by both sodium oxide content and total impurities. The first category is normal calcined aluminas with a soda content of greater than 0.1%. Total alumina content is generally 99.0 to 99.5%. A second category contains calcined aluminas, sometimes referred to as low-soda and/or thermally reactive aluminas, with an alumina content of about 99.7% and less than 0.1% soda. The third classification includes high-purity calcined aluminas that exhibit a minimum purity of 99.9% Al_2O_3. One major part of this classification is 99.99% pure alumina produced from aluminum salts and not from the Bayer process.

Except for the highest purity calcined alumina, all calcined aluminas are produced by heat treatment of aluminum hydroxide (gibbsite) which comes from the refining of bauxite by the Bayer process. There are almost 35 000 000 metric tons per year of alumina (on a calcined basis) produced throughout the world. The U.S. production is approximately 5 000 000 metric tons/year. Major outlets for this production are shown in Fig. 1.

Before 1987, alumina used for metal production sold for $100 to $150 per metric ton. The prices for various alumina chemicals depend on the market and form of the alumina. The pricing range for calcined aluminas is from $300 per metric ton, for some normal calcined aluminas, up to $20 per pound for the highest purity calcined alumina. The average price for high-volume, normal-soda alumina is approximately $500 per metric ton.

In the early 1900s, Bayer process plants (or bauxite refineries) were initially built to specifically produce smelter-grade alumina (SGA) as the raw material for aluminum metal production. Today, approximately

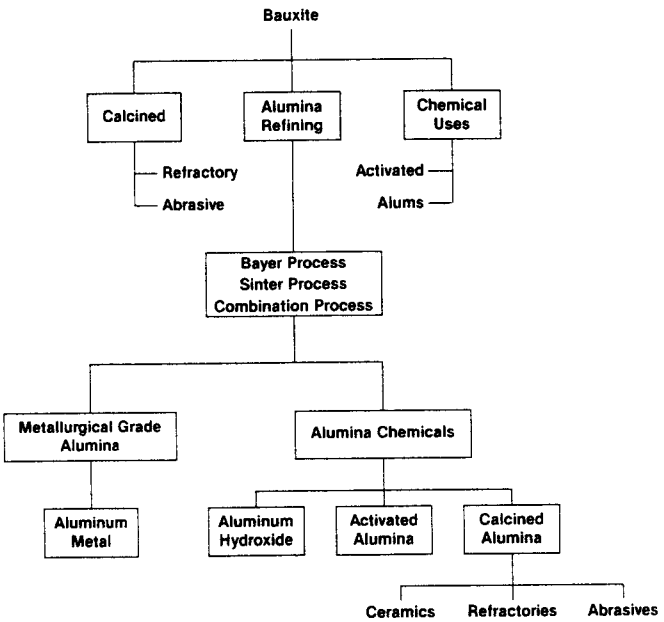

Fig. 1. Major outlets for alumina.

93% of all Bayer process equivalent alumina output goes into metallurgical or smelter-grade alumina.[3,5–7] Some Bayer plants have converted some or all SGA capacity to production of unique alumina chemicals and calcined aluminas. Since these "specialty" aluminas are all derived from the Bayer process, they resemble the basic properties of SGA.[5]

Typical properties of SGA are shown in Fig. 2.[6] These are very general properties. Smelter-grade alumina is produced in over 20 countries, with Bayer plants utilizing different bauxite sources and varying Bayer process parameters. These differences can result in calcined aluminas with inherent differences in chemical impurities, particle-size distribution, and particle morphology.

Particle size distribution, wt%	
+ 100 mesh (Tyler)	<5
+ 325 (44 μm)	>92
− 325	<8
Bulk density, kg/L	
loose	0.95–1.00
packed	1.05–1.10
Specific surface area, m^2/g	50–80
Moisture (to 573 K), wt%	<1.0
Loss on ignition (573–1473 K) wt%	<1.0
Attrition index (modified Forsythe-Hertwig method)	increase in <44 μm particles 4–15 wt%
α-Al_2O_3 content (by optical or X-ray method), %	<20
Chemical analysis	wt%
Fe_2O_3	<0.020
SiO_2	<0.020
TiO_2	<0.004
CaO	<0.040
Na_2O	<0.500

Fig. 2. Typical properties of metallurgical alumina. (Used by permission.)

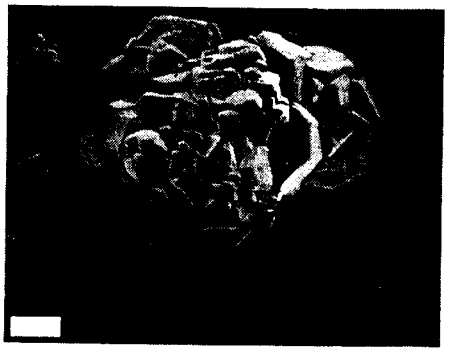

Fig. 3. Bayer alumina hydrate. (Bar = 15 μm.)

The remaining 7% of worldwide alumina production goes into alumina chemicals, as shown in Fig. 1.[3,5–7] Aluminum hydroxides and activated aluminas account for the majority (60%) of this production. The production processes and properties of these hydrated alumina chemicals are described by others in this book. Specialty calcined aluminas represent less than 3% of total worldwide alumina production. There are almost 100 varieties of calcined aluminas produced in the world.[8] The applications for these calcined aluminas include various ceramic, refractory, and abrasive products, which will be discussed in a later section. The production processes for various calcined and high-purity aluminas will be discussed next.

Production Processes

Normal- and Low-Soda Calcined Aluminas

Raw material for production of calcined alumina is Bayer-processed aluminum hydroxide (hydrate). Typical properties of hydrate were discussed in a previous chapter. Hydrate particles are 40 to 200 μm in size and are roughly spherical agglomerates, as shown in Fig. 3.[1,2,5] When dried, hydrate is very free flowing. The soda content of normal Bayer hydrate is 0.5%. A small portion (<0.1%) can be removed by washing, but most is trapped within the hydrate structure. Under different precipitation conditions in the Bayer refinery, hydrates can be produced with soda contents as low as 0.05%. It should be noted that these special process conditions increase production costs compared to those for normal-soda hydrate.

Hydrates of various soda contents are heated to form calcined aluminas.[1–3,6,7] The heat treatment is called calcination and can be accomplished in two ways. Rotary kilns have been the standard method for many years. A schematic diagram of a rotary kiln system is shown in Fig. 4.[14] They are large, refractory-lined, steel cylinders up to 10 feet in diameter and 250 feet long. They are horizontally mounted at an angle and rotate about an axis. Bayer hydrate slurry from the refinery is washed through filters, and the resulting cake is fed damp to the upper, or cold end of the kiln. As the kiln rotates, the hydrate particles slowly move down the kiln toward the lower end. At the lower end, a burner injects a hot flame (gas or oil) which heats the entire kiln, producing a thermal gradient along its length. The hydrate decomposes into transition-alumina phases and water vapor. The water vapor and combustion gases travel out the upper (cold) end by induced-draft fans. The alumina particles transform into alpha alumina in the hot zone near the burner and continue to tumble out the discharge or hot end of the kiln. Rotary coolers remove heat from the alumina so it can be transported and stored. Production rates depend on kiln size and the particular product being calcined. Typical rates can vary from 50–350 tons/day.

Stationary, or flash calciners were developed to replace rotary kilns. Their advantages are lower energy consumption, lower capital costs, lower maintenance costs, and lower manpower requirements. Figure 5 is a diagram of a commercial Alcoa unit.[6] The calciner consists of a series of fluidized beds which serve as surge hoppers and heating vessels. Drying, calcination, and particle cooling occur during dilute material transport through the system. These stationary units are capable of calcining 1500 tons/day. Calciners were primarily designed for large-volume production of SGA. One disadvantage of the system is that only lower alpha alumina content (<90%) alumina products can be produced at this time.

The goal of calcination is usually to convert hydrate into alpha alumina. However, there are applications for aluminas with 20 to 95% alpha alumina contents (partial conversion) which will be discussed later. Another goal of the calcination step is to produce calcined aluminas having various crystal sizes and chemistry. Both goals can be achieved by adjusting process variables such as calcination temperature, time, atmosphere, impurities in the hydrate, and known additions of mineralizing compounds.

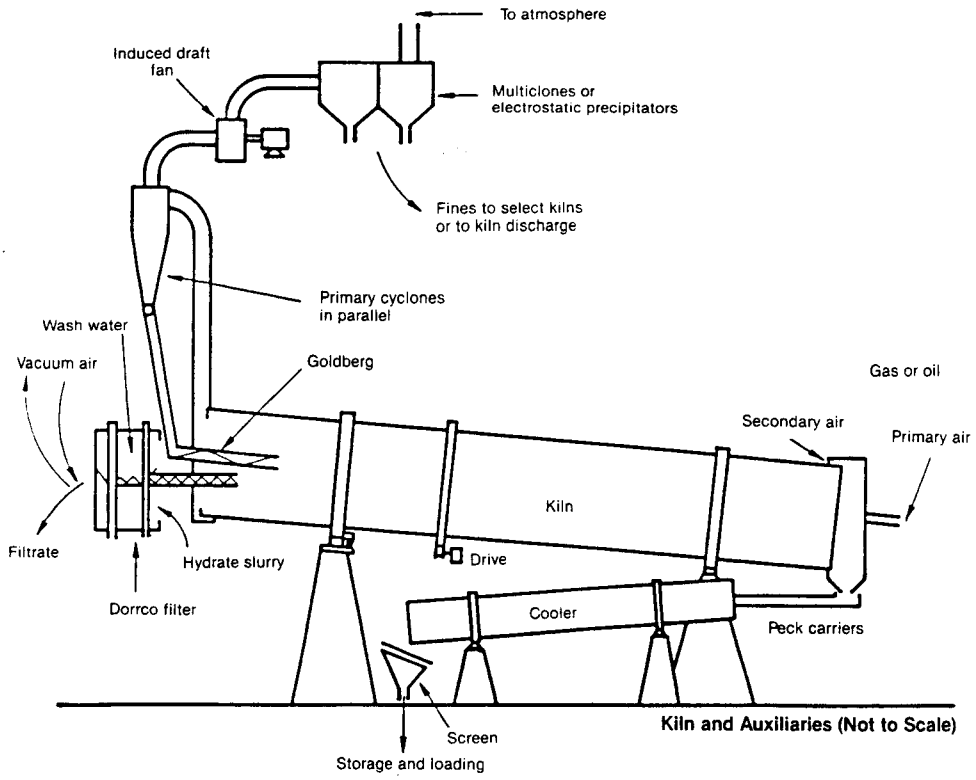

Fig. 4. Rotary kiln system.

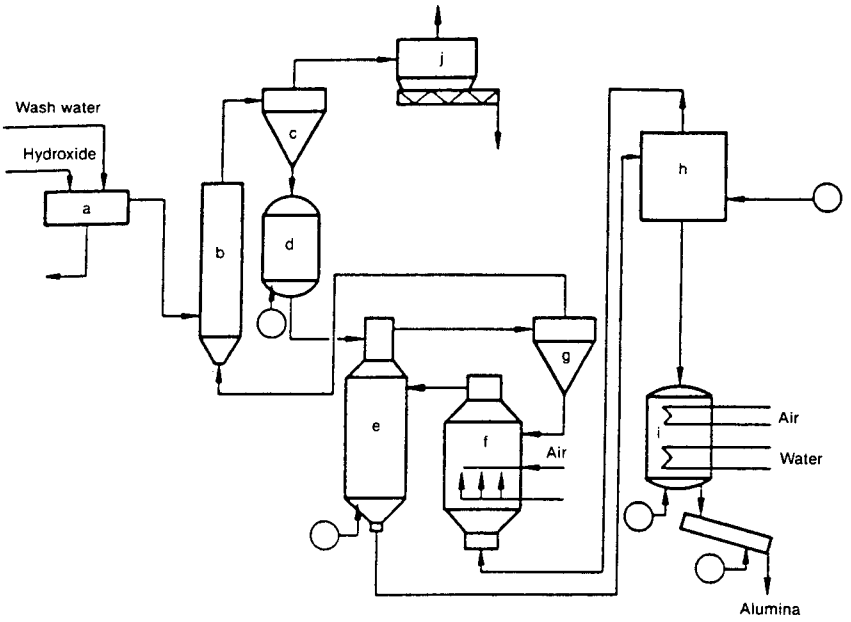

Fig. 5. Alcoa flash calciner: (*a*) filter; (*b*) flash dryer; (*c*) cyclone; (*d*) fluidized-bed dryer; (*e*) holding vessel; (*f*)furnace; (*g*) cyclone; (*h*) multistage cyclone cooler; (*i*) fluidized-bed cooler; (*j*) electrostatic precipitator

The exterior spherical hydrate particle is not disturbed as the hydrate particles, or agglomerates, are heated and transformed into alpha alumina, but the internal structure of the agglomerate is changed dramatically. While Bayer hydrate agglomerates exhibit groups of irregularly shaped blocks, the 100% alpha alumina agglomerates now exhibit a three-dimensional network of individual alpha alumina crystals, as shown in Fig. 6.[3,6–8,11,12] The internal precursor structure of the hydrate is lost. The structure of 20 to 90% alpha alumina will still show the blocky hydrate structure because the alpha alumina crystals are very small

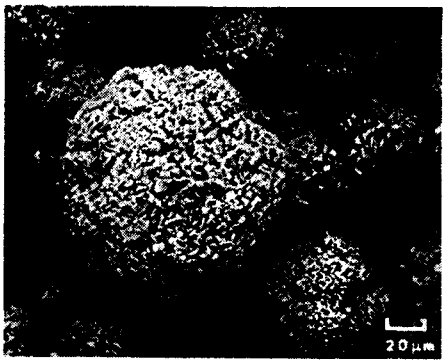

Fig. 6. A-12 alumina.

(<0.5 µm), as shown in Fig. 7.[3,6–8,11,12] The complete conversion to 100% alpha alumina usually occurs at 1200°C and is accompanied by a small exothermic reaction.

The effects of calcination temperature and time are well documented.[1–3] Lower calcination temperatures require longer calcination times to produce equivalent products as more normal higher temperatures and short times. As calcination temperature is increased to approximately 500°C, the Bayer hydrate decomposes, losing molecules of chemically combined water and forming an amorphous transition alumina. The removed water leaves a very porous, high-surface-area material (up to 300 m^2/g). As temperature increases from 500° to 1200°C, surface area gradually decreases as structural reordering occurs and higher density crystals of alpha alumina begin to form. Changes in surface area and specific density with temperature are shown in Fig. 8.[1–3]

Chemistry plays a large role in the production of calcined alumina. Soda content in the starting Bayer hydrate affects the transformation temperature of alpha alumina. At 1200°C and without chemical additives, alpha alumina generally forms less than 1 µm sized crystals. At very high calcination temperatures (>1500°C), crystal growth occurs, resulting in larger alpha alumina crystals (2 to 3 µm). To produce larger or equivalent-sized crystals at lower temperatures, crystal growth additives must be used. These additives

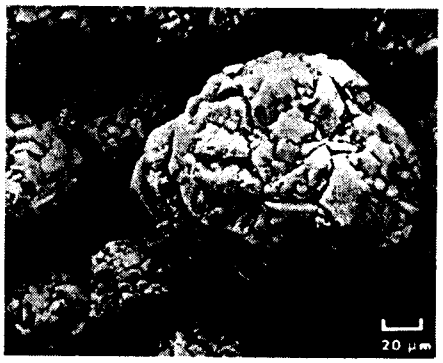

Fig. 7. A-13 alumina.

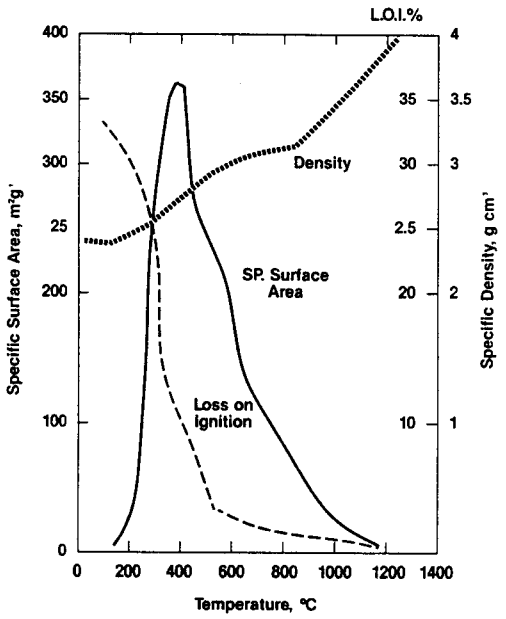

Fig. 8. Temperature effect on Bayer alumina properties.

are commonly called mineralizers.[1–3] They are usually salts or acids of boron, fluorine, or chlorine. When added to the calcination process in various ways, alpha alumina crystals can grow to as large as 10 to 20 µm. They are usually flat, hexagonal, platelike crystals with the average diameter being measured across the large face (see Fig. 9).[8]

The use of boron or chlorine also leads to a reduction in the soda content of Bayer hydrate during calcination.[1–3] Near final calcination temperatures, boron or chlorine reacts with soda to form easily vaporized chemical compounds. Normal hydrate can be calcined to as low as 0.05% soda in calcined alumina. However, this process results in residual boron or chlorine in the alumina and also results in a more severe processing condition. Otherwise, starting hydrates need to be below 0.1% soda in order to produce <0.1% soda calcined alumina without the use of mineralizers.

After calcined aluminas are produced, they can be further processed by separating the agglomerated par-

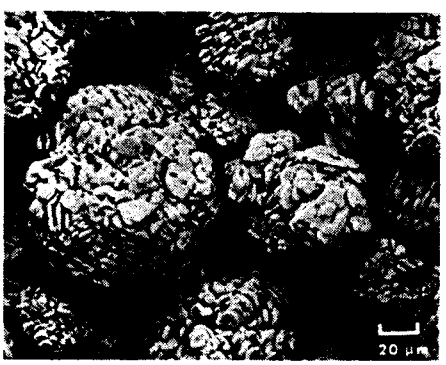

Fig. 9. A-10 alumina.

ticles into their individual crystals. Since the individual alumina crystals are not monosize, this results in some form of particle-size distribution. Alumina agglomerates are usually comminuted by continuously dry grinding in a ball mill or jet mill. Commercially available ground aluminas are usually sold as 95% −325 mesh or 99% −325 mesh (44 μm).[5] These agglomerated aluminas have not been completely separated into their ultimate crystals. In those applications where a more completely ground alumina is required, the customer may further grind the material or purchase superground (SG) alumina.[9,11,12]

Superground aluminas are ground in a batch ceramic-lined ball mill for extended periods of time. Grinding time can be more than 30 hours in order to fracture all alumina agglomerates into individual crystals. The smaller crystal size aluminas usually require the longest grinding time due to their denser agglomerate structure and stronger crystalline bond. Superground aluminas are also referred to as thermally reactive aluminas because the relatively high-surface-area fine crystals exhibit higher densification rates when compacted and sintered into ceramic products. Sintering temperatures required to completely densify ceramics made from fine superground aluminas are usually 200°C lower than those made from regular ground or coarse crystal size aluminas.[8]

High-Purity Alumina

A 99.9% alumina can be produced starting with a Bayer hydrate. The production process is the same as described in the previous section, except that additional processing steps are required to further remove major impurities of soda, silica, and iron oxide. This usually requires either reprecipitation or step precipitation and repeated washing of the alumina.

There are many methods for producing a 99.99% pure alumina.[1,2] They usually involve decomposition of a high-purity form of recrystallized aluminum salts (sulfates, chlorides, nitrates) or aluminum metal. A common method first requires the preparation of aluminum sulfate by digesting Bayer hydrate in sulfuric acid. The sulfate is then reacted with anhydrous ammonia to produce a pure recrystallized ammonium alum. When calcined, a 99.99% pure, fine crystalline alumina is obtained. The particle morphology and agglomeration are usually quite different from those of Bayer aluminas, as seen in Fig. 10.[8] Calcination time and temperature are adjusted to produce various surface-area aluminas. Alum-derived alumina is usually not ball milled, but deagglomerated in a jet mill since the crystals are weakly bonded together after calcination.

Properties

Normal-Soda Calcined Aluminas

These calcined aluminas have a soda content of 0.1 to 0.6%. Table I shows typical properties for some commercial grades. The major differences between these grades are soda content, surface area, alpha alumina content, ultimate crystal size, and loss on ignition (LOI). The highest surface area aluminas exhibit the lowest alpha content, as shown in Group A. In general, aluminas with a surface area above 5 m^2/g contain some non-alpha alumina phases. For example, a 10 m^2/g alumina will contain approximately 85% alpha alumina, while a 50 m^2/g calcined alumina will contain <20% of the alpha phase. The calcined aluminas in Group B exhibit controlled surface area in the range of 5 to 15 m^2/g. These aluminas have not been fully converted to alpha alumina. They also have very small ultimate crystals, less than 1 μm. These individual crystals can be distinguished only by microscopy at greater than × 10 000 magnification due to their submicrometer size.

The calcined aluminas in Group C have been converted to essentially 100% alpha alumina.[8] Due to the presence of a high amount of soda, one must expect that there is some beta alumina formed in these aluminas. As a result of the alpha transformation, the individual crystals have grown in size to 3 to 6 μm and exhibit a hexagonal platelike structure, as shown by the scanning electron micrograph in Fig. 6. The surface area has also decreased to less than 1 m^2/g due to the formation of coarse, dense crystals. The LOI

Table I. Typical Properties of Normal Calcined Aluminas

	A		B							C								
	Kaiser C-70	Alcan C-1	Alcoa A-13	Kaiser C-1	Alcoa Chemie CT-105	VAW 103-60	Martinswerk PN	Showa A-14	Sumitomo A-12	Alcoa A-12	Kaiser C-5R	Alcan C-71	Alcoa Chemie CT-19	VAW 105	Martinswerk DX	Pechiney GCT	Showa A-12	Sumitomo A-21
Ultimate crystal size (μm)	<1.0	<1.0	<1.0	<1.0	1	0.3		0.3	<1.0	3–5	4–6		4–5.5	1.5–3.0	6		5	2–4
Surface area (m^2/g)			6–12		6	6	8–15	5		0.5			0.5	0.5–1	0.3–0.7	0.5	0.6	
Al_2O_3 (wt%)	98.5	99.3	99.2	99.2	99.0	99.1	99.3	99.7	99.7	99.4	99.4	99.7	99.5	99.3	99.6	>99	99.7	99.7
Na_2O (wt%)	0.45	0.55	0.25	0.45	0.3	0.3	0.5	0.3	0.3	0.25	0.45	0.18	0.25	0.3	0.25	0.3	0.3	0.3
SiO_2 (wt%)	0.01	0.03	0.02	0.01	0.02	0.03	0.03	0.02	0.01	0.02	0.01	0.03	0.03	0.03	0.03	0.02	0.02	0.01
Fe_2O_3 (wt%)	0.01	0.03	0.04	0.01	0.03	0.03	0.03	0.01	0.01	0.04	0.01	0.03	0.03	0.03	0.03	0.03	0.01	0.01
Loss on ignition (%)	0.9	1.0	0.4	0.35	0.5	0.4		0.35	0.3	0.2	0.1	0.1	0.1	0.1	0.2	0.01	0.1	
Alpha Al_2O_3 (%)			65–90		>80	80	>60			98		98	98	98	>95	>88		

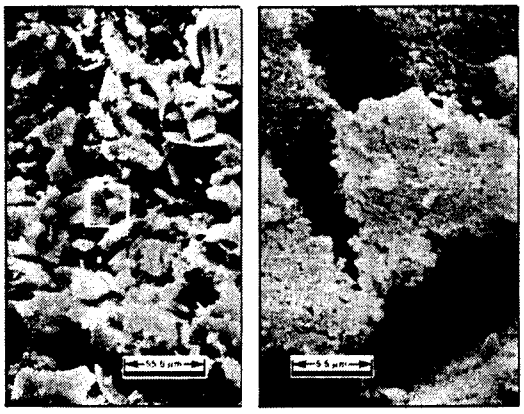

Fig. 10. Linde A alumina.

(species vaporized by heating to 1100°C) is near zero for Group C because low-surface-area materials have a low affinity for water vapor.

Low-Soda Calcined Aluminas

The calcined aluminas in this subgroup have a soda content of less than 0.1%. Table II depicts typical properties for some commercial grades. Table II is divided into two main groups. The low-soda calcined aluminas in Group A exhibit typically coarse ultimate crystals (between 2 and 10 μm). Most of these aluminas have been calcined in the presence of mineralizers to promote crystal growth and reduce soda levels to as low as 0.03% Na_2O. Essentially, all are 100% alpha aluminas. Surface area is typically less than 1 m^2/g, again indicative of the presence of coarse crystals. A scanning electron micrograph of one of these aluminas is shown in Fig. 9. While it is similar to the structure of a normal-soda alumina in Fig. 6, it does have larger diameters as well as thicker, platelike structures.

The low-soda aluminas in Group B are additionally designated as thermally reactive ground aluminas. These aluminas are usually sold in superground form and exhibit enhanced sintering activity. The crystal size of the aluminas ranges from 0.3 to 5.0 μm. This leads to surface areas from 10 to 2 m^2/g. The mean particle size given in Table II is the median size of ground material as it is sold. This number is usually close to the ultimate crystal size, indicative of grinding coarse agglomerated particles into their ultimate crystals. The finer crystalline, high-surface-area aluminas can have a small amount of non-alpha phase present. This is usually less than 10%. The variety of particle-size distributions that can be obtained due to grinding various crystal-size aluminas is shown in Fig. 11.[12] Since the higher-surface-area aluminas are finer in crystal size and contain some non-alpha phases, they require much longer grinding time to achieve ultimate crystal size.

The thermally reactive aluminas can also be characterized by their compaction behavior and sintering reactivity. Compaction behavior is quantified by pressing alumina in a steel die at high pressure without the use of organic binders and measuring the green bulk

Table II. Typical Properties of Low-Soda and Thermally Reactive Calcined Aluminas

A. Low-Soda Aluminas

	Alcoa				Alcan	Alcoa Chemie				VAW	Martinswerk			Sumitomo		Showa
						CIB Series										
	A-3500	A-4000	A-14	A-10	C-75	3	4	5/6	7	0625-25-10	ZS-6	ES-6	DS-6	AL-43	ACL-27	AL-15H
Ultimate crystal size (μm)	2.5	3–4	2–5	6–10		5.5	5	4	3	2.4	3.5	4.5	5.5	2–3	3–5	3.0
Surface area (m^2/g)	<1	<1	0.5	0.4		0.3	0.4	0.5	0.7	1.5	1.0	0.7	0.5			0.7
Al_2O_3 (wt%)	99.7	99.7	99.6	99.5	99.8	99.8	99.8	99.8	99.8	99.3	99.8	99.8	99.8	99.9	99.9	99.9
Na_2O (wt%)	0.08	0.08	0.03	0.1	0.05	0.03	0.05	0.07	0.10	0.1	<0.1	<0.1	<0.1	0.03	0.02	0.03
SiO_2 (wt%)	0.02	0.02	0.08	0.08	0.02	0.03	0.03	0.03	0.03	0.05	0.03	0.03	0.03	0.05	0.02	0.02
Fe_2O_3 (wt%)	0.02	0.02	0.04	0.04	0.03	0.04	0.04	0.04	0.04	0.03	0.03	0.03	0.03	0.01	0.02	0.02
LOI (%)			0.2	0.2	0.1	<0.1	<0.1	<0.1	<0.1					0.1	0.1	0.08
Alpha Al_2O_3 (%)	98	98	98	98		99	99	99	99	98	>95	>95	>95			

B. Low-Soda, Thermally Reactive Ground Aluminas

	Alcoa						Alcoa Chemie		Martins-werk	Sumitomo			Showa			
	A-16SG	A-152SG	A-15SG	A-17	A-1000SG	A-3000FL	CT-1000SG	CT-3000SG	CS-400M	ALM-41	AES-11	AL-31	L-45-1	AL-150SG	AL-160SG	AL-170SG
Ultimate crystal size (μm)	0.3–0.5	1.5	2–2.5	3–3.5	0.3–0.5	3–3.5	1.3	0.5	0.5	1.8	0.3	0.3–4	1.8	0.3–5	0.5	0.3–5
Surface area (m^2/g)	10	3	6	3	10	3	3	6	6–10				2	5	7	2.5
Al_2O_3 (wt%)	99.7	99.7	99.7	99.7	99.7	99.7	99.6	99.6	>99	99.9	99.8	99.9	99.8	99.9	99.9	99.8
Na_2O (wt%)	0.08	0.08	0.08	0.08	0.08	0.08	0.1	0.1	0.1	0.04	0.03	0.03	0.05	0.05	0.05	0.06
SiO_2 (wt%)	0.03	0.04	0.03	0.03	0.02	0.02	0.1	0.08	0.1	0.04	0.04	0.02	0.08	0.03	0.03	0.05
Fe_2O_3 (wt%)	0.01	0.04	0.01	0.01	0.02	0.02	0.03	0.03	0.03	0.01	0.01	0.02	0.02	0.02	0.02	0.02
LOI (%)							<0.5	<0.5	0.7	0.1	0.3	0.2	0.2	0.5	0.7	0.2
Mean particle size (μm)	0.5	1.5	2.0	3.0	0.5	3.0	1.3	0.5			0.4	2–3	1.8	2.0	0.6	2.0
Green density (g/cm^3)	2.15	2.25	2.50	2.50	2.15	2.50				2.20	2.23	2.60	2.30	2.60	2.25	2.55
Fired density (g/cm^3)	3.91	3.84	3.89	3.75	3.91	3.75				3.20	3.96	3.72	3.70	3.80	3.91	3.80
Compaction pressure (MPa)	345	345	345	345	345	345				300 kg/cm^2	300 kg/cm^2	300 kg/cm^2				
Sintering temperature (°C)	1540	1620	1670	1750	1540	1750				1600	1600	1700	1700	1700	1550	1700
Sintering time (h)	1	1	1	1	1	1				2	2	2	2	2	2	2

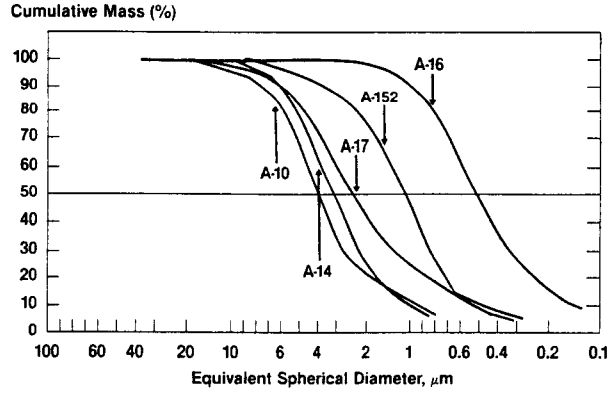

Fig. 11. Particle-size distribution of various fully ground aluminas.

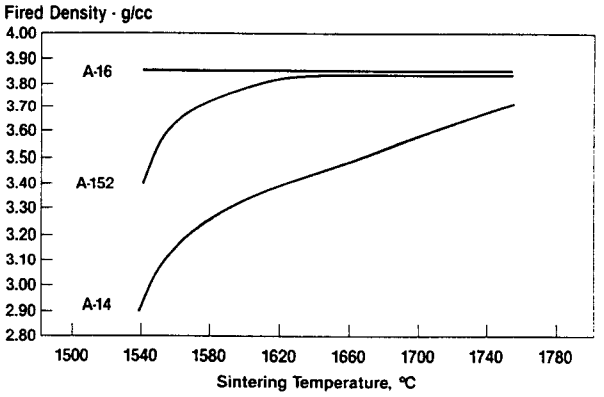

Fig. 13. Effect of sintering temperature on fired density of fully ground aluminas.

density of the pressed part. As shown in Table II, as alumina crystal size increases, green density increases. Also, as the crystal-size distribution is broadened, green density increases. A-17 is an example of a special grade produced to exhibit an extremely high green density to minimize shrinkage during sintering.

Sintering reactivity is measured by heating pressed compacts to some temperature and determining their fired density. The shrinkage behavior of compacts is shown in Fig. 12.[12] Coarse crystalline aluminas exhibit minimum shrinkage at 1500°C, while finer aluminas are in the final stages of sintering (shrinkage is complete) at this temperature. The fired density as a function of sintering temperature for various aluminas is shown in Fig. 13.[12]

For fully ground aluminas with crystal sizes greater than 1.5 μm, temperatures greater than 1600°C are required for maximum densification or fully dense structures with no open porosity. All of these sintering tests are made without fluxing additives or sintering aids which may cause liquid-phase sintering and thereby increase fired densities at lower temeratures.

A-16SG is representative of the most thermally reactive alumina.[8] It exhibits near-theoretical density (>3.90 g/cm^3) at as low a sintering temperature as

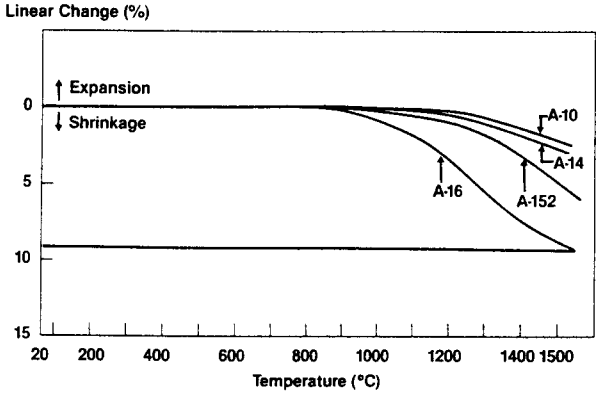

Fig. 12. Dilatometer analysis of various ground aluminas.

1540°C. It also exhibits the highest shrinkage due to its low green density.

The chemical analysis shows that these aluminas are typically 99.7 to 99.9% pure alumina. The most reactive grades usually have MgO dispersed in them by milling to act as a grain-growth inhibitor during sintering. This allows high fired densities to be achieved while maintaining small, uniform, fired crystals. This is an optimum microstructure for ceramic parts required to exhibit high abrasion resistance and strength.

High-Purity Aluminas

The commercial grades of high-purity aluminas available are summarized in Table III.[8] In some cases, a whole series of different surface-area aluminas are available, but only one is listed in the table. The 99.95% aluminas are produced from a Bayer hydrate precursor. Most 99.99% aluminas are produced from decomposition of various aluminum salts. In both cases, major impurities are soda, silica, and iron oxide. The aluminas with a surface area of 5 to 10m^2/g are typically 90% alpha, with ultimate crystals of less than 0.5 μm. These aluminas do not sinter as well as Bayer based aluminas at 1500 to 1600°C due to their crystal morphology and low green density.

The crystal morphology of 99.95% alumina Bayer-derived aluminas are similar to those in Fig. 7. The 99.99% alumina crystal shape is quite unique due to decomposition from an alum salt. These crystals are usually referred to as wormlike due to their agglomeration into long wormlike chains, as shown in Fig. 14.[8]

Applications

The major markets for calcined aluminas are refractories, ceramics, and abrasives.[5–13] It is estimated that worldwide usage of calcined aluminas is approximately 20% for abrasives, 25% for ceramics, 50% for refractories, and 5% miscellaneous.

Abrasives

Calcined aluminas are used in the abrasives market in two major ways. The largest use is as a raw

Table III. High-Purity Aluminas

	Alcoa		Reynolds	Baikowski CR Series	Criceram EXAL Series	Sumitomo		Showa UA Series	Union Carbide	Condea (Arco)
	Alumalux 39	Alumalux 49	RC-HP DBM	CR-6	A6Z	A-HPS30	A-HPT	UA-5055	Linde A	HPA
Ultimate crystal size (μm)	<0.5	<0.5	0.5	0.25		0.3	0.3	0.3	0.3	
Surface area (m^2/g)	7–10	6	7–10	5–7	5–7	5–7	5–6	5	10–18	5–30
Al_2O_3 (wt%)	>99.95	99.99	99.95	99.99	99.98	>99.95	>99.99	99.99	99.98	99.97
Na (ppm)	75 (Na_2O)	5 (Na_2O)	<80 (Na_2O)	20	48	30	15	10		44
Si (ppm)	200 (SiO_2)	60 (SiO_2)	120 (SiO_2)	18	40	50	8	6		93
Fe (ppm)	100 (Fe_2O_3)	20 (Fe_2O_3)	32 (Fe_2O_3)	10	10	20	7	4		21
Particle size (μm)	0.5	0.5		<0.6	0.6	0.4	0.4	0. 5		0.6
Green density (g/cm^3)	2.15	2.10	2.12	1.55		2.25	2.11	1.90		2.16
Fired density (g/cm^3)	3.91	3.91	3.96			3.95	3.95			3.95
Compaction pressure (MPa)	345	345	345	138		300 kg/cm^2				345
Sintering temperature (°C)	1540	1540	1510			1600				1510
Sintering time (h)	1	1	2							2

Fig. 14. Alum-derived alpha alumina crystals.

material for production of white fused alumina. Calcined aluminas are melted in large electric arc furnaces using graphite electrodes. The lowest-cost calcined aluminas are used as feedstock. They exhibit high soda content and high surface area, as shown in Table I, Group A. The amount of LOI, or water absorption, is critical, as well as the particle-size distribution, in order to prevent excessive dust losses in the furnacing operation.

Calcined aluminas are also used as abrasives themselves.[8] In this case, aluminas are mainly used for polishing and lapping applications. Aluminas are usually mixed into polishing compounds (i.e., pastes or suspensions) and used to alter surfaces of metals, plastics, glass, and stones. Industries such as cutlery, automobiles, computers, furniture, eyewear, semiconductors, and jewelry use polishing aluminas. Polishing aluminas are also used to coat surfaces, such as video tape.

All types of calcined aluminas are used for polishing applications, from the coarsest, high-soda type to the high-purity, fine aluminas. Coarse-crystal aluminas (2 to 20 μm) usually are used for their high cutting effect due to the large, hard crystals. The finer-crystal (<1 μm) aluminas give a higher polishing effect for surface luster, particulary for softer materials (i.e., plastic).

To prevent scratches and meet stringent surface-quality requirements, the particle-size distribution of all polishing aluminas is rigidly controlled. This requires grinding and classifying operations on a few feedstock alumina materials to obtain a broad spectrum of various-sized polishing aluminas. Because of the extra processing, polishing aluminas are sold at a premium.

Ceramics

The ceramics market encompasses a wide variety of applications for alumina, from glass and chinaware to spark plugs, bioceramics, and integrated circuits.[4,11–13] In the United States and Japan, electronic applications are dominant, while in Europe, mechanical applications are the majority. Electronic and mechanical alumina ceramics usually contain greater than 85% alumina. Other uses, such as glass, chinaware glazes, and porcelain insulators utilize 5 to 25% alumina additions.

In the electronics field, the largest use of alumina is in production of spark plug insulators. Coarse-crystal (2 to 10 μm) aluminas with 0.05 to 0.20% soda are usually used so that optimum dielectric, mechanical, and thermal shock properties are obtained. Optimum processability (low shrinkage) is also obtained with these aluminas. Insulator bodies are usually 85 to 95% alumina.

There are numerous specialty electronic applications, including vacuum tube envelopes, rf windows, rectifier housing, integrated circuit packages, and thick- and thin-film substrates. These applications usually require the low-soda and thermally reactive aluminas. Electronic alumina ceramics are being produced with increasing quality, reproducibility, surface finish, flatness, strength, etc. Low-soda, thermally reactive alumina must, therefore, have consistent chemical purity, compaction, and sintering characteristics. These ceramics can range from 90 to 99.5% alumina. For substrates having printed metal circuits and other metallization, alumina is usually doped with

fluxing additives to form a microstructure that is optimum for a metal-ceramic bond.

A very unique application for high-purity alumina is in the manufacture of sodium vapor lamp tubes. While traditional glass tubes allow significant sodium diffusion at high temperatures, high-purity alumina tubes have excellent long-term resistance. When processed under strict sintering conditions, total light transmission through polycrystalline alumina can exceed 96%. This translucent alumina ceramic would not be possible without the availability of 99.99% pure calcined aluminas. Key impurities that must be minimized are SiO_2, CaO, Fe_2O_3, and Na_2O.

Alumina is well suited for mechanical applications that require high wear resistance, strength at low and high temperatures, and corrosion resistance. Typical alumina products include cutting tools, seal rings, pump parts, bearings, nozzles, thread guides, grinding media, wear plates, armor, and many others. All varieties of calcined aluminas are used. When optimum hardness, density, and wear resistance are required, the thermally reactive aluminas are used in compositions that are 95% alumina or more. When lower performance is adequate and when cost needs to be minimized, the lower-priced normal-soda calcined aluminas are utilized in compositions as low as 85% alumina.

The use of alumina for cutting tools could be a potentially fast-growing market. This application requires the use of thermally reactive, high-purity aluminas. Recent developments include the use of zirconia or fibers to form composite alumina structures with improved mechanical strength, fracture toughness, and cutting behavior.

Lower-cost normal calcined aluminas are used in many miscellaneous ceramic applications, including production of chinaware and porcelain insulators, where alumina imparts strengthening characteristics. Since clays are the main constituent of these ceramics, wet processing is used, which requires the soluble soda of normal calcined alumina to be minimized, and the alumina to exhibit minimum shrinkage during firing. Coarse-crystal, high-alpha aluminas are used. Production of specialty glasses can use one of the normal-soda calcined aluminas for increased alumina content and purity.

Another special mechanical use of high-purity calcined aluminas is in the medical field. Alumina ceramics are fabricated for bone and joint replacement, such as hip joints and dental implants. High mechanical strength, fine surface finish, high density, and high purity are requirements needed for success.

Refractories

Refractories are composed of an aggregate phase (coarse sintered grains) that is bonded together by various binders. Calcined alumina is used as one binder to improve the refractoriness, high-temperature creep resistance, strength, and corrosion resistance of refractories.[9,10] For dry-processed refractories (pressed shapes) and traditional refractory castables, normal, coarse (2 to 5 μm)-crystal calcined aluminas that have been ground to 95% -325 mesh are used. The aluminas are essentially 100% alpha to provide volume stability, but at the same time react during sintering to bond aggregate materials and other binders together in a dense matrix.

For special refractories that require optimum density and corrosion resistance, finer-crystal, lower-soda aluminas are utilized, usually in small amounts (<10%).[9,10] Higher concentrations may cause excessive shrinkage of the refractory product which leads to cracking. In the emerging area of low-moisture, low-cement castables, fine alumina that exhibits high reactivity but low water demand are particularly useful. These are low-soda aluminas that exhibit high green compaction densities.

There are also refractories produced by fusing raw materials. These refractories are usually large fused cast blocks of alumina, silica, and zirconia. High-alpha, coarse-crystal, unground, normal-soda aluminas are used as the alumina source. These same aluminas are also used to produce insulating refractories, those that exhibit high-porosity and low-density structures. Calcined aluminas are also used as raw materials for production of tabular alumina aggregates and calcium aluminate cements.

Later chapters in this book address in more detail the role of calcined aluminas in abrasives and polishing compounds, advanced ceramics, biomedical products, catalysts, coatings, electronics, glass, refractories, and whitewares.

Future Trends in Aluminum Raw Materials

In the field of calcined aluminas, there have been few truly new aluminas developed over the past 10 to 15 years. One example may be the production of pure, 99.99% alumina powder from alkoxide precursors. Apparently this material is available in spherical form.

The most technically advanced applications of calcined aluminas will require aluminas which exhibit greater consistency and uniformity of properties within a given "batch" and between batches sold to customers. In the electronics arena, there may be a stronger push for aluminas that have low alpha emissions to prevent inadvertent switching of electronic signals due to alpha emitters. For mechanical and wear applications where high density and maximum flexural strength are needed, calcined alumina powders are needed that will sinter to theoretical density. This must be accomplished at as low a sintering temperature as possible so that fired crystal size can be minimized. Research continues in areas of evaluating aluminas with a monosize particle distribution (M.I.T. and others), or seeding of monohydrate precursors with fine alpha aluminas (Penn State). There is also research on alumina that is toughened with a dispersion of zirconia.

With the continuing research and development in areas such as automobile ceramics, bioceramics, cutting tools, electronics, and mechanical (wear components) ceramics, one must expect that calcined aluminas will continue to be challenged to meet new property goals. The role of low-soda, thermally reactive aluminas, plus high-purity alumina, should increase.

References

[1] W. H. Gitzen (ed), Alumina as a Ceramic Material. The American Ceramic Society, Inc., Columbus, Ohio, 1970; pp. 1–253.

[2] K. Wefers and G. M. Bell, "Oxides and Hydroxides of Aluminum," Technical Paper No. 19, Aluminum Company of America, Pittsburgh, PA, 1972; pp. 1–51.

[3] G. MacZura, T. L. Francis, and R. E. Roesel, *Interceram.*, **25** [3] 200 (1976).

[4] E. Dorre and H. Hubner, Alumina, Springer-Verlag. Berlin, 1984.

[5] C. Misra, Industrial Alumina Chemicals. ACS Monograph 184, The American Chemical Society, Washington, DC, 1986.

[6] L. Hudson, C. Misra, and K. Wefers, "Aluminum Oxide"; in Ullmann's Encyclopedia of Industrial Chemistry, Volume A1. VCH Publishers, Deerfield Beach, FL 1985.

[7] G. MacZura, K. Goodboy, and J Koenig, "Aluminum Oxide"; pp. 214–44 in Kirk-Othmer Encyclopedia of Chemical Technology, Vol. 2, 3rd ed. Wiley & Sons, New York, 1978.

[8] Alumina Product Data Bulletins:

(a) No. CHE920, CHE922, Alcoa, Bauxite, Arkansas
(b) Alcoa Chemie, Lausanne, Switzerland
(c) Alcan Chemicals, Cleveland, Ohio
(d) Kaiser Chemicals, Cleveland, Ohio
(e) Malakoff Ind. (Reynolds), Malakoff, Texas
(f) Baikowski, Charlotte, North Carolina
(g) Criceram (Pechiney), Cedex, France
(h) Union Carbide Specialty Powders, Indianapolis, Indiana
(i) Sumitomo Aluminum Smelting, Tokyo, Japan
(j) Showa Alumina Industries SAL, Tokyo, Japan
(k) VAW Aluminum, Germany
(l) Martinswerke, Germany
(m) Pechiney, France
(n) Arco Specialty Chemicals, Newton Square, Pennsylvania

[9] G. MacZura, V. Gnauch, and P. T. Rothenbuehler, "Fine Aluminas for High Performance Refractories," *Interceram.*, **33** [5] 27–32 (1984).

[10] J. A. Everts and G. MacZura, "High Purity Aluminas for the Refractory Industry," *Industrial Minerals Refractory Supplement*, April 1983.

[11] C. T. McLeod, J. W. Kastner, T. J. Carbone, and J. P. Starr, "Aluminas for Tomorrow's Ceramics," *Ceram. Eng. Sci. Proc.*, **6** [9-10] 1233-43 (1985).

[12] T. J. Carbone, "Aluminas for the Ceramic Industry"; presented at Brazilian Ceramic Society 29th Annual Meeting, April 1985, Santa Catarina, Brazil.

[13] S. Kayama and Y. Oda, "Alumina for Ceramics and Its Latest Developments," *Taikabutsu*, 36-665, 1984

[14] L. K. Hudson, Alumina Production, Alcoa Research Laboratory, Alcoa Center, PA.

Production Processes, Properties, and Applications for Tabular Alumina Refractory Aggregates

George MacZura
Alcoa 670
One Allegheny Square
Pittsburgh, PA 15212

This chapter presents the historical development of tabular alumina as a product of ceramic sintering, associated frontier developments on processing and sintering pure Al_2O_3 ceramics which were instrumental in accelerating early advances in mechanical and electronic alumina ceramics, the tabular alumina manufacturing process, the effect of sintering aids, and the chemical and physical properties of the various tabular alumina grades in their crushed, graded, and ground forms. Tabular alumina grain properties are characterized with regard to physical properties important to ensuring optimum performance as a refractory aggregate for refractory brick, shapes, and monolithics. Tabular alumina refractory properties are characterized in depth using sintered-mullite and H_3PO_4 bonds and hydraulic bonding with calcium aluminate cements in castable refractories ranging from low- to high-cement contents. Finally, the many applications for tabular alumina refractories are presented.

Tabular alumina[1] derives its name from the large, typically 50 to >400 μm, flat tabletlike corundum crystals constituting the sintered synthetic α-Al_2O_3 briquet/ball shapes. Crystal facets are visible on fractured surfaces of this highly fired, fully shrunk recrystallized α-Al_2O_3 product. Tabular alumina is distinctly different from other dense, fine-crystalline, sintered aluminas and the white/dark fused aluminas.

The first dense sintered tabular corundum was prepared in 1934 by Thomas S. Curtis under Alcoa contract using his patented shaft furnace, called a converter.[2] The following chronological history traces the early evolvement of pertinent tabular alumina technical and commercial developments.

1935 Alcoa's pilot Curtis converter produced sufficient tabular Al_2O_3 to enable development and manufacture of sintered tabular Al_2O_3 brick for constructing a kiln to fire pure Al_2O_3 refractory/ceramic shapes.

1936 Production of sintered tabular Al_2O_3 containing 0.2 to 0.4% Na_2O was commercialized by the Aluminum Ore Company of East St. Louis, Illinois (Alcoa wholly owned subsidiary).
Dense tabular alumina grade T-60 analyzed typically <10% H_2O absorption (WA) and <25% apparent porosity (AP); porous tabular alumina grade T-70 was 16 to 22% WA and 55 to 75% AP.

1937 A low-soda (<0.05% Na_2O) sintered tabular Al_2O_3 was developed for alumina spark plug insulators and electron tube element supports and spacers. (The lowest-soda calcined Al_2O_3 available for these applications at the time contained 0.15% Na_2O maximum.)

1938 The <0.05% Na_2O tabular alumina (dense grade T-61 and porous grade T-71) was produced commercially in tonnage quantities for electrical/electronic applications. Spectrographic methods were developed for analyzing 0.002 to 0.6% Na_2O in Al_2O_3.

1939 First use of rubber-lined ball mill was made to minimize impurities during dry grinding of tabular Al_2O_3.

1940 Tabular α-Al_2O_3 grades (typically 0.02 and 0.15% Na_2O) ground to 90% −325 mesh (Tyler) were made commercially available by the Aluminum Ore Company.

1945/50 Ball-forming techniques were perfected, with tabular alumina balls being produced in various sizes between ¼ and ¾ inch for use as heat-exchange media and inert bed support for chemical process reactors.
Dense and porous tabular alumina grades were improved and produced in various crushed, graded, and ground sizes having the following typical properties:

Grade	Na_2O (%)	WA (%)	AP (%)
T-60	0.25%(max)	1–4	3–13.5
T-61	0.05%(max)	1–4	3–13.5
T-74	0.07–0.30	7–10	23–30
T-75	0.02–0.07	5–8	15–24

1948 Alcoa Research Laboratories–East St. Louis (ARL/ESL) used the electron microscope to supplement light microscopy for particle-size counts on ground tabular alumina for product development in refractory/ceramic applications.

1949 Began using the Andreason pipette sedimentation method to characterize the subsieve particle size of ground tabular Al_2O_3.

1950 The Furnas theory[3,4] to obtain an ideal size

distribution for maximum packing was applied to Al_2O_3 refractories and ceramic test compositions using blends of Al_2O_3 having different particle-size distributions to optimize properties.

1952 The Bouyoucos hydrometer method was adopted for characterizing and controlling the particle size of ground tabular alumina.

1953/55 ARL/ESL developed and characterized phosphate-bonded tabular alumina (Phos-Tab) ramming and castable mixes having remarkable abrasion resistance over a wide range of temperature and excellent serviceability in the temperature range to 1870°C (3400°F).[5]

Phos-Tab-rammed monolithic refractory linings in Alcoa production shaft furnaces extended lining life more than fourfold over the less than six-month average service life of the best brick and monolithic refractory linings using other bond systems.

Besides significantly reducing costs for producing tabular, this converter lining application, among others, demonstrated the feasibility and practicality of using orthophosphoric acid (H_3PO_4) with proper safety precautions in the field to form a strong permanent $AlPO_4$ bond on reaction with the tabular grain in situ at 315° to 425°C (600° to 800°F).

The concept of phosphate bonding using H_3PO_4 and monoaluminum phosphate (MAP) evolved, thus rapidly expanding the market for tabular alumina not only in monolithic refractories, but also pressed brick and prefabricated shapes. Almost every field of application requiring high strength/abrasion resistance in the broad temperature range of 260° to 1925°C (500° to 3500°F) has since had phos-bonded refractories evaluated for performance acceptance where compatible environments exist.

1954/56 ARL/ESL designed the tabular alumina aggregate particle-size distribution for maximum density after Furnas for use in evaluating high-purity calcium aluminate cement (CAC) in standard Cal-Tab test castables.[6]

Cal-Tab and Phos-Tab type castables found immediate application as wear-resistant linings in aluminum melting furnaces and fluid catalytic cracking units[7] operated at intermediate temperatures of 540° to 1095°C (1000° to 2000°F) where CA-25 excelled in strength over other commercially available CAC.

During the intervening years there have been extensive process modifications and improvements to optimize the tabular alumina process with regard to economy, product quality characteristics, and consistency of production. Process engineering modifications were incorporated with each new plant design which came on-stream as follows: 1954—Bauxite, Arkansas; 1960—Arkansas plant expansion; 1968—Alcoa Chemie Nederland, Rotterdam; 1975—Moralco Ltd., Iwakuni, Japan; 1986—Alcoa Chemie GmbH, Ludwigshafen, Federal Republic of Germany. Besides the aforementioned Alcoa tabular alumina production facilities, the following companies have sintered/tabular Al_2O_3 production plants in operation, with Kaiser chemicals being the first to come on-stream following Alcoa in 1959: Vereinigte Aluminum-Werke (VAW) in Europe and Showa Denko KK and NAIGAI Refractory Co. in Japan started production during the 1970s. VAW ceased tabular Al_2O_3 production in 1989.

Not all sintered aluminas are tabular Al_2O_3 because the alpha alumina crystal size is not large enough to warrant such distinction. Tabular Al_2O_3 is here defined as sintered aluminas having a median α-Al_2O_3 crystal size which averages 50 μm and greater, with the occurrence of large flat tabletlike α-Al_2O_3 crystals. Because of the grain-boundary porosity entrapped during rapid sintering, tabular alumina has a particle bulk density, also called bulk specific gravity, in the range 3.40 to 3.65 g/cm^3 with characteristic closed spherical porosity typical of a fully sintered ceramic with secondary recrystallization.[8] The excellent thermal shock characteristic of tabular alumina is attributed in part to these <1 to >10 μm closed spherical pores, which apparently act as crack arresters. Open porosity is characteristically low, being <5.0% and typically 1 to 2%.

On the other hand, sintered aluminas that cannot be classified as tabular Al_2O_3 have α-Al_2O_3 crystal size medians in the range <5 to about 25 μm. They are normally manufactured in rotary kilns and, because of kiln temperature limitations, most contain small amounts of MgO, CaO, or other additives to aid sintering and densification. The sintering aids help to sweep the porosity from between the submicrometer alpha alumina crystal during sintering, resulting in a rather pore-free microstructure. As might be expected from the microstructure characteristics, these finely crystalline, dense, sintered aggregates are extremely strong, but lack the thermal shock resistance of tabular alumina.

Sintered aluminas are prepared from calcined alumina produced by the Bayer process, so soda exists in small amounts as the major impurity, usually being <0.3% Na_2O when using a typical 0.4 to 0.5% Na_2O alumina feedstock. Loss of Na_2O to evaporation during the sintering process accounts for the difference. The quantity of soda in the sintered product can be controlled by the quantity of Na_2O in the starting raw material and/or the use of additives, such as H_3BO_3, to enhance vaporization, which also enhances mineralization. Typical impurities include about 0.05% SiO_2, 0.05% Fe_2O_3, and <0.1 to 0.40% Na_2O, with the lower

level occurring in U.S. products and the higher level in Japanese and European products.

Today, dense tabular is available in numerous smooth ball sizes to about 25.4 mm (1 in.) diameter and in crushed and graded sizes from a top size of 12.7 mm (0.5 in.) to −325 mesh (44 μm). Extensive magnetic separation is required to remove iron from the crushed grains to minimize discoloration in refractory and ceramic products. The porous tabular alumina T-70 grades have not been manufactured since the mid-1960s.

Further details on the tabular alumina manufacturing processes, grades, and properties, and the new developmental tabular Al_2O_3 aggregates are presented in this chapter. Also, additional information on the various refractory products and applications involving tabular alumina are reviewed.

Tabular Alumina Manufacture—A Ceramic Sintering Process

The successful development of the Alcoa tabular alumina process required extensive R & D programs to develop the necessary analytical procedures and test methods for characterizing and optimizing the ground calcined α-Al_2O_3 feedstock and the finished sintered tabular alumina product. Likewise, techniques for fabricating, sintering, and testing pure α-Al_2O_3 ceramics had to be developed to appraise the potential of developmental sintered alumina products.

These frontier developments on processing pure alumina ceramics were shared with the ceramic industry as they occurred, and thus were very instrumental in the accelerated advances achieved by mechanical and electronic alumina ceramics from 1950 to 1960. Although some of these technical achievements were highlighted in the introduction, a few having specific impetus on advancing the refractory/ceramic technologies are further expanded during the following discussion on the tabular alumina process.

The production process for the manufacture of tabular alumina involves the basic unit operations used in ceramic processing to produce sintered alumina ceramics having utility. Raw material grinding, forming/shaping, drying, and sintering are also the necessary stages of processing in the manufacture of tabular alumina through the sintered ball stage, as shown in the tabular alumina process schematic (Fig. 1).

Tabular smooth balls have a uniform α-Al_2O_3 microstructure. The process has been controlled to minimize macrodefects so as to give corundum spheres which are highly resistant to thermal and mechanical shock. Outstanding performance is achieved as heat-exchange pebbles for transferring process energy in moving beds, stationary heating beds, catalyst bed support, fluid energy dispersion beds, and refractory aggregate. Tabular alumina dense smooth balls are made in several grades and are available in the following sizes: 6.4, 9.5, 12.7, 15.9, and 19.0 mm (¼, ⅜, ½, ⅝, and ¾ in.).

Alumina Grinding

The calcined alumina feedstock used for the production of tabular alumina has a controlled surface area. The fine crystalline α-Al_2O_3 feed aids sintering and densification, but only after dry grinding the 100–325 mesh Bayer agglomerates by continuous ball milling. Feedstock soda typically falls into the 0.2–0.4% Na_2O range while the SiO_2, Fe_2O_3, and CaO will each typically fall into the 0.01–0.05% range.

Ball Forming

The fine grind on the calcined Al_2O_3 feedstock is important not only with regard to densification on sintering, but also for ensuring successful forming of the green balls in the Alcoa proprietary pelletizing process which utilizes a rotating drum to grow the ¼ in. seed balls to the desired 1.0 to 1.25 in. diameter. The spheres grow by a layering process similar to that of rolling a snowball. The ball-forming process involves sequentially wetting the balls' surfaces with a fine water/binder spray, dusting the surface with the finely ground calcined alumina, and then rolling to compact the surface. Green balls must develop sufficient strength to avoid breakage during handling and transport to the dryer chamber, which is positioned above the Curtis shaft furnace. Sometimes starch or other organic binders are used to increase green strength. The strength of the green balls is also enhanced whenever H_3BO_3 is added to the binder solution.

Drying

Thermally efficient dryers have been designed for continuously drying the green balls to remove the nominal 15% moisture prior to being transferred to the top of the converter (500°C, 932°F). An induced-draft fan draws the hot exhaust gases from the top of the converter and through the bed of balls which pass countercurrent to the flow of hot gases in the dryer. Temperatures are continuously monitored and controlled to prevent thermal shock fracture of the green balls. Fractured balls impede the uniform gravity free flow of the ball bed through the dryer, cause channeling, and subsequent nonuniform drying with further worsening of the thermal shocking episodes.

Tabular Conversion/Sintering

The continuous Curtis converter used in firing tabular alumina at sintering temperatures of 1815° to 1925°C (3300° to 3500°F) is generally operated by combusting natural gas with air. Liquified petroleum gas (butane) is used where natural gas is not available.

The flow of the Al_2O_3 balls through the shaft furnace is controlled by a discharge table (Fig. 2). Flow of the theoretical gas/air mixture is balanced with the Al_2O_3 ball throughput to obtain proper drying rates and full conversion to the tabular alumina structure, as evidenced by the crystal development of the converter

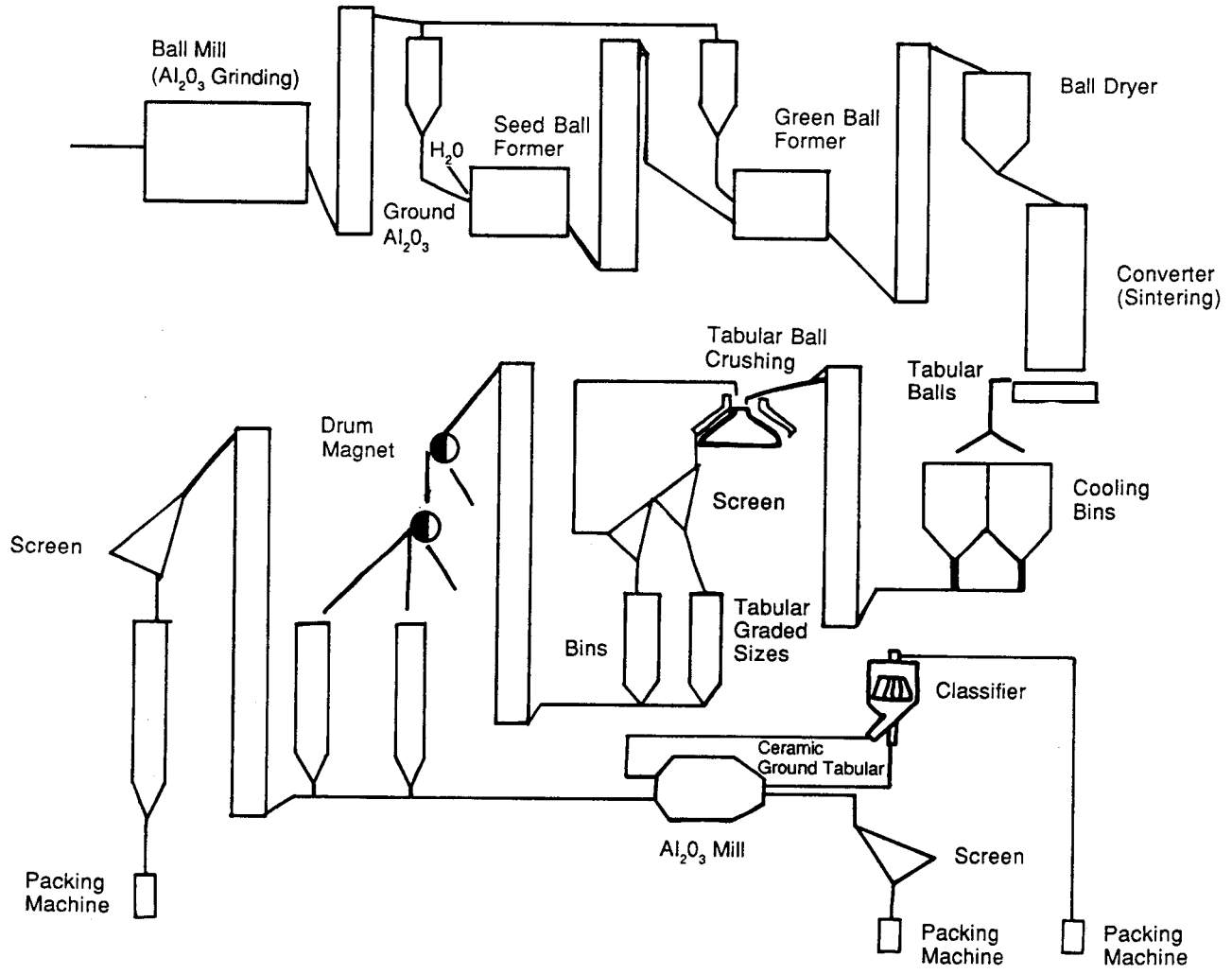

Fig. 1. Tabular production system.

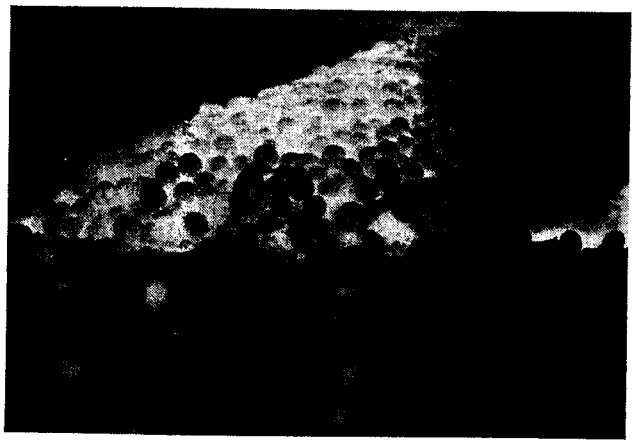

Fig. 2. White hot tabular Al_2O_3 spheres discharging from Curtis converter.

discharge. The α-Al_2O_3 crystals of properly fired tabular alumina can be seen in reflected light by the naked eye.

The crystal structure is appraised in comparison with standards for acceptability by visual inspection of the tabular alumina fractured surfaces with a lighted low-power magnifying glass after crushing the cooled sintered balls. Under- and overfired tabular exhibit open porosity that is readily detected and rejected by the operator using dye solutions common to the ceramic industry for evaluating porosity in dense fired ceramics. Acceptable quality tabular product in the cooling bins is further characterized by laboratory analysis to determine the BSG, AP, and WA to ensure that minimum specifications have been met prior to crushing or transfer to pack/ship for bagging or bulk shipment to customers.

Al_2O_3 Sintering Studies

Sintering studies on Al_2O_3 were cumbersome in the early 1930s because of the lack of adequate pro-

cessing equipment for grinding aluminas without contamination and the lack of laboratory high-temperature furnacing equipment with adequate hearth area for sintering studies on a rapid turnaround basis. Fine grinding of alumina with steel balls in steel mills required troublesome and cumbersome HCl leaching, followed by extensive washing, filter pressing, and drying, if powders were desired for dry-pressing test specimens. Organic binders were used to provide adequate green strength for handling. Researchers took advantage of the deflocculating characteristics of the HCl to make slipcast pure Al_2O_3 crucible cups and boats to act as containers for calcining alumina and for holding small test specimens during sintering studies.

The improved techniques developed and used by ARL/ESL through the 1930s and 40s were finally disclosed to industry in July 1951[9] to enhance the market development of alumina ceramic applications. The techniques developed by W. H. Gitzen and W. F. Graebe were given in detail. A 1.2 kg Al_2O_3 charge was ground with 900 cm^3 of distilled water and 6 cm^3 of HCl (37.5% concentration) using about a 55 vol% mill volume loading of 1 to 1.25 in. diameter sintered alumina balls for 4 hours in a one gallon rubber-lined ball mill rotated at 70 rpm. This lab grind avoids any iron contamination. Besides providing directions for processing and stabilizing the 1.85 specific gravity slip at pH 1 and slipcasting shapes in white dental plaster after deairing the slip, further details were given for proper stacking of crucibles and combustion boats to prevent warpage and cracking induced by shrinkage and plastic flow at maturing temperatures. It was recommended that "long slender tubes or other shapes, easily affected by thermal flow, must be suspended by supporting on a sintered alumina pin passing through a thickened or expanded portion of the shape which may later be diamond sawed to remove." This technique of suspension firing and modifications thereof are still being used as a common practice for firing alumina ceramic tubes.

The pure Al_2O_3 combustion boats were invaluable in sintering studies for characterizing the effect of small metal oxide additions on the sintering behavior of tabular alumina. Likewise, the laboratory-scale pot-type surface combustion furnace using natural gas and plant-source compressed air through a single burner provided rapid, daily turnaround firings. Pressed cyclinder and 9.38 by 9.38 by 75 mm (⅜ by ⅜ by 3 in.) bar specimens were housed in cylindrical saggers (1 in., 25 mm wall) fabricated with a graded tabular alumina particle-size distribution for maximum packing and bonded initially with aluminum sulfate. These saggers were subsequently replaced by the previously mentioned Cal-Tab and Phos-Tab formulations. Tabular alumina balls embedded the sagger chamber in the furnace cavity and provided the surface combustion media necessary to achieve a temperature of 1800°C (3272°F) within 1.5 to 2.0 hours. This 1900°C (3472°F) laboratory "workhorse" furnace was normally fired 4 hours at 1750°C, 2 hours at 1800°C, or 1 hour at 1850°C to obtain equivalent maturing of the pure alumina specimens sintered with available aluminas in 1951. Subsequent development of thermally reactive calcined aluminas by Alcoa in the mid-1950s reduced the heat treatment for <1 μm crystalline aluminas to only 1 hour at 1520°C (2770°F); thus the origin of the name reactive aluminas. Figure 3 is a later design of the laboratory Curtis-type furnace design as modified by L. D. Hart and coworkers.

Table I lists the results of one of many sintering studies conducted in this utility surface combustion laboratory furnace. Such studies provided direction in optimizing the proper calcined alumina feedstock for producing tabular alumina, enabled optimization of tabular alumina smooth ball compositions to eliminate macro- and microdefects, enabled thermal shock studies to proceed for optimizing the α-Al_2O_3 structure of tabular alumina (Table II), and aided in the development of high-alumina and pure alumina grinding media and accelerated their commercial production and availability for ceramic milling tabular and calcined aluminas to avoid metallic contamination.

The laboratory Curtis surface combustion furnace continues to be actively used for sintering studies. An example of such a study on the effect of different sintering aids on the bulk density and median crystal size of tabular alumina using pressed specimens with different metal oxide additions and a 0.47% Na_2O, 0.5 μm calcined Al_2O_3 is shown in Table III. The data confirm previous studies on the significant advantage

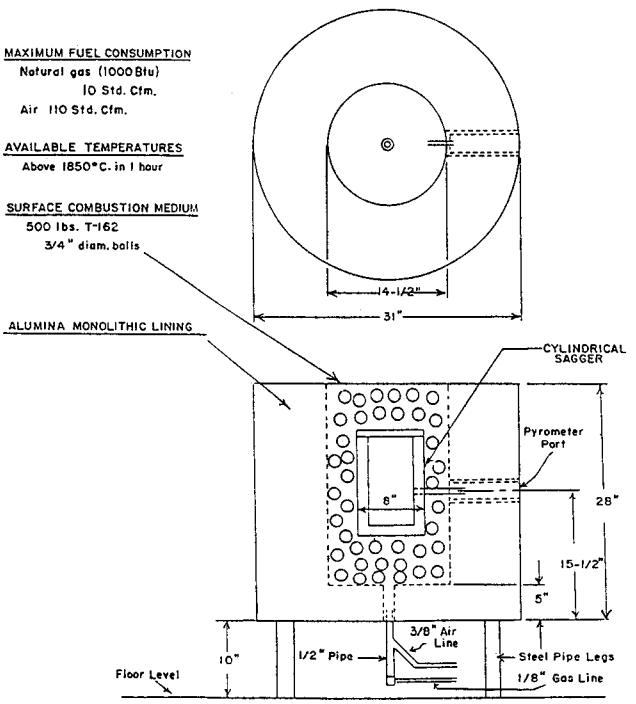

Fig. 3. Laboratory high-temperature surface combustion furnace.

Table I. Influence of Selected Additives on Sintered Alumina Properties

Exp. No.	Additive to Alumina Composition: Material	Additive to Alumina Composition: % in Al_2O_3	Green Body Density Dried at 110°C g/cc	Properties of Bodies Fired at 1800°C: Bulk Density (g/cm^3)	Linear Shrinkage (%)	Apparent Porosity (%)	Modulus of Rupture† lbs./sq.in.: Average	Modulus of Rupture† lbs./sq.in.: Std σ	Crystal Size (μm): Average	Crystal Size (μm): Max.	Crystal Size (μm): No. of Specimens
				Alumina A-303 Fired 2 hours at 1800°C in lab Curtis converter*							
4257-G	(Control) H_2O	10.0	1.86	3.71	20.1	0.17	19 050	2020	100	300	11
4325-G	$2MgO \cdot 3SiO_2$‡	0.5	1.79	3.78	21.3	0.24	36 280	4560	30	50	5
4326-G	$2MgO \cdot 3SiO_2$	1.0	1.76	3.74	21.5	0.24	34 430	3430	25	40	5
4322-G	$3Al_2O_3 \cdot 2SiO_2$	0.5	1.74	3.71	21.8	0.30	28 460	1860	60	110	4
4297-G	$3Al_2O_3 \cdot 2SiO_2$	1.0	1.82	3.67	21.6	0.25	22 490	1440	60	160	12
4298-G	$3Al_2O_3 \cdot 2SiO_2$	4.0	1.76	3.74	21.6	0.75	18 090	1630	90	350	13
4323-G	$3CaO \cdot 5Al_2O_3$	0.5	1.81	3.61	20.0	2.13	14 590	1690	80	150	6
4299-G	$3CaO \cdot 5Al_2O_3$	1.0	1.75	3.62	20.9	2.69	13 890	790	80	120	13
4300-G	$3CaO \cdot 5Al_2O_3$	4.0	1.79	3.49	19.8	5.12	14 290	1300	80	110	15
4324-G	TiO_2	0.5	1.74	3.74	21.5	1.33	12 010	2110	100	300	5
4301-G	TiO_2	1.0	1.75	3.76	22.3	1.27	10 050	970	100	330	13
4302-G	TiO_2	4.0	1.77	3.63	22.4	5.19	6 340	1740	150	350	9
				Alumina A-303 Fired 4 hours at 1700°C in lab Curtis converter*							
4345-G	(Control) H_2O	10.0	1.90	3.64	19.2	0.55	20 490	990	75	100	5
4354-G	$2MgO \cdot 3SiO_2$	0.5	1.77	3.80	22.1	0.19	38 410	3010	30	50	5
4347-G	MgO	0.5	1.87	3.79	22.1	0.12	28 360	6190	20	40	5
4360-G	MgO	4.0	1.81	3.67	22.0	0.49	28 050	1130	20	25	5
4351-G	MgF_2	0.5	1.79	3.82	21.6	0.26	27 200	4690	20	40	5
4358-G	MgF_2	4.0	1.78	3.60	19.5	2.24	19 050	2180	25	40	5
4350-G	$CoCl_2 \cdot 6H_2O$	0.5	1.84	3.85	21.7	0.12	28 110	3680	40	80	5
4363-G	$CoCl_2 \cdot 6H_2O$	4.0	1.85	3.66	19.4	2.27	22 000	1290	50	80	5
4355-G	$3Al_2O_3 \cdot 2SiO_2$	0.5	1.72	3.70	20.3	0.26	28 050	4090	60	100	5
4346-G	ZnO	0.5	1.80	3.77	19.5	0.61	22 140	1130	30	100	5
4357-G	ZnO	4.0	1.81	3.60	19.4	3.03	21 200	4000	35	60	5
4352-G	Al_2F_6	0.5	1.84	3.52	18.4	0.49	18 040	2580	75	100	5
4359-G	Al_2F_6	4.0	1.84	3.46	19.4	4.07	22 500	3860	40	80	5
4349-G	Cr_2O_3	0.5	1.80	3.70	20.1	0.44	18 800	2210	50	70	5
4362-G	Cr_2O_3	4.0	1.86	3.74	20.3	0.42	21 780	2320	50	110	5
4348-G	MnO_2	0.5	1.83	3.63	21.0	0.95	18 530	2210	60	100	5
4361-G	MnO_2	4.0	1.82	3.54	21.9	2.96	15 760	1950	75	100	5
				Alumina Grade A-11 Fired 4 hours at 1700°C in lab Curtis converter**							
4368-G	(Control) H_2O	10.0	1.78	3.61	21.0	2.50	28 300	2030	50	70	5
4339-G	$2MgO \cdot 3SiO_2$	0.5	1.77	3.84	22.5	0.07	37 260	4630	25	60	5
4407-G	$2MgO \cdot 3SiO_2$	1.0	1.83	3.78	22.8	0.20	38 400	1600	30	60	5
4408-G	$2MgO \cdot 3SiO_2$	2.0	1.81	3.69	22.5	0.22	37 800	2720	35	60	5
4409-G	$2MgO \cdot 3SiO_2$	4.0	1.78	3.58	22.2	0.18	33 800	1260	30	60	5
4369-G	MgO	0.5	1.69	3.85	21.2	0.16	34 700	1650	25	50	5
4404-G	MgO	1.0	1.90	3.83	23.8	0.23	32 500	1960	25	50	5
4405-G	MgO	2.0	1.86	3.79	22.8	0.26	31 300	1150	20	40	5
4406-G	MgO	4.0	1.86	3.72	22.5	0.45	31 700	3190	20	40	5
4334-G	$3Al_2O_3 \cdot 2SiO_2$	0.5	1.79	3.72	21.4	0.14	30 370	4660	50	75	6
4340-G	$3Al_2O_3 \cdot 2SiO_2$	4.0	1.78	3.72	21.0	0.28	27 560	1820	75	110	5
4337-G	$3CaO \cdot 5Al_2O_3$	0.5	1.78	3.65	20.6	0.42	20 880	1590	75	110	5
4336-G	$3CaO \cdot 5Al_2O_3$	4.0	1.96	3.62	18.1	0.39	18 160	830	70	110	5
4338-G	TiO_2	0.5	1.78	3.80	21.9	0.44	13 050	510	200	500	5

*Alumina A-303 Number S-2762-E, nominally 0.5% Na_2O, 0.5 μm α-Al_2O_3, plant-ground to 90.4% finer than 325 mesh.
†⅜" × 3" test bars, dry-pressed at 5000 lbs. per sq. inch
‡Analysis: MgO 19.84%, SiO_2 47.20%, L.O.I. 30.40%, Na_2O 2.07%.
**Alumina A-11, Number S-1553, nominally 0.20 to 0.25% Na_2O, 4μm α-Al_2O_3, laboratory dry-ground to 90% finer than 325 mesh.

Table II. Influence of Thermal Shock on Empirical Compressive Strength*

	3713-G				3714-G				3730-G				3731-G				3736-G				3737-G			
	Y				Y				Y				Y				Y				Y			
X	(1)	(2)	$\bar{Y}$	$\bar{Y}_4$	(1)	(2)	$\bar{Y}$	$\bar{Y}_4$	(1)	(2)	$\bar{Y}$	$\bar{Y}_4$	(1)	(2)	$\bar{Y}$	$\bar{Y}_4$	(1)	(2)	$\bar{Y}$	$\bar{Y}_4$	(1)	(2)	$\bar{Y}$	$\bar{Y}_4$
									Gradient: 500°C. to 100°C.															
0	5238†				5188†												6200‡				6140‡			
2	5750	1600	3675	4488	3750	2250	3000	3646									4000	3750	3875	3875	4000	3500	3750	3750
4	4600	4500	4550	3491	3250	2250	2750	2808									3600	3000	3300	3458	3500	2600	3050	3183
6	2500	2000	2250	3858	2750	2600	2675	2558									4100	2300	3200	3208	2500	3000	2750	2950
8	4800	4750	4775	3525	2500	2000	2250	2433									3250	3000	3125	3358	3500	2600	3050	3017
10	3600	3500	3550	4058	2500	2250	2375	2458									4000	3500	3750	3458	3250	3250	3250	3100
12	4100	3600	3850	3650	3250	2250	2750	2158									4050	3000	3500	3500	3500	2500	3000	3187
14	3600	3500	3550	3528	1750	1000	1350	1958									3250	3250	3250	3308	3000	3600	3300	3158
16	3500	2500	3000		1800	1750	1775										3250	3100	3175		3600	2750	3175	
									Gradient: 1000°C. to 100°C.															
0	5238†				5188†				6163†				5995†				6200‡				6140‡			
2	4000	2000	3000	3829	3300	2500	2900	3646	3300	3100	3200	4604	4000	3000	3500	4248	3300	2900	3100	4183	3500	2300	2900	2900
4	4250	2250	3250	3608	3250	1250	2250	2383	4600	4300	4450	4217	4250	3250	3750	3717	3250		3250	2933	2750	2500	2625	2733
6	4750	4400	4575	3642	2750	1250	2000	2783	5000	5000	5000	4300	4300	3500	3900	3558	2600	2360	2450	2775	3250	2100	2675	2708
8	3900	2300	3100	3842	3500	2300	2900	2383	4000	2900	3450	4067	3300	2750	3025	3283	3250	2000	2625	2800	2900	2750	2825	2250
10	5700	2000	3850	3108	2500	2000	2250	2428	4500	3000	3750	3400	3900	2250	2925	3442	3900	2750	3325	3442	2800	1500	2150	2075
12	3250	1500	2375	3083	2750	2000	2375	2167	4000	2000	3000	3175	4600	4250	4375	3583	3500	3250	3375	2775	3600	2500	3050	2783
14	3300	2750	3025	2850	2500	1250	1875	2183	3300	2250	2775	3133	3900	3000	3450	3483	2000	1250	1625	2558	3300	3000	3150	2850
16	3300	3000	3150		2500	2100	2300		4000	3250	3625		3250	2000	2625		3250	2100	2675		2600	2100	2350	

Y = Individual compressive strength at a specific cycle - lbs/cm-ball
$\bar{Y}$ = Average of individual compressive strengths at each cycle - lbs/cm-ball
$\bar{Y}_4$ = Running average of $\bar{Y}$ values over four cycle interval
X = Number of thermal shock cycles.
* Running averages begin at two cycles.
†Average of 20 determinations.
‡Average of 10 determinations.

of using small amounts of MgO as a sintering aid for alumina in restricting crystal growth and maximizing density.

Morgan and Koutsoutis[10] suggest that the soda level (0.4 to 0.5% Na_2O) in commercial Bayer aluminas used in TiO_2-doped sintering studies is sufficient to cause liquid-phase sintering to occur as low as 1350°C (2460°F). Ikegami et al.[11] provide a recent reference review on the use of MgO and TiO_2 for sintering Al_2O_3. They also confirm that TiO_2 greatly enhances the densification of Al_2O_3 in the initial and intermediate stages of sintering, compared to undoped and MgO-doped Al_2O_3. Their work supports the Morgan and Koutsoutis consensus of a transient liquid-phase occurrence in the 1350° to 1400°C range. However, MgO enhances the final stages of sintering at 1600°C compared to the undoped and TiO_2-doped Al_2O_3 and results in achieving a final density of 99% theoretical, compared to only 97 to ≈98% theoretical for the undoped and TiO_2-doped Al_2O_3 sintered samples, respectively.

Tabular Crushing/De-Ironing and Screening

The kiln discharge (KD) from the shaft converter is stored in cooling bins, then processed through the crushing, de-ironing, and sizing operations. The KD balls feed the Gyradisc crusher from storage bins. Crushed tabular is screened through two 1.2 by 3.0 m (4 by 10 ft) Derrick screens with the sized product passing through two magnetic drum separators in series for removing metallic iron pickup from the crusher. Highly wear-resistant, nonmagnetic hardened-alloy crusher plates cannot be used because of the inability to remove metallic contamination by de-ironing. The screened oversized tabular is cycled back to the Gyradisc for further size reduction. The graded tabular sizes are stored in needle bins. Some have been modified to evaluate the ability to minimize segregation. Likewise, transfer points have been especially designed to minimize segregation during transport of the product through processing to bagging. The crushed products are packaged in 100 pound multiwall paper bags and controlled to a net weight of 100 pounds ± 1.0 lb. The bags are automatically palletized and shrink-wrapped for shipping. The graded products are also available for bulk rail shipments.

Ceramic Milling

Tabular alumina grades −48 mesh and finer are primarily manufactured by ceramic milling using coarser crushed tabular alumina sizes as feedstock. The air-swept ball mills are currently lined with 90% Al_2O_3 abrasion-resistant mill-lining brick. Likewise, 90% Al_2O_3 abrasion-resistant ceramic balls are being used to avoid oxide contamination. These were upgraded in the 1960s to approach the wear resistance of the 99.8%

Table III. Effect of Sintering Aids on Al_2O_3 Density and Crystal Growth

Additive	Amount (wt%)	Bulk Density (g/cm^3)	Median Crystal Size (μm)
Calcined Al_2O_3 (control) (0.47% Na_2O, 0.5 μm α-Al_2O_3)		(3.70)	50–80
MgO	0.01	+0.10	
	0.02	+0.12	
	0.05	+0.13	20
	0.1	+0.14	
	0.2	+0.14	20
SiO_2	0.02	0	
	0.05	+0.01	
	0.10	+0.02	40
B_2O_3	0.3	−0.09	
	0.6	−0.05	80
	0.9	−1.0	
Y_2O_3	0.05	+0.04	
	0.1	+0.06	
	0.2	+0.06	40
La_2O_3	0.05	+0.04	
	0.1	+0.04	
	0.2	+0.05	50
NiO	0.2	0	
	0.05	+0.04	
	0.10	+0.10	
Fe_2O_3	0.02	0	
	0.05	0	
	0.10	+0.01	
	0.5	+0.06	
	1.0	+0.08	
	2.0	+0.12	25
Mn_2O_3	0.5	+0.08	
	1.0	+0.08	
	2.0	+0.06	80
TiO_2	0.5	+0.06	40
	1.0	+0.03	60
	2.0	−0.03	100
AlF_3	0.5	−0.30	30
	1.0	−0.50	30
	2.0	−0.60	30

Note: Calcined Al_2O_3 ground with and without additives to nominally 1 μm, 25 mm disks, die-pressed at 69 MPa (10 ksi) with 10 g Al_2O_3 and heated, 1750°C, 1 h in a laboratory Curtis converter.

Al_2O_3 grinding media developed by Alcoa[12] and commercially produced by ceramic manufacturers. The high-purity 99.8% Al_2O_3 grinding media can be economically justified for grinding the high-purity reactive aluminas currently available on the market, but not for grinding tabular.

Ceramic grinding of tabular alumina began in the 1950s with initial development beginning with the use of smooth tabular alumina balls as grinding media. This was followed by isostatically pressed 98% Al_2O_3 grinding media developed by Gitzen and Graebe with technology being transferred to commercial alumina ceramic producers for commercialization. Special tests[12] were developed for characterizing the wear resistance of alumina grinding media by Alcoa, which ultimately led to the further improvement of the 90% Al_2O_3 grinding media and improved performance over the previously developed 85% Al_2O_3 products.

Energy Requirements for Tabular Production

Fuel consumption for tabular alumina conversion in the vertical shaft furnace has been effectively improved in recent years with major capital investments. The furnace design was modified to improve heat recovery and feedstock was optimized to obtain more efficient tabular conversion at increased recovery by eliminating the boric acid used to aid reduction of Na_2O by volatilization during sintering. Fuel consumption is continuously being reduced in tabular alumina production. The energy requirement for tabular alumina conversion is less than the energy requirements for melting calcined alumina in the production of white fused products.[8]

Tabular Alumina Production Capacity

Tabular Al_2O_3 is produced in large-scale production centers having a capacity of 50 000 to 125 000 metric tons annually. In 1982, Everts and MacZura[13] estimated tabular Al_2O_3 worldwide production capacity for 1983 at about 240 000 metric tons (Fig. 4). Using a 10% annual growth rate and a 1982 tabular Al_2O_3 consumption of about 120 000 metric tons, adequate supply was projected until 1990.

The projected 10% growth did not occur and more closely approximated a 0% growth rate during the recession years through 1986. Cost-reduction programs netted increased efficiencies and production capacities during these years. Thus, worldwide tabular Al_2O_3 capacity appears more than abundant to supply the demand until the twenty-first century.

Patents Relative to Sintered Alumina Production

Except for the protection provided by the Curtis patent,[2] Alcoa sought no patent protection with regard to tabular alumina production. In 1937, Fessler[14] pat-

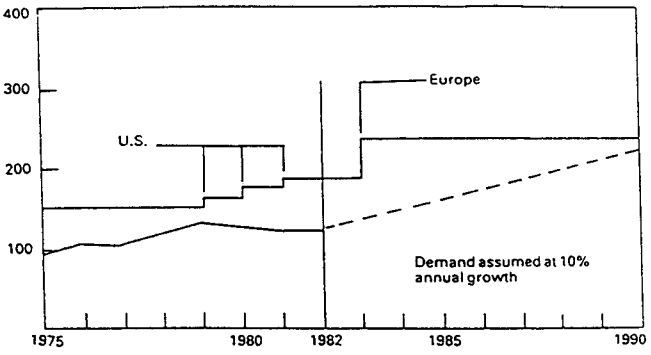

Fig. 4. Tabular alumina—estimated worldwide supply/demand (1975–1990).

ented the concept of using boric acid (H_3BO_3) in the molecular ratio of 4 B_2O_3 to 1 Na_2O to reduce the soda content of alumina on calcining it at a temperature of about 1400°C (2550°F) to remove the soda by volatilization as sodium borate compounds. Thompson[15] restricted crystal growth during Al_2O_3 calcination in the rotary kiln when using H_3BO_3 addition to reduce Na_2O by preventing the recycling of sodium tetraborate with the kiln dust.

Paul and House[16] discovered that a dense, high-purity alumina refractory grain can be made from gibbsite (aluminum trihydrate) by compacting the dry hydrate under a pressure of at least 414 MPa (60 000 psi), and firing. They found it preferable to subject the material to shear stresses during compaction, as in a roll-type briquetting press. This procedure eliminates the need for precalcining the hydrate prior to conversion sintering. The high-pressure compaction is the key (to the successful firing of the hydrate briquets without disintegration). For example, compacts pressed at 138 MPa (20 000 psi) exploded within seconds after being introduced statically into a furnace at 1000°C (1832°F), whereas compacts pressed at >552 MPa (>80 000 psi) had a >90% intact briquet survival rate after dropping 20 feet into the >1100°C (2010°F) feed-end of a rotary kiln and subsequently tumbling through the >1700°C (3090°F) hot zone and discharging.

Ring[17] patented a process for producing sintered alumina shapes or grains of low porosity and reduced Na_2O content by taking advantage of the synergistic reaction of a magnesium salt and a boron compound with calcined Al_2O_3 when sintering for 1 to 25 hours within the temperature range of about 1600° to 1900°C (2910° to 3450°F). The sintered Al_2O_3 product had a porosity of <3% by the Hg displacement technique and <0.03% Na_2O when using a 0.2 to 1.0% Na_2O calcined Al_2O_3 and about 0.01 to 0.3% Mg added as a magnesium salt and 0.1 to 1.0% B_2O_3 when added as a boron compound with all additions being based upon the Al_2O_3 weight. The calcined Al_2O_3 feedstock had an average particle size of 2 to 6 μm before being shaped into pellets of about 13 mm average diameter using water or water-soluble magnesium salts in water as the shaping liquid. The synergistic effect of reducing porosity and Na was not realized when using $Mg_3(BO_3)_2$ additions (boron-free magnesium salt).

Tabular Alumina Grades and Properties

Environmental emission control laws in Europe and Japan prevented the use of H_3BO_3 additions for Na_2O reduction in the tabular alumina T-60 grades manufactured in these countries since 1968 and 1975, respectively. Typical soda in the T-60 grades ranges about 0.25 to 0.30% Na_2O with a 0.40% Na_2O maximum for converter discharge (CD). The soda level is dependent upon that of the available calcined Al_2O_3 feedstock. Although this soda level has not been approved by some U.S. refractories manufacturers for production of 90 to 99+% Al_2O_3 brick and pressed shapes, the Japanese and European manufacturers have continued to use the available T-60 grades for the production of these products.

Properties of T-60 CD are compared in Table IV with the lower soda T-61, T-1061, and T-64 grades being available from the United States. Boric acid is

Table IV. Comparison of Properties among T-64, T-60, T-61, and T-1061

			Published Data		
		Alcoa T-64	Alcoa T-60	Alcoa T-61	Kaiser T-1061
Typical Properties (Converter Discharge)					
Al_2O_3	%	99.7+	99.5	99.5+	99.8
SiO_2	%	0.04	0.04	0.06	0.06
Fe_2O_3 (total)	%	0.06	—	0.06	0.03
Fe_2O_3 (acid soluble)	%	0.01	0.02	—	—
Na_2O	%	0.16	0.30	0.10	0.03
CaO	%	0.04	0.05	—	—
MgO	%	<0.001	—	—	—
B_2O_3	%	<0.001	—	—	—
Bulk density, packed, lb/ft³					
Converter discharge		128		125	
Granular, −14 mesh		138		135	
Powder, −325 mesh		143		140	
Specific gravity, bulk, g/cm³		3.50–3.65	3.6	3.40–3.60	3.40–3.56
Apparent porosity	%	3	4.0	5	5
Water absorption	%	0.8	1.5	1.5	2
Specifications for Shipment					
Na_2O (max)	%	0.22	0.40	0.20	0.20
Apparent porosity (converter discharge) (max)	%	7	8.0	10	10
Water absorption (converter discharge) (max)	%	2	4.0	4	4

very effective in significantly reducing the Na_2O level in sintered aluminas, that is, tabular alumina T-61 grade at one time was produced consistently at a <0.01% Na_2O level when using a 0.4 to 0.5% Na_2O calcined Bayer alumina feedstock. However, condensation of the sodium borate compounds in the cooler portion of the alumina bed at the top of the shaft furnace causes channeling and periodic over- and underfiring of the finished tabular alumina balls, thus causing excessive product variability and high rejection rates.

In 1984, economic studies by Alcoa determined the cost of reject to be excessive when using boric acid addition in the manufacture of tabular alumina, even when used in moderate additions. A major capital investment was justified to produce an intermediate Na_2O alumina feedstock for the production of the new tabular alumina grade T-64, having a typical soda in the range 0.15 to 0.20% Na_2O and a 0.22% Na_2O maximum, without the use of boron.

T-64 product quality and uniformity are greatly improved over that of T-61 because of the more consistent tabular alumina microstructure obtained during converter firing by the elimination of boron additions. The CD also crushes more uniformly and predictably by the minimization of over- and underfired CD balls. Typical properties and specifications for crushed and ground tabular aluminas are given in Table V.

Tabular Alumina Grain Properties

Good-quality tabular is characterized by its large α-Al_2O_3 crystalline structure (Fig. 5), high amounts of closed porosity, and very little open porosity and consequently low water absorption (Table V). On the other hand, over- and underfired tabular exhibits excessive open porosity and water absorption with greatly differing grain strength and high-temperature volume stability. Table VI[18] gives the characteristics of properly fired tabular Al_2O_3.

Under-fired tabular has the appearance of white chalk, but it is characterized by a very strong, finely crystalline and highly porous structure, typical of a partically sintered pure Al_2O_3 ceramic body. The porosity in under-fired tabular is primarily microporosity. Because of its high strength, under-fired tabular fractures into the large grain sizes. Besides having excessively high open-porosity/water-absorption values, these partially sintered grains exhibit poor volume stability and shrink upon further sintering when used in refractories. The resulting defect structure weakens the refractory and is a source of high porosity which limits corrosion/erosion resistance of the refractory in service.

The problem of under-firing tabular (high porosity) can be reduced with small additions of MgO which lowers the sintering temperature, enhances densification, and essentially eliminates the occurrence of open porosity.[12] Although higher densities and greater grain strength can be obtained by the use of MgO and other sintering aids, crystal growth is restricted to generally <25 μm. This dense finely crystalline structure exhibits poor thermal shock properties compared to the large (50 to > 400 μm) lower density crystalline tabular structure, as exemplified by results obtained during armament development studies in 1967–68 at Alcoa Labs.

A bed of dense (3.948 g/cm^3) Al_2O_3 spheres (25 mm, 1 in.) made with 0.05% MgO and having a nominal 5 μm crystal size (Fig. 6, sample IIA) shattered into thousands of pieces when contacted by 816°C (1500°F) molten aluminum after being preheated at 232°C (450°F). In contrast, similarly embedded tabular Al_2O_3 spheres (25 mm, 1 in.) remained whole, as observed by X ray. Additional tests by molten aluminum contact established that the dense, fine-crystalline 99.8% Al_2O_3 spheres fragmented at a 290C° (520F°) ΔT and remained whole but cracked at a 140C° (250F°) ΔT. The critical thermal rise fracture shock ΔT for tabular is >584C°, over twice the fracture shock ΔT (>140C°, <290C°) for the fine-crystalline, dense Al_2O_3 spheres. This work vividly demonstrates the thermal shock advantages of the lower density, coarse crystalline tabular Al_2O_3 structure over the dense, fine-crystalline Al_2O_3 structure.

The advantage of coarse crystalline Al_2O_3, similar to tabular grain size, has also been demonstrated in Al_2O_3 ceramic quenching shock tests. Hasselman's[19] predicted behavior of strength as a function of quenching temperature for a given material is shown in Fig. 7. Several researchers[20–24] have demonstrated that commercial Al_2O_3 ceramics' strength decreases instanta-

Table V. A. Typical Properties and Specifications for Ground T-64

	Tyler Standard Sieves	
	−325 mesh Standard	−48 mesh, −60 mesh −100 mesh, −325 mesh Low Iron
Typical Properties		
Al_2O_3 .....%	99.+	99.5+
SiO_2 .....%	0.1	0.05*
Fe_2O_3 (total).....%	0.3	0.07
Fe_2O_3 (acid soluble).....%	0.2	0.02
Na_2O.....%	0.2	0.16
CaO.....%	0.04	0.04
Specifications for Shipment		
SiO_2 (max).....%	0.25	0.2
Fe_2O_3 (acid soluble) (max).....%	0.3	0.05
Na_2O (max).....%	0.25	0.22
CaO (max).....%	0.12	0.12
Sieve analysis — See Note†		

*Increases to 0.1 for the finer mesh sizes
†5% maximum retained on screen of specified screen size (i.e., on −48 mesh 5% maximum +48; on −60 mesh 5% maximum +60; on −100 mesh 5% maximum +100; on −325 mesh 5% maximum +325).

Table V. B. Sieve Specifications of Crushed and Graded T-64

Crushed sizes	Tyler Sieve analysis 5 percent max on.	Graded granular sizes	Tyler Sieve analysis 2% max on —	5% max through
Minus ½ in.	½ in.*	½ in. to ¼ in.	½ in.*	4 mesh
Minus ¼ in.	¼ in.*	3 to 6 mesh	— See Note*	
Minus 6 mesh	6 mesh	¼ in. to 8 mesh	¼ in.*	10 mesh
Minus 8 mesh	8 mesh	8 to 14 mesh	8 mesh	20 mesh
Minus 14 mesh	14 mesh	14 to 28 mesh	14 mesh	35 mesh
Minus 28 mesh	28 mesh	28 to 48 mesh	28 mesh	65 mesh

*U.S. Standard Sieve Designation
†Sieve analysis for 3-6 mesh

Cumulative on No. 3 ..... 2% max
Cumulative on No. 3½ ..... 30% max
Cumulative on No. 4 ..... 30% min – 70% max
Cumulative through No. 4 ..... 30% min – 70% max
Cumulative through No. 5 ..... 7% max
Cumulative through No. 6 ..... 11% max
Cumulative through No. 8 ..... 5% max

Table V. C. T-64 Soluble Iron Specifications*

Mesh Size	Typical %	Specification %
3-6 m	0.005	0.015 max
¼"-8 m	0.005	0.015 max
8-14 m	0.005	0.015 max
14-28 m	0.005	0.015 max
28-48 m	0.01	0.03 max
– ¼"	0.005	0.015 max
– 6 m	0.005	0.015 max
– 8 m	0.005	0.015 max
– 14 m	0.01	0.02 max
– 28 m	0.02	0.03 max
– 48 m	0.02	0.05 max
– 60 m	0.02	0.05 max
– 100 m	0.02	0.05 max
– 325, low iron	0.02	0.05 max
– 325 m	0.2	0.3 max

*Crushing, sizing, grinding, and handling of tabular alumina imparts soluble iron to the material. The sizes listed here are magnetically de-ironed to minimize discoloring in ceramic and refractory products.

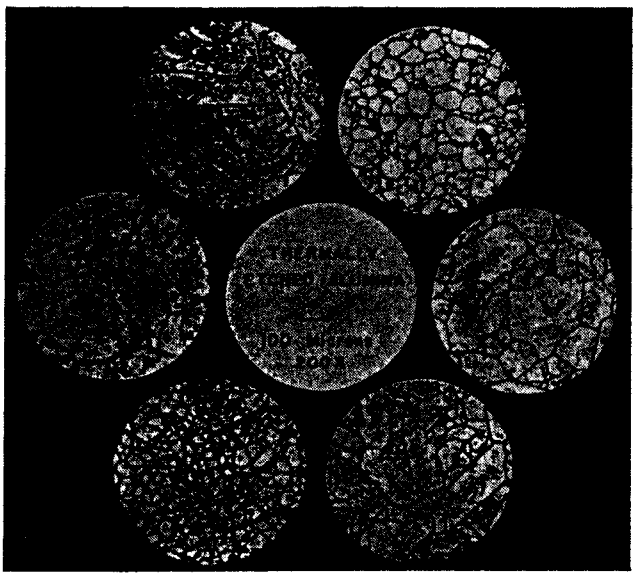

Fig. 5. Sintered α-Al_2O_3 microstructure (polished sections). Preferred tabular Al_2O_3 structure: large elongated crystals with closed porosity.

neously with quenching. Ainsworth and Moore[22] showed an appreciable strength decrease after a shock of 175C° (315F°) ΔT, when ice (H_2O) quenching 24 μm 99.5% Al_2O_3 rods of near theoretical density.

Gupta[25] showed that thermal shock damage resistance of dense polycrystalline α-Al_2O_3 improves with increased Al_2O_3 grain size. Cold MOR strength degradation of Al_2O_3 specimens quenched at increasing temperatures decreased continuously in Al_2O_3 samples of 10, 34, and 40 μm mean grain size after a sharp drop at 200C° (360F°) ΔT_c (Fig. 8). The strength decreased gradually in the 85 μm sample. His microstructural studies reportedly verified Hasselman's predicted behavior of ceramics subjected to thermal shock.[23,26,27] Strength degradation that occurs on shocking depends on the initial crack length of the material. Cracks propagate kinetically when the crack length is short; a quasi-static crack propagation occurs with long crack length. Gupta determined the crack length of his 85 μm sample to be >1000 μm, whereas the smaller crystal samples' crack length measured <1000 μm.

Many sintered Al_2O_3 refractory aggregate manufacturers must resort to the use of sintering aids, such as MgO, to achieve acceptable densification in rotary kilns. The resulting dense, fine, α-Al_2O_3 crystalline products suffer the same malady of poor thermal shock resistance compared to that obtained with a properly fired tabular structure. The thermal shock advantage of tabular over dense, coarser crystalline, fused Al_2O_3 aggregates involves differences in pore structure and is documented later.

Alumina Grain Characteristics Affecting Refractory Strength Properties

Heilich et al.[18] were the first to conduct a study to determine if the grain strength of refractory alumina

Table VI. Characteristics of Well-Fired Tabular Al_2O_3

Tabular Al_2O_3 Grain 3/4 Mesh							
Strength		Modified ASTM C373-56 Physical Properties					
Crushing Load kg (lb)		Particle Density	Apparent Specific	Porosity (%)			H_2O Absorption
$\bar{X}$*	CV(%)†	(g/cm^3)	Gravity	Open	Closed	Total	(%)
208(458)	35	3.64	3.68	1.1	7.5	8.6	0.3

*$\bar{X}$ = Average breaking load of 30 individual equant shaped grain using a 25 mm (1 in.) diamond steel mortar and strain rate of 1.25 mm/min. (0.05 in./min.) in a Dillon dynometer mechanical testing machine.
† Coefficient of variation (%) = std. dev. ÷ $\bar{X}$ (100)

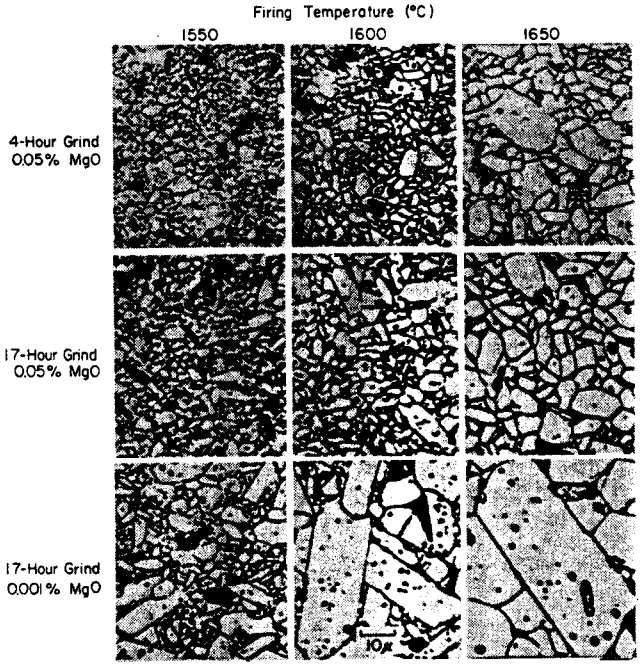

Fig. 6. Effect of grinding time, MgO addition, and firing temperature on 99.8% Al_2O_3 microstructure.

aggregates influences the strength of refractories. In 1968, the properties of Arkansas T-61 and Holland T-60 tabular Al_2O_3 aggregates were compared with European white fused Al_2O_3 from West Germany. Table VII shows that the chemistry of the European T-60 and white fused products is quite comparable, while the Arkansas T-61 is significantly lower in soda. The small amount of residual boron (B_2O_3–0.002/0.003%) confirms the use of boron compounds in the T-61 process to reduce soda. Ceramic milling is the source of the slightly higher SiO_2 and MgO in the −48 mesh T-60 and T-61 products.

Although the total porosities of the tabular and fused-Al_2O_3 aggregates are about the same level, there are marked differences in their grain porosity. The open porosity of the fused grain is two to three times greater than that of the tabular aluminas (Table VIII). Most of the porosity in the white fused Al_2O_3 consists of large open pores, whereas over one-half of the porosity in tabular are closed pores. Although the total

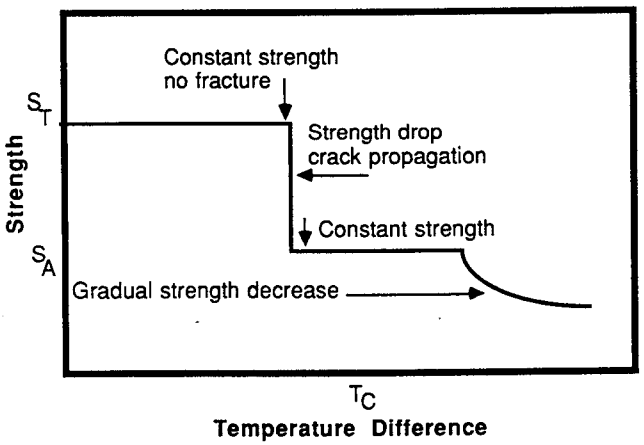

Fig. 7. Schematic of strength behavior in brittle ceramics vs severity of thermal shock as predicted by theory (Ref. 19).

porosity for the European fused in this initial study was 10 to 30% higher than that of tabular alumina, it does not account for the 50 to 75% higher grain strength exhibited by the tabular Al_2O_3.

The crushing strength of individual aggregate particles correlates with dried and fired concrete strengths, as shown in Table IX. The dense Cal-Tab 15 type castables fractured through the high-purity 80% Al_2O_3 cement matrix after moist curing for 24 hours with bend strength ranging 4.2 to 5.8 MPa (605 to 840 psi). As the cementitious matrix becomes stronger in the dried and fired states, a significant portion of the transverse strength fracture occurs through the coarse aggregate grains. The Heilich et al.[18] study suggests that the strength of refractories can be limited by the strength of the coarsest aggregate as the bond strength of the matrix becomes strong enough to cause fracture through the coarse grain. A transverse strength above about 7 MPa (1000 psi) is required to differentiate the effect of aggregate strength on the strength of the refractories.

The thin sections (Fig. 9) of the 4/8 mesh tabular and fused Al_2O_3 grains used in the Heilich et al.[18] study help to explain the poor performance of the

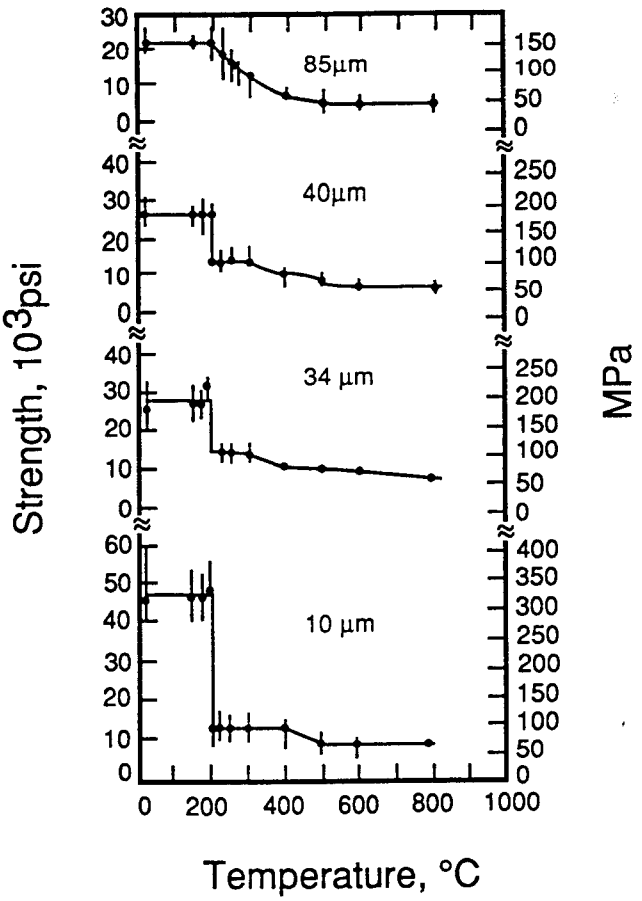

Fig. 8. Room-temperature strength of Al_2O_3 specimens of various grain sizes as function of quenching temperature.

white fused Al_2O_3. The porosity in the fused Al_2O_3 is concentrated in large, connecting, open pores. This grain structure apparently accounts for the lower grain strength of fused Al_2O_3 compared to the tabular Al_2O_3, which contains small closed pores distributed throughout its structure.

The mercury displacement method (ASTM 493–86) is the only valid method for totally characterizing the bulk density and porosity of granular aggregates, but the costs of properly maintaining an environmentally safe laboratory limit its use. A modified ASTM C373–56 method for determining porosity, water absorption, and density of ceramics based on the Archimedes principle is used to characterize tabular grain. Unfortunately, this technique is limited to the coarser grains, generally the +6 mesh aggregate fractions.

The gas comparison pycnometer method (ASTM C604–86) can be used for measuring the apparent specific gravity (ASG) of refractory aggregates throughout the entire particle-size range. The ASG provides a measure of closed porosity. Table X shows that ASG increases (closed porosity decreases) with decreasing particle size of tabular alumina. The tabular ASG does not become equivalent to that of white fused grain until the products reach a fineness of −325 mesh, suggesting that some porosity in tabular remains closed even in the intermediate particle sizes to just below 44 μm.

Additional characterization studies on white fused Al_2O_3 refractory aggregates from various countries confirm that the majority (65 to 90%) of the porosity in 4/10 mesh and coarser grain is composed of open interconnecting macropores (Table XI). In contrast, most of the porosity contained in tabular Al_2O_3 occurs primarily as spherical closed micropores as a result of intercrystalline porosity being entrapped and coalescing during α-Al_2O_3 recrystallization on sintering. The coarse open porosity in the white fused alumina grain originates as continuous pipes formed perpendicular to the solidification plane on cooling the large fused ingots. The relatively coarse, open porosity remaining after crushing is primarily concentrated in the +28 mesh white fused Al_2O_3 grains.

The nominal 0.2% Cr_2O_3 addition to white fused Al_2O_3 gives a characteristic pink fused Al_2O_3 exhibiting superior abrasive properties, but the physical characteristics as shown in Table XII are quite similar to the white fused Al_2O_3 grain characteristics. The grain strength of the 3/4 mesh particles is as good as the best white fused evaluated at the time of this study. The large amount of open porosity also typifies the white fused alumina products.

Brown fused Al_2O_3 grain is made using bauxite as the Al_2O_3 feed for fusion. Unlike the pink and white fused Al_2O_3 products, it exhibits a very high particle density (3.91 g/cm^3) and <2% porosity, as represented by the light and dark brown fused Al_2O_3 products from Germany in Table XII. Grain strength is about 1.5 to 3 times greater than the pink and white fused aluminas, but these light and dark brown fused Al_2O_3 grains are only about one-half as strong as the Holland tabular Al_2O_3.

Heilich et al.[18] ran comparative tests on dense CAC concretes (Table XIII) prepared with Holland tabular and the five strongest fused Al_2O_3 aggregates listed in Table XII to better clarify the grain/refractory strength relationship. Eight closely sized fractions composing the complete size range of the aggregates were weighed separately and then mixed with 15 wt% CAC to ensure identical maximum density distributions for each of the aggregate compositions.

The CAC matrix is strong enough in the dried and fired state to cause a significant portion of the transverse strength fracture to occur through the larger aggregate grains and, in effect, reflects the relative strength inherent in the alumina grains. The Holland tabular alumina concretes have significantly higher dried and fired strength than the average strengths for

Table VII. Quantometric Analysis of Al_2O_3 Aggregates (%)

	European White Fused		Holland T-60 Tabular		Arkansas T-61 Tabular	
	8–14 Mesh	Minus 48 Mesh	8–14 Mesh	Minus 48 Mesh	8–14 Mesh	Minus 48 Mesh
SiO_2	0.025	0.020	0.028	0.063	0.044	0.10
Fe_2O_3	0.024	0.032	0.026	0.037	0.070	0.076
TiO_2	0.003	0.002	0.002	0.002	0.004	0.004
Na_2O	0.30	0.30	0.31	0.22	0.008	0.007
CaO	0.027	0.027	0.030	0.027	0.029	0.035
Ga_2O_3	0.008	0.005	0.017	0.016	0.020	0.021
B_2O_3	<0.001	<0.001	<0.001	<0.001	0.002	0.003
MnO	0.0003	0.0007	0.0006	0.0005	0.0007	0.0009
Cr_2O_3	0.0008	0.0007	0.0003	0.0003	0.0005	0.0026
MgO	0.002	<0.0005	0.001	0.015	0.004	0.026
ZnO	0.002	0.003	<0.0005	<0.0005	<0.0005	0.001
CuO	0.001	0.0008	<0.0005	<0.0005	<0.0005	<0.0005
V_2O_5	0.001	0.0002	0.0007	0.0006	0.0003	0.0003

Table VIII. Physical Properties* of 4/8 mesh Al_2O_3 Grains

Property	European White Fused	Holland Tabular T-60	Arkansas Tabular T-61
Porosity (%)			
Open	12.8	6.1	3.8
Closed	1.2	6.4	6.9
Total	14.0	12.5	10.7
Water absorption (%)	3.7	1.7	1.1
Apparent specific gravity	3.94	3.71	3.70
Particle density (g/cm^3)	3.43	3.49	3.56
3/4 Mesh Grain			
Crushing load (kg (lbs))†	68(147)	104(229)	116(255)
Coef. of Var. (%)	40	66	43

*Grain-density properties determined by a modified ASTM C373-56 procedure.
†Average of 50 individual equant-shaped grains.

Table IX. Strength Comparison of Refractory Concrete and Coarsest Castable Aggregate

Coarse Al_2O_3 Aggregate (3/4 Mesh)		Caltab 15 Type—Dense Castable*		
		Cold MOR—MPa(psi)†		
Type	Grain Crushing Load kg (lb)	Moist Cured 24 h @32°C (90°F)	Dried 5 h @110°C (230°F)	Fired 5 h @866°C (1500°F)
Arkansas tabular T-61	116(255)	5.4(790)	9.8(1415)	12.0(1740)
Holland tabular T-60	104(229)	4.9(715)	9.1(1325)	11.6(1685)
European white fused	68(147)	4.9(705)	7.4(1070)	9.8(1425)

*Composition of ideal size distribution test concretes

Tyler Mesh Size	wt%	Tyler Mesh Size	wt%
3/4	4.4	28/48	8.5
4/8	17.0	48/100	9.3
8/14	10.2	100/325	12.7
14/28	10.2	Minus 325	12.7
		CAC cement	15.0

†Average of 4 sets of 4 bars (25 by 25 by 180 mm)

the brown fused concretes, which, in turn, have significantly greater dried and fired strength than the grouped values for the pink and white fused alumina concretes. These data strongly support the initial results shown in Table IX.

Additional tests were run to determine the water requirements for a pourable consistency for each of the aggregates, besides determining the strength values on specimens prepared using the water requirement for a good ball-in-hand consistency. A computer

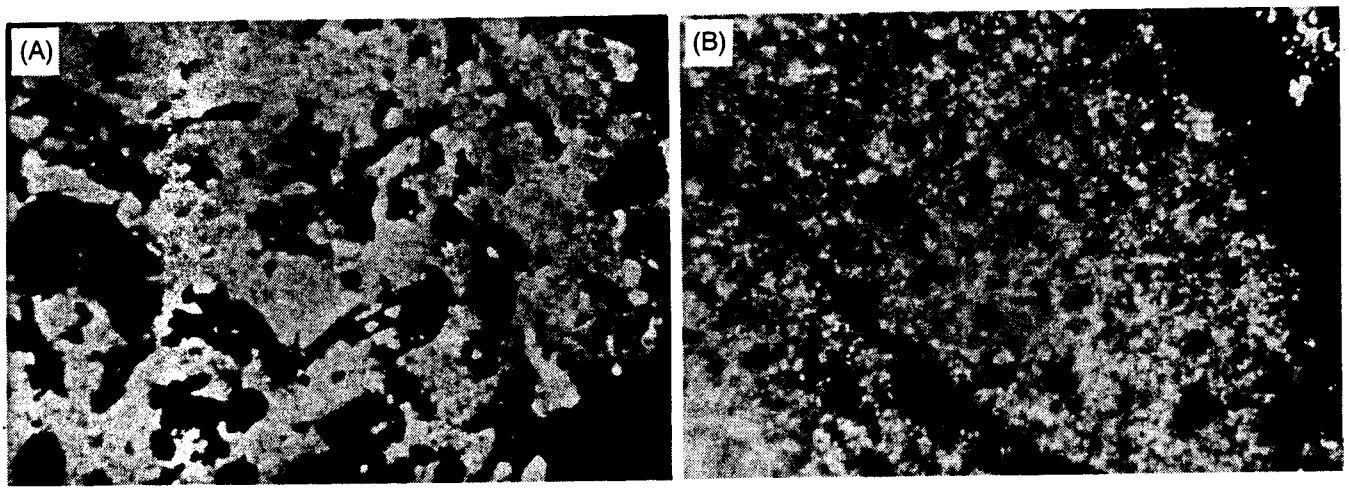

Fig. 9. Thin sections of 4/8 mesh tabular alumina and white fused Al_2O_3 grains magnified 60 diameters: (*a*) white European fused alumina; (*b*) Arkansas tabular.

Table X. Apparent Specific Gravity* of Al_2O_3 Aggregate

Tyler Mesh Size	German White Fused	Holland Tabular T-60	Arkansas Tabular T-61
3/4	3.87	3.72	3.66
4/8	3.94†	3.71†	3.70
14/28	3.91	3.75	3.77
48/100	3.92	3.80	3.79
100/325	3.96	3.89	3.88
Minus 325	3.92	3.91	3.90

*Gas comparison pycnometer method (ASTM C1–1604). True density is not obtained when α-Al_2O_3 grains contain closed porosity.
†Modified ASTM C373–56 method (Archimedian).

analysis of the resulting 112 individual strength specimens gives a multiple correlation coefficient of 0.93 for the following regression equation for dried strength based on aggregate crushing load and casting water:

$$Y_d \text{ MOR} = 2905 - 199W + 0.7C_1 \quad (1)$$

where

C_1 = −3, +4 mesh grain average (N = 50) crushing load (lbs)
W = casting water (%)
Y_d MOR = average dried MOR (N = 4)
S_{yx} = 0.5 MPa (73 psi)

A 0.95 multiple correlation coefficient was calculated for the regression curve of fired strength on aggregate crushing load and casting water as described by the following equation.

$$Y_f \text{ MOR} = 4300 - 327W + 0.7C_1 \quad (2)$$

where

Y_f MOR = average (N = 4) cold MOR after firing 5 hours at 816°C (1500°F)
S_{yx} = 0.6 MPa (88 psi)

Peretz et al.[28] also concluded that the strengths of individual aggregate particles can be very important in determining the overall strength of a refractory body. Their work on the strengths of mullite-matrix aluminosilicate refractories with aggregates of kaolin, andalusite, and tabular grains of identical aggregate grain distributions suggests that the finer aggregates are stronger than the coarser ones. Evaluation of spherical mullite and bauxite grains confirmed that the finer aggregates are stronger than the coarser ones. The magnitude of the aggregate strengths were described by Weibull analysis and were appropriate for the strength differences observed in the refractory bodies. The individual strength studies also revealed differences in the strength distributions that are related to the chemistry, mineralogy, and the manufacturing process applied to the aggregates, but these relationships are not clear. However, the sintered mullite and bauxite spheres were significantly stronger than their fused counterparts.

The aforementioned alumina aggregates (Heilich et al.[18]) were also appraised in a coarse-grog (−¼ in., −6.25 mm), heat-setting ramming composition using phosphoric acid to obtain a stronger bonding matrix than obtainable with CAC bonding. Transverse strength data on fired bars prepared using a dense ideal aggregate size distribution are summarized in Table XIII with the coarse aggregate properties listed for comparison.

Phos-bonded Holland tabular coarse-grog refractories are 20 to 80% stronger than those made with white fused or brown fused abrasive grains which are also used as alumina refractory aggregates. The 10 to 20 times greater coefficient of variation exhibited by the fused aggregates suggests that the Holland tabular provides a more uniform structure throughout the acid-bonded refractory. The combination of significantly higher strength and reduced variation in Holland Phos-Tab is ascribed to greater inherent strength of the tabular grain and to more efficient use of the phosphoric acid in developing a phosphate bond. The latter

Table XI. Characteristics of Alumina Grain

ASTM C20–46	Fused				Tabular Holland
	France	Japan	Germany	England	
Mesh Size	8–10	4–10	4–8	4–8	4–8
Open porosity (%)	4.7	6.2	7.5	11.5	1.3
Closed porosity (%)	1.5	3.3	2.8	2.3	8.0
Total porosity (%)	6.2	9.5	10.3	13.8	9.3
Water absorption (%)	1.3	1.7	2.1	3.4	0.4
Apparent sp. g.	3.9	3.9	3.9	3.9	3.7
Particle density (g/cm^3)	3.7	3.6	3.6	3.4	3.6
Grain strength					
Mesh Size		4–6	3–4	3–4	3–4
Load—lbs. $\bar{X}$		81	128	127	392
Std. deviation		30	53	51	153
Quantometric Analyses					
Particle size	8–10 m	4–6 m	1–3 mm	⅛"–1/16"	8–14 m
SiO_2	0.006	0.018	0.022	0.028	0.019
TiO_2	0.029	0.020	0.026	0.010	0.032
Fe_2O_3	0.003	0.005	0.003	0.003	0.006
Na_2O	0.20	0.15	0.26	0.44	0.25
CaO	0.003	0.011	0.014	0.048	0.013
MnO	0.0003	0.0003	0.0004	0.0005	0.0004
MgO	<0.0005	0.001	<0.0005	0.0007	<0.0005

Table XII. Coarse Al_2O_3 Aggregate/Dense Castable Property Effects

Al_2O_3 Aggregate	Grain Properties			Caltab 15 Type Dense Castable			
					Transverse Strength—MPa (psi)		
	Crushing* Load kg (lbs)	Bulk Density (g/cm^3)	Open Porosity (%)	GBIH H_2O (%)	Cured 24 h 90°F, >90% rh	Dried 24 h 110°C (230°F)	Fired 5 h 816°C (1500°F)
Rotterdam tabular	178(392)	3.61	1.3	7.8	4.8(700)	9.4(1370)	11.1(1610)
German dark brown fused	96(212)	3.91	1.2	7.6	4.9(705)	8.6(1250)	10.2(1480)
German light brown fused	92(202)	3.91	1.5	7.8	5.1(745)	9.1(1325)	10.7(1550)
German pink fused	61(135)	3.58	7.7	8.3	4.7(685)	8.4(1215)	9.7(1405)
German white fused	58(128)	3.57	7.5	9.4	4.8(695)	8.7(1265)	9.9(1430)
English white fused	58(127)	3.43	11.5	8.3	4.7(685)	7.9(1150)	9.9(1435)

*Average of 50 individual 3/4 mesh grains.
†Minimum H_2O to obtain a good-ball-in-hand consistency (GBIH)
‡Average of 3 sets made 8.5, 9.0 and 9.5% H_2O (n = 12)

could be the result of greater surface reactivity, lower open porosity, and/or lower Na_2O of the Holland tabular. Yet, the brown fused grains have lower Na_2O and, thus, would be expected to neutralize less H_3PO_4 and provide more phosphate ions for greater bonding. However, this was not the case, as demonstrated by the higher strength of the Holland Phos-Tab.

Although the grain strength of the brown fused grain is 1.5 times higher than the English white and German pink fused aluminas, their strengths are comparable in acid-bonded refractories. This suggests that the absorbed H_3PO_4 reacted on heating to increase the grain strength of the porous white and pink fused Al_2O_3. The one exception is the German white fused Al_2O_3. It had the lowest phosphate bond strength and the greatest strength variation. The fact that it required the largest casting water addition to develop a ball-

Table XIII. Comparative Strength Properties of Phosphoric Acid Bonded Fused and Tabular Alumina Refractories

Aggregate Type	*Transverse Strength MR—psi	
	Ave. −4	Coef. Var. — %
Holland tabular	3947	0.7
English white fused alumina	3243	6.6
German bauxite corundum—dark	3209	7.7
German pink fused alumina	2970	7.1
German bauxite corundum—light	2923	10.7
German white fused alumina	2120	15.8

Coef. of variation (%) = $\frac{\text{std. dev.}}{\text{average}} \times 100$

*One-inch bars were dry pressed at 1000 psi, dried 24 hours at 220°F and heat treated at 500°C to develop a permanent bond.

in-hand consistency in the CAC concretes implies that the 11 wt% H_3PO_4 was insufficient for the type of pore structure to increase the grain and refractory strength as much as the other porous grain. The greater phosphate bond strength in comparison to the CAC bond confirms some enhancement of the German white fused grain by H_3PO_4 absorption and reaction.

With comparable particle-size distributions, the amount, size, and shape of the open pores become important parameters in determining liquid requirements for bonding H_3PO_4 refractories. The diameter of the rather large open pores occurring in white fused Al_2O_3 can be as large as 150 to 200 μm and larger, as illustrated in Fig. 10. Besides limiting the strength values of the castables, this type of porosity provides a source of variability in castable H_3PO_4/H_2O requirements for proper placement. Absorption characteristics can be extremely different, depending on the use and type of vibration during installation. This 8/14 mesh particle had to be turned 90° to the horizontal to observe the continuous "pipes" after sprinkling the particles onto the flat SEM mount. The modified ASTM C373–56 method was ineffective in characterizing the open porosity because the absorbed water could not be retained by such large pores while determining the saturated weight of the particles. Similarly, H_3PO_4 and other liquid binders can be expected to drain from such large open pores and segregate by gravitation during storage of wet monolithic mixes. Ground calcined alumina, alumina hydrate, and/or raw clay additions can increase the cohesiveness of the plastic mass and impede the separation of the liquid binders from the large, open, fused alumina pores.

Formation of the aluminum phosphate bond in situ on the tabular alumina surfaces by use of concentrated H_3PO_4 gives much stronger bonds than achieved by aluminum phosphate additions.[5] The H_3PO_4-bonded monolithics, both heat-setting and cold-setting compositions, give excellent serviceability in the range to 1870°C (3400°F). Gitzen[29] cites additional references on phosphate bonding.

Lukasiewicz and Reed[30] give the most recent literature review on phosphate bonding. They studied the types of phosphate-bond development by reacting orthophosphoric acid with nine Bayer process aluminas varying in specific surface area, purity, and α-Al_2O_3 phase content after reacting at 450° to 800°C (840° to 1470°F). It was concluded that the reaction between H_3PO_4 and tabular Al_2O_3 formed mechanically strong specimens at temperatures as low as 450°C. Specimens reacted between 450° and 800°C contained both B-$AlPO_4$ and C-$AlPO_4$, identified as burlinite or the quartz polymorphic crystalline form of aluminum orthophosphate and the cristobalite form, respectively. Variscite was detected in the 450°, 650°, and possibly in the 800°C samples. No amorphous phosphate bonding phase was detected in the fabricated −100 mesh tabular alumina specimens with these heat-treatment conditions. The presence of a major amount of C-$AlPO_4$ in the powders reacted at 450°C is in contrast to the results of Gonzalez and Halloran.[31] Phosphate bonding reactions and phases produced at moderate temperatures and soak times cannot be simply predicted from the relative activity index, as developed by Gonzalez and Halloran, when using different types of Bayer process aluminas. The type of phosphate phase(s) formed depends on parameters other than the specific surface area, alkali content, and percent α-Al_2O_3 content.

Nishikawa[32] provides a practical reference on phosphate-bonded monolithic refractories and notes that storage life of phosphate-bonded monolithic refractories is quite long when using materials of high purity, such as tabular alumina. Even so, it is recognized that phosphate-bonded tabular alumina refractory storage life is generally shorter than that of ordinary plastic refractories. On the other hand, partial aging of Phos-Tab mixes can enhance strength development by as much as 50%.

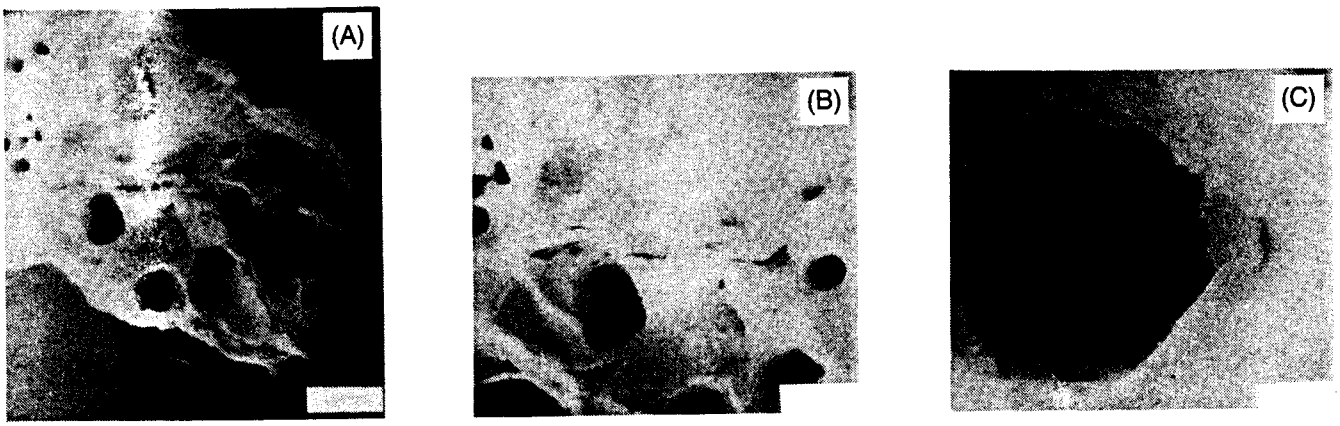

Fig. 10. Scanning electron micrographs of white fused Al_2O_3: (*a*) bar = 333 μm; (*b*) bar = 200 μm; (*c*) bar = 50 μm.

Strength increases with increasing PO_4^{3-} additions to the mix. However, the amount of H_3PO_4 addition is limited to a maximum that ensures good placement properties when being installed by ramming. The 400°C (715°F) strength of a fine Phos-Tab mix (65% −14 mesh and 35% −325 mesh tabular) is about 27.6 MPa (4000 psi). The strength increased to 41.4 MPa (6000 psi) after aging four weeks in sealed containers; the batch was remixed with an additional 0.5 wt% H_3PO_4 (85% concentration) without degrading placement properties. The aforementioned provides an example of the intrinsic properties of the alumina refractory grain that can dramatically affect the physical properties and ultimate performance of monolithic refractories.

The American Concrete Institute ACI 547 Committee on Refractory Concrete gives a current in-depth treatise on plastic and ramming monolithic refractories in their recent state-of-the-art report.[33]

Hot-Strength Properties of Tabular Alumina Refractories

Scanning electron micrographs (Fig. 11) of the −325 mesh tabular and white fused-alumina grains reveal significantly different surface characteristics. The 44 μm white fused-alumina particle shows a characteristic conchoidal fracture, typical of glass or supercooled liquids, and a relatively smooth surface. In comparison, the tabular particle shows a rough irregular surface containing shallow semispherical pores which should enhance reaction and mechanical interlocking with the bonding matrix to give greater refractory hot strength.

Creep studies in 1971 by Davidson and Willshee[34] confirm the better bonding surface of tabular alumina compared to white fused Al_2O_3 when using the Furnas ideal particle-size distribution in fabricating a mullite-bonded 90% Al_2O_3 fired brick. Figure 12 shows the deformation curves for tabular and white fused aluminas under steady state creep test conditions at 1550°C (2820°F) with a loading of 0.69 MPa (100 psi), after first holding for 6 hours at 1550°C. This substantiates the advantage of the more reactive interlocking surface of the tabular alumina with the bond phase on improving the performance of alumina refractories in comparison with white fused. Houseman[35] reports additional substantiating data on the more favorable bonding surface of tabular with pure Al_2O_3 and TiO_2 bonds in comparison with fused Al_2O_3. Figure 13 shows that the mullite-bonded 90% Al_2O_3 brick made with tabular alumina aggregate has compressive-creep resistance comparable to that of silica brick, which is known for its excellent creep resistance during extended long-term usage under load in blast furnace stoves. The lower compressive-creep resistances obtained for sintered mullite and 42% Al_2O_3 firebrick are shown for comparison purposes.

Bray[36] and Alder and Masaryk[37] give additional creep and compressive stress/strain measurements at high temperatures, along with updated references. Data are presented for various brick and monolithic refractories, but none exceed the creep performance of the aforementioned mullite-bonded 90% Al_2O_3 brick. Bray cited Alcoa internal creep test conditions for selecting refractories as being 100 hours at 1425°C (2600°F) under a stress of 1.72×10^5 Pa (25 psi). The creep performance of a CAC/tabular castable on initial heat-up and on reheating is shown in Fig. 14.[36]

The excellent creep properties exhibited by the mullite-bonded 90% Al_2O_3 refractory using tabular Al_2O_3 provided the basis for this composition and various modifications to be the industry standard for Al_2O_3 saggers and kiln furniture throughout the years since first being patented in 1959 by Ortman.[38] Ortman's thixotropically cast sagger compositions contain 66 to 78% tabular Al_2O_3, 4 to 12% clay, and 10 to 28% mullite. Subsequent drying and firing between about cone 14 and cone 30 cause sufficient reaction between the clay and tabular alumina fines to form a mullite bond.

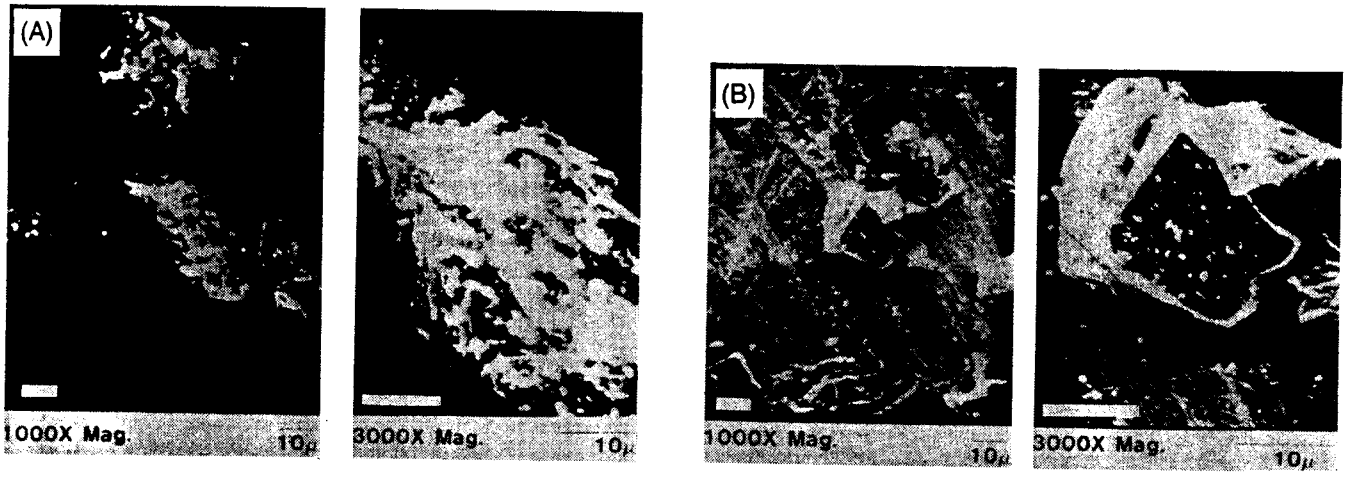

Fig. 11. Scanning electron micrographs of (*a*) Rotterdam tabular Al_2O_3; magnification 1000× (left), 3000× (right); and (*b*) European white fused Al_2O_3; magnification 1000× (left), 3000× (right). Bars = 10μ.

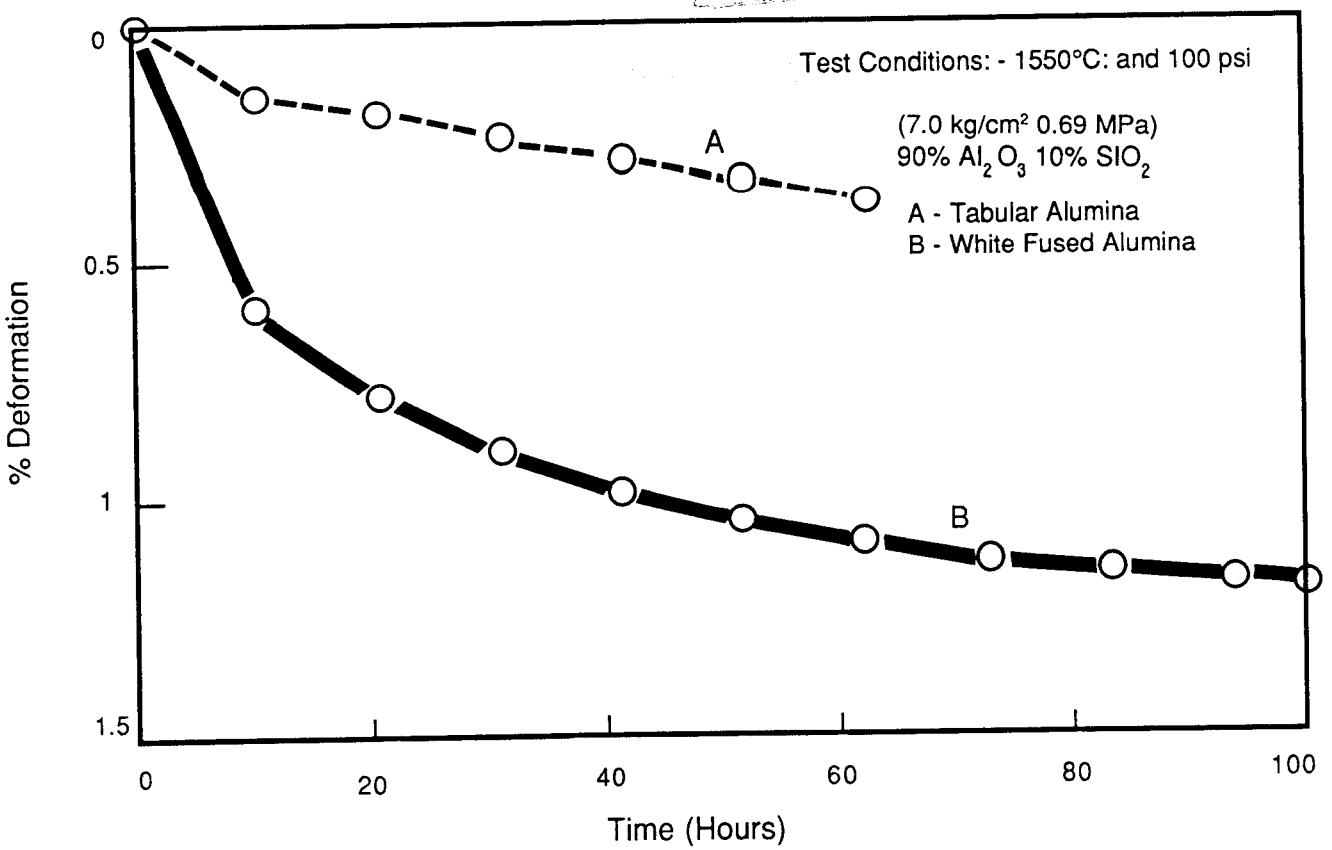

Fig. 12. Creep deformation of mullite-bonded 90% Al_2O_3 brick.

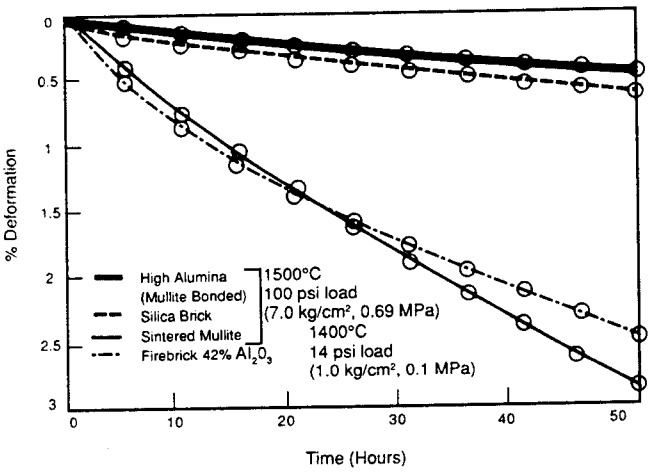

Fig. 13. Creep deformation of fired refractory brick.

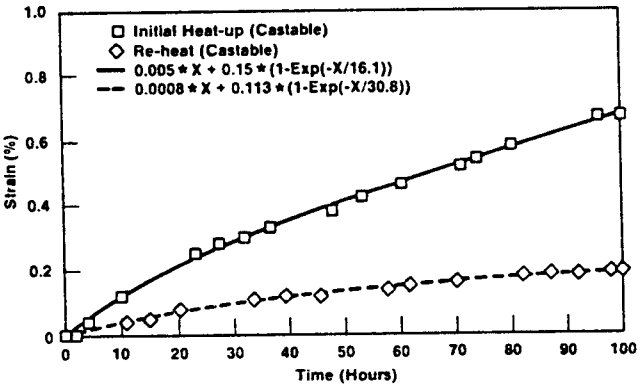

Fig. 14. Creep analysis for castable A, a high-alumina castable based on high-purity, CA cement and tabular Al_2O_3 tested at 1425°C under 1.72 × 10^5 Pa stress for 100 h.

In 1962, Miller[39,40] obtained greatly enhanced refractory properties when using from 1 to 10 wt% amorphous or volatilized SiO_2 with tabular alumina or in combination with tabular, fused mullite and calcined Al_2O_3 to form mullite-bonded pressed tabular alumina refractories on firing. Further improvement in the mullite-bonded 90% Al_2O_3 pressed refractories is claimed by Bakker[41,42] in which 0.01 to 0.5 wt% lithium compounds are capable of forming Li_2O during firing of a pressed-brick batch mix containing by

weight, 85 to 96% Al_2O_3, 2.99 to 13.99% SiO_2, and about 1 to 5% bentonite. The second patent[42] was obtained with 2 to 7% volatilized SiO_2 being used in place of bentonite. Hot MOR strength at 1500° and 1600°C (2730° and 2910°F) was essentially doubled by the addition of 0.05% Li_2O to the base composition or with 2 to 7% volatilized SiO_2 used in place of bentonite.

A further modification of mullite-bonded tabular alumina was reported in 1974 by Farris and Green.[43] A high-alumina refractory of improved resistance to deformation under a 172.4 kPa (25 ksi) load at 1600°C and resistance to slag penetration is claimed with a coarse fraction (+28 mesh) containing calcined flint clay and a fine fraction containing silica fume and tabular alumina. Manigault[44] claimed higher densities in a new alumina refractory composition comprising from 76 to 96.5% tabular Al_2O_3, 0 to 10% calcined Al_2O_3, 3 to 10% SiO_2, and 0.5 to 4% of a titanium compound selected from the group consisting of rutile TiO_2 and barium titanate after forming and firing at 1500° to 1650°C (2730° to 3000°F).

The aforementioned patents are the basis for the continued successful performance of tabular alumina refractories in mullite-bonded alumina slide gates, saggers and kiln furniture, pressed brick, and isopressed shapes.

Effect of Na_2O in Tabular on Refractory Hot Strength

In 1973,[45] Alcoa began a study to investigate the effect of Na_2O contents in tabular and calcined aluminas on the hot-strength properties of a 90% Al_2O_3/10% SiO_2 refractory composition. Standard size test brick were pressed at 70 MPa (10 ksi), after muller-mixing 5 wt% calcium lignosulfonate binder solution (1 : 4H_2O), using tabular aluminas with six different soda levels (0.008, 0.017, 0.035, 0.087, 0.11, and 0.28% Na_2O). Calcined aluminas A–2, A–12, and A–15, containing 0.45, 0.18, and 0.07% Na_2O, respectively, constituted the matrix alumina additions to enhance mullitization during the simulated commercial firing (10 hours at 1545°C, 2820°F). The complete composition based on the Furnas ideal particle size (6 mesh to 0.2 μm) distribution is listed in Table XIV.

Hot-load testing was conducted at 1760°C (3200°F) under 172.4 kPa (25 psi) for 24 hours to better differentiate the relative effects of the Na_2O impurity in the various tabular and calcined aluminas. No deformation occurred when using a 1.5 hour hold at 1650°C (3000°F) and 172.4 kPa (25 psi), the most severe conditions specified by ASTM C16–73. Statistical analysis of the subsidence data indicated that Na_2O in tabular accounts for 51% of the variance; apparent porosity in tabular is responsible for 28% variance; Na_2O in calcined Al_2O_3 is insignificant, causing <0.1% variance; and 20% was associated with fabrication variables which are critical in this formulation.

The effect of tabular Na_2O, particle bulk density and apparent porosity, and brick bulk density and total

Table XIV. Mullite-Bonded 90% Al_2O_3 Refractory Test Composition

Component	Tyler Mesh	wt%
Tabular Al_2O_3	6/8	7.3
Tabular Al_2O_3	8/14	13.2
Tabular Al_2O_3	14/28	11.7
Tabular Al_2O_3	28/48	10.4
Tabular Al_2O_3	48/100	9.2
Tabular Al_2O_3	100/200	8.1
Tabular Al_2O_3	200/325	5.4
Tabular Al_2O_3	−325	14.7
Calcined Al_2O_3	−325	10.0
SiO_2 Sand	−200	6.5
SiO_2 Fume	Fume	3.5
	Total	100%

Note: 5 wt% binder solution (1:4 NORLIG-41H:H_2O) mix-mulled prior to pressing 9 in. straights at 70 MPa (10 ksi).

Na_2O on hot-load deformation of the 90% Al_2O_3/10% SiO_2 refractories was appraised as first-order multipolynomial relationships by including the squared values of the independent variables as separate functions in a computer multiple linear regression analysis. Tabular Na_2O and apparent porosity accounts for 97.8% of the Y variance in the 17 hot-load tests conducted at 1760°C on 90% Al_2O_3 brick, according to the following curvilinear equation:

$$Y = 8.64 + 207\,S_t^2 + 0.54\,p^2 - 3.85\,p - 23.5\,S_t \quad (3)$$

where

Y = % deformation at 172.4 kPa (25 psi) loading for 24 hours at 1760°C

p = % apparent porosity (tabular alumina 4/8 mesh)

S_t = % Na_2O in tabular Al_2O_3

The standard error of estimate is ±0.58% with a multiple correlation coefficient of 0.989. These respective values were 1.77% and 0.912 for the best multiple linear regression analysis, which accounted for only 79% of the variance in the test.

The multipolynomial equation describes a curved chute which rises slightly at the bottom when plotted in three dimensions (Fig. 15). The bottom of the chute designates the minimum hot-load deformation for any tabular Na_2O level up to 0.28%. The lowest deformation (about 1.2%) is predicted with 0.06% Na_2O and 4% apparent porosity when pressing brick with 5% binder at 70 MPa (10 ksi) and firing for 10 hours at 1545°C (2820°F).

It is interesting to note that optimum amounts of Na_2O (0.02 to 0.1%) and apparent porosity (2 to 5%) in tabular alumina grain enhance the hot-load characteristics of mullite-bonded 90% Al_2O_3 brick. Neither lower nor higher Na_2O in the calcined Al_2O_3/SiO_2 bulk bonding matrix significantly influences the load-bearing resistance of these tabular brick. This suggests

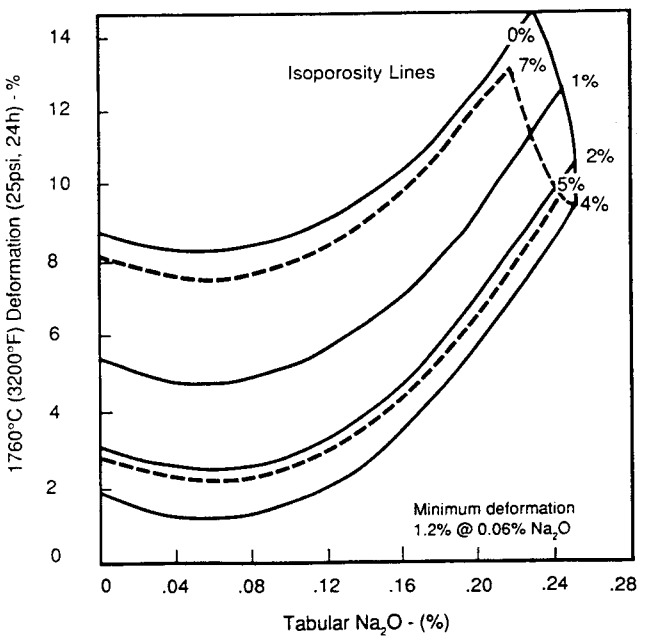

Fig. 15. Multipolynomial correlation effect of tabular Al_2O_3 and apparent porosity on hot-load properties of 90% Al_2O_3 brick.

that the reaction zone and/or degree of mullitization occurring at the surface of the tabular grain controls the deformation under load, rather than the bulk matrix. This emphasizes the importance of characterizing refractory grain surfaces and reaction kinetics with different bonding matrices.

The 1760°C deformation increases dramatically as tabular-grain open porosity drops below ≈2% and increases above 5%. Since brick fabrication characteristics were not significantly different for the various tabular grains, as indicated by pressed and fired densities, the mechanism by which open porosity affects hot-load deformation is yet to be defined. It may be (1) giving an indication of the tabular-grain surface roughness, providing a "keying mechanism" for mechanically interlocking the mullite crystals to the tabular surface and preventing slippage of the mullite boundary layer, (2) indicating a measure of tabular reactive surface area and the optimum amount for reacting to form mullite with the specific amount and size of available SiO_2 present in the composition, (3) indicating some other physicochemical effect, or (4) representing a combination of these.

The Na_2O in tabular Al_2O_3 evidently affects/controls the mullitization kinetics at the surface of the tabular grain. The Na_2O contained in α-Al_2O_3 crystals is known to migrate to the grain surface when sufficient heat energy (about 1150° to 1250°C) is applied. Bayer alumina, nominally 0.5% Na_2O and 100 to 325 mesh, can be reduced to <0.1% Na_2O by heating between 1100° and 1350°C (2010° and 2460°F) with 1 to 10% low-alkali SiO_2 and/or SiO_2 compounds that are coarse enough to be physically separated from the Al_2O_3 after thermally reacting with the Na_2O.[46,47] Conversion to α-Al_2O_3 occurs at these temperatures and very little Na_2O is lost to volatilization, either with or without SiO_2 present. Surprisingly, the Na_2O migrates to the surface of the Bayer α-Al_2O_3 grain, a very porous crystalline cluster, and combines with the larger SiO_2 particles.

In the present case, it may be assumed that the Na_2O migrates to the surface of the tabular grain and reacts with the SiO_2 fume on the tabular surface to form a sodium silicate which melts with increasing temperatures. It then reacts with the tabular Al_2O_3 at 1545°C to form mullite crystals in a boundary layer at the tabular surface. Insufficient Na_2O in the tabular does not permit liquid-phase sintering to occur, thus limiting the degree of mullitization in the 1545°C-fired 90% Al_2O_3 brick and increasing the deformation under load relative to that occurring with the enhanced mullitization on the 0.02 to 0.1% Na_2O tabular grain. Higher Na_2O levels in tabular grain can be expected to net a surface-boundary layer with excessive residual glass relative to its mullite content, thus increasing deformation.

The preceding assumes that Na_2O acts as a mineralizer in promoting the mullitization reaction between tabular Al_2O_3 and SiO_2 in a manner similar to that reported on the mullitization of mixtures of china clay and Al_2O_3.[48–50] It is claimed that the fluxing action of the mineralizers contributes to the mullitization of kaolinite. A small quantity of vitreous phase was found in clay/mineralizer mixtures, even though no visible fusion was observed. A liquid phase can be expected to expedite mullite formation, inasmuch as the Al_2O_3 and SiO_2 are brought in intimate contact by the liquid phase, enhancing solid state reaction. Experimentation with sintering temperatures, various soda levels in tabular Al_2O_3, and SiO_2 additions of varying grain sizing and amounts should maximize mullitization during initial firing of mullite-bonded 90% Al_2O_3 pressed refractory shapes and further enhance hot-strength properties.

Similar studies have been reported[51,52] but soda and porosity in tabular, if and when used, was not noted as a variable. Matsumura et al.[51] give a thorough discussion on the various factors affecting hot-load and creep properties of mullite-bonded high-alumina brick, including flux content; the size, shape, and distribution of pores; crystalline microstructure, particularly the mullite content of the matrix; and development of mullite crystallization. The crystalline microstructure, such as the particle bond and the coarse particle, were said to constitute an important factor.

Figure 16[51] shows the effect of alkali (Na_2O + K) on the creep deformation of fired mullite brick for 2 kg/cm loading at 1550°C for 50 hours. The creep deformation rapidly increases as the alkali content

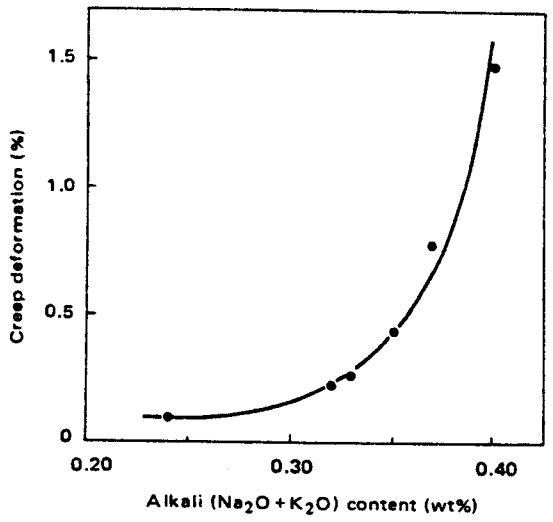

Fig. 16. Relation between alkali content and creep deformation (Ref. 51. Used by permission.)

exceeds ≈0.35 wt%. However, the lower 0.24% alkali brick shows a decided advantage over the 0.32% alkali product with increased loading. The 0.24% alkali mullite brick shows steady creep behavior despite extended 1700°C hold times on initial firing and increasing loads during testing (Fig. 17).

Thermal spall resistance of the 0.24% alkali brick was improved markedly by increasing the Al_2O_3 content from 73.3 to 86.7, with a simultaneous drop in alkalis to 0.19%. The creep resistance was affected only slightly (Fig. 18).

In 1971, Smith[52] reported an attempt to improve the plastic deformation, hot MOR, and thermal shock properties of a commercial >85% Al_2O_3 kiln furniture composition containing tabular Al_2O_3 and white mullite aggregate with a finely ground high-purity matrix. High firing and increased SiO_2 additions in the experimental bodies improved 1650° (3000°F) sag deformation and HMOR. The best 1427° and 1538°C (2600° and 2800°F) HMOR values were 13.5 and 11.6 MPa (1960 and 1680 psi), respectively. An intermediate SiO_2

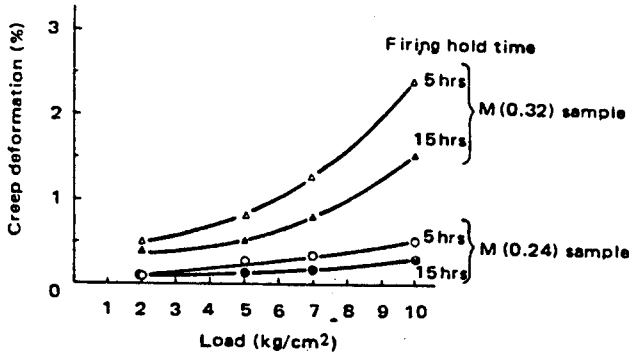

Fig. 17. Relation between load and creep deformation for specimens fired at 1700°C for 5 h and 15 h.

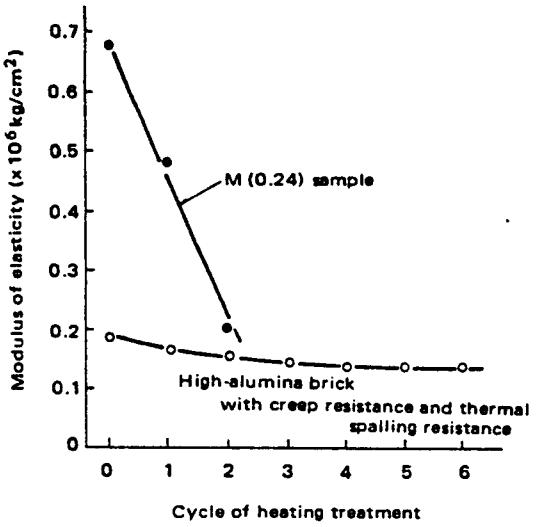

Fig. 18. Results of thermal spalling test for high-alumina brick with creep resistance and thermal spalling resistance and μ(0.24) sample.

addition showed the best thermal shock damage resistance. Similar studies in the future using tabular of varying Na_2O content and apparent porosities should prove fruitful.

The Na_2O level in the mullite-bonded 90% Al_2O_3 specimens made with different tabular and calcined alumina Na_2O levels in the Alcoa study had no significant effect on 1480°C (2700°F) (hot MOR) (HMOR) values. All compositions had excellent hot strengths, exceeding 13.8 MPa (2000 psi) HMOR. The A–15, A–2, and A–12 HMOR values averaged 20.1, 19.6, and 16.9 MPa (2910, 2850, and 2460 psi), respectively, when used in combination with the different tabular aluminas. Similarly, the bulk densities were 2.87, 2.85, and 2.82 g/cm^3 (179, 178, and 176 pcf). The slightly lower bulk density probably accounts for the significantly lower HMOR obtained with the intermediate soda A–12 alumina.

Skoog and Moore[53] give the most current literature review on mullite as a bonding phase in refractory and structural ceramics, in addition to mullite properties in selected uses. Melting behavior, structure, mullite starting materials, sintering parameters, and the influence of impurities on fabrication of properties are areas of specific interest covered in the review. Skoog[54] also studied the development of mullite in situ as a bond phase from α-Al_2O_3 and SiO_2 fume. Determination of mullite formation with temperature and composition are reported. Properties used to characterize the mullite formation are fired density, shrinkage and porosity, and quantitative mullite yield. Green densities were also measured and correlated. It was concluded that mullite forms as low as 1350°C when using a superground 1 μm Al_2O_3 and SiO_2 fume, but substantial amounts are not developed below 1400°C.

Lower mullite contents are produced with the coarser 3 μm aluminas. Maximum mullite yield is obtained in a compositional range around the 3 : 2 mullite stoichiometry. Both green density and firing shrinkage relate directly to maximum firing density. Additionally, it was concluded that an amorphous SiO_2 source should be used with α-Al_2O_3 to promote densification before mullitization of aluminosilicate matrices.

The superiority of the aforementioned experimental mullite-bonded 90% Al_2O_3 can be appreciated by comparing their 1480°C HMOR values with the typical 1370°C (2500°F) HMOR values for commercial 50 to 99% Al_2O_3 fired refractories charted in Fig. 19.[55] The dense high-CAC/tabular Al_2O_3 "ideal" castable compositions of differing coarseness are shown for comparison. They exhibit 1370°C HMOR values, after first firing at 1650°C (3000°F), 5 hours, that are equivalent to the best commercial mullite-bonded 90% Al_2O_3 fired brick. The increased hot strength that occurs with increasing aggregate size at the 25% CAC level confirms the importance of increasing the aggregate size to improve hot strength.

The hot-strength advantage of high-cement conventional −4 mesh CAC/tabular Al_2O_3 castables in comparison to low-cement CAC/tabular alumina castables containing 5% SiO_2 fume has been reported as shown in Table XV.[56] Although the 1650°C, 5 hour prefiring shows a 1370°C strength advantage for the 25% CAC castable, the bars prefired at only 815° (1500°F) and held for only 3 hours before loading at test temperature exhibit exceptional strength at 1370° and 1510°C of 15.2 MPa (2205 psi) and 15.6 MPa (2265 psi), respectively. These HMOR values are comparable to the previously reported 1480°C HMOR values for the mullite-bonded 90% Al_2O_3 fired brick.

In contrast, the low-cement (LC) castables containing SiO_2 fume show a rapidly decreasing HMOR above 1370°C and at 1370°C with increasing Na_2O content from the sodium polyphosphate dispersant. Recent work has shown that the 1400° and 1500°C HMOR can be significantly increased by substituting a newly commercialized dispersible superground submicrometer reactive alumina for SiO_2 fume (Table XVI).[57] Additional improvement in high-temperature strength

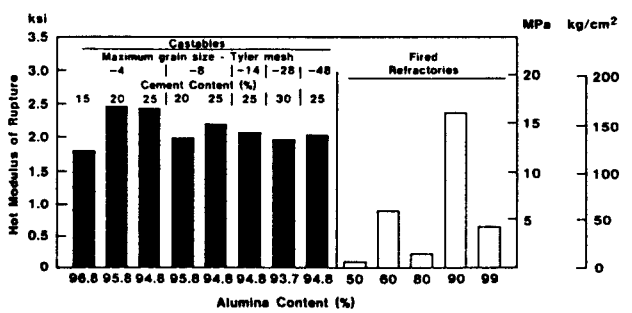

Fig. 19. Hot (1370°C (2500°F)) modulus of rupture (1 psi = 6.9 kPa).

properties of LC castables can be expected as these new dispersible calcined aluminas and tabular alumina castable compositions are optimized.

LC castables generally contain 3 to 8% CAC and typically require only 3 to 7% water for placement by vibration casting. LC castable technology[58–74] has contributed significantly to the advances made in processing technology by the iron and steel industries.

The low water requirement is accomplished by carefully grading the particle-size distribution so that the successively finer pores are filled with increasingly smaller particles, down to the submicrometer range below 0.1 μm diameter. Minimizing pore water requirements thus limits the mixing water for good fluidity to only that required to coat the surfaces of all particles. The surface water requirements can be further reduced by proper selection of deflocculants or dispersive additives. Consequently, with packing density maximized, the LC vibratable castables are characterized by their low porosity, high density, and exceptional hot strength which enhance erosion, corrosion, and spalling resistance. These characteristics provide superior performance over other monolithic refractories, such as ramming mixes, plastics, slinging materials, or gunning refractories. Durability is equal and sometimes superior to equivalent conventionally fired, dense refractory brick.

Because of the tight structure and low permeability, caution is required on initial heating to prevent disruptive steam spalling. Clay-bonded vibratable castables depend on deflocculation and subsequent coagulation[30] by the Ca^{2+} from the 1 to 2% CAC addition. These concretes have a pseudozeolithic bond which releases bond water slowly between 150° and 450°C (300° and 660°F), rather than within a narrow temperature range as do the hydrated phases of conventional concretes.[75] Thus, heating schedules are less critical in these ultra low-cement (ULC) castables than the LC and conventional castables. Nonetheless, some producers add about 2% organic, low-melting fibers to remove water more easily through the pores formed by the fibers. Metal powder has also been used to increase castable permeability by gas pipes formed during controlled H_2 release on reaction by the metal powder with the placement H_2O prior to set. This technique requires that precautions be taken to properly vent the H_2 to prevent formation of explosive atmospheres.

Submicrometer powders commonly used in LC and ULC castables include fumed-SiO_2 dust, Al_2O_3, Cr_2O_3, ZrO_2, TiO_2, SiC, clay minerals, and carbon. The ease of dispersion, availability, and cost effectiveness of SiO_2 fume has resulted in its common usage in many commercial LC castables. However, the sensitivity of the SiO_2-fume LC castables to water requirement and the unpredictably short working times and long setting times have caused mixed reactions regarding the total acceptance and full utilization. One problem seems to be that the various CAC types do not

Table XV. Hot Strength of Tabular Al_2O_3 Castables

Castable Type	CAC Al_2O_3 (wt%)	CAC Amount (wt%)	SPP (% twb)	GBIH H_2O (%)	Hot MOR, (MPa/psi)* 1370°C/2500°F	Hot MOR, (MPa/psi)* 1510°C/2750°F
Low-cement†	70	5	0	6.5	8.69/1260	0.31/45
Low-cement†	70	5	1.0	6.5	2.76/400	0/0
Low-cement†	70	5	2.0	6.5	0.83/120	0/0
Conventional	80	25	0	7.8	15.2/2205	15.6/2265
					18.7/2715§	16.9/2455¶
Conventional	90	20	0	8.3	ND**	8.31/1205
						11.7/1695¶
Conventional	90‡	20	0	6.9	ND**	12.4/1800
						14.7/2130¶

*25 mm (1-in.) bars prefired at 815°C (1500°F), except where noted, bars held 3 h before loading.
†Contains 5% fumed-SiO_2 dust and 5% Al_2O_3 (fully ground 3 μm median).
‡Experimental cement
§Prefired 5 h at 1650°C (3000°F), cooled, and reheated for testing.
¶Prefired 5 h at 1510°C (2750°F), cooled, and reheated for testing.
**Not determined.

Table XVI. Low-Cement Caltab 605 Castable Hot Strength using Developmental CAC and Calcined Aluminas*

LC Castable Composition				Castable Properties			
80% Al_2O_3 CAC Grade	CALTAB Type	Fine Components 1 μm	Fine Components 3 μm	GBIH H_2O (%)	VICAT WT (min)	Hot MOR-MPa(psi)* 1400°C (2550°F)	Hot MOR-MPa(psi)* 1500°C (2640°F)
LC	605S	SiO_2 fume	COM-3	4.5	34	2.6(380)	0.4(60)
LC	605S	SiO_2 fume	SA-3	5.4†	43	6.1(880)	4.7(680)
CFL	605A	DSG-1	COM-3	5.6†	30	3.8(560)	2.0(290)
CFL	605A	DSG-1	SA-3	6.0†	30	10.9(1580)	7.5(1087)

*Ref. 57. Used by permission.
*Preheated 12 h at temperature prior to testing
†Soft/BIH consistency

perform similarly in LC castables containing submicrometer SiO_2 fume.

As previously noted, refractoriness is another limiting factor in the use of SiO_2-fume LC castables. The CAC reacts with the SiO_2 fume to form anorthite ($CaO \cdot Al_2O_3 \cdot 2SiO_2$) and gehlenite ($2CaO \cdot Al_2O_3 \cdot SiO_2$),[75,76] which have low melting points, being respectively 1553°C (2827°F) and 1593°C (2900°F). A low-melting eutectic between these two compounds exists at 1380°C (2515°F) on the Al_2O_3 side of the triaxial $CaO \cdot Al_2O_3 \cdot SiO_2$ phase diagram (Fig. 20). An even lower eutectic can occur at 1335°C (2435°F) if $2CaO \cdot SiO_2$ is developed in the presence of $12CaO \cdot 7Al_2O_3$ and $CaO \cdot Al_2O_3$. Thus, hot strength is limited by the formation of a glass at temperatures above this eutectic. Although special LC castables containing submicrometer α-Al_2O_3 or Cr_2O_3 have excellent hot strength at 1500°C (2730°F) and higher, only the α-Al_2O_3 LC castables can be used safely without potential toxic complications such as hexavalent chrome, which can form from Cr_2O_3 in CAC castable refractories.[77]

Nonetheless, in spite of the high-temperature shortcomings of SiO_2-fume LC castables, their successful application by dedicated experienced crews and equipment continues to expand monolithic applications, exhibiting improved performance over fired brick.[78–86] Minimizing the amount of CaO by use of higher Al_2O_3 CAC enhances refractoriness of the SiO_2-fume LC castables.[56]

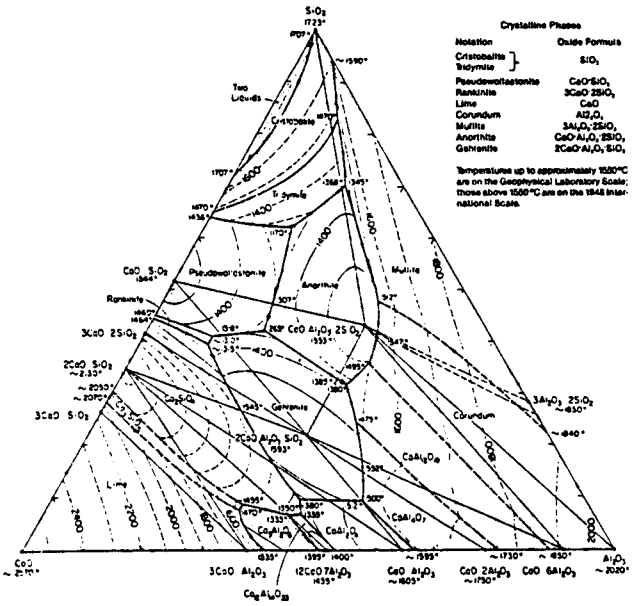

Fig. 20. System $CaO \cdot Al_2O_3 \cdot SiO_2$; composite.

Thermal Shock Properties of Tabular Alumina Refractories

As noted by Darroudi and Landy,[87] brittle materials such as ceramics, glass, and refractories generally exhibit a degradation in strength when subjected to constant or cyclic load,[88–91] as well as repeated thermal shock[92–94]; these phenomena are generally referred to as static, dynamic, and thermal fatigue, respectively. Probably the strength decrease is the result of growth of preexisting flaws in a slow or subcritical manner (slow crack growth, SCG). This SCG can lead to cumulative crack extension that can be sufficient to cause extensive spalling or even catastrophic failure in industrial applications subjected to repeated thermal and mechanical stresses.

They studied the strength/temperature patterns for relationships with several physical and chemical properties of a series of high-Al_2O_3 refractories. The SCG resistance parameter, N, was calculated from the room-temperature dynamic fatigue data and found to correlate directly with elastic modulus, E, and inversely with the amount of amorphous phase (Fig. 21), but not with Al_2O_3 content or crystalline phases present.

Although true for this 60 to 90% Al_2O_3 refractory brick series, the tabular 90% Al_2O_3 made with SiO_2 exhibited a much greater N value (87) than all others, including the tabular 90% Al_2O_3 brick made with clay which had the next highest N value (48). The 33 N-value difference is higher than the 27 N-value range between the 90% Al_2O_3 brick made with clay and the remaining refractories. This suggests either that the small mineralogy and Young's elastic modulus, E, differences (83 versus 85% α-Al_2O_3, 10 versus 8% mullite, 2 versus 4% cristobalite, 0 versus 1% quartz, 5 versus 2% amorphous, and 45.8 versus 54.3 GPa E value for clay versus SiO_2/90% Al_2O_3 brick, respectively) are critical or that other parameters, for example, matrix bonding to the tabular Al_2O_3 grain, are controlling. The HMOR advantage for the tabular 90% Al_2O_3/SiO_2 product over the tabular 90% Al_2O_3/clay composition is shown in Fig. 22 for reference.

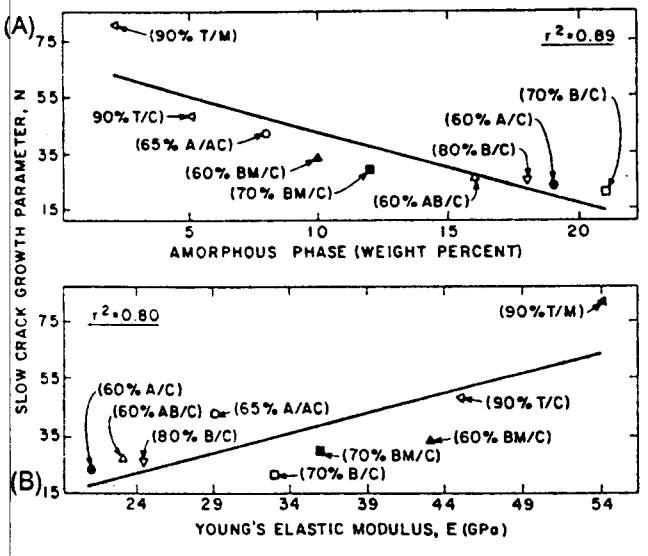

Fig. 21. Variation of SCG with (*a*) amorphous phase content and (*b*) Young's elastic modulus for Al_2O_3 refractories.

Thermal shock characteristics were determined on 25 mm (1 in.) bars cut from the aforementioned (Heilich et al.[18]) fired 90% Al_2O_3/10% SiO_2 test brick using a prism spall test procedure that was described previously.[95] A thermal shock cycle consisted of a rapid (2 second) transfer to a preheated muffle and a 0.5-hour hold at 816°C, a 2-second transfer to a fluidized Al_2O_3 bed, a 0.5-hour hold in the 60°C fluidized bed. After eight thermal shock cycles, all compositions showed that resonant frequency retention and bending strengths were similar or better than those of commercial mullite-bonded 90% Al_2O_3 brick. Resonant frequencies retention was 65 to 80% and bending strengths ranged from 8.6 to 13 MPa (1250 to 1890 psi), as illustrated in Fig. 23. Soda in tabular has no significant effect on the thermal shock properties of the mullite-bonded 90% Al_2O_3 test brick, based on the standard deviation for the averages of 15 bars being 11.6% of the mean. Likewise, Na_2O in the calcined Al_2O_3 had no significant effect.

Similarly, a correlation of Na_2O in tabular and fused Al_2O_3 aggregates bonded with 15% CAC could not be established with the thermal shock properties of the refractory concretes fired at 1650°C (3000°F), 5 hours prior to thermal shock testing.[95] Nondestructive sonic testing offers the advantage of being able to obtain an assessment of thermal shock damage after each shock cycle in the same specimen and indicates that the major shock damage occurs during the first four thermal shock cycles (Fig. 24). A reasonable correlation was established between the residual four-point bend strength after eight thermal shock cycles

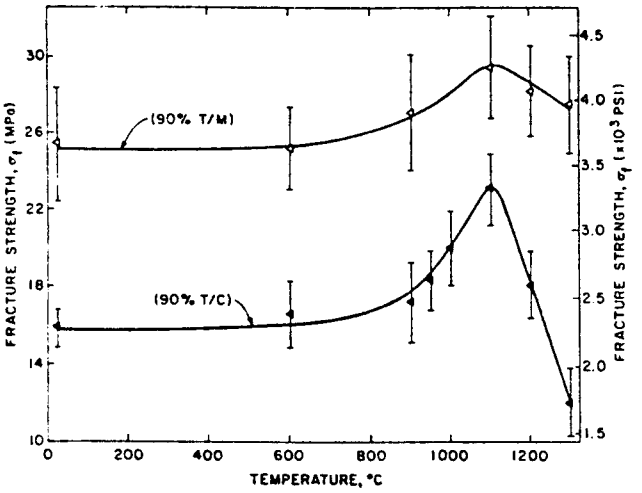

Fig. 22. Effect of temperature on the fracture strength of two tabular Al_2O_3-based refractories.

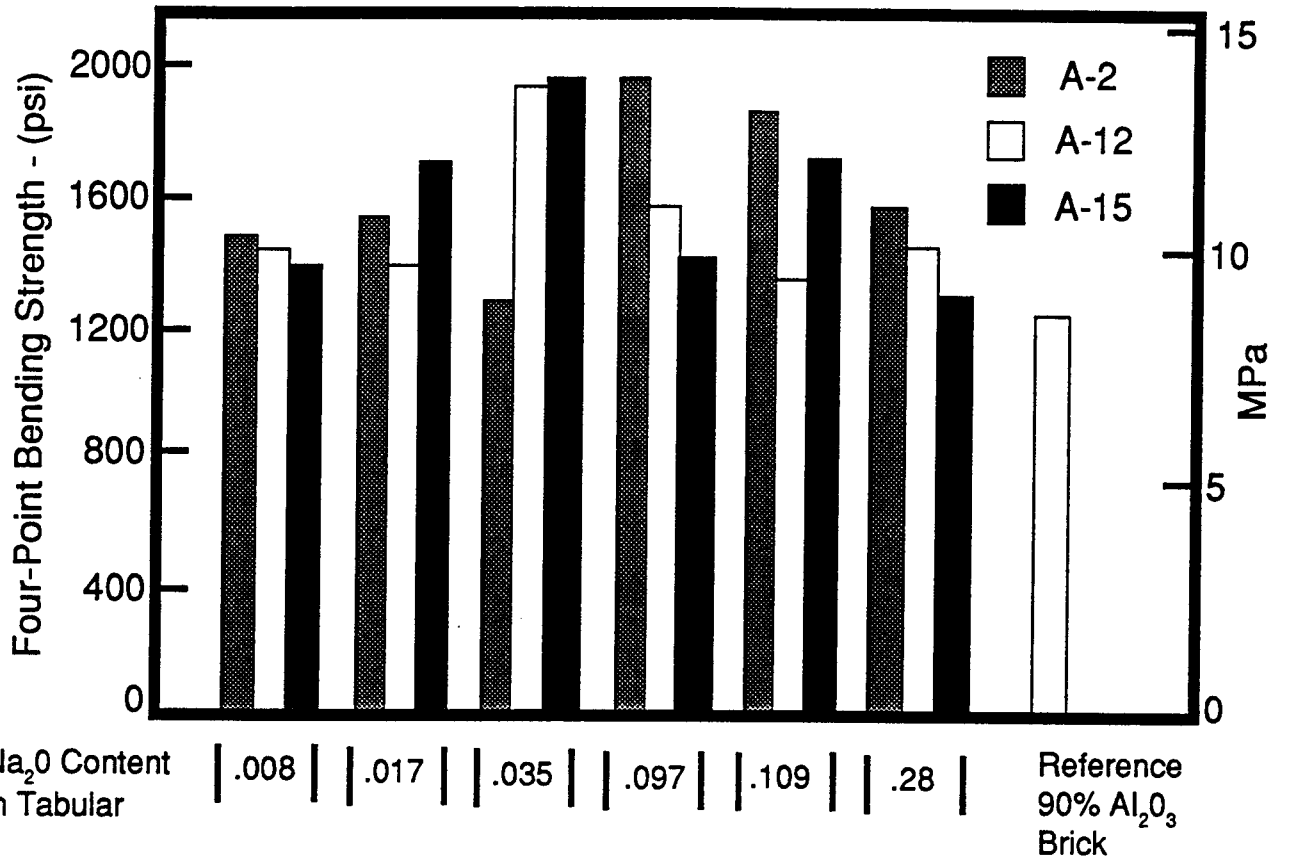

Fig. 23. Bending strength after eight thermal shock cycles between 816° and 860°C on 90% Al_2O_3-10 % SiO_2 refractory test brick.

with resonant frequency for high-Al_2O_3 refractory concretes according to the following equation based on the data listed in Table XVII:

$$S = 0.869f^2 \times 10^{-6} + 0.35 \text{ MPa} \quad (4)$$

$$\sigma = 1.01 \text{ MPa (146 psi)}$$

where

S = 4-point bending strength (MPa)

f = resonant frequency (Hz).

The correlation was established for one cement using four different types of alumina aggregates which had an "ideal" graded particle-size distribution (Fig. 25). The regression equation is expected to vary if another cement is used or if the experimental conditions are altered. Increasing the thermal shock test temperature has a dramatic effect on the retained specimen strength, but catastrophic failure did not occur on any of the 25 mm (1 in.) specimens. Surface cracks appeared after thermal shock cycling and were oriented perpendicular to all edges of the specimen, indicating cracking created by tensile stresses on cooling.

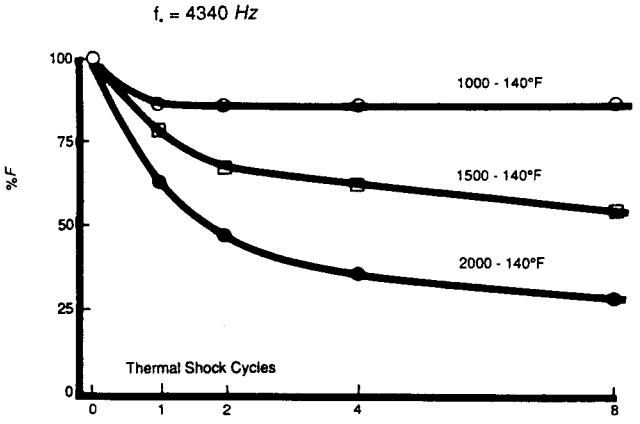

Fig. 24. Resonant frequency after thermal shock of high-Al_2O_3 refractory concrete (Cal-Tab 15 fired 5 h, 1650°C (3000°F)).

Figure 26 shows the effect of different heat treatments on the thermal shock damage resistance as represented by the transverse-strength depreciation of tabular- and fused-Al_2O_3 concrete bonded with 15 wt% CAC after eight shock cycles (60°–816°–60°C).[96] The unusually high, unshocked, cold MOR obtained on the tabular Al_2O_3 specimens fired at 1800°C (3270°F) sug-

Table XVII. Resonant Frequency and Four-Point Bending Strength Properties after Thermal Shock of Refractory Concretes Made from 85% Aggregate: 15% Calcium Aluminate Cement

	Aggregate				Caltab 15 — Properties			
		Porosity (%)		Bulk Density	Thermal Shock		Strength (psi)	
Type	Na_2O (%)	Open	Closed	(g/cm^3)	Test Temp(°F)	%F	S_8	σ
Tabular	0.01	5.3	5.4	3.57	1000 – 140	88	2380	300
					1500 – 140	56	1250	210
					2000 – 140	29	820	210
Tabular	0.24	1.3	8.2	3.61	1000 – 140	85	1970	270
					1500 – 140	58	1000	260
					2000 – 140	23	470	80
White fused	0.20	8.1	4.4	3.50	1000 – 140	76	740	80
					1500 – 140	49	480	270
					2000 – 140	14	170	10
White fused	0.45	12.3	2.4	3.41	1000 – 140	77	1290	286
					1500 – 140	46	480	150
					2000 – 140	17	390	80

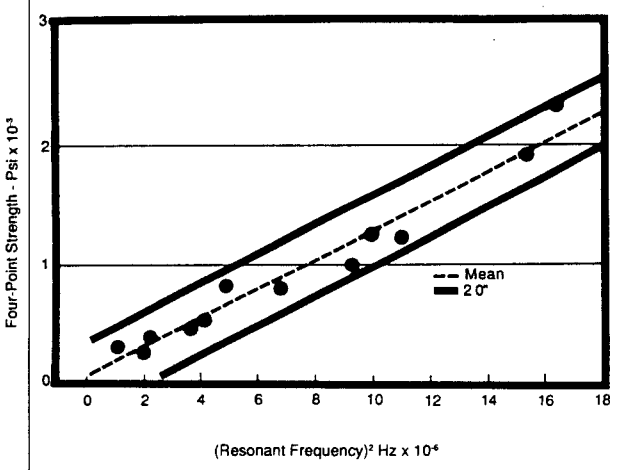

Fig. 25. Correlation of strength after thermal shock with resonant frequency for high-Al_2O_3 refractory concrete. $S = 126 f^2 \times 10^{-6} + 51$ psi; $\sigma = 146$ psi.

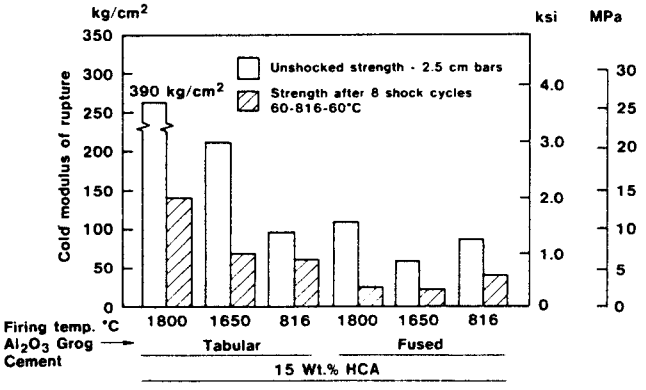

Fig. 26. Thermal shock damage resistance of tabular and fused Al_2O_3 castables bonded with high-purity CA cements.

gests the presence of a glassy bond. However, the retained strength after thermal shocking is highest for these specimens, suggesting the occurrence of a sintered, rather than a glassy, CA_6 bond.

The CAC/tabular concretes exhibit higher strengths than the equivalent white, fused-aggregate, refractory concretes for each test condition. Apparently, when the bend strengths of the cementitious bond exceed ≈6900 kPa (≈1000 psi), the castable strength becomes limited by the transgranular fracture through the coarse (4/8 mesh) white fused grain. The larger white fused particles contain rather large contiguous open pores (Fig. 27(*a*)) which reduce particle strength to <50% of equivalent-sized tabular particles.

The better thermal shock damage resistance of tabular is ascribed to (1) the large (>50 μm) α-Al_2O_3 crystals (see tabular alumina grain properties), (2) the <5 to 15 μm closed pores (Fig. 27(*b*)) which are thought to act as crack arresters (closed pores in tabular range to about 50 μm diameter), (3) better mechanical bonding to the rougher tabular fractured surfaces, and (4) more efficient use of the CA bond compared with the white fused Al_2O_3 wherein some of the high-purity CAC is lost in the large open pores of the coarse grain (Fig. 27(*a*)) and inefficiently used.

The advantage of closed porosity on improving thermal shock damage resistance has been documented by others. Smith et al.[97] studied the effect of 0 to 5% induced cylindrical, two-dimensional, and spherical porosity in dense fine-grained (nominally 2.0 μm) 99.9% Al_2O_3 ceramics on strength degradation on quench shocking at different temperatures. They commented that a pore in a ceramic matrix acts as a stress concentrator. When stressed, pores act to initiate fracture locally; therefore, they may be considered flaw activators. As pore volume increases, the number of pores or the number of possible fracture sites on the specimen surface increases. For a given severity of thermal shock, more cracks are propagated in a pore sample than in a nonpore one, as suggested by Has-

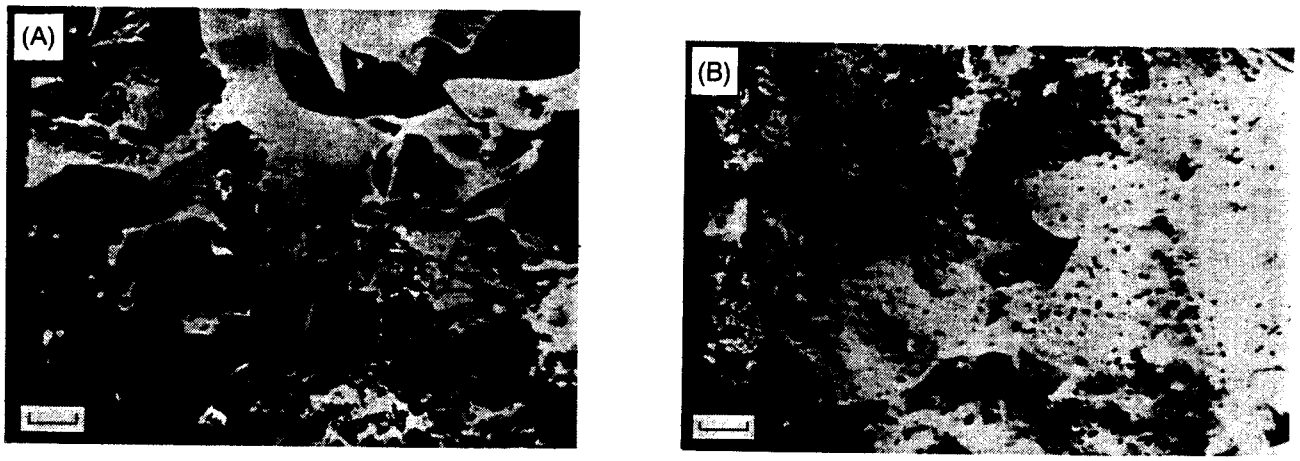

Fig. 27. Scanning electron micrographs of (*a*) white fused alumina grain and (*b*) tabular alumina grain. Bars = 50 micron.)

selman.[19] Pores may also act as crack arresters. When the crack front arrives at a pore, the crack may be forced to alter its path or even stop. The crack depth in thermally shocked samples decreased as the porosity was increased in Smith et al.'s work, suggesting that pores act as crack arresters or energy dissipators.

Organic pore-forming materials were used by Smith et al.[97] to induce 40 to 100 μm diameter spheres, 50 μm by 12 μm diameter fibers, and 100 μm (largest dimension) flakes in the polycrystalline Al_2O_3 ceramic on sintering. The strength decreased as the pore asymmetry increased from spherical to cylindrical to two-dimensional geometry. It was observed that pore shape also determines the degree of damage sustained on quench shocking. The fractional strength retained after shocking increased with increasing porosity and as the pore geometry became more asymmetrical. Crack density also increased with increasing porosity. Thus, excessive strength degradation in Al_2O_3 ceramics or aggregates can be avoided by processing in a manner which would increase porosity. Propagation of the maximum number of cracks will minimize damage and avoid catastrophic failure. Natural pores formed by incomplete sintering are cylindrical or spherical, depending on the degree of sintering. If pores are to be introduced by organic additions, they should be distributed homogeneously throughout the sample. Most ceramics require a usable strength after shocking; therefore, the amount of porosity that can be introduced is determined by the remnant strength needed for the specific application.

Homeny and Bradt[98] investigated the fracture behavior of CAC-bonded tabular Al_2O_3 refractory concretes after firing at 1200°C (2190°F). Theoretical thermal shock damage-resistance parameters derived from mechanical properties were correlated with the experimentally observed trends in the thermal shock behavior of tabular Al_2O_3 concretes. It was found that variations in cement contents and aggregate distributions were effective means of producing substantial modifications of certain physical and mechanical properties, as can be observed in Table XVIII.

The thermal shock damage-resistance parameter R_{st} was found to be inversely related to single-cycle thermal shock trends, while R'''' correlated directly with trends observed in the multiple-cycle thermal shock test. It was determined that bulk density, Young's elastic moduli, shear moduli, notched-beam fracture surface energies, and the work of fracture varied significantly with microstructure modifications due to variation in cement content and aggregate size distribution. Fracture strengths, Poisson ratios, and thermal expansion coefficients were affected to a much lesser degree. These microstructure variations also modified the behavior of different concrete systems during thermal shock testing. In laboratory thermal shock tests, the gap-sized systems showed increased resistance to thermal shock damage compared with the generic or continuously graded concretes. However, the retained flexural strength after 10 1200°C thermal shock cycles with the continuous distributions containing 25 and 30% CAC was about 6.2 MPa (900 psi), about 1.7 to 2 MPa (250 to 300 psi) higher than that retained by the gap-sized concrete for the same cement levels. The generic concrete containing 25% CAC retained 5.5 MPa (800 psi) after 10 cycles. The retained strengths for the 20% CAC continuous and gap-sized concretes were similar.

Developmental Tabular Al_2O_3 Refractory Aggregates

The ever-evolving technology on altering the chemical and thermal states of molten steel in ladle metallurgy constantly drives refractories to ever-increasing time/temperature and corrosion/erosion resistance requirements. New and improved refractory

Table XVIII. Mechanical Properties and Thermal Shock Damage Resistance Parameters of High Purity CAD Bonded Tabular Al_2O_3 Castables

A. Room-Temperature Data of Samples Fired at 1200°C and Tested at Room Temperature

Aggregate Dist. — Cement Content	ρ (g/cm^3)	α (°C^{-1})	E (MN/m^2)	G (MN/m^2)	ν	σ_f (MN/m^2)	γ_{NBT} (J/m^2)	γ_{WOF} (J/m^2)
Generic-25	2.59	7.0×10^{-6}	2.09×10^4	1.01×10^4	0.04	8.40 (±1.34)*	7.14 (±2.76)	44.22 (±5.61)
Continuous-20	2.69	6.3×10^{-6}	3.44×10^4	1.58×10^4	0.09	6.66 (±0.81)	2.80 (±0.25)	27.91 (±2.37)
Continuous-25	2.54	6.4×10^{-6}	2.79×10^4	1.28×10^4	0.09	9.14 (±0.89)	10.10 (±1.31)	61.85 (±4.78)
Continuous-30	2.51	6.5×10^{-6}	2.51×10^4	1.18×10^4	0.06	9.52 (±0.71)	10.52 (±1.26)	51.65 (±3.88)
Gap-Sized-20	2.83	6.5×10^{-6}	6.51×10^4	3.08×10^4	0.06	6.18 (±0.80)	4.85 (±0.79)	88.23 (±9.62)
Gap-Sized-25	2.72	6.5×10^{-6}	6.41×10^4	3.02×10^4	0.06	5.10 (±0.64)	2.76 (±0.27)	70.29 (±7.51)
Gap-Sized-30	2.62	6.8×10^{-6}	4.70×10^4	2.12×10^4	0.11	4.71 (±0.51)	2.58 (±0.31)	79.18 (±11.11)

*95% confidence intervals.

B. Elevated Temperature Data of Samples Fired and Tested at 1200°C

Aggregate Dist. — Cement Content	α (°C^{-1})	E (MN/m^2)	G (MN/m^2)	ν	σ_f (MN/m^2)	γ_{NBT} (J/m^2)	γ_{WOF} (J/m^2)
Generic-25	8.3×10^{-6}	1.50×10^4	0.78×10^4	0.05	6.86 (±0.90)*	6.52 (±2.08)	118.72 (±14.05)
Continuous-20	7.9×10^{-6}	2.47×10^4	1.13×10^4	0.09	7.65 (±0.89)	5.31 (±1.38)	196.51 (±43.31)
Continuous-25	7.6×10^{-6}	2.00×10^4	0.91×10^4	0.09	8.88 (±1.11)	6.86 (±1.86)	205.67 (±44.41)
Continuous-30	7.7×10^{-6}	1.83×10^4	0.86×10^4	0.06	10.72 (±0.97)	9.78 (±2.41)	233.50 (±24.55)
Gap-Sized-20	8.3×10^{-6}	4.71×10^4	2.23×10^4	0.05	3.96 (±0.84)	0.98 (±0.26)	110.02 (±28.64)
Gap-Sized-25	9.1×10^{-6}	4.60×10^4	2.16×10^4	0.07	6.49 (±0.82)	2.00 (±0.29)	251.49 (±56.75)
Gap-Sized-30	8.2×10^{-6}	3.37×10^4	1.50×10^4	0.11	5.34 (±0.80)	2.77 (±0.59)	234.60 (±41.27)

*95% confidence intervals.

raw materials must be researched and developed with a sustained ongoing effort to take advantage of the periodic advances in refractory material technologies in order to meet this continually changing need for new and improved refractory raw materials.

Future progress on improving refractory aggregates requires the development of additional testing procedures to better differentiate characteristic properties of the aggregates in order to show a measure of improvement. Bertrand et al.[99] continue to improve the interpretation of the mechanical properties of refractory aggregates by using Weibull statistics to analyze the room-temperature compressive strength results of individual grains. The fracture stress is calculated from the maximum test load at fracture and the average diameter of each grain using the Hiramatsu and Oka[100] equation:

$$\sigma_f = \frac{2.80\, p_{max}}{\pi d^2} \tag{5}$$

where

σ_f = fracture stress
p_{max} = load at failure
d = grain diameter

The strengths of two fused aluminas and two tabular aluminas were measured and compared by the application of Weibull statistics in the Bertrand et al.[99] study. The Weibull moduli of these grains were relatively low (1.17 ± 0.32 to 2.51 ± 0.70), indicating a wide strength distribution. Several different flaw populations appear to be present in these materials, as indicated by the shapes of the Weibull plots.

The two tabular aluminas, which deferred primarily in a Na_2O level (0.10 vs 0.16), exhibited fracture stresses consistently greater than those of the brown and white fused aluminas. Differences in grain microstructure are thought to be the reason for the tabular aluminas' higher strength. The fused Al_2O_3 grains are large individual crystals, often equal in size to the four grain sizes tested (4/6, 6/8, 8/10, and 10/14 mesh) with many large intergranular pores, whereas the polycrystalline tabular aggregate grains contained comparatively smaller crystallite sizes and only fine intergranular porosity. It was concluded, by consideration through the Griffith equation, that the tabular aggregate grains, which appear to have smaller intrinsic flaw sizes and also larger fracture toughnesses, may be expected to exhibit higher strengths than the fused grains. Scanning electron microscopy appraisal of the fracture surfaces substantiates their explanation of the strength differences.

A new refractory-grain thermal spalling resistance test procedure was developed to differentiate the properties of three developmental tabular Al_2O_3 aggregates in comparison with a developmental $MgO \cdot Al_2O_3$ spinel aggregate and commercial tabular Al_2O_3, white fused Al_2O_3, and brown fused Al_2O_3 aggregates (Table XIX).[101]

The refractory-grain thermal spalling resistance test procedure consists of selecting 300 approximately equiaxed 5 mm grains and thermal cycling 100 each for 10, 20, and 30 cycles between 20° and 1300°C (68° and 2370°F). The unfractured whole grains are counted and reported as percentage undamaged. Thirty of the remaining whole grains are then crushed individually to obtain a measure of thermal shock damage resistance of the refractory aggregates.

Table XIX. Refractory Aggregate Chemical and XRD Phase Analyses*

Analyses	Tabular	White Fused	Brown Fused	Spinel	Ca-Tab	Si-Tab	Zr-Tab
Chemical analysis (%)							
Al_2O_3	99.40	99.55	95.85	69.50	98.20	97.00	90.20
SiO_2	0.050	0.015	0.77	0.18	0.04	2.24	0.66
TiO_2	0.002	0.003	2.81	0.01	0.004	0.01	0.02
Fe_2O_3	0.14	0.037	0.18	0.34	0.61	0.52	0.09
CaO	0.040	0.009	0.07	0.38	0.83	0.06	0.02
MgO	0.010	0.009	0.26	29.50	0.040	0.010	0.02
Na_2O	0.29	0.39	0.03	0.06	0.24	0.10	0.09
K_2O	0.01	0.01	0.01	0.01	0.01	0.01	0.01
ZrO_2		0.01					8.80
Note: Ca-Tab and Spinel are not acid washed to remove Fe from crushing.							
XRD Phase							
Corundum	ST	ST	ST	VW	ST	ST	ST
B-Al_2O_3	W	M					VW
Illmenite			W				
MgO Spinel				ST			
Periclase				W			
$CaO \cdot 6Al_2O_3$					W		
Mullite						W	
Baddeleyite							M
ZrO_2 Cub/tetr							VW

Note: ST = strong, M = medium, W = weak, VW = very weak.
*Ref. 101. Used by permission

The results of the grain thermal spalling resistance test are compared in Table XX, along with additional grain physical characteristics.

The best grain thermal spalling resistance is demonstrated by both Ca-Tab and Zr-Tab with 91 and 87%, respectively, of the original 5 mm grain remaining undamaged after 30 cycles between 20° and 1300°C. These excellent results are significantly higher than the next best aggregate, tabular alumina, which is noted for its excellent thermal shock resistance in slide-gate plates and other steel contact refractories used in continuous casting. Si-Tab gives the next best thermal spalling resistance performance with spinel, white fused, and brown fused aggregates following in decreasing order and at significantly lower performance levels. For example, all of the brown fused grains were thermally fractured between 20 and 30 thermal shock cycles; thus no grain strength determination could be made after 30 cycles.

Zr-Tab exhibits the best thermal shock damage resistance of the refractory aggregates, as indicated by the strength of the remaining undamaged grains after thermal cycling. Tabular and Ca-Tab are equivalent and next best, followed by Si-Tab with spinel, white fused, and brown fused exhibiting very poor thermal shock damage resistance.

A more detailed study is required to establish the mechanisms involved during the sintering of Ca-Tab and Zr-Tab to explain their superior thermal shock characteristics over the other Al_2O_3 aggregates. The presence of $CaO \cdot 6Al_2O_3$ in the sintered tabular alumina structure may provide an advantage for Ca-Tab. Previously reported microcracking in $ZrO_2 \cdot Al_2O_3$ composites resulting from differential expansion characteristics of the two oxides (ZrO_2 and Al_2O_3) may provide the advantage for Zr-Tab. The thermal cycling between 20° and 1300°C precludes the publicized ZrO_2 martensitic tetragonal-to-monoclinic transition from being a controlling mechanism.

A sag deformation test[52,96] was used to determine the refractoriness of the developmental and commercial aggregates in a test castable containing 15% high-purity CAC (80% Al_2O_3). Table XXI lists the refractoriness ratings for the various aggregate/15% CAC-bonded test castables based on the test specimens exceeding a 1% sag deformation.

The sag deformation test gives a relative measure of hot strength by comparing the ability of 25 mm (1 in.) MOR specimens to resist gravity deformation or sagging when supported unrestrained on a 127 mm (5 in.) span. Percentage sag deformation is calculated by dividing the amount of deformation as measured between the center of the specimen and the 127 mm cord. Specimens are heated for 5 hours at different temperatures to establish the temperature at which a 1% sag deformation is exceeded. This level of deformation is

Table XX. Grain (5mm) Physical Properties of Developmental Technical Al_2O_3 Aggregates

Al_2O_3 Aggregate	Grain Physical Characteristics: Bulk Density (g/cm^3)	Apparent Specific Gravity (g/cm^3)	Apparent Porosity (%)	H_2O Absorption (%)	Thermal Spalling Resistance† % Undamaged 20°-1300°-20°C Shock Cycles: 10	20	30	Grain Strength Breaking Load kg	Grain Crushing Strength§ After Thermal Shocking Breaking Load (kg) 20°-1300°-20°C Shock Cycles: 10	20	30
Tabular	3.49	3.66	4.82	1.38	95	87	73	296	170	118	80
White fused	3.57	3.89	8.28	2.32	68	19	0	105	21	4	0
Brown fused	3.82	3.97	3.78	0.99	62	10	0	195	38	5	0
Spinel	3.17	3.26	2.73	0.86	82	53	20	242	43	30	12
Ca-Tab	3.46	3.70	6.37	1.84	100	99	91	236	122	96	73
Si-Tab	3.48	3.63	4.21	1.21	91	76	58	462	77	79	65
Zr-Tab	3.92	4.09	4.04	1.03	100	97	87	219	174	162	131

*Ref. 101. Used by permission.
†Thermal shock testing done on 300 grains with 100 used for each shocking cycle series.
‡Average of 30 individual grains.
§Average of 10 to 30 individual grains with strength test being conducted on available unfractured grain remaining from each 100 grain shock cycle series.

Table XXI. SAG Deformation Refractoriness Rating of Developmental Technical Al_2O_3 Aggregates in 15% CAC Test Castable*

Al_2O_3 Aggregate	15% CAC Castable Refractoriness: Max. Use Temperature (<1.0% SAG Deformation) (°C)
Tabular	>1700
White fused	>1700
Brown fused	1500–1550
Spinel	1500–1550
Ca-Tab	>1700
Si-Tab	1500–1550
Zr-Tab	1600–1650

*Ref. 101. Used by permission.

thought to indicate the maximum use temperature for the test castable at which sufficient hot strength exists [about 1.38 MPa (200 psi) MOR] to support its own weight.

Ca-Tab, tabular, and white fused Al_2O_3 produced the most refractory castables (>1700°C) with 15% CAC. The lower refractoriness of the brown fused, Si-Tab, and spinel confirms the physical property data obtained on these refractory concretes that indicated the development of a glassy bond when the bars were fired at 1650°C, 5 hours.

It was concluded that the two developmental technical refractory aggregates, Ca-Tab and Zr-Tab, exhibit grain and 15% CAC castable properties sufficiently comparable or superior to the best commercial Al_2O_3 refractory aggregates to warrant further development and appraisal by industry in severe applications requiring improved refractories performance. Although the spinel and Si-Tab grain did not meet the performance of tabular Al_2O_3, Ca-Tab, and Zr-Tab, these developmental aggregates did perform as well or better than white and brown fused, except for having less refractoriness than white fused Al_2O_3, but equivalent to brown fused, in CAC castables. Other bond systems should be considered to take advantage of Si-Tab superior grain strength and thermal spalling-resistant properties and the known corrosion-resistant properties of spinel.

Tabular Al_2O_3 Refractory Applications

Tabular alumina is a dense, fully shrunk, sintered Al_2O_3 with large (50 to >400 μm) well-developed α-Al_2O_3 crystals forming a strong aggregate structure. The predominantly tabletlike crystals contain a significant amount of closed porosity which is entrapped during rapid heating to sintering temperatures slightly below the fusion point of Al_2O_3. Tabular alumina finds significant use as a refractory raw material because of the following significant chemical and physical properties:

- High chemical purity—the sintering process produces tabular alumina of purity over 99.5% Al_2O_3.
- Extreme hardness of the ultimate crystals—Moh's scale, 9; Knoop hardness, 2000.
- Low apparent porosity—≈3% with 2 to 3 times higher closed porosity, ≈0.8% H_2O absorption, 3.97 true density,and 3.50 to 3.65 g/cm^3 particle density.
- High melting point—approximately 2050°C (3720°F).
- Chemical inertness—not attacked by most alkalis and mineral acids except hydrofluoric and phosphoric acids.
- Relatively high thermal conductivity for ceramic materials.
- Good thermal shock resistance—withstands repeated rapid changes of extreme temperature.
- High electrical resistivity—excellent electrical properties at ultrahigh frequencies and elevated temperatures.
- Excellent volume stability—since tabular alumina is fully shrunk there is a virtual absence of reheat shrinkage in refractories.

- Highly reactive surface for ceramic, chemical, and cement bonding.
- Absence of microcracks and gross internal porosity.
- High individual grain strength.

The aforementioned properties make tabular alumina an excellent refractory raw material and when incorporated into refractories enable the manufacturer to obtain the following advantages:

- High fusion point–high refractoriness
- Excellent hot-load strength–low creep
- High density–low permeability
- Good thermal shock resistance
- Good abrasion resistance
- Good resistance to chemical attack
- Low reheat shrinkage
- High purity

These merits of tabular alumina can be appreciated by comparing the properties of the 90 and 100% Al_2O_3 classes of high-alumina brick with other refractory brick listed in Table XXII.[102]

A measure of refractoriness is indicated by the pyrometric cone equivalent, or PCE tests, in which the softening behavior of small cones of the refractory are compared with that of standard pyrometric cones of known time-temperature softening behavior. The PCE is reported as the standard cone number which touches the supporting plaque simultaneously with a cone made of the refractory being investigated, when tested in accordance with the Standard Method of Test for Pyrometric Cone Equivalent (ASTM designation: C–24). The PCE values for various refractories and their corresponding softening temperatures when heated under standard test conditions are shown in Fig. 28.[103]

Although the PCE test provides a standard method of comparing the refractoriness of various compositions, the maximum service temperatures of most refractories are considerably below the PCE temperature. The Refractories Institute (TRI) provides a useful comparison of typical maximum hot-face working temperatures for various refractory brick linings, as shown in Table XXIII.[104]

The ASTM C–16 hot-load test gives another measure of the potential maximum use temperature of refractories when totally immersed in the thermal environment (Table XXII-B). The definite advantage of the mullite-bonded 90% Al_2O_3 brick class is obvious, typically showing only 0 to 1% deformation after heating at 1700°C (3090°F), 1.5 hours. The superior hot strengths of the dense mullite-bonded 90% Al_2O_3 brick are also shown in the classic hot-MOR chart shown in Fig. 29.[105]

Besides the aforementioned properties for refractories, thermal expansion and thermal conductivity characteristics are important in the design and use of refractory linings. Tabular alumina refractories are typically represented by the 90 and 100% Al_2O_3 class refractory characteristics illustrated in Figs. 30[103] and 31[102] for the linear thermal expansion and thermal conductivity properties, respectively.

Although the 90 and 100% Al_2O_3 class refractories typify the properties of tabular alumina refractories, tabular alumina is used extensively as an alumina enrichment addition to many of the other high-alumina classes of refractories, besides being a major ingredient in the Al_2O_3-C, Al_2O_3-SiC-C, and Al_2O_3-Cr_2O_3 refractories. Tabular-based or -enriched monolithic plastics, ramming and castable compositions are also extensively utilized by industry. They can be used with improved performance in substitution for any compositions containing brown or white fused aluminas, if the refractories are properly designed for optimum performance.

Generally, refractories are needed in production processes where temperatures are >590°C (1095°F), with a number of uses in the range 1430° to ≥1930°C (2605° to 3505°F).[106] Although the iron and steel industry continues to be the major user of refractory products, consuming about 50% of U.S. shipments,[107] the industry has experienced a sharp decline from its nominally 70% share as the result of rationalization and consolidation of unprofitable excess capacity. The western European steel industry has experienced a similar retrenchment, but refractory product shipments to the iron and steel industry still represent a 60 to 65%[108] share, as shown in Table XXIV.

There has also been a drastic decrease in refractories production in Japan, primarily attributable to the reduction of crude steel and cement output (Fig. 32), as well as a reduced specific consumption of refractories (Fig. 33).[109] Nonetheless, the iron and steel industry is projected to consume 65% of the total refractories (1 250 000 metric tons, 1 380 000 tons) in Japan, even after projecting a future reduction of crude steel production to 82 million metric tons (90 million tons) from a 1987 level of 98.5 million metric tons (108.4 million tons).[110] Specific consumption of the refractories is projected to be reduced to 11 kg/metric tons (10 kg/ton) from 21.1 kg/metric tons (19.1 kg/ton) in 1976 and 13.9 kg/metric tons (12.6 kg/ton) in 1986.[109] Some Japanese integrated iron and steel companies and those with recently installed electric furnaces currently have specific refractory consumption of 8.8 kg/metric tons (8.0 kg/ton) with monolithic refractories representing 70% of total consumption.

The 1986 sales of refractories by industry in Japan are shown in Fig. 34 with monolithic refractories accounting for 44.5% of refractory sales, according to Sakano and Takahashi.[109] They attribute the remarkable increase in monolithic production since 1980 to the development of ultrafine powders and cementless high-strength castables, along with mechanized application. The decrease in construction brick consumption for coke ovens, hot stoves, and blast furnaces accounts for the reduced sales of fireclay, silica, and dolomite brick. However, consumption of MgO-C and

Table XXII. A. Composition of Alumina, Silica, and Zirconia Refractories, %

Type	SiO_2	Al_2O_3	Fe_2O_3	TiO_2	CaO	MgO	Alkalies	ZrO_2
Silica	95–96	0.2–1.5	0.8–1.0	0.3–0.1	3.3–2.7	<0.1	<0.2	
Fireclay								
Semisilica	70–79	17–27	0.6–2.0	0.8–1.6	0.1–0.4	0.1–0.4	0.2–0.4	
Medium duty	56–70	25–36	1.8–3.4	1.3–2.7	0.2–0.4	0.4–0.6	1.0–2.7	
High duty	51–59	35–41	1.5–2.5	1.1–3.0	0.2–0.6	0.1–0.6	1.3–2.6	
Super duty	50–54	40–46	0.8–2.3	1.1–2.5	0.1–0.5	0.4–0.6	0.1–1.4	
High alumina								
50% Al_2O_3	40–47	47–57	0.9–1.6	2.2–2.4	0.5–0.6	0.3–0.6	0.8–1.3	
60%	27–37	58–67	0.9–2.7	1.7–3.0	0.1–0.3	0.2–0.7	0.2–1.2	
70%	19–28	68–77	0.9–2.2	2.0–3.3	0.1–0.3	0.1–0.7	0.2–1.2	
80%	8–17	78–87	0.7–1.7	2.5–3.2	0.1–0.2	0.1–0.4	0.1–1.0	
85%*	6–10	82–86	1.0–2.5	2.0–3.0	trace–0.2	trace–0.4	0.1–0.3	
90%	3–10	88–96	0.1–1.4	0.1–2.6	0.1–0.2	0.1–0.3	trace–0.9	
100%	0.2–1.1	97–99	0.1–0.3	trace–0.3	0.1–0.3	0.1–0.3	0.1–0.3	
Zircon	32	1	0.1	1.8	trace	0.1	0.02	64
Molten cast								
Al_2O_3–ZrO_2–SiO_2	11–13	50–51	trace–1.0	trace–1.0	trace	trace	1.0–1.5	33–35
Al_2O_3–SiO_2	18–22	57–70	1–4	3.0–4.5	0–1	0–1	0.0–1.5	
Al_2O_3 high soda	0.04	93.8	0.1	0.05	0.1	0.1	5.6	
Al_2O_3 low soda	0.10	99.2	0.1	0.05	0.1	0.1	0.3	

*Phosphate-bonded.

B. Typical Ranges of Physical Properties of Alumina, Silica, and Zirconia Refractory Brick

Type	PCE*	Modulus of rupture MPa†	Deformation under 172 kPa† % linear change after 1½ hours Temperature °C	Change (%)	Linear reheat change‡ at °C	(%)	Thermal spalling loss§ at °C	(%)	Bulk density (g/cm³)	Porosity (%)
Silica		2.8–11.2	1650	0					1.60–1.80	20–30
Fireclay										
Semisilica	27–31	2.1–4.2	1450	0.1–2			1480	0–10	1.80–2.10	20–30
Medium duty	29–31	7.0–11.2	1450	1–6			1600	2–6	2.11–2.20	17–21
High duty	31–33	2.8–21.0	1450	0.5–15	1600	0–1 S	1600	3–7	2.13–2.30	4–30
Super duty	33–34	2.8–24.0	1450	0–9	1600	0–1 S	1650	2–8	2.28–2.48	5–22
High alumina										
50% Al_2O_3	34–35	7.0–11.2	1450	2–6	1600	0–1 E	1650	8–12	2.27–2.43	14–18
60%	36–37	7.0–11.2	1450	1–4	1600	0–5 E	1650	1–5	2.10–2.49	13–28
70%	37–38	7.0–11.2	1450	1–3	1600	1–7 E	1650	3–7	2.20–2.66	14–28
80%	38–39	7.0–12.6							2.50–2.90	14–29
85%¶	38–39	21.0–35.0	1450	0.3–3	1600	0–2 E	1650	0–5	2.70–2.92	12–17
90%	40–41	14.0–35.0	1700	0–1	1700	0–1 E	1650	0–1	2.67–3.10	11–27
100%	41–42	12.6–21.0	1650	1–2	1700	0–0.5 S	1650	0–5	2.84–3.10	19–29
Zircon			1600	2–5	1540	0			3.77	20
Molten cast										
Al_2O_3–ZrO_2–SiO_2									3.70–3.74	0.8–3
Al_2O_3–SiO_2									3.00–3.20	1–3
Al_2O_3 high soda									2.89	
Al_2O_3 low soda									3.50	

*Pyrometer cone equivalent, as determined by ASTM C 24.
†To convert MPa to psi, multiply by 145; for kPa, multiply by 0.145.
‡S = Shrinkage; E = Expansion.
§As determined by ASTM C 38.
¶Phosphate-bonded
Ref. 102. Used by permission.

Al_2O_3-SiC-C brick is increasing rapidly and consumption of Al_2O_3 and carbon composites should grow. This scenario, perhaps, portends the future of refractories usage throughout the world, as advanced steelmaking technology is adopted and placed into service. If so, then the trends in raw material consumption in Japan provide an important reference in predicting future raw materials needs for the worldwide refractories industry (Table XXV).[111]

The trend of raw materials consumption by various countries throughout the world can be expected to differ from that of the Japanese, depending on the

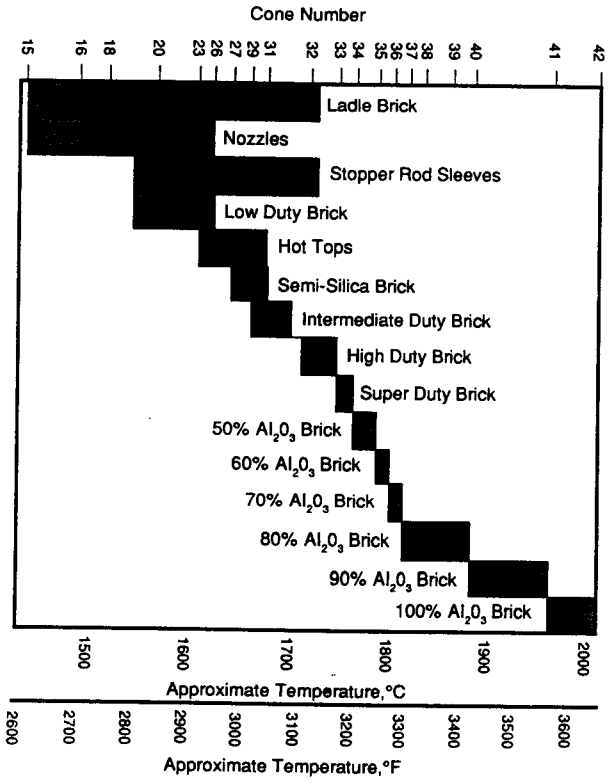

Fig. 28. Pyrometric cone equivalent (PCE) of various alumina-silica refractories.

Table XXIII. Typical Maximum Hot-Face Working Temperatures for Refractory Brick Classes*

Refractory Class	Typical Hot-Face Working Temperatures °F	°C
Low-duty fireclay	2600	1425
Medium-duty fireclay	2700	1480
High-duty fireclay	2800	1540
Superduty fireclay	3000	1650
High-alumina, 50% Al_2O_3	3000	1650
High-alumina, 60% Al_2O_3	3100	1705
High-alumina, 70% Al_2O_3	3250	1790
High-alumina, 80% Al_2O_3	3250	1790
High-alumina, 90% Al_2O_3	3400	1870
Basic chrome	2500	1370
Basic chrome-magnesite	3000	1650
Basic magnesite-chrome	3000	1650
Basic magnesite	3000	1650
Basic magnesite (periclase)	3300	1815
Fosterite ($MgO \cdot SiO_2$)	3000	1650
Silica	3100	1705

Note: The maximum working temperature of any refractory product varies with its unique composition and operating conditions; therefore, the above temperatures are approximate.
*Ref. 104. Used by permission.

availability of geographic natural resources and alternate refined synthetic materials. The increasing tabular alumina consumption in Japan from 28 900 metric tons (31 790 tons) in 1975, when tabular Al_2O_3 was first differentiated from fused Al_2O_3 usage, to 61 300 metric tons (67 430 tons) in 1983 emphasizes the

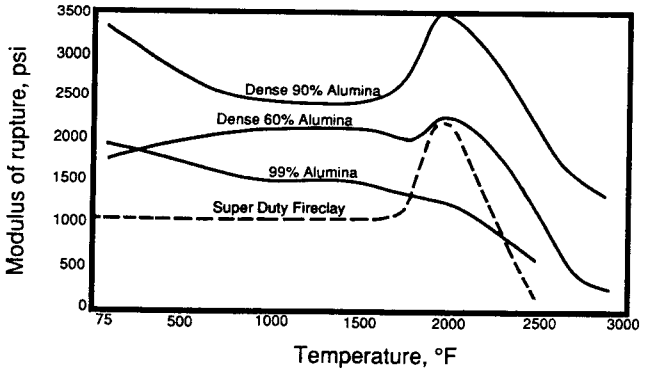

Fig. 29. Effect of temperature on modulus of rupture of new high-strength refractories (Ref. 105, Fig. 2. Used by permission).

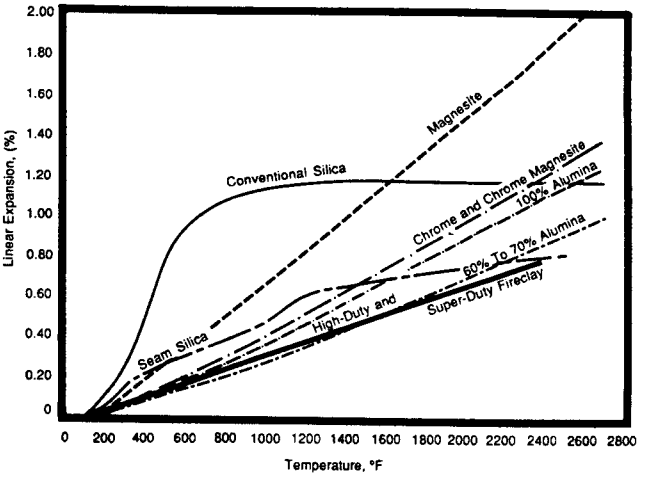

Fig. 30. Typical curves of linear expansion of various types of refractories (Ref. 103, Fig. 2–2. Used by permission).

important role tabular alumina has played in meeting the demand for higher quality and durability refractories to meet the more severe operational conditions imposed by the Japanese steelmaking companies. Tabular alumina's share of the synthetic Al_2O_3 raw materials consumption increased from 39 to 57% at the expense of fused alumina between 1975 and 1978. Their proportional usage remained relatively constant during the interim period which saw a significant increase in total consumption in 1979. The total Japanese refractories consumption dropped significantly during this period of growth and stable market consumption for tabular Al_2O_3 refractories, as did their refractories consumption for steelmaking (Fig. 32).

It is evident from the aforementioned that the iron and steel industry, as in the past, will be the primary market driving tabular alumina refractory consumption, because of the continuing effort to improve steel quality using higher temperature refining techniques. Nonetheless, there are many industrial applications

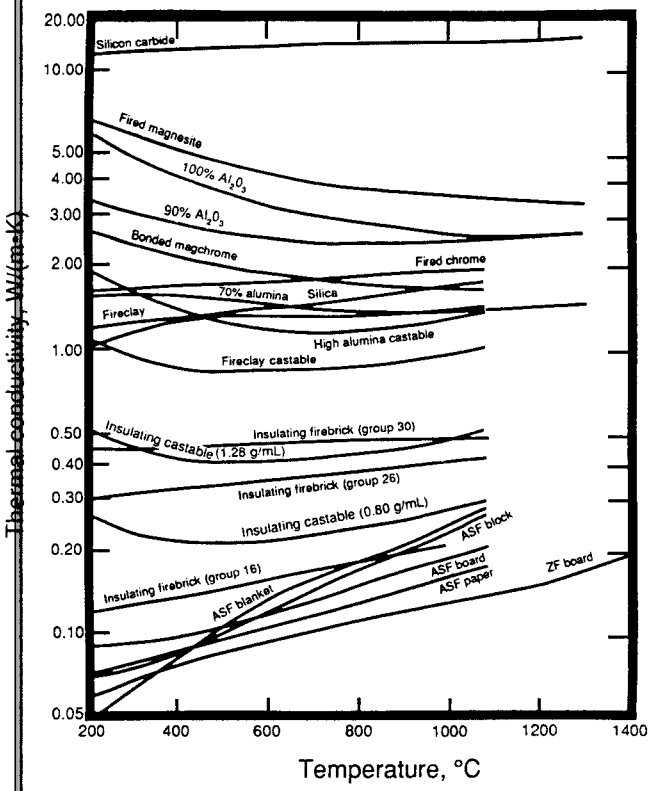

Fig. 31. Thermal conductivity of typical refractories (3,25). ASF = aluminosilicate fiber; ZF = zirconia fiber (Ref. 102, Fig. 2. Used by permission.)

Table XXIV. Refractory Product Shipments by End-Use Industry

End-Use Industry	Portion of shipments (%)
Iron and steel	60–65
Ceramics	5–8
Cement/lime	5–8
Glass	5–8
Nonferrous metal	3–5
Chemicals and petrochemicals	2–4
Energy generation	2–4
Room-heater brick	2–5

that have refractory needs that can best be served by tabular alumina refractories. References 32, 33, 66, 67, 102–106, and 109–127 describe the various applications for refractories in greater detail.

There have been tremendous advances in refractories during the past two decades that enabled the new iron and steel processes to be developed and improved for the more efficient production of higher quality steels. These advances far exceeded those of other industries. Thus, the following sections highlight tabular alumina refractory applications in iron and steel with the thought that many heat-process industries will benefit from this knowledge. Also, please refer to Section IV, chapters 20 and 24–29, which detail industrial applications that can take advantage of tabular Al_2O_3 refractory properties.

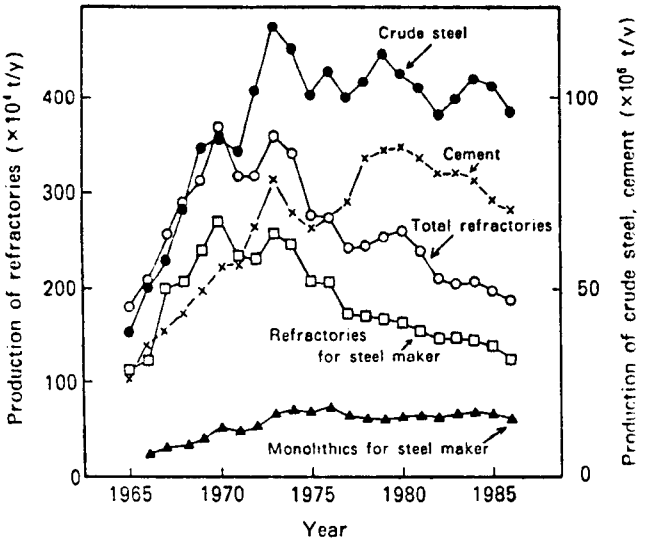

Fig. 32. Changes in annual production of refractories, crude steel, and cement.

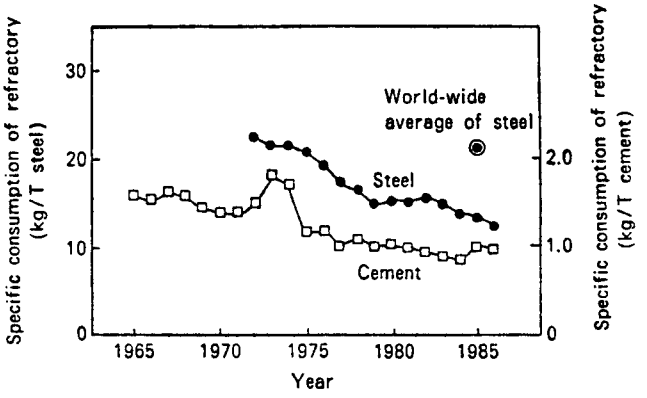

Fig. 33. Specific consumption of refractories for iron and steel use and for cement applications.

Tabular Alumina Refractories in Iron and Steel

Figure 35 shows a schematic of the unit operations for a steelmaking process which includes iron production in the blast furnace.[32] In 1982, Hubble and Kappmeyer[67] listed the current and future use of refractories in the steel industry and the corresponding demand for increased raw material usage according to specific unit operations (Table XXVI). Tabular alumina is included in the "alumina" refractory type designation and is also used for alumina enrichment in the "high-alumina" refractory types. Accordingly, tabular alumina refractories are expected to find increased usage in blast-furnace linings, iron and steel handling, degassers in secondary steelmaking, and in continuous

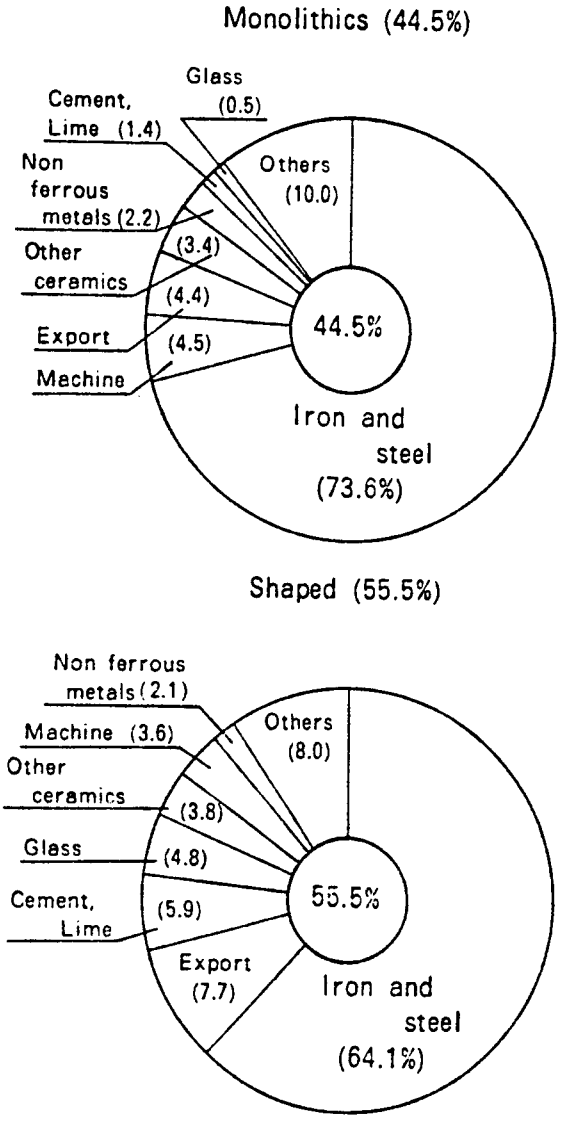

Fig. 34. Sales of refractories by industry, 1986.

casting. High-alumina shapes and monoliths, enriched with tabular Al_2O_3 additions, should find increased usage in blast-furnace stove shapes, iron-handling monolithics, and as brick, shapes, and monolithics in ladle linings.

Blast Furnaces for Ironmaking

The blast furnace (BF) (Fig. 36)[130] produces molten pig iron by reacting iron ore, coke, and limestone that are dumped into the top of the furnace and react with reducing gases in a fluidized high-pressure and high-temperature bed to smelt pig iron. Blast-furnace linings must be highly resistant to thermal shock and the abrasive action of the charge, as well as the corrosion action of alkalis and a reducing carbon monoxide atmosphere at temperatures that exceed 1760°C (3200°F). Daily iron production ranges from about 910 metric tons (1000 tons) to about 7300 metric tons (8000 tons) for the larger blast furnaces, which have hearth diameters up to 15 m (49 ft) and an overall height approaching about 60 m (200 ft) above ground level.

Zoning of refractories is a matter of routine in BF linings and very necessary to obtain an average life span between six and ten years. Improving the durability of the lower shaft and furnace bottom, said to be the weak points of BF linings, by preventing metal infiltration and carbon dissolution, significantly extend the BF's typical five- to six-year life. Gunning repairs from within the furnace and grouting repairs from outside the furnace were introduced in obtaining the extension of BF life. Copper cooling plates or cast iron staves at the shell protrude into the refractory wall, help conduct heat outwardly to the furnace shell, and enhance refractory life by minimizing alkali attack.

Noteworthy appraisal of two BF blow downs in Japan follows:[131]

1. If the design of the cooling plate is proper, even with fireclay bricks, a life of seven to ten years can be attained.
2. Alumina bricks have greater durability than fireclay bricks.
3. Large-furnace alkali absorption is small.

Smith et al.[132] provide a recent review of the performance of ultrahigh alumina products based on high-purity synthetic alumina or silicon carbide brick that are being used in the critical areas of BF linings. The relative advantages of each refractory based on both product R&D and experience worldwide in BF linings are presented. A mullite-bonded 90% Al_2O_3 brick lining in the bosh, belly, and lower stack of Nippon Steel Corporation's Kimitsu BF3 produced in excess of 30 million metric tons iron from November 1971 to May 1982, when using high-intensity internal copper cooling plates.[133] Kimitsu BF4, which uses a closer cooler spacing, achieved its metastable equilibrium thickness some two to three years later than BF3, indicating a potential 13 to 14 year campaign life.

The preceding verifies the traditional use of tabular alumina refractories in blast furnaces, which include the use of 90% Al_2O_3 refractory brick in the bosh and lower stack areas because of its good thermal conductivity, abrasion and chemical resistance, and hot-load strength. Dense, abrasion-resistant brickwork is also needed to withstand the abrasion in the raw material feeding section of the BF throat. Tabular alumina refractories also provide outstanding service as tuyere blocks, sinter notches, hearth bottom cooling wafers, and as stock line armor in the upper stack throat, bends, and nozzle tips of air blast systems.

Numerous investigators[132,134–136] have utilized the improved performance of ultrahigh Al_2O_3 refractories, particularly the 8 to 12% Cr_2O_3/Al_2O_3 brick made with high-purity corundum. This solid solution refractory has excellent hot strength with only slightly lower thermal shock resistance. The excess Cr_2O_3 concen-

Table XXV. A. Japanese Consumption (1000 Metric Tons) of Raw Materials for Refractories*

Year	Chrome Ore		Magnesia Clinker		Synthetic Mag-dolo Clinker	Dolomite Clinker	Spinel Clinker	Bauxite	Sillimanite, Kyanite, Andalusite
	Domestic	Imported	Domestic	Imported					
1973	26.0	68.5	357.6	10.2	89.9	49.3		101.5	15.2
1974	24.8	65.1	351.9	23.6	79.5	39.9		96.7	15.5
1975	19.2	40.5	285.5	29.6	59.0	28.6		75.1	15.5
1976	23.6	41.3	314.6	38.9	59.4	30.1		80.3	19.4
1977	15.2	41.8	301.2	14.3	53.8	23.8		78.6	15.8
1978	8.5	48.2	306.1	24.5	60.6	19.5		78.7	16.9
1979	15.0	36.4	329.3	46.4	56.3	17.7	3.4	78.6	17.1
1980	11.0	39.2	305.6	78.0	43.9	13.2	3.8	81.4	15.3
1981	9.4	39.5	276.7	98.8	32.4	12.2	4.1	80.7	16.6
1982	5.6	32.3	244.0	110.9	22.8	13.9	3.5	72.6	15.8
1983	8.1	28.3	243.0	122.3	16.5	16.3	3.6	72.9	14.2

B.

Year	Synthetic Mullite	Fused Alumina	Tabular Alumina	Chinese Bauxite	Fukushu Clay	Silica	Pyrophyllite		Shamotto	Pottery Rock
							Domestic	Imported		
1973	45.4	59.6		29.1	9.4	250.2	615.6	84.6	164.8	32.9
1974	46.7	76.3		41.4	17.1	251.7	537.8	98.6	135.1	18.5
1975	51.5	45.3	28.9	43.1	9.4	211.7	422.5	83.1	73.6	14.7
1976	43.2	45.7	40.3	46.3	14.0	148.2	471.1	91.1	62.5	12.7
1977	35.8	39.9	43.9	41.1	14.8	115.1	405.6	76.6	50.4	8.9
1978	32.8	37.1	48.7	46.8	15.6	109.2	415.8	89.2	48.0	6.9
1979	34.2	40.3	59.0	61.5	26.6	96.8	422.1	95.9	45.6	5.5
1980	35.5	42.7	57.7	75.8	33.2	116.4	396.9	110.6	48.7	5.2
1981	32.6	40.2	59.4	91.9	34.1	102.2	336.0	87.7	36.7	5.7
1982	23.6	42.5	55.8	82.2	26.8	83.8	303.9	54.4	30.7	3.6
1983	19.9	46.0	61.3	87.6	25.6	61.7	286.9	40.5	27.0	3.4

C. Shipments of Refractories to the Iron and Steel Industry in Japan*

Year	Output of Crude Steel (1000 metric tons) (A)	Quantity (1000 metric tons) and % of Refractories Shipments to the Iron and Steel Industry			B/A (kg/metric ton)	C/A (kg/metric ton)	D/A (kg/metric ton)
		Shaped (B)	Unshaped (C)	Total (D)			
1973	120 017	1 939 (71.1)	650 (71.9)	2 589 (71.7)	16.2	5.4	21.6
1974	114 036	1 755 (72.4)	706 (75.3)	2 460 (73.2)	15.4	6.2	21.6
1975	101 613	1 411 (74.8)	676 (76.9)	2 087 (75.4)	13.9	6.7	20.5
1976	108 325	1 344 (73.2)	723 (79.4)	2 067 (75.3)	12.4	6.7	19.1
1977	100 646	1 095 (68.1)	631 (74.4)	1 725 (70.3)	10.9	6.3	17.1
1978	105 059	1 098 (67.7)	610 (72.9)	1 707 (69.5)	10.4	5.8	16.3
1979	113 010	1 069 (64.5)	616 (70.8)	1 685 (66.7)	9.5	5.4	14.9
1980	107 386	1 023 (61.6)	620 (68.8)	1 543 (64.2)	9.5	5.8	15.3
1981	103 029	938 (60.3)	626 (70.1)	1 563 (63.9)	9.1	6.1	15.2
1982	96 299	869 (66.5)	626 (72.8)	1 491 (69.0)	9.0	6.5	15.5
1983	100 195	816 (67.1)	654 (73.8)	1 470 (69.9)	8.1	6.5	14.7

*Source: Japan Refractories Assn.

trates in the matrix as a result of the slower diffusion rate into the coarser corundum grains. These Cr_2O_3/Al_2O_3 refractories give improved resistance to slag attack and fluxing, because of their low solubility in most silicate and aluminosilicate melts.

Greater use of interim restoration of BF lining by pneumatic placement (gunning) of castables is practiced to obtain maximum furnace availability during periods of high demand to avoid substantial loss of iron production by a total reline.[137] This is particularly true now that fewer large blast furnaces are being used to achieve higher throughputs. Restoration by gunning relines requires 45 to 60 days, including taking the furnace down, scaling down, inspecting, gunning, and returning to service, compared to 90 to 120 days for conventional brick relines. Large quantities of castable are required for BF gunning repairs. In one case where an entire lining was gunned, the stack areas were lined to a thickness 0.6 m (24 in.) with 927 metric tons (1022 tons) of a selected 1538°C (2800°F) castable, and the stockline area to a thickness up 0.9 m (36 in.) with 388 metric tons (428 tons) of a more abrasion-resistant

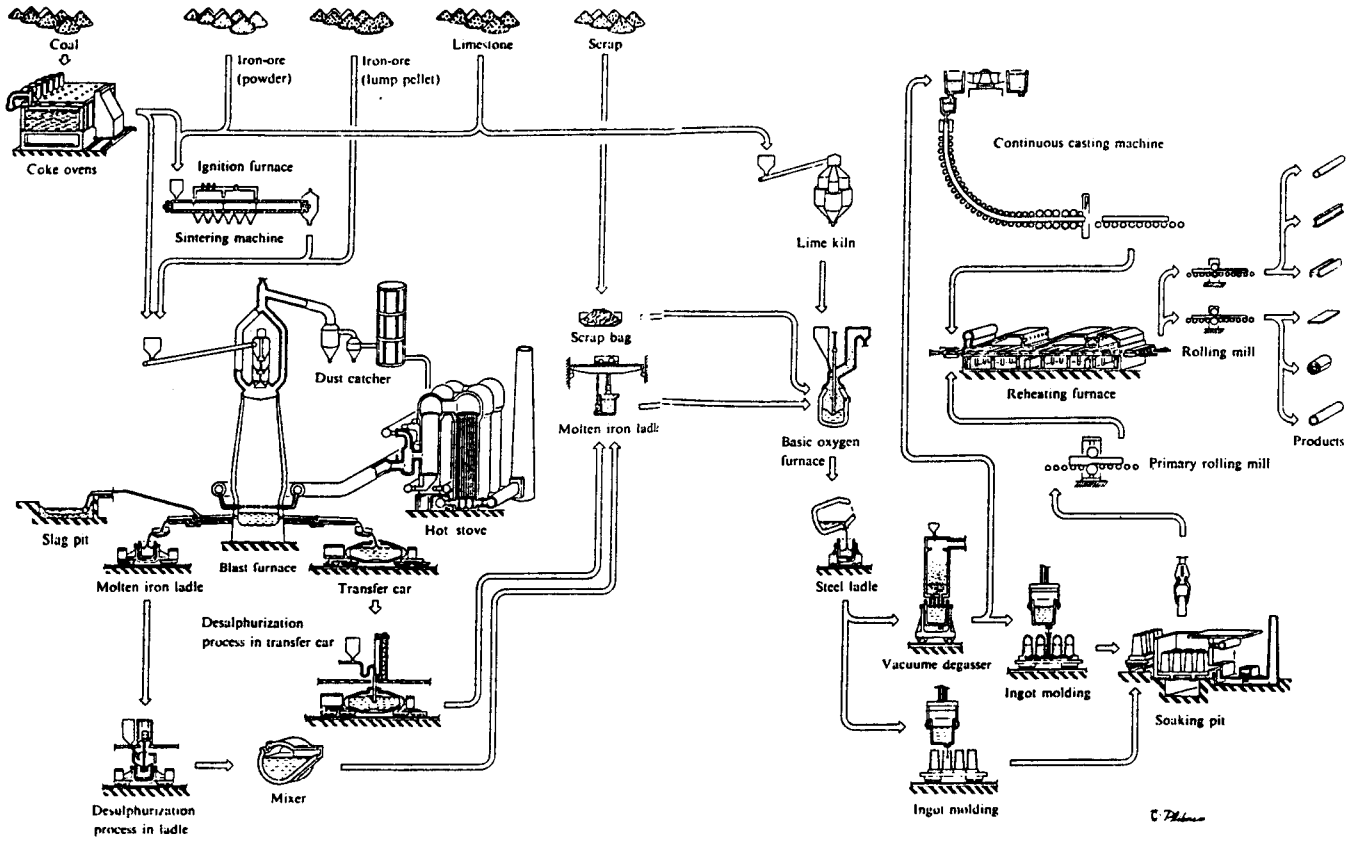

Fig. 35. Iron and steel flow diagram (Ref. 32, pp. 330–31. Used by permission.)

castable. Wessel notes that the furnace was gunned in 13 days, dried out in 5 days, and was out of service only 46 days for all repairs. This process may be repeated as much as three times until the hearth refractories are also spent. These high-purity CAC castables are formulated to average <25 wt% rebound on gunning, average 20-hour CO disintegration test ratings that shall not exceed surface popouts with no cracks, average <5.0% deformation after a 1350°C (2460°F) hot-load test and shall not exceed a ±1.5% average linear change after reheating at 1540°C (2800°F) to meet U.S. Steel refractory specification for BF castables.

Another technique being used to extend the operational life of the BF between major relines involves injection of refractory grouts into the hot BF lining from the outside during blowoff to remedy damage to belly or shaft section linings, as described by Egami.[138] The injection material, designed for a maximum service temperature of 1700°C (3090°F), is reported to contain 78% Al_2O_3, 15% SiO_2, and 7% other and requires 16 to 20 wt% H_2O for pressure injection into the hot BF through holes in the steel shell to fill the void in the lining or between the lining and the steel shell. Detail techniques are described by Egami for mixing and pumping the wet refractory mix to avoid segregation of the aggregate. He further described hot gunning repair of the BF upper shaft using a long gunning nozzle to make repairs of deteriorated lining exposed above the level of charge materials. These techniques are further described by Kreitz et al.[139]

Watanabe et al.[140] report successful use of a resol-type phenolic resin as a low-temperature binder for material injected during operation between stave coolers in the range from the lower part of the BF shaft to the bosh. A reliable premolded and dried panel repairing method is noted by Naruse.[141] The refractory panel is suspended from the BF top, over the lowered and banked burden, and positioned on the wall with the aid of supporting pipes projecting through the wall, after which castable is injected between the panel and BF steel shell.

BF Associated Equipment: Coke Ovens and Hot Blast Stoves

Reference 118 gives a thorough description of the design, operation, and typical refractory linings of coke ovens and hot stoves used in conjunction with BF operations (Fig. 35). Coke, made by carbonization of certain types of coals in enclosed chambers (coke ovens), is one of the primary carbon sources consumed in the BF when generating the CO atmosphere

Table XXVI. Current and Projected Use of Refractories in The Steel Industry

Item	Coke and Ironmaking				Steelmaking				Secondary Steelmaking			Casting, Shaping and Finishing		
	Coke Oven	Blast Furnace	Stoves	Iron-Handling	BOP	Electric	AOD	Open Hearth	Ladles	Degassers	Steel Handling	Continuous Casting	Ingot Casting	Shaping and Finishing
Conventional refractory	Silica, fireclay	Fireclay, high-alumina, alumina-carbon	Fireclay, high-alumina, silica	Fireclay, high-alumina, carbons	Periclase-carbon	Periclase-chrome, periclase,	Periclase-chrome dolomite high-alumina	Periclase-chrome, dolomite	Fireclay, high-alumina	Periclase-chrome, alumina	Fireclay, clay-graphite alumina, fused silica	High-alumina, fire-clay silica periclase-chrome	Fireclay, silica	Fireclay, high-alumina silica, periclase
Future refractory	Same	High-alumina SiC, carbon, fireclay	High-alumina silica, fireclay	High-alumina, SiC, graphite	Periclase-carbon periclase-graphite	Periclase-graphite, periclase chrome	Dolomite, periclase-chrome	Strong downward, most shops replaced by BOP	High-alumina dolomite, periclase-graphite	Periclase-chrome, alumina	Alumina, periclase alumina graphite, fused-silica	Periclase in monolithic form, high-alumina, alumina-graphite, zirconia	Fireclay silica	Same
Consumption trend, general	Constant	Constant, but material requirement more critical with fewer furnaces	Constant	Upward with more metal treatments and environmental requirements	Downward because of better life	Downward with use of water-cooled panels and better refractories	Lower with longer life	None	Upward with more ladle processing	Upward with more degasser use	Upward with more productive systems	Strong upward with more continuous casting	Downward with less ingot casting	Downward with less soaking pits
Consumption trend, overall	About the same with less in furnaces/stoves and more in iron handling				Strong downward with BOP replacing open hearth, use of water-cooled panels				Upward with more ladle-degasser processing			Upward with more complex materials required for casting		
Increased raw matererial usages	None, but possible shortage production capacity	SiC, alumina	High-alumina	High-alumina, alumina, SiC, graphite	Graphite	Graphite			High-alumina	Chrome ore alumina	Alumina, graphite	Alumina, graphite zirconia		
Possible substitute materials		Extended use of stove or dense plate coolers	Periclase,** silica alternate high-alumina sources	Periclase,** dolomite**	Periclase-carbon dolomite	Periclase or periclase-carbon, more water-cooled panels	Dolomite		Periclase or dolomite	Dolomite, periclase	Periclase-graphite**	Periclase-graphite**		

*Refractory Type	Raw Material Source
Silica	Domestic quartzites
Fireclay	Domestic clays, raw or calcined
High-alumina	Imported or domestic-fired bauxites, andalusite
Alumina	Synthetic tabular, fused, or calcined alumina from imported bauxite
SiC	Synthetic from silica and coke, domestic
Carbon	Domestic petroleum or metallurgical cokes, calcined anthracite, amorphous carbons
Graphite	Imported natural graphite
Periclase	Largely synthetic from domestic brine or seawater and domestic dolomite
Chrome ore	Imported natural chrome ores
Dolomite	Fired domestic raw dolomite
Fused silica	Synthetic from domestic sands or quartzite
Zircon	Domestic or imported sands
Zirconia	Synthetic from zircon sands — domestic or imported

**Relatively new application for materials.

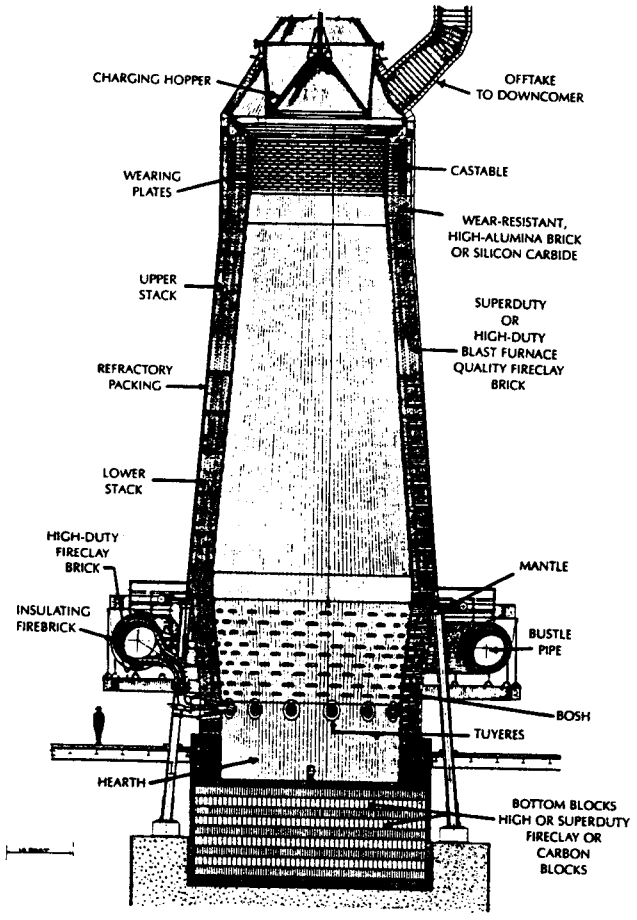

Fig. 36. Typical modern blast furnace for reducing iron ore to iron metal (Ref. 130, Fig. 1. Used by permission.)

necessary for chemical reduction of the iron ore. The primary coke-oven application for tabular Al_2O_3 is as an aggregate and/or for Al_2O_3 enrichment in high-purity CAC castables used to line coke-oven doors and standpipes.[137,142] Castable refractories and prefired shapes have been broadly accepted in replacing fireclay brick because of ease of fabrication with lower cost labor and proven performance. The best castable for coke-oven doors has high hot strength and the ability to retain this strength when exposed to cyclic conditions and to carbon monoxide, as specified by U.S. Steel.[137] These large coke-oven door plugs use either V-type anchors or other embedded steel hangers, along with metallic fiber reinforcement, ranging from carbon steel to AISI 400-grade stainless. Wessel[137] reported that field tests demonstrated a 10 to 400% improvement in plug life when metal fibers were added to the castables.

A typical BF stove having an internal combustion chamber is shown in Fig. 37 with the classic refractory brick and checker linings.[130] The scrub gases from the top of the BF enter the bottom of the BF stove combustion chamber, impinge on the dome, and then

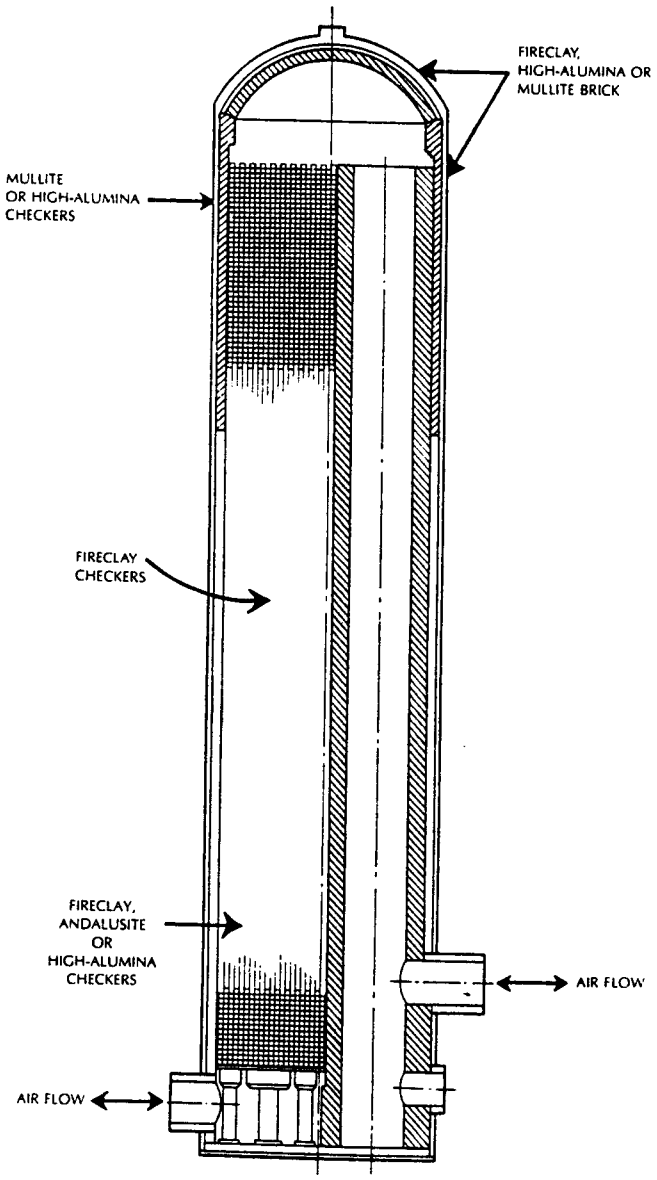

Fig. 37. Two-pass blast-furnace stove (Ref. 13. Used by permission.)

pass down through the checker work. Most integrated plants have three stoves for each BF. They alternately preheat the air going into the BF to a temperature of 815° to 1090°C (1500° to 1994°F) or more.

Nishina et al.[143] give an excellent review on a desirable direction of refractories for hot-blast stoves after following the progress of high-temperature blast stoves and surveying the results of dismantled furnaces. They note that the internal combustion hot stoves reached their high-temperature, high-pressure blasting capacity as blast furnaces became larger and were replaced by the external combustion-type hot-blast stoves with 3 to 4 kg/cm^2 normal blasting pressure and 1200° to 1300°C (2190° to 2370°F) blast temperatures. The dome and upper checker work must

run several hundred Celsius degrees hotter to provide these higher blast temperatures. To obtain 10 years of service, 80 to 90% Al_2O_3 brick with exceptionally high spalling resistance have been used at the upper ceramic burners in newly constructed and repaired stoves. Also, some bricks in the lower sidewalls in the combustion chamber suffered severe spalling due to temperature variations caused by alternate firing and blasting and thus were rebuilt using 90% Al_2O_3 brick with high creep and spalling resistance.

Cast House Refractories: Tap Hole Mixes and Trough/Runner Materials

With the increase of size, top pressure, and productivity of blast furnaces, inexpensive low-grade materials once used as cast house refractories have been replaced by high-performance materials which have an important bearing on ironmaking operations. The relative consumption of these refractories in an integrated steel works is relatively high, making cast house refractories an important factor in total refractory costs (Table XXVII).[144]

Costly thermosetting phenolic resins began to be used by the mid-1970s to eliminate the drawbacks (insufficient quick setting and black smoke emission) of coal tar as a binder for tap-hole (TH) mixes.[144–146] Also, extension of tapping duration required improved TH mix performance as BF increased in size and output. Depending on BF conditions, high-performance anhydrous, tar-bonded, and resin-bonded TH mixes are being used with high-grade refractory aggregates, such as tabular/fused Al_2O_3, SiC, SiO_2, and so on. High-SiO_2 and high-Al_2O_3 raw materials are used because of their outstanding corrosion resistance and high expansion properties. Table XXVIII lists properties of recent compositions used in Japan, with the SiO_2 mud being more popular because of workability and cost.[109]

The TH mix not only functions satisfactorily as a TH filling material, but also protects the BF bottom carbon lining. The TH mix must sinter and harden or carburize to form a carbon-bonded structure to plug the TH in a matter of minutes after placement. When the BF is tapped, the TH mix forms a passage through which hot metal and slag flow under high pressure and temperatures. Thus, TH mixes must be designed to withstand severe mechanical erosion, as well as chemical attack and wear by the hot metal and slag.

Table XXVII. Refractories Consumption at Integrated Steel Works (Typical)*

		kg/ton steel	%
Ironmaking	Taphole mix	0.62	6.3
	Trough	0.80	8.2
	Others	0.22	2.2
Steelmaking and casting	Basic oxygen furnace	1.99	20.3
	Ladle	2.98	30.4
	Continuous casting	0.89	9.1
	Others	2.24	22.8
	Others	0.07	0.7
	Total	9.81	100

*Ref. 144.

Iron troughs include the main trough, iron runner, slag runner, tilting trough, and others of which the main trough has seen especially marked changes in refractory materials during the past two decades.[144] Manual ramming was the predominant method of installation in lining fixed-type troughs with low-grade and -cost materials bonded with tar binders until the 1950s. Exchangeable trough systems evolved in the 1960s, in which the relining was done outside the cast house floor with high-grade refractory materials, such as SiC, Al_2O_3, and so on, being included in the trough ramming mixes tempered with water. During the 1970s, mechanization of relining exchangeable troughs began with automatic ramming machines and gunning was first tested as a method of lining repair.

The latter half of the 1970s proved to be a period in which development in trough material technology advanced most rapidly with technology offering an installation process that allows interim repairs to be carried out effectively and economically. The vibration forming (VF) method was the initial process of this new type to be developed which used the lowest possible water content to obtain high-density uniform linings by casting. This led to the development of various other new processes, including the dry-type vibration forming process, as well as a series of casting processes.[58,60–63,78–84,144,147–151]

Table XXIX[63] gives some of the installation characteristics and advantages of the various new casting methods developed in Japan, while Table XXX lists refractory properties of typical casting mixes in comparison to ramming mixes used in the main trough, iron runner, and tilting trough.

The corundum-based 57 to 71% Al_2O_3, 10 to 35% SiC, 3% C, and 2 to 18% SiO_2 casting mixes with lower apparent porosity and higher strength exhibit about three times longer life and ≈30% lower unit refractory consumption than the ramming mixes in Fukuyama No. 3 BF comparative trough tests. Additional advantages cited were an improved working environment, drastically reduced high-temperature hard labor because of the extended trough life and reduced local wear, and accordingly, less frequent relining and intermediate hot repair. The drawback for casting is that drying time after hot repairs is longer, but not prohibitively long for tapping.

Aluminum metal powder additions have been used to increase the permeability of the cast Al_2O_3-SiC-C refractories to ease and accelerate drying and firing.[63,77,81,151] The Al metal powder reacts with the placement H_2O to generate H_2 which forms in small pipes or passageways to the casting surface, thus providing passages for water vapor during dry-out. The metal powder addition also helps delay oxidation of the SiC and C in the mix by reacting with the

Table XXVIII. Properties of Taphole Mud

Material	A	B	C	D
Quality	High silica-silicon carbide-carbon			High alumina-silicon carbide-carbon
Chemical composition (%)				
SiO_2	37–41	29–33	28–31	19–23
Al_2O_3	6– 9	8–11	29–20	29–33
SiC	10–13	17–20	8–32	8–11
C	19–23	13–16	17– 8	17–20
Modulus of rupture (kgf/cm^2)				
After heating at 1400°C for 2 hours	20–40	30–60	80–110	35–65
Bulk density				
After heating at 1400°C for 2 hours	1.70–1.80	1.80–1.90	2.05–2.15	1.95–2.05
Remarks	Tar bond	Tar bond	Resin bond	Tar bond

Table XXIX. Summary of New Installation Methods for BF Troughs*

Method	Casting	VFP	SVP	Ramming
Characteristic of refractories	Water addition 5 ≈ 6% at mixing Deflocculation and flocculation by means of cation exchange of clay	Water content 4 ≈ 8% Thixotropic softening and hardening properties	Water content < 0.5% Nearly dry aggregate and dry body as installed	
Installation apparatus (for installation of 2 m length)	Mixer 1 (capacity 2 tons) Form Vibrator freq. 8 000 ≈ 10 000 vpm $n = 2 \approx 3$	VFP machine Weight 6 ≈ 7 tons Vibrator freq. 3 600 ≈ 12 000 vpm amplitude 0.2 ≈ 2.5 mm power 1.2 kW $n = 10$	SVP machine Weight 1.5 ≈ 2 tons Vibrator freq. 3 600 vpm amplitude 0.3 ≈ 0.8 mm power 1.2 kW $n = 8$	Air rammer freq. 600 vpm $n = 2 \approx 3$
Advantages	Very uniform lining Easy partial repair Easy to attain very long through life	Very dense and uniform lining Short installation time Easy hot partial repair	Simple process without skill No drying process and rapid preheating Easy hot partial repair	
Disadvantages	Drying time longer	Noisy Long drying time	Less dense upper side wall	

*Ref. 63. Used by permission.

available O_2 first, thus extending the advantages of having C in the lining during use. This is particularly true for pressed Al_2O_3-SiC-C brick made with Al metal powder additions.[152] These techniques have been extensively used in the broad-based ultralow- and low-cement castable applications, including the use of organic fibers.[153]

Table XXXI[109] gives a more recent listing of the Al_2O_3-SiC-C casting compositions used with proper trough design and installation to obtain longer service life and reduced specific consumption in Japan. However, specific consumption of trough materials is expected to increase as molten iron pretreatment and desiliconization is advanced upstream in the process to the trough. Specific consumption of a Kawasaki Steel BF trough increased about 19% from 1984 to 1987 after introducing desiliconization in the trough.

Table XXXII[150] lists the characteristics of the new BF trough lining and repair techniques developed in Europe using the Al_2O_3-SiC-C trough mixes. Suckow et al.[150] show a unique composite trough system which takes advantage of prefabricated inserts in the trough walls in combination with 80% Al_2O_3 refractory concrete, earth-dry ramming mixes, and dry-vibration mixes.

Similar trough casting and dry-vibrating mixes have been extensively used in the United States as well. Extensive efforts continue on characterizing and optimizing these Al_2O_3-SiC-C compositions by using better characterization techniques in an attempt to understand the wear mechanisms involved during metal/slag contact.[63,144,147–150,154–158]

The low-moisture castables used in BF trough systems were discussed earlier as ULC and LC castables. The term *no-cement* castables has also been described for mixes that set by flocculation and/or

Table XXX. Properties of Typical Casting Refractories for Troughs*

Properties	Materials		Main Trough			Iron Runner		Tilting Trough	
			Casting A	Casting B	Ramming	Casting	Ramming	Casting	Ramming
Chemical composition (%)	SiO_2		3	2	4	18	44	15	44
	Al_2O_3		71	57	62	68	11	70	11
	SiC		17	35	22	10	29	10	29
	C		3	3		3		3	
Water Content (%)			6.0 ≈ 6.3	5.5 ≈ 6.0	4.0	8.5 ≈ 9.0	4.6 ≈ 4.8	6.0 ≈ 6.5	4.6 ≈ 4.8
Bulk density		110°C × 24 h	2.58	2.70	2.65	2.50	2.15	2.70	2.15
		1100°C × 3 h	2.58	2.74	2.64				
		1500°C × 3 h	2.55	2.72	2.66	2.42	1.80	2.62	1.80
Apparent porosity (%)		110°C × 24 h	20.6	13.0	22.0	18.0	18.0	14.0	18.0
		1100°C × 3 h	23.8	19.0	23.0				
		1500°C × 3 h	24.3	20.0	21.5	24.0	27.0	19.0	27.0
Cold modulus of rupture (kg/cm^2)		110°C × 24 h	40	75				25	
		1100°C × 3 h	50	65					
		1500°C × 3 h	50	60				70	
Cold crushing strength (kg/cm^2)		110°C × 24 h	145	380	150	50	150	200	150
		1100°C × 3 h	200	400	130				
		1500°C × 3 h	260	380	110	180	100	450	100
Permanent linear change (%)		110°C × 24 h	0.06	−0.12	±0.0	±0.0		±0.0	
		1100°C × 3 h	+0.06	−0.15					
		1500°C × 3 h	+0.13	+0.08	+0.30	−0.30	+4.0	+0.10	+4.0
Hot modulus of rupture at 1400°C (kg/cm^2)			11	18			at 1300°C 6	at 1450°C 21	at 1300°C 6

* Ref. 63. Used by permission

Table XXXI. Blast-Furnace Trough Lining Techniques

Lining Method	Condition As-Delivered	Water Content On Installation (%)	Mode of Installation	Advantage	Disadvantage
Relining sand lining	Pit moist	4–6	Knocking	Cheap	Labor-intensive Time Consuming
Ramming	Earth-dry	approx. 6	Ramming	Increased life	Difficult handling
Wet vibrating	Dry	6–10	Vibrating	Easier to install, homogeneous texture-free compaction	Time-consuming preparation of mix, setting and drying
Dry vibrating	Dry	0	Vibrating	Compaction without lamination, simple lining method, no susceptibility to cracking, no drying, short heat-up time	Low initial strength
Prefabricated part	Dry	0	Hoisting gear	Rapid installation, possibility of prefabricating complex geometrics	Must be heated
Repair gunning, wet	Dry	approx. 10	Gunning	Long shelf life	Dusting possible, higher porosity, susceptibility to cracking
Gunning, earth dry	Earth-dry	approx. 6	Gunning	No re-wetting, higher compaction	Rebound loss, separation
Vibrating, wet	Dry	6–10	Vibrating	Easier to install	Peeling on hot repairs
Vibrating, dry	Dry	0	Vibrating	Short repair time, no drying time	Low intitial strength
Prefabricated part	Dry	0	Hoisting gear	Ease of replacement	Must be heated

Table XXXII. Properties of Casting Trough Material

Material	A	B	C	D	E	F	G
Application	Main trough Impact zone and skimmer zone	Main trough Impact zone and skimmer zone Slag line	Main trough Impact zone Metal line	Main trough Metal line	Tilting runner	Iron runner	Slag runner
Chemical composition (%)							
SiO_2	1–3	1–4	1–4	6–9	6–9	48–52	6–9
Al_2O_3	78–82	70–74	68–72	62–68	64–68	30–33	55–59
SiC	11–14	14–17	14–17	16–19	14–17	7–10	18–21
C	1–3	1–3	3–5	2–4	2–4	2–4	4–6
Modulus of rupture (kgf/cm^2)							
After drying at 110°C for 24 h	25–45	10–30	15–35	15–35	10–30	10–30	10–30
After drying at 1400°C for 2 h	90–130	90–120	70–100	60–90	30–60	30–60	70–100
Bulk Density							
After drying at 110°C for 24 h	2.97	2.76	2.71	2.39	2.48	2.15	2.36
After drying at 1400°C for 2 h	2.92	2.72	2.63	2.34	2.42	1.93	2.32

when using other binder systems. The complexity of these various casting systems can be better appreciated by reviewing the many materials and variables that can interact to affect the service performance of these new low-moisture vibrating mixes, as shown in Fig. 38.[63]

Hot-Iron Pretreatment and Transport

Pretreatment of molten iron in hot metal or torpedo rail cars as an unconventional refining system began in the early 1970s when it began to be used as a reaction vessel for desulfurization in addition to being used to transport and store molten pig iron. Normally, refractory wear is correlated with and increases linearly with desulfurization treatment.[131] Hot-metal pretreatment refers to hot-metal desiliconization (De-Si), dephosphorization (De-P), and desulfurization (De-S) and can be performed in several ways (Fig. 39).[159]

Service temperatures in refractory-lined 50 to 250 ton capacity hot-metal cars range from 1540° to 1600°C (2800° to 2900°F).[130] The temperature of the molten pig iron at the time of treatment is 1400° to 1500°C (2550° to 2732°F) when injecting the usual fluxing reagents for De-S : CaC_2, CaO, and Na_2CO_3; for De-Si : Fe_2O_3; for De-P : CaF_2 and CaO and injecting gas-N_2, air, or O_2 over 10 to 60 minutes.[131] Specific examples of flux composition are cited to gain an appreciation of the corrosive environment to which tabular Al_2O_3 refrac-

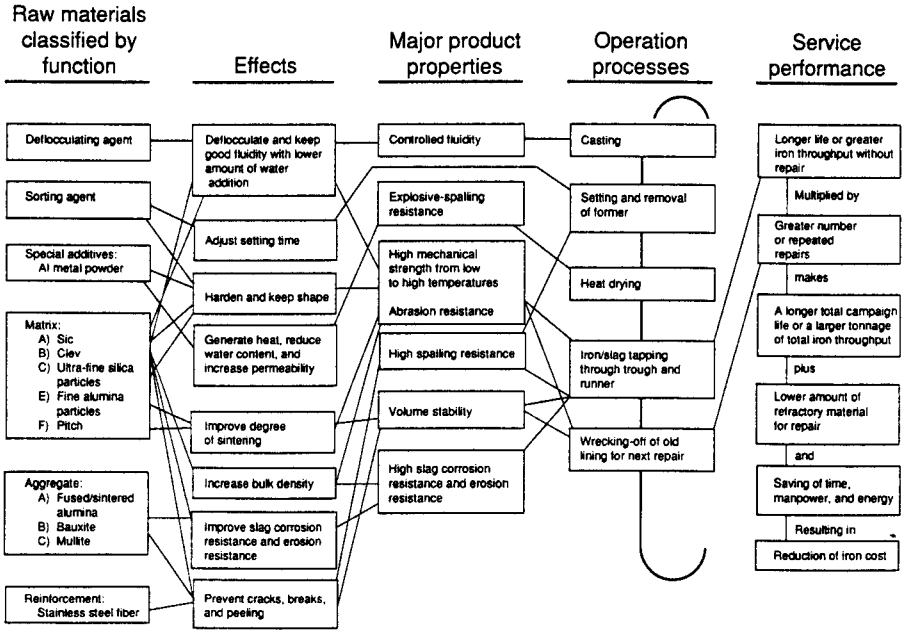

Fig. 38. Interrelations between raw materials, effects, major properties, operation processes, and service performance of blast-furnace trough linings (Ref. 63, Fig. 40. Used by permission.)

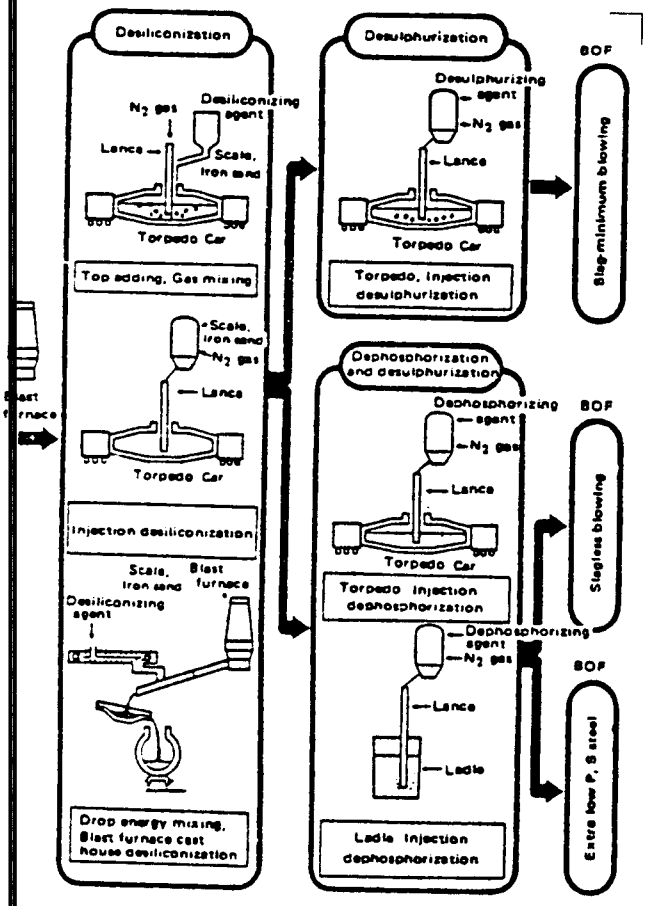

Fig. 39. Hot-metal pretreatment (Ref. 159, Fig. 9. Used by permission.)

tories are exposed during hot-metal treatment as noted by Hiragushi[131]:

	Flux Composition (wt%)				
Type	Fe-Oxide*	CaO	CaF_2	$CaCl_2$	Na_2CO_3
De-Si	55	35	5	2–5	
De-P	39	39	11		11

*Millscale

Al_2O_3-SiC-C bricks are the main refractories used for hot-iron pretreatment, including troughs, torpedo cars, iron ladles, and special furnaces in Japan.[141] These bricks have excellent resistance against wear by structural spalling caused by FeO-CaO-Na_2O-SiO_2-type slag and temperature fluctuations. The SiC protects the carbon from being oxidized by CO. In practice, the MgO-C bricks, which naturally have good corrosion resistance against >2C/S ratio slags, do not perform as well as the Al_2O_3-SiC-C bricks in practice.[141] Naruse[141] relates the inferior performance of the MgO-C bricks to their much larger thermal expansion and permanently linear change with the metal powder reinforcement used to obtain oxidation resistance and hot strength. The changes in torpedo-car refractory linings since about 1970 in Japan are

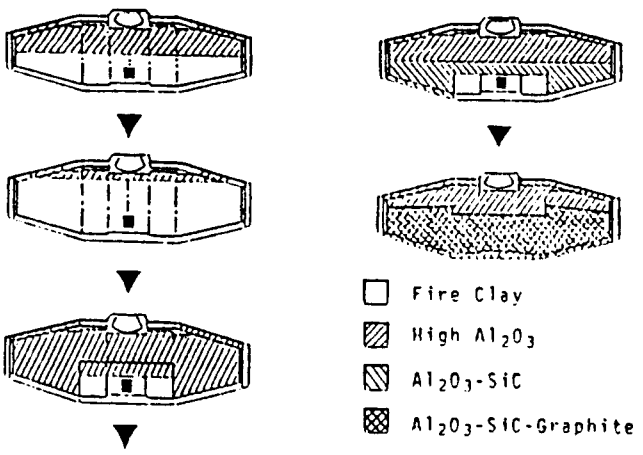

Fig. 40. Change in the lining profile of torpedo car (Ref. 148, Fig. 9. Used by permission.)

shown in Fig. 40.[160] The big, complex, special-shape mouth bricks, which are difficult to make and place, are being replaced by high-strength cementless castables reinforced with steel fibers to increase strength and toughness while improving spall resistance.

Koltermann[161] shows the torpedo-car refractories developments in West Germany, which track a pattern similar to the Japanese usage as molten iron temperatures increased and various metallurgical treatments began to take place in the torpedo car (Fig. 41). Resin-bonded corundum-SiC-C brick, as in Japan, is receiving increased usage in Europe. Table XXXIII lists its properties compared to new andalusite brick with various binders that are also receiving increased attention in comparison with standard brick and safety lining brick properties.

The U.S. ironmaking practice for hot-metal De-S by CaC_2 or CaO injection has also moved upstream to the torpedo ladle. Hubble shows the alternate paths available for demineralization of hot metal from the

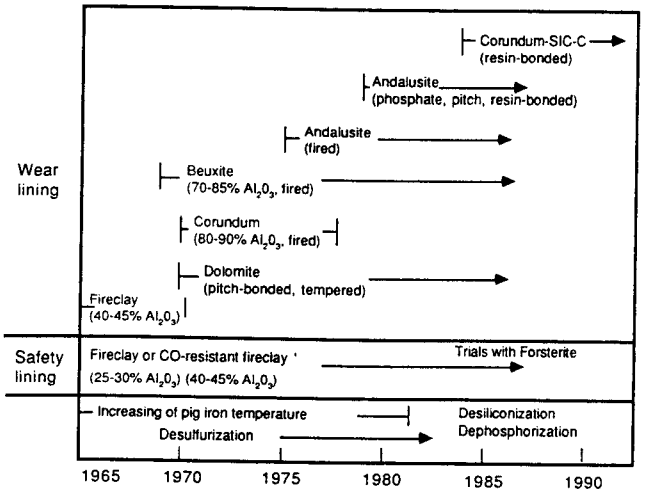

Fig. 41. Development of torpedo car refractories in West Germany (Ref. 161, Fig. 1. Used by permission.)

Table XXXIII. Values of Torpedo Car Bricks

	Standard bricks				Safety Lining			New Bricks			
	Andalusite	Bauxite	Corundum	Dolomite	Fireclay	Fireclay	Forsterite (Olivine)	Andalusite	Andalusite	Andalusite	Al_2O_3-SiC-C
Bonding	Fired	Fired	Fired	Pitch*	Fired	Fired	Fired	Pitch*	Phosphate*	Resin*	Resin*
Chemical analysis (%)											
SiO_2	37–38	7.7	13.0	<1.5	73.0	48.0	31.8	39	37.6	37–39	
Al_2O_3	60–61	86.5	81.7	<1.0	21.8	45.8	2.6	59	57.3	57–59	55–65
TiO_2	<0.5	3.1	0.9	<0.3	1.2	1.8	<0.1	<0.3	<0.3	<0.3	
Fe_2O_3	<1.0	1.7	1.4	<1.0	1.3	0.8	6.1	1.0	1.0	1.0	
CaO	<0.3	<0.2	0.2	<61.0	<0.2	<0.2	0.6	<0.2	<0.2	<0.2	
MgO	<0.5	<0.2	0.1	>36.0	0.3	0.9	55.6	<0.4	<0.4	<0.4	
Na_2O	<0.3	<0.2	0.3	<0.3	0.4	<0.2	<0.1	<0.2	<0.2	<0.2	
K_2O	<0.4	<0.2	0.3	<0.3	1.8	0.4	<0.1	<0.3	<0.3	<0.3	
Cr_2O_3	<0.1	<0.2					3.70				
P_2O_5	<0.1	<0.2	1.9				<0.1		1.9		
C				1.3–1.8				3–5	7–10		5–10
SiC											20–25
Bulk Density (g/cm^3)	2.5–2.6	2.96	2.80	2.85–3.0	2.3–2.4	2.1–2.2	2.7–2.8	2.7	2.4–2.5	2.5	2.8
Apparent porosity (%)	10–15	18–19	16–19	6–10	12–16	14–18	17–19	5–7	14–18	12–14	10–12
Cold crushing strength (N/mm^2)	60–100	80–110	90–160	>30	40–80	40–60	25–40	30–40	20–40	25–35	40–60
Hot crushing strength† (N/mm^2) at 1500°C	5–12	5–12	6–8		0	0	12–16	2–4	2–4	4–6	3–5
Length change after heating (%) 1500°C/12 hrs.	0.1	−0.2	1.3–1.5				0.5	1.3–1.6	1.6–1.8	1.5	1.2

*Tempered in the range 150°–400°C.
†Oxidizing atmosphere.
Ref. 161. Used by permission

BF to the steelmaking furnace in Fig. 42.[162] Kappmeyer and Hubble[163] note that hot metal is currently desulfurized externally in transfer ladles to optimize BF operation and steel quality. Because of the large availability of scrap in the United States, alternate pretreatment steps in torpedo cars will not be required until the price of scrap changes or lower levels of phosphorus are required.

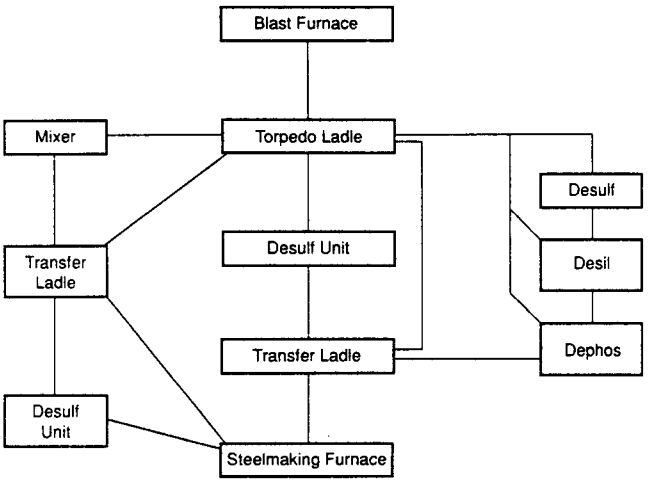

Fig. 42. Various routes for hot-metal handling and treatment between the blast furnace and steelmaking unit.

High-duty, superduty, high-Al_2O_3 or mullite bricks are the usual metal contact refractory, backed with insulating brick on top of a refractory packing next to the torpedo ladle steel shell.[130] Tabular Al_2O_3 bricks have traditionally been used in the bottom impact area and in the belly-band sidewalls, with plastic monoliths being used in the charging/pouring opening and for repair, along with gunning. Al_2O_3-SiC-C plastics or ram mixes have been used in the lance impact areas of torpedo ladles, because they have good thermal cycle resistance and resistance to metal and slag erosion/corrosion.[162] The Al_2O_3-SiC-C low-moisture castables have also been used in metal mixers because of their resistance to metal and slag erosion/corrosion.

Tabular Al_2O_3 has traditionally been used for monolithic construction of metal mixer pouring spouts, brick or monolithic lining of the total bath area, and plastic or gunned repair and maintenance of hard-wear zones. The IISI Committee on Technology projects gradual replacement of mixers by torpedo ladles because of the introduction of De-S and possible introduction of induction heating based on their 1980–82 refractories survey reported in 1985.[164]

Torpedo-car refractory linings in the United States can be expected to follow a path similar to that experienced in Japan as hot-metal pretreatment shifts to include De-Si and De-P in addition to De-S (Fig. 43).[152]

Miyagawa et al.[164] give specifics on improved Al_2O_3-SiC-C unburned brick that sufficiently withstands the combined flux injection during hot-metal

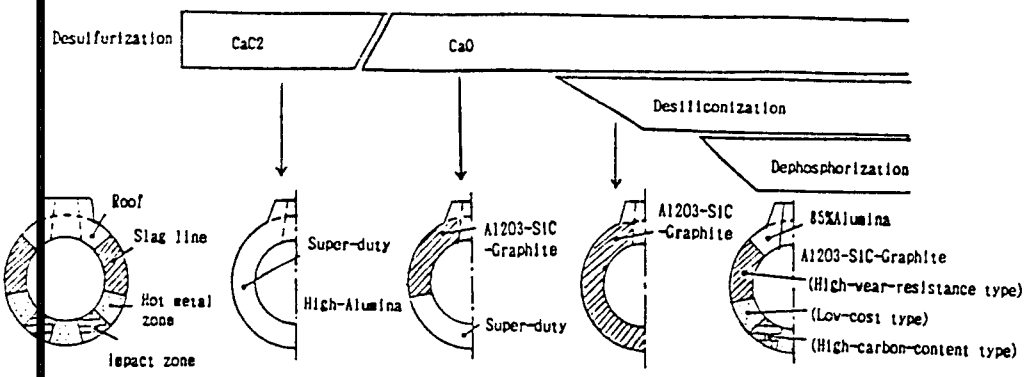

Fig. 43. Changes in process of hot-metal pretreatment and applied materials (Ref. 152, Fig. 1. Used by permission.)

pretreatment and stirring in torpedo cars. Brick shapes are molded using phenol resin as a binder for 3 mm or smaller Al_2O_3 grains, 1 mm or smaller SiC grains, and flake graphite. The technical optimal composition is ≥7[illegible]% Al_2O_3, 15% C, 5% SiC maximum, and 3% SiO_2 maximum. Since SiO_2 content does not contribute proportionately to refractory life, some cost benefits can be realized by appropriate use (zoning) of bricks containing 7 to 10% SiO_2, if attention is given to the mineral composition of the SiO_2 addition. Elemental X-ray images of the microstructure suggest the use of $Al_2O_3 \cdot SiO_2$ minerals to increase the SiO_2 content.

Shimada et al.[165] conducted studies that established the wear mechanism of ordinary Al_2O_3-SiC-C brick at the slag line in torpedo ladles subjected to hot-metal pretreatment to be:

1. Oxidation of C and SiC by the atmosphere in the ladle.
2. Slagging reaction by De-[Si], -[P], and -[S] slag.
3. Spalling from cracks due to repeated charging and tapping of hot metal.

With increased use, joint wear, and spalling, a decarbonized layer developed on the cold face which makes the lining reliability questionable. Lining life in a 350 ton torpedo ladle was doubled by small additions of borosilicate glass (2.0 wt%) and metallic powders (2.5 wt% Al, 1.0 wt% Si) to the Al_2O_3-SiC-C brick composition bonded with phenol resin. The borosilicate glass and metallic Al produce an oxidation-protective glassy film around the C and SiC grains on melting. Toughness increases and, consequently, spalling resistance improves. Borosilicate glass and metallic Al also cause a substitution reaction during use, making aluminosilicate glass and Si, which further reacts with carbon gas to form β-SiC whiskers in situ.

Chien et al.[166] reported 3 to 5 wt% Cr_2O_3 to be optimum in high Al_2O_3-Cr_2O_3 brick if Cr_2O_3 is added in the form of oxide and about 9 wt% Cr_2O_3 if in the form of chromite for torpedo ladle desiliconization refractories based on simulated service tests. Higher Cr_2O_3 additions in tabular Al_2O_3 brick improved corrosion resistance but reduced thermal shock resistance when tested in a gas-fired rotary slag test under the combined action of thermal shock and slag attack. Although the Al_2O_3-SiC-C brick tested best for desiliconization, the high Al_2O_3/Cr_2O_3 bricks are proposed for the charging pad, slag line, and above in the torpedo ladle because of lower thermal conductivity, good slag-attack resistance, and possible lower costs.

Steelmaking

As noted by Hubble in Table XXVI, basic refractories are used to line the primary steelmaking furnaces. These include the basic oxygen furnace (BOF) which rapidly burns carbon out of molten iron by blowing oxygen through a lance inserted from the top of the converter, the Q-BOP that blows oxygen through tuyeres located in the converter bottom, the combined blowing process which has a variety of lettered designations for the different types of processes using both top and bottom blowing of gases (Ar, N_2, CO_2, and O_2), the electric arc furnace (EAF) which can be constructed for acid or basic steelmaking processes, the argon-oxygen decarburizing (AOD) furnace, and the open hearth (OH).

The BOF has essentially replaced the OH furnace as the primary steelmaking furnace in most western countries with <1% crude steel production in 1987 being made by OH and about 68% by the BOF, according to the 1988 IISI statistics.[110] The BOF is largely used for decarburization in the combined blowing process with final refining being performed by secondary refining in the ladle when De-[Si], -[P], and -[S] are first performed by hot-metal treatment (Fig. 39). Naruse[141] shows the carbon content dropping about 1% during pretreatment of the hot iron and about 3% during BOF refining from about 3.5 to 0.15% C with further reduction of about 0.2% C during secondary refining. Tabular Al_2O_3 is used in the functional refractories required in the operation of the BOF. These include injection lances, porous plugs, and bottom blowing nozzles which will be described in a later section.

Although the OH furnace is no longer a significant factor in steel production, there are a number of large,

relatively modern OH shops still operating in the United States, with justification for operations being dependent on local situations, that is, high scrap availability at low costs or to supplement capacity during periods of high demand.[167] Traditional uses of tabular Al_2O_3 refractories in the OH using large amounts of oxygen and higher operating temperatures include critical wear areas using the zoned lining concept for special refractories. Plastic monoliths have been widely used in OH chill walls, in nosings, fantail roofs, and inwalls. Tabular Al_2O_3 mixes have performed especially well in slag pockets, uptakes, iron charging areas, and scrap charging doors, as well as the steel tapping spouts.

Tabular alumina refractories have traditionally been used in the delta section of the EAF roof as brick, preformed shapes, and monolithics in the form of castables, plastics, or ramming mixes.[103–106,112,118,119,130,167,158] Metal dam and tap-hole blocks of fired tabular Al_2O_3 shapes provide good wear resistance along with the monolithically lined pouring spout, charging and slagging doors, besides the monolithic shapes around the dust collector port and other areas of severe abrasion. Large preformed refractory delta sections are being fabricated from 80 to 97% Al_2O_3 castables for water-cooled panel roofs. Table XXXIV[168] lists high-alumina refractories used in EAF roofs in Europe and the United States, while Table XXXV[167] also identifies the raw material base used in United States refractories for EAF roofs.

Secondary Refining in Ladles and Continuous Casting

Proper mix design and compounding of tabular alumina refractories provides an opportunity for a significant reduction in the 3.60 kg/metric ton (7.9 lbs/ton) projected 1990 U.S. refractory usage in integrated steel plant ladles using ladle metallurgy and 4.05 kg/metric ton (8.9 lbs/ton) for EAF plants (Table XXXVI).[163] With ladle metallurgy, the partly refined heat of steel is tapped from the steelmaking furnace into a ladle and refined by one or a combination of ladle refining processes that may include argon steering, induction steering, lance injection, wire feeding, alloy trimming additions, synthetic slags, ladle arc reheating, chemical reheating, vacuum casting, vacuum degassing, and vacuum oxygen decarburization, as noted by Orehoski and Gray.[169] They detail and illustrate the many ladle refining processes being used by the steel industry to produce the highest quality steel grades being specified by the end-user. Figure 44[159] summarizes the special processing used by one steel works to meet the rigid requirements for high-grade steel specified for various applications.

The secondary refining processes extend hot-steel contact time with the ladle refractories to several hours. The protective slag layer becomes extremely corrosive when superheated to temperatures of 1760° to 1850°C (3200° to 3300°F) while being stirred during electric arc heating.[163] Although basic refractories with improved slag resistance resist the highly damag-

Table XXXIV. High-Alumina Refractories for Electric Arc Furnace Roofs

	Europe				U.S.			
	1	2	3	4	5	6	7	8
Chemical Composition								
Al_2O_3	77.20	86.30	92.00	96.60	71.80	70.00	72.00	86.00
SiO_2	16.70	7.60	6.50	2.70	22.90	25.40	24.00	9.60
TiO_2	2.50	3.00	0.30	0.04	2.90	2.90	2.60	2.80
Fe_2O_3	1.80	1.80	0.70	0.10	1.50	1.00	1.00	1.20
CaO				0.20	0.20	0.10	0.10	0.10
MgO				0.02	0.20	0.10	0.10	0.10
Alkali				0.30	0.50	0.10	0.20	0.20
Total (%) aux. oxides	6.10	6.10	1.50	0.70	6.00	4.40	4.00	4.40
Bulk density (g/cm^3 or t/m^3)	2.75	2.96	3.00		2.57	2.57	2.63	2.99
Apparent density (%)	20.00	18.00	15.00	13–17.00	20.00	17.00	13.60	17.80
Cold crushing strength (kg/cm^2)	700	900	950					
Differential subsidence (0.5%)	1,460	1,550	1,650					
Hot strength (%) (*)								
1,450°C					1.50	−0.20	−0.20	−0.40
1,650°C					−11.00	−7.00	−1.80	−8.50
Modulus of rupture (kg/cm^2)								
1,260°C				70	71	153	229	197
1,480°C	1,500 8	1,500 43	1,500 80	42	21	50	75	89

(*) ASTM C 16
Ref. 168. Used by permission.

Table XXXV. Properties of EAF Roof Brick

Type	Burned High Alumina			Burned Super Alumina	
Usual application	Main roof			High-wear areas; electrode rings	
Raw material base	Bauxite	Bauxite & bauxitic kaolin*	Bauxitic kaolin*	Bauxite	Tabular alumina
Chemical analysis (%)					
Al_2O_3	72.0	70.5	69.2	82.9†	91.6
SiO_2	23.2	24.2	26.2	12.6	8.0
Fe_2O_3	1.3	1.6	1.3	1.4	0.2
TiO_2	2.0	2.9	2.9	3.0	trace
Alkalies	1.0	0.4	0.2	0.1	0.2
Bulk density (g/cm^3)	2.61	2.56	2.55	2.81	2.99
Apparent porosity (%)	19.0	19.0	17.0	15.0	15.0
Modulus of rupture (kg/cm^2)	91	95	144	190	211
1500°C linear reheat change (%)	+4.0 to +4.5	+3.5 to +6.0	−0.2 to +1.0	+2.7 to +6.5	+1.0 to +2.5 (at 18.15°C)

*Bauxitic kaolin produced in southeastern U.S.
†Includes AIPO. Ref. 167. Used by permission.

Table XXXVI. Projected U.S.A. Refractory Usage — 1990

Area	Consumption			
	Integrated Plant		Nonintegrated Plant	
	kg/ton	lb/ton	kg/ton	lb/ton
Coke oven	0.40	0.9		
Blast furnace	0.45	1.0		
Casthouse	2.55	5.6		
Hot-metal transfer and treatment	2.25	5.0		
Steelmaking	3.05	6.7	5–10*	16.5
Steel ladles & ladle metallurgy	3.60	7.9	4.05	8.9
Gates or rods/tubes	0.65	1.5	1.05	2.3
Tundish	1.25	2.8	1.65	3.6
Finishing	1.25	2.8	1.25	2.8
Total	15.45	34.2	13–18.00	34.1

*Depends on production rate and usage of water-cooled panels and roof.

ing effects of CaO-Al_2O_3 slags superheated 280° to 550°C (500° to 1000°F) above their melting point at the ladle slag line, in most cases a variety of higher-quality high-Al_2O_3 ladle refractories with minimal free SiO_2 are adequate for lining the balance of the modern ladles used for secondary refining. Low-Al_2O_3 and/or high-SiO_2 refractory can interfere with the desirable metallurgical reactions in the production of high-quality steels by releasing oxygen to the steel at the wrong time, resulting in silicon pickup and aluminum loss.

Yoshino[62] cites the transition of ladle brick materials from the high siliceous to zircon, semizircon, 75 to 85% Al_2O_3, Al_2O_3/Cr_2O_3, and basic refractory material sources. Monolithic ladle linings evolved in attempts to overcome joint problems, increase lining performance, and decrease costs. The success of the automatic ramming machine, "sand slinger" concept for installing low-moisture siliceous mixes in ladle sidewalls in Japan and Europe justified low- and ultralow-cement monolithic ladle lining performance evaluations because of the ease of installation compared to the ramming mixes.[170] Japan continues using Roseki and zircon as a material base, Europe concentrates on the higher Al_2O_3 materials, principally andalusite, whereas the United States pursues other readily available Al_2O_3 materials.

Prendergast[170] lists the raw material used in various ladle castable products in Table XXXVII. He notes that almost all alumina materials are based on calcium aluminate bonding, although clay and phosphate bonds have been tried, whereas the basic products require different bonds, ranging from organic to phosphate. Although all these castables are installed using similar techniques (Fig. 45),[170] only the alumina monolithic linings appear to be amenable to repair in North America.

Yoshino[62] details the installation methods used in Japan for installing ladle casting refractories. The placement techniques are quite similar to those described previously for trough casting refractories and require experienced personnel, specifically designed placement equipment, and proper curing and heating schedules to obtain optimum performance. To obtain adequate service life with the low-cement/no-cement monolithics, the primary raw materials are limited by their physical properties, particularly particle sizing and porosity, besides refractoriness. These are very important with regard to water control in obtaining the correct ratio for proper placement and optimum performance. Any factor which affects the critically low water requirement (5% or less H_2O is common) will certainly decrease the optimization of their performance.[170] Figure 46[62] outlines the hardening mecha-

Equipment		Molten metal pretreatment		BOF	Secondary refining					Casting	
		ORP	SIDP	LD-OB	DH	PIM	LF	VOD	CAS/CAB	Vertical-type CC	Bending-type CC
Sketch											
Function		Molten metal de-Si, Mn; Molten metal de-P,S		De-C De-P	De-C De-H	De-S Inclusion control	De-S Raising temperature	De-C,S,H Raising temperature	Inclusion float CAS raising temperature	Molten steel temperature control	
High-purity steel	Good formable cold rolling mill			○	○					○	○
	Electrical sheet	○		○	○					○	○
	Heavy plate, SML	○		○	○	○				○	○
High-clean steel	DI tin plate			○					○(CAS)	○	○
	Valve spring steel			○					○(CAB)	—	○
High alloy steel	High alloy steel		○	○			○			○	○
	High-Mn steel		○	○				○		○	○

Fig. 44. Processes for high-grade steel (Nippon Steel's Yawata Works) (Ref. 159, Table 7. Used by permission.)

Table XXXVII. Ladle Castable Products and Their Raw Materials*

	High Alumina		Low Alumina		
	60 + Al_2O_3	80 + Al_2O_3	<40%	Al_2O_3	Basic
Zircon			X		
Roseki			X	X	
Andalusite	X				
Mulcoa	X		X		
Bauxite	X	X			
Tabular		X			
Chrome ore					X
Magnesia					X
Mag-chrome					X
Spinel					X
North American	X	X	X		X
Japan	X	X	X	X	X
Europe	X	(X)	X		X

*Ref. 170. Used by permission.

nism of the various low-/no-cement ladle casting refractories.

Nosbisch et al.[171] presented the development of castable-lined ladles from castable bottom trials to a totally cast steel ladle and compared the advantages and disadvantages to the previous practice of brick ladles. The ultralow-cement, low-moisture castables (clay-bonded, 85% Al_2O_3, 95% Al_2O_3, and $Al_2O_3 \cdot Cr_2O_3$) were evaluated in the ladles using the 95% Al_2O_3 castable in the bottom and the 85% Al_2O_3 castable in the barrel with mag-chrome brick at the slag line. This nets a 20% material savings compared to a total brick lining because the castable can be scaled down and repaired by patching.

Initial trials with a clay-bonded trough castable containing SiC caused excessive deskulling losses although the castable had successfully withstood the eroding action of the steel in the high-wear impact area. Examination showed that the SiC in the castable had dissolved in the steel and promoted the sticking of the castable to the steel skull. It was concluded that a stronger, lower thermal conductivity mix without SiC

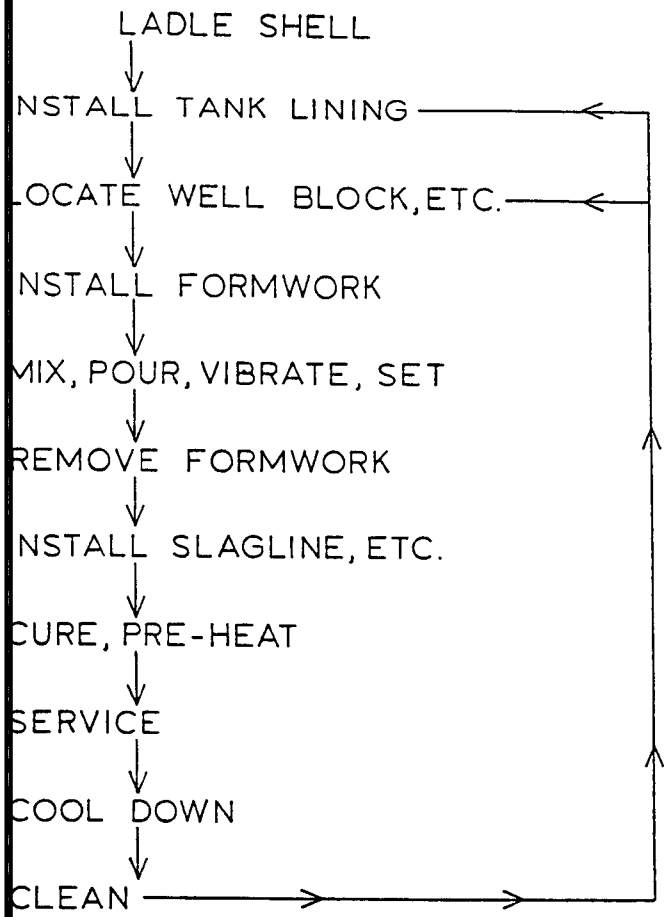

Fig. 45. Process flow (Ref. 170, Fig. 4. Used by permission.)

was required and led to the successful use of the other compositions listed. Tabular Al_2O_3 base castables are being used in the most severe wear applications, including ladle bottoms and precast shapes, including impact pads, well blocks, seating blocks, and so on.

Prendergast[172] notes the improved refractory performance provided by a 95% Al_2O_3 castable pad compared to various Al_2O_3 brick in a variety of steel ladle bottom shell designs, as shown in Table XXXVIII. Lalancette and Rigaud[173] present the trends in steelmaking ladle refractories in Canada based upon results of a survey covering 15 steelmaking plants during 1986. Ladle refractory consumption is averaging 2.8 kg/ton of steel produced with >70% Al_2O_3 brick being the most popular.

Continuous casting (CC) continues to be a strong growth area for tabular alumina refractories, because there is a large amount of conversion yet to take place. Although the U.S. 1987 crude steel production by CC was 47.2 million metric tons (about 59% CC), the remaining 33 million metric tons of steel production is potential for future conversion to CC. This is second only to the U.S.S.R. and China which have about 137 and 36 million metric tons raw steel, respectively, unconverted to CC, as seen in the following listing derived from the 1987 IISI Statistics.[110]

1987 Raw Steel by CC		1987 Raw Steel CC Conversion Potential	
Country	Million Tonnes	Country	Million Tonnes
Japan	91.9	U.S.S.R.*	137.4
U.S.	47.2	China*	46.0
F.R. Germany	33.5	U.S.	33.1
U.S.S.R.*	24.0	Poland*	15.3
Italy	20.5	India	13.1
France	16.5	Brazil	12.1
Republic of Korea	14.0	Romania*	10.0
United Kingdom	11.3	Canada	7.5
Brazil	10.1	Japan	6.6
China*	10.0	United Kingdom	6.1
Canada	7.2	Australia	3.3

*Estimated

In spite of Japan's high conversion (93.3%) to CC, it still ranks in the top ten countries having the most raw steel production potential yet to be converted to CC. Conversion of 100% to CC is unlikely in major steel-producing countries, because enameled steel has not yet been produced by the CC process as it requires a fair amount of oxygen which increases the refractory wear rate excessively (Fig. 47).[159] The refractory which can withstand such wear has not yet been developed. Every effort must be made to suppress air oxidation in removal of nonmetallic inclusions from the molten steel by floating separation in the tundish and mold of proper construction in the last stage of molten steel solidification during CC.

Tabular Alumina Functional Refractories

A variety of tabular Al_2O_3 special refractories have been developed for ladle impact pads, stirring and injection devices, seat blocks, nozzles and plates for casting ladle and tundish slide gate systems, ladle/tundish and tundish/mold shrouds to minimize steel oxidation and temperature loss, tundish dams, weirs, and impact pads as partially illustrated in Figs. 48–52.

The importance of the functional special refractories to the successful performance of CC in making the best steel quality is evident by the extensive literature reported on the subject.[116,118,119,123,126,127,129–131,141,160,162,163,169,174,176,179–182]

Slide Gate Valves (SV)

The various SV systems that have been developed to accurately control the flow of hot metal has been one of the technological breakthroughs that was necessary to enable the continuous casting concepts in aluminum to be more rapidly adapted by the steel manufacturers. Likewise, tabular alumina refractories played an important role in the successful development in the form of SV plates to control the flow of hot steel. Although the SV concept was first patented in

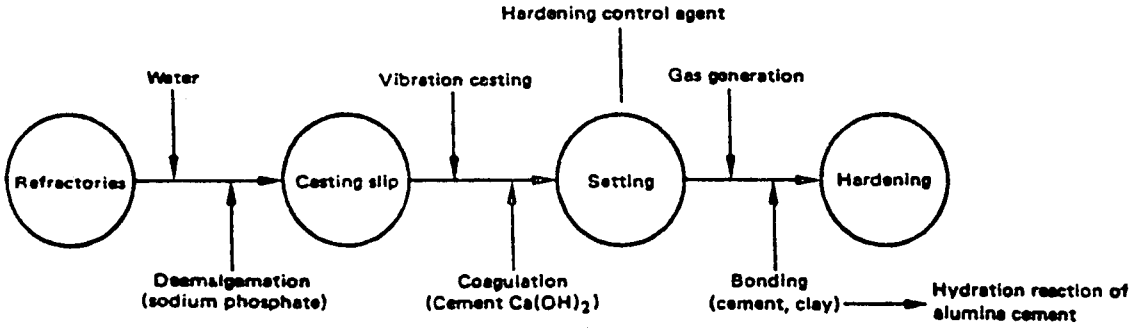

Fig. 46. Outline of hardening mechanism of ladle casting refractories (Ref. 62, Fig. 1. Used by permission.)

Table XXXVIII. Refractory Performance versus Ladle Bottom Shell Design*

Ladle Capacity (tons)	Integrated Steel Mills					
	210	250	220	290	280	250
Ladle shape	Round	Obround	Obround	Round	Round	Round
Ladle bottom		Dished			Flat	
Reinforcing (bottom)		None			Ribs	
Performance (9-in. wear lining) (No. of heats)						
Bloating fireclay		15–20	15–20			
70% alumina brick	15–20	15–20	15–20	35–40	50	40–45
80% alumina brick	15–20	15–20	15–20	70–75		
95% alumina						
Castable pad	20–30	20–30	20–25		>90	>100

*Ref. 172. Used by permission.

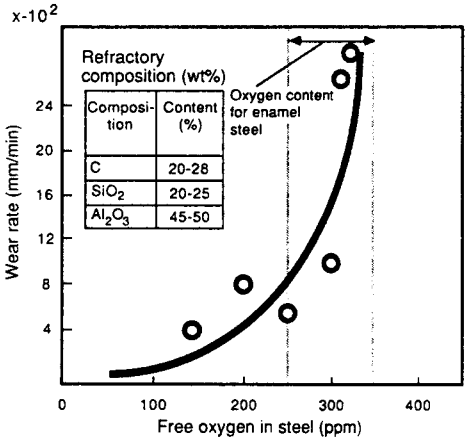

Fig. 47. Relation between free oxygen in steel and refractory wear rate (Ref. 159, Fig. 34. Used by permission.)

1884, it was not used until 1961 on an experimental basis by Benteler Steel Works, Paderborn, W. Germany, some 89 years later.[176] In 1958 there were only 17 continuous casting plants outside the U.S.S.R., but by 1965 their popularity began growing rapidly after the successful introduction of SV gates at Benteler Steel Works in 1964.[117,178]

In 1981, SV were normally manufactured from high-alumina refractories, usually tabular alumina (85 to 90% Al_2O_3) with possible additions of mullite and zirconia. A magnesite variety is being developed which has better corrosion resistance to steel processed with the more basic slags. Jeschke reported that SV plates in West Germany are mainly high alumina with the mullite-bonded, nominally 90% Al_2O_3 compositions being the standard. Nearly all alumina plates are pitch-impregnated and preferably tempered to partially convert the pitch into fixed carbon and eliminate odor. He notes that magnesia plates are used for CC low-carbon steels, where alumina is not good enough for severe chemical attack. Mutsaarts[179] lists the common European community Al_2O_3 plate compositions: 89 to 91% Al_2O_3/5.5 to 6.5% SiO_2/2.7 to 3% Cr_2O_3, 87% Al_2O_3/11% SiO_2, and 93 to 95% Al_2O_3/4.5 to 5.5% SiO_2.

New refractory material developments for SV systems are shown in Table XXXIX.

Yoshino[180] gives a current detailed discussion on the use of SV refractories in Japan since it was first introduced in 1967. The SV has experienced the most rapid progress as a flow control system for ladles and tundishes in Japan. It has been the impetus behind the development of the ladle refining processes and continuous casting technology because of its excellence in controlling flow, ease of being operated automatically, and its superiority to the nozzle stopper system with regard to effects of casting time, compositions of slags, and other operating conditions. In Japan the tundish SV (TD-SV) is being used in most slab and bloom

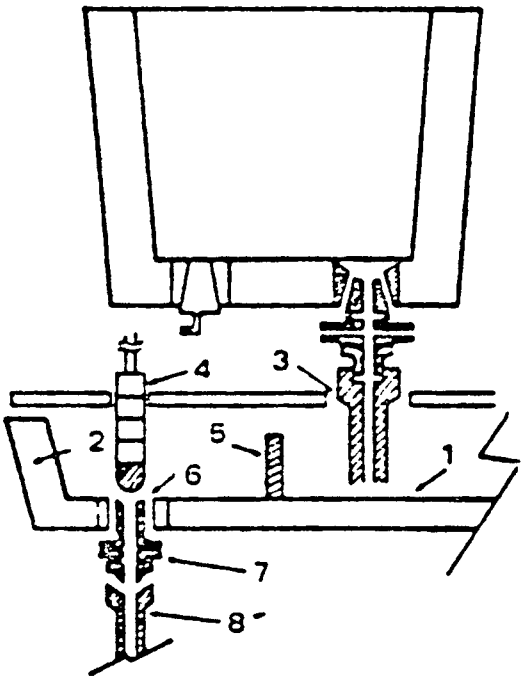

No.	Part name	Material
1	Inner cooting material(Board)	Magnesia
2	Tundish lining	Semi-zircon (monolithic)
3	Long nozzle	Alumina-graphite
4	Stopper	High alumina
5	Dam	High alumina
6	Upper nozzle	High alumina
7	Sliding nozzle	High alumina
8	Immersion nozzle	Alumina-graphite

Fig. 48. Construction of CC refractories (Ref. 159, Fig. 31. Used by permission.)

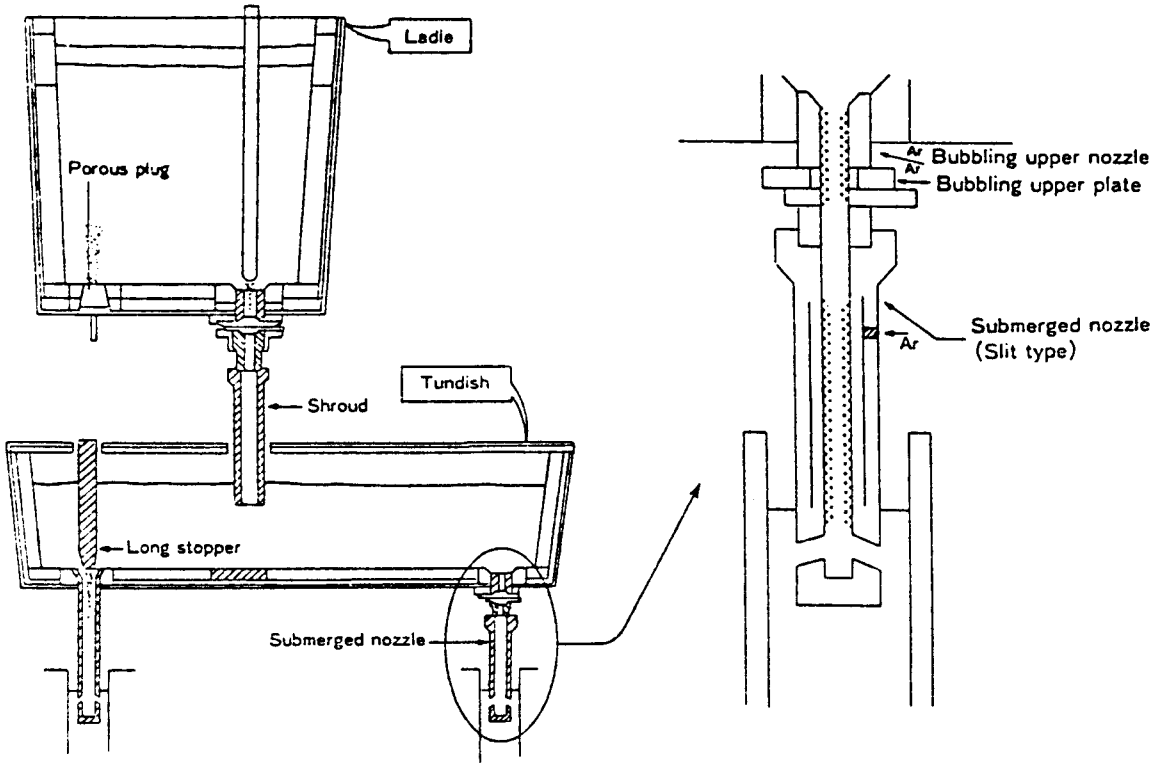

Fig. 49. Gas bubbling in continuous casting processes (Ref. 141, Fig. 15B. Used by permission.)

casting mills, but its use in billet casting is just beginning. Alumina-mullite was the first SV plate refractory used in Japan and is generally impregnated with tar before use. The refractory consists primarily of sintered Al_2O_3 with added portions of mullite, andalusite, sillimanite, or zirconia-mullite to improve spalling resistance and $Cr_2O_3$to improve slag corrosion resistance. Figure 53 confirms that the refractories

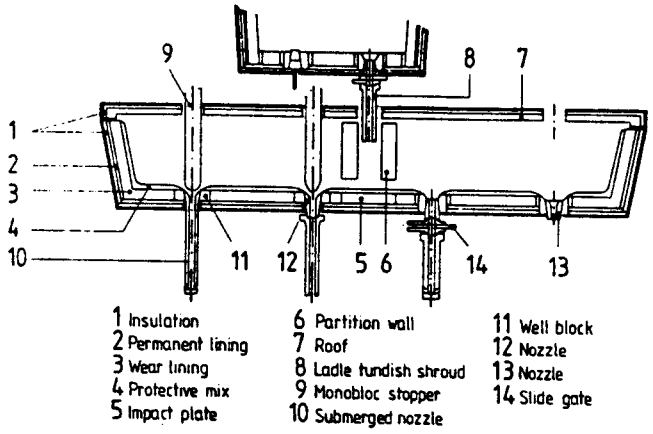

Fig. 50. Refractory parts in continuous casting system (Ref. 174, Fig. 27. Used by permission.)

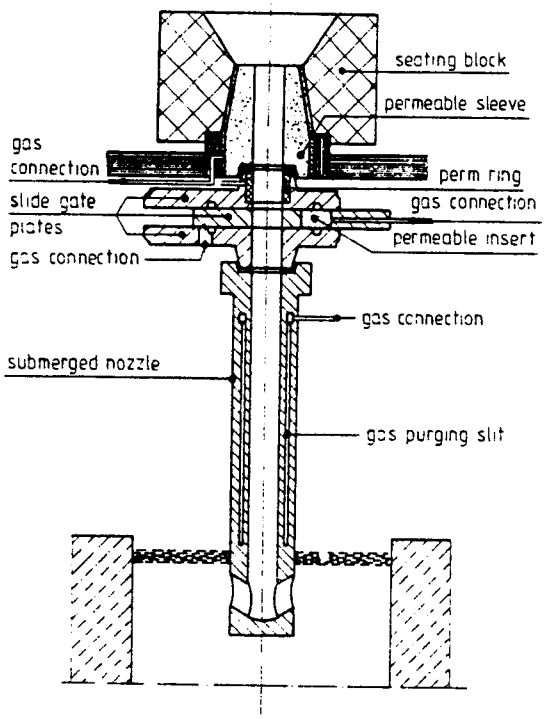

Fig. 51. Injection of purging gases in a tundish slide gate (Ref. 174, Fig. 29. Used by permission.)

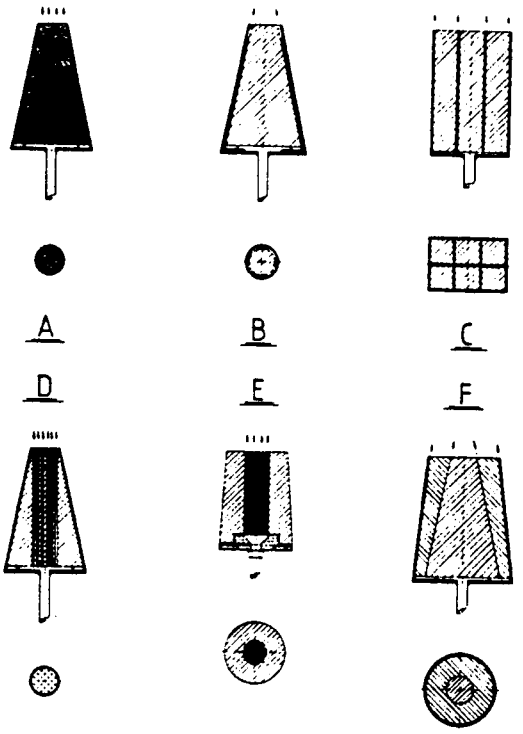

Fig. 52. Gas purging systems (Ref. 174, Fig. 14. Used by permission.)

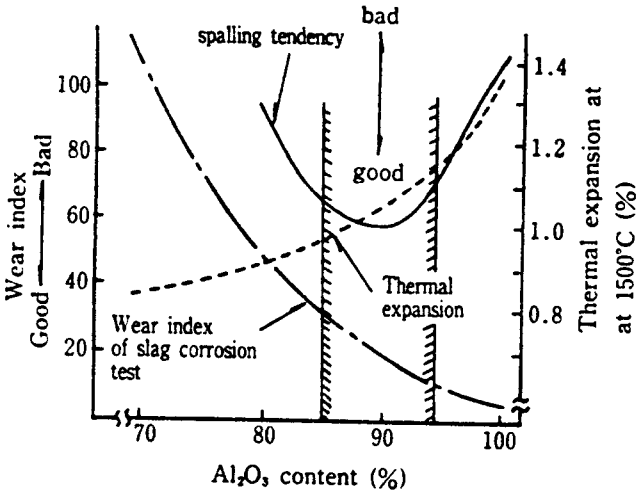

Fig. 53. Relationship between Al_2O_3 content and qualities of high-Al_2O_3 plates (Ref. 175, Fig. 11A, B and Table 3. Used by permission.)

should contain about 90% Al_2O_3 to equilibrate corrosion resistance with spalling resistance.

Non-tar, carbon-bonded Al_2O_3/C SV plates were developed and marketed in the late 1970s because of problems with smoking and embrittlement of the tar-impregnated Al_2O_3 and MgO plates. At present, Al_2O_3/C plates are predominately used for SV in Japan because of their excellent corrosion/spalling resistance and strength at high temperatures, as shown in Table XL.

Al_2O_3/C plate refractories are burned in a reducing atmosphere after pressing the mix of sintered Al_2O_3 and carbon with organic binders, such as phenol resin, after which the burned plates are tar-impregnated and tempered to densify and strengthen the texture, according to Yoshino.[180] Additions of mullite, andalusite, and other materials having a lower thermal expansion are effective in improving spalling resistance. He also references zirconia-mullite and zirconia-corundum as being more stable than mullite or andalusite additions to Al_2O_3/C plates to lengthen plate life.

Table XXXIX. Refractory Material for Slide Gates*

Part	Characteristic	Type of Bond	Chemical Analysis Al_2O_3 %	ZrO_2 %	Cr_2O_3 %	C %	Physical Values R g/cm³	KBF N/mm²	P· %
Well block	Chrome Corundum	Hydraulically	83		10		3.2		
Purging sleeve	Sintered corundum (permeable)	Ceramically	88		2		2.87		2:
Slide gate plates	High-alumina/ graphite	C bonding	80	7		+10	2.8	15	1(
	Zircon oxide	Ceramically		96			4.8	35	1{
LTS/SMN	High-alumina/ graphite	C bonding	74			+30	2.3	7	2:

LTS = ladle tundish shroud
SMN = submerged nozzle
R = bulk density
KBF = cold modulus of rupture
Po = open porosity
*Ref. 174. Used by permission.

Table XL. Properties of Plate Refractories

Quality	High Alumina SVR-90AC	SVR-85A	SVR-65A	Magnesia SVR-A4	Alumina-Carbon SVR-A85G	SVR-V1	SVR-A65GZ	SVR-S21
Chemical composition (%)								
Al_2O_3	87	86	69	5	85		64	87
SiO_2	7	12	27		4	4	14	
MgO	(Cr_2O_3) 3			94				
ZrO_2						6	9	3
C					8	9	10	4
Apparent porosity (%)	16.0	16.0	16.5	13.8	11.5	6.5	12.0	8.9
Bulk density	3.05		2.50	2.99	3.05	3.10	3.05	3.20
Crushing strength (kgf/cm²) {MPa}	1400{140}	1300{130}	1000{100}	1000{100}	1200{120}	1600{160}	1200{120}	1170{11.5}
Modulus of rupture at RT (kgf/cm²) {MPa}	210{21}	200{20}	200{20}	180{18}	250{25}	230{23}	200{20}	180{18}
at 1400°C	95{9.3}	80{8}	60{6}	130{13}	185{18}	170{17}	140{14}	230{23}
Thermal expansion at 1500°C	1.1	1.0	0.9	1.4	1.1	0.9	0.9	1.2
Character								
Wear resistance	○	Δ	×	□	□	○	○	□
Spalling resistance	○	○	Δ	×	Δ	□	○	Δ
Others		Tar impregnation				Nontar		Unburned nontar
Application	for all	TD-SV	TD-SV	EAF-SV	EAF-SV	for all	TD-SV	EAF-SV

□ Excellent ○ Good Δ Average × Inferior

Yoshino comments that various carbon or graphite materials, which differ in crystallization ratio and particle size, can be used, for instance, flake graphite, coke, carbon black, and so on, in Al_2O_3/C plates. Graphite is superior in corrosion resistance, and amorphous carbon is superior in bonding strength, erosion resistance, and tar permeability. About 5 to 12 wt% of these carbon-source raw materials are used in the production of Al_2O_3/C plates.

Although the Al_2O_3/C plate refractories have very low gas permeability because of their smaller pore diameters than those of high-Al_2O_3 plates (0.01 to 1.0 vs 1.0 to 10 μm pore diameters), they are easily oxidized and corroded with multiple uses or with high-[O] steel casting; SiC, B_4C, silicon, or aluminum are added to prevent oxidation. Aluminum powder additions to unburned Al_2O_3/C plates especially show excellent resistance to high-[O] steel and are being put into production, because of their high affinity for oxygen, as referenced by Yoshino.

In an effort to reduce refractory costs, some ladle SV plates are used after being repaired by inserting an Al_2O_3 or ZrO_2 ring to reshape the bore and reconditioning the plate surface with cement-bonded or phosphate-bonded high-Al_2O_3 mortar. In some cases recyclable used plates are selected and reused with no repair for the TD-SV, while others are selected for reuse after polishing the sliding surface and completely

equipping it with cushions, according to Yoshino,[180] who lists the production performance of ring-inserted plates in Table XLI.

SV Nozzles

Nonporous nozzle refractories for the ladle SV must have excellent wear resistance to withstand the attack by slags and lanced oxygen. The 85 to 95% Al_2O_3 plate refractory compositions are also used for high-Al_2O_3 upper and lower nozzles in Japan, with the lower nozzles requiring steel encasement or tar impregnation to improve spalling resistance. Al_2O_3/C upper and lower nozzle refractories are made with 3 to 7 wt% C, depending on the type of steel and thermal balance of the SV required. Use of Al_2O_3/C nonporous nozzles is expanding with the improvement of SV plate life and with the increase of corrosive steel manufacture, as can be seen by the increasing wear rate of high-alumina plates with increasing Mn or decreasing C steels (Fig. 54).[180]

Yoshino shows the improvement in production life (charges or heats) and wear resistance of Al_2O_3/C upper and lower SV nozzles for varying sized ladles in Table XLII.[180]

TD-SV Porous Nozzles, Nozzle Stopper, and TD Nozzle

Sequential castings, closed starts, and on-line successive casting of several types of steels have necessitated the technological development of using Ar gas injection in the TD-SV to prevent Al_2O_3 from adhering to the nozzle bore, to prevent molten steel solidification in the bore when the SV is shut, and to agitate the molten steel surface in the mold. Tabata et al.[181] give a more thorough in-depth discussion on the inert gas injection technology being developed for preventing nozzle clogging caused by Al_2O_3 adherence and molten steel solidification in the SV. Usually, high-Al_2O_3 porous refractories of about 90% Al_2O_3 are used for optimum wear and spalling resistance and exhibit properties, as shown in Table XLIII.

The complexity of engineering and operational design with extremely close tolerances to enable the use of good sealing methods and prevent gas leakage can be appreciated by reviewing the schematic of a TD-SV system shown in Fig. 51.

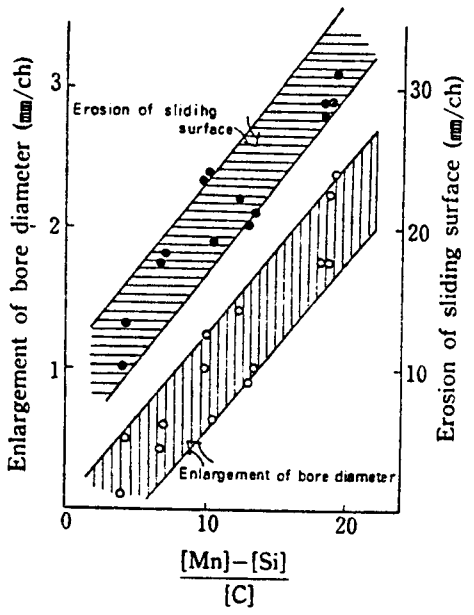

Fig. 54. Wear rate of high-alumina plate bricks in various steel casting (Ref. 180, Fig. 22. Used by permission.)

Isostatically pressed monoblock Al_2O_3/C refractory nozzle stoppers are commonly used in Japan to control the steel flow through a TD nozzle for billet casters because the nozzle bore diameter is too small for the SV system. Yoshino also notes that the nozzle stopper and the SV are sometimes used together in order to prevent molten steel from solidifying in the nozzle bore when casting starts or when different types of steel are successively cast. Monoblock stoppers are isostatically pressed corundum-graphite, which can be used several times after cleaning and regrinding of the stopper head.[178]

CC Long Nozzles (LN) (Shrouds)/ Submerged Nozzles

Figure 50 shows a ladle tundish shroud attached to a ladle SV for feeding steel into the center of a tundish between two alumina weir plates (partition walls). Three flow control systems from the tundish

Table XLI. Results of Practically Used Ring-Inserted Plate

User	A (250t, LD)	B (60t, EF)	C (70t EF)
Type	Ring exchange type	High-quality ring type	
Plate refractory	High-alumina	Alumina carbon	
Ring refractory	High-alumina	Zirconia	
Ring exchange times	2		
Life			
Ring type	10 ch	14 ≈ 15 ch	10 ≈ 12 ch
Ordinary type	6 ch (High-alumina)	10 ≈ 12 ch (Alumina-carbon)	8 ≈ 9 ch (Alumina-carbon)

*Ref. 180. Used by permission.

Table XLII. Comparison of the Practical Results of Alumina-Carbon and Ordinarily High Alumina Nozzles*

Usage	User	Life of High-Al_2O_3 (ch)	Life of Al_2O_3-C (ch)	Wear Rate Index (High Al_2O_3 = 100)
Upper nozzle	A (70t ladle)	11 ≈ 12	14 ≈ 15	55
	B (90t ladle)	9 ≈ 10	14 ≈ 15	65
	C (250t ladle)	4	6 ≈ 8	60
Lower nozzle	D (120t ladle)	2	3	60
	E (70t ladle)	4 ≈ 5	6<	70
	F (250t ladle)	1	2 ≈ 3	60

*Ref. 180. Used by permission.

Table XLIII. Properties of Porous Refractories*

Quality	ALP-A90M	ALP-A90CM	ALP-A75MA
Chemical composition (%)			
Al_2O_3	89	87	77
SiO_2	9	9	20
Cr_2O_3		2	1
Apparent porosity (%)	22.0	21.0	22.5
Bulk density	2.75	2.80	2.45
Crushing strength (kgf/cm^2) {MPa}	700{69}	700{69}	750{74}
Thermal expansion at 1000°C (%)	0.6	0.6	0.5
Gas permeability ($\times 10^{-2}$C.G.S.)	50	40	20
Average pore diameter (μm)	40	30	20

*Ref. 180. Used by permission.

are shown with submerged nozzles designed for each specific flow control device.

The most important role of the LN is to protect the stream of molten steel from reoxidation and nitrogen pickup by air contact while flowing into the tundish from the ladle. A submerged nozzle (submerged entry nozzle) is used for nonoxidation casting of steel from the tundish to the mold as illustrated in Fig. 51. It has two additional important functions besides that of the LN: enhancing the rise of nonmetallic inclusions and the prevention of mold powder entrapment in the steel by control of molten steel flow in the mold.[180] Yoshino lists the properties of continuous casting nozzles that are necessary to realize these functions:

1. High thermal spalling resistance.
2. High mechanical strength to withstand the molten stream and vibration.
3. Good sealing property on the contact surface with lower nozzle of the slide valve.
4. High resistance to corrosion and erosion from the molten steel flow.
5. High resistance to corrosion from the tundish and mold fluxes.

The CC nozzles have shifted from the highly thermal shock-resistant fused SiO_2 refractories to the Al_2O_3-graphite (AG) or ZrO_2-graphite compositions with excellent corrosion/erosion resistance. Isostatically pressed AG nozzles have excellent properties but tend to clog because of their high thermal conductivity, whereas high-fired vacuum-extruded AG nozzles have medium thermal conductivity because of the orientation of the graphite particles and thus have a lower tendency to clog.[178] The fused SiO_2 nozzles do not tend to clog by Al_2O_3 deposition because of their lower thermal conductivity, but their application is now being limited to the casting of ultralow-carbon grades of steel because of their consistently shorter service life.

Yoshino[180] notes that the main constituents for AG nozzles are Al_2O_3, fused SiO_2, and graphite. The compositions are designed to take advantage of the low thermal expansion coefficients of fused SiO_2 and graphite, along with the high thermal conductivity of the graphite to provide the good thermal spalling resistance required for CC nozzles. Although the Al_2O_3 has rather high thermal expansion, it is superior in corrosion to molten steel. The corrosion resistance of AG nozzles tends to decrease with the increase of fused SiO_2 and graphite contents, as shown in Figs. 55 and 56.

Yoshino[180] comments that the corrosion resistance has been improved by experimenting with the grain-size distribution of the matrix, the Al_2O_3/SiO_2 ratio, and the oxide/graphite ratio. The corrosion resistance of the AG nozzles has also been improved by replacement of the pitch binder with phenol resin. The physical properties of the AG nozzle are also affected by the inner texture, which is controlled by the grain-size distribution, type of binders, and other additives. Some metals, carbides, or nitrides are generally added to the AG nozzles for the suppression of oxidation or the prevention of strength reduction at higher temperatures. Resin-bonded AG nozzles have

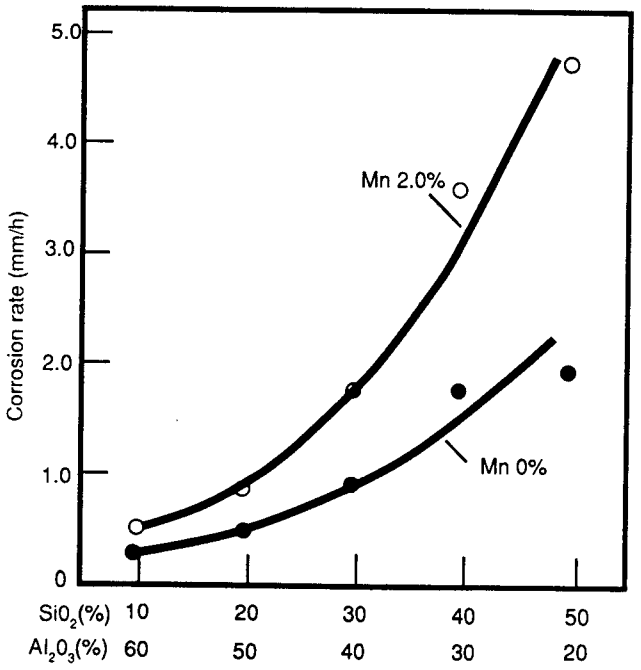

Fig. 55. Effect of silica content on the corrosion resistance of alumina-graphite nozzle by molten steel (C = 30%) (Ref. 180, Fig. 31. Used by permission.)

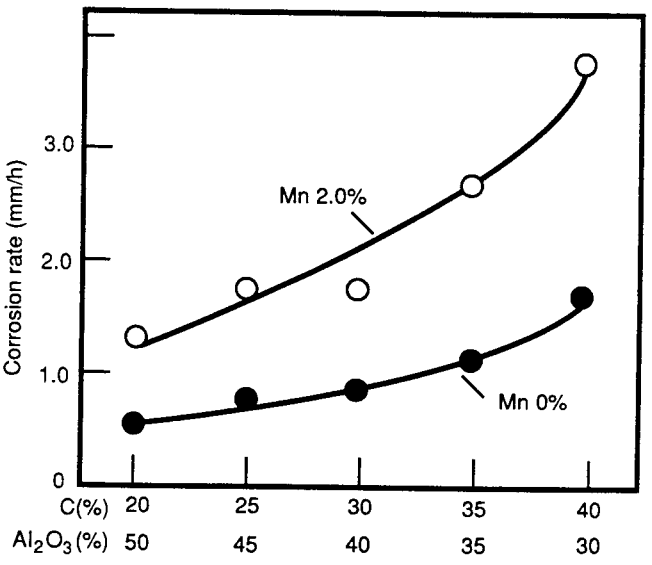

Fig. 56. Effect of graphite content on the corrosion resistance of alumina-graphite nozzle by molten steel (SiO_2 = 30%) (Ref. 180, Fig. 32. Used by permission.)

higher oxidation resistance due to their denser texture and smaller pore size and better abrasion resistance because of higher bonding strength, all of which results in excellent corrosion resistance. The wear rate of resin-bonded AG nozzles has recently been reduced in Japan to 1 mm/heat or less, even in the most damaged part of the LN, under ordinary casting conditions such as normal Al-killed steel with 250 to 300 metric ton ladles.[180] Properties of these long nozzles and submerged entry nozzles are shown in Table XLIV.

Kyoden et al.[182] provide a thorough study on the factors affecting the alumina buildup in submerged entry nozzles for CC of steel and preventative methods against the buildup from the viewpoint of the material for the interior liner of the nozzle and the nozzle configuration. These include BN-Si_3N_4-ZrO_2 interior liners and ZrO_2/C slag line insets in the Al_2O_3/C submersion nozzles.

Table XLIV. Properties of Long Nozzles and Submerged Entry Nozzles*

	Long Nozzle			Submerged Entry Nozzle			
	Main body		Cap part	Main body		Slag zone	
Brand name	G-28H	G-32D	CP-1	G-28D	G-28C	G-3Z	G-5Z
Apparent porosity (%)	14.0	14.0	14.5	14.0	15.0	15.0	14.5
Bulk density (g/cm^3)	2.35	2.25	2.45	2.35	2.50	3.35	3.70
Modulus of rupture (kgf/cm^2) {MPa}	95{9.3}	85{8.3}	120{12}	90{8.8}	90{8.8}	75{7.4}	70{6.9}
Modulus of elasticity (kgf/mm^2) {MPa}	1100{110}	950{93}	1350{132}	1150{113}	1100{110}	900{88}	850{83}
Thermal expansion at 1000°C (%)	0.29	0.24	0.36	0.29	0.39	0.44	0.46
Chemical composition (%)							
SiO_2	24	28	23	24	8		
Al_2O_3	47	40	55	47	60		
ZrO_2						69	78
C + SiC	28	31	20	28	30	26	19
Remarks	For pre-heating use	For non-preheating use	Reinforcement of the joint to ladle lower nozzle.	Standard	High corrosion resistance (low-SiO_2)	Standard	High corrosion resistance (high-ZrO_2)

*Ref. 180. Used by permission.

Yoshino concludes that, with the development of CC technology, refractories for CC have also evolved into functional refractories with high reliability and stability, which are designed to meet the diversified operational conditions which exist today.

References

[1]J. R. Wall, "Contributions to Research by Alcoa Research Laboratories—East St. Louis Division," Internal Alcoa Research Laboratories Report, September 8, 1959.

[2]T. S. Curtis, "Converter," U.S. Pat. No. 2 065 566, 1936.

[3]C. C. Furnas, "Grading Aggregates: I," *Ind. Eng. Chem.*, **23** [9] 1052–58 (1931).

[4]F. O. Anderegg, "Grading Aggregates: II," *Ind. Eng. Chem.*, **23** [9] 1058–64 (1931).

[5]W. H. Gitzen, L. D. Hart, and G. MacZura, "Phosphate-Bonded Alumina Castables: Some Properties and Applications," *Am. Ceram. Soc. Bull.*, **35** [6] 217–23 (1956).

[6]W. H. Gitzen, L. D. Hart, and G. MacZura, "Properties of Some Calcium Aluminate Cement Compositions," *J. Am. Ceram. Soc.*, **40** [5] 158–67 (1957).

[7]C. R. Venable, Jr., "Erosion Resistance of Ceramic Materials for Petroleum Refinery Applications," *Am. Ceram. Soc. Bull.*, **38** [7] 363–68 (1959).

[8]G. MacZura, K. P. Goodboy, and J. J. Koenig, "Aluminum Compounds–Aluminum Oxide (Alumina)," Kirk-Othmer: Encyclopedia of Chemical Technology, Vol. 2, 3rd ed. Wiley, New York, 1978.

[9]H. P. Bonebrake, "Slipcasting Alumina Shapes," Alcoa Chemicals Division ALCHEMEMO, July 1951.

[10]P. E. D. Morgan and M. S. Koutsoutis, "Phase Studies Concerning Sintering in Aluminas Doped with Ti^{4+}," *J. Am. Ceram. Soc.*, **68** [6] C-156–C-158 (1985).

[11]T. Ikegami, K. Kotani, and K. Eguchi, "Some Roles of MgO and TiO_2 in Densification of Sinterable Alumina," *J. Am. Ceram. Soc.*, **70** [12] 885–90 (1987).

[12]A. Pearson, J. E. Marhanka, G. MacZura, and L. D. Hart, "Dense, Abrasion-Resistant, 99.8% Alumina Ceramic," *Am. Ceram. Soc. Bull.*, **47** [7] 654–58 (1968).

[13]J. A. Everts and G. MacZura, "High Purity Aluminas for the Refractory Industry," Industrial Minerals Refractory Supplement, April, 1983.

[14]A. H. Fessler, "Alkali-Free Ceramic Materials and Method of Making Same," U.S. Pat. No. 2 069 060, 1937.

[15]J. F. Thompson, "Process of Producing Alumina," U.S. Pat. No. 2 469 088, 1949.

[16]D. E. Paul and L. M. House, "Method of Making Alumina Refractory Grain," U.S. Pat. No. 3 795 724, 1974.

[17]T. A. Ring, "Process for Producing High Density Sintered Alumina," U.S. Pat. No. 4 045 234, 1977.

[18]R. P. Heilich, F. J. Rohr, R. H. Goheen, and G. MacZura, "Comparison of Alcoa Tabular Alumina and European Fused Alumina Refractory Castables," Alcoa Research Laboratories—E. St. Louis Progress Report 3-A-1 (1-15-69).

[19]D. P. H. Hasselman, "Unified Theory of Thermal Shock Fracture and Crack Propagation in Brittle Ceramics," *J. Am. Ceram. Soc.*, **52** [11] 600–604 (1969).

[20]R. W. Davidge and G. Tappin, "Thermal Shock and Fracture in Ceramics," *Trans. Br. Ceram. Soc.*, **66** [8] 405–22 (1967).

[21]J. H. Duncan, D. T. Trigg, and W. E. C. Creyke, "Abrasion, Thermal Stress Resistance, Texture, Bulk Density and Strength of Aluminous Ceramics," *Trans. Br. Ceram. Soc.*, **64** [2] 121–36 (1965).

[22]J. H. Ainsworth and R. E. Moore, "Fracture Behavior of Thermally Shocked Aluminum Oxide," *J. Am. Ceram. Soc.*, **52** [11] 628–29 (1969).

[23]D. P. H. Hasselman, "Strength Behavior of Polycrystalline Alumina Subjected to Thermal Shock," *J. Am. Ceram. Soc.*, **53** [9] 490–95 (1970).

[24]W. P. Rogers, A. F. Emery, R. C. Bradt, and A. S. Kobayashi, "Statistical Study of Thermal Fracture of Ceramic Materials in Water Quench Test," *J. Am. Ceram. Soc.*, **70** [6] 406–12 (1987).

[25]T. K. Gupta, "Strength Degradation and Crack Propagation in Thermally Shocked Al_2O_3," *J. Am. Ceram. Soc.*, **55** [5] 249–53 (1972).

[26]D. P. H. Hasselman, "Thermal Stress Resistance Parameters for Brittle Refractory Ceramics: A Compendium," *Am. Ceram. Soc. Bull.*, **49** [12] 1033–37 (1970).

[27]D. P. H. Hasselman, "Elastic Energy at Fracture and Surface Energy as Design for Thermal Shock," *J. Am. Ceram. Soc.*, **46** [11] 535–40 (1963).

[28]I. Peretz, S. Perrella, and R. C. Bradt, "Aggregate Particle Strengths and the Strength of Aluminosilicate Refractories"; pp. 549–59 in Proceedings First International Conference on Refractories. Technical Association of Refractories, Tokyo, Japan, 1983.

[29]W. H. Gitzen, Alumina as a Ceramic Material. The American Ceramic Society, Columbus, OH, 1971.

[30]S. J. Lukasiewicz and J. S. Reed, "Phase Development on Reacting Phosphoric Acid with Various Bayer-Process Aluminas," **66** [7] 1134–38 (1987).

[31]F. J. Gonzalez and J. W. Halloran, "Reaction of Orthophosphoric Acid with Several Forms of Aluminum Oxide," *Am. Ceram. Soc. Bull.*, **59** [7] 727–31, 738 (1980).

[32]A. Nishikawa, Technology of Monolithic Refractories. Plibrico Japan Co., Ltd., Tokyo, Japan, 1984.

[33]"Refractory Plastics and Refractories, State-of-the-Art Report," ACI Committee 547 Report ACI 547.1R-90. American Concrete Institute, Detroit, MI, 1990.

[34]J. S. C. Davidson and J. C. Willshee, G. R.-Stein Refractories Ltd.; private communication, January 24, 1972.

[35]D. H. Houseman, "Performance of High-Alumina in Selected Steelmaking Refractories," *J. Br. Ceram. Soc.*, **74** [6] (1975).

[36]D. J. Bray, "Creep of Refractories: Mathematical Modeling"; pp. 69–80 in Advances in Ceramics, Vol. 13. The American Ceramic Society, Columbus, OH, 1985.

[37]W. R. Alder and J. S. Masaryk, "Compressive Stress/Strain Measurement on Monolithic Refractories at Elevated Temperatures," pp. 97–109 in Advances in Ceramics, Vol. 13. The American Ceramic Society, Columbus, OH, 1985.

[38]C. D. Ortman, "Kiln Refractory," U.S. Pat. No. 2 895 840, 1959.

[39]E. D. Miller, "Alumina Refractories," U.S. Pat. No. 3 067 050, 1962.

[40]E. D. Miller, "Alumina Refractories," U.S. Pat. No. 3 226 241, 1965.

[41]W. T. Bakker, "High Alumina Refractories," U.S. Pat. No. 3 640 739, 1972.

[42]W. T. Bakker, "Alumina Refractories," U.S. Pat. No. 3 652 307, 1972.

[43]R. E. Farris and M. E. Green, Jr., "High Alumina Refractory," U.S. Pat. No. 3 841 884, 1974.

[44]E. L. Manigault, "Alumina Refractory Composition," U.S. Pat. No. 3 808 013, 1974.

[45]R. P. Heilich, F. J. Rohr, G. V. Givan, and G. MacZura, "Na_2O in Refractories," Alcoa Research Laboratories, E. St. Louis, IL. Monthly Summary Reports 4/73 to 2/74.

[46]G. Holder, O. Helmboldt, and P. Vogt, "Process for Preparing Sodium-Free Alumina," Ger. Pat. No. 1 092 457, 1960.

[47]D. R. Watson, A. Lippman, and D. V. Royce, Jr., "Method for Reducing the Soda Content of Alumina," U.S. Pat. No. 3 106 452, 1963.

[48]H. Moore and M. R. Prasad, "Effects of Various Mineralizing Agents in Promoting Recrystallization in Mixtures of Clay and Alumina During Firing," *J. Soc. Glass Technol.*, **39**, 314–50T (1955).

[49]S. P. Chaudhuri, "Role of Mineralizers on the Size of Mullite Crystals," *Ind. Ceram.*, **14** [4] 111–16 (1969).

[50]S. P. Chaudhuri, "Induced Mullitization of Kaolinite-A Review," *Trans. J. Br. Ceram. Soc.*, **76** [5] 113–20 (1977).

[51]I. Matsumura, Y. Hayashi, Y. Hiyama, and A. Ijiri, "Refractoriness Under Load and Hot Creep Measurements," *Takabutsu Overseas*, **2** [2] 36–42 (1982).

[52]T. M. Smith, "Sonic Test for Thermal Shock Resistance," *Am. Ceram. Soc. Bull.*, **50** [4] 434 (1971).

[53]A. J. Skoog and R. E. Moore; "Refractory of the Past for the Future: Mullite and Its Use as a Bonding Phase," *Am. Ceram. Soc. Bull.*, **67** [7] 1180–85 (1988).

[54]A. J. Skoog, "An Investigation of In Situ Formed Mullite for Ceramic Matrices," M.S. Thesis in Ceramic Engineering, University of Missouri-Rolla, 1988.

[55]R. P. Heilich, G. MacZura, and F. J. Rohr, "Precision Cast 92–97% Alumina Ceramics Bonded with Calcium Aluminate Cement," *Am. Ceram. Soc. Bull.*, **50** [6] 548–54 (1971).

[56]G. MacZura, J. E. Kopanda, F. J. Rohr, and P. T. Rothenbuehler, "Calcium Aluminate Cements for Emerging Castable Technology"; pp. 285–301 in Advances in Ceramics, Vol. 13. The American Ceramic Society, Columbus, OH, 1985.

[57]G. MacZura et al., "Developmental Technical Refractory Materials—Part II"; Proceedings Latin-American Association of Refractory Manufacturers (ALAFAR) XVII Congress on Refractories. ALAFAR, Montevideo, Uruguay, 1988.

[58]T. Ochiai, H. Itoi, and Y. Hoshiide, "Vibration Forming Troughs," *Ironmaking Proc.*, **35**, 61–68 (1976).

[59]K. E. Granitzki and K. Takeda, "New Refractory Materials for Blast Furnaces," *Interceram*, **27** [1] 60–63 (1978).

[60]L. Prost and J. Pinon, "Higher Performance Castables for Reheating and Heat Treatment Furnaces," XXII International Colloquium on Refractories, Aachen, Germany, September 27–28, 1979.

[61]M. Nishi and A. Miyamoto, "Lining Materials and Installation Methods for Blast Furnaces," *Taikabutsu Overseas*, **1** [1] 26–39 (1981).

[62]S. Yoshino, "Recent Trends in Steel Ladle Linings in Japan," *Taikabutsu Overseas*, **1** [1] 49–55 (1981).

[63]T. Taniguchi, M. Otani, and I. Iwasaki. "Studies on Trough Lining Refractories for Large-Capacity Blast Furnaces," *Taikabutsu Overseas*, **2** [1] 78–89 (1982).

[64]K. Umeya, "Rheological Approaches to Monolithic Refractories-I," *Taikabutsu Overseas*, **2** [2] 49–54 (1982).

[65]K. Umeya, "Rheological Approaches to Monolithic Refractories-II," *Taikabutsu Overseas*, **2** [2] 55–60 (1982).

[66]Papers from the Proceedings of the XXVth International Colloquium on Refractories (October 14–15, 1982) Aachen, Germany.

[67]D. H. Hubble and K. K. Kappmeyer. "Future Raw Material Requirements for Steel Plant Refractories." Workshop on Critical Materials, Vanderbilt University, Nashville, TN (October 4–7, 1982), to be published in *U.S. Bureau of Standards Bulletin* (1983).

[68]B. Cooper, "Continuous Casting of BSC Port Talbot Works," *Steel Times*, 235–40 (May 1983).

[69]B. Cooper, "Conquest Keeps BSC Stockbridge at the Forefront of Technology," *Steel Times*, 242–47 (May 1983).

[70]J. Mitchell, "Scunthorpe Completes Concast Trio," *Steel Times*, 249–53 (May 1983).

[71]W. Welburn, "Developments in Continuous Casting of Special Steels," *Steel Times*, 254 (May 1983).

[72]K. Yamamoto, "Some Properties and Applications of Low-Moisture Castables," reviewed at the ACI Refractory Concrete Committee 547 Workshop—Seminar IV on Refractory Concrete at Carnegie-Mellon University, Pittsburgh, PA (June 7–9, 1983).

[73]G. MacZura, V. Gnauck, and P. T. Rothenbuehler, "Fine Aluminas for High Performance Refractories." *Interceram*, December 1984.

[74]B. Clavaud, J. P. Kiehl, and R. D. Schmidt-Whitley, "Fifteen Years of Low Cement Castables and Steelmaking"; 589–606 in Proceedings First International Conference on Refractories. Technical Association of Tokyo, Japan, 1983.

[75]A. Seltveit, G. S. Dhupia, and W. Kroenert,"Microstructural Aspects of Microsilica-Blended High Alumina Castables," *Ceram. Eng. Sci. Proc.*, **7** [1–2] 243–60 (1986).

[76]B. Monsen, A. Seltveit, B. Sandberg, and S. Bentsen, "Effect of Microsilica on Physical Properties and Mineralogical Composition of Refractory Concretes"; pp. 201–10 in Advances in Ceramics, Vol. 13. American Ceramic Society, Columbus, OH, 1985.

[77]D. J. Bray, "Toxicity of Chromium Compounds Formed in Refractories," *Am. Ceram. Soc. Bull.*, **64** [7] 1012–16 (1985).

[78]R. Stieling, H.-J. Kunkel, and V. Martin, "Vibrated Castables with a Thixotropic Behavior"; pp. 211–18 in Advances in Ceramics, Vol. 13. The American Ceramic Society, Columbus, OH, 1985.

[79]E. P. Weaver, R. W. Talley, and A. J. Engel, "High-Technology Castables"; pp. 219–29 in Advances in Ceramics, Vol. 13. The American Ceramic Society, Columbus, OH, 1985.

[80]C. Richmond and C. E. Chaille, "High-Performance Castables for Severe Applications"; pp. 230–44 in Advances in Ceramics, Vol. 13. The American Ceramic Society, Columbus, OH, 1985.

[81]Y. Naruse, S. Fujimoto, S. Kiwaki, and M. Nishima, "Progress of Additives in Monolithic Refractories"; pp. 245–56 in Advances in Ceramics, Vol. 13. The American Ceramic Society, Columbus, OH, 1985.

[82]S. Banerjee, R. V. Kilgore, and D. A. Knowlton, "Low-Moisture Castables: Properties and Applications"; pp. 257–73 in Advances in Ceramics, Vol. 13. The American Ceramic Society, Columbus, OH, 1985.

[83]B. Clavaud, J. P. Kiehl, and J. P. Radal, "A New Generation of Low-Cement Castables"; pp. 274–84 in Advances in Ceramics, Vol. 13. The American Ceramic Society, Columbus, OH, 1985.

[84]R. A. Howe and J. A. Kaniuk, "The Effects of Curing Temperature and Times on Low-Moisture Trough Castables," *Ceram. Eng. Sci. Proc.*, **7** [1–2] 261–66 (1986).

[85]C.-H. Liu, J. L. Mendoza, and R. E. Moore, "Effect of Dopants on the Creep Behavior of Low and Ultra-Low Cement Refractory Concretes," *Ceram. Eng. Sci. Proc.*, **8** [1–2] 1–8 (1987).

[86]J. L. Mendoza, R. E. Moore, and C.-H. Liu, "Low-Cement/No Cement Monolithics—Their Potential for Ladle Metallurgy," Proceedings 23rd ACerS St. Louis Section Refractories Symposium, "Refractories for Ladle Metallurgy," St. Louis, MO, April 10, 1987.

[87]T. Darroudi and R. A. Landy, "Effects of Temperature and Stressing Rate on Fracture Strength of a Series of High Al_2O_3 Refractories," *Am. Ceram. Soc. Bull.*, **66** [7] 1139–43 (1987).

[88]R. J. Charles, "Static Fatigue of Glass," *J. Appl. Phys.*, **29** [11] 1549–60 (1958).

[89]J. E. Ritter, Jr. and C. L. Sherburne, "Dynamic and Static Fatigue of Silicate Glasses," *J. Am. Ceram. Soc.*, **54** [12] 601–605 (1971).

[90]T. E. Adams, "Dynamic Fatigue of Alumina Refractories at Room Temperatures," M.S. Thesis in Ceramic Science. The Pennsylvania State University, August 1980.

[91]T. E. Adams, D. J. Landini, C. A. Schumacher, and R. C. Bradt, "Micro- and Macrocrack Growth in Alumina Refractories," *Am. Ceram. Soc. Bull.*, **60** [7] 730–35 (1981).

[92]J. White, "An Assessment of Recent Research on Refractories, Part I," *Refract. J.*, **52** [11–12] 10–19 (1976).

[93]C. A. Schumacher, "Crack Propagation and Thermal Fracture of Alumina Refractories," M.S. Thesis in Ceramic Science. The Pennsylvania State University, August 1980.

[94]D. R. Larson, J. A. Coppola, D. P. H. Hasselman, and R. C. Bradt, "Fracture Toughness and Spalling Behavior of High Al_2O_3 Refractories," *J. Am. Ceram. Soc.*, **57** [10] 417–21 (1974).

[95]G. V. Givan, G. MacZura, R. P. Heilich, and F. J. Rohr, "Thermal Shock Testing of Calcium Aluminate Bonded Refractory Concretes," *Am. Ceram. Soc. Bull.*, **54** [7] 650–53 (1975).

[96]G. MacZura, L. D. Hart, R. P. Heilich, and J. Kopanda, "Refractory Cements," *Ceram. Eng. Sci. Proc.*, **4** [1–2] 46–67 (1983).

[97]R. D. Smith, H. U. Anderson, and R. E. Moore, "Influence of Induced Porosity on the Thermal Shock Characteristics of Al_2O_3," *Am. Ceram. Soc. Bull.*, **55** [11] 979–82 (1976).

[98]J. Homeny and R. C. Bradt, "Aggregate Distribution Effects on the Mechanical Properties in Thermal Shock Behavior of Model

Monolithic Refractory Systems"; pp. 110–30 in Advances in Ceramics, Vol. 13. The American Ceramic Society, Columbus, OH, 1985.
[99]P. T. Bertrand, S. E. Laurich-McIntyre, and R. C. Bradt, "Strengths of Fused and Tabular Alumina Refractory Grains," *Am. Ceram. Soc. Bull.*, **67** [7] 1217–21 (1988).
[100]Y. Hiramatsu and Y. Oka, "Determination of the Tensile Strength of Rock by a Compression Test of an Irregular Test Piece," *Int. J. Rock. Mech. Min. Sci.*, **3**, 89–99 (1966).
[101]G. MacZura, D. V. Ruhs, R. J. Rohr, P. T. Rothenbuehler, V. Gnauck, R. Carvalho, and T. Fujioka, "Developmental Technical Refractory Materials—Part I"; Proceedings 2nd International Conference on Refractories. Technical Association of Refractories, Tokyo, Japan, 1987; 1125/Supplement.
[102]H. D. Leigh, "Refractories," Encyclopedia of Glass, Ceramics, and Cement. Edited by M. Grayson, Wylie & Sons, New York, 1985.
[103]H. E. McGannon, Making, Shaping and Treating of Steel. U.S. Steel Corporation, Pittsburgh, PA, December 1970.
[104]Refractories, Fire Brick-Specialties, Uses in Industrial Importance. The Refractories Institute, Pittsburgh, PA, 1975.
[105]Harbison-Walker Refractories Company Technical Staff, "Refractories for Iron and Steel Plants," Watkins Cyclopedia of the Steel Industry, 1969.
[106]"Refractories," The Refractories Institute, No. 7901, p. 4, 1979.
[107]C. G. Marvin, "Refractories—An Overview," *Am. Ceram. Soc. Bull.*, **66** [7] 1101–1102 (1987).
[108]H. Longin, "Trends in the European Refractories Industry," *Am. Ceram. Soc. Bull.*, **67** [7] 1161–62 (1988).
[109]Y. Sakano and H. Takahashi, "Outlook for the Refractories Industry in Japan." *Am. Ceram. Soc. Bull.*, **67** [7] 1164–75 (1988).
[110]"International Iron and Steel Institute Statistics," *Iron Steel Maker, AIME-ISS*, **15** [13] 2–16 (1988).
[111]A. Kadano, "Trends of Japan's Refractory Industry," *Am. Ceram. Soc. Bull.*, **63** [9] 1124–27 (1984).
[112]Modern Refractories Practice. Harbison-Walker Refractories Company, 4th ed. Pittsburgh, PA, 1961.
[113]F. H. Norton, Refractories, 4th ed. McGraw-Hill, New York, 1968.
[114]Proceedings of XXVth International Colloquium on Refractories, Aachen, W. Germany, October 14–15, 1982, *Interceram*, **32**, 3–146 (1983).
[115]"Refractories in the Cement Industry," *Interceram*, **33**, 3–82 (1984).
[116]*Proc. of 1st International Conference on Refractories*, November 15–18, 1983, Technical Association of Refractories-Japan, Tokyo, Japan, 1983.
[117]K. Shaw, Refractories and Their Uses. Halstead Press Division, Wiley & Sons, New York, 1972.
[118]W. T. Lankford, et al. (eds.). The Making, Shaping and Treating of Steel, 10th ed. United States Steel Company, New York, 1985.
[119]C. W. Hardy, et al. Committee on Technology—Special Study Team on Refractories, Refractory Materials for Steelmaking. International Iron and Steel Institute, Brussels, Belgium, 1985.
[120]R. J. Fruehan, Ladle Metallurgy Principles and Practices. AIME-ISS, Pittsburgh, PA, 1985.
[121]"New Developments in Monolithic Refractories," Advances in Ceramics, Vol. 13, R. E. Fisher, ed. American Ceramic Society, Columbus, OH, 1985.
[122]C. R. Beechan, et al. ed., "Applications of Refractories," *Ceram. Sci. Eng. Proc.*, **7** [1–2] 1986.
[123]"Refractories for Continuous Casting," Proceedings of XXIXth International Colloquium on Refractories, Aachen, W. Germany, October 9–10, 1986.
[124]*Foundry Industry Scoping Study*, Center for Metals Production Report No. 86–5, Pittsburgh, PA, November 1986.
[125]J. E. Kopanda, et al., "Application of Refractories," *Ceram. Sci. Eng. Proc.*, **8** [1–2] 1987.
[126]Proceedings of 2nd International Conference on Refractories, Vols. 1–2. The Technical Association of Refractories, Tokyo, Japan, 1987.
[127]Proceedings of International Symposium on Advances in Refractories for the Metallurgical Industries, Vol. 4. Edited by M. A. J. Rigaud, et al., Pergamon, New York, 1988.
[128]J. M. Benzel, et al. ed., "Applications of Refractories," *Ceram. Sci. Eng. Proc.*, **9** [1–2] 1988.
[129]"Special Issue on Continuous Casting," Shinagawa Technical Report 31, Shinagawa Refractories Co. Ltd., Tokyo, Japan, 1988.
[130]Refractories. The Refractories Institute, Pittsburgh, PA, 1987.
[131]K. Hiragushi, "Refractories for the 80's—Actual Position and Tendencies in Japan," Proceedings of ALAFAR Congress XIV, Canela, Brazil, November 4–7, 1984.
[132]P. L. Smith, J. White, and P. G. Whiteley, "Ultra High Alumina or Silicon Carbide Refractories for Critical Areas in Blast Furnace Linings"; pp. 101–17 in Proceedings of the 2nd International Conference on Refractories, Vol. 1. The Technical Association of Refractories, Tokyo, Japan, 1987.
[133]W. Ishikawa, T. Yamamoto, Y. Abe, and K. Okuda, *Proc. Europ. Iron Congress 1986*, Vol. 3, Paper V-2.
[134]J. M. Bauer and J. P. Kiehl, "Refractories for Iron-Making," *Proc. Br. Ceram. Soc.*, **29** [10] 191 (1980).
[135]R. Eschenberg, W. Keyk, G. Klages, W. Kowalski, and L. Smeets, "Development of the Refractory Lining of Blast Furnaces at Thyssen AG," *Interceram*, **32**, 19–24 (1983).
[136]J. M. Bauer, R. D. Schmidt-Witley, D. Dumas, B. Du Mensnildot, and J. P. Kiehl, "New Solutions for Problem Areas of Blast Furnace Linings," *Interceram*, **32**, 25–32 (1983).
[137]R. L. Wessel, "Selection and Use of Refractory Concretes in the Steel Plant," ACI SP-57 Refractory Concrete, 179–222. American Concrete Institute, Detroit, MI, 1978.
[138]A. Egami, "Repair Methods and Materials for Blast Furnaces in the Hot Condition," *Taikabutsu Overseas—Special Topics: Refractories for Iron Making*, **2** [1] 71–77 (1982).
[139]L. P. Krietz, R. Woodhead, S. Chadhuri, and A. Egami, "The Use of Monolithics in Blast Furnaces"; pp. 323–30 in Advances in Ceramics, Vol. 13. The American Ceramic Society, Columbus, OH, 1985.
[140]A. Watanabe, T. Okamura, Y. Mizuta, J. Kariya, and H. Takadachi, "Development of Resin Bonded Injection Material for Blast Furnace Repairing"; pp. 118–32 in Proceedings of 2nd International Conference on Refractories, Vol. 1. The Technical Association of Refractories, Tokyo, Japan, 1987.
[141]Y. Naruse, "Future Trend and Development of Refractories Industry in Japan"; pp. 3–60 in Proceedings of 2nd International Conference on Refractories, Vol. 1. The Technical Association of Refractories, Tokyo, Japan, 1987.
[142]W. Kroenert, "Recent Progress in the Use of Monolithic Refractories in Europe"; pp. 21–45 in Advances in Ceramics, Vol. 13. The American Ceramic Society, Columbus, OH, 1985.
[143]T. Nishina, S. Takehara, and M. Terao, "Recent Trends of Refractories for Hot Blast Stoves," *Taikabutsu Overseas—Special Topics: Refractories for Iron Making*, **2** [1] 98–109 (1982).
[144]K. Sugita and Y. Shinohara, "Refractories Technology for Blast Furnace Tapholes and Troughs," *Interceram*, **32**, 111–18 (1983).
[145]*Ironmaking Proc.—Symposium on Taphole Mixes*, AIME **35**, 79–96, St. Louis, MO (1976).
[146]J. A. Cummins, S. A. Nightingale, and I. N. Mackay, "The Development of an Improved Quick Curing High Strength Resin Bonded Blast Furnace Taphole Clay"; pp. 133–46 in Proceedings of 2nd International Conference on Refractories, Vol. 1. The Technical Assoc. of Refractories, Tokyo, Japan, 1987.
[147]H.-P. Ruther, "Investigation Into Causes of Wear in the Blast Furnace Trough Systems and Measures to Improve the Service Life of the Refractory Trough Linings," *Interceram*, **32**, 119–26 (1983).
[148]G. Gelsdorf and F. Wirth, "Blast Furnace Trough Lining Techniques and Trends of Development in Germany," *Interceram*, **32**, 127–31 (1983).
[149]K. E. Granitzki, P. Schiefer, M. Ackermann, K. Thomas, and F. Trager, "Application of a New Type of Casting Method for

the Lining and Repair of Blast Furnace Main Trough," *Interceram*, **32**, 132–36 (1983).

[150]A. Suckow, L. Dotsch, and H. Hoffgen, "Experience With Various Blast Furnace Trough Lining Techniques," *Interceram*, **32**, 137–40 (1983).

[151]T. Taniguchi, M. Otani, I. Iwasaki, and M. Ishikawa, "Development of Castable Refractories with Powder Aluminum for Blast Furnace Troughs and Runners," *Interceram*, **32**, 141–46 (1983).

[152]Y. Kimura, H. Shikano, and K. Hiragushi, "Progress of Alumina Silicon Carbide Graphite Refractories for Hot Metal Pretreatment"; pp. 239–53 in Proceedings of 2nd International Conference on Refractories, Vol. 1. The Technical Assoc. of Refractories, Tokyo, Japan, 1987.

[153]S. Yamamoto, Y. Owada, S. Naigai, T. Yamaguti, and H. Hasimoto, "Castable Refractories for Tundish Lining," *Taikabutsu Overseas*, **6** [3] 14–21 (1986).

[154]R. A. Howe, J. W. Kelley, and T. A. Dannemiller, "Designing a Cast House for Preformed Shapes"; pp. 305–12 in Advances in Ceramics, Vol. 13. The American Ceramic Society, Columbus, OH, 1985.

[155]S. Nishizawa and A. Kondo, "Application of Dry-Forming Method to Blast Furnace Troughs"; pp. 313–22 in Advances in Ceramics, Vol. 13. The American Ceramic Society, Columbus, OH 1985.

[156]S. B. Bonsall and D. K. Henry, "Wear Mechanisms in Alumina-Silicon Carbide-Carbon Blast Furnace Trough Refractories"; pp. 331–40 in Advances in Ceramics, Vol. 13. The American Ceramic Society, Columbus, OH 1985.

[157]Y. Toritani, T. Yamane, S. Yamasaki, I. Nishijima, T. Kawakami, and Y. Kadota, "Progress in Casting Trough Materials and Installing Techniques for Large Blast Furnaces"; pp. 341–54 in Advances in Ceramics, Vol. 13. The American Ceramic Society, Columbus, OH 1985.

[158]C. M. Jones, "Comparison of Monolithic Refractories for Blast Furnace Troughs and Runners"; pp. 355–62 in Advances in Ceramics, Vol. 13. The American Ceramic Society, Columbus, OH 1985.

[159]N. Moritama, "Recent Progress of Steelmaking Technology and Expectation for Refractories," *Taikabutsu Overseas*, **6** [2] 18–36 (1986).

[160]T. Hayashi, "Recent Developments of Refractory Technology in Japan"; pp. 5–34 in Proceedings of 1st International Conference on Refractories. Tokyo, Japan, 1983.

[161]M. Koltermann, "Torpedo Ladle Refractories in West Germany," *Taikabutsu Overseas*, **5** [2] 35–40 (1985).

[162]D. H. Hubble, "Performance of Monoliths in Industrial Applications," Presented at NICE "Workshop on Performance of Monoliths in Industrial Applications," The American Ceramic Society, 89th Annual Meeting, Pittsburgh, PA, April 26, 1987.

[163]K. K. Kappmeyer and D. H. Hubble, "The Continuing Challenge for Steel-Plant Refractories"; presented at the Refractories Institute 38th Annual Spring Meetings at Kiawah Island, S.C., June 23–25, 1988.

[164]S. Miyagawa, M. Yokoi, A. Mastuo, T. Morimoto, and T. Kawakami, "Refractories for Torpedo Cars," *Ceram. Eng. Sci. Proc.*, **7** [1–2] 58–74 (1986).

[165]K. Shimada, A. Doi, and K. Kono, "Development of Refractories for Torpedo Ladles with Hot Metal Pretreatment"; pp. 266–80 in Proceedings of 2nd International Conference on Refractories, Vol. 1. The Technical Association of Refractories, Tokyo, Japan, 1987.

[166]Y. T. Chien, C. C. Chou, H. C. Pan, and Y. C. Ko, "Evaluation and Selection of Refractory Materials for Desiliconization in Torpedo Ladles"; pp.254–65 in Proceedings of 2nd International Conference on Refractories, Vol. 1. The Technical Association of Refractories, Tokyo, Japan, 1987.

[167]M. L. Van Dreser and J. E. Neely, "Refractories for Steelmaking in the U.S.A.—Current Practice and Future Trends"; pp. 35–62 in Proceedings of 1st International Conference on Refractories. The Technical Association of Refractories, Tokyo, Japan, 1983.

[168]P. Marshall, et al. EAF Study Team, The Electric Arc Furnace. International Iron and Steel Institute, Brussels, Belgium, 1983.

[169]M. A. Orehoski and R. D. Gray, "Ladle Refining Processes," *AISE Iron Steel Eng.*, **63** [1] 40–52 (1986).

[170]I. D. Prendergast, "Developments in Monolithic Ladle Linings"; presented at The 42nd Annual Forum, Pennsylvania Ceramic Association, The Pennsylvania State University Park Campus, State College, September 11–12, 1987.

[171]T. L. Nosbisch, R. M. Wardrop, J. A. Kaniuk, and I. D. Prendergast, "Development of Monolithic Steel Ladles at Gary Works"; pp. 289–98 in *Proceedings of International Symposium on Advances in Refractories for the Metallurgical Industries*, Vol. 4. Pergamon, New York, 1988.

[172]I. D. Prendergast, "Practical Aspects of Refractory Selection and Performance in Steel Ladles"; pp. 163–80 in Proceedings of International Symposium on Advances in Refractories for the Metallurgical Industries, Vol. 4. Pergamon, New York, 1988.

[173]G. Lalancette and M. Rigaud, "Trends in Steelmaking Ladle Refractories in Canada"; pp. 155–62 in Proceedings of International Symposium on Advances in Refractories for the Metallurgical Industries, Vol. 4. Pergamon, New York, 1988.

[174]M. Oberbach, G. Zingel, and B. Schiefer, "Modern Refractories—A Key to Improved Economy in Steelmaking"; pp. 71–104 in Proceedings of International Symposium on Advances in Refractories for the Metallurgical Industries, Vol. 4. Pergamon, New York, 1988.

[175]Y. Sasajima and M. Kogiso, "Refractories for Lance Pipe"; pp. 291–306 in Proceedings of 2nd International Conference on Refractories, Vol. 1. The Technical Association of Refractories, Tokyo, Japan, 1987.

[176]"Slide Gate Valve Systems Gaining a Foothold in the U.S.?", *Thirty-Three Magazine*, April 1973.

[177]E. M. Dickson, "Refractories—Practice and Trends," Raw Materials for the Refractories Industry—an "Industrial Minerals" consumer survey. Metal Bulletin Ltd., London, 1981.

[178]P. Jeschke, "Recent Tendency of Refractories for the Steel Industry in West Germany," Industrial Minerals Refractory Supplement. April 1983.

[179]P. Mutsaarts, "Continuous Casting Technologies in European Community," Shinagawa Technical Report—Special Issue on Continuous Casting, No. 31, pp. 1–30, 1988.

[180]S. Yoshino, "Present Situation of Continuous Casting Refractories in Japan," Shinagawa Technical Report—Special Issue on Continuous Casting, No. 31, pp. 31–74, 1988.

[181]K. Tabata, T. Kakehi, M. Terao, and N. Tsukamoto, "Gas Injection Methods at Tundish Slag Gate Valve for Continuous Casting," Shinagawa Technical Report—Special Issue on Continuous Casting, No. 31, pp. 97–110, 1988.

[182]H. Kyoden, Y. Namba, and E. Iida, "Prevention of Alumina Buildup in Submerged Entry Nozzle for Continuous Casting of Steel," Shinagawa Technical Report—Special Issue on Continuous Casting, No. 31, pp. 85–96, 1988.

Production Processes, Properties, and Applications for Calcium Aluminate Cements

J. E. Kopanda* and G. MacZura
Aluminum Company of America
Pittsburgh, PA 15212

This chapter describes the historical development of calcium aluminate cements, raw materials currently used in the manufacturing processes, chemical and physical properties, and the hydration/dehydration/ceramic reactions associated with these cements. Also discussed are the effects of various additives on properties of calcium aluminate cements used as hydraulic binders in refractory concretes. Refractory and nonrefractory applications of calcium aluminate cement concretes are discussed in other chapters of this book.

Discovery of calcium aluminates, their behavior, production into cements, and ultimate usage covers a span of 140 years. The following chronological history was reported and referenced primarily by Robson.[1,2]

1848: Ebelman produced a calcium aluminate compound by heating alumina and lime or marble.

1856: Deville mixed calcium aluminates with water and corundum aggregate to mold high-temperature crucibles. During the same year, Winkler published information on the hydraulic properties of calcium aluminates.

1865: Fremy and Michaelis (1869) prepared fused calcium aluminate compounds which were found to be useful as structural units, and investigated their setting and hardening properties.

1882: Roth was awarded a German patent for a cementitious material made from bauxite, lime, and siliceous materials.

1888: Snelus et al. obtained a British patent for making calcium aluminate-type cements by combining Irish bauxite and lime into a fritted brick and adding blast furnace slag. They promoted their product for nonrefractory cementitious applications.

1906: Schott demonstrated that calcium aluminates have high-strength development capabilities.

1908–09: Bied received French and British patents for a method to produce a calcium aluminate cement with bauxite and lime in a cupola furnace.

1918–19: LaFarge manufactured this cement according to Bied and marketed it as a feasible sulfate-resistant product for concrete seawater corrosion resistance.

Mid-1920s: Investigators began applying the high-temperature properties of these cements with suitable aggregates to line high-temperature furnaces.

1924: Atlas Aluminate Cement Co. began manufacturing a calcium aluminate cement in the United States for use as a binder in refractory mixes. The development of both refractory aggregates and the data on cement aggregate mix designs for various high-temperature applications led to prepackaging these dry mixes by refractory manufacturers. These dry packaged materials are called "castables," a proportioned mixture of selected cements, aggregates, and special property-inducing ingredients.

1951: Alcoa and Lafarge began developing high-purity cement types made from alumina and lime.

Today, there are low, intermediate, and high-purity calcium aluminate cements that include a wide range of compositions. They are manufactured in many countries. These cements are made from bauxite and/or alumina plus limestone raw materials by fusing or sintering the raw mix in rotary or shaft kilns, or batch-type furnaces.

Nomenclature

Calcium aluminate cements are generally referred to as high-alumina cements (HAC), aluminous or aluminate cements (AC), or calcium aluminate cements (CAC). We prefer the latter designation because calcium is a principal component, and it distinguishes between these cements and the portland or calcium silicate cements (CSC). The three types of calcium aluminate cements are abbreviated throughout this chapter as: LP CAC for low-purity, IP CAC for intermediate-purity, and HP CAC for high-purity calcium aluminate cements.

Raw Materials

Bauxite is the principal raw material source of the alumina necessary for production of CAC clinker. Gibbsite, diaspore, and boehmite are the primary alumina-bearing minerals present in bauxites found throughout the world.

Kaolinite, an aluminum silicate, can also contribute some alumina to the CAC composition, but the siliceous impurity, along with the iron oxide hematite, detracts from the desirable properties achieved in CAC made from higher purity raw materials.

*Deceased October 28, 1987.

The various types of bauxites are generally present in tropical or subtropical climates. Australia, Indonesia, China, Surinam, Guyana, Brazil, the southern United States, Jamaica, Africa, southern France, Yugoslavia, Hungary, the U.S.S.R., and India are primary sources of bauxites for use in alumina extraction and refractory applications. Not all are suitable for direct use as raw materials to produce CAC. Those containing high iron oxide and silica impurities require refining into alumina before use. Typical raw material analysis is given in Table I.[3]

Bauxites predominate in the following hydrous alumina minerals:

Diaspore, β-$Al_2O_3 \cdot H_2O$, a mineral that is difficult to grind. Heat will remove the water of crystallization and cause decrepitation, which helps in the grinding process to prepare a fine CAC raw material for use in the sintering process. A non-processed lump form would be more suitable for a melted process that uses vertical or shaft-type kilns.

Boehmite, α-$Al_2O_3 \cdot H_2O$, a softer mineral that is more easily ground into a fine raw kiln feed.

Gibbsite, α-$Al_2O_3 \cdot 3H_2O$, a soft mineral typifying South American bauxites.

Alumina, Al_2O_3; purified or refined alumina in hydrous or calcined form can be used as a raw material for high-purity CAC. Minimal contaminants in these processed aluminas and use of higher purity limestones provide the basis for manufacturing high-purity CAC.

The lime source for producing CAC is primarily derived from calcium carbonate in the calcite or aragonite mineral variety. Limestone is an economical material conveniently located in most areas of the world.

The major concern in using any of these mineral-derived constituents to produce CAC is the quantity of impurities retained in the finished cement product. Disproportionate amounts of silica, ferrites, magnesia, titania, and alkalis affect the types of compounds formed in the burning process and the eventual performance of CAC. These compound formations and effects will be discussed later.

Table I. Typical Chemical Analysis Ranges of Raw Materials

	CaO Source	Al_2O_3		
		Calcined	Dried Bauxites	
Oxide Constituents	Limestone (%)	Al_2O_3 (%)	Domestic (%)	Foreign (%)
Al_2O_3	0.2–0.3	99.0	49–56	50–63
CaO	54–55	0.1	0.1–0.6	0.01–0.03
SiO_2	0.4–0.6	0.1	5–13	0.25–9.0
Fe_2O_3	0.2–0.3	0.1	3.5–7.5	0.9–19.0
MgO	0.2–0.4	0.1		
Na_2O	0.3–0.5	0.5		
LOI (1100°C)	41–43	1.0	27–31	27–34

By-product slags from various elemental production and other processes utilizing alumina and lime-bearing raw materials can be used as a raw material source for producing CAC clinkers and cements of different purities. Their composition, treatment, and economics determine the extent of their suitability as potential raw material and cement products.

Manufacturing Processes

Raw-material dryers, ball-mill grinding equipment, and fuels (natural gas, oil, coal, oxygen-enrichment, wood chips, etc.) are similar to those used in the portland cement industry.

Robson[1] describes various melting-process operations for producing CAC by either the vertical shaft kiln or rotary kiln operations. Electric arc resistance furnaces are also being used to produce CAC in countries where electrical energy is relatively cheap. However, sintering in a rotary kiln has proved to be a more viable option for producing more uniform and consistent products of every purity type of CAC, from low to high.

Compounds formed during sintering generally proceed dynamically in a nonequilibrium manner. High-lime calcium aluminates form initially with ferrites and silicates. Gradually, the uncombined lime and alumina continue to react with the high-lime products and form lower-lime or higher-alumina compounds, according to the phase diagram developed by Nurse et al.[4] (Fig. 1). These reactions continue in the kiln until the mix is

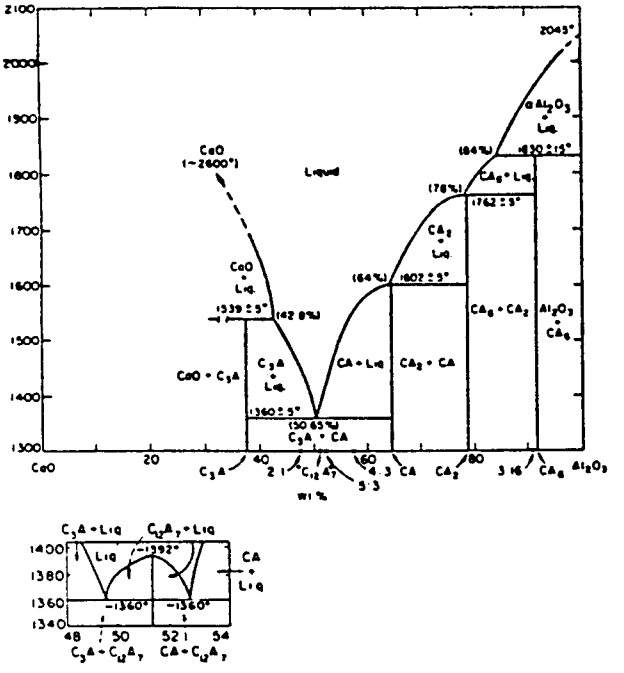

Fig. 1. The system CaO-Al_2O_3, according to Nurse et al. (Ref. 4) (*a*) Moisture-free atmosphere; (*b*) atmosphere at ordinary humidity.

completely combined below the melting point as follows.

$$C + A \rightarrow C_3A \rightarrow C_{12}A_7 \rightarrow CA \rightarrow CA_2 \rightarrow CA_6^{\dagger} \quad (1)$$

The major hydrating phase present in all commercial CAC clinkers is CA; the others occur as secondary phases, except for CA_2. It also occurs as a major phase for clinker compositions exceeding 70 wt% Al_2O_3 (<28% CaO).[5]

The sinter or clinker is ground in a ball mill to specific finenesses with or without admixtures such as slag or alumina and/or blended with or without additives such as set control and property modifiers. Generic types are described below under "Additives."

Finely powdered CAC is generally packaged in 22.7 to 45.4 kg (50 to 100 lb) paper bags containing a vapor barrier and 454 to 908 kg (1000 to 2000 lb) top or bottom discharge cloth supersacks. Bulk shipments are also made by rail and truck.

Low/Intermediate-Purity CAC

Sintering high-iron bauxites for LP CAC clinker production can also be accomplished in a "shock-sintering" rotary kiln operation[6] by adding calcium sulfate[7] to the raw mix. This addition extends the sintering range by forming suitable compounds at relatively low temperatures. "Shock-sintering" bypasses the slow formation of calcium aluminate compounds by rapidly combining the lime and alumina into desirable compositions. This is accomplished by providing a rapid movement of the finely ground and pelletized raw mix from the calcining zone of ≈870°C (1600°F) to a hot-zone temperature ranging from ≈1345° to ≈1480°C (2450° to 2700°F), depending on the composition, in a short time.

Melting limestone and alumina-bearing minerals has advantages and disadvantages. Coarse, unground raw materials are burned in vertical kilns until a molten pool collects near the base. This melt can then be analyzed for appropriate compositional control before tapping into molds. Calcium aluminates form on cooling from this equilibrium-type condition. Molten tapping temperature and both the type and rate of cooling will determine the calcium aluminate compounds that form in the mold as cement clinker and their characteristic properties. Grinding of this clinker obtained from a molten condition usually requires more energy than is required for a sintered composition.

High-Purity CAC

High-purity CAC sinters readily, even though very refractory high-purity limestone and Bayer calcined alumina (Table I) are used as raw materials in rotary kiln calcination. A 1360°C (2480°F) eutectic occurring at ≈50 wt% CaO/Al_2O_3 enhances liquid-phase sintering of these refractory oxides. The properties of some HP CAC compositions in the 64 to 86% alumina portion of the system lime-alumina are described by Gitzen et al.[8] Reaction of CaO and Al_2O_3 at 1425°C (2600°F) in a gas-fired atmosphere was considered to be practically complete when free CaO was found to be <0.15% and loss on ignition <0.5% at 1100°C (2010°F).

A well-converted HP CAC clinker having a maximum of 0.25% free lime immediately after calcination will have acceptable working-time and strength properties when using between 0.1 and 1.5% sodium citrate on the cement weight basis (cwb) to retard the $C_{12}A_7$ phase in the CAC, according to Hart.[9] It is reported that marginally converted clinker, having about 0.5% free lime after the heating operation, exhibited normal setting properties in the retarded CAC. However, within a short time, the free lime in the CA clinker increased to above 1%, enough to cause a reduction in cement working time and flash set. Grossly underconverted clinker will contain even more free lime and exhibit flash setting properties as-manufactured. According to this invention, the aforementioned instability problems with free lime can be offset by the addition of 0.05 to 3% (cwb) sodium bicarbonate and 0.1 to 1.5% (cwb) sodium citrate to ensure the production of HP CAC having normal working-time and strength properties.

Sadran[10] identified a composition and process for making a highly refractory aluminous cement consisting of an admixture of ≈60 wt% clinker, ≈40 wt% Al_2O_3, 2 wt% $AlNa_3F_6$, and ≈0.18 to 2.5 wt% sodium citrate and having a grain size distribution in which about 90% of the particles are under 30 μm. The clinker is formed by burning 98% purity Al_2O_3 and 99% purity $CaCO_3$ to obtain a mixture of CA and CA_2 in the ratio of approximately 1:1. Sadran claimed to have overcome the problem of low/intermediate-temperature (1000°C, 1832°F) strength by including a flux such as cryolite, ($AlNa_3F_6$), which melts at intermediate temperatures and helps create a ceramic bond.

Masaryk[11] noted a shortcoming in the Sadran patent as follows: "Such cements (U.S. 3 617 319) have shortcomings in that addition of the flux ($AlNa_3F_6$) makes them (CAC) less creep resistant, and also reactive with silica, forming silicon fluoride gas. Therefore, they cannot be used with refractory aggregates containing silica, for example, the very commonly used aluminosilicate aggregates." In other words, "cements containing fluoride fluxes should only be used with low silica aggregates." The Masaryk invention provides "a CAC of good refractoriness, rapid hardening, and good strength, both at room temperature and at intermediate temperatures."

U.S. Patent No. 3 963 508 by Masaryk[11] details a process for making an improved HP CAC involving admixing from 40 to 60% of a CA clinker containing at

---

† The following compound formulations used throughout this chapter are cement chemistry abbreviations: C = CaO, A = Al_2O_3, S = SiO_2, F = Fe_2O_3, M = MgO, T = TiO_2, $\bar{S}$ = SO_3, N = Na_2O, $\bar{K}$ = K_2O, and H = H_2O. For example, $C_{12}A_7$ = $12CaO \cdot 7Al_2O_3$, $C\bar{S}$ = $CaSO_4$, and $C\bar{A}H_{10}$ = $CaO \cdot Al_2O_3 \cdot 10H_2O$. Other chemical designations are spelled out.

least 80% CA phase with from 60 to 40% Al_2O_3 having a specific surface of 1 to 30 m^2/g and grinding to 80% −325 mesh. Known grinding aids, for example, triethanolamine or napthenic acid in amounts from 0.01 to 1 wt%, improved milling efficiency and achieved a preferred finer grind of 90% -325 mesh. Likewise, sodium citrate, a known retarder, was effective in controlling the rate of set of refractory castables when used in an amount of 0.1 to 1 wt%.

Schmitt and Mathieu[12] described a CAC binder having improved strength properties at an intermediate temperature of 1100°C (2012°F) and specified the use of pentasodium-tripolyphosphate, in addition to sodium citrate, CA phases, and calcined alumina. Specifically, they claim "a process for preparing a ground refractory hydraulic binder containing calcium aluminates which comprise: mixing from 45 to 65% clinker particles containing 45 to 72% CA phase, the balance being almost exclusively constituted by CA_2 phase, 55 to 35% alumina particles, 0.01 to 0.3% sodium citrate, and 0.01 to 0.3% pentasodium-tripolyphosphate, the percentages being by weight of the entire mixture wherein the clinker and the alumina are both ground before or after mixing." The preferred clinker contains 64 to 66% CA phase, an alumina having 2 to 15 m^2/g and at least 30%, preferably 55%, particles <2 μm, 0.1% (CA clinker and Al_2O_3 wt) sodium citrate, and 0.15% (CA clinker and Al_2O_3 wt) pentasodium-tripolyphosphate.

CA Clinker Mineral Compositions

The $CaO \cdot Al_2O_3 \cdot SiO_2$ equilibrium phase diagram (Fig. 2) provides the basis for the difference in mineral constitution between CAC and portland cement.[13] CA cements occur in a region of higher Al_2O_3 (lower CaO and SiO_2) than portland cement, a factor accounting

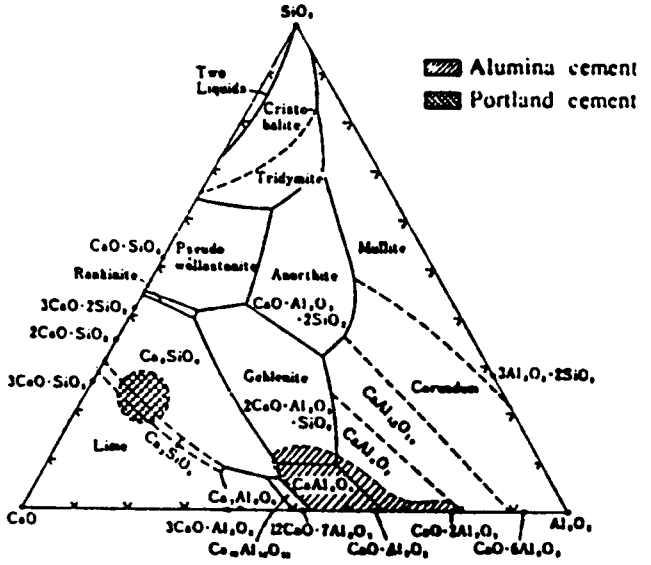

Fig. 2. Position of CAC and portland cements in the system $CaO-Al_2O_3-SiO_2$.

for their higher melting point and use as a refractories binder. The major hydrating phase present in all commercial CAC clinkers is CA; the others occur as secondary phases, except for CA_2. It also occurs as a major phase for clinker compositions exceeding 70 wt% Al_2O_3 (<28% CaO).[5]

As stated previously, calcium aluminates are formed by solid state combination of lime and alumina in either a sintering process or during cooling of a melt under equilibrium conditions.

In sintering, these raw-mix combinations generally progress into higher alumina phases as the material temperature increases in the kiln. Both lime/alumina ratio and temperature will determine the amount and type of calcium aluminate phases formed in the sinter.

Similar crystalline phases form in melting the raw mix, but glass and crystal products depend on the liquid temperature from which they are cooled and the type of cooling—slow or fast, and air or water quench.

Impurities in the raw materials or admixtures will also combine with the principal lime and alumina compositions during the heating process to form additional compounds:

SiO_2		C_2S or C_2AS
Fe_2O_3 + CaO + Al_2O_3	→	C_2F or C_4AF
TiO_2		CT
SO_3		Ca sulfide or $3(CA) \cdot C\bar{S}$

Reducing conditions in the kiln will affect the color but not the performance properties of the clinker. Iron oxides, reduced to the FeO state, will darken the clinker considerably. Color intensity will depend on the amount of iron oxide present in the raw mix.

Phases formed in the burning process have specific setting-behavior characteristics during hydration:

Fast setting:	C_3A, $C_{12}A_7$, C
Moderate setting:	CA, $3(CA) \cdot C\bar{S}$
Slow setting:	CA_2, C_2S, C_4AF
Minimal or nonsetting:	CA_6, C_2AS, C_2F, CT, α-A, calcium sulfide

This setting behavior is discussed below under description of the various types of cement and hydration reactions. Characteristics of the major CA hydrating compounds in CAC are listed in decreasing order of reactivity in Table II.

C_3A is not listed because it does not normally occur in CAC. C and α-A are listed for reference only. $C_{12}A_7$ hydrates very rapidly and can be used to control the setting rate of CAC when used in small quantities.

CA is the most important component of alumina cements because it generally occurs in large amounts and develops the highest strength among the phases listed during the relatively short time allotted for hydrating refractory concretes and has a relatively high melting point (mp).[1,4,13] It takes some time to start setting, but hardens rapidly after the initial set.

Table II. Characteristics of CAC Mineral Constituents

Mineral	Chemical Composition (%) CaO	Al_2O_3	Fe_2O_3	SiO_2	mp (°C)	Molecular Weight (g)	Density (g/cm^3)	Crystal System
C	99.8				2570	56.1	3.25/3.38	Cubic
$C_{12}A_7$	48.6	51.4			1360–1390	1387	2.69	Cubic
CA	35.4	64.6			1600	158	2.98	Monoclinic (triclinic)
CA_2	21.7	78.3			1750–1765 (decomposition)	260	2.91	Monoclinic
C_2S	65.1			34.9	2066	172	3.27	Monoclinic
C_4AF	46.2	20.9	32.9		1415	486	3.77	Orthorhombic
C_2AS	40.9	37.2		21.9	1590	274	3.04	Tetragonal
CA_6	8.4	91.6			1830	668	3.38	Hexagonal
α-A		99.8			2051*	102	3.98	Hexagonal

Ref. 17.

CA_2 takes an excessively long time to set with relatively low strength after curing 24 hours.[5,8,13] Jung[5] concluded that the hydration rate and hardening process for CA_2 are accelerated by the presence of CA. CAC containing 30% CA : 70% CA_2 developed compressive strengths about equivalent to 100% CA after one-day hydration and exceeded the CA reference after three-days hydration. These fused-CAC product results are not confirmed by the sinter-product data of Gitzen et al.[8] Cured, dried, and fired room-temperature strengths were maximum for the CA products and decreased with increasing CA_2 content, as noted by the combined Al_2O_3/CaO ratio for heat treatments up to 816°C (2000°F). Transverse strength after firing to 1400°C (2550°F) favored the higher CA_2 composition as the only exception.

C_2S and C_4AF are common to portland cement, but can also occur in the high-silica/iron-rich LP CAC. C_2AS shows little tendency to hydrate unless it contacts a lime solution or is present in an amorphous state.[13] It is an undesirable component of alumina cement which limits refractoriness and hot-strength properties.

CA_6 is the only nonhydrating phase in the pure CA system and is often a reaction product in alumina castables bonded with HP CAC. Thus, the mp can be misleading. Addition of finely ground Al_2O_3 to CA cements and/or castables enhances reactive sintering and conversion of the lower Al_2O_3 phases to the more refractory ones during initial heating of CAC furnace linings.

Criado et al.[14] used dilatometry to study the reaction of CA and α-A to form CA_2 and CA_6, as well as CA_2 and α-A to form CA_6. CA and α-A begin sintering at about 1100°C (2012°F), as indicated by a slight shrinkage, and then react to form CA_2, as noted by the large, nominally 1% expansion between 1200° (2192°) and 1400°C (2552°F) when using a 5°C/min heating rate. The 1.7% contraction on further heating to 1500°C (2732°F) indicates sintering and densification of the CA_2 specimen. Conversion to CA_2 was 90% complete on the first cycle and pure CA_2 was obtained after the fifth heating cycle, as confirmed by XRD. The thermal expansion (TE) coefficient decreased with each cycle and increasing CA_2 content.

Addition of α-A to CA to form stoichiometric CA_6 did not produce CA_6, but only CA_2 and α-A, on repeat cycles to above 1400°C in the dilatometric equipment. However, CA_6 was formed when using CA_2 and sufficient α-A to form CA_6 on repeated heatings. Thus, it may be concluded that CA_6 is most readily formed when using CA_2 as a precursor.

The TE coefficient of the various CA phases was developed in a previous paper by Criado et al.,[15] as shown in Table III. The TE data for C, C_3A, and α-A (corundum) are after Rigby and Green.[16] The corun-

Table III. Average Thermal Expansion Coefficient from 20°C (X10-6)

	200°	300°	400°	500°	600°	700°	800°	900°	1000°	1100°	1200°	1300°	1400°	1500°
CaO	12.4	12.5	12.7	12.9	13.0	13.3	13.5	13.6	13.6	13.5	13.6			
$3CaO \cdot Al_2O$	7.8	8.1	8.8	9.0	9.3	9.6	9.8	10.0	10.2	10.3	10.5			
$12CaO \cdot 7Al_2O$	4.9	5.2	5.3	5.5	5.5	5.7	5.9	6.0	6.2	6.4	6.5	6.3	5.5	
$CaO \cdot Al_2O$	6.7	6.7	6.8	6.9	7.0	7.2	7.3	7.4	7.6	7.8	7.8	7.7	5.9	
$CaO \cdot 2Al_2O$	1.7	1.4	1.4	1.6	1.9	2.3	2.6	2.9	3.3*	3.7	4.0	4.3	4.4	
$CaO \cdot 6Al_2O$	6.8	6.9	7.0	7.2	7.4	7.6	7.7	7.8	8.0	8.2	8.3	8.4	8.5	
Al_2O_3	7.7	8.0	8.0	8.0	8.0	8.1	8.0	8.0	8.1	8.0	8.0			

*Mendoza et al. reports 6.2 × 10^{-6} for CA_2 (Ref. 15*a*).

dum TE coefficient is lower than more recent data developed on sintered calcined alumina (99% Al_2O_3), as reviewed by Gitzen.[17] Average TE coefficients in the range of 20° to 1200°C and 25° to 1500°C are: (9.50 and 9.6) $\times 10^{-6}$/°C. These values are considered to be representative of the α-A currently being used in CA cements and castables.

The average TE coefficients for 20° to 1000°C from Table III are illustrated in Fig. 3, except for use of the data for α-A after Gitzen and the 6.20×10^{-6} TE coefficient value for CA_2 reported more recently by Mendoza et al.[15a] The changes in TE coefficient and densities associated with the phase changes occurring during reactive sintering with α-A to form the higher-Al_2O_3 CA phases should be critically considered when designing large CAC-bonded refractory castable shapes and thick linings for large process vessels.

As noted earlier, all CAC dehydration products in the bond phase will transist from $C_{12}A_7$ through CA to CA_2 and CA_6 if sufficient α-A is present in the castable.[3] Table IV summarizes the dimensional changes associated with these CAC phase changes and the lowest reaction temperatures at which an increase in

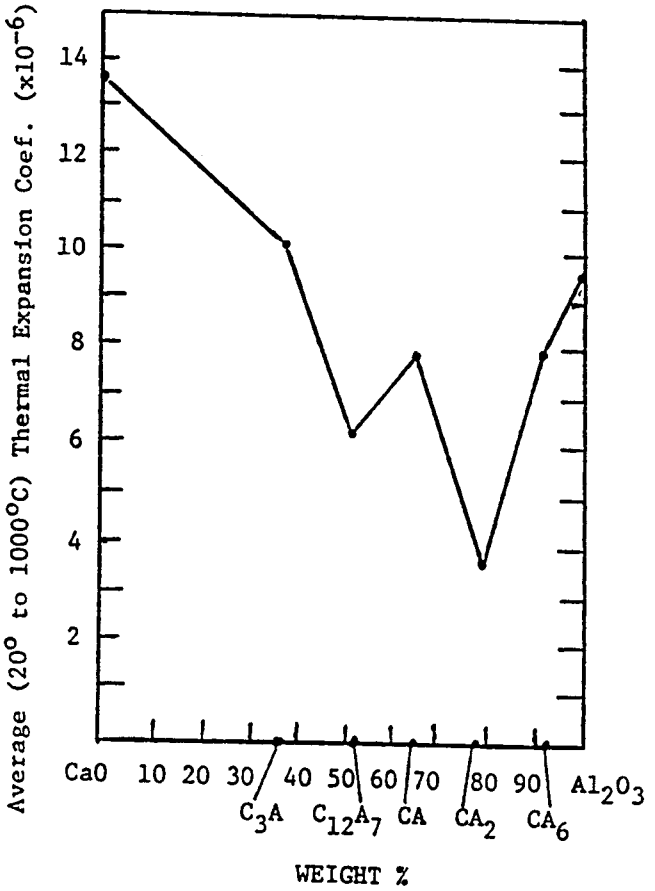

Fig. 3. Thermal expansion coefficient variation of CAC phases. After Mendoza, et al. (Ref. 15a).

Table IV. CAC Reactions and Associated Permanent Dimensional Changes

Reactions	Dimensional Change (%) Volume	Linear
(1) $C_{12}A_7 + 5A \rightarrow 12CA$	−1.17	−0.39
(2) $CA + A \rightarrow CA_2$	+13.6	+4.76
(3) $CA_2 + 4A \rightarrow CA_6$	+3.01	+1.01

Lowest Reaction Temperatures Showing an Increase in Phase

20% CA-25 Cement/80% Tabular (−6 Mesh) Ideal Castable, Hydrated and Heated*

(1) CA : 816°C (1500°F), 5-h hold
(2) CA_2 : 1100°C (2010°F), 5-h hold
(3) CA_6 : 1370°C (2465°F), 5-h hold

20% CA-25/80% Tabular (14–28 Mesh) Castable, Hydrated, and Heated†

(1) CA : 700°C (1290°F), ≈ 10-h hold
(2) CA_2 : 900°C (1650°F), ≈ 9-h hold
(3) CA_6 : 1300°C (2370°F), ≈ 8-h hold

*Ref. 18.
†Ref. 19.

that phase is detected by XRD in CAC-bonded tabular alumina castables.

The CA_6 phase is finally receiving the attention that it deserves with regard to being properly characterized to fully utilize its potential as an important nonhydrating bond phase in monolithic refractories, a strong thermal-shock-resistant refractory aggregate, and/or an advanced thermal/mechanical ceramic.[20–22] The sintering studies by Criado et al.[20,21] determined CA_6 sintering characteristics, microstructure, and mechanical properties (transverse strength and K_{IC} fracture toughness).

Using $CaCO_3/Al_2O_3$ mixtures formulated to the stoichiometric compositions for 0, 4.21, 6.37, 12.69, and 25.15 vol% CA_6, Criado et al.[20] conducted sintering studies in air at 1500° to 1650°C (2730° to 3000°F) using pressed compacts fabricated from the ground mixes. The controlled-rate heating shrinkage and shrinkage-rate curves showed two different sintering behaviors as a function of the calcium content. The two lower-C compositions showed a sintering behavior similar to that of α-A, but also exhibited a discontinuous expansive effect with the formation of the different calcium aluminate phases. The shrinkage curves for the two higher-C samples were explained in terms of a sintering process passing through a transitory liquid phase at about 1370°C (2500°F). The shrinkage-rate curves always showed a minimum at about 1500°C (2730°F), ascribed to the CA_6 formation.

The difference in microstructures between the two low- and two high-C compositions was also attributed to the transitory liquid phase, which enhanced grain growth of the CA_6 in the higher-C compositions. The CA_6 plank-shaped grains were 3 to 4 and 5 to 7 μm long for the low- and high-C compositions, respectively, and had an aspect ratio (L/d) of about 10 after sintering at 1550°C (2820°F) for 2 hours. The reference

sintered single-phase hexagonal α-A grains were 1.55 μm, slightly larger than the 1.25 to 1.35 μm α-A grains in the CA_6 compositions, except for the 12.69 vol% CA_6 sample, which averaged 1.7 μm.

The presence of CA_6 in the >97% theoretical density (<5% porosity) specimens formed by reaction between the $CaCO_3$ and α-A did not affect the fracture toughness. All K_{IC} values fell within the range of the alumina sample value (4.5 ± 0.1 MPa • $m^{-1/2}$). The significantly lower flexural strength of the CA_6 samples relative to α-A was attributed to the anisotropic grain growth of the CA_6 phase. Further, an increase in CA_6 sample K_{IC} values when normalizing for differences in porosity values in CA_6/α-A composites, compared with α-A alone, relates to an increase in the critical flaw size because of the abnormal CA_6 grain size and shape.

In a more recent CA_6 sintering study by Criado et al.,[21] a <1 μm CA_6 powder prepared at 1600°C (2910°F) and a mixture of $CaCO_3/Al_2O_3$ compounded to stoichiometric CA_6 were used for comparison. The transitory liquid phase at about 1350°C (2430°F) is believed responsible for the higher densities and two times faster sintering rate exhibited by the latter. The crystal habit resembles the elongated planks observed in the previous study and corresponds to grain growth from a liquid phase, whereas the former microstructure is typical of the controlled grain growth obtained with solid state sintering. The plank grains were about 4 to 6 μm long and had a smaller aspect ratio (L/d = 3) compared to the previous study, which contained less CA_6 (only up to 25.15 vol% CA_6). The solid state sintered CA_6 hexagonal crystals averaged 1.0 to 1.6 μm. Intergranular porosity was observed in both cases.

The mechanical properties are summarized in Fig. 4. The differences observed in density (ρ/ρ_{th}), fracture energy (K_{IC}), and flexural strength are attributed to the differences in microstructure. These results show that CA_6 has outstanding mechanical properties when properly sintered, for example, flexural strength = 300 MPa and fracture toughness, K_{IC} = 4.5 MPa • $m^{-1/2}$.

Mendoza et al.[22] also obtained K_{IC} = 4.5 MPa • $m^{-1/2}$ for CA_6 in sintering studies using different raw materials. A commercial CAC‡ and $Ca(OH)_2$ initially formed CA_6 at 1370° and 1400°C, respectively, when compounded to the stoichiometric CA_6 composition using 0.5 and 3 μm finely ground reactive aluminas. These compositions are being used to study the effects of alumina crystal size on the formation rates of calcium hexaluminate at different temperatures.

For characterization, CA_6 was made by heating compacts of the aforementioned compositions at 1700°C (3090°F) for 12 hours, followed by crushing, grinding, and pressing compacts again and refiring for 12 hours at 1700°C. Table V lists the physical properties of CA_6 as characterized by Mendoza et al. The properties of α-A are listed for comparison.

‡Alcoa CA-25 cement

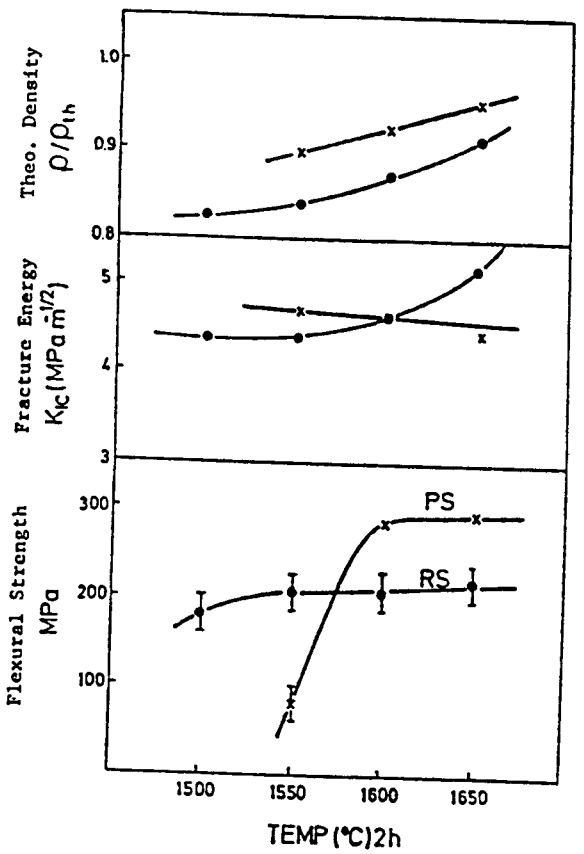

Fig. 4. Sintered CA_6 mechanical properties; PS = presintered; RS = reaction sintered.

Table V. CA_6 Characteristics

Property	CA_6	α-A
Density (g/cm³)	3.38	3.98
Young's modulus (GPa)	145	379
(x10⁶ psi)	21	55
Modulus of rupture (MPa)	159	345
(ksi)	23	50
Fracture toughness (K_{IC}) (MPa•$m^{-1/2}$)	4.5	2.1(*a*), 4.0(*b*)
Mean TE coef. (0°–1000°C) (x10^{-6}/°C)	8.5	9.6
Thermal shock (T_c) (°C)	200–240	220–250
Creep properties: 1400°–1500°C 0.31–0.38 MPa (45–55 psi)		
Steady state strain rate (x10^{-4} cm • cm • h)	2–50	0.5–200

Notes: *a* = Single-crystal sapphire
b = MgO-doped polycrystalline Al_2O_3

Although the 159 MPa MOR for CA_6 is only about one-half that reported for α-A, it is over 1.5 times greater than that reported for dense MgO, MgO • Al_2O_3 spinel, ZrO_2, and mullite. CA_6 thermal-mechanical properties are sufficient to approximate the critical thermal shock temperature (ΔT_c) for α-A at 200° to 240°C. The 2 to 50 × 10^{-4} cm • cm • h steady state creep rate at 1400° to 1500°C under 0.31 to 0.38

MPa (45 to 55 psi) loading falls within the range of that reported for α-A. These data reinforce the potential of CA_6 as a strong thermal-shock-resistant refractory aggregate and a good candidate as an advanced ceramic material.

Cements

Chemical and physical properties of the individual cement types are controlled by the producers during processing of the products. Customers may require certain properties for their applications and specify these on a mutually agreeable basis with the producer. While some countries do have standard classifications for these cements, there are no ASTM-type standard specifications applied to CAC in North America.

The American Concrete Institute's Refractory Concrete Committee 547 has described [23] the chemical and physical property ranges of these cements that are similar to those indicated in Table VI.

Color of these cements, ranging from black to white, depends on the impurities present and on the iron oxide quantity and oxidation state. Reducing conditions during the burning process will darken the cements containing iron compounds, while oxidation will produce a lighter, tannish color. The high-purity cements are white.

Generally, the characteristics of CAC binders are associated with the amount of alumina, lime, and impurities present in the products. Increased percentages of alumina will provide higher refractoriness, while a high lime content in the cement will produce an increase in cured strength. Iron impurities lower the carbon-monoxide-resistant capabilities at high temperatures[25–29] and siliceous compounds reduce resistance to hydrogen atmospheres under similar conditions.[30]

Hydration

The hydration process commences on initial contact of binder with water. Primary reactions form crystalline calcium aluminate hydrates and a hydrated alumina, present as either a crystal or a gel.

Table VI. Characteristics of Calcium Aluminate Cement Binders

	Low Purity	Intermediate Purity	High Purity
Al_2O_3 (%) (ASTM C114)*	39–50	55–66	70–90
CaO (%)	35–42	26–36	9–28
Fe_2O_3 (total iron) (%)	7–16	1–3	0.0–0.4
SiO_2 (%)	4.5–9.0	3.5–6.0	0.0–0.3
Surface area (m^2/g):			
Wagner (ASTM C115)*	0.14–0.16	0.16–0.24	0.22–0.30
Blaine (ASTM C204)*	0.26–0.44	0.32–1.00	0.36–1.50
B.E.T.	0.60–1.00	0.80–5.00	0.60–18.00
Specific gravity	3.05–3.25	2.95–3.10	3.00–3.30
Vicat initial set (h:min) (ASTM C191)*	3:00–9:00	3:00–12:00	0:30–6:00

*Ref. 24.

Ambient temperatures can have a major effect on the behavior of the binder, both during mixing and subsequent property development. Therefore, an understanding of the temperature effect on both the mix-water requirements and the hydration process during curing is essential.

Water is essential for hydrating the cement binder and for lubricating the dry grains to consolidate the concrete. Too much will lower strength development and increase shrinkage of the structure. Too little inhibits good consolidation of the concrete and may prevent completion of the hydration process.

Initial mix water and castable (binder + aggregate) temperatures affect the amount of water and handling time necessary for placement. Lower material temperatures require less water and extend working times for obtaining a satisfactory mix consistency, as illustrated by Given et al.[18] in Fig. 5 for an HP CAC/tabular alumina composition.

An investigation into the amount of water necessary to combine with the calcium aluminates at the curing temperatures described below was reported by MacZura et al.[3] and is presented in Table VII. Water requirement during application is limited by the consistency necessary for proper placement. A casting consistency can be obtained with 8.5 to 9.5% water when using the HP CAC shown in the table. The placement water indicated is adequate to completely hydrate the 20 to 30% CAC concretes when cured at temperatures above 21°C (70°F), but not when cured below 21°C. Attempts to moisten the concrete surface with a fine water spray should be avoided, because this procedure will dilute the surface pore water that is concentrated with Ca^{2+} and Al^{3+} ions, thus reducing hydration and causing low strengths and poor abrasion resistance at the surface.

Results in Fig. 5 and Table VII suggest that lowering the mixing water and solids temperature for

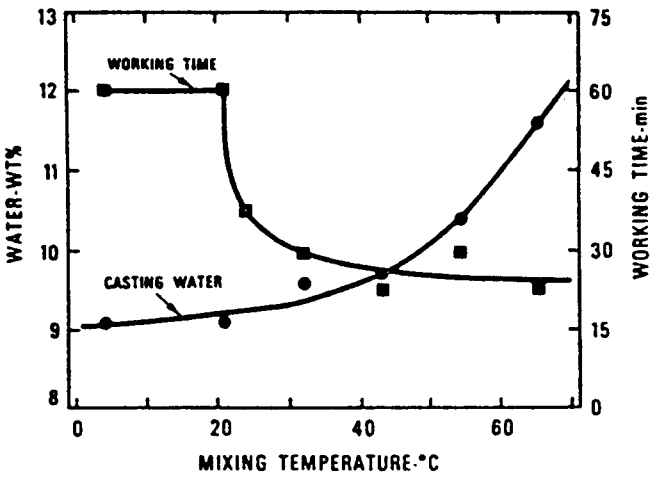

Fig. 5. Effect of mixing temperature on casting water and working time of a 20% high-purity cement: tabular alumina mix.

Table VII. Effect of Curing Temperature on Water Requirements of Calcium Aluminate Phases in High-Purity Cement*/Tabular Alumina Mixes

Curing Temperature			Water Requirements For Complete Hydration		
°C	°F	Hydration products	100% Cement	20% Cement	30% Cement
21	70	CAH_{10} + AH_x (gel)	58	11.6	17.4
21–35	70–95	C_2AH_8 + AH_3 (gel)†	32	6.4	9.6
35	95	C_3AH_6 + AH_3 (crystal)	23	4.6	6.9

*18.5% CaO cement.
†Gel crystallizes between 27° and 32°C (81° and 90°F) as detected by X-ray diffraction.

good mixing and longer placement time, in combination with increasing the curing temperature and maintaining a moist atmosphere after placement, will provide ideal concrete properties. (Note: High-temperature and high-humidity curing conditions have caused poor strength development in some low and ultralow castables; see previous chapter low-moisture/low-cement castable developments.)

The types of stable hydration products formed from the initial sintered mineralogical phases and their crystalline structures generally develop within 3 to 6 months under ambient conditions, or within the first 24 hours if curing is performed under high temperatures, as shown schematically in Fig. 6[3] and by the following reactions:

$C_{12}A_7/CA/CA_2$ + H (2)

<24°C (<75°F) → CAH_{10} (metastable hexagonal prisms) + AH_x (gel)

>24°C<35°C (>75°F <95°F) → C_2AH_8 (metastable hexagonal plates) + AH_x + AH_3

>35°C (>95°F) → C_3AH_6 (stable cubic trapezohedrals) + AH_3

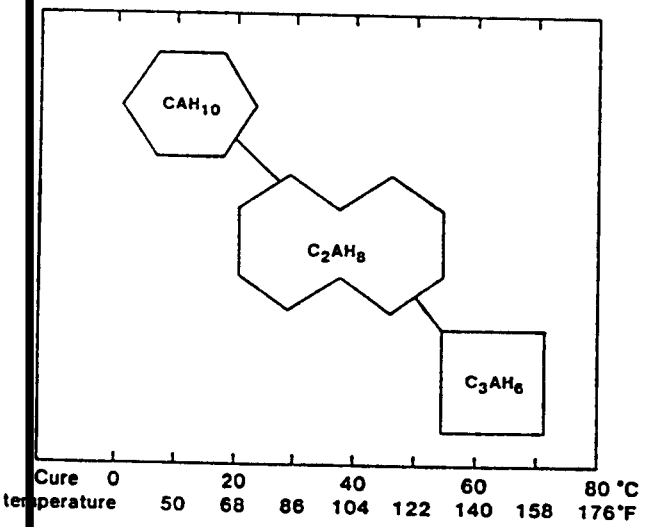

Fig. 6. Principal crystalline hydration phases in CAC during curing.

The transitional crystalline change from one calcium aluminate hydrate to another is commonly referred to as "conversion."

CAH_{10}/AH_x + time/temperature → $C_2AH_8/AH_x/AH$ + time/temperature → C_3AH_6/AH_3 (3

When the CAH_{10} is allowed to form during low temperature curing, the metastable hexagonal prism and gel solidify and, as shown by Mehta and Lesnikof in Figs. 7 and 8,[31] will eventually convert to the stable trapezohedral cubic type with time and/or temperature. This considerable internal volume change is disruptive to a rigid structure because both the crystal restructuring and decreased volume, indicated in Table VIII,[3] of these phases in the concrete contribute to a lower strength development.

Therefore, the conversion process can be controlled without strength retrogression by subjecting the newly placed concrete to a curing temperature environment suitable for preventing formation of CAH_{10} and AH_x gel.

Drying of the concrete at 104° to 110°C (220° to 230°F) is necessary to remove all superficial or free water. This also fully converts any metastable phases into the cubic hydrate and crystalline gibbsite, and provides a higher compressive strength development for the binder/aggregate system cured 24 hours at the higher temperatures, as indicated in Fig. 9[3] for an IP

Fig. 7. Scanning electron micrograph of CAH_{10} crystals (bar = 2 μm).

Fig. 8. Scanning electron micrograph of C_3AH_6 crystals (bar = 4 μm).

Table VIII. Effect of Temperature on Hydration Products of CAC

Curing T°		Hydration Products	Density (g/cm^3)	Volume Change* (%)
°C	°F			
<21	<70	CAH_{10}	1.72	
21–35	70–95	$C_2AH_8/AH_x/AH_3$	1.95/2.42	−37
>35	>95	C_3AH_6/AH_3	2.52/2.42	−53

*From CAH_{10}

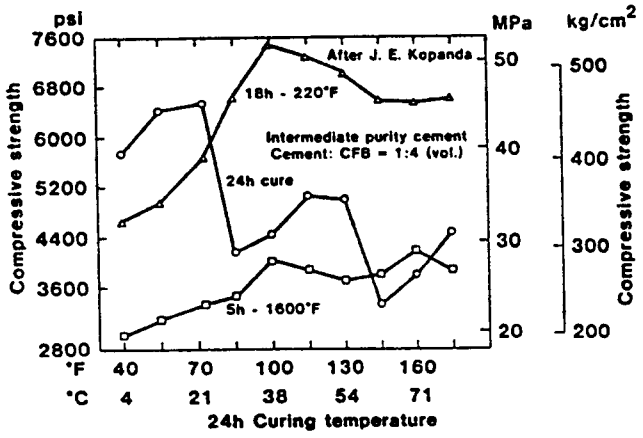

Fig. 9. Effect of curing temperatures on compressive strength of an intermediate-purity CAC/calcined flint clay mix.

CAC binder/calcined flint clay mix that was cured at 4° to 80°C (40° to 175°F), then dried and fired.

Additional improvements in refractory concrete properties were reported by Gitzen and Hart.[32] Their investigations, presented in Fig. 10, show that explosive steam spalling of concrete linings is related to the low curing temperatures that affect permeability and modulus of rupture after firing the installation.

The explosion temperature of a 64-mm (2.5-in.) cube specimen, cast from a 15% HP CAC/tabular alumina mix, increased from about 593°C (1100°F) after curing at 4°C (40°F) to about 1040°C (1900°F) when cured at 21°C (70°F). Significantly, better explosion resistance was demonstrated at higher curing temperatures by the survival without explosion of cured but undried test cubes that were instantly subjected to 1650°C (3000°F). Therefore, steam spalling of refractory CAC concretes can be averted by controlling the ambient curing temperatures, preferably at >27°C (31°F), to avoid AH_x gel formation with associated low permeability.

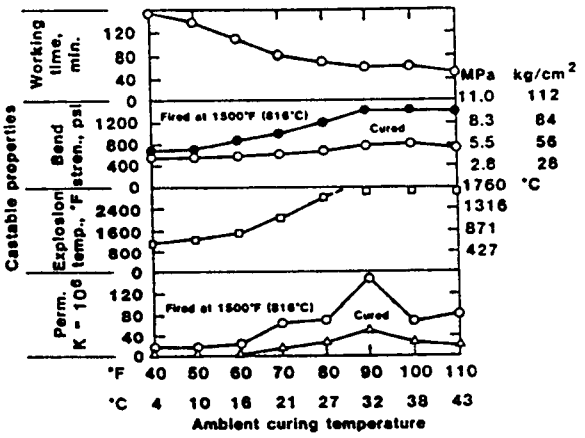

Fig. 10. Effect of curing temperatures on fired properties of HP CAC/tabular alumina mixes.

In nonrefractory applications, conversion can be prevented by either continuously maintaining the concrete at temperatures below 21°C (70°F) or by initially curing at >35°C (>95°F) for 24 hours.

As temperature is increased, dehydration continues by dissociating the water of crystallization from calcium aluminate and alumina hydrates. Thick linings may develop hydrothermal pressures that can form $C_4A_3H_3$ and boehmite (AH), as reported by Farris and Masaryk[33] and shown in Table IX.

This dehydration process continues with increasing temperature until all phases lose their water of crystallization. Lime and alumina reappear, and recombine similarly to the original sintered raw materials in the kiln. Calcium aluminates again form with increasing temperature and continue to react with each other until a ceramic reaction occurs between the binder components and aggregate, as shown schematically in Fig. 11[3] for an HP CAC/tabular alumina mix. A horizontal line can be drawn across the chart to denote the phases present in a CAC concrete lining at any stage of the curing/firing process. Phase changes

Table IX. Thermal Decomposition Temperatures for CAC Phases

Compound	Temperature Range °C	Temperature Range °F	Peak Reaction Temperature °C	Peak Reaction Temperature °F
AH_3	210–240	410–464	230	446
C_3AH_6	240–370	464–698	315	600
AH	480–565	896–1049	525	977
$C_4A_3H_3$	565–620	1049–1148	600	1112

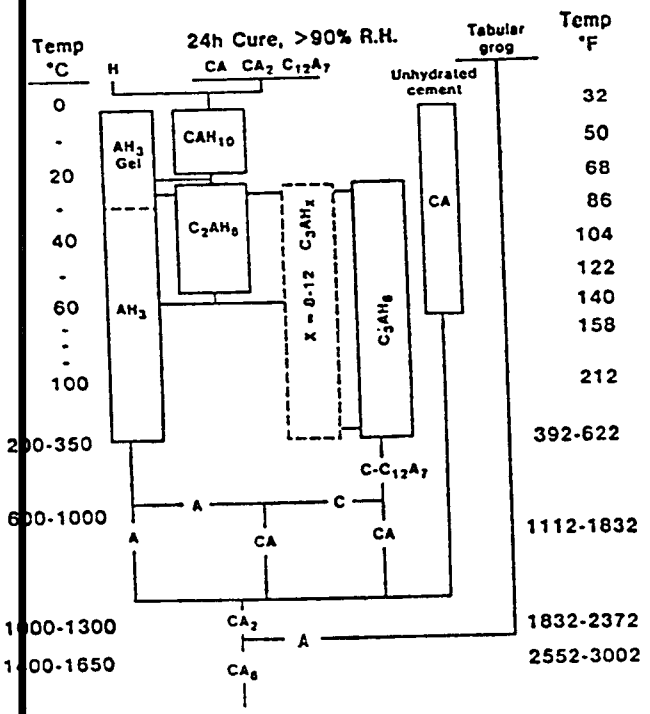

Fig. 11. Hydration/dehydration reactions in a high-purity CAC/tabular alumina mix.

are noted by the reaction paths as temperatures increase (moving down the chart). The CAC phases formed within a furnace lining can be estimated by assuming that the cold face is at the top of the figure and the hot face at the bottom.

Lower purity cements and aggregates can form similar hydration/dehydration/ceramic reaction products to those illustrated in Fig. 11. The compounds will vary, depending on the initial composition of the mix. Impurities that hydrate and subsequently dehydrate do not affect the curing/drying process to any great extent, but do react differently with the aggregates at the higher temperatures to form calcium aluminum silicates, ferrites, and titanates. Formation of these compounds usually reduces the refractory properties. Generally, these binders do not interreact with the aggregates at low temperatures to form different phases.

When used in refractory applications, cement binders are subjected to three main stages of dynamic reactions: curing, drying, and firing.

Proper moist curing produces a high strength development (60 to 70% of potential in the first 24 hours) by permitting the cement to form desirable hydrates.

Typical placement conditions are:

a. Cold weather (2° to 16°C, 35° to 60°F) (prevent water from freezing).

b. Ideal placement (16° to 27°C, 60° to 80°F) (prevent surface water from evaporating).

c. Hot weather (27° to 38°C, 80° to 100°F) (cool to prevent evaporation and fast setting of mix).

The following recommendations are offered:

a. Subject the concrete to a temperature of 32° to 50°C (90° to 120°F) as soon as possible after placement, and cure for 24 hours or more.

b. Cool thick sections to below 93°C (200°F) if steam is being generated by the binder heat of hydration.

c. Apply a membrane-type curing compound, a fine water spray, or a plastic covering on the concrete surface after placement to prevent moisture from evaporating during the initial 24 hours of curing.

Drying

Expose the cured concrete at 104° to 110°C (220° to 230°F) for at least 24 hours (longer for thick sections) to remove all free moisture and to fully convert the hydration products to stable phases.

Firing

Heating rates depend on the thickness of the concrete structure. A rate of 28° to 55°C (50° to 100°F)/h to either the expected operating temperatures or to a minimum of 593°C (1100°F) should suffice for the initial firing schedule of the 32° to 50°C (90° to 120°F) cured and dried structure. This will enable the hydration products to dehydrate completely and eventually react with the aggregates to form ceramic bonds at the higher temperatures. Lower curing temperatures require slower heating rates to prevent explosive spalling.

Caution should be used when patching furnace linings that have been taken out of service for repairs. To avoid explosive spalling, a higher curing temperature should be used throughout the patch and original lining. Those CAC phases present in a fired lining will rehydrate when wetted to form the same hydrated phases developed in a new lining (depending on the temperatures used for curing).

Additives

An additive is considered as a material interground or blended with the cement during the manufacturing process to control or modify the properties of the binder. However, some additions may be required in the field to control setting behavior or plasticity due to ambient conditions. These additions would be made prior to or during mixing of the concrete.

Listed below are generic descriptions of chemicals[23] that have been found to accelerate (Table X) or retard the set (Table XI), or provide water reduction and plasticity to the overall mix (Table XII). Behavior may vary, depending on individual cement characteristics and ambient placement conditions. Therefore, these additions must be tested in a small batch of a specific mix under ambient conditions before use in the installation.

The accelerators and retarders listed in Tables X and XI also function in the described manner when

Table X. Set Accelerators of Calcium Aluminate Cement Binders

Alkalis and Alkaline Compounds	Hydrated lime (see calcium hydroxide)
Anhydrite	Lime, hydrated
CAC, prehydrated and ground	Lithium salts
Calcium hydroxide, dilute	Plaster of paris (see calcium sulfate hemihydrate)
Calcium sulfate (0.5–1.0%)	Portland cement
Calcium sulfate hemihydrate	Potassium carbonate
Calcium sulfate dihydrate (0.5–1.0%)	Potassium hydroxide, dilute
Gypsum (see calcium sulfate dihydrate)	Potassium silicate
Hemihydrate (see calcium sulfate hemihydrate)	Sodium carbonate
	Sodium hydroxide, dilute
	Sodium silicate
	Sodium sulfate
	Sulfuric acid, dilute
	Triethanolamine (TEA)

Table XI. Set Retarders of Calcium Aluminate Cement Binders

Acids and acidic compounds	Hydrochloric acid, dilute
Acetic acid, dilute	Hydroxy-carboxylic acid salts: citric, gluconic, tartaric
Air-entraining agents	Isopropyl alcohol
Aluminum chloride hydrate	Lead salts
Anhydrite (see calcium sulfate)	Lignosulfonates
Barium chloride	Magnesium chloride
Barium hydroxide	Magnesium hydroxide
Borax	Muriatic acid (see hydrochloric acid)
Boric acid	Phosphates
Calcium chloride*	Seawater
Calcium sulfate (0.25%)	Sodium chloride
Casein	Sodium sulfate
Cellulose products	Starch
Flour	Sugar
Glycerine	Water-reducing agents
Glycols	
Gypsum (see calcium sulfate dihydrate)	

*Deleterious to CAC concrete.

introduced into a mix inadvertently. This may occur by contamination from a water supply, contact with installation equipment and other materials, or from various environmental sources. Specifically, a commonly occurring problem is the failure to properly clean equipment previously used to mix and handle portland cement concretes. The residual portland cement in the equipment reacts with the CAC to cause rapid set.

Special properties are obtained from some admixtures (Table XIII) added to the cement/aggregate system. The overall mix composition may be proprietary but some desirable properties and applications, such as low-cement castables, enhanced tensile strength from fibers, and high-temperature molten metal and slag resistance, are promoted by the refractory producers.

Table XII. Water Reducers and Plasticizers for CAC Concrete Mixes

Water-Reducing Agents	Plasticizers and Superplasticizers
Gluconic acid	Air-entraining agents (AEA)
Sodium citrate	Bentonite (2–3%)
Sodium gluconate	Fire clay, raw (5–15%)
	Fly ash, low-alkali
	Melamine formaldehyde sulfonate
	Naphthalene formaldehyde sulfonate
	Slag, finely ground, granulated

Table XIII. Special Admixtures for CAC Refractory Concrete Mixes

Alumina	Cryolite	Silica, fumed
Alumina, colloidal	Fibers	Silicon carbide
Aluminum fluoride	Frits	Spinel reactive powder
Aluminum powder	Graphite	Zircon
Barium sulfate	Nonwetting additives	Zirconia
Carbon	Silica, colloidal	
Chromic oxide		

The above-tabulated materials can react with the CAC binders at either low or high temperatures. Their addition to the binder or concrete mix controls the initial behavior of the mix during placement or enhances specific properties.

Aggregates have a different function in the total mix design of the concrete. A description of the variety of aggregates used in refractory applications and their basic function are included in the chapter on "Alumina Aggregates."

References

[1]T. D. Robson, High-Alumina Cements and Concretes. Wiley & Sons, New York, 1962.

[2]T. D. Robson, "Refractory Concretes: Past, Present, and Future," Refractory Concrete, SP-57. American Concrete Institute, Detroit, MI, 1978.

[3]G. MacZura, L. D. Hart, R. P. Heilich, and J. E. Kopanda, "Refractory Cements," *Ceram. Sci. Eng. Proc.*, (1983).

[4]K. M. Parker and J. H. Sharp, "Refractory Calcium Aluminates," *Trans. J. Br. Ceram., Soc.*, **8** [2] 29–56 (1982).

[5]M. Jung, "Hydraulic Properties of High-Alumina Cements," International Symposium on Refractory Concretes, Czechoslovakia, 1971.

[6]H. O. Nickelsen, J. E. Kopanda, and F. J. Piasecki, "Method of Making Cement Clinkers," U.S. Pat. No. 3 677 781, 1972.

[7]H. O. Nickelsen, J. E. Kopanda, and F. J. Piasecki, "Method of Sintering Calcium Aluminate Raw Mixes," U.S. Pat. No. 3 944 426, 1976.

[8]W. H. Gitzen, L. D. Hart, and G. MacZura, "Properties of Some Calcium Aluminate Cement Compositions," *J. Am. Ceram. Soc.*, **40** [5] 158–67 (1957).

[9]L. D. Hart, "Improvements Relating to Calcium Aluminates," Brit. Pat. 1 002 368, 1965.

[10]G. H. Sadran, "Highly Refractory Aluminous Cement and Process for Manufacture," U.S. Pat. No. 3 617 319, 1971.

[11]J. S. Masaryk, "Calcium Aluminate Based Refractory Hydraulic Binder and Its Process of Preparation," U.S. Pat. No. 3 963 508, 1979.

[12]Schmitt and Mathieu, U.S. Pat. No. 4 162 923

[13]A. Nishikawa, Technology of Monolithic Refractories. Plibrico Japan Co., Ltd., Tokyo, Japan, 1984.

[14]E. Criado, D. A. Estrada, and S. De Aza, "Dilatometric Study of the Formation of CA_2 and CA_6 in Cements and Refractory Concretes," *Bull. Sp. Ceram. Glass Soc.*, **15** [5] 319–21 (1976).

[15]E. Criado, S. De Aza, and D. A. Estrada, "Dilatometric Characteristics of Calcium Aluminates," *Bull. Sp. Ceram. Glass Soc.*, **14** [3] 271–73 (1975).

[15](*a*) J. L. Mendoza, A. Freeze, and R. E. Moore, "Thermomechanical Behavior of Calcium Aluminate Composites"; pp. 294–311 in Advances in Refractories Technology (Ceramic Transactions Volume 4), edited by R. E. Fisher. The American Ceramic Society, Westerville, OH, 1989.

[16]G. R. Rigby and A. T. Green, "The Thermal Expansion Characteristics of the Calcium Aluminates and Calcium Ferrites," *Br. Refr. Res. Assoc. Bull.*, No. 80 (1941).

[17]W. H. Gitzen, Alumina as a Ceramic Material. The American Ceramic Society, Columbus, OH, 1971.

[18]G. V. Given, L. D. Hart, R. P. Heilich, and G. MacZura, "Curing and Firing High Purity Calcium Aluminate-Bonded Tabular Alumina Castables," *Am. Ceram. Soc. Bull.*, **54** [8] 710–13 (1975).

[19]W. Kronert, "Studies of the Development of the Ceramic Bond in High Alumina Refractory Concretes Using SEM and XRD Analysis," Refractory Concrete, SP-57. American Concrete Institute, Detroit, MI, 1978.

[20]E. Criado, A. Caballero, and P. Pena, "Microstructural and Mechanical Properties of Alumina-Calcium Hexaluminate Composites"; presented at the World Congress on High Tech Ceramics, Milan, Italy, June 23–28, 1986.

[21]E. Criado, A. Caballero, and P. Pena, "Influence of Process Methods on Mechanical Properties of Calcium Hexaluminate"; presented at the XXVII Annual Meeting of the Spanish Ceramic and Glass Society, Merida, Spain, May 25–26, 1987.

[22]J. L. Mendoza, A. Freese, and R. E. Moore, "Morphological Characterization of Calcium Hexaluminate," *Am. Ceram. Soc. Bull.*, **66** [3] 583 (1987).

[23]Refractory Concrete, State-of-the-Art Report, ACI Committee 547 Report ACI 547R-79. American Concrete Institute, Detroit, MI, 1979.

[24]Annual Book of ASTM Standards, 04.01, ASTM, Philadelphia, PA, 1986.

[25]B. Osann, "Experimental Proof of the Disintegration of Linings and Charges in the Blast Furnace by the Decomposition of Carbon," *Stahl Eisen*, **27**, 1626–28 (1907).

[26]C. M. Vogrin and H. Heep, "High-Temperature Stability of Insulating and Refractory Castables in Reducing and Oxidizing Atmospheres," *Trans. Am. Soc. Mech. Eng.*, **78**, 1021–29 (1956).

[27]T. F. Berry, R. N. Ames, and R. B. Snow, "Influence of Impurities and Role of Iron Carbides in Deposition of Carbon from Carbon Monoxide," *J. Am. Ceram. Soc.*, **39** [9] 308–18 (1956).

[28]W. H. Gitzen, R. P. Heilich, and F. J. Rohr, "Carbon Monoxide Disintegration of Calcium Aluminate Cements in Refractory Castables," *Am. Ceram. Soc. Bull.*, **43** [7] 518–22 (1964).

[29]J. J. Brown, Jr., "Investigation of Carbon Monoxide Disintegration of Refractories in Coal Gasifiers," Final Report (10-1-80/9-30-83), DOE Contract No. DE–ACOI–80 ET 13702 (July 1984).

[30]M. S. Crowley, "Hydrogen-Silica Reactions in Refractories," *Am. Ceram. Soc. Bull.*, **46** [7] 679–82 (1967); **49** [5] 527–30 (1970).

[31]P. K. Mehta and G. Lesnikoff, "Conversion of $CaO \cdot Al_2O_3 \cdot 10H_2O$ to $3CaO \cdot Al_2O_3 \cdot 6H_2O$," *J. Am. Ceram. Soc.*, **54** [4] 210–12 (1971).

[32]W. H. Gitzen and L. D. Hart, "Explosive Spalling of Refractory Castables Bonded with Calcium Aluminate Cement," *Am. Ceram. Soc. Bull.*, **40** [8] 503-507, 510 (1961).

[33]R. E. Farris and J. S. Masaryk, "Mineralogy of Curing and Drying of a Refractory Concrete"; p. 277 in Ceramic Processing Before Firing. Wiley & Sons, New York, 1978.

Gallium

A. Pearson and C. N. Cochran
Aluminum Company of America
Alcoa Technical Center
Alcoa Center, PA 15069

The history, properties, manufacturing methods, and uses of gallium are reviewed with special emphasis on primary production methods and electronic applications. Applications for gallium compounds are growing rapidly in the electronic area. Improved manufacturing techniques for gallium-based devices and improved recovery methods for primary gallium are being developed to keep up with the growing demand.

This chapter was included because gallium has chemical properties quite similar to those of aluminum, and its production is closely tied to the alumina refining industry. Also, interest in and demand for gallium is growing as applications in electronic devices expand and diversify. Manufacture of these new devices is providing interesting challenges to ceramic and materials scientists. This chapter is not intended to be a comprehensive treatment of gallium but is more of an overview with special emphasis on production methods and electronic applications.

Historical Background

Gallium was first isolated by the French chemist LeCoq de Boisbaudran in 1875 and was named in honor of his native country. Before the discovery of gallium, however, its existence and some of its key properties were predicted by Dmitri I. Mendeleev. He called the unknown element eka-aluminum, and its subsequent discovery provided early support for his periodic system of classifying the elements.

Commercial use of gallium has been a fairly recent phenomenon. From its discovery until about 1940 it was recovered on a very small scale from various raw materials and it has been estimated that the total production during this time was about 50 kg.[1] During and shortly after World War II, small production facilities were installed, and gallium became "commercially" available in the United States with Eagle-Picher beginning in 1943[2] and Alcoa beginning in 1946. During 1946, Alcoa production of gallium was about 3 kg at a production cost of $5580/kg. By 1947, Alcoa's production rate had increased to about 50 kg/year, and the selling price was $4000/kg.[3] Since that time, as applications were developed, operating scale increased and recovery technology improved, resulting in a steady downward trend in gallium's price. By 1982, world demand for gallium was estimated at 25 000 kg/year and growing at a rate of 20%/year.[4] The price of electronic-grade gallium at that time was about $500/kg.

Properties

Gallium is a silvery-blue metallic element with several unusual physical properties. It has a very low melting point (30°C) yet a high boiling point (2403°C), resulting in the widest liquid range among the elements. It has the ability to be supercooled and, in the absence of seeding, will remain liquid for long periods of time at temperatures well below its freezing point. On freezing, it can form well-developed orthorhombic crystals which float in liquid gallium. Physical properties of gallium are shown in Table I.

The chemical properties of gallium are similar to those of zinc and aluminum. Like aluminum it is amphoteric and forms a protective oxide coating when exposed to oxygen or water vapor. Gallium oxide exists in several crystalline forms, the most stable of which is β-Ga_2O_3, a corundum structure which is obtained by heating above about 600°C.[5] For more detailed information on chemical and physical properties of gallium and its compounds, excellent reviews are available.[6,7]

Uses

Gallium has been used to a limited extent for high-temperature thermometry, for high-temperature lubrication, for electrically conductive rotary seals, and in dental alloys and mirrors. These applications have not become important because of the high price of gallium and problems with its chemical reactivity. It has also been advocated as a component in cracking[8] and reforming[9] catalysts. Gallium oxide has been investigated in a large variety of glass compositions[10–14] and as a constituent of a seal for high-alumina ceramics.[15,16]

One interesting application is the detection of solar neutrinos using concentrated gallium chloride solution. This has been proposed as an experiment to test current physical theories about solar reactions and will constitute the largest single use of gallium (up to 50 tons) if funding can be obtained for the experiment.[17]

Table I. Physical Properties of Gallium

Atomic number	31
Atomic weight	69.72
Atomic structure	K shell-2 L shell-2, 6 M shell-2, 6, 10 N shell-2, 1
Isotopes	Ga-69 ..... 60.2% Ga-71 ..... 39.8%
Crystal structure	Orthorhombic a = 0.45 μm (4.524Å) b = 0.76 μm (7.661Å) c = 0.45 μm (4.523Å)
Melting point (°C)	29.78
Boiling point (°C)	2403
Specific gravity	
solid (29.6C)	5.904
liquid (29.8C)	6.095
(32.38C)	6.093
(301C)	5.095
(600C)	5.720
(806C)	5.604
(1100C)	5.445
Solidification expansion	3.2%
Linear coefficient of thermal expansion of solid (/°C)	
Crystallographic axis	
a	1.66×10^{-5}
b	1.15×10^{-5}
c	3.10×10^{-5}
Volume coefficient of thermal expansion	
(0 to 30C) solid	5.8×10^{-5}
100C liquid	12.0×10^{-5}
900C liquid	9.7×10^{-5}
Vapor pressure (mm Hg)	
600C	0.0000000044
800C	0.0000059
1000C	0.00082
1200C	0.030
1400C	0.45
1600C	3.8
1800C	21
2000C	86
2200C	280
2403C	760
Thermal conductivity (watts/meter • Kelvin)	
50C	33.1
100C	42.5
150C	53.8
200C	54.5
250C	57.3
Specific heat (cal/g • °C)	
−268.9C (solid)	0.0000291
−257.1C (solid)	0.0046
−213.1C (solid)	0.042
0 to 24C (solid)	0.089
12.5C to 200C (liquid)	0.095
Latent heat of fusion (cal/g)	19.16
Latent heat of vaporization at B.P. (cal/g)	930.4
Viscosity, poises (cgs units)	
97.7C	0.01612
1100C	0.00578
Volume resistivity of liquid (microhms • cm)	
0C	25.2
20C	25.6
40C	26.0

Table I. Continued

Volume resistivity of solid (microhms • cm)

	a Axis	b Axis	c Axis
29.7C	54.3	17.4	8.1
0C	48.0	15.4	7.16
−195.6C	10.1	3.08	1.43
−268.9C*	0.00138	0.00068	0.00016

−272.06C Superconducting transition temperature

*Value for 99.9999% Ga, higher for less pure materials

Magnetic susceptibility (cgs units)	
solid (18C)	-0.24×10^{-6}
liquid (100C)	-0.04×10^{-6}
Standard electrode potential	
Ga to Ga^{3+}	−0.52v
Hydrogen overvoltage	
(solid)	0.31v
(liquid)	0.44v
Electrochemical equivalents	
(Ga^{3+})	4.15 coulomb/mg
Heat of combustion	2Ga to Ga_2O_3 + 258 kcal
Spectral lines (strong)	287.4 μm (2874Å) 294.4 μm (2944Å) 403.3 μm (4033Å) 417.2 μm (4172Å)
Ionic radius	0.06 μm (0.62Å)
Covalent radius	0.13 μm (1.25Å)
Atomic radius in metals	0.12 μm (1.22Å)
Hardness (Mohs scale)	1.5-2.5

Electronic Applications

The principal uses for gallium are in semiconducting compounds from Groups III and V of the Periodic Chart, such as GaAs, GaP, GaSb, GaAlAs, GaInP, GaAsP, GaInAs, etc.[18] These compounds have unusual electrical properties, such as larger band-gap energies for higher operating temperatures than are available with silicon devices,[19] higher carrier mobility, and electron saturation drift velocities for transistors with higher speeds or lower power dissipation.[20] In addition, direct band gaps make possible efficient light-emitting devices such as lasers and light-emitting diodes. Resistance to radiation damage is higher than for silicon devices,[21] which is important in GaAs photovoltaic cells used in satellites. Their efficiency in converting sunlight to electricity is unrivaled by silicon photovoltaic cells.[22]

These properties are enabling the development of much higher speed, more compact computers, more powerful and efficient microwave receivers, amplifiers and transmitters for satellites,[23] and optoelectronic links and amplifiers in optical fiber circuitry.[24] Furthermore, alloying or mixing of these compounds allows properties to be varied continuously over a wide range for matching to specific needs in each application.

Gallium oxide in the form of gadolinium gallium garnet is used as a substrate in bubble domain memories, compact devices not requiring the storage power used by other memory devices.[25]

These additional capabilities over silicon are driving the development of gallium devices though they will probably continue to be more expensive than silicon devices. The development of highly integrated gallium devices is generally tracking 10 years behind silicon.[26]

Gallium compounds can be synthesized as bulk compounds or deposited epitaxially on various substrates from liquid or gas phases or from molecular beams.[27-29] Crystals synthesized by the Bridgman technique are probably best suited for optical applications. Microwave and high-speed digital devices which require higher dislocation densities[30] are usually made from crystals obtained by the liquid-encapsulated Czochralski technique. Epitaxial techniques are used to deposit layers of gallium compounds on oriented substrates of the bulk crystals to make devices.

Occurrence

Gallium is a relatively abundant element, comprising an estimated 15 ppm of the earth's crust. This is about the same concentration as lead and higher than antimony, silver, bismuth, molybdenum, and tungsten.[2]

In spite of its abundance, it does not occur in high concentration in any known natural ores. The richest ores apparently are small African deposits of germanite and renierite, which contain about 1% gallium. Gallium is widely distributed as a trace impurity in natural minerals, usually in association with aluminum or zinc, at concentrations of less than 0.01%.[31] Commercially, the most important mineral source is bauxite, which contains 0.003 to 0.008% gallium.[32]

Gallium Availability

It has been estimated that approximately 5000 Mt/year of gallium are extracted from bauxite in the course of worldwide alumina refining,[33] yet only about 1% of this amount is recovered as primary gallium. The remainder leaves the refining operations as an impurity in alumina or in bauxite residues. The reason for the low recovery rate is that extraction of gallium is relatively expensive and market demand has not been large enough to be interesting to most alumina refiners. It is clear, however, that there is a large potential reserve of gallium available.

Gallium Production Processes

Since the most important processes for primary gallium production are tied to aluminum refining operations, they will be emphasized here. In alumina refining by the Bayer process, bauxite is contacted with hot caustic liquor, which dissolves the alumina and gallium. The insoluble residue is separated, then the liquor is cooled and contacted with gibbsite crystals, causing a portion of the supersaturated alumina to precipitate in a relatively pure form. The purified gibbsite crystals are separated and the liquor is recycled to dissolve more bauxite. During this operation the gallium tends to accumulate in the liquor and, if no gallium is extracted (other than that which leaves as an impurity in the gibbsite), at equilibrium the gallium/aluminum ratio in the spent liquor will be about 2 times the gallium/aluminum ratio in the bauxite. Thus the gallium undergoes a "free" concentration step in every alumina refinery.[34]

Even though the gallium has been concentrated, it is still a very minor component in the liquor stream. A typical U.S. refining plant liquor might contain 150 g/l NaOH, 75 Al_2O_3, and only 0.12 Ga. The trick then is to separate the small amount of gallium from the other components of this strongly alkaline solution.

Early processes for recovery of gallium from Bayer-process liquors involved staged precipitation of alumina. It was found that, by various reactions, most of the alumina could be precipitated from the liquor but most of the gallium would remain in solution. After the precipitate was filtered out, the liquor was rapidly gassed with CO_2. This treatment neutralized the remaining caustic, causing the rest of the alumina and gallium to precipitate. The precipitate was leached with caustic to preferentially remove the gallium and the resultant sodium gallate solution was electrolyzed to recover crude gallium.[34] The early commercial U.S. process used CaO to effect the first step of alumina reduction,[35] while the competing French process used carbonation.[36] A more recently patented variation discloses the use of sodium silicate.[37] The reaction products of these three variations are calcium aluminate, gibbsite, and zeolite, respectively. The main problem of this process is that a large amount of caustic must be neutralized to recover a small amount of gallium. Some improvement in economics is available at sinter plants where sodium carbonate and alumina are being thermally reacted for alumina recovery from difficult bauxites.

Another approach to recovering gallium is direct electrolysis of Bayer-process liquor using an agitated mercury cathode.[38] In normal electrolysis, gallium cannot be recovered from caustic solutions if the gallium concentration is below about 0.3 g/L Ga. This is because, at low concentrations, the electrolytic deposition rate is very slow and consequently the gallium redissolves as fast as it is electrolyzed. The mercury cathode process solves this problem by collecting the gallium in the liquid mercury during electrolysis. When the gallium content in the mercury reaches about 1%, the metal is leached with sodium hydroxide and the resulting sodium gallate solution is electrolyzed. This process is widely used in Europe but not in the United States because U.S. aluminum refining operations generally have high organic contamination and low gallium concentrations in the liquor compared to European practice. The problems associated with this type of process are low current efficiencies and environmental concerns due to the mercury. (Environmental concerns caused this pro-

cess to be abandoned in Japan.) A variation of this process is the use of low-melting-point metal alloys in place of mercury.[39] A further variation is to use a solid cathode into which the gallium can diffuse. Periodically the cathode is removed and the gallium-containing portion removed by etching or grinding.[40] A nonelectrolytic "cementation" process has been described where finely divided aluminum is mixed with Bayer liquor.[41] The gallate ion is reduced by metallic aluminum, causing gallium to be deposited onto the aluminum particles. The aluminum is then removed and dissolved to recover the gallium.

Recently two processes based on selective separation techniques were introduced. The first is liquid/liquid extraction.[42,43] In this process, the liquor is mixed with a water-immiscible organic solvent containing a chelating agent which specifically reacts with the gallium. By this process, the gallium passes from the liquor into the organic phase. The organic and aqueous phases are then separated by decantation and the gallium is stripped from the organic phase by mixing with an aqueous acid solution. The gallium can be separated from the acid by direct electrolysis or by further chemical treatment. The second process is ion exchange.[44] Specific resins have been reported which are stable in the hot, highly alkaline liquor and which are selective for gallium. The gallium is stripped from the resins by acid and recovered. These more sophisticated extraction processes appear promising and will probably change the face of the primary gallium industry if problems with thermal and chemical compatibility can be overcome.

Another source of gallium in the aluminum industry is fine alumina dust generated in some smelting plants. One commercial operation to recover gallium from this source has been announced.[45] The process probably involves leaching with acid and separating gallium by ion exchange.[46]

Primary gallium is also recovered commercially as a by-product of zinc manufacturing. Although this was one of the earliest gallium recovery methods, it is now a minor source compared to the aluminum operations described above. In this process, the zinc sulfide ores are roasted and the zinc is then distilled, leaving a residue containing most of the gallium. The residues are leached with acid to dissolve trace elements, including gallium. After several additional processing steps, the gallium eventually reports to a hydrochloric acid solution from which it is recovered by liquid/liquid extraction or ion exchange.[31,47]

A commercial facility to recover gallium, germanium, copper, zinc, and silver has been announced.[48,49] This operation reportedly uses previously mined material from an abandoned copper mine. The ore, which contains 0.025% Ga, is leached with acid and then the gallium is separated by liquid/liquid extraction.

Secondary recovery from gallium arsenide scrap constitutes a major source of gallium.

Summary

Gallium appears to be on the verge of a dramatic increase in use. The outstanding properties of electronic materials containing gallium are driving it into a wide variety of applications and the technology of device manufacture is rapidly improving. The combination of desirable properties and improved extraction methods should ensure a bright future for this interesting metal.

References

[1]P. de la Breteque, Gallium, Properties Principales, Bibliographie, June 1962, Aluminum-Industrie-Aktien-Geselschaft.

[2]E. Chin, "Gallium," Mineral Facts and Problems, U.S. Bureau of Mines, 1975 ed.

[3]Aluminum Co. of America; private communication.

[4]*Chemical Week,* September 21, 1983.

[5]R. Roy, V. G. Hill, and E. F. Osborn, *J. Am. Chem. Soc.*, **74**, 719 (1952).

[6]I. A. Sheka, I. S. Chaus, and T. T. Mityureva, The Chemistry of Gallium. Elsevier, New York, 1966.

[7]K. Wade and A. J. Banister, "The Chemistry of Aluminum, Gallium, Indium and Thallium"; Ch. 12 of Comprehensive Inorganic Chemistry. Pergamon, New York, 1973.

[8]J. S. Roberts et al., U.S. Pat. No. 4 377 504, March 22, 1983.

[9]A. I. Foster et al., U.S. Pat. No. 4 224 192, September 23, 1980.

[10]F. Branda et al., "Glass Transition Temperatures of Soda-Silica Glasses Containing M_2O_3 Oxides (M = Aluminum, Gallium, Indium, Selenium, Yttrium, Lanthanum), *Phys. Chem. Glasses*, **22** [3] 68–69 (1981).

[11]S. Barnier et al., "Study of Chalcogenide Glasses Containing Divalent Europium in the Europium Monosulfide-Gallium Trisulfide-Germanium Sulfide System," *Mater. Res. Bull.*, **15** [6] 689–705 (1980).

[12]W. H. Grodkiewicz et al., "Gallium Sesquioxide-Germanium Dioxide-Arsenous Oxide (As_2O_5) Glasses," *J. Non-Cryst. Solids*, **44** [2–3] 405–408 (1981).

[13]P. W. Angel, C. S. Ray, and D. E. Day, "Glass Formation and Properties in the System Calcia-Gallia-Germania," *J. Am. Ceram. Soc.*, **68** [11] 637–40 (1985).

[14]J. L. Piguet, J. C. Papp, and J. E. Shelby, "Transformation Range Behavior of Lithium Galliosilicate Glasses," *J. Am. Ceram. Soc.*, **68** [6] 326–29 (1985).

[15]R. H. Arendt, U.S. Pat. No. 3 736 222, May 29, 1973.

[16]R. H. Arendt, U.S. Pat. No. 3 833 349, September 3, 1974.

[17]*Chemical and Engineering News,* September 24, 1979; pp. 37–38.

[18]R. P. Mandal, "III-V Semiconductor Integrated Circuits, A Perspective," *Solid State Technol.*, **1**, 94–103 (1982).

[19]R. C. Eden, A. R. Livingston, and B. M. Welch, "Integrated Circuits: The Case for Gallium Arsenide," *IEEE Spectrum*, **2**, 30–37 (1983).

[20]J. M. Woodall, "III-V Compounds and Alloys: An Update," *Science*, **208** [5] 908–15 (1980).

[21]W. P. Rahilly, "Radiation Effects on Solar Cells," *Prog. Astronaut. Aeronaut.*, **71**, 365–85 (1980).

[22]H. W. Brandhorst, D. Flood, and I. Winberg, "Gallium Arsenide Solar Cells — Status and Prospects for Use in Space"; pp. 409–15 in Proceedings of the Intersociety Energy Conversion Engineering Conference, Vol. 1. American Institute of Aeronautics and Astronautics, NY, 1981.

[23]T. Andrade, "Manufacturing Technology for GaAs Monolithic Microwave Integrated Circuits," *Solid State Technol.*, **2**, 199–205 (1985).

[24]W. Sponsler, "Lightwave Sources and Detectors," *Solid State Technol.*, **3**, 93–101 (1981).

[25]Encyclopedia of Chemical Technology, Kirk Othmer, 1977 ed., Vol. 11; p. 619.

[26]J. G. Posa, "Innovative Circuit Techniques Propel Digital GaAs Devices Toward LSI and VLSI Densities," *Electronics*, February 24, 1982; pp. 112–16.

[27]M. J. Haves and D. V. Morgan, (eds), Gallium Arsenide, Materials, Devices, and Circuits. Wiley & Sons, New York, 1985.

[28]D. K. Ferry (ed), Gallium Arsenide Technology. Howard W. Sams & Co., Inc., Indianapolis, Indiana, 1985.

[29]Properties of Gallium Arsenide. INSPEC Institution of Electrical Engineers, New York and London, 1986.

[30]A. D. Weiss, "Substrates Review: Silicon, Sapphire, and GaAs," Semiconductor International, pp. 66–71, 1983 June.

[31]"Gallium: Long Run Supply," CRA Report 483, Prepared Under Contract XS-9-8258-1 for Photovoltaic Analysis and Evaluation Branch, SER Charles Rivers Associates, Inc., June 1980.

[32]"Survey of Availability and Economical Extractability of Gallium from Earth Resources," Alcoa, Pittsburgh, PA, October 1976.

[33]R. L. Watts et al., "The Evaluation of Critical Materials for Five Advanced Design Photovoltaic Cells With an Assessment of Indium And Gallium," Preliminary Report Prepared Under DOE Contract EY–76–C–06–1830, Battelle Pacific Northwest Laboratory, February 1980.

[34]L. K. Hudson, "Gallium as a By-Product of Alumina Manufacture," *J. Met.*, September 1965.

[35]F. C. Frary, U.S. Pat. No. 2 582 378, January 15, 1952.

[36]M. Beja, U.S. Pat. No. 2 574 008, November 1951.

[37]J. L. Dewey et al., U.S. Pat. No. 3 890 427, June 17, 1975.

[38]P. de la Breteque, Swiss Pat. Nos. 333 169 and 333 264, November 29, 1958. See also *J. Met.*, 11, 1528–29 (1956).

[39]G. Sinka et al., U.S. Pat. No. 4 362 606, December 7, 1982.

[40]C. G. Honey et al., Can. Pat. No. 1 072 043, February 1980.

[41]W. Westwood et al., Br. Pat. No. 1 519 452, July 1978.

[42]P. de la Breteque et al., U.S. Pat. No. 3 887 681, June 3, 1975.

[43]J. Helgorsky and A. Leveque, U.S. Pat. No. 3 971 843, July 27, 1976.

[44]Y. Kataoka et al., U.S. Pat. No. 4 468 374, August 28, 1984.

[45]*American Metal Market*, May 3, 1985, p. 1.

[46]Mitsui Aluminum, Japanese Patent Application JP85 166 224A–KoKai, February 3, 1984.

[47]H. Abe et al., "Recovery of Gallium and Indium at Dowa Mining"; presented at Fourth Joint Meeting MMIJ-AIME 1980, Tokyo.

[48]*Chem. Eng.*, February 20, 1984; p. 17.

[49]Mineral Commodity Summaries, U.S. Bureau of Mines, 1986.

Analytical Procedures for Alumina Chemicals

Editor's Note

Unforeseen circumstances made it impossible to complete this important chapter before publication of the book. Following are some general recommendations on where to find information on analytical methods.

The best sources of information on analytical methods for alumina chemicals are the major producers of these products. Firms such as Alcoa, Alcan, and Kaiser have spent many years and large sums of money developing and publishing analytical methods for characterizing the wide range of alumina chemicals and the myriad of end-products derived from these basic raw materials. These procedures include elemental and compound analyses by a large number of techniques, physical test methods, engineering properties determinations, and surface characterization methods.

Information on analytical methods can also be found in the literature published by organizations such as the International Standards Organization (ISO), the American Society for Testing Materials (ASTM), the Australian Standards Organization (ASO), and the American Ceramic Society (ACerS). Misra[1] briefly summarized analytical procedures for aluminum hydroxides and activated aluminas. There are some references to analytical methods in the various chapters of this book.

It is hoped the next edition of this book will include a chapter with comprehensive information on analytical procedures for these products.

Reference

[1]C. Misra, *Industrial Alumina Chemicals*. ACS Monograph 184; Washington, D.C., 1986.

SECTION IV

State of the Art Assessments *in* Applications Utilizing Alumina Chemicals

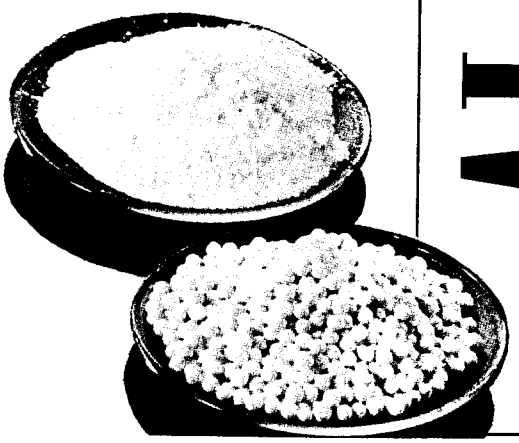

Alumina Chemicals as Additives for Paper, Dentifrices, Paints, Coatings, Rubbers, and Plastics with Emphasis on Fire-Retardant Products

Larry L. Musselman
AMAX Technical Center
Apollo, PA 15613

In the follow-up to earlier chapters covering selected applications of the various alumina chemicals, this chapter covers the details of major commercial additive uses in paper, dentifrice systems, paints, coatings, rubbers, and plastics. In addition, some of the less well-known applications like adhesives, pharmaceuticals, cosmetics, waxes, and polishes are mentioned.

The major direct chemical applications using aluminum hydroxide as the base reactant in sodium aluminate, zeolite, alum, aluminum fluoride, and titanium dioxide manufacture were discussed in previous chapters. The closest to an alumina chemical use as a true *additive* from this group was the TiO_2 pigment application. The real additive in that case, however, is the titanium dioxide since alumina is used only to enhance TiO_2 properties. This section will deal primarily with systems in which an alumina chemical is defined as an additive because it gives higher value properties to a matrix without changing chemically or structurally. Specific alumina chemical product forms, properties attained in the matrices, and methods of application are reviewed.

Early production of alumina chemical additive products was first carried out in a small scale experimental plant by the Aluminum Company of America from 1920 to 1948. The first larger scale production of the forerunners of today's coarse, white precipitated hydrate* and fine precipitated hydrate* products began in an East St. Louis plant in 1944 and 1946, respectively. By 1960, these materials[1] were being widely used as pigments, embodying agents, and reinforcing additives in paper, rubber goods, and mild abrasives. The real growth with these types of additives has come more recently with the increased usage of high-gloss, high-brightness, and carbonless types of paper and with the phenomenal sustained growth rates of the polymer industries over the last twenty years.

Uses of Aluminum Hydroxide in Paper

Once the larger scale commercial capacity for fine aluminum hydroxide was established in 1946, domestic paper use grew rapidly to over five million pounds annually by the early 1950s. Two major paper application categories evolved after a second major expansion in production facilities allowed tighter quality control on hydroxide particle size, impurity levels, and whiteness in the early 1960s. These categories were (1) as an embodying filler and (2) eventually as a paper coating pigment or additive. Expansions in these applications led to an estimated usage in the U.S. paper industry of over 70 million pounds by the late 1970s. The growth was attributed to the value in paper established by improvements in process technology involving hydroxide product brightness and uniformity.

All of the product grades shown in Table III of "Production Processes, Properties, and Applications for Aluminum-Containing Hydroxides" have been used in various forms of paper. Median particle sizes ranging from 0.5 to nearly 2 μm have found the largest volume use in specific paper applications. Some aluminum hydroxide products are specially prepared for wet end papermaking processes; others are shipped in bulk (by agglomerating with dispersants) to papermaking locations. Historically, only a relatively sharp (narrow)† distribution, precipitated alumina trihydrate had been used in paper processing; however, recently much broader, ground grades have been approved for use at some major paper mills. This reevaluation of hydroxide type first began occurring in the United States in the early to mid-1980s. This was followed by some conversion more recently in Europe and other nondomestic locations.

In the filler application, extremely good dispersability and very high retention are noted as the main advantages of aluminum hydroxide. In fact, addition of certain hydroxide grades improves retention of the other fillers and pigments, including clay and TiO_2. Improved ink receptivity[2,3] is also noted. In coatings, in addition to retention and ink receptivity, aluminum hydroxide has been documented to increase opacity, gloss, brightness, and smoothness[4,5] of the paper. Some of these advantages are summarized in Table I.

*See Tables II and III in "Production Processes, Properties, and Applications for Aluminum-Containing Hydroxides".

†All particles in the distribution are very close to the median.

Table I. Advantages of Alumina Trihydrate in Paper Coating*

Higher brightness (Tappi T–452)
Higher gloss (Tappi T–480)
Higher smoothness (Sheffield test)
Better hiding for opacity level
Better ink receptivity
Better flame retardancy

*Using a 62% solids casting (50% clay, 10% TiO_2, 40% H–705) in 17% casein-latex binder.

In the early 1960s, optical brighteners or special types of dyes began to be widely used to increase visual brightness of white paper over that obtainable by bleaching or using fillers.[6] Because of the high ratio of hiding power to opacity of aluminum hydroxide and decreased ultraviolet radiation degradation compared to titanium dioxide and $CaCO_3$ in paper, aluminum hydroxide grades were used at that time to displace part of the TiO_2 and all of the calcium carbonate in many coating systems.[7,8] Optical brighteners depend on ultraviolet radiation for activation. This radiation is potentially degrading to polymers and other papermaking ingredients. Aluminum hydroxide does not absorb in the uv range and, therefore, does not contribute to polymer degradation. Aluminum hydroxide was used when lower binder usage was required or when one of the other properties noted above specifically needed improvement. Aluminum hydroxide has even been used to displace some of the low-cost primary paper filler and china clay.

In these applications, two precipitated aluminum hydroxide grades have stood out over the years — the 1.0 μm median (6–8 m^2/g) and 0.5 μm median (10–18 m^2/g) grades. In filled sheet, the optical properties are similar for the 1.0 and the 0.5 μm grades. However, in coatings the 0.5 μm material gives better brightness and higher calendered gloss and printability. Both grades can give over a 30% reduction in the supercalendering pressure.[8] This usually also results in an appreciable increase in tear strength. Specific tests with 0.3 to 0.5 μm median aluminum hydroxide showed as much as a 60% reduction in supercalendering pressure over a similar calcium carbonate coating.[8] The smoothness and calendered gloss at these lower pressures were similar or better. The same results were found with a 25% substitution of 0.3 to 0.5 μm median aluminum hydroxide for TiO_2.

Table II shows an example of a pilot coater test formulation to compare properties of a 0.3 μm aluminum hydroxide with a 0.25 μm similarly shaped calcium carbonate.[8] The pressures needed for the ATH (alumina trihydrate) coatings were about one-third that needed for calcium carbonate. Less steam was required also. The ATH coatings were significantly brighter, had greater ink receptivity, and ink absorption was more uniform.

Table II. Coating Formulations and Properties

	Coating C	Coating A
Formulation		
No. 1 clay, parts	50	50
$CaCO_3$, 0.25 μm, parts	40	
Alumina ATH, 14 m^2/g, parts		40
TiO_2 (anatase), parts	10	10
Binder (casein-SBR latex), % on pigments	17	17
Properties		
Percent solids	61.8	62.1

Supercalendering Conditions for 40% Alumina Trihydrate (14 m^2/g) Coating and 40% Calcium Carbonate Coating

	Coating C (calcium carbonate)		Coating A (alumina trihydrate)	
Pressure, lb/in.	500	1320	165	380
Steam, lb/h	2	2	1	1.5
Number of nips	4	4	4	4

Physical and Optical Properties of Supercalendered Sheets, 40% Alumina Trihydrate (14 m^2/g) Coating and 40% Calcium Carbonate Coating

Coat weight, lb/3300 ft^2	6.4	6.4	6.0	6.0
Specular gloss (75°), T480	51	68	49	62
Brightness, T452	84.1	82.6	86.2	85.7

Printing Properties of Supercalendered Sheets, 40% Alumina Trihydrate (14m^2/g) Coating and 40% Calcium Carbonate Coating

Ink receptivity (K&N), RC-19	70.6	77.0	59.6	60.8
Gloss ink holdout	84.0	86.3	78.3	84.0
Freedom from ink mottle	0	0	100	75

Table III shows that 25% substitution of ATH for TiO_2 in extended coatings gives little or no loss in optical properties, and gains in smoothness, gloss, and printability were observed.[8]

Coating binder demand, high shear viscosity, and handling of fine powders can be problems in high-volume, high-solids-concentration coatings. In addition to the standard dry forms of hydroxide, a precipitated spray-dried product containing dispersant is available for easier handling and slurried forms from 55 to 70% solids have been recently reintroduced to the market for enhanced processing into paper applications. Typical dispersants include sodium polyacrylates, diammonium phosphates, and sodium hexametaphosphates, as well as several organic complexes. Dispersant concentrations can range from 0.2 to 2% and depend on the product particle size, surface area, and shipping/handling requirements.

The largest growth application for aluminum hydroxide in paper coating applications in the last 15 to 20 years has been in carbonless paper. The future growth potential appears to be in fire-retardant grades of paper products. Because of the higher value of aluminum hydroxides in other applications and higher production costs compared to modified clays and special calcium carbonates, consumption of hydroxides in paper has decreased in recent years. Currently, pricing on competitive products is increasing which may reverse this trend although a complete comeback is unlikely.

The Use of Aluminum Hydroxide in Dentifrice Applications

The earliest uses of domestic commercial large volume aluminum hydroxide in dentifrice systems which were documented previous to the late 1950s primarily described only uses of the 1 μm median particle size grades.[1] One use was as bodying agents to increase the thixotropy of new pastes. The idea was to increase the viscosity at low shear to keep pastes from running off the brush. Another earlier application was in tooth powder, where the soft, smooth texture and absence of grit were the most desirable features. These attributes of the fine precipitated hydrate grades also made them natural components of early cosmetic base creams.

The major aluminum hydroxide use in current dentifrice applications is as a mild abrasive in therapeutic and nontherapeutic pastes and powders for tooth cleaning, gum massage, and other mouth hygiene applications. Dentrifices for oral hygiene date back to ancient Egyptian literature where vague formulas were used for removal of objectionable mouth tastes and odors and for reducing dental pain. However, not until modern times (1930s) was the polishing of tooth surfaces the major emphasis. It has been even more recently (since the 1950s) that therapeutic concepts like fluoride as well as other caries, plaque, and tartar breakdown/prevention aids have been connected to the mild abrasives in dentrifices. For these applications, slightly coarser, broader particle-size distribution aluminum hydroxides were the first to be used. Initially, some of the largest volume usages were with 7 to 10 μm median ground grades. Specific applications have also made use of combinations of precipitated and ground hydroxide grades for unique results.[9]

The properties that make aluminum hydroxide uniquely suited as a mild abrasive in dentifrice include: the whiteness of certain grades, Mohs hardness of 2.5 to 3.5 (well below that of tooth enamel, cementum, and the softer dentin found under the gum line), relatively low flavor, and therapeutic additive adsorption,[10] a more palatable texture than light chalks or other calcium carbonates and a unique particle wear phenomenon that cleanses by rounding edges of hydroxide particles rather than roughing up the tooth surface.[‡] Table IV shows the results of this phenomenon in a comparison test of brushing actual extracted human teeth. One of the lowest reductions in tooth material loss, as measured in millimeters, was found with aluminum hydroxide (hydrated alumina), yet adequate polishing and tooth cleansing is maintained.

Although all domestic dentifrice pastes now use polymer or polymer inside coated tubes or other plastic consumer packaging containers, one early drawback to hydroxide use in pastes was a possible paste stability problem that was loosely connected to corrosion in unlined aluminum containers. This problem

[‡]Most of these same attributes allow slightly coarser ATH grades (6–8 μm) to be used in cleaning type waxes and polishes.

Table III. Properties of Alumina Trihydrate (1.0 μm) Extended Coatings

Clay (%)	TiO_2 (%)	ATH (%)	Br. Gain	Op. Gain	75° Gloss Gain	Smoothness Gain (s)	Larocque Printability
90	10.0	0	14.0	5.3	15.0	132	92.0
90	7.5	2.5	15.0	5.0	22.4	148	92.2
90	5.0	5.0	13.7	4.8	26.0	150	92.8
90	0	10.0	12.7	4.3	24.0	156	92.7

Uncoated paper base–35# Coating Rawstock: BR = 52.3, Op = 89.1
Binder composition–8% starch + 8% SBR latex
Coating weight–8 lb/3300 ft^2. Supercalendered 2x at 1500 PLI

Table IV. Rotary Brush Abrasion of Human Teeth

Abrasive	Abrasion Loss (mm)
Calcium carbonate, extra dense	0.012
Light chalk, USP -	0.003
Extra light chalk, USP	0.003
Bentonite	0.006
Flour of pumice	0.300
Calcined alumina	0.300
Hydrated alumina (aluminum hydroxide)	0.002
Dibasic calcium phosphate, anhydrous	0.021
Tribasic calcium phosphate, $Ca_3(PO_4)_2$	0.001
Stannic oxide, CP	0.083
Zinc oxide	0.003
Calcium pyrophosphate, $Ca_2P_2O_7$	0.005
Magnesium trisilicate	0.009

was solved in a number of ways but one simple solution is the incorporation of 1% calcium carbonate with 34 to 59% aluminum hydroxide in the dental cream.[11] In a related concept, improvement in the free fluoride for therapeutic pastes is accomplished by addition of insoluble sodium metaphosphate[12] to the aluminum hydroxide abrasive package. Other proprietary unpublished techniques have been used to improve the compatibility of alumina mild abrasives in specific applications. Work on surface treatments to make hydroxides compatible with various inorganic[13] and organic mediums is continuing.[14]

The domestic dentifrice industry is made up of four major suppliers who in 1985 had approximately 95% of the market and perhaps as many as 20 smaller share suppliers. The growth rate of dentifrices in the 1980s has been astounding, growing more in the most recent five-year period studied than it did in the previous 15 years put together. Dentifrice products usage in the United States alone passed the $1 billion mark in 1985 and made selected use of mild polishing aids at loadings from 20 to 60% by weight. The dentifrice market share lead has traditionally shifted every so often with two leaders hovering around 30% share each, followed by the next two largest share suppliers at 17 to 18% each.

Dentifrice paste is generally processed in large batch mixers with combination or separate deaeration systems. A 3000 liter blender would be typical, with special ports and dispensing units for the precise metering of additives in small quantities uniformly throughout the mix. The newer systems can operate under vacuum, pressure, or atmospheric conditions and are jacketed for temperature control. Mixing is accomplished by agitator mechanisms as simple as a Hobart blender design to complex combinations of anchor stirrers, blade stirrers, and homogenizing turbines all rotating at once. When processing is complete (may be up to 14 hours/batch), the material is discharged to large (up to 100 gallon) drums for storage or pumped to extrusion lines for packaging into tubes.

Techniques for aluminum hydroxide introduction into dentifrice vary and are proprietary, as are the specific grades and concepts used to make hydroxide surfaces compatible with other component chemistries. The trends are toward very specialized higher technology materials unique to each type of dentifrice application. Examples of early nonfluoride and fluoride formulations using aluminum hydroxide are shown in Tables V and VI, respectively.

The volume of aluminum hydroxide used in the dentifrice industry should continue to grow with the projected increases in dentifrice usage. Major increases beyond this will have to be preceded by continued research and further implementation of the current knowledge base in alumina surface technology. Specifics will have to include making systems using aluminum hydroxide more stable with new therapeutic aids, flavors, and other functional additives. The high purity available and other properties mentioned above with the highly refined aluminum hydroxides used in FDA approved dentifrices allows many other pharmaceutical applications like aluminum chlorohydrate production for antiperspirants and use in several leading stomach antacid products.

Aluminum Hydroxide in Paint and Coating Applications

The earliest use of aluminum hydroxide in coatings was as a bodying agent in varnish and oil paint where 1 μm grades were used to increase viscosity.[§] Because of its lower refractive index compared to TiO_2, for example, low-level use in varnishes did not substantially reduce the clarity. In water-based paints, on the other hand, there was some early use as an opacifying agent at higher loadings.

This opacifying power led to paint research in the 1960s to determine the effects of aluminum hydroxide as a pigment in latex paints. It was determined that 0.5 μm (14–20 m^2/g) precipitated aluminum hydroxide could be substituted for up to 25% of the titanium dioxide in vinyl acetate latex coatings without reducing the opacity of the formulation.[15] Efficient hiding power, higher gloss, higher brightness, and lower costs are all advantages of this phenomenon. Part of the mechanism postulated in Ref. 15 for the effectiveness of aluminum hydroxide is related to both particle

[§]A combination of the cold cleansing action mentioned earlier and the bodying and opacifying effects of the high-purity 1 μm grades of aluminum hydroxide led to use as a base for several cosmetic creams and makeups, also.

Table V. Example of a Nonfluoride Toothpaste Formulation

Hydrated alumina (%)	50.00
Water	21.25
70% sorbitol	12.50
Glycerin	12.50
Sodium lauryl sulfate	1.50
Magnesium aluminum silicate	1.00
Flavor	1.00
Cellulose gum	0.25

Table VI. Example of a Fluoride Toothpaste Formulation

Hydrated alumina (%)	50.00
Water	17.94
Glycerin	15.00
Sorbitol	13.00
Sodium lauryl sulfate	1.00
Sodium carboxymethylcellulose	1.00
Flavor	0.90
Sodium monofluorophosphate	0.76
Sodium monohydrate phosphate	0.25
Sodium benzoate	0.10
Sodium saccarin	0.05

reflection and the spacing of TiO_2 particles due to the geometries and size of the aluminum hydroxide.

While titanium dioxide primarily contributes to opacity and hiding because of its high refractive index, aluminum hydroxide's contribution to hiding is secondarily due to refractive index. The more important effects with small particle size hydroxide are due to the reflection, light scattering, and light diffraction properties when combined with titanium dioxide. The theory is based on the fact that hiding power of titanium dioxide is increased as the spacing between particles approaches one TiO_2 particle diameter. This effect evidently reaches a maximum at a loading of one part aluminum hydroxide to three parts titanium dioxide in vinyl acetate coatings. Beyond that concentration too much dilution of the higher refractive index material must take place, as shown in Fig. 1.[15]

Figure 1 is simply the brightness of the paint film measured against a black background contrasted to the same measurement against a white background. Figure 2 clearly shows that the effect is more efficient with aluminum hydroxide (0.5 μm hydrated alumina in a 3 mil wet film) than 100% titanium dioxide or the same ratio of similarly sized calcined clay or calcium carbonate. This same effect has been demonstrated in acrylic latex coatings using up to 28% aluminum

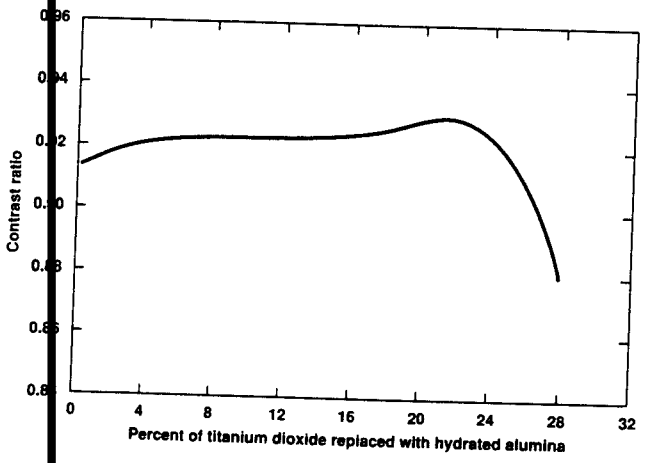

Fig. 1. Effect on contrast ratio of substituting hydrated alumina for titanium dioxide at a 3 mil wet-film thickness level.

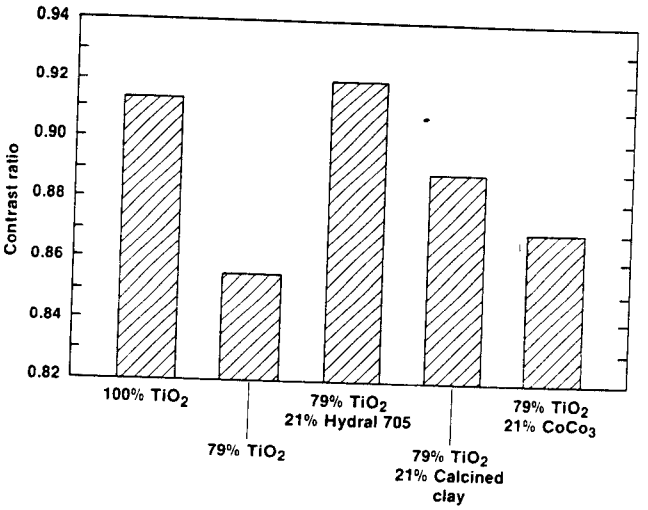

Fig. 2. Effect on contrast ratio of replacing 21% of the titanium dioxide with hydrated alumina at 3 mil wet-film thickness level.

hydroxide,[16] as has the good scrubbability, sheen, gloss, viscosity, pH stability, and enamel holdout. In addition, Table VII shows that aluminum hydroxide reduces the pigmenting color needed in tinted paints to maintain the same shade and hiding power. This phenomenon allows a 25% ATH/75% TiO_2 loading to be even more cost-effective than simply reducing the titania concentration. Since titanium dioxide is such a strong whitener, it takes more expensive coloring pigment to overcome the whitening power of 100% TiO_2 or the opacifier blends mentioned earlier than the ATH/TiO_2 blend with the same hiding power.

The effects shown in the table are true regardless of tint color. The table data were measured in a gray tint. Other tints showed similar differences. All of the data noted above were rechecked with reproducible results on 4-, 6-, and 12-month storage samples. In addition, confirming data are also available using similar sized aluminum hydroxide in polyvinyl acetate, butadiene-styrene, and semigloss enamel systems.[17] Table VIII shows a typical example of an aluminum hydroxide use as a titanium dioxide extender in PVA.[18]

Aluminum hydroxide has been documented in a wide range of fire-retardant coatings including ablative, sublimative, intumescent, and reflective. Generally they are described as mastics, reactive systems, or nonreactive nonflaming fire barriers. In terms of the total volume of coatings, these fire-retardant coatings

Table VII.* Color Variation in Tinted Paints†

Pigment Extender	Color Change
Aluminum hydroxide	0.2
Calcium silicate A	2.5
Calcium silicate B	1.4
Sodium silicoaluminate	2.4

*Ref. 15.

†Compared to a TiO_2 control.

Table VIII. Hydral 705 as TiO_2 Replacement in a Latex Coating

Formulation	Pounds Per Hundred of Formulation
PVA	16.71
Hydral 705	3.30
TiO_2	12.09
Tamol 731	0.70
2½% natrosol solution	19.79
KTPP	0.09
Colloid 581 B	0.26
Phenyl mercury acetate	0.04
Ethylene glycol	1.32
Carbitol solvent	0.88
Duramite	17.59
Glomax LL	6.60
Tergitol NPX	0.18

are very small volume; however, their value is high and increasing. The largest markets for these types of coatings have been petrochemical plants, government and defense applications, and general construction uses.

Mastics have generally been used in construction/roofing applications. A typical example of a fire-retarded acrylic mastic roof coating is shown in Table IX. Intumescent coatings usually protect wood, steel, or aluminum in construction. Ablative or sublimative coatings are used in more exotic situations like the

Table IX. Acrylic Roof Coating

Cowles Grind*	lbs/100 gal.
Water	140.0
Ethylene glycol	25.6
Foamaster VL	4.0
KTPP	1.5
Rhoplex EC-1895 (61%)	116.4
R-960 (TiO_2)	88.8
Duramite ($CaCO_3$)	387.9
Kadox 515 (ZnO)	59.2
7–8 μ	145.0
Natrosol 250 MR	3.5
Letdown	
Rhoplex EC-1895 (61%)	315.4
Foamaster VL	6.0
Texanol	7.8
Skane M-8	2.3
Ammonium hydroxide (28% NH3)	7.1
% solids by weight	73.1
% solids by volume	56.7
Pigment/binder	2.58/1
PVC	48.1
Wgt./gal.	13.0
pH/viscosity (KU)	9.9/102

*Add in order as specified to facilitate pigment addition. Grind at high speed for 15 min, then letdown with minimum agitation. Before letdown reduce speed to slow and position impeller just below the surface of the grind. Stop the impeller and add the EC-1895 and Foamaster VL, resume agitation at low speed, and continue adding the other letdown ingredients.

finish on missile or rocket firing aircraft or as protection against reentry heat generated by atmospheric friction. Many of the fire-retardant classification and application terms are used interchangeably by paint or coating manufacturers and much more discipline will have to come to the nomenclature as this area grows.

An example of an ablative system showing the synergistic effect of aluminum hydroxide and borate compounds as fire retardants was demonstrated in an epoxy/polysulfide coating resin that also used refractory fibers to withstand 2801°C (5100°F) short duration and 1093°C (2000°F) longer duration tests, and then finally full service tests of the Zuni 5-inch rocket on the AH-IT helicopter.[18] The self-curing coating, which is easily applied to existing structures, forms a rigid ceramic char as part of the system melts/vaporizes away with considerable absorption of heat in a fire situation. A similar concept is described for use on wire and cable jacketing based on an acrylic resin emulsion and polyamidemide fibers in Ref. 19. Clark[20] reviewed another ceramic char-forming system, combining water-soluble borate and aluminum hydroxide in a vinyl acrylic latex binder, for coating fiberglass for FR thermal insulation.

Many aluminum hydroxide fire-retardant applications have been defined in coatings and adhesives for construction boards and other building products. Examples abound in the literature including: vinyl acetate on polyester fiberboard,[21] synergistic effects between aluminum hydroxide and antimony oxide in formaldehyde-melamine-phenol for cellulosic board,[22] aluminum hydroxide coupled to the substrate with titanate/zirconate surface treatments,[23] aluminum hydroxide in urea resin with chlorinated paraffin as a fire-retardant synergist,[24] and so on.

Coatings that bond as well as supplying fire protection with aluminum hydroxide are described for wood substrates layered with aluminum foil[25] and for general use in multilayer construction boards,[26] as well as for fabrics layered with flexible PVC[27] or rigid fabrics stiffened by impregnation with high loadings of aluminum hydroxide in acrylimide ethylene vinyl chloride copolymers.[28]

Fire-retardant coatings can also be used on more flexible substrates such as ordinary use fabric. Unfortunately, most systems of this type with enough aluminum hydroxide to be effective lose some of the "hand" or flexible feel we are used to and are higher density than their nonfire-retardant counterparts. Typical examples found in the literature include: aluminum hydroxide in binders like acrylic acid-butadiene-styrene copolymers,[29] ATH in neoprene-based latex covers for cotton upholstery,[30] styrene butadiene rubber-based latexes generally mixed 50/50 with aluminum hydroxide,[31] polyvinyl chloride- or PVC/ATH-filled binders or coatings for substrates from cloth to electrical cable base fabrics,[32–34] aluminum hydroxide in urea coating compounds,[35,36] and ATH mixed with other fire retardants like phosphorus-based liquids.[37]

Although polyurethane foams do not fall into the "fabrics" coatings category, three examples are included here because they fall closer to the coated substrates concept than a normal compounded polymer category. The first is a layered effect using a higher density foam coating of tougher polymers that are more forgiving to higher loadings of aluminum hydroxide to protect polyurethane foam moldings.[38] Second, aluminum hydroxide has been documented to protect polyurethane substrates by using high loadings in neoprene latex coatings.[39] Finally, flexible, high-resiliency polyurethane foam can be made flame-resistant by saturating the open-celled foam with a dispersion of aluminum hydroxide in a flexible halogenated coating. The higher the aluminum hydroxide loading in the binder, the higher the flame retardancy. Loadings of 150 to 200 parts hydroxide to 100 parts binder, then adding a 1 to 1 by weight ratio of this mixture to the polyurethane foam, provided adequate flame ratings.[153] This halogenated latex binder concept has also been applied to fabrics in the same way as reported in several earlier references using varying loadings of aluminum hydroxide, chlorine content, and other particulate fire retardants like antimony oxide to show the increased flame retardancy with both higher loadings and synergistic combinations of these three types of components.[40–42]

Paints and coatings have taken these discussions from TiO_2 extender applications to fire-retardant applications. Before venturing into the complex high-volume uses in other polymer applications, some more detail on aluminum hydroxide, fire/smoke, and arc/track mechanisms will be useful.

Fire Retardance of Aluminum Hydroxide in Polymers

The basic mechanisms by which aluminum hydroxides retard fire and suppress smoke in elastomers and plastics were reviewed in the earlier chapter "Production Processes, Properties, and Applications for Aluminum-Containing Hydroxides," Eqs. (2) and (3), and Figs. 22 through 25.[43] It is important to look again at some specific aspects of that phenomenon in terms of polymers and polymer processing. Heat capacity followed by hydroxyl release/endothermically converting to water in air was the basis for that retardance. From the formula $Al(OH)_3$ for aluminum hydroxide, Newsome et al.[44] determined that approximately three moles of water would be formed per mole of alpha alumina (α-Al_2O_3) on complete dehydration. Based on this, they plotted the time/temperature histories of the residual moles of water left in aluminum hydroxide per mole of alumina that would be formed by thermal dehydroxylation at specific temperatures over time. We know from Fig. 24 in this chapter,[43] that at a heating rate of 20°C per minute there is very little aluminum hydroxide degradation until 230°C under normal conditions for polymers that process below that temperature. However, Fig. 3[44]

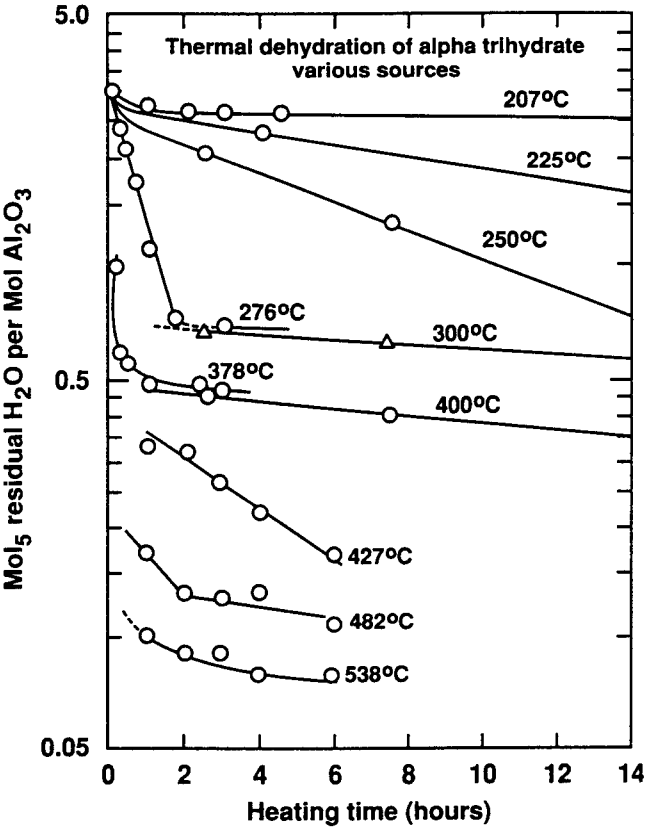

Fig. 3. Thermal dehydration of aluminum trihydroxide in relation to time and temperature.

shows that aluminum hydroxide will degrade at lower temperatures if held at a high temperature for long periods of time.

Normal final polymer part processing takes only seconds and very rarely more than minutes, but if conditions are such that an extremely long polymer working time at temperatures above 200°C can occur in final product forming, it is possible that hydroxide release can contribute to free moisture in the compound and surface defects on finished products.

The fire-retarding and smoke-suppressing mechanisms of aluminum hydroxide do not interfere with other fire retardants and, in fact, can act synergistically in polymers. Proof of this will be given in later sections on unsaturated polyesters and PVC. Some of the reasons for this include the fact that there are two distinct phases in polymer burning or degradation: (1) the *condensed* phase which involves the solid (or virgin) polymer (and the degrading or melting surface if thermoplastic) and (2) the *gaseous* phase which involves the flame caused by the burning of volatiles (or fuel) that is emitted from the polymer surface. A third area (3) is the *interface* between these two phases which may be used to form a barrier (or char) between the phases. This barrier can slow burning by causing a break in the cyclic combustion process. Figure 4 shows an artist's conception of a burning polymer

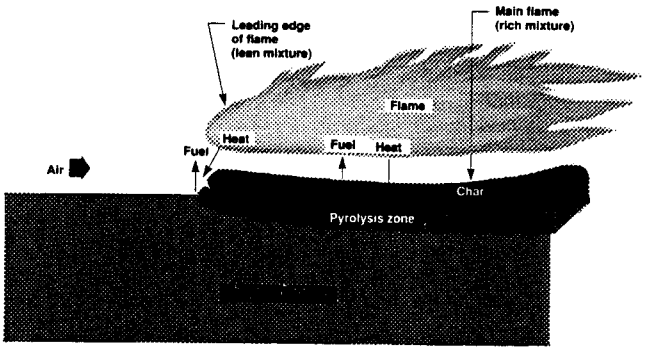

Fig. 4. Schematic of burning polymer.

surface,[42] detailing the solid polymer, char, and fuel zones.

Individual fire retardants can successfully act in any one of these three areas. Since most other high-volume fire retardants act either in the gaseous phase or surface barrier area, and aluminum hydroxide acts in the condensed phase or solid polymer, it does not generally interfere with other fire-retardant mechanisms. In certain cases, hydroxides have been shown to actually enhance the effects of other materials. On the other hand, later in the section on PVC, data are reviewed that show nonhydroxide fire retardants can actually react antagonistically toward each other and give a reduced fire rating when combined.

Figure 5 simplistically describes the cyclic polymer combustion/pyrolysis process. As noted in the

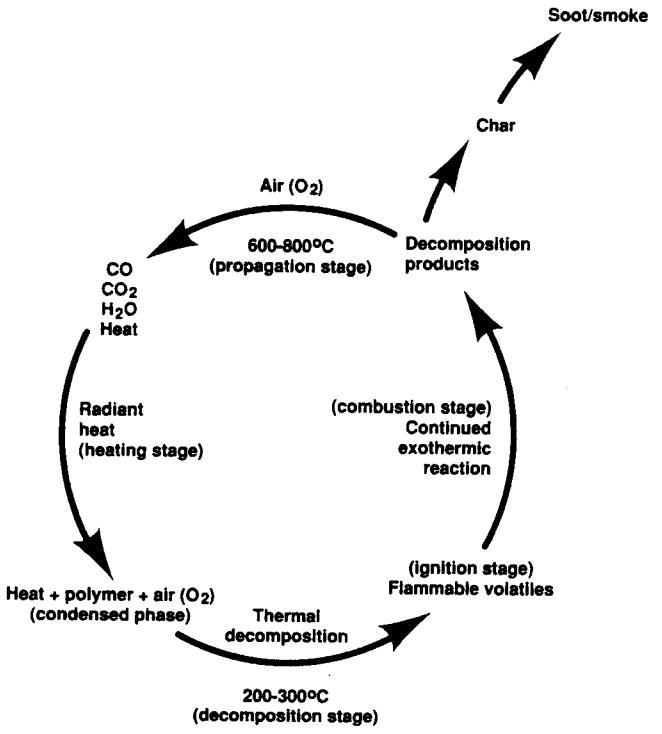

Fig. 5. The cyclic process of fire propagation in polymers.

Hydroxides chapter, Fig. 23, and more explicitly here in Fig. 5, the polymer pyrolysis reaction can be self-propagating if allowed to initiate and continue without inherent or added flame retardance. This retardance is obtained by modifying either one of the phases mentioned above or the surface between the phases.

We have already described the heat capacity/heat sink and endothermic reaction mechanisms of hydroxides in the earlier chapter. By adding aluminum hydroxide to the polymer, we have modified the condensed phase (virgin polymer) with an endothermic additive. The surface between the phases may also be modified by the addition of char formers like the phosphates and borates mentioned previously. In a fire situation these materials can form tough, glassy char layers between the polymer and the heat source, cutting off the gaseous phase or fuel phase from evolving and thereby breaking the fire-propagation cycle. A third way to retard fire is by modifying the gaseous phase. This can be accomplished with halogens alone, by free gas-phase radical scavenging[45] or by gas radical recombination.[46]

Free radical scavenging can be explained most simply by using methane (CH_4) as a model for a polymer burning. Oxidation of methane forms OH– and H– free radicals instantly which react with other CH_4 molecules to form CH_3, water (H_2O), and H_2. Further oxidation forms CH_2O and H, which continues the propagation using more oxygen, liberating more OH and H radicals until CO and finally CO_2 is formed. The propagation is broken by free radical scavenging when a halogen (Br, Cl, etc.) is liberated and ties up H as in HBr, for example, then further reaction with OH forms H_2O and the less reactive Br free radical.

The propagation can also be broken by "free radical recombination" when a material like sodium bicarbonate ($NaHCO_3$) or antimony oxide (Sb_2O_3) in combination with a halogen is added. At flame temperature, either the sodium radical reacts with OH to form sodium hydroxide (NaOH), H_2O, and CO_2 gas or antimony reacts with HCl gas or HBr to form SbOCl or the bromine analog. SbOCl or SbOBr then decomposes above 170°C to form volatile $SbCl_3$ that oxidizes in the flame back to fine but heavy Sb_4O_6 particles, which in turn form sites for H and OH recombination and HCl formation. In either case, the reduction of H and OH concentration slows the burning process. The unfortunate part of either the char formation or antimony and halogen use for radical scavenging or recombination is the dark, sooty, smoky particles created as the char develops or the antimony oxide precipitates with its trapped free radicals. Halogens further complicate this picture with the formation of HBr and HCl corrosive gases. This vision-obscuring/smoking phenomenon is demonstrated visually in the following sections on elastomeric carpet backing and unsaturated polyesters.

On the other hand, aluminum hydroxide, which evolves water, is noncorrosive and of itself adds no toxic or smoky fumes to a fire situation. Hydroxides dilute the smoke from burning polymers, extending escape time by allowing visual clarity to temporarily see exit signs in fire situations. Mechanisms which involve free radicals have become the center of many serious debates recently,[47] including claims that certain types of free radicals can be the cause of death where heat, flames, or known toxins like carbon monoxide gas have been shown *not* to have been inhaled.[48]

Arc and Track Resistance of Aluminum Hydroxide in Polymers

After fire retardancy, the second largest technical use for aluminum hydroxide in polymers is for suppressing electrical arcing and tracking. In the early 1950s, Rostone Corporation employees[49] discovered that high loadings of ATH could reduce formation of conductive carbon paths or carbon tracking that occurs when polymer surfaces break down in the presence of electrical charge. Kessal[50] described the action of aluminum hydroxide as a carbon scrubbing mechanism. The formation of this carbon on the polymer surface concentrates the electrical field, causing further carbonization and leading to a complete breakdown between positive and negative terminals in a standoff insulator or switch enclosure, for example.

Figure 6 shows a typical insulator that is not under load. Figure 7 shows that system breaking down due to arcing. To protect against this problem, small amounts of aluminum hydroxide degrades locally at the polymer surface as the polymer begins to degrade into carbon. The hydroxide oxidizes the carbonaceous particles to carbon dioxide and the resulting aluminum

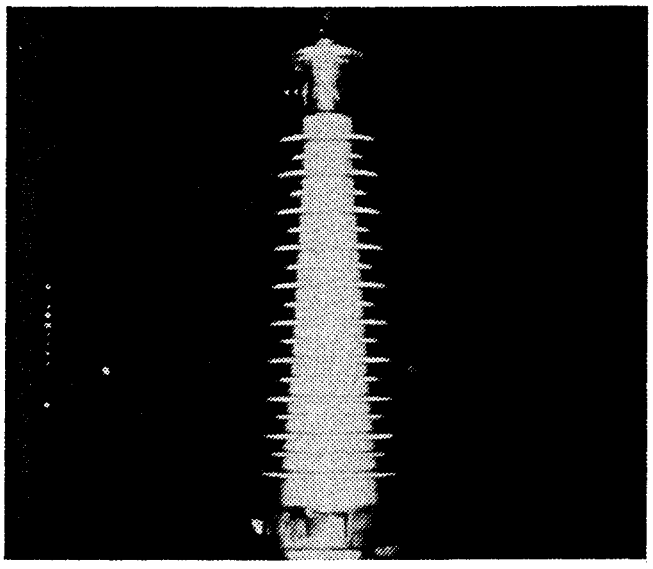

Fig. 6. Insulator not under load.

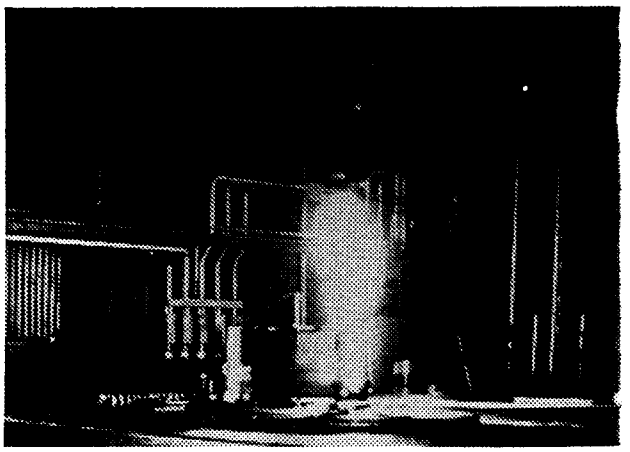

Fig. 7. Insulator of Fig. 6 in flashover condition due to carbon arcing without ATH.

oxide particles formed act as a catalytic agent t indirectly promote further oxidation.[51] The coolin action of the hydroxyl release also helps retard carbo formation. Without the "track" of free carbon, th polymer degradation ceases and the electrical insula tion integrity of the polymer part is maintained. Figur 8 shows an insulator compounded with aluminun hydroxide under very severe conditions of carbo buildup and salt fog. As arcing begins, the hydroxid goes to work and prevents the complete breakdow that was shown in Fig. 7.[52] After Kessal's origina work showed the reduction of tracking in butyl rubber he followed up with successful formulations in ther moset epoxies[52] and polyesters.[53] Formulations usin aluminum hydroxide for arc and track resistance wil be shown in the sections covering each of thos polymer types. Table X lists the various tests fo resistance to tracking.

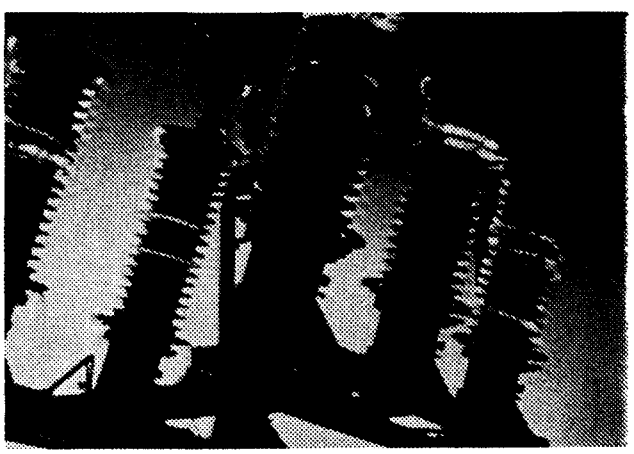

Fig. 8. Similar insulators to Fig. 7 under very severe conditions of arcing in a salt fog with ATH stopping complete breakdown.

Table X. Arc/Track Tests

ASTM Test	Subject
D–495	High voltage, low current dry arc resistance of solid electric insulation
D–2132	Dust and fog tracking and erosion resistance of electrical insulating materials
D–2302	Differential wet tracking resistance of electrical insulating materials with controlled water to metal discharges
D–2303	Liquid contaminant inclined plane tracking and erosion of insulation
D–3638	Comparative tracking index of electrical insulation materials

These tests measure the track resistance in terms of

1. The length of time for which tracking proceeds to a point between electrodes at a constant voltage.
2. The applied voltage at which continuous tracking is initiated.
3. The voltage (tracking index) which causes failure with 50 drops of electrolyte.
4. The total time of test operation until all parts of the surface between the electrodes are carrying current.

Aluminum Hydroxide in Rubber (Elastomer) Applications

Natural Rubber

The word "rubber" is loosely used many times to describe a more universal class of polymers that are more accurately defined as elastomers. Actual natural rubber (sometimes called India rubber) is essentially cis 1,4 polyisoprene, a very narrowly defined, high molecular weight class of materials made from the sap of particular trees and plants. Taken from plantations in damp, warm climates in just a few parts of the world, the raw material is usually shipped as a latex (rubber dispersed in water) or as sheets made by milling gel from the latex that has been set up with coagulation aids and dried.

Aluminum hydroxide is easily added to the latex form since it also disperses readily and is stable in water. The sheet form of rubber can be slit and masticated (subjected to severe mechanical working), during which the rubber becomes a soft, gummy mass. Compounding ingredients like aluminum hydroxide can be added to this mass before it is cured. After compounding, the material is vulcanized or cross-linked. Vulcanization is a chemical reaction initiated by addition of sulfur or other active ingredients (oxidizing agents or free radical generators). Vulcanization can decrease plastic flow, increase elasticity, substantially increase tensile strength, make the compound less soluble, and substantially reduce surface tackiness by the formation of a network of cross-links between the long, tangled polymer chains.

Synthetic Rubbers

In this section we will address use of aluminum hydroxides in the original or "natural" rubbers as part of the broader group of elastomers which also includes "synthetic" rubbers. These are loosely defined as polymers that can be stretched to over twice their normal length and, when released, will return to their approximate original lengths immediately, but cannot be repeatedly softened and hardened by heating and cooling like thermoplastics. Materials usually considered to be in this group are listed in Table XI.

The applications for these materials are extremely varied, from films and latex paints to packaging and electric cable wraps to mine belting, tires, shoe soles, carpet backing, hose, fuel tanks, wire insulation, inner tubes, and sheet stock on industrial roofing, to name just a few of the more common uses. The value of shipments of industrial rubber products will continue to grow to over $7.2 billion by 1991.[232] The use of aluminum hydroxide in these materials will grow with the use of the base polymers. By far the greatest current use of hydroxides is in the synthetic rubbers with SBR, nitrile rubber, neoprene, and EPDM being the largest volume applications.

In most elastomer processing systems, aluminum hydroxide is added during or right after the solids mastication step in a Banbury or similar mechanical working device or during blending of other additives in a latex mix. Calendering, extrusion, or other mixing/forming/foaming operations usually take place before vulcanization and final curing. Depending on the form of aluminum hydroxide and the application, ATH is added to minimize the difficulty in handling the elastomer mix, for better tack (or surface texture and abrasion resistance), for electrical arcing and tracking resistance, for better stiffness, for flame retardance, for smoke suppression, or some combination of these effects. All of these phenomena distinguish aluminum hydroxide from inert fillers such as clays, calcium carbonate, and barytes which have little effect on any property except handling characteristics.

The best-known hydroxide uses are for flame, smoke, and electrical tracking resistance. Although there are particular applications for which ATH always stands out as the best additive for one of the other properties listed above, there are sometimes more economical alternatives to obtain a particular property. For example, carbon black is also an outstanding stiffening or reinforcing additive for natural and synthetic elastomers. The mechanism for this reinforcement by carbon black and fine particle size ATH is not well understood, but they seem to add many relatively weak bond points to the network of strong primary bond cross-links formed during vulcanization. The cross-linking restrains the large movements of entire polymer molecules but leaves small local segments free to move. The reinforcing additives seem to stiffen and toughen by reducing this local freedom of movement of the molecules.

Table XI. Common Elastomers

Abbreviation	Common Name	Technical Name
ABR (AR)	Acrylic rubber	Polyacrylate
AU	Urethane rubber (UR)	Polyurethane (polyester)
BR	CBR, PBd	Polybutadiene
CO	Hydrin (CO, ECO)	Polyepichlorohydrin
CPE (CM)	Plaskon CPE	Chlorinated polyethylene
CR	Neoprene	Chloroprene polymers
CFM		Fluorocarbon
CSM	Hypalon (HYP)	Chlorosulfonyl polyethylene
ECO		Ethylene oxide epichloro hydrin
EOT	Thiokol B	Ethylene ether polysulfide
EPDM	EP elastomer	Ethylene propylene terpolymer
EPM (EPR)	EP elastomer	Ethylene propylene copolymer
ET	Thiokol A	Ethylene polysulfide
EU (u)	Urethane rubber (UR)	Polyurethane (polyether)
FPM	Viton, Fluorel, Kel-F	Fluorinated hydrocarbon
FVSi (FMQ)	Silastic LS	Fluorosilicone
Hytrel	Hytrel	Copolyester
IIR	Butyl, chlorobutyl rubber	Isobutylene-isoprene
IR	Synthetic rubber	Polyisoprene, synthetic
Kraton	Kraton "G"	SBS block copolymer
MQ	Silicone RuBoCr	Silicone
NBR	Buna N, nitrile rubber	Butadiene-acrylonitrile copolymer
NR	Natural rubber	Polyisoprene, natural
Profax	Profax SB814	Olefinic elastomer
PSBR		Butadiene styrene vinyl pyridine
SBR	GR-S, Buna S, Solprene	Styrene-butadiene copolymer
Si	Silicone rubber	Organopolysiloxane
Telcar	Telcar	Polyolefin copolymer
T		Polysulfide
TNP	Thermoplastic Nordal	Proprietary
TPO		PE-Butyl graft copolymer
TPR	Thermoplastic Rubber*	Proprietary

*Shell Chemical Co., Houston, TX.

As with stiffness and toughness, the tensile strength, impact strength, abrasion resistance, tear resistance, hardness, fire retardance, and smoke suppression (mechanisms noted in Chapter 1, Section III) all generally increase at least marginally with decreasing particle size, whereas processing characteristics become poorer as the particle size decreases. Because of this, processing and final physical property balance are always a trade-off and must be fully evaluated. For example, one may find that all of the above physical and chemical properties of a 7 to 10 mil calendered polymer sheet will go up in the laboratory when going from a 1.0 μm median to a 0.5 μm median particle size aluminum hydroxide (everything else remaining equal). But the conversion to a 0.5 μm grade ATH may still not be possible in production because of higher localized processing viscosities during calendering. The viscosity increase can create higher localized sheet temperatures and excessive localized polymer working or tearing, which in turn can cause microscopic holes that ultimately reduce physical properties of the production sheet.

An example of a recently documented wall covering material that could be calendered in this fashion is described in a German patent[54] that discusses copolymers of ethylene and propylene with vinyl acetate and aluminum hydroxide to give good compressive strength and flexibility while being fire resistant and yet produces no corrosive gases or much smoke. An application that could be included here or in the coatings section is combinations of EPR and ethylene-vinyl acetate copolymers or vinyl acetate-vinyl chloride copolymers with aluminum hydroxide to make coverings or coatings for automotive carpet backing.[55] An unrelated example is fire-resistant urethane elastomer sheets that have been prepared with 150 to 400 parts aluminum hydroxide to 100 parts of resin for electrical applications.[56]

Another recently documented high-loading electrical application uses over 250 parts $Al(OH)_3$ in an acrylic acid-ET acrylate-ethylene copolymer/silicone rubber mixture for cable insulation.[57] An additional example of a more rigid formulation based on an elastomeric-based compound is a 500 to 10 000 molecular weight polybutadiene compound that uses a combination of aluminum hydroxide and red phosphorus to make a flame-retardant, crack-resistant potting compound for flyback transformers.[58] A more flexible

composition (EPDM rubber), that also combines aluminum hydroxide and red phosphorus in a fire-resistant rubber compound, was recently patented in Japan.[59] The problems with using red phosphorus include: it is flammable itself (ignites under friction), can cause dust explosions in handling, and colors the polymer compound red. Therefore, there are many similar compositions in the literature simply using higher loadings (up to 400 parts) of aluminum hydroxide in EPDM or EPR compounds. Table XII shows an example of high-loading ATH in an EPDM electrical arc resistant/fire-retardant compound. On the other hand, where particular properties require lower loadings of ATH, dark colors (i.e., pigmented with carbon black pigment) and special handling techniques have been used with red phosphorous to obtain adequate ignition resistance.

Another elastomer application using synergy between fire retardants was recently developed by Fujikara Cable Works.[60] Here the application was air- and water-tight seals using polyurethane/polybutadiene with phosphate ester, halogen, ATH, and antimony oxide for flame retardance. They developed a similar composition to make a sealant using chloroprene rubber (neoprene) with aluminum hydroxide, antimony oxide, and chlorinated paraffin for flame retardance.[61] Showa Electric Wire and Cable Company Ltd. put together similar application formulations using epoxidized butadiene with ATH, antimony oxide, and dechlorine plus chlorinated compounds.[62] While all these combinations do truly have the potential to allow higher fire ratings with lower levels of aluminum hydroxide synergistically (more than could be obtained with equivalent amounts of $Al(OH)_3$ added alone), in a later section we will show how the reduction of ATH levels and additions of even small amounts of some of these synergists can increase smoke tremendously. In fact, the terminology "halogen free" has become used more and more in recent years (especially in electrical applications) to advertise low-smoke, low-toxic-gas, and low-corrosive gas evolving formulations of all types[63–65,81–87,167,224–231] that use aluminum hydroxide and other metal salts.

Table XII. Nontracking Compound–High Corona Resistance

Compound	Units
Epsyn 5508 (EPDM)	50.0
Epsyn 40-A	50.0
Hydral 710	340.0
Sunpar 2280	60.0
Zinc oxide	20.0
Agerite resin D	1.5
Silane A-172	1.0
Butazate	3.0
Mots #1	3.0
Sulfasan R	1.0
Tellurac	0.5
Sulfur	1.0
Zinc stearate	2.0

While not in the synergist category that will be discussed later, a visual comparison of smoke using current competitive commercial systems is shown in Figs. 9 and 10. Figure 9 shows a qualitative comparison of carpet backing strips ignited with a Bunsen burner in a glass cylinder topped with filter paper to allow the generated smoke to be contained. Figure 10 shows a more quantitative analysis of two of the systems shown in Fig. 9, along with some others. The ATH/SBR and PVC carpet backing systems can be compared visually for smoke density in Fig. 9 and as the area under the curve from test data taken from the National Bureau of Standards Smoke Chamber (ASTM E-662) in Fig. 10. Both graphics clearly show the reduced smoke density with ATH commercial carpet backing formulations[235] compared to calcium carbonate in SBR or a commercial PVC backing under the same conditions.

The bulk of the literature written on aluminum hydroxide in elastomeric applications center around 12 to 14 major elastomers including: Natural rubber[133,134,139,193–195] (a natural rubber formulation fire retarded with ATH and PVC is shown in Table XIII), neoprene or chloroprene[61,71,95,96,109,122,132,140,148,149,158,163,164,169,176,178,180–187,190,196–199] (two neoprene formulations for conveyor belts are shown in Table XIV), butadiene rubber or copolymers with butadiene,[60,62,68,69,77,78,81,93,94,98–101,104,107,108,117–119,121,129,130,134–136,137,141,152,157,161,162,172] EPDM[59,63,67,97,114,145,150,176,198,200,201] (Table XV shows two EPDM wire insulation compounds,[43] EPR[65,66,70,79,80,88,105,115,171,189,201,202] (a fire-retardant EPR roofing compound is shown in Table XVI), silicone rubbers,[123–128,139,144,147,165,166,188,203,204] SBR,[112,141,174,176,205–211] polyphosphazene,[192,212,213] urethane,[56,74,90,91,102,103,159,160,168] nitrile rubber,[146] acrylic rubber,[76,173] mixed copolymers[111,133,155,175,176,191,407,408,410,411,413,414,416] (an ethylene acrylate rubber insulation compound is shown in Table XVII), Hypalon,[214,197,198,215] and other chlorinated polyethylenes.[55,216–218]

While aluminum hydroxide use in elastomers has continued to grow over the last ten years, there has been very little growth in the use of rubber materials generally during this time. However, 1987 was a growth year and the International Institute of Synthetic Rubber Producers** projects reasonable growth through 1992. Unlike the spectacular growth that will continue in plastics, the rubber industry seems to be mature and 2 to 3% per year growth rates are likely according to IISRP. They feel this will reach nearly 16 million metric tons of synthetic and natural rubber in use by 1992. They also project the largest gain in tonnage used will be in Europe and Asia. SBR contin-

**(IISRP) — 51 producers that comprise over 95% of noncommunist world rubber production.

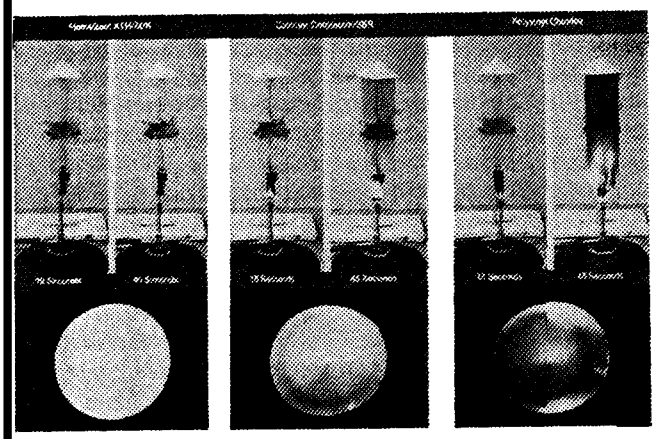

Fig. 9. ATH/SBR vs PVC smoke.

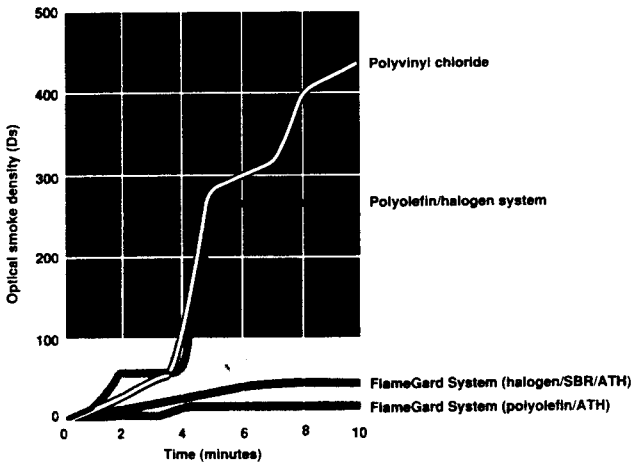

Fig. 10. ATH/SBR vs PVC NBS chamber smoke buildup.

Table XIII. Natural Rubber Fiber/Latex Binder Automotive Seat Cushioning

	Volume Percent
Natural rubber	60
PVC	20
Hydrated alumina	15
Antimony oxide	5
Compression recovery	60
MVSS 302 fire test	Pass

Latex-to-fiber ratio ranges 1:1 to 0.43:1

ues to be the leading volume elastomer used, followed by polybutadiene and EPR materials. SBR use grew 7.4% in the United States in 1987,[232] butadiene 10%, and EPR 11%.

SBR maintains its lead because of its important use in tiremaking but also because it mixes so well with other compounding materials like carbon black, calcium carbonate, aluminum hydroxide, and so on. Whether as a milled, masticated, continuous band to smooth extrusion for specific products, or even distribution on rolls for latex backing applications, ease of processing seems to be the primary reason this syn-

Table XIV. Fire-Resistant/Anti-Static Conveyor Belt

Cover	Phr*
Polychloroprene rubber	100
Hydral	40
SCF black	30
70% chlorinated wax	15
MgO	4
Stearic acid	0.5
Skim	
Polychloroprene	95
Polybutadiene	5
Hydral	35
Soft clay	35
70% chlorinated wax	25
MgO	5
Stearic acid	1

*Parts per hundred resin.

Table XV. Low-Voltage Insulation EPC Compound (Halogen-Free, Low Smoke, Flame-Retardant)

	Units
Vistalon 3708 (EPDM)	14.0
XQ 92.36 (27% VA) Exxon	14.5
PD-064 (PP) Herculon	14.0
Sunpar 2280 oil	2.5
Hydral 710B (ATH)	52.5
Stearic acid	1.0
Irganox 1010	1.0
DLTDP	0.5
Specific gravity	1.35
Physical Properties	
Hardness, Shore A	95.0
200% modulus (psi)	900.0
Tensile strength (psi)	1350.0
Elongation (%)	600.0

EPDM/LDPE Compound–Class EPCV (UL 44)

	Units
Vistalon 1721	50.0
Escorene LD-411.09	50.0
Zinc oxide	5.0
TRD-90	5.0
Paraflint H1	5.0
Hydral 710	50.0
Burgess KE clay	50.0
A-172 Drimix	1.5
Vulkanox ZMB-2	2.0
Aminox	1.0
Dicup R	2.8
Physical Properties	
Hardness, Shore A	97.0
Tensile strength (psi)	1500.0
Elongation (%)	325.0
Aged Physical Properties	7 days/150°C
% tensile retained	110.0
% elongation retained	80.0

Table XVI. Roofing

Material	Phr*
Vistalon 4608 (EPR)	100.0
Hydral 710	75.0
Hypalon 40	5.0
Hi-Sil 215	50.0
Titanox AMP	15.0
DEG	3.0
Flexon 766 oil	20.0
Zinc oxide	10.0
Magnesium oxide	5.0
Stearic acid	1.0
Sulfur	2.0
TMTDS	2.0
MBT	1.0

*Parts per hundred resin.

thetic rubber polymer maintains its volume lead. As in tires, most noncarpet backing SBR applications like molded and extruded items, seals, grommets, belts, hoses, gaskets, solid wheels, footwear, fabric coatings, and wire/cable coatings are primarily blends of SBR and other elastomers to give specific properties. Polybutadiene fits this blend category and is mixed with SBR to give wear resistance, crack reduction, and lower heat buildup in working applications. EPR and EPDM materials find uses from automotive white walls and all the hose, seal, weather stripping applications already mentioned to exterior automotive body parts, wire and cable jacketing, and single-ply roof sheeting, as shown in the tables. While wire and cable have traditionally been high-volume applications for ATH, this last application (roofing) has grown the most in recent years.

Specialty elastomers include nitrile rubber, polyurethanes, silicones, thermoplastic elastomers, and fluorocarbons. Urethanes are by far the most widely used specialty elastomers and can be formed into parts by casting as well as all types of molding and milling techniques. Specialty elastomers have the widest array of cost and performance characteristics and, while they do not impact the total rubber production picture very heavily, they are the most profitable. Generally they are combined with high-grade additives to give their unique performance characteristics in seating, electrical, automotive, aerospace, and medical applications. Figure 11 shows the comparative 1986 major elastomer volume categories in metric tons.

Foamed Polymers

Carpet Applications

Although most polymers can be foamed, the use of aluminum hydroxide in foams will be covered in this section only because elastomers constitute the widest use of ATH in foamed polymer systems. Actually the first large-volume use for aluminum hydroxide as a fire retardant began in the 1960s in natural and synthetic rubber adhesives and foams that were used for backings on carpet. The market growth at that time was created by a domestic movement on a federal level to pass legislation requiring carpets to meet flame-test specifications. This led to widespread and sometimes excessive use of aluminum hydroxide to replace calcium carbonate in carpet applications.

By the early 1970s, usage in carpet peaked as uniform flame-test procedures were developed and, at this time, ATH volumes to carpet began a steady decline that continued until the mid-1980s, when a growing awareness of the value of hydroxides as smoke suppressants began to reverse the trend. Public, insurance and regulatory pressures all played a role in this change. A major turning point came in 1987 when investigations turned up carpet in public schools that did not meet the systems specification guidelines.[233,234] This set off a federal probe. It also helped put ATH in carpet back in the growth trend that had continued for other polymer systems for the last 20 years.

Carpet foamed elastomers and carboxylated latex adhesives still use more aluminum hydroxide than any other single polymer application. However, in recent years use in synthetic stone-look polymer kitchen sanitary ware and building product applications has grown close. If fiberglass-reinforced polyester sinks, vanities, tubs, and tub/shower units, which will be covered later, are included with the synthetic stone sanitary application areas, domestic use of ATH in carpet would be moved to a distant second in total volume. These latter two applications will be covered in sections on thermoset plastics.

Carpet backing elastomeric formulations can range from 100 to 550 parts aluminum hydroxide to 100 parts of dry rubber. A typical carpet backing adhesive formulation is shown in Table XVIII. Example polymers used in backings can be SBR latex, natural rubber latex, PVC latex, or polyurethane foams. The latex mix of polymer, water, hydroxide, calcium carbonate, thickeners, and surfactants can be foamed or frothed with a pin mill-type aerator before being applied to the back of a precoated carpet with roller applicators as wide as the carpet roll by using continuous takeup lines. If the polymer is SBR or natural rubber, the carpet is then drawn through a curing oven at 120° to 150°C.

Typical fire and smoke tests required to be run on carpet, depending on the application use area, include: the Flooring Radiant Panel Test ASTM E–648, the Steiner Tunnel Test ASTM E–84, the NBS Smoke Density Chamber Test ASTM E–662, and the Methenamine Pill Test (DOC FF1–70). Flammability, smoke, and toxicity tests may be also run on the carpet precoat, adhesive foam, or separate cushioning underlayment for informational purposes, but the only data usable by specifiers are those collected on the complete carpet construction. To go into detail on all these specific tests for carpet and the bench scale tests which usually precede them would be beyond the

Table XVII. Low-Smoke Ethylene Acrylate Rubber for Insulation/Jacketing

Vamac N-123	100 phr	123 phr	123 phr	123 phr
Santowhite powder		2	2	2
Hydral 710	165	150	150	120
FEF carbon black (N-550)				10
Stearic acid		0.5	1.5	1.5
Armeen 18D		0.5		
Hystl B-2000	1.6		2	2
Di Cup 40C	5.7	7	5	5
HVA #2	1.6	2		
Diak #1			1	1
3/64 Insulation on No.12 AWG Aluminum Cured 60 s in 225 psi steam				
Stress/Strain-Original				
2000% modulus (psi)		940	840	820
Tensile strength (psi)		1000	1000	1220
Elongation at break (%)		240	480	460
UL Vertical Flame Test–VW–1				
Results	Passed	Passed	Passed	Failed
Smoke	Nil	Nil	Nil	Nil
Flame travel	Nil	Nil	Nil	Nil
Limiting oxygen index	40	38	38	38

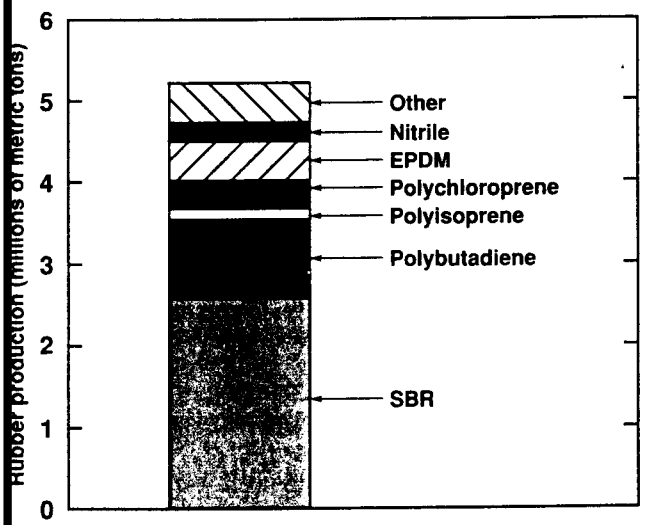

Fig. 11. Rubber production.

scope of this review. However, the Flooring Radiant Panel Test is one of the most important tests currently used for carpet and will be discussed here to gain some insight into the concepts behind the thousands of polymer fire test procedures developed. This test was initiated to understand the burning characteristics of carpet in rooms, hallways, and exit ways that might be used for egress in a fire situation. Information of this type is especially important for carpet used in hospitals, homes for the aged, and other public buildings.

The method measures the critical radiant flux of horizontally mounted carpet samples exposed to a flaming ignition source in a graded heat energy chamber. The full carpet construction should be laid out with the cushion system in place as it is to be used in actual practice. The radiant flux of heat from a ceiling-mounted, 45° angle, gas-burning panel simulates the thermal radiation levels likely to be projected on the floor of a room or hallway for which the upper surfaces are already heated by flames and hot gases from a fully developed fire in a nearby location. The test chamber is 50 by 140 by 71 cm high. The critical flux is calculated from the distance down the sample any burning or smoldering travels. A calibration curve (regularly checked with a transducer) is used to record the energy needed for burning at any distance. For public facilities the specification generally used is 0.45 W/cm^2 minimum. Ignition is attempted using a small gas flame source at the heated panel end of a 107 cm long carpet construction sample. Carpets for which the flame travels to a lower critical flux than 0.45 or which burn their full length fail the specification. Of course, carpets which self-extinguish at a higher critical radiant flux (or distance closer to the panel than the specification) pass the test. As with all small-scale tests, disclaimers must be used indicating that no test method can cover all the possible variables that can occur in an actual fire situation.

The literature is very detailed on the use of aluminum hydroxide in carpet applications.[91,106,110,156,174,177,179,193,194,205–211] Basically, the face carpet fiber is attached to the primary carpet backing (usually either imported jute or woven polypropylene) with an adhesive that can contain ATH. Then a secondary backing comprised of either (a jute or a polypropylene fiber with a latex coating) or (an SBR foam latex, urethane foam, EVA- or PVC-type cushion backing) are adhered to the primary backing. The coatings and foams can all contain ATH. Example suppliers are: polypropylene backings — Amoco, Exxon, Wayn-Tex, Synthetic Industries, and General Fibers; adhesives —

Table XVIII. Typical Elastomer/Aluminum Hydroxide Carpet Backing Adhesive

		82% FR Adhesive				
		Dry/Wt.	Wet/Wt.	Cost per lb.		Total
Polymer X-1986	53%	100.0	188.68	$ 0.55	=	$55.00
Water			29.60			
T.S.P.P.		0.50	0.50	0.12		0.06
FlameGard (aluminum hydroxide)		300.00	300.00	0.1125		33.75
Whiting (calcium carbonate)		150.00	150.00	0.0125		1.88
Thickener		0.36	3.00	0.10 wet		0.30
	Totals:	550.86	671.78			90.99

Dry lb. cost $90.99 − 550.86 = $0.16518
Cost per square yard @ 24 oz. add on wt. ($0.16518 × 24 oz.) = $0.24777

		82% Regular Adhesive		19-30 oz. coating/sq. yd.	
Polymer X-1986	53%	100.00	188.8	0.55	$55.00
Water			29.60		
T.S.P.P.		0.50	0.50	0.12	0.06
Whiting		450.00	450.00	0.0125	5.63
Thickener		0.36	3.00	0.10 wet	0.30
	Totals:	550.86	671.78		$60.99

Dry lb. cost $60.99 − 550.86 = $0.11072 lb.
Cost per square yd. @ 24 oz. add on wt. ($.11072 × 24 oz.) = $0.16608

FR jute adhesive cost	$.24777
Regular jute adhesive cost	$.16608
FlameGard add-on cost	$.08169 per square yd.*

Manufacturing cost

Add-on material cost for coating a 12′ × 18′ (24 sq. yds.) piece of carpet with a 300 part FlameGard adhesive is $1.96. This cost is based on a coating weight of 24 oz. per sq. yd. and an alumina value of $0.1125/lb.

*Less than 10¢/square yard

Reichhold, Polysar, Goodyear, GTR, and Air Products; SBR latex — Goodyear and Polysar. Urethanes are supplied by Dow and Mobay. Amoco by far is the world's largest supplier of woven carpet backings, with Goodyear and Polysar sharing the SBR foam backing lead and Dow leading in the urethane backing arena. Compounding and coating companies as well as the carpet mills themselves do the combining of aluminum hydroxide into the various systems for fire retardance at the expense of calcium carbonates and clays.

The SBR latex foam share of the secondary U.S. backing market has dropped considerably in recent years due to quality problems but still holds high shares in Canada and Europe where quality against urethane foam and woven backings has been maintained. Urethane foam markets have continued to increase and some inroads have been made by PVC and PVDC latex backings.

Cushioning Applications

Of greater potential for polyurethane foams usage of ATH than in carpet backings in recent years is use in foam cushioning for bedding and seating. More emphasis on fire-retarding urethanes in these applications was brought about in the early 1980s with the media connotation that referred to some unfire-retarded urethane polymers as "solid fuel." This led to some specific fire-retardant foam requirements in California and other localities. Much has been done to change this image by foam producers, the most notable being the development of CMHR[72,92,154] (combustion-modified high-resiliency foams) by Mobay Chemical Company and similar concepts by others including Dunlop[113,120,134] in Europe.

Literature abounds on the use of aluminum hydroxide in flexible polyurethane foams.[73,75,116,131,138,142,143,151,153,168–170,185,219–223] The two most commercially viable systems use entirely different mechanical technologies. The first and more widely used is the Mobay technology, which incorporates coarser aluminum hydroxide materials internally into the polyol portion of the two-component, open-cell, flexible urethane foam forming mix. This is done before reacting the polyol with polyisocyanate. The same technology can be applied to closed-cell (rigid) polyurethane foams and basically entails balancing the fire-retarding properties of ATH with the dispersion viscosity (processing properties) of the mix by controlling ATH particle size. Higher loading level and smaller particle sizes increase flame retardance, while larger particle sizes and reduced loading levels aid dispersion viscosity

reduction and can create easier processing. Particle-size distribution optimums were found with sharp distributions in the 20 μm median particle size range but best results usually require the use of ATH with FR synergists because high loading levels of ATH can degrade physical properties.

The second method developed by Alcoa and Dunlop involves first compounding fine particle size (1 μm) ATH into a polymeric binder like vinylidene chloride or neoprene and coating the previously formed open-cell foam followed by squeeze-out and drying. This approach allows a higher degree of fire retardancy based on ATH alone but requires a two-step procedure which increases processing time. The Alcoa and Dunlop techniques differed in that the first saturated the entire foam bun stock while the second created a highly fire-retarded external layer of foam but has an internal core of lower density, nonfire-retarded foam.

Insulating Applications

There is a wide range of elastomeric insulating applications in current use from water pipe and hot water tank covers to high-frequency sound-absorbing linings for equipment compartments. PVC/nitrile rubber blends are one of the most interesting examples of foam for this type of use. Generally, nitrile elastomer is added to rigid-type PVC polymer along with selected plasticizers to lower the viscosity. The mix can be a 50/50 blend to which roughly a 30% loading of a very uniform 1 μm precipitated aluminum hydroxide can be added. The nitrile in weighed sheets, followed by ATH and PVC in pellets or powder, are usually hot-mixed in a Banbury-type operation which then can be dropped onto calendering rolls for further mixing with catalysts and other additives before extruding into a final shape. Generally, chemical blowing agents are used for foaming. Care must be taken in compounding, curing, and blowing to balance the core and expansion rate of these polymers. The resultant parts can have an extremely good balance of flame resistance, insulating value, weather resistance, chemical resistance, and stability in oily and solvent-laden atmospheres.

For the rest of these discussions we will generally classify polymers into three distinct groups: elastomers, thermoset plastics, and thermoplastics. We have already defined elastomers. *Thermoset plastics* are loosely defined as those plastics that set up with heat and *thermoplastics* are defined as plastic materials that can be worked or formed by heating to a unique temperature range above ambient. Thermoplastics will then set up on cooling without degrading. Table XIX lists typical thermoset and thermoplastic materials already used with ATH. The thermoset plastics and elastomers can take several times their polymer weight in hydroxide loading without special particle-size or surface modification. Elastomers, unlike thermoset plastics, maintain physical properties at these high loadings due to forgiving, pliable structures. Generally, however, addition of a nonfibrous particulate like aluminum hydroxide degrades final part physical properties. Thermoset plastics use fibrous reinforcement with high loadings of aluminum hydroxide to overcome physical property problems, while thermoplastics require reduced loading levels or ATH surface modification to make the inorganic surface more compatible with the organic matrix.

Table XIX. Plastic Systems Using Alumina Trihydrate as an Additive

Thermoset	Thermoplastic
Epoxy	Acrylic
Acrylics	
Phenolic	PVC
Polyester	Polyethylene
Spray-up	Polypropylene
Hand lay-up	Various copolymer
Foam	
SMC	
BMC	
Ethylene copolymers	
Polyurethane	
Dialkylphthalates	
Melamine/formaldehyde	

Thermoset Plastics

Polyesters

Following the rapid, large-volume growth of aluminum hydroxide use in carpet applications in the late 1960s and early 1970s, thermoset polyesters became the second largest early high-volume application for aluminum hydroxide. The first documented hydroxide cases in thermoset polyesters for arc and track resistance in the early 1950s were possibly the first real "ATH in polymer" application,[49] as noted in earlier sections on electrical arc and track mechanisms. Those applications were followed in the late 1950s by hydroxide use in polyester for its esthetic (translucent/fire retardant) pigmenting value.[236] This in turn was followed in the 1960s by use in premix polyester (molding compounds) as well as in laminating polyester (spray up compounds) primarily as a fire retardant.[237] However, it wasn't until major international[238] and domestic[239] standard setting organizations endorsed tests in the early 1970s specifically showing the value of aluminum hydroxide as a fire retardant in fiberglass reinforced bathtubs and shower stalls that the major growth of ATH in polyesters began.

Compared to the sophisticated toxicity, ignition and heat release tests which clearly show the value of ATH today, these early torch tests did not yield much analytical data. What they did show was a clear capability of aluminum hydroxide to make thermoset polyesters self-extinguishing to a plumber's torch. These endorsements began a voluminous stream of literature that continues today on aluminum hydroxide in general unsaturated polyester uses[240,110,188,241–273,276–315,531] and in premix sheet molding/SMC and bulk

molding (BMC) compounds.[274,275,278,316–328,334] The endorsements were brought about after some fires in newly framed construction that occurred when workmen inadvertently ignited nonfire-retarded polyester bathtubs or shower stalls while sweat-fitting the copper pipe joints with a plumber's torch. Without walls to contain the fire, the hot-burning polyester quickly ignited the wood 2 × 4 framing and soon the roofs and exposed plywood floors were in flames.

The difficult portion of the technology development was the maintenance of adequate processing and surface properties in these rapidly evolving polymer systems. Flame inhibition, smoke reduction, and arc/track resistance were easily demonstrated in these systems at high ATH loadings (45 to 65% by weight). But the resin industry had to develop special low-viscosity, faster-cure resins and the fiberglass industry had to modify their glass-reinforcing products to allow for adequate wet-out of all the inorganic systems.[310] Luckily, because of the high glass loading in these reinforced products, final physical properties were not unmanageably affected by the loading and particle size of the aluminum hydroxide.[315]

Most spray-up resins performed somewhat similarly in viscosity tests. Within a certain range, viscosity curves like Fig. 12 were independent of the resin manufacturing location when checked with various particle size aluminum hydroxides.[329] However, other resin processing parameters varied widely from resin to resin. Gel and cure times versus particle-size curves, for example, could have a positive, negative, or zero slope, depending on the additive package the resin supplier used to stabilize, accelerate, or otherwise proprietarily control resin properties. This created a need to develop application curves like that shown in Fig. 13[329] to establish particle sizes for each location to optimize viscosity, gel time, cure-time characteristics, and so on.

It also created a market for viscosity-improving additives like DMMP, triethyl phosphate, and other water-soluble phosphate derivatives. These materials also added to the fire retardancy but adversely affected smoke properties.[293] Disadvantages of using ATH included more wet-out time, somewhat reduced strength as compared to systems more highly filled with fiberglass, higher stiffness, and greater density (heavier parts). None of these disadvantages slowed the use of ATH because of the improved flammability at lower cost than other fire retardants. Examples of the two fabrication techniques most affected by roll-out (wet-out) problems with aluminum hydroxide are shown in Figs. 14 and 15.[330] In both hand lay-up and spray-up, rollers and other techniques are needed to distribute fibers and particulates evenly and ensure complete resin contact with all the inorganic additives and reinforcements.

Much work has been done to determine the optimum particle-size distributions and ratios of round particles to fibers for maximum packing conditions in systems like these.[331–333] The ATH suppliers have taken advantage of this information to help customers approximate optimum conditions in their systems by adjusting the particle-size distributions of the aluminum hydroxide products available. As Fig. 13 showed, optimum median particle size for spray-up (depending on the slope of the resin gel and cure time curves) is between approximately 8 and 15 μm. Adjustment of

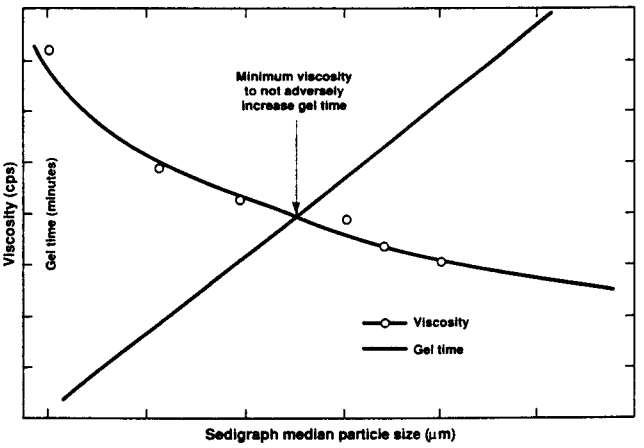

Fig. 13. UP viscosity/gel vs particle size.

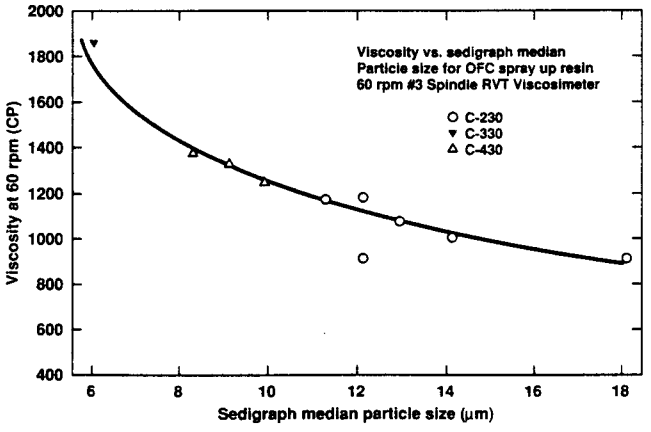

Fig. 12. UP viscosity vs particle size.

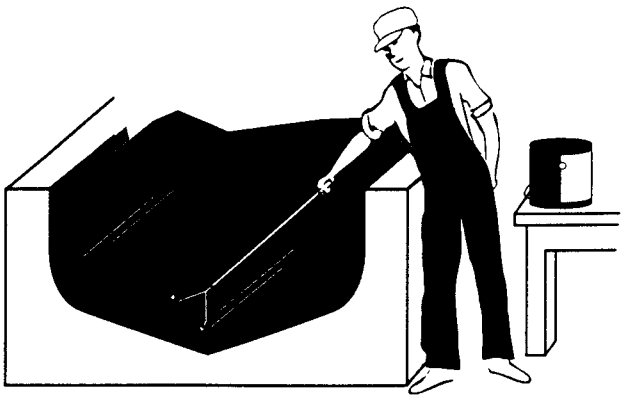

Fig. 14. Hand lay-up.

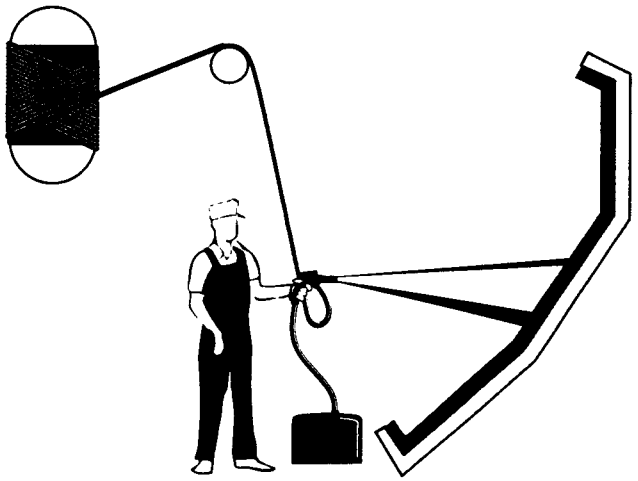

Fig. 15. Spray-up.

Table XX. Typical Spray-Up Formulation

	Weight Percent
General purpose unsaturated polyester	35
Aluminum hydroxide	47
Figerglass (1 inch chopped)	18

the aluminum hydroxide particle-size distribution around this median can optimize thixotropy — a good balance between low viscosity at high shear (as the mix goes through the spray gun) and high viscosity at low shear (once the mix hits vertical walls of the mold). A typical spray-up formulation is shown in Table XX.

The optimum particle-size distributions for premix unsaturated polyester systems like SMC and BMC[††] are very different. Unlike spray-up and hand lay-up applications where often the fines are classified out, in SMC and BMC applications the fines are an important part of the viscosity control mechanism as well as contributing appreciably to the fire retardancy. In some cases bimodal distributions of two or more products are used to obtain the effect desired. The ATH mixture may be a 2 to 1 blend of a 7 μm median broad distribution particle size aluminum hydroxide with a sharper distribution 1 μm material. The BMC/SMC polymer compounds usually are very thick mixes, almost like a bread dough consistency. Figures 16 and 17 show typical molding mechanisms used to make final parts. Compression molding requires a preweighed premix while injection molding systems use a screw or ram to meter the mix into the mold. Sheet products are also made by wetting out fiberglass mat or chopped glass layers with catalyzed resin on continuous lines between thin sheets of polyethlene or other suitable films to contain the mix until the unsaturated polyester has cured. Typical premix and SCM formulations are shown in Table XXI.

[††]Sheet and bulk molding compounds.

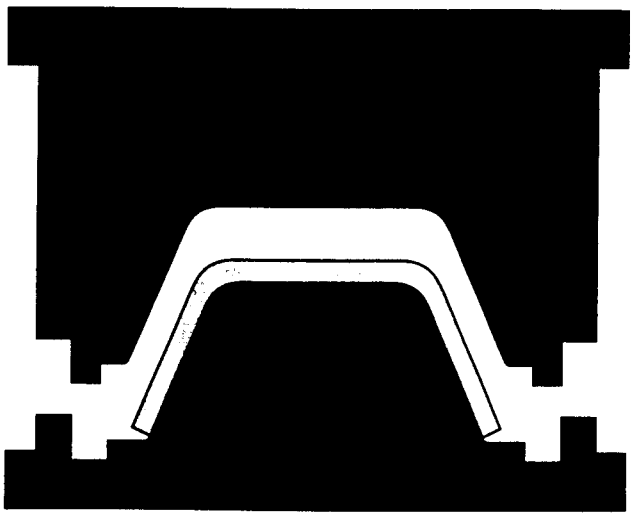

Fig. 16. Compression molding.

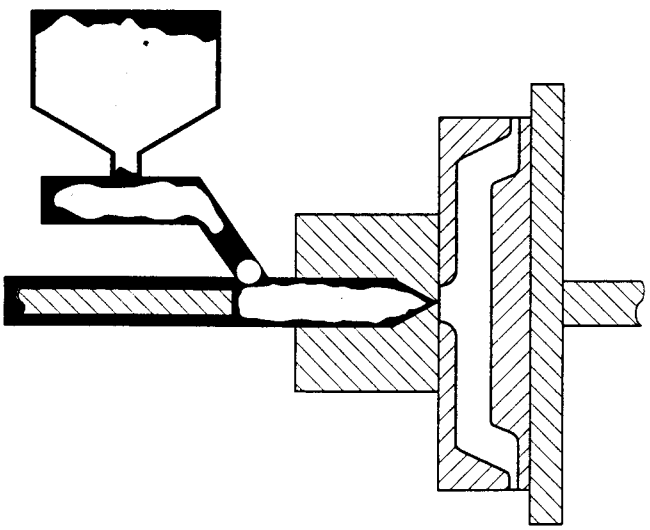

Fig. 17. Injection molding.

Two other large-volume fabrication techniques used with unsaturated polyesters are pultrusion, as shown in Fig. 18 and continuous lamination (Fig. 19). Pultrusion is the technique used to make structural members like I-beams and bar stock. An interesting application of this fabrication technique that caught early attention was the production of fire-retardant sowy slats to compete with specially shaped aluminum extrusions used in the floors of hog houses that allowed waste to fall through without pinching the hog's hooves. Continuous lamination equipment is used in the production of circuit boards, for example. Both of these systems are based on wet-out of continuous fiberglass strands, rope, or mats with a highly filled liquid resin system. Although, as a group, these high-volume applications for aluminum hydroxide in

Table XXI. Typical Premix and SMC Formulations

Premix Components	Weight Percent
General purpose unsaturated polyester resin	30.0
Benzoyl peroxide post	0.6
C-330 (7 μm ATH)	38.0
H-710 (1 μm ATH)	15.0
Glass fiber, ¼ inch	15.0
Zinc stearate	1.4
SMC Components	**Phr***
Halogenated unsaturated polyester resin	100.0
Styrene	5.0
Microthene FN 500	5.0
t-butyl perbenzoate	0.8
Zinc stearate	3.0
Aluminum hydroxide	125.0
Pigment paste	5.0
Magnesium oxide	1.2
1-inch chopped fiberglass coving	70.0

*Parts per hundred resin.

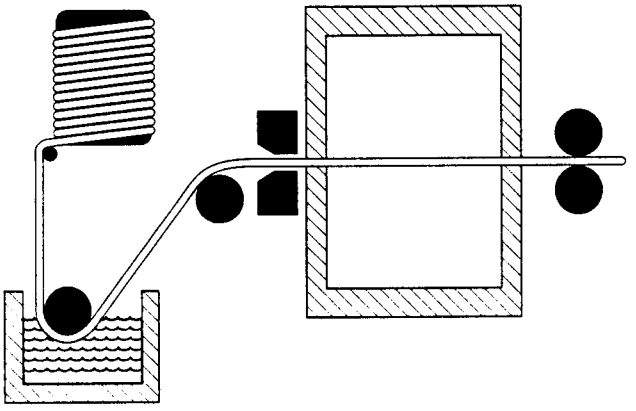

Fig. 18. Pultrusion.

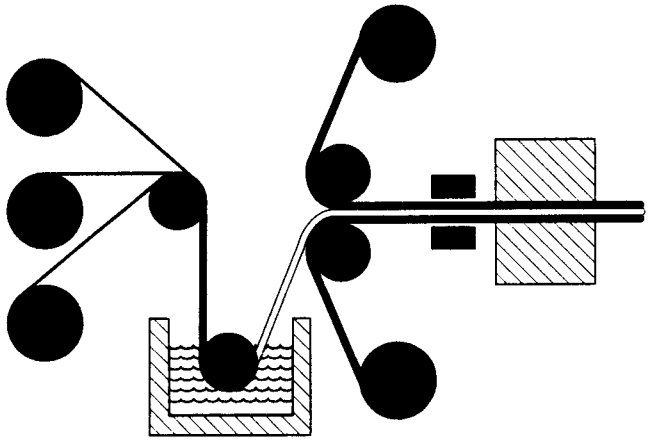

Fig. 19. Continuous laminating.

unsaturated polyester resin continue to grow, the percentage used in spray-up bathtubs and shower stalls has decreased due to relaxed FR regulatory

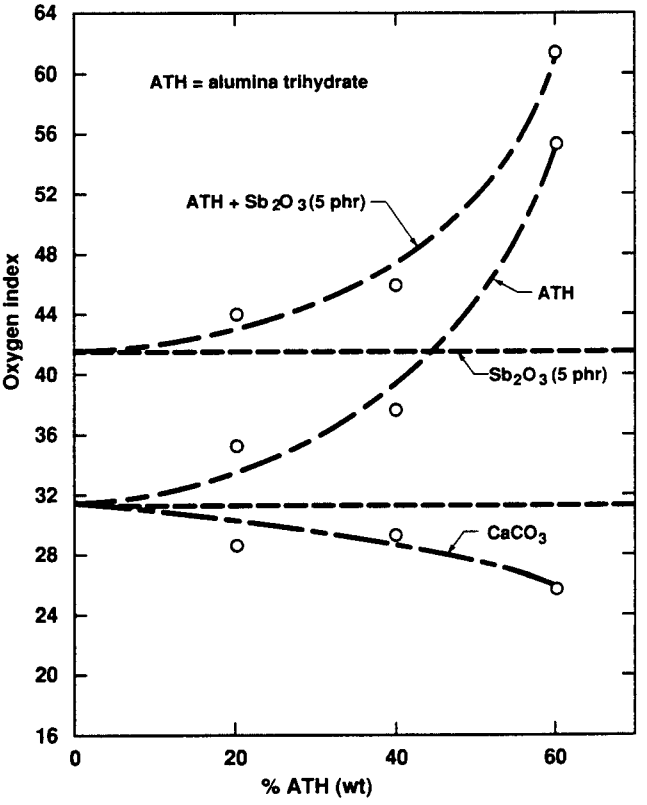

Fig. 20. Oxygen index of filled chlorinated polyester resin (Hooker 435P).

enforcement, foaming operations for some components, and the use of mixtures with calcium carbonate and gypsum.

Synergism with Other Fire Retardants

The synergistic effects of other fire retardants with aluminum hydroxide in unsaturated polyester resins are shown in Fig. 20.[283] The higher the oxygen index, the higher the fire rating. The resin shown is a halogenated resin. Since chlorine is a fire retardant in its own right, the oxygen index starting point at zero ATH additive percent is higher than it would be if just a general purpose (nonchlorinated) polyester resin were used. The graph shows that fire rating continues to go up as the ATH loading is increased. However, if a further synergist, 5 parts Sb_2O_3 (antimony oxide) per 100 parts of resin is added, the fire rating is increased even further. These compound increases are more than that expected due to the additive effect of each of the fire retardants individually. In this example, calcium carbonate addition seems to reduce fire rating. While this is not always the case with other systems, it is clear that inert fillers like calcium carbonates and clays do not add to the fire rating.

Some phosphorous-containing additives (Fig. 21) can also be shown to increase the fire rating with ATH.[283] These effects have allowed partial use of aluminum hydroxide in applications where a full load-

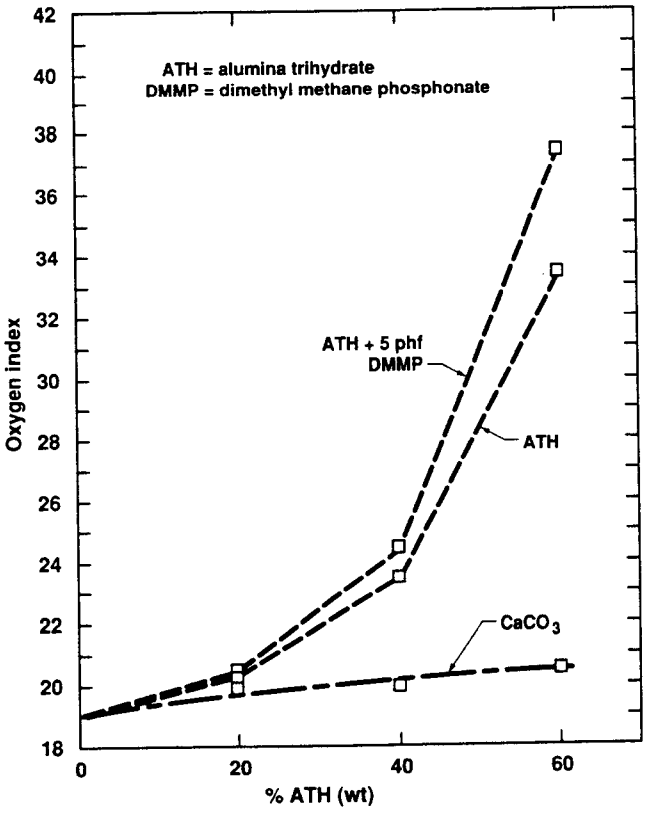

Fig. 21. Oxygen index of filled GP polyester resin (Kopper's B–304–60).

ing would have changed processing parameters and final physical properties to the point where initial use of ATH alone may have been prohibited. As manufacturers learned more about how to work with aluminum hydroxide and advances have been made in organic surface modification[273,306,317,318,335,338] and resin modification,[336,337] the loadings have been increased in several applications.

Unfortunately, this synergism using other fire retardants to obtain higher fire ratings with lower loadings of ATH has become a good news/bad news situation for many applications. The fire hazard emphasis in the 1980s has grown from just the 1970s requirement to raise fire (ignition and flame spread) ratings to an increased emphasis on smoke and toxicity also. Figure 22 is an unretouched photograph of a qualitative, visual, smoke-density comparison of the compounds using the synergistic fire-retardant additive combinations shown in Fig. 20. The simplistic nonscientific technique used was simply an attempt to ignite small, equally sized strips of material compounded as depicted in the photograph with a Bunsen burner for an equal length of time in a glass cylinder, capped with a filter paper hat. Of course the first sample, not being fire retarded, burned profusely and created dark, dense, black smoke (on the left in Fig. 22) that accumulated on the filter paper. The second

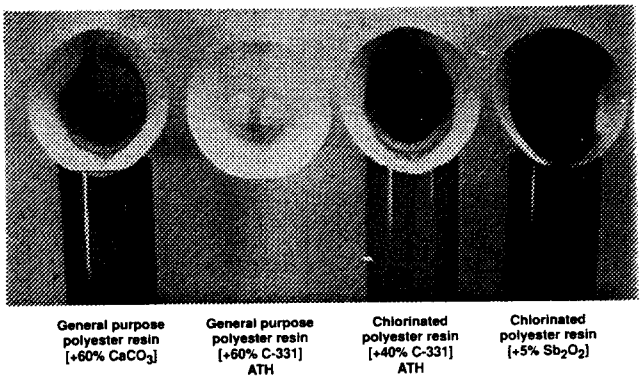

Fig. 22. Smoke-filled glass tubes (polyester).

sample, highly loaded with ATH, did not burn much at all and emitted very little dark smoke. The third sample, with reduced aluminum hydroxide and a halogen synergist to maintain the same fire rating by oxygen index, indicates a much higher level of dark smoke emission as well as more particulate collected on the filter paper. The last sample (on the right in Fig. 22), with ATH completely removed and an antimony oxide synergist used with the halogenated system, appears to show more dark smoke than even the first (nonfire-retarded sample).

This concept was verified scientifically in the National Bureau of Standards Smoke Chamber (Fig. 23); the data are shown graphically in Fig. 24.[339] The total smoke density increases as the amount of aluminum hydroxide is reduced and the fire-retarded system using the other synergists alone (without ATH) actually did produce more smoke in this case than the nonfire-retarded system. New fire-retardant synergist packages are always being developed, and over time smoke levels for these types of systems alone will be reduced. However, the use of aluminum hydroxide to fill this requirement has been clearly recognized. The ATH technology, however, must continue to advance with new products to allow this need to be met without processing and final polymer part physical property problems.

In addition to the electrical insulator, bathtub, shower stall, and flat sheet construction applications, aluminum hydroxides-loaded unsaturated polyester resins have found their way into thousands of home, commercial, and industrial applications. Items like handles for home appliances such as toasters, coffee pots, skillets, mixers, irons, full housings for hair dryers, power drills, and saws; commercial items like computer terminals, CRT casings, copy machine housings, cash registers, and air conditioner housings; and industrial uses in noncorroding ductwork, wall panels, large tanks, people mover interiors, auditorium seating, electrical boxes, switches, and bus bar connections are examples.

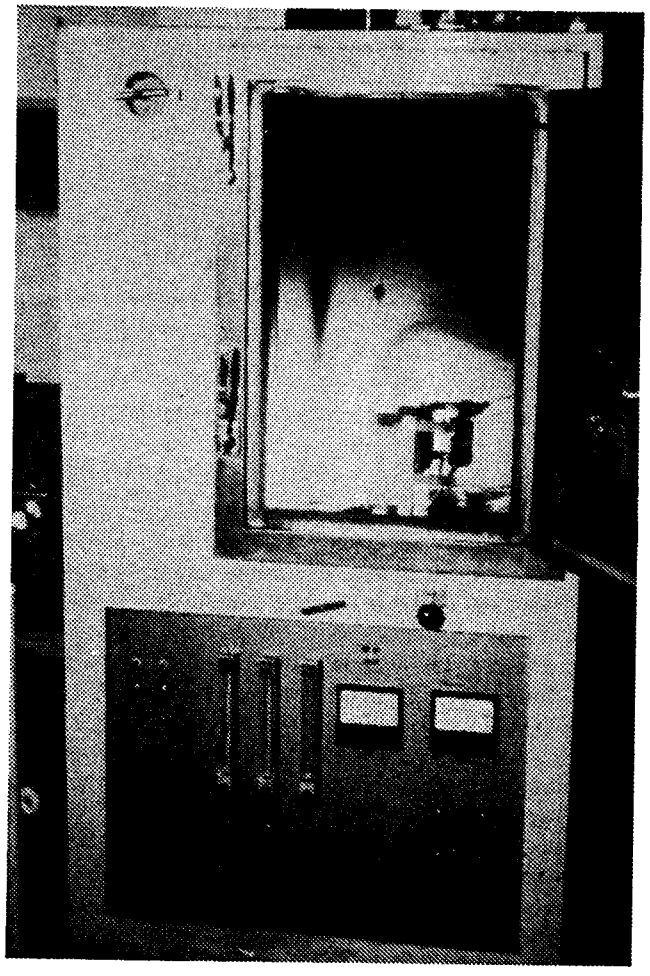

Fig. 23. NBS smoke chamber.

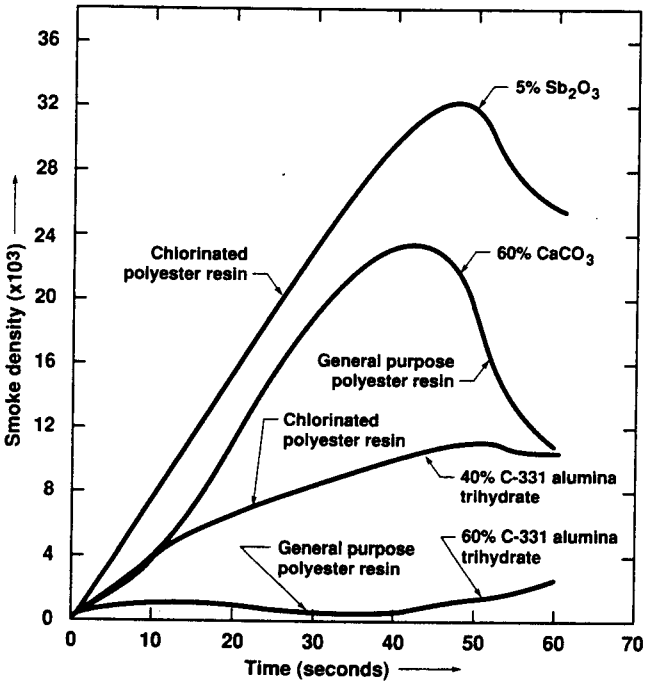

Fig. 24. Smoke density of flame-exposed, filled polyester resins.

Cultured Onyx/Marble

The synthetic marble industry has gone through tremendous growth since its tiny beginning in the late 1960s. The major application area initially was bathroom counter tops but now architects and builders have expanded the commercial and residential applications into sophisticated new areas. Recently increased heights of consumer interest in luxurious new and remodeled bathrooms, kitchens, and other marble interior decor areas has raised the demand for the premier products this industry has to offer. Two distinctly different types of products have emerged. The older polyester product and less capital-intense fabrication technique simply involves mixing clear, white polyester resin, white aluminum hydroxide, catalyst, and extremely small amounts of pigment in slow-speed, batch, dough kneading-type mixes, the contents of which are poured into open-air vibrating molds. Each mold has been precoated with a thin polyester gel which serves as a waterproof surface on the finished piece.

The mixing technique, time addition of pigments, and exact matrix formula vary from manufacturer to manufacturer, each seeking to replicate the delicate veining and translucence of polished stone. After several hours of chemical curing, which can be accelerated by heat, followed by a cool-down period, the product is trimmed, cleaned, ground, and buffed. While early growth in this segment was with the use of calcium carbonate, pulverized crushed marble, alkali mixtures, and other nonfunctional fillers, ATH has been predominate in onyx looks over the past decade or so because of its unique performance benefits and visual properties. The visual effects are created by the close approximation of the ATH refractive index to that of polyester resin, giving a beautiful in-depth look. These synthetic parts have many advantages over natural marble in weight, lower cost, more stain resistance, less brittleness, good color, hardness control and, of course, customization of shape without seams.[340]

The newer type of polyester product has been loosely dubbed "fully densified" and requires not only more rigorous control during fabrication, including lower viscosity resins, more intense mixing, and vacuum deaeration during mixing and forming, but is also more optimally produced in continuous operations. This type of product generally requires specialty white aluminum hydroxide products that vary from manufacturer to manufacturer. While the general onyx industry had been moving along slowly with little help from the primary alumina manufacturers for nearly 18 years even though the volumes have been substantial for the last 10 to 13 years, it wasn't until the last several years that a domestic product line was specif-

ically formulated to address the requirements of this industry. Needed product specifics included guaranteed consistency in color, elimination of dark particle contamination, consistency in particle size, and ease of pigmentation to accentuate the polyester translucency and increase the manufacturer's color and appearance control. This required higher levels of chemical purity and consistency and a completely nonreactive product. Fire resistance, smoke suppression, and no toxicity in and of itself were extra benefits. All this required starting from the ore source with raw material selection up through all the changes that can occur during the manufacturing process as well as working with the individual manufacturers to develop optimal resin systems, catalyst and promoter systems, and mixing techniques for best dispersion and optimization of all the process equipment, materials of construction, and process conditions.[341] The fully densified onyx product is slightly more opaque, uses less veining, and is more conducive to granite and other stone looks in addition to the original onyx appearance.

Previous to these recent efforts by the base aluminum hydroxide producers, most effort to support the industry had been put forth by the resin suppliers, distributors, and the Cultured Marble Institute (CMI). Selected resin manufacturers and mold manufacturers have continued to educate final part manufacturers in resin technology[342,343] and train them in good manufacturing principles.[344] The CMI's main thrust has been to coordinate industry technology exchange, develop certification and standardization programs, and promote marble systems to building regulators, architects, and trade groups.[345] A typical example of an onyx casting formula is given in Table XXII.[346] The veining mix could also contain titanium dioxide or other pigments and the casting resin could contain a small amount of glass spheres for weight reduction or frit for appearance effects.

Table XXII. Onyx Mix Formulas and Casting Techniques

100% Onyx Castings	
Base mix:	Silmar S-793C or S-40 casting resin
	1 part by weight
	½–1% AZOX peroxide OR (NOT BOTH AT SAME TIME)
	½ — 1% FS-100 peroxide
	3.0 parts by weight C-31 coarse grind ATH
	Mix may be used natural or tinted with dye.
Veining mix:	Silmar S-793C casting resin 1 part by weight
	1% AZOX Peroxide
	2.0 parts by weight C-31 regular ATH
	Mix should be lightly pigmented.

Veining can be achieved by slightly mixing veining mix into base mix using a Hobart dough mixer. The veining mix is thicker than the base mix and will, therefore, produce well-defined streaks. The mix then should be poured into the mold and vibrated just long enough for air removal (1–3 min). The veining neither rises or settles during vibration. *Excess vibration will result in the loss of definition of the veining.*

The advances by hydroxide manufacturers, distributors,[‡‡] resin producers, mold manufacturers, and fabricators in the recent past have moved this industry forward in California, Florida, Texas, and other regional markets. The leading companies have tended to be small, local, independent entrepreneurs. The trend now is toward national growth and will come with the stronger network of national and international companies putting facilities and distribution systems in place generally to market the fully densified type of onyx product described above. Despite their small size, the local companies will also continue to grow with the strong front they present through organizations like the CMI. CMI-supported test programs examine quality of workmanship, structural integrity, thermal shock resistance, color fastness, stain resistance, chemical resistance, cleanability, wear, and cigarette burn resistance. CMI standards also include installation, care, and maintenance instructions. The CMI estimates that 40 to 50% of the bathroom lavatory market and 8% of the tub and wall panel market is cultured marble. New trends are in archways, toilets, window sills, ash trays, planters, picture frames, and so on. The possibilities are endless for this esthetic product. Even synthetic onyx marble dog dishes for high class canines are on the market today.

Thermoset Acrylics

A natural follow-up to the description of the "fully densified" polyester products is the use of aluminum hydroxide in cross-linked acrylics for applications that include kitchen counters, commercial counters, bathroom sinks, vanity tops, and wall panels. All of the attributes needed for the hydroxide and all of the advantages of the finished products described above for polyester synthetic marble applications also fit methyl methacrylate (acrylic) resin systems. Actually, the commercial appearance of these types of products falls[347] in between what was described earlier as the original cultured onyx polyester synthetic marble products and the current emergence of "fully densified" polyester synthetic marble products. The additional attributes that allowed the acrylic marble-type products to rapidly outstrip the original batch-cast polyester applications are the primary reasons for the attempts to develop the newer, fully densified polyester products. These include: ease of installation, on-site shape modification and finishing with normal woodworking type procedures, durability during shipping and handling over long distances, precise color matching, uniformity of final physical properties, and economies of scale available only with large continuous processing procedures.

[‡‡]In addition to the major distributors listed in Chapter 1, Section III, R. J. Marshall, Inc., Detroit, MI, has contributed to the onyx industry.

Although the original work with aluminum hydroxide in polymethyl methylacrylate was done in the late 60s,[347,348] and finally patented in 1974[349] in the United States, new concepts and improvements are still evolving.[350,351] The original use was described as building products with low flame spread, increased resistance to stress cracking, resistance to chemical etching, and high translucency. Except for the extremely important additional toughness/durability attributes, these are basically the qualities described in the first patent on highly aluminum hydroxide-filled polyester.[236] The early polyester products were successful in custom-built construction where the molding shop had cast them to fit a custom-built rough structure, but due to the hard, thin, gel-coated surface they could not be cut, drilled, sanded, or routed by regular construction workers without special chemicals and knowledge of reaction and curing techniques. On the other hand, even the early acrylic building products were relatively uniform throughout and allowed all of the normal construction finishing techniques with little instruction.

Advances have continued in the methyl methacrylate products cross-sectional uniformity for finishing, color, and matching capability and in the variety of stone-look appearances available. This has allowed these types of products to maintain a substantial lead in the high end of the regular domestic and commercial construction markets. Typical formulations can involve 55 to 80 percent by weight aluminum hydroxide and other pigmenting additives with the balance possibly being a 3 to 1 ratio of methyl methacrylate homopolymer in monomer and normally 1% or so of a cross-linking agent like ethylene dimethacrylate and less than 1% of a polymerization initiator. There has been very little written documentation of other aluminum hydroxide applications in thermosetting acrylic systems.[352]

Phenolics

Phenolic resins are one of the oldest plastic systems in current use today and, while they have some inherent fire retardancy, it was recognized[358,359] early on that additives could improve phenolic FR characteristics. Some of the early use products included automotive, radio, television, and other electrical appliance parts. More important fire retardant uses today are for construction plates, paper and chipboard laminates, putties, adhesives, translucent decorative panels, and other fire-retardant building and mass transportation interior sheetstocks.[229,241,353–354,361] Two vastly different applications using high loadings of aluminum hydroxide in phenolic resins are shown in Table XXIII. Generally, however, much less ATH is used proportionately with phenolics because of their inherent fire retardancy.

Table XXIII. Phenolic Formulations

Fire-Retardant Top Layer of a Three-Ply Decorative Laminate Panel*	
Aluminum hydroxide	70.0%
Phenolic novalak resin	7.5
Calcium carbonate	15.0
Zeolite	5.0
Glass fiber	2.5
Fire-Resistant Putty†	
Aluminum hydroxide	61.5%
Phenolic resol	22.0
Asbestos fibers	7.7
Lexa bromobenzene	4.4
Vinyon fibers	4.4

*Ref. 356.
†Ref. 355.

Epoxy Plastics

Epoxies were probably one of the first resins in which extensive mechanism studies were completed to determine exactly how the various alumina products worked to improve thermal conductivity,[362] arc/track resistance,[363,364] and fire retardancy.[365] Starting from their first introduction in 1947 and two million pounds being produced in 1950, epoxies have grown to 430 million pounds being produced annually in the United States alone by 1987. The oldest aluminum hydroxide use in epoxy that was uncovered was the 1950s work patented in 1961 by Kessal and Norman (G.E.) for arc and track inhibiting applications discussed earlier.[52] This was followed by Bayes (Shell) showing the increase in thermal conductivity, surface hardness, and modulus of epoxies with fine tabular alumina in 1964 and Union Carbide work[366,367] in 1968 that again showed the value of aluminum hydroxide in arc and track epoxy applications for high-voltage electrical systems. Examples of the conductivity and arc/track results from these latter two reports are shown in Tables XXIV and XXV, respectively.

Both of these tables indicate the high loadings of aluminas used in some epoxy applications. Figure 25 shows the effect that particle size can have on physical properties of epoxy systems. Physical properties also drop off in a similar manner with increases in loading levels but viscosities increase as the loading level goes up. This is complicated even more by the fact that Fig. 25 shows the advantage of going to finer particle sizes in epoxies,[43] but the finer the particle the higher the processing viscosity. These viscosity complications can be controlled by optimizing the distribution of particles and using process aid-type surface treatments. Physical properties on the other hand can be improved by using coupling agent-type surface treatments.[368,381] In addition to the advantages of using fine aluminum hydroxides, low soluble content is also desirable.[364,369] An example of a current application of fine precipitated aluminum hydroxide in a

Table XXIV. Thermal Conductivity of Filled Epoxy Resins*

Filler	Phr	Wt.% of Total	Vol.% of Total	K
None				0.13
Aluminum oxide†	325	73	48	0.82
Atomized aluminum‡	200	63	45	0.94
Iron powder§	300	72	30	0.52
Copper powder¶	1200	91	60	0.94
Silica**	150	56	39	0.44
			Steel	26.0
			Aluminum	116.0
			Copper	244.0

*Epon 828 with 20 phr curing agent Z.
Cure schedule:2 h @ 85°C (135°F) plus 2 h @ 150°C (300°F)
†Grade T-61, 325 mesh, Alcoa.
‡Grade mD-101, Metals Disintegrating Co.
§Grade MD180, Metals Disintegrating Co.
¶Venus-A, U.S. Bronze Co.
**No. 27, Whittaker, Clark & Daniels Co.

Table XXV. Arc/Track Resistance Properties

Formulation	Parts by Wt.
ERRA-4090	50
ERL-4211	50
Hexahydrophthalic anhydride (HHPA)	67
Hydrated alumina, C-331*	250
Benzyldimethylamine	1.0
Arc/Tract Properties	
Arc resistance (s) (ASTM D-495)	>400
Arc/track resistance, 3500 V, min† (ASTM D-2303)	No failure
Erosion rate (cm^3/h)	0.0049

*Aluminum Company of America, Pittsburgh, PA.
†Test conditions:

Stress level	1.75 kV/in
Time under test	1000 min
Contaminant	0.1% aqueous NH_4Cl
Surface preparation	Lightly sanded and cleaned with methanol

typical epoxy circuit board formulation is shown in Table XXVI.[43]

Other examples of aluminum hydroxide use in epoxy resins systems with casting, potting, compression molding, encapsulation, laminating, and coil impregnation techniques for high-voltage insulators, circuit breakers, television components, circuit boards, heat-resistant parts, and transformers are detailed in the literature.[73,110,241,370–385] One of the most interesting newer applications and currently the fastest growing in the composites field is pultrusion.[386] Pultruded products are used in applications like oil field sucker rods and ladder rails, potential framing for space platforms, wiring box covers, third rail covers for mass transit systems, and a variety of rods, angles, and trough profiles as well as specialty tubing and pipe. Epoxies are used more for the high-end advanced composite pultruded products. These include high-strength, aerospace, and other high-tech applications. Recent work has also been completed to evaluate the synergism of aluminum hydroxide with phosphorus fire retardants in epoxies.[84,376,380]

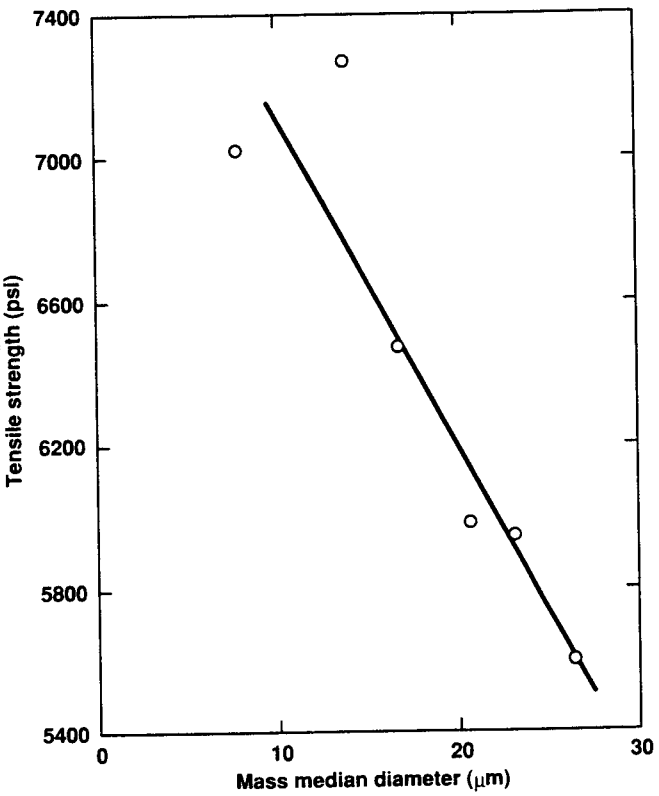

Fig. 25. Tensile strength vs particle size for various grinds from C-31 coarse–60% in epoxy resin.

Ethylene Vinyl Acetate and Other Cross-Linkable Ethylene Copolymers

This polymer grouping includes some of the highest volume single-application areas for aluminum hydroxide in electrical or electronic use today. These types of polymers generally fit better with the needs of the thermoplastic polymeric materials than the typical thermosetting resins based on the physical and chemical property characteristics of the hydroxides that have been used successfully. Although the resin combination possibilities and variations of hydroxides for new improved compound properties are still being

Table XXVI. Example Formulation Solvent Cast Upstaged Epoxy Resin

Formulation	Phr*
Glycidyl ether of brominated bisphenol A	100
Hydral PGA-B	45
Acetone or methylcellosolve with DMF	25
Dicyandiamide	3–4
Benzyldimethylamine	0.2–0.3

*Parts per hundred resin.

Applied with Burlington Glass Material.

heavily researched,[387–394] the initial work in this area was documented over 20 years ago.[395,396] Almost every grade of aluminum hydroxide available has been used in these types of systems for various applications. However, the largest volume, most successful uses generally require sharp or narrow distributions of precipitated 0.8 to 1.8 μm median particle sizes with either in situ or pretreatment types of chemical surface modifications. A typical application formula using in situ surface treatment is shown in Table XXVII.

This type of formulation, which can be used in appliance and automotive wiring insulation, has been one of the highest growth electrical applications. In the future, cross-linked polyethylene building wire and conduit applications for aluminum hydroxide have the potential to take the electrical application area growth lead. Much of the research has been completed and specific formulation approvals by code bodies and electrical standard setting organizations[400,401] are moving forward. In both cross-linked EVA copolymers and polyethylene, some property trade-offs may have to take place when high loadings of hydroxides are used. However, the combination of adequate physical properties with low smoke, fire retardance, and no corrosive off gases is a major advantage in electrical applications. The fire retardant basis for this advantage is well documented in the literature.[64,85,111,224,225,406,409,412,415,417–441]

Aluminum hydroxide incorporation in these types of systems is usually accomplished by melt compounding. This can be achieved by premixing ATH in polymer pellets or powder or by direct introduction of both components with other ingredients to a Banbury-type operation or compounding extruder. These steps can be followed by strand extrusion and pelletizing for shipping and handling. When the pellets go through final processing (wire coating extrusion, conduit extrusion, part molding, etc.), care must be taken to process below the time/temperature decomposition curve for aluminum hydroxide. This is generally not a problem for polyethylene-based materials but can be a serious problem for polypropylene, as will be shown in the section on thermoplastics. Applications other than electrical insulation and conduit for the EVA and cross-linkable copolymer systems that use aluminum hydroxide include automotive carpet backing, thermally insulating packaging, roofing material, building facing material, sheathings for optical fibers, fire-retardant wall covering linings, adhesives, and protective foams.

Table XXVII.

	Phr
EVA copolymer	100.0
Hydral PGA ATH	125.0
Stearate	2.0
Cross-linking agent	1.7
Vinyl silane	1.5
Antioxidant	1.0

Polyurethane and Other Thermosetting Polymers

Urethanes are extremely versatile polymers and therefore have already been partially covered under specific application portions of the previous elastomer foams and carpet sections. The flexible applications[442] for aluminum hydroxide in urethanes have realized more success and have a high potential for future growth as hydroxide particle size and surface modification advances take place. Urethane systems not referenced earlier, including some still in the research stages, involve laminant building materials, automotive exterior applications, thermally insulating materials, protective coatings, and so on.[219,442–448,456,457,461,463–465,468,470,471,474] While some use has already occurred in these applications, future growth will depend on research efforts to improve final physical characteristics of each application.

Other thermoset applications in similar need for follow-up research include compounds based on diallyl phthalate for building products and other uses,[479,480,483] phenol/formaldehyde, melamine formaldehyde, and phenol butyraldehyde systems.[451–454,466,478,484,548] These are molding compounds or binders for extremely highly loaded applications. A host of copolymer resins, grafted resin systems, and otherwise modified thermoset polymer systems not covered elsewhere,[360,449,450,455,458–560,462,467,469,472,473,476,477,481,482,485,526,545,580,581] for binder applications, foam building products, sealant applications, insulator applications, laminates, intumescent coatings, and circuit boards can also be found in the literature.

Thermoplastic Materials

Research on aluminum hyroxide in thermoplastic applications has made great strides in recent years but there is still much to be done before general acceptance in a wide range of thermoplastic polymers occurs. The most dramatic successes have been accomplished by making special modifications to both the hydroxide and the polymer systems. The most important customizing changes required of the hydroxide are in the particle-size median, particle-size distribution, and surface modification. Some of the more important changes required of resin may involve tailoring process aids, copolymerization, the use of blends

to adjust melt index, or incorporation of plasticizing additives for viscosity and physical property adjustments. These modifications are often unique to the specific application involved[336,496] and it appears that tailoring each of the components in the system will continue to be much more important for success of hydroxides in thermoplastics than in thermoset plastics or elastomers. While hydroxide surface modification usually is beneficial in all polymers, the benefit-to-cost ratio is much higher in thermoplastics, for example.

Another key to the success of hydroxides in thermoplastics, as with all polymer systems, is balancing or matching the processing temperature ranges and decomposition characteristics of the polymers and hydroxides. For example, thermoplastic systems involving some polystyrenes may decompose too fast for typical aluminum hydroxide.[397] Other thermoplastic materials like PVC, polyethylene, EVA, and so on seem to match fairly well with standard Bayer aluminum hydroxide both in processing temperature limits and decomposition characteristics, while materials like polypropylene, PBT, acetate, and so on can be processed inside or outside the decomposition range of normal ATH and therefore are compatible only if extreme care is taken in processing. However, some thermoplastic materials like nylon 66, PET, and fast cycling polycarbonate are definitely outside the gibbsite aluminum hydroxide decomposition range and are candidates for higher temperature decomposing hydroxides. Polymers from each of these groups will be discussed in the following section.

Polystyrenes

Many references ranging from insulation board to synthetic wood-look applications that claim the use of aluminum hydroxide for flammability and smoke reduction in polystyrene foams can be found in the literature.[399,475,503,574] A few also reference direct incorporation of aluminum hydroxide in high-impact polystyrene[336,535] applications. However, other references note ways to fire-retard polystyrene with aluminum hydroxide without direct incorporation by using other, perhaps more compatible, resins as binders or in a protective coating. This may be because the apparent effectiveness of ATH as a flame retardant/smoke suppressant compounded directly into polystyrene varies with the type of test.[336,397] The oxygen index and other vertical burn test results on polystyrene samples can be substantially improved using ATH[336,397] as can the early smoke hazard,[336] but horizontal burn tests and total smoke generated appear to be unaffected by normal loading levels. This phenomenon has been ascribed to a possible mismatch in the endothermic reaction rate and decomposition temperature of ATH to the temperature and rate of polystyrene pyrolysis. Vertical orientation and extremely high loadings may give better results because more of the endothermic by-products of aluminum hydroxide decomposition are available in the flame zone to reduce the rate of the eventual exothermic polystyrene combustion reaction step.[397]

Polyvinyl Chloride

PVC and PVDC applications have used aluminum hydroxide as a fire retardant/smoke suppressant since the early 1970s. However, new research still continues to evolve better fire-retardant combinations today.[575,576,628] The widest use of ATH in vinyls has been in flexible PVC applications and, while now surpassed by the volume of polyolefin and polyfin copolymer literature, flexible PVC data were the subject of more of the early available literature reports on aluminum hydroxide/polymer combinations than any other thermoplastic system. Some of the most significant early work that led to large-volume usage of aluminum hydroxide was in communication wiring insulation and jacketing.[636,637] In general, the largest portion of published PVC work is involved with wire and cable applications.[575,579,583,584,593–601,604,607,608,610,611,613,616,620–625] PVC coating applications also made up a good portion of the literature. Fabric coatings, metal coatings (aluminum siding), wall coverings, floor coverings, and upholstery coatings have been heavily funded in terms of PVC/hydroxide compound research efforts.[576,586,588,602,604,614,617,618,630,641–643] While vinyl foams are much more difficult applications to fire retard with ATH, some major successes have been noted even in this field.[578,591,615,638,640,644–646] Only a few large-volume applications have been reported in rigid PVC applications. This remains one of the most fertile areas for future research with a high potential for success.[577,587,589,590,606,612,626] Methods to maintain physical properties and good processibility are the primary challenge.

Smoke reduction in PVC with aluminum hydroxide has been a major advantage.[582–585,592,603,608,611,619,622,624,631] Because of the chlorine in its structure, polyvinyl chloride is somewhat inherently fire-retardant. Smoke levels can be improved even further by combining additives like ferric oxide, zinc borate, or molybdenum compounds with ATH.[592,611,633,638] However, some synergistic smoke-suppressant additives like ferric oxide can reduce flammability ratings[638] and some ignition-improving additives can increase smoke production, like fire-retardant phosphates.[630,631] This problem was also noted for halogen fire retardants in the section on unsaturated polyester thermoset plastics. Combinations of other fire retardants/smoke suppressants with aluminum hydroxide, while important in some cases to meet certain specifications, can cause a trade-off in other fire-related properties.

There were no data uncovered in the literature of polymer flammability rating reduction by the addition of aluminum hydroxide to already fire-retarded polymers. However, fire test data antagonism between other (nonhydroxide) fire retardants has been noted in

several polymer systems.[647–651] The reduction of PVC fire rating possible when a phosphorous-based fire retardant plasticizer and an antimony oxide fire retardant are used together is shown in Table XXVIII.[647] Notice the drop in oxygen index flammability rating when five parts Sb_2O_3 per 100 resin parts are added to two PVC compounds using a phosphate plasticizer to boost the fire rating. Some speculate that this antagonism is due to the fact that the two fire retardants act in the same phase in a burning polymer system (see the section on Fire Retardance of Aluminum Hydroxide in Polymers), that is, that they compete in the gas phase. It is possible that phosphorus renders the Sb_2O_3 useless by converting it to $SbPO_4$. A more plausible explanation is that these two fire retardants compete from different phases, each hindering the mechanism of the other. Phosphates have been shown to be effective fire-retardant char formers.[652] Antimony, on the other hand, works in the gaseous phase.[45,46] If the char forms first and does not allow the antimony to vaporize, the antimony may be useless as a fire retardant. On the other hand, if some antimony does break through the char, causing discontinuities in the char layer, the effectiveness of the phosphorus fire-retardant char mechanism to protect the polymer would be reduced. The result in any case is a diminished fire retardancy.

This antagonism must be taken into account when considering combination systems to use with ATH. In addition to being synergistic rather than antagonistic with most other fire retardants, the natural fire-retardant mechanism of ATH continually increases the fire rating as the concentration of ATH is increased in most polymer systems (this was shown for polyesters in Figs. 20 and 21). However, Fig. 26 shows that the increase in fire retardancy created by increased loadings of antimony oxide and zinc borate (Fire Brake ZB) reaches a maximum at 5 to 8 parts antimony per 100 parts of resin in flexible PVC systems.[608] This characteristic holds true in other systems as well. It follows then that any amount of antimony over this level can be replaced by an appropriate grade of aluminum hydroxide to achieve higher fire ratings.

The grades of aluminum hydroxide most often used successfully in PVC are in the 0.5 to 1.5 μm median particle size range. Sharp or narrow particle-size distributions of 1 μm median precipitated aluminum hydroxide have found the widest acceptance in PVC. Example formulations of two of the larger volume types of vinyl applications are shown in Tables XXIX and XXX. Table XXIX, top, is an example of a typical formulation that might be used as the basis to make fire-retardant shower curtains, laminated tarpaulins, or seat covering constructions.

Table XXVIII. Flammability of PVC Compounds

PVC	100	100	100	100
Triaryl phosphate, phr	65	65	65	65
Antimony oxide, phr		5		5
Calcium carbonate, phr			20	20
Antioxidants, phr	5	5	5	5
Oxygen index	31.8	29.1	32.1	31.8

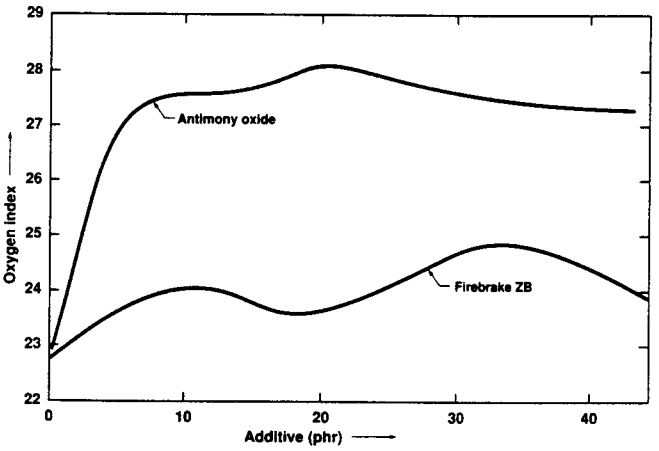

Fig. 26. Variation of oxygen index with additive concentration in flexible PVC.

Table XXIX. Calendered Sheet PVC

Material	Phr*
Medium M.W. PVC resin	100.0
Hydral 710	25.0
Phosphate plasticizer	14.0
DOP	5.0
DIDP	20.0
Alkyl phthalate	8.0
Fungicide	3.0
Liquid BaCdZn stabilizer	2.0
Solid BaCd stabililzer	1.0
Cheltor	0.5
Stearic acid	0.3
Banbury/Extruded Stock	
Medium M.W. PVC Resin	100.0
Hydral 710	15.0
DOP plasticizer	70.0
Synpron 1438 stabilizer	1.0
Stearic acid	0.5
Color concentrate	0.5

*Parts per hundred resin.

An alternate formulation for the extruded sheet uses a high molecular weight resin, 40 phr DOP, and 5 phr lead stabilizer in place of the similar components listed above.

Table XXX is an example of the current trends in wire and cable toward reduced smoke and reduced HCl emission formulations. Formulations with lower levels of the nitrile (Hycar) would normally not use as much of the Winnofil S filler, but similar formulas were used here for comparison.[654]

Production of PVC and copolymers of PVC reached nearly eight billion pounds in 1987.[653] A large portion of that total is compounded into systems in which aluminum hydroxide could be substituted for other less functional additives or fillers. Research in each application area is still required to allow the high loadings of aluminum hydroxide needed for dramatic

Table XXX. PVC/Nitrile Rubber Jacketing with Phosphate and Epoxy Plasticizers for Low-Smoke/ Low-HCl Evolution

PVC	100	80	60
Hycar 35/80	0	20	40
Reofos 50 phr	35	35	35
Reoplast 39	22	22	22
Winnofil S	60	60	60
Alcoa 710	60	60	60
Tribasic lead sulfate	6	6	6
Paraffin wax	1	1	1
LOI(%)	36.5	33.0	31.5
HCl evolution (%)	8	4	2
Tensile strength (Mn/m^2)	25.8	8.2	6.3
Elongation at break (%)	160	315	470
Volume resistivity (Ohm · cm × 10^{-12})	4.8	2.8	0.4
NBS smoke–flaming	223	162	126

reductions in smoke in many flexible and rigid PVC compounds. A good example of combined effects due to aluminum hydroxide in rigid PVC is shown in Table XXXI.[43]

In PVC siding a 0.5 μm median particle size, precipitated aluminum hydroxide was used to improve impact strength, weatherability, and processing of PVC exterior house siding. Research is continuing to further fire-retard and smoke-suppress this type of application based on slightly coarser, surface-treated hydroxide grades. Electrical conduit and pipe are other fertile rigid PVC application areas for the use of ATH to reduce smoke and HCl emissions. However, specific data and educated voices are needed to show the value of hydroxide-filled PVC as building products. This need has been created by the growing movement by many local officials to ban PVC plastics generally from new construction based on general and sometimes emotionally biased information about the hazards associated with nonfire-retarded/nonsmoke-suppressed PVC.[655,656]

Polyolefin Thermoplastics

The polyolefins (polyethylene, polypropylene, polybutylene, and their copolymers) have been the most heavily researched polymer group in terms of fire retardance and smoke suppression with aluminum hydroxide in recent years. The bulk of the pertinent literature involving ATH has occurred since 1980 and dramatic advances are still being made today.[388] This group of materials is finding increased usage as replacements for polymer systems that create more smoke in fire situations because of their cleaner burning characteristics. With aluminum hydroxide, polyolefin flammability is reduced without increasing smoke obscuration dramatically.[336,514,559–561]

It appears that for most olefin applications a combination of parameters must be changed to obtain optimum combinations of smoke, fire, processing, and final physical properties for each system. First, high loadings of ATH are needed, typically 35 to 65%. Second, the inorganic must usually be surface-modified (most often with an organic) for compatibility. Third, if the system is originally based on a homopolymer, it is likely a blend with a copolymer or a special rheology grade of a compatible polymer may be necessary to reduce melt index at the low processing temperatures required by the aluminum hydroxide and to increase some physical properties like impact strength. Finally, it is likely that optimum processing conditions will be obtained only with a processing additive package

Table XXXI. PVC Siding Formulation

	Parts
PVC (K = 65)	100.0
Hydral 705	6.0–12.0
TiO_2 (Rutile)	2.0–12.0
Calcium stearate	0.8– 2.0
Paraffin wax 165°F	1.2– 1.0
Processing aid	1.0– 0.3
Butyltin mercaptide stabilizer	1.5
Modified acrylic modifier	3.0– 5.0

Effect of modifier type on reinforcement with hydrated alumina (Formulation first column above with impact modifer as shown)

	Phr										
Variable	1	2	3	4	5	6	7	8	9	10	11
Hydrated alumina	6.0		6.0		6.0		6.0		6.0		6.0
Modified acrylic		5.0	5.0								
All-acrylic				5.0	5.0						
MBS						5.0	5.0				
CPE								5.0	5.0		
ABS										5.0	5.0
Izod impact (ft-lb/in notch)	1.0	14.3	22.6	2.6	13.9	5.3	8.4	1.5	20.9	2.5	9.4

specially designed for the specific applications in question.[336,388,496]

Polyethylene

A good portion of the literature and currently the highest volume uses for aluminum hydroxide in polyethylene and PE copolymer systems are in electrical applications. Wire insulation, wire jacketing, electrical conduit, plug moldings, and connectors are the primary application areas. High-molecular-weight/high-density polyethylenes were involved in some of the earliest successes with ATH. Insulating foams, panels, and a wide range of molded products make up the bulk of the more rigid uses for PE/aluminum hydroxide systems, while the newest nonelectrical applications involve adhesive copolymers and putties for small opening fire barriers and heavily loaded copolymer sheets for large surface area fire barriers.[388,494–497,499,501,502,504–506,508–517,519,520,524,525,527–531,536–538,541–544,547,551,552,555,558–567] Polyethylene, because of its high volume, low cost, relatively low processing temperatures, and capability to take high loadings of particulate and still maintain physical properties by cross-linking or copolymerization, has found the widest ATH acceptance of all the polyolefin-based systems.

Polybutylene/Polybutene

These materials are specialty polymers by comparison with polyethylene applications. Systems using these polymers have much less total usage of aluminum hydroxide because of their low-volume/higher cost base. However, there is still good potential in butadiene hot melt adhesive systems and butylene pipe and tubing applications. In addition, copolymers with ethylene using ATH have been used successfully as wire and cable insulation materials.[512,518,533,557] The pipe and fittings application is an extremely interesting one. While relatively low volume overall, one of the highest potential volume applications is in mobile homes, motor homes, and other part-time living or vacation quarters where unprotected plumbing made from normal polymers, copper, or steel can be damaged by freeze/thaw conditions. The butylene materials have the same good balance of pipe properties as PVC but also maintain those properties at very low temperatures and can take a hard freeze expansion without bursting. Because of the part-time use of vacation homes and other temporary facilities, there is also a higher risk of undetected fire propagation. The combination of these factors points to a potential need for some specific fire-retardant work in this area.

Polypropylene

Aluminum hydroxide applications in polypropylene generally parallel the types of uses in polyethylene but propylene is required because of some extra but critical property not available with polyethylene to justify the higher base cost of using this resin. Examples include sheet oriented to give higher strength in one direction, cabinet materials matching final physical properties of high-impact polystyrene but with lower smoke characteristics, electrical applications requiring better dielectric properties, part constructions needing special foaming characteristics, parts requiring good injection molding, processability or better weathering characteristics, or higher thermal stability, and so on.[336,398,498,500,507,523,532,534,539,540,546,549,550,553,554,556,568–573,657]

Over 6.6 billion pounds of polypropylene were produced in 1987, but very little of this was compounded with aluminum hydroxide even though the literature shows that some compounding and final part processing technology is available and the fire and smoke benefits are clear. It is possible that an educational program must be undertaken to get the literature and hands-on experience to those who need it. Clearly the research-expanding technology to allow ATH use in other polypropylene applications must continue.

The major drawback to any aluminum hydroxide approach is the wide range of processing temperatures that operators are accustomed to using with polypropylene and the bad experiences some have had when the upper aluminum hydroxide limits of 200°C bulk, 230°C local, compound processing temperatures have been inadvertently exceeded. Crackling and popping in extruders, surface splay on injection-molded parts and extruded sheet/conduit/wire insulation or under extreme conditions, and enough steam pressure build-up in nonvented systems to open injection molds have all occurred. Even in cases where the processing temperature limits for aluminum hydroxide have been strictly followed, the high loadings of particulate required to meet some fire standards have sometimes caused problems by reducing production rates due to the extra power requirements to extrude normal rates at these lower temperatures. While current and future research efforts will expand the range of polypropylene applications that will be able to use aluminum hydroxide through better process aids, copolymers/blends, and better processing technology, there will always remain some polypropylene applications that will require hydroxides that process at higher temperatures than standard Bayer process aluminum hydroxide.

Tables XXXII and XXXIII[336] show the balance of properties attainable with a polypropylene/aluminum hydroxide system when required to meet the properties of a halogen fire-retarded high-impact polystyrene but have lower smoke characteristics. This compound was the result of a research program to make a low smoke injection, moldable, thin-walled electric cabinet

Table XXXII. Polypropylene/Aluminum Hydroxide Composite 231

Hercules 7823	18.5%
Hercules 6523	18.5
Alcoa lubral 710 IS	62.0
Emery E-132	1.0

Table XXXIII. Physical and Electrical Properties of Polypropylene/Aluminum Hydroxide Composite 231

Property	Value
Specific gravity	1.45
Oxygen index (D2863-77)	30
U/L VBT (0.094" at 73°F)	V-O
Izod impact (0.125" at 73°F; Notched)	1.5 ft-lb/in [2.81 × 10^{-2} J/m]
Tensile yield strength (D638-77a)	2800 psi (1.93 × 10^{1} MPa)
Elongation	15.5%
Flexural modulus (D790-71)	3.68 × 10^{3} MPa (534,000 psi)
Flexural strength (D790-71)	4.04 ¼ × 10^{1} MPa (5,860 psi)
Gardner impact (1.125" at 73"F)	150 in-lb
Heat-distortion temperature (66 psi)	105"C (222"F)
Heat-distortion temperature (264 psi)	62"C (144"F)
Smoke obscuration number (SON)	4.0
Arc resistance (D495)	No failure; samples melted–4 min
Dielectric strength–short time (D149)	510 V/mil
–step-by-step	350 V/mil
Volume resistivity (D257)	1.42 (10^{12} ohm/cm)
Surface resistivity (D247)	6.94 (10^{12} ohm/cm)
Dielectric constant (D150)	
at 10^{2}, 10^{3}, 10^{6} Hertz	4.71; 4.15; 3.23
at 10^{2} Hertz	0.09056
at 10^{3} Hertz	0.08335
at 10^{6} Hertz	0.02026

material. Molding trials have shown acceptability for pump housings, electric fan housings, fire-retardant vent covers, and electrical connectors.

Higher Temperature Processing Thermoplastics

There are very few reported data involving gibbsite aluminum hydroxide in thermoplastics that normally process at temperatures above 230°C because of the degradation of ATH above that temperature. The only well-documented work involves low-temperature casting of coatings in lattices, in monomers, or other special processing techniques. Polyamides have been specially processed with aluminum hydroxide and other fire retardants by preparing a latex coating adhesive for fabrics[541] or by plasma spraying to make a refractory coating.[586,588] Polyoctanes have been monomer cast with aluminum hydroxide to make fire-retardant foams from E-caprolactam.[660]

Two notable exceptions to these lower temperature ways to use higher temperature polymers have been claimed in the literature but no commercial follow-up has been uncovered. There are reports of normal higher temperature processing of ABS and polyphenylene oxide with aluminum hydroxide. Studies on both polymer systems discuss advantages of flame retardance and/or smoke suppression but none go into detail on processing, amount of degradation, or final physical properties obtained.[486–493] It is suspected that, with the exception of aluminum monohydroxide, there would be considerable degradation in commercial practice of the regular gibbsite aluminum hydroxides noted in these studies. In addition, the reduction in ABS physical properties caused by the current commercially available grades of ATH could be dramatic. The same processing temperature problems in practice could occur with the claimed fire-retardant advantages in injection-molded polyphenylene oxide.[658,659]

To overcome these problems, higher temperature, decomposing, aluminum-containing hydroxide systems have been and continue to be the subject of much research in thermoplastics. In the last few years, work has again started with magnesium aluminum carbonate hydroxides, for example, in applications from polyolefins to silicones.[66,85,99,126,402–405,667] Earlier work with these types of potential fire retardants covered polymer applications from PVC to polyester and ABS.[662–664] Of the previous systems studied, thermoplastic polyesters and ABS polymers have the greatest need for tailoring of these types of potential fire-retardant compounds to match each polymer's degradation and processing properties. Initial updated studies in this area should also include materials like polypropylene and nylon. Current and future fire-retarding hydroxide programs will have to address deficiencies in each polymer system, including the final polymer physical properties, to be successful. This type of aluminum- and carbonate-containing hydroxide material is noted because of its rearrangable anionic clay structure.[673–677] The rearrangement of this structure to give critical properties is relatively simple[678–680] and can produce a wide variety of aluminum and nonaluminum hydroxides or hydrates.[673,674]

There is also a substantial volume of work available on sodium aluminum carbonate hydroxides in polymer systems ranging from polyolefins to higher temperature processing materials like polyacrylnitrile.[99,397,662,663,665–670,679,681,690] These types of aluminum-containing hydroxides are all viable starting

points for successful fire retardants and smoke suppressants in higher temperature processing polymers because they react in an endothermically similar manner to Bayer gibbsite aluminum hydroxide but over different higher temperature ranges.[682,703–706] This second material, for example, can be widely varied in crystal form to give anything from spherical agglomerates to high-aspect-ratio fibers. The fibers have been found to give excellent fire-retarding properties as well as increased heat-deflection temperature and increased tensile strength, while reducing melt flow in higher temperature processing polymers specifically needing those properties, such as propylene and ABS.

Two other types of aluminum-containing hydroxides that have some potential to fill lower temperature processing or specialty niches in a fire-retardant family for thermoplastics are ammonium aluminum carbonate hydroxide and one or more of the calcium aluminate hydroxides. These materials have been tested loosely in systems that range in decomposition characteristics from polystyrene to polypropylene and ABS.[662,663,671,672] Each has been found to improve the fire retardancy of the specific polymers where the exothermic decomposition reaction rate and initiation temperature are matched to reaction rate and temperature range of the endothermic decompositions of the individual hydroxides.

The volume of higher temperature processing polymers, which includes the engineering-grade resins, is over 10 billion pounds per year.[653] While not all of these polymers produced need to be fire retarded and smoke suppressed, the applications that do, continue to grow, especially for the hydroxide-type materials. This is in part because of the current emphasis on halogen-free and low-smoke/fire-retardant polymer products. Success in each application will require tailoring both the hydroxide and the polymer composite to be able to meet the demands of current and future specifications. The process of upgrading polymer compounds with hydroxides is really one of developing design aids that allow designers and specifiers to select materials with precise performance properties. These include fire retardance, smoke suppression, toxicity reduction, higher temperature processability, coloring, ease of handling, physical property improvement, processing property improvement, weathering property improvement, and so on. This concept is crudely shown schematically in Fig. 27.

Aluminum Hydroxide Surface Modification for Design Properties

After tailoring particle size and shape, the next most important aspect to compatibility of the inorganic aluminum hydroxides to the organic polymer matrix is the tailoring of the hydroxide particle surface chemistry. Depending on the particle size and shape, and the treatment used, surface modification can increase the hydroxide price from 5 to 50 cents per pound. Typical types of treatments include fatty acids, organosilicone chemicals, deactivating inorganic chemicals, wetting

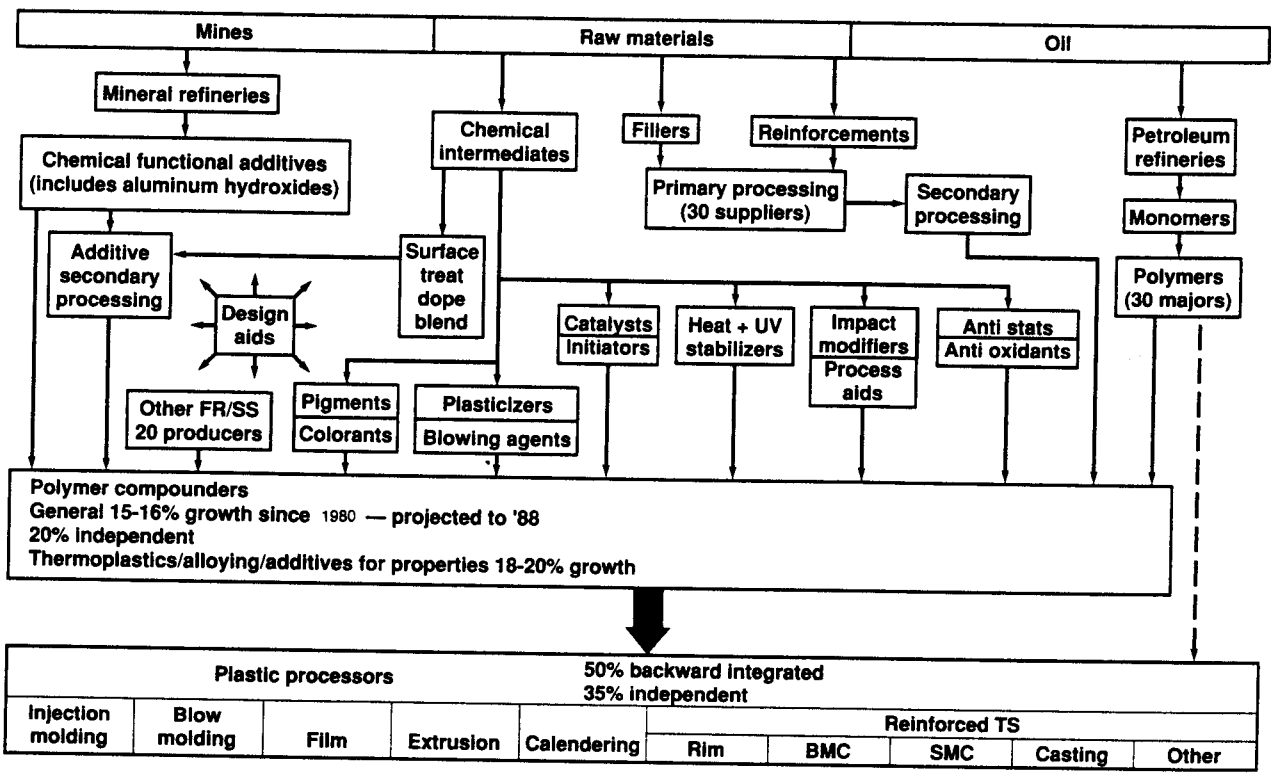

Fig. 27. Aluminum hydroxides as part of the design aids concept for polymer compounds.

agents, liquid flame retardants, and catalysts. Generally they can be classified into two categories: coupling agents and compatibilizing agents. If original manufacturer treatments, captive treatments, and in-process treatments are collectively considered, at least 30 million pounds of the domestic U.S. production of aluminum hydroxide requires surface treatment for polymer applications. In practice, between 0.5 and 2% surface-treating chemical by weight of the aluminum hydroxide is usually added. This is much more than monolayer coverage would require.[683] Unfortunately, the state of the art of commercial surface-treatment technology is not yet at a level that allows adequate encapsulation of every particle at monolayer coverage. This requires higher concentrations to be applied than theoretically needed to obtain optimum results in polymer.[336,684–686]

The hydroxide and the polymer matrix are of course very different. The inorganic is hydrophilic and ionically bonded, the polymer is hydrophobic and covalently bonded. Each has widely differing physical properties but their differences show up most emphatically where they interface. This is the weakest link in the polymer/ATH compound matrix, and it is at this contact region where electrical, physical, or chemical breakdown occurs. Compatibilizing agents tend to decouple the hydroxide particles from each other, allowing the inorganic phase of the matrix to be dispersed in or wet out by the polymer phase. Compatibilizing agents usually react with one phase only if any. Coupling agents, on the other hand, are supposed to react with both phases and therefore usually have different functional groups for each type of polymer involved.[687,688] Because of this cross-linking effect by the coupling agents, they can increase tensile strength, compressive strength, and wet-tested electrical properties tremendously. However, they tend to make the system more rigid and brittle, reducing elongation and impact strengths.

In the opposite manner, the compatibilizing or decoupling agents tend to act as process aids, plasticizers, or lubricants. Energy of impact can be absorbed by some slip at the interface now that rigid chemical bonds described with coupling agents do not have to break. Some of these types of surface treatments, like isostearic acid, react and tightly bond with the hydroxide surface but the long hydrocarbon chain tail simply protrudes into the polymer phase. A series of molecules, head attached at the hydroxide particle and tails sticking out into the polymer, may appear as advertisements which have shown soap molecules drawn around dirt particles in water. The long tails entangle with the polymer chain molecules while keeping individual hydroxide particles separated; however, under impact shock some disentangling can take place without breaking bonds and rupture. Combining these two concepts of coupling and compatibilizing in one mixed treatment appears to give the best of both worlds.[684]

The widest use of surface treatment with aluminum hydroxides is in thermoset and thermoplastic polymers, although there is some use in elastomers, adhesives, and other polymer base applications. The earliest successes were in elastomers and thermoset polyester systems to allow increased loadings of aluminum hydroxide. Later the use of surface treatment to improve electrical properties of hydroxide-filled systems was discovered. Now surface treatments can be specified that will individually improve process viscosities, tensile strengths, impact strengths, and many other critical application properties. The growing portion of the use of surface treatments for hydroxides in plastics is for these final physical properties although uses for processing and electrical property improvement also continue to play a role. Elastomers on the other hand, use surface treatments with hydroxides primarily for better wet-out of the particulate. This usually also translates into improved bonding and better wet electrical properties. In low-viscosity adhesive and sealant applications, surface treatments are sometimes used as suspension aids, especially in systems where a shear thinning effect can take place if remixing would be needed to avoid settling out of the aluminum hydroxide.

Over one-third of the use of surface-treated aluminum hydroxides has been in thermoplastic, wire and cable applications. Thermoset compound moldings comprise the next largest group of polymeric uses for surface-treated ATH, followed by elastomeric cable insulation and jacketing applications. Polyethylene copolymers and PVC applications are the largest volume thermoplastic uses. Epoxies are the highest volume thermoset plastic use and EPDM the larges volume elastomeric use of surface-treated hydroxides. These are only a few of the larger volume uses o treatments with ATH. An in-depth look at the history and all application uses will have to be the topic o another discussion.[273,278,306,317,318,335,338,642,689–702]

References

[1]Alcoa Product Data, Hydrated Aluminas Series C-30, C-300 and Hydral 700. Aluminum Company of America, Alumina and Chemicals Division, East St. Louis, IL, 1959.

[2]Hentchel, H. Wochenbl, Papierfaer 1968, 23/24, 851–854.

[3]E. Bohn, Allg. Paper, Rundsch 1964, 24, 1987–1991.

[4]J. J. Koenig, *TAPPI* (1964). **48** [12] 123A–124A.

[5]H. H. Murray, "Paper Coating Pigments," Monograph Series No. 30, New York, 1966.

[6]W. H. Bureau, Paper . . . From Pulp to Printing. Graphic Arts Publishing, Chicago, 1968.

[7]J. W. Newsome, H. W. Heiser, A. S. Russell, and H. C Stumpf, "Alumina Properties," Technical Paper No. 10, Aluminum Company of America, Pittsburgh, 1960.

[8]J. J. Koenig and G. G. Tauth, "Paper Coating Pigments."

[9]R. Hoyles, "Toothpaste," U.S. Pat. No. 4 212 856, July 15 1980.

[10]R. L. Mitchell, "Dental Cream," U.S. Pat. No. 4 046 872 September 6, 1977.

[11]R. L. Mitchell and W. J. Chang, "Dental Cream Composition," U.S. Pat. No. 4 152 417, May 1, 1979.

[12]L. T. Murray and G. M. Salmann, "Dentifrice Compositions," U.S. Pat. No. 3 822 345, July 2, 1974.

[13]L. L. Musselman and L. F. Weiserman, "Surface Treated Aluminas for Reduced Halide Application," U.S. Patent No. 4 781 982, November 1, 1988.

[14]L. L. Musselman and T. L. Levendusky, "Surface Modified Alumina Trihydrate," U.S. Pat. No. 4 711 673, December 8, 1987.

[15]J. E. Williams, "Hydrated Alumina Extenders," *Paint Varnish Production*, June 1967.

[16]J. E. Williams, "Hydral 705 in Water-Based Acrylics," Alcoa Laboratories, March 1968.

[17]H. W. Ritter, W. A. Blose, and T. A. Demski, *J. Paint Technol.*, **38** [500] (1966).

[18]AH l_T (TOW), Final Trials Phase Service Acceptance Trials ("Zuni Rocket Blast/Airframe Protective Coating Test," Naval Air Test Center Report No. RW–19R–80, July 24, 1980.

[19]D. K. K. Tatsuta, "Paint Composition," Jpn. Pat. No. J58120675–A, July 18, 1983.

[20]V. P. Clark, "Coating Compositions," U.S. Pat. No. 3 945 962, March 23, 1976.

[21]H. Mizushima and K. Oshio, "Flameproofed Fiberboards," Jpn. Pat. No. 7528582, July 3, 1975.

[22]M. Ito, T. Nakai, and C. Matsui, "Laminated Materials," Jpn. Pat. No. 7311827, April 16, 1973.

[23]S. T. Monte, G. Sugermen, and D. J. Seeman, "Titanate Coupling Agents — Update 1977," 32nd Annual Tech. Conf., SPI Reinforced Plastics Institute, Paper 4-E, 1977.

[24]H. L. Becher, "Fire Resistant Sheet," U.S. Pat. No. 2 611 694, September 23, 1952.

[25]M. Ueoa, T. Duehi, and T. Horike, "Fire Resistant Boards," Jpn. Pat. No. 7527397, March 20, 1975.

[26]F. G. Alfeis and R. W. Goldsmith, "Fire Resistant Webs and Internal Treatment Therefore," U.S. Pat. No. 4 032 393, June 28, 1977.

[27]M. W. Hart, Jr., "Bonding Fabric and Other Carriers to Highly Plasticized PVS Using a Fire Retarding Adhesive," U.S. Pat. No. 3 814 661, June 4, 1974.

[28]J. G. Bergome, Jr., "Flame Resistant Compositions of Ethylene/Vinyl Chloride Interpolymers and Hydrated Alumina," U.S. Pat. No. 3 827 997, August 6, 1974.

[29]H. Uejima, K. Kudo, T. Nanba, T. Ida, H. Yamamura, and Y. Echigo, "Fire Resistant Polyamide Fabrics," Jpn. Pat. No. 75152097, December 6, 1975.

[30]DuPont, "Fire Resistant Neoprene Interlayers for Upholstered Furniture," Netherlands Pat. No. 2 244 597, April 25, 1974.

[31]H. Uejina, K. Kudo, T. Nanba, T. Ida, H. Yamamura,and Y. Echigo, "Fireproofed Pile Textiles," Jpn. Pat. No. 7455995, May 30, 1974.

[32]I. Okuda, "Fireproofing of Synthetic Nonwoven Textiles," Jpn. Pat. No. 7548272, April 30, 1974.

[33]J. W. Pedlow, "Arc and Fireproofing Tape," U.S. Pat. No. 4 018 962, April 19, 1977.

[34]I. Yoshitake, A. Sakai, and H. Takabe, "Synthetic Paper," Jpn. Pat. 74116378, November 7, 1974.

[35]H. Uejima, K. Kuko, T. Nanba,and H. Yamamura, "Fire Resistant Polyamide Fabrics," Jpn. Pat. No. 75152096, December 6, 1975.

[36]H. Uejima, K. Kudo, T. Nanba, and H. Yamamura, "Fire Resistant Polyamide Fiber Products, Jpn. Pat. No. 75152096, December 6, 1975.

[37]T. Miwa and H. Akazawa, "Fireproofed Textiles with Increased Retention of Tensile Strength," Jpn. Pat. No. 7582399, July 3, 1975.

[38]F. X. Chancler, "Polyurethane Foam Molding,' Ger. Pat. No. 2 450 508, May 15, 1975.

[39]S. Kumasaki, S. Tada, and G. Yoneyama, "Fireproofing of P.U. Foams," Jpn. Pat. No. 7509674, October 3, 1975.

[40]L. L. Musselman and P. V. Bonsignore; unpublished Alcoa Customer Application Presentations, 1978.

[41]P. V. Bonsignore, "Alumina Trihydrate as a Component of Flame Retardant Coating Systems for Cellulosic Materials," FRCA Conference, October 30, 1977.

[42]L. L. Musselman and P. V. Bonsignore; unpublished customer applications presentations, Alcoa, 1979.

[43]L. L. Musselman and T. L. Levendusky, "Precipitated Alumina Trihydrate for Polymers," SPE 1984, RETEC, Georgia Institute of Technology, October 22, 1984.

[44]J. W. Newsome, H. W. Heiser, A. S. Russell, and H. C. Stumpf, Alumina Properties Technical Paper No. 10, Aluminum Co. of America, 1960.

[45]P. C. Warren, Polymer Stabilization. Wiley & Sons, New York, 1972.

[46]K. Akita, Aspects of Degradation and Stabilization of Polymers. Elsevier, Amsterdam, 1978.

[47]SPE Technical Program Literature — PVC: The Issues, Vinyl Division Retec, Bally's Park Place Hotel, September 15–17, 1987.

[48]S. Hattangadi, "Free Radicals — A Chemical Clue to Mystery Deaths," *Ind. Chem.*, October 1987.

[49]P. W. Jones and R. E. Wilkinson, U.S. Pat. No. 2 768 264, October 23, 1956.

[50]R. S. Norman and A. A. Kessal, "The Internal Oxidation Mechanism for Non Tracking Organic Insulation," *AIEE*, (1958).

[51]A. A. Kessal and R. S. Norman, U.S. Pat. No. 2 997 526, August 22, 1961.

[52]A. A. Kessal and R. S. Norman, U.S. Pat. No. 2 997 527, August 22, 1961.

[53]A. A. Kessal and R. S. Norman, U.S. Pat. No. 2 997 528, August 22, 1961.

[54]A. Schellmoeller, H. Mussenbach, and H. Will, "Covering Material," Ger. Pat. No. 3 306 776, August 23, 1984.

[55]Denki Kaguku Kogzo K. K., "Fire Resistant Backing Compositions," Jpn. Pat. No. 83186675, October 31, 1983.

[56]Hitachi Cable Ltd., "Fire Resistant Rubber Compositions," Jpn. Pat. No. 83225116, December 27, 1983.

[57]I. Bartholomeus, H. A. Mazer, W. Muno, and D. S. Parmer, "Polymer Compositions for Cable Insulation," African Pat. No. 83/4185A, February 29, 1984.

[58]Hitachi Ltd., "Potting Compositions for Flyback Transformers," Jpn. Pat. No. 84/191206, October 30, 1984.

[59]Shin-Etsu Chemical Company, "Fire Resistant Rubber Compositions," Jpn. Pat. No. 84/140242, August 11, 1984.

[60]Fujukara Cable Works, Ltd., "Flame Retardant Polyurethane Compositions," Jpn. Pat. No. 84/86619, May 18, 1984.

[61]Fujikara Cable Works Ltd., "Fireproofing Putty Compositions," Jpn. Pat. No. 84/89371, May 23, 1984.

[62]Showa Electric Wire & Cable Co. Ltd., "Fire Resistant Putty," Jpn. Pat. No. 84/1428, January 12, 1984.

[63]J. Hardvick et al., "Fire Resistant Material," Nowegian Intl. Pat. No. 83/4041, November 24, 1983.

[64]Sumitomo Electric Industries Ltd., "Nonflammable Low-Smoke Polyolefin Compositions," Jpn. Pat. No. 84/117549, July 6, 1984.

[65]Hitachi Cable Ltd., "Flame Retardant Electric Insulator Compositions," Jpn. Pat. No. 84/118006, July 6, 1984.

[66]Furukawa Electric Co. Ltd., "Flame Retardant Polyolefin Resin Compositions," Jpn. Pat. No. 84/227935, December 21, 1984.

[67]P. C. Laurenson, "Fire Resistant Thermoplastic Mixtures and Their Use on Electric Cables," Fr. Pat. FR2538401A1, June 29, 1984.

[68]Hitachi Ltd., "Potting Compositions for Flyback Transformers," Jpn. Pat. No. 84/100509, June 9, 1984.

[69]Hitachi Ltd., "Thermosetting Rubber Compositions," Jpn. Pat. No. 83/160309, September 22, 1983.

[70]P. Galli, S. Danesi,and T. Simonazzi, "Polypropylene Based Polymer Blends," *Polymer Eng. Sci.*, **24** [8] 544–54 (1984).

[71]Denki Kagaku Kogzo K. K., "High Filled Fire Retardant Sealants," Jpn. Pat. No. 83/171468, October 6, 1983.

[72]J. F. Szabat and J. A Gaetano, "CMHR Foam for High Risk Occupancies," SPI 6th Tech/Mark. Conf., New York, NY, Polyurethane Div. Proceedings, p. 326–31. 1983.

[73]J. G. Schuhmann, "Improved Furniture and Mattress Fire Safety Through the Use of Combustion Modifying Polyurethane Foam," SPI 6th Tech/Mark. Conf., New York, NY, Polyurethane Div. Proceedings, p. 307–15, 1983.

[74]P. A. Isaacs, "Flame Retardant Thermoplastic Polyurethanes," SPI 6th Tech/Mark. Conf., New York, NY, Polyurethane Div. Proceedings, p. 499–502, 1983.

[75]J. Z. Keating, "The Use of Hydrated Alumina as a Flame and Smoke Suppressing Filler for Flexible Urethane Foams," *J. Fire Retardant Chem.*, **9** [4] 215–20.

[76]Eaton Corp., "Fire Resistant Elastomer Composition," Jpn. Pat. No. 83/217513, December 17, 1983.

[77]Denki Onkyo Co. Ltd., "Impregnants for Flyback Transformers," Jpn. Pat. No. 83/21403, April 30, 1983.

[78]Nippon Leon Co. Ltd., "Potting Compositions," Jpn. Pat. No. 83/93717, June 3, 1983.

[79]Hitachi Cable Ltd., "Fire Resistant Insulated Electric Wire," Jpn. Pat. No. 83/87709, May 25, 1983.

[80]Hitachi Cable Ltd., "Fire Resistant Insulated Electric Wire," Jpn. Pat. No. 83/87710, May 25, 1983.

[81]Osaka Packing Mfg. Co. Ltd., "Fireproof Putty Compositions," Jpn. Pat. No. 83/84881, May 21, 1983.

[82]E. Ruehl and J. Thenner, "Nonflammable Rigid Polymeric Foam and Its Use as a Construction Material," Ger. Pat. No. DE 3244779C1, April 12, 1984.

[83]Hitachi Ltd., "Epoxy Resin Compositions," Ger. Pat. No. A2 84/78268, May 7, 1984.

[84]Fujikura Cable Works, Ltd., "Polyethylene Flame Retardant Compositions," Jpn. Pat. No. 83/49739, March 24, 1983.

[85]Furukawa Electric Co., "Fire Resistant Polyolefin Composition," Jpn. Pat. No. 84/2022431, November 16, 1984.

[86]A. C. Kingston, "Faced Masonry Units and Facing Compositions Therefor," U.S. Pat. No. 4 499 142A, February 12, 1985.

[87]J. Hordvik, W. L. Persson, N. S. Pedersen, and A. Kristiansen, "Fire Resistant Material," *Appl.* **83** [17] May 4, 1983.

[88]Fujikura Cable Works Ltd., "Fire Resistant Polyethylene Compositions," Jpn. Pat. No. 83/63738, April 15, 1983.

[89]Fujikura Cable Works Ltd., "Fireproofing Polyethylene Blends," Jpn. Pat. No. 83/49738, March 24, 1983.

[90]Nippon Iron Co. Ltd., "Fire Resistant Polyurethane Composition," Jpn. Pat. No.

[91]L. D. McKinney, "Polyurethane Composition for Carpet Backing," U.S. Pat. No.

[92]J. F. Szabat, "Combustion–Modified Flexible Polyurethane Foam," U.S. Pat. No. 4 381 351A, April 26, 1983.

[93]Hitachi Ltd., Hitachi Chemical Co. Ltd., "Castable Electric Insulators," Jpn. Pat. No. 82/212222, December 27, 1982.

[94]Hitachi Ltd., Hitachi Chemical Co. Ltd., "Castable Electric Insulators," Jpn. Pat. No. 82/212223, December 27, 1982.

[95]Hitachi Cable Ltd., "Fire Resistant Sealing Compositions," Jpn. Pat. No. 82/209980, December 23, 1982.

[96]Denki Kagaku Kogyo K. K., "Fire Resistant Two-Liquid Type Sealants," Jpn. Pat. No. 82/192482, November 26, 1982.

[97]Shin-Etsu Chemical Industry Co. Ltd., "Fire Resistant Rubber Electric Insulators," Jpn. Pat. No. 82/195757, December 1, 1982.

[98]J. F. Porter and D. G. Hayashi, "Coating Composition for a Flame Retardant Cable Jacket," Can. Pat. No.1116797A1, January 19, 1982.

[99]Hitachi Cable Ltd., "Nonflammable a-olefin Resin Compositions," Jpn. Pat. No. 82/170941, October 21, 1982.

[100]Hitachi Cable Ltd., "Nonflammable a-olefin Resin Compositions," Jpn. Pat. No. 82/170942, October 21, 1982.

[101]Hitachi Cable Ltd., 'Fire Resistant Polyolefin Compositions with Low Smoke Damage," Jpn. Pat. No. 82/165437, October 12, 1982.

[102]W. Goyert, W. Fleige, H. G. Hoppe, and H. Wagner, "Flame Retardants for Thermoplastic Polyurethane Rubbers with Low Halogen Contents," Ger. Pat. No. DE 31133851A1, October 21, 1982.

[103]Hitachi Cable Ltd., "Fire Resistant Polyurethane Compositions," Jpn. Pat. No. 82/121021, July 28, 1982.

[104]Hitachi Ltd., "Insulators for Flyback Transformers," Jpn. Pat. No. 82/96507, June 15, 1982.

[105]Fujikura Cable Works Ltd., "Fire Resistant Olefin Polymer Compositions," Jpn. Pat. No. 82/92037, June 8, 1982.

[106]A. A. Davies, "Fire Resistant Molded Rubber Foams," Eur. Pat. Appl. EP55081A1, June 30, 1982.

[107]Takiron Co. Ltd., "Fire Resistant Foams," Jpn. Pat. No. 82/633334, April 16, 1982.

[108]Mitsubishi Chemical Industries Co. Ltd., "Curable Polymer Compositions," Jpn. Pat. No. 82/76019, May 12, 1982.

[109]J. Oda, "Refractory Putty," Ger. Offen. DE 3204387A1. August 12, 1982.

[110]D. J. Braun, "Effect and Application Range of Aluminum Hydroxide as a Flame Retardant Filler," *Plastverarbeiter*, **33** [7] 711–4 (1982).

[111]I. Bartholomeus, P. Daljit, and H. A. Mayer, "Fire Resistant Polymer Cable Insulation," Eur. Pat. Appl. EP54424A2, June 23, 1982.

[112]J. E. Betts, A.C.Bruhin, and R. P. Hoeppner, "Fire Resistant Insulated Multiconductor Electric Cable," Can. CA 1104677A1. July 7, 1981.

[113]Dunlop Ltd., "Flame Retardant Foam Cushions," Neth. Appl. NL80/4257A, February 16, 1982.

[114]Furukawa Electric Co. Ltd., "Fire Resistant Rubber Electric Insulators," Jpn. Pat. No. 82/18744, January 30, 1982.

[115]Fujikura Cable Works Ltd., "Fire Resistant Ethylene Propane Rubber Compositions," Jpn. Pat. No. 82/5736, January 12. 1982.

[116]M. P. Pcolinsky, Jr., "Intumescent Flexible Polyurethane Foam," U.S. Pat. No. 4 317 889A, March 2, 1982.

[117]Hitachi Ltd., Hitachi Chemical Co. Ltd., "Epoxy Terminated Butadiene Rubber Electric Insulator Coating Compositions," Jpn. Pat. No. 82/12037, January 21, 1982.

[118]Matsushita Electric Industrial Co. Ltd., "Fire Resistant Butadiene Rubber Casting Compositions," Jpn. Pat. No. 82/8231. January 16, 1982.

[119]Mitsubishi Electric Corp., "Fire Resistant Electric Insulators," Jpn. Pat. No. 81/133327, October 19, 1981.

[120]J. C. J. Fallows and R. G. Harvey, "Flame Retardant Polyurethane Foam Crumb," Br. Pat. No. 6B1594474A, July 30. 1981.

[121]R. K. K. Sunyu, "Fire Resistant Urethane Polymer Electric Insulation," Jpn. Pat. No. 81/122821, September 26, 1981.

[122]Hitachi Cable, Ltd., "Electric Cable Sheathings," Jpn. Pat. No. 81/104983, August 21, 1981.

[123]W. J. Bobear, "Flame-Retarding Silicone Rubber Compositions," Fr. Demande FR 2472591, July 3, 1981.

[124]D. Wolfer and A. Schiller, "Fire-Resistant Elastomers Or Crosslinkable Compositions From Organopolysiloxanes After The Addition of a Crosslinking Agent," Ger. Pat. No. DE 3018549A1. November 19, 1981.

[125]Hara Dingen K. K., "Fire-Resistant Silicone Rubber Foam Sealants," Jpn. Pat. No. 82/141476, September 1, 1982.

[126]Shin-Etsu Chemical Industry Co., Ltd., "Fireproof Silicone Rubber Compositions," Jpn. Pat. No. 83/65751, April 19, 1983.

[127]V. Abolins, J. E. Betts, and F. F. Holub, "Flame-Resistant Thermoplastic Blends of Polyoryphenylenes," U.S. Pat. No. 4 497 925A, February 5, 1985.

[128]B. A. Ashby, "Silicone Flame Retardants For Nylon," U.S. Pat. No. 4 496 680A, January 29, 1985.

[129]Mitsubishi Electric Corp., "Castable Electric Insulator Compositions," Jpn. Pat. No. 81/103806, August 19, 1981.

[130]Mitsubishi Electric Corp., "Castable Electric Insulator Compositions," Jpn. Pat. No. 81/103805, August 19, 1981.

[131]P. V. Bonsignore, "Alumina Trihydrate As a Flame Retardant For Polyurethane Foams," *J. Cell. Plast.*, **17** [4] 220–25 (1981).

[132]J. P. Hons-Olivier, T. LeThanh, and F. M. Devanz, "Fireproof Elastic Packing Material," U.S. Pat. No. 4 266 039, May 5. 1981.

[133]H. R. Bennett and G. M. Dymonds, "Flame Retardant Electric Cables," Br. UK Pat. No. 6B2059140, April 15, 1981.

[134]Mitsubishi Electric Corp., "Fire-Resistant Liquid Rubber Compositions," Jpn. Pat. No. 81/79121, June 29, 1981.

[135]Mitsubishi Electric Corp., "Fire-Resistant Liquid Rubber Compositions," Jpn. Pat. No. 81/79120, June 29, 1981.

[136]Mitsubishi Electric Corp., "Fire-Resistant Liquid Rubber Compositions," Jpn. Pat. No. 81/76428, June 24, 1981.

[137]Mitsubishi Electric Corp., "Fire-Resistant Liquid Urethane Rubber," Jpn. Pat. No. 81/61424, May 26, 1981.

[138]R. S. Park, "Polyether-Based Polyurethane Foams Including a Flame Retardant System Containing Antimony Trioxide, A Chlorinated Paraffin and Alumina Trihydrate," U.S. Pat. No. 4 266 042, May 5, 1981.

[139]A. Nakamura, "Hardenable Mixture For Self-Extinguishing Organopolysiloxane Elastomers," Ger. Pat. No. DE3043815, July 2, 1981.

[140]Hitachi, Ltd., "Chloroprene Rubber Compositions For Molding of Sheath Heater Ends," Jpn. Pat. No. 80/164231, December 20, 1980.

[141]W. P. Whelan, "Flame-Retarded Hydrocarbon Diene Elastomer," Eur. Pat. EP22365, January 14, 1981.

[142]R. M. Murch, P. I. Meyer, and J. J. Eagan, "Flame-Retardant Polyurethane Foams," U.S. Pat. No. 4 230 822, October 28, 1980.

[143]Kodo Co., Ltd., "Fire-Resistant Polyurethane Foams," Jpn. Pat. No. 80/135126, October 21, 1980.

[144]Toshiba Silicone Co., Ltd., "Fire-Resistant Silicon Rubber Compositions, Jpn. Pat. No. 80/108454, August 20, 1980.

[145]Sumitomo Bakelite Co., Ltd., "Fire-Resistant Resin Compositions," Jpn. Pat. No. 80/104336, August 9, 1980.

[146]Hitachi Chemical Co., Ltd., "Flexible Printed Circuit Boards," Jpn. Pat. No. 80/75292, June 6, 1980.

[147]Matsushita Electric Industrial Co., Ltd., "Fire-Resistant Silicone Compositions," Jpn. Pat. No. 80/80460, June 17, 1980.

[148]Sumitomo Electric Industries, Ltd., "Fireproofing Tapes," Jpn. Pat. No. 80/15229, April 22, 1980.

[149]Hitachi Cable, Ltd., "Fireproofed Cable Sheathings," Jpn. Pat. No. 80/69679, May 26, 1980.

[150]Fujikura Cable Works, Ltd., "Fire-Resistant Sheaths For Electric Cables," Jpn. Pat. No. 80/62988, May 12, 1980.

[151]R. Murch, "Organic-Inorganic Composite Urethane Foams," *Adv. Urethane Sci. Technol.*, 7, 115–46 (1979).

[152]K. K. Renji Sunya, "Fire-Resistant Electric Insulator Casting Compositions," Jpn. Pat. No. 80/62918, May 12, 1980.

[153]P. V. Bonsignore, "Flame Retardant Flexible Polyurethane Foam By Post-Treatment With Alumina Trihydrate/Latex Binder Dispersion Systems," *J. Cellulas Plastics*, May/June (1979).

[154]J. F. Szabat and W. J. Eicher, "Fire Behavior of Polyurethane Foam Materials for Mattresses," Proc. S.P.T. Annu. Urethane Div. Tech. Conf. 25th/Polyurethanes: Looking Ahead Eighties, 1979.

[155]J. Foerster, H. A. Mayer, H. Briem, and W. Krestel, "Flame-Resistant Halogenfree Polymer Mixtures," Ger. Pat. No. DE2849940, June 12, 1980.

[156]A. G. Bayer, "Flame-Resistant Polymer Foam," Ger. Pat. No. DE2849649, June 4, 1980.

[157]N. Imamura and K. Yamanaka, "Liquid Resin Compositions For Electric Insulation," Jpn. Pat. No. 80/43168, March 26, 1980.

[158]Y. Matsuga, S. Sato, J. Suemori, T. Kakihana, and K. Takahashi," Fire Resistant Sheaths for Electric Cables," Jpn. Pat. No. 80/18416, February 8, 1980.

[159]T. Ishikawa, "Bonding Hard Substrates With Thermal Insulator Panels," Jpn. Pat. No. 80/31813, March 6, 1980.

[160]R. Schlatter and A. Grass, "Composite Sheet With Two Covering Layers and an Intermediate Core," Ger. Pat. No. DE2842858, May 6, 1980.

[161]R. Muneno, S. Kondo, and K. Karya, "Fireproofing Agents For Electric Insulators," Jpn. Pat. No. 79/139647, October 30, 1979.

[162]K. Kariya, S. Kondo, and R. Muneno, "Liquid Rubber Casting Compositions for Fire-Resistant Electric Insulators," Jpn. Pat. No. 79/138044, October 26, 1979.

[163]G. Bertelli, R. Locatelli, and P. Roma, "New Intumescent Char-Forming Additives for Flame-Retardant Thermoplastic Polyolefin Elastomers," Proc. Int. Rubber Conf., 924–33. Int. Rubber Conf. 1979: Milan, Italy.

[164]P. Barruel, "Influence of the Formulation of Polychloroprene Compounds on the Reaction to Fire of Their Vulcanizates." Proc. Int. Rubber Conf., 903–12. Int. Rubber Conf. 1979: Milan, Italy.

[165]C. Shimizu, "Self-Extinguishing Room Temperature Curable Polysiloxane Compositions," Jpn. Pat. No. 79/90349, July 18, 1979.

[166]A. Hirai, K. Nishimoto, and H. Kuroki, "Flame Retardant Silicone Composition Having X-Ray Shielding Ability," Br. UK Pat. No. GB2008136, May 31, 1979.

[167]H. Briem, J. Foersterk, W. Krestel, and H. A. Mayer, "Flame-Resistant Halogen-Free Polymer Mixtures," Ger. Pat. No. DE2809294, September 13, 1979.

[168]P. V. Bonsignore, "Flame Retardant Flexible Polyurethane Foam By Post-Treatment With Alumina Trihydrate/Latex Binder Dispersion Systems," Ger. Pat. No. DE2754313, June 7, 1979.

[169]H. Esser, H. W. Illger, H. Mueller, W. Kost, and A. C. Gonzalez-Doerner, "Flame-Resistant Polyurethane Foam," Ger. Pat. No. DE2754313, June 7, 1979.

[170]W. R. Grace & Co., "Fire-Resistant Polyurethane Foams," Jpn. Pat. No. 79/13594, February 1, 1979.

[171]M. Tabana, N. Sekine, T. Mitsuni, and K. Mitsui, "Fire-Resistant Polyolefin Compositions," Jpn. Pat. No. 79/22451, February 20, 1979.

[172]S. Katayama, F. Tanaka, and K. Jin, "Fire-Resistant Electric Insulators," Jpn. Pat. No. 79/21487, February 17, 1979.

[173]L. H. Smiley, "Rigidized Acrylic Articles," U.S. Pat. No. 4 145 477, March 20, 1979.

[174]F. R. Davis, "Flame-Retardant Rubber Flooring Compositions," U.S. Pat. No. 4 131 592, December 26, 1978.

[175]H. Hentschel and B. Schreiber, "New Possibilities for Reducing the Flammability of Plastics," *Rev. Plast. Mod.*, **36** [269] 679–81 (1978).

[176]H. Hentschel and R. Wingenbach, "Flame Retardant Finishing Using Aluminum Hydroxide," *GAK Gummi Asbest. Kunstst.*, **31** [11] 863–64, 866 (1978).

[177]J. L. Schwartz and R. E. Mayer, "Flame Retardant Carpet," U.S. Pat. No. 4 097 630, June 27, 1978.

[178]W. P. Whelan and M. I. Jacobs, "Flame-Resistant Neoprene Foam With Low Smoke Development,' Ger. Pat. No. DE2812398, September 28, 1978.

[179]H. Hentschel, "Aluminum Hydroxide as an Antiinflammatory Agent For Covering Carpet Backing," *Hule Mex. Plast.*, **33** [388] 23–24 (1978).

[180]A. C. M. Griffiths, "Flame Resistant Foams," Br. G.B. Pat. No. 1499168, January 25, 1978.

[181]T. Jmai, S. Kawata, S. Kobayashi, N. Takahata, S. Sato, and H. Tachikara, "Fireproofing of Electric Cables," Jpn. Pat. No. 78/39382, April 11, 1978.

[182]T. Jmai, S. Kawata, S. Kobayashi, N. Takahata, S. Norio, and H. Tachihara, "Fire Resistant Tapes for Electric Cables," Jpn. Pat. No. 78/39383, April 11, 1978.

[183]L. Parts, R. D. Myers, C. A. Thompson, and N. F. May, "Flame and Smoke Retardant Polymer Systems," *Gov. Rep. Announce. Index (U.S.)*, 168 **78** [10] (1978).

[184]K. Marushashi and T. Tadeda, "Fire Resistant Neoprene Rubber," Jpn. Pat. No. 78/8645, January 26, 1978.

[185]K. Katsuki, "Fireproofing of Rigid Polyurethane Foams," Jpn. Pat. No. 78/5269, January 18, 1978.

[186]T. Takahashi and S. Horikoshi, "Fireproofing of Cellular Rubber," Jpn. Pat. No. 77/142768, November 28, 1977.

[187]M. Ohta, Y. Yamamoto, H. Nishizawa, M. Nishiumi, and S. Suyama, "Fireproofing Adhesive Tapes," Jpn. Pat. No. 77/132045, November 5, 1977.

[188]H. Hasegawa, I. Hashi,and N. Kita, "Fire Resistant Unsaturated Polyester Compositions," Jpn. Pat. No. 77/141874, November 26, 1977.

[189]H. Kimura and A. Miyoshi, "Fire Resistant Polyolefin Compositions," Jpn. Pat. No. 77/130842, November 2, 1977.

[190]H. Nishizawa, K.Kuroda, M. Ota, and M. Nishiumi, "Fire Resistant Tape," Jpn. Pat. No. 77/119645, October 7, 1977.

[191]F. Sakaguca, I. Yamasaki, and M. Suzuki, "Arc and Fire Resistant Butene-Ethylene Copolymer with High Tear Strength," Jpn. Pat. No. 77/78255, July 1, 1977.

[192]A. E. Obeaster and J. C. Vicic, "Naphthalenic Derwatized Plasticizers for Polyphosphazine Polymers," U.S. Pat. No. 4 567 211, January 28, 1986.

[193]Anonymous, "Carpet Foam Backing Flame Retardant Formulations," *NR Technol.*, 7[3] 74 (1976).

[194]H. Schaper, H. Steeg, and M. Suches, "Sound Deadening and Heat Insulating Mat for Motor Vehicles," Ger. Pat. No. 2 214 282, November 10, 1973.

[195]I. T. Gridunov, "Evaluation of the Fire Resistance of Rubber," *Izv. Vysshikh Uchebn. Zavedenii, Khim. ikhim Technol.*, **9** [2] 322 (1966).

[196]C. W. Stewart, R. L. Dawson, and P. R. Johnson, "Effect of Compounding Variables on the Rate of Heat and Smoke Release from Polychloroprene Foam," *Rubber Chem. Technol.*, **48** [1] 132 (1977).

[197]C. E. McCormack, "Flame Resistance of Composition of Neoprene and Hypalon via the Oxygen Index Method," *Rubber Age*, **6**, 27 (1972).

[198]P. R. Johnson et al., "Elastomers and Flammability," 106th Meeting Div. of Rubber Chem. Am. Chem. Soc., Paper 10, Philadelphia, PA. 1974.

[199]D. C. Thompson, J. F. Haganan, and N. N. Mueller, "Flame Resistance of Neoprene — Effects of Compounding Ingredients," *Rubber Age*, **83** [5] 819 (1958).

[200]F. Woods, "Use of Hydrated Alumina as a Filler for EPDM Elastomers,' SGF Publications, 47 (IV), 1975.

[201]N. Nishizawa, S. Kon, and J. Fukabori, "Fire Resistant Electric Insulating Adhesive Tapes," Jpn. Pat. No. 74/124149, November 27, 1974.

[202]K. Yamamoto, M. Aoshima, and I. Katagiri, "Rubber Compositions Containing a Modified Aluminum Hydroxide," Jpn. Pat. No. 74130440, December 13, 1974.

[203]V. I. Treshchalov and V. N. Fomin, "Silicone Rubber Based Composition," USSR Pat. No. 555 122, April 25, 1977.

[204]M. Bargain, "Self Extinguishing Siloxane Rubber," Ger. Pat. No. 2 308 595, August 30, 1973.

[205]G. G. Jaisinghani, "Fire Retardant Carpet," U.S. Pat. No. 3 663 345, May 16, 1972.

[206]P. R. Johnson, R. Parisen, and J. J. McEvoy, "Elastomers and Flammability," 106th Meeting Div. of Rubber Chem. Amer. Chem. Soc., Paper 10, Philadelphia, PA, 1974.

[207]D. F. Lawson, E. L. Kay, and D. T. Roberts, Jr., "Mechanism of Smoke Inhibition by Hydrated Fillers," *Rubber Chem. Technol.*, **48** [1] 124 (1975).

[208]F. Pitts and M. H. Chubley, "Fire Resistant Rubber Foam," Ger. Pat. No. 2 339 722, February 14, 1974.

[209]J. Stroetzen, "Nonflammable Latex Mixtures," Ger. Pat. No. 2 206 690, August 16, 1973.

[210]G. A. Geppert and R. D. Woosley, "Fire Retardant Composition," U.S. Pat. No. 3 874 889, April 4, 1975.

[211]J. J. Bayerl, "Flameproof Rubber Compositions," Belg. Pat. No. 645 879, July 16, 1964.

[212]E. J. Quinn and R. L. Dieck, "Flame and Smoke Properties of the Polyphosphazenes, III. Polyacrylvayphosphazene Copolymer Foams," *J. Cellular Plastics*, **13** [2] 96 (1977).

[213]K. A. Reghard and J. C.Vicic, "Polyphosphazene Wire Coverings," U.S. NTIS AD REP., AD–A028872, 1976.

[214]C. E. McCormick, "Flame Resistance of Neoprene and Hypalon via the Oxygen Index Method," *Rubber Age*, **6** 27 (1972).

[215]H. Abe and T. Morimoto, "Fire Resistant Chlorosulfonated Polyethylene," Jpn. Pat. No. 7466740, June 6, 1974.

[216]E. L. Kay, "Smoke Retardant for Chlorinated Polyethylene and Vinyl Chloride Polymers," U.S. Pat. Appl. B561 387, February 10, 1976.

[217]K. Motoyama and K. Yamaguchi, "Fire Resistant Rubber Compositions," Jpn. Pat. No. 74103944, November 2, 1979.

[218]K. Motoyama and K. Yamaguchi, "Fire Resistant Composition," Jpn. Pat. No. 7337976, November 11, 1973.

[219]C. L. Kehr, R. M. Murch,and N. S. Marans, "Smoke and Flame Retardant Hydrophillic Urethane Ruber," U.S. Pat. No. 3 897 372, July 29, 1975.

[220]T. Kishimoto, O. Fujii, H. Wakabazashi, and M. Numabe. "Non-Flammable Polyurethane Foam," Jpn. Pat. No. 75/04236. February 17, 1975.

[221]S. Kashahara and F. Hayashi, "Fire Resistant Polymer Foams," Jpn. Pat. No. 75/74671, June 19, 1975.

[222]C. Anorga, Jr. and S. Chess, "Flame Resistant, Flexible Polyurethane Foam," Ger. Pat. No. 2 512 345, October 2, 1975.

[223]H. Haga and Y. Ohtsuka, "Fire Resistant Polyurethane Foams," Jpn. Pat. No. 74/67953, July 2, 1974.

[224]S. Tanigucci, Y. Sakuma, and T. Yoshii, "Flame Retardant Additives Based on Alumina Trihydrate and Ethylene Polymer Compositions, Containing Same, Having Improved Flame Retardant Properties," Eur. Pat. Appl. EP77055A1, April 20, 1983.

[225]T. Sullivan and J. E. Braddock, "Transportation Systems and Electric Cables for Use in Them," U.S. Pat. No. 4 370 076A, January 25, 1983.

[226]L. M. Narkevich, N. I. Grishko, L. V. Rynskova, S. P. Dashko, and Y. S. Shenkin, "Aluminum Compounds as a Filler and Fireproofing Compound for Production of Polyurethane Foam," *Deposited Doc.*, **VINITI**, 3096–80 (1980).

[227]Sumitomo Electric Industries Ltd., "Fire Resistant Compositions," Jpn. Pat. No. 81/20040, February 25, 1981.

[228]Mitsubishi Electric Corp., "Fire Resistant, Low-Smoking Unsaturated Polyester Compositions," Jpn. Pat. No. 81/10549, February 3, 1981.

[229]B. Newitzki, "Noncombustible Material Based on Phenolic Resins and Furfuryl Alcohol," Ger. DE 2 825 295, November 8, 1979.

[230]W. Mylich and W. Albert, "Flame Resistant Polystyrene Foam," Eur. Pat. Appl. EP4578, October 17, 1979.

[231]A. Okuno, "Fireproofed Epoxy Impregnants," Jpn. Pat. No. 79/93044, July 23, 1979.

[232]B. F. Creek, "Modest Growth Ahead for Rubber," *C&EN*, March 21, 1988; p. 25.

[233]M. Connell, "School Delays Opening Due to Carpet Failing Tests," *Dalton Daily Citizen News*, April 24, 1987.

[234]A. Richardson, "Feds To Get Results on Carpet Testing Tomorrow," *Washington Dateline, Dalton Daily Citizen News*, May 7, 1987.

[235]L. L. Musselman, "Where There's Fire There Isn't Always Smoke," Alcoa FlameGuard Publication F35–14860, November 1987.

[236]J. K. Allen, "Flame Resistant Translucent Molded Articles," Ger. Pat. No. 1 006 154, April 11, 1957.

[237]W. J. Connolly and A. M. Thornton, "Alumina Hydrate Filler in Polyester Systems," *Modern Plastics*, 1965.

[238]IAMPMO Standard PS 11–72, International Association of Plumbing and Mechanical Officials, 1972.

[239]ANSI Standard Z124.1–1974, American National Standards Institute, 1974.

[240]Nippon Shokubai Kagaku Kogyo Co. Ltd., "Fire Resistant Glass Fiber Reinforced, Cured Polyester Moldings," Jpn. Pat. No. 85/32833, February 20, 1985.

[241]Nippon Chemical Industrial Co. Ltd., "Fire Proofing Composition Containing Red Phosphorus," Jpn. Pat. No. 84/170176, September 26, 1984.

[242]C. T. Domide, "Fire Resistant Polyester Composition," Romanian Pat. No. R082743B, October 3, 1983.

[243]C. T. Domide et al., "Fire Proofed Polyester Composition," Romanian Pat. No. R082744B, October 30, 1983.

[244]D. Braun and R. Rohlmann, "Filler Based on Aluminum Hydroxide," Ger. Pat. No. DE3 308 023A1, September 13, 1984.

[245]P. H. Liu and T. C. Wu, "Study on Flame Retardancy of Glass Fiber-Reinforced Unsaturated Polyester Resins," Fang Chih Kung Cheng Hsueh Kan. 9, 131–57, Textile Engrg. Graduate School, Feng Chin University, 1982.

[246]Ferro Enamels Ltd., "Unsaturated Polyester Flame-Resistant Sheets," Jpn. Pat. No. 83/38729, March 7, 1983.

[247]T. Kobayashi et al., "Nonflammable Dynamoelectric Machine Having Coil Windings and Core Encapsulated with Unsaturated Polyester Resin Filler Composition," U.S. Patent No. 4 387 311, June 7, 1983.

[248]Tanner Chemical Co., "Unsaturated Polyester Lightweight Panels," Jpn. Pat. No. 82/63319, April 16, 1982.

[249]E. Vasatko, "Self-Extinguishing Mixture of Additives with Unsaturated Polyester Resin," Czech Pat. No. 192703B, September 30, 1981.

[250]J. Greber and D. J. Braun, "Combustion Protection with Aluminum Hydroxide," *Din 4102, Plastverarbeiter*, **33** [1] 43–46 (1982).

[251]V. I. Salomatov, "Polymer Concrete Slurry," USSR Pat. No. 854913, August 15, 1981.

[252]D. Scholz, "Flame Retardant Low Smoke GR-UP Laminates Based on Low Viscosity UP Resins," *Plastverarbeiter*, **32** [12] 1621–24 (1981).

[253]J. Greber and D. J. Braun, "Flame Retardation with Aluminum Hydroxide," Vorabdruck-Deff. Jahrestag Arbertsgem Verstaekte Kunstst 17, 6/1–6/5, 1981.

[254]Matsushita Electric Industrial Co. Lt., "Fire Resistant Thermosetting Resin Compositions," Jpn. Pat. 81/2347, January 12, 1981.

[255]Matsushita Electric Industrial Co., Ltd., "Fire Resistant Unsaturated Polyester Compositions," Jpn. Pat. 80/161845, December 16, 1980.

[256]C. J. Del Valle and R. A. Hunter, "Alternate Flame Retardant Systems for Polyester Spray-Up Applications," Proc. Int. Conf. Fire Safety 5, 227–40, 1980.

[257]J. M. Makhlouf and E. E. Parker, "Low Smoke Density Fire Retardant Resins," U.S. Pat. No. 4 246 163, January 20, 1981.

[258]Asahi Chemical Industry Co., "Fire Resistant Electrically Insulating Sheets," Jpn. Pat. No. 80/136413, October 24, 1980.

[259]C. H. Lin and Y. T. Chang, "FRP Fire Retardant Additives," *Ying Yung Chieh Mien Hua Hsueh*, **9**, 23–25 (1980).

[260]W. Glaser, "Copolymers of Inorganic and Organic Components," Ger. Pat. No. DE2 816 504, April 24, 1980.

[261]V. S. Gorshkov and V. B. Polyakov, "Use of Hydrate Containing Fillers as Flame Retardants," *Plast. Massy.*, **8**, 42–43 (1980).

[262]Matsushita Electric Industrial Co. Ltd., "Fire Resistant Unsaturated Polyester Compositions," Jpn. Pat. No. 80/94918, July 18, 1980.

[263]Matsushita Electric Industrial Co. Ltd., "Fire Resistant Unsaturated Polyester Compositions," Jpn. Pat. No. 80/80422, June 17, 1980.

[264]J. F. Greber and G. Winkhaus, "Flame Resistant Composite Material," Ger. Pat. No. DE2 852 273, June 4, 1980.

[265]W. Glaser, "Copolymers from Inorganic and Organic Components," Ger. Pat. No. DE2 916 504, April 24, 1980.

[266]J. M. Self, "Highly Extended Unsaturated Polyester Resin Syrup Compositions," U.S. Pat. No. 4 192 791, March 11, 1980.

[267]Y. Oda, "Fillers for Plastic Composites," Jpn. Pat. No. 79/132641, October 15, 1979.

[268]P. V. Bonsignore and W. L. Burton, "ATH as SS Adjunct to FR Halogenated Polyester Resins," Proc. Amer. Conf., Reinf. Plast/Comp. Inst. Soc. Plast. Ind. 34th 14E, 1979.

[269]Y. Hatogai, "Fire Resistant Polyesters," Jpn. Pat. No. 79/50087, April 19,1979.

[270]H. P. Hsieh, "Reducing Gel and Cure Times for Polyester ATH Dispersions by Blending Therewith Small Quantities of Act Alumina," U.S. Pat. No. 4 159 977, July 3, 1979.

[271]H. K. Kenady-Shipton and T. Robertson, "Fire Resistant Additives for Hardenable Resin Compositions," Ger. Pat. No. DE2 853 827, June 28,1979.

[272]S. Kirah and Y. Elisov, "Aluminum Hydroxide as a Fire Retardant for Plastics," *Polim. Vehomarim Plast.*, **8** [1] 4–7 (1978).

[273]S. E. Berger, B. Prokai, E. G. Schwarz, and M. Montague, "The Role of Silanes in the Processing and Properties of Reinforced Plastics," Mfg. Qual. Reinf. Plast. Congr. 159–66, Br. Plast. Fed., London, England 1978.

[274]P. V. Bonsignore, "ATH and Other Inorganic Flame Retardant Additives for Glass Fiber-Reinforced Polyester Plastics," FRCA/SEP Conf. Proc. 101–27, 1978.

[275]E. Vasatho, "Self-Extinguishing Filler for Plastics," Czech Pat. No. CS175781, December 15, 1978.

[276]H. Hasegawa et al., "Fire Resistant Polyester Moldings," Jpn. Pat. No. 78/128686, November 9, 1978.

[277]H. Hasegawa et al., "Fire Resistant Unsaturated Polyester Panels," Jpn. Pat. No. 78/98379, August 28, 1978.

[278]K. E. Atkins et al., "Silane Treated Alumina Trihydrate," *Polymer Eng. Sci.*, **18** [2] 73–77 (1978).

[279]H. Hasegawa et al., "Fire Resistant Laminated Unsaturated Polyesters," Jpn. Pat. No. 78/43782, April 20, 1978.

[280]G. Bilandzic and H. Hentschel, "The Use of Additives for Reducing the Viscosity of UP Resin/Aluminum Hydroxide Systems," *Kunststoffe*, **68** [2] 62–64 (1978).

[281]H. Hasegawa et al., "Fire Resistant Polyester Sheets," Jpn. Pat. No. 77/124091, October 18, 1977.

[282]H. Hasegawa, "Fire Resistant Polyester Sheets," Jpn. Pat. No. 77/124092, October 18, 1977.

[283]P. V. Bonsignore and J. M. Manhart, "ATH as a Flame Retardant and SS Filler in Reinforced Polyester Plastics," 29th Annual Tech. Conf. Plast/Comp. Inst., SPI 23-C, 1974.

[284]S. M. Byrd, Jr., "Flame Retardant Polyester — Two Approaches," 29th Annual Tech. Conf. Reinf. Plastics/Composites Inst. SPI 23-D, 1974.

[285]G. Bockmann, "Self-Extinguishing Moldings Based on Unsaturated Polyesters," Ger. Pat. No.2 159 757, June 7, 1973.

[286]W. J. Connolly and A. M. Thorton, "New Polyester Resin and Filler System Producing Excellent Flame Resistance and Heat Aging Properties," 20th Annual Tech. Conf. Reinf. Plast/Comp. SPI 11-B, 1965.

[287]W. J. Connolly and R. M. Thorton, "ATH Filler in Polyester Systems," *Modern Plastics*, **43** [2] 154, 156, 202 (1965).

[288]L. P. Connors et al., "FRP Third Rail Protective Cover Systems," 31st Annual Tech. Conf., Reinf. Plast./Comp. Inst SPI 10C (1976).

[289]H. Date, "Fire Proofing of Chlorine-Containing Polyesters," Jpn. Pat. No. 75/34043, April 2, 1975.

[290]S. M. Dragunov, "Fire Resistant Polyester Compositions," Def. Publ. U.S. Pat. No. 903 019, March 10, 1972.

[291]S. M. Dragunov et al., "Comparative Evaluation of Fire Brake ZB with Antimony Oxide Using Various Fire Testing Methods," 26th Annual Tech. Conf. Reinf. Plast/Comp. Inst. SI 2-8, 1971.

[292]S. M. Dragunov, "Fire Resistant Halogenated Polyester Resin Products," Ger. Pat. No. 2 105 444, February 10, 1972.

[293]S. M. Dragunov, "Flame Resistant Additives for Synthetic Resin Products," Ger. Pat. No. 2 105 443, March 9, 1972.

[294]O. K. Goins and Y. C. Chae, "Tetrachlorophthalic Anhydride Polyester Flame Retardancy, UV Stability and Reduced Smoke," 27th Annual Tech. Conf., Reinf. Plast/Comp. Inst. SPI 19-A, 1972.

[295]R. C. Hopkins, "Alumina Trihydrate Clean Low-Cost Fire Retardant," *Polymer Age*, **6** [5] 130 (1975).

[296]A. H. Horner, "Acrylic Composite Sanitary Ware, The Economies of Extended Resin Reinforcement," 30th Annual Tech. Conf. Reinf. Plast./Comp. Inst. SPI 3-B, 1975.

[297]J. Ibata et al., "Thermosetting Resin Molding Comp.," Jpn. Pat. No. 76/133339, November 19, 1976.

[298]J. Z. Keating, "Filler Management in Polyester Resin Systems," 31st Annual Tech. Conf. Reinf. Plast./Comp. Inst. SPI 8-C, 1976.

[299]C. V. Lundberg, "Hydrated Alumina as a Fire Retardant Filler in Styrene Polyester Casting Compounds," Advances in Chem. Ser., ACS Monograph BX Chapt. 18, 1974.

[300]J. Z. Keating, "Flame and Smoke Management in Polyester Resin Systems," 32nd Annual Tech. Conf. Reinf. Plast./Comp. Inst. SPI, 13-F, 1977.

[301]T. J. McHugh, Jr., "A Novel Approach to the Manufacture of RP/C Shapes via Solid Vinyl Monomers," 29th Annual Tech. Conf. Reinf. Plastics/Comp. Inst. SPI 9-O, 1974.

[302]J. H. Mallinson, "Fire Retardancy-Duct Systems in the Chemical Industry," 30th Annual Tech. Conf. Reinf. Plastics Comp. Inst. SPI Paper 2-C, 1975.

[303]D. F. Miller et al., "An Evaluation of Some Factors Affecting the Smoke and Toxic Gas Emission from Burning Unsaturated Polyester Resins," 31st Annual Tech. Conf. Reinf. Plast./Comp. Inst., SPI Paper 20-C, 1976.

[304]I. Okado et al., "Molded Articles Made of Water Containing Polyesters," Jpn. Pat. No. 73/93689, December 12, 1973.

[305]K. Parvin, "Polyester Resins of Reduced Fire Hazard," 30th Annual Tech. Conf. Reinf. Plast./Comp. Inst., SPI, 1975.

[306]B. P. Pleuddemann and G. L. Stock, "Silane Coupling Agents for Alumina Trihydrate," 31st Annual Tech. Conf. Reinf. Plast./Comp. Inst., SPI 6-D, 1976.

[307]M. A. Rizzi, "Total System Approach to Mixing and Injection Molding Glass Reinforced Polyester Compounds," 27th Annual Tech. Conf. Reinf. Plast./Comp. Inst., SPI 16-D, 1972.

[308]M. Silvergleit et al., "Flammability Characteristics of Fiber Reinforced Organic Matrix Composites," 32nd Annual Tech. Conf. Reinf. Plast./Comp. Inst., SPI 9-G, 1977.

[309]I. Sobolov, E. A. Woycheshin, Alumina Trihydrate. Van Nostrand Reinhold, New York, 1978.

[310]T. K. Sprow et al., "Filled Polyester Spray-up Systems Offering Improved Fire Hazard Classifications," 28th Annual Tech. Conf. Reinf. Plast./Comp. Inst., SPI 7-D, 1973.

[311]R. H. Trampenan and T. R. Evans, "Fire Resistant FRP in Construction," 28th Annual Tech. Conf. Reinf. Plast./Comp. Inst., SPI 4-C, 1973.

[312]P. W. Vaccarella and J. E. Selley, "New Fire Retardant Resins for Corrosion Resistance," 32nd Annual Tech. Conf. Reinf. Plast./Comp. Inst., SPI 13-A, 1977.

[313]R. H. Trampenan and T. R. Evans, "FRP Means Performance in Construction," 29th Annual Tech. Conf. Reinf. Plast./Comp. Inst., SPI 7-B, 1974.

[314]F. D. Wampnor, "ATH Average Particle Size Effect on Flammability and Physical Properties of Fiber Glass Reinforced Plastics and Bulk Molding Compound," 31st Annual Tech. Conf. Reinf. Plast./Comp. Inst., SPI 3-C, 1976.

[315]E. A. Woycheshin and I. Sobolev, "Effect of Particle Size on the Performance of Alumina Trihydrate in Glass Reinforced Polyesters," 30th Annual Tech. Conf. Reinf. Plast./Comp. Inst., SPI 4-B, 1975.

[316]F. J. Armpthor and C. H. Kroekel, "Developments in Low Profile SMC for Flame Retardant and Electrical Application," 27th Annual Tech. Conf. Reinf. Plast./Comp. Inst., SPI 8-E, 1972.

[317]K. E. Atkins et al., "Improved ATH Filled FRP," High Perf. Plast., Natl. Tech. Conf. SPE, p. 102, 1976.

[318]K. E. Atkins et al., "Silane Treated ATH," 32nd Annual Tech. Conf. Reinf. Plast./Comp. Inst., SPI 4-D, 1977.

[319]R. H. Bradley and F. M. Haminski, "A New Low Shrink Polyester Resin for Color Applications," 28th Annual Tech. Conf. Reinf. Plast./Comp. Inst., SPI 2-B, 1973.

[320]W. J. Connolly and A. M. Thorton, "New Polyester Resin and Filler System Producing Excellent Flame Resistance and Heat Aging Characteristics," 20th Annual Tech. Conf. Reinf. Plast./Comp. Inst., SPI 11-B, 1965.

[321]T. R. Evans et al., "Formulated Fire Retardant Polyester Systems for Press Molded Laminates," 27th Annual Tech. Conf. Reinf. Plast./Comp. Inst., SPI 19-C, 1972.

[322]C. B. Frankhof et al., "Bulk Molding Compound," 24th Annual Tech. Conf. Reinf. Plast./Comp. Inst., SPI 3-B, 1969.

[323]C. Kato and K. Matsushima, "Non-Burning Composites," Jpn. Pat. No. 75/03156, January 14, 1975.

[324]E. L. Livingston and J. M. Kring, "Polyester Impregnated Glass Fiber Reinforced Sheet," U.S. Pat. No. 3 881 978, May 6, 1975.

[325]J. S. McNally et al., "Low Shrinkage Plus Flame Retardance," 27th Annual Tech. Conf. Reinf. Plast./Comp. Inst., SPI 5-C, 1972.

[326]G. A. Sundstrom et al., "Low Density Sheet Molding Compound," CSMC and BMC, 30th Annual Tech. Conf. Reinf. Plast./Comp. Inst., SPI 1-B, 1975.

[327]K. Takaijhi et al., "Unsaturated Polyester Compositions," Jpn. Pat. No. 74/103986, November 2, 1974.

[328]G. L. Williams, "A New Approach to SMC-SEM Molding," 31st Annual Tech. Conf. Reinf. Plast./Comp. Inst., SPI Paper 2-D, 1976.

[329]L. L. Musselman, "Application Tools to Use Hydrated Alumina in Spray-up Resins"; unpublished Alcoa Customer Presentation, 1978.

[330]L. L. Musselman and J. P. Starr, "Fabrication Techniques for Systems Highly Filled with Alumina Trihydrate"; unpublished Alcoa Customer Presentation, 1979.

[331]J. V. Milewski, "A Study of the Packing of Fibers and Spheres," Ph.D. Thesis, Rutgers University, 1973.

[332]J. V. Milewski, "Identification of Maximum Packing Condition in the Bimodal Packing of Fibers and Spheres," 29th Annual Tech. Conf. Reinf. Plast./Comp. Inst., SPI 10-B, 1974.

[333]J. L. Greenzweig and T. L. Pickering, "Flow Properties of Calcium Carbonate in Filled Polyester Resins," 31st Annual Tech. Conf. Reinf. Plast./Comp. Inst., 1976.

[334]H. E. Selley et al., "Formulating Fire Retardant SMC," 28th Annual Tech. Conf. Reinf. Plast./Comp. Inst., SPI 18-E, 1973.

[335]L. L. Musselman and T. L. Levendusky, "Surface Treatment of ATH for a Better Resin System," *Modern Plastics*, February 1983.

[336]L. L. Musselman and T. L. Levendusky, "ATH as a Fire Retardant and Smoke Suppressant Additive in the Development of a Commercial Fire Retardant Polypropylene," SPE 38th Annual Tech. Conf., Chicago, May 2, 1983.

[337]J. Z. Keating, *Plastics Compounding*, **7**, 23 (1986).

[338]L. L. Musselman and T. L. Levendusky, "Combination of Surface Modifiers for Powdered Inorganic Additives," U.S. Pat. No. 4 711 673, December 8, 1987.

[339]L. L. Musselman, P. V. Bonsignore, and J. P. Starr, "Smoke and Flammability Comparisons"; unpublished oral applications presentations, Alcoa, 1978.

[340]L. L Musselman and T. J. Austin, "New Chemical Products Enhance Appearance and Performance of Cultured Marble," Alcoa Publication F35–14682, Cultured Marble Institute Convention, Houston, TX, February 1987.

[341]L. L. Musselman, "A Breakthrough for the Cultured Marble Industry," Alcoa Publication F35–14659, Cultured Marble Inst. Convention MarbleCon '85, Pine Mountain Resort, GA, February 1985.

[342]O. Zaske, "Reactivity of Current Commercial Peroxide Catalysts with Cultured Onyx Matrix," Dymatec Conference, Los Angeles, CA, September 13, 1985.

[343]W. Schramm, "A New Generation of Marble Resins," CMI MarbleCon '85, Pine Mountain Resort, GA, February 1985.

[344]J. Petty and I. Eckbreth, "Solving Problems on the Shop Floor," Dymatec Conf., Los Angeles, CA, September 14, 1985.

[345]R. A. Brewer, "CMI-NAHB/RF Certification Program," Plumbing Inspection Conf., Savannah, GA, September 1987.

[346]O. Zaske, "Technical Report Cultured Onyx," Silmar Technical Data Bulletin, September 1983.

[347]R. B. Duggins, "Flame and Impact-Resistant Methyl Methacrylate Polymers or Copolymers Containing Aluminum Hydroxide," Ger. Pat. No. 2 006 197, July 22, 1971.

[348]R. B. Duggins et al., "Polymethyl Methacrylate Articles Containing a Filler," Ger. Pat. No. 2 316 638, October 10, 1973.

[349]R. B. Duggins, "Use of ATH on a Polymethyl Methacrylate Article," U.S. Pat. No. 3 847 865, November 12, 1974.

[350]T. Hashimoto, T. Iwaki, M. Katatani, and M. Nikki, "Highly Filled Curable Acrylic Compositions and Articles From Them," Eur. Pat. Appl. EP 211657AZ, February 25, 1987.

[351]Kyowa Hakko Kogyo Co. Ltd., "Fire Resistant Resin Compositions," Jpn. Pat. No. 82/141445, September 1, 1982.

[352]S. Okada, T. Fukuda, and N. Ando, "Thermosetting Compositions Containing Acidic Aluminum Phosphate," Jpn. Pat. No. 74/30280, March 18, 1974.

[353]Sumitomo Bakelite Co. Ltd., "Phenolic Resin Compositions," Jpn. Pat. No. 83/149939, September 6, 1983.

[354]Toshiba Chemical Products Co. Ltd., "Fire Resistant Phenolic Resin Impregnated Paper Laminates," Jpn. Pat. No. 84/54545, March 29, 1984.

[355]Furukawa Electric Co. Ltd., "Fire Resistant Putty Compositions," Jpn. Pat. No. 83/65780, April 19, 1983.

[356]Takiron Co. Ltd., "Nonflammable Decorative Inorganic Panels," Jpn. Pat. No. 81/31260, July 20, 1981.

[357]Toshiba Chemical K. K., "Fire Resistant Laminates," Jpn. Pat. No. 81/65028, June 2, 1981.

[358]D. E. Baldwin and R. H. Runk, Westinghouse, U.S. Pat. No. 2 801 672, 1957.

[359]J. M. Black, "Forest Products Laboratory Report R1427," U.S. Dept. of Agriculture, Forest Service, March 1943.

[360]C. Kato, K. Kamei, K. Matsushima, and M. Hirakawa, "Nonburning Lightweight Composites," Jpn. Pat. No. 75/03451, January 14, 1975.

[361]J. A. Holderried, "Flame Retardants," Modern Plastics Encyclopedia, 1974–75.

[362]R. E. Bayes, "Epoxy Resins," Modern Plastics Encyclopedia, 1964.

[363]H. Lee and K. Neville, Handbook of Epoxy Resins. McGraw-Hill, New York, 1967.

[364]P. Bruins, Epoxy Resin Technology. John Wiley, New York, 1968.

[365]F. J. Martin and K. R. Price, "Flammability of Epoxy Resins," *J. Appl. Polymer Sci.*, **12**, 143 (1968).

[366]E. T. Patrick, Jr. and C. W. McGary, Jr., "Cycloaliphatic Epoxy Resins in Electrical Insulation," 24th Annual Tech. Conf. SPE, 1966.

[367]Union Carbide Technical Information Bulletin, "Bakelite ERRA-4090/ERL–4221 Electrical Insulation System," April 1969.

[368]J. J. Stevens, Jr., "Improved Cycloaliphatic Epoxy Systems for High Voltage Applications," 9th Electrical Insulation Conf. IEEE, September 10, 1969.

[369]J. J. Stevens, Jr., "Improved Cycloaliphatic Epoxy Systems for High Voltage Applications," U.S. Pat. No. 3 647 742, March 7,1972.

[370]A. S. Burhaus, "Improved Liquid Cycloaliphatic Epoxy Casting Systems," 32nd Annual Tech. Conf. SPE, 1974.

[371] Editor, Insulation/Circuits, "Epoxy Resins Replace Porcelain in Power Circuit-Breaker Applications," October 1974.

[372]Sumitomo Bakelite Co. Ltd., "Dimensionally Stable Thermosetting Resin Laminates," Jpn. Pat. No. 85/18339, January 30, 1985.

[373]Shin-Etsu Chemical Industry Co. Ltd., "Incombustible Epoxy Resin Compositions," Jpn. Pat. No. 84/33319, February 23, 1984.

[374]Nippon Zeon Co. Ltd., "Potting Agents for Electric Insulation," Jpn. Pat. No. 83/138724, August 17, 1983.

[375]Matsushita Electric Industrial Co. Ltd., "Epoxy Resin Molding Materials," Jpn. Pat. No. 83/138727, August 17, 1983.

[376]Matsushita Electric Industrial Co. Ltd., "Heat Resistant Thermosetting Resin Compositions," Jpn. Pat. April 3, 1981.

[377]J. G. Robinson, "Epoxy Resin Compositions and Their Use in Impregnating Glass Fiber Strips," Ger. Pat.No. DE3 026 709, February 5, 1981.

[378]K. Pol, "Fire Inhibition Effect of Aluminum Oxide Trihydrate on the Combustibility of Plastic Materials." *Maunzag Gumi, (Budapest)*, **17** [17] 204–207 (1980).

[379]Y. Hira, R. Sudo, T. Takamoto, and T. Isogai, "Flame Retardant Epoxy Resin Compositions," U.S. Pat. No. 4 145 369, March 20, 1979.

[380]K. Sumi,M. Shwsaki, and N. Hata, "Fire Resistant Epoxy Resin Compositions," Jpn. Pat. No. 79/3152, January 11, 1979.

[381]C. Snyder, "ATH, A New Generation," Plastics Compounding, p. 41, July/August 1985.

[382]R. C. Hopkins, "Alumina Trihydrate Clean, Low-Cost Flame Retardant," *Polymer Age*, **6** [5] 130 (1975).

[383]Y. Ota, "Use of a Flame Retardant Aluminum Hydroxide Filler for Epoxy Resins," *Purasuchikkusu*, **22** [9] 65 (1971).

[384]W. M. Rinehart, "A New Approach to High Voltage Outdoor Polymer Insulation," 27th Annual Tech. Conf. Reinf. Plastics/Comp. Inst., SPI Paper 8-C, 1972.

[385]M. Silvergleit, J. G. Morris, and C. N. LaRosa, "Flammability Characteristics of Fiber-Reinforced Organic Matrix Composites," 32nd Annual Tech. Conf. Reinf. Plast./Comp. Inst., SPI 9-G, 1977.

[386]E. Galli, "Pultrusion Pulls its Weight in Composites," *PM&E*, p. 43, April 1988.

[387]Y. Shingo, T. Matsuda, A. Yoshino, H. Sunazuka, M. Hasegawa, and H. Kobayski, "Flame Retardant Crosslinked Compositions for Cables," U.S. Pat. No. 4 549 041, October 22, 1985.

[388]R. R. Reitz, "Ethylene Copolymers with Enhanced Fire Resistant Properties," U.S. Pat. No. 4 678 607, July 7, 1987.

[389]J. F. Gobbi, "Polymeric Compositions Containing Hydrated Inorganic Fillers," Br. Pat. Appl. GB2 176 491 A1, December 31, 1986.

[390]S. H. Vande Ven and A. J. Dallavia, Jr.,"Alumina Trihydrate in Crosslinked EVA," Fall Conf. FRCA, 1986.

[391]L. M. Panzer, "Non-Halogen Flame Retardant Technology with Significantly Improved Combustion Toxicity," FRCA/SPE PMAD Joint Mtg., 1985.

[392]J. E. Betts, I. Fredland, and E. V. Wilkins, "Polyolefin Insulation for Conductors with Good Thermal Stability," Eur. Pat. Appl. EP 163 819 AZ, December 11, 1985.

[393]M. Hasegawa, H. Kobayoshi, H. Sunazuka, A. Yoshino, T. Matsuda, and Y. Shingo, "Flame Retardant Crosslinked Composition and Flame Retardant Cable," Br. Pat. Appl. GB2 156 825, October 23, 1985.

[394]K. Sano and H. Ishitani, "Radiation Crosslinked Polyolefin Insulated Wire," *Radiat. Phys. Chem.*, **25** [4–6] 849–59 (1985).

[395]P. Burton, "Fire Resistant Polyethylene," Belg. Pat. No. 688 540, February 21, 1966.

[396]P. Burton, "Fire Resistant Polyethylene," U.S. Pat. No. 3 741 929, 1973.

[397]I. Sobolev and E. A. Woycheshin, "Alumina Hydrate as a Flame Retardant Filler for Thermoplastics," *J. Fire Flame/FRCA*, 1, [2] 13 (1974).

[398]I. Sobolev and E. A. Woycheshin, "Modified Alumina Hydrate Flame Retardant Filler for Polypropylene," U.S. Pat. No. 3 826 775, July 30, 1974.

[399]J. Rodish, "Flame Retardant Additive for Foamed Polystyrene," U.S. Pat. No. 4 182 799, January 8, 1980.

[400]M. Keogh, "Compounding and Processing of Flame Retarded Moisture Curable Polyolefin Compounds," FRCA Fall Conf., Kiawah Island, October 22, 1986.

[401]M. Keogh, "Halogen versus Non-Halogen Flame Retardance Questions in Wire and Cable Applications," FRCA Spring Conf., Grenelefe, FL, March 21, 1988.

[402]Sumitomo Electric Industries Ltd., "Low Smoking Fire Resistant Sheathings for Optical Fiber-Insulated Metal Wire Composite Cables," Jpn. Pat. No. 84/226413, December 19, 1984.

[403]Sumitomo Electric Industries Ltd., "Electric Wire Coated with Fire Resistant Low Smoke Polyolefins," Jpn. Pat. No. 84/160911, September 11, 1984.

[404]Furukawa Electric Co. Ltd., "Flame Retardant Polyolefin Compositions," Jpn. Pat. No. 84/217741, December 7, 1984.

[405]Furukawa Electric Co. Ltd., "Flame Retardant Olefin Polymer Compositions," Jpn. Pat. No. 84/221345, December 12, 1984.

[406]E. Koehnlein and L. Koessler, "Flame Resistant and Radiation Resistant Thermoplastic Molding Compositions for Cable Insulation," Ger. Pat. No. DE 3 334 703 A1, October 11, 1984.

[407]U. Lauterbach, K. H. Schnickel, and T. E. C. Utteren, "Wallpaper Backing with an Adhesive Surface Layer," Eur. Pat. Appl. EP 109 663 AZ, May 30, 1984.

[408]K. K. Latex, "Durable Backing for Tile-Shaped Carpet," Jpn. Pat. No. 84/55218, March 30, 1984.

[409]Fujihura Cable Works Ltd., "Fire Resistant Polyolefin Electric Insulators," Jpn. Pat. No. 83/109596, June 29, 1983.

[410]N. L. Tutaeva, W. J. Komarov, A. Y. Morkisa, M. M. Revyako, and M. D. Belyakova, *Zh. Prikl. Khim. (Leningrad)*, **56** [10] 2324-8 (1983).

[411]Nisshan Kogyo Co. Ltd., "Flexible High Strength Fire Resistant Roofing Material,' Jpn. Pat. No. 83/65655, April 19, 1983.

[412]Furukawa Electric Co. Ltd., "Flameproof Resin Compositions," Jpn. Pat. No. 83/117237, July 12, 1983.

[413]Joban Kashatsu K. K., "Wall Decorative Compositions," Jpn. Pat. No. 83/65771, April 19, 1983.

[414]Lioka K. K., "Fire Resistant Carpets," Jpn. Pat. No. 83/5312, January 29, 1983.

[415]P. Liptak and K. Chaternuchova, "Modification of the Properties of Filled Crosslinked Polyethylene with Ethylene-Vinyl Acetate Copolymer," *EKT, Elektrorzolacna Kablova Tech.*, **36** [1] 17–22 (1983).

[416]Fon Seal Corp., "Wall Paper," Jpn. Pat. No. 83/4879, January 12, 1983.

[417]Furukawa Electric Co. Ltd., "Fire Resistant Resin Composition," Jpn. Pat. No. 82/212247, December 2, 1982.

[418]Furukawa Electric Co. Ltd., "Inorganic Compound Filled Foam Manufacture," Jpn. Pat. No. 82/115432, July 17, 1982.

[419]Sumitomo Electric Industries Ltd., "Fire Resistant Electric Wire," Jpn. Pat. No. 82/36688.

[420]D. Alt and J. Siewert, "Insulating Mixture for Electrical Cables," Ger. Pat. No. DE 3 106 147 AL, September 9, 1982.

[421]N. L. Tuteave et al., "Fillers Containing Aluminum Hydroxide for Polymeric Compositions," USSR Pat. No. 927 837, May 15, 1982.

[422]Nippon Zeon Co. Ltd., "Fire Resistant Resin Composition," Jpn. Pat. No. 82/99644, March 23, 1982.

[423]A. West and D.B. Radadia, "Low Smoke Polyolefin Jacket Composition for Electrical Wire," U.S. Pat. No. 4 327 001, April 27, 1982.

[424]J. W. Biggs and M. F. Maringen, "Fire Retardant Polymer Coating Compositions for Electrical Conductors," Belg. Pat. No. 890270, March 8, 1982.

[425]H. Nakae, I. Noguchi, and M. Kondo, "Crosslinked EVA Copolymer Foam Containing an Inorganic Material and Its Production," Br. Pat. Appl. 2070021, September 3, 1981.

[426]Furukawa Electric Co. Ltd., "Highly Filled Fire Resistant Resin Compositions,' Jpn. Pat. No. 81/67363, June 6, 1981.

[427]R. J. Penneck and R. S. Skipper, "Polymer Composition Containing Hydrated Alumina Particles Useful for Electric Insulation," Braz. Pat. No. 80/7125, May 5, 1981.

[428]Furukawa Electric Co. Ltd., "Fire Resistant Resin Compositions for Cable Sheaths," Jpn. Pat. No. 81/18636.

[429]Furukawa Electric Co. Ltd., "Heat Resistant Resin Compositions Highly Filled with Inorganic Materials," Jpn. Pat. No. 80/164235, December 20, 1980.

[430]Showa Electric Wire & Cable Co., "Fire Resistant Compositions," Jpn. Pat. No. 80/160067, December 12, 1980.

[431]Furukawa Electric Co. Ltd., "Fire Resistant Thermoplastic Compositions," Jpn. Pat. No. 80/127446, October 2, 1980.

[432]G. Pfirromann et al., "Flame Resistant Thermoplastic Molding Compositions," Ger. Pat. No. 2 909 498, September 18, 1980.

[433]M. R. C. Johnson and R. S. Skipper, "Flame Retardant Covering for Elongated Substrate," Ger. Pat. No. 2 947 332, June 4, 1980.

[434]I. Noguchi, H. Nakae, and M. Hasebe, "Fire Resistant Resin Compositions," Jpn. Pat. No. 80 34226, March 10, 1980.

[435]M. F. Maringen, L. A. Meeks, and W. K. Hanna, "Flame Retardant Polymeric Materials," U.S. Pat. Appl. 865 833, March 13, 1976.

[436]S. Yamamoto and M. Nishumura, "Fire Resistant Ethylene Copolymer Compositions," Jpn. Pat. No. 78/141353, December 9, 1978.

[437]T. Ohta, "Fire Resistant Paper Substitutes," Jpn. Pat. No. 77/96701, August 13, 1977.

[438]J. A. North and G. W. Kackro, "Flameproofing Polymeric Materials for Coating Electrical Conductors," Ger. Pat. No. 2 228 978, January 18, 1973.

[439]J. A. North and G. W. Kackro, "Flame Retardant Compositions," U.S. Pat. No. 3 922 442, November 25, 1975.

[440]R. B. Walters, "Polymer Compositions for Insulation," Ger. Pat. No. 2 439 490, March 6, 1975.

[441]I. Aishima, Y. Tahashi, Y. Katagama, and K. Matsumoto "Fire Resistant Resin Compositions, Jpn. Pat. No. 4032393, June 28, 1977.

[442]John F. Szabat, "Fire Resistant Flexible Polyurethane Foam," U.S. Pat. No. 4 546 117, October 8, 1985.

[443]P. V. Bonsignore and T. L. Levendusky, "Alumina Trihydrate as a Flame Retardant and Smoke Suppressive Filler in Rigid High Density Polyurethane Foams," *J. Fire Flammability*, 8 [1] 95 (1977).

[444]C. Elwert and G. Goeze, "Polymer Foam Insulators," Ger. Pat. No. 2 244 597, April 25, 1974.

[445]H. Zunker, "Construction Panel of Rigid Polyurethane Foam," Ger. Pat. No. DE 3 401 509 A1, October 25, 1984.

[446]N. S. Marans, C. L. Kehr, and R. M. March, "Hydrophillic Polyurethane Compositions with Flame Retarding Properties," Ger. Pat. No. 2 447 943, April 4, 1975.

[447]R. C. Hopkins, "Alumina Trihydrate, Clean, Low-Cost Flame Retardant," *Polymer Age*, **6** [5] 130 (1975).

[448]K. Yagura and H. Lugihara, "Fireproofed Polyisocyanate Foams," Jpn. Pat. No. 75/29700, March 25, 1975.

[449]R. B. Gallagher, G. A. Harpell, E. R. Kamans, and V. R. Kamath, "Properties, Processing, Applications of Polyester Foams," 32nd Assn. Tech. Conf. Reinf. Plastics Komp. Inst., SPI 3-C, 1977.

[450]T. Yamoshita and R. Imaizumi, "Graphite Fiber-Reinforced Foams," Jpn. Pat. No. 73/40055, November 28, 1973.

[451]C. Kato, K. Kanei, K. Matsushima, and M. Hirakawa. "Nonburning Lightweight Composites," Jpn. Pat. No. 75/03451, January 14, 1975.

[452]C. Kato, K. Kanei, K. Matsushima, and M. Hirakawa. "Fire Resistant Lightweight Composites Having Patterns," Jpn. Pat. No. 75/05471, January 21, 1975.

[453]C. Kato, "Fire Resistant Composite Boards," Jpn. Pat. No. 74/131244, December 16, 1974.

[454]C. Kato, K. Kannei, K. Matsushima, and M. Hirakawa. "Nonflammable Decorative Stone Substitutes," Jpn. Pat. No. 74/120978, November 11, 1974.

[455]Asahi Chemical Industry Co. Ltd., "Vinylidene Chloride Resin Compounds," Jpn. Pat. No. 84/215345, December 5, 1984.

[456]Nippon Zeon Co. Ltd., "Flame Retardant Thermal Insulation," Jpn. Pat. No. 84/141454, August 14, 1984.

[457]A. Kaminski, "Flammability as a Criterion of the Applicability of Polyester Laminate in the Construction of Passenger Cars," Polimery (Warsaw), **29** [4–5] 196–99 (1984).

[458]K. K. Renzi Sunyu, "Flame Resistant Epoxy Resin Compositions," Jpn. Pat. No. 84/98123, June 6, 1984.

[459]Sumitomo Bakelite Co. Ltd., "Fire Resistant Copper-Clad Polyester Laminates," Jpn. Pat. No. 84/57744, April 3, 1984.

[460]Editor, "The Bathroom Also-Ran Now Sets the Pace," *Modern Plastics Magazine*, March 1975.

[461]L. E. Tyaglova, D. Kh. Kulev, N. K. Perepelkina, V. S. Slichkin, G. N. Gregorev, and L. Yu Esipov., "Lowering the Flammability of Rigid Polyurethane Foams," *Plast. Massy*, **9**, 46–48 (1983).

[462]Hitachi Cable Ltd., "Nonflammable Thermosetting Resin Composition," Jpn. Pat. No. 83/98360, June 11, 1983.

[463]K. Kita, "Fireproofing of Aluminum-Coated Polyester Fibers," Jpn. Pat. No. 83/13774, January 26, 1983.

[464]V. S. Gorshkov et al., "Rigid Polyurethane Foams, USSR Pat. No. SU 872529A1, October 15, 1981.

[465]P. V. Bonsignore, "Alumina Trihydrate as a Flame Retardant for Polyurethane Foams," *Adv. Urethane Sci. Technol.*, **8**, 253–62 (1981).

[466]H. Petersen, K. Fischer, and H. Z. Kurt, "Crosslinkable Condensation Product Based on Phenol-Butyraldehyde Resins and Thermoplastic Materials," Ger. Pat. DE 2 941 635, April 23, 1981.

[467]C. J. Del Valle, "Resin Compositions," U.S. Pat. No. 4 267 095, May 12, 1981.

[468]Kodo Co. Ltd., "Fire Resistant Polyurethane Foams," Jpn. Pat. No. 81/20018, January 25, 1981.

[469]Matsushita Electric Industrial Co. Ltd., "Fire Resistant Thermosetting Resin Compositions," Jpn. Pat. No. 81/2340, January 12, 1981.

[470]Henderson's Industries Ltd., "Fire Resistant Semirigid Polyurethane Foams with High Resilience," Jpn. Pat. No. 80/145720, November 13, 1980.

[471]D. C. Priest, "Polyether-Derived Polyurethane Foam Impregnant," U.S. Pat. No. 4224374, September 23, 1980.

[472]R. L. Dieck, "Modified Polyester Compositions," Ger. Pat. DE 3 004 942, August 21, 1980.

[473]Mitsui Petrochemical Industries Ltd., "Phenolic Resin Foam Laminate," Jpn. Pat. No. 80/63255, May 13, 1980.

[474]R. M. Murch, P. I. Meyer, and J. J. Eagan, "Fire Resistant Polyurethane Foam," Ger. Pat. No. DE 2 940 749, April 30, 1980.

[475]J. Tintner, E. Urinann, P. Maillard, and F. Leschchorn, "Molded Composition Made from Foamed Polystyrene, Specifically Foam Polystyrene Sheets," Ger. Pat. No. DE 2 729 493, November 23, 1978.

[476]J. Aoki, "Aluminum Hydroxide as a Flame Retardant for Plastics," *Porima Daijesuto*, **30** [3] 27–43 (1978).

[477]P. Hamelin and G. Debicki, "Study on Variations of Mechanical Properties of Various Glass-Resin Laminates Subjected to Operation Cycles Defined by the Flame Reaction Test," *Verre Text., Plast. Rein.*, **16** [7] 25–29 (1978).

[478]K. M. Foley, F. P. McCombs, and R. H. Bell, "Molding Composition Containing A Heat-Hardenable Resin and a Cement," Belg. Pat. No. BE 835555, March 1, 1976.

[479]Y. Ninomiya and H. Hashimoto, "Fire-Resistant Decorative Panels," Jpn. Pat. No. 77/130881, November 2, 1977.

[480]Y. Ninomiya and H. Hashimoto, "Fire-Resistant Decorative Panels," Jpn. Pat. No. 77/130880, November 2, 1977.

[481]Y. Haneda, "Fire-Resistant Thermosetting Resin Compositions," Jpn. Pat. No. 74/34940, March 30, 1974.

[482]Y. Haneda, "Fire-Resistant Electrical Insulation," Jpn. Pat. No. 75/139838, November 8, 1975.

[483]J. L. Thomas, U.S. Pat. No. 3 826 777, FMC, 1974.

[484]H. Talsma, U.S. Pat. No. 3 786 041, Standard Oil, 1974.

[485]T. Saheki and M. Ueda, Okura Ind. Co., Jpn. Pat. No. 74/92139, 1974.

[486]Y. Toi, "Fire Proofed Resins," Jpn. Pat. No. 73/29882, April 20, 1973.

[487]T. Ono, S. Negishi, U. Yonemura, and T. Hagashi, "Fire Resistant Resin Composites Containing Aluminum Hydroxide," Jpn. Pat. No. 73/96640, December 10, 1973.

[488]S. Kobayshi, H. Takeachi and I. Yamazaki, "Vinyl Resin Composites Containing Gibbsite," Jpn. Pat. No. 74/75655, July 22, 1974.

[489]T. Sasono and H. Hirate, "Impact and Fire-Resistant Resin Moldings," Jpn. Pat. No. 73/76985, October 16, 1973.

[490]M. M. Hirschler and O. Tsika, "The Effect of Combinations of Aluminum (111) Oxides and Decabromobiphenyl on the Flammability of and Smoke Production from Acrylonitrile-Butadiene-Styrene Terpolymer," *Eur. Polym. J.*, **19** [5] 375–80 (1983).

[491]F. K. Antia, C. F. Cullis, and M. M. Hirschler, "Binary Mixtures of Metal Compounds as Flame Retardant for Organic Polymers," *Eur. Polym. J.*, **18** [2] 95–107 (1982).

[492]S. Salman, D. Klempner, and F. B. McGregor," Alumina Hydrate As a Flame Retardant Filler For Thermoplastics," *Soc. Plast., Eng., Tech. Pap.*, **25** , 937–41 (1979).

[493]G. L. Deets and Y. C. Lee, "Smoke Reduction Studies on Selected Vinyl Polymers," *J. Fire Flammability*, **10** [1] 41–51 (1979).

[494]D. E. Malloy, Jr. "Formulating Compounds For Electron-Bream Cross-Linking," *Plast. Eng.*, **40** [12] 33–36 (1984).

[495]H. Jan, P. Wilfred, N. P. Skaar, and K. Arvid, "Fire Resistant Material," Br. Pat. No. GB 2 130 223 A1, May 31, 1984.

[496]S. C. Vick, D. Fairhurst, and A. Sorio, "Organosilicon Chemicals in Alumina Trihydrate-Filled Polyolefins," *Gummi Fasern Kunstst.*, **37** [7] 336–40 (1984).

[497]O. M. Lejnek, M. Lacuska, and P. Liptak, "Gas and Gel Permeation Chromatographic Investigation of Polyethylene Modification in Model Chemical Reactions," *J. Chromatogr.*, **286**, 301–309 (1984).

[498]B. R. Frye, "A New Silicon Flame Retardant System For Thermoplastics," *Polymer. Mater. Sci. Eng.*, **51**, 235–39 (1984).

[499]K. K. Latex, "Fire-Resistant Wallpaper," Jpn. Pat. No. 84/43198, March 10, 1984.

[500]N. K. Jha, A. C. Misra, and P. Bajaj, "Flame Retardant Additives For Polypropylene," *J. Macromolecular Sci., Rev. Macromol. Chem. Phys.*, **C24** [1] 69–116 (1984).

[501]Ube Industries, Ltd., Daiichi Chemical Industry Co., Ltd., Nippon Kyoiku Sozai K. K., "Preparation of Fire Resisting Cellular Polyethylene Resin," Jpn. Pat. No. 83/129026, September 10, 1983.

[502]Matsushita Electric Industrial Co., Ltd., "Flame Retardant Adhesives," Jpn. Pat. No. 83/41318, September 10, 1983.

[503]R. Murai, A. Iwata, S. Fukushima, Y. Shimura, and M. Hayashi, "Fire Resistant Synthetic Wood," Jpn. Pat. No. 76/06270, January 1, 1976.

[504]Y. Catrain, C. Guerrier, and J. R. Claude, "Composite Material Useful In Reinforcing Insulating Panels," Fr. Pat. No. 2 534 185 A1, April 13, 1984.

[505]Showa Electric Wire And Cable Co., Ltd., "Flame Resistant Crosslinked Polyolefin Composition," Jpn. Pat. No. 83/118828, July 15, 1983.

[506]Japan Atomic Energy Research Institute; Furukawa Electric Co., Ltd., "Flame Retardant Polyolefin Moldings," Jpn. Pat. No. 83/38736, March 7, 1983.

[507]T. L. Levendusky and W. L. Burton, "Flame Retardant Filled Polypropylene Compound With Improved Properties," U.S. Pat. No. 4 390 653A, June 28, 1983.

[508]B. Ivanfy, W. Muno, H. A. Mayer, and D. S. Parmar, "Thermoplastic Flexible Polymer Mixture," Ger. Pat. No. DE 3 150 798A1, June 30, 1983.

[509]Furukawa Electric Co., Ltd., "Fire-Resistant Resin Compositions," Jpn. Pat. No. 83/1741, January 7, 1983.

[510]W. A. Muelle, J. D. Ingham, and W. W. Reilly, "Elastomer Coated Fillers and Their Composites Comprising at Least 60% By Weight of a Hydrated Filler and an Elastomer Containing an Acid Substituent," U.S. Pat. No. 4 373 039A, February 8, 1983.

[511]Hitachi Cable, Ltd., "Fire-Resistant Resin Compositions," Jpn. Pat. No. 82/174349, October 27, 1982.

[512]E. Koehnlein and D. Moorwessel, "Flame-Resistant Thermoplastic Molding Compositions Based on Polyolefin-Bitumen Mixtures Useful as Sealing Strips," Ger. Pat. No. DE 3 117 672A1, November 25, 1982.

[513]M. Maeda, N. Watanabe, and K. Fujitani, "Polyolefin Composition," Eng. Pat. No. EP 62 252 A1, October 13, 1982.

[514]C. C. Ndubizu and B. T. Zinn, "Soot Suppression in Noncharring Polymer Diffusion Flames," *J. Fire Flammability*, **13** [3] (1982).

[515]F. K. Antia, C. F. Cullis, and M. M. Hirschler, "The Inhibition of Polymer Combustion By Metal Oxides." Colloq. Int. Berthelot-Vieille-Mallard-Le-Chatelier, (Actes), 1st. Volume 2, 602-7, Sect. Fr. Combust. Inst: Orleans, Fr., 1981.

[516]K. Ogino, N. Hashimoto, and H. Takahashi, "Study on the Thermal Behavior of the Polymer Composite Materials. Polyethylene-Aluminum Hydroxide System," *Trans. Jpn. Soc. Compos. Mater.*, **7** [2] 52–57 (1981).

[517]Dainippon Ink and Chemical Inc., "Fire-Resistant Resin Compositions," Jpn. Pat. No. 82/102941, June 26, 1982.

[518]Hitachi Cable, Ltd., "Flexible and Flame Resistant Ethylene-Butene Copolymer Compositions," Jpn. Pat. No. 82/87010, May 31, 1982.

[519]Hitachi Cable, Ltd., "Vinyl Polymer Compositions and Plugs," Jpn. Pat. No. 82/42759, March 10, 1982.

[520]Hitachi Cable, Ltd., "Graft Copolymer Electric Insulators for Plugs," Jpn. Pat. No. 82/40548, March 6, 1982.

[521]Dainippon Ink and Chemicals, Inc.," Fire-Resistant Unsaturated Polyester Molding Compositions," Jpn. Pat. No. 82/40519, March 6, 1982.

[522]K. Nakatani, S. Watanabe, and Y. Kaneshige, "Flame Retardant Compositions of Polyethylene and Ethylene-Vinyl Acetate Copolymer," *Toyo Soda Kenkya Hokoku*, **26** [1] 17–24 (1982).

[523]T. Handa, T. Nagashima, H. Yamamoto, S. Miyanishi, N. Ebihara, and S. Orihashi, "The Synergistic Effects of Antimony Trioxide and Other Metal Oxide or Hydroxide in Plasticized Flame Retardant Polypropylene and Plasticized PVC.," *J. Fire Retard. Chem.*, **8** [4] 171–92 (1981).

[524]J. W. Biggs and M. F. Maringer, "Fire-Retardant Polymer Coating Composition Hardenable by Irradiation," Belg. Pat. No. BE 890 269A1, March 8, 1982.

[525]Furukawa Electric Co., Ltd., "Polyethylene Compositions," Jpn. Pat. No. 81/166246, December 21, 1981.

[526]D. Scholz, "Flame-Retarding and Low-Smoke GF-UP Laminates Based on Low-Viscosity Resins," *Vorabdruck-Oeff. Jahrestag. Arbeitsgem. Verstaerkte Kunstst.*, **17**, 5/1–5/5 (1981).

[527]K. K. Denko Showa, "Flame-Retardant Polyolefins," Jpn. Pat. No. 81/127643, October 6, 1981.

[528]Japan Atomic Energy Research Institute: Furukawa Electric Co., Ltd., "Fire-Resistant Polyolefin Compositions," Jpn. Pat. No. 81/84732, July 10, 1981.

[529]Showa Electric Wire and Cable Co., Ltd., "Fire-Resistant Electric Wire," Jpn. Pat. No. 81/102006, August 15, 1981.

[530]K. K. Denko Showa, "Fireproofing Conductive Chlorinated Polyethylene," Jpn. Pat. No. 81/53142, May 12, 1981.

[531]E. G. Howard, B. L. Glazar, and J. W. Collete, "Homogeneous Composites of Ultrahigh Molecular Weight Polyethylene and Minerals. 2 Properties," *Ind. Eng. Chem. Prod. Res. Dev.*, **20** [3] 421–28 (1981).

[532]B. Cheval, "Highly Filled Polyolefins," Fr. Pat. No. 2 440 382, May 30, 1980.

[533]Sumitomo Electric Industries, Ltd., "Fire-Resistant Electric Cables," Jpn. Pat. No. 80/136406, October 24, 1980.

[534]W. A. Mueller, J. D. Ingham, and W. W. Reilly, "Development of Flame And Smoke Retardant Thermoplastic Molding Compounds," *J. Fire Flammability*, **11** [10] 275–83 (1980).

[535]T. Susano and H. Hirato, "Flame Resistant High Impact Polystyrene," Jpn. Pat. No. 74/125453, Risso Corp., 1975.

[536]H. Nakae, I. Noguchi, and M. Hasebe, "Ethylene-a-Olefin Copolymer Compositions Having High Contents of Inorganic Fillers and Good Elongation Properties," Jpn. Pat. No. 80/25405, February 23, 1980.

[537]H. Nakae, I. Noguchi, and M. Hasebe, "Polyethylene Resin Compositions Having High Content of Inorganic Fillers," Jpn. Pat. No. 80/31871, March 6, 1980.

[538]E. J. Augustyn, "Flame-Retardant Thermoplastic Composites Made From Polyethylene," 1979.

[539]T. Handa, N. Ebihara, T. Nagashima, H. Yamamoto, H. Tsushima, S. Miyanishi, and S. Orihashi, "The Synergistic Effects of Antimony Trioxide and Other Metal Oxide or Hydroxide in the Flame Retardant Polypropylene and Soft PVC," *Proc. Int. Conf. Electr. Electron. Mater.*, **1**, 75–122 (1980).

[540]K. Saito, M. Kinoshita, T. Sano, and S. Suganuma, "Reformed Red Phosphorus," Jpn. Pat. No. 80/10462, January 24, 1980.

[541]K. Nishimoto and A. Hirai, "Fire-Resistant Adhesive Compositions," Jpn. Pat. No. 79/83939, July 4, 1979.

[542]G. Braun and J. Theyssen, "Ultrahigh Molecular Weight Polyethylene A Material and its Modification," *Kunststoffe*, **69** [8] 434–39 (1979).

[543]K. Nishimoto and A. Hirai, "Fire-Resistant Adhesives," Jpn. Pat. No. 79/8643, January 23, 1979.

[544]R. G. Angell Jr., L. H. Gross, and S. E. Berger, "Injection Molding Reduced Combustibility High Impact Strength Polyethylene Articles," U.S. Pat. No. 4 107 258, August 15, 1978.

[545]K. Sumi, M. Shiosaki, and N. Hata, "Fire-Resistant Epoxy Compositions," Jpn. Pat. No. 79/3151, January 11, 1979.

[546]N. Maeda, T. Wakahata, T. Sakairi, and F. Iwami, "Fire-Resistant Polypropylene Composites," Jpn. Pat. No. 78/82845, July 21, 1978.

[547]A. G. Hoechst, "Fire-Resistant, Thermoplastic Molding Compositions," Belg. Pat. No. BE 854858, November 21, 1977.

[548]B. A. Murashev, "Synthetic and Natural Hydrates and Prospects of Their Introduction as Fillers and Fireproofing Compounds," Napolnitel Polimer Material or 156-61 From: Ref. ZH., Khim. 1977, Abstract No. 13T54, 1977.

[549]H. Goto, Y. Sato, M. Hori, and Y. Okiishi, "Fire-Resistant Polypropylene Composite Electric Insulators," Jpn. Pat. No. 77, 121058, 1977.

[550]T. Murata, "Fire-Resistant Thermoplastic Resin Compositions," Jpn. Pat. No. 77/108447, September 10, 1977.

[551]H. Staendeke, F. J. Dany and J. Kandler, "Flame-Resistant Molding Compositions From Thermoplastic Synthetic Materials," Ger. Pat. No. DE 2 623 112, December 1, 1977.

[552]M. Kamikado, T. Ogawa, and H. Ishii, "Fire-Resistant Thermoplastic Tube," Jpn. Pat. No. 77/100549, August 23, 1977.

[553]L. K. Ojiauw and R. D. Icenoyle, "Low Smoke Polypropylene Insulation," U.S. Pat. No. 4 622 352, November 11, 1986.

[554]L. Keating and S. Petrie, "Hydroxide, A Halogen Free Flame and Smoke Suppressant for Polypropylene," Fire Safety Use Flame Retardant Polymer, FRCA Meeting, 1985.

[555]C. T. Jacobsen, "High Temperature Polymeric Fire Barriers," *Plant Operations Progress*, **5** [3] 148–54 (1986).

[556]L. Keating, S. Petrie, and G. Beekman, "Magnesium Hydroxide: Halogen Free Flame Retardant and Smoke Suppressant for Polypropylene," *Plast. Compounding*, **9** [4] 40, 42, 44 (1986).

[557]K. Ohtsuka, T. Takahashi, and T. Tanaka, "Fire Resistant Resin Compositions," Jpn. Pat. No. 74/125453, November 30, 1974.

[558]E. G. Howard, B. L. Glazur, and J. W. Collette, "Ultra High Molecular Weight Polyethylene/Mineral Composites," High Performance Plast. Natl. Tech. Conf., SPE, p. 36, 1976.

[559]G. L. Nelson, "Smoke Evolution: Thermoplastics," *J. Fire Flammability*, **5**, 125 (1974).

[560]F. Sakaguchi, "Repoc, A Pollution Free General Purpose Composite Resin," *Japan Plast. Age.*, **12** [4] 44 (1974).

[561]F. Sakaguchi, "Repoc, Pollution-Free Composite Materials," *Japan Plast. Age*, **20** [2] 77 (1974).

[562]H. Yui, S. Moriwaki, and T. Watanabe, "Self-Extinguishing Resin Composition," Jpn. Pat. No. 75/34643, April 3, 1975.

[563]T. Kimura, "Thermal Insulators and Foams of Resins Containing Inorganic Polymers," Jpn. Pat. 75/87164, July 14, 1975.

[564]T. Kimura, "Foams and Heat and Fire Resistant Reinforced Resins Containing Inorganic Polymers," Jpn. Pat. No. 75/87166, July 14, 1975.

[565]K. Sumi, "Hard to Flame Polyethylene Composition," Jpn. Pat. No. 73/18570, June 7, 1973.

[566]N. Tanaka, S. Hayashi, and I. Morimoto, "Foamable Polyethylene Extrusion Molding Compositions," Jpn. Pat. No. 75/92360, July 23, 1975.

[567]M. Tomikawa, A. Tsunoda, H. Ohkawa, K. Hazashi, K. Kaneda, and Y. Mugino, "Fire Resistant Polyethylene Foam Compositions," Jpn. Pat. No. 74/05171, January 7, 1974.

[568]A. W. Carlson, "Flame Retardant Polypropylene Compositions," U.S. Pat. No. 4 006 114, February 1, 1977.

[569]H. Matsubara et al., "Development of New Fire Proof Wire and Cable," 24th Intl. Wire & Cable Symposium, 1975.

[570]F. Sakaguchi, K. Takemura, H. Takouchi, and T. Suzuki, "Thermoplastic Resin Sheets," Jpn. Pat. No. 73/102176, December 22, 1973.

[571]F. Sakaguchi, K. Takemura, H. Takouchi, and T. Suzuki, "Olefinic Resin Composition Having Softness and Fire Resistance," Jpn. Pat. No. 75/35449, April 2, 1974.

[572]H. Yashima, "Amorphous Polypropylene Nonsticking Resin," Jpn. Pat. No. 73/14424, May 7, 1973.

[573]H. Yui, S. Moriwaki, and T. Watanabe, "Self Extinguishing Resin Compositions," Jpn. Pat. No. 75/34643, April 3, 1975.

[574]Y. Harada, H. Takawa, and A. Kakizaki, "Fire Resistant Polystyrene Foams," Jpn. Pat. No. 74/103957, October 2, 1974.

[575]R. J. Hoelzer, "Insulation Jacketing Material," U.S. Pat. No. 4 544 685, October 1, 1985.

[576]R. G. Spain, "Fire Retardant Coatings," U.S. Pat. No. 4 666 960, May 19, 1987.

[577]C. Yoshida Kogyo K. K., "Fire Resistant Packing for Window Frames," Jpn. Pat. No. 84/52192, December 18, 1984.

[578]Fuji Chemical Industry Co. Ltd., ABC Trading Co. Ltd., "Nonflammable Foam," Jpn. Pat. No. 84/215331, December 5, 1984.

[579]S. Kobayoshi, H. Takeuchi, and I. Yamazaki, "Vinyl Resin Composites Containing Gibbsite," Jpn. Pat. No. 75/09674, October 3, 1975.

[580]Hitachi Ltd., Hitachi Chemical Co. Ltd., "Potting Compositions for Flyback Transformers," Jpn. Pat. No. 84/160910, September 11, 1984.

[581]Hitachi Ltd., Hitachi Chemical Co. Ltd., "Potting Compositions for Flyback Transformers," Jpn. Pat. No. 84/143313, August 16, 1984.

[582]R. J. Brown, "Smoke Retardant Vinyl Halide Polymer Compositions," Eur. Pat. Appl., EP 94 602A2, 1983.

[583]H. P. Desai and R. D. Deanin, "Smoke Suppressants for Plasticized Poly (Vinyl Chloride)," *J. Vinyl Technol*, **6** [1] 25–27 (1984).

[584]Dainichi Nippon Cables Ltd., "Soft PVC Compositions with Reduced Smoke," Jpn. Pat. No. 83/37039, March 4, 1983.

[585]G. L. Nelson, "Smoke Evolution: Thermoplastics," *J. Fire Flammability*, **5**, 125 (1974).

[586]S. George and T. H. George, "Refractory Coated and Dielectric Coated Flame Resistant Insulating Fabric Composition," U.S. Pat. No. 4 396 661A, August 2, 1983.

[587]Associated Lead Manufacturers Ltd., "Improved Stabilizers for Vinyl Resins," Belg. Pat. No. BE 894 788 A1, February 14, 1983.

[588]S. George and T. H. George, "Refractory Coated and Conductive Layer Coated Flame Resistant Insulating Fabric Composition," U.S. Pat. No. 4 375 493A, March 1, 1983.

[589]C. Loeffler and R. Wingenbach, "Possibilities for Making PVC Flame Retardant," *GAK, Gummi Asbest. Kunstst.*, **35** [11] 604, 606–607 (1982).

[590]T. Akamura and H. Jrifune, "Flame Retardant Construction Materials," Fr. Pat. No. 2 500 437A1, August 27, 1982.

[591]V. S. Gorshkov et al., "Plastic Foam," USSR Pat. No. SU937478A1, June 23,1982.

[592]K. K. Shen and R. W. Sprague, "Zinc Borate as a Flame Retardant and Smoke Suppressant in PVC," *J. Vinyl Technol*, **4** [3] 120–23 (1982).

[593]C. P. Yang and J. F. Hwang, "The Effect of Additives on Arc Resistance of Polymers (PVC and PE)," *J. Chin. Inst. Chem. Eng.*, **13** [1] 35–44 (1982).

[594]Fujikura Cable Works Ltd., "Fire Resistant Poly(Vinyl Chloride) Compositions," Jpn. Pat. No. 82/49640, March 23, 1982.

[595]Hitachi Cable Ltd., "Poly (Vinyl Chloride) Based Electric Insulators for Plugs," Jpn. Pat. No. 82/40542, March 6, 1982.

[596]Hitachi Cable Ltd., "Poly(Vinyl Chloride) Electric Insulators for Plugs," Jpn. Pat. No. 82/40541, March 6, 1982.

[597]Hitachi Cable Ltd., "Graft Copolymer Electric Insulator Composition for Plugs," Jpn. Pat. No. 82/40543, March 6, 1982.

[598]Hitachi Cable Ltd., "Vinyl Polymer Composition for Electric Plugs," Jpn. Pat. No. 82/40546, March 6, 1982.

[599]Furukawa Electric Co. Ltd., "Fire Resistant Composite Tapes," Jpn. Pat. No. 81/164843, December 18, 1981.

[600]Cainichi Nippon Cables Ltd., "Fire Resistant Wire Covering," Jpn. Pat. No. 81/59856, May 23, 1981.

[601]Dainichi Nippon Cables Ltd., "Fire Resistant Wire Covering," Jpn. Pat. No. 81/59855, May 23, 1981.

[602]V. S. Gorshkov et al., "Polymeric Composition," USSR Pat. No. SU817036, March 30, 1981.

[603]P. Peurasuro, A. Litja, and V. Tammela, "Improvement of the Fire Resistance of Poly (Vinyl Chloride)," *Kem.-Kemi*, 7 [11] 657–62 (1980).

[604]K. K. Densen Tokai, "Fire Resistant Electric Insulators," Jpn. Pat. No. 80/108108, August 19, 1980.

[605]H. Hentschel, "Fireproofing of Plastics with Aluminum Hydroxide," *Kunstst, Bau*, **15** [3] 127–29 (1980).

[606]H. Severus-Laubenfeld, "Composite Panels which Are not Easily Combustible," U.S. Pat. No. 4 221 835, September 9, 1980.

[607]W. Popp and J. Sedivy, "Plasticized Poly(Vinyl Chloride) Compositions and Their Use," Ger. Pat. No. DE2 905 011, August 14, 1980.

[608]P. V. Bonsignore and P. L. Claassen, "Alumina Trihydrate as a Flame Retardant Filler for Flexible Vinyl Compounds," *J. Vinyl Technol.*, **2** [2] 114–18 (1980).

[609]A. Ossin and E. A. Welsh, "Ablative Radome Material Screening," Natl. SAMPE Symp. Exhib., (Proc.), 25, 1980's (Nineteen Eighties)-Payoff Decade Adv. Mater., 728–36, 1980.

[610]K. K. Shokusen Hiraoka, "Fire Resistant Films," Jpn. Pat. No. 80/4582, January 31, 1980.

[611]F. W. Moore and G. A. Tsigdinos, "Advances in the Use of Molybdenum Additives as Smoke Suppressants and Flame Retardants for Poly (Vinyl Chloride)," Fire Retard., Proc. Intl. Symp. Flammability Fire Retard., 160–72, 1978.

[612]S. Orihashi et al., "Fire Resistant Poly(Vinyl Chloride) Composition," Ger. Pat. No. DE2 937 482, March 27, 1980.

[613]M. Shinmon and H. Ishii, "Wire and Cable Sheath," Jpn. Pat. No. 80/1020, January 7, 1980.

[614]C. Loeffler and R. Wingenbach, "Coated Fabrics — A Contribution to Flame Resistant Finishing," *Coating*, **12** [10] 275–78 (1979).

[615]M. Yamamoto and J. Yamamoto, "Polyurethane Foams Laminated with Fire Resistant Films," Jpn. Pat. No. 79/70383, June 6, 1979.

[616]K. Furukawa et al., "Fire Resistant Resin Compositions," Jpn. Pat. No. 79/37152, March 19, 1979.

[617]P. V. Bonsignore, "Alumina Trihydrate as a Component of Flame Retardant Coating Systems for Cellulosic Materials," Life Prop. Prot., Pap., Semi-Annual Mtg., Fire Retard. Chem. Assoc., 319–30, Fire Retardant Chem. Assoc., Westport, CT 1977.

[618]H. Taniuchi and N. Hayashi, "Fire Resistant Water-Repellent Sheets," Jpn. Pat. No. 79/3180, January 11, 1979.

[619]E. Cox, "The Role of Flame Retardant Additives in PVC," Probl. Solutions: Conf./Workshop, Jt. Mtg. Soc. Plast. Eng. Fire Retard. Chem. Assoc., 315–25, Fire Retardant Chem. Assoc., Westport, CT, 1978.

[620]P. V. Bonsignore, "Alumina Trihydrate as a Flame Retardant Filler for Flexible Vinyl Compounds," Life Prop. Prot., Pap., Semi-Annual Mtg., Fire Retard. Chem. Assoc., 253–59, 1977.

[621]H. R. Bennett, "Plastics Coatings for Electric Cables," Br. Pat. No. GB1519781, August 2, 1978.

[622]M. Sato, N. Takahata, and K. S. Norie, "Prevention of Hydrochloric Acid and Smoke in Burning of Plasticized Poly(Vinyl Chloride)," Jpn. Pat. No. 79/3862, January 12, 1979.

[623]S. Kaufman and M. M. Yocum, "The Behavior of Fire Resistant Communication Cables in Large Scale Fire Tests," Plast. Telecommun., Int. Conf., 2nd Paper No. 8, 16 pp., Plast. Rubber Inst., London, England, 1978.

[624]D. F. Lawson, "Smoke Retardant Chlorinated Polymer Compositions," U.S. Pat. No. 4 096 116, June 20, 1978.

[625]K. Furukawa, A. Sugiyama, and H. Matsumoto, "Fire Resistant PVC Compositions for Cable Sheaths," Jpn. Pat. No. 78/43740, April 20, 1978.

[626]W. Moros and P. Pavlowski, "The Oxygen Index — A Quantitative Determination Index for the Combustion Behavior of Plastics," *Chem. Kunstst., Aktuell*, **32** [2] 70–72 (1978).

[627]H. Baumgaertel, D. Heinrich, and R. Saffert, "Plasticizer Containing Fireproof Molding Compositions and Articles Made from Them." Ger. Pat. No. DE2 644 079, April 6, 1978.

[628]L. L. Musselman; private communication, B.F. Goodrich Technical Center Personnel; Avon Lake, Ohio, June–September 1987.

[629]Y. Ota, "Flame Resistant Filler for PVC Resin II," *Purasuchukkusn*, **23** [5] 163 (1972).

[630]A. W. Morgan, T. C. Mathes, and F. D. Hinchen, "Use of Phosphate/ATH Systems in Flame Retarding Vinyl Compositions," 30 ANTEL SPE, 1972.

[631]T. C. Moths and J. D. Hinchen, "Effect of Phosphate Ester/Filler Interactions on the Flammability and Smoke Generation of PVC," 31st ANTEC SPE, 1973.

[632]S. Kobayoshi, H. Takanchi, and I. Yamazaki, "Vinyl Resin Composites Containing Gibbsite," Jpn. Pat. No. 74/75655, July 22, 1974.

[633]E. L. Kay, "Smoke Retardant for Chlorinated PE and PVC Polymers," U.S. Pat. Appl. B561 387, February 10, 1976.

[634]S. Kawawata, N. Takahashi, and M. Sorisnachi, "PVC Comp.," Jpn. Pat. No. 74/114657, November 1, 1974.

[635]S. Kawawata, N. Takahashi, and M. Sorisnachi, "Fire Resistant PVC Comp.," Jpn. Pat. No. 74/113845, October 30, 1974.

[636]S. Kaufman and C. A. Landreth, "Development of Improved Flame Resistant Interior Wiring Cables," 24th Int. Wire & Cable Symposium, 1975.

[637]S. Kaufman and M. M. Yocum, "Balancing Flame Retardancy and Low Temperature Properties in PVC," Int. Symp. Flammability Fire Retardants, 1975.

[638]J. Kimura, "Resin Foams Containing Aluminum Oxide," Jpn. Pat. No. 75/85668, July 10, 1975.

[639]C. E. Hoke, "Compounding Flame Retardance Into Plastics," *SPE J.*, **29**, 36 (1973).

[640]J. Kimura, "Fire Resistant Plastic Materials," Ger. Pat. No. 2 420 093, November 28, 1974.

[641]J. P. Hamilton, "Reducing Flammability in PVC Plastisols with Triaryl Phosphate Plasticizer," *Modern Plastics*, **49** [10] (1972).

[642]S. J. Monte, G. Sugerman, and D. J. Sieman, "Titanate Coupling Agents Update 1977," 32nd Annual Tech. Conf. Reinf. Plast./Comp. Inst. SPI Paper 4E, 1977.

[643]G. Schoenefeld and J. Walter, "Aluminum Hydroxide, Fire Retardant Filler for PVC Plastisols," *Gummi Asbest. Kunstst.*, **27** [5] (1974).

[644]J. Kimura, "Heat Insulating Foams and Resins Containing Inorganic Materials," Jpn. Pat. No. 75/86562, July 11, 1975.

[645]J. Kimura, "Fire Resistant Heat Insulating Foams and Resins Containing Inorganic Materials," Jpn. Pat. No. 75/86561, July 11, 1975.

[646]J. Kimura, "Resin Foams Containing Aluminum Oxide," Jpn. Pat. No. 75/85668, July 10, 1975.

[647]R. T. Flaherty, J. P. Hamilton, J. Litwin, and C. A. Lynch, SPE Technical Papers, 29th ANTEC XVII, 412, 1971.

[648]C. P. Fenimore, "Flammability of Polymeric Materials," Conf. on Flammability Characteristics of Polymeric Materials, Univ. of Detroit, 1970.

[649]Celanese, "Formulating Epoxy Compounds with Low Flame Spread Ratings," Tech. Bulletin 0667, Celanese Resins Div. of Celanese Coatings Co., 1973.

[650]J. R. Darby, J. K. Sears, and N. W. Touchette, *SPE J.*, **27** [4] 7 (1971).

[651]G. S. Learmonth and D. G. Thwaite, *Br. Polymer J.*, **1**, 154 (1969).

[652]A. J. Papa and W. R. Proops, *J. Appl. Poly. Science*, **16**, 2361 (1972).

[653]Editor, "Polymer Output Records Fifth Consecutive Annual Rise," *Chem. Eng. News*, April 11, 1988.

[654]L. L. Musselman; private communication-Cieba Geigy, 1985.

[655]J. Schmitz, "City Urged to Ban Plastic Building Materials as Toxic to Firefighters," *The Pittsburgh Press*, October 31, 1984.

[656]J. Schmitz, "Council Approves Plastic Pipe Ban," *The Pittsburgh Press*, November 20, 1984.

[657]L. L. Musselman and T. L. Levendusky, "Fire Retarding Oriented Polypropylene Sheet with Alumina Trihydrate"; Alcoa unpublished data, 1985.

[658]N. Yoshii and M. Chono, "Fire Resistant Resin Compositions," Jpn. Pat. No. 79/94539, July 26, 1979.

[659]N. Yoshii and M. Chono, "Fire Resistant Resin Compositions," Jpn. Pat.No. 79/64541, May 24, 1979.

[660]R. B. Duggins, "Fire Retardant Polylactam Polymers," U.S. Pat. No. 3 733 283, 1973.

[661]S. Miyota, "Synthetic Resin Composition Having Reduced Corrosion and Coloration Causing Tendency," Eur. Pat. Appl. 189 899 AZ, 1986.

[662]I. Sobolev and E. A. Woyshissin, "ATH and Other Endothermic Flame Retardants," *172nd ACS Mtg., Div. Org. Coatings and Plastics Chem.*, **36** [2] 497 (1976).

[663]I. Souma, H. Wakano, and H. Takahashi, "The Filler Effect of Dawsonite and Hydrotalcite on PVC," *Nippon Gomu Kyohaishi* **49** [1] 35 (1976).

[664]T. Murata, "Smoke Reduction in ABS Blends," Jpn. Pat. No. 78/00251, 1978.

[665]R. H. Greenhalgh and P. R. Snowdon, "Polymer Compositions and Electric Cables Made from Them," Br. Pat. No 1 420 977, January 14, 1976.

[666]S. Horie, T. Hasegawa and H. Suzuki, "Flame Resistant Polyester Composites," Jpn. Pat. No. 74/34935, March 30, 1974.

[667]T. C. Mathis, G. W. Mappes, and C. M. Calvert, SPE Tech Papers 23, 190, 1977.

[668]K. C. Hecker, R. E. Fruzzetti, and E. A. Sinclair, *Rubber Div. Chem. Technol.*, **45** [1692] (1972).

[669]M. Mosesnan and J. D. Ingham, 113th Rubber Div. American Chemical Soc., Montreal, May 1978.

[670]S. Metna, "Dawsonite as a Reinforcement for Thermoplastics," M.S. Thesis, University of Lowell, January 1977.

[671]E. A. Woycheskin, R. J. Rigge, and I. Sobolev, "Flame Retardant Polymeric Compositions," U.S. Pat. No. 3 878 166, April 15, 1975.

[672]M. Fukuda, H. Okai, K. Nakagawa, and I. Kishi, "Fireproofed Resin Compositions," Jpn. Pat. No. 74/111994, November 24, 1974.

[673]W. T. Ruchle, "Anionic Clay Minerals," *Chem. Tech.*, **5**[1] (1986).

[674]L. L. Musselman and H. Greene, U.S. Pat. Appl. No 287070, 1988.

[675]H. F. W. Taylor, *Miner. Mag.*, **39**, 377–89 (1973).

[676]R. Allmann and H. P. Jepson, Neves Jahib. Mineral Monatah, 544–51, 1969.

[677]R. Allmann, *Acta. Crystallogr., Sect. B*, **24**, 972–77 (1968).

[678]W. T. Reichle, "Catalyst for Aldol Condensations," U.S. Pat. No. 4 458 026, July 3, 1984.

[679]S. Myota, *Clays Clay Miner.*, **28**, 50–56 (1980).

[680]D. L. Bish, *Bull. Mineral.*, **103**, 170–75 (1980).

[681]T. C. Mathes and R. W. Morgan, "Smoke Retardant Halogen-Containing Polymer Systems," U.S. Pat. No. 3 869 420 March 4, 1975.

[682]C. W. Huggins and T. E.Green, "Thermal Decomposition of Dawsonite," *Am. Mineral.*, **58**, 548–50 (1973).

[683]L. L. Musselman, T. L. Levendusky, and L. Weiserman "Surface Modified Alumina," Soc. of the Plastics Industry 40th Annual Tech. Conf., Jan. 28, 1985.

[684]L. L. Musselman and T. L. Levendusky, "Combination of Surface Modifiers for Powdered Inorganic Additives," U.S. Pat. No. 4 711 673, December 1987.

[685]L. L. Musselman and L. Weiserman, "Surface Treatment for Reduced Halide Adsorption," U.S. Pat. Appl. 126 244.

[686]Union Carbide, "Ucarsil FR Organosilicone Chemical for Flame Retardant Polyolefin Application," Bulletin SC-415B, Union Carbide Corp., Danbury, CT, 1987.

[687]Union Carbide, "Silane Coupling Agents in Mineral Reinforced Elastomers," Union Carbide Corp., Danbury, CT, April 1979.

[688]S. J. Monte and G. S. Sugerman, Bulletin No. KR–10846. Kenrich Petrochemicals Inc., Bayonne, NJ, February 1985.

[689]A. C. Kingston, "Faced Masonry Units and Facing Composition Therefore," U.S. Pat. No. 4 499 142, February 12, 1985.

[690]V. Abolins, J. E. Betts, and F. F. Holub, "Flame Resistant Blends of Polyoxyphenylenes," U.S. Pat. No. 4 497 925, February 5, 1985.

[691]Hitachi Ltd., "Potting Composition for Flyback Transformers," Jpn. Pat. No. 84/160910, September 11, 1984.

[692]Hitachi Ltd., "Potting Composition for Flyback Transformers," Jpn. Pat. No. 84/143313, August 16, 1984.

[693]T. S. Smith and R. J. Murphy, "Fire Proofing Cable Jacketing," Eng. Pat. Appl. 2 128 394A1, April 26, 1984.

[694]Toya Soda Mfg. Co., "Aluminum Hydroxide Fillers for Polyolefins," Jpn. Pat. No. 84/20336, February 2, 1984.

[695]Toyo Pulp Co. Ltd., "Paper Useful as Electrical Insulation," Jpn. Pat. No. 84/71490, April 23, 1984.

[696]Eaton Corp., "Plenum Cable Jackets Fire Resistant Elastomer Compositions," Jpn. Pat. No. 83/217531, December 17, 1983.

[697]N. L. Tutreva, "Building and Facing Materials Prepared with Modified Minerals for Fire Resistant Composition," *Zh. Priki, Khim. (Leningrad)*, **56** [10] 2324–28 (1983).

[698]T. Kobayashi et al., "Nonflammable Dynamoelectric Maching Having Coil Windings and Core Encapsulated with Unsaturated Polyester Resin Filler Composition," U.S. Pat. No. 4 387 311, June 7, 1983.

[699]A. Stoloff, "Small Particle Size Hydrated Alumina as an Impact Synergist for Impact Modified Vinyl Halide Polymers," Eur. Pat. Appl. EP80 837A2, June 8, 1983.

[700]P. Liptak and K. Chaternuchova, "Aluminum Hydroxide Treated with Tris (2-Metho-Polyethylene Ethoxy) Vinylsilane in Crosslinked Polyethylene with Ethylene-Vinyl Acetate Copolymer," *Elektroizolocna Kablova Tech.*, **36** [1] (1983).

[701]B. A. Ashby, "Silicone Flame Retardants for Nylon," U.S. Pat. No. 4 496 680, January 29, 1985.

[702]D. A. Harbourne and E. M. Lundhild, "Fire Retardant Sheet Material," U.S. Pat. No. 4 722 858, February 2, 1988.

[703]L. L. Musselman and H. L. Greene, "Materials for Use as Fire Retardant Additives," U.S. Pat. Appl. Serial No. 287070, December 21, 1988.

[704]M. E. Tarquini and C. R. Andrews, "A Novel Flame Retardant Additive for Thermosets Requiring High End-Use Temperatures," 42nd Annual Conf. SPI, February 1987.

[705]J. M. Huber, "Experimental Inorganic Flame Retardant" CAS No. 11097–59–9 Property Sheet, J. M. Huber Corp. 1988.

[706]M. E. Tarquini and C. R. Andrews, "Flame Retardant Thermosets Having Lower Smoke Generation," 43rd Annual Conf. SPI February 1988.

Activated Alumina Desiccants

R. Dale Woosley
Aluminum Company of America
Vidalia, LA 71373

The transition forms of aluminum oxide are highly porous, high-surface materials referred to as activated alumina. The large number of both acidic and basic sites produces an affinity for polar molecules of sufficient magnitude to make them valuable as economical desiccants. Current manufacturing technology is responsible for the abundance of products available to the field of dehydration with promises of further improvements in product quality and applications. Important new uses for traditional alumina desiccants include coadsorption with both unwanted contaminants and stream components of high value when isolated. At least four major world producers are active in the production of commercial alumina desiccants and they, along with other investigators, are at work to improve the application of their products through the development of reliable predictive computer models for adsorption.

Although activated aluminas are currently used in a wide variety of adsorbent applications, the original products were valued most as desiccants. The first commercial products were granular in form, contained significant amounts of inorganic impurities, and were of low sorptive capacity by current standards. Physical strengths were low, leading to high abrasion losses and frequent downstream problems in large dehydrators. As manufacturing techniques were improved to take advantage of more active, higher purity raw materials, spherical products of high physical strength and high adsorptive capacity were developed to meet the demands of expanding gas- and liquid-phase dehydration. This chapter reviews the past and current technology involved in the use of activated alumina desiccants for drying both gases and liquids. The improvement of dehydration processes in the future, led by recent successful attempts to develop and verify computer models for dehydration and other related processes, is also presented.

History of Activated Alumina as a Desiccant

Thermal treatment of clays and bauxites to produce porous materials in the early 1930s led to development of the first "high-purity" activated alumina. Using as a raw material the scale formed in thick layers on the walls of precipitator vessels in the Bayer refining process, investigators at Alcoa's research facility in East St. Louis, Illinois produced small quantities of a porous product which exhibited higher sorptivity than clays and bauxites, but which initially was more of a laboratory curiosity than a commercial product. In a few short years, this granular activated alumina was developed into an excellent desiccant, competing with silica gel in the removal of water from many gases and a few selected liquids.

One of the earlier comprehensive papers which heralded the new solid adsorbent appeared in 1938.[1] In this paper, Derr answered many of the questions concerning the ability of F-1 Activated Alumina® to adsorb water to a low level, citing tests in which effluent dew points of compressed air were as low as −70°C (−94°F). With cyclic water loadings in the range of 12 to 14 wt%, this new product promised to provide an economical means of drying gases. Regeneration was said to be accomplished easily by flowing hot air through the bed in the reverse direction to that of the air being dried, a design principle which remains in effect today. Derr also measured the rise in desiccant bed temperature because of the "heat of adsorption" and documented the changes in heat-front profiles during the regeneration process as water was desorbed. Perhaps the most informative section of this paper was the description of new dehydration systems for applications other than the air/water binary system. Specifically mentioned were water removal from hydrogen, ammonia, natural gas, and carbon dioxide with warnings against drying carbon dioxide at pressures near the critical pressure where condensation of carbon dioxide in the pores of the desiccant would reduce adsorption of water.

The ability of activated alumina to provide very dry air over many years of service is illustrated well in the use of F-1 in large wind tunnel dryers at NASA's Lewis Research Center in Cleveland, Ohio. The initial charge of 1.04 MM • kg (2.3 MM • lb) of the ¼ inch by 8 mesh product was made in 1952; it is still in use in 1987, providing dry air for space-age testing.[2]

During the 1940s, granular F-1 was the only commercial activated alumina desiccant available. As evidenced by the large number of gases and liquids commercially dried by F-1, it was a highly successful desiccant. However, F-1 was unable to compete to a significant degree in the rapidly expanding field of natural gas processing because of its high pressure-drop potential and its much lower sorptive capacity than rounded silica gel, such as Sorbeads R. In 1952, Alcoa began commercial production of a new spherical activated alumina with high sorptive capacity at high relative saturations of water.[3] This product, known as

H-151 Alumina Gel®, had a bulk density of about 835 kg/m^3 (52 lb/ft^3), giving it a net sorptive capacity for a given bed volume as high as silica gel of lower density. H-151 was capable of yielding effluent dew points below −60°C (−80°F), even as low as −100°C (−150°F),[4] making it suitable for essentially all gas dehydration applications then in operation, particularly for high-pressure natural gas drying where F-1 was less than ideal.

The base material for H-151 was prepared by rapid neutralization of sodium aluminate liquor with sodium bicarbonate, followed by washing, drying, and thermal activation of the colloidal precipitated gel into an active powder. After the ball-forming process, a second activation was carried out. This unique production process resulted in an alumina of unsurpassed hydrothermal stability. H-151 was used extensively as a catalyst support in addition to its primary role as a solid adsorbent.[5] This product was destined to remain a premium adsorbent and catalyst support until 1985 when it was withdrawn from the market because of intolerably high production costs in aging facilities.

As will be explained later in this chapter, the activation of alumina base materials to produce high-surface area, highly sorptive products is a thermal process carried out on small particles of aluminum trihydroxide. In a process which replaced the traditional lengthy thermal activation process with one lasting only a few seconds, Pechiney-St. Gobain of France in the early 1960s found that essentially all of the inactive boehmite transition alumina form could be made active while generating the pore sizes and surface sites conducive to high sorptivity for polar molecules and to high dew point depression.[6] Known as Type A® activated aluminas, the Pechiney products were revolutionary and offered excellent, unprecedented desiccant performance at economical prices. Pechiney-St. Gobain eventually became Rhone-Poulenc, the name by which it is known today,[7] and the company offers alumina catalyst supports and special adsorbents to industry in addition to Type A desiccants.

In the late 1960s, production of similar activated aluminas was begun in the United States by Kaiser Aluminum and Chemical Corporation. The initial product was called A-101®; later products for dehydration are A-1, A-2, A-201, and A-204.[8] From the technology used in A-101 manufacture, Kaiser expanded their high-surface-area, high-porosity aluminas into Claus-process sulfur-recovery catalysts, a field in which Kaiser products remain a dominant force. Essentially all current alumina desiccants are referred to as "crystalline" activated aluminas, in recognition of the nature of the gibbsite base material, just as the earlier name H-151 Alumina Gel reflected its origin.

In more recent years, other new activated alumina desiccants have been introduced for gas and liquid dehydration, with more complete technical information from suppliers. Discovery Chemical Company[9] began producing DD420, DD430, and DD440, a series of high-purity balled desiccants of high bulk density, unique in today's marketplace. Discovery markets these high-capacity products as having strength suitable for pneumatic handling into applications where dust cannot be tolerated or where it is advantageous to increase the net sorptive capacity of a bed via the higher density of their desiccants. Alcoa produces two new adsorbents[10,11] at a new facility; these products, known as F-200 and H-152, are also classified as high-strength, high-capacity desiccants which can withstand the rigors of pneumatic handling.

Alcoa still makes granular F-1 activated alumina for dehydration, although the current prominent uses for F-1 are for selective adsorption and water treatment. Rubel and Woosley[12] reported removal capacities exceeding 2500 g fluoride/m^3 media from potable water at the Gila Bend, Arizona, municipal plant. A later study for the U.S. Environmental Protection Agency by Rubel and Williams[13] determined criteria for simultaneous removal of fluorides and arsenic from potable water.

As shown in Table I, activated aluminas are offered in a variety of closed mesh sizes to better meet adsorption and pressure-drop requirements.

Other new high-alumina adsorbents are produced by Engelhard Corporation.[14] These granular products are specially made for contending with difficult process problems such as corrosion. Driocel® comes in three mesh sizes with bulk densities ranging from 880 to 930 kg/m^3 (55 to 58 lb/ft^3) and is the standard product of the series. The higher bulk density compensates to some degree for the lower water adsorptivity of the product line. Driocel S is a chemically treated product for dealing with the corrosive nature of sulfur compounds in a process stream. Driocel E is an extruded product pneumatically conveyable and used for many dehydration applications. Dynocel is a new Engelhard desiccant containing 89% Al_2O_3 with SiO_2, Fe_2O_3, and TiO_2 as major impurities, and with significantly higher sorptive capacities than the Driocel products.

Development of Activated Alumina Properties

The physical integrity of commercial activated alumina desiccants depends significantly on the properties of an intermediate activated powder which is the feed stock for the forming process used by the manufacturer. The base material for the active powder is known mineralogically as gibbsite and chemically as aluminum trihydroxide, $Al(OH)_3$. A thermal treatment, the temperature and length of which are a matter of the producer's technology, removes 28 to 31% of the 35% water of crystallization from the gibbsite, leaving a loss on ignition of 4 to 7 wt%. While this process is sometimes referred to as a partial dehydration, the more nearly correct term is "dehydroxylation" since it is the loss of hydroxyls that determines the

Table I. Physical Properties of Commercial Activated-Alumina Desiccants

Type	Producer	Application	Form	Sizes	PBD*	Strength
A-1	Kaiser	Gas/liquid	Spher.	¼ × 8 m	45	—
				5 × 8 m		20
A-2	Kaiser	Gas/liquid	Gran.	8 × 14 m	42	
				12 × 32 m		—
A-201	Kaiser	Gas/liquid	Spher.	½″ × ¼″	48	—
				¼″ × 8 m		—
				3 × 6 m		—
				5 × 8 m		35
				7 × 12 m		—
A-204	Kaiser	Gas/liquid	Spher. Promoted	½″ × ¼″	50	—
				3 × 6 m		—
				5 × 8 m		20
				8 × 14 m		—
A	Rhone-Poulenc	Gas/liquid	Spher.	2 × 5 mm	48	29
				5 × 10 mm		55
F-200	Alcoa	Gas/liquid	Spher.	⅛″	48	30
				3/16″		55
				¼″		70
H-152	Alcoa	Gas/liquid	Spher.	— Same as F-200 —		
DD420	Discovery Chemical	Gas/liquid	Spher.	¼″ × 5 m	52	40
				5 × 8 m		—
				8 × 14 m		—
DD430	Discovery	Gas/liquid	Spher.	¼″ × 5 m	56	45
				5 × 8 m		
				8 × 14 m		

nature of the surface sites involved in adsorption. This mechanism was described in detail by Wefers and Bell,[15] who showed, as in Fig. 1, well-defined relationships among treatment temperature, loss on ignition, specific surface area, and alumina density. Particle density may sometimes be a factor in desiccant performance via its relationship with total pore volume, but surface area is almost always a critical factor in any adsorption process.

The thermal treatment is carried out at 375° to 450°C for 2 to 3 hours if done in rotary kilns or tunnel

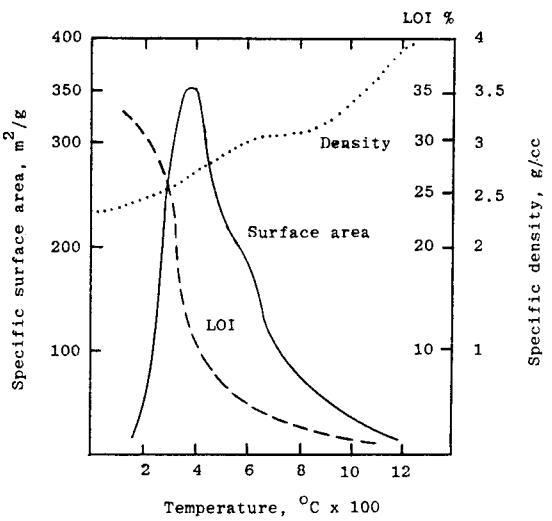

Fig. 1. Surface area, density, and loss on ignition vs temperature.

activators, or 3 to 10 seconds if done in hot gas cyclones. In the rapid dehydroxylation there is beneficially no opportunity for changes in macrocrystallinity but, in either procedure, the resulting active powder becomes highly porous and has a high surface area on which several species of ions can be found. For example, Al^{3+} and O^{2-} ions can be present in different packing arrangements and at least five forms of hydroxyls have been identified. A discussion of the nature of these hydroxyl sites can be found in two references by Peri[16,17] and a good discussion of the physical and chemical nature of the alumina surfaces can be found in a paper by Bowen et al.[18]

The proportion of different forms of hydroxyls and, indeed, the total number of hydroxyls, can be manipulated by the thermal treatment; higher treatment temperatures reduce the number of hydroxyls via the dehydroxylation mechanism already mentioned. Such manipulations alter the proportion of Lewis and Brönsted acid sites, the former increasing with increasing temperature of activation and the latter decreasing. The net result on basicity is a decrease with increasing temperature. Figure 2 shows a relationship of site modification via temperature control as it influences the acidity and basicity of the surfaces and the resultant affinity for water vapor.

The manipulation of hydroxyl sites in the preparation of the active powder is specifically aimed at creating a base material of proper activity for bonding particles together with water as the sole or primary binder medium. The forming operation causes some of

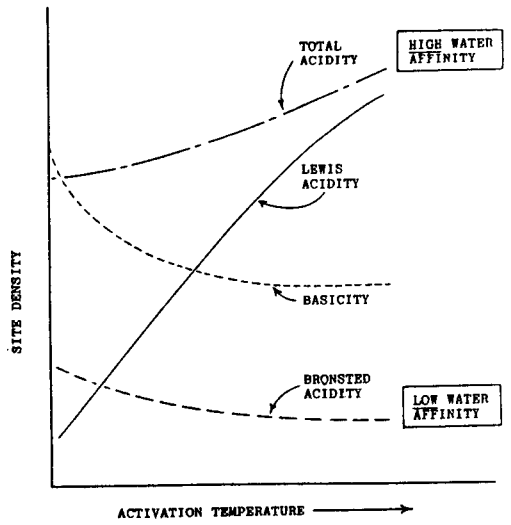

Fig. 2. Effect of activation temperature on site densities and affinity for water.

the active sites to become inactive or otherwise unavailable for adsorption in the formed product. Thus it is necessary to perform a second thermal treatment on the formed product to reactivate inactive sites. Since this is the final treatment, it establishes the alumina's performance as a desiccant, controlling the surface sites to enhance the selectivity for the adsorbate. The final activated product will usually be produced with a loss on ignition of between 4 and 8% and, within that range, the performance of a desiccant can be modified drastically. For a more detailed discussion of the generation, nature, and benefits of site modification, see the chapter on "Selective Adsorption Processes" in this book.

Laboratory procedures for determining the types and densities of the various active sites are lengthy and subject to many pitfalls. It has become customary to characterize the activated, or "transition" aluminas by use of X-ray diffraction (XRD) analysis even though the structures are defect structures which are frequently poorly organized and may appear to be amorphous to XRD analysis. The best-known transition form is the gamma form with its defect spinel structure. Another form, eta, is less frequently seen in commercial manufacture and finds its most significant uses in the field of catalysis where the preponderance of acid sites is a benefit to catalytic activity. Other forms, such as chi and rho, may appear in XRD readouts at times, but are generally considered to be of minor consequence in adsorption mechanisms.

The pore-size distribution of activated aluminas can be varied and controlled in commercial production to alter intraparticle diffusion, retention or rejection of adsorbates based on molecular size, and pore volume levels. Activated aluminas do not inherently possess the high degree of selectivity of molecular sieves, which can separate isomers, for example, but activated aluminas can be enhanced or retarded in affinity through modifications in pore-size distributions as well as by the proportions of acid and base sites. Present activated aluminas can be produced with mono-, di-, and trimodal pore-size distributions.

Table II shows some surface and adsorptive properties of commercial activated alumina desiccants. Although the specific surface area and sorptive capacity for desiccants may depend to some degree on the particle size, it is generally considered that actual attractive forces for polar adsorbates do not vary significantly with size. However, particle size influences significantly the dynamic performance of a desiccant. Note that surface areas of current products are well above 300 m^2/g, with total pore volumes typically in the range 0.3 to 0.7 cm^3/g. Loss on ignition values are based on the loss of weight between 250° and 1100°C. Weight losses below 250°C are generally considered to be "moisture" or readily desorbed water.

Table II. Surface and Adsorptive Properties of Activated-Alumina Desiccants

Types	Producer	Loss on Ignition	Surface Area m^2/g	Total Pore Vol., cm^3/g	Equilibrium Cpacity at 10% rh	60% rh	90% rh	Range 60% rh
A-1	Kaiser	6.0	240–325			17		16–21
A-2	Kaiser	6.0	280–350			18		17–21
A-201	Kaiser	6.0	280–360	0.46		20		19–22
A-204	Kaiser	6.0	200–300			18		15–20
A(2-5)	Rhone-Poulenc	3–5	345	0.40	8	22	35	
A(5-10)	Rhone-Poulenc	3–5	315	0.40	7	20	35	
F-200	Alcoa	6.5	325–355	0.50	7	19	40	17–21
H-152	Alcoa	4.0		0.50	12	22	40	20–23
DD420	Discovery Chemical	6.0	325	0.45		20		
DD430	Discovery Chemical	6.0		0.40		22		

Adsorptive Characteristics

The solid adsorbents most widely used as desiccants are activated alumina, molecular sieves (zeolites), and silica gel, each of which can remove water from a wide variety of streams with high efficiency. All conform well to the general requirements of desiccants, that is, a desiccant should not undesirably alter the stream which it is drying, and it should in turn strongly resist being harmed by a chemical or physical property of the stream.

The adsorption process depends initially on attractive forces to get adsorbate molecules to the active sites. The more polar the adsorbate molecule, the higher this attraction. The first layer of adsorbate molecules is held with high energy, typically in the range of chemisorption, 30 to 50 kcal/mol.[19] Beyond the first layer, the energy of adsorption decreases drastically until, within 4 to 6 layers, it is essentially the heat of condensation. This energy release is the "heat of adsorption" or "heat of wetting" and depends on the nature of the adsorbate as well as the nature of the desiccant. For water adsorbed on activated alumina the integral, or total heat of wetting, is approximately 830 cal/g of H_2O (1500 BTU/lb of H_2O).[19]

Water adsorbed on the solid surfaces has a vapor pressure which relates to the water vapor pressure in the environment around the surface. When equilibrium is approached and the amount of water in the adsorbed phase remains essentially constant, there still is an on-going process of desorption and adsorption, sometimes involving diffusion mechanisms which are quite complicated. For activated alumina, the amount of water in the adsorbed phase increases continually with increasing concentration of water vapor in the environment.

The simplest plot of the relationship between the adsorbed and mobile water molecules is the adsorption isotherm. To overcome the problem of having a separate data plot for every temperature of interest, it is common practice to use percent relative saturation (of water vapor) as the abscissa. Figure 3 shows the typical adsorption isotherms for silica gel, molecular sieves, and activated alumina.

The adsorption of water molecules at low relative saturation (low water vapor pressure) takes place as a monolayer and is represented by the low end of the curves. For activated alumina having a surface area of 330 m^2/g, the weight of water corresponding to a monolayer is 16.5% of the alumina weight. The upper end of the isotherms represents the phenomenon of capillary condensation, or pore filling, and it can be seen that the pore-filling mechanism accounts for much of the ability of activated alumina and silica gel to adsorb large amounts of water in streams of high water saturation.

In 1938, Brunauer et al.[20] published a classic paper on multimolecular layer adsorption from gases,

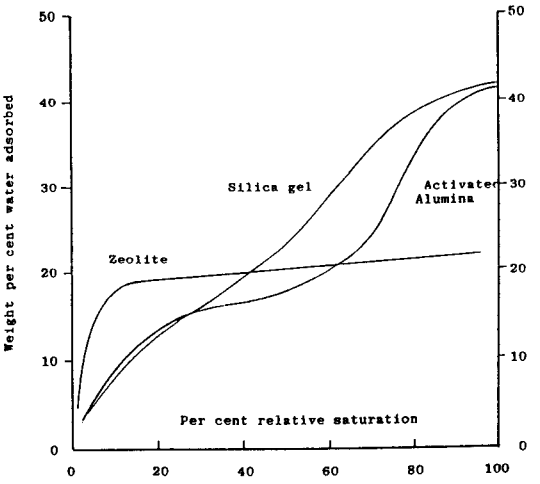

Fig. 3. Equilibrium adsorption isotherms.

building on the work of Langmuir, who had published in 1915[21] his definitive analysis of monolayer adsorption. Langmuir's work was so original that the accepted name for the relationship by which surface loadings can be predicted is known as the "Langmuir equation." In the 1938 paper, Brunauer et al. proposed five isotherm shapes as being descriptive of various multilayer adsorption mechanisms. In Fig. 3, the Type I isotherm is represented by the plot for molecular sieves which, by nature of the zeolite structure, is incapable of a significant amount of pore filling. The Type IV isotherm is represented by activated alumina and silica gel. Brunauer et al. also applied the Kelvin equation to estimation of pore-filling quantities.

Adsorption isotherms are usually determined for equilibrium conditions in the laboratory by exposing small, regenerated desiccant samples to constant-humidity chambers for 24 to 48 hours. They are not easily adapted to predicting dynamic performance of desiccants, but they can be used to make comparisons as to the expected behavior of different adsorbents as water vapor pressure is varied. Another method of presenting desiccant properties is the isostere, not shown in this chapter, which relates the temperature and water vapor pressure of regeneration to the expected equilibrium dew point during the next drying cycle.

Any reduction in vapor pressure of the water surrounding the "saturated" desiccant begins the process of desorption, the second half of the performance of a desiccant that makes it a cyclical, economical means of dehydration of a stream. Because of the high affinity between the desiccant and the water vapor, desorption requires a driving force. It may be a thermal driving force, as in dryers that have a heating circuit, or it may be attained through a drastic reduction in system pressure, as is done in pressure-swing dryers where little or no additional thermal energy is put into the system to accomplish desorption. Activated alumina typically demonstrates a hysteresis effect

on desorption,[7] as shown in Fig. 4. It is possible to modify the severity of hysteresis which in part determines the ease of desorption for a given application.

Industrial Dehydration Systems

The need for dry gases and liquids ranges from such practical situations as the prevention of freezing of distribution lines during cold weather to more exotic applications such as the elimination of interference with polymerization of organic monomers due to trace amounts of water. All solid desiccants provide economical, cyclic dehydration of a wide variety of gases and liquids but, in specific instances, there are circumstances which dictate the choice of one type of solid desiccant over another. There also are applications, however, which do not have a regeneration step because of the coadsorption with water of a compound which cannot be removed from the desiccant. These "one-shot" uses provide a valuable service in specific difficult applications despite the loss of economy because of nonregeneration.

Table III lists a wide variety of gases and liquids which have been successfully dried with activated alumina. In many applications involving these and similar streams, activated alumina may also be removing one or more adsorbates which act as contaminants or recovering a valuable component item such as a heavy paraffin hydrocarbon useful for plastics feedstock.

The two general classifications of regenerative dryers are pressure swing (gases only) and thermal regeneration (gases and liquids). The latter type can be designed for any one of several methods of regeneration and for adsorption cycles from an hour to several days, while pressure-swing dryers use cycle times of about 4 to 12 minutes and regenerate only with a dry purge flow at near-atmospheric pressure. Activated alumina desiccants work efficiently and economically in both types.

In dehydration practice, the ability to reduce the water in the stream to a constant level is of paramount

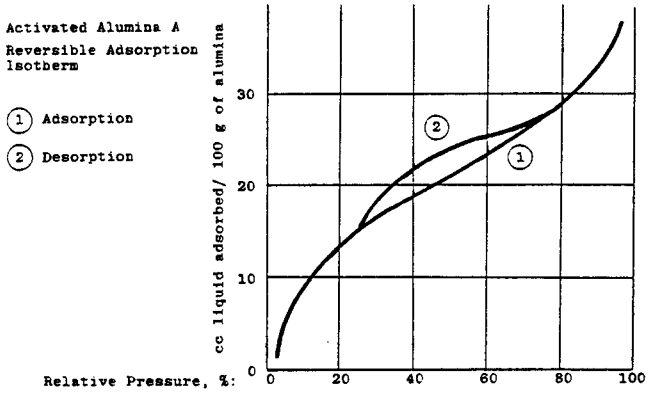

Fig. 4. Hysteresis effect of water adsorbed on activated alumina. (Ref. 7, used by permission.)

Table III. Substances Successfully Dried by Activated-Alumina Desiccants

Gases	
Acetylene	Hydrogen chloride
Air	Hydrogen sulfide
Ammonia	Methane
Argon	Natural Gas
Carbon dioxide	Nitrogen
Chlorine	Oxygen
Ethane	Propane
Ethylene	Propylene
Furnace gas	Refrigerants
Helium	Sulfur dioxide
Hydrogen	
Liquids	
Benzene	Lubricating oils
Butane	Naphtha
Butene	Nitrobenzene
Butyl acetate	Pentane
Carbon tetrachloride	Pipe-line products
Chlorobenzene	Propane
Cyclohexane	Propylene
Ethyl acetate	Refrigerants
Gasolines	Styrene
Heptane	Toluene
Hexane	Transformer oils
Hydraulic oils	Vegetable oils
Jet fuel	Xylene
Kerosene	

importance. Once a dryer is in operation, there usually are few practical remedies if the desired dew point is exceeded.

In thermally regenerated dryers, there is an additional concern, not of great significance in pressure-swing dryers, for the amount of water retained in a cycle by the desiccant. Typically, there are two desiccant beds (towers) in a dryer, one of which is adsorbing water from the stream as it passes through the desiccant and the other is regenerating, by whatever means is selected for the system. At the end of a preset adsorbing time, or, alternatively, when water has "broken through," switching is done to reverse the roles of the beds and operation continues in this manner until some circumstance of system or desiccant performance forces replacement of the desiccant. Depending on many circumstances, this service time may vary from a few months to several years.

Figures 5(*a*) through 5(*e*) show flow diagrams for common dryer designs. The two-tower schematics in Figs. 5(*a*) and 5(*b*) illustrate a basic choice between "wet" gas and "dry" gas for regeneration. In Fig. 5(*a*), the use of wet inlet gas for regeneration saves the cost associated with having dried the gas which might be vented off after its passage through the spent desiccant, but the effluent dew point from the system will be higher than that of Fig. 5(*b*) because the desiccant will be in equilibrium with a higher water vapor pressure and this is carried over into the next drying step. Both 5(*a*) and 5(*b*) follow a generally

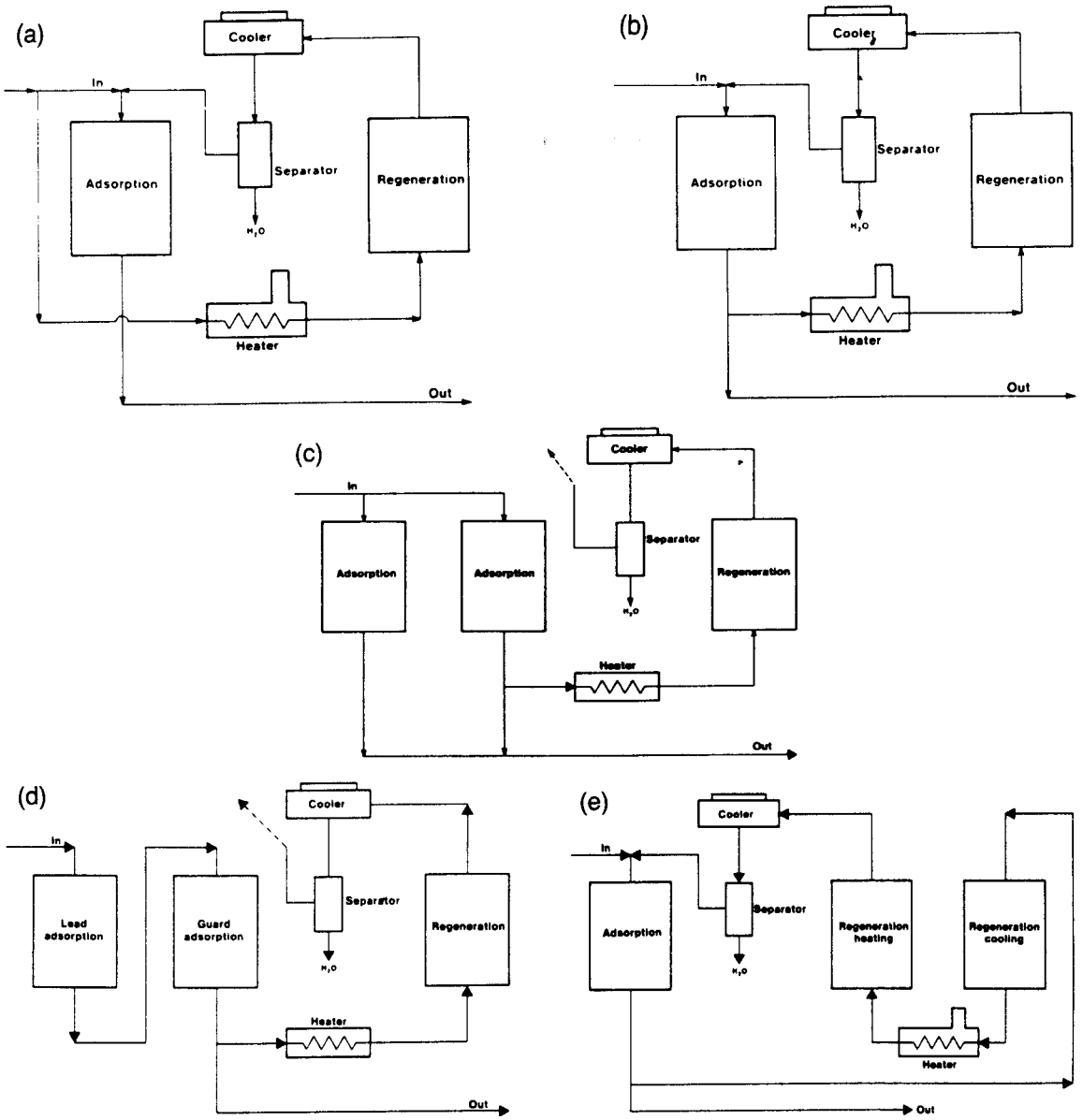

Fig. 5. (*a*) Two-tower dehydration wet gas regeneration; (*b*) two-tower dehydration dry gas regeneration; (*c*) three-tower dehydration split flow; (*d*) three-tower dehydration lead-guard; (*e*) three-tower dehydration series regeneration for heat recovery.

accepted rule of thumb for the use of activated alumina in that heating is countercurrent to the drying flow direction. If the heating flow were to be cocurrent with drying, the entire load of sorbed water would be pushed through each desiccant cycle at high temperature and the desiccant life would be shortened by premature rehydration of the active sites, a recognized cause of deactivation of alumina which is well compensated for in countercurrent designs.

An additional choice is the direction of cooling gas flow if "wet" gas is used for cooling. Countercurrent flow with wet gas has the same end result as with the heating gas flow in that the exit end of the bed for drying tends to equilibrate with the vapor pressure of water in the gas and thus has a dramatic effect on the next drying step dew point. If the direction with wet cooling gas is cocurrent with drying, the worst that can happen is a small amount of water preloading ahead of the next drying step.

Figures 5(*c*), 5(*d*), and 5(*e*) illustrate some of the flexibility that can be built into a three-tower system. In Fig. 5(*c*), a gas flow too great for one drying tower is split between two towers. In large natural gas plants, as many as ten towers can be found in one system. Figure 5(*d*) is a three-tower system with two unique advantages. For any type of gas flow, the "lead-guard" arrangement allows a higher cyclic water loading by running the lead tower until saturation, with the

guard tower protecting the dew point. For gas streams which may present problems—as, for example, olefins which adsorb on alumina—running the lead tower until water saturation displaces most of the unwanted carrier gas from the alumina. Finally, the capture of waste heat from a cooling bed, followed by booster heating for regeneration, is shown in Fig. 5(*e*).

There are numerous variations on these flow schemes. It is the task of the system design engineer to match the best performance characteristics of the desiccant to the particular stream, its conditions, and the user's needs.

Effluent moisture content, expressed as either parts per million water or as the dew point (related to pressure or to one atmosphere), depends on the surface properties of the desiccant, the stream composition, the temperature and humidity of regeneration, and to certain design parameters such as contact time. The typical air dryer used for instrument controls and general plant cooling requires that effluent moisture be at least as low as a dew point of −40°C at pressure. All solid desiccants can achieve this level easily in a properly designed, constructed, and operated system. In more stringent applications, such as the drying of gas-phase hydrocarbons which will undergo cryogenic separation, the effluent dew point requirement may be in the range of −70° to −100°C (−100° to −150°F), and extraordinary care must be taken in designing, constructing, and operating a system for that purpose. In between are applications in which dew points of −40° to −70°C (−40° to −100°F) are wanted.

The designer of a dehydration system must take into account the adsorption and desorption characteristics of a desiccant in all cases, relate them to the flow sheet and hardware to be used and choose those parameters which ensure that the effluent moisture will be within specifications. Especially important in this procedure is how regeneration temperature and humidity affect the equilibrium conditions established at the end of the desiccant bed which will be the exit end during drying.

Special Dehydration Factors

Activated alumina is particularly useful in drying nonpolar liquids, such as propane and butane. The broad pore-size distribution of activated alumina promotes intraparticle diffusion of water molecules to interior pores. For streams in which "heavy" hydrocarbons (C_8 and up) are present, water loadings may be reduced slightly but, typically, activated alumina can be loaded to 6 to 10 wt% water in liquid hydrocarbon drying. The effect of the heavy hydrocarbons is to resist desorption as vapor and carbonize in the pore structure, blocking active sites.

In drying olefinic streams, activated alumina acts as a catalyst for breaking the double or triple bonds between carbon atoms, allowing the formation of dimers, trimers, and tetramers which resist thermal desorption and which may reform into waxy matter. Although the degree of bond breakage is very small, it is a cumulative process which shortens the service life of the desiccant, unless the degree of premature decline is anticipated in the design and water loadings are down-graded for long-term usage. This effect is severe if an olefinic gas is in contact with the activated alumina during the heating part of regeneration. If such is the case, polymerization can be retarded, but not eliminated, by using the lowest regeneration temperature consistent with attaining the desired dew point. A helpful procedure is to purge the olefins from the desiccant with a cool, nonolefinic gas prior to heating with the same gas.

Activated alumina is used successfully to dry "sour gases," such as H_2S, CO_2, SO_2, and CS_2. Design practice should strive toward reducing the relative saturation (of water) in the stream by raising the temperature to reduce capillary condensation. In this maneuver, the solution of acid gas in liquid water is reduced or eliminated and thus corrosive attack on the desiccant surfaces is prevented. As a matter of experience, water loadings for acid gas streams are usually no higher than 6 wt%. Effluent water levels of 2 to 5 ppm(v) can be reached.

The drying of CO_2 by activated alumina has been a long-term application made even more important in the 1980s as the use of fermentation-produced CO_2 has grown. Activated alumina is tolerant of carryover contaminants in the gas, but in many installations follows a bed of activated carbon for scavenging. The ability of activated alumina to withstand high drying pressures of over 170 atm has been demonstrated well in a large CO_2 dryer at Sand Hills, MS.[21] After three years of service, the F-200 desiccant still achieves a dew point of below −60°C (−76°F).

Removal of small amounts of water from monomer streams such as vinyl chloride, styrene, and propylene takes advantage of the ability of activated alumina to yield low water levels without contaminating these materials, which are destined for polymerization into high-value flexible and rigid polymers.

Modeling of Dynamic Systems

In lieu of useful models for dynamic dehydration systems developed by mass and heat balance solutions, it has been the practice for a multitude of engineers to use what might be termed an "empirical guidelines" approach to describing what takes place in their systems. In this concept, the engineer ends up having to assign some key performance factors on the basis of similar experience and field reports of operating units. At best, the predictive ability from this approach is usually a conservative guess based on what is working and tends to retard the improvement of the combination of desiccant quality and the design of the flowsheet to get the very best performance for the most reasonable cost. There are numerous papers detailing methods of calculating loading capacities, pressure drop, regeneration heat duty, and similar

system parameters, all based more on field observation than on a rigorous modeling treatment. Few of these papers deal with intraparticle diffusion effects, heat of wetting effects, and other effects related to desiccant microproperties. As "how-to" papers, they serve a useful purpose, both in terms of making it attractive for other engineers to delve into system design and in terms of presenting dehydration practice in contexts more familiar to operating engineers.

No definitive papers have been found which model dynamic dehydration systems in which there are multiple adsorbates as might be found in mixed paraffinic and olefinic streams. For the water/air binary system, two papers[23,24] were found which developed a model around the rate constant, defined as

$$dw/dt = K(P - P_E) \quad (1)$$

where w = amount of water adsorbed, in kg of water per kg of desiccant; t = vapor time in hours; P = partial pressure of water vapor in the gas to be dried; P_E = partial pressure of the water vapor in the gas at equilibrium with the desiccant, for the amount of water adsorbed; K = adsorption rate coefficient in kg of water per kg of desiccant per h • atm.

In the first of the papers,[23] Papee et al. found that K is practically independent of (*a*) the amount of water already on the desiccant; (*b*) the gas velocity, provided the Reynolds number is over 50; (*c*) temperature and pressure; and (*d*) aging of the desiccant.

It was also concluded that K is dependent on the nature of the gas and is inversely proportional to desiccant particle size. Both mass balance and heat balance were considered in developing the model. Using breakthrough water loadings as the criteria in pilot tests carried out over a pressure range of 1 to 100 Pa, it was found that differences of less than 5% were observed between calculated and experimental capacities. A digital computer was used for much of the data processing.

The second paper,[24] by Ping in 1984, accepted as general assumptions the findings of the paper by Papee et al.[23] and included Type 4A molecular sieves run alone and in a split-bed configuration with A-201 activated alumina (2 : 1 alumina : sieves). Good agreement was found between observed and calculated breakthrough times and capacities. One of the significant findings of this work was that "field-aged" and laboratory-aged samples had significantly different rate coefficients when laboratory samples were aged by a single mechanism of rehydration, while field-aged samples included a fouling history as well as rehydration history. Field samples were found to have less constant rate coefficients.

Ping's paper[24] also attempted to predict lowest effluent water concentrations. Perfect agreement between predicted and observed values was not obtained, but at the extremely low levels to which the test columns produced effluent water, the discrepancies may not be significant.

A predictive model associated with one of the most innovative developments in desiccant usage was presented by Oliker.[25] His patented[26] "Four Front System (4FS)" proposed to reduce energy consumption by terminating the heat to a desiccant bed before the entire bed became hot and utilizing the heat stored in the bed to complete regeneration. Optimizing the timing of the heater shutdown to provide enough heat for regeneration while conserving energy was part of the patent technology. The requirements for a 4FS system included a desiccant bed sufficiently deep to allow a small amount of residual water in the inlet end of the bed, countercurrent heating, and dry gas regeneration. Oliker's patent followed or was coincidental with a rigorous development of an adsorption model using equilibrium front mechanics.[27] The 4FS system was installed and successfully operated in several different dehydrators in the United States.

These papers were chosen for this discussion from a small number of papers on the subject of dynamic modeling. The improvement in instrumentation and especially computer data treatment in recent years suggests that the field of dynamic modeling of dehydration systems, once considered too formidable to penetrate, will see new models verified by new tests. From this progress will come improvements in current desiccants and new desiccant types not yet produced.

The Future of Alumina Desiccants

Current R&D work in the area of activated-alumina desiccants involves improvements in and modifications to existing commercial products as well as the development of new desiccants. Target improvements include increasing the hydrothermal stability of alumina to resist rehydration effects which speed up the aging process, increasing selectivity by site modifications, and retaining current sorptive capacity levels while removing trace contaminants from gas and liquid streams.

New alumina desiccants will probably include a superstable product capable of high dew point depression in the heat-of-compression dryers, which are a present challenge to activated alumina because of high humidities and low temperatures of regeneration. Development of alumina composite products to take advantage of the best properties of distinctly different adsorbent components is virtually a reality today, and promises to be a way of the future.

Note Added in Press: In mid-1988, Kaiser Chemicals was sold to LaRoche Chemicals, who will continue the production and sale of products referenced in this chapter.

References

[1]R. B. Derr, "Drying Air and Commercial Gases with Activated Alumina"; p. 384 in *Industrial and Engineering Chemistry*, Vol. 30. 1938.

[2]Private communications; NASA Lewis Research Center, Cleveland, Ohio, 1986, 1987.

[3]R. J. Getty, C. E. Lamb, and W. C. Montgomery, "A New Desiccant for Drying Natural Gas," *Petroleum Eng.*, 8, (1953).

[4]W. Swerdloff, "Dehydration of Natural Gas"; Paper No. A-2, *Proceedings of the Gas Conditioning Conference*, The University of Oklahoma, April 1969.

[5]Aluminum Company of America, Pittsburgh, PA., "*Activated and Catalytic Aluminas*," Bulletin GB2A, July 1969.

[6]Pechiney-St. Gobain, Paris, France, Technical Brochure on Activated Aluminas, no other title, 1967.

[7]Rhone-Poulenc Specialties Chimiques, Technical Brochure, 1982.

[8]Kaiser Aluminum and Chemicals Corporation, Baton Rouge, LA. Bulletin IC-117R, May 1978.

[9]Discovery Chemical Company, Baton Rouge, LA. Product Data Sheets, 1986–1987.

[10]Aluminum Company of America, Product Data Sheet CHE-946 for F-200, April 1986.

[11]Aluminum Company of America, Product Data Sheet CHE-044 for H-152, April 1985.

[12]F. Rubel, Jr. and R. D. Woosley, "The Removal of Excess Fluoride from Drinking Water by Activated Alumina," *J. Am. Water Works Assoc.* 1, 45–49 (1979).

[13]F. Rubel, Jr. and F. S. Williams, "*Pilot Study of Fluoride and Arsenic Removal from Potable Water*," EPA-600/2-80-100 (August 1980).

[14]Engelhard Corporation, Seven Hills, Ohio, Specialty Chemicals Division Bulletin T1-775 et al., 1987.

[15]K. Wefers and G. M. Bell, "*Oxides and Hydroxides of Aluminum*," Technical Paper 19, Alcoa Research Laboratories, 1972.

[16]J. B. Peri, "Infrared and Gravimetric Study of the Surface Hydration of Gamma Alumina," *J. Phys. Chem.*, **69** [1] 211 (1965).

[17]J. B. Peri, "A Model for the Surface of Gamma Alumina," *J. Phys. Chem.*, **69** [1] 220–30 (1965).

[18]J. H. Bowen, R. Bowrey, and A. S. Malin, "A Study of the Surface Area and Structure of Activated Alumina by Direct Observation," *J. Catal.*, 7, 209–16 (1967).

[19]V. M. Stowe, "*Activated Alumina: Heat of Wetting by Water*," *J. Phys. Chem.* **56**, 484 (1952).

[20]S. Brunauer, L. S. Deming, W. E. Deming, and E. Teller, "On a Theory of the van der Waals Adsorption of Gases," *J. Am. Chem. Soc.*, **62**, 1723–32 (1940).

[21]I. Langmuir, "Chemical Reactions at Low Pressures," *J. Am. Chem. Soc.*, **37**, 1139–67 (1915).

[22]Personal communications with Adsorption Engineering, Inc., Houston, Texas, 1984–1987.

[23]D. Papee, C. Meniere, A. Bellier, and F. Jouanneault, "*Optimize Alumina Gas Drying System*," *Hydrocarbon Processing*, **46** [10] 142–46 (1967).

[24]W. Ping, "*Use of Computer Model Optimization of Gas Drying Tower Design*," Petroenergy '84, Conference, Houston, Texas, September 1984.

[25]M. D. Oliker, "*The Four Front System - A Revolution in Adsorption Bed Operation and Design*," Petroenergy '85, Houston, Texas, September 1985.

[26]U.S. Pat. No. 4 324 564, "*Adsorption Beds and Methods of Operation Thereof*," April 13, 1982.

[27]Personal communications, M. D. Oliker, Near Equilibrium Research Association, Amesbury, MA, 1982–1986.

Selective Adsorption Processes

H. L. Fleming and K. P. Goodboy
Aluminum Company of America
Pittsburgh, PA 15219

The use of aluminum oxides and hydroxides as adsorbents in chemical separations is surveyed. Properties necessary in commercial adsorption processes are discussed in the context of the chemical and physical characteristics of these materials. A chronology is presented of their early manufacture and use, through today, with comments regarding trends for the future.

Aluminas have been in use for many years as adsorbents. Introduced commercially in 1932 by Alcoa for water adsorption,[1] since that time, activated aluminas have traditionally been known as desiccants for the chemical process industries. As early as 1901, references can be found for the use of synthetic aluminas in the chromatographic purification of biological compounds.[2] In recent years aluminas have found widespread usage in applications as diverse as municipal wastes, polymers, and pharmaceuticals. Novel design of these materials is extending their separations capability into even more nontraditional areas of adsorption technology.

This chapter surveys current applications of aluminas as adsorbents. Advances in materials design and adsorption process technologies are also discussed, relating recent trends in applications of adsorbent aluminas to developing specialty process requirements. The ability of these materials to selectively remove desired compounds from the remainder of the process stream has greatly accelerated their use in recent years.

History of Adsorption with Aluminas

To place current events in their proper perspective, it is advantageous to briefly examine the chronological development of the use of aluminas in adsorption technology. The earliest known use of adsorbent alumina was in the chromatographic separation of liver extracts by Folkers and Shovel in 1901.[2] Beginning in the 1930s, when laboratory-scale chromatography became a common analytical technique, aluminas were the packing material of choice. [3,4] Chromatography using aluminas continued to develop through the late 1950s until celluloses and dextran materials were synthesized and were perceived as having greater versatility in separations.[5,6] Continued research in alumina-based media was virtually halted and this group of materials has been largely ignored since that time. There were many successful analytical separations with aluminas, however, which can be found in surveys on small-scale chromatography.[6]

As shown by Table I, the only large-scale application of adsorbent aluminas prior to 1940 was as desiccants. Both air and natural gas dehydration were being routinely performed with waste-heat regeneration of the alumina columns. In later years, dehydration with aluminas was extended to cracked gas and heavier hydrocarbon streams, as well as those containing carbon dioxide and ammonia. Liquid dehydration of aromatic and paraffinic hydrocarbons, halogenated hydrocarbons, and gasoline—among others—became common in the 1960s. Even today, drying applications are being extended to include cold bed adsorption, more complex liquid dehydration, and pressure swing operation.[7]

Use of aluminas was extended in the 1950s and 1960s to isotopic separation of a number of the actinide series compounds, as well as some specialty organics. In the 1960s, additional uses were the impurity separation of halogenated compounds from aqueous streams and organic acids from hydrocarbons. Degenerative carboxylic acids from lubricating oils is an example of such a separation.

In recent years the variety and complexity of applications have become extensive. On a volume basis, desiccant usage now accounts for less than one-half of the total adsorbent alumina consumption each year in this country (Fig. 1). Section III of Table I is a representative listing of current large-scale generic applications. With the advent of more stringent conservation requirements in the early 1970s, removal of phosphate, mercaptan, and fluoride compounds in ground and drinking waters became successful applications of alumina adsorbents.[8,9] The passage of the Clean Air and Clean Water acts in the late 60s and early 70s led to several large-scale alumina adsorption processes in aqueous streams.

Environmental concerns also established new applications for aluminas in gas treatment. Although not of the magnitude of air purification with activated carbon, adsorption of acid gases and sulfur species in petroleum-related industries constituted a significant portion of adsorbent alumina utilization in the 1970s. These areas have received even greater attention in the 1980s and are included in Table I. Unfortunately, it is a fact of almost every industry using aluminas that the

Table I. Commercial Alumina Adsorption Applications

		Molecular Weight	Gas Phase		Liquid Phase	
			Impurity	Product	Impurity	Product
I.	Pre 1940	Low	Water			
		High				
II.	1960s	Low	Water		Water	
			Isotopes	Isotopes	Halogens	
					Color bodies	
		High			Organometallics	
III.	1980s		Water		Water	
			Isotopes		Halocarbons	
		Low	SO_2	Flavors	Halogens	
			H_2S	Fragrances	Phosphates	
			Acid gases	Xylenes	Inorganic acids	
			Amines	Aromatics	Ketones	
					Carboxylic acids	
					Mercaptans	
					Alcohols	
					Sulfides	
					Metals	Metals
					Color bodies	
		High			Organometallics	
					Pharmaceutical	Pharmaceutical
					>C5 paraffins	Sugars
						Vitamins

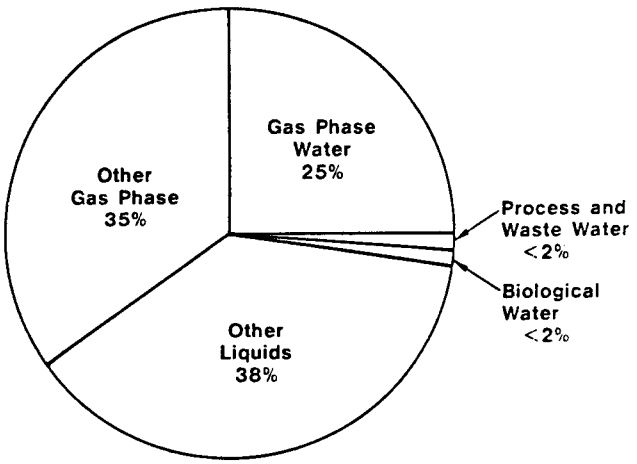

Fig. 1. Alumina adsorption applications (volume of aluminas).

application is proprietary. The examples presented here are a few representatives of the broad range of applications.

A second major driving force for the use of alumina-based chemicals as selective adsorbents has been the cost of energy. In the petrochemical industry, for example, processes which have traditionally used distillation are employing adsorption as the primary mechanism for separation. Figure 2 illustrates this trend. The purification of ethylene dichloride, a commodity feed material for the production of polyvinyl chloride, is now being handled by a new process

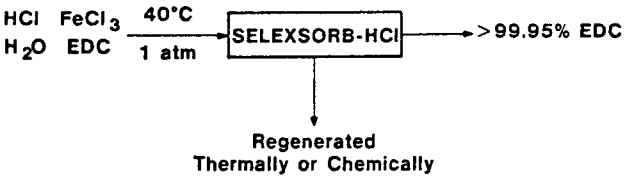

Fig. 2. Ethylene dichloride cleanup process.

utilizing a selective alumina-based adsorbent. Trace chloride and iron contaminants are effectively removed to undetectable limits from the liquid without the need to change the process temperature nor volatilize any of the stream to effect the separation.

Alumina Structure and Surface Chemistry

Considering the longevity of alumina usage in the catalysis and adsorption industries, it is surprising to note how many misconceptions still exist concerning its physical-chemical properties. Because the surface structure of an adsorbent essentially determines its adsorptive characteristics, an understanding of the surface chemistry of aluminum oxides is necessary to comprehend selective adsorption properties.

Alumina is a commonly used term for aluminum oxides and hydroxides, which exist as at least five thermodynamically stable phases and many more metastable transition forms. Other chapters include discussions of the physical forms of these materials and their methods of production. With the exception of some alpha aluminas, all forms possess surface hydroxyls which can have a certain degree of activity in adsorp-

tion. The treatise by Wefers and Bell is considered to be a good review of aluminum oxide phase chemistry.[10] The crystallographically stable oxides and hydroxides are not usually considered useful as adsorbents since they have little porosity and low surface area. Some of these aluminas are useful in water treatment and are reviewed in a separate chapter. Because the primary mechanisms of separation are usually quite different, this discussion is limited to the use of aluminas as adsorbents in all applications other than water.

Transition forms of alumina constitute the largest group used as adsorbents. Usually formed via thermal decomposition from the hydroxides, the loss of hydroxyls results in defect structures in the aluminum and oxygen lattice. Depending on the particular transition form, the Al^{3+} and O^{2-} ions can be either tetrahedrally or octahedrally coordinated in cubic or hexagonal close-packed systems. For example, gamma alumina, the best-known form, has a defect spinel structure in which the oxygens are in cubic close packing. The oxygen sublattice is fairly well ordered, although there is significant disorder in the tetrahedral aluminum sublattice.

As an example of the complexity of the alumina system, eta alumina, a transition form with a spinel structure similar to that of gamma alumina, has a strong one-dimensional disorder of the cubic close-spaced lattice. This distortion results in a greater concentration of surface acid sites (and strengths) in eta than in gamma alumina. This is an important consideration in adsorption systems, such as water and amines, which require these functionalities.

Depending on the synthetic methodology, the initial form in producing transition aluminas can be amorphous (or at least indifferent, as determined by X-ray diffraction). In fact, a number of commercial products that are sold as "gamma alumina" are amorphous. It is also generally recognized that a large portion of the catalysis and adsorption literature using "gamma alumina" that was not well characterized is actually data on an amorphous material, or at least poorly formed gamma. As a rule, amorphous transition aluminas (as distinguished from amorphous hydroxide aluminas) have greater concentrations of defect structures, i.e., greater chemical activity than the more crystalline transition aluminas.[11] In the amorphous-to-crystalline transition, octahedral Al^{3+} must reorder to tetrahedral with considerable rearrangement of the oxygen lattice. Large numbers of defect structures can be envisioned during this process, which result in active sites for adsorption. Most commercial transition materials fall somewhere between amorphous and more structured.

Gelatinous aluminas comprise an additional group of materials which can be important as adsorbents. As a group, these materials possess only short-range lattice order and can be prepared in numerous ways, ranging from precipitation to hydrolysis reactions. Their extremely high surface areas and chemical activity make alumina gels of continued interest in catalysis and adsorption. The poorly crystallized pseudoboehmite, for instance, exhibits good adsorptive properties for phosphates and arsenates in aqueous streams.

Another group of materials which exhibits adsorptive properties is the beta aluminas, which consist of alkali-substituted aluminates and their related compounds. The best known is beta sodium aluminate. Dawsonite (Na_2O-Al_2O_3-$2CO_2$-$2H_2O$) is a related compound which, with beta sodium aluminate, is the principal component of the so-called "alkalized alumina" process for desulfurizing flue gas.[12] Dawsonite can be synthesized as both crystalline and gelatinous and appears to have interesting chemical activity. Neither dawsonite nor the beta aluminas have received much attention for their adsorptive properties.

To be complete, alpha alumina should be included in this list. Although not normally considered reactive because of almost total dehydroxylation, low surface area, and virtually no porosity, alpha alumina exhibits greater Lewis acidity per unit surface area than the transition aluminas and can be shown to have strong adsorptive properties through this acidity. For example, halides, water, and inorganic acids can be adsorbed well on alpha alumina.[13]

The chemical nature of the active sites responsible for adsorption phenomena on aluminas is still not well understood. Defect structures formed via surface dehydroxylation result in localized regions of adsorptive and catalytic activity. The activity cannot be completely attributed to anion vacancies. Depending on the particular alumina, various concentrations of at least five distinct sites have been identified. They are sometimes listed as the A, B, E, I, and X sites, following the catalysis model,[14] and roughly correspond to distinct surface hydroxyls. Depending on their synthesis, geometric orientation, and concentration, they can possess differing degrees of both acidic and basic character in adsorption. Although not complete, a good discussion of the hydroxyl properties can be found in the papers by Peri[15,16] and the review by Knozinger and Ratnasamy.[14]

For adsorption, active aluminas can be considered as possessing both Lewis and Bronsted acidic and basic sites of various strengths and concentrations. Acidity is contributed by lattice Al^{3+} ions, protonated hydroxyls, and some acidic hydroxyls. Basicity is a result of O^{2-} anion vacancies and basic hydroxyls. A useful schematic representing the various surface functionalities is shown in Fig. 3.[15]

Because of the variation of alumina surface properties with hydroxyl concentration and type, adsorption behavior can be modified in numerous ways on the materials. A relatively easy method, for example, is thermal dehydroxylation. As shown in Fig. 4 for two levels of hydroxyl content, the acidic and basic site concentrations can be made quite different. This trend is summarized in Fig. 5 for transition aluminas as a

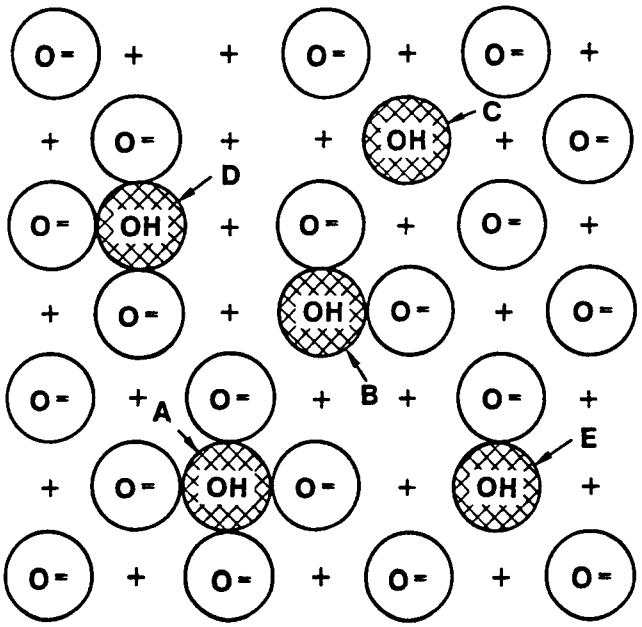

Fig. 3. Transition aluminas' surface functionalities (Ref. 15). (Used by permission.)

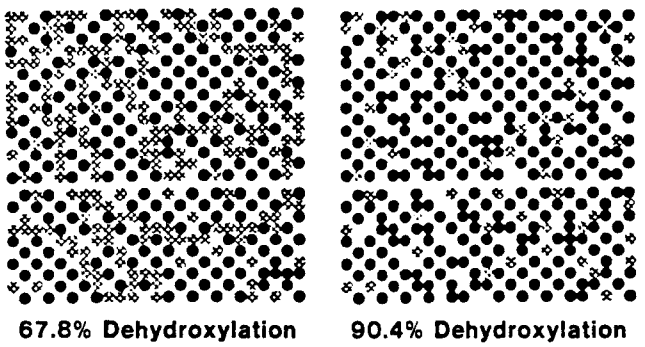

Fig. 4. Transition alumina dehydroxylation (Ref. 15). (Used by permission.)

function of final activation temperature in the synthesis process. Higher temperatures tend to eliminate surface hydroxyls, which increase the number of Lewis acid sites, thus increasing total acid sites on a surface-area basis.

A complicating factor in the design of alumina surface chemistry for adsorption is the tremendous complexity of the surface due to the simultaneous presence of numerous distinct sites. Termed surface heterogeneity, this distribution of sites with different energies on a surface typically inhibits selectivity and makes specific design of a material for a particular application more difficult. There will always be, for example, some residual hydroxyls which act as basic sites, rather than the bulk of the hydroxyls which are acidic, ready to donate their protons in the attached hydrogen atoms. This phenomenon is demonstrated in Fig. 6, where the site-energy distributions of various aluminas for gas-phase ammonia adsorption are given.

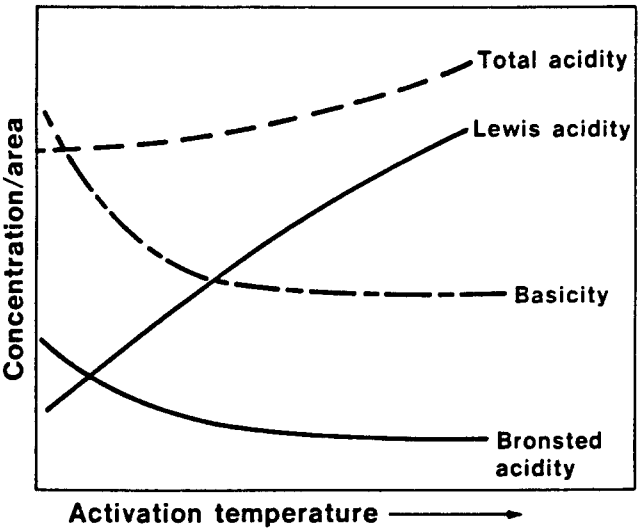

Fig. 5. Transition aluminas (acid-base modifications).

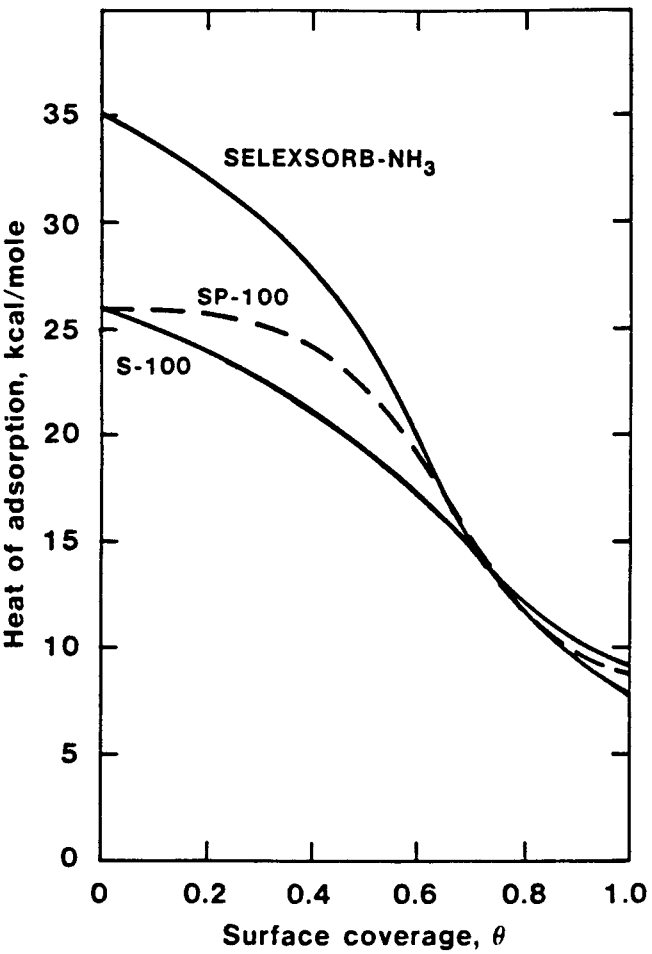

Fig. 6. Surface heterogeneity of aluminas (NH_3 desorption, 25°C).

As measured by the heats of interaction, it is seen that the surface of each of these commercial alumina-based materials is quite different, and each is heterogeneous

in its interaction with ammonia. There are some sites which bind very strongly (>20 kcal/mol), while others only physically interact with Van der Waals forces (<10 kcal/mol). Both SP-100 and SELEXSORB-NH_3 are aluminas whose surfaces have been chemically modified.

In addition to surface effects, there are other ramifications of changing activation temperature in design of the adsorbent. As seen in Fig. 7, total surface area is a sensitive function of temperature, as well as pore distribution and total pore volume. In gas-phase separation of small molecules with fast pore transport, surface area is critical for good uptake capacities. Viscous liquids such as large hydrocarbons, on the other hand, tend to require more macroporosity, i.e., inherently lower surface areas, with well-designed surface chemistries. Optimum selection of an alumina will depend on the relative importance of these factors to the end user.

Advances in pore-structure control of the porous active aluminas have resulted in major improvements in commercial adsorbents. Zeolites have their pore structures determined simultaneously with the precipitation process and are constrained in size by the configuration of the sodalite cage. In contrast, active alumina porosity is relatively independent of the bulk-phase formation process and is usually engineered following material synthesis. Microporosity is controlled via kinetics of the dehydroxylation process, whereas macroporosity is usually developed in the agglomeration process.

A preeminent theme in current adsorption requirements is the move toward greater specificity of separation with more complex streams. In the past there was a tendency to classify aluminas as nonspecific with limited adsorption capability. More recently, development efforts have begun to generate materials of a better-characterized, highly specific nature. Several transition alumina forms are now available in commercial quantities for particular applications. At last count, they included gamma, chi, and eta, as well as amorphous. Alcoa's CP and CPN grades are examples of amorphous and transition forms, respectively.

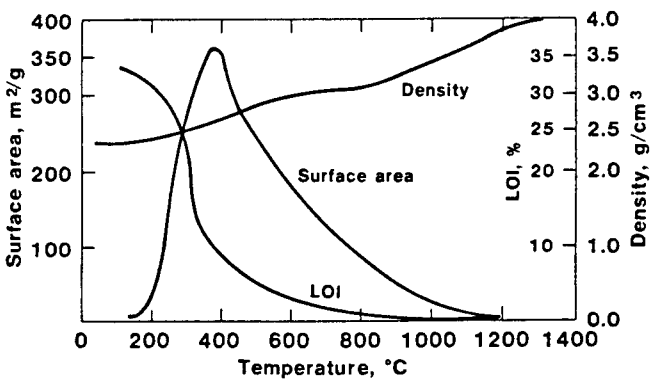

Fig. 7. Surface area vs temperature (Ref. 10). (Used by permission.)

Because of the influence of impurities on adsorption performance, greater attention is being given to chemical purity. Good examples are the ultrapure pseudoboehmites Catapal* and Dispural.† Most manufacturers now offer varying grades of chemical purity for differing adsorption requirements. There are two reasons for this trend. First, more aluminas are being produced that are not products of a Bayer stream. Consequently, they are not constrained by the purity limitations of the Bayer liquor. Catapal and Dispural are prominent examples, as is fumed alumina. The second factor in improved chemical purity is the increased process control now being associated with Bayer precipitation. Greater care is being taken to achieve acceptable chemical purities for the technical aluminas.

Increased understanding of these phenomena, in conjunction with greater control of initial particle size, has allowed engineering of pore-size distributions and degree of porosity. Representative pore distributions of various commercial transition aluminas are given in Fig. 8. They cover the range of 3 to 100 000 nm (30 to 1 000 000 Å) in bi-, tri-, and monomodal distributions. Total pore volumes ranging from 0.3 to 0.8 cm^3/g are not uncommon, with some experimental materials having porosity up to 1 cm^3/g.

Currently, more manufacturers are tailoring pore structures to meet specific process requirements than was the case in the past, where only commodity materials were available. Within practical constraints, the technology is now in place for generation of both microporous and macroporous aluminas in any derived structural form. In addition, there is little question that the future in adsorbent alumina manufacture is in the direction of greater control of pore structures, particularly for liquid-phase adsorption of deactivating species such as organometallics. Controlled pore structures can also be beneficial for more-efficient regeneration of difficult adsorbates. A primary example is deposition of elemental sulfur, where the frequency of cyclic regeneration can be controlled by strong pore-diffusion resistances.

Modification of alumina surface chemistry to enhance selective adsorption of particular compounds has become more prevalent in recent years. Active aluminas are multifunctional materials with ratios of surface sites. Engineering the alumina to contain advantageous surface functionalities while reducing undesired sites is fast becoming a science and is a powerful tool in the design of selective adsorption units.

The most common approach to surface modification with transition aluminas is through control of the thermal treatment. As shown in Figs. 5 and 7, it is quite easy to alter the total surface Lewis and Brönsted acidity and basicity via control of the hydroxyl concentration. To some extent this technique has been

*Vista Chemical Co., Houston, TX
†Condea, Martinswerk, Federal Republic of Germany.

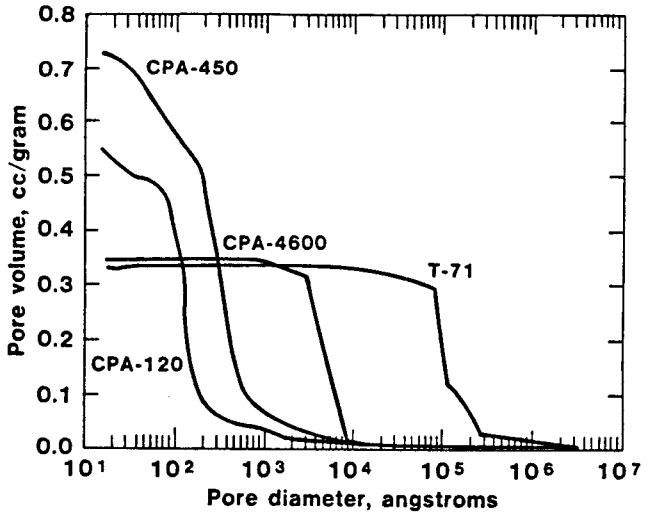

Fig. 8. Adsorbent pore distribution.

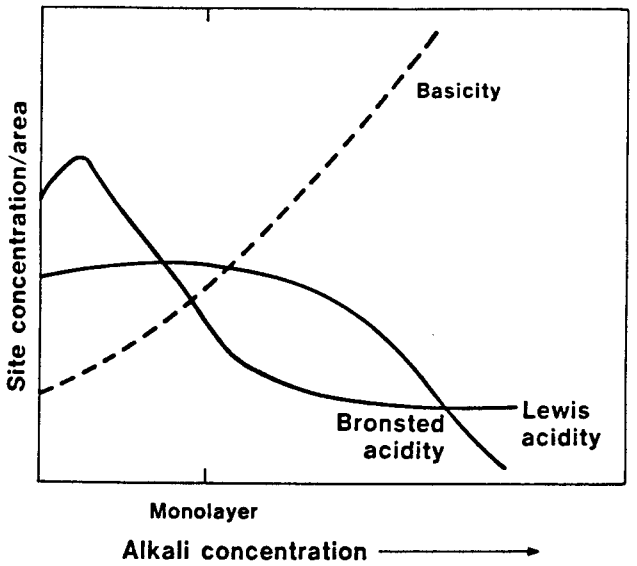

Fig. 9. Transition aluminas (acid-base modifications).

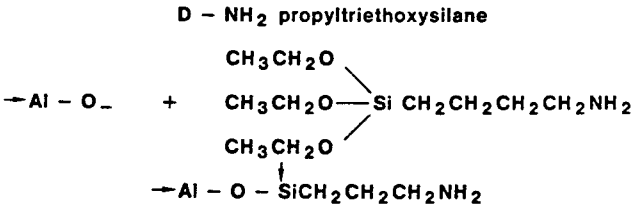

Fig. 10. Silanization.

used since the early 1950s, particularly in chromatographic aluminas. The so-called Brockmann scale[3] for rating aluminas is based on thermal history, and commercial materials are available today in the various Brockmann grades. Only recently has the concept been applied to large-scale adsorption systems.

A more complex approach to enhancement of surface properties is the addition of chemical modifiers which increase the concentration of the existing desired functionalities. Adsorption of acids or bases which alter the concentration and reactivity of alumina surface hydroxyls is a good example.

Although the basic technology has existed for over 20 years and is used routinely in catalysis, adsorbent aluminas have been noticeably neglected and are only today coming on-stream in commercial systems. However, most of the applications are proprietary and the materials have been designed with the particular user in mind.

A simple example of chemical modification of transition aluminas is shown in Fig. 9 for the addition of alkali cations. It is that total surface basicity is increased as alkali is impregnated on the alumina surface. It is also of interest to note that both Lewis and Brönsted acidity decrease, but only after an increase at low alkali concentration.

Because the variety of chemical functional groups that can be adsorbed on aluminas is so diverse, a third group of surface modifications is becoming more popular. They involve chemical treatment of the alumina surface in order to introduce new functionalities which can enhance adsorption. An example of such a modification is given in Fig. 10. A transition-alumina surface is silanized through a condensation reaction with a commercial triethoxysilane. The synthesized surface exhibits quite different properties than the base alumina and can be used for applications such as reversed phase chromatography.

Although not modified to increased adsorption capacity, the first commercial example is the cobalt chloride-impregnated transition alumina marketed by Alcoa in the 1950s for water adsorption. Calcium, sodium, and potassium salts have also been used commercially for various reasons. The most recent published example is the modified alumina used to separate mercury from natural gas streams in the Arabian oil countries. A related example is the permanganate impregnation of a transition alumina for simultaneous adsorption and oxidation of selected air pollutants. Most of the material modifications have been done for specific proprietary applications and are not available for public disclosure.

Adsorption Processes

Aluminas tend to adsorb species via chemisorption, a form of chemical reaction. As such, the affinity is usually quite strong, with large heats of uptake, as well as desorption. Because of this property, aluminas have a distinct advantage over other materials, such as carbons and ion-exchange resins, that operate by alternative mechanisms in certain applications. First, they are particularly good at removing trace quantities of substances from a bulk stream. This is illustrated in Fig. 11. There is a very favorable isotherm, or affinity, for species that do adsorb at low concentrations. Other

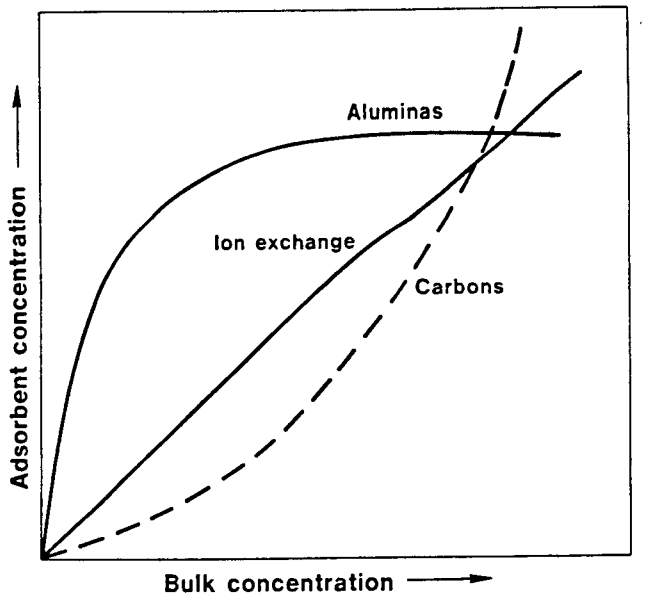

Fig. 11. Adsorption isotherms.

materials become competitive at higher concentrations (typically >1000 ppm). Second, aluminas remove components of streams very selectively. When it is necessary to either purify or remove a product from a stream with multiple components, aluminas are generally applicable. A general outline of their affinity for species, as defined by functional group, is shown in Fig. 12 for a number of common chemicals. Although difficult to generalize, this may represent a rough consensus of correct thought regarding chemisorption of these species.

Although many methods of contacting the alumina adsorbent with the multicomponent stream of interest are possible, most processes today still use packed beds. A packed bed offers high efficiency of separation per volume, is easy to control, and has low capital and operating costs. Typical operation is outlined in Fig. 13. A gas, liquid, or multiphase stream passes through the bed, with the component(s) of interest being removed. A mass transfer zone of the adsorbate remaining in the fluid phase is established which moves through the bed until it breaks through the end and is detected in the effluent. The bed is then considered spent and is either regenerated or discarded.

Two general techniques are used for regenerating beds. When possible, thermal desorption via an inert gas at a high temperature is used to strip the adsorbate from the alumina for reuse. Typical temperatures for regeneration range from 150° to 400°C, depending on the affinity of the adsorbate for the alumina surface. The concentrated adsorbate can be either reused or vented. Chemical energy can be used instead of thermal energy in certain instances. For example, a liquid can be contacted with the bed which displaces the

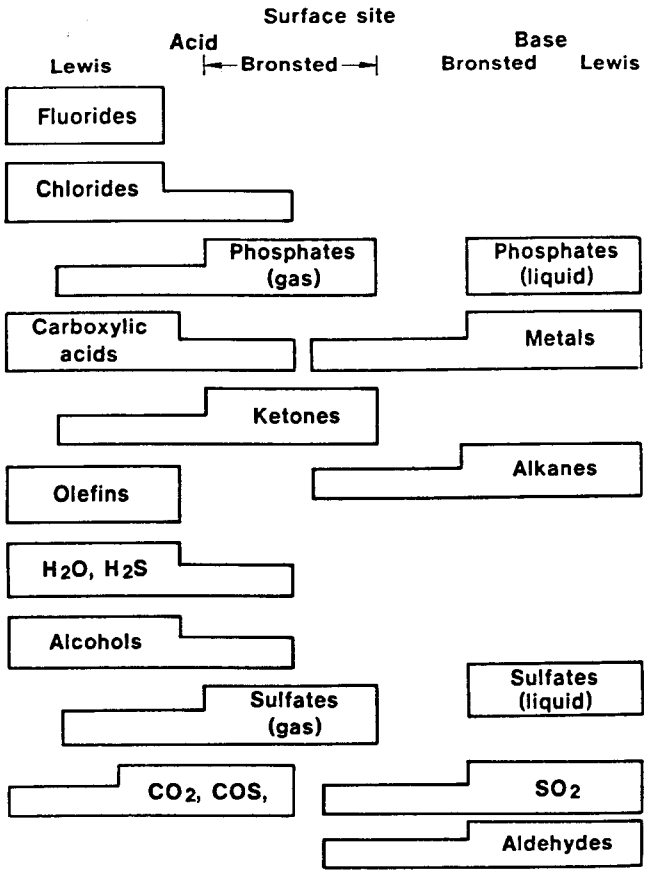

Fig. 12. Transition aluminas (functional group adsorption).

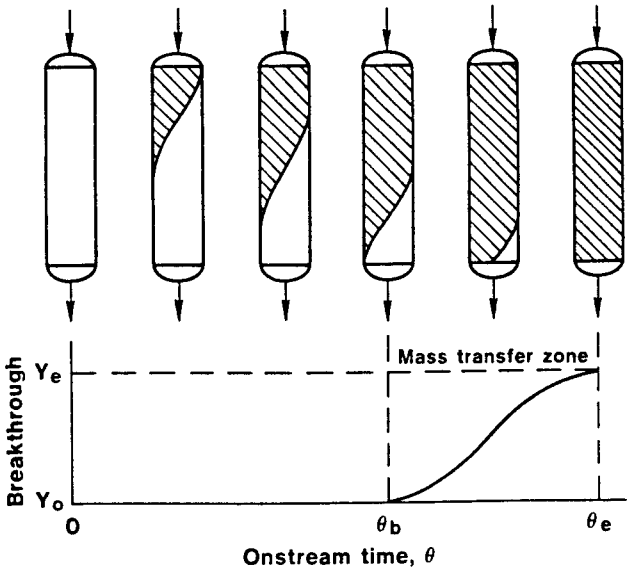

Fig. 13. Adsorption dynamics.

adsorbate and serves the same purpose as the hot gas in regenerating the bed. In either case, the alumina remains intact and is immediately reusable. These

techniques are generally applicable in all applications, except aqueous streams.

Current Commercial Applications

Because of the unique versatility of aluminas, and a greater current understanding of their properties, these materials have moved into industries not formerly considered as applicable adsorption opportunities. In the past, petrochemical applications of alumina adsorption accounted for virtually all of the adsorbent alumina market. Today the list encompasses specialty chemicals, polymers, metals, waste management, and biological processing, among others.

An exhaustive compilation regarding the use of aluminas for chemical separations would be quite an undertaking. As shown in Fig. 12, the broad range of surface affinities allows these materials to be used to remove a wide range of chemical functionalities. Adsorption of C1 to C5 alcohols on aluminas in gas and liquid phase is common.[17,18] Selective removal of alcohols and thiols and their interaction has been examined.[19]

Sulfides and thiols can be separated.[20,21] There are references to the removal of substituted phenols from various mediums and phases.[22,23] The selectivity of aluminas for different species from streams containing alcohols, carboxylic acids, and amines has been reported.[24,25] Selectivity has been shown for carboxylic acids from phenols, and vice versa.[26–28]

Polyaromatic compounds, such as porphyrins and naphthalenes, are being removed from heavy oils.[29] Large nitrogen-containing hydrocarbon species in oils are being considered in processes similar to that of the porphyrins.[30] Even small hydrocarbons, both saturated and olefinic, are being removed in both gas and liquid phases.[31,32] Acid and organic chlorides are routinely removed from streams as diverse as inert gases to heavy hydrocarbon liquids.[33,34] Species as diverse as cyanide[35] and hydrogen[36–38] can be adsorbed to some extent on aluminas.

Most applications of aluminas are proprietary and are generally not contained in the preceding list. Also, applications in water treatment are excluded because of the discussion in another chapter. Neither can one get a sense of the trends in the use of these materials from a scattered sampling. A few selected cases are offered to illustrate current trends.

Removal of carbonyl sulfide from propylene, a key step in the production of polypropylene, can be accomplished via adsorption on aluminas. Figure 14 features some representative data on COS removal with three aluminas which are quite different, both chemically and physically. SELEXSORB-COS is a material produced by Alcoa with specific affinity to carbonyl sulfide.

Similar needs for purification are found in petroleum processing, where synthetic hydrocarbons are produced. Hydrochloric acid is a typical impurity which affects downstream catalytic processing. As

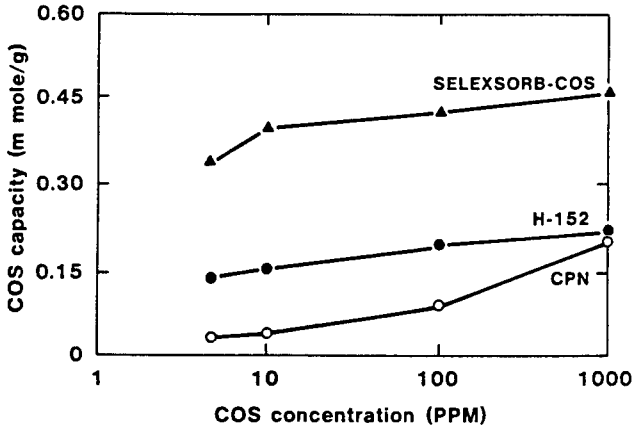

Fig. 14. COS/adsorption isotherms for various alumina-based adsorbents (25°C).

shown in Fig. 15, aluminas have the potential to handle this separation problem. SELEXSORB-HCl is a chemically modified alumina used commercially in these types of applications.

Selective removal of carbon dioxide from water, as well as the converse, is typical in petrogas drying. These two species are mutually compatible in their adsorptive behavior, in that selectivity can be obtained by modification of surface Lewis acidity. This is represented in Fig. 16 for a series of commercial aluminas and depicts the power of selectivity available to the design engineer.

An example of selectivity in the liquid phase is given in Fig. 17. Silver and copper in water can be recovered individually by the choice of the correct alumina, as is commercially practiced in the catalyst manufacturing industry. Acidic and basic CPN simply refers to transition aluminas which have been chemically modified so that their zero point of charge (zpc) falls on positive and negative sides of the solution pH, respectively.

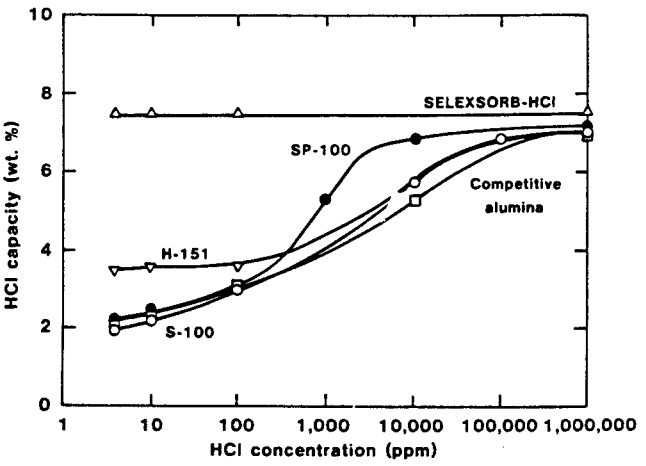

Fig. 15. HCl adsorption isotherm (25°C, 1 atm, dynamic excess flow).

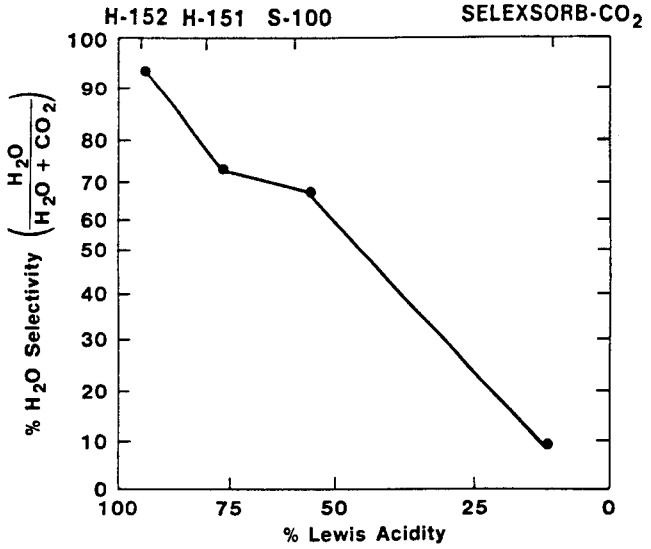

Fig. 16. CO_2/H_2O selective adsorption (25°C, 1 atm, He dynamic flow, 50 ppm each).

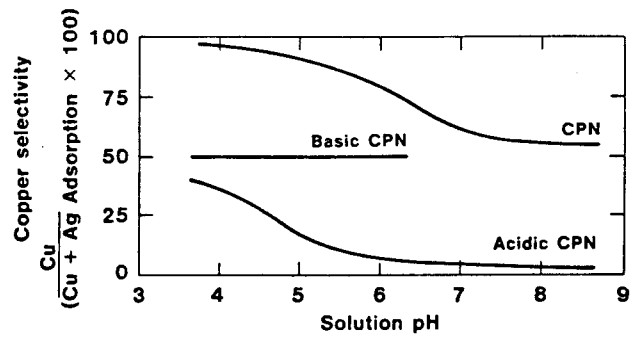

Fig. 17. Cu^{2+}/Ag^{+} adsorption selectivity.

An additional field in which alumina adsorption technology has made inroads recently is biological processing. Because of the ability to modify surface characteristics, define pore structures, and exhibit good physical and chemical stability with consistency, aluminas are finding successful application in commercial processing of biological materials. A representative list of demonstrated bulk separations is given in Table II. Although systems of pharmaceutical interest comprise the largest portion of the applications, a broad spectrum of biomolecules is included which encompasses foods, agriculture, medical, and specialty chemicals in addition to pharmaceuticals. Some of the larger volume commercial separations, all of which are chromatographic, include steroids, proteins, and vitamins.

Aluminas have found applications in virtually every type of commercial chromatographic process. Adsorption chromatography in aqueous systems comprises a large portion of alumina usage because of the specific affinity of aluminas for a variety of chemical functionalities. Ion-exchange chromatography is possible, particularly at high pH. The purification of proteins is an obvious example and is demonstrated in Fig. 18.

Depolarization of active alumina surfaces and modification of the Brockmann number by many techniques may make their use possible in high-performance liquid chromatography and reversed-phase chromatography, respectively. Molecular exclusion chromatography has been demonstrated on aluminas with large concentrations of macropores. There is even some evidence to indicate that affinity chromatography for very specific attachment of biological functionalities may be successful via covalent ligand addition to particular alumina structures.

As the entire field of biotechnology continues to expand, with its associated requirements for greater separations processing, more specific aluminas with tailored properties are expected to be generated which meet specialty demands. It is interesting to note that the whole area of biological separations seems to have made a complete circle in its direction. For some of the same reasons that aluminas were first investigated and used for analytical purifications in the original work on aluminas over 40 years ago—namely physical stability and strong affinity for a wide variety of biomolecules—they are being rediscovered and further refined in the context of present-day needs.

Chromatographic adsorption with aluminas is gaining acceptance as a viable kinetic separation alternative to molecular sieve zeolites and carbons. Although traditionally associated with biological systems, large-scale chromatography is rapidly finding application in various industries, including nuclear and specialty chemicals. In fact, one of the largest chromatographic columns in commercial practice uses aluminas to produce various flavors and fragrances. In another industry, separations of isomers, such as meta- and orthoxylene, which are impossible by distillation, are easily accomplished using high-affinity chromatographic aluminas.

Aluminas have traditionally been considered to be limited to impurity separations of the minor stream components. With the advent of successful, continuous large-scale chromatographic technology, numerous bulk separations have become practical which would not have been considered in the past. The same properties of commodity aluminas which were considered detrimental—e.g., strong affinity for a wide range of components—is usually advantageous for alumina chromatographic processing. An example of the wide range of separation possibilities is included in Table III.[6] This compilation of the elutropic series of solvents on a transition alumina is illustrative of the considerable versatility potentially available for chromatographic processing.

As successful large-scale chromatographic technology continues to be demonstrated, the trend toward use of aluminas in greater numbers of bulk, as well as

Table II. Representative Biological Chromatographic Purifications Using Aluminas

Separation	Technique	Ref.
Basic drugs	Ion-exchange chromatography	39, 40
Hypnotic antiepileptic drugs	Liquid chromatography	41
Antipyretic drugs/aspirin	Liquid chromatography	42
Alkaloids	Thin-layer chromatography High-performance liquid chromatography	39, 43
Proteins	High-performance liquid chromatography Ion-exchange chromatography	44
Catecholamines	Reverse-phase liquid chromatography High-performance liquid chromatography	44, 45
Triglycerides/lipids/oils	Liquid chromatography	46, 47
Estrogens	Liquid chromatography	48, 49
Testosterones	Thin-layer chromatography	32
Steroids	High-performance liquid chromatography	48, 50
Cyclic nucleotides	Liquid chromatography	48, 51
Peptides	High-performance liquid chromatography	52
Mucopolysaccharides/heparin	Liquid chromatography	49
Phospholipids	High-performance liquid chromatography	53
Streptomycins	Liquid chromatography	54
Glucoamylases	Adsorption chromatography	55
Quinones	Liquid chromatography	56, 57
Aminohydrolases	High-performance liquid chromatography	58
Fatty acid methyl esters	Thin-layer chromatography	59
Staphylocci	Liquid chromatography	

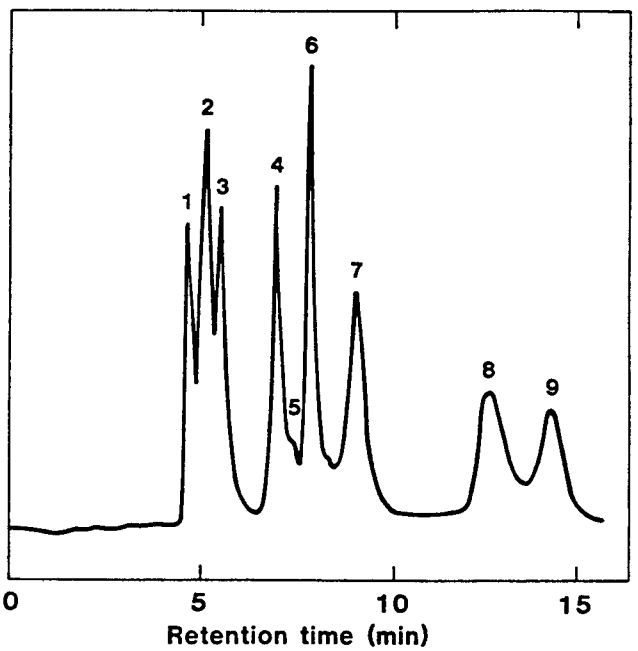

Mobile phase: 0.25 M Na_2PO_4 (pH 9).
Solutes: 1 and 2 = bovine albumin; 3 = ovalbumin; 4 = myoglobin; 5 = unknown; 6 = arginine vasopressin; 7 = trypsinogen; 8 = lysozyme; 9 = chymotrypsinogen.

Fig. 18. Chromatographic separation of standard proteins on CG-20.

impurity, separations is expected to increase. The simulated moving bed process developed by UOP, the Oak Ridge annular rotating, multiple extraction system, as well as other designs for continuous chromatography, will provide additional options in commercial separations other than those that exist today. Thorough reviews on these and other large-scale chromatographic technologies are given by Sussman[60] and Rendell.[61]

The Future in Selective Adsorption

Virtually every trend present in separations technology today points toward selectivity as a key criterion. The demand for higher quality chemicals and feed streams, the energy-driven need to remove trace contaminants from the desired bulk component, and growth and awareness of pollution-abatement requirements, are all major driving forces for development of separations processes which are highly specific. Adsorption, particularly using aluminas, will be a front-runner in this movement. As forming technology becomes more controllable, advances in understanding of the surface chemistry will lead to molecularly engineered surfaces which should considerably expand the horizons for aluminas in selective adsorption processes.

References

[1]J. B. Barnitt, U.S. Pat. No. 1 868 869. July 26, 1932.
[2]K. Folkers and J. Shovel, U.S. Pat. No. 2 573 702, 1901.
[3]H. Brockmann, *Disc. Faraday Soc.*, 7, 58 (1949).
[4]P. Reichstein and C. W. Shoppee, *Disc. Faraday Soc.*, 7, 305 (1949).
[5]Polesuk, *J. Am. Lab.*, 27 [5] (1970).
[6]J. Sherma, Handbook of Chromatography. CRC, Boca Raton, FL, 1971.
[7]S. Joshi and J. Fair, *Ind. Eng. Chem. Fund.* (3rd Quarter, 1986).
[8]F. Rubel and R. D. Woosley, EPA Tech. Rep. 570/9–78–001 (1978).
[9]W. C. Yee, *JAWWA*, 239 [2] (1966).

Table III. Elutropic Series of Common Solvents on γ-Alumina*

Solvent	$E°(Al_2O_3)$	Viscosity
Fluoroalkanes	−0.25	
n-pentane	0.00	0.23
Hexane	0.00	
Isooctane	0.01	
Petroleum ether, skellysolve B, etc.	0.01	0.3L
n-decane	0.04	0.92
Cyclohexane	0.04	1.00
Cyclopentane	0.05	0.47
Diisobutylene	0.06	
l-pentene	0.08	
Carbon disulfide	0.15	0.37
Carbon tetrachloride	0.18	0.97
Amyl chloride	0.26	0.43
Butyl chloride	0.26	
Xylene	0.26	0.62–0.81
l-propyl ether	0.28	0.37
l-propyl chloride	0.29	0.33
Toluene	0.29	0.39
n-propyl chloride	0.30	0.35
Chlorobenzene	0.30	0.80
Benzene	0.32	0.65
Ethyl bromide	0.30	
Ethyl ether	0.38	0.23
Ethyl sulfide	0.38	0.45
Chloroform	0.40	0.57
Methylene chloride	0.42	0.44
Methyl-*l*-butylketone	0.43	
Tetrahydrofurane	0.45	
Ethylene dichloride	0.49	0.79
Methyl ethyl ketone	0.51	
l-nitropropane	0.53	
Acetone	0.56	0.32
Dioxane	0.56	1.54
Ethyl acetate	0.58	0.45
Methyl acetate	0.60	0.37
Alyl alcohol	0.61	4.1
Dimethyl sulfoxide	0.62	2.24
Aniline	0.62	4.4
Diethyl amine	0.63	0.38
Nitromethane	0.64	0.67
Acetonitrile	0.65	0.37
Pyridine	0.71	0.94
Butyle cellusolve	0.74	
l-Propanol, *n*-propanol	0.82	2.3
Ethanol	0.88	1.20
Methanol	0.95	0.60
Ethylene glycol	1.11	19.9
Acetic acid	Large	1.26
Water	Larger	
Salts and buffers	Very large	

*Ref. 6.

[10]K. Wefers and G. Bell, "Oxides and Hydroxides of Aluminum, Technical Paper 19," Aluminum Company of America, Pittsburgh, PA, 1972.

[11]S. J. Teichner, et al., *Bull. Soc. Chim. Fr.*, **7–8**, 1226 (1974).

[12]D. Bienstock, et al., USBM Report of Investigations 7021, Part 3 (7/67).

[13]R. R. Bailey and J. Wightman, *J. Colloid Interface Sci.*, **70** [1] 112 (1979).

[14]H. Knozinger and P. Ratnasamy, *Catal. Rev.-Sci. Eng.*, **17** [1] 31 (1978).

[15]J. B. Peri, *J. Phys. Chem.*, **69**, 231 (1965).

[16]J. B. Peri, *J. Phys. Chem.*, **70**, [10] 3168 (1966).

[17]H. Knozinger and B. Stubner, *J. Phys. Chem.*, **82** [13] 1526 (1978).

[18]A. V. Deo, et al., *J. Phys. Chem.*, **75** [2] 234 (1971).

[19]J. Travert, et al., *Proc. Int. Conf. Vibrat. Surfaces*, 333 (1982).

[20]R. W Glass and R. A. Ross, *J. Phys. Chem.*, **77** [21:] 2576 (1973).

[21]T. L. Slager and C. H. Amberg, *Can. J. Chem.*, **50**, 3416 (1972).

[22]D. R. Taylor and K. H. Ludlum, *J. Phys. Chem.*, **76** [20] 2882 (1972).

[23]G. L. Mundhara, et al., *J. Ind. Chem. Soc.*, **LVII**, 306 (1980).

[24]S. D. Williams and K. W. Hipps, *J. Catal.*, **78**, 96 (1982).

[25]J. Koubek, et al., *J. Catal.*, **38**, 285 (1975).

[26]G. L. Mundhara and J. S. Tiwari, *Ind. Chem. Soc. J.*, **56**, 737 (1979).

[27]L. I. Vladyko, et al., *Kinet. Catal*, UDC 541.124.03 + 541.183, 1200 (1982).

[28]E. A. Nechaev and G. V. Zvonareva, *Kolloidnyi Zhurnal*, **42** [3] 511 (1980).

[29]A. Chantong and F. E. Massoth, *A.I.Ch.E. J.*, **29** [5] 725 (1983).

[30]C. D. Ford, et al., *Anal. Chem.*, **53**, 831 (1981).

[31]W. J. Nelson and D. G. Walmsely, *Proc. 2nd Int. Conf. Birat. Surfaces*, 471 (1982).

[32]H. Tamon, et al., *J. Chem. Eng. Jpn.*, **14** [2] 136 (1981).

[33]M. Tanaka and S. Ogasawara, *J. Catal.*, **16**, 157 (1970).

[34]E. B. Krasnyy and L. M. Iozefson, *Trudy Kazanskogo Khimiko- Tekhno. Inst.imeni S. M. Kirova*, **40** [1] 273 (1969).

[35]S. L. Regen, et al., *J. Am. Chem. Soc.*, 101 [25] 7629 (1979).

[36]Y. P. Borisevich, et al., *Zhurnal Fizicheskoi Khimii*, **56**, 1298 (1982).

[37]Y. Amenomiya, *J. Catal.*, **22**, 109 (1971).

[38]S. W. Weller and A. A. Montagna, *J. Catal.*, **21**, 303 (1971).

[39]C. Laurent, et al., *Chromatographia*, **17** [5] 253 (1983).

[40]C. Laurent, et al., *Chromatographia*, **12** [7] 395 (1983).

[41]M. Sarsunova and T. H. Ba, *Cesk. Farm.*, **15** [10] 522 (1966).

[42]S. Gocan, et al., *Stud. Univ. Babes-Balyeii, Ser. Chem.*, **22** [2] 42 (1977).

[43]L. N. Slepova, et al., *Tr. Leningred. Khim.-Farm. Inst.*, **28**, 69 (1969).

[44]B. Westerink, et al., *Clin. Chem.*, **28**, 1745 (1982).

[45]W. Drell, *Anal. Biochem.*, **34** [1] 142 (1970).

[46]S. D. Gusekova, et al., *Khim. Prir. Soedin*, **3**, 310 (1978).

[47]E. Pescucci and G. Ventura, *Rass. Chim.*, **24** [3] 124 (1972).

[48]T. Ivanov, *Nauch. Tri.*, **21**, 55 (1971).

[49]M. K. Pal and J. Neth, *Anal. Biochem.*, **57** [2] 395 (1974).

[50]S. White, *Methods Enzymol.*, **38** [C] 41 (1974).

[51]G. Fluoret and O. Hechter, *Anal. Biochem.*, **58** [1] 276 (1975).

[52]I. Bartley, et al., *Biochem. J.*, **126** [1] 251 (1972).

[53]M. G. Luthra and A. Sheltawy, *Biochem. J.*, **126** [1] 251 (1972).

[54]G. P. Mueller, *J. Am. Ceram. Soc.*, **69**, 195 (1947).

[55]J. Cormon, U.S. Pat. No. 3 332 851, July 25, 1967.

[56]O. P. Mitsan, et al., *Visn. L'viv. Politekh. Inst.*, **112**, 69 (1977).

[57]A. Steward, *Disc. Faraday Soc.*, **7**, 65 (1949).

[58]C. Baron, et al., *Anal. Biochem.*, **124** [1] 84 (1982).

[59]C. Marutoiu, et al., Romanian Pat. No. R 071 380B, September 9, 1980.

[60]M. V. Sussman, *Chemtech*, **6** [4] 260 (1976).

[61]M. Rendell, *Proc. Eng.*, **66** [4] (1975).

[62]M. Yakovleva, *Endokrinopatii Lech. Ikh. Gromonami*, **5**, 216 (1970).

[63]E. Z. Naugol'nykh, *Lab. Delo.*, **9**, 539 (1978).

[64]F. Orlandi, et al., *Biochim. Biol. Sper.*, **5** [2] 281 (1966).

Water-Treatment Products and Processes

Hubert L. Fleming
Alcoa Laboratories
Aluminum Company of America
Pittsburgh, PA 15219

The use of aluminum oxides and hydroxides in water treatment is reviewed. Fundamental bulk and surface chemistry of these materials in aqueous media is discussed, relative to properties desired in water treatment. Representative examples of commercial products and processes are given, with some considerations for future trends in this field.

Alumina chemicals have found wide application in the treatment of industrial and municipal waters. For over 100 years, aluminum sulfate (alum) has been used as a primary coagulant for removal of various metals, particulates, and organics from industrial wastewaters. To a limited degree in the United States, and much more in Europe, aluminum trihydroxide (gibbsite, in particular) and monohydrates (pseudoboehmites, in particular) have found acceptance as flocculants in drinking-water treatment. On a lesser scale, transition forms of alumina are used as adsorbents for removal of undesired contaminants in both municipal and industrial waters.

This chapter reviews the technology of water treatment using alumina chemicals. Examples of current applications are used to illustrate commercial technology. An understanding of the interaction of alumina chemicals with dissolved species in water leads to speculation on the potential use of alumina chemicals in emerging water-treatment processes.

Aluminum Sulfate and Hydroxides

Millions of pounds of hydrated aluminum sulfate, $Al_2(SO_4)_3 \cdot 12H_2O$, are used annually in the United States as a chemical coagulant to clarify municipal and industrial water supplies. Solid aluminum sulfate is added to the water, which then forms a gelatinous precipitate of aluminum oxyhydroxide and carries suspended particles down to the bottom with it. The reaction of the cationic Al^{3+} is shown simplistically in Reaction (1).

$$Al^{3+}(aq) + 3H_2O \rightarrow Al(OH)_3(s) + 3H^+(aq) \quad (1)$$

The water passes through a filtration operation to remove the remaining suspended material prior to further chemical treatment.

Depending on the particular application, one of three mechanisms is operative in alum coagulation. Flocculation of suspended solids can occur on the precipitated aluminum hydroxide, as shown in Reaction (1). Dissolved species, particularly cations at higher pH, can also adsorb on the hydrated alumina. Currently, this approach is emphasized more in Europe than in the United States, and uses monohydrated alumina gels as the treatment chemical rather than alum.[1]

A third, frequently used mechanism in the use of alum is the direct precipitation in the sulfate form of undesired contaminants in the water. Most of the Group 2A and Row 4 elements form insoluble sulfates.[2] Aluminum sulfate can be added to water containing lead, for example, and precipitate lead sulfate, $PbSO_4$, while Al^{3+} remains in solution.

$$Pb^{2+}(aq) + SO_4^{2-}(aq) \rightarrow PbSO_4(s) \quad (2)$$

Given a K_{sp} of $PbSO_4 = 1 \times 10^{-8}$, precipitation is effective in removing the lead from solution to very low effluent concentrations. The corresponding hydroxyalumino species are quite soluble and are not toxic to humans at levels found in fluids used for general consumption. Sulfates and hydroxides tend to be mutually complementary precipitating agents. As a general rule, the hydroxides, such as lime, are more effective for heavy metals, whereas the sulfates remove lighter, nontransition elements.

Alums are a general group of hydrated sulfate salts containing aluminum, but not limited to $Al_2(SO_4)_3 \cdot 12H_2O$. Possessing the general formula $MAl(SO_4)_2 \cdot 12H_2O$, M may be practically any common univalent, monoatomic cation, except for lithium, which is too small. These materials are not commonly available, however. For commercial purposes, only the dialuminum compound is widely used for water treatment.

In conjunction with lime precipitation, followed by polishing with adsorption, alum is used extensively in a number of commercial applications. The following examples illustrate the breadth and type of use.

Barium from explosives-manufacturing wastewaters and related industries is removed by precipitation as barium sulfate via addition of either alum or iron sulfate.[3] Barium sulfate is relatively insoluble, having a minimal theoretical solubility of 1.4 mg/L at stoichiometric concentrations of barium and sulfate.[4] Table I lists results of a pilot-plant study of barium removal via iron sulfate, alum, and lime treatments. The use of alum required more sulfate, but resulted in lower effluent concentrations of barium.[5,6]

Table I. Comparative Treatment for Barium Removal*

System	Coagulant	pH	Sulfate Dose (mg/L)	Effluent Barium (mg/L)
Iron	45 mg/L $FeSO_4$	6.0	92.2	0.27
Alum	200 mg/L $Al^2(SO_4)_3$	6.4	164.5	0.04
Low lime	260 mg/L lime 20 mg/L $FeSO_4$	10.0	36.5	0.03
High lime	600 mg/L	11.5		0.94

*Refs. 5 and 6.

Following reduction of hexavalent chromium, Cr^{3+} can be treated by precipitation. Table II summarizes various treatment schemes, including electrolysis and a number of precipitating agents. Although lime is more typically used, alum results in lower concentrations of chromium in the effluent. The chromic hydroxide or sulfate sludge is dewatered by vacuum filtration, or directly landfilled.

Table III summarizes coagulation processes for treatment of copper-bearing municipal wastewaters.[11] The use of alum proved to be advantageous over iron, lime, and combinations of other precipitating agents in terms of attaining effluent limits of 0.02 mg/L. It has been shown, however, that most coagulants, including alum, are not as effective with complexed copper in wastes.[12]

Aside from precipitation of metals, alum and aluminum hydroxides have been utilized for primary clarification of organic wastes. Although generally less effective for organics than metals because of the higher solubilities, coagulation has proved to be cost-effective as a first step toward concentration reduction. For example, concentration of total organic nitrogen in conventional municipal wastewaters is shown in Table IV for various processes.[13] The use of alum was as effective as ion exchange for nitrogen reduction.

Destabilizing oil droplets and destroying emulsions via the addition of alum or aluminum hydroxide coagulants has been shown to be effective as a pretreatment to an ultrafiltration unit to separate oil and grease.[14] Table V summarizes typical options in the primary settling step. In some instances, the separation is good enough to use air flotation to gravity-filter the flocs in order to eliminate the requirement for the expensive ultrafilter.[15]

Table II. Comparative Treatment for Trivalent Chromium

System	pH	Cr^{3+} Conc. (mg/L) Initial	Final	Ref.
Lime	8.8	650	18	7
	7–8	140	1.0	8
Lime with sand filtration	8.5	7400	1.3–4.6	9
Electrolysis		2.1	0.1	10
Alum	6.4	0.7	0.017	6
Alum with carbon adsorption			0.006	6

Transition-Alumina Adsorption Chemistry

Transition forms of aluminum oxides have been used as adsorbents in water treatment. In contrast to the use of hydroxides as flocculants, where adsorption capacity is of secondary importance as a separation mechanism, the use of packed beds of adsorbents requires high affinities for waste compounds by the adsorbent media.

Alumina is a generic name for the oxides and hydroxides of aluminum. The phase chemistry is complex, with five thermodynamically stable phases (gibbsite, bayerite, nordstrandite, diaspore, and alpha), plus many metastable and transition forms. Sorption behavior varies extensively, depending on the morphology and synthesis methodology of the particular material. Most relevant for water treatment are the transition forms. Their surface chemistry, as related to adsorption phenomena in nonaqueous environments, has been discussed by the authors[16] and others,[17,18] as well as in other chapters in this book.

Adsorption of molecular species on aluminas from a bulk liquid-water medium represents a special case in adsorption with aluminas. It has been established[16] that affinity for water on aluminas is stronger than for virtually all other species. For this reason, the water-treatment industry typically assumes that the competition with water by all nonaqueous species is too strong and the resulting capacities will be low. This is a popular misconception and is typically incorrect for reasons to be discussed.

Initial contact of water with a well-degassed transition alumina results in irreversible chemisorption to form surface hydroxyls. A second layer of water is bound to the surface via hydrogen bonding of the water molecules to the surface hydroxyls and is sometimes described as quasi-chemisorption. Additional water molecules are physically adsorbed in multilayers onto the hydrogen-bound molecules. A schematic representation of this ordering is shown in Fig. 1. Considerable evidence for this structure on oxides, including heats of immersion,[19] dielectric dispersion measurements,[20] integral entropy of adsorption calculations,[21] and nuclear magnetic resonance studies[22] have shown the decreasing mobility of water with proximity to the surface.

Because of the inherent heterogeneity of aluminas, the formed hydroxyls exhibit a distribution of functionalities, ranging from very basic to partially acidic.

Table III. Treatment of Copper Wastewater*

Process	Chemical Addition	pH	Copper Conc. (mg/L)	
			Influent	Effluent
Alum	220 mg/L	6.4	0.7	0.022
Iron	45 mg/L Fe at $FeSO_4$	6.0	5.0	0.155
Low lime	260 mg/L lime, 20 mg/L Fe at $FeSO_4$	10.0	5.0	0.170
High lime	600 mg/L	11.5	5.0	0.352

*Ref. 11.

Table IV. Organic Nitrogen Removal

Process	% Soluble Organic Nitrogen Removed			% Soluble COD Removed		
	Avg.	Max.	Min.	Avg.	Max.	Min.
Lime (pH 11)	33	43	26	24	36	13
Alum (pH 6)	29	35	23	28	46	17
$FeCl_3$ (pH 6)	40	48	30	32	40	19
Anion exchange	12	20	9	30	34	23
Cation exchange	11	12	9	4	12	0
Activated carbon	71	92	52	81	93	68
Chlorination	42	48	39	18	28	10
Ozonation	14	28	6	46	53	41

*Ref. 13.

Table V. Oil and Grease Removal by Coagulation*

Industry	Treatment Chemical	Oil and Grease (mg/L)		
		Influent	Effluent	% Rem.
Paint manufacture	Sodium aluminate	1260	22	98
	Alum	1810	11	99
	Alum + lime	830	16	98
	Alum + lime + $FeCl_3$	393	91	77
	Alum + lime + polymer	980	22	98
	Alum + polymer	1700	880	48
Commercial laundry	Alum + polymer	15	4	73
Steel pickling	Lime	3	1	66
	Lime + polymer	650	6	99

*Ref. 15.

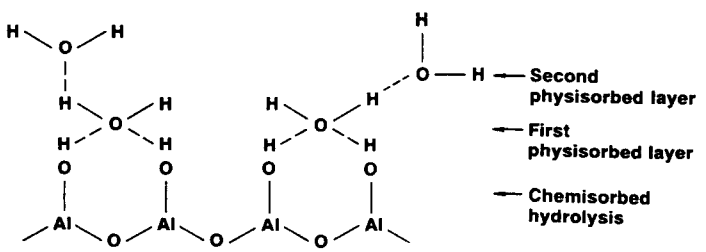

Fig. 1. Interfacial ordering of water (Ref. 20).

Coupled with the coordinatively unsaturated lattice sites, the resulting alumina surfaces are quite complex.

Adsorption on aluminas in aqueous systems, however, can be generally characterized by three mechanisms. Somewhat analogous to the gas phase, sorbing species can chemisorb to form a surface complex via covalent attachment to the alumina. To a degree, the hydroxylated alumina can be treated as a polymeric

oxyacid or base. Then, specific surface-coordination reactions (Reactions (3) and (4)) can occur by liquid exchange.

$$\text{Al-OH} + M^{z+} \rightleftarrows \text{Al-OM}^{(z-1)} + H^+ \quad (3)$$

$$2(\text{Al-OH}) + M^{z+} \rightleftarrows \text{Al-O}_{\text{Al-O}}\text{M}^{(z-2)} + 2H^+ \quad (4)$$

$$K_1 = \frac{[\text{Al-OM}^{(z-1)}]\,[H^+]}{[\text{Al-OH}]\,[M^{z+}]} \quad (E1)$$

$$\beta_2 = \frac{[(\text{Al-O})_2\,M^{(z-2)}]\,[H^+]^2}{[\text{Al-OH}]^2\,[M^{z+}]} \quad (E2)$$

The associated equilibrium expressions are given in Eqs. (1) and (2). In many cases, adsorbing species can be bound even against electrostatic repulsion. Obviously, the chemical binding energy must predominate over coulombic repulsion. Examples of metallic cation binding via chemisorption are given by the stability constants in Table VI, as modified by Schindler.[23] Coordination of selenium (as selenate) is an example of anion chemisorption with ligand exchange (Reaction (5)).[24]

$$\text{Al-OH} + SeO_4^{2-} \rightarrow \text{Al-O-SeO}_3^- + OH^- \quad (5)$$

For protonated anions, such as selenite, surface deprotonation of the ligand may occur with exchange (Reaction (6)).

$$\text{Al-OH} + SeO_2(OH)^- \rightarrow \text{Al-O-SeO}_2H + OH^- \rightarrow \text{Al-O-SeO}_2^- + H_2O \quad (6)$$

A second mechanism of adsorption, which is always present to some extent, is the electrostatic charge derived by surface protonation. As demonstrated in Reactions (7) and (8), all aluminas are amphoteric.

$$\text{Al-OH} + H^+ \rightleftarrows \text{Al-OH}_2^+ \rightleftarrows \text{Al}^+ + H_2O \quad (7)$$

$$\text{Al-OH} + OH^- \rightleftarrows \text{Al-O}^- + H_2O \quad (8)$$

Surface hydroxyls can be protonated to form positively charged surfaces (Reaction (7)) in an acidic medium and deprotonated (Reaction (8)) for a negative surface in a basic medium. The extent of charging and the point of zero charge (zpc) on a particular alumina are determined by the degree and type of hydroxyls and the extent of chemical modification of the surface.

Typical zpcs for aluminas range from pH 5 to 10,[25,26] but can be extended over a broader pH range by chemical modification. In Fig. 2, for example, the surface charge (as represented by zeta potential) for Alcoa CPN as a function of solution pH is shown to vary dramatically. Particular acidic or basic modification results in aluminas which can retain complete negative or positive charges, respectively. In this respect, transition aluminas are analogous to other transition-metal oxides with potential-determining ions adsorbed to their surface.[23]

Table VI. Representative Stability Constants for Surface Metal Complexes on a Transition Gamma Alumina*

Metal	log K_1	log β_2	I
Ca^{2+}	−6.1		0.1M $NaNO_3$
Mg^{2+}	−5.4		0.1M $NaNO_3$
Ba^{2+}	−6.6		0.1M $NaNO_3$
Pb^{2+}	−2.2	−8.1	0.1M $NaClO_4$
Cu^{2+}	−2.1	−7.0	0.1M $NaClO_4$

*Ref. 23.

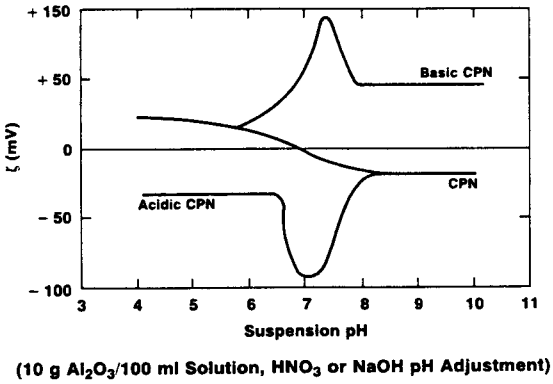

Fig. 2. Zeta potential of acid-base CPN.

The importance of electrostatic charging and the electric double layer as an adsorption mechanism are shown by example in Fig. 3. Adsorption of silver cations on various commercial alumina adsorbents, primarily a charge phenomenon under the given process conditions, as a function of solution pH, exhibits widely different efficiency, depending on the surface charge.

Adsorption on Alcoa CPN, a commercial transition alumina (amorphous and gamma with a 6 wt% hydroxyl content), increases dramatically as the zpc of 6.8 is overcome by the solution pH. Alcoa CP-7 (amorphous transition form, 5 wt% hydroxyls) and a basic CPN, materials with positive charges over most and all of the pH range, respectively, exhibit low

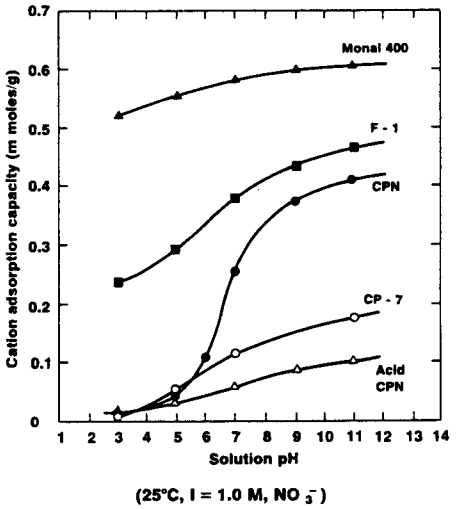

Fig. 3. Ag^+ adsorption isotherm for various alumina adsorbents.

adsorption affinities. There is very strong adsorption, however, on Alcoa Monal 400, a nontransition (pseudoboehmite) alumina with a strongly negative charge.

An example of anionic electrostatic adsorption is given in Fig. 4. Isotherms for the anionic dyes Orange II (OD) and Napthol Blue-Black (NB) are given as a function of pH for an HCl-modified alumina[12] and Alcoa CPN. Adsorption behavior is as expected for anions as predicted by the Gouy-Chapman-Stern-Graham model of electrostatic adsorption.[13]

The pH-zpc dependence of electrostatic adsorption can be utilized to obtain selectivity in multicomponent systems. In Fig. 5, for example, virtually pure copper (chemisorbing) or silver (electrostatic adsorption) can be recovered from each other by the proper choice of adsorbent and pH.

The third mechanism for adsorption with aluminas is ion exchange. Reactions (9) and (10) represent the primary exchange mechanisms for cation M^{2+}.

$$\text{Al-OH} \overset{OH^-}{\rightleftarrows} \text{Al-O}^- + H^+OH^- \overset{+M^{z+}}{\rightleftarrows} \text{Al-OM}^{(z-1)} + H^+OH^- \quad (9)$$

$$\text{Al-OH} \overset{H^+}{\rightleftarrows} \text{Al-OH}_2^+ \overset{X^-}{\rightleftarrows} \text{Al-OH}_2^+ \, X^-H \rightleftarrows \text{Al-X} + H^+OH^- \quad (10)$$

Exchange occurs via surface protons and hydroxyls and is favored for aqueous anions at low pH and cations at high pH. Although not usually considered to be important because of low exchange capacities (0.1 to 0.4 meq/g),[29,30] aluminas do have certain advantages. Compared with organic exchangers, aluminas can be more selective for certain ions (metals, sulfates, halides); they resist oxidation; they do not swell; and they offer superior physical properties in terms of

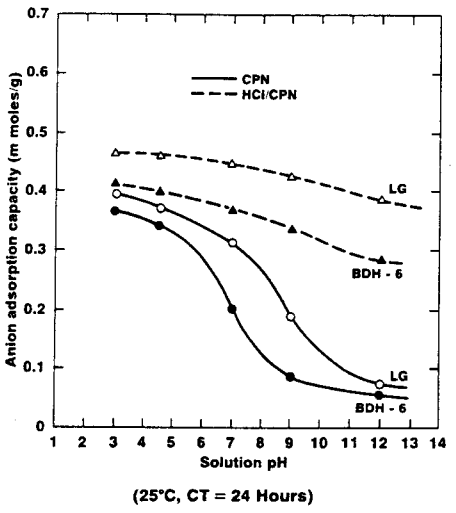

Fig. 4. Anionic dye adsorption isotherms (BDH 6 and Lissamine Green BN).

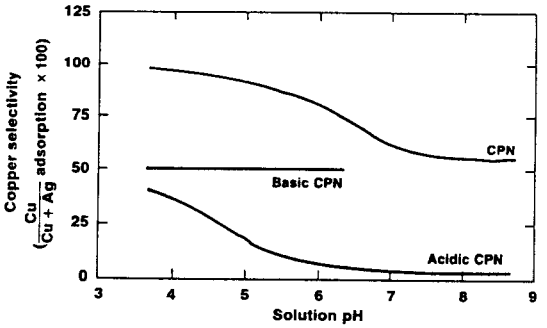

Fig. 5. Cu^{2+}/Ag^+ adsorption selectivity.

crushing strength, abrasion resistance, and minimal chemical solubility. Via chemical modification, their inherently low exchange capacities can be increased up to 1.2 meq/g. Although not intended as an ion exchanger, Alcoa SELEXSORB-W, for example, is a chemically modified alumina which possesses 0.75 meq/g exchange capacity with strong selectivity for certain cations.

Cation and anion exchange series for typical ions on transition aluminas are given in Table VII. As an example of ion-exchange separation of similar functionalities, various amines are fractionated by an acidic alumina in Fig. 6.[18]

Current Commercial Applications

Relative to activated carbon and ion exchange resins, aluminas are currently not used extensively in process and wastewater separations. Their strengths have historically been utilized in processing of specialty gases and organic liquids. Distribution of aluminas on a volume of adsorbent basis to their various application segments is shown in the related chapter on selective adsorption processes. Today, less than 2% of all aluminas are used in process and wastewater. Although outside the scope of this paper, another small segment (<2%) is utilized in product purification from water solutions in biological systems. Processing of organic liquids accounts for the single greatest segment (38%), although the distribution between usage in gases versus liquids is still in favor of the gas phase (60 vs 40%).

Table VII. Cation and Anion Selectivity Series on Transition Aluminas*

Cations
Th(II), Al(III), U(IV) > Zr(II), Ce(IV) > Fe(III), Ce(III) > Ti(III) > Hg(II) > UO_2(II) > Pb(II) > Cu(II) > Ag(I) > Zn(II) > Co(II), Fe(II) > Ni(II) > Tl(I) > Mn(II)
Anions
$OH^- > PO_4^{3-} > C_2O_4^{2-} > F^- > SO_3^{2-}$, $Fe(CN)_6^{4-}$, $CrO_4^{2-} > S_2O_3^{2-} > SO_4^{2-} > Fe(CN)_6^{3-}$, $Cr_2O_7^{2-} > NO_2^-$, $CNS^- > I^- > Br^- > Cl^- > NO_3^- > MnO_4^- > ClO_4^- > CH_3COO^- > S^{2-}$

*Refs. 12, 25, 31.

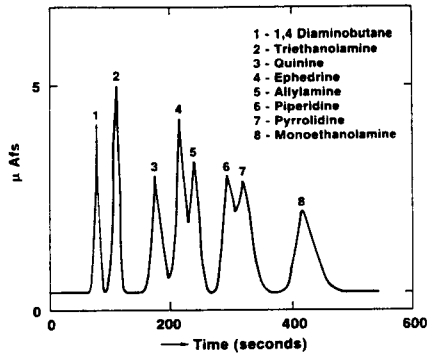

Fig. 6. Separation of actionic compounds on CG-20 alumina.

Removal of excess fluoride ion from municipal waters via a transition alumina is commercially accepted technology and is a good example for illustrating alumina adsorption processes in water. A schematic of the continuous removal of fluoride is given in Fig. 7. Typically, dual bed adsorbers are used for continuous separation. One bed adsorbs the fluoride while the other is in a regeneration mode. Once the first bed is spent and the second is reconditioned, feedwater flow is switched to the opposite beds and the process is continued.

Unlike gas-phase operation, spent alumina beds in water treatment can be regenerated by more than one step. Operation of fluoride units for regeneration is atypical in that both backwash and neutralization steps are necessary. Most water applications require only some type of regeneration (e.g., pH swing) and a minimal rinse.

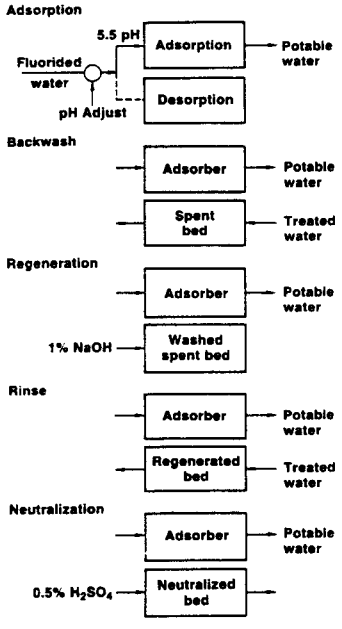

Fig. 7. Fluoride adsorption.

Typical performance for a unit removing fluoride from a municipal water supply is 1400 bed volumes with Alcoa F-1 alumina of 5 mg/L fluoride with an effluent of less than 0.8 mg/L.[35] Capacities are somewhat increased through the use of an adsorbent designed specifically for fluoride, such as Alcoa AG-1. An economic comparison of adsorption with lime precipitation and alum treatment for fluoride treatment[36] concluded that adsorption with aluminas is competitive with alum treatment down to 10 mg/L and is both technically and economically superior for effluents which must be discharged below 10 mg/L.

An application sometimes related to fluoride treatment is the removal of arsenic from water supplies. Typically, trivalent and pentavalent arsenic have been treated with Alcoa F-1 (a granulated amorphous/gamma form designed for liquid-phase adsorption) of an inlet stream of 0.1 mg/L arsenic with removal to less than 0.01 mg/L with a capacity of more than 900 bed volumes.[37] The regeneration cycle is similar to that of fluoride, except for a backwash, and is completely reversible. This capacity can be increased by almost an order of magnitude, however, by adjustment of the stream pH to 3 to 5,[38] or further by the use of a synthetic alumina.

Speciation of the arsenic is intimately related to its adsorption behavior. Depending on the arsenic source, both 3+ and 5+ oxidation states of As exist in species ranging from H_3AsO_4 to AsO_4^{3-}. Adsorption being most effective for the pentavalent $H_2AsO_4^-$ and H_3AsO_3 species, removal capacity can be increased by preoxidation of the inlet water by chlorine, for example.[39]

Adsorption with aluminas has been used to eliminate colloidal silica which fouls ion-exchange columns in high-silica California waters. There is evidence to suggest that $Si(OH)_3O^-$ is the species being adsorbed.[40] Optimum removal is accomplished at a pH of 7 to 8 with a specific adsorbent, such as Alcoa CPN-800 (acidic gamma form, large pores). Under typical conditions, capacities range up to 0.3 mmol/g with a totally regenerable (by 1*M* NaOH) system. There is little interference from competing ions.

Inorganic phosphates, including orthophosphates ($H_2PO_4^-$, HPO_4^{2-}, and PO_4^{3-}), pyrophosphate ($P_2O_7^{4-}$), tripolyphosphate ($P_3O_{10}^{3-}$), and hexametaphosphate ($(PO_3)_6^{3-}$), are being removed from municipal and groundwaters using aluminas. Using F-1, Yee[41] and others[42,43] showed that large-scale treatment costs of $64/million gallons were realized with a total phosphate removal of greater than 90%. Use of an acid-treated Alcoa CPN, with a stream pH adjusted to 7.5, increases the phosphate loading to greater than 1000 bed volumes with a removal down to less than 0.5 mg/L from 20 mg/L. The use of an alumina in phosphate treatment is straightforward, with the conversion of total phosphorus to orthophosphate (the most

effective adsorbing species), followed by a lime precipitation of the concentrated phosphate wastes.

Removal of anionic dyes from textile and pulp wastewaters via alumina adsorption has been of considerable interest in recent years. As shown in Fig. 8 for the representative dyes Orange G (OG) and Lissamine Green BN (LG), adsorption capacities of greater than 0.3 mmol/g can be obtained with the chemically modified alumina Alcoa SELEXSORB-D. Capacities of an order of magnitude lower are found with F-1, a more generic adsorbent in this application. In both cases, removal of greater than 90% is accomplished with wastewaters containing from 5 to 20 mg/L dye with an effluent of <0.5 mg/L. Regeneration is complete and is usually accomplished with an alkaline salt, such as Na_2SO_4, rather than a base.

Removal and reclamation of trace quantities of waste metals from catalyst production facilities has been a commercial application of adsorption with aluminas over the past 10 years. Representative metals include silver, copper, and cobalt, which are usually present in wastewaters at concentrations below 10 ppm. Silver removal is exemplified in Fig. 3. Although F-1 is a typical commercial adsorbent for this application with good capacity (0.46 mmol/g), it can be seen that the proper choice of alumina adsorbent, as well as pH, is necessary. Reclamation is usually accomplished with a base desorption followed by precipitation of the metal from the concentrated regenerate stream.

Most metals of interest are removed with higher efficiencies than silver. Although not as good as the SELEXSORB series, typical capacities on CPN for copper and cobalt are 0.52 and 0.82 mmol/g, respectively. Following adjustment to the appropriate pH, an example of selective removal of catalyst waste metal recovery was given in Fig. 5 for virtually complete separation of pure copper and silver from a wastewater. Such a process typically requires at least two beds with selective adsorbents for each component to be recovered in each bed.

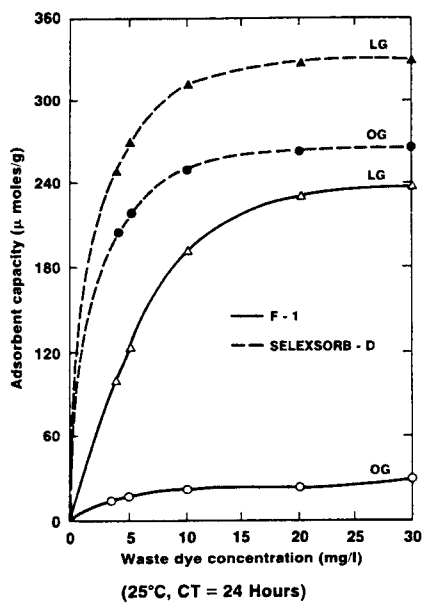

Fig. 8. Dye adsorption isotherms.

Removal of mercury from well waters represents an interesting alumina adsorbent application. Typical mercury capacities on transition aluminas are not economically attractive (0.08 mmol/L on Rhone-Poulenc* CR-30 for <50% recovery). The formation of a sulfide surface on the alumina allows reactive adsorption to occur, with the formation of mercuric sulfide. Although not regenerable, the capacity is then upward of 0.5 mmol/g, with a removal to less than 0.1 mg/L from waters of 2 to 5 mg/L mercury.

Potential Applications

Because of the tremendous versatility in selecting adsorption efficiency offered by current alumina modifications technology, there would appear to be strong potential for use of these materials in solving water problems. It is important, however, to distinguish between commodity alumina adsorbents, which are designed for general use with no strong affinity or selectivity for any functional groups, and selective materials with high concentrations of relevant active sites. An example of a generic material would be Alcoa F-1, for liquid-phase application. The SELEXSORB series, chemically modified for particular affinities, is specific to applications. Use of generic aluminas for tertiary water treatment is quite limited, while the application of engineered aluminas is potentially attractive.

A discussion of all possible applications would be unwieldy due to the diversity of water-treatment problems. The following examples will serve to illustrate potential processes using specialty aluminas for wastewater treatment.

Selenium removal from groundwater presents a challenge in certain geographical areas of the United States today. Concentrations as great as 200 ppb Se (preferably Se^{4+}, but also possible with Se^{6+}) can be economically removed using alumina adsorption technology. Literature published to date by the EPA and others[24,44] places removal efficiency at 1200 bed volumes at pH 5 for an efficiency of greater than 98% with Alcoa F-1. However, because of the high chemical impurity level in F-1, resulting in a high zpc, coupled with its inherently low chemisorption capacity, this material is a poor choice as an adsorbent for selenium in any form. Neither the adsorbent nor process are optimized in this technology. Work at Alcoa has resulted in a material which, when combined with the proper process chemistry and oxidation state adjustment, results in major improvements in capacity. Additionally, because the adsorbent is selective for selenium, the influence of competing ions (e.g., sul-

*Rhone-Poulenc, Paris, France

fate) is markedly reduced, and chelated selenium, such as that found in disposal sites, may be addressed.

Removal of dissolved organics from water has traditionally been considered the domain of activated carbon. It is true that, for the vast majority of organic substances, the high degree of van der Waals interactions of carbon surfaces with solute carbon skeletons makes carbon attractive as a separation media. There are, however, many organic species which might be better separated with selective aluminas. Examples are given below.

There are substituted phenols which present many environmental problems in a number of industries. Phenols are chemisorbed to Lewis acid sites on selective aluminas[45] through the oxylinkage of the phenol with great affinity. Examples of their affinity are shown in Fig. 9. A good carbon for liquid-phase adsorption of 2,4 dinitrophenol is shown for reference. The capacity is good, rising somewhat linearly up to 50 mmol/g at 100 mg/L DNP. Monal-400 is a highly efficient alumina for phenols, with almost an order of magnitude increased capacity over carbon at low DNP concentrations. Because of the different adsorption mechanisms between carbons and aluminas, the isotherms for aluminas are very favorable at low concentrations. There is less concentration sensitivity because the affinity for covalent bonding is as great at low concentrations of the solute as at high levels. For comparison, CPN, a nonselective alumina, is shown to have as good a capacity as the carbon. Yet, it exhibits only 40% of the capacity of that observed with Monal 400.

Alumina-based adsorbents preferentially adsorb the phenols over benzene and certain derivatives.[46] This can be useful when selective recovery is of interest, and is another major difference from carbon. Regeneration is accomplished in situ by either chemical desorption with methanol, salts, or caustic, or can be done thermally for gas-phase evolution of the phenol. The aluminas are not affected by the thermal treatment and are ready for a second cycle.

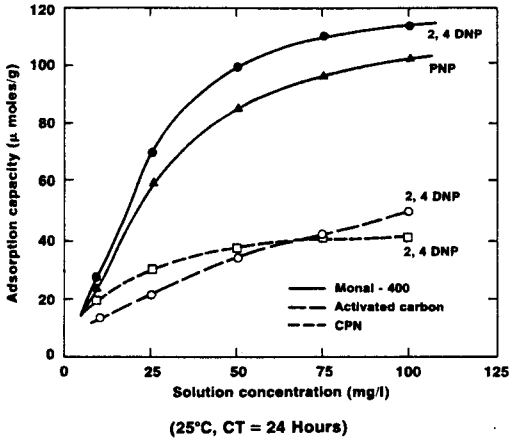

Fig. 9. Adsorption isotherms–substituted phenols.

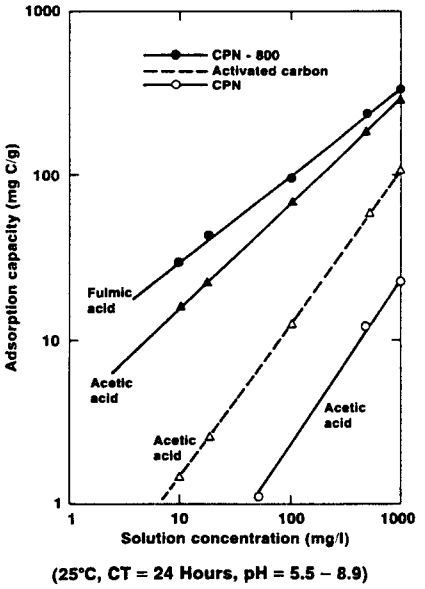

Fig. 10. Adsorption isotherms of organic acids in water.

Organic acids, particularly carboxylic acids, have good potential for removal by aluminas from water. Their affinity for aluminas is greater than for carbons, primarily due to their strong covalent attachment through carboxylate to the oxide surface. This may become significant in water applications for three reasons. First, at high carbon number, their affinity increases with carbon number up to approximately 20 000 molecular weight. The opposite is true for low carbon number, C = 1 to 10. The affinity for aluminas is greater at C = 1 than at C = 8, for example. Of course, the affinities for activated carbon increase with increasing carbon number in this range.

This is opposite to carbons in this range and implies that aluminas have a niche in high molecular weight compounds, those generally found in groundwaters, that carbon cannot handle. Second, the mechanism is primarily chemisorption, so that they have a good affinity at low concentrations. This is demonstrated in Fig. 10 for acetic acid on CPN-800. The liquid-phase carbon not only exhibits lower capacity across the concentration range, it is more sensitive to concentration changes. Third, humates in water are becoming more of a problem. Proper aluminas can address the problem. An isotherm for humic acid is given for CPN-800 which shows capacity actually better than the lower-order acetic acid. It should also be noted that capacities over three orders of magnitude can be obtained with a poor choice of media, as demonstrated by CPN.

Utilizing the strengths of both carbon and aluminas would appear to have merit. A front bed of a selective alumina for removal of lower-order humates and other organic acids, followed by carbon for paraffinic compounds, should be a useful concept in groundwater treatment, for example. Eberle et al.[47] demonstrated

pilot-plant success using a nonspecific alumina (Compalox)[†] lignin derivative in the pulp and paper industry without the use of carbon.

Trihalocarbons (THCs) are of growing concern in groundwater contamination. Their volatility and low affinity with conventional adsorbents have resulted in a lack of sufficient separation procedures for environmental safety. Based on proprietary alumina-based adsorbents, two potential cleanup processes are depicted in Fig. 11. In the first, THC is adsorbed from groundwater, followed by hydrothermal decomposition to acid and CO_2. The acid is subsequently removed in a second adsorption step with a selective material. In the second potential scheme, THC is first decomposed by ozonation, followed by adsorption (enhanced by ozonation) onto an alumina selective for the degraded acidic products. Regeneration here requires either a salt-splitting step, acid neutralization, or concentration for reuse as a valuable by-product. In practice, however, adsorption capacities have been found to be quite low. It is questionable whether such a process is economically viable.

As touched on earlier, heavy metals as a group constitute a potential area of future adsorptive separations using aluminas. Virtually any transition or lanthanide series metallic species can be adsorbed onto aluminas, as well as most other transition-metal oxides. Affinities are particularly strong at low concentrations and for transition metals. Although not an optimum material, isotherms for various metals on CPN are given in Fig. 12. Both adsorption and surface-induced precipitation are operable mechanisms in metals removed with aluminas.

An example application is the conceptual process for polishing of chromium electroplating wastes given in Fig. 13. The metal-containing wastewater enters the adsorption unit, which is selective for the metals of interest. Depending on the stream, some pH or valence adjustment (i.e., Cr^{6+} reduced to Cr^{3+}) chemistries are applied prior to the column. The effluent water can either be reused in the process or discharged. The metal is regenerated from the spent bed by chemical desorption and is recovered either as the metal (electrolytically) or as a useful salt (precipitation from the concentrate).

This generic process is applicable to most metal-containing systems. Selective recovery of one metal from others can be accomplished in certain cases. Organically chelated metals in chemical waste dumps also have potential for treatment by this mechanism.

One final application worthy of note is the treatment of amine-containing waters. The chemical industry and municipal treatment facilities, among others, require removal of low-level ammonia and methylamines. A chemically modified alumina, called SELEXSORB-NH3, has been developed to remove amines. Not only does it provide a strong affinity at

[†]Aluswisse, Martinswerk, Federal Republic of Germany.

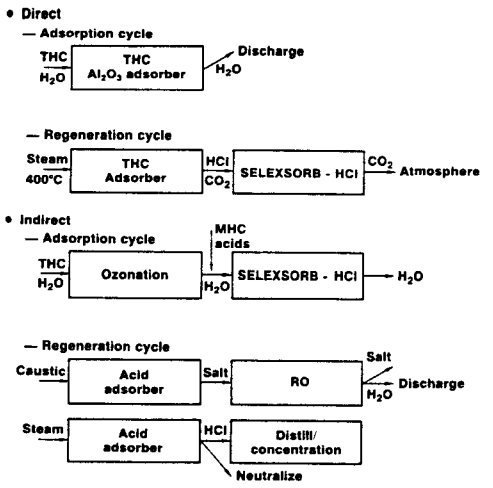

Fig. 11. Conceptual trihalocarbon separation process.

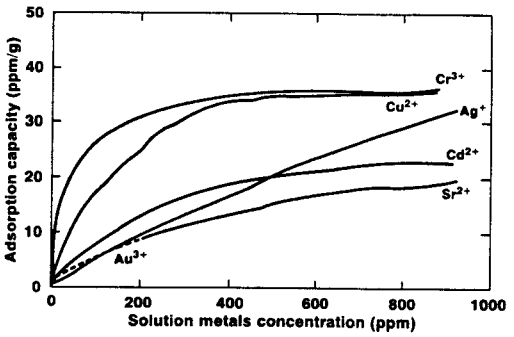

(10 g Al_2O_3/100 g solution, 25°C, pH 5.0, Alcoa CPN, No_3^-)

Fig. 12. Metals removal isotherms.

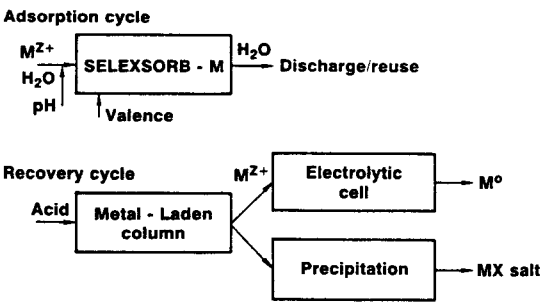

Fig. 13. Metal adsorption recovery process.

low concentrations, but is selective over some competing salts and ionic species. In the Alcoa process, the ammonia is stripped as volatile ammonia or is recovered for reuse as an ammonium salt.

One alternate concept should be discussed briefly. Previous application examples have focused on the requirement for chemically modified surfaces for preferential attachment. An additional requirement in alumina manufacture is the need for optimum pore structures. Inefficient diffusion to the surface to accomplish the separation would result in unfavorable economics. In Fig. 14, this concept is illustrated for humic acid.

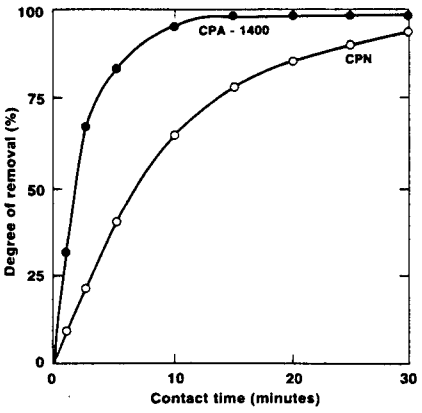

Fig. 14. Kinetics of humic acid elimination.

Good kinetics on CPA-1400, a controlled macroporous transition alumina with pores of 140 μm (1400 Å) is shown to be favored over the more microporous CPN with an average pore diameter of 6.2 μm (62 Å). In addition, the equilibrium removal efficiency is greater in the material with greater pore size, possibly due to steric limitations of the high molecular weight humate fractions.

Conclusions

Alumina-based chemicals represent a major constituent of the water-treatment industry. Uses are varied and range from primary coagulation of high-concentration effluents to polishing of drinking water to meet EPA discharge requirements. Because of the versatility of alumina chemicals, and the increasing understanding of their properties, the use of these materials should continue to grow. As environmental requirements for water conservation and management grow more stringent, alumina chemicals will find novel applications.

References

[1]J. Y. Bottero, F. Thomas, and A. Leprince, *Aqua*, **2**, 73 (1983).

[2]W. L. Masterton and E. J. Slowinski, Chemical Principles, 3d ed. W. B. Saunders Co., Philadelphia, 1973.

[3]The Economics of Clean Water, Vol. 3, Inorganic Chemicals Industry Profile, USDI, Washington, D.C., 1970.

[4]L. G. Sillen and A. E. Martel, Stability Constants of Metal-Ion Complexes, 2d ed. Special Publication 17, Chemical Society, London, 1964.

[5]T. Maruyama, S. A. Hannah, and J. M. Cohen, *J. Water Pollut. Control Fed.*, **47**, 962 (1975).

[6]S. A. Hannah, M. Jelus, and J. M. Cohen, *J. Water Pollut. Control Fed.*, **49**, 2297 (1977).

[7]L. K. Wang, et al., *Water Wastes Eng.*, **10**, 20 (1973).

[8]P. I. Aurutskii, *Chem. Abstr.*, **70**, 206 (1969).

[9]E. H. F. Stone, Proceedings of the 22nd Industrial Waste Conference, Purdue University, 848 (May, 1967).

[10]I. F. T. Kennedy and S. D. Gupta, *Fin. Manag.*, 7 (July, 1978).

[11]T. Maruyama, S. A. Hannah, and J. M. Cohen, *J. Water Pollut. Control Fed.*, **47**, 962 (1975).

[12]K. J. Yost and A. Scarfi, *Fin. Manag.* (July 19–24, 1978).

[13]S. J. Randtke, et al., USEPA 600/2–78–030 (1978).

[14]W. Cawley (ed.) Treatability Manual, Vol. III, Technologies for Control/Removal of Pollutants, USEPA 600–8–80–042–C (July 1980).

[15]D. A. Roberts and D. S. Yeaple, 48th Annual Meeting of Water Pollution Control Federation, Miami Beach (October 6, 1975).

[16]K. P. Goodboy and H. L. Fleming, *Chem. Eng. Prog.*, **80** [1] 63 (1984).

[17]K. Wefers and G. M. Bell, "Oxides and Hydroxides of Aluminum," Technical Paper No. 19, Aluminum Company of America, Pittsburgh, PA, 1972.

[18]H. Knozinger and P. Ratnasamy, *Catalysis Rev.-Sci.Eng.*, **17** [1] 31 (1978).

[19]F. Dumont and A. Watillon, *Disc. Faraday Soc.*, **52**, 352 (1971).

[20]E. McLafferty and A. Zettlemoyer, *J. Colloid Interface Sci.*, **34**, 452 (1970).

[21]E. McLafferty and A. Zettlemoyer, *Trans. Faraday Soc.*, **66**, 1732 (1971).

[22]R. T. Pearson and W. Derbyshire, *J. Colloid Interface Sci.*, **46**, 232 (1974).

[23]W. Stumm, H. Hohl, and F. Dalang, *Croatica Chem. Acta*, **48** [4] 491 (1976).

[24]M. M. Ghosh, J. R. Yuan, R. J. Schlicher, and S. M. Hornung, *Proc. Water Poll. Cont. Fed. Conf.*, New Orleans (9/84).

[25]G. A. Parks, *J. Phys. Chem.*, **66**, 967 (1962).

[26]R. Fricke and H. Keefer, *Naturforsch.*, **4A**, 76 (1949).

[27]G. L. Mundhara, M. P. Tiwari, and J. S. Tiwari, *J. Ind. Chem. Soc.*, **LVII**, 404 (1980).

[28]R. O. James and T. W. Healy, *J. Colloid Interface Sci.*, **40**, 42 (1972).

[29]M. J. Fuller, *Chromat. Rev.*, **14**, 45 (1971).

[30]E. Lederer and M. Lederer, Chromatography, Elsevier, Amsterdam, 1957.

[31]C. P. Huang and W. Stumm, *J. Colloid Interface Sci.*, **43** [2] 409 (1973).

[32]F. H. Pollard and J. F. W. McOmie, Chromatographic Methods of Inorganic Analysis, Butterworths, London, 1953.

[33]H. Kulbi, *Helv. Chim. Acta*, **30**, 453 (1947).

[34]C. Laurent, H. A. H. Billiet, and L. deGalan, *Chromatographia*, **17** [5] 253 (1983).

[35]F. Rubel and R. D. Woosley, EPA 570/9-78-001, U.S. Environmental Protection Agency, Washington, D.C., 1978.

[36]C. L. Parker and C. C. Fong, *Indust. Wastes*, **23** (11–12/75).

[37]E. Bellack, *J. AWWA*, 454 (7/71).

[38]M. M. Ghosh, et al., *Proc. Water Pollut. Control Fed. Conf.*, New Orleans (9/84).

[39]Y. S. Shen, *J. AWWA*, **65**, 543 (1973).

[40]D. Clifford, J. Mason, and R. Kennedy, University of Houston Lecture (1979).

[41]W. C. Yee, *J. AWWA*, **58**, 239 (1966).

[42]R. D. Neufield and G. Thodos, *Eng. Sci. Technol.*, **3** [7] 661 (1969).

[43]L. L. Ames and R. B. Dean, *J. Water Pollut. Control Fed.*, **42**, 161 (1970).

[44]R. R. Trussell, A. Trussell, and P. Kreft, EPA–600/2–80–153 (8/80).

[45]D. R. Taylor and K. H. Ludlum, *J. Phys. Chem.*, **76** [20] 2882 (1972).

[46]G. L. Mundhara and M. P. Tiwari, *J. Ind. Chem. Soc.*, **LVII**, 306 (1980).

[47]S. H. Eberle, et al., U.S. Dept. Commerce NTIS PB–265 359–T, 380 (1976).

Claus Catalysts and Alumina Catalyst Materials and Their Application

Judith C. Downing and Kenneth P. Goodboy
Aluminum Company of America
Pittsburgh, Pennsylvania 15219

Aluminas, in their many phases and forms, have unique characteristics that allow them to be the most versatile and widely used heterogeneous catalyst support and optimum catalyst in certain applications. The properties, manufacturing processes, and applications are discussed for major alumina catalyst markets.

Aluminas used in catalysis are usually prepared through the dehydroxylation of various aluminum hydroxides, as described in previous chapters. This material preparation creates various crystalline forms, depending on the time/temperature/environment history during production. The aluminas vary in impurities, primarily sodium, silicon, titanium, and iron, depending on the manufacturing process and selection of raw materials. These impurities have a bearing on the selection and suitability of aluminas as a catalyst or catalyst support. Some forms of alumina have the unique characteristic of being self-binding and, with the right forming technology, will form a very strong pellet or sphere.

The major phases of alumina that are used in catalytic processes are eta and gamma transitional phases, which are characterized by high surface area and relatively high thermal stability over the temperature range of application (50°–70°C). They are similar in structure and cannot be easily distinguished by X-ray diffraction procedures.

Eta alumina is preferred over gamma alumina in acid-catalyzed reactions such as isomerization due to the higher number of Lewis and Bronsted acid sites (exposed Al^{3+} and OH^- sites, respectively). For catalytic hydrotreating, gamma alumina is preferred because of the high thermal and hydrothermal stability.

Alpha alumina and high-order transitional phases are also used but in smaller quantities. Alpha alumina offers high strength and ultra thermal stability as a catalyst support for high-temperature reactions such as ethylene oxide, steam reforming, or CO-shift catalysts.

Other catalysts and catalyst supports may use combinations of alumina phases. Claus catalysts and some hydrogenation catalyst supports utilize moderately pure activated alumina made from Bayer process-quality aluminum trihydroxide. Made through processes described in other chapters, this alumina is in the form of chi, rho (amorphous), and eta alumina. The three phases in combination yield a very high-strength, high-surface-area (275–375 m^2/g) support.[1–4]

Alumina as a Catalyst Support

Alumina catalyst supports are found in a wide variety of applications. Two of the largest applications are hydrotreating (hydrodenitrogenation and hydrodesulfurization) of petroleum feedstocks and auto exhaust oxidation catalysts. Other significant market applications are ammonia synthesis, petroleum reforming, hydrocracking, hydrogenation of edible and inedible oils, dehydrogenation, methanation, and oxychlorination.[5] The volume of alumina extruded catalyst supports is estimated as 50 million pounds annually. An additional significant volume is spheroidized, tableted, or formed in other manners.

Alumina catalyst carriers vary significantly in properties, depending on the application and role they play in the reaction. Berrebi and Bernusset[6] place the carriers in the following categories:

1. *Inert Carriers*. These are alpha aluminas having a low surface area (<20 m^2/g) and can withstand severe process conditions because of high strength and chemical and thermal resistance. Due to their inert properties, this carrier does not promote undesirable side reactions or loss of selectivity.
2. *Interacting Carriers*. The catalyst component reacts with the alumina surface, thus promoting surface dispersion and resulting in maximum catalytic active surface sites. This promotes stability by retarding migration of the catalytic agent during use.
3. *Synergistic and/or Bifunctional Carriers*. This type of carrier not only serves as a support for the active catalyst but also contributes to the catalyst's performance. For example, in reforming catalysts the acid surface sites of the alumina aid the isomerization reaction, while the precious metal promotes dehydrogenation. Bifunctional catalysts are often supported on gamma-phase alumina and have surface areas of 200 to 300 m^2/g.

Critical properties to consider in selecting an alumina support are listed in Table I. Surface area is important since the rates of some catalytic reactions depend to a large extent on the number of available active sites. Porosity and pore-volume distribution

Table I. Critical Properties of Alumina Catalyst Supports

Chemical Impurities
Na
Si
Cl
Fe
Mo
Ni
Co
S
Ca
Mg
Ti
Physical Properties
Surface chemistry and acidity
Surface area, BET
Pore volume (H_2O)
Pore volume (H_g) > 3 nm diameter
Pore volume (N_2)
Pore volume distribution (Hg)
Compacted bulk density
Apparent bulk density
Pellet size
Pellet shape
Crush strength
Attrition resistance
Abrasion resistance
Particle-size distribution
Bed void fraction
Thermal stability
Hydrothermal stability

determine accessibility of reactants to the active catalyst sites as well as catalytic stability, resistance to fouling, heat transfer, and ease of impregnation of the catalytic agent on the support. Surface area and porosity can be varied independently within a limited range. Figures 1 and 2 give some examples of how these properties may be modified. Alcoa's CSS and LDS are commercial alumina supports that can be

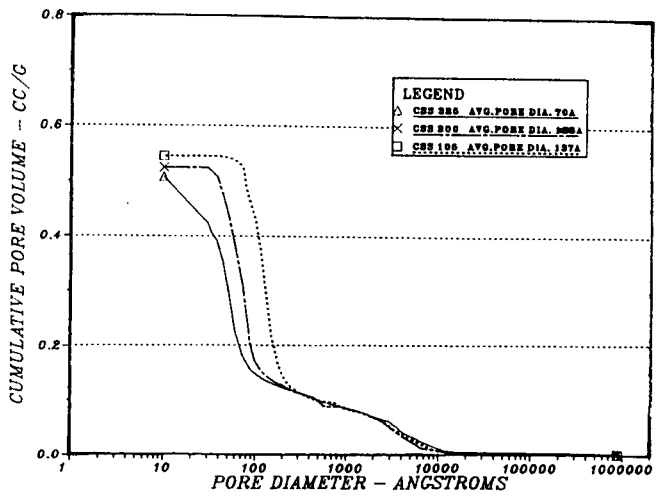

Fig. 1. Cumulative pore distributions of CSS spheres.

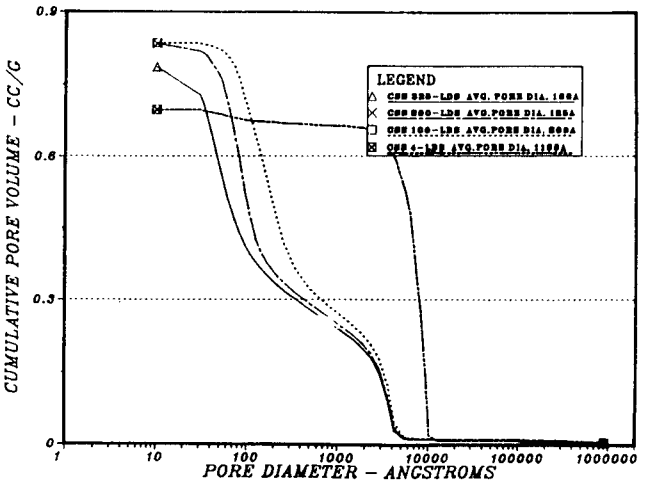

Fig. 2. Cumulative pore distributions of low-density spheres.

custom processed to yield desired surface area and pore-volume distribution requirements.

Pores in the range of 2 to 50 nm (20 to 500 Å) are formed in the alumina dehydration process and are often of importance in catalyst performance. Larger pores are formed during the agglomeration of finer particles. The function of pores <2 nm is determined by the application. These pores may advantageously provide size selectivity to molecules entering the interior of the catalyst or detrimentally be rapidly blocked by carbon deposition. Reaction products may not be able to diffuse out of these micropores and subsequently undergo secondary reactions. For this reason, catalyst pore distribution is often optimized in the 10 to 50 nm diameter region in reactions such as hydrodesulfurization.

Strength and physical integrity requirements are also determined by the application. Attrition resistance is critical in a fluid or ebullating bed process but of lesser importance in a fixed bed process unless there is a risk of loss of precious metals from the catalyst surface. Crushing strength can determine the maximum allowable depth of the catalyst in a reactor.

Thermal and hydrothermal stability becomes critical in applications involving high temperature or water vapor, particularly if a high-surface-area support is employed. Thermal deactivation occurs by the further dehydroxylation or the sintering of fine crystallites, characterized by loss of surface area or collapse of micropores. The rehydration of dehydroxylated phases of alumina is a result of hydrothermal instability in high-temperature, steam-containing processes. Hydroxyl groups attach to the active sites and cause phase transformation to aluminum oxide hydroxide (AlOOH) or aluminum trihydroxide [$Al(OH)^3$].

Because of space limitations, only a few major applications of alumina catalyst supports, their catalytic components, and important alumina properties

will be discussed here. A broader list of alumina catalyst support applications may be found in Table II.

Automotive Exhaust Catalysts

Federal legislation in the United States went into effect for 1975-model automobiles to control the emissions of three pollutants: hydrocarbons, CO, and NO_x. These emissions may be reduced to some extent by internal combustion engine modifications and precise control of air/fuel ratios. But, with a few exceptions,the specified emission levels could be met only by the use of a catalyst.

Until recently, the automobile exhaust catalyst market was focused in the United States. With the increase in foreign car imports to the United States and pending emission control regulations throughout the world, the demand for alumina as an automotive catalyst support has grown to as much as 20 million pounds annually.

Automotive exhaust catalysts are produced in two forms, monolith and pelleted. The two subsequent chapters provide in-depth information on monolith and pelleted catalyst systems, respectively.

The monolith is a cordierite (magnesium aluminum silicate) or metal honeycomb, coated with a high-surface-area layer of alumina. To prepare a monolithic support, the monolith is dipped into a pseudoboehmite, boehmite, or gamma alumina slurry, then dried or, in the case of the monohydrate coating, is calcined to a gamma-phase alumina. Important characteristics of the alumina are pore structure, thermal stability of the surface area, and the capability of producing high-solids, low-viscosity slurries for processing ease.

The other type of catalyst is produced using a 3.5-mm, highly porous alumina sphere. Important characteristics include pore structure, thermal capacity, thermal stability of the surface area, and resistance to attrition and abrasion.

Platinum, palladium, and rhodium are applied as catalytic agents on the alumina surface. The reaction is highly mass transfer-limited after the engine reaches operating temperature and the catalyst surface is 400° to 700°C. Also, the catalyst surface tends to be poisoned by fuel impurities and carbon. The most effective use of the precious noble metals is the application of a thin layer slightly below the outer surface of the support.

Table II. Major Catalyst Support Applications for Alumina

Refinery Catalysts
Claus
Hydrocracking
Hydrogenation
Hydrotreating
Reforming
Isomerization
Fluid catalytic cracking
Chemical Catalysts
Ethylene oxide
Hydrogenation
Isomerization
Oxychlorination
Pollution Control
Automobile exhaust
SO_x

Platinum is more active for the oxidation of paraffinic hydrocarbons, palladium for the oxidation of carbon monoxide and unsaturated hydrocarbons. The more stringent limitations for NO_x emissions were set in 1981 and later years forced development of the three-way catalyst, which employs rhodium in combination with the platinum to control reduction of the NO_x to N_2 (and not NH_3).

$$CO + 0.5\,O_2 \rightarrow CO_2$$
$$C_3H_6 + 4.5O_2 \rightarrow 3CO_2 + 3H_2O$$
$$NO + CO \rightarrow CO_2 + 0.5N_2$$

Hydrotreating Catalysts

The sulfur, nitrogen, and metal content of crude oil varies significantly with its origin. Highly paraffinic crudes from North Africa may have 0.2% sulfur and 3 ppm metal content, while the Venezuelan crude contains as high as 4% sulfur and 500 ppm metals. The selection of crude oils for refinery processing is determined by crude availability, economics, refinery capabilities, and products desired.

Reduction of sulfur, nitrogen, and metal content of petroleum fractions is necessary for protection of reforming, isomerization, and hydrocracking catalysts, meeting air pollution standards for fuel oils, minimizing catalytic cracker SO_x generation, and corrosion reduction. The process to accomplish this is hydrotreating, or, specifically, hydrodesulfurization (HDS), the catalytic treatment of the petroleum fraction with hydrogen to convert the various sulfur compounds to hydrogen sulfide.

The sulfur in crude oils is primarily present in the form of thiols (mercaptans), sulfides, disulfides, and various thiophenes. The following reactions are examples of mercaptans and sulfides reacting to form H_2S and hydrocarbons (R and R′ and various hydrocarbon groups).

$$RSR' + 2H_2 \rightarrow RH + R'H + H_2S$$
$$RSSR' + H_2 \rightarrow RH + H_2S$$
$$RSH + H_2 \rightarrow RH + H_2S$$

Additional reactions occur during this process. Some desirable reactions are hydrogenation of diolefins, hydrodenitrogenation, and hydrogenation of multiring aromatics to single-ring compounds.[7]

Operating conditions of a hydrotreating unit will vary significantly with the particular distillate fraction to be treated and the severity of other reactions required. Low and middle boiling point distillates require less severe temperatures and pressures than

residual oils, for instance. The catalyst also is typically developed for specific fractions and processing conditions.

Hydrotreating catalyst manufacture consumes the highest volume of alumina catalyst supports in the petroleum refining industry, annually estimated to be 65 to 90 million pounds worldwide. The catalysts are most commonly cobalt-molybdenum or nickel-molybdenum oxides supported on alumina extrusions. Some specialty catalysts are spherical or may be alumina/silica supported.[8]

Catalysts for use in distillate hydrotreating applications typically have the major pore volume in pores smaller than 10 nm in diameter. Most hydrotreating catalysts, however, have more open porous structures and possess a significant volume of pores larger than 100 nm in diameter to improve thermal and hydrothermal stability and aid diffusion of larger hydrocarbon molecules.

The desired combination of pore-volume distribution, surface area, strength, and surface acidity determines the type of alumina catalyst support precursor and processing techniques. Boehmite or pseudoboehmite aluminas are available in a range of purity and capacity to produce varied pore distributions. Dispersibility of the alumina to colloidal-sized particles in an acid environment determines the meso- and macropore structure of the extrudate. Further manipulation can be accomplished by thermal treatments and modification of the mulling conditions (water and acid contents and level of shear).[9]

A typical process to produce an extruded hydrotreating catalyst incorporates a mix-mulling step where the pseudoboehmite is mixed with water and a monovalent acid to form a doughlike substance. The mulled alumina mixture is fed to an extruder, forcing the alumina through a die to produce spaghetti-like extrusions of various shapes. The shapes are either cut to the proper length with a knife blade or are broken in further processing.

The extrudates are then dried and calcined to a high surface area gamma-phase structure (400°–700°C). The catalytic metals are applied either through impregnation of solutions to incipient wetness where adsorption is predominant or through dipping the catalyst into the solution, incorporating both adsorption and ion exchange.

A critical step is the final calcination of the impregnated extrusion. The metals are then oxidized and dispersed on the surface. Placement of both molybdenum and promoter (Ni or Co) can either improve or destroy the catalytic sites.

Ethylene Oxide Catalyst

Ethylene oxide is a petrochemical used in the production of ethylene glycol antifreeze and polyester. Prior to 1960, ethylene oxide was produced by the chlorohydrin process but, due to the fluctuating supply and cost of chlorine, availability of improved technology, and thermodynamics, oxidation is now the preferred method of production.

The oxidation of purified ethylene is carried out with air or oxygen over a silver-coated, low-surface-area alpha-alumina support. The process is typically operated at about 260° to 280°C with air oxidation and about 230°C with oxygen. Contact time with the catalyst is about 1 second and the pressure is maintained at 1 to 3 MPa. Industrial reactors are shell-and-tube type. The heat of reaction is removed by an organic coolant system flowing tube side.

The desired reaction is believed to proceed via a Rideal mechanism in which ethylene is strongly adsorbed onto a previously adsorbed diatomic oxygen ion, O_2^-. This complex splits at the O–O bond to form ethylene oxide, leaving an adsorbed oxygen atom.

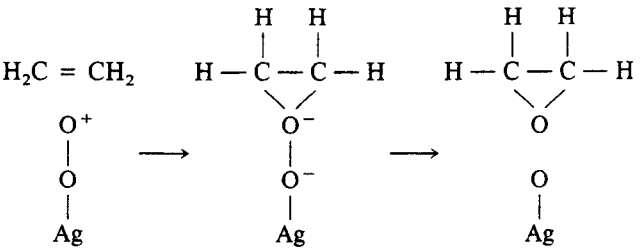

To support ethylene oxide production, an estimated 3 to 6 million pounds of catalyst per year are used worldwide. Performance requirements of the ethylene oxide catalyst are high activity, high selectivity, and high durability. The chemical and physical characteristics of the support and finished catalyst have a major influence on this performance. The catalyst is typically an extrusion 6 to 9 mm in diameter. An irregular surface is advantageous to expel the high heat of reaction.

A low-surface-area alpha alumina is preferred to reduce the side reactions and possibility of ethylene combustion promoted by high surface areas. Traditional catalyst supports used in commercial operations have surface areas less than 1 m^2/g. Catalysts with slightly higher surface areas have been developed in the effort to promote selectivity.

It is thought that rapid removal of the ethylene oxide from the surface is desirable to minimize oxidation to CO_2 and H_2O. Furthermore, theory predicts that, in a high-pressure environment, the heat of reaction may be rapidly dissipated using large pores to allow free passage of process gas.

The catalyst is produced by extruding alpha-alumina particles of controlled particle-size distribution. Binder, sintering, and extrusion aids can be added. The green support is then dried and calcined above 1000°C to produce an alpha-alumina-phase carrier with 0.2 to 0.4 cm^3/g total pore volume. Selection of sintering temperature is critical to generate the appropriate pore diameter.

An organosilver compound is then coated or impregnated onto the support to an 8 to 15% Ag content. Addition of an alkali promotor such as cesi-

um[10] enhances and stabilizes the activity of the catalyst. The catalyst is finally dried to remove any residual water.

Claus Catalyst

The Process

With increasing shortages of sweet natural gas, the development of technology to refine heavier crude oils, and the importance placed on reduction of sulfur pollutants in air and water, a greater emphasis has been placed on the operation of the Claus process.

The Claus process was originally developed in Germany in 1883 to convert hydrogen sulfide into elemental sulfur and water. The original process (reaction (1)) was a single step of passing H_2S over a catalyst at high temperatures (Fig. 3). This process limits sulfur yields to 80 to 90% (at 3 h^{-1} GHSV) because the heat of reaction could be dissipated by radiation alone.

$$3H_2S + 3/2O_2 \rightarrow 3/xS_x + 3H_2O + 620\ kJ \quad (1)$$

A major modification was made around 1937, increasing significantly the processing capacity as well as allowing the recovery of energy through heat recovery. In the modified Claus process (Fig. 4), reaction (1) is carried on in two stages. The first is a thermal oxidation of one-third of the H_2S to SO_2 and the second stage is a reaction of residual H_2S with SO_2 at a 2:1 ratio, as in reactions (1) and (3).

$$3H_2S + 3/2O_2 \rightarrow SO_2 + 2H_2S + H_2O + 520\ kJ \quad (2)$$

$$2H_2S + SO_2 \leftrightarrow 3/xS_x + 2H_2O + 93\ kJ \quad (3)$$

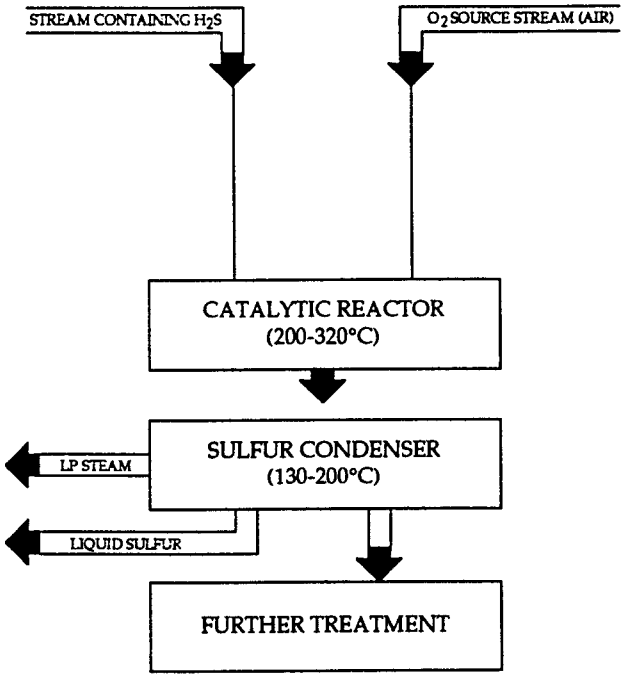

Fig. 3. Claus process.

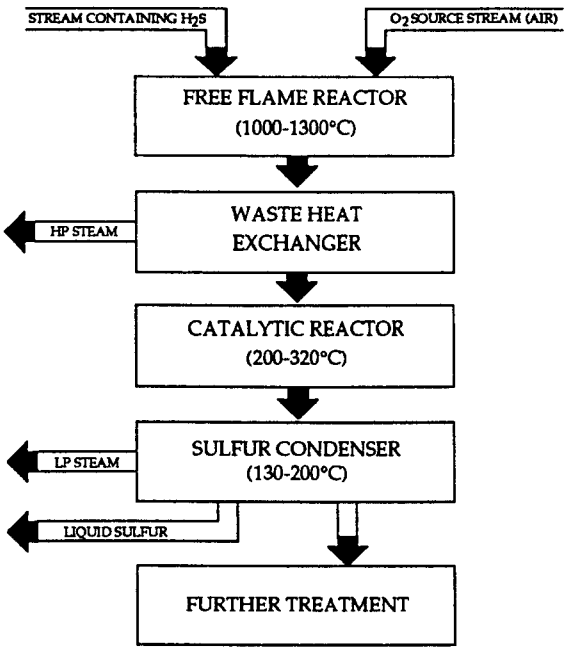

Fig. 4. Modified Claus process.

The fundamental design (Fig. 5) of the modified Claus process can be best understood by reference to the thermodynamic equilibrium curve (Fig. 6) for the basic reaction.[11] The theoretical degree of conversion is at a maximum at low temperatures, falls off rapidly and passes through a minimum at 540°C, and then increases slowly at higher temperatures.

The oxidation and rapid H_2S/SO_2 reaction occurs in the reaction furnace yielding 60 to 70% sulfur conversion, depending on the H_2S concentration of the feed gas. This reaction occurs in the thermal region of the equilibrium curve and a catalyst is not required to accelerate the reaction.

The gases leaving the reaction furnace must be rapidly quenched to avoid reduction of the sulfur yield due to a reverse reaction. Mechanically, this typically occurs in a waste heat boiler followed by a shell-and-tube sulfur condenser. The elemental sulfur is

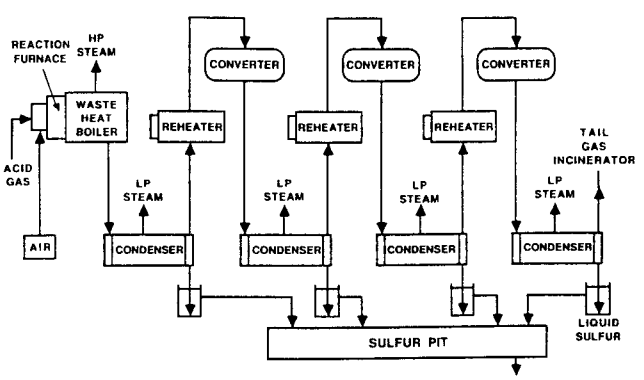

Fig. 5. Typical three-stage sulfur plant.

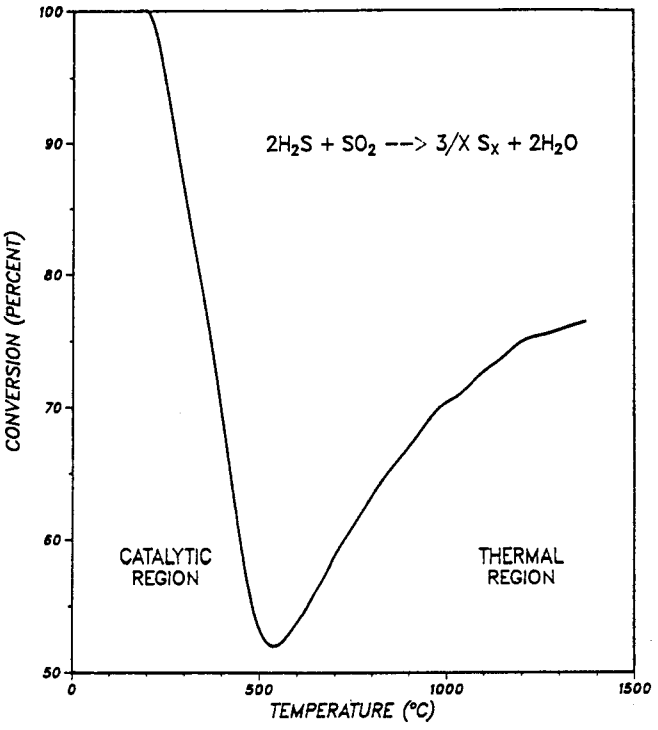

Fig. 6. Equilibrium conversion of H_2S to sulfur (Ref. 11).

removed from the gas stream in the liquid phase and stored in pits. To convert more of the H_2S and SO_2 to elemental sulfur, the conversion must be continued at lower temperatures in the catalytic region of the equilibrium curve.

The thermodynamic curve dictates that the catalytic unit should be operated at as low a temperature as possible, provided that the gases remain above the sulfur dewpoint and the rate of reaction is fast enough. To avoid sulfur deposition on the catalyst, the gas is reheated 25° to 50°C above the sulfur dewpoint and then passed through a 0.9 to 1.4 m (3 to 4.5 ft) depth bed of catalyst at gas hourly space velocities between 500 and 1200 h^{-1}. The Claus reaction is exothermic, creating a temperature increase as the gases pass through the bed. The gas is again cooled and the sulfur condensed to yield 88 to 93% total sulfur conversion.[12]

To achieve higher conversions (up to 97 to 98%), the gas is processed through two or three additional reheat, catalytic, and condensing stages at lower reactor temperatures. The residual H_2S in the gas is then incinerated to SO_2 or further processed in chemical or solid bed tail gas treating units. One general type of tail gas treating unit is a continuation of the Claus process utilizing an alumina catalyst. In this process, the catalytic beds are operated below the sulfur dewpoint, thus maximizing the equilibrium conversion. The sulfur product condenses within the pores of the alumina catalyst. When the pores are saturated, the catalyst bed is regenerated using hot process gas. The sulfur is condensed and recovered. When a tail gas process is employed, sulfur recovery of 99.0 to 99.9% can be achieved. Figure 7 is a photograph of a small-scale Claus sulfur recovery unit.

In the presence of CO, CO_2, and hydrocarbons in the acid gas feed to the reaction furnace, COS and CS_2 may be formed in the reaction furnace by reactions (4) through (8).

$$CH_4 + SO_2 \rightarrow COS + H_2O + H_2 \quad (4)$$

$$CO + S \rightarrow COS \quad (5)$$

$$CO_2 + H_2S \rightarrow COS + H_2O \quad (6)$$

$$CH_4 + 2S_2 \rightarrow CS_2 + 2H_2S \quad (7)$$

$$2CO + S_2 \rightarrow CO_2 + CS_2 \quad (8)$$

These carbon/sulfur compounds are destroyed to some extent in the first converter, either by hydrolysis to H_2S (reactions (9) and (10)), then subsequently reacted with SO_2 (reaction (3)) or by direct reaction with SO_2 (reactions (11) and (12)).[13]

$$COS + H_2O \rightarrow CO_2 + H_2S \quad (9)$$

$$CS_2 + 2H_2O \rightarrow CO_2 + 2H_2S \quad (10)$$

$$2COS + SO_2 \rightarrow 2CO_2 + 3S \quad (11)$$

$$CS_2 + SO_2 \rightarrow CO_2 + 3S \quad (12)$$

All of the reactions to decompose the carbon/sulfur compounds are kinetically limited and therefore typically occur only in the lower portion of the first reactor and can be accelerated by higher bed temperatures. Total conversions of these compounds are dependent on reactor temperature, catalyst type and activity, and gas composition.

Claus Catalyst History

The original modified Claus-process catalysts were a granular form of activated bauxite. Bauxite is a high-alumina natural mineral containing significant amounts of iron oxide and silica, which are catalytically undesirable in the Claus reaction. The activated bauxite also has a relatively low surface area, negatively affecting conversion potential. In the 1960s, a

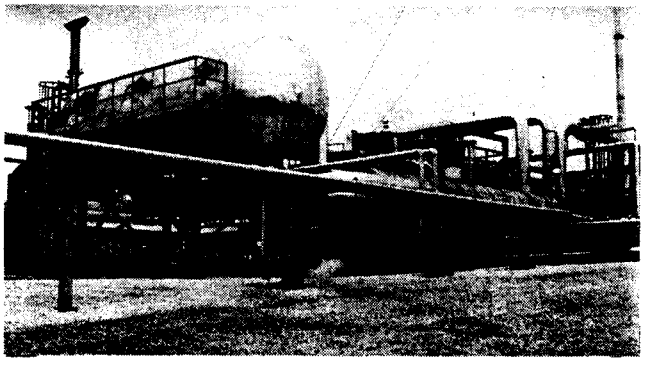

Fig. 7. Claus sulfur recovery unit. (Photo courtesy Alcoa.)

spherical form of the refined activated alumina was introduced, capable of meeting the then-current environmental demands of 90%+sulfur recovery.

Since that time, Claus catalysts have undergone improvements to increase physical strength, allowing handling of the catalyst without dust generation prone to causing increased pressure drop. Promoted forms of activated alumina and nonalumina catalysts have been developed to fill certain market niches. These improvements include resistance to sulfate poisoning, increased conversion of carbon-sulfur compounds, and resistance to carbon fouling.

Types and Properties of Claus Catalysts

Several standard activated aluminas are marketed, providing most users adequate conversions under nonrigorous operating conditions and are usually most cost-effective. The catalyst provides theoretical conversions for the period of time prior to significant deactivation (mechanism to be discussed later). Important properties include high surface area, controlled porosity, high physical integrity, and thermal and hydrothermal stability.

Since the Claus unit is operated at only 1.42–1.49 atm (7 to 8 psig), pressure drop is a critical consideration in selecting a catalyst and in operating conditions. Pressure drop is minimized by the use of a catalyst that has a nominal particle diameter. This reduces the initial pressure drop and also minimizes the increased pressure drop due to carbon plugging because of the inherent larger interstitial voids.

The standard activated alumina catalyst, such as S-100, is the cost-effective catalyst to be used in most applications. These catalysts, in a fresh state, have an excess of active sites, capable of producing theoretical conversion of the H_2S/SO_2 for two to five years in a refinery and three to eight years in a gas processing plant. Standard activated aluminas comprise approximately 80% of the annual Claus catalyst market.

Impregnated or promoted activated aluminas, such as SP-100, are used to enhance COS and CS_2 hydrolysis when the achievement of environmental requirements is dependent on maximizing the conversion of the carbon/sulfur compounds. These plants typically have high CO, CO_2, or hydrocarbon contents of the inlet acid gas, or no tail gas unit, or one that operates subdewpoint. These second-generation catalysts also maintain activity under high sulfating conditions. SP-100 uniquely is capable of resisting deactivation caused by the cracking of aromatic hydrocarbons on the surface of the alumina. Sales of the second-generation catalyst comprise about 17% of the annual market and cost an average of 50% more than standard aluminas.

The most recent catalyst introduced in the 1980s is a titanium oxide extruded catalyst designed to convert as much as 90 to 95% CS_2. This high-activity catalyst is used primarily in the bottom half of the first reactor where the operating temperature is maximized. The catalyst costs about seven times the standard alumina, makes up 3% of the market, and is usually applied in applications where CS_2 hydrolysis is critical to meet environmental requirements.

Typical properties of the Alcoa catalysts may be found in Table III.

Table III. Typical Properties of Alcoa Claus Catalysts

Typical Physical Properties S-100 and SP-100 4.8 mm (3/16 in.)	S-100	SP-100
Surface area	340 m^2/g	325 m^2/g
Total pore volume	0.55 cm^3/g	0.55 cm^3/g
Alumina XRD phase	Amorphous, chi and gamma	Amorphous, chi and gamma
Crush strength	25 kgs (55 lbs)	27 kgs (50 lbs)
Abrasion loss	0.1 wt%	0.1 wt%
Bulk density	0.72 g/cm^3 (45 lbs/ft^3)	0.74 g/cm^3 (46 lbs/ft^3)
Typical Chemical Properties S-100 and SP-100 4.8 mm (3/16 in.)		
Al_2O_3	95.1 wt%	91.6 wt%
SiO_2	0.02 wt%	0.02 wt%
Fe_2O_3	0.02 wt%	0.02 wt%
Na_2O	0.35 wt%	0.35 wt%
LOI (250°–1200°C)	4.5 wt%	4.0 wt%
Promotor, oxide basis	0 wt%	4.0 wt%
Sizes available:	7.9, 6.4, 4.8, 3.2 mm (5/16, 1/4, 1/8 in.)	
SRU ½ in. High-Surface-Area Bed Support		
Surface area	240 m^2/g	
Crush strength	57 kg (125 lb)	
Bulk density	0.80 g/cm^3 (50 lb/ft^3)	

Deactivation Mechanisms of Claus Catalysts

Claus catalysts have initial excess activity but are deactivated at a rate dependent on the design and operating procedures of the sulfur recovery unit and the acid gas feed. The five major mechanisms controlling the activity of the catalyst are:

1. Thermal loss of surface area.
2. Hydrothermal loss of surface area.
3. Sulfation or SO_2 chemisorption.
4. Sulfur deposition.
5. Carbon deposition.

Loss of Surface Area. Loss of surface area due to thermal or hydrothermal deactivation is unavoidable and irreversible. The loss is caused by operation of the catalyst at high temperatures (220° to 400°C) in a water-containing atmosphere. The rate of deactivation can be accelerated by temperature excursions due to sulfur fires, poor regeneration techniques, or excessive use of steam during start-up or shut-down procedures.

Sulfation or SO_2 Chemisorption. Surface sulfation is due to oxygen carryover from the reaction or direct-fired reheat burners between converter stages. The oxygen combines with SO_2 to form SO_3, which can then be adsorbed or reacted on the surface of the alumina. Chemisorbed SO_2 and sulfation are equilibrium phenomena primarily dependent on operating temperatures, H_2S/SO_2 ratios, and oxygen leakage caused by corroded, poorly designed, or improperly operated reheat burners. These deactivation mechanisms can be partially reversed by a rejuvenation procedure that incorporates high reactor temperatures and higher H_2S/SO_2 ratios.

Sulfur Deposition. Since operating close to the sulfur dewpoint enhances Claus activity, the risk of sulfur deposition in the pores is chronic in sulfur plant operations. Sulfur deposition is caused by operating too close to or below the sulfur dewpoint or inefficient sulfur condenser operations initiating sulfur misting or fogging in the gas fed to the reactors. Sulfur deposition can be reversed by a heat soak method in which the reactor inlet temperature is raised 25° to 50°C above the normal operating temperature for 24 hours.

Carbon Deposition. The first type of carbon deposition is formed by incomplete combustion of lighter hydrocarbons in the reaction furnace or reheat burners. This type of carbon is described as "powdery" and tends to collect on the top surface of the catalyst bed. Although this type of carbon does not directly deactivate the catalyst, it may form a crust with sulfur and generate preferential flow characteristics and increased pressure drop through the bed. The effect of this can be minimized with the use of larger catalyst particles or the use of a nominal-sized spherical catalyst that offers larger interparticle voids. Once the carbon is above tolerable levels, the top layer of the catalyst bed is usually removed and replaced. Some operators have success in performing an oxidation burnoff to remove the carbon. Often temperature excursions will occur during this procedure, so careful precautions must be incorporated.[14]

Carbon deactivation is caused by the presence of aromatic hydrocarbons in the acid gas feed. These hydrocarbons will crack on the acid surface of the alumina, leaving a "glossy" carbon deposition that blocks access to the alumina active sites. This mechanism has been found to be resisted by the use of SP-100 in which the acidic surface sites of Al^{3+} are masked by the promoting agent. Oxidative regeneration procedures have also been used for this type of carbon.

Additional information concerning Claus catalyst deactivation mechanisms can be found in Refs. 14 and 15.

Catalytic Dehydration of Alcohols

Alumina is one of many oxides that are efficient catalysts to dehydrate alcohols, yielding olefins and ethers or both. Activated alumina can initiate synthesis in which H_2O may be the reactant or product. Activated alumina is the catalyst of primary industrial importance at typical operating conditions of atmospheric pressure, 250° to 400°C, and 1 to 5 m^3 of liquid per h/m^3 of catalyst. The most severe operating conditions are required for primary alcohol dehydration.

Primary and secondary alcohols can also form olefins via an intermediate ether and, by lowering the reactor temperature, a significant increase in the formation of ether can be observed. Ethers of secondary alcohols are more difficult to produce and they are not formed from tertiary alcohols. Furthermore, the percent olefin production increases with the alkali content of the alumina, whereas the amount of ether formation usually decreases as a function of reactor run time.

References

[1]B. C. Lippens, "Structure and Texture of Aluminas," Ph.D. Thesis, Delft University of Technology, The Netherlands, 1961.

[2]W. H. Gitzen, Alumina as a Ceramic Material. The American Ceramic Society, Columbus, Ohio, 1970.

[3]K. Wefers and C. Misra, "Oxides and Hydroxides of Aluminum," Technical Paper 19 Revised, Alcoa Laboratories, 1987.

[4]G. MacZura, K. P. Goodboy, and J. J. Koenig, "Aluminum Compounds, Aluminum Oxide (Alumina)," Kirk-Othmer Encyclopedia of Chemical Technology, Vol. 2, 3rd ed., 1978.

[5]The Kline Guide to the Chemical Industry. Charles H. Kline & Co., Inc., New Jersey, 1980.

[6]G. Berrebi and Ph. Bernusset; pp. 13–39 in Preparation of Catalysts, Vol. I. Edited by B. Delmun, P. A. Jacobs, and G. Poncelet. Elsevier, Amsterdam, 1976.

[7]E. I. Shaheen, Catalytic Processing in Petroleum Refining. Penn Well Publishing Co., Tulsa, OK, 1983.

[8]"Catalysts, Meeting New Challenges in a $2.5 Billion Global Business," *Chemical Week*, 26, 138 (1986).

[9]R. K. Oberlander, "The Extrusion of High Surface Area Aluminas"; presented at the 17th Biennial Conference, the Institute of Briquetting and Agglomeration, September 1981.

[10]Charles N. Satterfield, Heterogeneous Catalysis in Practice. McGraw-Hill, New York, 1980.

[11]B. W. Gamson and R. W. Elkins, *Chem. Eng. Prog.*, **49**, 203 (1953).

[12]"Sulfur Recovery by the Modified-Claus Process," Seminar Manual, Western Research, 1986.

[13]K. P. Goodboy, "Catalyst Increases COS Conversion," *Oil Gas J.*, February 18, 1985.

[14]J. C. Downing, H. L. Fleming, and K. P. Goodboy, "Sulfur and Carbon Deposition on Claus Catalyst Examined," *Oil Gas J.*, November 4, 1985.

[15]G. R. Schoofs, "Sulfur Condensation in Claus Catalyst," *Hydrocarbon Processing*, February 1985.

Monolithic Catalyst Systems

Irwin M. Lachman
Corning Glass Works
Sullivan Park, DV-01-9
Corning, NY 14831

Monolithic catalyst systems consisting of a cellular ceramic coated with high surface area gamma alumina and noble metal catalysts are now widely used for automotive emissions control. The use of alumina chemicals in this application and others developed subsequently are discussed. They include stationary emissions control by selective catalytic reduction and various high-temperature applications. The latter are of interest for high-temperature automotive use, catalytic combustion, catalytic supports in the chemical processing industries, and as molten metal filters. High surface area cellular gamma alumina and spinel compositions are now being intensively developed and evaluated for applications in the chemical process industries and refining industries. They can minimize reactor volume and have the additional advantages of cellular ceramics, i.e., low pressure drop, large geometric surface area, and short diffusion paths.

Monolithic catalyst systems were intensively developed in the early 1970s for automotive emissions control and were commercially utilized starting with 1975 model-year cars. Such catalyst systems consisted of a cellular ceramic structural element coated with high surface area gamma alumina containing noble metal catalysts. Thermal stabilizers and cerium oxide for three-way catalysis are also added to the gamma alumina coating as needed. Figure 1 is a photograph of several such extruded cellular ceramic monoliths. Figure 2 is an optical photomicrograph of a polished section of a typical automotive convertor. It shows the cellular ceramic monolith coated with a noble metal-catalyzed gamma alumina washcoat.

Cellular ceramics have been fabricated and used for various purposes since about 1950.[1–18] Wrapped or laid-up configurations[4–7,9,10,13] were widely used in early model years, 1975–1978, for oxidation of automotive exhaust gases, but were then completely superseded by extruded cellular ceramics[14–18] (Fig. 1). The traditional bead- or pellet-filled reactor was also used starting in 1975 but is now being gradually displaced by extruded cellular ceramics. Pellet convertors now account for only about 3% of the 1989 model-year convertor-equipped vehicles.

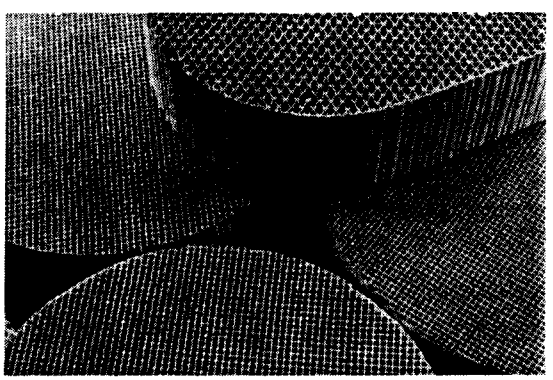

Fig. 1. Extruded cordierite cellular ceramic monoliths.

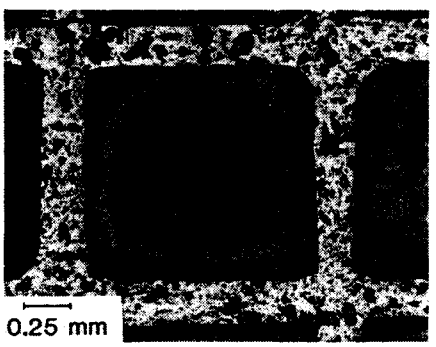

Fig. 2. Optical photomicrograph of an automotive convertor showing: (*a*) cordierite cellular ceramic, (*b*) noble metal-catalyzed gamma alumina washcoat, and (*c*) open cellular channel.

The following sections will discuss the use of alumina chemicals in presently used automotive emissions control catalysis as well as in compositions for new applications. In all these catalytic applications, the unique cellular thin-wall configuration makes possible the combination of low pressure drop, large geometric surface area, and short diffusion paths into and out of the active catalyst/substrate material.

Cordierite Compositions for Automotive Emissions Control

The synthetic-ceramic-phase cordierite was identified initially as the best practical material for the cellular ceramics used in automotive convertors and is still the dominant material. The cordierite cellular ceramic functions as a structural element. It carries the high surface area gamma alumina coating and noble metal catalysts, as described above and illustrated in Fig. 2.

Cordierite is a magnesium aluminosilicate, $2MgO \cdot 2Al_2O_3 \cdot 5SiO_2$, combining relatively low thermal expansion with both high thermal shock resistance and adequate refractoriness. Equilibrium peritectic melting occurs at 1465°C for pure cordierite. Cordierite compositions for automotive use are formulated to be stoichiometric or slightly rich in magnesia and alumina in order to minimize thermal expansion, as shown in the compositional diagram of Fig. 3.[19] Typical formulations of cordierite compositions and their chemical analyses are shown in Tables I and II, respectively.[19]

Fabrication of monolithic cellular cordierite ceramics is described in Refs. 19 and 20. The clay, talc, alumina, and silica compositions of Table I are dry-mixed with a temporary binder, methylcellulose, and then plasticized with water in a muller-type apparatus commonly used in clay technology. The plasticized batch can then be extruded through the specialized dies[20] used for forming cellular monolithic ceramics.

The alumina chemicals used must be pure enough that they will not interfere with the formation of oriented cordierite which is essential to low expansion and thermal shock resistance.[20] They must also be fine enough to enable the reaction to proceed to completion. Calcined aluminas ground to −325 mesh and hydrated aluminas have proved to be practical in this regard. Alkalis and calcium oxide are especially deleterious and must therefore be limited.[20]

Due to regulations, automotive emissions control is now concentrated in the United States and Japan, but a wide international market is developing. In Europe, West Germany is encouraging the use of catalytic convertors through tax incentives for new and retrofitted cars. Switzerland required convertors in late 1986 with Sweden, Norway, and Austria following in 1987. The European Economic Community as a whole is also proposing standards for new cars some time in the near future. Australia imposed standards for 1986 model-year cars and Korean control standards will go into effect for 1988 model-year cars.

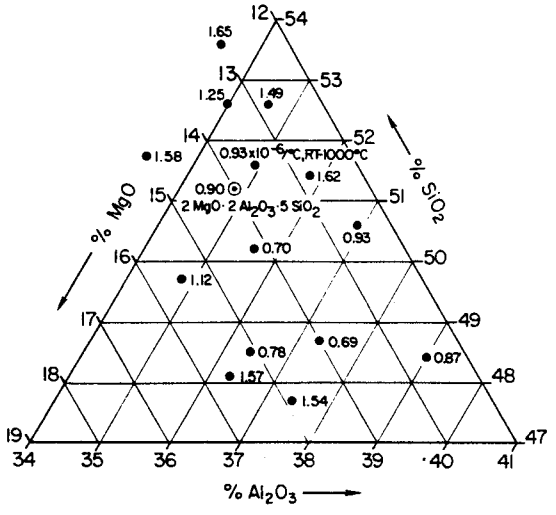

Fig. 3. Thermal expansion coefficients (25°–1000°C) of extruded cordierite compositions in relation to stoichiometry (Ref. 19).

Table I. Extruded Ceramic Cordierite Compositions (wt%)

Raw Material	A	B
Kaolin	21.74	40.2
Talc, raw	39.24	19.4
Alpha alumina	11.23	3.68
Hydrated alumina	17.80	16.9
Silica	9.99	
Talc, calcined		19.8

Table II. Typical Chemical Analyses of Cordierite Compositions (wt%)

Constituent	A	B
SiO_2	50.5	49.2
Al_2O_3	34.9	35.2
MgO	13.8	14.5
Fe_2O_3	0.34	0.38
TiO_2	0.16	0.47
Na_2O	0.11	0.25
K_2O	0.10	0.05

Stationary Emissions (NOX) Control

Cordierite cellular ceramics, as described above, and alpha alumina cellular ceramics have been used for selective catalytic reduction (SCR) of nitrogen oxides by coating with various catalyst systems, noble metal as well as base metal.[21–28] Coatings based on the hydrogen form of the zeolite mordenite[28] have also been used effectively for the selective catalytic reduction of nitrogen oxides. In SCR, ammonia is injected into nitrogen oxide-containing exhaust gases and, in the presence of a catalyst at moderate temperature (250° to 450°C), they react to form nitrogen and water vapor.

Stationary emissions control is a relatively new application for catalysis and is expected to grow significantly, especially as governments enact legislation for emissions limits. In the United States, regulations are in force under the Clean Air Act but, in most cases, they are not strict enough to require secondary controls like SCR. More stringent regulations have been enacted at the state and county levels in California, Texas, and Oklahoma. West Germany has strict national regulations for power plant emissions so that SCR was actively implemented in 1986. Nitric acid plants already use emissions control but incineration units, power plants, and stationary source engines are growth areas for industrial emissions control.

High-Temperature Compositions

High-temperature cellular ceramic compositions have been developed for automotive emissions control,[29–33] for catalytic combustion,[9,34–43] for catalytic supports for oxidation reactions in the chemical pro-

cess industries,[44–49] and as molten metal filters.[50–52] Varying degrees of thermal shock resistance are needed so that traditional alumina-containing refractory compositions have been used as well as ones designed to utilize microcracking for enhanced thermal shock resistance.

A long-used catalytic combustion application is the control of nitric acid tail gas from nitric acid plants.[53,54] A fuel such as natural gas or methane is added to nitric acid tail gas to increase the stream temperature, which is then passed over a noble metal catalyst supported on a cellular ceramic monolith. This reduces the red nitrogen dioxide to NO or nitrogen, depending on the gas mixture and catalysts used.

The use of cellular ceramic supports in the manufacture of HCN, the Andrussow process, is another example of the application in the chemical process industries. In their Andrussow process, a platinum-alloy gauze is supported on alumina or alumina-containing cellular monoliths and a reaction mixture of methane, ammonia, and air is passed through at 1100° to 1150°C. The products, HCN and water vapor, are quenched in a heat exchanger to prevent further reaction to undesired compounds.

Future applications may include other catalytic oxidation reactions such as the production of ethylene oxide and catalytic ammoxidation for the production of nitric acid. The oxidation reaction of ethylene to ethylene oxide is highly exothermic and requires the simultaneous removal of heat by an exchanger. Therefore the cellular support will need to be designed for heat-exchanger reactor geometry.

Cordierite cellular ceramics have been applied to catalytic incineration[42] and to catalytic combustion for woodburning stoves,[43] both of which have become very important for air pollution prevention. Catalytic incineration has been used in the refining industries to eliminate pollutants as well as to conserve energy. Catalytic combustion for woodburning stoves has the benefits of preventing air pollution, preventing creosote deposits and chimney fires, and maximizing combustion efficiency.

In most cases, a ceramic honeycomb is used as a structural element for carrying the catalyst/high surface area coating. However, some patents describe the option of including catalytically active phases in the honeycomb itself.[38,39] Table III lists the generic high-temperature compositions described in the literature or already in use and indicates the area of application. Cordierite is included in Table III because its use overlaps with the more refractory compositions. In these compositions, alumina exists in the high-temperature alpha form or else reacts with other constituents during manufacture. Therefore, calcined alpha alumina is the raw material of preference. It minimizes firing shrinkage and is available in relatively high purity, which is necessary for maximum refractoriness.

High Surface Area Compositions

Cellular ceramics fabricated substantially or entirely from high surface area compounds or precursors are now being intensively developed for applications in the chemical process industries and for stationary emissions control.[55–66] They are based on gamma alumina and spinel, as well as other traditional catalytic substrate compounds and mixtures. Research, development, and commercialization efforts are very active now but the initial research goes back at least a decade.[67,68]

Gamma alumina cellular ceramics are fabricated from pseudoboehmite and/or gamma alumina, which is usually derived from calcined pseudoboehmite. Temporary binders are used,[19] as well as a variety of alumina precursor compounds that result in permanent binders.[56] Therefore, cellular ceramics composed entirely of gamma alumina are available, as well as ones in which additives are present for specific purposes. It is especially useful to incorporate compounds or precursors, such as silica, to increase thermal stability.[57,69] Lanthanum oxide precursor has also been added to gamma alumina precursors to form the stable high surface area lanthanum beta alumina phase.[70] The literature contains a good deal of information on this subject.[34,36–39]

Figure 4 shows BET surface area as a function of heat-treatment temperature for three gamma alumina cellular ceramic compositions, 100% gamma alumina, 7% silica, and 12% clay. The increased thermal stabil-

Table III. High-Temperature Cellular Ceramic Compositions and Areas of Application

Phase Composition	Automotive Emissions Control	Catalytic Combustion	Chemical Process Industries	Molten Metal Filters
Cordierite	x	x	x	
Mullite			x	x
Spinels		x		
Alumina			x	x
Zircon		x	x	x
Alumina + silica			x	
Aluminum titanate	x	x		
Mullite + aluminum titanate	x	x	x	
Zirconia + spinel				x
Zircon + mullite		x		

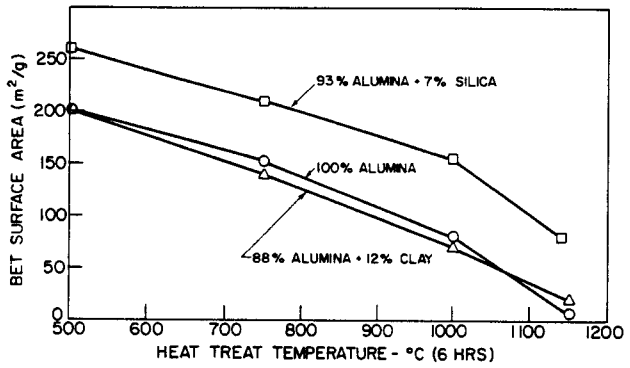

Fig. 4. BET surface area vs heat-treatment temperature for gamma alumina cellular ceramic substrates.

ity imparted by the 7% silica is evident in the 80 m^2/g after the 1150°C heat treatment.

Pore size varies as a function of heat treatment in the 100% alumina and the 7% silica compositions (Fig. 5). With increasing temperature sintering, pore coarsening and the usual phase transformations occur in the 100% alumina composition. However, X-ray diffraction analyses show that the 7% silica prevents formation of alpha alumina at 1150°C and, at the same time, causes a bimodal pore distribution. The stabilizing effect of silica results in only a small incremental increase in the average pore size of the fine porosity in going from the 1000° to the 1150°C heat treatment. However, the pore size of the 100% alumina changes radically from 14.5 nm (145 Å) to 105 nm (1050 Å) over the same temperature range (not shown in Fig. 5). The total open porosity of the 100% alumina changes only from 60.0 to 54.8% in going from the 500° to the 1150°C heat treatment.

Spinel cellular ceramics can be formulated with spinels of widely varying ratios of alumina to magnesia

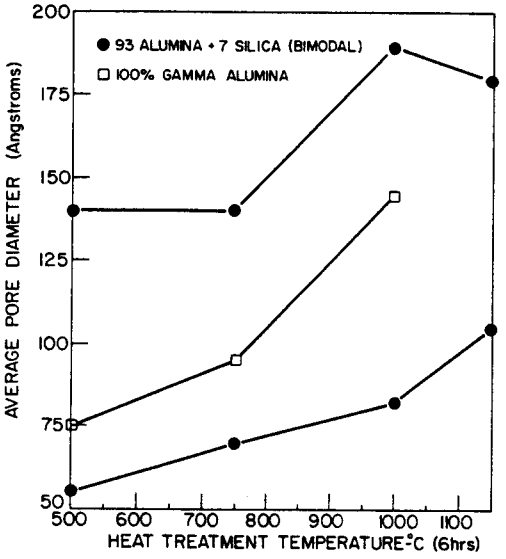

Fig. 5. Average pore diameter (by nitrogen desorption) of gamma alumina and alumina-silica cellular ceramics.

and this ratio has an important effect on the thermal stability.[71] Useful spinels or spinel precursor materials must be prepared by coprecipitation, hydrolysis of alkoxides,[72] or similar methods so that the compound is easily formed at a low temperature and high surface area is obtained. The BET surface area of a cellular ceramic fabricated from a coprecipitated spinel with an Al/Mg ratio = 2.84 is shown in Fig. 6 as a function of heat-treatment temperature. After the 1150°C heat treatment, it still retains one-half of the initial surface area, thus indicating good thermal stability. Mercury porosimeter analyses on material fired up to 1000°C measures about 60% porosity and a median pore size of 42 nm (420 Å).

High surface area alumina and spinel cellular ceramics will minimize reactor volume and give the advantages of low pressure drop, large geometric surface area, and short diffusion paths for reactants and products. These geometric variables can be coupled with controlled material properties, BET surface area, porosity, pore-size distribution, and chemical purity to obtain unique cellular catalytic substrates.

Future applications for alumina and spinel are possible where fixed-bed reactors are now used in petroleum refining, steam reforming, and the chemical process industries. Some reports of experimental work in these areas have already been published.[67,69]

References

[1]H. Cohen, "Heat Exchanger and Method of Making the Same," U.S. Pat. No. 2 552 937, May 15, 1951.

[2]V. Stopka, "Method of Producing Ceramic Bodies Having Longitudinal Passages," U.S. Pat. No. 2 506 244, May 2, 1950.

[3]R. P. Forsberg et al., "Ceramic Structure and Method of Making Same," U.S. Pat. No. 2 977 265, March 28, 1961.

[4]R. Z. Hollenbach, "Method of Making Ceramic Articles," U.S. Pat. No. 3 112 184, November 26, 1963.

[5]L. L. Johnson, W. C. Johnson, and D. L. O'Brian, "The Use of Structural Ceramics in Automobile Exhaust Converters," *A.I.Ch.E. Chemical Engineering Progress Symposium Series*, 57 [35] 55–67 (1961).

[6]G. R. Smith, "Reaction Milieu and Afterburner Incorporating Same," U.S. Pat. No. 3 088 271, May 7, 1963.

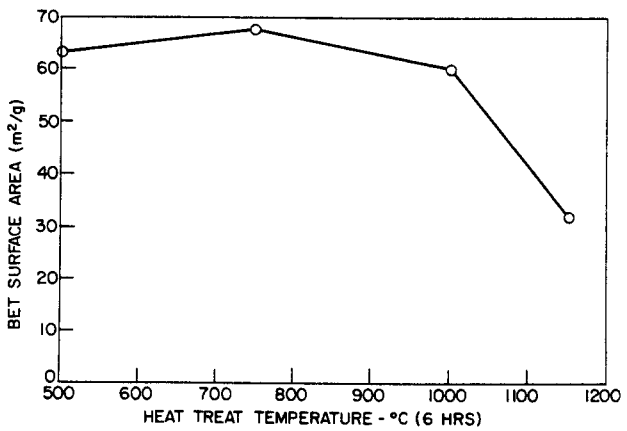

Fig. 6. BET surface area vs heat-treatment temperature for spinel cellular ceramic substrates.

[7]G. P. Smith and G. E. Strong, "Structural Ceramic Bodies and Method of Making Same," U.S. Pat. No. 3 272 686, September 13, 1966.

[8]J. M. Nowak and J. C. Conti, "Development of Lightweight Ceramic Honeycomb Structure," *Am. Ceram. Soc. Bull.*, **41** [5] 321–25 (1962).

[9]C. D. Keith, P. M. Kenah, and D. L. Blair, "Coated Film of Catalytically Active Oxide on a Refractory Support," U.S. Pat. No. 3 565 830, February 23, 1971.

[10]C. D. Keith, T. Schreuders, and C. E. Cunningham, "Apparatus for Purifying Exhaust Gases of an Internal Combustion Engine," U.S. Pat. No. 3 441 381, April 29, 1969.

[11]H. C. Andersen, W. Green, and P. Romeo, *Engelhard Tech. Bull.*, **1**, 100 (1966).

[12]D. J. Cassidy, M. Esper, and D. J. Ronnie, Ger. Pat. No. DT2 349 472.

[13]F. J. Sergeys, "Porous Ceramic-Exhaust Oxidation Catalyst," U.S. Pat. No. 3 755 204, August 28, 1973.

[14]J. J. Benbow and W. L. Lord, "Catalyst Support," U.S. Pat. No. 3 824 196, July 16, 1974.

[15]R. D. Bagley, "Extrusion Method for Forming Thin-Walled Honeycomb Structures," U.S. Pat. No. 3 790 654, February 5, 1974.

[16]J. S. Howitt, "Ceramics Clean Automobile Exhaust," *Ceram. Ind.*, February 1975

[17]J. P. DeLuca and L. E. Campbell, "Thin Wall Ceramics as Monolithic Catalyst Supports"; Chap. 10 in Advanced Materials in Catalysis. Academic Press, New York, 1977.

[18]J. S. Howitt, "Thin Wall Ceramics as Monolithic Catalyst Supports," SAE Tech Paper No. 80082, 1980.

[19]I. M. Lachman and R. M. Lewis, "Anisotropic Cordierite Monolith," U.S. Pat. No. 3 885 977, May 27, 1975.

[20]I. M. Lachman, R. D. Bagley, and R. M. Lewis, "Thermal Expansion of Extruded Cordierite Ceramics," *Am. Ceram. Soc. Bull.*, **60** [2] 202– [21]"Catalyst Useful in Reduction of Nitrogen Oxides," Mitsubishi Heavy Ind., 1978. Rept. No. JP 53 138 992.

[22]"Catalyst Useful in Reduction of Nitrogen Oxides," Mitsubishi Heavy Ind. Rept. No. JP 840 150 185, 1984.

[23]"Catalytic Reduction of Nitrogen Oxides in Waste Gas," Mitsubishi Chem Ind. Rept. No. JP 500 628 615, 1975.

[24]"Catalytic Reduction of Nitrogen Oxides in Waste Gas," Mitsubishi Chem Ind. Rept. No. JP 800 176 195, 1980.

[25]B. Harrison, A. F. Diwell, and M. Wyatt, "Controlling Nitrogen Oxide Emissions from Industrial Sources," *Platinum Met. Rev.*, **29** [2] 50–56 (1985).

[26]C. H. Bartholomew, "Reduction of Nitric Oxide by Monolithic Supported Palladium-Nickel and Palladium-Ruthenium Alloys," *Ind. Eng. Chem. Res. Dev.*, **14**, 29 (1975).

[27]M. Engler and K. Unger, "Effect of Impregnation and Activation Conditions of Al_2O_3/CuO Supported Monolith Catalysts in the Reduction of NO"; p. 29 in Preparation of Catalysis II. Edited by B. Delmon, et. al. Elsevier, New York, 1979.

[28]J. R. Klovsky, P. B. Koradia, and C. T. Lim, "Evaluation of a New Zeolitic Catalyst For NO_x Reduction with NH_3," *Ind. Eng. Chem. Prod. Res. Dev.*, **19** [2] 218–25 (1980).

[29]I. M. Lachman and R. N. McNally, "High-Temperature Monolithic Supports for Automobile Exhaust Catalysis," *Ceram. Eng. Sci. Proc.*, 2 [5–6] 337–51 (1981).

[30]J. P. Day and I. M. Lachman, "Aluminum Titanate-Mullite Ceramic Articles," U.S. Pat. No. 4 483 944, November 20, 1984.

[31]I. Oda and T. Matsuhisa, "Low-Expansion Ceramics and Method of Producing the Same," U.S. Pat. No. 4 307 198, December 22, 1981.

[32]I. Oda and T. Matsuhisa, "Low-Expansion Ceramics and Method of Producing the Same," U.S. Pat. No. 4 316 965, February 23, 1982.

[33]I. Oda and T. Matsuhisa, "Low-Expansion Ceramics and Method of Producing the Same," U.S. Pat. No. 4 306 909, December 22, 1981.

[34]S. G. Hindin and J. C. Dettling, "Compositions and Methods for High Temperature Stable Catalysts," U.S. Pat. No. 3 956 188, May 11, 1976.

[35]C. B. Lundsager, "Porous Ceramic Structure," U.S. Pat. No. 3 963 504, June 15, 1976.

[36]S. G. Hindin and G. R. Pond, "Method of Combustion Using High Temperature Stable Catalysts," U.S. Pat. No. 3 966 391, June 29, 1976.

[37]S. G. Hindin, L. M. Polinski, and G. W. Roberts, "Catalys System," U.S. Pat. No. 4 089 654, May 16, 1978.

[38]M. J. Angwin and W. C. Pfefferle, "Catalytic Monolith Method of its Formulation and Combustion Process Using the Catalytic Monolith," U.S. Pat. No. 4 337 028, June 29, 1982.

[39]M. J. Angwin and W. C. Pfefferle, "Catalytic Monolith and Method of its Formulation," U.S. Pat. No. 4 295 818 October 20, 1981.

[40]"Catalytic Burner," Matsushita Elec Ind. Rept. No. JP 600 537 115, 1985.

[41]R. Prasad, L. A. Kennedy, and E. Ruckenstein, "Catalytic Combustion," *Catalysis Rev.-Sci. Eng.*, **26** [1] 1–57 (1984).

[42]E. Kenson, "Catalytic Incineration in Cogeneration Systems," *Chem. Eng. Prog.*, **81** [11] 57–62 (1985).

[43]J. Vara, "Woodburning: the Catalytic Combustor Comes of Age," *Country J.*, **11**, 92–99 (1982).

[44]J. A. Cox, Jr., G. G. Glaser, Jr., and M. J. Shoger, "Catalyst System for Making Hydrogen Cyanide," U.S. Pat. No. 3 545 939, December 8, 1979.

[45]D. M. Sowards, "Dispersed Phase Activated and Stabilized Metal Catalysts," U.S. Pat. No. 3 666 412, May 30, 1972.

[46]E. I. du Pont de Nemours and Company, "Carrying out Reactions in the Presence of Metal Catalysts," Br. Pat. No. 1 281 943, October 14, 1969.

[47]D. M. Sowards, "Composite Articles of Manufacture and Apparatus for Their Use," U.S. Pat. No. 3 505 030, April 7, 1970.

[48]G. A. Jarvi, K. B. Mayo, and C. H. Bartholomew, "Monolithic Supported Nickel Catalysts: I. Methanation Activity Relative to Pellet Catalysts," *Chem. Eng. Commun.*, **4**, 325–41 (1980).

[49]E. L. Sughrue and C. H. Bartholomew, "Kinetics of Carbon Monoxide Methanation on Nickel Monolithic Catalysts," *Appl. Catal.*, **2**, 239–56 (1982).

[50]D. J. Bak, "Ceramic Filter Solves Casting Problem," *Design News*, March 1981.

[51]J. P. Day and H. Kind, "Filtration of Irons with Cellular Ceramic Filter," *Modern Casting*, April 1984.

[52]J. P. Day and H. Kind, "The Development and Application of Cellular Ceramic Filters for Gray and Ductile Iron," *Am. Foundry Soc. Trans.*, **92**, 339–45 (1984).

[53]C. N. Satterfield; pp. 229–30 in Heterogeneous Catalysis in Practice. McGraw-Hill, New York, 1980.

[54]O. J. Adlhart, S. G. Hindin, and R. E. Kenson, "Processing Nitric Acid Tail Gas," *Chem. Eng. Prog.*, **67** [2] 73–78 (1971).

[55]I. M. Lachman, "New Monolithic Honeycomb Supports for Catalysis"; in Abstracts of the Ninth North American Meeting of the Catalysis Society, Houston, Texas, March 17–21, 1985.

[56]I. M. Lachman and L. A. Nordlie, "Method of Producing High-Strength High Surface Area Catalyst Supports," European Patent Application No. 8630134.0-; filed 24.02.86.

[57]I. M. Lachman and L. A. Nordlie, "Improved Monolithic Catalyst Support Material," European Patent Application No. 86 301 957.6-; filed 18.03.86.

[58]I. M. Lachman and T. P. DeAngelis, "Preparation of Monolithic Catalyst Supports Having an Integrated High Surface Area Phase," European Patent Application No. 86 301 315.7-; filed 24.02.86.

[59]P. Bardhan, I. M. Lachman, and L. A. Nordlie, "Preparation of Monolithic Catalyst Support Structures Having an Integrated High Surface Area Phase," European Patent Application No. 86 301 582.2-; filed 06.03.86.

[60]C. M. Golino and I. M. Lachman, "Preparation of High Surface Area Agglomerates for Catalyst Support and Preparation of Monolithic Support Structures Containing Them," European Patent Application No. 86 301 313.2-; filed 24.02.86.

[61]K. Mori et al., "Catalyst for Removing Nitrogen Oxide from Exhaust Gas," Jap. Pat. No. 1980-17 621 (55–17 621), January 31, 1975.

[62]Jap. Pat. No. 8 195 035, "Steam Reforming on Honeycomb Ceramic," Matsushita, 1981.

[63]Hap. Pat. No. 83-049 602, "Steam Reforming of Hydrocarbons," Matsushita, 1983.

[64]Jap. Pat. No. 81 187 760, "Reforming Catalyst," Matsushita, 1981.

[65]Jap. Pat. No. 54 138 005, "Gamma-Alumina Honeycomb Manufacture," NGK Spark Plug, 1979.

[66]K. Abe, S. Tamura, and T. Nakatsuji, "Method for Preventing the Wear of a Monolithic Catalyst by Dusts," U.S. Pat. No. 4 294 806, October 13, 1981.

[67]J. Scinta and S. W. Weller; pp. 279–86 in Catalytic Hydrodesulfurization and Liquefaction of Coal. Elsevier, Amsterdam, 1977/1978.

[68]D. S. Soni and B. L. Crynes, "A Comparison of the Hydrodesulfurization and Hydrodenitrogenation Activities of Monolithic Alumina Impregnated with Cobalt and Molybdenum and a Commercial Catalyst"; p. 56 in Upgrading Coal Liquids. Edited by R. F. Sullivan. ACS Symposium Series. The American Chemical Society, Washington, DC, 1981.

[69]Alcoa Technical Paper No. 10, 2d rev., 1960; p. 61.

[70]S. Matsuda, A. Kato, M. Mizumoto, and H. Yamashita, "A New Support Material for Catalytic Combustion Above 1000°C," German Soc. for Chemical Apparatus (DECHEMA), Proceedings of the Eighth International Congress on Catalysis, 1984, VCH Pubs.

[71]R. D. Bagley and H. K. Bowen, "Effect of MgO and Alumina on Grain Growth of Magnesium Aluminate Spinel," *Am. Ceram. Soc. Bull.* **56** [8] 732 (1977).

[72]M. Matsui and T. Takahashi, "Polycrystalline Transparent Spinel Sintered Body and Method of Producing the Same," U.S. Pat. No. 4 543 346, September 24, 1985.

Pelleted Catalyst Systems

W. S. Briggs
Consultant Services
35 Franklin Drive
Bridgeton, NJ 08302

Seventy million pounds of alumina are used in the form of pelleted catalyst each year in three major commercial applications—catalytic reforming, hydroprocessing, and auto emission control. The unique properties of alumina: high thermal stability, high and stable surface area, tailored pore structure, surface acidity, purity, and crystalline structure have contributed to these successful uses. Control of one or more of these properties has made possible poisoning resistance, thermal sintering, and improved performance in each process. Investigators have been able to improve thermal and hydrothermal stability and maintain surface area to temperatures as high as 1200°C through the use of stabilizers such as lanthanum and silica. Significant progress has been made in forming technology to offer structures which provide a high geometric surface-to-volume ratio with strength characteristics to resist mechanical breakage and maintain low pressure drop.

Pellets formed from alumina have been widely used for many years as supports for catalysts in a variety of chemical and petroleum processes. Alumina's usefulness is derived from its many chemical, physical, and economic characteristics. First, it is readily available in large quantities at reasonable prices; second, it can be prepared in high-purity form with surface properties ranging from slightly acidic to mildly basic, and third, it can be produced with a range of surface areas and pore structures and in several structural shapes with good strength and excellent thermal stability. Aluminas are generally prepared initially as powders, but can be formed by tabletting, extrusion, disk granulation, or oil drop technology into cylinders, spheres, and special shapes such as polylobes or miniliths. This chapter is concerned only with high surface area aluminas, those which have been arbitrarily defined as having a specific surface area greater than 100 m^2/g. We will also be turning our attention to the transition aluminas originating from gibbsite (α-trihydrate), bayerite (β-trihydrate), boehmite (α-monohydrate), or pseudoboehmite. These phases (Alcoa 1930 nomenclature) have been well described and defined in several publications.[1–3]

While there are many commercially available aluminas in powder, tablets, spheres, or extrudates, it is rare that an investigator is able to translate them into a successful catalyst in the initial experiments. Instead, it normally requires an extensive program to define the specific parameters which will be of prime interest. It is then often necessary to modify the available aluminas to optimize those parameters. Three commercial systems, representing the three largest uses of alumina pellets, reflect the situation described in the previous sentence. These are catalytic reforming, hydroprocessing, and auto emission control.

Catalytic Reforming

Catalytic reforming, a process for upgrading the octane number of straight-run naphthas or the naphtha cut from hydrocracking, was introduced in the late 1940s and consumes from 8 to 10 million pounds per year of alumina.[4] Initially this catalyst was based on a gamma-type alumina prepared by a precipitation process and washed thoroughly to remove impurities, especially soda (Na_2O) and iron, to a very low level. This product was formed into spheres or tablets and calcined to the gamma form. Because of the slightly acidic surface of such a material, it readily accepts metals like platinum from salt solutions; one example is chloroplatinic acid. The platinum disperses to a high degree over the surface area available, ≈250 m^2/g, and presents a new catalyst type, the dual-function catalyst with both hydrogenation and acidic capability.[5,6] This maximizes aromatics production from a naphtha charge stock, thus producing high octane gasoline. The application was a commercial success with long sustained life of the catalyst possible, that is, 50 to 75 barrels per pound of catalyst was easily achieved. This system was also sufficiently stable to undergo regeneration procedures, further extending the life.

In succeeding years, preparations of ultrahigh purity were developed, starting with 99.9 pure aluminum metal. Two procedures are used: (1) conversion of the aluminum to an alkoxide followed by hydrolysis to an alumina hydrate and (2) conversion to a salt through an amalgam process with subsequent neutralization to a hydrate form. It is possible to control process conditions to produce specific crystalline forms such as beta trihydrate or bayerite. Careful dehydration and calcination of this material led to the eta transition form, characterized by a high surface area, ≈300 m^2/g, with a large fraction contained in pores of less than 5 nm (50 Å) diameter. This provided a support for reforming the catalyst which gave an extended service life, reaching as high as 200 barrels per pound of catalyst.

Progress continued and alumina preparations containing controlled proportions of mixed alumina phases such as eta, nordstrandite, and gamma were formu-

lated during neutralization. This gave flexibility in process conditions with specific-yield octane benefits. Representatives of all these systems are still currently in use. Other modifications such as smaller particle size 3.18 mm (⅛ in.), 1.59 mm (1/16 in.), and 0.79 mm (1/32 in.) are all available and bimetallic compositions such as Pt-Re for lower pressure operation have been developed. Improvement of catalytic systems is a never-ending process.

Hydroprocessing

Hydroprocessing, in a specific sense hydrotreating, is the largest catalytic use of alumina pellets, consuming some 40 to 50 million pounds annually.[7] This process was developed in the same time period as reforming and was used as a preliminary step in providing a saturated low-sulfur naphtha feed to the reformer. Early samples were of gamma alumina, impregnated as a powder in the boehmite state with cobalt and molybdenum. These were extruded and calcined to the final gamma form, with a 225 m^2/g surface area and a pore volume of 0.50 cm^3/g. This resulted in a catalyst having a bulk density of 0.85 g/cm^3, a rather heavy material by today's standards. This catalyst was the industry standard until the pseudoboehmite aluminas became available.[8] The pseudoboehmites offered much higher pore volumes and the system cobalt-molybdenum now was available at a much lower bulk density, 0.60 g/cm^3, and a pore volume of 0.75 cm^3/g. At the same surface area of 225 m^2/g, this catalyst was characterized by a larger average pore diameter. This new system was extended to nickel-molybdenum and nickel-tungsten compositions and to use with heavier feed stocks, practical with the improved pore structure.

A large family of catalysts are now available. They are, however, based on the pseudoboehmite precursor, but each has a pore structure which has been specially tailored for use with different charge stocks. Uses range from the lighter feedstocks where sulfur removal is of major interest, to the heavier gas oils where both sulfur and nitrogen removal is required, such as feed to catalytic cracking units, to residual oil treating where sulfur, nitrogen, and metals such as nickel and vanadium must all be removed. The ability to control the pore structure is the foundation of this technology. Not only has particle-size reduction been possible in hydroprocessing, the introduction of polylobe extrudates has improved geometric area per unit catalyst volume with little or no penalty on pressure drop.

Auto Emission Control

In no other application was the specific need for a catalyst carrier with unique properties more evident than in that of a catalyst for automobile emission control.[9] Contrasted with the previous examples, where carefully controlled process conditions and moderate temperatures (500°C) exist, the automotive system swings wildly from ambient at cold start to a nominal level at about 600° and to an upper range which may easily reach 1000°C and above. Operation of the vehicle in normal service moves rapidly and cyclically throughout this range of temperatures with equally wide variations in gas flow.

Experience in California during the late 1950s and early 1960s showed that several properties were necessary. Some of these are a highly stable surface area in the range of 100 to 150 m^2/g; a large pore volume with both micro (less than 60 nm (600 Å) diameter) and macro (60 to 1000 nm (600 to 10 000 Å)) diameter pores; a crystalline phase and structure stable to thermal and hydrothermal conditions; and a particulate form, such as spheres or extrudates, which is strong enough to resist both crushing and abrasive action. The target life in California was one year or 12 000 miles and the supports shifted from boehmite toward the early precipitated pseudoboehmite precursors developed in the hydroprocessing area. Even so, loss of catalyst through abrasion was a serious problem and not totally overcome at that time. Although qualified by the State Air Resources Board, none of the certified catalyst systems reached commercialization. With the Clean Air Act of 1970, research programs on catalyst systems for automobiles were reactivated and directed toward a lead-free environment. The requirement of longer service duty, five years or 50 000 miles, imposed even more severe conditions.

An early experiment, using a catalyst product from the California program, indeed lasted for 50 000 miles with reasonable activity retention but, while no weight loss was observed, the catalyst chamber was only 50% full. Severe thermal exposure over prolonged time periods, one excursion to 2000°C, had caused an interaction of the alumina support with the active catalytic components, in this case copper and manganese, with resulting spinels of much greater density and lower bulk volume. This lead to the inclusion of a thermal screening test consisting of 24 hours at 982°C (1800°F) in which specifications were set. Minimum values were specified for surface area, crush strength, and attrition resistance following this exposure and maximum values for shrinkage of 5 vol% were set. In addition, no detectable levels of alpha alumina were permitted. This test required modifications to the alumina in order to meet the specified values and one method was stabilization with rare-earth mixtures. This changed the surface properties and much work was necessary to regain activity performance with base-metal compositions.

Test procedures, promulgated by the EPA, dictated an emphasis on cold-start activity and led to the exclusive use of noble metals, platinum, palladium, and rhodium as the active component in these systems. This approach opened the door for thermal stabilization of the improved pseudoboehmite aluminas against the rigors of the shrinkage test. Calcination of particles formed from pseudoboehmite, under con-

trolled conditions, moved through the transition series to the theta phase, retaining 100 to 125 m^2/g surface area and gave less than 3 vol% shrinkage with no detectable alpha alumina in the test at 982°C. Careful control of crystalline size by treating pseudoboehmite precursors allowed thermal stabilization in the gamma phase. This gave good shrinkage resistance to the thermal test, but the surface areas were 20 to 25 m^2/g less than the previous method and showed a greater tendency toward alpha alumina formation.

This thermal stabilization procedure was the basis for the initial commercial catalysts in 1975. These were both spherical and extruded cylinders with an average bulk density of 0.70 g/cm^3. Beginning in 1975 and continuing for the next two years, pelleted catalysts were used in about 70% of all automobiles manufactured for U.S. or Japanese domestic use. By 1978, the emission standards had been tightened[8] and a greater emphasis on light off activity was introduced.

Additional work on the preparation of alumina permitted modifications in the pseudoboehmites to give a distinct dual pore structure and, by control of reaction conditions,[10] to give the desired surface reactivity so that peptization could be managed to provide physically strong particles without sacrificing the dual pore system. This allowed the production of lower density particles of 0.50 g/cm^3 density, resulting not only in better light off activity but the retention of overall activity in the face of extended use with poisons.[11,12] Use rapidly shifted to this type of support and, while the monolith system gained market share, pellets continued to supply a significant fraction of the market through 1982.

Progressively more severe standards, effective in 1981, introduced additional performance requirements to the catalyst, specifically the need for NO_x reduction and the wider use of three-way catalyst (TWC) technology, either as a single-bed or dual-bed configuration. The successful application of pellets to the automobile was made possible in part by a well-designed and engineered container, developed and patented by General Motors, which has performed well in two sizes since its introduction. The advent of dual catalyst systems, a TWC as the first bed and an oxidation catalyst as bed two, imposed a tough design problem for pellets. Models were introduced and enjoyed excellent catalytic performance, but the increased use of smaller and V-6 engines with higher rpm operation and vibrational frequencies, combined with higher thermal excursions, created sufficient catalyst breakage to cause blockage and deterioration of engine performance.

Dual-bed configuration uses a rich air-fuel ratio (oxygen-deficient) as the fuel mixture for the first bed in order to reduce NO_x content, with added air between the beds for final removal of CO and HC. This design in both pellet and monolith systems often produces thermal excursions because of interactions at the bed interfaces. With pellets, this created mechanical expansion which produced crushed pellet and with monolith systems it produced the meltdow phenomenon. Crushed pellets resulted in pressur buildup, prompting driver complaint and correctiv action (recall), whereas monolith destruction by melt down failed open or safe from the frequency of drive complaint. In either case, the higher thermal loa imposed more severe thermal requirements on th system and improved aluminas, stabilized for bot pellets and washcoat, were required. Despite excellen catalyst performance, in many respects superior t monoliths, the use of pellets in dual-bed converter came to an end and at present perhaps only 20% of th market is supplied by pellets.

Single-bed operation continues as TWC system require modifications such as the use of ceria an additional stabilization against thermal deactivation. I has been found that individual rare earths, for exam ple, lanthanum, impart a high degree of thermal sta bility. As shown in Table I, gamma aluminas may los surface area at 1000°, special aluminas derived fro pseudoboehmite retain significant amounts at 1100°. while lanthanum stabilization may allow retention o as much as 50 m^2/g at 1200°C. Little interference wit catalytic performance is observed with lanthanum. Stabilization can also be achieved with silica an surface area retention may be 25 m^2/g higher at given temperatures. However, silica imparts a stronger acid surface to the alumina and may interfere in some reaction systems.

Significantly, the extension of strict standards to light and medium trucks puts a premium on thermal stability since these vehicles, on the average, operate under load conditions which increase the thermal load on the catalyst. The thermal resistance of alumina makes this ideal for such service and the surface area stabilizers allow performance durability not previously observed.

As noted in the cases of reforming and hydroprocessing, aluminas permitted the downsizing of the catalyst particle to as small as 0.79 mm (1/32 in.) and the introduction of special shapes such as polylobes. So too with emission control, a case in which mass transfer is the controlling factor in conversion, an increase in activity is gained through greater geometric area as opposed to specific surface area. Figure 1 shows that the geometric area per unit volume increases as particle diameter decreases and shows comparison points for commercial monoliths. This shows that

Table I. Thermal Stability of Aluminas*

Source	1000°C	1100°C	1200°C
Bayerite/gibbsite	20	5	1
Pseudobhoehmite	120	60	5
Pseudoboehmite w/lanthanum	150	90	50
Pseudoboehmite w/silica	175	115	75

*Surface area (m^2/g) six hours at temperature shown.

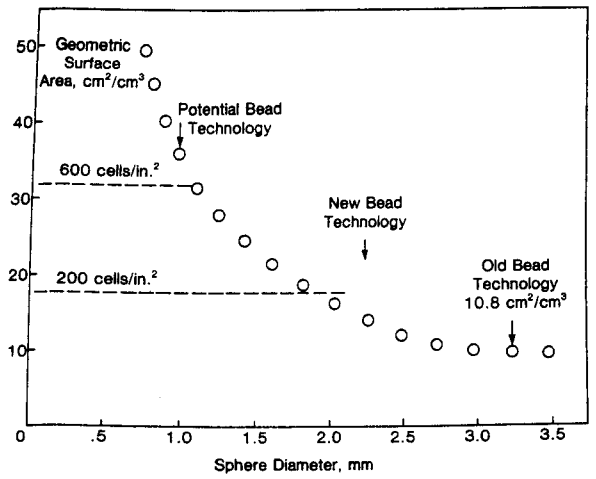

Fig. 1. Spherical-bead geometric surface area as a function of bead diameter.

equivalent geometric areas can be achieved with pellets in a practical particle-size range. External factors such as pressure drop come into play as particle size decreases, indicating the range of design features which must be considered in a catalytic system. The impact of geometric area on hydrocarbon conversion is shown in Fig. 2, where values for both fresh catalyst and 50 000-mile-aged catalyst are plotted. While the effect is real and significant, the total picture is discussed in detail in Ref. 13, where factors including pressure drop and optimum pore structure are considered.

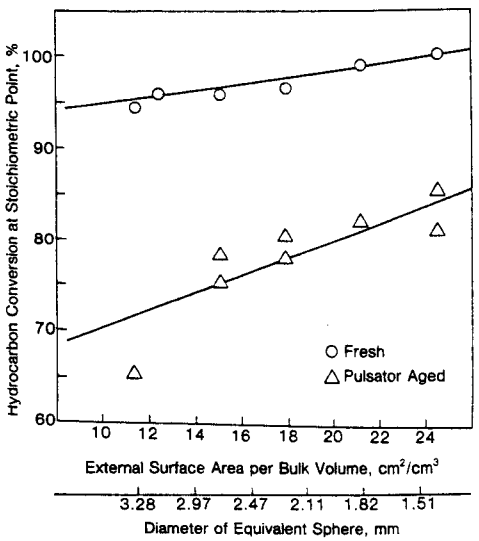

Fig. 2. Effect of external surface area on HC conversion at stoichiometry.

Conclusion

Alumina has inherent chemical and physical properties that make it an ideal material as a catalyst support for particulate or pelleted systems. Many of the properties of alumina can be modified and optimized for specific applications where critical parameters are poisoning thermal stress, physical stress, and mass transfer control. A necessary part of a successful catalytic application is understanding the relationship and influence of external factors such as flow, pressure drop, reactor pressure, temperature, and space velocity. When these factors can be properly engineered into the design, pelleted catalysts offer the best solution in most cases. Where size conditions (frontal area and bed depth) and pressure drop become controlling, monolith configurations offer much potential. In the case of monolithic emission control catalysts, the active substrate is the washcoat of alumina. The characteristics of this washcoat are as critical as the properties of pellets used as catalyst supports.

References

[1]A. S. Russell, et al., "Alumina Properties," Technical Paper No. 10 Alcoa, Pittsburgh, 1953.

[2]K. Wefers and G. M. Bell, "Oxides and Hydroxides of Aluminum," Technical Paper No. 19, Alcoa, Pittsburgh, 1972.

[3]K. Wefers and C. Misra, "Oxides and Hydroxides of Alumina," Alcoa Laboratories, 1987.

[4]M. D. Edgar, Catalytic Reforming of Naphtha in Petroleum Refineries, Vol. 1, Applied Industrial Catalysis, 1983

[5]F. G. Ciapetta, "Isomerization of Saturated Hydrocarbons—Nature of the Catalyst and Mechanism of the Reaction," *Ind. Eng. Chem.*, **45**, 162 (1953).

[6]G. A. Mills, H. Heinemann, T. H. Miliken, and A. G. Oblad, "Houdriforming Reactions-Catalytic Mechanism," *Ind. Eng. Chem.*, **45**, 134 (1953).

[7]D. C. McCulloch, Catalytic Hydrotreating in Petroleum Refining, Vol. 1, Applied Industrial Catalysis, 1983

[8]R. K. Oberlander, Aluminas for Catalysts, Vol. 3, Applied Industrial Catalysis, 1984.

[9]W. S. Briggs, Catalysts and the Automobile—25 Years Later, Vol. 3, Applied Industrial Catalysis, 1984.

[10]*(a)* M. G. Sanchez and N. R. Laine, "Process for Preparing Alumina," U.S. Pat. No. 4 154 812, May 15, 1979.

(b) M. G. Sanchez, M. V. Ernest, and N. R. Laine, "Process for Preparing Spheroidal Alumina Particles," U.S. Pat. No. 4 179 408, December 18, 1979.

(c) M. G. Sanchez and N. R. Laine, "Alumina Compositions," U.S. Pat. No. 4 371 513, February 1, 1983.

(d) M. G. Sanchez and J. E. Herrera, "Extruded Alumina Catalyst Support having Controlled Distribution of Pore Sizes," U.S. Pat. No. 4 301 037, November 17, 1981.

[11]L. L. Hegedus and J. C. Summers, "Improving the Poison Resistance of Supported Catalysts," *J. Catal.*, **48**, 345–53 (1977).

[12]J. R. Adomaitis, J. E. Smith, and D. E. Achey, "Improved Pelleted Catalyst Substrates for Automotive Emission Control," SAE Paper No. 800084, February 25–29, 1980.

[13]C. J. Pereira, G. Kim, and L. L. Hegedus, "A Novel Catalyst Geometry for Automobile Emission Control," *Catal. Rev.-Sci. Eng.*, **26** [3–4] 503–23 (1984).

Electrical Properties of Alumina Ceramics

Robert H. Insley
Champion Spark Plug Company
Ceramic Division
Detroit, MI 48234

Alumina is a dominant ceramic material not only because of its superior mechanical, thermal, and chemical properties, but also because of outstanding electrical properties that make it an excellent low-tension and high-tension insulator. The electrical properties make it adaptable for use in applications ranging from electronic substrates to spark plug insulators to MHD power generators. Resistivity is affected by phases present, secondary-phase distribution, alkali content, and temperature. Dielectric strength is a function of temperature, specimen thickness, porosity, and silicate glass-phase concentration and distribution.

The excellent electrical insulating properties of alumina were recognized early and were first applied in technical ceramics in the manufacture of spark plug insulators. Gerdian and Reichmann prepared an insulator composition in 1927 which was substantially pure alumina and Reichmann subsequently patented this technology.[1] Shortly after, Kohl[2] published work that was done at Siemens-Halske to develop a spark plug insulator of sintered alumina and the technology was soon advanced in the United States by several manufacturers.[3] It was necessary to have an alumina raw material with a low iron content for the successful development of alumina ceramics for electrical applications; this was achieved in the early and middle 1920s. The technical superiority of alumina for many applications, ranging from high-tension insulators to electronic substrates, has lead to its widespread use. It is the dominant ceramic material in use today and is predicted to remain in this position into the next century.

Volume Resistivity

Alumina has high electrical resistance over a broad range of temperatures. A typical 95% alumina composition will have a room-temperature volume ac resistivity of $>10^{14}\ \Omega \cdot$ cm that will drop to around $7 \times 10^5\ \Omega \cdot$ cm at 1000°C. The T_c value (temperature at which the volume resistivity is 1 M$\Omega \cdot$ cm is typically between 950° and 1000°C. Alumina content of the ceramic has a significant influence on the resistivity. Normal glass-bonded alumina ceramics will have resistivities that vary with temperature, as shown in Fig. 1. It is difficult to measure precisely the electrical resistance of a polycrystalline ceramic and the data for alumina have shown differences of several orders of magnitude. Complete information with regard to purity, solute concentration, nonstoichiometry, experimental techniques, firing conditions (particularly partial oxygen pressure), grain size, grain-boundary conditions, etc. is necessary to interpret the results. The resistivity/conductivity characteristics of ceramic systems result from the contributions of the phases

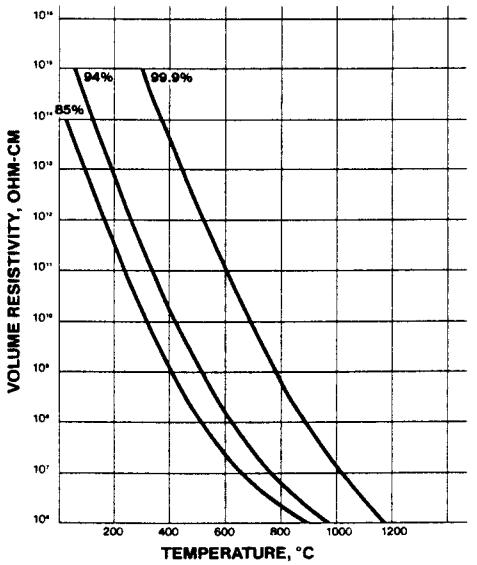

Fig. 1. The effect of alumina content and temperature on the volume resistivity of alumina ceramics. Data courtesy of Coors Porcelain Co.

present, e.g., pores, glass phase, secondary crystalline phases, etc. Substantial effects can result from changes in composition at grain boundaries. For alumina ceramics there is almost invariably a silicate glassy phase at the grain boundaries, causing a separation of the grains. This results in a two-phase system with the minor phase being the continuous one. The resulting resistivity depends on relative conductivity values of the individual phases. As temperature increases, the resistivity of the silicate phase drops more rapidly than that of the major alumina phase. Compositions whose resistivities drop most at moderate temperatures are those that have an appreciable glassy phase.

The negative thermal coefficient of resistance is typical of ionic- or homopolar-bonded ceramic materials as opposed to metallic-bonded materials, which have a positive thermal coefficient. The resistivity will

also be dependent on the purity of the raw material; alkali, iron, and titania impurities are the most influential. Presently, commercial-grade calcined aluminas are readily available with <0.05% Fe_2O_3 and <0.10% Na_2O. These impurity levels are too low to have any significant effect on conductivity or dielectric losses for most commercial applications. The effect of soda content on the T_e value of a 90% glass-bonded alumina ceramic is shown in Fig. 2. Kröger and others have studied the effects of several dopants on the properties and structure of alumina[4–8] and Kröger summarized the effects on the electrical properties.[9] Kemp and Moulson[10] showed that Fe_2O_3 in solid solution with Al_2O_3 had no effect on the conductivity but Fe^{2+} increased conductivity by an electron-hopping mechanism associated with oxygen vacancies. Gitzen[11] cited numerous references on the resistivity and conductivity of alumina and alumina ceramics.

Pappis and Kingery[12] reported that single-crystal alumina exhibits intrinsic semiconductivity above 1600°C at low to moderate oxygen pressures. They also noted that polycrystalline alumina specimens behaved similarly to single crystals except that intrinsic conduction is masked by impurity- or structure-sensitive defects. There was a frequency dependence of resistivity and dielectric constant.

Alumina has been primarily noted for its high electrical resistance, but there is a form, β-alumina, that exhibits exceptionally high ionic conductivity and that has become of great technological interest. The β-aluminas are hexagonal structures with the approximate composition $AM_{11}O_{17}$, in which the mobile ion A is a monovalent ion such as Na or K and M is a trivalent ion, normally Al. There are related structures, β′-AM_7O_{11} and β″-AM_5O_8, the latter having extremely high conductivities and currently of interest as a ceramic electrolyte for the sodium-sulfur battery for electrical propulsion or off-peak power storage.

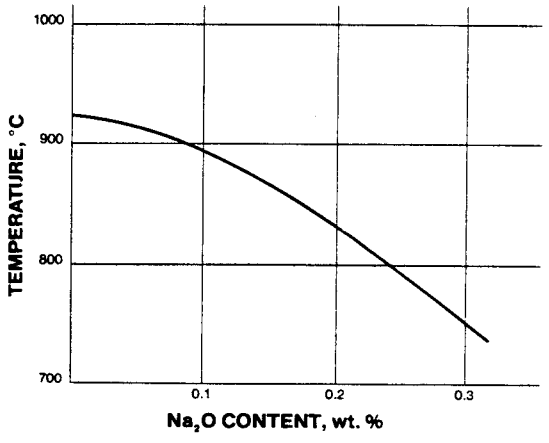

Fig. 2. The effect of Na_2O content on the T_e value of a 90% Al_2O_3 ceramic. Champion Spark Plug Company internal communication.

Dielectric Constant

The dielectric constant of a material is the measure of the storage capacity of a dielectric and is equal to the capacitance when the plates are separated by a thickness of the dielectric compared to the capacitance when the plates are separated by the same thickness under vacuum. Dielectrics can be generally classed[13] as insulators with dielectric constant below 12 and capacitors with dielectric constant above 12. The dielectric constant of alumina places it well within the insulating range with a value of 8.8 at 1 MHz. The single-crystal values show an anisotropy of 10.6 parallel to the *c* axis, as compared to 8.6 perpendicular to the *c* axis. Alumina's loss factor is about 0.001, again low enough that it satisfies conditions for insulating applications. The influence of temperature and frequency on the dielectric constant and loss factor of alumina ceramics is illustrated in Fig. 3. Alumina ceramics with the crystalline α-alumina separated by a vitreous silicate boundary layer have properties between those of single-crystal Al_2O_3 and glasses. The dielectric constant and the loss factor increase with temperature, particularly at the lower frequencies. The glassy phase is the main contributor to dielectric losses and its composition is the controlling factor. To obtain low-loss materials, alkali-containing fluxes, such as feldspars, are avoided by using clays, talcs, and alkaline earth oxides, such as calcite or dolomite. Alumina ceramics have properties suitable for most dielectric applications. As a guide, the minimum requirements for the joint Army and Navy specifications

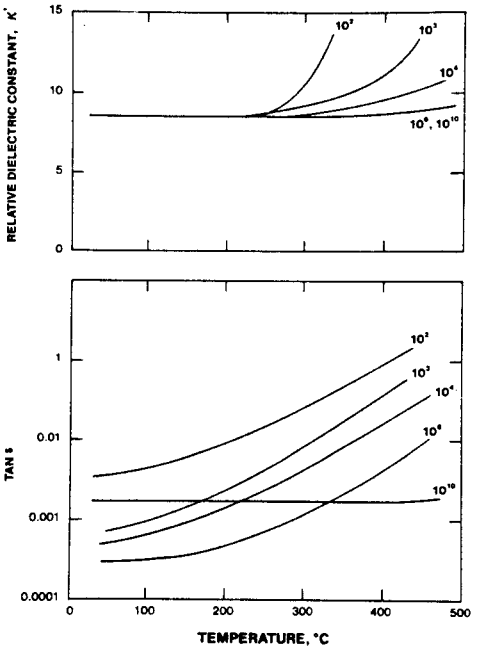

Fig. 3. Effect of frequency and temperature on the dielectric constant and tan δ of an alumina ceramic. See Ref. 13. (Used with permission.)

for ceramics to be used as insulators in electronic devices are given in Table I.

Dielectric Strength

The dielectric or electrical breakdown strength of alumina is an important property because of the key role of this ceramic as a high-tension insulator at ambient and high temperatures. From spark plug insulators to new energy technologies such as MHD power generators, there is a requirement for good electrical insulation between electrodes at moderate to high temperatures—up to 1800°C. Electrical conductivity has been studied extensively but electrical breakdown, particularly at high temperatures, has received less attention. Dielectric strength is the dielectric breakdown of insulating materials under an applied electric field. It can take place by an electronic mechanism, which is referred to as the intrinsic dielectric strength, or by a heating mechanism by which ceramic materials usually fail. Under an applied electrical stress, local overheating arises from local electrical conduction and increases to a point where instability occurs, permitting a rush of current, melting, and puncture—a result of thermal breakdown. Thermal breakdown increases with an increase in temperature or an increase in the time a voltage is applied. Glass and polycrystalline ceramics such as alumina follow similar behavior. Vermeer[15] showed that the apparent dielectric strength for Pyrex* glass is decreased by three orders of magnitude when the impulse time is increased from 10^{-5} to 30 seconds. The absolute value of dielectric breakdown strength is highly dependent on the test method used, electrode materials, electrode configurations, nonhomogeneous fields, testing medium, etc.

A study on sapphire and 99.5% polycrystalline alumina by Yoshimura and Bowen[16] showed that the strength was identical for both materials, and dc measurements on the sapphire in thicknesses of 2.5 to 10 μm showed a dielectric strength of 600 kV/mm (15 000 V/mil). They concluded that the breakdown was thermal and that, in addition to the intrinsic factors of low electrical conductivity and high thermal conductivity of materials, high electrical strengths increase with the elimination of surface and bulk defects. They also showed that the relationship between resistivity and breakdown strength is a straight-line function with a slope of one-half when a log-log plot is used.

Probably the most commonly used dielectric strength test procedure for commercial ceramic materials is ASTM D-116. It specifies a disk of the test material and brass or stainless steel cylinders with rounded edges for electrodes. It also specifies the procedure for determining the dielectric strength of the testing medium, usually transformer-grade insulating oil. When the oil becomes contaminated, it will become more conductive and energy loss in the oil will result in an apparently higher dielectric strength of the test material. In addition to flat disks, samples with machined wells, shrouds on the edges, or pressure-sealed flanges have been used to increase the flashover path. The sample thickness has a significant effect on the dielectric strength as a thicker sample will require more time to rupture, thus increasing the heating. The effect of sample thickness on dielectric strength is shown in Fig. 4. The test-specimen thickness should be representative of the thickness of material in the commercial application. Thus, spark plug insulator ceramics are generally tested in thicknesses of 1.25 to 1.5 mm. Modern, high-energy ignition systems are capable of developing 20 kV and insulator walls can be as thin as 1.25 mm, requiring dielectric strengths as great as 16 kV/mm (400 V/mil).

A method for rapidly testing ceramics for spark plug insulators as a process control function, with test specimen geometry and wall thickness and voltage application representative of service conditions, has been used routinely.[17] Cylindrical specimens 5.75 cm long with a 1.27 mm wall and 6.35 mm OD are isostatically pressed, turned, and fired under the same conditions as the in-service insulator. They are insert-

Table I. JAN-I-10 Minimum Requirements for Insulating Ceramics, Radio, Class L

Porosity:	No liquid penetration at 70 MPa pressure
Thermal stress resistance:	
Type A:	withstand 20 cycles from 100°C into 0°C water
Type B:	withstand 5 cycles from 100°C into 0°C water
Transverse strength:	>21 MPa
Dielectric strength:	>7.2 kV/mm
Dielectric constant:	<12 after 48-h water immersion/
Loss factor (κ′ tan δ):	Grade L-1 <0.150
	L-2 <0.070
	L-3 <0.035
	L-4 <0.016
	L-5 <0.008
	L-6 <0.004

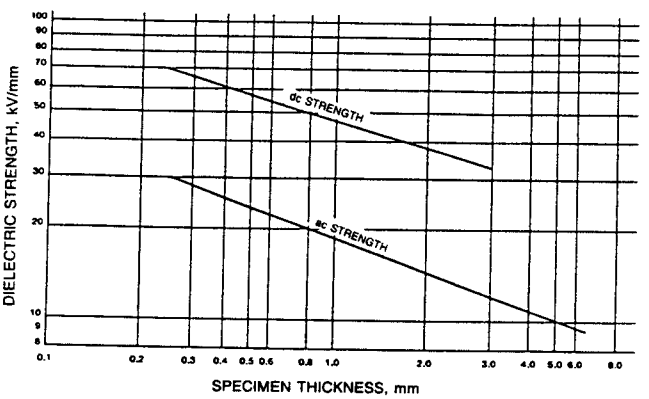

Fig. 4. The effect of specimen thickness on the dielectric strength of alumina ceramics. Data courtesy of Coors Porcelain Co.

*Corning Glass Works, Corning, NY.

ed in an insulating oil bath over a wound, fine-coiled stainless steel spring and into a woven wire sheath that contacts the outer wall opposite the spring. The spring is unwound to contact the inner wall. Alternating current voltage is applied at a rate of 1 kV/s until rupture occurs. The large current drawn at the time of rupture trips a circuit breaker, and the rupture voltage is displayed on a dial readout. Whatever the test sample and electrode material, the volume of sample exposed to the electrical stress should be great enough to account for a representative sampling of defects in the test material. Just as 4-point bending in modulus of rupture (MOR) is preferred over 3-point because it samples a larger volume of material, so should dielectric strength determinations sample a significant volume of material. Illustrative of this is the fact that, when a sample has been electrically ruptured in insulating oil and then retested, a higher value will be obtained as the rupture will fill with insulating oil and in the subsequent test the next weakest spot will fail.

The heating effect is dramatically shown in Figs. 5 and 6. This was a breakdown in a 92% Al_2O_3 ceramic under 21 kV through a 1.27 mm wall at a voltage increase rate of 1 kV/s. The dielectric strength was 16.5 kV/mm (420 V/mil). The melting effect is clearly shown in the smooth walls of the tubular breakdown path. The heating effect, even for the very short duration, is very intense. An energy dispersive X-ray probe of the walls of the hole indicated that the component remaining was primarily alumina, indicating that the silica, calcia, and magnesia used to flux this particular ceramic had vaporized. The hole is about 20 μm in diameter.

Temperature also has a significant effect on dielectric strength. Figure 7 shows the effect of testing two specimen thicknesses at temperatures up to 1100°C. The high temperature accelerates the heating that occurs when the voltage is applied, resulting in very low dielectric strengths at high temperatures. The

Fig. 5. View into a dielectric puncture of a 92% Al_2O_3 ceramic (× 2400). Champion Spark Plug Company internal communication.

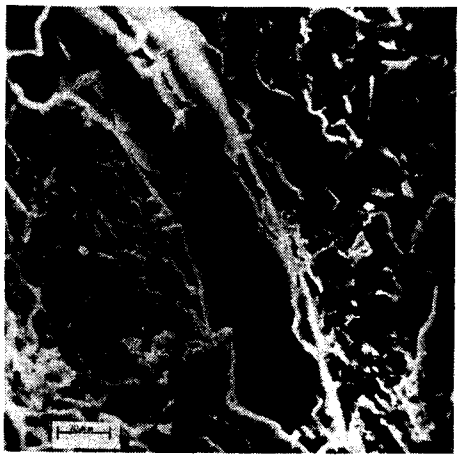

Fig. 6. View along the path of a dielectric puncture at 21 kV of a 92% Al_2O_3 ceramic (× 2400). Champion Spark Plug Company internal communication.

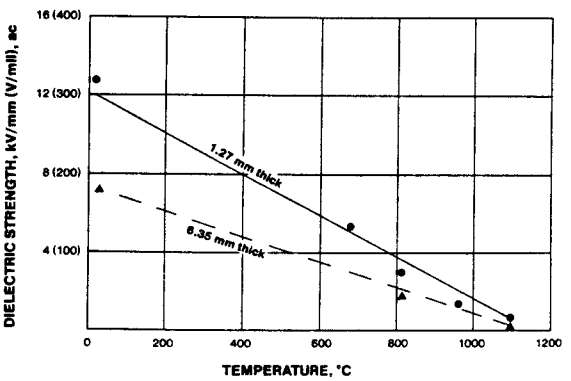

Fig. 7. The effect of temperature and thickness on the dielectric strength of a 92% Al_2O_3 ceramic. Champion Spark Plug Company internal communication.

dielectric strength of the medium in which the article is operating (in the case of the spark plug insulator, the combustion chamber atmosphere) is also decreasing, however, letting the ceramic material remain as an effective insulator.

Porosity also has a significant effect on dielectric strength, as would be expected. A 90% alumina ceramic was underfired to produce varying degrees of porosity, and then tested for dielectric strength. There was a 50% drop in dielectric strength between 5 and 12% closed porosity, as shown in Fig. 8. An identical relationship with porosity for hot-pressed alumina was found by Morse and Hill.[14]

The dielectric strength of alumina ceramics can be significantly increased in several ways. Insley and Barczak[18] showed that the dielectric strength of an 89% Al_2O_3 ceramic was increased 32% by rapid cooling after reheating to near the normal maturing temperature. A similar increase was observed for the physical strength (MOR), indicating a restoration of the integrity of the material following exsolution that occurs on normal kiln cooling. The reheating and

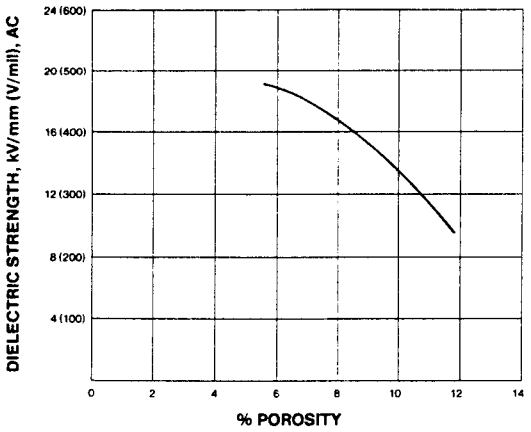

Fig. 8. The effect of porosity on dielectric strength of a glass-bonded 90% Al_2O_3 ceramic. Champion Spark Plug Company internal communication.

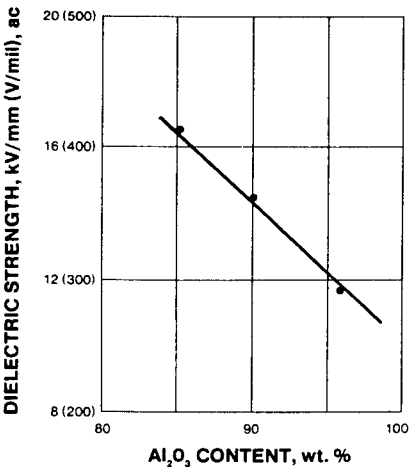

Fig. 9. The effect of silica glass-phase content on the dielectric strength of high-alumina ceramics. Champion Spark Plug internal communication.

quick cooling left more of the glass phase in the vitreous state and minimized the grain-boundary stresses that occur with exsolution. Vitreous glasses have higher dielectric strengths than crystalline ceramic materials and increasing the glass phase in a polycrystalline alumina increases the dielectric strength. Changing the alumina content from 96 to 85% by increasing the silicate flux content, and thus the glass content, increased the dielectric strength from 11.6 kV/mm (295 V/mil) to 16.5 kV/mm (418 V/mil), a 42% increase (Fig. 9).

Acknowledgments

The support of Champion Spark Plug Company in providing facilities for reproduction of the figures, F. E. Simms for the micrographs, and P. E. Rempes for aid in literature search is acknowledged with appreciation.

References

[1]R. Reichmann, "Spark Plug," U.S. Pat. No. 1 799 225, April 7, 1931.

[2]H. Kohl, "Vitreous Corundum, a New Ceramic Material of Pure Alumina," *Ber. Dtsch. Keram. Ges.*, **13** [2] 70–85 (1932).

[3]J. S. Owens, J. W. Hinton, R. H. Insley, and M. E. Poland, "Development of Ceramic Insulators for Spark Plugs," *Am. Ceram. Soc. Bull.*, **56** [4] 437–43 (1977).

[4]B. V. Dutt and F. A. Kröger, "High Temperature Defect Structure of Iron-Doped α-Alumina," *J. Am. Ceram. Soc.*, **58** [11–12] 474-76 (1975).

[5]L. D. Hou, S. K. Tiku, H. A. Wang, and F. A. Kröger, "Conductivity and Creep in Acceptor-Dominated Polycrystalline Al_2O_3," *J. Mater. Sci.*, **14** [8] 1877–89 (1979).

[6]B. V. Dutt, J. P. Hurrell, and F. A. Kröger, "High-Temperature Defect Structure of Cobalt-Doped α-Alumina," *J. Am. Ceram. Soc.*, **58** [9–10] 420–27 (1975).

[7]S. K. Mohaptra and F. A. Kröger, "Defect Structure of α-Alumina Doped with Magnesium," *J. Am. Ceram. Soc.*, **60** [9–10] 381–87 (1977).

[8]M. M. El-Aiat and F. A. Kröger, "Yttrium, an Isoelectric Donor in α-Alumina," *J. Am. Ceram. Soc.*, **65** [6] 280–83 (1982).

[9]F. A. Kröger, "Electrical Properties of α-Al $_2O_3$"; pp. 1–15 in Advances in Ceramics, Vol. 10. Edited by W. D. Kingery. The Amerian Ceramic Society, Columbus, OH, 1984.

[10]J. L. Kemp and A. J. Moulson, "The Effect of Iron Additions on the Electrical Properties of Alumina Ceramics," *Proc. Br. Ceram. Soc.*, **18**, 53–64 (1970).

[11]W. H. Gitzen (ed), Alumina as a Ceramic Material. The American Ceramic Society, Columbus, OH, 1970.

[12]J. Pappis and W. D. Kingery, "Electrical Properties of Single Crystal and Polycrystalline Alumina at High Temperatures," *J. Am. Ceram. Soc.*, **44** [9] 459–64 (1961).

[13]W. D. Kingery, H. K. Bowen, and D. R. Uhlmann; pp. 847–974 in Introduction to Ceramics. Wiley & Sons, New York, 1975.

[14]C. T. Morse and G. J. Hill, "The Electric Strength of Alumina: The Effect of Porosity," *Proc. Br. Ceram. Soc.*, **18**, 23–36 (1970).

[15]J. Vermeer, "Impulse Breakdown Strength of Pyrex Glass," *Physica*, **20**, 313–26 (1954).

[16]M. Yoshimura and H. K. Bowen, "Electrical Breakdown Strength of Alumina at High Temperatures," *J. Am. Ceram. Soc.*, **64** [7] 404–10 (1981).

[17]P. E. Rempes, D. H. Pratten, and R. H. Insley, "Process Control Dielectric Strength Testing of High Alumina Ceramics," *Am. Ceram. Soc. Bull.*, **51** [4] 414 (1972).

[18]R. H. Insley and V. J. Barczak, "Thermal Conditioning of Polycrystalline Alumina Ceramics," *J. Am. Ceram. Soc.*, **47** [1] 1–4 (1964).

Electronic Ceramics

Bernard Schwartz
IBM Corporation
East Fishkill, NY 12533-0999

The use of alumina ceramics in high-density electronic packaging of integrated circuits has been highly successful, with the most advanced embodiments being used in the IBM 3080 and 3090 systems. Those embodiments are described after a discussion of previous achievements that led to their development. Then, criteria for future ceramics, metallurgies, and processes are presented.

Ceramic-based "headers" or "modules" have been used for the past three to four decades to provide an intermediate level of interconnections between microelectronic chips and printed circuit cards or boards. The initial use of ceramics in the packaging of electronic devices was for interconnections and environmental protection.[1-3] Eventually these uses were expanded so that a ceramic substrate became a functional part of the system using it. As large-scale systems became more complex, the packaging had to be compatible with these changes. This chapter describes packaging ceramic developments during the past 30 years and illustrates the growth of substrate technology.

Early headers were made from glass metal bases and ceramic disks and contained from 3 to 14 leads, as shown in Fig. 1. A cap (not shown) was subsequently welded to the flange. Figure 2 shows a 16-lead package, with a flange extending from the pin area, to which a cap could be welded. In Fig. 3, a package is shown with 60 leads and, in this case, a cap could be soldered to the flange. Figure 4 portrays a flat pack with 32 leads which was typically sealed with a solder glass. Other types of packages included leadless chip carriers (LLCC), leaded chip carriers (LCC), and multichip carriers.

A flow sheet for the dry-pressing process for fabricating a typical substrate is shown in Table I. This process included the ball milling of an alumina-glass slurry with a binder, lubricant, and water. This suspension was then spray-dried to a fine alumina-glass powder with binders and lubricants adhering to the surfaces of the particles. The powder was then dry-pressed in dies, and these parts were sintered in air at temperatures between 1450° and 1600°C. The final step, metallizing of these parts, could be done either at the plants which produced them or at the receiving locations.

Figure 5 summarizes the improvement of circuit performance and densities from 1965 to 1980. Note that the circuit delay times decreased over one order of magnitude and circuit densities at the module level

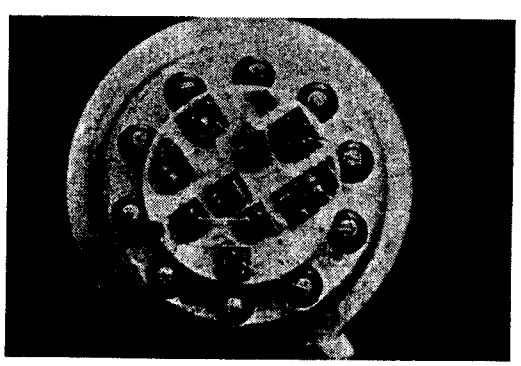

Fig. 1. Hermetically sealed glass-metal header with ceramic insert.

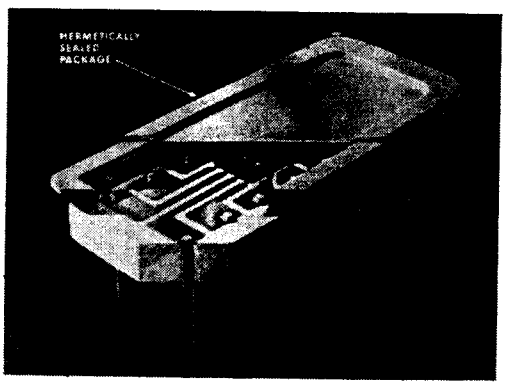

Fig. 2. Hermetically sealed sixteen-pin dual in-line package.

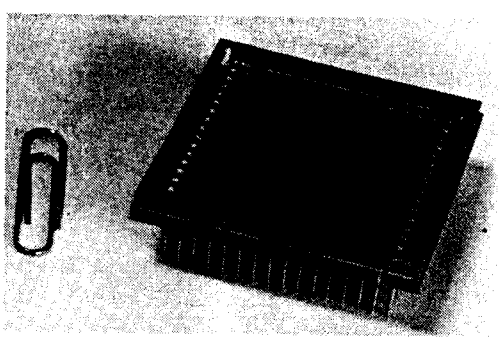

Fig. 3. Hermetically sealed sixty-pin substrate.

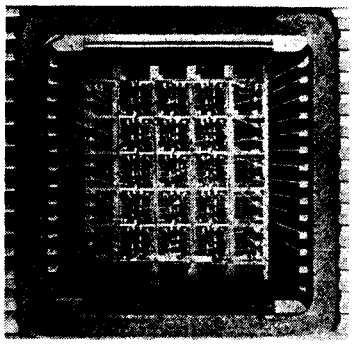

Fig. 4. Hermetically sealed thirty-two leaded flat pack.

Table I. Steps in the Dry-Press Process

1.	Ball mill slurry
	Alumina
	Glass
	Binders and lubricants
	Solvents
2.	Spray-dry slurry
3.	Press parts
4.	Sinter parts
5.	Metallize parts

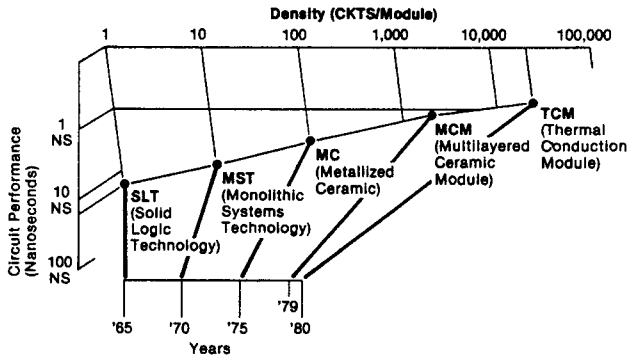

Fig. 5. Evolution of density/performance of IBM modules.

increased over four orders of magnitude during this time. The improvements were also occurring in much shorter time intervals.

The first module developed at IBM was the solid logic technology (SLT) module, which is pictured in Fig. 6. It consisted of a 12.7-mm square, 96% alumina ceramic substrate which was metallized with thick noble metal pastes. Each substrate contained up to 16 holes into which copper pins were swaged. Resistors were screened onto these substrates to provide for the connections. Silicon device chips were then connected to the solder-coated conductors by using solder-coated copper balls. The alumina substrates provided the supporting structures for these elements. This technology was introduced in 1965.

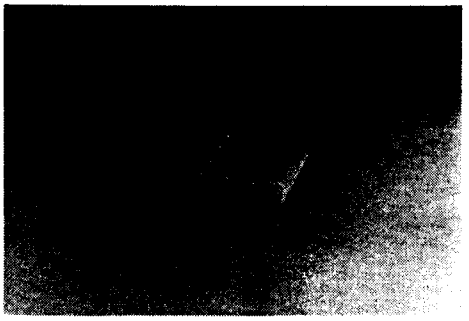

Fig. 6. Solid logic technology (SLT) module.

In 1970, IBM produced the monolithic systems technology (MST) modules. The chips used in this development contained logic and memory circuits. For these chips, the solder-coated copper balls were replaced with 95% Pb-5% Sn solder pads. This module is shown in Fig. 7.

IBM announced the metallized ceramic (MC) modules in 1975; in this development, use was made of Cr/Cu/Cr thin-film surface patterns. The MC modules required 28 by 28 mm or 36 by 36 mm substrates to support additional pins and larger integrated circuit chips. These modules used aluminum covers with crimped seals at the base of the (96% alumina) substrates. The MC module is still being produced by IBM, and is pictured in Fig. 8.

IBM's multichip module (MCM) contained 23 layers of wiring, had nine chips, was 50-mm square, used a sealing ring on the top surface, and had 361 I/O pins. The MCM used a 90% alumina and 10% glass substrate with Mo metallization. An enhanced version of the MCM had 64 chips and the same ceramic and metallurgical composition.

The thermal conduction module (TCM) was manufactured with the same alumina, glass, and Mo metallization as the MCM. These modules were 90 by 90 mm, had 33 layers (5.5-mm thick), and contained up to 133 chips and 1800 I/O pins. IBM still produces TCMs in plants in the United States and Germany, and uses them for the IBM 3080 systems. Approximately 350 000

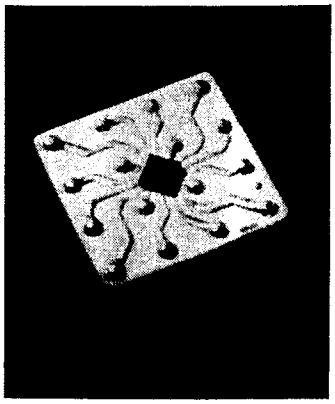

Fig. 7. Monolithic systems technology (MST) module.

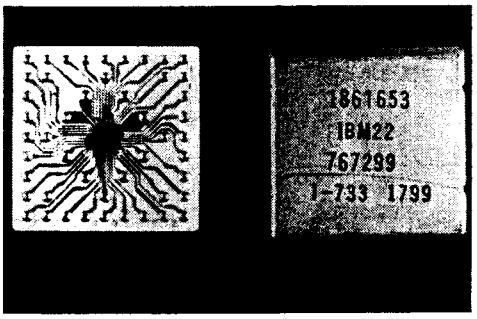

Fig. 8. Metallized ceramic (MC) module.

vias, holes through the layers which were filled with a molybdenum paste, and 130 m of internal wiring, were used to interconnect the various layers.[4] Typically, 25 000 circuits and 60 000 array bits were interconnected on one module. This is the same number of circuits contained in an entire IBM System/370 Model 145.

Balderes and White[5] reported how an entire level of packaging could be eliminated from the IBM 3080 computer system. They were able to cut the delay times in half with the use of the TCM.

In 1985. IBM introduced a new TCM which was made with the same material combination as the first TCM. It had 36 layers, up to 100 chips, and 1800 I/O pins. The size of this substrate was 107 by 118 mm, and the cover was then attached directly to the substrate with the same type "C" ring. These substrates will be described more fully in the following sections.

Multilayer Ceramic Technology Development

Laminated ceramics were originally developed to meet the special capacitor needs of the Micromodule Project for the U.S. Army Signal Corps and the Radio Corporation of America. Based on the titanate materials available in 1958, at least 11 layers, each 0.025-mm thick, would be needed to produce these capacitors. Each capacitor had three notches on each side.

The two critical problems to be solved were how to produce 0.025-mm layers and how to laminate them into a monolithic structure. Doctor blading was selected as the first choice because it was the most efficient in regard to casting thin green sheets. At that time thick plasticized green titanate sheets were being made for capacitors. Fortuitously, the paint industry was then producing a plasticized copolymer of polyvinyl chloride acetate, which could be used as a binder. The interactions of ceramic powders, plasticized binder, deflocculants, and solvents were optimized to produce a stable slurry with a high specific gravity that could be used for doctor blading thin green sheets.[6]

The layer-to-layer connections for the capacitors were made by extending palladium metallization to the notches on wafers, and then painting the notches with vertical stripes of the palladium electrode material. A completed capacitor could then be sintered and made available for the micromodule. The lamination was done using a heated press.[7] A capacitor was 7.62-mm square and over 0.0508-mm thick. The capacitors were sintered in air between 1250° and 1400°C. Table II provides the equation for calculating the capacitances of these capacitors. This technology marked the beginning of the multilayer capacitor industry.

In 1960, the Micromodule Project needed hermetic alumina packages for quartz crystal oscillators. In this application a plasticized polyvinyl butyral binder was used for the thicker green sheets. This three-layer alumina package used a molybdenum-manganese type of metallization in order to achieve hermeticity. This package had to be sintered in a wet hydrogen atmosphere between 1500° and 1600°C. A metal cap was ultrasonically soldered to the nickel- and gold-plated sealing ring on the top surface of the substrate. The quartz crystal oscillator had to be hermetically sealed to keep out contaminants from the package. Its significance lay in an engineer's ability to cast, screen, laminate, and sinter the new three-layer substrate. This was the first MLC alumina package produced in the industry.[8]

Similar micromodule multilayer packages were made for transistors and diodes. The far right side of Fig. 9 shows a stack of micromodule wafers, produced for the micromodule, which are connected with 12 riser wires. To the left of this stack is a laminated module, which provided for a remarkable reduction in the size of the substrate.

In 1961, a request came from the RCA Laboratories to make a package that would house many unipolar transistors. At this time the development of the via provided a major breakthrough in the ability to make crossovers any place in the planes of the green sheets.[9] Vias are holes in which Mo-Mn pastes are screened to

Table II. Calculations for Capacitance of Multilayer Capacitors

$$C = \frac{0.009 \times \epsilon \times A \times n}{t} \text{ (pF)}$$

Precision capacitor:

ϵ = 30
A = 25.8 mm^2
n = 11 layers
t = 0.0254 mm
C = 3000 pF at 50 Vdc rating

General-purpose capacitor:

ϵ = 3000
A = 25.8 mm^2
n = 11 layers
t = 0.0254 mm
C = 300,000 pF at 50 Vdc rating

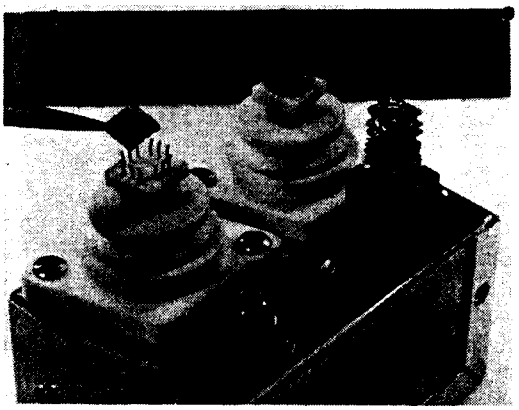

Fig. 9. Micromodule wafers and laminated micromodule.

make connections under or over other signal lines. Each via was attached to another by a screened Mo-Mn paste line, as shown in Fig. 10. The top of this substrate had etched thin-film surface patterns which were used to interconnect these unipolar transistors. This was a remarkable achievement.

In 1962, the Micromodule Project ended. However, the technologies developed in this project were to become the basis for future products in regard to computers and other electronic systems. From 1963 to 1979, thick- and thin-film technologies were utilized to create new processes for the ensuing electronics era.

Among the most widely used processes developed in this time span was the doctor blading of green sheets. A slurry was prepared with an alumina-glass powder and a polyvinyl butyral binder with two solvents. This slurry was mixed in a ball mill, which was cast in a large continuous caster to make the alumina green sheets (Fig. 11). These green sheets, nominally 0.28-mm thick, had to be carefully dried in the drying chamber. The solvents were evaporated from the

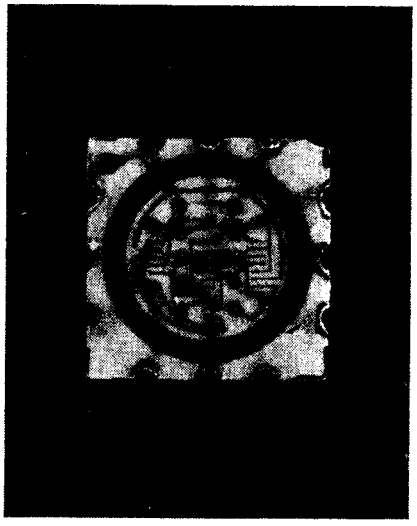

Fig. 10. Laminated micromodule package showing the vias and thin-film lines.

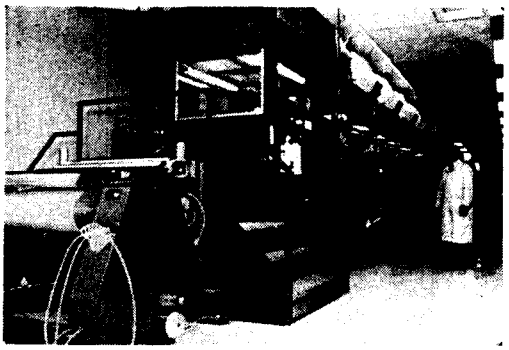

Fig. 11. Doctor blading system.

slurry while the tape was passing through the drying sections of the large tunnel. Finally, the dried green sheets were loaded onto several spools and made available for the next process.

After spooling, the tapes were inspected for defects, which could be distinguished on the blanking tool, as seen in Fig. 12. This machine has a laser scanner, which could locate defects in the tape and then advance them out of the range of the punch. The blanking tool provided holes for both alignment of the sheets and orientation. After the 185-mm^2 blanks were prepared, they were sent to a via punch. This tool contained a cluster punch, which could produce up to 100 holes at a time and up to 36 000 holes in any single sheet. After punching, each sheet was inspected for plugged or missing holes by using inspection masks and light tables.

The specific patterns in a TCM had to be made with different Mo pastes which were designed specifically for their purposes. Several Mo pastes were specified for the various layers. These pastes consisted of powders uniformly dispersed in resins and solvent mixtures. They were extruded through metal masks as a dispensing nozzle transversed the green sheets.

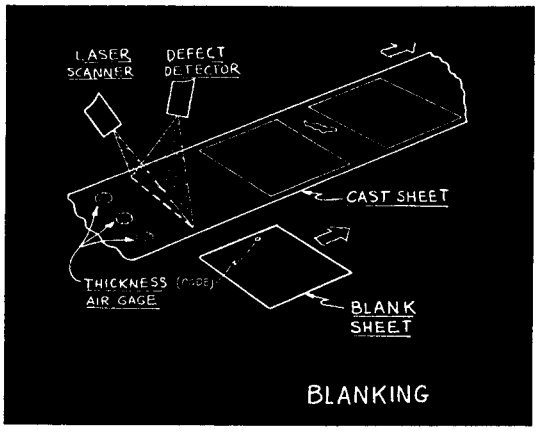

Fig. 12. Blanking tool, showing the laser scanner with defect detector.

The masks had to be cleaned after each use, and the holes in the green sheets were used to align the sheets for the screener. The pastes were screened onto the sheets, and were then dried in an oven. With proper process control, line widths of 0.1 mm on 0.2-mm spacings could be achieved with high yields (see Fig. 13). Each pattern was fully inspected with a laser scanning system.

The green sheets were then ready for lamination into a substrate. During stacking, each sheet had to be placed in its proper position, as shown in Fig. 14. A typical lamination cycle occurred at 75°C and 25 MPa pressure. The laminate was cut to size while going through the lamination cycle, and, if necessary, it was sized with a saw blade. After lamination, the substrate was ready for sintering.

The sintering of a substrate is a complex process. First the binders are driven off. Then water is added to the atmosphere to burn off the residual carbon as CO or CO_2. The burn-out ranges for the binders are measured by thermal gravimetry (TG) and differential thermal analysis (DTA). In the case of the Mo metal pastes, the partial pressures of oxygen have to be carefully controlled in the furnace atmosphere. The metal and ceramic powders start to sinter concurrently. The shrinkage of the metal and the ceramic are carefully matched throughout the entire sintering cycle to provide for good bonding between the alumina and the Mo. The glass in the substrate wets the molybdenum oxide surface in order to achieve a good bond. The substrates are sintered to complete density, and during cooling the thermal cycle must be carefully controlled to avoid camber or cracking. A cross section of a substrate is pictured in Fig. 15.

After the substrates were sintered, they were prepared for plating. First, a low-stress Ni film was electrolessly plated on the exposed patterns. This

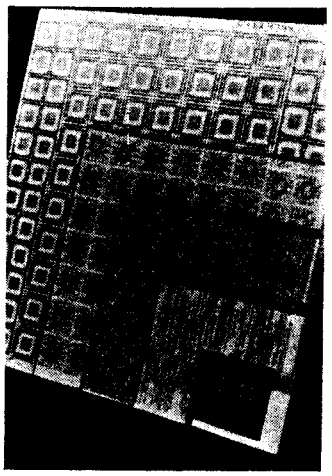

Fig. 13. Various metallized patterns for the TCM (top layer). Vias for chip connections and E-C pads; fan-out patterns; reference planes; signal lines; and power distribution layers (bottom layer).

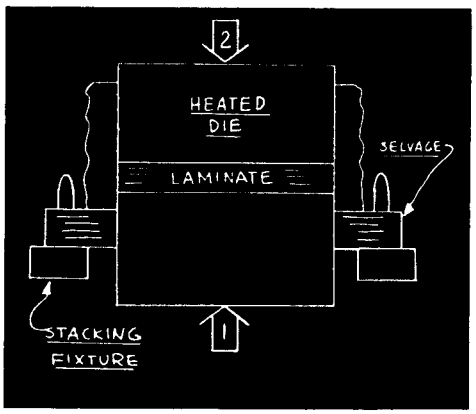

Fig. 14. Lamination fixture.

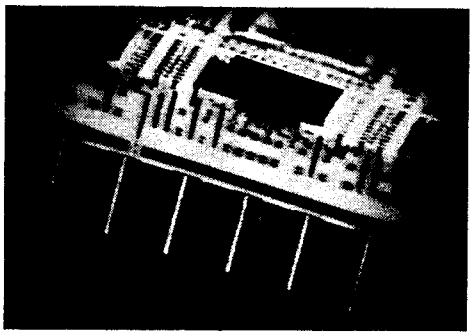

Fig. 15. Cross section of a TCM module, showing the chip connections to the solder pads, the fan-out patterns, the reference planes, the signal lines, the power planes, and the pin attachments.

deposition was then followed by a thin Au plating which protected the nickel surface from oxidation. The heavy gold was needed as a bonding agent for the "E-C" wires which interconnected the various pads on the top surface of the substrate, as shown in Fig. 16. See Table III for a full description of the MLC process.[10]

Another important process developed during this period was the "controlled-collapse-chip-connection," usually referred to as the "C-4" process.[11] This process permitted many solder joints to be made in a single thermal process. These joints had to be exceedingly reliable in regard to the size of the chips. Contact pads on the chips were then coated with a 95% Pb-5% Sn solder. The actual process began with a tool that positioned the chips with a water-soluble white-rosin flux to hold them in place on the substrate vias. When passing through a reflow furnace in a nitrogen atmosphere, the surface tension of solder aligned the pads. The cycle time through the furnace was approximately 30 minutes and the temperature was held at 350°C. The vias were used to interconnect the various layers of circuitry beneath the surface layer in order to transfer pulses of information, as indicated in Fig. 17.

Another accomplishment of this period was the brazing of the pins and flange to the substrate. The

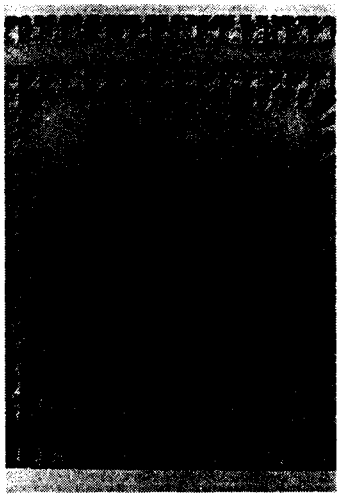

Fig. 16. Top view of gold-plated 120-via connections and E-C pads.

Table III. Steps in Laminated MLC Process*

1.	Artwork generation
2.	Raw material procurement
	Alumina and glass
	Binder and plasticizer
	Deflocculant
	Solvents
3.	Raw material qualification
4.	Ceramic-slurry preparation
5.	Metal paste preparation
6.	Ceramic tape casting
7.	Tape blanking and inspection
8.	Registration hold punching
9.	Via punching
10.	Hole inspection
11.	Metallurgy screening
11a.	Paste-drying
12.	Screen layer inspection
12a.	Screening rework
13.	Stacking
14.	Lamination
15.	Sizing
16.	Inspection
17.	Sintering
18.	Refiring and/or flattening
19.	Plating
20.	Shorts/opens testing
21.	Pinning
22.	Top-surface wiring
23.	Chip attachment
24.	Electrical testing
25.	Encapsulation

*From Ref. 10.

pins were brazed with an 80% gold-20% tin alloy paste, and the flange used the same alloy but in strip form. The substrates were then passed through a furnace at 400°C in a hydrogen atmosphere. A schematic drawing of a TCM is shown in Fig. 18.

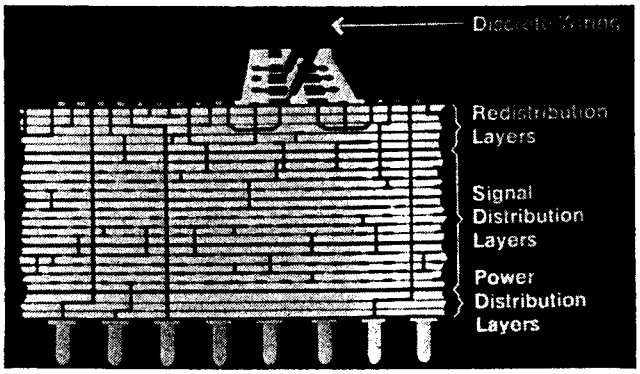

Fig. 17. Multilayer multichip module.

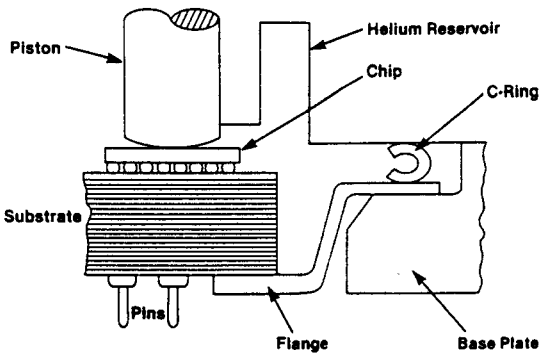

Fig. 18. TCM module cross section.

In 1985, IBM developed a new substrate in which the flange was eliminated from the module. In this case the superstructure was attached directly to the substrate in order to remove the heat from these devices.

The TCM module can no longer serve only as a connector between the chips and the board; it must also provide all the functions listed in the third section of this chapter.

Module Performance

The functions which the latest thermal conduction module (TCM) must perform include: (1) intraconnections, (2) engineering changes, (3) cooling, (4) environmental protection, and (5) power distribution. Each of these items will be discussed separately.

Intraconnections

An important property of the ceramic material is the distance a signal must travel through the substrate and its dielectric constant, which is measured by the delay time (*Td*) as:

$$T_d = \sqrt{\epsilon} \times l/c \text{ nanoseconds per cm} \quad (1)$$

where the delay time is determined by the square root of the dielectric constant ϵ, the distance l the signal must travel through the substrate, and the speed of light, c. Typical values per unit length are listed in

Table IV. These time delays (per signal) may appear to be quite small, but the total time for many megabits of information, which have to travel through large computer systems, can be quite significant. It is desirable, therefore, to reduce the distance and dielectric constants as much as possible, without compromising the other properties of the substrate.

The dielectric constants of ceramics, in general, will vary with their electronic, dipole, and ionic polarizabilities and inversely with their bond strengths and densities. Glasses, therefore, tend to have lower values than corresponding crystalline structures. Any technique that increases the specific volume of a solid would be beneficial. The constraints, however, could be lower strengths and thermal conductivities.

The characteristic impedance (Z_0) of the material also depends on the dielectric constant of the ceramic, as well as the geometry of the wiring, according to the following equation:

$$Z_0 = \sqrt{L/C} \text{ ohms} \quad (2)$$

where L is the inductance and C is the capacitance of the line. Semiconductor circuits generally require a line impedance of between 35 and 100 ohms. Referring to the equation for C in Table II, by lowering the thickness of the dielectric, ϵ also has to be reduced to maintain the same impedance.

The constraint in reducing the dimensions of the substrate is the electrical conductivity of the metallurgy which will also have to be increased. Decreasing the linewidth and thickness increases the resistance of the line, according to the following equation:

$$R = \frac{\rho \times l}{A} \text{ ohms} \quad (3)$$

where ρ is the resistivity of the metal, l the length of the line, and A the cross-sectional area of the line. The higher line resistances produce voltage drops and localized heating which can affect device switching behavior. As line dimensions are further reduced, higher electrical conductivity metals must be used in multilayer structures to keep the power loss down.

Engineering Changes

As mentioned earlier, a module containing an average of 35 000 circuits must provide the means for making wiring and chip changes during the initial debug stages. The TCM has two such methods. Rewiring is done on the surface of the module. Each wiring pattern is brought to the surface where it could be opened by laser deletion. Afterward, a gold-clad copper wire is ultrasonically bonded to the desired "E-C" pad for the new wiring connections, as shown in Fig. 19.

The chips can also be replaced with the combined use of a mechanical tool and a hot gas desoldering and dressing tool. The new chips are replaced in a normal "C-4" chip-joining reflow cycle or an individual thermal replacement.[12]

Cooling

The MST and MC modules transfer heat out of the chips through the solder pad interconnections to the substrate. Making the solder pad diameters larger and the heights shorter will aggravate the stress problems. The moderate, yet adequate, thermal conductivity and superior strength of high-alumina ceramics were predominant reasons for their selection as the first substrates. Heat transfer sets up thermal gradients and stresses which are reduced by the thermal conductivity of the alumina. The strengths of the aluminas also help them withstand both the thermal and mechanical stresses.

Therefore, a completely new cooling system had to be used for the TCM. Heat is removed from the back of the silicon chips, as shown in Figs. 18 and 20. Each chip is contacted by a separate 5.5-mm diameter aluminum spring-loaded piston and the heat produced in each chip is conducted through the piston and walls of the chamber by contact and through the helium gas fill. A hermetic seal provides for containment of the helium and enables the transfer of heat to a water-cooled cover. This module can dissipate up to 300 watts and maintain all the chip junction temperatures between 40° and 85°C. Up to four watts per chip can be cooled by this method. Successful operation of the TCM depends strongly on the gas fill in the chamber. The thermal resistance of the solid aluminum piston is 4.4°C/W and the helium is 3.5° C/W, providing for a total of 7.9°C/W. Chilled water flows continuously through the channels in the cover, removing heat from the chips.[13,14]

Environmental Protection

In 1980, the TCM was used for the IBM 308X systems. Its cover was clamped directly to the flange,

Table IV. Ceramic Material Properties

Alumina (%)	Glass (%)	Dielectric Constant (ϵ)	Thermal Conductivity (W/mK)	Thermal Expansion (10^{-6}/°C)	Flexural Strength (MPa)	Delay Time (10^{-9}/cm)
96	4*	10.2	20.9	7.1	276	0.686
90	10†	9.5	16.7	6.9	315	0.660
55	45‡	7.5	4.2	4.2	296	0.610

*Kyocera
†IBM
‡NEC

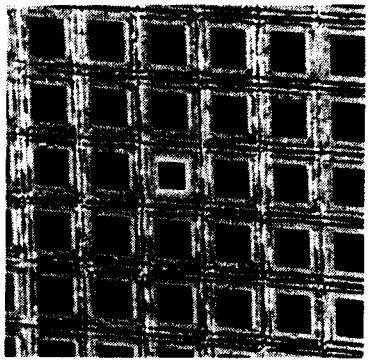

Fig. 19. Multiple chips with E-C wires.

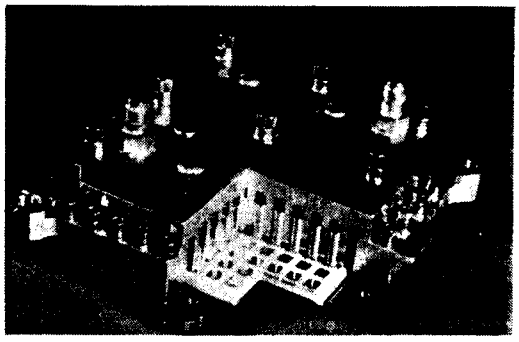

Fig. 20. TCM substrate with chips attached, aluminum pistons, and water-cooling cover.

which was brazed to the substrate. A cross section of this substrate is shown in Fig. 18. Figure 20 portrays a TCM module showing the water-cooled housing. Each piston extracts heat from a chip it contacts and transfers it to the water-cooled superstructure (or cover).

The TCM for the IBM 309X systems, introduced in 1985, does not have a flange. The cover is clamped directly to the bare ceramic substrate using the same C-ring; thus the flange and braze materials are unnecessary.

Power Distribution

An emerging problem is how to handle the increasing current requirements for higher speed devices in ever-decreasing spaces. Although the size of the power planes and vias are being increased at each module change, this process will be self-limiting because it increases the total dimensions of the substrate.

Stresses in Solder Pads

Stresses occur in the solder pads each time the computer is turned on and off, when the module is heated and cooled. The resulting strain is measured by the following equation[15]:

$$\epsilon_p = \frac{\Delta\text{TCE} \times \Delta T \times D_{np}}{H} \text{ cm/cm} \qquad (4)$$

where ΔTCE is the difference in thermal expansions between the silicon and the ceramic material, ΔT the change in temperature, D_{np} the distance from the neutral point on the chip, and H the height of the solder pads. The Coffin-Manson equation relates the number of cycles to failure (N_f) by the following equation[16]:

$$N_f = A/(\epsilon p)^2 \qquad (5)$$

where A is a constant determined by each system. As large-scale integrated circuit chips become larger, it will become important to find new ceramic materials with thermal expansions more closely matched to that of silicon.

Properties of Materials

Current Materials

Throughout the electronic ceramic industry, varying materials are being used in the manufacture of multilayer ceramic substrates. The following discussion describes some of the materials being used by major producers in this field.

The multilayer ceramic technology currently being used by the Kyocera Corporation is a 96% alumina

Table V. Metallurgies for Substrates

Metals	Melting Points (°C)	Electrical Resistivity (10^{-6} Ω • cm)	Thermal Expansion (10^{-6}/°C)	Thermal Conductivity (W/mK)
Ag	960	1.6	19.7	418.4
Au	1063	2.2	14.2	297.1
Cu	1083	1.7	17.0	393.3
Pd	1552	10.8	11.0	71.1
Pt	1774	10.6	9.0	71.1
Mo	2625	5.2	5.0	146.4
W	3415	5.5	4.5	200.8
Ni	1455	6.8	13.3	92.1
Cr	1900	20.0	6.3	66.9

- 4% glass-ceramic with the use of a tungsten metallization for the MLC structures. The properties of these materials are specified in Tables IV and V. The mechanism of bonding the tungsten to the alumina and glass is the oxidation of the tungsten powders, which are subsequently wet by the glass in the ceramic material. The tungsten can then be bonded to the ceramic by the glass in the ceramic which causes the adhesion between the tungsten and glass with the formation of oxygen bonds at their interfaces. After these bonds are made, the glass in the ceramic will wet the oxide surfaces and secure the tungsten powders to the ceramic. These substrates were sintered in a wet hydrogen atmosphere between 1450° and 1600°C. A nickel and gold plating on the surface of the tungsten powders prevents the tungsten from oxidizing. The gold coating on the nickel provides a good surface for the solders and brazes to wet the gold.[17]

The properties of IBM's alumina and molybdenum TCM are given in Tables IV and V. The mechanism of adhesion between the alumina and molybdenum was described in the section on MLC Technology Development.

The NEC Corporation manufactures a 55% alumina-45% lead borosilicate glass substrate with a gold metallurgy. The properties of this module are given in Tables IV and V. The gold is bonded to the glass in the ceramic by wetting of the gold in the paste, which causes adherence to the glass-ceramic substrate. These substrates were sintered in air or a neutral atmosphere at temperatures of about 900°C.

Future Materials

In regard to future materials, there are several mixtures to be considered; these combinations are listed below.

Watanabe et al.[19] reported the use of alumina and mullite green sheets. This patent described how the mullite layers increased the transmission speed of the signals through the substrate, and the alumina layers on the surface increased its strength.

In another paper, presented at the 1987 Electronics Components Conference, Shimada et al.[20] described a substrate which uses a silver-palladium conductor system with a low firing temperature multilayer glass-ceramic multicomponent ceramic substrate. In this case, mixtures of a lead borosilicate glass with either 55% alumina, 45% cordierite, or 35% silica were used. The metal paste was a 95% Ag-5% Pd, which had a resistivity of about 3.5 $\mu\Omega \cdot$ cm. The flexural strength of the alumina substrate is about 3500 kg/cm^2. The other substrates have lower flexural strengths due to pores in the ceramics. The dielectric constants of the alumina, cordierite, and silica ceramics were 7.8, 5.0, and 3.9, respectively, at 1 MHz. The dissipation factor was less than 0.5%. The linear shrinkages were about 13.0, 13.7, and 13.9% and the delay times were about 9.8, 8.3, and 7.0 nsc/m for the alumina, cordierite, and silica substrates.

At an ISHM '87 meeting, a new substrate was described, which included a 60% (CaO-Al_2O_3-SiO_2-B_2O_3)-40% alumina ceramic, with ruthenium dioxide resistors, 85%Ag-15%Pd and Ag conductors which were cofired in air at about 880°C. A second firing was performed at 600°C in nitrogen using a copper conductor paste. The copper conductor had a conductivity of about 2.4 $\mu\Omega \cdot$ cm, and the ceramic had a dielectric constant of about 7.7.[21]

The properties of copper, gold, and silver are described in Table V. These metals can be used to increase the electrical conductivity of the conductors.

There are other papers in the literature, which describe other combinations, but these substrates represent the latest in the area of ceramics and metals.

Summary and Conclusions

This chapter described how ceramics were first used to produce multilayer capacitors. Within three decades, the manufacture of these MLC capacitors became a major industry. The application was the expanding semiconductor business which required small-volume, high-capacitance, low-voltage, and high-quality capacitors. It soon became apparent that this technology might also be useful for semiconductor packaging.

Future technical directions are toward lower dielectric constant ceramics, matching thermal expansions to that of silicon and processes capable of finer resolutions. Beyond these goals, it would be desirable to increase the strength and thermal conductivities of the ceramic materials. Processing will become more important as dimensions become smaller and fewer defects can be tolerated. Therefore, new methods for synthesizing improved precursor materials, clean-room operations, and optical processing will become necessary to expand the applications for the multilayer ceramic technology.

The role of ceramics for packaging of microelectrics will continue to be challenging. Future needs will become increasingly complex and will require additional ingenuity by engineers working in this area. Alumina ceramics will continue to be important materials for packaging integrated circuits.

References

[1]B. Schwartz, "Microelectronics Packaging," Electronic Ceramics, Am. Ceram. Soc., Publication #3, pp. 12-25 (May 3, 1969).

[2]B. Schwartz, "Microelectronics Packaging: II," *Am. Ceram. Soc. Bull.*, **63** [4] 577–81 (1984).

[3]B. Schwartz, "Review of Multilayer Ceramics for Microelectronics Packaging," *J. Phys. Chem. Solids*, **45** [10] 1051–68 (1984).

[4]A. J. Blodgett, Jr., and D. R. Barbour, "Thermal Conduction Module: A High-Performance Multilayer Package," *IBM J. Res. Develop.*, **26** [1] 30–36 (1982).

[5]D. Balderes and M. L. White, "Package Effects on CPU Performance of Large Commercial Processors," IEEC Proc. ECC 1985, pp. 351-55.

[6]R. E. Mistler, D. J. Shanefield, and R. B. Runk, "Tape Casting of Ceramics"; pp. 411-48 in Ceramic Processing Before

Firing. Edited by G. Y. Onoda, Jr. and L. L. Hench. Wiley & Sons, New York, 1978.

[7]W. J. Gyurk, "Methods for Manufacturing Monolithic Ceramic Bodies," U.S. Pat. No. 3 192 086, June 29, 1965.

[8]"Micro-Module Crystal Units," Signal Corps Contract No. DA-36-039-SC-85046, Dept. of the Army Project No. 3A99 15-001-02 (March 31, 1961).

[9]H. Stetson, "Method of Making Multilayer Circuits," U.S. Pat. No. 3 189 978, June 22, 1965.

[10]W. S. Young, "Multilayer Ceramic Technology"; pp. 403-24 in Ceramic Materials for Electronics. Edited by R. C. Buchanan. Marcel Dekker, New York, 1986.

[11]L. F. Miller, "Controlled Collapse Reflow Chip Joining," *IBM J. Res. Develop.*, **13** [3] 239-50 (1969).

[12]K. Puttlitz, "Chip Replacement by Hot-Gas Site Dressing," *Solid State Technol.* **23** [11] 48-50 (1980).

[13]R. C. Chu, O. P. Hwang, and R. E. Simons, "Conduction Cooling for an LSI Package: A One-Dimensional Approach," *IBM J. Res. Develop.*, **26** [1] 45-54 (1982).

[14]S. Oktay and H. C. Kammerer, "A Conduction-Cooled Module for High Performance LSI Devices," *IBM J. Res. Develop.*, **26** [1] 55-66 (1982).

[15]L. S. Goldmann, "Geometric Optimization of Controlled Collapse Interconnections," *IBM J. Res. Develop.*, **13** [1] 251-65 (1965).

[16]S. S. Manson, Thermal Stress and Low Cycle Fatigue. McGraw-Hill, New York, 1966.

[17]M. Terasawa, S. Minami, and J. Rubin, "A Comparison of Thin Film, Thick Film, and Co-Fired High Density Ceramic Multilayer with the Combined Technology: T & T HDCM," 36th ACerS Pacific Coast Regional Meeting, San Diego, CA.

[18]Y. Shimada, K. Utsumi, M. Suzuki, H. Takamizawa, M. Nitta, and T. Watari, "Low Firing Temperature Multilayer Glass-Ceramic Substrate," *IEEE Trans.*, **CHMT-6, [4]**, 382-85 (1983).

[19]Y. Watanabe, F. Kobayashi, S. Ogihara, and Y. Ohzawa, "Multi-Layer Ceramic Substrate and Method for the Production Thereof," U.S. Pat. No. 4 624 896, November 25, 1986.

[20]Y. Shimada, Y. Yamashita, Y. Shiozawa, M. Suzuki, and H. Takamizawa, "Low Dielectric Constant Multilayer Glass-Ceramic Substrate with Ag-Pd Wiring for VLSI Package," 1987 ECC, pp. 398-405.

[21]S. Nishigaki, J. Fukuta, S. Yano, H. Kawabe, and M. Fukaya, "A New Low Temperature Fireable Ag Multilayer Substrate Having Post-Fired Cu Conductors," *Int. J. Hybrid Microelectron.*, **10** [2] 36-46 (1987).

Alumina Usage in Electric Power Generation and Storage

Wate T. Bakker

Electric Power Research Institute
Palo Alto, CA 94303

Present use of alumina and alumina-containing ceramics in the electric power industry is limited, because of the widespread use of water-cooled structural components and heat-exchanger elements. Alumina is used in insulators for the transmission of electric power. This application of alumina is discussed in the chapter on electrical ceramics. Minor amounts of alumina-containing refractories are used in steam boilers. A more significant use of alumina is in alumina boron-carbide burnable poison rods used in nuclear power plants to assist in optimum core burnup. A potentially large market for alumina may develop if the present development of sodium sulfur batteries for electric vehicles (EVs) and energy storage becomes commercial. The use of high-energy density batteries will increase the range of EVs from the present 80 to 96 km (50 to 60 miles) to well over 160 km (100 miles), and thus will make their use attractive for many applications.

Prior to the energy crisis in the early 1970s, the electric power industry showed a predictable pattern of an almost steady 6 to 7% annual growth, combined with an equally steady decrease in the price of its product: kilowatt hours. This happy scenario was brought about by evolutionary improvements and economies of scale of electric power plants, consisting of fossil-fueled boilers and steam turbines driving electric generators, and the stable price of fossil fuels. Little or no alumina-containing ceramics or refractories were used in these plants, due to the extensive use of water cooling of the high-temperature boiler walls.

Radical changes occurred in the electric power industry in the early 1970s, which led to a rapid escalation of electricity cost to consumers, a slow-down of the yearly growth rate to 2 to 3%, and a much greater uncertainty in the future growth of electricity. The major factors behind the change were: (1) rapid escalation of fossil fuel costs following the Arab oil embargo; (2) the introduction of nuclear power and subsequent cost escalation thereof due to safety concerns; (3) the need to address the environmental impact of burning fossil fuel; and (4) high interest rates.

The electric power industry responded to these challenges by participating in various developments aimed at reducing the cost of electricity production, reducing effluents from fossil plants, and diversifying its sources of fuel. Apart from nuclear power, the following new or improved technologies are presently being developed.

1. *Fluidized-Bed Combustion (FBC):* Here the coal is burned in the presence of limestone in a fluidized bed at 816° to 927°C (1500° to 1700°F). The limestone removes about 90% of the sulfur in the coal and the low bed temperature prevents the formation of excessive NO_x. Thus, air pollution is greatly reduced without the use of costly flue-gas desulfurization equipment. Several 100 to 200 MW plants are presently under construction. A variation of FBC is pressurized fluidized-bed combustion (PFBC). In this technology, the boiler is pressurized and the pressurized flue-gas is expanded through a power turbine to produce additional electricity. Thus, the size of the equipment is reduced and its efficiency increased.

2. *Integrated-Gasification-Combined-Cycle Power Plants (IGCC):* Here the coal is first gasified under pressure. The hot raw syngas is cooled in a pressurized boiler (called syngas cooler) and subsequently scrubbed to remove particulates and water-soluble impurities such as chloride and ammonia. After scrubbing, sulfur is removed as H_2S and converted to elemental sulfur, a saleable by-product. The clean syngas is combusted in a gas turbine.

Additional steam is raised in a heat-recovery steam generator (HRSG) and combined with steam raised in the syngas cooler to drive a steam turbine. In this manner, electricity can be produced at about the same cost as in a conventional pulverized-coal boiler with a greatly reduced air pollution. Experiments at a 100 MW demonstration plant in California have shown that emission as low as 10 ppm SO_x and 35 ppm NO_x are possible using high-sulfur (2 to 4%) coal. Future use of catalytic combustors will reduce the NO_x content to less than 10 ppm. Thus, this technology allows the use of coal, while producing fewer air pollutants than with natural gas.

3. *Fuel Cells:* Fuel cells convert the chemical energy of fuels directly into electricity. This is accomplished by oxidation of the fuel inside the cell. Since no fuel is burned, less waste heat and almost no emissions are generated. Since there are no moving parts in a power plant using fuel cells, it is also very quiet.

Fuel-cell power plants, using a phosphoric acid electrolyte and graphite electrodes impregnated with a noble metal catalyst, have been demonstrated in sizes up to about 5 MW. It is expected that 10 MW fuel-cell power plants will be available in the mid-90s for use with clean hydrocarbon fuels such as natural gas. The

lack of emissions and noise allows siting in or near urban areas. The efficiency of fuel-cell plants is generally higher than that of conventional steam plants, which makes the use of a premium fuel feasible.

4. *Storage Batteries:* Daily and weekly use of electricity is highly cyclical, whereas the production cost of electricity is lowest when the power plants are operated continuously near capacity. To provide extra energy during peak periods, less-efficient power plants must be used or excess electricity produced during periods of low demand must be stored. Traditionally, this has been done by pumped hydroelectric storage. Here the excess electricity is used to pump water from a low reservoir to a higher one. Later, the water is allowed to flow down through turbines which generate extra electricity during peak hours. This method is limited topographically.

The use of storage batteries is universally applicable, and potentially more efficient. However, the energy density of presently available—mostly lead-acid—batteries is relatively low and their reliability needs improvement. The use of sodium-sulfur batteries, which use a solid sodium-beta alumina electrolyte, may provide a much more suitable battery for energy storage as its energy density and cost are potentially much lower.

Use of Alumina in Electricity Production

In general, very little alumina is being used in the generation and transmission of electricity. Nuclear power plants operate at relatively modest steam temperatures—generally well below 500°C—and therefore do not use ceramic materials except for the UO_2 fuel and burnable poison rods. The latter may be a small, but significant, near-term market for alumina and will be discussed in more detail later.

Conventional pulverized-coal-burning power plants rely heavily on water-cooled alloy steel walls to contain the high-temperature combustion products and generate high-pressure steam. The use of refractories in these plants is very small and generally limited to plastics and ramming mixes to protect water walls in areas subject to slag impingement, refractory concrete-lined ash hoppers, and similar minor applications. Only small amounts of calcium aluminate cement and alumina are used here.

Potential use of alumina in future power-generation technologies is also relatively low. Pressurized fluidized-bed combustors may use ceramic air filters, which may be made from alumina-silica fibers or packed beds containing alumina or calcined fireclay granules. A preferred technology has not yet been developed.

Entrained-flow, slagging gasifiers probably will need a refractory lining. Refractories with 60 to 80% chromia are presently preferred. The balance of the refractory composition could be either Al_2O_3 or MgO.

Fuel cells as such do not require alumina components. However, when hydrocarbon fuels are used, the fuel-cell power plant requires a reformer where the hydrocarbon is converted to a mixture of H_2 and CO. These units will require high-alumina insulating materials.

The only potentially large use of alumina is in energy storage plants using sodium sulfur batteries, as these batteries use a beta alumina solid electrolyte. The potential for alumina usage may become even greater when electric vehicles using the same battery become commercial. The use of beta alumina in batteries will also be described in a separate section.

Considerable quantities of alumina are also used in electrical insulators for the transmission of electricity. The use of alumina in this application is described more fully in the chapter on electrical ceramics.

Use of Alumina in Alumina-Boron Carbide Burnable Poison Rods

Light-water nuclear reactors (LWRs) use burnable poison rods in their fuel assemblies to prevent early power peaking and to assist in power shaping and optimum core burnup.[1] Burnable poison rods consist of a small quantity (1 to 5%) of neutron absorbers such as B_4C, contained in an inert matrix. Pressurized water reactors (PWRs) presently use mostly sintered or hot-pressed Al_2O_3 rods containing up to 4 wt% B_4C. Boiling-water reactors use UO_2-Gd_2O_3 burnable poison rods. Borosilicate glass rods have been used in the past. Rods consisting of BZr-coated UO_2 pellets are presently being tested. All burnable poison rods are clad with Zircaloy.* The total use of Al_2O_3 for this application is relatively small. Burnable poison rods usually last for three refueling cycles, and only 2% of the fuel consists of burnable poison. Thus, assuming that Al_2O_3-B_4C is preferred material, a maximum yearly consumption of 360 000 to 540 000 kg (80 000 to 120 000 lbs) of alumina for this application is anticipated.

The Al_2O_3-B_4C pellets are made by standard processes to produce oxide ceramics, mostly by cold pressing and sintering or by hot-pressing. Sintering or hot-pressing must be done in an inert atmosphere to prevent formation of the relatively volatile B_2O_3, which will result in boron losses. Due to interactions between B_4C and Al_2O_3, the density of the pellets produced is less than 90%. Sintered pellets are usually ground to size. Drying of the porous pellet prior to cladding is of critical importance to remove entrapped moisture which can lead to hydriding of the Zircaloy cladding during service.

Operating experience with Al_2O_3-B_4C burnable poison rods has generally been satisfactory. The rod can be used for up to three fuel cycles. Two types of problems have occurred:

1. Abnormal rod elongation and bowing due to pellet-cladding interactions. This problem has been alleviated by a different rod design, but may become

*Westinghouse Electric Corp., Blairville, PA.

problem again, when advanced rods with a higher B_4C content are introduced.

2. Internal hydriding of the Zircaloy cladding, causing cladding failure. This is caused by moisture in the pellets prior to assembly and can be prevented by appropriate quality control.

Use of Alumina in Sodium Sulfur (NAS) Batteries

General

The sodium-sulfur (NAS) battery is the result of a fundamental discovery by J. T. Kummer and N. Weber of Ford Motor Co.[2] that sodium beta alumina is an excellent ionic conductor for sodium ions. This makes it possible to use beta alumina as a solid electrolyte in a battery having molten sodium as the negative and sulfur as the positive electrode. The major advantage of this battery over conventional lead-acid batteries is its much higher energy density.

Lead-acid batteries have energy densities ranging from 41 to 48 W • h/kg, while NAS batteries have energy densities of 100 to 150 W • h/kg. This feature will make it possible to produce electric vehicles (EVs) with twice the range and considerably more power than those using lead-acid batteries. For electric load-leveling applications, the use of NAS batteries should provide lower-cost energy storage. The main drawback of sodium sulfur batteries is their high operating temperature (about 350°C). This requires highly insulated containment in electric vehicles and complicated insulation and heat-management schemes in load-leveling batteries.

Active development of NAS batteries has been carried out since the early 1970s in the United States, England, Germany, and Japan. Most efforts have been concentrated on EV batteries. Several experimental vans have been successfully road-tested. Limited production of delivery-type vans for urban use may occur as early as 1992.

The market for alumina for this application could be huge. The EPRI projects that additional installed energy storage capacity by the year 2000 could be as high as 8000 MW.[3] If an acceptable NAS battery is available by 1992, 2000 to 3000 MW of this capacity may be in the form of battery storage. This would require 2 to 3 $\times$ 10^6 kg alumina. An NAS battery for a typical electrical vehicle would require about 50 kg of alumina per vehicle. Production of only 100 000 EVs per year would thus represent 5 $\times$ 10^6 kg of alumina per year. A recent economic study by the Electric Vehicle Development Corporation and EPRI indicates that, by the year 2000, the production of EVs may exceed 1 $\times$ 10^6 vehicles, mainly delivery vans, a year, if their range exceeds 100 miles. Advanced batteries such as the NAS battery are required to achieve this goal.[4] The present literature on NAS batteries is voluminous but ably summarized by Sudworth and Tilley.[5]

Requirements for Beta Aluminas in NAS Batteries

Electric Properties: The lower the ionic resistivity of the electrolyte, the lower the overall cell resistance and the higher the cell efficiency will be. Research on beta alumina has shown that its structure is composed of alternating slabs of close-packed oxides and layers with a low atom density containing mobile cations (typically sodium). There are two main subgroups which differ in the stacking sequence of layers along the unique *c* axis, labeled β′- and β″-Al_2O_3. The β″-Al_2O_3 has a significantly higher ionic conductivity than β′-Al_2O_3, and is now preferred by all developers of NAS batteries. State-of-the-art polycrystalline β″-Al_2O_3 electrolytes containing >90% β″-Al_2O_3 have a resistivity in the 3 to 7 Ω • cm range. The β″ structure is stabilized by the addition of Mg and/or Li ions. Ionic resistivity and other properties are highly dependent on the chemical composition.

A widely used formulation is 90.4 wt% Al_2O_3-8.85 wt% Na_2O-0.75 wt% Li_2O. The electric resistivity and the electrochemical behavior of β″-Al_2O_3 are also influenced by low levels of impurities such as CaO, SiO_2, and K_2O. Aluminas derived from Bayer-process hydrate have generally acceptable levels of SiO_2 and K_2O, provided no SiO_2 is introduced during grinding. Calcia is generally not controlled by the raw material producer, and can reach unacceptably high levels, depending on which bauxite and which variant of the Bayer process are used. The CaO content of all raw materials should in general be below 100 ppm and preferably below 50 ppm.

Microstructure: During sintering, β-Al_2O_3 tends to develop a duplex microstructure with large euphedral crystals embedded in a fine-grained matrix. Whether or not the large grains are detrimental to the performance of β″-Al_2O_3 in NAS cells has not been resolved at this point, although a more fine-grained structure is generally preferred. Recent experiments aimed at transformation toughening of β″-Al_2O_3 by the addition of zirconia have shown that 5 to 15% ZrO_2 additions prevent the formation of large crystals, which is an unexpected benefit of zirconia toughening.

Mechanical and Physical Properties: The β″-Al_2O_3 is usually produced in tubular form and sintered to near theoretical density, usually in the 3.18 to 3.24 g/cm^3 range. It should also be helium-tight. The strength of β″-Al_2O_3 is, like all ceramics, dependent on the stressed area of the specimens tested. Typical strength data are: diametral compression test, 250 MPa (36 ksi); 4-point bend bar, 193 MPa (28 ksi); and burst test of 24 mm OD by 230 mm long by 1.5 mm wall thickness tube, 130 MPa (19 ksi). Weibull moduli typically range from 6 to 9. It is not clear at this point if mechanical strength is a life-limiting factor for β″ electrolytes. However, during cell manufacture the electrolyte may be exposed to mechanical stresses of various kinds; a strong electrolyte is therefore pre-

ferred. The major electrochemical failure mechanism indicates that fracture toughness (K_{IC}), and surface flaws are important factors controlling service life. The fracture toughness of β''-Al_2O_3 ranges from 1.6 to 2.3 MPa • $m^{1/2}$.

Various developers have attempted to apply transformation toughening to β''-Al_2O_3. It has been demonstrated that both the strength and the fracture toughness of β''-Al_2O_3 can be increased substantially, without markedly increasing the resistivity, by adding 15% ZrO_2 to the standard formulation.[6] Tests in sodium sulfur batteries are now underway to determine if the improved mechanical properties and microstructure also increase service life.

Production of β''-Al_2O_3 Electrolytes

At present, all NAS battery cells under development require a tubular electrolyte. A typical electrolyte size for an electric vehicle battery is: 34 mm OD by 262 mm long by 1.5 to 2.0 mm wall thickness. For electric energy storage batteries, it is advantageous to make the cell as large as the electrolyte manufacturing process allows. Tubes as large as 50 mm OD by 600 mm long, with a wall thickness of 2.5 mm, have been produced.

There are two major forming processes used: isostatic pressing and electrophoretic deposition. Both prereacted powders and mixtures of the individual ingredients (α-Al_2O_3, Na_2O, Li_2CO_3, etc.) are used to prepare spray-dried powders for isostatic pressing. When electrophoretic deposition is used, uniform prereacted powders are needed. After drying, the green electrolytes are sintered in batch or continuous furnaces. When unreacted powders are used, a bisque firing at 700° to 1000°C is generally needed prior to the main firing at 1550° to 1650°C. To control secondary crystal growth, the hold time at 1550° to 1650°C is kept short and is generally followed by an annealing treatment at a lower temperature to increase conversion to β''-Al_2O_3 and thus reduce the resistivity.

Manufacture and Testing of NAS Cells

Sodium sulfur batteries consist of numerous individual cells: about 500 for an electric vehicle battery and 10 000 or more in load-leveling storage batteries. A typical large NAS cell is pictured in Fig. 1,[7] which shows a central sodium cell, with the sodium electrode inside the β'' electrolyte and the sulfur electrode on the outside. Configurations in which the sodium is on the outside are also being developed.

A typical NAS cell is rather complex and is manufactured in many steps, which eventually must be automated to reduce production cost. The first step is to attach an insulating α-Al_2O_3 header to the electrolyte, using a compatible sealing glass, which resists attack by sodium. The final step is to add liquid sodium at 300° to 350°C. At this point, the cell is ready for testing.

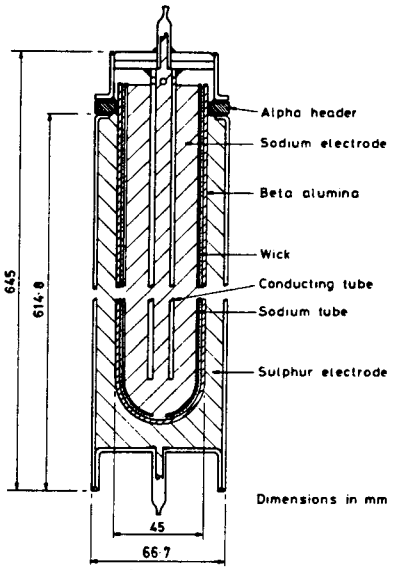

Fig. 1. Schematic of large central sodium cell for a load-leveling, electric storage battery (Ref. 7).

Testing consists of discharging and charging individual cells at a typical current density of 100 to 200 mA/cm^2. Typical charge and discharge times are three to five hours each; thus two to three cycles are completed each day. Since cells are complex components, they may fail for many reasons in a random manner, with a typical Weibull modulus of one. Thus, large groups of cells (30 to 60) must be tested, to draw statistically correct conclusions. For practical application, individual cells must be able to withstand at least 1000 cycles before a significant number of failures occurs. This makes testing lengthy and costly.

Efforts have been made to accelerate testing by increasing the charge and discharge current and/or using sodium/sodium cells. In this manner, the same amount of current can be passed through a cell in a much shorter time. These tests are useful in weeding out unsuitable compositions and raw materials, but an exact correlation between accelerated testing and service-life testing in NAS cells has not been obtained so far.

Failure Mechanisms of β'' Electrolytes

The most common failure mode of a β'' electrolyte in an NAS cell is the formation of a crack through the wall thickness. This will cause the cell to short out and fail. Fracture mechanics calculations have shown that a sodium-filled crack can propagate due to the pressure generated by the flow of sodium out of the crack during charging (Poiseuille pressure). A current density threshold (i_{cr}) must be exceeded before the crack will propagate catastrophically. Calculations show that the critical current density is several orders of magnitude higher than the typical charging current of 100 mA. It is also proportional to K_{IC} (Ref. 4).

Charging experiments, using acoustic emission to detect cracking, indicate initiation of cracking at charge currents of 200 to 300 mA. After long service, electrolytes generally show degraded (corroded) layers on the sodium side. This may lead to a local lowering of the K_{IC} and slow crack growth, for which there is also some evidence.[8] The fracture toughness of β″ is also anisotropic. Thus, large grains may crack preferentially if oriented poorly.

There are many other factors, which will not be discussed here, which affect the degradation and failure of an electrolyte. However, the average and maximum cell life have been increasing rapidly over the last several years. Average cycle life is now well over 1000 cycles, while maximum life is well in excess of 3000 cycles, representing several years of service.

Economic Considerations

To succeed commercially, NAS batteries must be able to compete with conventional lead-acid batteries and other advanced batteries now under development. Electric vehicles (EVs), their most promising application, must be able to compete with conventional gasoline-powered vehicles, with the possible exception of mandated use of EVs in cities, where air pollution is severe. This means that their life-cycle cost must be comparable to conventional vehicles.

Studies by EPRI and EVPC[4] have shown that an electric delivery van can compete with conventional vans if its initial cost is not more than 30% greater than that of a conventional vehicle. The reason is that maintenance and fuel costs of EVs are significantly lower than those of conventional vans, even at gasoline prices of $0.85/gallon. Since NAS batteries promise to double the range of EVs from the present 50 to 60 miles to well over 100 miles, they should be able to replace lead-acid batteries if they can be produced at about the same cost. This means that the individual cells in the battery should cost $8 or less; β″ electrolytes, fully assembled with an alumina header, for such cells should cost about $2 to $3. A study by Miller and Gordon[9] indicates that this is possible, provided fully automated production processes are used and the alumina raw material—a major cost factor—does not exceed $1 per kg.

It will be a challenge to the ceramics industry to develop the appropriate high-volume, low-cost production process and to the alumina producers to provide high-purity, highly uniform raw material. At the moment, this appears feasible, as reactive aluminas derived from Bayer hydrate are suitable, provided their CaO content can be kept below 100 ppm.

Summary

Development of sodium sulfur batteries for electric vehicle and electric storage use represent an exciting large-volume application of alumina in the future, while offering significant conservation of liquid fuels and reduction of air pollution. Over 15 years of development have brought the battery from a laboratory curiosity to an advanced stage of development in all major developed countries.

References

[1]A. Roberts, p. 122 in Structural Materials in Nuclear Power Systems. Plenum, New York, 1981.

[2]J. T. Kummer and N. Weber, p. 37 in Proc. 21st Annual Power Sources Conf., 1967.

[3]A. Fickett, "Batteries for Electric Utilities, Will There be a Market?" pp. 1–9 in Proc. DOE-EPRI Beta Battery Workshop, EPRI Report EM–3631–SR, December 1984.

[4]J. Cohen, "Fleet Vans Head The Way for Electric Vehicles," *EPRI J.*, July/August, 22 (1986).

[5]J. L. Sudworth and A. R. Tilley, The Sodium Sulfur Battery. Chapman and Hall, New York, 1985.

[6]R. S. Gordon and G. H. Miller, "Overview of Ceramatec's R&D Activities," pp. 2–55 in Proc. DOE-EPRI Beta Battery Workshop, EPRI Report EM–3631–SR, December 1984.

[7]J. Bast, EPRI Rept. EM–2579, Project 128-6, 1982.

[8]L. C. de Jonghe, "Degradation of β″ Alumina Electrolytes," EPRI Rept. EM–4151, July 1985.

[9]R. G. Miller and R. S. Gordon, "Manufacturing Cost Reduction of Beta″ Alumina," pp. 7–179 in Proc. DOE-EPRI Beta Battery Workshop, EPRI Report EM–3631–SR, December 1984.

Alumina in Electrical Porcelain

Ronald H. Lester, PE
Indiana University of Pennsylvania
Indiana, PA 15705

Alumina as an ingredient in electrical porcelain is traced in history from 1921 to the present state-of-the-art technology. Typical raw materials, compositions, properties, and forming methods are reviewed. A reference list is provided for further study.

The use of alumina as a substitute for flint in electrical porcelain seems to have been pioneered by General Electric Company, as disclosed by Twells and Lin[1] in 1921. Although this laboratory accomplishment showed technical advantages, neither economic justification nor supply of raw materials was adequate to pursue the alumina porcelain development on a commercial basis.

In 1935, Thiess[2] continued these investigations but again, the material available, calcined diaspore, could not justify the commercial applications.

Work at Battelle sponsored by the Aluminum Company of America was published in 1946 by Austin et al.[3] This investigation covered the use of calcined ground Bayer process alumina in hotel chinaware, electrical porcelain, cooking ware, and sanitaryware bodies. It is this most significant contribution that was later picked up by the electrical porcelain and hotel chinaware industries.

In 1953, Batchelor[4] reported further progress at the British Ceramic Research Association, and in 1954 Pearch[5] at Locke Insulator Division of General Electric perfected the development of the first commercial alumina porcelain for the U.S. electrical utility industry.

In 1955, Locke design engineers introduced a line of high-strength electrical insulators. The demand for extra-high voltage (EHV) transmission lines had created the need for higher strength compact tower designs, and the alumina porcelain fulfilled this need. The design engineers not only had to address the need for higher mechanical strength with lighter compact insulators, but also had to fulfill the electrical requirements of dielectric strength and electrical flashover.

The first U.S. commercial alumina insulator was a 111.2 kN (25 000 lb) M&E rated suspension insulator color-coded with a gray compression glaze since this unit was the same shape and size as a 44.5 kN (10 000 lb) M&E rated insulator. The smaller, lighter weight insulator gave the EHV designers a 2.5 times factor for mechanical loading, and hence an insulator string that was much lighter in weight.

As higher and higher transmission voltages (ultra-high voltages (UHV)) were demanded, the alumina porcelain product lines were extended to up to 355.9 kN (80 000 lb) M&E rating. When economic justifications permitted, all major suppliers of electrical porcelain adopted the new alumina ceramics.

Through the late 1950s, Crosley et al.,[6] Selsing,[7] Blodgett,[8] and other researchers throughout the porcelain industry continued ceramic development to improve the alumina ceramics or to develop more economic blends of flint and alumina.

Lester[9] at Locke Insulator investigated the ball milling and vibro-energy milling of the basic matrix composition and found a 30% improvement in mechanical strength and a 35% improvement in dielectric strength. Thus, a combination of matrix improvement by process changes and select fillers was offered as a means of further improving the strengths of electrical porcelain. Because of the high investment in milling equipment and the departure from standard shrinkage allowances, hence duplicate tooling, this approach was not adopted.

In the 1960s, Batchelor and Dinsdale[10] reported their further progress and Floyd et al.[11–16] at Reynolds Metals Company contributed to the basic research. Carithers et al.[17] showed that commercially available calcined bauxite ground to 325 mesh could be substituted for calcined alumina with similar properties. The EPRI, in 1978, sponsored work by Knickerbocker et al.,[18] which was directed toward improvements in alumina porcelains so that larger conductors could be carried by insulator strings and station insulators could be developed with higher resistance to short-circuit forces.

This study centered on refinement of the body by vibro-energy milling, material substitution, and adjustment of the clay/flux ratio. Significant improvements using a 50% alumina body are reported. This body was adapted by Victor Insulator for line post insulators.

Raw Materials and Body Preparation

The basic raw material is prepared by the Bayer process shown in Fig. 1. Typical particle-size analysis is shown in Table I.

Grinding of calcined alumina is either by steel balls, ceramic balls, or fluid energy milling. The degree of calcining and type of milling affect the vitrification properties of the porcelain. For a given grind, higher

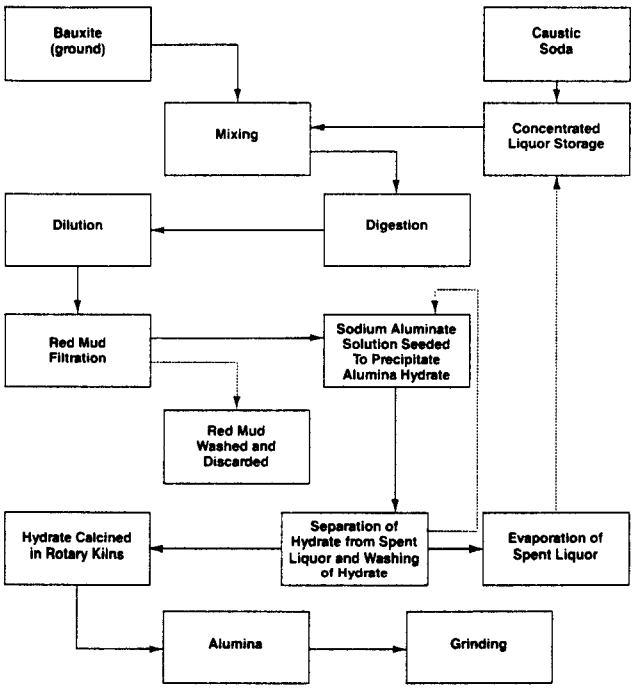

Fig. 1. Bayer process for the production of alumina.

calcining temperature and grinding with steel balls produces earlier vitrification and higher strengths. At coarser particle sizes, the calcined alpha alumina, containing more crystal agglomerates, proved to be more refractory, weaker, and more resistant to firing deformation than monocrystals. At finer particle sizes, the calcined alumina, containing finer crystal agglomerates, yielded properties similar to those of fused alumina. Leachable soda content is extremely important for slip and filter-cake stability. Highly leachable soda causes deflocculation of the clay or delayed breakdown of the filter cake. Additional processing steps to remove the soluble soda or higher calcining can help alleviate this situation.

Table I. A Typical Calcined Alumina for Electrical Porcelain

Size (μm)	X, % <L.E.S.D.	3σ
44	96	2.8
20	93	4.6
15	90	6.4
10	84	7.9
8	78	11.3
6	65	17.5
4	34	26.7
2	10	8.3

*Percent finer than equivalent spherical.

Typical Body Preparation

Clays are either premixed with water or may be directly batched with the nonplastics. Heated water aids mixing. Temperatures of 43° to 49°C (110° to 120°F) are common.

After blunging, the mixture is lawned to remove coarse lignite. Prior to filter pressing, the body mixture is flocculated with divalent or trivalent salts such as calcium chloride, magnesium chloride, or aluminum chloride and filter-pressed at pressures from 551 to 1378 kPa (80 to 200 psi). Alumina bodies are usually colored with an organic dye to prevent mixing of the body with the standard triaxial porcelain.

Electrical Porcelain Formulations

The basic criteria for introduction of the alumina porcelains are:

1. Forming by the commercial processes of extrusion, then plunging or turning, and by the slip casting process.
2. Orton Cone 9 to 12 vitrification so as to fire alumina porcelain side by side with conventional porcelain.
3. Manufacturing losses equivalent to flint-feldspar clay triaxial porcelain.
4. Total design economics to favor a body substitution.

Electrical insulators require a porcelain body composition with the characteristics shown below:

1. Consistency as a function of filter cake or slip age.
2. Formability without stretch cracks under the rotational dies or extrusion process.
3. Good turning characteristics to avoid tool chatter or clay cracks.
4. Equivalent drying characteristics so flint and alumina porcelain can be mixed in the dryer on a common drying cycle.
5. Drying and firing shrinkages so common molds and tooling can be used for flint and alumina porcelains.
6. Equivalent vitrification characteristics so that flint- and alumina-bearing porcelains can be fired side by side.
7. Equivalent dielectric properties.

The basic substitution of flint for alumina is a volume-for-volume substitution; for example, (3.09/2.65) × (% flint). This will give a matrix of glass and mullite with an equal volume of alumina substituted for flint. Since the finer flint particles dissolve into the glassy matrix, this is only an approximation.

Table II shows the compositions and effect of alumina additions on the fired modulus of rupture of 0.0191 m (¾ in.) diameter test rods as compared to standard porcelain. The span was 0.1270 m (5 in.) and the load rate 2.7 kN (600 lb) per minute.

All of these compositions were fired to cone 10 to 11 down approximately 1249°C (2280°F). All gave good working properties and vitrification. Similar results

Table II. Compositions

	Flint	A	B	C	D	E	F
Ball clay (%)	30	30	27.2	26.6	25.8	25.0	30.9
China clay (%)	20	19	17.3	16.0	14.6	13.2	4.6
Feldspar (%)	30	31	28.2	27.4	26.6	25.8	25.5
Calcined alumina (%)	20	20	27.3	30.0	33.0	36.0	39.0
X unglazed modulus of rupture, MPa	75.2	93.8	108.9	111.0	117.9	120.7	131.7
(kpsi)	(10.9)	(13.6)	(15.8)	(16.1)	(17.1)	(17.5)	(19.1)
X glazed modulus of rupture, MPa	103.4	102.0	141.3	158.6	164.1	168.2	175.1
(kpsi)	(15.0)	(14.8)	(20.5)	(23.0)	(23.8)	(24.4)	(25.4)

are reported by Gales[19] for an exchange of a 25 mass percent quartz by 35 mass percent alumina. The strengths are increased by the use of standard compression glazes.

Depending on processing and testing variables, a 5 to 10% coefficient of variation is typical. Composition F, 39% alumina addition, was selected for commercial application and additional properties were evaluated.

Impact Strength

This test is made using a 0.0191 m (¾ in.) diameter by 0.1524 m (6 in.) long test specimen. Rods are placed in the sample holder of a Charpy impact tester, at a 0.0762 m (3 in.) span. A weighted pendulum is dropped on the specimens at intervals of 0.113 J (1 in. • lb) until the sample ruptures. (See Table III.)

Thermal Shock Resistance

The test rods are heated slowly to 649°C (1200°F) and then brought back to room temperature by air cooling. The standard modulus of rupture test is then performed. (See Table IV.)

Dielectric Strength, Dielectric Constants Loss Factor (Unglazed) (Tables V and VI).

The physical and electrical properties in Tables V and VI are fairly typical for alumina electrical porcelains in use today. The particle size of the materials greatly affects all properties. Ball milling of the clays and fluxes can (as will the use of fine alumina powders) greatly increase the strength. Improved properties are a trade-off with respect to forming and processing problems; for example, higher shrinkages and cracking.

Table III. Impact

	Unglazed *X*	Glazed *X*
Flint porcelain	0.43 J	0.61 J
	(3.8 in. - lb)	(5.4 in. - lb)
39% alumina	0.82 J	1.00 J
	(7.2 in. - lb)	(8.8 in. - lb)

Table IV. Thermal Shock

	X Initial Strength (Glazed)	*X* Shocked Strength
Flint porcelain, MPa	107.6	74.5
(kpsi)	(15.6)	(10.8)
39% Alumina, MPa	184.1	175.8
(kpsi)	(26.7)	(25.5)

Table V. Electrical Properties

	K	% Power Factor	% Loss Factor	Dielectric Strength, MV • m^{-1}
Flint porcelain	5.1	0.80	4.1	9.02 (229 V/mil)
39% alumina	6.8	0.59	4.0	9.57 (243 V/mil)

Table VI. Coefficient of Expansion, 50° to 70°C

Flint porcelain	6.54×10^{-6} $°C^{-1}$
39% alumina	7.25×10^{-6} $°C^{-1}$

Compositions higher than 39% alumina require additional processing or composition changes but are certainly feasible should economics so dictate. Ball milling and higher firing temperatures are two approaches that will work. The trade-off is the lack of compatibility with the standard flint porcelain; hence tooling and processing modifications are required.

In applications where the use of an alumina porcelain is not justified, a combination of alumina and flint can be used. Lester investigated such compositions in 1958 and these properties are shown in Table VII.

Selsing obtained a patent[7] in 1959 which claimed a beneficial strength increase by using nepheline syenite

Table VII. Compositions and Properties of Alumina-Flint Combination

	A	B	C
Ball clay (%)	30.5	30.5	31.0
China clay (%)	11.8	6.8	0.0
Feldspar (%)	28.2	28.2	29.0
Flint (%)	10.0	15.0	20.0
Alumina (%)	19.5	19.5	20.0
Unglazed modulus of rupture,* MPa	98.6	98.6	93.8
(kpsi)	(14.3)	(14.3)	(13.6)
Glazed modulus of rupture, MPa	137.2	140.0	130.3
(kpsi)	(19.9)	(20.3)	(18.9)

*Test rods 0.0191 m (¾ in.) diameter, 0.1270 m (5 in.) span.

in place of feldspar. This substitution was designed to reduce the number of particles of quartz, which lowered the strength of the product, as shown in Table VIII. This product was not a commercial success, since the nepheline syenite caused excessive cracking during forming and drying operations. This adverse reaction is caused by deflocculation of the filter cake when the soda is released from the nepheline syenite and alumina.

Extending the alumina content beyond 50% requires ball milling or auxiliary fluxes. These additional processing steps allow the alumina content to be extended to 75%, yet still fire at conventional cone 10 temperatures. A typical composition and properties are given in Table IX.

The EPRI[18] reported that an attempt was made to use vibratory milling and talc as an auxiliary to alumina porcelains but that only a 10% improvement in strength was noted. Their efforts then centered on materials replacements to reduce the free quartz and lignite.

A composition of 50% Alcoa A-12 alumina, 30% Ajax P kaolins, and 20% Minex 10 nepheline syenite exhibited significant gains in flexural strength. No specimen size or load rate is reported but a mean value of 304 MPa (44 100 psi) is given for a 1.22 clay-flux ratio. This ratio was found to be dependent upon the percentage by weight of alumina. The greater the alumina content, the lower the clay-flux ratio to obtain higher flexual strengths. The key to commercial realization of such compositions is the fineness of the body without excessive losses from the forming and drying operations.

Table VIII. Residual Quartz as a Function of Flux Ratios

Weight Ratio Nepheline Syenite: Feldspar in Ceramic Mix	% Quartz in Fired Product	Modulus of Rupture, MPa (psi)
0:35	3.0	110.3 (16 000)
15:20	1.2	122.7 (17 800)
20:15	0.6	132.4 (19 200)
25:10	0.5	134.5 (19 500)
30:5	0.2	138.6 (20 100)
35:0	0.0	162.7 (23 600)

Table IX. Typical Composition and Properties of Electrical Porcelains Made with 75% Alumina

	Dry Weight (%)
Ball clay	4
Bentonite	3
Nepheline syenite	18
Alumina	75
Unglazed modulus of rupture,* MPa	289.6
(kpsi)	(42.0)
Glazed modulus of rupture, MPa	310.3
(kpsi)	(45.3)

*0.0191 m (¾ in.) test rods, 0.1270 m (5 in.) span.

To date, the electrical porcelain industry has not moved forward with higher strength alumina porcelains. This author feels that commercial production is possible should economics so dictate. Electrical restraints may overcome the mechanical advantages; for example, flashover geometry and dielectric strength.

Major Methods of Forming High-Voltage Insulators

Schematics for the major forming methods are shown in Figs. 2 through 5.

Extrusion

Depending on the forming process to be used following extrusion, filter cakes of "clay" mixture are formed by dewatering the ceramic slip to 16 to 22% moisture. The "clay" cakes are fed into a vacuum deairing pug mill which shreds or noodles the clay through a sealing die into a vacuum chamber. The deaired clay is then carried by an auger through an extrusion barrel and then through a nozzle or die to form billets or cylinders of compacted "clay." The design and control of the extrusion process is well

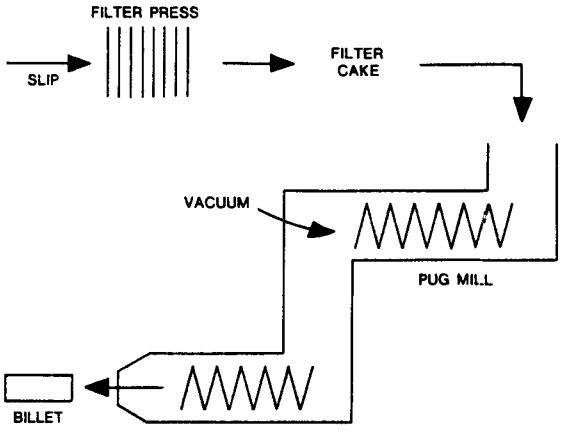

Fig. 2. Extrusion.

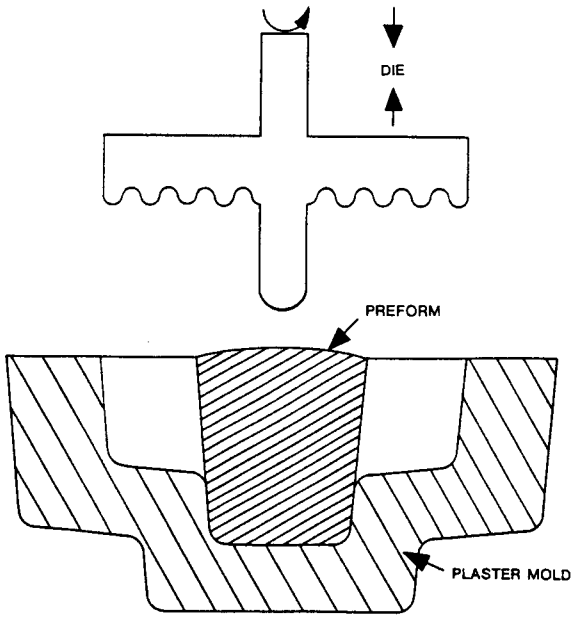

Fig. 3. Pressing.

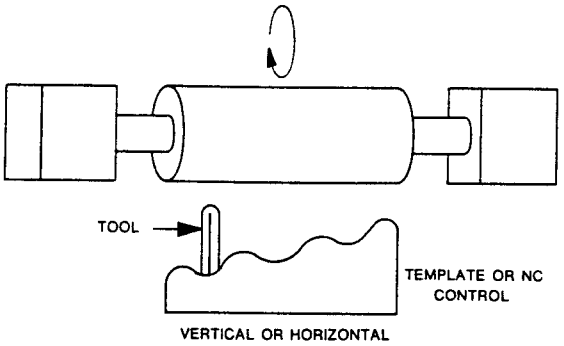

Fig. 4. Turning.

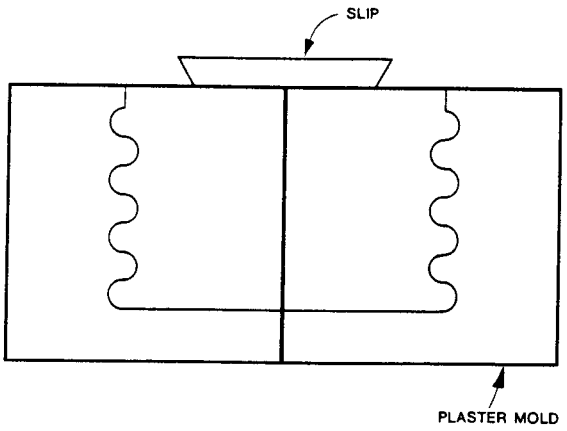

Fig. 5. Slip casting.

documented by Lester.[20] No special equipment or procedures are needed when alumina is substituted for flint. The extruded billets are then conditioned or dried and formed into electrical insulators using one of the processes shown in Figs. 2 through 5 and described in the following paragraphs.

Hot-Pressing

Billets of clay with moisture contents from 19 to 20% (wet basis) are preformed and then pressed into intricate shapes for suspension, switch, multipart, and pintype insulators. The preforms are placed into plaster molds to form the external contour and a heated rotating die, "plunger," is pushed into the preforms to press the "clay" and fill the mold. Oil is applied to the surface of the preforms to aid die release. Dies can be heated internally by steam or external heat may be applied by gas flame or heat gun. After pressing, the mold is placed into a mold release drier and, after sufficient shrinkage has occurred, the part is lifted by vacuum or dumped from the mold. The shaped piece is then further conditioned or dried for final contouring by green or dry finishing techniques.

Cold-Pressing/Jiggering

Cold pressing is performed with clay in 19 to 21% moisture content. Vacuum may be applied when plaster male and female dies are used. Generally male dies are not rotated and in the jiggering process, a narrow segmented steel profile of the desired shape is pressed into the clay as the mold and preform are rotated. The jiggering tool is gradually immersed into the "clay." Fuse cutouts and guy strain insulators are often formed by the use of male and female plaster dies, while large switch and multipart pintype insulators are jiggered.

Turning

Extruded billets of clay called "pugs" are turned using techniques similar to wood turning. The lathes are in either a vertical or a horizontal mode. Green finishing, semidry, or dry turning finishing options are available. Green finishing is a preferred method because of lower turning cost, health considerations, lower capital investment, and tooling costs. The tradeoff is lower dimensional fidelity. When green finishing, extruded billets are either electrically dried by applying electrodes to each end or conventionally dried to a "leather-hard" state at moistures of 14 to 17%. Spring steel or carbide tooling are used in contouring the pug. When dry finishing, the pugs are dried to less than 4% moisture and ceramic or carbide tools are utilized. Semidry finishing at moistures from 8 to 13% offers a compromise in dimensional control, tool life, and employee health considerations.

Key variables in forming insulators by the turning process are as follows:

1. Proper support of the hollow or blind end extrusions so as to avoid excessive internal gripping pressures from the expansion pads or internal chucking device.
2. Sufficient green or dry strength of the extruded part. This is a function of the body formulation and

retained moisture. Too low a moisture can lead to tool vibration and chipping.

3. Proper selection of feeds and speeds for the turning machine and cutting tool.

4. Proper cutting tool design and maintenance.

5. Proper template design. Both single or multipath tooling options are used. Tools may trace the pattern in multiple or a single-plunge cutting tool path. In green finishing, the quickest method is plunge cutting, using a tool shaped to the desired contour which is fed into the rotating pug.

In dry turning, an NC program or template can be used to trace rough and finished cuts. The rough cuts may be multiple to avoid deep chips out of the clay and resulting fracture paths below the surface of the finish cut. Turned and dried parts can be monitored with fluorescent dye and black light to control the quality of the finished ware. Preglaze inspection is desirable.

Slip Casting

Casting compositions needed for complex shapes such as radio tower insulators for long-wave transmissions are produced by slip casting in plaster molds. A typical casting composition is shown in Table X and a comparison to standard porcelain is shown in Table XI.

A clay slurry is made using an electrolyte such as 0.03 to 0.04% sodium silicate (dry basis) and at a specific gravity of 1.8 to 1.95. The slip is poured into plaster molds and when sufficient thickness is obtained, the slip is drained or poured from the mold. Solid casting utilizes an internal plaster mold so casting proceeds from two directions until a solid cast is obtained. Medium-pressure casting is performed by pumping the slip into a battery of molds at pressures of 300 kPa (3 bars). High-pressure casting at 2500 kPa (25 bars) is done on steel-jacketed plaster, ceramic, or plastic molds. The higher the pressure, the faster the casting rate.

Glazing

Glazing techniques are as used for conventional triaxial porcelain; for example, spray, dip, and flooding. Aqueous suspensions of glass-forming and coloring oxides can be applied by conventional paint-spraying techniques, including robotics. Parts may also be dipped into the glaze or the glaze may be pumped over the rotating part. After glazing, the part is dried below 1% moisture prior to firing.

Table X. Typical Casting Composition*

	Dry Wt (%)
Ball clay	19.0
China clay	15.0
Feldspar	25.5
Alumina	39.0
Talc	1.5

*Slip specific gravity = 1.948.

Table XI. Properties of Cast 39% Mass Alumina Porcelain

	Standard	Alumina
Dry modulus of rupture, MPa	2.7	2.2
(psi)	(385)	(325)
Unglazed modulus of rupture, MPa	71.0	113.8
(kpsi)	(10.3)	(16.5)
Glazed modulus of rupture, MPa	100.0	172.4
(kpsi)	(14.5)	(25.0)
Specific gravity	2.39	2.81
Dry shrinkage	3.4%	3.3%
Fired shrinkage	10.3%	13.3%
Total shrinkage	13.7%	16.6%

Firing and Firing Range of Alumina Porcelain

Typical firing ranges are from cone 10 tip to cone 12 down. This is a good cone more than conventional triaxial porcelain. As a typical flint porcelain is fired, the quartz dissolves into the matrix and lowers the body expansion. The high glass content with lower expansion reduces the advantage of the compression glaze. Hence, both unglazed and glazed alumina bodies are superior. Dye penetration is a method of evaluating firing range. A test specimen is immersed in fuscine dye and alcohol and subjected to 68.9 MPa (10 000 psi) for six hours. Results for a typical flint and alumina porcelain are as follows:

Flint	no penetration	
	1249° to 1277°C:	Range 28°C
	(2280° to 2330°F):	Range (50°F)
Alumina	no penetration	
	1232° to 1360°C:	Range 128°C
	(2550° to 2480°F):	Range (230°F)

The crystal makeup of these bodies shows less glass and increased mullite for the alumina porcelain.

	Mullite	*Glass*	*Quartz*	*Alumina*
Flint porcelain	19.0%	70.2%	10.8%	none
Alumina porcelain	27.8%	40.5%	trace	31.7%

Future Growth of Alumina in Electrical Porcelain

Due to the decrease in demand for electrical energy, little volume growth is projected in the next decade. The demand for improved properties awaits the economic justification for the added cost of higher alumina contents or additional processing costs. Any development that can reduce costs, such as a moderately calcined ground bauxite, could open up the doors for wider use of alumina porcelain. Body color is not a major criterion for electrical porcelain, so less-refined raw materials could offer attractive alternatives to the more expensive Bayer process alumina.

Inroads of polymer insulators utilizing a lightweight polymer shed and a fiberglass rod core permit the tower designer greater weight reductions and better tower economics. Hence, the overall growth opportunity for alumina in electrical porcelain is not promising.

References

[1]R. Twells, Jr., and C. C. Lin, "The Effect of the Replacement of Free Silica by Alumina and Zirconia in Electrical Porcelain," *J Am. Ceram. Soc.*, **4**, 195–205 (1921).

[2]L. E. Thiess; unpublished private communication, General Electric Co., Porcelain Manufacturing Div., Schnectady, NY, 1935.

[3]C. R. Austin, H. Z. Schofield, and N. L. Haldy, "Alumina in Whiteware," *J Am. Ceram. Soc.*, **29** [12] 341–54 (1946).

[4]R. W. Batchelor, "Some Physical Properties of Porcelain Bodies Containing Corundum, Part II-The Use of Calcined Run Materials High in Alumina," Research Paper No. 212, The British Ceramic Research Association, Stoke-on-Trent, August 1953.

[5]H. C. Pearch; unpublished private communication, General Electric Co., Locke Insulator Dept (1954).

[6]Crosley, Williams, Lester, unpublished private communications; General Electric Co., Locke Insulator Dept (1956–1959).

[7]J. Selsing, "Ceramic Products," U.S. Pat. No. 2 898 217 (1959).

[8]W. E. Blodgett, "High Strength Alumina Porcelain," *Am. Ceram. Soc. Bull.*, **39** [4] 247 (1960).

[9]Lester, R. H.; unpublished private communications, General Electric Co., Locke Insulator Dept (1960).

[10]R. W. Batchelor and A. Dinsdale, "Some Physical Properties of Porcelain Bodies containing Corondum"; pp. 31–38 in Transactions of the VII International Ceramic Congress, London, 1960.

[11]J. R. Floyd, J. H. Sterne III, and J. S. Deutscher, "The Strength of Whiteware Bodies - Test Technique Makes a Difference," *Ceramic Age*, **81** [4] 60, 62–68 (1966).

[12]J. R. Floyd, D. Royce, Jr., and A. Lippman, Jr., "Alumina Versus Flint in Whiteware Bodies," *Am. Ceram. Soc. Bull.*, **45** [4] 463 (1966).

[13]J. R. Floyd, "The Strength of Whiteware Bodies - Alumina Additive Makes a Difference," *Ceramic Age*, **82** [4] 61, 70–74 (1967).

[14]J. R. Floyd, "Alumina Improves Properties of Whiteware Bodies," *Ceramic Ind.*, April (1967).

[15]J. R. Floyd, "Calcined Bauxite for the Whiteware's Industry," Test Report 1R1667-1 Alumina Research Div., Reynolds Metals Co., 10 pages, January 1967.

[16]J. R. Floyd, "A Potential Inexpensive Raw Material for Strengthening Vitreous Whiteware Bodies," *Am. Ceram. Soc. Bull.*, **48** [4] 493 (1969)./L

[17]V. G. Carithers, D. R. Watson, and R. L. Johnson, "Comparison of Commercially Calcined Bauxite, Calcined Alumina and Flint in a Vitreous Whiteware Body," *Am. Ceram. Soc. Bull.*, **48** [4] 493 (1969).

[18]I. O. Knickerbocher, J. E. Funk, W. Curtis, D. Miller, and G. Steere, "Improvement of Electrical Porcelain Insulators," EPRI Report EL–721–54, Project 424–1, April 1978.

[19]F. Gales, Ceramic Monographs—Handbook of Ceramics. Verlag Schmid Gmblt, Freiburg i. Br., 1987.

[20]R. H. Lester, "Pugmill Perfection Provides Porcelain Profits"; pp. 141–57 in Technical Innovations in Whitewares, Alfred University Press, New York, 1982.

Dinnerware Manufacture and Use in the United States

Robert J. Beals
Hall China Co.
East Liverpool, OH 43920

The domestic production of dinnerware in the United States is described. The effect of foreign imports on production and usage together with the health concerns of heavy metals in glazed dinnerware, are discussed.

The earliest use of ceramic articles for storing, cooking, and serving foodstuffs goes back through history to the time when man discovered that clay could be hardened by fire. Since those early times, pottery making has developed as an art rather than a science. Much of the ceramic dinnerware of today is manufactured in much the same way as it was 200 years ago. However, innovative approaches and refined techniques are being investigated and used to bring modern technology into dinnerware manufacture.

Definitions of Dinnerware

Ceramic tableware is produced in almost every country in the world, either for local use or for export. Quality ranges from the most primitive of shapes to the most refined and beautiful chinaware. A variety of names and definitions describing the same product have caused confusion in the minds of the user. The following definitions,[1,2] while not rigorous, permit a clearer understanding of the various categories of dinnerware.

Pottery. As a generic name, pottery includes all fired clayware produced. As a specific name, it describes low-fired, porous ware which is usually colored. The term is properly applied to the clay products of primitive peoples or to decorated art products made from unrefined clays and by unsophisticated methods.

Ceramic products acquire strength, rigidity, and durability through the application of heat. The chemical composition of the raw materials used determines, with the heat applied, the strength, porosity, and vitrification of the fired product. Primitive pottery, often baked in the sun and composed of unrefined, local clays has low strength and high porosity.

Earthenware. This is a porous type of ceramic body fired at comparatively low temperatures, producing an opaque body, less strong than stoneware or china and lacking the resonance of those products when struck. The product may be glazed or unglazed.

Crockery. This is a term, often used synonymously with earthenware, to describe a porous opaque body for domestic use. Because of its moisture permeability, or porosity, it is normally glazed. Shapes are normally thick-walled and may be colored.

Stoneware. This is a nonporous (or very low-porosity ceramic composition made of unprocessed clays o clays with flux additives, fired at high temperatures. I is quite durable but lacks the translucence and white ness of china. It is resistant to chipping and ring clearly when struck. It differs from porcelain chiefly i that it is colored, generally as a result of iron and othe inclusions in the clay.

Ironstone china. This is a historic term for durabl English stoneware. The composition and properties are similar to those of porcelain except that the body i not translucent and may be off-white. In the Unitec States today, this term is used to describe a number o other products, including semivitreous dinnerware.

Cooking ware. This is a broad term applied to earthenware, porcelain, and china when the shapes are designed for cooking or baking as well as for serving. The ware has a smooth glazed surface where food may contact it and is strong and resistant to thermal shock.

Fine china. This is a term applied to thin, translucent, vitrified bodies, generally fired twice: first at a relatively high temperature to mature the purest mixture of flint, clay, and flux materials; and, second, to develop the high gloss of a beautiful glaze. It is the highest quality tableware manufactured for the domestic or retail market. It includes bone china, frit china (or Belleek), and some feldspar chinas.

Porcelain. This term is used synonymously in Europe and the Orient to describe china. European porcelain, like china, is fired twice. In the United States and the Orient, porcelain may be fired in a one- or two-stage process. Porcelain is a hard, nonabsorbent, high-strength body, which is white and translucent in thin section. European porcelain is made primarily for the retail market.

Bone china. The term applies to a specific type of fine china manufactured primarily in England but duplicated in other parts of the world. The body consists of a high proportion (>25%) of bone ash to develop greater translucency, whiteness, and strength. It is primarily for the retail trade.

Restaurant china. This china is a uniquely American blending of fine china and porcelain designed and

engineered specifically for use in commercial restaurant operations. The body was formulated to give high impact strength and durability, with the low absorption that is required for public food service. Decorations are applied between the body and the glaze, or in the glaze, thereby protecting the decoration during commercial use. In the United States, the terms "hotel china," "commercial china," "restaurant china," "institutional china," and "American vitrified china" are used synonymously.

In the manufacturing processes of the United States, most of the ware is subject to a high-temperature first firing and a lower-temperature second, glaze firing. Some of the ware is manufactured, as it is in the Orient, in one-fire operations wherein the body and the glaze mature in the same time and at the same temperature. Like fine china, American restaurant china is vitrified, that is, has a water absorption of less than 0.5%.

Absorption

The physical property most often used to characterize the various classes of table and dinnerware is the percentage of water absorption—the weight gain which results when the ware is properly impregnated[3] with the maximum amount of water it will hold. Typical values of absorption are given in Table I.

Areas of Manufacture

In the earliest years of the United States, most (if not all) of the ceramic tableware used was produced in and imported from England and Europe. There had been a viable pottery industry in America for many years, but it was not until the early 1870s[4] that domestic manufacturers in East Liverpool (Ohio), Trenton, New York City, Baltimore, Cincinnati, and St. Louis began to make inroads on British imports. For example, the Staffordshire potteries exported 199 782 "packages" to America in 1866 but only 45 378 units in 1874. Further, the Morrill Tariff of 1861 was a highly protective duty rate of 40%. As world trade increased, ceramic tableware was imported from the Orient and South America as well as from England and Europe. The ceramic tableware industry in the United States was never able to expand to meet the full expectations and needs of its markets. The temporary encouragement and protection given by World War II quickly fell away and England, Western Europe, and Japan reestablished themselves. Foreign manufacturers are estimated to provide more than 70% of the market's needs.[5] The decline in present U.S.-manufactured tableware can be traced, in large part, to the loss of production facilities and to the success of generally lower priced imported ware.

Table I. Absorption Values of Different Classes of Dinnerware

Dinnerware Type	Percent Absorption
Earthenware	10 – 15
Stoneware	0 – 0.5
Ironstone ware	0 – 0.5
Semivitreous ware	4 – 9
Fine china	0 – 0.5
Porcelain	0 – 0.5
Bone china	0 – 0.5
Restaurant China	0 – 0.5

The ceramic tableware industry, as defined by the Tariff Schedule of the U.S. Department of Commerce (TSUS),[6,7] consists of two major groups—the earthenware industry and the vitreous chinaware industry. In 1977, the earthenware industry in the United States was composed of 23 establishments. Of these, 17 employed more than 20 employees. As a result of consolidations and closings, the number of companies decreased to 15 by 1982 (the last year for which TSUS data are published). These plants, mostly privately held, are concentrated in the Appalachian region (Pennsylvania, West Virginia, Ohio) and California. The four largest firms accounted for 70 to 80% of domestic earthenware production in 1980. Total employment was estimated[7] at 3600 production workers. By 1982, this figure had diminished to 2600 workers. Declines in pottery employment have continued as the American public has turned to less-expensive imported ware, particularly from the People's Republic of China.

The vitreous chinaware industry has remained relatively stable over the past few years, at 28 factories, 14 of which employ 20 or more persons. Most are producing commercial chinaware. One company (Lenox China) dominates the household chinaware sector. In 1980, there were 6700 production workers; in 1982, there were only 5500 production workers in this industry.

Estimated U.S. consumption of table- and kitchenware fluctuated during 1980 to 1982,[8] rising from $622.7 million in 1980 to $696.7 million in 1981 and then declining to $680.2 million in 1982. During this time, imports accounted for about 53% of the apparent annual consumption. Apparent consumption of earthenware or stoneware table- and kitchenware articles rose from around $269.6 million in 1981 to $303.5 million in 1981, then decreased to $289.7 million in 1982. Imports accounted for an estimated 67% of the apparent yearly consumption. Consumption of chinaware or subporcelain table- and kitchenware articles increased from an estimated $352.8 million in 1980 to $393.2 million in 1981, then fell slightly to $390.5 million in 1982. Imports accounted for about 43% of these annual consumptions.

In 1978, Japan lead the importers (with an import share of around 53%)[7] of all categories of table- and kitchenware into the United States with the United Kingdom a distant second. By 1982, the People's Republic of China had emerged as the second largest source of imports, with a 33% share of the import market. In 1981, the U.S. International Trade Com-

mission stated, "Imports from the People's Republic of China of ceramic household articles chiefly used for preparing, storing, or serving food or beverages, or food or beverage ingredients, did not result in market disruption with respect to an article produced by a domestic industry."[9] Yet, the United States experienced a trade deficit in ceramic table and kitchen articles which rose from $309 million in 1980 to $353 million in 1981, then declined slightly to $342 million in 1982. There are indications[10] that the dinnerware and fine china industry lost further ground by 1986. Sales on domestic production were approximately $222 million in 1982, had fallen to $182 million in 1985, and further to $146 million in 1986, apparently caused by increased imports.

Raw Materials

Pottery, earthenware, crockery, and some stoneware are generally manufactured from locally available, relatively unrefined raw materials used singly or in simple mixtures.

The batch formulas for semivitreous ware, fine china, porcelain, and American vitrified china are more complex. Generically speaking, the body materials are classified as flint, clay, feldspar, and auxiliary fluxes. Few of the raw materials are found in deposits near the manufacturing site, which is generally chosen to be near markets or fuel sources or for similar reasons.

Flint

The so-called flint used in the United States is a ground quartz sand, principally a widely distributed deposit of St. Peter's sandstone outcropping in Pennsylvania, Ohio, West Virginia, Illinois, and Oklahoma. This material has a low iron content and yields quartz of high purity. Commercial flints are available, ground with 50% of the materials <30 μm. The particle size is carefully controlled since the drying and firing properties of the body and its thermal shock resistance are influenced by the flint. Most whiteware manufacturers utilize a single source of flint.

Clay

Most U.S. whiteware manufacturers utilize a variety of kaolins, china clays, and ball clays in their bodies. The word kaolin is derived from the Chinese words "kao ling" (high ridge). It is used to identify the relatively pure, white-burning clay found in the United States. The term "china clay" is used to identify a similar material in England. The word kaolin will be used here to mean either kaolin or china clay.

Kaolin is found as (*a*) residual kaolin, where the clay replaces the pegmatite rock formed by weathering or other alterations and (*b*) sedimentary kaolin, composed of clay particles transported from the original point of formation by stream action and settled in deposits at the bottom of bodies of quiet water, such as lakes.

For use in whiteware in the United States, the only domestic deposits of value are (*a*) the residual kaolin deposits in the Spruce Pine region of North Carolina, (*b*) the sedimentary kaolin deposits of Georgia and South Carolina, and (*c*) the fine-grained kaolins of Putnam County, Florida. Probably 90% of U.S. production comes from the Georgia-South Carolina deposits. Although used less today than formerly, the china clays from the Cornwall region of England are still used by some U.S. manufacturers because of their unique properties.

Semivitreous dinnerware and hotel china rely, for the most part, on ball clays to provide plasticity and dry strength to the formed ware. Little or no ball clay is used in fine china and bone china, because of its effect on translucency and color. Ball clays are used (*a*) to provide increased workability of the body in the plastic state, especially when jiggering; (*b*) to develop increased green strength, reducing handling losses; (*c*) to increase fluidity in casting slips; and (*d*) to increase fluxing of the clay to give a "tighter" fire. In the United States, commercially important deposits consist of lower Eocene (tertiary) beds of secondary origin running through western Kentucky and Tennessee and some deposits in Mississippi. The well-known deposits in the Devon region of England are used to a lesser degree in domestic dinnerware.

Feldspars and Other Fluxes

Domestic feldspars are the principal fluxes in semivitreous and most of the vitrified china produced in the United States. They form the glassy phase and promote vitrification and translucency. They are also a source of alkali and alumina in the glazes. They are relatively inexpensive and are one of the few sources of water-insoluble alkali compounds. The potash-albite spars are the principal spars used. Commercial deposits of spar are found in California, Connecticut, North Carolina, and South Dakota. Most are supplied in fine-ground form, froth-floated to remove quartz and other undesirable materials.

Some U.S. manufacturers, particularly for semivitreous dinnerware, use nepheline syenite as an active flux, especially for lower-temperature firing. Large deposits of this mineral are found in the Province of Ontario, Canada.

Some manufacturers use talc, a hydrated magnesium silicate, as an auxiliary flux in combination with feldspar. In some cooking ware bodies, where resistance to thermal shock is important, talc is added to develop cordierite. The principal talc deposits in the United States are found in New York, Vermont, California, Montana, and Texas.

Bone ash is one of the few manufactured fluxes in use. It is used principally in the manufacture of bone china in the United Kingdom, replacing feldspar and other fluxes. Cattle bones, principally from the Netherlands and Sweden, are processed, calcined, and ground to produce bone ash.

Alumina

Alumina occurs naturally in the ball clays, kaolins, feldspars, nepheline syenite, and talcs used as raw materials in the dinnerware industry. Alumina is added* by some U.S. manufacturers as a ground calcined alumina in quantities around 10 to 20%, primarily to increase fired strength of the body. One domestic manufacturer of cooking ware uses a 50% addition of calcined alumina to produce an exceptionally strong, highly thermally shock resistant body. Secondary benefits derived by adding calcined alumina to dinnerware compositions include extension of the firing range, increased whiteness of the body, and a reduction in flaws resulting from the quartz inversion.

Manufacturing Methods

Each dinnerware manufacturer uses some methods which are unique to his operation, but most of the procedures are common to the entire industry. Automation and process control are gradually replacing manpower but the dinnerware industry is still a highly labor-intensive operation.

Raw Material Storage and Batching

Increased governmental regulations, high labor costs, and increased automation have resulted in improved handling and storage of ceramic raw materials. Today, most raw materials are shipped in hopper cars or trucks, unloaded by pneumatic or belt conveyors into enclosed silos, automatically or semiautomatically batched into enclosed weigh hoppers with dust collectors, then charged into enclosed blungers. Dust and the problem of airborne contamination are minimized. A dinnerware batch formulation may contain from 10 to 12 ingredients, perhaps one flint, one or two feldspars, one or more auxiliary fluxes, two ball clays, two or three kaolins, one or more china clays, and possibly alumina. The multiple-source raw materials minimize variations inherent in any natural raw material. As the degree of automation increases, there is a greater need for uniformity of raw materials.

It is common throughout the industry to water-wash the raw materials to remove organic impurities and to permit the removal of iron-bearing material. Following the water wash, the body materials are consolidated in a recessed-chamber filter press. While presses may be manually unloaded, increasingly manufacturers are turning to automatically unloaded, conveyor-carried filter presses. The processed filter cake will contain 20 to 25% water.

Forming Methods

Two major methods are used in the manufacture of all types of dinnerware: plastic forming and slip casting. Several European sources have suggested dry pressing as a viable alternate, but this has not become a widely accepted procedure inasmuch as it is limited to relatively flat ware.

Plastic Forming: About 85% of the dinnerware manufactured is produced by jiggering. In earlier times, round and oval shapes were hand-jiggered but, today, semiautomatic or automatic machines have replaced the manpower attendant on hand-jiggering.

The filter cake is prepared for use in the plastic forming process by a vacuum pugmill. The extruded, deaired clay, of varying consistency and water content, is fed to the jigger machine, cut to size, and formed to shape on a rotating plaster head. Whereas in early days, and still in some manual jiggering, a profiled metal blade formed the ware, today steel or aluminum roller tools, often heated to prevent sticking of the clay, or polyurethane or other plastic roller tools are widely used. The formed piece, in the plaster mold, is passed through an infrared, microwave, or hot-air dryer, removed from the mold, fettled, trimmed, and finally dried. Much of this can be accomplished automatically.

To be readily jiggered, the piece should be round or oval. When other shapes are desired, slip casting or plastic pressing may be used. Several specialty manufacturers use the plastic-press process in which the plastic clay is formed to shape between plaster dies, trimmed, sponged, and dried. The process is relatively rapid but is seldom automated. Most plates, cups, saucers, bowls, and similar items are manufactured by jiggering.

Slip Casting: About 15% of the dinnerware production is by slip casting. There has been little change in the procedure in about 200 years. Although there have been improvements in the plaster of Paris used for the molds and new electrolytes have been formulated, the basic process still depends on the skilled craftsman for forming the ware. Automatic casting machines have been devised and microwave casting has been advocated, but they are less successful than the automatic jiggering machines.

The previously prepared filter cake is blunged, together with appropriate electrolytes, to form a casting slip. Sodium carbonate and sodium silicate are the most commonly used electrolytes, generally in combination—perhaps 0.1% of each, depending on the cation exchange equivalent of the clays. There are also several polymeric materials used as electrolytes. The casting slip is adjusted to a density of 1.65 to 1.95 $g \cdot cm^{-3}$. Equally important to the process is the viscosity of the slip, which is the key to proper slip control. Controls normally include the measurement of slip viscosity, together with the determination of thixotropy of the slip.

Each manufacturer adjusts the physical characteristics of his casting slip to give the desired rate of casting. The casting rate is slowed by fine-grained

*Austin et al.[11] reported a comprehensive investigation on adding calcined alumina to a variety of whiteware bodies including dinnerware.

clays and increased by coarser nonplastics. Slip casting remains the slowest of the forming methods, with a cast time of about 30 minutes. Some fine china shapes may be cast in 3 to 5 minutes, but they are composed of essentially ball clay-free materials.

Once the desired thickness of cast wall is attained, the molds are inverted, either manually or automatically, and the remaining slip is drained. The cast body remains in the plaster mold to set, then the mold is opened, the piece removed from the mold, trimmed, fettled, sponged, and dried. While any dinnerware piece may be formed by the casting process, irregular shapes such as sugars, creamers, gravy boats, platters, and teapots are slip cast.

Bisquing

Once the formed pieces are completely dried, they are transferred to a kiln for bisque firing. Most of the semivitreous and vitreous ware produced in the United States is bisque-fired before glazing. For many years the tunnel kiln, with its heavy refractories and slow firing schedules, was used to fire dinnerware. Within the past five to seven years, the advent of the roller hearth kiln and the wide hearth, low thermal mass kilns have replaced the tunnel kiln. These kilns, because of their low mass, permit rapid schedules approaching 5 hours instead of the 25 to 30 hours of the tunnel-kiln era.

Most whiteware is fired in a slightly oxidizing atmosphere. For bisque firing, open settings on mullite or cordierite slabs are prevalent. Some fine china is fired in setters of cordierite or mullite to accommodate deformation during firing. Bisquing temperatures vary among manufacturers, but Cone 8 (about 1300°C) is the general range for semivitreous ware and Cone 9—10 (1320° to 1330°C) is common for hotel ware. Some frit porcelains and bone china may be fired as low as 1250°C.

Glazing

The typical dinnerware manufacturer compounds his glazes using one or more commercially prepared frits, feldspar, whiting, flint, clays, and other materials in his batch formula. Some add compounds of lead, although this is most often accomplished in one of the fritted materials.

The traditional method of grinding the glaze to the desired fine particle size has been the use of the pebble mill. More and more, the vibrating mill, with alumina grinding media, is used to reduce grinding time by at least an order of magnitude.

Glaze Application: As automation in body preparation has increased, so has the use of continuous spray or "waterfall" machines for applying glaze to the bisque body. Some holloware and special pieces may be hand-dipped or hand-sprayed, but these are minimal.

Glost Firing: Just as the tunnel kiln is being replaced in the bisquing operation by roller hearth or wide hearth kilns, so is the glost firing. Firing temperatures of lead-containing glazes are around Cone 5 (1220°C). although there are departures from these temperatures.

Decoration

The use of an underglaze decoration, applied by decalcomania, silk screen, stencil spraying, or direct printing on the bisque, provides a decoration unaffected by conditions of use. Much of the semivitreous ware and hotel china is so decorated.

Fine-china decorations are most often fired over the glaze, having been applied by slide-off decal, hand- or machine lining, or stamping. The applied decals are fired onto the ware at temperatures of 700° to 800°C in a relatively short time. The detail and colors available for overglaze decalcomania are somewhat greater than in underglaze decoration. Recently, the advent of in-glaze decals, in which the decal is applied over but fired into the glaze, have provided increased flexibility for decoration of U.S. dinnerware.

One-Fire China

A manufacturing process in which the body and the glaze are matured at the same time and the same temperature finds application in the manufacture of cooking and baking ware. Here, the green ware is glazed and the body and glaze fired at Cone 12–13 (1310° to 1320°C). There are problems associated with this procedure. There can be little support of the shapes during firing, except for an unglazed foot or base. The higher firing temperature necessary to mature the body restricts the range of colors available in the glaze. Underglaze decoration, except for engobes, is difficult. However, the higher fire eliminates the use of lead-containing compounds in the glaze and minimizes the use of other fluxing agents. Development of the glaze and body in this one-fire operation yields a very strong, hard, and abrasion- and chip-resistant shape. Overglaze or in-glaze decorations may be applied to the ware.

Heavy Metals in Glazes

It has long been the practice to use lead-containing compounds in dinnerware glazes. The presence of these compounds gives a brilliant, hard, durable glaze when properly fired on the dinnerware. However, if the glaze is not properly matured, there can be problems with solubility of lead in the glaze in food acids. The first reported incidence of lead poisoning occurred in the United States in 1960.[12] To prevent repetition of such an occurrence, agencies in the United States and in other parts of the world began research programs to identify and control lead and cadmium release from ceramic foodware. The U.S. Food and Drug Admin-

istration (USFDA), ASTM, and others worked with and through the World Health Organization, starting in 1974, to develop standards[13] and testing procedures[14] concerning lead and cadmium release from foodware surfaces. As a result of this two-decade activity in research and development of the stability of lead and cadmium ions in glasses and glazes, manufacturers have developed better procedures and greater understanding of the problem.

The USFDA has established release standards (using a 4% acetic acid leachant for 24 hours)[14] as follows:

Type of Ceramic Ware	*Unit*	*Lead*	*Cadmium*
Flatware	ppm	7.0	0.5
Small hollow-ware	ppm	5.0	0.5
Large hollow-ware	ppm	2.5	0.25

The U.S. manufacturers of dinnerware, and most of the developed countries of the world, have subscribed to the World Health Organization and USFDA standards for heavy-metal release. Their quality control and evaluation of their fired glazes by independent laboratories assure the user of safe ware. However, some of the developing nations, including Mexico, the People's Republic of China, Taiwan, and others, are negligent in their control of glazing and firing, and imported ware which violates the USCFDA limits, but which may be imported undetected, threatens the health of the using public. Vigilance in using ware from such nations is necessary if the resultant health hazards are to be avoided.

References

[1]R. J. Beals, "Manufatura de louca de mesa los estados unidos," *Ceramica*, **29** [166] 259–69 (1983).

[2]R. J. Beals, "Dinnerware"; pp. 1195–99 in Encyclopedia of Materials Science and Engineering, Pergamon, New York, 1986.

[3]"Standard Test Method for Water Absorption, Bulk Density, Apparent Porosity and Apparent Specific Gravity of Fired Whiteware Products," ASTM Standard C373.

[4]W. C. Gates, Jr., The City of Hills and Kilns. East Liverpool Historical Society, East Liverpool, Ohio, 1984; p. 76.

[5]R. L. Smyth and R. S. Weightman, The International Ceramic Tableware Industry. Croom Helm, London, 1984; p. 123.

[6]"Summary of Trade and Tariff Information, Ceramic Table and Kitchen Articles," USITC Publ. 841, Control No. 5-2-6, November 1981.

[7]"Summary of Trade and Tariff Information, Ceramic Table and Kitchen Articles," Control No. 5-2-6 (Supplement), February 1984.

[8]R. J. Beals, "Manufacture and Importation of Ceramic Tableware in the U.S.," *Am. Ceram. Soc. Bull.*, **64** [1] 47–50 (1985).

[9]"Certain Ceramic Kitchenware and Tableware from the People's Republic of China," USITC Publ. 1979, August 1982.

[10]"Giants in Whiteware," *Ceram. Ind.*, **129** [2] 47 (1987).

[11]C. R. Austin, H. E. Schofield, and N. L. Haldy, "Alumina in Whiteware," *J. Am. Ceram. Soc.*, **29** [12] 341–54 (1946).

[12]J. S. Nordyke, Lead in the World of Ceramics. The American Ceramic Society, Columbus, Ohio, 1984.

[13]International Standard ISO 6486/1, "Ceramic Ware in Contact with Food—Release of Lead and Cadmium—Part 1: Method of Test; Part 2: Permissible Limits," 1981.

[14]"Lead and Cadmium Extracted from Glazed Ceramic Surfaces," ASTM Standard C738.

Advanced Ceramics Involving Alumina

John B. Wachtman, Jr. and Richard A. Haber
Rutgers, The State University of New Jersey
Piscataway, NJ 08854

An excellent summary of the properties of existing alumina ceramics was published recently by Dorre and Hubner. In the present paper we shall therefore discuss trends in the development of alumina ceramics, especially trends in the processing methods which promise to produce alumina ceramics with improved properties. In some cases (such as whisker-reinforced alumina cutting tools) the new materials are already on the market; in others the new materials are still in the research and development stage.

Several trends are apparent in the continuing development of advanced ceramics involving alumina. They include (1) improvements in the mechanical properties of alumina ceramics closely related to conventional whitewares through improved microstructure and composition; (2) transformation toughening of alumina ceramics to give high strength combined with high toughness; (3) use of submicrometer powders to alter sintering kinetics and to produce very fine-grained bodies; (4) development of a novel process to produce alumina composites by direct oxidation of molten aluminum; (5) development of fiber-reinforced alumina ceramics with very good mechanical properties; (6) development of partially sintered microporous alumina ceramics for applications such as filtration; and (7) application of combinations of such advances to produce advanced alumina ceramics for such applications as cutting tools, wear parts, electronic substrates, sensors, filters, etc.

Transformation-Toughened Alumina

The properties of transformation-toughened ceramics, including alumina, were reviewed recently by Cannon[2] and the papers from the Transformation Toughening Workshop in Lorne, Australia in 1985 have been published.[3]

Zirconia has three polymorphic forms, cubic, tetragonal, and monoclinic, whose stability is governed by either temperature or a stabilizing agent. For instance, the stable room-temperature form for pure zirconia is monoclinic, while its high-temperature stable form is tetragonal. The transformation from the high-temperature tetragonal to room-temperature monoclinic phase is inhibited by constraining the low-modulus zirconia in a high-modulus matrix such as alumina. When the tetragonal form is constrained it is subject to stress-induced transformation toughening. In the enhanced stress field near the crack tip, the tetragonal zirconia particles become unstable and transform to their stable monoclinic form by way of a martensitic or diffusionless transformation. This is accompanied by a volume increase of approximately 3 to 5% and a shear strain of approximately 8% at the unit cell level. Together, these qualities produce residual strains which allow the rapid, localized buildup of significant compressive stresses in response to the stress field associated with the propagating crack front.

McMeeking and Evans[4] showed that this phenomenon would result in an increase in fracture toughness which could be described by:

$$\Delta K^T = (0.22/1 - \nu)Ee^T h^{-1/2} \quad (1)$$

where E is the elastic modulus, e^T the transformation strain arising from the volume increase, and h the transformation zone width.

Claussen[5] found that, for hot-pressed mixtures of alumina and zirconia powders, toughness values as high as 10 MPa • $m^{1/2}$, combined with fracture strengths of 470 MPa, were obtained.

Becker[6] demonstrated that a large improvement in thermal shock behavior for a similar material could result. In addition, it was observed that a 10 vol% addition of zirconia to alumina resulted in peak toughness values, while a peak in strength was found at slightly higher zirconia content, around 12 vol%. Quenching into 100°C water caused no strength deterioration up to temperatures of 800°C, as opposed to a beginning of strength deterioration at 200°C quenching temperature for alumina without zirconia.

Details of the behavior of different mechanical properties depend in complex ways on the amount of zirconia, which includes the amount of each phase and the size and distribution of the particles. These in turn depend in complex ways on the processing.[7,8]

The good mechanical properties of transformation-toughened alumina are comparable to those of transformation-toughened zirconia. The lower cost of the alumina powder and lower firing temperatures associated with alumina make it attractive, but the need to hot-press increases the cost. Wilfinger and Cannon[9] reported success with slip casting and pressureless sintering of transformation-toughened alumina. Strength values of 850 MPa were achieved with 10 vol% zirconia additions.

Traditional Whiteware Alumina Ceramics

Alumina has been used successfully in traditional ceramic compositions for many years. Floyd et al.[10] showed that the addition of 30 wt% alpha alumina to a whiteware body could increase the flexural strength of the body by 80%, from 170 to 310 MPa. While increases of this magnitude were significant for whiteware bodies, there were significant disadvantages to the composition of these materials for advanced applications. These disadvantages specifically focused on the high alkali content, sodium and potassium, associated with the flux additions, for example, feldspar or nephaline syenite, to the body.

As the performance requirements for higher-alumina ceramics increased, the composition changed. From being primarily a mullite, alkali-containing glass matrix with small amounts of alumina additions, the higher-alumina bodies changed to skeletons of alumina particles with interstitial, low-alkali, high-alumina glass and possibly minor secondary crystals such as mullite. Although the composition of the glassy phase varies among manufacturers, it is most commonly a calcium or magnesium aluminosilicate occasionally containing minor additions of chromium, cobalt, and manganese.[11]

Table I shows the electrical and physical properties of seven commercially produced alumina ceramics, noted by their alumina content. These compositions include additions of kaolin, talc, $MnCO_3$, and/or flint to make up the remainder of the compositions. When possible, it is desirable to use additions of clay or talc to promote plasticity in the green body. When this is not possible, plasticizers and lubricants must be added, stemming from the nonplastic and abrasive character of the alumina grain.[12]

In a modification of the common wet mix-press-fire processing of alumina, Smoke[13] and Smoke and Snyder[14] found that strength and microstructure could be improved by using an initial prereaction step prior to final firing. It was found that, for a prereacted 90% alumina, 6% clay, and 4% talc body, strengths of 50% (420 versus 276 MPa) greater than typically prepared wet mix-press bodies were obtained for the same composition. This was attributed to an increase in bulk density and a more uniform microstructure that resulted from prereacting the materials.

The prereaction technique entailed mixing and pelletizing the batch, followed by an initial firing. During this firing the compact was partially sintered and the additional ingredients allowed to react. Once fired, the pellets were ground to a predetermined particle-size distribution, dried, slip cast or pressed, and fired again. This technique has permitted large shapes such as radomes to be produced by slip casting without affecting the initial alumina grain size, which is critical for fired properties such as strength and fracture toughness.

Glass-Bonded Alumina Composites

The mechanical properties of alumina ceramics have been examined and modeled in a vast number of investigations. In these studies a variety of individual microstructural features have been attributed to increases and decreases in mechanical properties, in

Table I. Properties of Selected High-Alumina Ceramics

Property	Alumina Content (%)						
	79*	85†	88*	90†	94†	95*	96†
Type of body	Alumina-mullite	Alumina	Alumina	Alumina	Alumina	Alumina	Alumina
Color	White	White	White	Black	White	Brown	White
Specific gravity	3.33	3.41	3.61	3.69	3.62	3.88	3.72
Water absorption	None	None	None	None	None	None	None
Linear coefficient of thermal expansion/°C							
$\times 10^{-6}$ 25–100°C	4.40	5.3	5.33	6.4	6.3	3.60	6.0
$\times 10^{-6}$ 25–400°C	5.72	6.2	6.85	7.3	7.1	6.11	7.4
$\times 10^{-6}$ 25–700°C	6.42	6.9	7.42	8.0	7.6	7.29	8.0
Coefficient of thermal conductivity, cal/s/cm²/°C	0.0095	0.035	0.0144	0.030	0.043	0.0180	0.059
Tensile strength (MPa)	73	155	91	228	193	107	193
Compressive strength (MPa)	826	1930	995	2413	2103	1288	2068
Flexural strength (MPa)	192	296	199	365	352	248	358
Dielectric strength (v/mil)	200	240	203	135	220	202	210
Dielectric constant (1 MHz)	7.0	8.2	8.4	9.8	8.9	9.2	9.0
Power factor (1 MHz)	0.0014	0.0009	0.00086	0.0200	0.001	0.00035	0.0011
Loss factor (1 MHz)	0.010	0.007	0.007	0.200	0.004	0.003	0.001

*Values taken from Frenchtown Ceramics Co., Frenchtown, NJ.
†Values taken from Coors Porcelain Co., Golden, CO.

particular, strength, fracture toughness, and elastic modulus. The specific interactions discussed will be those associated with the physical configuration of the microstructure, i.e., thermal expansion mismatch, grain size, and volume fraction of glassy phase, and those associated with chemical interactions between the phases, i.e., relative reactivity between phases. Borom[15] provides an excellent overview of these studies for this system.

The effect of residual glass content on the mechanical properties of alumina ceramics has been well documented. Hasselman and Fulrath[16,17] postulated that the strength of an alumina-glass composite is governed by the size of the critical flaw, which is in turn governed by the particle spacing and volume fraction. They concluded that, at high volume fractions of glass, the average flaw size was statistically reduced independent of the size of the dispersed phase, whereas at low volume fractions of glass the average flaw size of an alumina-glass ceramic was governed by the average distance between particles dispersed in the matrix. Observed strengths for alumina-glass composites were generally two to three times less in magnitude than theoretical strength, which was attributed to structural flaws which acted as sources of weakness.

Lange[18,19] examined the fracture strength of a similar system as a function of both volume fraction and alumina particle size. He found that the larger particles strongly influenced the increase in composite fracture energy. He cited increases in fracture energy for a 10 vol% addition of alumina to glass of 10 600 to 15 600 ergs/cm for a 3.5 and 44 μm alumina, respectively. However, he disagreed with Hasselman and Fulrath,[16,17] stating that particulates increased rather than limited flaw size, e.g., approximately 1 to 3 times the average particle size of the alumina. Thus, increases in fracture strength could be attributed to a balance between an increase in the composite fracture energy and an increase in crack size.

Frey and Mackenzie[20] studied the effect of differences in elastic modulus to determine their effect on strength for alumina and zirconia-glass composites. They found that, in addition to residual stresses occurring because of differences in thermal expansion, differences in elastic constants between the inclusion and matrix resulted in stress concentrations related to the applied stress.

Nicholson[21] found that a large difference in elastic constants was desirable to enhance composite strength if the elastic modulus of the inclusion was greater than that of the matrix; for example, alumina inclusions with a higher modulus than the matrix would increase strength, while a pore with lower modulus than the matrix would decrease strength.

Miyata and Jinno[22] hypothesized that the fracture mechanism involved in alumina-glass systems was a direct result of differences in elastic modulus. They stated that fracture occurs due to crack nucleation and crack propagation around the dispersed alumina particles. At lower volume fractions of particulate, macroscopic fracture occurred as a result of the growth of the microcracks originating near the inclusion. At higher volume fractions, where further crack propagation is prohibited by the higher-modulus alumina particulate, the process of crack propagation around (or deflection) is probably the overriding mechanism. In this case strength would be an increasing function of volume fraction.

Fulrath[23] and Davidge and Green[24] examined the significance of thermomechanical stresses evolving from differences in thermal expansion between the glassy phase and alumina. They described how differences in the coefficient of thermal expansion between the matrix glass and alumina produced residual stresses on cooling of the ceramic. Utilizing the expression derived by Selsing,[25] which was derived for an isotropic linear elastic continuum containing inclusions. they showed how a spherical particulate inclusion will be subjected to a pressure p. This pressure could be described as

$$P = \Delta\alpha\Delta T[(1 + \nu_m)/2E_m + (1 - 2\nu_p)/E_p]^{-1} \quad (2)$$

where $\Delta\alpha$ is the thermal expansion difference, ΔT the temperature drop from the set point to ambient, ν the Poisson ration, and E Young's modulus. Subsequently the stresses exerted by this inclusion could be expressed as $\sigma = PR^3/r^3$ and $-PR^3/r^3$ for radial and tangential stresses, respectively, where R is the radius of the inclusion and r is the distance from the center of the particle to a point in the matrix. Experimentally it was found that, if the expansion of the matrix was significantly higher than that of the inclusion, radial cracking occurred, whereas if the expansion of the matrix was significantly lower than that of the inclusion, tangential cracking occurred. In either case a lowering in the composite strength was observed. There was no noticeable change in strength when the difference in thermal expansion between the particle and matrix was small or negligible. They concluded that differences in thermal expansion coefficient detrimentally affected strength.

Borom[15] showed how the stresses surrounding particles diminished as the distance from the matrix-inclusion interface increased. This produced a state of variable compressive stress throughout the matrix which opposed crack propagation.

Haber[26] studied a number of microstructural variations concurrently for the alumina-glass system. In these studies a series of glasses with higher, lower, and similar thermal expansion coefficients to alumina was examined as a function of volume fraction. In this case it was reported that, for 90% alumina, 10% borosilicate glass having initially a similar thermal expansion, composite strengths in excess of 722 MPa were observed. It was shown that a sharp change in expansion, either higher or lower, at the particle-matrix interface would cause spontaneous microcracking and lower

total composite strength. However, a graded thermal expansion interface could be produced by prereacting alumina and glass where there was dissolution of alumina into the glass, creating a matrix glass of variable composition ultimately leading to an enhancement in strength. Table II shows the strength as a function of weight percent of alumina for three matrix glasses, similar in composition but varying in thermal expansion coefficient. In addition, it was observed that there existed a critical loading of glass, approximately 75% alumina, after which complete densification was achieved and residual porosity became quite evident.

Table II. Transverse Strength of Alumina-Glass Composites*

	Flexural Strength (MPa)		
Alumina (wt%)	Glass 1 (−4.35)	Glass 2 (+0.50)	Glass 3 (+4.65)
95	420	620	722
90	413	722	653
85		578	460
80	372	543	474
75	248	268	295
70	275	302	294
60	275	247	
50	237	144	179

*Ref. 25.
( ) Denotes differences in coefficient of thermal expansion between the alumina and the matrix glass, values in 10^{-6}cm/cm • °C.

Alumina Composites Made by Direct Oxidation of Aluminum

A new process for making alumina-aluminum composites has been patented under the tradename of Lanxide.* This process involves the direct oxidation of molten aluminum alloyed with one or more dopants under controlled conditions of temperature and atmosphere ($T < 1200$°C). During the process the molten metal alloy will react with the environment to form a ceramic oxide product. This oxide product is then grown continuously as molten metal is fed through channels which form in the product toward the reactive environment.

The volume fraction of the residual metal and ceramic, the scale of the microstructure, the porosity, and the degree of interconnectivity of the respective phases in the composite depend on the processing conditions chosen. The ceramic phase is usually interconnected in all three dimensions and, in the case of alumina, is high purity with little or no glass at the grain boundaries. The degree of interconnectivity of the metal can be varied from isolated to continuous.

Successful growth has been reported[27] from aluminum melts containing 3 wt% Si combined with 1 to 10 wt% Mg. The process produces Al_2O_3 in the corundum phase in a columnar growth morphology. The orientation is nearly constant within each column, although there is a substructure involving crystallites with a spread in orientation of approximately five degrees. Materials can be grown at lower temperatures and carried to high specific weight gains and a high degree of oxidation of the aluminum, developing a microstructure of porous alumina with interconnected porosity.

Composites up to 10 cm thick and 18 kg in weight have been demonstrated. The process is said to be capable of producing a wide variety of shapes and sizes in alumina and other ceramics with the appropriate metal. For alumina/aluminum composites, resistivity values from less than 1 to more than 10^{11} Ω • cm can be produced.

Urquhart et al.[28] showed that this technology can also be used to produce reinforced alumina/aluminum composites. Composites reinforced with SiC particulate have exhibited flexural strengths of 480 MPa and fracture toughness values of 8.0 MPa • $m^{1/2}$. Similar alumina matrix composites filled with 11 vol% Nicalon† SiC fibers have produced composites with room-temperature strengths of 364 MPa and toughness values of 18 MPa • $m^{1/2}$. It should also be emphasized that these materials exhibited good high-temperature mechanical properties. For example, approximately one-half the room-temperature strength was retained at 1500°C.

Fiber-Reinforced Alumina Ceramics

Great interest and activity in the use of fiber-reinforced ceramic-matrix composites has followed the development[29] of high-toughness composites of SiC fibers in glass matrices. For lithium aluminosilicate glass with 50 vol% loading of aligned, continuous SiC fibers, critical stress intensity values of 17 and 25 MPa • $m^{1/2}$ at 22° and 1000°C, respectively, were reported. These measurements were made using notched beams with cracks propagated perpendicular to the aligned fibers.

Care must be taken in interpreting high "toughness" results because the dependence of the critical stress intensity factor on crack length in continuous fiber-reinforced composites can be quite different from that in ceramic particulate microstructures. In fact, the critical stress intensity factor can be independent of crack length for some regimes of behavior associated with matrix cracking without fiber failure.[30] Nevertheless, the high energy absorptions and gradual failure exhibited by these composites make them of great interest and potential. The subject of ceramic matrix fiber-reinforced composites was reviewed recently.[31]

Reinforcement of alumina by continuous, aligned fibers is an area of interest[32,33] but the published work on reinforced alumina has proceeded primarily in a different direction. Chopped whiskers, rather than

*Lanxide Inc., Newark, DE.

†Nippon Carlson Co., Tokyo, Japan.

continuous fibers, have been used for material in commercial application.

SiC whiskers are made by Arco, Los Alamos National Laboratory, and Tateho. For 20 vol% SiC whiskers in alumina, toughness values of 5.1 and 7.8 MPa • $m^{1/2}$ and flexural strength values of 535 and 700 MPa, respectively, have been reported for samples with Tateho and Arco whiskers.[34]

Silicon carbide fiber-reinforced alumina ceramics with substantial improvements in toughness have been developed.[35,36] Samples were made using single-crystal SiC whiskers derived from rice hulls and having an average diameter of 0.6 μm and lengths ranging from 10 to 80 μm. They were mixed with alumina powders with average particle sizes of 0.2 to 0.3 μm. Theoretical density was achieved by hot-pressing at 1850°C under 59 MPa for 45 minutes.

Samples made from the finest alumina powders with no fibers had critical stress intensity values of 4.6 MPa • $m^{1/2}$ as measured by the double cantilever technique. The mechanical properties of the composites were anisotropic. With the crack plane parallel to the hot-pressing direction, the value of K_{Ic} was 8.7 MPa • $m^{1/2}$ but it was 5.4 MPa • $m^{1/2}$ when the crack propagated along a plane perpendicular to the hot-pressing direction. The strength in flexure was 805 MPa at 25° and 520 MPa at 1200°C for the most favorable orientation, i.e., the tensile stress direction perpendicular to and the tensile surface of the test specimen parallel to the hot-pressing direction.

Microporous Alumina Ceramics

Sol-gel techniques for producing ceramics have been reviewed.[36,37] Most of the research has concerned preparation methods and character of the films with relatively little on physical properties. One very interesting property is the very low thermal conductivity obtainable in microporous bodies made by sol-gel techniques. Values of thermal conductivity as low as 2×10^{-3} W/m • K have been obtained in microporous silica gels.[38]

Microporous alumina should have very low thermal conductivity values and should be usable below its sintering temperature. Attempts to make bulk ceramics by sol-gel techniques are limited by the tendency of the bodies to crack, which worsens as the pore size decreases. Encouraging results with drying control additives have been reported[39] but no apparent physical properties of this material have been reported.

Alumina coatings made by the sol-gel process using aluminum sec-butoxide can be produced with variable surface area and porosity by firing on dense alumina substrates at 700° to 1000°C. These coatings are found to have large (over 100 MPa) compressive stresses and to cause a small but significant strengthening of the substrate. The surface area decreases within this firing range, while both the internal stress and strengthening effect increase with increasing firing temperature.

Dense coatings have long been used to enhance the properties of materials. Increased wear and thermal shock resistance, greater hardness and strength, and resistance to chemical or other environmental attack have caused increased usage of coatings in applications such as engine components, cutting tools, electronic components, and optical components. Porous plasma-sprayed coatings have been used for thermal protection of metals, i.e., to reduce the surface temperature.[40]

High porosity is desirable to give good thermal protection but other desirable properties, including mechanical properties, are usually degraded by increased porosity such that a trade-off is involved. Optimum material design requires better knowledge of the dependence of properties on the amount and character of the porosity. Photon conductivity becomes important at high temperatures. A decrease in pore size should give lower conductivity, in contrast to

Table III. Properties of Single- and Multidipped Porous Alumina Coatings on Alumina Substrates as a Function of Firing Temperature*

Property	1× Dip (700°C)	1× Dip (800°C)	1× Dip (900°C)	1× Dip (1000°C)	1× Dip (700°C)	1× Dip (800°C)	1× Dip (900°C)	1× Dip (1000°C)
Thickness (μm)	1.89	2.11	1.98	1.79	4.41	4.39	4.24	4.20
Surface area (m^2/g)	125	102	96	82	131	109	101	76
†Stress (MPa)	113	110	149	176	106	116	129	189
‡Strength (MPa)								
no indent	318	338	348	356	323	314	353	364
1 kg indent	281	288	310	336	312	320	332	339
3 kg indent	220	236	236	250	228	216	263	245
§Coefficient of friction	0.23	0.09	0.15	0.15	0.61	0.10	0.13	0.14

*Ref. 57.
†Stress measurement based in technique of Lawn and Fuller (Ref. 58). Technique relates internal stress to behavior of indentation fracture. All coatings were observed to have compressive stresses.
‡Strength of an uncoated sample was found to be 308 MPa.
§Friction determination was made using a stainless 0.5 cm steel ball under a 105 g load. Reciprocating tester was used, measurement taken for a single pass.

phonon conductivity which should be pore-size-independent for a given total pore volume.[41] The microporous character of oxide coatings made by the sol-gel process makes them interesting candidate materials for thermal protection.

The basic aspects of preparation of inorganic gels and their use as coatings has been reviewed extensively.[42,43] Methods for preparing aluminum hydrous oxide sols[44] and a process for making transparent alumina coatings[45–48] have been developed. These reports concern processing, structure, and selected properties, especially optical properties.

Phase changes, sintering, and microstructure developments in similar alumina coatings have been studied by several researchers[49–54] and a few studies of processing of composite coatings involving alumina have appeared.[55,56] The thermal and mechanical properties of alumina coatings made by sol-gel techniques have not been extensively studied, however. Results on some physical properties of alumina coatings made by the Yoldas et al. process were reported recently.[57] Table III illustrates a number of physical properties for two thicknesses of alumina coatings on alumina substrates.

References

[1]E. Dorre and H. Hubner, Alumina—Processing Properties, and Applications. Springer-Verlag, New York. 1984.

[2]W. R. Cannon, "Transformation Toughened Ceramics for Structural Applications" in Structural Ceramics. Edited by J. B. Wachtman, Jr. Academic Press; in press.

[3]A. H. Heuer, F. F. Lange, M. V. Swain, and A. G. Evans, "Transformation Toughening: An Overview," *J. Am. Ceram. Soc.*, **69** [3] i-iv (1986).

[4]R. M. McMeeking and A. G. Evans, "Mechanics of Transformation Toughening in Brittle Materials," *J. Am. Ceram. Soc.*, **65** [5] 42–46 (1982).

[5]N. Claussen, "Fracture Toughness of Al_2O_3 with an Unstabilized ZrO_2 Dispersed Phase," *J. Am. Ceram. Soc.*, **59** [1–2] 49–51 (1976).

[6]P. F. Becker, "Transient Thermal Stress Behavior in ZrO_2-Toughened Al_2O_3," *J. Am. Ceram. Soc.*, **64** [1] 37–39 (1981).

[7]S. Hori, M. Yoshimura, and S. Sómiya, "Strength-Toughness Relations in Sintered and Isostatically Hot-Pressed ZrO_2-Toughened Al_2O_3," *J. Am. Ceram. Soc.*, **69** [3] 169–72 (1986).

[8]M. Rühle, N. Claussen, and A. H. Heuer, "Transformation and Microcrack Toughening as Complementary Processes in ZrO_2-Toughened Al_2O_3," *J. Am. Ceram. Soc.*, **69** [3] 195–97 (1986).

[9]K. Wilfinger, and W. R. Cannon; unpublished work.

[10]J. S. Floyd, D. V. Royce, and A. Lippman, Jr., "Alumina Improves Properties of Whiteware Bodies." *Ceram. Ind.*, **4**, 108–39 (1966).

[11]*a*. D. W. Luks, "High Alumina Ceramics," *Mach. Design*, **5**, 54–59 (1954).

b. N. L. Haldy, H. Z. Schofield, and J. D. Sullivan, "High-Alumina Porcelains," *Am. Ceram. Soc. Bull.*, **35** [9] 351–55 (1956).

[12]E. J. Smoke, "Work with Dense Ceramic Bodies," *Ceramic Age*, **69**, 32 (1957).

[13]E. J. Smoke and N. H. Snyder, "Prereacted Raw Materials Technique for Attaining High Quality Ceramics," U.S. Pat. No. 3 360 203, 1967.

[14]M. P. Borom, "Dispersion Strengthened Glass-Matrices, Glass-Ceramics, A Case in Point," *J. Am. Ceram. Soc.*, **60** [1–2] 17–21 (1977).

[15]D. P. H. Hasselman and R. M. Fulrath, "Effects of Alumina Dispersions on Young's Modulus of Glass," *J. Am. Ceram. Soc.*, **48** [4] 218–19 (1965).

[16]D. P. H. Hasselman and R. M. Fulrath, "Micromechanical Stress Concentration in Two-Phase Brittle Matrix Ceramic Composites," *J. Am. Ceram. Soc.*, **50** [8] 399–404 (1967).

[17]F. F. Lange, "Fracture Energy and Strength Behavior of a Sodium Borosilicate Glass-Alumina Composite System," *J. Am. Ceram. Soc.*, **54** [12] 614–24 (1971).

[18]F. F. Lange, "The Interaction of a Crack Front with a Second Phase Dispersion," *Philos. Mag.*, **26**, 1327–44 (1972).

[19]W. J. Frey and J. D. MacKenzie, "Mechanical Properties of Selected Glass-Crystal Composites," *J. Mater. Sci.*, **2**, 124–30 (1967).

[20]P. S. Nicholson, "Crack Paths and the Toughening of Brittle Materials by Second Phase Particles," *High Temp. Sci.*, **13**, 279–97 (1980).

[21]N. Miyata and H. Jinno, "Theoretical Approach to the Fracture of Two-Phase Glass-Crystal Composites," *J. Mater. Sci.*, 7, 973–82 (1972).

[22]R. M. Fulrath, "Internal Stresses in Model Ceramic Systems," *J. Am. Ceram. Soc.*, **42** [9] 123–28 (1959).

[23]R. W. Davidge and T. J. Green, "The Strength of Two Phase Ceramic/Glass Materials," *J. Mater. Sci.*, **3** 629–34 (1968).

[24]J. Selsing "Internal Stresses in Ceramics," *J. Am. Ceram. Soc.*, **44** [8] 419–23 (1961).

[25]R. A. Haber, "The Effect of Controlled Glass Additions on the Strength of High Alumina Ceramics"; Ph.D. Thesis, Rutgers University, 1984.

[26]M. S. Newkirk, A. W. Urquhart, H. R. Zwicker, and E. Breval, "Formation of Lanxide® Ceramic Composite Materials," *J. Mater. Res.*, **1** [1] 81–89 (1986).

[27]A. W. Urquhart, M. S. Newkirk, D. R. White, H. D. Lesher, and C. R. Kennedy, "Fabrication of Ceramic Matrix Composites by Direct Oxidation of Molten Metals," *Am. Ceram. Soc. Bull.*, **66** [3] 550 (1987).

[28]K. M. Prewo and J. J. Brennan, "High-Strength Silicon Carbide Fiber-Reinforced Glass-Matrix Composites," *J. Mater. Sci.*, **15** [2] 463–68 (1980).

[29]D. C. Marshall, B. N. Cox, and A. G. Evans; unpublished work.

[30]R. L. Lehman, Ceramic Matrix Fiber Composites in Structural Ceramics. Edited by J. B. Wachtman, Jr. Academic Press, New York, 1987.

[31]J. J. Lanutti and D. E. Clark, "Sol-Gel Derived Ceramic-Ceramic Composites Using Short Fibers"; pp. 369–74 in Better Ceramics Through Chemistry. Materials Research Society Symposia Proceedings, Vol. 32, 1984.

[32]J. J. Lanutti and D. E. Clark, "Long Fiber Reinforced Sol-Gel Al_2O_3 Composites"; pp. 375–81 in Better Ceramics Through Chemistry. Materials Research Society Symposia Proceedings, Vol. 32, 1984.

[33]T. N. Tiegs, P. F. Becher, J. W. Geer, and W. H. Warwick, "Dispersion Toughened Oxide Composites," Progress Report to DOE Office of Transportation Systems, February–March 1986.

[34]P. F. Becker and C. Wei, "Toughening Behavior in SiC-Whisker-Reinforced Alumina," *J. Am. Ceram. Soc.*, **67** [12] C-267–C-269 (1984).

[35]G. C. Wei and P. F. Becher, "Development of SiC-Whisker-Reinforced Ceramics," *Am. Ceram. Soc. Bull.*, **64** [2] 298–304 (1985).

[36]L. C. Klein, "Sol-Gel Technology: A Review," *Glass Ind.*, **14** [1] (1981).

[37]L. C. Klein, Sol-Gel Technology: Processing Glassy Films, Fibers and Shapes, Noyes Publications, Park Ridge, NJ, 1986.

[38]J. Fricke, "Thermal Insulation Materials from the Sol-Gel Process," in Sol-Gel Technology: Processing Glassy Films, Fibers and Shapes. Edited by L. C. Klein. Noyes Publications, Park Ridge, NJ, 1986.

[39]J. J. Lanutti and D. E. Clark, 8th Annual Conference on Composites and Advanced Ceramic Materials Jan. 15-18, 1984, Cocoa Beach, FL.

[40]P. A. Siemers and L. Mehan, *Ceram. Eng. Sci. Proc.*, **4** [5–6] 828 (1983).

[41]W. D. Kingery, H. K. Bowen, and D. R. Uhlmann; p. 638 in Introduction to Ceramics 2d ed. Wiley & Sons, New York, 1975.

[42]S. J. Teichner, G. A. Nicolaon, M. A. Vicarini, and G.E.E. Gardes, *Adv. Colloid Interface Sci.*, **5**, 245 (1976).

[43]H. Dislich, "Glassy and Crystalline Systems from Gels: Chemical Basis and Technical Application," *J. Non-Cryst. Solids*, **57**, 371–88 (1983).

[44]D. L. Catone and E. Matijevic, *J. Colloid. Interface Sci.*, **48**, 291 (1974).

[45]B. E. Yoldas, "Alumina Sol Preparation from Alkoxides," *Am. Ceram. Soc. Bull.*, **54** [3] 286–88 (1975).

[46]B. E. Yoldas, "Deposition and Properties of Optical Oxide Coatings from Polymerized Solution," *Appl. Opt.*, **21**, 2960 (1982).

[47]B. E. Yoldas, "Effect of Variations in Polymerized Oxides on Sintering and Crystalline Transformations," *J. Am. Ceram. Soc.*, **65** [8] 387–93 (1982).

[48]B. E. Yoldas, "Alumina Gels That Form Porous Transparent Al_2O_3," *J. Mater. Sci.*, **10**, 1856–60 (1975).

[49]L. J. Nikolic, J. E. Bailey, and M. M. Ristic; p. 168 in Sintering-Theory and Practice, Elsevier, Amsterdam, 1982.

[50]J. M. Zivkovic and M. M. Ristic; p. 257 in Sintering Theory and Practice. Elsevier, Amsterdam, 1982.

[51]A. C. Pierre and D. R. Uhlmann, "Super-Amorphous Alu mina Gels," *Mater. Res. Soc. Symp. Proc.*, **32**, 119 (1982).

[52]B. I. Lee and L. L. Hench, "Effect of Aging on Electroph retic Behavior of Sol-Gel Derived Aluminas," *Mater. Res. Soc Symp. Proc.*, **32**, 307–12 (1984).

[53]F. W. Dynys, M. Ljungberg, and J. W. Halloran, "Micr structural Transformations in Alumina Gels," *Mater. Res. Soc Symp. Proc.*, **32**, 321–26 (1984).

[54]M. Kumagai and G. L. Messing. "Controlled Transforma tion and Sintering of a Boehmite Sol-Gel by α-Alumina Seeding," *J Am. Ceram. Soc.*, **68** [9] 500–505 (1985).

[55]J. Martinsen, R. A. Figat, and M. W. Shafer, "Preparation o Thin Composite Coatings by Sol-Gel Techniques," *Mater. Res Soc. Symp. Proc.*, **32**, 145–50 (1984).

[56]D. W. Hoffman, R. Roy, and S. Komarneni, "Diphasi Xerogels, A New Class of Materials: Phases in the Systen Al_2O_3-SiO_2," *J. Am. Ceram. Soc.*, **67** [7] 468–71 (1984).

[57]M. F. Gruninger, B. F. Lawn, E. N. Farabaugh, and J. B Wachtman, Jr., "Measurement of Residual Stresses in Coatings o Brittle Substrates by Indentation Fracture," *J. Am. Ceram. Soc.*, 7 [5] 344–48 (1987).

[58]E. R. Fuller, B. R. Lawn, and R. F. Cook, "Theory o Fatigue for Brittle Flaws Originating from Residual Stress Concen trations," *J. Am. Ceram. Soc.*, **66** [5] 314–21 (1983).

Alumina as a Biomedical Material

John W. Boretos
National Institutes of Health
Biomedical Engineering and Instrumentation Branch
Bethesda, Maryland 20892

Surgical implants depend on an array of properties for success. Almost every class of man-made material has been investigated for use in the body. Only within the past decade has medical science realized the promise that is offered by ceramics. Devices such as artificial heart valves, dental implants, tissue augmentation implants, and prosthetic knees and hips are relying on ceramics to resolve design problems. Alumina has been at the forefront of this effort. Successful performance with thousands of patients suggests continued use of alumina with possible new areas of treatment envisioned.

Ceramics for medical use have come into prominance within the past decade. Prior to that time, little interest was shown for these materials, possibly because they were considered too brittle for most applications. A bone plate or an orthopedic hip must, by necessity, be fracture-resistant. Consequently, metals and plastics dominated the field. Imaginative researchers realized that specific ceramics and composites possessed unique combinations of properties not often found in a single material. Some forms possess chemical structures similar to that of natural bone. One of the first areas that has met with wide acceptance is the use of pyrolytic carbon in artificial heart valves.[1] Their inertness and great wear resistance have extended the lives of literally tens of thousands of patients with heart disease. With the discovery that bone tissue would grow into ceramics, such as alumina,[2] hydroxylapatite,[3] tricalcium phosphate,[4] and others, if they possessed appropriate porosity, new uses were devised.

One of the most promising is the possibility of implanting an artificial hip or tooth implant coated with a porous ceramic material that would achieve permanent fixation through bone in-growth without the need for the usual polymethylmethacrylate cement. This is of particular advantage since the polymer cement can fail in some cases. Alveolar bone ridges can now be reconstructed in shape and height so that dentures may be worn comfortably.[5] Composites of ceramics and polymers are opening whole new opportunities for tissue augmentation and bone reconstruction.[6] Alumina has played a major role in all of this development and will continue to do so. This paper will review the impact that this otherwise commonplace material has made on medical science.

Alumina A Bioceramic

The total volume of alumina consumed worldwide for medical implant construction is miniscule compared to the total annual production. To achieve physiological inertness, only 99.9% pure grade is used. Fabrication techniques must be exacting, with absolute control over physical properties and physical form. Special applications require special characteristics. Depending on how it is processed, alumina can be made porous, monocrystalline, or multicrystalline. Where the high-density single-crystal forms are required, aluminum oxide powder is compressed under isostatic pressure and fired at 1500° to 1700°C. Table I shows typical mechanical properties of single-crystal alumina.

Chemical polishing using molten fluxes hardens the surface, increasing its resistance to wear and lowering its coefficient of friction. These are essential traits for devices such as artificial knees and hip joints where spherical gliding contact under heavy load is involved.

Total Hip Prostheses

Total hip replacement systems are indicated for treatment of the natural femoral-pelvic (hip) joints in patients who can no longer function adequately due to pain, decreased range of motion, and/or destruction or abnormality of the joint structures. The symptoms can be caused by several conditions, including osteoarthritis, rheumatoid arthritis, post-traumatic arthritis, avascular necrosis, trauma, osteomyelitis, and fracture-dislocation. A hip prosthesis can consist of an alumina femoral head (ball) which articulates with an alumina acetabulum (cup) (Fig. 1). The stem is inserted into the head of the femur, whereas the cup is fixed into the hip socket. With every movement of the leg, and every step that is taken over a recipient's lifetime, the two

Table I. Physical Properties of Alumina*

Property	Value
Density, g/cm^3	3.97
Hardness, Mohs	9
Flexural strength	
MPa	900
psi	130 500
Modulus of elasticity	
MPa	390 000
psi	56 550 000

*Single-crystal sapphire form (Ref. 7).

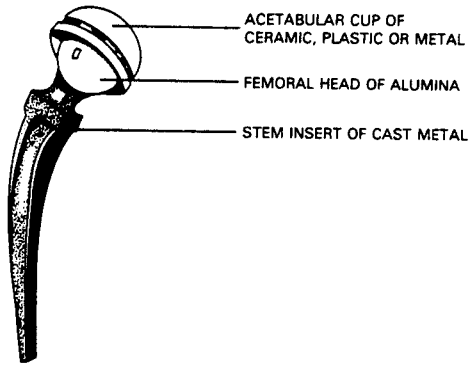

Fig. 1.

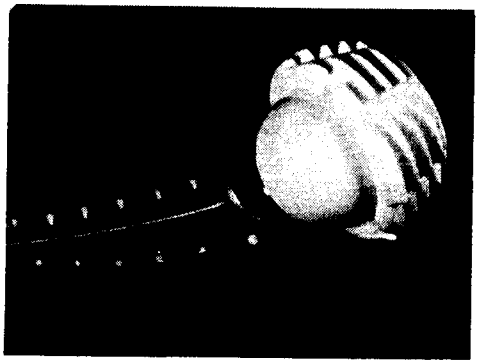

Fig. 2.

surfaces are stressing each other. Fortunately, the single-crystal sapphire type now being used exhibits an order of magnitude greater wear resistance than has been seen by previous combinations of materials, such as metal-to-polyethylene.[8] The coefficient of static friction is also lower between alumina and polyethylene than it is between polyethylene and metal (see Table II).

Perhaps the inert characteristic of alumina is equally responsible for its surgical acceptance. Alumina is corrosion-resistant, since it exists in the highest oxidation state that aluminum metal can possess, and has the potential for microstructural control of the interface without formation of toxic corrosion products. This may also explain why its porous and nonporous forms are so predisposed for cement-free anchorage to bone. Figure 2 shows a commercially available hip prosthesis with mating surfaces made from alumina. Thousands of these units have been implanted by European doctors.

Until recently, most hip prostheses were cemented in place with polymethylmethacrylate. However, this method of fixation is being challenged by the principle of stabilization through tissue in-growth (i.e., bone attachment) into porous alumina surfaces. Hulbert et al.[10] showed that, by controlling the porosity of alumina to within a 75 to 100 μm pore size, connective tissue infiltration with initiation of bone growth into the ceramic would occur. Bone was found to penetrate to depths of 100 μm. Unfortunately, for patients who may be undergoing chemical and radiation therapy, bone in-growth into the ceramic can be severely inhibited; Szycher and associates[11] reviewed the tissue in-growth phenomena with most of the applicable porous materials.

Table II. Coefficient of Friction for Various Artificial Hip Materials*

Material	Coefficient of Friction, Static†
UHMW-PE:‡/titanium alloy	0.180
UHMW-PE/CoCrMo	0.137
UHMW-PE/Al_2O_3	0.100

*Ref. 9.
†Pin and disk method.
‡Ultrahigh molecular weight polyethylene.

Dental Implants

Single-crystal alumina exhibits an elastic modulus 20 times greater than that of cortical bone but is prone to fracture if sufficient shear forces are imposed. Regardless, when carefully designed and used in the proper circumstances, alumina implants are practical and serviceable. Since tooth implants are short, compact, and require mainly compressive strength, alumina is suitable. Thousands of successful dental implants have been performed over the past 10 years. McKinney and Koth[12] found that the single-crystal dental implant exhibits hard- and soft-tissue biocompatibility when used in the mouth. Clinical experience based on five years of study showed that the material would support fixed dental prostheses and function under the occlusive stresses that normally occur in the oral environment.[13] Ultrastructural evidence showed that an attachment complex between gingival epithelium and alumina exists that is analogous to that seen around natural teeth. This suggests that a viable seal can develop and provide support.[14]

Alumina dental implants are available for all tooth areas. They also serve as anchors for bridges and dentures. Figure 3 shows the various shapes required,

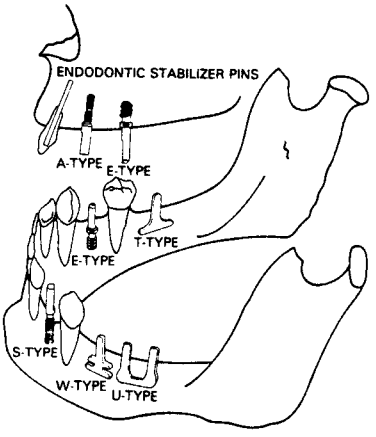

Fig. 3.

depending on their location and function within the mouth. U-type and T-type implants are for edentulous sites and for large interdental spaces. S-type implants must be threaded into alveolar bone and serve for edentulous sites where only a few teeth are missing. Blade-type implants (usually carbon with alumina coating) function similarly to U-type implants and serve as anchors for posterior bridge work. W-type implants are for the posterior region where the jaw is usually narrow. A-type implants are somewhat different in that they have the coronal portion made of polycrystalline alumina and are mainly threaded into anterior bone. For this latter implant, the polycrystalline form of alumina is soft enough to be contoured to match adjacent teeth once the implant has stabilized itself within the bony ridge. Conventional dental machine tools can be used. Figure 4 is a typical A-type tooth implant that uses the single-crystal alumina as the main body with a crown of the multicrystalline form. Figure 5 shows the threaded and nonthreaded varieties. White portions are multicrystalline, whereas clear structures are of the sapphire form.

For a successful outcome, precise fit is essential so that tissue adaptation can occur. To fit an A-type implant, for example, a fissure bur is used to drill a "body" hole to accommodate the prosthetic root. A "washer" bur is then used to make a counterbore that houses the offset at the base of the crown. Finally, a guide tap followed by a bone tap ensures that a tightly threaded union is formed between the bone and the alumina. Experience has shown that, if tight compressive-type opposition is not achieved, the implant will fail. Ceramic cones merely pressed into fresh sockets without a positive fit over the entire surface (not just random point contact) are readily rejected.

Tissue Augmentation

Perhaps the most versatile ceramic material for tissue augmentation is a porous composite of alumina/polytetrafluoroethylene and graphite/polytetrafluoroethylene.[15] The white alumina version has the advantage of color when used near the surface of light-colored skin. This low-modulus and resilient material is available as blocks, sheets, and preformed implants for facial and temporomandibular joint reconstruction, middle ear ossicular replacements, and custom ligament implants. It can be coated onto metal prosthetic parts to serve as a resilient interface between an unyielding surface and bone. This characteristic is said to accommodate micromovements of a device that otherwise might generate pain. The composites are chemically and biologically inert. Pore sizes range from 50 to 400 μm, with interpore connections of approximately 50 μm. The actual surface area is 1200 times the apparent surface area and is easily wetted by cells. These features promote rapid in-growth of tissue and vascularization.[16]

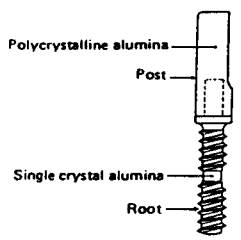

Fig. 4.

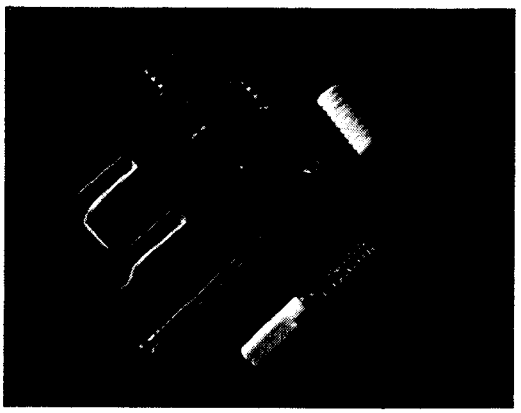

Fig. 5.

Other Applications of Alumina

Spinel ($MgAl_2O_4$), in conjunction with corundum (α-Al_2O_3), is being used to produce porcelain for posterior as well as anterior teeth. These 70% alumina crowns are said to offer a more precise fit than provided for by those previously available since they undergo minimal shrinkage during firing. Durability is improved over past materials used in this application.

Multichannel systems requiring implantable receivers or electronic stimulators and pacers all require protection from the adverse effects of the body's moist environment. Due to the inherent water permeability of most insulating coatings made from plastics and rubber, the length of service for these units is limited before shorting and/or physical breakdown occurs. However, hermetically sealed alumina cases and feedthroughs provide reliable insulation as well as an impermeable barrier to body fluids. Alumina is consequently replacing polymers in some electrical implant applications and is continuing to be explored for others.

Summary

Ceramic materials are at the forefront of medical implant technology. Alumina has contributed to this present posture as much as any other. Hard, wear-resistant, and low-friction surfaces of alumina are now providing for enduring orthopedic and dental implants. Porous forms encourage bone and tissue in-growth for permanent fixation. As experience progresses with this physiologically stable substance, applications will increase and patient health and comfort will benefit.

References

[1]A. Haubald, H. S. Shim, and J. C. Bokros, "Carbon in Medical Devices"; in Biocompatibility of Clinical Implant Materials, Vol. II. Edited by D. E. Williams, CRC Press, Boca Raton, FL, 1981.

[2]S. F. Hulbert, L. L. Hench, D. Forbes, and L. S. Bowman, "History of Bioceramics"; pp. 3–29 in Ceramics in Surgery. Edited by P. Vincenzini, Elsevier, New York, 1983.

[3]M. Jarcho, C. H. Bolen, M. B. Thomas, J. Bobich, J. F. Kay, and R. H. Doremus, "Hydroxylapatite Synthesis and Characterization in Dense Polycrystalline Form," *J. Mater. Sci.* **11**, 2027–35 (1976).

[4]K. de Groot, "Calcium Phosphate Ceramics: Their Current Status"; pp. 477–91 in Contemporary Biomaterials: Material and Host Response, Clinical Applications, New Technology and Legal Aspects. Edited by J. Boretos and M. Eden. Noyes, Park Ridge, NJ, 1984.

[5]J. N. Kent, J. H. Quinn, M. F. Zide, L. R. Guerra and P. J. Boyne, "Alveolar Ridge Augmentation Using Nonresorbable Hydroxylapatite With or Without Autogenous Cancellous Bone," *J. Oral Maxillo. Surg.*, **41** [10] 629–42 (1983).

[6]C. A. Holmsy, "Biocompatibility of Perfluorinated Polymers and Composites of These Polymers"; pp. 59–79 in Biocompatibility of Clinical Implant Materials, Vol. II. Edited by D. F. Williams. CRC Press, Boca Raton, FL, 1982.

[7]Data sheet; Bioceramic Div., Kyocera International, Inc.

[8]P. Griss and G. Heimke, "Biocompatibility of High Density Alumina and its Applications in Orthopedic Surgery"; pp. 155–98 in Biocompatibility of Clinical Implant Materials, Vol. I. Edited by D. F. Williams. CRC Press, Boca Raton, FL, 1982.

[9]K. W. J. Wright, "Clinical and Laboratory Experience with the Use of Titanium and Titanium Type 318 Alloy for Bone and Joint Replacement"; in Biomedical Materials. Edited by J. M. Williams, M. F. Nichols, and W. Zingg. Materials Research Symposium Proceedings, Vol. 55. Pittsburgh, PA, 1986.

[10]S. F. Hulbert, F. A. Young, R. S. Mathews, J. J. Klawitter, C. D. Talbert, and F. H. Stelling, "Potential of Ceramic Materials as Permanently Implantable Skeletal Prostheses," *J. Biomed. Mater. Res.*, **4**, 433–56 (1970).

[11]M. Szycher, B. D. T. Daly, and K. A. Dasse, "Use of Porous Biomaterials for Tissue Ingrowth." pp. 493–522 in Contemporary Biomaterials: Material and Host Response, Clinical Applications, New Technology and Legal Aspects. Edited by J. W. Boretos and M. Eden. Noyes, Park Ridge, NJ, 1984.

[12]R. V. McKinney and D. L. Koth, "The Single-Crystal Sapphire Endosteal Dental Implant: Material Characteristics and 18 Month Experimental Animal Trials," *J. Prosthet. Dent.*, **47**, 69–84 (1982).

[13]R. V. McKinney and J. E. Lemons, The Dental Implant: Clinical and Biological Applications. PSG, Littleton, MA, 1985.

[14]R. V. McKinney, D. E. Steflik, and D. L. Koth, "Evidence for a Junctional Epitheleal Attachment to Ceramic Dental Implants," *J. Peridont.*, **56** [10] 580–91 (1985).

[15]R. L. Westfall, C. A. Homsy, and J. N. Kent, "A Comparison of Porous Composite PTFE/graphite and PTFE/Aluminum Oxide Facial Implants in Primates," *J. Oral Maxillofacial Surg.*, **40**, 771–75 (1982).

[16]Data sheet, Vitek, Inc.

Alumina In Coatings

Lisa A. Ketron*
The American Ceramic Society
Columbus, OH 43081-2821

The hardness, wear resistance, dielectric characteristics, and chemical inertness properties of alumina make it an ideal coating material. Some applications of alumina thin films include cutting tools, optical coatings, refractive coatings, and electrical devices such as capacitors, transistors, and semiconductors. When designing for these devices, a wide variety of methods can be utilized to apply Al_2O_3 coatings which yield the desired material properties.

A coating is defined as a near-surface region with properties that differ significantly from the bulk of the substrate. Significant purposes for coatings are: corrosion resistance against chemical erosion, high-temperature degradation (oxidation or structural stability) protection, mechanical action or abrasion resistance, and prevention of electrical losses (due to lack of insulation). Not only can a coating maintain the integrity of the bulk material, but it can enhance the properties of the bulk by combining the desirable properties of both the film and the coated material.

The hardness, wear resistance, dielectric characteristics, and chemical inertness properties of alumina make it an ideal coating material. Important roles of alumina thin films include cutting tools, optical coatings, refractive coatings, and electrical devices such as capacitors, transistors, and semiconductors. These devices are fabricated using a wide variety of methods.

All coating methods consist of three basic steps: (1) synthesis or generation of the coating species or precursor at the source, (2) transport from the source to the substrate or item to be coated, and (3) nucleation and growth of the coating on the substrate.[1] The scheme selected to classify the deposition processes is founded on the dimensions of the depositing species, for example, atomic (or molecular) deposition, particulate deposition, bulk coating, or surface modification.

Atomistic (Molecular) Deposition

Atomistic (molecular) deposition can transpire in several environments. They include (1) chemical-vapor environment, which takes in chemical vapor deposition (CVD) and spray pyrolysis; (2) plasma environment, encompassing activated reactive evaporation (ARE) and sputter deposition; and (3) vacuum environment, involving ion-beam deposition.

Chemical Vapor Deposition

High-quality alumina coatings can be produced by chemical vapor deposition (CVD).[2] Generally, CVD consists of two parallel processes.[3] The first is largely chemical and involves dissociation of the incoming reactants and their subsequent reaction to solid product, the coating, and gaseous reaction products, which leave the reactor.[3] The second process, which is mainly physical, proceeds simultaneously. This is the process of adsorption, surface diffusion, and nucleation and growth. The various steps of this second process are principally the same as those occurring in physical vapor deposition (PVD).[3] However, the quantitative difference between the two processes becomes very complex and depends on which gas radicals are adsorbed, which immediate products surface-diffuse, and which of the immediate products react to form the final solid product.[3]

Alumina CVD coatings can be prepared by either hydrolysis[2–16] or pyrolysis.[17–21] The hydrolysis case involves reacting an aluminum halide, i.e., $AlCl_3$ or $AlBr_3$,[4] with CO_2-H_2. The $AlCl_3$ is obtained by reacting chlorine (or HCl) with an excess of aluminum chips at 250°C.[2] The $AlCl_3$ vapor stream is then admitted into the CVD reaction chamber through heated tubing to avoid condensation. The $AlCl_3$ mixes with H_2-CO_2 just above the substrates to be coated.

The substrates are heated with a radio frequency (rf) generator, the induction coil being outside the CVD chamber.[2] The hydrolysis of $AlCl_3$ results from the reduction of CO_2 by hydrogen at high temperatures,[2] proceeding according to the generally accepted overall chemical mechanism:

$$H_2(g) + 3CO_2(g) \rightleftarrows 3H_2O(g) + 3CO(g) \quad (1)$$

$$2AlCl_3(g) + 3H_2O(g) \rightleftarrows Al_2O_3(s) + 6HCl(g) \quad (2)$$

$$2AlCl_3(g) + 3H_2(g) + 3CO_2(g) \rightleftarrows Al_2O_3(s) + 3CO(g) + 6HCl(g) \quad (3)$$

It is assumed that, when equilibrium is reached, $AlCl_3$ is quantitatively reacted into Al_2O as long as the initial gas mixture contains enough hydrogen and CO_2 to form the required amount of water.[2] Kinetics have been found to play an important role in CVD of alumina.[2,5] The coating grows from nuclei whose density on the substrate surface has been determined

*Currently affiliated with International Pressure Service, Inc.

by the process conditions. These nuclei grow and finally coalesce to form a continuous coating.

Hydrolysis of $AlBr_3$ also has been used to yield CVD alumina coatings. The decomposition reaction $AlBr_3 + NO + H_2$ takes place in a resistance-heated furnace (at 910°C) with a forming-gas atmosphere.[4] This process is very similar to one developed by Rand[22] for depositing SiO_2 films from $SiBr_4 + NO + H_2$.

Another CVD method for producing alumina coatings onto silicon substrates has been by pyrolysis of organoaluminum compounds such as aluminum triisopropoxide, $Al(OC_3H_7)_3$. The alkoxide vapors are transported to the rf-heated substrates by bubbling helium through the molten alkoxide at 125°C.[19] This gas is subsequently mixed with nitrogen and oxygen at a deposition temperature of approximately 420°C.

The pyrolysis technique also has been used with the compound trimethyl aluminum, which is mixed with nitrous oxide to deposit a film of aluminum oxide via chemical vapor.[23] A high-resistivity aluminum oxide film that is amorphous and can be etched by conventional hydrofluoric acid systems is produced by this method for coating semiconducting devices. This aluminum oxide film is dense, substantially free of pinholes, and covers the surface of the semiconductor material uniformly.[23]

The important question in the production of coatings is which of the parameters are the critical ones in the process.[11] Alumina CVD coatings have been the subject of many investigations. Deposition parameters of importance include temperature,[2,3] pressure,[2,3] initial gas mixture composition, gas flow rate,[2] the nature of the substrate,[2,3] nucleation and growth conditions, and thermodynamic analysis.[5]

Temperature Effects

Deposition rate and film properties such as structure, composition, index of refraction, dielectric strength, and electrical conductivity have been found to be dependent on temperature.[13] The nuclei density (number of nuclei formed per unit area) has been found to be a significant factor in the adherent strength of the alumina coating to a substrate. The nuclei density increases as the deposition temperature decreases.[3,10] Yet nuclei growth[7,13,21] and deposition rate[13] increase with the substrate temperature. Therefore, for the best results a medium temperature (≈1000°C) is desirable.[2] Amorphous, polycrystalline, and epitaxial single-crystal films on the substrate can be obtained by varying substrate temperature.[21] The deposition temperature (temperature of the reaction chamber) also controls the film structure. With electron diffraction patterns, Kamoshida et al.[8] found that films were amorphous at low temperatures (700°C) and polycrystalline at high temperatures (850°C). Silvestri et al.,[13] using low-angle X-ray diffraction, found that the γ-alumina (amorphous) to α-alumina (crystalline) transformation takes place at 900°C. Iida and Tsujide[7] documented a crystalline structural change with increased index of refraction (via ellipsometry) with increased temperature.

Following the deposition process comes the heat-treatment process where once again temperature comes into play.[9] Heat treatments at high temperature cause the alumina coating to crystallize to the α-alumina structure.[7,9] This structural change at high temperatures can lead to a thermal expansion mismatch between the substrate and coating, as seen with silicon and alumina, resulting in a damaged coating.[7,19] Another cause for damage to the coating comes from the etching done by HCl formed by the reaction between hydrogen gas and the chlorine contained in the film when deposited at low temperature.[7] Several examinations of chlorine impurity in CVD alumina coatings have been made via X-ray analysis, MeV He^+ ion backscattering, and X-ray fluorescence, indicating that the $AlCl_3$ does not completely decompose at low temperatures (850°C). In the case of Al_2O_3 coatings on Si substrates, an SiO_2 film may also develop between the coating and the substrate.[7,9] The temperature of the substrate during heat treatment can affect coating thickness.[9]

Temperature also has an effect on the dielectric strength; it decreases when the deposition temperature increases and this may affect Al_2O_3 grain size.[13] The dielectric strength of films is optimized in the temperature range 700° to 900°C.[13] In the case of alumina coatings on alumina (coated material had increased wear resistance), the deposited coatings were gray and found to be conducting (electrical resistance 2.5×10^3 Ω) via the In-Ga alloy probe technique.[2] This conductivity is due to vacancies in the oxygen substrate which are eliminated when the coating is heat-treated in air (1 hour at 650°C), yielding a white coating with a resistance of 10×10^8 Ω.[2]

Pressure Effects

Pressure has also been known to have an effect on the properties of Al_2O_3 coatings. Deposition rate could be increased with increased reactant partial pressures[13] and flow rates.[6] Yet, Colmet and Naslain[2] found that low partial pressure, 6 kPa (0.06 atm), gave the best results: good adherence and wear resistance. A phenomenon called supersaturation has been described as the driving force for nucleation.[10] Supersaturation relates the input partial pressure of components to the equilibrium partial pressure.[3,10] The evaluations demonstrate that, when the input partial pressure of CO_2 decreases, the nuclei density decreases,[3] whereas a reduction in input partial pressure of $AlCl_3$ results in an increase in nuclei density.[3]

The initial gas-phase composition has a marked effect on the deposition rate of alumina.[2] This composition also has an influence on the coating microstructure.[2] While deposits are generally composed of black nonstoichiometric α-Al_2O_3, it has been found that white corundum can be obtained when the partial

pressure of CO_2 is very low or partial pressure of $AlCl_3$ ($pAlCl_3$) very high.[2] Kornmann et al.[10] examined the nuclei density at 850° and 1000°C and found that it increased as supersaturation increased. Funk et al.[6] determined that deposition rate decreases slightly as the $pAlCl_3$ increases and the same pattern is observed with partial pressure of hydrogen (pH_2). The deposition rate increases approximately proportionally with pCO_2.[6] When initial compositions are extremely rich in $AlCl_3$, almost no alumina deposition is detected.[2] Alumina coatings are chemically vapor deposited at

$$\alpha = (\text{initial } pH_2) / (\text{initial } pCO_2) = 1 \qquad (4)$$

for cemented carbide cutting tools and $\alpha > 1$ for other applications, such as semiconducting materials.[5]

The effect of gas input rates on deposition rate and film properties such as structure, composition, index of refraction, dielectric strength, and electrical conductivity must be evaluated.[13] Doo and Tsang[21] found that whether or not the alumina coating was amorphous, polycrystalline, or even epitaxial single crystal depends on flow rate.

Effect of Substrate

How well the alumina serves as a coating is affected by the substrate and its handling. Multiphase substrates have been found to be unsuitable for coating due to the unique coating adherence pattern for each phase.[3,6,10] For example, with cemented WC-Co, the Co phase has poor adherence with large nuclei clusters, whereas the carbide phases have good adherence with small nuclei clusters.[10] Therefore, a precoating is recommended; TiC and TiN are suggested precoatings for WC-Co cemented carbides.[6]

Another factor is the pre- and postheat treatment of the substrate. For TiC precoated cemented carbide inserts, the quality of the deposited alumina can be increased significantly if the substrate is heated before deposition.[2] Alumina coatings on silicon are examples of where postheat treatments provide the desired adherence.[9]

Scanning electron microscopy has been used to examine the nuclei cluster pattern.[3,10] The studies conducted to date indicate that the larger the nuclei density, the stronger the adhesion of the coating to the substrate.[11] Therefore, nucleation is important for determining the adhesion and type of subsequent growth of desired layers.[6,10,11]

Thermodynamic study shows that Al_2O_3 can be deposited over a wide range of temperatures, total pressures, and initial compositions.[5] The activation energy for deposition has been determined to be between -95.4 kJ/mol (-22.8 kcal/mol)[13,21] and -130 kJ/mol (-31.2 kcal/mol).[5] However Iida and Tsujida[7] determined a value of -237 kJ/mol (-56.7 kcal/mol), which could be explained by impurities. The main conclusion of thermodynamic study on the formation of Al_2O_3 coatings by CVD is that dynamic factors such as mass transport in the vapor phase and/or kinetic considerations play an important role in the CVD of alumina.[5]

Uses

The CVD of alumina has recently led to several applications in the electronic component and cutting tool industry.[5] A CVD alumina coating has also been used as light-diffusing layers for the internal surface of electric lamps.[24,25] This layer has a minor lumen loss and compresses a thin layer of vapor-formed spherical particles having a particle-size range of 40 to 500 nm in diameter.[5,7]

Alumina coatings are preferred to SiO_2 coatings for the passivation of semiconducting components due to their excellent dielectric properties[5] and to their higher efficiency as barriers against contamination (i.e., moisture).[17] Alumina CVD coatings in electronic devices have been found to be useful in protection against sodium-ion migration in silicon devices because the sodium penetration of Al_2O_3-coated silicon is much less than sodium diffusion in silica alone.[16] In addition, Al_2O_3 makes the silicon surface more *p*-type due to the negative charge.[17] Alumina film has a higher dielectric strength ($\approx$7.5) and density (3.5 to 4.0 g/cm^3) than SiO_2 film with corresponding values of 3.8 and 2.20 g/cm^3.[19] Other electronic evaluations, such as dielectric, strength, capacitance-voltage,[15,16] and current-voltage (*I-V*) characteristics, indicate that alumina films are suitable as insulators in nonvolatile field-effect memory devices.[15] The dielectric breakdown strength of alumina-coated capacitors, where CVD alumina is produced via pyrolysis of Al-isopropoxide, has been found to be independent of temperature (100° to 140°C) and Al_2O_3 thickness (20 to 600 nm).[19] The dielectric properties of these alumina films compare favorably with those of anodized Al_2O_3 films.[17]

Alumina coatings having both impressive hardness and excellent behavior toward oxidation considerably increase the lifetime of cemented carbide cutting tools at high temperature. Machining tests carried out with cast iron and steel have shown that the presence of alumina coatings increases the lifetime of the tool insert, reduces the number and size of "cutting microholes" on the work pieces, and decreases the amount of heat generated.[6] The wear of uncoated or TiC-coated tools is greater than that of Al_2O_3-coated tools.[5,6] Chemically vapor-deposited Al_2O_3 coatings on AlN were found to have superior characteristics for use as high-speed cutting tools (with very good lifetimes) compared to uncoated AlN.[14] Alumina has also been deposited with titanium oxide to yield, via CVD, coatings that provide dense protective coatings on wear surfaces.[26] Alumina-coated materials can be used where high thermal stability and high abrasive resistance are required, such as die shafts, bearings, ball bearings, and mechanical seal rings.[14]

Methods of Evaluation

The methods of evaluation of the various alumina coatings are:

1. Ellipsometry-measured refractive index,[13,15,16] thickness of the film,[15] and relative permittivity[15] (compared to anodized Al_2O_3 films).
2. Growth rate, evaluated by weighing the substrate.[2,5]
3. Scanning electron microscopy evaluation of the morphology of the coatings.[2,5]
4. Etch rates.[7,8,12,15,16]
5. Adherence to substrate estimated via the Rockwell C hardness test with a 1471 N load[2] or the Vickers scratching test with a 29.4 N load.[2]
6. MeV He^+ ion backscattering[8,13] measures the stoichiometry of the Al_2O_3 coating and residual ions such as Cl^-.

Reactive Evaporation (Thermal Evaporation) Technique

Alumina coatings have also been prepared by reactive evaporation (RE), which is sometimes referred to as thermal evaporation. The process occurs in a vacuum chamber with the substrate and its heating element (radiative furnace) positioned at the top.[27] The reactive evaporation of aluminum oxide is performed as follows[27]:

1. Very pure aluminum powder is evaporated from a beryllia crucible by heating.[27]
2. An oxidizing gas, such as water vapor,[27] oxygen,[28,29] or air,[30] is injected into the system above the aluminum source. The reaction between the evaporated aluminum particles and the oxidizing gas is confined in a chimney in order to maintain a high oxidizing gas concentration.
3. A shutter, which has been positioned between the substrate and the reaction chimney, is then opened and the oxidized alumina is allowed to deposit on the substrate. The deposition rate is monitored by a quartz crystal oscillator.
4. Following deposition, the alumina layer is annealed.

The quality of the alumina film produced in this manner depends on the reactive process itself and on the evaporation source materials.[27]

As the deposition rate increases in reactive processing, the film becomes increasingly dense.[27] However, a maximum is reached at the rate of 1.5 nm/s, above which the density decreases rapidly, indicating that the layer is no longer a pure dielectric film but contains nonoxidized aluminum. This nonstoichiometry (excess aluminum or oxygen vacancies) may also be controlled by deposition pressure, rate of source evaporation, and the distance from the source.[29] Another factor related to the reactive process is that H^+ ions or OH^- ions may be present as contaminants on the oxide film and affect the electronic behavior of the film. Other contaminants may result from impurities in the aluminum source or from the reaction chamber.[27] When an excess of aluminum is present, the alumina film has a "positive charge."[27,28] Antula[27] found that this positive charge diminished during the aging process due to oxidizing of aluminum in the ambient air surroundings.[28]

Reactively evaporated alumina films have been evaluated for such properties as density, dissolution rate, dielectric constant (via a capacitance bridge)[27,30] and electrical breakdown as a function of deposition parameters.[27] Other properties include film thickness (using a Talysurf),[27] index of reflection (using Brewster angle technique), infrared transmittance (using infrared spectrophotometry, optical transmittance of an He-Ne laser,[29] capacitance-voltage curves involving an MIS device,[29] and current-voltage (*I-V*) curves which show metallic conductivity. The electronic properties are highly dependent on the amount of metallic aluminum in the film.[29]

Activated Reactive Evaporation

The activated reactive evaporation (ARE) process (first conceived in 1971[31] and now classified as a plasma-enhanced deposition process) is similar to the RE process in that evaporated aluminum reacts with an oxidizing gas in the vacuum chamber. The difference between the processes is that the vaporized metal atoms (heated and melted by high-acceleration voltage electron beam)[31] and gas molecules are activated and/or partially ionized by a low-pressure plasma generated in the space between the source and the substrate with the help of a positively biased probe.[31,32] The advantage of this process is that the stoichiometry of the compound deposited can be easily varied and controlled.[32]

When Al_2O_3 coatings are made in this fashion, several forms of alumina have been detected via X-ray diffraction. As the deposition temperature increases, more α-Al_2O_3 is produced (as in the case for CVD coatings). All the deposits had a milky white appearance, were porous, and flaked easily.[32] The deposition rate is much greater at low deposition temperatures (700° to 800°C) than at higher temperatures (1100° and 1200°C).[32] The structure and microhardness (500 to 800 kg/mm^2 VHN) are comparable with those produced by direct evaporation and sputtering.[32]

Activated reactive evaporation processes have been used for coating cutting tools which endure considerable abrasive wear.[31] These processes are comparable with chemical vapor deposition and physical vapor deposition processes which produce equally good results for coating cutting tools used in continuous cutting operations.

Electron-Beam Evaporation

Aluminum oxide films can be coated onto substrates such as aluminum by means of electron-beam evaporation of alumina in an oxygen atmosphere.[33] To evaporate a film of Al_2O_3, the aluminum oxide source

is positioned on a horizontal, water-cooled hearth (Fig. 1).[34] The electron beam is emitted horizontally from the electron gun and deflected downward toward the Al_2O_3 source by a magnetic beam. The inverted substrate is positioned above the Al_2O_3 source to prevent the buildup of aluminum oxide films which can flake off and fall on exposed surfaces.[31] A shutter is positioned between the substrate and electron beam evaporator so that the material flux can be regulated. All of these components are positioned in a vacuum chamber.

Standard operating procedure consists of evacuating the reaction chamber to the mid-100 μPa (10^{-6} torr) range.[33] Following chamber evacuation, the substrates are heated (if desired), the electron gun preheated, and the Al_2O_3 source heated to the desired evaporation rate.[33] Once the desired evaporation rate is achieved, oxygen is leaked into the chamber and the shutter opened so that the substrate is coated. When the desired film thickness is achieved, the shutter is closed and the system allowed to cool. The evaporation rate and the thickness are controlled by a quartz-crystal oscillator monitor.[35,36]

The predominant use of these coatings has been in the area of electronics to form integral dielectric (insulator) components on semiconductors.[33–36] The properties and characteristics of electron-beam evaporated Al_2O_3 coatings have been the subject of several investigations. Areas which have been investigated include dielectric (constant[36] and loss factor[35]) measurements; breakdown field[33,34]; index of refraction[34,36]; etch rates of various acids such as HF,[33,34] hot HCl,[34] H_3PO_4,[34,36] hot HNO_3,[34] NaOH,[34] HNO_3-HF,[33] and HF-H_3PO_4[34]; density[33,34,36]; direct current (dc) resistivity[34]; band gap[34]; stoichiometry (via electron beam microprobe)[34]; and structure (amorphous via X-ray).[33,34] These properties have also been compared to other films such as Si_3N_4 and SiO_2[34] or mixtures/combinations of Al_2O_3-SiO_2.[36] Various structures were fabricated to test the qualities of the alumina film. Examples are metal-insulator-metal (MIM), metal-insulator-semiconductor (MIS), and metal-oxide-semiconductor (MOS). (Note: MAS represents metal-alumina-semiconductors, a special case of MOS.) The capacitance versus voltage (*C-V*) curves taken from the devices produced data concerning interface properties between oxide and silicon, as well as conduction of the Al_2O_3 with applied bias conditions.[33,34]

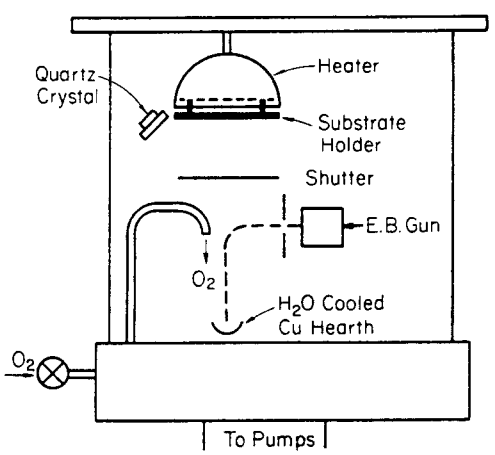

Fig. 1. Schematic of a vacuum deposition system.

The growth and uniformity of the deposited films (and its effect on the dielectric properties) has been found to be highly dependent on type of substrate used,[33] evaporation rate,[33,35] substrate temperature,[33,35] and atmospheric conditions in the reaction chamber.[33,35] The dielectric constant tends to increase up to 7 to 8 with evaporation rate; at the same time the loss factor decreases to 2×10^{-3}.[35] In addition, the dielectric properties are nearly independent of substrate temperature.[35] A high rate of evaporation decreases the influence of impurities (H_2O, N_2) due to residual atmosphere in the reaction chamber; thus a small loss factor is obtained.[35] Osipov et al.[37] observed that adding O and H to the reaction chamber during precipitation of films affects the electrophysical characteristics.

The refractive index, as measured by ellipsometry, has been found to depend on deposition parameters[33]; the values range from 1.55 to 1.77.[33,36] A lower refractive index is probably the result of a large amount of oxygen present in the film.[33,36] (Note: In the case of ARE of Al_2O_3 films, a lower n is measured because of the incorporation of oxygen from the oxygen plasma.[36] In turn, a higher refractive index suggests that either a nonstoichiometric film (oxygen-deficient) or a low-density film exists.[33]

Etch-rate investigation may be used on these films to measure homogeneity and quality of films.[36] For example, the etching of films in buffered HF suggests some degree of porosity.[33]

Measurements of refractive index, relative permittivity, density, and hardness reveal that films produced by this process have a more porous structure than sapphire crystals.[34] Another point is that properties of these films depend more on the source of the Al_2O_3 than on the method of deposition when comparing electron-beam evaporation-, reactive evaporation-, and activated reactive evaporation-produced films.[36]

Sputtering

Dielectric alumina films deposited on semiconductor substrates in solid state devices[38] can also be prepared by sputtering techniques. Sputtering is a process in which material is removed from a source or target (the cathode), carried by a plasma, and deposited on the substrate (the anode).[39] Energetic particles impinging on the surface of the target cause the emission of target particles and erosion of the surface.[40]

Targets have been positioned above,[38,41,42] below,[43] and around[44] the substrate. This type of deposition process can be divided into two categories: (1) chemical, which entails reactive and dc reactive sputtering and (2) physical, which encompasses radio-frequency (rf) sputtering. The physical sputtering process also has been compared to the evaporation coating process.[45] Reactive sputtering is used to convert coating material to another compound by using a reactive gas mixed with argon.[46]

Typical applications involve introducing oxygen mixed with argon while sputtering a metal such as aluminum to deposit a thin film of aluminum oxide.[43,47] This is a method used to produce capacitors and resistors.[43,46] Frieser[43] observed that the deposition rate decreased as the partial pressure of oxygen (pO_2) increased in the oxygen-argon mixture of sputtering gas. Other factors influencing the deposition rate are sputtering voltage, sputtering gas pressure, and current density; the latter two both have a direct influence, while electrode separation has an indirect influence.[43]

Depending on the experimental conditions, two types of alumina films could be deposited.[43] One type is polycrystalline γ-alumina film which dissolves with difficulty in HF and is the result of conditions favoring high deposition[43] rates and substrate temperatures. Amorphous alumina also can be deposited with this process at low substrate temperature. It generally is an HF-soluble film.

Good-quality Al_2O_3 films are deposited by rf sputtering from an Al_2O_3 target in an argon atmosphere.[38,44,48–50] In this case, power density has the predominate influence on rate of deposition (linear relationship), etch rate, density, dielectric constant, conductivity, and surface characteristics.[38] As the power density decreases, the rate of etching (in $HF\text{-}HNO_3$) increases, which indicates the formation of porous films.[38] An increase in power density results in an increased density which, in turn, may be related to index of refraction (1.55 to 1.65 with power density of 1 W/cm^2 and 8.5 with 2.5 W/cm^2, both at a thickness of 0.5 μm) and dielectric constant.[38] However, low-angle electron diffraction shows an amorphous structure which is independent of power density.[38] In general, high-power density sputtering is preferred, but has the major detrimental effect of deterioration in surface properties, i.e., surface charge becomes a problem.[38]

The structure of the film is affected by the substrate temperature as observed by Thornton and Chin.[44] As-deposited structures are noncrystalline for substrate temperatures ≤500°C. Alpha Al_2O_3 is obtained at temperatures above 1100°C.[44] Intermediate temperatures yield polymorphic phases.[44]

Sputtering is competitive with the evaporation process since it yields more consistent sheet resistivity and improved temperature coefficient of resistance.[39] The disadvantages of sputtering as compared with vacuum evaporation are the higher cost of equipment and operation, more complex equipment, and slower deposition rates.[39]

Particulate Deposition

Particulate deposition can be described as a melt-spraying process and is achieved by thermal spraying. Alumina coatings are prepared by projection of a stream of molten particles at high velocity against the material to be coated and are widely used to provide wear, thermal, or corrosion protection.[51] The droplet spray may be produced either by passing suitable powders or a rod through a combustion flame, called flame spraying, or by injection of powder into a direct current plasma jet, called plasma spraying. The two processes are identical in principle; however, the high temperatures and gas velocities in a plasma result in a higher velocity molten-particle spray without practical limitations imposed because of melting point of the sprayed material. The microstructure of both flame- and plasma-sprayed coatings consists of a series of overlapping lamellas (or solidified splats) produced by the spread and rapid solidification of the impinging droplets.[51,52]

The crystal structure of plasma- and flame-sprayed coatings depends on the conditions under which the liquid droplets spread and solidify on impact with the substrate, and their subsequent thermal history. Under most conditions, flame- and plasma-sprayed coatings contain some α-alumina in addition to γ-Al_2O_3.[50] Other metastable forms of alumina, δ-Al_2O_3 and ϑ-Al_2O_3, have been observed via X-ray diffraction.[51]

Heat treatment can be used to transform the metastable alumina forms to α-Al_2O_3,[52,53] which has a higher conductivity.[52] The phase transition due to heat treatment is accompanied by volume shrinkage, which in turn leads to cracks caused by differences in thermal expansion coefficients between coating and substrate.

The temperature of the substrate on application of the coating is a significant feature. For example, if the substrate is heated above the $\gamma \rightarrow \alpha$ phase-transition temperature, it is possible to obtain α-Al_2O_3 during spraying.[53,54] Microcracks could develop due to thermal shock when applying coating to a cold substrate.[52]

Use

Flame spraying has been used to form a hard, dense, optically stable alumina coating that reflects light diffusely and has a reflectance that varies less than 4% over the spectral range of 0.3 to 3.0 μm.[55]

Plasma-sprayed coatings can be used to coat substrates of virtually any composition, including silica glass, metals, and plastic, which can be used in fuel cells, batteries, laboratory test work, and other applications.[56] A plasma arc-spraying technique has been used to produce a high-emittance coating onto radioisotope containment vessels.[57]

Plasma-deposited coatings (thickness range 0.1 to 1.0 mm) on nickel substrates have an electrical strength range of 6 to 12 kV/mm at normal temperatures, falling steadily with use in temperature to 1 to 2 kV/mm at $T \approx 1500$ K.[58] The resistivity of these materials up to 1200 K is substantially lower than that of monolithic alumina at the same temperatures.[58] The thermal cycling behavior of Al_2O_3 coatings has been evaluated using an acoustical emission (AE) technique.[59] This technique can evaluate morphological changes within coatings, such as crack initiation and crack growth either within the coating or at the coating-substrate interface.[59]

Bioceramics are another area in which alumina coatings applied by particulate deposition techniques have been investigated. The feasibility of alumina-coated prostheses have been investigated from the standpoint of physiological compatibility[60–62] and in growth of natural bone into the porous ceramic.[61–63] Alumina coatings have been thermally sprayed, both plasma[61] and flame,[60] to yield coatings with a porosity which can be regulated by processing conditions.[60] These coatings have potential in nonload-bearing situations where muscle tissue fixation can occur. Load-bearing situations have not been successful due to the low strength of the ceramic-to-metal bond.[60]

Bulk Coating

In the bulk coating process, alumina coatings are joined to the substrate by a wetting process which includes painting, spraying, soaking, dipping, suspending, or otherwise immersing the substrate. Some materials to be coated have surfaces of limited accessibility, therefore necessitating a process to coat the surfaces uniformly. An example is coating a catalytic convertor which has a monolithic skeletal structure composed of thin laminated sheets of corrugated ceramic material which provide many adjacent, parallel, and unidirectional channels; it is commonly called honeycomb.[64–66]

Another example is coating a three-dimensional network cellular structure having many interconnected voids without obstruction in any direction.[67] Bulk coating techniques can be utilized for these complex substrates.[64–66] Several coating procedures have been utilized for various substrate structures.

The coating procedure for the honeycomb structure is as follows.

1. An alumina sol is prepared by digesting an excess of aluminum in aqueous hydrochloric acid under flux conditions (98° to 115°C). This sol is then mixed with polyethylene glycol plasticizer and polyoxyethylene alcohol nonionic surfactant.[64] Other alumina sol recipes have been tried.[66]

2. The ceramic honeycomb structure is immersed in the alumina sol with a gently reciprocating movement in the direction of parallel channels to ensure contact and even distribution of sol on the honeycomb surface. The impregnated honeycomb is removed and blown free of excess sol with a stream of air. The piece is then dried (150°) and calcined (540°C).[64]

A method has been devised for controlling the uniformity and repeatability of coating a catalytic support system which has at least 100 axially aligned tubular passageways to the square inch. The catalytic support system is subjected to a vacuum which draws the slurry through the passageways and removes plugging and excess slurry.[64] The amount of slurry left on the monolith is controlled by the purge time and the vacuum pressure.[64] In operation, the coating is accomplished in an earlier station by pouring, spraying, painting, or immersing the support.[65,66] The vacuum system is started once the support is positioned in the purging station.[65] Following the purge, the coated support is dried and then fired.[66]

The cellular network device mentioned earlier can be used as a filter for molten metal by adsorbing molten impurities such as hydrogen, sodium, and the like onto an activated alumina layer.[67] This layer is applied by impregnating the network system into an alumina slurry, followed by drying and firing processes.[67]

In Al_2O_3 coating of the fibers or whiskers to be used in composites using organic starting materials, three techniques have been employed: (1) coating, (2) multiple dipping, or (3) freezing[68] in an alumina sol-gel.[69] The coating process consists of aluminum sec-butoxide which was hydrolyzed with dionized water at 80°C. Following hydrolysis, acetic acid was added and allowed to react at 90°C until a clear sol was obtained (approximately one week).[69] Coating and dipping methods with the organic are self-explanatory but freezing deserves a brief explanation.

The freezing technique involves the abrupt change in the sol viscosity that occurs near gelation. The prewetted whiskers are added to the sol and the resulting solution is boiled and stirred vigorously until gelation is imminent. At this point, the solution is cast,[68] gelled, and dried.

The wetting process also has been used to coat particles by preparing a slurry of aluminum salt (aluminum nitrate ($Al(NO_3)_3 \cdot 9H_2O$), aluminum sulfate, or aluminum chloride) and water.[70] The particles to be coated, such as CrO_2, are added to the coating material and agitated in a controlled-temperature environment. Careful monitoring of the temperature and pH allows a water-soluble base, e.g., NaOH, KOH, LiOH, Na_2CO_3, NH_4OH, or gaseous NH_3 to be added until the pH has reached the desired value (about 4.5 to 8). The slurry continues to be stirred to ensure equilibrium of the hydrous alumina coating. The coated particles are separated from the mother liquid by filtering, washed, dried with acetone in air, and finally heated.[70]

Beta alumina films suitable for use as a ceramic electrolyte in high-energy, high-density sodium sulfur batteries[71] also can be formed by the sol process and applied by any of the bulk coating application methods, e.g., dipping, spraying, etc.

The sol preparation consists of two stages:

1. Sodium hydroxide reacts with an aluminum alkoxide, $Al(OR)_3$, such as aluminum sec-butoxide, $Al(OC_4H_9)_3$.

$$Na(OH) + Al(OR)_3 \rightleftarrows Na\text{-}O\text{-}Al(OR)_2 + ROH \quad (5)$$

2. The remaining alkyl groups are removed with an excess of water.

$$Na\text{-}O\text{-}Al(OR)_2 + 2H_2O \rightleftarrows Na\text{-}O\text{-}Al(OH)_2 + 2ROH \quad (6)$$

This is applied to the substrate and heat-treated at 500°C to convert film to essentially organic-free amorphous oxide. On further heating to 1200°C, transformation to β-Al_2O_3 occurs.[71] The bulk coatings technique covers a wide variety of sizes and shapes.

Surface Conversion Coating

A coating may be produced by altering the surface material to produce a surface layer composed of the added and substrate material. This is called conversion or surface-modification coating. Surface modification of aluminum can result in an aluminum oxide film. Two methods utilized are thermal oxidation and electrochemical anodization. Thermal oxidation can occur when an aluminum substrate is exposed to air at high temperatures (500°C). This coating can serve in its present form or can function as a precursor for the anodized coatings.[72] In the case of alumina thermal oxidation or electrochemical anodization, an aluminum substrate surface can be transformed into an alumina coating.

Aluminum oxide films are also obtained when aluminum is anodized electrochemically.[73] Characteristics and growth rates of such films depend on the crystallographic orientation,[74,75] anodizing voltage,[73,74,76] current density,[73,74,77] electrolyte and its concentration,[73,76,77] and operating temperature.[73–75,77] These films are formed primarily to protect aluminum coatings from corrosion or for insulation. The dielectric strength of these coatings varies with the electrolyte used.[78] Impedance characteristics and dissolution behavior have been the subject of several studies.[78]

Anodic spark deposition is another electrochemical anodization method and an unconventional process for forming ceramic coatings on conductive substrates.[78] As the name implies, the coating is deposited on an electrode of an electrolytic cell by a mechanism involving a spark.[78] The alumina coatings formed in this fashion are crystalline in nature: primarily α-Al_2O_3 with minor amounts of β and γ forms. The β form is the result of using the electrolytic solutions: sodium aluminate ($NaAlO_2$)[78,79] and sodium silicate.[78] The latter yields a glassy coating, while the former results in a more crystalline surface.[78]

Another feature of the anodic deposition technique is that other ions can be incorporated into the alumina barrier films via the selection of electrolytic solution. Cocke et al.[80] studied solutions containing MoO_4^{2-}, WO_4^{2-}, CrO_4^{2-}, or MnO_4^- and found that the later two were more evenly distributed throughout the alumina because the ionic radii were closer to Al^{3+} than W^{6+} or Mo^{6+}. These ions dramatically affect the structure, electronic properties, and stability of the alumina formed.

Plasma anodization differs from ordinary anodization in that the electrolyte solution is replaced by an oxygen plasma.[81] As a method of producing dielectric films, it is of particular interest in the fabrication of electronic devices since it is compatible with other vacuum processing steps.[81] In other words, these insulating films are amorphous,[82,83] with a low dissipation factor (0.02 at 1 kHz), a high breakdown strength,[83] and a dielectric constant of 7.6 (at 1 MHz).[82] The index of refraction as measured by ellipsometry is between 1.67 and 1.70 depending on exact fabrication conditions. Also, ionic motion at high temperatures makes aluminum oxide an excellent gate insulator for MOS transistors.[82]

Plasma anodization is carried out in a vacuum system where dry oxygen is admitted to the system and a plasma is ignited between the anode and cathode.[83,84] The specimen to be coated is inserted into the plasma near the cathode but facing away from it to avoid picking up sputtered cathode material.[81] Following oxidation, the sample is annealed for about an hour at 300°C in an inert (N_2, He) ambient gas to produce film thicknesses between 50 and 70 nm.[82,83]

The basic reaction chamber for electrochemical anodization consists of a glass beaker containing electrolytic solution, a cathode (usually platinum), the anode (aluminum), a power supply which controls the voltage, and a current supply which connects the electrodes.[73,78] An end of each electrode is positioned in an electrolyte solution.[78] The chamber is surrounded by a heating mantle for temperature control.[73,78] The type of electrolyte utilized has been either acidic and/or alkaline. The list includes: sodium tetraborate, sodium carbonate, sodium citrate, oxalic acid, ammonium dihydrogen phosphate, ammonium citrate (acid/base), ammonia solution, potassium sodium tartrate, sodium aluminate ($NaAlO_2$), sodium silicate (Na_2SiO_3), sodium hydroxide (NaOH), ammonium pentaborate (25°C), sulfuric acid, and tartaric acid and ammonia.

The oxide film produced does not have a uniform density throughout its thickness.[76] It consists of a very thin, dense (nonporous) barrier layer adjacent to the metal surface and a thick porous oxide (partially hydrated) layer adjacent to the barrier layer.[73,77]

Barrier thickness is primarily a function of forming voltage and is affected to a minor degree by the type of electrolyte. Films formed below 40 V (70°C) were found to be a combination of amorphous and crystalline oxide (γ'-alumina),[85] while films formed above 60 V were essentially completely crystalline with a higher density and field strength[74] than typical amorphous, anodic oxide barrier layers.[75]

An ordered amorphous oxide may be a precursor of the crystalline oxide.[74,75] The crystalline sites are nucleated only during the early growth of the films and have a strong initial preferred orientation on non-(100) substrates.[74,75] The number of these sites is dependent on the electrolyte temperature,[74,75] current density,[74] and crystallographic orientation of the electropolished aluminum substrate[74,75]; they increase with increased temperature.[74] As anodization continues, the crystalline sites grow larger, but do not increase in number; eventually, the individual sites grow together to form a continuous sheet.[75] Growth of nucleated Al_2O_3 is optimized by high electrolyte temperature, low current density, and high anodization voltage.[74] A low current density primarily decreases the rate of oxide growth and increases the time required for total anodization; this, apparently, favors crystalline oxide growth.[74] The overall growth rate of Al_2O_3 films is dependent on current density and current transport properties.[73] This growth of the oxide film results in increased electrical resistance at the anode.[73] The exact growth process is not known; the crystalline oxide may grow by conversion of amorphous oxide, by direct crystal growth, or by a combination of the two.[74] Crystalline films which have γ'-Al_2O_3 crystal structure had a higher capacitance, were thinner, and contained fewer impurity ions than largely amorphous films anodized to the same voltage.[74]

Some electrochemical anodization processes may be preceded by a thermal oxidation of the aluminum in air at high temperature (500°C).[74,85] This thermal treatment produces platelets of γ-Al_2O_3, which act as effective nucleation sites for the growth of crystalline anodic oxide.[74]

Applications

This section describes uses of alumina coatings which have not been discussed previously.

In the area of cutting tools, several principal properties are required, including good wear resistance, toughness, chemical stability under high temperature, large forces, and sufficiently high flow strength. Although it is not possible to achieve all these properties with a single material, alumina has been investigated as a possible candidate.[85,86] An alumina coating over a TiC coating has been found to enhance wear and crater resistance appreciably. Failure of tools used for cutting at high speeds is due to wear, plastic deformation, or rupture of the tool.[6]

Alumina coatings have been utilized on the space shuttle tile to reflect sunlight. While in orbit, overheating of the shuttle tile can be prevented by relying on the optical properties of alumina coatings which reflect sunlight.[87] Alumina films also have served as one of the components in an antireflective coating for infrared transmission materials.[88,89]

Alumina coatings, when coupled with tungstic oxide, can self-destruct modules which are circuited to cause ignition of a thermite layer, thus destroying the circuit before it falls into enemy hands. The wide variety of methods which can be used to apply alumina coatings provides an excellent opportunity to select a procedure which yields the desired material properties.

Overall, the critical aspects of the coating process involve adherence to the substrate, residual stresses arising from thermal expansion mismatch, or growth stresses caused by imperfections in the coating that are built in during film growth. These are major considerations when designing alumina-coated materials and they must be considered carefully.

References

[1]Page 719 in Encyclopedia of Glass, Ceramics, and Cement. Edited by M. Grayson. Wiley & Sons, New York, 1985.

[2]R. Colmet and R. Naslain, "Chemical Vapour Deposition of Alumina on Cutting Tool Inserts from $AlCl_3$-H_2-CO_2 Mixtures: Influence of the Chemical Vapour Deposition Parameters and the Nature of the Inserts on the Morphology and Wear Resistance of the Coatings," *Wear*, **80**, 221–31 (1982).

[3]T. R. Johannesson and J. N. Lindstrom, "Factors Affecting the Initial Nucleation of Alumina on Cemented-Carbide Substrates in the CVD Process," *J. Vac. Sci. Tech.*, **12** [4] 854–57 (1975).

[4]J. A. Aboaf, D. R. Kerr, and E. Bassous, "Charge in SiO_2-Al_2O_3 Double Layers on Silicon," *J. Electrochem. Soc.*, **120** [8] 1103–1106 (1973).

[5]R. Colmet, R. Naslain, P. Hagenmuller, and C. Bernard, "Thermodynamic and Experimental Analysis of Chemical Vapor Deposition of Alumina from $AlCl_3$-H_2-CO_2 Gas Phase Mixtures," *J. Electrochem. Soc.*, **129** [6] 1367–72 (1982).

[6]R. Funk, H. Schachner, C. Triquet, M. Kornmann, and B. Lux, "Coating of Cemented Carbide Cutting Tools with Alumina by Chemical Vapor Deposition," *J. Electrochem. Soc.*, **123** [2] 285–89 (1976).

[7]K. Iida and T. Tsujide, "Physical and Chemical Properties of Aluminum Oxide Film Deposited by $AlCl_3$-CO_2-H_2 System," *Jpn. J. Appl. Phys.*, **11** [6] 840–49 (1972).

[8]M. Kamoshida, I. V. Mitchell, and J. W. Mayer, "Influence of Deposition Temperature on Properties of Hydrolytically Grown Aluminum Oxide Films," *Appl. Phys. Lett.*, **18** [7] 292–94 (1971).

[9]M. Kamoshida, I. V. Mitchell, and J. W. Mayer, "Influence of Heat Treatment on Aluminum Oxide Films on Silicon," *J. Appl. Phys.*, **43** [4] 1717–24 (1972).

[10]M. Kornmann, H. Schachner, R. Funk, and B. Lux, "Nucleation of Alumina Layers on TiC and Cemented Carbides by Chemical Vapor Deposition," *J. Cryst. Growth*, **28**, 259–62 (1975).

[11]J. N. Lindstrom and T. R. Johannesson, "Nucleation of Al_2O_3 Layers on Cemented Carbide Tools," *J. Electrochem. Soc.*, **123** [4] 555–59 (1976).

[12]I. V. Mitchell, M. Kamoshida, and J. W. Mayer, "Channeling-Effect Analysis of Thin Films on Silicon: Aluminum Oxide," *J. Appl. Phys.*, **42** [11] 4378-89 (1971).

[13]V. J. Silvestri, C. M. Osburn, and D. W. Ormond, "Properties of Al_2O_3 Films Deposited from the $AlCl_3$, CO_2, and H_2 System," *J. Electrochem. Soc.*, **125** [6] 902–907 (1978).

[14]H. Tanaka and Y. Yamamoto, "Aluminum Nitride Sintered Body Coated with Alumina," U.S. Pat. No. 4 203 733.

[15]T. Tsujide, S. Nakanuma, and Y. Ikushima, "Properties of Aluminum Oxide Obtained by Hydrolysis of $AlCl_3$," *J. Electrochem. Soc.*, **117** [5] 703–707 (1970).

[16]S. K. Tung and R. E. Caffrey, "Pyrolytic Deposition and Properties of Aluminum Oxide Films," *J. Electrochem. Soc.*, **114** [11] 275C–276C (1967).

[17]J. A. Aboaf, "Deposition and Properties of Aluminum Oxide Obtained by Pyrolytic Decomposition of an Aluminum Alkoxide," *J. Electrochem. Soc.*, **114** [9] 948–52 (1967).

[18]J. A. Aboaf, D. R. Kerr, and E. Bassous, "Charge in SiO_2-Al_2O_3 Double Layers on Silicon," *J. Electrochem. Soc.*, **120** [8] 1103–1106 (1973).

[19]J. E. Carnes and M. T. Duffy, "Self-Healing Breakdown Measurements of Pyrolytic Aluminum Oxide Films on Silicon," *J. Appl. Phys.*, **42** [11] 4350–56 (1971).

[20]M. T. Duffy and A. G. Revesz, "Interface Properties of Si-(SiO_2)-Al_2O_3 Structures," *J. Electrochem. Soc.*, **117** [3] 372–77 (1970).

[21]V. Y. Doo and P. J. Tsang, "Morphology, Structure, and Properties of Pyrolytic Aluminum Oxide," *J. Electrochem. Soc.*, **116** [3] 118C (1969).

[22]M. J. Rand, "A Nitric Oxide Process for the Deposition of Silica Films," *J. Electrochem. Soc.*, **114** [3] 274–77 (1967).

[23]L. H. Hall, "Method and Device Employing High Resistivity Aluminum Oxide Film," U.S. Pat. No. 3 698 071.

[24]D. C. Henderson and K. M. Maloney, "Alumina Coatings for an Electric Lamp," U.S. Pat. No. 3 842 306.

[25]L. H. Hall, "Method and Device Employing High Resistivity Aluminum Oxide Film," U.S. Pat. No. 3 698 071.

[26]F. Fomzi, "Method of Co-Deposit Coating Aluminum Oxide and Titanium Oxide," U.S. Pat. No. 4 112 148.

[27]E. Ferrieu and B. Pruniaux, "Preliminary Investigations of Reactively Evaporated Aluminum Oxide Films on Silicon," *J. Electrochem. Soc.*, **116** [7] 1008–13 (1969).

[28]J. Antula, "Effect of Positive Ionic Space Charge on Electrical Capacitance and Schottky Current in Thin Al_2O_3 Films," *Thin Solid Films*, **4**, 281–89 (1969).

[29]H. Birey, "High-Field Transport Properties of Aluminum-Embedded Aluminum Oxide Films," *Appl. Phys. Lett*, **23** [6] 316–18 (1973).

[30]H. Birey, "Thickness Dependence of the Dielectric Constant and Resistance of Al_2O_3 Films," *J. Appl. Phys.*, **48** [12] 5209–12 (1977).

[31]R. F. Bunshah, "The Activated Reactive Evaporation Process: Developments and Applications," *Thin Solid Films*, **80**, 255–61 (1981).

[32]R. F. Bunshah and R. J. Schramm, "Alumina Deposited by Activated Reactive Evaporation," *Thin Solid Films*, **40**, 211–16 (1977).

[33]D. Hoffman and D. Leibowitz, "Al_2O_3 Films Prepared by Electron-Beam Evaporation of Hot-Pressed Al_2O_3 in Oxygen Ambient," *J. Vac. Sci. Tech*, **8** [1] 107–11 (1971).

[34]W. M. Gosney and R. S. Muller, "Aluminum Oxide Films Made from Evaporated Sapphire," *Thin Solid Films*, **14**, 255–66 (1972).

[35]M. Le Contellec and F. Morin, "An Investigation of Metal-Insulator-Semiconductor Structures with Al_2O_3 Insulating Layers Obtained by Electron Gun Evaporation," *Thin Solid Films*, **52**, 63–68 (1978).

[36]J. Vanfleteren and A. van Calster, "A Comparative Study of Evaporated Al_2O_3, SiO_2, and SiO_2-Al_2O_3 Thin Films," **139**, 89–94 (1986).

[37]K. A. Osipov, T. L. Borovich, and I. I. Orlov, "Films of Alumina Obtained by Electron-Beam Method," *Izv. Akad. Nauk. SSSR Neorg. Mater.*, **7** [11] 1970–74 (1971).

[38]C. A. T. Salama, "RF Sputtered Aluminum Oxide Films on Silicon," *J. Electrochem. Soc.*, **117** [7] 913–17 (1970).

[39]Page 478 in Kirk-Othmer Concise Encyclopedia of Chemical Technology. Wiley & Sons, New York, 1985.

[40]M. B. Bever; p. 4322 in Encyclopedia of Materials Science and Engineering, Vol. 6. MIT Press, Cambridge, MA, 1986.

[41]M. C. Chen, "Some Charge Phenomena in D-C Reactivity Sputtered Alumina Films on Silicon," *J. Electrochem. Soc.*, **118** [4] 591–96 (1971).

[42]J. F. Henrickson, G. Krauss, R. N. Tauber, and D. J. Sharp, "Structure and Properties of Sputtered Ta-Al_2O_3 Cermet Thin Films," *J. Appl. Phys.*, **40** [13] 5006–14 (1969).

[43]R. G. Frieser, "Phase Changes in Thin Reactively Sputtered Alumina Films," *J. Electrochem. Soc.*, **113** [4] 357–60 (1966).

[44]J. A. Thornton and J. Chin, "Structure and Heat Treatment Characteristics of Sputter-Deposited Alumina," *Am. Ceram. Soc. Bull.*, **56** [5] 504–508, 512 (1977).

[45]Page 723 in Encyclopedia of Glass, Ceramics, and Cement. Edited by M. Grayson, Wiley & Sons, New York, 1985.

[46]M. B. Bever; p. 4563 in Encyclopedia of Materials Science and Engineering, Vol. 6. MIT Press, Cambridge, MA, 1986.

[47]T. Tanaka and S. Iwauchi, "The Characteristics of Al-Al_2O_3-Si Structures Formed by Reactive Sputtering," *Jpn. J. Appl. Phys.* **7**, 1420 (1968).

[48]R. Jarvinen, T. Mantyla, and P. Kettunen, "Improved Adhesion Between a Sputtered Alumina Coating and A Copper Substrate," *Thin Solid Films*, **114**, 311–17 (1984).

[49]S. Krongelb, "Stability of Aluminum Oxide Films on Germanium Devices," *J. Electrochem. Soc.*, **116** [9] 1583–84 (1969).

[50]I. H. Pratt, "Growth and Electrical Characteristics of RF Sputtered Aluminum Oxide," *Thin Solid Films*, **3**, R23–R26 (1969).

[51]R. McPherson, "On the Formation of Thermally Sprayed Alumina Coatings," *J. Mater. Sci.*, **15**, 3141–49 (1980).

[52]G. F. Hurley and F. D. Gac, "Structure and Thermal Diffusivity of Plasma-Sprayed Al_2O_3," *Am. Ceram. Soc. Bull.*, **58** [5] 509–11 (1979).

[53]V. S. Thompson and O. J. Whittemore, "Structural Changes on Reheating Plasma-Sprayed Alumina," *Am. Ceram. Soc. Bull.*, **47** [7] 637–41 (1968).

[54]I. R. Kozlova, "Structural Transformation in Sprayed Aluminum Oxide," *Izv. Akad. Nauk. SSSR Neorg. Mater.*, **7** [8] 1372–76 (1971).

[55]J. M. Davies and W. Zagleboyle, "Flame Spraying Aluminum Oxide to Make Reflective Coatings," U.S. Pat. No. 3 610 741.

[56]F. D. Rizzelli and K. Papadopoulos, "Alumina Coating," U.S. Pat. No. 4 395 432.

[57]J. L. Blumenthal, D. F. Carroll, and J. R. Ogren, "Plasma Arc Sprayed Modified Alumina High Emittance Coating for Noble Metals," U.S. Pat. No. 3 751 295.

[58]D. Y. Dudko, A. V. Primak, N. I. Fal'kovskii, D. M. Karpinos, Y. I. Morozov, V. G. Zil'berberg, and K. I. Yakovlev, "High-Temperature Electric Insulating Characteristic of Plasma-Deposited Alumina Coatings," *Sov. Powd. Metall. Met. Ceram. (Engl. Transl.)*, **21** [2] 150–53 (1982).

[59]N. R. Shankar, C. C. Berndt, H. Herman, and S. Rangaswamy, "Acoustic Emission from Thermally Cycled Plasma-Sprayed Oxides," *Am. Ceram. Soc. Bull.*, **62** [5] 614–19 (1983).

[60]C. M. Baldwin and J. D. Mackenzie, "Flame-Sprayed Alumina on Stainless Steel for Possible Prosthetic Application," *J. Biomed. Mater. Res.*, **10**, 445–53 (1976).

[61]J. L. Drummond, M. R. Simon, S. D. Brown, and R. J. Blattner, "Degradation of Plasma-Sprayed Alumina on Metal Substrates in Physiological Media," *J. Am. Ceram. Soc.*, **64** [8] C-109–C-110 (1981).

[62]S. F. Hulbert, H. L. Richbourg, J. J. Klawitter, and B. W. Sauer, "Evaluation of Metal-Ceramic Composite Hip Prosthesis," *J. Biomed. Mater. Res.*, **6**, 189–98 (1975).

[63]S. F. Hulbert, F. A. Young, R. S. Mathews, J. J. Klawitter, C. D. Talbert, and F. H. Stelling, "Potential of Ceramic Materials as Permanently Implantable Skeletal Prostheses," *J. Biomed. Mater. Res.*, **4**, 443–56 (1970).

[64]J. Hoekstra, "Method of Depositing a High Surface Area Alumina Film on a Relatively Low Surface Area Support," U.S. Pat. No. 3 767 453.

[65]J. R. Reed, T. Way, and R. A. Leal, "Method for Coating Catalyst Supports," U.S. Pat. No. 4 208 454.

[66]T. Kato, T. Ikemi, and T. Sagawa, "Method for Forming Activated Alumina Coating on Refractory Article and Article Thereby Produced," U.S. Pat. No. 4 213 900.

[67]T. Naramlya, "Cordierite, Alumina, Silica Porous Ceramic Bodies, Coated With an Activated Alumina Layer," U.S. Pat. No. 4 258 099.

[68]J. J. Lannutti and D. E. Clark, "Sol-Gel Derived Coatings on SiC and Silicate Fibers," *Eng. Ceram. Sci. Proc.*, **5** [7–8] 574–82 (1984).

[69]B. E. Yoldas, "Alumina Sol Preparation from Alkoxides," *Am. Ceram. Soc. Bull.*, **54** [3] 289–90 (1975).

[70]D. G. Pye, "Method of Coating CrO_2 with Alumina," U.S. Pat. No. 3 736 181.

[71]B. E. Yoldas and D. P. Partlow, "Formation of Continuous Beta Alumina Films and Coatings at Low Temperatures," *Am. Ceram. Soc. Bull.*, **59** [6] 640–42 (1980).

[72]J. Antula, "Thickness Study of Thermally Oxidized and Anodized Thin Al_2O^3 Films," *Thin Solid Films*, **3**, 183–88 (1969).

[73]H. Lasser, G. Robinson, and B. Almaula, "Preparation of Semiporous Wafers of Aluminum Oxide By High Voltage Anodization," *Am. Ceram. Soc. Bull.*, **50** [2] 165–69 (1971).

[74]C. T. Chen and G. A. Hutchins, "Crystalline Anodic Oxide Growth on Aluminum Foil in an Aqueous Ammonium Dihydrogen Phosphate Anodization Electrolyte," *J. Electrochem. Soc.*, **132** [7] 1567–74 (1985).

[75]G. A. Hutchins and C. T. Chen, "The Amorphous to Crystalline Transformation of Anodic Aluminum Oxide During Anodization in an Ammonium Citrate Electrolyte," *J. Electrochem. Soc.*, **133** [7] 1332–37 (1986).

[76]R. Greef and C. F. W. Norman, "Ellipsometry of the Growth and Dissolution of Anodic Oxide Films on Aluminum in Alkaline Solution," *J. Electrochem. Soc.*, **132** [10] 2362–69 (1985).

[77]J. Hitzig, K. Juttner, and W. J. Lorenz, "AC-Impedance Measurements on Corroded Porous Aluminum Oxide Films," *J. Electrochem. Soc.*, **133**, 887–92 (1986).

[78]S. D. Brown, K. J. Kuna, and T. B. Van, "Anodic Spark Deposition from Aqueous Solutions of $NaAlO_2$ and Na_2SiO_3," *J. Electrochem. Soc.*, **54** [8] 384–90 (1971).

[79]L. B. Sis, S. D. Brown, T. B. Van, and G. P. Wirtz, "Polymorphic Phases in Anodic-Spark-Deposited Coatings of Al_2O_3," *J. Am. Ceram. Soc.*, **57** [3] 108 (1974).

[80]D. L. Cocke, C. A. Polansky, D. E. Halverson, S. M. Kormali, C. V. Barros-Leite, O. J. Murphy, E. A. Schweikert, and P. Filpus-Luycks, "The Extent of the Phenomenon of Oscillary Anion Incorporation in Alumina Barrier Films," *J. Electrochem. Soc.*, **132** [12] 3065–66 (1985).

[81]W. L. Lee, G. Olive, D. L. Pulfrey, and L. Young, "Ionic Current as a Function of Field in the Oxide During Plasma Anodization of Tantalum and Niobium," *J. Electrochem. Soc.*, **117** [9] 1172–76 (1970).

[82]A. Waxman and K. H. Zaininger, "Al_2O_3-Silicon Insulated Gate Field Effect Transistors," *Appl. Phys. Lett.*, **12** [3] 109–10 (1968).

[83]K. H. Zaininger and A. S. Waxman, "Radiation Resistance of Al_2O_3 MOS Devices," *IEEE Trans. Elec. Devices*, **Vol. ED-16** [4] 333–38 (1969).

[84]R. Morgan, "The Microstructure Of Plasma-Anodised Alumina Films," *J. Mater. Sci. Lett.*, **6**, 1227–28 (1971).

[85]K. Kobayashi, K. Shimizu, and H. Nishibe, "The Structure of Barrier Anodic Films Formed on Aluminum Covered with a Layer of Thermal Oxide," **133** [1] 140–41 (1986).

[86]A. K. Chattopadhyay and A. B. Chattopadhyay, "Wear and Performance of Coated Carbide and Ceramic Tools," *Wear*, **80**, 239–58 (1982).

[87]H. Nakano, "Particle Size Analysis of the Coating for Space Shuttle Tiles," *Am. Lab.*, **13** [12] 57–60 (1981).

[88]K. B. Steinbruegger, J. S. Schruben, and Lyle H. Taylor, "Broadband Antireflection Coating for Infrared Transmissive Materials," U.S. Pat. No. 4 436 363.

[89]K. Shioya, "High Emissivity Refractory Coating, Process for Manufacturing the Same, and Coating Composition Therefor," U.S. Pat. No. 4 469 721.

Alumina as a Composite Material

Greg Fisher*
Consultant

Alumina is finding increased use in advanced-application ceramics, primarily because of the great knowledge already amassed on its properties, processability, and chemical durability. Composite materials are one of the advanced-application areas for which alumina is seriously being considered, and it will most likely find wide application in this area. The development of those composite materials which use alumina either as matrix phase or as a reinforcing phase is summarized. Concentration is on those composites which have high alumina contents and those using high-alumina reinforcing phases.

Author's Comment

The following article was completed in 1986. It describes the status of the technology for the use of alumina in composite materials for the time period 1970 through 1986. Several significant developments have occurred in the use of alumina in composites since 1986, in particular, the development of SiC whisker reinforcements for cutting tools and other structural components employing alumina as a matrix material. The reader should be aware that the patents covering this group of composites and their impact on the future of alumina composites have not been considered in the production of this article. The reader may await future updates of this publication or explore these developments through patents issued to the Department of Energy, including U.S. Pat No. 4 657 877 issued April 14, 1987, describing SiC whisker-reinforced ceramics, articles in the open literature, and information available from those companies supplying components based on this technology.

Improved understanding and technical development concerning the nature of ceramic materials have occurred since the first accounting of alumina as a ceramic material was completed. One of the major developments has been the use of ceramics in fibrous form to reinforce materials other than plastics and epoxy compounds, such as was being designed with glass fibers in 1970, the upper limit of coverage for the first compilation on alumina. Alumina materials are among those candidates for strengthening and being strengthened. In many cases, it is considered the most important ceramic engineering material, not because of its well-known properties as a refractory or high abrasion-corrosion-erosion-resistant material with moderate strength and fracture toughness, but due to the possibilities of improving some of these properties for specific applications at relatively low cost as compared to some of the monolithic materials under development for similar applications.

In a discussion of composites involving alumina, three general categories can be identified: composites involving alumina as a fiber or whisker, composites involving alumina and metallic materials in nonfibrous form, and composites involving alumina and other ceramics where at least two phases of ceramic remain distinct, i.e., low reactivity between the alumina and second ceramic material. A fourth type of composite does exist, involving the bonding of alumina to dissimilar materials such as metallized alumina substrates in electronic substrates and packages, and alumina coatings used in various applications. Both of these composites are considered in other reports within this volume and will not be elaborated on here.

Continuous Alumina Fibers

The first aspect of composites involving alumina fibers or whiskers that must be examined is the properties of the fibers or whiskers and how they make the alumina fiber a candidate for reinforcement in various matrix materials. However, there is another application for high-alumina fibers and whiskers that does not involve their use as a matrix reinforcement. This application is fibrous refractories and represents the widest use of high alumina-content fibers in the current market.

The first *Alumina as a Ceramic Material*[1] was compiled prior to the widespread application of refractory alumina fibers in industrial furnaces and other high-temperature insulating areas. However, U.S. Patents 3 082 051,[2] 3 082 099,[3] and 3 096 144,[4] issued to Wainer and Beasley; Beasley and Johns; and Wainer and Mayer, respectively, in 1963, and identified in *Alumina as a Ceramic Material*, are the beginnings of the technology for producing high-purity-alumina and high-alumina continuous fibers in production quantities. The second two patents pertain to the development of fibers from a substrate, but the first patent—involving the production of these fibers from spinneret extrusion of alumina paste—describes the same production elements found in many of the high-alumina fiber production processes used today. Also, in 1966 Lockhart and Wainer[5] produced spun alumina monofilaments (U.S. Pat. No. 3 271 173). However, the mass production of such fibers was delayed because

*Now with The Chemical Abstracts Division of The American Chemical Society.

potential applications for the fibers required lower cost products with higher production rates. But the technology of spinning fibers has revolutionized the refractory industry through the application of high-alumina fibers.

Most of the production of high-alumina fibers today goes into the fabrication of high-temperature refractory blanket, board, bundles, mat, paper, and loose fiber as produced by a number of refractory manufacturers. Typically, the composition of such fibers is aluminosilicate-based, with higher silica content leading to lower refractoriness for the fiber refractory.[6] Table I describes the various chemistries and use-temperature limitations of alumina fibers available today. The direct correlation between alumina content and refractoriness is modified only by the glass-forming ability of the other constituents. For instance, aluminoborosilicate fibers (patented by 3M Co.[7,8] and tradenamed Nextel) have a lower use temperature than aluminosilicate fibers with lower Al_2O_3 because of the glass-forming B_2O_3 present. However, this material replaces aluminosilicate fibers in many lower temperature applications because the B_2O_3 content inhibits crystal growth in the fibers over time at temperature—the eventual failure mechanism of fibrous aluminosilicate refractories.

The initial production of aluminosilicate fibers utilized a melt-forming method of producing fibers and stemmed from the production of high-alumina, chemical-resistant glasses in fiber form. Higher alumina content additions produced more refractory products, although the desired result was better alkali-resistant glasses.

Attempts to improve the refractoriness and crystalline stability of aluminosilicate fibers by Galushkin et al.[9] using Cr_2O_3 found problems with shot production using melt-spinning processes, but the Cr_2O_3 additions did produce fibers with lower shrinkages than straight high-alumina fibers produced from melt spinning.

Experiments with wider ranges of Cr_2O_3 content (1 to 35%) fiber at 3M Co.[10] took a different production route—extruding the materials and firing after matting. The process of producing fibers through the use of organic precursors also took hold around this time, even though initially conceived in 1963. Patents granted to ICI[11] in 1976 describe the formation of alumina fibers without silica. Today, they are tradenamed Saffil and have been used primarily in refractory applications.[12]

The main goal for these refractory alumina fibers was the development of a low-mass, highly insulating refractory[13,14] which could withstand continuous high-temperature exposure to combustion gases and by-products of combustion, as well as the outgassing of volatiles from sintering materials, with the aim of fuel savings (generally found to be between 25 and 40% over conventional refractory insulating firebrick[15]). A large number of engineering studies on refractory fiber products have been conducted since their introduction in the early 1970s and most manufacturing industries using high-temperature processes have tried utilizing these refractory fibers as insulation.[16,17]

The development process for high-alumina fiber with essentially refractory applications as their only use continued well past the initial development of the 95% Al_2O_3 fiber by ICI. Gaodu et al.[18] reported the melt production of a fiber with 80% Al_2O_3 content from electric arc melting of commercial-grade Al_2O_3 and quartz. The 80% Al_2O_3 fibers produced were reported to have refractoriness of 1870°C.

Low alpha Al_2O_3-content fibers also continued to be developed. Ekdahl[19] produced refractory fibers containing 5 to 35% alpha alumina fibers with the intent of making fibers from melts at lower temperature without loss of refractoriness as compared to fibers having 75 to 90% alpha alumina content.

However, those fibers suitable for consideration as reinforcement in composites require high strengths and modulus of elasticity in order to act as reinforcement to a matrix material.[20] Typically, reinforcement (continuous) fibers must have an elastic modulus twice that of the matrix material. Table II shows the physical properties of high-alumina fibers that have been considered for reinforcements for composites.

Gribkov et al.[21] reported literature values for the modulus of elasticity of alpha alumina ranging from 190 to 2300 GPa, depending on the orientation of the crystals tested. However, they determined values of 440 to 490 GPa for (0001), (10$\bar{1}$1), (21$\bar{1}$0), and (10$\bar{1}$0) crystal orientations by using ultrasonic vibration measuring techniques on alpha alumina whiskers grown by gaseous-phase deposition.

Table I. Chemistry versus Uses for Alumina-Containing Fibers*

Composition (wt%)							
Al_2O_3	SiO_2	B_2O_3	ZnO_2	ZrO_2	Other	Use Temperature (°C)	Application
25	60		15		1	985	Low temperature
43.9	50.1			5.1	0.7	1200	Refractory
56	38				6	1425	Mod. refractory
95	5					1650	Refractory
62	24	14				1204	Ref. textile
25	60			15	0.2	1090	Acid refractory

*Ref. 6. Used by permission.

Table II. Properties of Alumina-Containing Fibers

Property	Fiber FP	Saffil	Sumitomo Alumina	Nextel 440	Nextel 312	Fibermax
Composition (%)						
Al_2O_3	99+	95	85	70	62	72
B_2O_3				2	14	
SiO_2		5	15	28	24	27
Density (g/cm^3)	3.95	2.8	3.25	3.1	2.7	3.0
Diameter (μm)	20	3	17	11	11	2–3.5
Tensile strength (GPa)	1.39	1.03	1.79	1.72	1.72	
Elastic modulus (GPa)	378	103	210	241	151	
Use temperature (°C)	1315	1400	1248	1425	1200	1650
Liquidus temperature (°C)	2040	1980		1870	1800	1870
Coeff. therm. exp (10^{-6}/°C)			8.8		3.5	
Elongation (%)	0.35		0.85			
Dielectric constant					5	
Continuous	X		X	X	X	
Discontinuous		X		X	X	X
Supplier	du Pont	ICI-B&W	Sumitomo Chemical	3M	3M	Carborundum

Since the requirement for fiber-reinforced composites of a fiber modulus of elasticity twice that of the matrix somewhat governs the combinations of materials that can be produced as composites, the development of alumina fibers having near the maximum modulus of elasticity has been the goal of research, i.e., to maximize the range of matrix materials suitable. (The relation between fiber and matrix modulus is held such that, as the matrix material fails under tensile loading, the load is supported by the fiber reinforcement long enough to permit identification and replacement of the failing component.) Because of this need and the concomitant high chemical purity of the fiber, methods of producing fibers via polymer spinneret processing, as first patented in 1963, are again being considered for alumina fiber production.

The renewed investigations into the production of high-alumina fiber via nonmelt processing includes the work at Bayer AG[22] on dry spinning an aluminum compound containing polyethylene oxide and sizing the fiber with polyvinyl acetate before heat-treating. In this process, the fibers were preferably spun with silicon or other modifiers—leading to fibers not necessarily designed for reinforcement.

Battelle Development Corp.[23] devised a process of melt-forming Al_2O_3 fibers, but the process required temperatures above the melting point of Al_2O_3 in order to form a liquid drop of the material, with a viscosity between 10^{-4} and 10^{-1} Pa • s and surface tension of 10 - 2500 dynes/cm, which could be drawn into fiber form.

Researchers at Hepworth and Grandage Ltd.[24] utilized carbon to initiate a reaction to purify alumina-containing materials in an attempt to produce alumina whiskers which could be used as three-dimensional reinforcement for matrix materials without the problems of fiber lay-up. In the reaction, the alumina-bearing material is reacted with the carbon and gaseous aluminum trihalide. The reaction gases are then rereacted, i.e., the aluminum monohalide and CO formed in the first reaction precipitated Al_2O_3, carbon, and aluminum trihalide. At this stage, the alumina may be precipitated on a metallic surface or other suitable substrate for collection.

Gribkov et al.[25] also discovered the growth of alpha alumina whiskers during oxidation of Al in moist H_2. The mechanism for whisker growth was noted as a vapor-liquid-solid reaction as the aluminum alloy begins to melt. Volkadov[26] continued these pursuits by examining the role of moisture in the oxidation of Al metal and the growth of whiskers from the reaction surface.

At the same time, U.S. researchers pursued the production of continuous alumina fibers. Hayes and Sobel[27] patented a process of producing alumina fibers from an alumina sol and hexamethylenetetramine mixtures using organic precursor methodology. However, Pearson and Marhanka[28] pursued traditional methods of producing ceramic polycrystalline materials and patented a process that produced alumina fibers from an alumina slip of high solids content—similar to the extrusion processes developed in 1963.

The successful production of a polycrystalline alumina fiber having an alpha alumina content approaching 99% and its incorporation into a metal matrix is described by Dhlagre[29] in U.S. Pat. No. 4 036 599. The fibers were reported to have 1.5 GPa tensile strengths with diameters of 15 to 25 μm. Although the production methodology for the fibers is not disclosed in the patent, the small fiber diameter and smoothness of the fibers (roughness of 0.23 to 0.30 μm with 0.85 μm period) could not have been produced through either extrusion processes or recrystallization of a melt-produced fiber. Also, only the organic precursor processing has proved capable of yielding fiber with greater than 90% alpha alumina content. The

fibers produced by E. I du Pont de Nemours and characterized in this patent are tradenamed FP. To date, these are the only high-alumina fibers that have been used successfully in composite structures.

A process for production of precursors that lead to alumina fiber was disclosed by Takeshi et al.[30] in U.S. Pat. No. 4 348 341. The polymeric precursor material is gelled to a viscosity between 0.5 and 2 Pa • s before subjecting the material to a form of spray dryer with a funnel-shaped disk.

The development of alpha alumina from polymeric precursors is described by Birchall[31] for aluminum chloride precursors, but other anions have similar processing. He indicates that, for continuous fiber production, a viscosity of 10 to 100 Pa • s is required for the polymer. Drying of the fiber and dehydrating is a three-stage process. The first stage involves conversion of the gel to a crystalline form without disturbing the fiber structure. Here temperatures of 300° to 400°C are used to generate eta and gamma alumina fibers. The second stage further dehydrates the fiber and completes organic burnout. The delta and theta phases of alumina appear during this stage with heat treatments at 400° to 1000°C. The final heat treatment converts the theta-phase to alpha-phase alumina. This generally is a rapid transition at the 1000°C temperature point, but depends on the conversion to theta phase. Birchall reports that, as crystallization progresses, the tensile strength of the fiber decreases, with the eta-phase fiber having the highest tensile strength. Table III shows the change in properties for a 96% alumina-4% silica fiber produced from aluminum chloride precursors as the crystalline phase changes. The inclusion of grain-growth inhibitors, such as Si, B, P, and Zr oxides, can be made in the precursor stage by the addition of appropriate salts to the solution and can limit grain-boundary mobility, thus allowing the high-temperature conversion to alpha phase to take place without grain growth.

Alumina Fiber Composites

For continuous fibers, the incorporation of these alumina fibers into a matrix material to form a composite requires fiber lay-up, followed by some form of permeation of the fibers by the matrix material. When ceramic matrix materials are used, the methods of infiltrating the fibers with matrix material generally involve powders of the matrix which can be coated on the fiber prior to lay-up in the form of a slurry coating.

Miedaner and Kucheria[32] developed a process for impregnating an alumina/alumina composite by blending colloidal alumina, aluminum chlorohydrate, and an inorganic acid (either hydrochloric or nitric) with water, and infiltrating the alumina fiber network with the resulting slurry. To convert the aluminum chlorohydrate to alumina, a drying and calcining cycle is incorporated into the processing. After lay-up, the coated fiber is hot-pressed to form the dense composite.

Some researchers are using glass powders[33] to produce zero-porosity composites with high fiber loading. However, in the case of alumina fibers, the reactivity of the matrix powder and the fiber must be considered; glass matrix materials have been found to be reactive with alumina fibers. Alternate methods of infiltration include polymer pyrolysis of organic materials, leading to a ceramic matrix, and CVD deposition of the ceramic materials from gaseous reaction and infiltration of the fiber network.

Kimura and Yasuda[34] explored the effect of $Mg_3(PO_4)_2$ materials as matrices for alumina fiber and found that a reaction zone formed at 20 μm out from the fiber surface. The reaction product was determined to be $MgO \cdot Al_2O_3$ spinel, formed after a 1250°C, 2-hour hot-pressing cycle. The effect of the reaction between fiber and matrix is a weakening of the fiber and loss of reinforcement for the composite.

Rice et al.[35] reported success in preventing the reaction of Al_2O_3 fibers with matrix materials through BN coatings applied to the fibers. Experiments comparing the effect of the coating on strength retention showed that Al_2O_3 fibers without coatings had strengths of 130 MPa, while those that were coated had strengths of 250 MPa. The coating thicknesses used were approximately 0.2 μm and the researchers believe that thicker coatings would improve the performance of the fibers. Coating the composite not only prevents the reaction between the fiber and matrix but, because of this reduced reaction, the fibers exhibit pull-out during failure of the matrix, adding to the strain elongation of the composite, i.e., strain to

Table III. Property Changes for Alumina Fibers with Crystalline Phase

Phase	Crystal Size (nm)	Crystal-linity (%)	Alpha Alumina (%)	Porosity Volume (mm^3/g)	Shrinkage at 1400°C (%)	Tensile Strength of 3.0 μm Fiber (MPa)	Elastic Modulus of 3.0 μm Fiber (GPa)
eta	6	50	0	200	18	2200	110
eta/gamma		62	0		17		
gamma		68	0	187	14		
gamma/delta		77	0	121	8	2150	
delta	500	79	0–5	73	6.5	2100	280
delta/theta		86	5–10		2.0	2050	300
delta/alpha/mullite	1000	97	20–50	0	0.5	1550	320 (20% alpha)
alpha/mullite	2000+	100	90	0	0	1200	360

failure, as well as reducing the interaction of crack fronts with the fiber, adding to the fracture toughness of the composite. Four times the fracture resistance and twice the strength of uncoated fiber composites have been reported for Al_2O_3/SiOC composites.

Colmet et al.[36] developed an alumina fiber/alumina composite material using chemical vapor infiltration (CVI) to produce a matrix phase in the fiber network. They reported that the alpha alumina fibers, having the best mechanical properties, were difficult to work with because of large diameters and high Young's modulus, but were the most promising. Optimum CVI parameters for the reaction: $2AlCl_3(g) + 3H_2(g) + 3CO_2(g) \rightarrow Al_2O_3(s) + 3CO(g) + 6HCl(g)$ were reported at temperatures of 900° to 1000°C, pressures of 2 to 3 kPa, and gas flow rate (D) = 100 cm^3/min. Fired porosities after CVI were reported as low as 12% with 40 vol% fiber. In these tests, high bonding characteristics between the fiber and matrix were one of the causes of low flexural strengths. The fibers were not coated with nonreacting materials. Flexural strength values for low-porosity composites were reported as 200 MPa at room temperature.

Pierre et al.[37] reported production of ceramic/ceramic composites having either alumina or SiC fibers and either alumina or zirconia matrices by immersion of the fibers in a sol or gel of the matrix material. This process utilizes the fluid condition of the sol to penetrate the fiber network. Gellation of the sol and drying before sintering create the ceramic/ceramic composite. These researchers indicated that the mechanical properties of the composites utilizing alumina were poor after heat treatment. No indication of the use of fiber coatings was given.

Chokshi and Porter[38] studied alumina matrices with 15 wt% SiC whisker reinforcement and found that the whiskers improved the creep resistance of the polycrystalline alumina matrix at 1773 K. The composites were produced by hot-pressing at 1300 K.

In other research involving alumina in ceramic/ceramic composites, Karpinos et al.[39] utilized a dry-mix Al_2O_3 and mullite single-crystal whiskers hot-pressed at 1.5 to 2 MPa and 1500°C in a graphite mold. They claimed that the mullite crystals do not react with the polycrystalline alumina under these conditions and remain distinct whiskers with mullite composition.

Sheldon and Lewis[40] inverted this relation between the chemistry of the fibers and matrix in composites utilizing mullite matrices and high-alumina fiber (the fibers were actually aluminosilicate with a composition similar to that of mullite). They found that, although there was almost a doubling of the Young's modulus for the composite utilizing 11.5% fibers over the unreinforced mullite matrix, the 13 MPa strength of the composites falls significantly short of the 80 MPa desired to use the material for bioceramic applications. These researchers felt that higher alumina content in both the fiber and matrix would improve the properties.

Barta et al.[41] examined alumina matrix materials reinforced with mullite, SiC, and graphite fibers added in 5 to 10 vol%. They used reactive alumina as the matrix in all cases and hot-pressed the composites at 1400°C and 18 MPa for 30 minutes. In their processing, they found that the highly reactive alumina matrix reacted with the mullite fibers such that no evidence of the mullite fibers could be found after hot-pressing. They also found high bonding between the SiC fibers and the matrix, but the graphite fiber additions did tend toward increased fracture toughness for the composite.

Investigations on alumina matrix materials reinforced with SiC fiber conducted by Tiegs and Becher[42] have shown that fabrication of these composites is possible without pressure sintering when fiber volumes are kept below 20%. These researchers also worked on the combination of whisker reinforcement of alumina and mullite matrices with transformation toughening using zirconia materials. Potential applications of the materials are in the high-stress areas of heat engines where good thermal shock properties also are required.

The most advanced composites utilizing alumina fibers are those having metal matrices. The incorporation of alumina fibers in a magnesium metal matrix was patented[29] along with the development of the 99% alpha alumina fiber developed at E. I. du Pont de Nemours. As in the case of the ceramic matrix composites, infiltration of the alumina fiber can be achieved in several ways: a slurry coating or infiltration using powder metals instead of ceramics, melt infiltration, and deposition. The first process may be the more promising, but requires the production of powder metal, slurry formation, and calcining and sintering in reducing atmospheres. Without protective coatings on the alumina fiber, severe degradation of the fiber can be expected using this process. Melt infiltration of the alumina-fiber network is the more common practice and can be achieved either by pouring molten metal into the fiber lay-up network or by hot-pressing a sandwich of alumina-fiber network and metal film. Deposition techniques that are being explored are dissimilar to those being used in ceramic matrix cases. The more common practice for metal deposition is direct deposition of the metal onto the individual fiber prior to lay-up and using liquid-phase sintering to consolidate the matrix. Experiments have also been conducted on infiltration techniques using deposition processes.

Two primary metals are being examined for reinforcement with Al_2O_3 fibers. The first development was that by Dhlagre,[29] using Mg metal films to infiltrate the fiber FP developed in 1977. However, since that time many other low-temperature-melting metals have been examined as matrices for these composites.

Hartman[43] developed a technique for coating lead onto alumina fibers by reducing lead oxide that is deposited on a glass coating on the alumina fiber. The glass coating prevents the degradation of fiber during reduction of the lead oxide while also giving added strength to the fiber.

Alumina metal-matrix composites are receiving the most attention and have the greatest potential for application to date. One product under development, reported by Folgar et al.[44] involves the use of alumina-fiber reinforcement of aluminum in the production of connecting rods for automotive engines. The products involve 30 to 50 vol% of alumina fibers and are 35% lighter (leading to reduced inertia) than steel counterparts. These components are being further developed by Toyota Motor Corp.,[45] but they are not the only Japanese manufacturer examining the potential use of these composites.

The first indication of the effects of Al_2O_3 content in aluminum metal is found in reports from Kothari.[46] He found that, in hot-pressing of aluminum, final densities for the metal were affected by the presence of oxide. Densification of the metal was found to be more difficult with increasing oxide content ranging from 1 to 10% Al_2O_3 as a coating on the metal grains.

Researchers at Sumitomo Chemical Co.[47] produced an alumina-fiber-reinforced aluminum composite by beginning with fibers produced by calcining polyaluminoxane and silicon compounds (no alpha-alumina phase is produced) and vacuum impregnating these fibers with a melt of aluminum metal at 800°C or depositing the metal directly onto the fibers by vapor deposition, plasma spraying, or chemical plating before laminating.

Yamatsuta and Nishio[48] described the use of an alumina fiber containing silica as reinforcement for an aluminum alloy containing Cu, Si, Mg, and Zr. The advantages of the alloying ingredients are lower melting temperature of the alloy and thus a lower temperature heat-treatment schedule.

Cornie et al.[49] report that Al-Li and Al-Mg alloys have been used with alumina fiber, indicating that the alloys generally exhibit secondary phases nucleated at the fiber/metal interface. They also report that commercial Mg alloys also have been used to infiltrate fiber FP alumina.

Dinwoodie et al.[50] report that staple fibers of alumina-4% silica have been used to reinforce aluminum in the production of metal-matrix materials that act as reinforcements for automotive pistons. They used Al-9Si-3Cu and Al6061 alloys in the development, and powder metallurgy techniques for infiltrating the 29 vol% staple fiber. Higher fiber volume loadings were reported to be possible, but only with decrease in the length of the staple fibers.

Cornie et al.[51] however, reported that composites containing 42 and 40 vol% of 20 μm diameter continuous alumina fibers or 140 μm SiC fibers, respectively, can be accommodated in Al-4.5%Cu alloys when pressure-casting processes are used to infiltrate the fiber network.

Page and Leverant[52] produced composites containing 35% continuous alumina fibers in pure Mg, magnesium alloy ZE41A (Mg-4.25%Zn-0.5%Zr-1.25%RE), and Al_3Li, showing that the fiber orientation controls the ultimate tensile strength, Young's modulus, and elongation before failure for the composite. Orientations at 0° to the tensile direction yielded the largest strengths and Young's modulus for the composites. The largest elongations were generally found when fibers were oriented 45° to the tensile stress.

Nunes et al.[53] worked with fiber concentrations of continuous alumina fiber up to 55 vol% in ZE41A matrices produced by liquid infiltration. They found that a 0.25 μm wide reaction zone between the fiber and matrix is produced in the process. The reaction zone is composed of spinel $MgO \cdot Al_2O_3$ precipitates. They also found that the Young's modulus and ultimate tensile strength of the composites increase with increasing fiber volume percent and that 0° orientations to the tensile stress produced the highest values for these two properties.

The reaction zone formed when alumina fiber is used as a reinforcement in metal-matrix composites actually improves the properties of the composite. This is in direct contrast to ceramic-matrix composites having ceramic fibers. The thin reaction zone surrounding the alumina fibers found in cases of Mg alloy matrices (and also occurring in Al matrix cases, but quite often disguised because of the chemistry of the reaction products) bonds the fiber to the matrix both chemically and physically. This allows the fiber to toughen the matrix with regions of higher hardness and to increase fatigue creep resistance of the metal.

Metal Ceramic Particulate Composites

The earliest utilization of ceramic and metal combination was in the form of cermets, so named because of the mixture of ceramics and metals that make up their microstructure. The greatest use of these materials has been in cutting tools—the most notable of which is WC-Co cemented cermets. However, alumina as the ceramic phase has been very prominent in the research in these materials, particularly for potential structural applications where high thermal shock resistance is required.

Most of the research that has been performed since the publication of *Alumina As A Ceramic Material* has been directed toward this same goal of a structural ceramic with excellent thermal shock and oxidation resistance. However, some research has been directed toward the electronic properties of alumina-containing cermets. Pakswer and Stevens[54] investigated the secondary electron emission of cermets produced from alumina and thin films of gold. They found that the secondary electron emission is dependent on the dielectric properties of the ceramic

and, of the materials tested, the Au-Al_2O_3 cermet was second only to Au-$BaTiO_3$ in secondary electron yield.

Gualandi and Jehenson[55] patented a process for the production of a structural composite using Al-Mg and Al_2O_3-MgO, which was meant for the high-temperature thermal-shock conditions of fission reactors.

Many of the cermets using alumina ceramic developed during the 1970s involved the use of Ni and the modification of the metallic alloy to allow wetting of the ceramic by the metal. Guazzi et al.[56] devised a method of electrodepositing Ni-Al_2O_3 composite cermets in an effort to attain good bonding between the metal and ceramic.

Ownby and Lahmann[57] determined that the partial pressure of oxygen during sintering of chromium-alumina cermets affects the mechanical properties of the cermet. When the oxygen partial pressure is maintained well above the equilibrium value, the strength of the cermet is 40% higher than at equilibrium partial pressures. This factor is unique to cermets containing chromium because of the multiple valency of the metal and its potential to reduce alumina.

Jangg et al.[58] found that they could produce cermets using porous alumina with a wide variety of metals regardless of the natural tendencies of those metals not to wet the alumina. They resorted to a process of coating the alumina with layers of metals in the pores of the ceramic. The coating process can also be achieved by infiltrating the ceramic with liquid metals to reduce the alumina along the pore surfaces. Thereafter, the ceramic can be metallized. They used Cu, Al, Ni, Fe-Ti, Zr, and other alloys in their infiltration experiments.

A patent issued to Roparco[59] describes a seal produced from plasma spraying Al-Al_2O_3 onto a substrate. The cermet produced from this process is comprised of 55 to 80% Al or Al alloy and 20 to 45% Al_2O_3 and is used for automotive engine wear seals.

Aluminum cermets with alumina ceramic have also been developed for their electrical properties. Hirai et al.[60] patented a process for producing an Al-Al_2O_3 dispersion composite that can be used as a conductive material, and Wilson[61] patented a process of combining spinel ($MgO{\cdot}Al_2O_3$) with aluminum metal.

Crispin and Nicholas[62] determined that nickel alloys could be made to wet alumina to produce Ni-Al_2O_3 cermets when additions of 1 to 2 wt% Cr or 0.02 to 0.08 wt% Y are added to the nickel. Further additions of either of these metals was found to cause a weaker bond to be formed.

Kislyi et al.[63] took another approach to producing cermets with high refractoriness and high thermal shock resistance. They combined W and Al_2O_3 at temperatures above 1800°C. They claimed that the reaction intensifies in the presence of molten alumina, but the reaction also causes strong bonding of the two species with the formation of WO_3 and metallic Al at the Al_2O_3 grain surfaces.

The difficulty in producing dense Cr-Al_2O_3 cermets, which was addressed by oxygen partial pressure control during sintering, was also examined by Cho and Puerta.[64] They found that up to 1 wt% additions of TiO_2 also improved the shrinkage, bulk density, and microhardness of the Cr-Al_2O_3 cermets (70% Al_2O_3). They found they could produce cermets with 84.5% and 87.4% densities using 1 and 5 wt% TiO_2 additions, respectively, with 1500°C, 10-hour sintering in air.

The use of molybdenum as the metallic phase for alumina-containing cermets has also been explored to produce refractory ceramics with good thermal shock properties. Goad and Moskovits[65] explored the bonding of colloidal metals in Al_2O_3 including Mo, by examining the specular reflectance spectra. Skidan et al.[66] examined cermets with up to 30% Mo and determined a mathematical relation for determining the optimum heat treatments for producing the maximum in mechanical properties for the cermet.

Bahat and Chu[67] found that glass-ceramics based on Ta_2O_5 and $BaO \cdot Al_2O_3 \cdot 2SiO_2$ and $Al_2O_3 \cdot Ta_2O_5$ could be combined with Mo to form cermets that have refractoriness when processed above 1400°C.

Yamamoto and Sendai[68] produced an electric heating element using $MoSi_2$-Al_2O_3 with less than 20 wt% $MoSi_2$. They found that a transition from resistive to conductive material occurs with $MoSi_2$ equal to 50 vol% and that strength of the electrical resistance heater was greater with the Al_2O_3 than without.

Kelly[69] utilized Mo at 50 wt% to produce cermets for bonding electrical feedthrough pins in insulator materials such as Al_2O_3. These cermets are produced by isostatically pressing and then sintering at 1620°C for 3 hours in wet hydrogen.

Morgan et al.[70] explored both Al_2O_3-Pt and Al_2O_3-Cr cermets for thermal shock resistance and toughness characteristics. In order to include Cr in the ceramic, they used chromium compounds such as $Cr(NO_3)_3 \cdot 9H_2O$ and reduced them by coating the Al_2O_3 powders with paraffin and firing in an H_2 atmosphere at 1300°C for 10 minutes before hot-pressing. The cermets formed were examined microscopically; it was found that cracks produced during thermal shock cycling were diverted by the metal inclusions in the ceramic. These researchers concentrated on Al_2O_3-Cr because grain growth during sintering of Al_2O_3-Pt left the Pt dispersed within the Al_2O_3 grains. These cermets are used as hermetic seals in reflood sensors located in nuclear fission reactor chambers.

Ceramic Particulate Composites

The great interest in developing new ceramic-metal composites using alumina has largely been displaced by the newer technologies of producing composite materials. The fiber composites already described contribute in part to the redirected interests, but another group of ceramics is the main reason that interest and research are no longer heavily focused on

cermets. This group of ceramics is the last category of alumina composites, namely, those alumina ceramics containing a second, discrete ceramic phase that is not a fibrous (or whisker) component, yet acts as a reinforcing agent for the alumina matrix. The reinforcement in this case is a particulate material that, through unique properties, can relieve stress energy in the alumina and thus give the composite much greater flexural strength than the unreinforced matrix alumina. The mechanism of stress relief demonstrated by the particulate reinforcement, i.e., in the case of ZrO_2, phase transformation accompanied by volume changes, also acts to inhibit crack propagation, yielding higher fracture toughness for the composite in relation to unreinforced alumina materials. However, the absorption of the stress energy need not take place in the form of transformation of the particulate reinforcement phase. It can be partially absorbed by the reinforcement phase, leading to crack deflection. This can occur even if only a variation in crystal structure or density is found in the reinforcement phase.

Samdani et al.[71] explored combinations of 75, 50, 25 wt% TiO_2 with 25, 50, and 75 wt% Al_2O_3 to determine the effects of combined diverse ceramic phases on density, phase change, and strength. In their preliminary examination, only the low-alumina-content composite had good strength characteristics. They also found that the ceramic phases did not remain distinct under sintering conditions, but combined to produce Al_2TiO_5, especially at a 1000°C soak of 3 hours. Solid solutions of Al_2O_3 and TiO_2 have more recently been experimented with in applications of ceramics in automotive engines because of their thermal shock characteristics.[73] However, their relatively low modulus of elasticity and strength characteristics make them poor candidates for application as compared to other materials under consideration.

Krylov[73] established the possibility of producing dense ceramics from combinations of Al_2O_3 and TiB_2. In these experiments, the highest densities were produced when 20% TiB_2 was added to the Al_2O_3 and sintering temperatures of 1500° to 1700°C were used.

Studies of the inclusion of ZrO_2 in an alumina matrix began in 1974 with Claussen's[74] examinations of the effects on alumina fracture toughness with inclusion of 15 vol% ZrO_2 in the alumina matrix. Fracture toughness values of 10 MPa • $m^{1/2}$ were produced when the ZrO_2 powders placed in the matrix had particle sizes averaging 4 μm. The volume fraction of ZrO_2 was determined to be optimum at 15%.

Sorrell and Sorrell[75] looked at the phase stability of the ZrO_2 in the alumina matrix by investigating the system ZrO_2-Al_2O_3-SiO_2. Their studies dealt mainly with the range of compositions containing from 30 to 70 wt% ZrO_2 and low Al_2O_3 content and focused on the production of $ZrSiO_4$ from reaction of the end-members in the system.

Greve et al.[76] examined composites having particulate ZrO_2 at 16 vol% dispersed in an alumina polycrystalline matrix. Their examination of the thermal conductivity/diffusivity of the composite led to the conclusion that microcracking which occurs on cooling at temperatures around 800°C is caused by the phase transformation of ZrO_2 from tetragonal to monoclinic and the subsequent 3% volume increase, and that on cooling from below 800°C, no hysteresis is seen in these properties because the cracks induced from the volume change do not close due to the expanded ZrO_2. These researchers inferred that the lack of thermal hysteresis effects should also be apparent in mechanical properties for these materials. Fracture toughness values of 7.14 MPa • $m^{1/2}$ were obtained for composites produced in their experiments. This is in comparison to values of 5.06 MPa • $m^{1/2}$ for alumina.

Iordanov et al.[77] observed changes in the electrical characteristics of alumina with the addition of 0.5 wt% ZrO_2 and a glass phase based on the composition 23.3 CaO, 14.7 Al_2O_3, 62 SiO_2. The breakdown voltage was identified as increasing from 20 to 24 kV/mm, while the dielectric loss decreased and the electrical resistivity and dielectric constant increased. Impact and flexural strengths of these 95% Al_2O_3 ceramics also increased with increasing ZrO_2 content.

Claussen and Jahn[78] examined mixtures of alumina and zircon reacted in situ to produce mullite and zirconia and found a dependence on the sintering time at 1400° to 1500°C on the percent tetragonal phase present in the mullite matrix. The transformation of some of the tetragonal phase to monoclinic from heat treatment was reported to reverse on cooling, leading to microcracking. Samples of these materials were reported to have fracture toughness values of 4.5 MPa • $m^{1/2}$ and strengths of 400 MPa (hot-pressed mullite strengths are 269 MPa).

Boch et al.[79] report that the formation of the mullite-ZrO_2 composite from Al_2O_3 and $ZrSiO_4$ is not easy to control due to competition effects between the reaction and densification of the ceramic. Their research examined powder characterization and process control aimed at producing dense ceramics.

Burden[80] reported that the consideration of Al_2O_3-ZrO_2 as a ceramic cutting tool is underway, where 10 to 20% ZrO_2 is added to the Al_2O_3. This is based on modulus of rupture values of 690 to 1035 MPa and fracture toughness values from 5.1 to 10.0 MPa • $m^{1/2}$.

Other mechanisms for toughening alumina matrices have also been examined. For instance, Noma and Sawaoka[81,82] have experimented with the addition of a dispersed diamond phase in alumina. The diamond is transformed to graphite during sintering and a correlation in the percent of diamond phase to the increase in fracture toughness was made. While the increases in fracture toughness are attributable to a transformation of the diamond to graphite, this holds true only for 5 vol% diamond content. Higher concentrations of diamond did transform to graphite in heat treatment but did not exhibit toughening. Fracture toughness values

of 6.7 MPa • $m^{1/2}$ were reported for 75% diamond-to-graphite conversions.

The inclusion of HfO_2 with the ZrO_2 as a solid solution in alumina matrices was first reported by Claussen et al.[83] The HfO_2 addition was believed to enhance the transformation rate for the ZrO_2 in going from tetragonal to monoclinic phase. Since then, Schioler et al.[84] have added Cr_2O_3 at 15 mol% to the alumina matrix as a solid solution in order to reduce the thermal conductivity of the alumina. In their research, up to 15 vol% ZrO_2:HfO_2 solid solutions were dispersed in the matrix. The best fracture toughness for these materials was reported as 5.29 MPa • $m^{1/2}$ for 10 mol% Cr_2O_3 in Al_2O_3, 10 mol% HfO_2 in ZrO_2, and 10 vol% dispersed phase. On heat treating to 1000°C for 500 hours, the best fracture toughness was reported for 20 mol% Cr_2O_3 in Al_2O_3, 10 mol% HfO_2 in ZrO_2, and 10 vol% dispersed phase.

Experiments by Biel and Tien[85] to optimize the HfO_2 content in the ZrO_2 determined fracture toughness values of 6.75 MPa • $m^{1/2}$ for 10 mol% HfO_2 and 5.8 MPa • $m^{1/2}$ for no HfO_2 content. These specimens were aged as long as 300 hours at 1200°C.

Recent reports by Shin et al.[86] on the densification of Al_2O_3/ZrO_2 composites indicates that two primary mechanisms occur during hot isostatic pressing. The low-temperature densification is described as an intergranular, glassy-phase, shear mechanism. High-temperature densification was reported to be controlled by plastic deformation of the grains.

Wang and Stevens[87] reported forming Al_2O_3/ZrO_2 composite ceramics with 99% theoretical density using conventional sintering techniques. Strength was correlated to the microstructure of the ceramic and an explanation of the 12 MPa • $m^{1/2}$ toughness attributed the value to low grain size and low defect content.

Other complex combinations of materials have been added to alumina matrices to enhance the fracture toughness and strength of the material. The combination of materials being examined by Inoue et al.[88] involves both ZrO_2, partially stabilized with 2 mol% Y_2O_3, and SiC whiskers. A fracture strength of greater than 1300 MPa was reported for the combination of 70 vol% Al_2O_3/15 vol% SiC whiskers/15 vol% ZrO_2, which was attributed to both load transfer and toughening mechanisms.

Claussen[89] also reports using the SiC whisker and yttria-stabilized tetragonal zirconia polycrystalline material as reinforcement for alumina. To accommodate the thermal mismatch between the SiC whiskers and Al_2O_3, some of the ZrO_2 was left in the unstabilized form. The unstabilized ZrO_2 transforms at 750°C, yielding compressive stresses in the matrix which compensate the tensile stresses of the SiC whiskers.

The effect of particulates on the strength behavior of materials was studied by Risbud[90] using a 50 vol% glass composition based on 70 wt% SiO_2, 14 wt% B_2O_3, 16 wt% Na_2O, and 50 vol% Al_2O_3 particulates. While this study was directed mainly at the effects of surface grinding on the strength of the composite, work by Lange[91] using the same glass and 10 to 40 vol% Al_2O_3 was aimed at determining the effect of particulate doping on the fracture energy of the homogeneous glass. He found that increased volume fraction of particulate dispersant led to higher fracture energy as well as increased strength. The fracture energy also increased with increasing dispersant size, but flexural strength did not follow the same pattern and larger dispersant-phase particles were shown to possibly lead to lower flexural strength.

Mussler and Shafer[92] examined a cordierite glass containing ZrO_2 precipitates and reported that these glasses had constant fracture toughness values while the zirconia remained in solution, independent of ZrO_2 content. However, when the glass was heat-treated and cordierite and ZrO_2 crystallized, the fracture toughness increased. Increases in fracture toughness were found to be directly dependent on the heat treatment and varied microstructure formed during the heat treatment and not transformation toughening due to ZrO_2 transformation. The mechanism for increased fracture toughness was proposed as crack deflection since the ZrO_2 was believed to be fully stabilized by the MgO present in the glass composition.

Alumina-containing composite materials are the most diverse of engineering ceramics being studied and applied today. The basic material's compatibility with other oxide and nonoxide materials lends it to be combined for trial development of newer, more exotic composites. While the combinations of materials and the research already described point out what has been recently explored in the development of alumina composites, the possibilities of new combinations of materials with alumina still exist. Of those composites identified, most likely to be in mass production by the beginning of the 21st century are Al_2O_3/Al fiber-reinforced metal-matrix composites and ZrO_2/Al_2O_3 particulate-reinforced ceramic-matrix composites. But greater strength and fracture toughness application requirements still exist and future combinations of alumina and other ceramics will have to be studied to meet these needs.

References

[1]Alumina as a Ceramic Material. Edited by Walter H. Gitzen. The American Ceramic Society, Inc., Columbus, OH, 1970.

[2]E. Wainer and R. M. Beasley, "Fiber Forming Process," U.S. Pat. No. 3 082 051, March 1963.

[3]R. M. Beasley and H. L. Johns, "Inorganic Fibers and Method of Preparation," U.S. Pat No. 3 082 099, June 9, 1963.

[4]E. Wainer and E. F. Mayer, "Method of Making Inorganic Fibers," U.S. Pat. No. 3 096 144, July 2, 1963.

[5]R. J. Lockhart and E. Wainer, "Preparation of Alumina Monofilaments," U.S. Pat. No. 3 271 173, September 6, 1966.

[6]W. L. Shepard, Jr., "Ceramic Fibers"; pp. 505–507 in Corrosion and Chemical Resistant Masonry Materials Handbook. Edited by W. L. Shepard, Jr. Noyes Publication, Park Ridge, NJ 1986.

[7]Minnesota Mining and Manufacturing Co., "Nonfrangible Alumina-Silica Fiber," Br. Pat. No. 1 580 973, December 10, 1980.

[8]K. A. Karst and H. G. Sowman, "Nonfrangible Alumina-Silica Fibers," U.S. Pat. No. 4 047 965, September 13, 1977. Assigned to 3M Co.

[9]A. P. Galushkin, K. Ya. Sal'nikov, and V. I. Kys'kov, "High-Thermostability Aluminochromosilicate Fiber," *Refractories*, **16** [5] 318 (1975).

[10]Minnesota Mining and Manufacturing Co., "Alumina Chromia-Metal (IV) Oxide Refractory Fibers Having a Microcrystalline Phase," Br. Pat. No. 1 479 639, July 13, 1977.

[11]Imperial Chemical Industries Ltd., "Alumina," Br. Pat. No. 1 425 934, February 2, 1976.

[12]M. R. Harris, "First Experiences with Aluminum Oxide and Zirconium Dioxide Fiber Insulating Materials," *Sprechsaal*, **109** [7] 405 (1976).

[13]H. J. Siebeneck, R. A. Penty, D. P. H. Hasselman, and G. E. Youngblood, "Thermal Diffusivity and Thermal Conductivity of a Fibrous Alumina," *Am. Ceram. Soc. Bull.*, **56** [6] 572–73 (1977).

[14]E. I. Aksel'rod, I. I. Vishnevskii, D. B. Glushkova, et al., "Thermal Conductivity of High-Porosity Insulating Materials Made from High-Alumina Refractory Fibers," *Ogneupory*, **10**, 8–13 (1979).

[15]R. Harris and M. J. Sherrard, "Alumina Fibers for Fast Firing Tunnel Kiln Sledges," *Ind. Ceram.*, **727**, 270–75 (1979).

[16]Y. Maruyama and G. Kurihara, "Durability of Alumina Fiber-Quality Evaluation of Alumina Fiber in Reheating Furnace After 2 Years Use," *Taikabutsu Overseas*, **4** [4] 33–36 (1984).

[17]R. E. Pawel, D. L. McElroy, F. J. Weaver, and R. S. Graves, "High Temperature Thermal Conductivity of a Fibrous Alumina Ceramic," July 31, 1985 Report on U.S. Department of Energy Contract No. DE-AC05-840R21400.

[18]A. N. Gaodu, I. G. Subochev, and M. M. Mirak'yan, "Production of High-Alumina Ceramic Fibers," *Proizvod. Spets. Ogneuporov*, **3**, 53–57 (1976).

[19]W. G. Ekdahl, "Method of Producing Alumina-Containing Fiber and Composition Therefore," U.S. Pat. No. 4 251 279, February 17, 1981. Issued to Johns-Manville Corp.

[20]G. Fisher, "Composites: Engineering the Ultimate Material," *Am. Ceram. Soc. Bull.*, **63** [20] 360–64 (1984).

[21]V. N. Gribkov, A. A. Muskaseev, and B. V. Shchetanov, "Normal Modulus of Elasticity of Ceramic Whiskers," *Sov. Powder Met. Metal Ceram.*, **3**, 243–46 (1970).

[22]"Processing of Aluminum Oxide Fibers," Br. Pat. No. 1 432 506, April 22, 1976.

[23]"Method and Apparatus for Making Filamentary Material," Br. Pat. No. 1 470 103, April 14, 1977.

[24]"Production of a Form of Alumina Whiskers," Br. Pat. No. 1 489 346, October 19, 1977.

[25]V. N. Gribkov, A. S. Isaikin, E. L. Umantsev, and B. V. Shchetanov, "Growth of Alpha-Alumina Whiskers During the Oxidation of Aluminum," *Izv. Akad. Nauk SSSR Neorg. Mater.*, **8** [7] 1249–53 (1972).

[26]G. I. Volkodav, "Role of Water in the Production of Alpha-Al_2O_3 Whiskers," *Izv. Akad. Nauk SSSR Neorg. Mater.*, **8** [7] 1254–58 (1972).

[27]J. C. Hayes and J. E. Sobel, "Making Alumina Fibers from a Mixture of Alumina Sol and Hexamethylenetetramine," U.S. Pat. No. 3 532 709, January 4, 1972. Assigned to Universal Oil Products Co.

[28]A. Pearson and J. E. Marhanka, "Producing Sintered Alumina Fibers from an Alumina Slip of Very High Solids Content," U.S. Pat. No. 3 705 223, December 5, 1972. Assigned to Aluminum Company of America.

[29]A. K. Dhlagre, "Polycrystalline Alumina Fibers as Reinforcement in Magnesium Matrix," U.S. Pat. No. 4 036 599, July 19, 1977. Assigned to E. I. du Pont de Nemours & Co.

[30]F. Takeshi, U. Yoshihisa, and K. A. Ohmi, "Process for Production of Precursor of Alumina Fiber," U.S. Pat. No. 4 348 341, September 7, 1982. Assigned to Denki Kaguku Kogyo Kabushiki Kaisha.

[31]J. D. Birchall, "The Preparation and Properties of Polycrystalline Aluminum Oxide Fibers," *Proc. Br. Ceram. Soc.*, **33**, 51–62 (1983).

[32]P. M. Miedaner and C. Kucheria, "Alumina Binder for Fiber Containing Alumina," U.S. Pat. No. 4 349 637, September 14, 1982. Issued to Kennecott Corporation.

[33]K. M. Prewo and J. J. Brenner, "Fiber-Reinforced Glasses and Glass-Ceramics for High Performance Applications," *Am. Ceram. Soc. Bull.* **65** [2] 305–313, 322 (1986).

[34]S. Kimura and E. Yasuda, "Preliminary Study of Ceramic Fiber/Magnesium Phosphate Composite," Report of the Research laboratory of Engineering Materials, Tokyo Institute of Technology, **6**, 55–61 (1981).

[35]R. W. Rice, J. R. Spann, D. Lewis, and W. Coblenz, "The Effect of Ceramic Fiber Coatings on the Room Temperature Mechanical Behavior of Ceramic-Fiber Composites," *Ceram. Eng. Sci. Proc.*, **5** [7–8] 614–24 (1984).

[36]R. Colmet, I. Lhermitte-Sebire, and R. Naslain, "Alumina Fiber/Alumina Matrix Composites Prepared by a Chemical Vapor Infiltration Technique," *Adv. Ceram. Mater.*, **1** [2] 185–91 (1986).

[37]A. C. Pierre, D. R. Uhlmann, and A. Hordonneau, "Ceramic Composites Made by Sol-Gel Processing," Societe Nationale Industielle Aerospatiale report SIAS-852-430-103 (1985).

[38]A. H. Chokshi and J. R. Porter, "Creep Deformation of an Alumina Matrix Composite Reinforced with Silicon Carbide Whiskers," *J. Am. Ceram. Soc.*, **68** [6] C-144–C-145 (1985).

[39]D. M. Karpinos, V. M. Grosheva, Yu. L. Pilipovskii, and E. P. Mikhashchuk, "Effect of Mullite Single-Crystal Whiskers on the Thermal Stability of Al_2O_3 Products," *Ogneupory*, **2** 56–57 (1973).

[40]D. A. Sheldon and D. Lewis, "Fabrication and Proper Ties of a Ceramic Fiber-Ceramic Matrix Composite," *J. Am. Ceram. Soc.*, **59** [7–8] 372–74 (1976).

[41]J. Barta, W. B. Shook, and G. A. Graves, "Impact Strength of Alumina Composites," *Am. Ceram. Soc. Bull.*, **51** [5] 464–70 (1972).

[42]T. N. Tiegs and P. F. Becher, "Alumina-SiC Whisker Composites, "Department of Energy Conference Report CONF-8510103-5 (1985).

[43]H. Hartman, "Lead Coated Alumina Fiber and Lead Matrix Composites Thereof," U.S. Pat. No. 4 282 922, August 11, 1981. Issued to E. I. du Pont de Nemours & Co.

[44]F. Folgar, W. H. Krueger, and J. G. Goree, "Fiber FP/Metal-Matrix Composites in Reciprocating Engines," *Ceram. Eng. Sci. Proc.*, **5** [7–8) 643–53 (1984).

[45]T. Dohnomoto and M. Kubo, "Composite Materials Made from Matrix Metal Reinforced with Mixed Alumina Fibers and Mineral Fibers, U.S. Pat. No. 4 595 638, June 17, 1986. Issued to Toyota Motor Corp.

[46]N. C. Kothari, "Density and Mechanical Properties of Hot-Pressed Aluminum-Aluminum Oxide Composite Materials," *Sci. Sintering*, **6** [1–2] 25–35 (1974).

[47]"Composite Material Comprising Reinforced Aluminum or Aluminum-Base Alloy," Br. Pat No. 1 484 980, August 9, 1977.

[48]K. Yamatsuta and K. Nishio, "Aluminum Alloy Reinforced with Silica Alumina Fiber," U.S. Pat. No. 4 444 603, April 24, 1984. Issued to Sumitomo Chemical Company Ltd.

[49]J. A. Cornie, Y-M. Chiang, D. R. Uhlmann, A. Mortensen, and J. M. Collins, "Processing of Metal and Ceramic Matrix Composites," *Am. Ceram. Soc. Bull.*, **65** [2] 293–304 (1986).

[50]J. Dinwoodie, E. Moore, C. A. J. Langman, and W. R. Symes, "The Properties and Applications of Short Staple Alumina Fiber Reinforced Aluminum Alloys"; p. 671 in Fifth International Conference on Composite Materials, ICCM *V* Proceedings. The Metallurgical Society, Pittsburgh, PA, 1985.

[51]J. A. Cornie, A. Mortensen, M. N. Gungor, and M. C. Flemings, "The Solidification Process During Pressure Casting SiC and Al_2O_3 Reinforced Al-4.5% Cu Metal Matrix Composites"; p. 809 in Fifth International Conference on Composite Materials, ICCM *V* Proceedings. The Metallurgical Society, Pittsburgh, PA, 1985.

[52]R. A. Page and G. R. Leverant, "Relationship of Fatigue and Fracture to Microstructure and Processing in Al_2O_3 Fiber Reinforced Metal Matrix Composites"; p. 867 in Fifth International Conference on Composite Materials, ICCM *V* Proceedings. The Metallurgical Society, Pittsburgh, PA, 1985.

[53]J. Nunes, E. S. C. Chin, J. M. Slepetz, and N. Tsangarakis, "Tensile and Fatigue Behavior of Alumina Fiber Reinforced Magnesium Composites"; p. 723 in Fifth International Conference on Composite Materials, ICCM *V* Proceedings. The Metallurgical Society, Pittsburgh, PA, 1985.

[54]S. Pakswer and M. T. Stevens, "Secondary Electron Emission from Thin-Film Gold-Metal Oxide Cermets," *J. Appl. Phys.*, **42** [13] 5853–54 (1971).

[55]D. Gualandi and P. Jehenson, "Process for the Production of a Composite Material Al-Mg-Al_2O_3-MgO," U.S. Pat. No. 3 619 894, November 16, 1971. Issued to European Atomic Energy Community (Euratom).

[56]F. Guazzi, B. Verdini, G. P. Cammarota, E. Lanzoni, et al., "Preparation and Study of Electrodeposited Ni-Al_2O_3 Composites," *Met. Ital.*, **65** [4] 201–207 (1973).

[57]P. D. Ownby and C. P. Lahmann, "Influence of Oxygen Partial Pressure on the Physical Properties of Chromium Alumina Cermets," *Powder Metall. Int.*, **7** [4] 172 (1975).

[58]G. Jangg, W. Wruss, and A. Stumreich, "Manufacture of Cermets Based on Al_2O_3 by Infiltration," *Ber. Dtsch. Keram. Ges.*, **52** [12] 367–72 (1975).

[59]"Seal Members," Br. Pat. No. 1 415 507, November 26, 1975. Issued to Roparco Ltd.

[60]M. Hirai, T. Takahashi, K. Arita, G. Yamauchi, et al., Production of Aluminum-Aluminum Oxide Dispersion Composite Conductive Material and Product Thereof," U.S. Pat. No. 3 982 906, September 28, 1976. Issued to Nippon Telegraph & Telephone Public Corp.

[61]L. E. Wilson, "Making Spinel and Aluminum-Base Metal Cermet," U.S. Pat. No. 3 973 977, August 10, 1976. Issued to Corning Glass Works.

[62]R. M. Crispin and M. Nicholas, "Wetting and Bonding Behavior of Some Nickel Alloy-Alumina Systems," *J. Mater. Sci.*, **11** [1] 17–21 (1976).

[63]P. S. Kislyi, B. D. Storozh, P. A. Verkhovodov, et al., "Nature of Phase Binding in the al_2O_3 -W Cermet," *Izv. Akad. Nauk SSSR Neorg. Mater.*, **13** [7] 1258–61 (1977).

[64]S.-A. Cho and M. Puerta, "Effect of Ti on Sinterability of 70% Al_2O_3 -30% Cr Cermets," *Am. Ceram. Soc. Bull.*, **57** [11] 1056–57 (1978).

[65]D. G. W. Goad and M. Moskovits, "Colloidal Metal in Aluminum Oxide," *J. Appl. Phys.*, **49** [5] 2929–34 (1978).

[66]B. S. Skidan, G. A. Fomina, and I. A. Shepilov, "Effect of Processing Factors on the Properties of Alumina-Molybdenum Cermets," *Sov. Powder Metall. Met. Ceram.*, **17** [5] 402–404 (1978).

[67]D. Bahat and G. P. K. Chu, "High Temperature Glass-Ceramics of the BaO-Al_2O_3-SiO_2-Ta_2O_5 System and Molybdenum Metal Composites," *J. Mater. Sci.*, **14** [11] 2637–41 (1979).

[68]H. Yamamoto and S. Sendai, "Sintered Composite of $MoSi_2$-Granular Al_2O_3," *Yogyo-Kyokai-Shi*, **87** [2] 76–80 (1979).

[69]M. D. Kelly, "Cermet-Bonded Metal Pins for Weldable Electrical Feedthroughs in Alumina," *Ceram. Eng. Sci. Proc.*, **2** [7–8] 520–25 (1981).

[70]C. Morgan, A. J. Moorhead, and R. J. Lauf, "Thermal-Shock Resistant Alumina-Metal Cermet Insulators," *Am. Ceram. Soc. Bull.*, **61** [9] 974–81 (1982).

[71]S. G. Samdani, M. N. Chary, and A. Ali, "Studies on Densification Behavior and Phase Changes in TiO_2-ZrO_2," *Trans. Ind. Ceram. Soc.*, **29** [4] 109–12 (1970).

[72]M. E. Woods, W. F. Mandler, Jr., and T. L. Scofield, "Designing Ceramic Insulated Components for the Adiabatic Engine," *Am. Ceram. Soc. Bull.*, **64** [2] 287–93 (1985).

[73]Yu. I. Krylov, "Composite Material Based on the System TiB_2-Al_2O_3," *Izv. Akad. Nauk SSSR Neorg. Mater.*, **12** [9] 1684–85 (1976).

[74]N. Claussen, "Fracture Toughness of Al_2O_3 with an Unsta bilized ZrO_2 Dispersed Phase," *J. Am. Ceram. Soc.*, **59** [1–2] 49–5 (1976).

[75]C. A. Sorrell and C. C. Sorrell, "Subsolidus Equilibria an Stabilization of Tetragonal ZrO_2 in the System ZrO_2-Al_2O_3-SiO_2," *Am. Ceram. Soc.*, **60** [11–12] 495–99 (1977).

[76]D. Greve, N. E. Claussen, D. P. H. Hasselman, and G. E Youngblood, "Thermal Diffusivity/Conductivity of Alumina with Zirconia Dispersed Phase," *Am. Ceram. Soc. Bull.*, **56** [5] 514–1 (1977).

[77]G. Iordanov, T. Mitev, T. Dimova, et al., "Effect of ZrO_2 o the Physicochemical Characteristics of an Al_2O_3 Ceramic Synthe sized with the Liquid Phase of the System CaO-Al_2O_3-SiO_2," *Stoit Mater. Silik. Prom-st.*, **18** [8] 11–12 (1977).

[78]N. Claussen and J. Jahn, "Mechanical Properties of Sintered In Situ-Reacted Mullite-Zirconia Composites," *J. Am. Ceram. Soc.*, **63** [3–4] 228–29 (1980).

[79]P. Boch, J. P. Giry, and P. D. D. Rodrigo, "Reactior Sintering of Mullite and Zirconia-Mullite Ceramics," Presented at Second International Symposium on Ceramic Materials and Components for Engines, Lubeck-Travemunde, Federal Republic of Germany, April 14–17, 1986.

[80]J. Burden, "Ceramic Cutting Tools," *Ceram. Eng. Sci. Proc.*, **3** [7–8] 351–59 (1982).

[81]T. Noma and A. Sawaoka, "Toughening in Very High Pressure Sintered Diamond-Alumina Composite," *J. Mater. Sci.*, **19**, 2319–22 (1984).

[82]T. Noma and A. Sawaoka, "Effect of Heat Treatment on Fracture Toughness of Alumina-Diamond Composites Sintered at High Pressures," *J. Am. Ceram. Soc.*,, **68** [2] C-36–C-37 (1985).

[83]N. Claussen, F. Sigulsinski, and M. Ruhle, "Phase Transformation of Solid Solutions of ZrO_2 and HfO_2 in an Al_2O_3 Matrix"; pp. 164–67 in Science and Technology of Ceramics: Advances in Ceramics, Vol. 3. Edited by A. H. Heuer and L. W. Hobbs. The American Ceramic Society, Inc. Columbus, OH, 1981.

[84]L. J. Schioler, R. N. Katz, T. Brog, and T. Y. Tien, "Mechanical Properties of Zirconia-Toughened Alumina," *Ceram. Eng. Sci. Proc.*, **6** [7–8] 822–25 (1985).

[85]J. P. Biel and T. Y. Tien, "Toughened Ceramics in the System Al_2O_3:Cr_2O_3/ZrO_2:HfO_2: Effect of HfO_2 Contents in the Dispersed Particles on Mechanical Properties of the Composites"; work in progress under Department of Energy contract.

[86]D. W. Shin, H. Schubert, G. Petzow, K. K. Orr, et al., "Microstructure Development of Al_2O_3-ZrO_2 System in Final Stage HIP Process," Presented at Second International Symposium on Ceramic Materials and Components for Engines, Lubeck-Travemunde, Federal Republic of Germany, April 14–17, 1986.

[87]J. Wang and R. Stevens, "Design, Fabrication and Microstructure-Property Relationships of Duplex Al_2O_3-ZrO_2 Ceramic," Presented at Second International Symposium on Ceramic Materials and Components for Engines, Lubeck-Travemunde, Federal Republic of Germany, April 14–17, 1986.

[88]S. Inoue, K. Niihara, and T. Hirai, "Al_2O_3/SiC (whisker)/ZrO_2 (PSZ) Ceramic Composites," Presented at Second International Symposium on Ceramic Materials and Components for Engines, Lubeck-Travemunde, Federal Republic of Germany, April 14–17, 1986.

[89]N. Claussen, "Whisker Reinforcement of Transformation-Toughened Ceramics," Presented at Second International Symposium on Ceramic Materials and Components for Engines, Lubeck-Travemunde, Federal Republic of Germany, April 14–17, 1986.

[90]S. H. Risbud, "Influence of Surface Condition on the Strength of Glass-Al_2O_3 Composites," *Ceram. Eng. Sci. Proc.*, **2** [7–8] 702–11 (1981).

[91]F. F. Lange, "Fracture Energy and Strength Behavior of a Sodium Borosilicate Glass-Al_2O_3 Composite System," *J. Am. Ceram. Soc.*, **54** [12] 614–20 (1971).

[92]B. H. Mussler and M. W. Shafer, "Preparation and Properties of Cordierite-Based Glass-Ceramic Containing Precipitated ZrO_2," *Am. Ceram. Soc. Bull.*, **64** [11] 1459–62 (1985).

Alumina in Glasses and Glass-Ceramics

John F. MacDowell
Corning Incorporated
Research and Development
Corning, NY 14831

This review article explains the use of alumina in glassmaking, and its effect on structure, properties, and formation of glasses and glass-ceramics. The critical role of Al_2O_3, even in small amounts, in dramatically improving the properties of silicate glasses is emphasized. It is shown that high (>10%) alumina glasses and glass-ceramics are meeting the increased demands of our society for materials that are (1) stronger, (2) better dielectrics, (3) more refractory, and (4) lower in thermal expansion. New processes such as sol-gel and viscous sintering/crystallization are also mentioned as ways to expand the usefulness of high-alumina glass-derived materials. It is predicted that alumina will play an increasingly vital role in the higher performance materials systems of the future.

Alumina comprises about 16% of the earth's crust, as calculated by Clarke and Washington.[1] It is the second most abundant oxide after SiO_2 and is concentrated mainly in the hydrolysates (clay minerals), through the decomposition of the feldspars in granite and basalt, and in mineral species derived from these primary rock types.[2]

Tropical weathering of Al_2O_3-containing rocks often produces aluminum hydroxides rather than hydrated aluminum silicates, and high-alumina clays and bauxites result.

Since glass is a metastable state of matter that can occur only with rather rapid quenching from the molten state, natural glasses are uncommon except near volcanic activity or in meteorites or tektites.[3,4] The presence of glasses in Precambrian rocks (>500 million years old) is essentially unknown, since, given enough time, and under the right conditions, most glasses are driven to transform to their lower, free-energy crystalline counterparts. The presence of water, fluorine, or high temperatures or pressures are conditions prevalent in the geologic history of the earth's crust and they all dramatically increase the rate of nucleation and crystallization of natural glasses.

The alumina content of natural glasses (mainly rhyolitic obsidians) is about 12 to 16 wt%.[5] The high stability of these high-silica (70 to 77% SiO_2) glasses against devitrification is due to their high melt viscosities and their highly polymerized structure consisting of cross-linked hexagonal rings of SiO_4 tetrahedra. The exact origin of the tektite glasses is still the subject of considerable controversy, but the lunar volcanic and terrestrial impact theories are currently considered most likely by serious researchers.[6] Although man first began to make glass about 5000 years ago, the ancient caveman used natural glass (obsidian) for tools many thousands of years before.[7] Because natural silicate glass is based on the composition of feldspar rock, and contains at least 15% Al_2O_3, it was much too refractory to be melted and shaped by the primitive wood fires of ancient man. In fact, glasses containing substantial amounts of Al_2O_3 did not appear until the 19th century.

Effect of Al_2O_3 on Glass Structure

The essence of the role of alumina in glass can be understood by examining the position of the aluminum ion in a simplified two-dimensional diagram of the aluminosilicate glass structure shown in Fig. 1. It is seen that the replacement of a silicon ion by an aluminum ion in a silicate glass structure allows the network to maintain its stable polymerized three-dimensional structure while accommodating one singly charged cation.[9] This substitution is geometrically possible because the radius ratio between aluminum and oxygen is 0.43, a value that allows aluminum to assume either 4- or 6-coordination. In the dominant mineral class known as feldspars (alkali and alkaline-earth aluminosilicates), aluminum occupies a fourfold position. In many other minerals, e.g., mullite, the spinels, corundum, bauxite, the clay minerals, etc., aluminum is 6-coordinated with respect to oxygen. In glasses, the tetrahedral role for aluminum is much more common because it is generally more difficult to

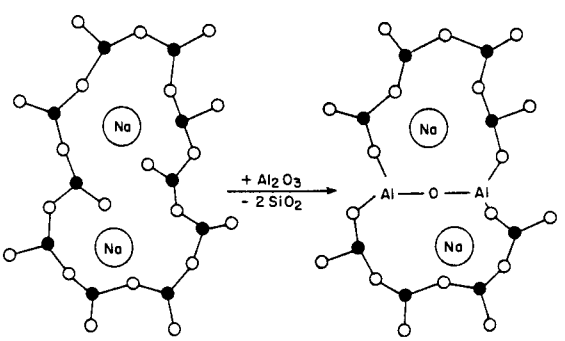

Fig. 1. Elimination of nonbridging oxygen in alkali silicate glasses by introduction of alumina (Ref. 8). (Used by permission.)

crystallize (and rearrange) the rigid, strongly bonded covalent tetrahedral oxygen-based network than it is a loosely bonded, largely ionic octahedral network that can rearrange itself without expending much energy.

Because a single positive charge is required to maintain electrical neutrality each time a $(AlO_4)^{5-}$ tetrahedron replaces a $(SiO_4)^{4-}$ tetrahedron, binary Al_2O_3-SiO_2 glasses have a very narrow range of stability. MacDowell and Beall[10] estimated that stable binary glasses are able to contain only about 7 wt% Al_2O_3. Above this amount, an unmixing occurs, causing a liquid phase high in Al_2O_3 to separate from a continuous high-silica glass matrix. The region of immiscibility in the system Al_2O_3-SiO_2 extends to about 55 mol% Al_2O_3, as shown in Fig. 2. The high-alumina dispersed phase readily crystallizes to mullite (plus a residual glass) when reheated to over 900°C, whereas the high-silica glass matrix in these glass-ceramic materials crystallizes above about 1200°C to cristobalite. The instability of silicate glasses containing such a small amount of Al_2O_3 is attributed by MacDowell and Beall to the formation of "triclusters" of AlO_4 tetrahedra which do not readily combine with the SiO_4 network. Lacy's tricluster model is represented in Fig. 3.[11] If Al^{3+} ions are to replace Si^{4+} ions in tetrahedral coordination without charge compensation by modifying ions, one oxygen ion must tribridge three tetrahedra for every Al^{3+} for Si^{4+} replacement. The tribridging of oxygens must necessarily produce a local tightening of the tetrahedral rings of the glass network. Figure 3 shows that the net effect of forcing Al^{3+} into a corner-shared tetrahedral array is to produce severe densification. This bimodal regime of high-Al_2O_3 (dense) and high-SiO_2 (less dense) regions apparently leads to separation into two phases.

In view of the recent work of Aksay et al.[12] and Morikawa et al.[13] using X-ray scattering intensity and emission spectra data, the best current model of binary

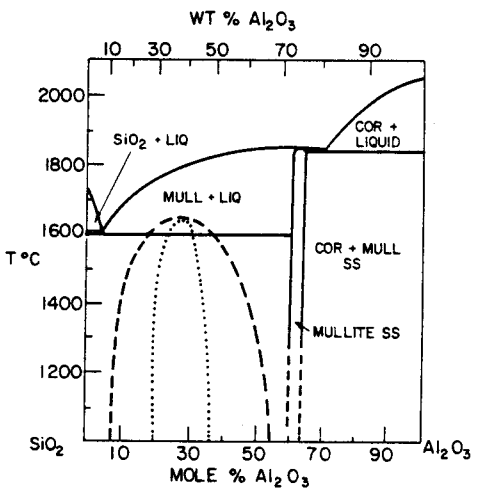

Fig. 2. The Al_2O_3-SiO_2 phase diagram showing schematic region of metastable immiscibility (Ref. 10).

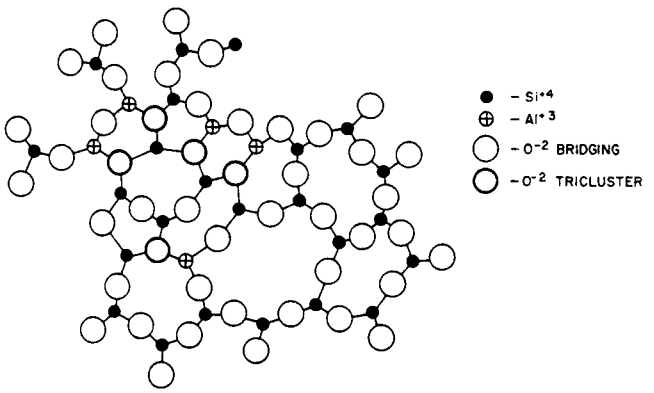

Fig. 3. Two-dimensional structural model showing the possible effect of additions of alumina to silica glass (Ref. 11). (Used by permission.)

SiO_2-Al_2O_3 glasses would include the presence of both triclustered AlO_4 tetrahedra and AlO_6 octahedra.

Lacy[11] also demonstrated that Al_2O_3 additions to Na_2O-SiO_2 binary glasses enhanced the oxygen densities, leaving insufficient oxygen atoms for the formation of octahedrally coordinated Al^{3+}. To explain the oxygen shortage, he postulated the formation of tribridging oxygens. Triclusters appear to form increasingly within ternary glasses at high Al/Si ratios from an equilibrium distribution of modifying ions, SiO_4 tetrahedra with one nonbridging O, AlO_4 groups, and AlO_6 octahedral groups tied to SiO_4 groups. Changes in the diffusion coefficient of Na^+ in Na_2O-Al_2O_3-SiO_2 glasses have also been attributed to structural changes in accord with Lacy's model.[13]

Another complex model involving the structure of alkali silicate glasses as Al_2O_3 is substituted for SiO_2 is proposed by Yoldas.[14] It postulates octahedral coordination at low concentrations of Al^{3+}. The models of both Lacy and Yoldas are supported by the conductivity data of Hayward,[15] especially for glasses near Al/Na = 1 and in the Na_2O-SiO_2 region of immiscibility.

In other regions of the system Na_2O-Al_2O_3-SiO_2, the conventional concept linking AlO_4 replacement of SiO_4 with subtraction of a nonbridging oxygen, as in Fig. 1, correlates well with property data.

Because of the much larger ionic radius of Al^{3+} vs B^{3+} (0.5Å vs 0.2), direct substitution of boron for aluminum occurs rarely. In boroaluminosilicates, Al^{3+} takes the fourfold O sites and B^{3+} is forced to occupy trigonal sites.[16]

In boroaluminate glasses containing alkaline-earth modifier ions, B^{3+} and Al^{3+} compete for tetrahedral sites, with most going to Al^{3+}.[17] Individual $(AlO_6)^{9-}$ and $(BO_3)^{3-}$ groups also exist in these glasses, contributing to a dense fragmented melt structure and low viscosities. "Cabal" glasses, as calcium boroaluminate glasses are called, are among the least conductive glasses in existence because of their dense, complex structure.[18]

Although Al_2O_3 does not form glass in bulk by itself, CaO and Al_2O_3 together form some fairly stable glasses.[19] Within a narrow composition range near 12 CaO:7 Al_2O, good glasses can be obtained without rapid quenching with liquidi near 1400°C. Most Al^{3+} in these glasses is tetrahedrally coordinated, as determined by Raman spectroscopy[20] and the radial distribution function methods.[21] Several model structures have been proposed, two of which are (1) $(CaAl_2) \cdot O_4$, analogous to the SiO_4 cristobalite polymeric structure, and (2) $5CaO \cdot 3Al_2O_3$, a crystalline sheet structure with both AlO_4 and AlO_6 groups. Despite considerable research, calcium aluminate remains among the least understood of all glass structures.

In SiO_2 glasses, the presence of P_2O_5 causes unmixing, forming an emulsion of a high-P_2O_5 and a high-SiO_2 glass that scatters light (opal). The addition of Al_2O_3 to binary silicophosphates greatly suppresses phase separation, increases chemical durability, and increases viscosity. The unusual feature of aluminophosphosilicate glasses is a structure wherein all three cations (Al^{3+}, P^{5+}, Si^{4+}) assume a tetrahedral coordination with oxygen.[22] The Al–O–P bond length is nearly identical to the Si–O–Si linkage and neutralization of the single negative charge on the (AlO_4) group by the positive charge on the (PO_4) yields a polymerized three-dimensional structure closely resembling an SiO_2 glass network (Fig. 4).

Aluminum phosphate glasses entirely SiO_2-free and based on aluminum metaphosphate [$Al(PO_3)_3$] can be prepared with supplementary oxygens contributed by the alkaline earths, ZnO, or PbO. These glasses resist attack by hydrofluoric acid, a nemesis to all silicate glasses.[23]

Aluminum fluoride (AlF_3) has been the key to finding glasses less toxic than BeF_2, but still maintaining a low (linear and nonlinear) index of refraction. An example of an early glass containing AlF_3 is (in wt%), AlF_3 40, PbF_2 24, SrF_2 12, MgF_2 24.[24]

The structure of AlF_3 glasses may consist of AlF_4 groups, with a tetrahedrally coordinated Al^{3+} network structure. AlF_3 can be added in large quantities to aluminum metaphosphate [$Al(PO_3)_3$] glasses, producing stable, low-index materials suitable for high-energy lasers.[25] The following is a typical composition (in mol%): $Al(PO_3)_3$ 4, AlF_3 36, MgF_2 10, CaF_2 30, SrF_2 10, and BaF_2 10.

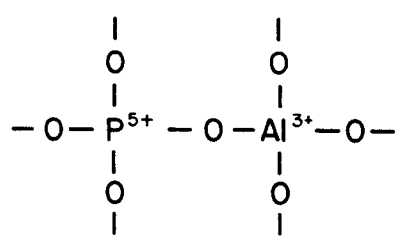

Fig. 4. Charge-balanced $AlPO_4$ polymeric unit.

Effect of Al_2O_3 on Glass Properties

Phase Separation and Crystallization

Since Al_2O_3 assumes a vital position within th three-dimensional backbone of the silicate glass net work, it also has a profound effect on the properties o these glasses.

Perhaps the most dramatic effect of Al_2O_3 addi tions to silicate glasses is on their phase separation anc crystallization behavior. In small amounts up tc 2 wt%, Al_2O_3 suppresses immiscibility in binary $MO-SiO_2$ systems[26] and in borosilicate glasses. In the system soda-lime-silica, where by far the largest volume of commercial glasses resides, small (<3 wt% Al_2O_3 additions expand the glass stability region[27] anc dramatically reduce the tendency for devitrification o phase separation to occur. Alumina also reduces liquidus temperatures when added to binary silicate glasses in amounts up to 10%.

The influence of Al_2O_3 on the tendency for phase separation or crystallization, however, varies widely depending on the base system. In Cabal ($CaO-B_2O_3-Al_2O_3$) glasses, for example, a phase separation consisting of a continuous high-alumina phase and a dispersed-borate phase occurs throughout the system.

Although additions of Al_2O_3 to highly phase-separable binary alkali oxide, CaO, and MgO silicate glasses eliminates liquid unmixing, when the Al_2O_3 modifier ratio exceeds 1, phase separation and crystallization are triggered because of the appearance of unstable structural groups that tend to cluster outside the tetrahedral glass framework.

Glass-Ceramics (Cordierite): The controlled crystallization of glasses to produce ceramics with fine and uniform crystal size was first introduced by Stookey.[28] Although Stookey began his studies of crystallizable glasses with lithium silicate glasses that could be photonucleated, subsequent discoveries were almost exclusively in aluminosilicate systems. A very fine-grained cordierite ($2MgO \cdot 2Al_2O_3 \cdot 5SiO_2$) ceramic was first synthesized in the middle 1950s via internal nucleation and crystallization of a magnesium aluminosilicate glass containing TiO_2 as a nucleating agent.[29] Because of its excellent strength, toughness, and resistance to thermal shock (low thermal expansion), this glass-ceramic forms the basis for a substantial business and is still the material of choice for several radar-transmitting missile nose cones. (See Fig. 5.) The glass-ceramic is strengthened via alkali fortification. Corning Commercial Code 9606 glass-ceramic contains about 20 wt% Al_2O_3. Barry et al.[30] have done a thorough study on the rather complex crystallization sequence involving eight crystalline phases that occur during transformation of the $MgO-Al_2O_3-SiO_2$ glasses into cordierite glass-ceramics.

$Li_2O-Al_2O_3-SiO_2$ Glass Ceramics: Subsequently, Stookey synthesized glass-ceramics in the system $Li_2O-Al_2O_3-SiO_2$.[28] They turned out to be the most

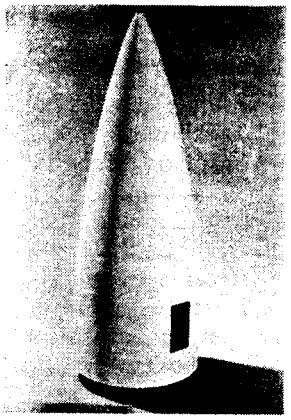

Fig. 5. U.S. Navy surface-to-air missile nose cone made of Corning Code 9606 cordierite glass-ceramic.

commercially significant of all glass-ceramics. He found that a β-spodumene-type crystal could be nucleated within a lithium aluminosilicate glass to yield a microcrystalline ceramic material whose thermal expansion coefficient approached zero! This "β-spodumene" crystal is actually a "stuffed derivative" of the silica polymorph keatite,[31] where Li^+ and Al^{3+} ions directly substitute for Si^{4+} in the silica structure. Typically, about 18 wt% Al_2O_3 is utilized in commercial compositions. This glass-ceramic type now abounds in modern American homes and is known as the Corningware® line of cooking dishes. In addition to cookware, the β-spodumene glass-ceramics have found use as stovetops, architectural cladding, and microwave oven shelves. A slight (≈10%) excess of Al_2O_3 over the Al_2O_3/modifier ratio of 1 in many of these glass-ceramics is added to produce a final crystal phase of mullite ($3Al_2O_3 \cdot SiO_2$) that precipitates at the glassy grain boundaries and prevents excessive grain growth of the major crystalline phase.

The lithium aluminosilicate system has another important microcrystalline solid solution—that of the stuffed β-quartz glass-ceramics.[31] Typically, this SiO_2 derivative has a very high nucleation efficiency when crystallized using TiO_2 or ZrO_2 as a nucleating agent. As a result, a crystallite size of less than 0.1 μm can be maintained with a high degree of crystallinity. Almost completely transparent β-quartz glass-ceramics have thus been produced in this system and are now being used as transparent cookware, wood-stove windows, and see-through electric range tops. Large quantities of β-quartz solid solution glass-ceramic is now being sold in the form of Visions® cookware. (See Fig. 6).

The stuffed β-quartz and keatite Li_2O-Al_2O_3-SiO_2 materials are highly crystalline, but there is extensive solid solution capability within the tetrahedral network between Al_2O_3 and SiO_2 in these structures.

The fact that crystal compositions between $Li_2O \cdot Al_2O_3 \cdot 4SiO_2$ (stoichiometric spodumene) and $Li_2O \cdot Al_2O_3 \cdot 10SiO_2$ all have about the same structure and properties allows the use of a relatively stable and

Fig. 6. New Visions® B-quartz solid solution glass-ceramic cookware manufactured by Corning Incorporated.

manufacturable parent glass (generally about $Li_2O \cdot Al_2O_3 \cdot 6.5SiO_2$). Glass quality and workability (and lower-cost batch) are also aided by up to one-third molar substitution of Mg^{2+} and/or Zn^{2+} for Li^+ ions in the keatite and β-quartz solid solution crystals.[31]

Mullite ($3Al_2O_3 \cdot 2SiO_2$) Glass-Ceramics: As discussed earlier, binary Al_2O_3-SiO_2 glasses are unstable with respect to two-liquid emulsion formation and devitrification. However, if enough modifying ions are present (at least 5 mol%), excellent monophase glasses can be obtained that crystallize on heat treatment to very fine-grained mullite glass-ceramics.[32] Figure 7 shows a typical mullite glass-ceramic in three stages of heat treatment. The modifying ions accomplish two things: (1) allow the melts to be quenched without phase separation or devitrification and (2) prevent cristobalite formation in the residual glass subsequent to the mullite crystallization.

These refractory high-alumina (>35 wt%) glass-ceramics must be melted above 1700°C, but show promise for use in high-temperature structures. They also have low thermal expansion coefficients (≈35 × 10^{-7} /°C) and excellent dielectric properties.[33]

Nepheline Glass-Ceramics: Glass-ceramics containing about 30 wt% Al_2O_3 and principally consisting of nepheline ($Na_2O \cdot Al_2O_3 \cdot 2SiO_2$) and celsian (BaO •

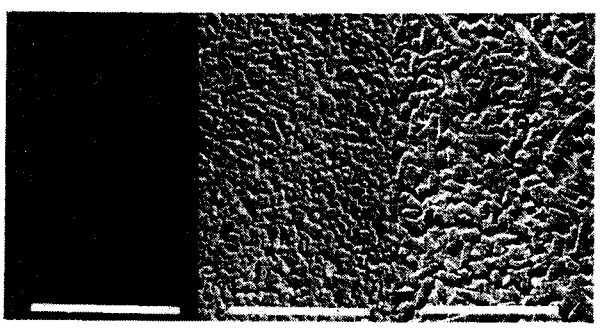

Fig. 7. Crystallization sequence of a mullite ($3Al_2O_3 \cdot 2SiO_2$ to $2Al_2O_3 \cdot SiO_2$) glass-ceramic. Bar = 1 μm.

$Al_2O_3 \cdot 2SiO_2$) have been produced commercially in the form of glazed tableware by Corning Glass Works since 1962.[34] Titania is added as the nucleating catalyst. Celsian is necessary to reduce the average thermal expansion coefficient to below 100×10^{-7}/°C, thus avoiding severe thermal shock problems inherent in high-expansion, pure sodium nepheline materials. The excellent serviceability of this commercial tableware material is made possible by applying a lower expansion glaze to the glass-ceramic body. This expansion differential creates a high-compression surface layer that results in high impact strengths and a modulus of rupture of 276 MPa (40 000 psi) (measured on abraded ware). Because of its economy of performance, the Hilton Hotel chain has carried this commercial tableware line almost exclusively for over 20 years. Perhaps the most unique feature of this material is its excellent coupling to microwave energy. This property was attributed to large sites in the nepheline lattice normally occupied by potassium in natural nephelines, but only loosely filled by sodium ions in the synthetic structure.[35] Apparently the resonant frequency of sodium ions in the large sites is in the microwave region ($\approx 2.45 \times 10^9$ Hz).

Machineable Glass-Ceramics Based on Fluorophlogopite: Glass-ceramics containing 30 to 50% SiO_2, 3 to 20% B_2O_3 10 to 20% Al_2O_3, 4 to 12% K_2O, 15 to 25% MgO, and 4 to 10% F and major amounts of fluorophlogopite ($KMg_3AlSi_3O_{10}F_2$) were developed during the early 1970s.[36] One of these glass-ceramics was marketed under the name Macor® and is still being sold by Corning for applications requiring excellent dielectric (insulating) properties, theoretical density (no porosity), dimensional stability, and machinability with conventional metal-working tools.

A large number of diverse applications include precision electric insulators, seismograph bobbins, windows for microwave tube parts, and boundary retainers on the space shuttle.

The machineability is attributed to the "house of cards" microstructure (see Fig. 8), where randomly oriented tiny flakes of mica allow only local fracturing to occur.

Ceramics Via Viscous Sintering and Crystallization of Glass Particulates: Although to date most glass-derived ceramics have been formed via internal (or bulk) nucleation and crystallization, a growing number of useful high-Al_2O_3 glass-ceramics are being formed via viscous sintering of fine glass particulates, followed (or accompanied) by surface nucleation and crystallization. If the initial particle diameter is on the order of a few micrometers, then the final crystal size in the densified ceramic is usually about 1 μm. One such application involves the use of keatite (*ss* glass-ceramics for heat regenerators in turbine engines.[37] In use, these honeycomb ceramics see a variety of conditions, including those of severe thermal shock and highly acid environments generated by high-sulfur fuels.

Fig. 8. Scanning electron micrograph of fracture surface of a machineable fluorophlogopite glass-ceramic. "House of cards" structure is the key to machineability.

To eliminate cracking of the heat exchangers due to stress produced during exchange between the hydrogen ions generated in combustion and the lithium ions in the keatite solid solution, the heat exchangers are "pre-exchanged" by treating the finished wheel in hot sulfuric acid.

The resulting "H^+-keatite" or H_2O-Al_2O_3-SiO_2 material is then stabilized by controlled heating to ≈1000°C to remove water. The converted "aluminous keatite" ($\approx Al_2O_3 \cdot 5.5SiO_2$) glass-ceramic material contains about 25 wt% Al_2O_3 and retains the original low-expansion keatite structure, but without its potential to destabilize via ion exchange.

Cordierite ($2MgO \cdot 2Al_2O_3 \cdot 5SiO_2$) contains about 35% Al_2O_3 and is another glass-ceramic that can be made via a glass-particulate sintering/crystallization process.

Electronic substrates are now being made experimentally via this process,[38] the principal advantages over the commercial pure Al_2O_3 substrate being a silicon-matching thermal expansion and low-temperature sintering. Sintering below 1000°C makes cofiring of many substrate layers possible, complete with low-temperature metal (Cu, Ag, Au) conductor patterns. The lower dielectric constant of cordierite (≈5.5 vs 9.0 for Al_2O_3) is also a distinct advantage, allowing substantially higher circuit densities. For these reasons, the drive to replace Al_2O_3 electronic substrates with cordierite glass-ceramics and other materials is intensifying.

Another potentially important application of high-alumina viscous-sintered glass-ceramics is in high-temperature ceramic-matrix composites reinforced with refractory fibers or whiskers.[39] SiC, carbon, boron, α-Al_2O_3, and mullite reinforcements have been used with cordierite, osumilite, anorthite ($CaO \cdot Al_2O_3$

• $2SiO_2$), β-spodumene, and other aluminosilicate glass-ceramic matrices.[40] Utilizing powdered glass as a raw material, densification of the matrix and wetting of the reinforcing fibers can be achieved at relatively low temperatures and pressures. These composites show remarkable strength and toughness, especially at high temperatures. Modulus of rupture values of >690 MPa (>100 000 psi) at temperatures exceeding 1000°C and toughness values (K_{ic}) of >10.0 MPa • $mm^{1/2}$ at an SiC fiber loading of about 25 vol% have been reported on these remarkable materials. Their place is almost ensured in the powerful, efficient, high-temperature aircraft (and spacecraft) engines of the future.

Sol-Gel Glasses and Glass-Ceramics: Although much research on glasses derived from sols and gels has been done over the past half-century, by far the preponderance of this work has occurred during the past five years.

The driving force for this effort has been threefold: (1) low-temperature firing (energy efficiency), (2) ultrahigh purity, and (3) dense, fine-grained, uniform (reliable) ceramics. Excellent glasses (and glass-ceramics) have been obtained through the thermal decomposition of alkoxides and other organic-based silicon and aluminum compounds.[41,42]

As yet, no major commercial applications have been found for sol-gel derived glasses. Optical fibers (including couplers), corrosion-resistant coatings, and other applications requiring one- and two-dimensional configurations remain the most likely future opportunities for these materials, since they are so difficult to dry and fire in bulk without cracking.

A substantial market has existed for several years for gel-derived mullite fibers (Nextel®) developed by the 3M Company.[43]

Chemical Durability

Trivalent aluminum is particularly beneficial with respect to water durabilty of certain important glasses. In sodium borosilicate glasses used for pharmaceutical and body fluid containment, it is important that the alkali extraction values are predictably low. When the Na_2O level is below 12 mol%, about 2 mol% Al_2O_3 strongly reduces the extraction loss.[44] In a study of soda-lime-silica glasses[45] between 14 and 21% Na_2O and 8 and 13% CaO, the following conclusions have been drawn: (1) alkali metal extraction reaches a minimum value between 2 and 3 wt% Al_2O_3, or when the Al_2O_3 content is equal to about one-eighth of the Na_2O content; (2) improvement in water (or weak acid) durability is greatest as the alkali content of the glasses increases; and (3) as the Al_2O_3 content approaches 10 mol%, the alkali extraction values begin to increase.

The chemical resistance of Na_2O-CaO-SiO_2 glasses to acids is also improved by Al_2O_3. However, a primary determinant in this case appears to be the SiO_2 level.[46] Some authors contend that acid durability should be optimum at $Na_2O/Al_2O_3 = 1$ or the ratio of the number of oxygen atoms in the network to the number of silicon + aluminum should be 2:1[47] (i.e., a completely polymerized tetrahedral network).

It is common knowledge, however, that sodium nepheline ($Na_2O \cdot Al_2O_3 \cdot 2SiO_2$) glass or "permutite" ($Na_2O \cdot Al_2O_3 \cdot 3SiO_2$) glass (used for water softening) has much lower acid resistance than albite ($Na_2O \cdot Al_2O_3 \cdot 6SiO_2$) glass.

The effect of Al_2O_3 on chemical durability of Na_2O-CaO-SiO_2 glasses in alkaline solutions is negligible.

Phase Separation

When Al_2O_3 is added to a borosilicate or phosphosilicate glass, the tendency toward phase separation is substantially reduced. Up to 3 wt% Al_2O_3 reduced immiscibility in binary alkaline-earth silicate[26] and in Pyrex® (Corning Code 7740)-type borosilicate glasses.[48] Without Al_2O_3, the borosilicates display uncontrolled two-liquid unmixing during cooling and/or annealing resulting in poor durability and otherwise unpredictable properties. As the SiO_2/B_2O_3 ratio is increased, less Al_2O_3 is needed to suppress phase separation. As little as 1 wt% Al_2O_3 is required to control immiscibility in a borosilicate glass containing 84% SiO_2.[49]

Binary SiO_2-P_2O_5 glasses phase-separate over broad regions of the system. The introduction of Al_2O_3 with equimolar amounts of P_2O_5, however, results in single-phase glass based on the $AlPO_4$ structure that is isomorphous with SiO_2. The neutralization of the free negative charge on the AlO_4 group by the excess charge on the PO_4 group and an Al–O–P distance identical to Si–O–Si allows complete miscibility with the silicate network.[50] Pure phosphate glasses based on $AlPO_4$ (P_2O_5 60–80, Al_2O_3 10-20 wt%) with up to 30 wt% ZnO or PbO strongly resist hydrofluoric acid attack.[51]

Solubility

The lower valency of Al^{3+} than Si^{4+} favors the stability of F^- (and other halide ions) in aluminosilicate glasses.[52] In like manner, Al^{3+} also binds OH^- groups in glass. This solubility may result in the scumming (foaming) of certain commercial soda-lime-silica glasses during melting, especially when feldspar is used as a batch material source of Al_2O_3.[53]

The solubility of Ag^+ in soda-lime-silica glasses is very small, but a few percent Al_2O_3 solubilizes it dramatically. The formation of aluminum oxoanions $(Ag[AlO_{4/2}])^{4-}$ similar to $(Na[AlO_{4/2}])^{4-}$ is believed to be the reason.[54]

Increased silver solubility may also explain the fact that photosensitive glasses (requiring a very limited solubility of Ag^+, Au^+, or Cu^+) do not normally contain significant amounts of Al_2O_3.

Ionic Conductivity

When tetrahedrally coordinated Al_2O_3 increases the ionic conductivity of binary silicate glasses,[55] the modifying cation is bound as an oxygen donor to the $[AlO_4]$ tetrahedron, and thus is more mobile in an electric field than when bound to a nonbridging oxygen atom. This explanation is supported by the fact that the conductivity of Na^+ in Na_2O-Al_2O_3-SiO_2 glasses is observed to reach a peak at $Al^{3+}/Na^+ = 1$, when the glass is completely polymerized and all Na^+ ions are bound to $[AlO_4]$ groups as oxygen donors.[56] Similarly, ion-exchange strengthening, depending on replacing a small ion at the surface of a glass with a larger one by diffusion, is maximized at a modifier/Al_2O_3 ratio of 1.0. When a smaller ion, e.g., Na^+ is replaced by a larger one, e.g., K^+ in a molten potassium salt, the surface tries to expand under the chemical potential gradient, and a compressive stress is thereby generated. Most ophthalmic glass lenses in the United States are currently strengthened via $K^+ \rightarrow Na^+$ exchange by immersing them for about 16 hours in a molten KNO_3 bath at about 400°C.[57]

In a similar manner, it is possible to prestress high-alumina glass-ceramics via ion exchange. Even higher stresses are possible with crystalline materials because of (1) higher strain points (temperatures at which stress release may occur) and (2) the possibility of phase transformations to produce stress. For example, nepheline (K_2O, Na_2O-Al_2O_3-$2SiO_2$) glass-ceramics can be ion-exchanged (K^+ for Na^+) to trigger a surface-phase transformation from nepheline to kalsilite.[34] The resulting volume expansion (density decrease) that occurs when kalsilite forms is nearly 10%. This results in abraded modulus of rupture values after crystallization and ion exchange of over 1380 MPa (200 000 psi). Large-diameter fibers of prestressed nepheline glass-ceramics have been used experimentally to reinforce polymer matrices.[58] Besides their very high strengths, these fibers have shown remarkable resistance to failure through surface-flaw generation or fatigue.

Glass Viscosity

Because of the strong network-forming role of Al_2O_3 in ternary aluminosilicate glasses, their viscosities over a wide range of temperatures increase as the Al_2O_3/M_2O + MO ratio increases up to a value of 1. Above this value, the viscosity curve is displaced to lower values and the liquidus increases precipitously. At a constant Al_2O_3/modifier ratio, viscosities increase further with increasing SiO_2. The alkaline-earth aluminosilicate system forms the basis for several commercial high-Al_2O_3 glasses.[59] Although the aluminosilicate glasses generally have high melting temperatures, their high low-temperature viscosities (i.e., annealing and strain points) allow strengthening via physical tempering and use at high temperatures without deformation or loss of stress. Because of the generally high liquidi in the system CaO-Al_2O_3-SiO_2, the commercial compositions center around the major low-melting eutectics, as described in Fig. 9 and Table I. Eutectic 2 has been the basis for "E"-glass fibers, tungsten-halogen lamp envelopes, and the skin glass for Corelle® laminated dinnerware.

Effect of Al_2O_3 on Other Properties

1. *Liquidus:* Small amounts of Al_2O_3 decrease the liquidi of binary silicate glasses but larger amounts increase them. Most ternary aluminosilicate phase diagrams have a region of rapidly increasing liquidus just over the Al_2O_3/modifier ratio of 1. All but the system CaO-Al_2O_3-SiO_2 also have a region of increasing liquidus values below about 40 wt% SiO_2.

2. *Density:* Since the $[AlO_4]$ and $[SiO_4]$ tetrahedra groups occupy approximately the same space in the silicate network and the densities of the Si and Al atoms are about the same, densities do not change with increasing Al_2O_3 content.

3. *Modulus/Strength:* Al_2O_3 has a positive effect on modulus of elasticity and therefore additions increase strength, according to the relationships developed by Griffith.[60]

4. *Hardness:* Since there is a direct relationship between hardness and viscosity, high-Al_2O_3 glasses display high hardness values, especially the alkaline-earth aluminosilicates. Their hardnesses can exceed that of soda-lime-silica glasses by as much as 50%.[61] Large-for-small ion exchange can also produce significant increases in scratch hardness by preventing the generation and propagation of small surface cracks.[56]

5. *Optical Properties:* Four-coordinated Al^{3+} substituted for Si^{4+} does not significantly change the refractive index of alkali silicate glasses. The 6-coordinated structural form of Al_2O_3, however, is denser and causes the refractive index to increase sharply as the Al_2O_3/alkali ratio exceeds one.[62] Aluminate glasses near the $12CaO \cdot 7Al_2O_3$ stoichiometry

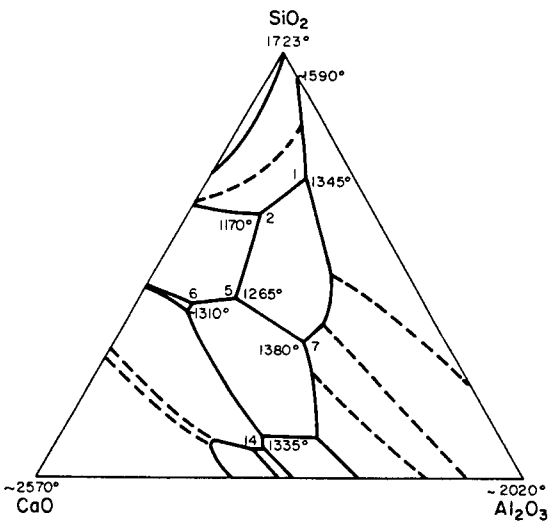

Fig. 9. Ternary diagram showing eutectics in the calcium aluminosilicate system (after Ref. 59).

Table I. Eutectic Glasses of the Calcium Aluminosilicate System*

Eutectic No.	1	2	5	6	7	14
SiO_2 }	70.4	62.1	42.0	41.0	31.7	6.95
Al_2O_3 } Wt%	19.8	14.6	20.0	11.8	39.1	43.35
CaO }	9.8	23.3	38.0	47.2	29.2	49.70
Exp. coeff. (25°–300°C) × 10^7/°C	33.1	54.7	76.5	88.7	59.5	84
Anneal. pt., °C	883	772	781	770	832	822
Strain pt., °C	831	728	746	738	800	~796
Temp of 1000 poises, °C	1612	1323	1166		1230	
log ρ (Ω • cm) 250°C	12.7	14.2	16.1	14.8	18.0	15.8
350°C	10.6	11.8	13.3	12.3	15.0	13.0
Dielectric const., 10 kHz, 25°C	6.3	7.1	9.3	9.9	8.9	12.5

*After Ref. 59.

are quite stable. The infrared transmission of these SiO_2-free glasses is excellent out to about 6.0 μm, making them candidates to replace sapphire in military infrared sensing systems.[63]

6. *Melting Rate:* Al_2O_3 additions generally decrease the melting rate of glass batches, primarily due to three factors: *(a)* increase in viscosity, *(b)* increase in liquidus temperature, and *(c)* lower reaction rates and higher reaction temperatures of Al_2O_3 batch materials as compared to SiO_2.

Raw Materials for Glass Batches

Because of the generally negative effect of Al_2O_3 additions on the melting rate of glass compositions, it is imperative that alumina-containing batch materials be chosen so that optimum melting rates are obtained. When Al_2O_3 is introduced to Na_2O-CaO-SiO_2 glass batches in the form of an aluminosilicate crystal such as feldspar [(Na,K)$AlSi_3O_8$] and/or nepheline [$KNa_3Al_4Si_4O_{16}$], the melting reaction rates are increased because these materials are homogeneous, melt readily below 1500°C, and fuse more easily than sand or limestone. Besides being relatively pure and low in iron oxides, these alkali aluminosilicates represent a sort of "homogenized batch" where their effect on melting is similar to that of cullet.[47] Thus, when making soda-lime-silica glass, the feldspars and feldspathoids, when economical, are currently the preferred source of alumina.

In the high-alumina glass-ceramics, aluminosilicates with three-dimensional tetrahedral structures are also preferred batch materials when available. Petalite (Otavi, from Africa) or low-iron α-spodumene (e.g., from Kings Mountain, North Carolina, or Tanco, Manitoba, Canada pegmatites) are the preferred sources of alumina for the ultralow-expansion β-spodumene (Corningware®) or β-quartz solid solution (Visions®) cookware materials, although lithium carbonate, calcined alumina, and sand can be used when cullet ratios are substantial. In the other glass-ceramics (e.g., cordierite (radomes), nepheline-celsian (tableware), phlogopite (machineables), calcined alumina plus carbonates and sand are used because the appropriate aluminosilicates (without Fe) are too costly or unavailable.

Kaolin, besides being generally too high in Fe_2O_3 for common untinted glass applications, tends to fuse into beads which ultimately result in batch stones in the glass product. This effect does not occur in alkali-free glass batches.[64]

Other high-Al_2O_3 minerals such as bauxite, kyanite, and gibbsite are also too high in iron for most glass batches, and are not known for their high reactivity with silica.

In glasses where purity level is of prime importance, either chemically purified calcined alumina or alumina hydrate is used as the source of alumina.[65]

Summary and Conclusions

Alumina is present in most natural glasses, averaging 12 to 16 wt%. Trivalent aluminum is a network-forming ion in glass, readily replacing Si^{4+} in tetrahedral coordination with oxygen when enough alkali or alkaline-earth ions are available to complete charge and bonding requirements.

Alumina has a profound effect on the properties of glass and is a critical ingredient in at least 90% of all glasses produced.[66]

Soda-lime-silica glass (for container and window glass products) has excellent chemical durability and resistance to devitrification, largely due to the ≈2 wt% Al_2O_3 it contains. Borosilicate glasses for chemical, pharmaceutical, and cookingware uses owe their stability against phase separation to small amounts (<10 wt%) of alumina. Refractory high-alumina glasses are used extensively for fiberglass, high-temperature lamp envelopes, and strengthened glass products.

The important family of high-alumina glass-ceramics for cookware, tableware, missile nose cones, and machineable dielectrics depends on alumina for the ability to crystallize in a controlled manner and thereby achieve unique and useful properties. Some important commercial high-alumina glasses and glass-ceramics are listed in Table II. New high-alumina glass ceramics for reinforced ceramic-matrix composites and cofired multilayer electronic substrates promise to play a revolutionary role in the 21st century. As the unique features of alumina are better understood in the glasses and glass-ceramics of today, we can begin to apply this knowledge to shaping tomorrow's world of performance-dominated materials.

Table II. Commercial High-Alumina Glasses and Glass-Ceramics*

Commercial Designation*	Composition System	Approximate wt% Al_2O_3	Properties	Applications
C-7059	BaO-Al_2O_3-B_2O_3-SiO_2	10	High ann. pt., durable	LCD substrates
C-0331	Na_2O-Al_2O_3-SiO_2	21	Strengthenability	Aircraft windows, laser disks, tape reels
OC E-Glass, S-Glass	CaO, MgO-Al_2O_3-SiO_2	15	Excellent dielectric properties, steep viscosity/temp. curve	Fiberglass
C-9754, BS 37A	CaO-Al_2O_3-GeO_2, SiO_2	39	Hardness, ir transmission	Infrared transmitting radomes, windows
C-1724, GE 180, OI EE-2, S-8252	CaO-Al_2O_3-SiO_2	20	High strain point, low thermal expansion	Tungsten halogen lamp envelopes
	Major Crystalline Phases			
C-9606	$2MgO \cdot 2Al_2O_3 \cdot 5SiO_2$ (cordierite)	20	Strong, transparent to microwaves	Radomes
C-9608, NE-11 (Narumi)	$Li_2O \cdot Al_2O_3 \cdot 6.5SiO_2$ (β-spodumene (ss))	18–22	Thermal shock-resistant, durable	Cookware
C-9609	$Na_2O \cdot Al_2O_3 \cdot 2SiO_2$ (nepheline) + $BaO \cdot Al_2O_3 \cdot 2SiO_2$ (celsian)	30	High strength with compression glaze	Tableware
C-9455	$Li_2O \cdot Al_2O_3 \cdot 5.5SiO_2$ (aluminous keatite)	23	Low expansion, high thermal stability	Heat exchangers
C-9607	$Li_2O \cdot Al_2O_3 \cdot 6.5SiO_2$ (β-quartz (ss))	19	Transparency, low thermal expansion	Top-of-stove ware
S-Zerodur®, O.I. Cer-Vit. C101	$Li_2O \cdot Al_2O_3 \cdot 6SiO_2$ (β-quartz (ss))	25	Low thermal expansion, dimensional stability	Telescope mirrors
S-Robax®	$Li_2O \cdot Al_2O_3 \cdot 6SiO_2$ (β-quartz (ss))	18	Low expansion, transparent	Stove tops, wood stove windows
C-9458	$KMg_3AlSi_3O_{10}F_2$ (fluorophlogopite mica)	17	Machineability, dielectric properties	Precision electrical parts
Slag-Sitall (U.S.S.R., Hungary)	Calcium silicate	8–14	Inexpensive, durable	Architectural

*Refs. 31, 59, and 67.
C = Corning Incorporated; OC = Owens Corning Fiberglass; S = Schott (West Germany); GE = General Electric Co.; OI = Owens Illinois Co.; NE = Nippon Electric; BS = Barr and Stroud Co.

References

[1]F. W. Clarke and H. S. Washington, "The Composition of the Earth's Crust," *U.S. Geol. Survey Profess.*, Paper 127 (1924); pp. 117.

[2]C. S. Ross. "Minerals and Mineral Relationships of the Clay Minerals," *J. Am. Ceram. Soc.*, **28**, 173–83 (1945).

[3]B. Mason. The Principles of Geochemistry. Wiley & Sons, 1952.

[4]D. Turnbull and M. H. Cohen, "Concerning Reconstructive Transformation and Formation of Glass," *J. Chem. Phys.*, **29**, 1049 (1958).

[5]N. L. Bowen. The Glassy Rocks, Chap. VIII, p. 125 in The Evolution of Igneous Rocks. Dover Publications, New York, 1956.

[6]J. A. O'Keefe, "Natural Glass," *Non-Cryst. Solids*, **67**, 1–17 (1984).

[7]A. L. Day, "Developing American Glass," *Proc. A.S.T.M.*, **36**, II (1936).

[8]N. J. Kreidl, "Inorganic Glass-Forming Systems"; Chap. 3, pp. 187–88 in Glass: Science and Technology. Edited by D. R. Uhlmann and N. J. Kreidl. Academic Press, New York, 1983.

[9]W. H. Zachariasen, "The Atomic Arrangement in Glass," *J. Am. Chem. Soc.*, **54**, 3841 (1932).

[10]J. F. MacDowell and G. H. Beall, "Immiscibility and Crystallization in Al_2O_3-SiO_2 Glasses," *J. Am. Ceram. Soc.*, **52** [1] 17–25 (1969).

[11]E. D. Lacy, "Aluminum in Glasses and Melts," *Phys. Chem. Glasses*, **4** [6] 234 (1963).

[12]I. A. Aksay, J. A. Pask, and R. F. Davis, "Densities of SiO_2-Al_2O_3 Melts," *J. Am. Ceram. Soc.*, **62** [7–8] 332–36 (1979).

[13]H. Morikawa, S. Miwa, M. Miyake, F. Marumo, and T. Sata, "Structural Analysis of SiO_2-Al_2O_3 Glasses," *J. Am. Ceram. Soc.*, **65** [2] 78–81 (1982).

[14]B. E. Yoldas, "The Nature of the Coexistence of Four- and Six-Coordinated Al^{3+} in Glass," *Phys. Chem. Glasses*, **12**, 28 (1971).

[15]P. Hayward, "The Electrical Conductivities and Cation Mobilities of Na_2O-Al_2O_3-SiO_2 Glasses," *Phys. Chem. Glasses*, **18** [6] 121 (1977).

[16]A. Appen, "The Aluminoboron Anomaly in Some Properties of Silicate Glasses," V Int. Cong. Glass, Session VI, p. 23, Glastech. Ber., Munich, 1959.

[17]P. Bray, The Structure of Glass, Vol. 7. Edited by E. Porai Koshits. Consultant Bureau, New York, 1966.

[18]A. Owen, "Properties of Glasses in the System $CaO-B_2O_3-Al_2O_3$," *Phys. Chem. Glasses*, **2** [87] 152 (1961).

[19]H. Rawson; p. 249 in Inorganic Glass-Forming Systems. Academic Press, New York, 1967.

[20]F. Seifert, B. O. Mysen, and D. Virgo, "Three-Dimensional Network Structure of Quenched Melts (Glass) in the Systems $SiO_2-NaAlO_2$, $SiO_2-CaAl_2O_4$ and $SiO_2-MgAl_2O_4$," *Am. Mineral.*, **67**, 696 (1982).

[21]H. Morikawa, F. Marumo, T. Koyama, M. Yamane, and A. Oyobe, "Structural Analysis of $12CaO \cdot 7Al_2O_3$ Glass," *J. Non-Cryst. Solids*, **56**, 355 (1983).

[22]H. Huettenlocher, "Kristellstruktur des Aluminiumorthophosphates $AlPO_4$," *Z. Krist.*, **90**, 508 (1935).

[23]D. Morgan, "Chemically Resistant Aluminophosphate Glasses," U.S. Pat. No. 3 746 556 (1973).

[24]K. Sun, "Aluminate Glasses," *Glass Ind.*, **30** [199] 232 (1949).

[25]M. Weber, "Glass for Neodymium Fusion Lasers," *J. Non-Cryst. Solids*, **42**, 189 (1980).

[26]E. M. Levin and S. Block, "Structural Interpretation of Immiscibility in Oxide Systems: III, Effect of Alkalies and Alumina in Ternary Systems," *J. Am. Ceram. Soc.*, **41** [2] 49–54 (1958).

[27]G. W. Morey, "The Effect of Boric Oxide on the Devitrification of the Soda-Lime-Silica Glasses. The Quaternary System, $Na_2O-CaO-B_2O_3-SiO_2$," *J. Am. Ceram. Soc.*, **15**, 457–75 (1932).

[28]S. D. Stookey, "Catalyzed Crystallization of Glass in Theory and Practice," *Ind. Eng. Chem.*, **51** [7] 805 (1959).

[29]S. D. Stookey, "Method of Making Ceramics and Product Thereof," U.S. Pat. No. 2 920 971 (1960).

[30]T. I. Barry, J. M. Cox, and R. Morell, "Cordierite Glass-Ceramics–Effect of TiO_2 and ZrO_2 Content on Phase Sequence during Heat Treatment," *J. Mater, Sci.*, **13**, 594 (1978).

[31]G. H. Beall and D. A. Duke, "Glass-Ceramic Technology"; p. 403 in Glass: Science and Technology, Vol. 1. Edited by D. R. Uhlmann and N. J. Kreidl. Academic Press, New York, 1983.

[32]J. F. MacDowell, "Nucleation in Glasses," *Ind. Engr. Chem.*, **58** [3] 38 (1966).

[33]J. F. MacDowell, "Semicrystalline Body and Method of Making It," U.S. Pat. No. 3 236 662; issued February 22, 1966.

[34]D. A. Duke, J. F. MacDowell, and B. R. Karstetter, "Crystallization and Chemical Strengthening of Nepheline Glass-Ceramics," *J. Am. Ceram. Soc.*, **50** [2] 67 (1967).

[35]J. F. MacDowell, "Microwave Heating of Nepheline Glass-Ceramics," *Am. Ceram. Soc. Bull.*, **63** [2] 282 (1984).

[36]G. H. Beall, "Structure, Properties, and Applications of Glass-Ceramics"; Advances in Nucleation and Crystallization of Glasses. Edited by L. L. Hench and S. W. Frieman. Am. Ceram. Soc. Spec. Publ. No. 5 (1972).

[37]D. G. Grossman and J. G. Lanning, "Aluminous Keatite Ceramic Regenerators," *Am. Ceram. Soc. Bull.*, **56** [5] 474 (1977).

[38]A. H. Kumar, P. W. McMillan, and R. R. Tummala, "Glass-Ceramic Structures," Br. Pat. Appl. GB2 013 650, August 15, 1979.

[39]J. J. Brennan and K. M. Prewo, "Silicon Carbide Reinforced Glass-Ceramic Matrix Composites Exhibiting High Strength and Toughness," *J. Mater. Sci.*, **17**, 2371 (1982).

[40]K. M. Prewo, J. J. Brennan, and G. K. Layden, "Fiber Reinforced Glasses and Glass-Ceramics for High Performance Applications," *Am. Ceram. Soc., Bull.*, **65** [2] 305 (1986).

[41]H. Dislich, "New Routes to Multicomponent Oxide Glasses," *Ange. Chemie (International Edition)*, **10** [6] 363 (1971).

[42]D. M. Kroll and J. G. van Lierop, "The Densification of Monolithic Gels," *J. Non-Cryst. Solids*, **63** 131 (1984).

[43]K. A. Karst and H. G. Sowman, "Non-Frangible Alumina-Silica Fibers," U.S. Pat. No. 4 047 965; issued September 13, 1977.

[44]L. Marchesini, C. Moretti, and M. Moretti. Parma at 21st Mostra Internationale Delle Industric per le Conserve Alimentari (1966); p. 81.

[45]A. K. Lyle, W. Horak, and D. E. Sharp, "The Effect of Alumina upon the Chemical Durability of Sand-Soda-Lime Glasses," *J. Am. Ceram. Soc.*, **19**, 142–47 (1936).

[46]W. König, "Ü ber die Säurebeständigkeit hochtonerdehaltiger Flaschengläser," *Glastech. Ber.*, **21**, 255 (1943).

[47]M. B. Volf; p. 298 in Chemical Approach to Glass. Elsevier, New York, 1984.

[48]G. O. Jones, Glass. Methuen's Monographs on Physical Subjects. Wiley & Sons, New York, 1956.

[49]M. B. Volf; p. 132 in Technical Glasses. Sir Isaac Pitman and Sons, Ltd., London, 1961.

[50]P. W. McMillan; pp. 68–69 in Glass-Ceramics. Academic Press, New York, 1964.

[51]A. G. Pincus, U.S. Pat. No. 2 577 627; *Glass Ind.*, **33**, 31 (1952).

[52]W. Fraser and L. Upton, "Optical Fluor-Crown Glasses," *J. Am. Ceram Soc.*, **27** [4] 121–28 (1944).

[53]D. Enright. P. Marshall, and J. Poole, "Effects of Major and Some Minor Constituents on Glass Melting," *J. Am. Ceram Soc.*, **32** [11] 351–55 (1949).

[54]I. Westermann, "Über die Ausnahme von Silberoxyd Durch Oxyde und Oxydverbindungen bei Hoheren Temperaturen," *Z. Anorg. Allgem. Chem.*, **206** 97 (1932).

[55]H. Moore and R. C. DeSilva, "A Study of the Electrical Properties of Alkali-Lime-Silica Glasses, Some Containing Boric Oxide or Alumina, in Relation to Glass Structure," *J. Soc. Glass Technol.*, **36**, 5 (1952).

[56]A. J. Burggraaf and J. Cornelison, "The Strengthening of Glass by Ion-Exchange: Part I. Stress Formation by Ion Diffusion in Alkali Alumino-Silicate Glass," *Phys. Chem. Glasses*, **5**, 123 (1964).

[57]R. F. Bartholomew and H. M. Garfinkel, "Chemical Strengthening of Glass"; p. 266 in Glass: Science and Technology, Vol. 5. Edited by D. R. Uhlmann and N. J. Kreidl. Academic Press, New York, 1980.

[58]J. F. MacDowell, K. Chyung, and K. Gadkaree, "Fatigue-Resistant Glass and Glass-Ceramic Macrofiber Reinforced Polymer Composites," Proceedings of the 40th Annual Conference, Reinforced Plastics/Composites Institute, Society of Plastics Industry, January 21–February 1, 1985.

[59]W. H. Dumbaugh and P. S. Danielson, "Aluminosilicate Glasses"; pp. 115–32 in Advances in Ceramics, Vol. 18. Edited by J. F. MacDowell and D. C. Boyd. The American Ceramic Society, Columbus, OH, 1986.

[60]A. A. Griffith, *Phil. Trans. Royal Soc.*, "The Phenomena of Rupture and Flow in Solids," **221 (A)**, 163 (1920).

[61]A. E. Pavlich and J. Mockrin, "Development of Hard Glass," *J. Am. Ceram. Soc.*, **30** [2] 54–63 (1947).

[62]J. F. Shairer and N. L Bowen, "Melting Relations in the Systems $Na_2O-Al_2O_3-SiO_2$ and $K_2O-Al_2O_3-SiO_2$," *Am. J. Sci.*, **245**, 193 (1947).

[63]J. R. Davy, "Development of Calcium Aluminate Glasses for Use in the Infrared Spectrum to 5 μm." *Glass Technol.*, **19** [2] 32 (1978).

[64]C. W. Parmelee and W. B. Silverman, "The Effect of Alumina on the Melting Rate of a Soda-Lime-Magnesia-Silica Glass," *Glass Ind.*, **17**, 111 (1936).

[65]J. R. Taylor, "Raw Material Sources for Alumina in Glass," *Glass Technol.*, **23** [6] 251 (1982).

[66]"Alumina in Glass"; p. 169, Chap. 21 in Alumina as a Ceramic Material. Edited by W. H. Gitzen. The American Ceramic Society, Columbus, OH, 1970.

[67]G. H. Beall, "Commercial Glass-Ceramics"; p. 232 in Advances in Ceramics, Vol. 18. Edited by J. F. MacDowell and D. C. Boyd, The American Ceramic Society, Columbus, OH, 1986.

Alumina Powder Production by Aerosol Processes

Toivo T. Kodas
University of New Mexico
Chemical and Nuclear Engineering Department
Albuquerque, NM 87131

Ajay Sood
Aluminum Company of America
Alcoa Laboratories
Alcoa Center, PA 15069

A review of experimental and theoretical studies of aerosol methods for alumina powder production is presented. Flame, plasma, condensation, and reaction processes which rely on gas-to-particle conversion, and spray pyrolysis processes which rely on chemical reaction in particles generated by atomization are considered. These processes have not previously been used extensively to produce powders other than SiO_2, TiO_2, and carbon black. The understanding of aerosol processes, however, has increased sufficiently in recent years to allow the rational design and operation of aerosol systems for large-scale production of alumina and various other ceramic powders.

Aerosol processes are used for the large-scale production of alumina, silica, carbon black, uranium dioxide, and titanium dioxide powders.[1] Aerosol methods, however, have not yet been exploited fully for production of ceramic powders. In the past, this was due to the lack of empirical or theoretical bases for the design and operation of aerosol systems. However, systematic studies in recent years have considerably increased our understanding of aerosol processes. Enough theoretical and experimental results are now available to allow the rational design and operation of various aerosol systems for powder production.

This work first describes some applications of alumina and other ceramic powders and discusses the powder properties needed for these applications. The properties of currently available alumina powders are described. Various aerosol processes for alumina powder production are introduced. The powder characteristics obtained with aerosol processes are compared with those obtainable with competing processes. A brief review of the general theory for aerosol systems is then presented. The remainder of the work reviews some of the theoretical and experimental studies of the main types of aerosol processes—flame, plasma, condensation, reaction, and spray pyrolysis—used for production of alumina and other ceramic powders.

Alumina Powder Properties Required for Production of Advanced Ceramic Parts

Alumina powder is used for production of integrated circuit substrates, high-pressure sodium-vapor lamps, catalyst supports, cutting tools, heat- and wear-resistant materials, and the shielding material in radioactive systems.[2] A common use of alumina and other ceramic powders is for the production of ceramic parts.[3] The properties needed from the finished part determine the criteria used for selecting the starting powder. For most advanced ceramic applications, the powder's purity, average size, particle-size distribution, and particle shape determine the component's performance.[4]

Powder purity strongly influences properties such as strength, oxidation resistance, and stress rupture life. Impurities play an even more important role in determining electrical, magnetic, and optical properties. These properties are usually carefully customized for a specific application by precisely controlled addition of a dopant. Small changes in the concentration or distribution of the dopant or the presence of undesirable impurities can alter the properties significantly and cause the device to function improperly.

The average particle size strongly influences the properties of the finished part. Small particles are required for manufacture of high-strength components. Very small particles, approximately 1 μm in diameter or less, can be compacted into a porous body and sintered at relatively low temperatures to near-theoretical density; e.g., transparent polycrystalline alumina used for sodium-vapor-lamp envelopes. The particle size also influences the temperature and time required for sintering. Typically, the finer the powder the lower the temperature and the shorter the time needed for densification. This can have an important effect on strength since long sintering times result in increased grain growth and lower strength.

A narrow particle-size distribution is required to achieve maximum, reproducible strength. The strength is determined by flaws in the material. Particles which are significantly larger than other particles can become the critical flaws that limit the strength of the component. Similarly, large voids resulting from broad particle-size distributions may not be eliminated during sintering and may become the strength-limiting flaws.

Particle shape plays an important role in the production of ceramic parts. Aggregates, clusters of fused particles, are undesirable since they limit attainable green density, interfere with microstructure de-

*Current address: Bettis Laboratory, P.O. Box 79, West Mifflin, PA 15122

velopment, impede initial sintering kinetics, and limit the potential benefits of fine particles on final-stage sintering.[5]

The ideal powder for production of ceramic parts would have high purity, small (submicrometer) particle size, narrow size distribution, and unagglomerated spherical particles.[6–8]

Characteristics of Currently Available Alumina Powders

Alumina is made commercially using the Bayer process, in which aluminum hydroxide is extracted from bauxite ore. The purity of the hydroxide is roughly 99.5%, with Na_2O, Fe_2O_3, SiO_2, and TiO_2 being the major impurities. The hydroxide generally has a median particle diameter of 10 μm and a broad particle-size distribution with a typical range of 0.1 to 60 μm for commercially ground hydroxides.[9] Some calcined aluminas prepared from the Bayer hydroxides exhibit somewhat higher purities. For example, Alcoa's commercially available A-16 calcined alumina has a typical purity of 99.7%. However, its particle-size distribution is also quite broad, ranging from 0.1 to 3 μm, with a median diameter of 0.5 μm. In addition, the particles are not spherical but have an irregular shape, as shown in Fig. 1.

A common method for production of submicrometer alumina powder is grinding of coarser alumina particles, followed by classification. The advantages of this process are that it is simple, has a wide range of applicability, and produces unaggregated powders. Grinding followed by classification, however, has several disadvantages: (1) The product may be contaminated by the grinding media during processing (grinding media of sufficient purity and abrasion resistance are not currently available). (2) Most grinding and classification schemes produce a broad size distribution. (3) Submicrometer grinding and classification are generally expensive unit operations and require high energy consumption per unit of throughput. (4) The particles are not spherical or equiaxed, but are irregular in shape. (5) Grinding does not permit addition of dopants dispersed uniformly in the alumina matrix.

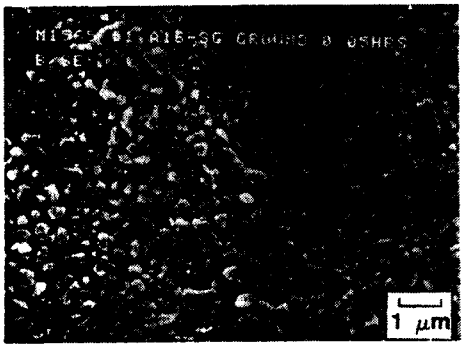

Fig. 1. Typical electron micrograph of finely ground calcined alumina (bar = 1μm).

Aerosol Processes for Powder Production

Aerosol processes for powder production are grouped in this paper as flame, plasma, condensation, reaction, and spray pyrolysis processes. This is a convenient way to group them since theoretical and experimental work in the literature has been organized in this manner. The characteristics of the powders that can be produced by these processes are presented in Table I.

By using high-purity reactants, all the processes can provide purities much higher than can be obtained using grinding methods. Aerosol processes can easily produce submicrometer particles; grinding processes cannot easily produce particles smaller than about 1 μm. For appropriate operating conditions, aerosol processes can also produce narrow size distributions; grinding followed by classification cannot easily produce monodisperse powders. In addition, spherical particles can be obtained using many aerosol processes; grinding produces aspherical particles.

Although this work will focus on alumina production, the methods can also be applied to other advanced ceramic materials such as the nonoxide ceramics, viz., nitrides (Si_3N_4), carbides (SiC, B_4C), borides (TiB_2), and superconductors ($YBa_2Cu_3O_7$).

General Theory for Aerosol Processes

The theories for flame, plasma, condensation, and reaction processes have a common basis since they all involve (1) formation of a single or multiple gaseous species that can condense or react to form particles or deposit on the walls, (2) particle formation (nucleation), and (3) particle growth. Coagulation may also be important, depending on the operating conditions. Friedlander[10] and Hidy and Brock[11] discussed the theories of particle formation, growth, and coagulation; Hinds[12] presented a more simplified explanation of these mechanisms. The processes of particle formation, growth, and coagulation are related in that each can be described by a single equation that, under limiting conditions, reduces to the equations used as a starting point for the separate theories.[13]

Particle formation is described using different theories, depending on the details of the process. Particle formation by condensation of a single condensable species is typically described using classical

Table I. Characteristics of Powders Produced by Aerosol Processes. (All processes can produce high-purity powders with narrow particle-size distributions.)

Process	Particle Diameter	Particle Shape
Flame	0.001 to 0.5μm	Aggregates
Plasma	0.001 to 1μm	Spherical or aggregates
Condensation	0.001 to ~10μm	Spherical
Reaction	0.001 to ~10μm	Spherical or aggregates
Spray pyrolysis	0.1 to 10 μm	Spherical or broken shells.

Becker-Doring or Lothe-Pound nucleation theory.[14] Particle formation by condensation of two species can be described by heteromolecular nucleation theory.[15–17] For many ceramic materials of practical interest, particle formation occurs by reaction on the surface of subcritical clusters (unstable nuclei). Katz and Donohue[18] have described particle formation in such systems when the rate of particle formation is limited by chemical reaction at the surface.

In some systems of practical importance, the concentration of the condensing species may change too rapidly to allow a steady state cluster size distribution to develop and permit the use of classical nucleation theory.[19] Sutugin et al.[20] presented a model that describes particle formation in such systems by solving for the time evolution of the subcritical cluster- and supercritical particle-size distributions.

Seigneur et al.[21] presented a comparative review of mathematical models for condensational particle growth and coagulation without particle formation. These models were derived assuming spatially uniform conditions. However, actual systems are spatially nonuniform due to mass and heat transfer effects and complex flow patterns. Kodas et al.,[22a,b] Pratsinis et al.,[23a,b,c] and Pesthy et al.[24] examined the effect of mass transfer of the condensing species on tubular flow reactor behavior. Pesthy et al. and Pratsinis et al.[23c] studied particle formation by condensation in tubular flows with radial heat and mass transfer. Kodas et al.[22b] evaluated the effect of reactant mixing on the aerosol dynamics in tubular flow reactors with radial mass transfer of reactants. Pratsinis et al.[23b] examined the effect of aerosol reactor residence-time distribution on product aerosol characteristics. Crump and Seinfeld[25] and Pratsinis et al.[23d] studied the aerosol dynamics of systems with exponential residence-time distributions.

In addition to particle formation, growth, and coagulation, and the effects of heat and mass transfer and the distribution of residence times, several other phenomena may influence the behavior of an aerosol process. Two of the more important mechanisms are particle deposition by thermophoresis in nonisothermal systems and particle losses by turbulent deposition. Friedlander[10] and Hinds[12] provide an introduction to these phenomena. Particle transport by thermophoresis in laminar and turbulent flows was studied in detail by several investigators.[26,27] Particle transport in turbulent flows has been examined extensively.[10,28] Crump and Seinfeld[29] developed a theory for the turbulent deposition and gravitational sedimentation of particles in a vessel of arbitrary shape.

This section has discussed the theory for the relatively complex aerosol processes relying on gas-to-particle conversion. In contrast, the theory for spray pyrolysis processes is much simpler. In the spray pyrolysis process, particles are formed by passing a solution containing powder precursors through an aerosol generator to form droplets. These droplets are then passed through a heated reactor where the solvent evaporates and the precursors decompose to produce the product. Thus, the critical step which determines the spread in the particle-size distribution and the average particle size is aerosol generation. Hinds[12] discusses the characteristics of a number of commercially available aerosol generators.

Monodisperse Powder Production in Aerosol Processes

Monodisperse powders are desirable for many ceramic applications.[6] In all of the processes discussed here, except for spray pyrolysis, molecular or atomic precursors condense homogeneously or react on the surface of clusters to form particles. Each particle then grows at a certain rate, depending on the conditions to which it is exposed while in the system.

Qualitatively, production of monodisperse aerosol requires that four conditions be met[30]: (1) Particle formation and growth must be separated to ensure that initial differences in particle size become negligible as the particles grow. (2) The residence-time distribution must be narrow to ensure that all particles have the same time to grow. (3) All particles must encounter the same conditions during their residence time in the system to ensure that they grow to the same final size. (4) Coagulation must be eliminated since it broadens the particle-size distribution.

Flame Processes

Flame processes are used for the large-scale production of SiO_2, TiO_2, and carbon black.[1] In a typical flame process, reactants are introduced into a flame where they react rapidly to form gaseous products (Fig. 2). Maximum flame temperatures are as high as 2500 K. The gaseous products condense homogeneously or react on the surface of clusters to form a

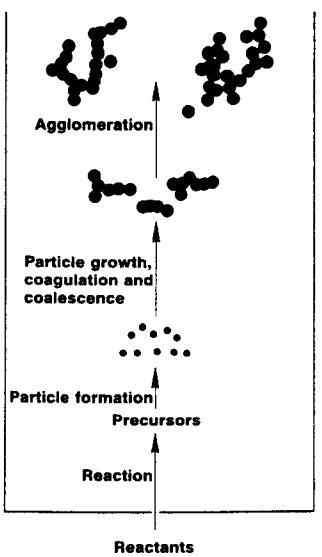

Fig. 2. Flame process.

high concentration of particles. The particles then coagulate, coalesce, and grow and may eventually form agglomerates (Fig. 2). In some processes, the particles exist as aggregates, flocs of small particles, throughout their existence.[31] Flame processes have been termed *pulse reactors* because the condensable material is generated in a short time relative to the characteristic times for subsequent processes such as particle formation, growth, coagulation, and coalescence.[32]

Variations of this basic process have been used to produce alumina powders. Buchanan et al.[33] produced ultrafine mixed-oxide powders based on alumina using an oxygen-acetylene flame. Atomized alcoholic solutions of aluminum isopropoxide doped with suitable metal acetates, alkoxides, or oxides were oxidized in the flame to form the product powder. Sokolowski et al.[34] formed alumina powder by oxidizing aluminum acetylacetonate ultrasonically sprayed into a hydrocarbon-oxygen flame. Formenti et al.[35] formed alumina and other oxide particles by reacting metal chloride vapors in an oxygen-hydrogen flame.

Alumina and other powders are typically produced in flames by introducing a metal-containing compound into the flame. The compound reacts rapidly to form molecular products. Alumina nuclei are probably formed by reaction of molecular species on cluster surfaces.[36] Katz and Donohue[18] studied the theory of particle formation limited by chemical reaction. The particle formation process is at present poorly understood.

The product particle-size distribution from flame processes is essentially independent of the distribution resulting from homogeneous nucleation.[37,38] Growth, coagulation, and particle fusion quickly change the initial size distribution and determine the final size distribution (Fig. 2). As a result, product particle-size distributions in flames tend to be broad and follow self-preserving theory.[37,39] Seigneur et al.[21] reviewed models for coagulation and growth of particles that coalesce instantly after colliding. Ulrich and Subramanian[38] examined systems where the particles do not instantly coalesce after colliding.

One advantage of flame processes is that a large variation (0.001 to 0.5 μm) can be obtained in the size of the primary particles that form aggregates (Table I). The aggregates can range from single particles to about 1000 primary particles, depending on the operating conditions. Another advantage of flame technology is that the effluent streams can be processed easily; by-products can be removed easily and recycled and the powder can be efficiently and economically collected on fabric filters. One disadvantage of flame processes is the relatively high cost of the reactants. However, this is often compensated for by the high purity and other desirable characteristics of the product. Another disadvantage of flame processes is that product particle-size distributions tend to be broad since they are determined by the effects of coagulation. Also, the particles are usually not spherical due to incomplete coalescence of particles after collisions.

Plasma Processes

Plasma processes are the most complicated of all aerosol methods for powder production because of the complexities associated with the plasma; plasmas are created by passing a current through a gas, thereby heating the gas to between 5000 and 25 000 K and ionizing the gas. In the tail flame of the plasma, downstream of the plasma arc, the temperature drops sharply to much lower values. Similarly, the temperature drops sharply between the arc and the walls, which are often water-cooled.

The theory for plasma aerosol systems exists in a fragmented form. Various workers have studied chemical reactions in plasmas.[40,41] Particle formation, growth, coagulation, thermophoresis, and other important aerosol phenomena have been studied extensively, as discussed earlier. Temperature and velocity profiles have been calculated for some plasma systems. Very little work, however, has focused on incorporating all the pertinent theoretical and experimental information into a complete description of plasma aerosol processes.

Figure 3 shows three types of plasma aerosol processes that have been examined experimentally. The individual steps in the process are drawn sequentially. In actual processes, however, many of the steps occur simultaneously. In the first process (Fig. (3A)), a material in particulate form is vaporized in a plasma. The vapor then cools and condenses to form particles. The vapor may also deposit on the reactor walls. The particles grow and may deposit on the walls by thermophoresis or other mechanisms. The particles, depending on their concentration and the residence-time distribution, may also coagulate or agglomerate. This type of plasma process was used by Pickles and McLean[42] to make ultrafine alumina particles. Yoshida

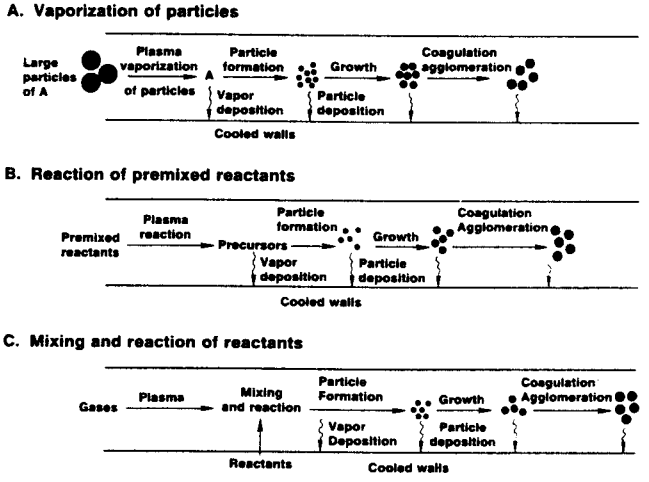

Fig. 3. Plasma processes.

et al.[43] used this type of system to produce ultrafine iron particles. Tarroni et al.[44] produced monodisperse iron particles using this method. Vissokov and Brakalov[45] produced aluminum nitride particles by reacting aluminum particles with nitrogen.

In the second process (Fig. 3(B)), premixed gaseous reactants are reacted in the plasma to form molecular precursors to the particles. The mixture is then cooled, resulting in particle formation followed by processes similar to those in Fig. 3(A). This type of plasma reactor has been operated by Gani and McPherson[46] and Aivazov et al.[47]

In the final type shown (Fig. 3(C)), gaseous reactants are introduced into the tail flame of the plasma. The reactant gas streams then mix with the main stream and react to form molecular precursors to the particles. Hollabaugh et al.[48] injected silane, methane, and hydrogen into the tail flame of an argon plasma to form silicon carbide powder. Zyatkevich et al.[49] formed AlN powders by introducing ammonia into a plasma containing aluminum vapor. Rezchikova et al.[50] produced TiN-Mo composite powders by injecting $TiCl_4$ and $Mo(CO)_6$ into a low-temperature nitrogen plasma.

Plasma processes have been used to produce various alumina-based powders. Aivazov et al.[47] formed alumina powder by oxidation of $AlCl_3$ and combustion of Al powder. Gani and McPherson[46] made Al_2O_3-TiO_2 powders by oxidation of Al_2Br_6 and $TiCl_4$ in an oxygen-argon high-frequency plasma. Silica powders doped with alumina have been produced by vaporizing and oxidizing silicon and aluminum powders and then condensing the vapor.[51]

The theory for the aerosol dynamics in plasma processes is similar to that for flame and reaction processes. For this reason, only a short discussion will be presented here.

Several processes may determine the product particle-size distribution in plasma systems. For systems in which high particle concentrations are formed, as in flames, broad particle-size distributions are produced by the effects of coagulation. This type of plasma reactor operation has been studied by Canteloup et al.,[51] Gani and McPherson,[46] and Yoshida et al.[43]

For plasma systems with broad residence-time distributions, the particle-size distribution may be determined by the reactor residence-time distribution. Pratsinis et al.[23b] showed that broad residence-time distributions produce broad particle-size distributions. Kodas et al.[22b] showed that reactant mixing in aerosol reactors can produce broad residence-time distributions and, as a result, broad particle-size distributions. This problem has not been investigated extensively.

For systems with narrow residence-time distributions, in which coagulation is unimportant, monodisperse particles can be produced by minimizing diffusion of the condensing species and separating nucleation and growth. This type of plasma reactor was used by Boffa and Pfender[52] to produce monodisperse carbon particles in the submicrometer range and by Tarroni et al.[44] to produce monodisperse iron particles.

One advantage of plasma processes is that high temperature phases of compounds can be obtained by rapid quenching. Superconducting and amorphous metals and compounds have been produced using this technique. Another advantage is that effluent streams are easily handled; the product powder can be collected on filters while gaseous by-products can be removed easily. One disadvantage of plasma processes is their complexity. Some other disadvantages are that particle-size distributions are often broad and the reactants can be relatively expensive.

Condensation Processes

Vapor condensation processes can be divided into two broad categories (Fig. 4). The individual steps are shown sequentially, but many of the steps occur simultaneously in actual systems. In the first category, a hot vapor of the product is condensed to form the solid product particles (Fig. 4(A)). The maximum temperature is of the order of the melting temperature of the product which, for some compounds, can be greater than 3000 K. In the second category, a hot vapor of a precursor to the product is condensed to form liquid droplets. Temperatures in this step are typically less than 500 K. The droplets are then reacted with a gas-phase reactant or thermally decomposed to form the solid product (Fig. 4(B)).

Particle production by direct vapor condensation of metal and oxide vapors has been studied by numerous investigators. Homma et al.[53] produced monodisperse lead, tellurium, bismuth, and indium aerosol by condensing vapors generated in a furnace. Ramsey and Avery[54] produced alumina and other ceramic powders by evaporating the bulk oxides and then condensing the vapors.

Particle formation by vapor condensation and subsequent chemical reaction has been used to produce alumina on a laboratory scale using aluminum

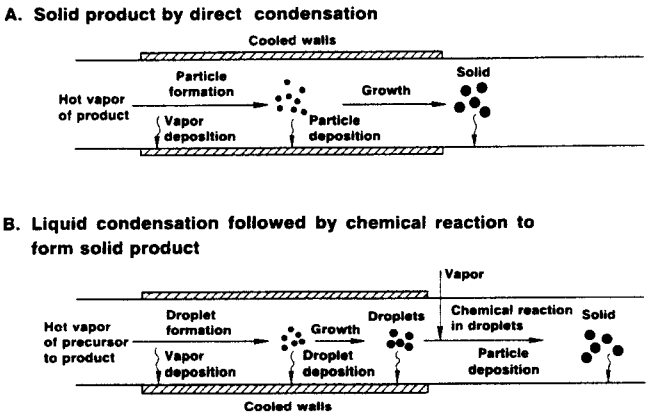

Fig. 4. Condensation processes.

alkoxides as the starting material.[22c,55] The alkoxide liquid is heated and vaporized into a carrier gas. The gas mixture is cooled, resulting in the formation of liquid droplets by homogeneous nucleation or by heterogeneous nucleation onto seed particles. The liquid droplets are then reacted with water vapor to form the solid product. Narrow particle-size distributions have been produced using this process.[56] Figure 5 is a scanning electron micrograph of alumina powder produced using this method.[22c] The versatility of this process has been demonstrated by producing monodisperse polymer[57] and TiO_2[58] particles of high purity. Mixed titania/alumina powders have been produced by hydrolysis of mixed aluminum-sec-butoxide-titanium ethoxide aerosol droplets.[59]

The steps that determine the spread of the product particle-size distribution are liquid particle formation and growth (Fig. 4). For this reason, experimental and theoretical work has focused on these steps. Davis and Liao[60] modeled particle growth in tubular condensers with a no-flux boundary condition for the vapor at the walls. Their theoretical analysis pointed out the importance of heat transfer in controlling product particle-size distributions; enhancing heat transfer relative to mass transfer produced narrower particle-size distributions. With sufficiently rapid heat transfer relative to mass transfer, radial redistribution of the condensing species was minimized, resulting in uniform conditions for particle growth in the reactor.

Pesthy et al.[24] examined the same problem, but assumed a saturation ratio of unity at the wall and examined the use of different nucleation theories to describe particle formation. They concluded that most of the condensing species would be lost to the condenser walls for certain operating conditions.

Pratsinis et al.[23c] examined the theory of vapor condensation in annular, parallel plates and tubular geometries. The reactor geometry did not significantly influence the product particle-size distribution for systems with narrow residence-time distributions. The analysis, however, suggested that turbulent flow processes may produce broader particle-size distributions than laminar flow processes for certain conditions. Rates of heat and mass transfer were comparable in turbulent flow systems, leading to significant redistribution of the vapor in the condenser and resulting in nonuniform particle growth. Nadkarni and Mahalingam[61] numerically solved the equations for aerosol behavior in temperature-gradient fields in tube flows. Their model can be used to estimate particle-wall losses in nonisothermal systems.

Almost all reported vapor condensation experiments were conducted under laminar flow conditions at low Reynolds numbers. Recently, however, Kodas et al.[22c] experimentally studied alumina powder production in a turbulent flow system. Product particle-size distributions were relatively narrow but broader than those obtained from laminar flow systems. The particles were porous, spherical, and of high purity. Their results show that large quantities of powder can be produced by turbulent-flow aerosol condensation processes.

Ingebrethsen and Matijevic[56] studied the kinetics of hydrolysis of metal alkoxide aerosol droplets in the presence of water vapor (Fig. 4(B)). They concluded that the process was controlled by reaction in the droplet or diffusion of reactants and/or products in the droplet.

The results from the literature suggest that monodisperse particles can be produced by condensation processes when four conditions are satisfied.[30]

1. Nucleation and growth must be separated. Also, the condenser must have enough residence time to allow complete condensation of the vapor. Otherwise, any remaining vapor may react in subsequent steps to form very fine particles, leading to a bimodal particle-size distribution. This may require long condensers for high gas flow rates.[22c]
2. The residence-time distribution must be narrow. Free convection must be minimized and the condenser geometry must be carefully chosen to avoid any recirculation.
3. All particles must consume the same amount of the condensable species. This requires eliminating diffusion of the condensing species by using a carrier gas with high thermal diffusivity relative to the vapor diffusivity. This results in rapid uniform cooling and

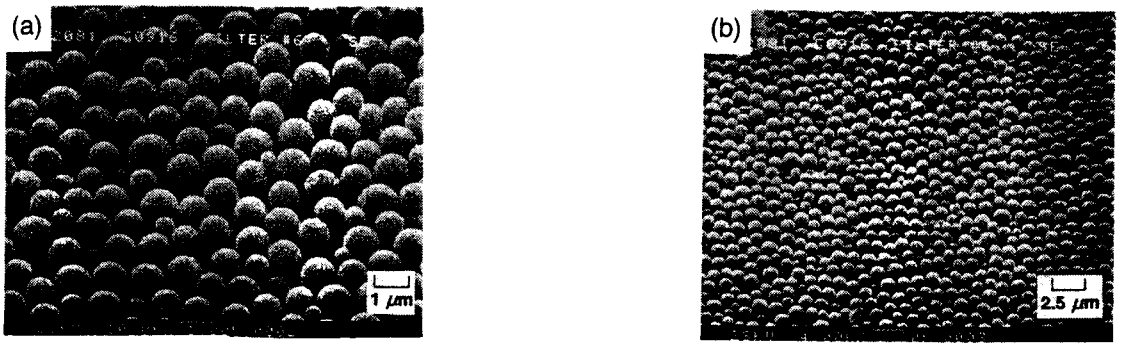

Fig. 5. Alumina powder produced by condensation of aluminum-sec-butoxide to form liquid droplets, followed by reaction of droplets with water vapor to form solid particles. (Bar = (*a*) 1 μm; (*b*) 2.5μm.)

rapid particle formation across the condenser. The surface area of the particles then consumes the vapor, minimizing diffusion of the vapor to the walls.

4. Coagulation must be eliminated. This requires production of sufficiently low particle concentrations by controlling the vapor concentration and cooling rate.

Advantages of condensation methods are that the product particles have a narrow particle-size distribution and are spherical, of high purity, and unaggregated. Another advantage is the simplicity of the system; the powder is produced using standard unit operations such as vaporization of a liquid into a carrier gas, condensation of the vapor, chemical reaction, and powder collection. A disadvantage is that relatively expensive reactants are usually required.

Reaction Processes

Reaction processes are a versatile method for powder production. The systems considered here rely on chemical reactions to produce species which then condense or react to form particles. Typical maximum operating temperatures range from room temperature up to roughly 2000 K, depending on the process and operating conditions.

Figure 6 is a schematic of a typical reaction process. In general, two or more reactants must be mixed in the reactor. These components react to form gaseous products. These gaseous species then deposit on the walls and either (1) condense homogeneously to form particles or (2) react on the surface of clusters to form particles, depending on the specific chemical system. The particles then grow and may also deposit on the reactor walls. Under certain operating conditions, the particles may coagulate or agglomerate. Although the steps are shown separately, many of them may occur simultaneously in actual systems.

Alumina powder production by reaction methods has not been studied extensively. Many other powders, however, have been produced. Silicon powders have been made by thermal decomposition of silane in a tubular flow reactor with heated walls.[62,63] Silicon and SiC powders have been formed by laser thermal decomposition of silane.[64,65] Carbide and nitride particles have been produced by chemical reaction in a tubular flow reactor.[66] Suyama and Kato[67] reacted $TiCl_4$ with oxygen to form TiO_2. Prochazka and Greskovich[68] reacted silane and ammonia in a tubular flow reactor to produce silicon nitride powder. Mazdiyasni et al.[69] made ultrahigh-purity submicrometer zirconia particles by thermal decomposition of zirconium alkoxide vapor. Mazdiyasni and Cooke[70] produced Si_3N_4 by reaction of $SiCl_4$ with ammonia.

The aerosol dynamics in the process shown in Fig. 6 can be described by the general dynamic equation (GDE).[10] Numerical and analytical solutions have been obtained for the GDE for various limiting cases, mostly for isothermal systems. Two approaches to solving the GDE accounting for particle formation and growth without assuming a form for the particle-size distribution are the sectional approach of Gelbard and Seinfeld[71] and the moment approach of Friedlander.[13]

The sectional approach is a method of solving the GDE by approximating the aerosol size distribution as consisting of size sections.[71] So far, the sectional approach has been applied only to batch systems or flow systems with a flat velocity profile and no radial vapor concentration gradients. Henry et al.[72] and Sutugin et al.[20] have also presented models for the aerosol dynamics in batch reactors in which the particle-size distribution is divided into sections. The power of these approaches is their ability to solve for detailed particle-size distributions accounting for particle formation, growth, coagulation, and deposition.[21]

The moment approach of Friedlander[13] involves reducing the partial differential equation of the GDE (without coagulation) to a set of coupled nonlinear ordinary differential equations for moments of the particle-size distribution. The resulting equations are relatively simple yet provide the spread of the particle-size distribution; aerosol yield; and the total particle concentration, area, and volume. Using this approach, particle formation and growth have been studied in various reactor geometries taking into account the residence-time distribution and diffusion of molecular reactants and products and mixing of reactants.[22a,b,23a,b,e] A related method in which the aerosol is assumed to be monodisperse has been used to predict aerosol concentrations resulting from a burst of particle formation in batch reactors.[73] Warren and Seinfeld[19] used this approach to study the more general problem of particle formation and growth from a continuously reinforced vapor in a batch reactor. Stern et al.[74] used this approach to study the effect of spatial inhomogeneities on the rate of particle formation in batch reactors.

Kodas and Friedlander[30] identified the operating conditions required for production of monodisperse particles in tubular aerosol flow reactors:

1. Particle formation and growth must be separated. This allows all particles to grow to the same final size since initial differences in particle size become negligible as particles grow. Particle formation and growth can be separated by operating with a sufficiently high rate of formation of the condensing species.

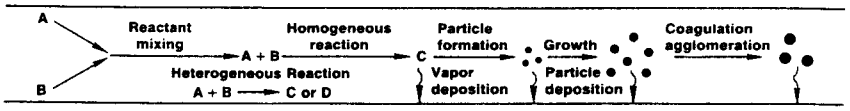

Fig. 6. Reaction process.

2. The reactor residence-time distribution must be narrow. This gives all particles roughly the same length of time to grow.

3. Radial diffusion of the condensing species must be minimized to produce equal depletion of the condensing species by all particles. Radial diffusion of the condensing species can be minimized by operating with sufficiently high rates of formation of the condensing species, high pressures, and large reactors.

4. Coagulation must be eliminated since it broadens the particle-size distribution and can lead to the formation of aggregates. Coagulation can be eliminated by operating below a critical value of the rate of formation of the condensing species.

One advantage of reaction methods is that a large range of particle diameters can be obtained (Table I). Particles of silicon as large as 10 μm have been produced by thermal decomposition of silane.[63] Another advantage is that reaction processes are simple; an aerosol reactor can consist of a reactant introduction system, a reactor tube, and filters to collect the product. The primary disadvantage is, as with the other aerosol processes, that relatively expensive reactants are required.

Spray Pyrolysis

The spray pyrolysis or evaporative decomposition process is a simple and versatile method for powder production. In this process, one or more precursors are dissolved in a solvent which is passed through an aerosol generator. The droplets that are formed are then sent through a heated-wall reactor where the solvent evaporates and the precursors decompose in the particles to yield the product powder.

This process has been used to produce alumina[75–77] and alumina-zirconia powders,[78] in addition to a variety of other materials including ZrO,[79] MgO,[80] NiO,[81] Y_2O_3,[82] ternary sulfides,[83] and superconductors, $YBa_2Cu_3O_7$.[84,85] As mentioned earlier, the particle-size distribution is determined primarily by the characteristics of the aerosol generator. Thus, nearly monodisperse particles have been produced by using the appropriate aerosol generator system.

The primary advantages of the spray pyrolysis process are its simplicity, the ability to produce multicomponent powders using inexpensive reactants, and the ability to provide a broad range of average particle diameters. The primary disadvantage is that this process usually produces highly porous particles because of the solvent evaporation step. As a result, it is often difficult to sinter the powders to near theoretical densities.

Summary

Experimental and theoretical studies of flame, plasma, condensation, reaction, and spray pyrolysis aerosol processes for powder production have been reviewed. These processes can produce monodisperse, spherical, unaggregated particles of high purity ranging in size from molecular clusters to roughly 10 μm. Currently, the most widely used type of aerosol process on an industrial scale is reactions in flame. This process is currently used to make TiO_2, SiO_2, and carbon-black powders. Plasma, reaction, and condensation processes, however, are not used regularly on an industrial scale. This has been due, in the past, to a lack of a basic understanding of aerosol systems. However, the understanding of aerosol processes has advanced sufficiently to allow the rational design and operation of aerosol systems for fine-particle production. This should allow aerosol processes to find more applications for the production of alumina and various other powders.

References

[1]G. D. Ulrich, *C&EN*, August 6, 1984; pp. 22–29.

[2]G. B. Kenney and H. K. Bowen, *Am. Ceram. Soc. Bull.*, **62** [5] 590–96 (1983).

[3]H. J. Sanders, *C&EN*, July 9, 1984; pp. 26–40.

[4]D. W. Richerson, Modern Ceramic Engineering. Marcel Dekker, New York, 19282.

[5]W. H. Rhodes, *J. Am. Ceram. Soc.*, **64**, 19–22 (1981).

[6]H. K. Bowen, *Mater. Sci. Eng.*, **44**, 1–56 (1980).

[7]R. L. Pober, E. A. Barringer, M. V. Parrish, N. Levoy, and H. K. Bowen, "Dispersion and Packing of Narrow Size Distribution Ceramic Powders," MIT Report No. 5-7-83.

[8]E. A. Barringer and H. K. Bowen, *J. Am. Ceram. Soc.*, **65** [12] C-199–C-201 (1982).

[9]C. Misra, "Industrial Alumina Chemicals," American Chemical Society Monograph 184, Washington, DC, 1986.

[10]S. K. Friedlander, Smoke Dust and Haze. Wiley-Interscience, New York, 1977.

[11]G. M. Hidy and J. R. Brock, The Dynamics of Aerocolloidal Systems. Pergamon, New York, 1970.

[12]W. C. Hinds, Aerosol Technology. Wiley-Intersciences, New York, 1982.

[13]S. K. Friedlander, *Ann. New York Acad. Sci.*, **404**, 354–64 (1983).

[14]G. S. Springer, *Adv. Heat Trans.*, **14**, 281–346 (1978).

[15]W. J. Shugard, R. H. Heist, and H. Reiss, *J. Chem. Phys.*, **61**, 5298–5305 (1974).

[16]P. Mirabel and J. L. Katz, *J. Chem. Phys.*, **60**, 1138–44 (1974).

[17]H. Reiss, *J. Chem. Phys.*, **18**, 840–48 (1950).

[18]J. L. Katz and M. D. Donohue, *J. Colloid Int. Sci.*, **85**, 267–77 (1982).

[19]D. R. Warren and J. H. Seinfeld, *Aerosol Sci. Technol.*, **3**, 135–53 (1984).

[20]A. G. Sutugin, A. N. Grimberg, and A. S. Puchkov, *J. Colloid Int. Sci.*, **98**, 229–35 (1984).

[21]C. Seigneur, A. B. Hudischewskyj, J. H. Seinfeld, K. T. Whitby, E. R. Whitby, J. R. Brock and H. M. Barnes, *Aerosol Sci. Tech.*, **5**, 205–22 (1986).

[22]*(a)* T. T. Kodas, S. E. Pratsinis, and S. K. Friedlander, *J. Colloid Int. Sci.*, **111**, 102–11 (1986).

(b) T. T. Kodas, S. E. Pratsinis, and S. K. Friedlander, *Ind. Eng. Chem. Fund Res.*, **26**, 1999–2007 (1987).

(c) T. T. Kodas, A. Sood, and S. E. Pratsinis, *Powder Technol.*, **50**, 47 (1987).

[23]*(a)* S. E. Pratsinis, T. T. Kodas, M. P. Dudukovic, and S. K. Friedlander, *Ind. Eng. Chem. Proc. Des. Dev.*, **25**, 634 (1986).

(b) S. E. Pratsinis, T. T. Kodas, M. P. Dudukovic, and S. K. Friedlander, *Chem. Eng. Sci.*, **41**, 693–700 (1986).

(c) S. E. Pratsinis, T. T. Kodas, and A. Sood, *Ind. Eng. Chem. Res.*, **27**, 105–10 (1988).

(d) S. E. Pratsinis, A. Pearlstein, and S. K. Friedlander, *AIChE J.*, **32**, 177–85 (1986).

(e) S. E. Pratsinis, T. T. Kodas, M. P. Dudukovic, and S. K. Friedlander, *Powder Technol.*, **27**, 17–23 (1986).

[24]A. J. Pesthy, R. C. Flagan, and J. H. Seinfeld, *J. Colloid Int. Sci.*, **91**, 525–45 (1983).

[25]J. G. Crump and J. H. Seinfeld, *AIChE J.*, **26**, 610–16 (1980).

[26]M. C. Weinberg, *J. Am. Ceram. Soc.*, **66**, 439–43 (1983).

[27]R. L. Byers and S. Calvert, *Ind. Eng. Chem. Fund.*, **8**, 646–55 (1969).

[28]G. A. Sehmel, *Aerosol Sci.*, **4**, 125 (1972).

[29]J. G. Crump and J. H. Seinfeld, *J. Aerosol Sci.*, **12**, 405–15 (1981).

[30]T. T. Kodas and S. K. Friedlander, *AIChEJ.*, **34**, 551–57 (1988).

[31]G. D. Ulrich and J. W. Riehl, *J. Colloid Int. Sci.*, **87**, 257-65 (1982).

[32]S. K. Friedlander, *Aerosol Sci. Technol.*, **1**, 3–13 (1982).

[33]R. K. Buchanan, P. J. Grose, and M. S. J. Gani, *Proc. Aust. Ceram. Conf. 9th, Aust. Ceram. 80, Sydney Aust.*, 102–104 (1980).

[34]M. Sokolowski, A. Sokolowska, A. Michalski, and B. Gokieli, *J. Aerosol Sci.*, **8**, 219–30 (1977).

[35]M. Formenti, F. Juillet, P. Meriaudeau, S. J. Teichner, and P. Vergron, p. 45 in Aerosols and Atmospheric Chemistry. Edited by G. M. Hidy. Academic Press, New York, 1972.

[36]R. W. Hermsen and R. Dunlap, *Comb. Flame*, **13**, 253–61 (1969).

[37]A. P. George, R. D. Murley, and E. R. Place, *Faraday Symp. Chem. Soc.*, **7**, 63–70 (1973).

[38]G. D. Ulrich and N. S. Subramanian, *Comb. Sci. Technol.*, **17**, 119–26 (1977).

[39]G. D. Ulrich, *Comb. Sci. Technol.*, **4**, 47–57 (1971).

[40]M. I. Boulos, *Mater. Res. Soc. Symp. Proc.*, **30**, 53–60 (1984).

[41]J. Szekely, *Mater. Res. Soc. Symp. Proc.*, **30**, 1–11 (1984).

[42]C. A. Pickles and A. McLean, *Am. Ceram. Soc. Bull.*, **62** [9] 1004–1009 (1983).

[43]T. Yoshida, A. Kawasaki, and K. Akashi, *Comm. Symp. Int. Chim. Plasmas*, 3d ed. P. Fauchais, 3, paper S.3.3 (1977).

[44]G. Tarroni, V. Prodi, C. Melandri, G. F. Bompare, T. DeZaiacomo, and M. Formignani, *J. Aerosol Sci.*, **6**, 305–10 (1975).

[45]G. P. Vissokov and L. B. Brakalov, *J. Mater. Sci.*, **18**, 2011–16 (1983).

[46]M. S. J. Gani and R. McPherson, *J. Mater. Sci.*, **15**, 1915–25 (1980).

[47]M. I. Aivazov, V. V. Volod'ko, B. A. Evseev, and Y. N. Nikulin, *Sov. Powder Metall. Met. Ceram.*, **20**, 1–3 (1981).

[48]C. M. Hollabaugh, D. E. Hull, L. R. Newkirk, and J. J. Petrovic, *J. Mater. Sci.*, **18**, 3190–94 (1983).

[49]D. P. Zyatkevich, T. Ya. Kosolapova, G. N. Makarenko, G. S. Oleinik, A. W. Pilyankevich, and D. D. Pokrovskii, *Porosh Kovaya Metallurgiya*, **7**, 70–73 (1978).

[50]T. V. Rezchikova, I. A. Domashnev, V. N. Troitskii, V. I. Torbov, and Y. M. D. Shul'ga, *Sov. Powder Metall. Met. Ceram.*, **22**, 869–73 (1984).

[51]J. Canteloup, R. Tueta, and M. Braguier; pp. 438–43 in Conference Proceedings of an International Symposium on Plasma Chemistry, 4th ed. Edited by S. Veprek and J. Hertz, (1979).

[52]C. V. Boffa and E. Pfender, *Aerosol Sci.*, **4**, 103–12 (1973).

[53]K. Homma, K. Kavai, and K. Nozaki; p. 361 in Generation of Aerosols and Facilities for Exposure Experiments. Edited by K. Willeke. Ann Arbor Science Publishers, Ann Arbor, MI, 1980.

[54]D. F. Ramsey and R. G. Avery, *J. Mater. Sci.*, **9**, 1681–88 (1974).

[55]B. J. Ingebrethsen and E. Matijevic, *J. Aerosol Sci.*, **11**, 271–80 (1980).

[56]B. J. Ingebrethsen and E. Matijevic, *J. Colloid Int. Sci.*, **100**, 1–16 (1984).

[57]E. Matijevic, *Langmuir* **2**, 2 (1986).

[58]M. Visca and E. Matijevic, *J. Colloid Int. Sci.*, **68**, 308–19 (1979).

[59]B. J. Ingebrethsen, E. Matijevic, and R. E. Partch, *J. Colloid Int. Sci.*, **95**, 228–39 (1983).

[60]E. J. Davis and S. C. Liao, *J. Colloid Int. Sci.*, **50**, 488–502 (1975).

[61]A. R. Nadkarni and R. Mahalingam, *AIChE J.*, **31**, 603–14 (1985).

[62]J. J. Wu, R. C. Flagan, and O. J. Gregory, *Appl. Phys. Lett.*, **49**, 82–84 (1986).

[63]M. K. Alam and R. C. Flagan, *Aerosol Sci. Tech.*, **5**, 237–48 (1986).

[64]G. W. Rice and R. L. Wooden, *SPIE*, **458**, 98–107 (1984).

[65]W. R. Cannon, S. C. Danforth, J. H. Flint, J. S. Haggerty, and R. A. Marra, *J. Am. Ceram. Soc.*, **65** [7] 324–30 (1982).

[66]A. Kato, J. Hojo, and Y. Okabe, Memoirs of the Faculty of Engineering, Kyushu University, No. 41, 1981; pp. 319–34.

[67]Y. Suyama and A. Kato, *J. Am. Ceram. Soc.*, **59**, 146–49 (1976).

[68]S. Prochazka and C. Greskovich, *Am. Ceram. Soc. Bull.*, **57** [6] 579–86, (1978).

[69]K. S. Mazdiyasni, C. T. Lynch, and J. S. Smith, *J. Am. Ceram. Soc.*, **48** [7] 372–75 (1965).

[70]K. S. Mazdiyasni and C. M. Cooke, *J. Am. Ceram. Soc.*, **56** [12] 628–33 (1973).

[71]F. Gelbard and J. H. Seinfeld, *J. Colloid Int. Sci.*, **68**, 363–82 (1979).

[72]J. H. Henry, A. Gonzalez, and L. K. Peters, *Aerosol Sci. Technol.*, **2**, 321–39 (1983).

[73]D. R. Warren and J. H. Seinfeld, *J. Colloid Int. Sci.*, **105**, 136–42 (1985).

[74]J. E. Stern, J. J. Wu, R. C. Flagan, and J. H. Seinfeld, *J. Colloid Int. Sci.*, **110**, 533–43 (1986).

[75]M. I. Ruthner; p. 515 in Ceramic Powders. Edited by P. Vincenzini. Elsevier, Amsterdam, 1983.

[76]A. Kato and Y. Hirata, *Memoirs Faculty Eng., Kyoto Univ.*, **45**, 251–71 (1985).

[77]D. M. Roy, R. R. Neurgaonkar, T. P. O'Holleran, and R. Roy, *Am. Ceram. Soc. Bull.*, **56** [11] 1023–24 (1988).

[78]D. W. Sproson and G. L. Messing, *J. Am Ceram. Soc.*, **6** [5] C-92–C-93 (1984).

[79]T. Q. Liu, O. Sakurai, N. Mizutani, and M. Kato, *J. Mater. Sci.*, **21**, 3698–3707 (1986).

[80]T. J. Gardner and G. L. Messing, *Thermochim. Acta*, **78**, 17–27 (1984).

[81]T. J. Gardner, D. W. Sproson, and G. L. Messing, *Mater. Res. Soc. Symp. Proc.*, **32**, 227–32 (1984).

[82]H. Ishizawa, O. Sakurai, N. Mizutani, and M. Kato, *Am. Ceram. Soc. Bull.*, **65** [10] 1399–1404 (1986).

[83]D. L. Chess, C. A. Chess, and W. B. White, *J. Am. Ceram. Soc.*, **66** [11] C-205–C-207 (1983).

[84]T. T. Kodas, E. M. Engler, V. Y. Lees, R. Jacowitz, T. H. Baum, K. Roche, S. S. P. Parkin, W. S. Young, S. Hughes, J. Kleder, and W. Auser, *Appl. Phys. Lett.*, **52**, 1622–24 (1988).

[85]T. T. Kodas, Angew. Chemie: *Int. Ed. in Eng.*, **28**, 794–807 (1989).

Refractory Ceramic Fiber

Russell D. Smith
The Carborundum Company
Fibers Division
Niagara Falls, NY 14302

Both amorphous and polycrystalline refractory ceramic fiber forms and their method of manufacture are presented. Properties of the fiber are reviewed. Traditional applications such as thermal insulation and nontraditional applications such as composites are discussed.

Increasing energy costs have fueled the need for more-effective insulation and for lighter-weight, higher-performance materials. Refractory ceramic fibers are alumina-containing fibers developed to serve a wide variety of these industrial applications. The compositions are essentially free of alkali and alkaline earths that are present in fiberglass. Refractory ceramic fibers can be of two general types: (1) amorphous fibers attenuated from a melt or (2) polycrystalline fibers produced from a solution chemistry or sol-gel route. Both types of fiber technologies can yield a multitude of fiber compositions and end-product forms.

The amorphous types of fibers were developed in the early to mid-1940s per U.S. Patents 2 467 889 and 2 557 834. Compositions are generally aluminosilicates with small amounts of modifiers such as B_2O_3 or ZrO_2. These fibers were first commercialized as high-temperature thermal insulation as they offered lower thermal conductivity, better thermal shock resistance, and lower heat storage than conventional refractories. Widespread commercialization did not occur until the 1970s, when energy prices increased and the fiber product forms began to be cost-competitive with hard refractories. Today, widespread commercial acceptance of refractory ceramic fiber product forms has occurred in specialty insulation, metals processing, petrochemical, fire retardation, and other market segments. In addition, the product forms are being utilized in emerging composite opportunities.

Solution chemistry approaches have allowed the development of fiber compositions and fiber forms that cannot be produced by the amorphous fiber technology. These alternate technologies were developed and commercialized in the 1970s and 1980s. Market acceptance has grown for higher temperature product forms in insulation markets and for specialty textiles in a wide variety of applications. In emerging composite applications, these fibers can be viewed as low-cost alternatives to other high-performance fibers, e.g., boron, SiC, carbon.

Amorphous Fibers

Manufacture

To produce amorphous refractory ceramic fiber, an aluminosilicate raw material is fused. The alumina source may be either naturally occurring (calcined kaolin or others) or a Bayer-processed alumina. The alumina source is blended with the appropriate silica source and minor ingredients such as ZrO_2, Cr_2O_3, B_2O_3, and others to yield the targeted composition.

The raw materials can be fused by several methods. Originally, the fusion occurred in traditional abrasive-producing furnaces. More commonly today, the fusion takes place in a modified de Bussey furnace, adapted from the fiberglass industries.[1] This furnace produces a continuous stream of melt; hence, it can be tied to continuous fiber processing systems.

The molten stream, produced by the furnace, is attenuated into fiber form by either impacting the molten stream with a high-velocity jet of air and/or steam, or by flowing the molten stream onto a series of rotating wheels.

Once refractory ceramic fiber is produced, it is processed into blanket, paper, felts, boards, textiles, and other forms. Figure 1 shows typical ceramic fiber product forms. In general, these postfiberization processes can be classified into air and wet-laid systems.

Fig. 1. Typical refractory ceramic fiber product forms.

Blankets and textiles are examples of products made by an air-laid system. Papers, felts, and boards are produced by wet-laid systems.

Traditional paper-forming processes such as a Fourdrinier, a cylinder machine, or Rotoformer are used to produce paper or felts. The fiber is dispersed in water and dewatered on the paper-forming equipment. As opposed to papers produced from cellulosic fibers, binders are required to impart handleability to the final product. Fillers may be also added to achieve desired properties.

Refractory ceramic fiber can be processed into boards and special shapes via vacuum casting. In this process, as in the paper process, refractory ceramic fiber is slurried in water with organic and/or inorganic binders. Fillers can be added to impart property enhancement such as improved strength. The slurry is dewatered onto molds via a vacuum. Simple flat shapes can be processed continuously by traditional papermaking techniques.

Textile products are made on traditional textile equipment. Due to the brittle nature of refractory ceramic fiber, organic fibers are blended with the fiber so that improved processing and yields can be achieved. Inserts of continuous fibers are added to yarns to impart strength in final product forms. The yarns are processed into a wide variety of cloths, ropes, and braids.

Blankets are generally produced in a continuous process directly tied to the fiberization system. The fibers are air-laid in a mat form. The mat is needled with barbed needles that interlock the mat together. The resultant needled blanket has sufficient handling strength to be utilized as a furnace-lining material.

Properties

Refractory ceramic fiber is produced in a variety of compositions. Table I shows the commercially available chemistries and their resultant physical properties, as reported by their manufacturers.

In general, refractory ceramic fiber is discontinuous, has 2 to 5 μm mean fiber diameter, contains up to about 50% unfiberized material (shot), and has good tensile and Young's modulus. A photomicrograph of refractory ceramic fiber and its diameter distribution is shown in Fig. 2.

In addition, refractory ceramic fiber has unusual thermal properties. Lightweight refractory ceramic fiber forms have low thermal conductivities. The thermal conductivities of the various types of ceramic fiber forms are compared in Fig. 3.

Another important parameter for refractory ceramic fiber is thermal stability—the temperature to which the product can be used. Many factors, both product- and application-related, determine the product's thermal stability. Product-related parameters include chemistry, crystallization behavior, viscosity of remnant glass, fiber-to-fiber sintering, and others.

When refractory ceramic fiber is exposed to high temperatures, the fibers crystallize to form mullite and cristobalite.[2–4] The crystallization of refractory ceramic fiber has been detailed in the literature.

Olds et al.[5] showed that additions of Cr_2O_3 to aluminosilicate melt yield a product with less thermal shrinkage, due to minimal fiber-to-fiber sintering.

Patents and literature have demonstrated that ZrO_2 additions to an aluminosilicate melt will produce a refractory ceramic fiber with improved thermal stability, improved chemical durability, and improved processing.[6–9]

Impurities such as those found in naturally occurring minerals yield products with lower maximum-use temperature. For example, the maximum-use temperature of products made with kaolin is lower than that for a product produced from pure raw materials.

Table I. Commercially Available Amorphous Refractory Ceramic Fiber

	Standard Temperature		High Temperature		
Raw Material(s)	Kaolin	Al_2O_3 SiO_2	Al_2O_3 SiO_2	Al_2O_3 SiO_2 Cr_2O_3	Al_2O_3 SiO_2 ZrO_2
Typical Composition, %					
SiO_2	52	52	45	55	50
Al_2O_3	45	48	55	41	35
Fe_2O_3	1				
TiO_2	2				
Cr_2O_3				4	
ZrO_2					15
Physical Properties*					
Mean fiber diameter (μm)	2–3.5				
Unfiberized material (%)	≈50				
Young's modulus (GPa)	83–103				
Tensile strength	483–1725				

*Most refractory ceramic fibers made by these processes have similar physical properties.

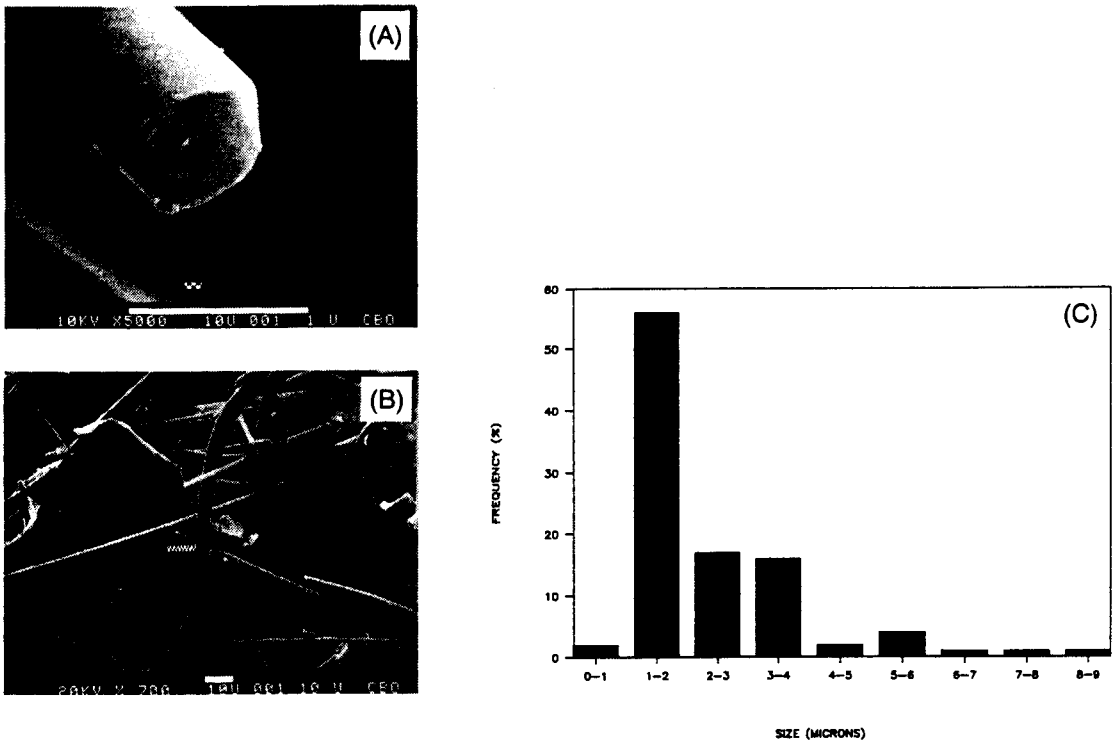

Fig. 2. Amorphous refractory ceramic fiber. (*a*) Low magnification (× 700; bar = 10 μm); (*b*) high magnification (× 5000; bar = 10 μm); (*c*) diameter distribution.

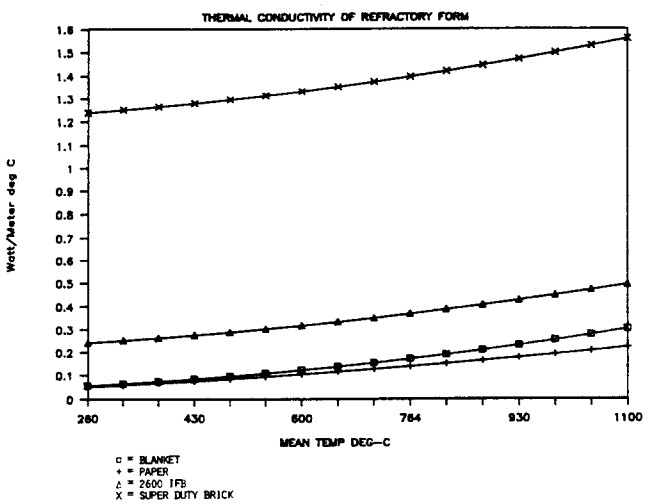

Fig. 3. Thermal conductivity of refractory form □ = blanket; + = paper; Δ = IFB; X = super-duty brick.

Applications

As a result of its physical and thermal properties, refractory ceramic fiber has found commercial use as a high-temperature insulation in iron and steel, petrochemical, aluminum, and metals processing applications. In these applications, refractory ceramic fiber offers low thermal conductivity (less heat loss), lower thermal mass (less heat storage), and improved thermal shock resistance. The literature describes these traditional applications.[10,11]

An important component of the cost of refractory ceramic fiber furnace lining is the installation cost. In recent years, the installation labor has been reduced. In the late 1970s, modular (preformed insulation blocks) lining techniques reduced installation time.[12,13] Recently, sprayable systems have been introduced that further reduce installation time. A sprayable consists of a refractory ceramic fiber that is sprayed. along with a liquid binder, directly onto the furnace substrate.[14,15]

In recent years, refractory ceramic fiber has found acceptance in specialty insulation applications such as automotives and appliances. In the automotive area, refractory ceramic fiber felts/blankets provide insulation between the catalytic converter and the passenger compartment. For ceramic monolith converters, a paper composed of refractory ceramic fiber and raw vermiculite is utilized as a gasket between the monolith and converter housing.[16] Other automotive applications include insulation in mufflers/silencers and heat shields around the passenger compartment. Appliance applications include vacuum-cast shapes for smooth-top ranges, catalytic heaters, and parts for ovens, dryers, etc.

Refractory ceramic fiber has also been used for fire retardation. Examples include fire protection of railroad tank cars, penetration seals in commercial

construction, and fire protection of electrical cables in nuclear power plants.

Due to its fibrous nature, low cost, and mechanical properties, refractory ceramic fiber is currently being evaluated in many applications that previously used asbestos, e.g., friction or brake parts. Many refractory ceramic fiber forms, such as specialty papers, boards, and textiles, are being utilized as substitutes for products that contained asbestos. Many other alternate approaches are being evaluated to replace asbestos forms. Only the cost-effective approaches will be successful.

In addition, refractory ceramic fiber is being evaluated as a cost-effective addition to high-performance fibers. Emerging opportunities are in metal[17] and organic composites for metal and plastic reinforcement.[18] In metal composites, refractory ceramic fiber provides improved properties over aluminum in diesel pistons. In special organic composites, refractory ceramic fiber offers advantages in mechanical properties after thermal exposure.

Economics

The selling price of refractory ceramic fiber products depends on the product form, its density, and the base fiber utilized in that product. Currently, bulk refractory ceramic fiber sells from about $1.50/pound for low-temperature to about $3.50/pound for high-temperature grades. The price of blanket, the product form with the largest commercial usage, ranges from a low cost of $1.00/bd. ft. for low-density, low-temperature blanket to a high of about $5.00/bd. ft. for high-density, high-temperature blanket. Other product forms utilize more specialized manufacturing technology and hence have higher costs. See the appendix for manufacturers who may be contacted for current market prices.

Health and Safety

The health and safety aspects of refractory ceramic fiber are currently under investigation. See the appendix for manufacturers who will inform the user in the safe handling practices of refractory ceramic fiber.

Sol-Gel-Derived Fibers

The properties of traditional amorphous refractory ceramic fiber limit its maximum-use temperature of approximately 1400°C, and limit its use in advanced composites. Additives that could improve the base fiber's properties alter the melt temperature and melt viscosity/surface tension such that the compositions cannot be fiberized successfully. Compositions with these improved properties have been formed by solution chemistry approaches. As in the traditional fusion process, both solution (melt) parameters and process parameters are critical to achieve fiber formation.

Commercial short staple fibers utilize an aluminum oxide precursor, usually a salt such as aluminum oxychlorite, formate, etc.; a silica source, usually colloidal silica, an organosilane, etc.; and modifiers, to alter the fiberization characteristics of the sol. The solution must be adjusted to achieve the proper amount of solids, viscosity, surface tension, and gel time. Examples of commercially viable solution chemistries are provided by U.S. Patents 3 503 765, 3 793 041, 3 950 478, 3 992 498, 4 125 406, and 4 159 205.

Two basic types of fiberization techniques for discontinuous sol-gel fibers are practiced. Kenworthy et al.[19] describe the process for production of Saffil*—a 95% Al_2O_3/5% SiO_2 fiber.

An alternate process for production of Fibermax† (a mullite) fiber was disclosed by Sweeting (U.S. Pat. No. 4 277 264). This process uses a rotary spinning process to attenuate the solution into a fiber form.

The solution chemistry approach also lends itself to formation of continuous filaments. In this type of process, the solution is spun/extruded through a small orifice, attenuated, and "gelled" into a filament. In the commercially practiced technologies, the sol may be composed of alumina particles, an alumina precursor, and modifiers as in du Pont Fiber F.P.,‡ composed of a silicon-based material additional to an organoaluminum compound as in Sumitomo's fiber,§ or composed of a B_2O_3 precursor in an alumina/silica-containing sol as in Nextel 312 fiber.¶

After formation, the fiber must be dried to remove residual water. The green fiber is then calcined to remove volatiles (Cl^-, etc.), to nucleate crystals, and to grow the crystals to the desired crystallite size. Each solution chemistry has its own optimum calcining conditions to achieve strong, handleable, thermally stable fibers. The conditions can be altered to produce specific properties. For example, a fiber for thermal insulation may be calcined in a different cycle than a fiber that would be utilized as a reinforcement. The calcination of Saffil fiber is described by Birchall et al.[20]

The process to convert a continuous filament from a gelled state to a polycrystalline state is more complex than for discontinuous fibers. The fiber must maintain adequate strength during processing such that its integrity is maintained. The process technology must also be capable of compensating for the linear shrinkage that occurs during the densification process.

While sol-gel-processed fibers have property advantages over amorphous refractory ceramic fibers, the manufactured cost for polycrystalline refractory ceramic fiber is generally one to two orders of magnitude higher than for amorphous refractory ceramic fiber.

---

*ICI United States, Inc., Wilmington, DE.
†The Carborundum Company, Niagara Falls, NY.
‡E. I. du Pont de Nemours & Co., Wilmington, DE.
§Sumitomo Industries Ltd., Hyogo, Japan.
¶3M Co, St. Paul, MN.

Table II. Commercially Available Polycrystalline Refractory Ceramic Fibers

Product/Trade name Form	Saffil Discontinuous	Fibermax Discontinuous	F.P. Continuous	Nextel 312 Continuous	Sumitomo Continuous
Composition (%)					
Al_2O_3	95	72	100	62	85
SiO_2	5	28		24	15
B_2O_3				14	
Specific Gravity	2.8	3.0	3.95	2.7	3.2
Mean fiber diameter (μm)	3	3	20	11	17
Young's modulus (GPa)	315	N.A.	379	152	210
Tensile strength (MPa)	1000–2000	N.A.	1000–2000	1000–2000	1000–2000

N.A. - Not available.

Properties

The properties of commercially available sol-processed fibers are listed in Table II. Commercially available fibers vary in Al_2O_3 content from 62 to essentially 100%. As opposed to traditional amorphous refractory ceramic fiber, discontinuous polycrystalline fibers contain essentially no unfiberized material (shot). In general, the fiber diameter distribution is narrower for polycrystalline fibers than for amorphous refractory ceramic fiber, as shown in Fig. 4. Due to the crystalline nature, sol-processed fibers have a larger surface area and more surface texture than amorphous fibers.

The tensile strength of polycrystalline fibers depends on the manufacturing process. The batch components, fiberization, drying, and calcination techniques impart flaws (defects) into the fiber that control the fiber's tensile strength. Birchall et al.[20] demonstrated the influence of crystalline phase on the tensile strength of Saffil fiber. For a 3 μm fiber, the tensile strength varied from approximately 900 to 1000 to 1250 MPa as the alumina phase changed from eta to gamma to delta. They further demonstrated that, as the amount of α-Al_2O_3 increased, the tensile strength decreased. After thermal exposure in which the α-Al_2O_3 phase

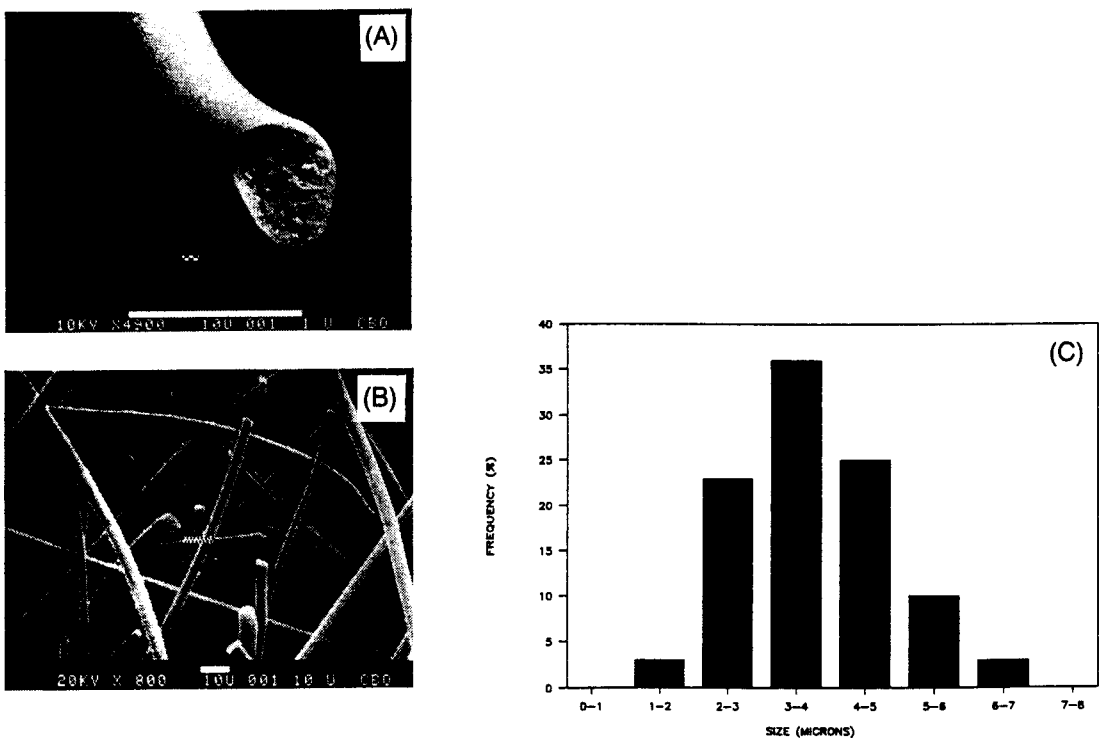

Fig. 4. Polycrystalline refractory ceramic fiber. (*a*) Low magnification (× 800; bar = 10 μm); (*b*) high magnification (× 4900; bar = 10 μm); (*c*) diameter distribution.

can grow, the fiber's tensile strength would be substantially reduced.

The discontinuous polycrystalline fibers have higher melting points than traditional amorphous refractory ceramic fiber. Due to this high melting point and polycrystalline nature, processed fiber can be utilized to higher temperatures.

Like amorphous refractory ceramic fiber, forms made from polycrystalline ceramic fiber have low thermal conductivity, good thermal shock resistance, and low heat storage; hence, they are also excellent products for thermal insulation.

Applications

Sol-gel fibers have found commercial acceptance in both high-temperature thermal insulation and composites. In many ways, these applications are similar to or expansions of those of amorphous refractory ceramic fiber applications.

The discontinuous high-Al_2O_3 fibers have been used as high-temperature insulation to temperatures of 1649°C (3000°F).[21–23] To be cost-effective, the polycrystalline fibers are usually blended with lower-cost amorphous refractory ceramic fiber. Smith[24] showed that the shrinkage (thermal stability) of the blended product form is dependent on the ratio of polycrystalline-to-amorphous fiber. For example, the linear shrinkage of a ceramic fiber product decreased from 6 to 4 to 2 to < 1% as the content of polycrystalline fiber increased from 0 to 20 to 40 to 60%.

The blended fibers can be processed into a variety of insulation forms—boards, felts, modules, papers, etc., via the technologies detailed above. These product forms are installed and utilized in a manner similar to that of amorphous refractory ceramic product forms.

Polycrystalline fiber mats also have found use in specialty insulation forms. Bradbury[25] disclosed use of Saffil fiber as a gas-tight packing between the ceramic monolith and the metal housing in automotive catalytic converters.

Nextel 312 fiber has been utilized in conjunction with silica fiber in the insulation tiles for the space shuttle. Other polycrystalline fibers have been used in different versions of these tiles.

Textile-type product forms have found acceptance in such specialty insulation applications as furnace belts, seals, gaskets, etc.

Chang and Lips[26] detailed the use of textiles, composed of either polycrystalline or amorphous fibers, as a filter medium for filtration of gas streams above 260°C (500°F).

As with the traditional refractory ceramic fiber, the mechanical properties of polycrystalline fibers have allowed it to be utilized in composite applications.

Dhingra[27] described aluminum, magnesium, lead, glass, and resin composites containing Fiber F. P.; Sowman and Johnson[28] described high-temperature polymer composites containing Nextel fiber. Pipes et al.[29] disclosed use of Nextel fiber in epoxies.

Of recent interest is the use of amorphous and polycrystalline refractory ceramic fibers in the reinforcement of aluminum. Donomoto et al.[29] discussed the use of refractory ceramic fiber as a reinforcement for diesel pistons. They cited improved wear properties, reduced thermal distortion, and reduced weight.

In production of a ceramic-fiber-reinforced piston, a ceramic fiber form (preform) is inserted into the mold of a squeeze-casting machine. Under pressure, the aluminum infiltrates and wets the preform. Preforms can be made of either amorphous or polycrystalline fibers. Typical preforms are shown in Fig. 5. The volume fraction of fiber and the orientation of the fiber are controlled to yield the desired composite properties.

The improvement in ultimate tensile strength of fiber-reinforced aluminum over the base alloy as a function of temperature was reported by Dinwoodie et al.[31] Refractory ceramic fiber reinforcement improved the ultimate tensile strength of the alloy at 300°C by over threefold.

Refractory ceramic-fiber-reinforced metals are being evaluated in pistons, connecting rods, wear parts, aerospace, and other applications. Commercial success in this or other composite applications will depend on the economic viability of the technology.

Economics

As with the more traditional refractory ceramic fiber product forms, the cost of polycrystalline fiber products can vary significantly between the different product forms.

For use in thermal insulation, polycrystalline fibers are generally blended with traditional refractory ceramic fiber. As such, the cost of the final product form depends on the product form (i.e., felt, board, modules), its density, and the ratio of polycrystalline fiber-to-refractory ceramic fiber.

Continuous filament polycrystalline product forms are currently available from about $6.00/ft^2 for woven product forms. For current prices, the appropriate manufacturer should be consulted.

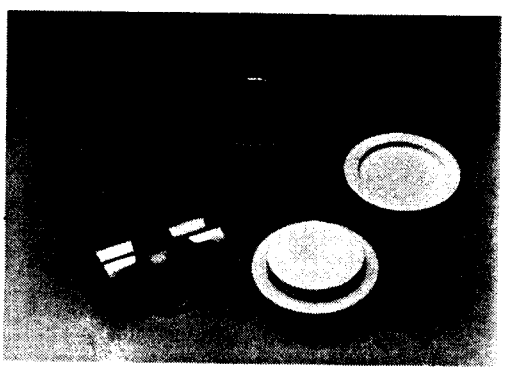

Fig. 5. Fiber-reinforced pistons and ceramic fiber preforms.

Appendix

Manufacturers from whom product information may be obtained are:

1. A. P. Green Refractories Co., Green Blvd., Mexico, MO 65265.
2. Thermal Ceramics, 2102 Old Savannah Rd., Augusta, GA 30903.
3. Combustion Engineering, Inc., 900 Long Ridge Rd., Stamford, CT 06902.
4. E. I. du Pont de Nemours & Co, Wilmington, DE 19898.
5. Imperial Chemical Industries, Ltd., Wilmington, DE 19897.
6. Industrial Furnaces Service, Inc., Box 2039, 10380 State Rt. 43, Streetsboro, OH 44241.
7. Manville Service Corporation, Box 5108-RF, Denver, CO 80217.
8. The Carborundum Company, Box 156, Niagara Falls, NY 14302.
9. 3M Co, 3M Center, Bldg. 225-4N-07, St. Paul, MN 55144.

References

[1]J. G. Mohr and W. P. Rowe, p. 7 in Fiberglass, Van Nostrand Reinhold Company, New York, 1978.

[2]A. Jager, Z. Stadler, and J. Wernig, "Investigations on Microstructural Changes Undergone by Ceramic Fibers at Elevated Temperatures, Particularly as Regards the Formation of Cristobalite, *Ceram. Forum Int.*, **61** [3] 143 (1984).

[3]S. Karlsson, R. Lundberg, and R. Carlsson, "Thermal and Environmental Effects on Ceramic Fibres"; pp. 9–11, presented at Science of Ceramics 13, Japan, 1985.

[4]R. Ganz and W. Kronert, "Crystallization Behaviour of High Temperature Ceramic Fibres of the Al_2O_3-SiO_2 System." *Interceram.*, **2**, 136–44 (1982).

[5]L. E. Olds, W. C. Miller, and J. M. Pallo, "High Temperature Alumina-Silicate Fibers Stabilized with Cr_2O_3," *Am. Ceram. Soc. Bull.*, **59** [7] 739–41 (1980).

[6]W. G. Ekdahl, A. R. Chaudhuri, and W. C. Miller, "High Temperature Refractory Fiber," U.S. Pat. No 4 555 492, November 26, 1985.

[7]W. G. Ekdahl, A. R. Chaudhuri, and W. C. Miller, "Chemically Resistant Refractory Fiber," U.S. Pat. No. 4 558 015, December 10, 1985.

[8]"Insulation Blanket," *Ceram. Ind.*, **11**, 27 (1985).

[9]J. C. McMullen, "Refractory Fibrous Material," U.S. Pat. No. 2 873 197, February 10, 1959.

[10]F. H. Fidler, "Ceramic Fiber in Ceramic Kilns: Past, Present, and Future," *Interbrick*, **1** [5] 1432–36 (1985).

[11]R. M. Lonero, "Recent Advances in Ceramic Fiber Technology," *Am. Ceram. Soc. Bull.*, **62** [9] 1000 (1983).

[12]R. A. Sauder, G. A. Kendrick, and J. R. Mase, "Method for Providing High-Temperature Internal Insulation," U.S. Pat. No. 3 993 237, November 23, 1976.

[13]C. O. Byrd, Jr., "Furnace Lining Apparatus," U.S. Pat. No. 3 952 470, April 27, 1976.

[14]W. H. Smith, "Method for Applying a Layer of Fiber on a Surface," U.S. Pat. No. 4 547 403, October 15, 1985.

[15]J. M. Cerdan-Diaz, M. J. Sanders, and M. E. Wellar, "Spray-Applied Ceramic Fiber Insulation," U.S. Pat. No. 4 640 848, February 3, 1987.

[16]R. A. Hatch and J. R. Johnson, "Intumescent Sheet Material," U.S. Pat. No. 3 916 057, October 28, 1975.

[17]Toyota Motor has Developed the World's First Fiber," *Jpn. Econ. J.*, **8**, 7 (1982).

[18]M. J. Wirtner, "Short Ceramic Fiber as Filler/Reinforcement," *Plastics Compounding* (Jan/Feb 1986).

[19]J. S. Kenworthy, M. J. Morton, and M. D. Taylor, "Process for Producing Alumina," U.S. Pat. No. 3 950 478, April 13, 1976.

[20]J. D. Birchall, J. A. A. Bradbury, and J. Dinwoodie, "Alumina Fibres: Preparation, Properties and Applications"; in Handbook of Composites, Vol. 1. Edited by W. Watt and B. V. Perov. Elsevier, Amsterdam, 1985.

[21]K. Sonobe and K. Tato, "Ceramic Fiber Felt," U.S. Pat. No. 4 269 887, May 26, 1981.

[22]"Saffil Fibers Application Report," Imperial Chemical Industries, November 1975.

[23]C. E. Chaille, R. C. Oxford, and G. C. Caudill, "Ceramic Fiber Board Linings for Furnaces Operating at 1200°-1480°C." *Am. Ceram. Soc. Bull.*, **60** [7] 695–99 (1981).

[24]R. D. Smith, "Thermal Stability of Polycrystalline Fiber/Ceramic Fiber Blended Product Forms," in Proceedings of the First Refractories Conference of Japan, Tokyo, Japan, 1983.

[25]J. A. A. Bradbury, Vol. 1, Paper No. 3, Proc. Int. Sym. Automotive Technol. and Automation, Wolfsburg, 1977.

[26]R. Chang and H. Lips, research performed at Acurex Corporation, Ceramic Fabric Material Testing — Draft Final Report, Acurex Project Rept. No. 7150, May 3, 1985.

[27]A. K. Dhingra, "Metal Matrix Composites Reinforced with Fibre FP (α-Al_2O_3)," *Philos. Trans. R. Soc. (London)*, **A294**, 559–64 (1980).

[28]H. G. Sowman and D. D. Johnson, "Ceramic Oxide Fibers," *Ceram. Eng. Sci. Proc.*, **6** [9–10] 1221–30 (1985).

[29]R. B. Pipes, (Center for Composite Materials, Univ. of Delaware, Newark, Delaware) and D. D. Johnson and K. Karst (Ceramic Fiber Products, 3M Company, St. Paul Minnesota), "Nextel 312 Ceramic Fiber Polymeric Composites."

[30]T. Donomoto (Toyota Motor Corp.) et al., "Ceramic Fiber Reinforced Piston for High Performance Diesel Engines," SAE, 1983.

[31]J. Dinwoodie et al., "The Properties and Applications of Short Staple Alumina Fibre Reinforced Aluminum Alloys"; p. 676 in Proceedings of the Fifth International Conference on Composite Materials ICCM-V, United States, 1985.

Fused Alumina—Pure and Alloyed—as an Abrasive and Refractory Material

Pawel Cichy
Sohio Electro Minerals Co. (retired)
Buffalo, NY 14226

The development of the fused alumina industry from its inception up to the most recent times is presented on the basis of published literature. A brief outline of its production is given, with reference to the furnaces used. Different varieties of fused alumina are mentioned and peculiarities in their production are pointed out. The utilization of fused alumina as an abrasive in the loose state and in bonded and coated applications is reviewed briefly. The additional use of fused alumina in bonded refractories and its alloys with SiO_2, ZrO_2, and MgO is discussed. Finally, the development and production of fused cast refractories consisting of alumina and alumina compositions in excess of 45% are described.

Fused alumina, due to its high hardness and high melting point, is an excellent abrasive and refractory. Its production on an industrial scale was initiated out of need to reproduce and improve the qualities of natural corundum and emery, used since prehistoric times as an abrasive.[1] By fusing alumina-containing natural materials, fused alumina (otherwise called artificial corundum or electrocorundum) was first made by Wehrlein[2] in France and Hasslacher[3] in Germany in 1893 and 1894, respectively.

After introducing some control in product-cooling, Jacobs[4] obtained a somewhat better quality fused alumina. A further step in improving the quality was the addition of iron borings to the bauxite-coke charge, as proposed by Hall,[5] which yielded a product free of metal particles. The final development occurred when Higgins[6] replaced the brick- or carbon-lined batch furnaces with a water-cooled steel shell protected by a thin congealed fused-alumina layer.

It is interesting to note that alumina was first fused in 1837 by Gaudin,[7] to make synthetic rubies in a laboratory arc furnace powered by batteries.

The emergence of the abrasive industry after 1890 with the advent of cheap electrical energy is described by Jacobs,[8] Eardley-Wilmot,[9] and Collie.[10] The latter gave a detailed account from the pioneer days to the period shortly after the Second World War. The many applications of fused alumina and other abrasive materials in the bonded form as wheels, and in the coated form as sandpaper and sanding belts, were summarized in treatises by Jacobs,[8,11] Lewis and Schleicher,[12] and Kleinschmidt.[13]

Many varieties of fused alumina appeared on the market. They differ mainly due to composition (alumina content and kind and amount of alloying oxide) and crystal size (being a function of melt solidification rate).

The different varieties of fused alumina are: (1) brown; (2) white; (3) pink and ruby; (4) monocrystalline; (5) zirconia modified with varying amounts of zirconia, e.g., 10, 25, and 43%; and (6) black.

Table I gives the composition, raw materials used, and some of the physical properties, e.g., hardness and friability, of the above varieties.

The high melting temperature of alumina makes it a good refractory material and, as soon as it was well established as an abrasive, producers extended its application into the refractory field. Its utilization as a refractory has been two-pronged:

1. Loose grain, made from fused crude by crushing and sizing, is rebonded using conventional ceramic bonding materials.
2. Fused cast refractory shapes made from molten alumina (either pure or modified with additions of SiO_2, ZrO_2, Cr_2O_3, and MgO).

Different fused aluminas and their modifications used in bonded refractories are given in Table II and those used as fused cast refractories are given in Table III.

When dispersed from a molten stream with compressed air or steam under pressure,[14,15] fused alumina forms bubbles, which are used for abrasive and refractory applications.

Adding from 37 to 50% silica to alumina and dispersing the molten mixture by a swift current of compressed air produces fibers[16,17] which replace the banned asbestos.

Fused alumina furnaces can also be adapted to make calcium aluminate cement from bauxite, aluminous materials, and lime.[18,19]

Raw Materials

The raw material for all fused alumina varieties is either directly or indirectly bauxite. The genesis of bauxite,[20] its composition,[21,22] and its deposits and sources[23–25] are given in the references.

Table I. Fused Alumina Abrasives

Raw Materials	Calcined Alumina	Calcined Alumina-Chrome ore	Calcined Alumina-Chromium Oxide	Bauxite	Bauxite, Iron Borings, Coke, Pyrite, Lime or Sodium Carbonate	Bauxite, Iron Borings, Coke, Reverts		Bauxite, Iron Borings, Coke, Reverts		1. Calcined Alumina, Baddeleyite, or Zirconia	2. Bauxite, Coke, Iron Borings, Baddeleyite, or Zirconia	3. Bauxite,* Zircon Sand, Coke, and Iron Borings
						Low Titania or (Semi-Friable)		High Titania or (Regular)		Alumina-Zirconia		
	(White)	(Pink)	(Ruby)	(Black)	(Mono-crystalline)	Slow Cooled	Chilled	Slow Cooled	Chill Cast	10% ZrO_2	25% ZrO_2	40% ZrO_2
Composition %												
Al_2O_3	99.53	98.79	96.77	71.7	99.27	96.80	96.66	94.12	94.19	86.15	70.84	53.80
TiO_2		0.28	0.25	4.25	0.57	2.10	2.30	3.05	3.30	2.25	0.91	1.50
SiO_2	0.04	0.18	0.11	12.00	0.03	0.50	0.60	1.65	1.30	1.25	0.94	1.50
Fe_2O_3	0.10	0.33	0.18	8.30	0.08	0.20	0.30	0.20	0.30	0.23	0.27	0.27
Na_2O	0.33	0.23	0.61		0.05	0.02	0.02	0.03	<0.01			
Cr_2O_3		0.07	2.03						0.12			
MgO			0.04	1.20		0.02	0.12	0.55	0.15			
CaO		0.12	0.01	2.60				0.40	0.45	10.10	27.04	43.00
C	0.03	0.02				0.05		0.04	0.05		0.06	0.05
Physical Properties												
Color	White	Bluish pink	Ruby	Black	Gray	Red-brown	Brown	Brown-black	Black-brown	Dark-gray	Gray	Light-gray
Fired color	White	Pink			Pink-Beige	Light-blue	Blue	Blue	Blue			
Av. crystal (μm)	2500		1000			600	200	1000	300	100	20	
Std. friability												
14 grit (%)	69–54	65–46	35.4		37.7	50	30	45	30	12	8	15
20 grit (%)	65–62				48–46		39–37		38–36	25		
Bulk density												
14 grit	1.62–1.76	1.75–1.95	1.92		1.90		2.10		2.10	2.14	2.18	2.30
20 grit	1.75–1.83				1.91–2.03	2.03	2.00-2.06	2.03	2.03–2.11	2.10		
Hardness K 100	1965	2000	2200		2000	2090	2100	2090		2200		1140
Shape	Sharp-edged Blocky	Blocky Sharp-edged			Blocky	Sharp-edged Blocky	Blocky	Sharp-edged Blocky	Blocky	Blocky	Blocky	Blocky

*Any of the three combinations can be used to make alumina-zirconia.

Table II. Fused Alumina and Alumina Compositions for Refractory Grain

	White Fused Alumina	Brown		Mullite				Zirconia-Mullite	Magnesia-Spinel
		(High TiO_2)	(Low TiO_2)	Black		White			
Composition									
Al_2O_3 (%)	99.50	96.00	98.41	98.17	76.00	77.70	75.60	45.80	70.63
Fe_2O_3	0.08	0.10	0.25	0.15	0.90	0.12	0.10	0.15	0.10
SiO_2	0.02	0.80	0.40	0.50	20.00	21.80	23.30	17.50	0.07
TiO_2	0.01	2.50	0.60	0.90	2.50	0.05	0.03	0.17	0.01
ZrO_2		0.20						36.00	
CaO	0.02	0.08	0.14	0.12					0.28
MgO	0.01	0.22				0.35	0.10		28.83
Na_2O	0.30	0.02	0.08	0.03	0.10		0.31	0.25	0.08
T.C	0.05	0.10							0.06
S		0.01							
Melting point (°C)	2050	2000 or above				1850	1850	1750	2135
Density ($g \cdot cm^{-3}$)	3.97	3.92	3.94			3.08	3.05	3.58	3.56

With regard to mineral composition, two main types of bauxites are found: (1) the boehmitic or diasporic type (Al_2O_3-H_2O) and (2) the gibbsitic or hydrargillitic type ($Al_2O_3 \cdot 3H_2O$). Crystalline plus free water present in the mined ore can exceed 40%. This high water content makes raw bauxite an undesirable feed for the high-temperature melting furnaces. Therefore, the bauxite has to be calcined. After crushing the raw bauxite to minus 50 mm in size, it is fed to rotary kilns operating at about 1100°C to reduce the total water content to 1% or less. Modern calciners have grate coolers to increase thermal efficiency.[26,27]

Table IV gives compositions of different calcined bauxites used and also mentions the U.S. government specifications.[28] The higher the alumina content, the more desirable the bauxite; however, other lower grade bauxites have been used. Kistler[29] gave the limits of bauxite compositions used in actual industrial practice. With increasing amounts of impurities, the energy requirement per unit of fused alumina increases. Walker[30] linked the bauxite impurities like SiO, Fe_2O_3, and TiO_2 to increased requirements in energy consumption. With an increase in the latter, the cost of fused alumina increases.

The CaO and MgO content in bauxite should not be higher than 0.4% for each. Burbott[31] cites a limit for CaO of 0.3%. Since some semifriable fused aluminas contained up to 1.2% CaO without detriment to wheel performance, this subject is somewhat ambiguous.

Instead of calcined bauxite, sintered bauxite[32,33] can be used, which improves the energy efficiency of the smelting operation. Dwight-Lloyd-type[34] sintering

Table III. Properties of Fused Cast Refractories*

Component	Mullite Corundum	Alpha A1	Alumina A2	Alpha-beta Alumina	Beta Alumina	Chrome-Alumina	(33%) Zirconia-Alumina	(36%) Zirconia-Alumina	(41%) Zirconia Alumina
Composition									
Al_2O_3 (%)	73.55	99.34	98.80	94.81	94.43	60.40	49.69	50.72	47.33
ZrO_2	1.01						33.24	36.37	40.97
SiO_2	18.57	0.08	0.60	1.09	0.12	1.77	15.29	11.34	10.61
Cr_2O_3						27.26			
FeO-Fe_2O_3	1.02	0.06	0.09	0.06	0.06	4.21	0.19	0.16	0.15
TiO_2	4.12				0.03		0.18		
CaO	0.39	0.13		0.28	0.12				
MgO	0.47			0.15	0.06	6.05			
Na_2O-K_2O	0.87	0.39	0.03	3.59	5.17	0.31	1.26	1.25	0.84
B_2O_3			0.50				0.15	0.16	0.15
Approximate Petrographic Composition (%)									
Component									
Alpha alumina (with included zirconia)							76	77	73
Alpha alumina (no zirconia inclusions)	34	92	97	44					
Beta alumina		8		55	100				
Mullite	45								
Chrome-alumina						63			
Spinel (Fe, Mg, Cr)						37			
Zirconia dendrit.							6	9	14
Titania crystals	4								
Inter cryst. glass	16		3	1			18	14	13
Physical Properties									
Bulk density:									
$kg \cdot m^{-3}$	3444	3524	3556	3172	2884	3444	3444	3524	3685
$lb \cdot ft^{-3}$	215	220	222	198	180	215	215	220	230
Thermal conduct.									
$\frac{Btu \cdot in.}{ft^2 \cdot °F \cdot h}$	35	49	50	34	24	35	20	21	23
$\frac{g \cdot cal \cdot cm}{cm^2 \cdot °C \cdot s}$	0.0120	0.0169	0.0172	0.0117	0.0083	0.0120	0.0069	0.0072	0.0079
Linear thermal expansion at 1093°C (2000°F) (%)	0.63	0.88		0.85	0.72	0.89	0.83	0.90	0.89
Electrical resistivity at $\Omega \cdot cm$ 1400°C (2550°F)		715		18	44	82	90	114	130
Apparent porosity (%)	2.55	1.06	1.5	1.91	4.09	4.23	0.45	0.61	1.34

*According to Ref. 363.

machines can be used to make a jagged porous sinter. Alternatively, pellets can be made in special shaft furnaces[35] from the fine-size portion of the bauxite and from the reverted dust originating from abrasive production.

To upgrade bauxite from an approximate Al_2O_3 content of 85 to 87% to about 96 to 97% in producing brown fused alumina, reducing agents like coke and anthracite are used to reduce oxides like Fe_2O_3, SiO_2, and TiO_2 (in part) to metal. The thus formed metal impurities can be separated easily from the alumina slag if the density difference between the alloy formed from the impurities and the molten alumina is large enough—in excess of 3 g/cm^3. If this difference is

Table IV. Composition of Calcined Bauxites

Country	Al_2O_3(%)	Fe_2O_3	SiO_2	TiO_2	CaO	MgO	Cr_2O_3	ZrO_2	MnO	K_2O	Na_2O	SO_3	C	LOI	H_2O (moisture)
Guyana															
Surinam															
Typical	86.83	5.23	3.02	3.01	0.06	0.01	0.07	0.18	0.01					1.58	0.45
Range	84.9–88.9	4.09–7.00	2.30–4.45	2.60–4.20										0.76–2.30	0.37–0.50
Demerara															
Typical	90.00	1.50	5.50	2.50	0.05	0.01	0.07	0.12				0.03	0.08	0.25	
Range	87.0–92.0	1.2–5.00	3.40–11.24	2.52–3.40										0.2–1.70	
Australia															
Typical	83.45	7.05	4.99	3.62	0.02	0.03	0.05	0.25	0.01	0.01	0.01		0.08	0.54	
Range	82.3–84.0	4.90–12.9	3.80–9.40	2.60–3.77										0.25–1.00	0.12–0.30
Guinea															
Typical	88.51	4.86	1.15	4.43	0.03	0.02	0.12	0.12	0.01	0.02	0.01			0.90	0.93
Range	88.00–90.0	3.50–4.5	1.00–2.0	2.50–5.2										0.51–1.2	0.33–0.5
China															
Typical	87.95	0.86	4.96	3.75	0.13	0.23	0.06	0.16	0.01	0.24	0.01		0.20	0.27	0.30
Range		0.80–1.80	4.90–7.00	3.60–4.20											
USA															
Arkansas															
Typical	79.15	8.00	7.00	4.00										1.50	
Alabama															
Typical	74.33	0.66	21.71	1.32	0.20	0.33								0.40	0.03
India															
Typical	88.92	2.86	2.31	4.45	0.31	0.07	0.09	0.14	0.05					0.80	
Range		22.80–5.40	1.36–2.40	4.00–4.50	0.14–1.10									0.26–1.15	
Brazil															
Typical	79.50	12.37	5.16	1.40											
Range	73.5–86.2	6.10–15.3	.45–6.9	1.00–2.3											
Malaya															
Typical	80.02	10.33	8.30	0.64										0.50	
US Government Specifications	80 min.	8 max.	7 max.	3.5 min.	0.4 max.	0.4 max.									

smaller, iron borings or cast iron chips have to be added according to the method first used by Hall[5] to prepare pure alumina from bauxite as a feed for the Hall-Heroult electrolytic cells.

Cast iron chips and steel turnings compositions are given in Table V. The chips and turnings might oxidize quite rapidly in outside storage, as is evident from the data reported by Donis.[36] Once the turnings are oxidized to Fe_3O_4, it takes five times as much energy to reduce the oxide and melt the iron than it does to melt an equivalent amount of nonoxidized iron.

Table VI gives coke and coals which have been used as reducing agents to remove impurities.[37]

Table V. Composition of Cast Iron Borings and Steel Turnings

	Cast Iron (%)	Borings (%)	Steel Turnings (%)
Fe	92.80	94.71	86.6
Si	1.03	0.47	
Al	0.84	0.78	
Mg	<0.10	<0.10	
Cr	0.27	0.09	
Cu	0.10	<0.10	
Mn	0.75	0.73	
Ti	0.10	<0.10	
C	1.27	0.74	

The raw material for white, pink, and ruby fused alumina is calcined alumina obtained by the Bayer process from bauxite.[38–40] The composition range of calcined aluminas is as shown in Table VII.

The raw materials used to modify the properties of fused alumina abrasive and refractory crudes are: (1) silica[41]; (2) chromium oxide and/or chrome ores[42,43]; (3) zirconia or baddeleyite[44,45]; (4) zircon or zirconium

Table VI. Composition of Reducing Agents

	Coke (%)	Coal (%)	(%)
	Moisture Content		
	5–14	3.64	0.75
Dry Basis			
V.M.	3.72	8.87	7.89
Ash	13.67	9.99	8.42
F.C. + S	82.61	81.19	83.69
S	0.62	0.77	1.32
F.C.	81.99	80.42	82.37
	Ash Analysis		
Fe_2O_3	28.81	5.92	4.4
SiO_2	32.10	52.42	54.0
Al_2O_3	18.53	30.17	39.3
CaO	15.86	10.32	
MgO	3.92	0.68	
TiO_2			0.63

Table VII. Chemical Analysis and Properties of Calcined Alumina

	Typical (%)	Range (%)	Maximum (%)
Al_2O_3	99.0		
Na_2O	0.50	0.24–0.58	0.75
Fe_2O_3	0.03	0.01–0.04	0.04
SiO_2	0.03	0.02–0.05	0.05
TiO_2	0.01	0.003–0.016	
CaO			0.05
MgO			0.05
LOI, 1100°C	0.75	0.05–1.36	1.25
SO_3	0.008	0.008–0.015	0.01
Bulk density packed		108.8 kg/m^3 (lb/per ft^3, 68).	
Bulk density loose		88 kg/m^3 (lb/per ft^3, 55).	

silicate[46,47]; (5) magnesite[48,49]; and (6) kyanite, andalusite, and sillimanite.[50,51] A most informative source book on ceramic raw materials and ceramic processing was written by Singer and Singer.[51]

Physicochemical Principles

The reactions taking place in a furnace producing fused alumina are quite complicated.[37,52] Much can be learned from direct reduction of bauxite,[53–57] if consideration is limited to the bauxite impurities, leaving the alumina untouched or reducing it only slightly.

The simplified reactions taking place when bauxite with, say, an 85% alumina content, is upgraded in the arc furnace to 94% alumina and higher are:

$$Fe_2O_3 + 3C = 3CO \quad (1)$$

$$SiO_2 + 2C = 2CO \quad (2)$$

$$TiO_2 + 2C = 2CO \quad (3)$$

The ease of reduction of the above reactions is illustrated by their change in free energy.[37] The most difficult to reduce is TiO_2. The removal of TiO_2 below 1% is accompanied by an increasing alumina reduction to aluminum metal, which goes into the ferrosilicon-titanium alloy. Therefore the composition of the alloy depends on the fused alumina purity, as indicated in Table VIII.

The melting temperatures of alumina, bauxite, and fused alumina products must be known, so the producer uses the proper equipment and takes the necessary safety precautions. The melting point of the pure material is 2054° ± 6°C.[58–60] Also, knowledge of the molten alumina density is desirable for calculation of the furnace contents; a few investigators[61–63] supply it.

Kamentzev[64] correlated the melting points of different calcined bauxites with their composition.

See the following references for binary phase diagrams for different alumina alloying oxides: alumina-silica (Refs. 65–68), alumina-zirconia (Ref. 69 and 70), alumina-chromia (Ref. 71), alumina-titanium sesquioxide (Ref. 72), alumina-titania (Ref. 73), alumina-calcia (Refs. 74 and 75), alumina-magnesia (Refs. 76 and 77), alumina-sodium oxide (Refs. 78 and 79).

Ternary phase composition diagrams important for the study of abrasives and refractory materials based on alumina are available for: alumina-silica-titania (Refs. 80 and 81), alumina-silica-zirconia (Refs. 81 and 82), alumina-zirconia-magnesia (Refs. 83 and 84), alumina-silica-calcia (Ref. 85), alumina-silica-sodium oxide (Ref. 86).

From 50° to 100°C of superheat should be added to the actual melting points found from the phase diagrams to obtain the proper operating temperature of fusion furnaces.

The theoretical heat requirements can be calculated from the furnace operating temperature using thermodynamic tables.[87,88] Actual figures of theoretical heat requirement for high-temperature refractory compounds were given by Finlay.[89] Theoretical energy consumptions are given in Table IX for alumina and its oxides such as SiO_2, TiO_2, Fe_2O_3, ZrO_2, Cr_2O_3, CaO, MgO, and Na_2O. These impurities are present either in the raw material or as required additions for a certain product. The furnace efficiencies can be calculated from the theoretical energy requirements; actual ranges of furnace efficiencies are given in Table X.

Furnaces Used

The furnaces used are of the arc-resistance type, based on the skull principle. The solidified melt or skull confines the melt; thus no contamination of the melt occurs. The skull is held within a shell, which may or may not be lined. Where there is no danger of forming metallic melts, e.g., in white fused alumina, no lining is necessary. In cases where metal cannot be avoided, as during the production of brown fused alumina, the shell is protected by a graphite or carbon lining.

It is extremely important that the skull thickness remain constant to prevent a break through the steel shell. Thus melting must be performed at steady state conditions, where the heat losses must equal the heat input at the skull-melt interface. To maintain a relatively thin skull, the steel shell is cooled by a film of

Table VIII. Ferrosilicon Composition

Alumina in Slag (%)	Si (%)	Fe (%)	Ti(%)	Al(%)	C(%)
94–95	12–16	73–80	1.5–3.5	1.5–3.0	0.2–0.7
95–97	14–18	74–77	3.0–4.5	2.5–5.0	0.5–1.0
>99	8–10	68–72	5–8	8–11	1–2

Table IX. Theoretical Energy Consumption

For Assumed Melt Temperatures (°C)	kW • h/kg Oxide				
	2050	2100	1950	1900	2185
To melt:					
Al_2O_3	1.03	1.05			
Fe_2O_3 (Fe_3O_4)*	0.70	0.71			
Fe_2O_3 (FeO)*	0.78	0.80			
SiO_2	0.67	0.69			
TiO_2	0.72	0.73			
TiO_2 (Ti_2O_3)*	1.18	1.19			
$3Al_2O_3 \cdot 2SiO_2$			0.95		
$Al_2O_3 \cdot ZrO_2 \cdot SiO_2$				0.73	
$Al_2O_3 \cdot MgO$					1.12
To reduce to metal:					
Al_2O_3	4.45	4.47			
Fe_2O_3	1.39	1.41			
SiO_2	4.00	4.02			
TiO_2	3.27	3.30			
To fume off as suboxides:†					
Al_2O_3	3.44	3.45			
SiO_2	3.61	3.62			
To melt:					
Fe	0.46	0.47			
Si	0.95	0.97			

*To melt and to reduce to a lower oxide.
†After reducing Al_2O_3 to AlO and SiO_2 to SiO.

running water over its outside surface and by impinging sprays at the bottom. Thick-walled skulls backed by a refractory, e.g., magnesia, are sometimes used,[90] making water-cooling at the shell redundant.

The type of furnace depends on the mode of operation. The original furnaces were small and of the batch type. Their energy input was around 1000 kW, with a few exceptions reaching an input of 2000[91] and 3700 kW.[92] As demand increased, plants expanded by building many small furnaces (more than 20 in individual plants).

To reduce operating costs, Lonza[27,91] introduced a continuous melting furnace before or during the Second World War. This was an adaptation of an old 2500 kW carbide furnace of rectangular construction with electrodes in line. After 1945, good sense prevailed and the Carborundum Company introduced continuous furnaces of the tilting type, with inputs up to 3500 kW. Nine such furnaces were in operation until a 12 000 kW furnace was started in 1976.

In the U.S.S.R., 7500 kW furnaces were already operating by 1965[92] and a 12 000 kW furnace was being designed.[93] Furnaces in the U.S.S.R. are of the stationary tapping type. The melt exits through a tapping hole located at the lower part of the furnace shell, identical with furnaces used in ferroalloy or calcium carbide production.

The furnaces used in Canada and the United States are of the tilting type, where the melt leaves the furnace from a pouring spout placed at the top of the furnace shell. The relative merits of each type were discussed by Cichy.[37]

Brown Fused Alumina

Brown fused alumina, which becomes blue when roasted, is produced mainly in two modifications: (1) regular or high-titania and (2) semifriable or low titania.

The TiO_2 concentration in regular is between 3.0 and 3.50% and in semifriable from 2.0 to 2.7%. The silica is also higher in regular, as its lower limit is 1%. For semifriable, the SiO_2 content is less than 1%, and is customarily around 0.5%. Regular is a somewhat tougher material and is made mostly in block furnaces. Nevertheless, a continuous tapping furnace was designed by Upper[94] to pour smaller pigs and thus obtain a crude with smaller crystals (average 300 μm) than those obtained from 5 to 10 tonne blocks. In the past this material was used for heavy-duty snagging and coated abrasives. It is becoming less significant and the semifriable variety is taking over. Large continuous furnaces, reaching inputs of 14 000 kW, are being used for production of the semifriable product. For information about installations of pouring and tapping furnaces, see Refs. 37, 95, and 96.

In the production of brown fused alumina, it is important to calculate the charge properly to approach the optimum carbon ratio. The latter is difficult to achieve due to the variance in bauxite composition, even when from the same source, as the ranges given in Table IV attest. Illustrations for charge calculations are given by Upper[97] and Litvakovskii.[98] Their methods take into account the stoichiometric relations available from Eqs. (1), (2), and (3) and adjust the addition of iron borings to yield a 15% Si-containing ferrosilicon-titanium alloy.

The calculated amount of carbon required is inaccurate as it does not allow for (1) carbon burnoff on the charge surface, (2) carbon reacting with the variable moisture content in the raw material, (3) ambiguity of how much SiO_2 is reduced to silicon metal and what amount volatilizes as SiO, and (4) how much alumina is reduced to metal. The operator must therefore learn to modify his ratio by control analyses of the TiO_2 and by determining the ratio of Si:SiO from overall material balances. Previously, the TiO_2 content was observed from the color of iron rod samples. However, since 1958, X-ray fluorescence analysis, as applied by Dimond and Walker,[99] has given quick results for immediate corrections of the bath.

A typical plant installation to make brown alumina, consisting of a battery of 3500 kW furnaces, was described in rough outline[37] and a somewhat shortened version is given as follows:

Calcined bauxite is supplied in railway or dump trucks to covered track hoppers. Belt conveyors and bucket elevators carry the bauxite to the top of concrete silos, each holding about 1000 tons. Bauxite is withdrawn from the silos into storage bins, which are located in the mix preparation building. There are also

Table X. Energy Requirements and Furnace Efficiencies

Product	Furnace Size (kW)	Energy per Unit* (kW • h per Mt)	Approximate Efficiency (%)	Remarks
Brown fused alumina	1500–12000	3000–2450		Lower grade bauxite
	2000–12000	2650–1930		Higher grade bauxite
White fused alumina	1600	1500	70	
(applies also to pink	3000	1350	78	
and ruby)	5000	1280	82	
Mullite	150	1750	54	
	1000	1350	70	
	2000	1250	76	
Zirconia	400	1400	52	
Mullite	2000	1150	63	

*Where no range is given the figures apply for well-controlled operations.

storage bins for iron borings, coke, reverts, and other materials. All the materials are weighed on batch-weight scales. A collector belt conveyor takes the material from the scales and dumps them into a rotating batch mixer. From the mixer, the batches are carried by bucket elevator and belt conveyors to the furnace feed tanks. Wilkinson[100] gives further details on the installation.

The furnace has an input of 3500 kW; its constructional features were described under the section on furnaces. A typical charge consists of Surinam bauxite, 1000 kg, iron borings, 146 kg, coke, 40 kg, reverts, 100 to 600 kg. Instead of Surinam bauxite, other bauxites mentioned in Table IV can be used, either by themselves or in combination. In the latter case, the preceding coke and iron borings ratio has to be changed to correspond to the bauxite composition applicable.

Reverts from the grain-crushing operations, magnetic fractions from the magnetic separation, dust-collector materials, and other materials are added in amounts depending on their availability and compatibility with satisfactory furnace operation.

The dust-collector material composition is given in Table XI. Due to its fineness, if reverted to the furnace unagglomerated, less than 25% of it will be melted and metallurgically upgraded. The remaining 75% will be shortcircuited and blown out before reaching the molten stage. Also, it will make determination of the proper carbon ratio more difficult. To avoid shortcircuiting, pelletizing was tried. However, pellets must be calcined at a temperature of at least 1000°C.

Drying them to only 300° to 400°C will not remove the bound water and the pellets, containing 4 to 6% water, will disintegrate into the original fine dust when thrown onto the hot charge.

The charge is fed from two or more feed tanks, located overhead on both sides of the furnace, onto a short belt which discharges into a funnel-shaped receptacle. From this receptacle, the charge flows into a swinging chute. This chute can be swung by the operator around the electrodes over a 150° angle, thus enabling the furnace to be charged in all vital points.

The front of a 3500 kW furnace is shown in Fig. 1, together with the spout and mold. The molds can be of two-fold construction. The lined molds have a 25 mm steel shell with a 100 to 200 mm thick lining of either baked carbon paste or a mixture of calcined bauxite, clay, anthracite, and binder. These molds require no water cooling. The bare molds, similar to the mullite molds,[121] are water-cooled and no lining is required. The bare molds cannot be used when ferrosilicon is expected. In the latter case, carbon-lined molds are an absolute necessity. Bare molds, holding up to 15 tonnes of brown fused alumina, filled in 5 to 10 minutes, are in operation for at least nine years.

The cross section of a brown fused alumina furnace is shown in Fig. 2. The lining, made up of congealed alumina within a steel shell, contains two distinct liquids: the lighter brown alumina slag and the heavier ferrosilicon at the bottom. The ratio of slag-to-metal varies with the raw materials, but is usually 1:9 to 2:8. Thus the ferrosilicon accumulates and has to be drained from time to time; e.g., in a 3500 kW furnace this happens after four to five alumina slag pours, each weighing about 5 tonnes.

When filled, the lined molds are cooled for two to three days, after which the pigs are ejected or dumped. On the unlined molds, a minimum film of cooling water is maintained from 16 to 24 hours before the pigs are dumped. Then the stripped pigs are air-cooled for another two days on the cooling floor.

The products from the molds from a 3500 kW furnace are:

First-grade semifriable fused alumina	65 to 75%
Second-grade and reverts semifriable fused alumina	10 to 20%
Ferrosilicon	10 to 17%

The second-grade material must be further handled to remove porous, sugary, and ferrosilicon pieces. For large furnaces, exceeding 10 000 kW input, the second-grade material is reduced to 1% or less, which is an additional advantage.

The pigs are broken into large pieces by a dropping steel ball and the pieces of less than 400 mm are fed to a large jaw crusher to be broken down to minus 150 mm. The crushed material passes a sorting belt where porous, sugary, and ferrosilicon pieces are

Table XI. Composition of Dust-Collector Material from Brown Alumina Furnaces

	Block Method (%) Typical		Continuous 2000–4000 kW Typical	Tilting Furnace 10 000 kW or Higher (%)		
				Typical		Range
	1	2	(%)	1	2	
Al_2O_3	33.60	38.03	59.40	69.28	63.20	54–75
Fe_2O_3	3.58	2.33	4.75	5.68	5.15	2–8
Cr_2O_3			0.08	0.09	0.10	
SiO_2	59.60	56.74	27.40	17.16	23.14	11–27
TiO_2	0.16	0.18	1.74	3.19	2.41	1–4
ZrO_2			0.05		0.08	
CaO			0.12	0.16	0.10	
MgO			0.46	0.18	0.26	
MnO					0.52	
Na_2O			1.20†	0.53	0.50	
K_2O					1.41	0.5–3
T • C			2.80	3.43	2.41	2–4
P_2O_5			0.25			
SO_3						
LOI			4.80	3.77	4.60	3–5
H_2O			0.35	0.40	0.35	

Size Range	(%)
250 μm and larger	2–3
150 μm	3–7
7 μm	7–12
2 μm	15–25
2 μm and less	50–70

Bulk Density (kg/m³)	
801–1.041	Vibrated
450–500	As-collected

*Composition depends on the kind of bauxite used, its size, and the amount of dust-collector material recycled.
†Indicates that the furnace was fed with recycle material high in Na_2O.

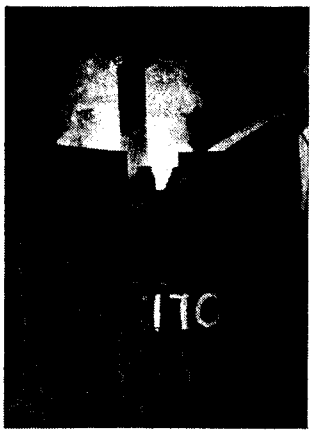

Fig. 1. Brown fused alumina furnace, tilt type, showing furnace spout and mold.

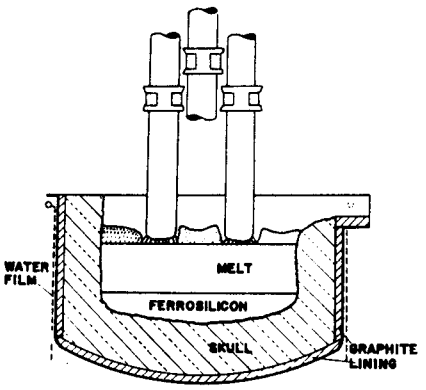

Fig. 2. Cross section of pouring-type brown fused alumina furnace.

removed by hand. The sorted crude is then fed to gyratory crushers to be reduced to minus 75 mm in size.

The minus 400 mm crude from the large furnace goes directly to a huge jaw crusher without previous sorting. The exiting material is fed to gyratory crushers; then it goes over a magnetic separator which removes ferrosilicon. The material collects in a silo from which the fused alumina crude is withdrawn into trucks or railway cars to be transported to the grain processing plant.

In the grain processing plant, the minus 75 mm crude is fed to a specially designed jaw crusher. From there, the material goes over screens to remove the fine sizes. The oversize pieces from the screens are fed to roll crushers; then the crushed material goes to impact crushers or pan mills for rounding. From the rounding operation the grain passes a magnetic separator to remove the iron picked up during size reduction. The magnetically treated grain is passed over screens to obtain the closely controlled grit sizes of the final grain. This grain is then sold to manufacturers of bonded and coated abrasives.

Figure 3 is a flow sheet for producing brown fused alumina grain from calcined bauxite. With the exception of monocrystalline alumina, the flow sheet after furnacing applies essentially to all fused alumina crudes.

The ferrosilicon, which is a by-product, is removed from the mold as described above. The fused alumina is separated from the ferrosilicon, which is then broken by the dropping ball; the large chunks are reduced to minus 250 mm in a jaw crusher. The 50 to 250 mm fraction is sold to the metallurgical industry as an additive. The minus 50 mm fraction is milled to very fine sizes (48, 65, 100, 200 grits) and, as such, is used as "heavy medium" (density 6.7 g/cm^3) in sink-float separation for upgrading iron and other ores.

The semifriable alumina, which is cooled slowly in the large carbon-lined molds, produces crude with

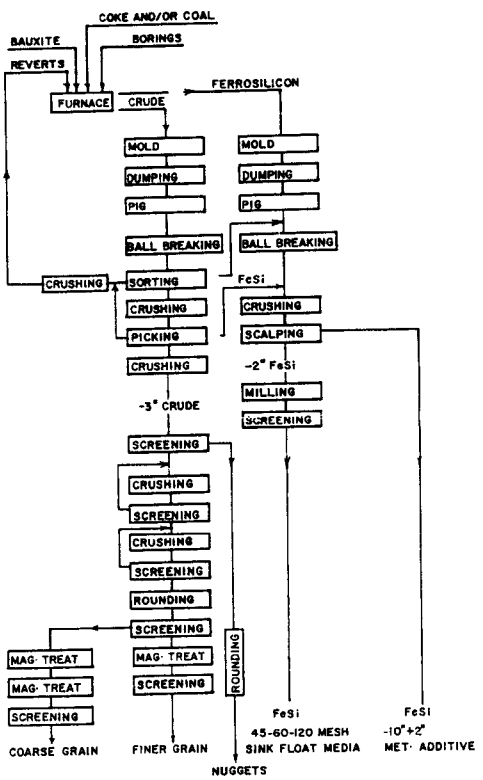

Fig. 3. Simplified flow sheet for production of semifriable fused alumina grain.

an average crystal size of 1600 μm. If crude of the same composition, or perhaps 0.5% higher in its silica content, is poured into water-cooled steel pans (2440 mm in diameter) in a layer not thicker than 150 mm, a finer crystalline crude results, from which grain is made for heavy-duty snagging. This material has an average crystal size of 200 μm. As shown in Table I, the semifriable alumina with the finer crystals has a higher resistance to breakdown, as measured by the ball-mill friability.[101]

The difference in friability between semifriable "slow-cooled" and semifriable "chilled fused alumina" disappears between 70 and 80 grits. As the grit size 70 corresponds to 200 μm, both above varieties of semifriable fused alumina below the above-mentioned size are composed of fragments of single crystals; hence, the convergence of physical properties is not surprising.

The preceding discussion indicates that the crystal size of an abrasive determines its grinding characteristics. To improve them, the final products were studied petrographically, since the products can be considered analogous to an igneous magma solidified at different cooling rates. Taking brown fused alumina of the composition 95.7% Al_2O_3, 3% TiO_2, and 1.25% SiO_2, and inserting it into the ternary diagram by Galakhov,[80] it seems logical that about 90% of the original melt will separate on solidification as primary alpha alumina crystals until the composition path intersects the boundary line between alpha alumina and titanium aluminate (Al_2TiO_5).

The path then changes direction and follows the boundary curve so that secondary alpha alumina and Al_2TiO_5 precipitate. This would take place as long as the quaternary invariant point for mullite, alpha alumina, Al_2TiO_5, and liquid is not reached. With increased SiO_2, the final liquid will freeze and form a glass primarily. When minor amounts of iron, magnesium, and calcium oxides are added, the final microstructure will still be alpha alumina, siliceous glass, and alumina-titania microcrystalline phases.

In high-titania fused alumina, Baumann[102] identified ferrous titanate, which is capable of taking up either 12% TiO_2 or 20% Al_2O_3 into solution. During production of brown fused alumina, carbon reduces some of the TiO_2 to Ti_2O_3, which is to some extent soluble in alumina.[72,102,103] Baumann[102] and McKee and Aleshin[103] set the solubility of Ti_2O_3 at 1.0, 1.8, and 2.5 mol% at 1400°, 1600°, and 1700°C. With increased titanium oxide content, a very small expansion of the alumina lattice occurs, and the hardness of the alumina decreases. Schrewelius[104] and Winkler et al.[105] found by cathodoluminescence that both Ti^{3+} and Ti^{4+} are present in alumina in air-fired samples.

Filonenko and Borovkova[106] identified the phases in brown alumina with incident light. Further, exhaustive work on microstructures of abrasives was done by Filonenko and Lavrov[107] and Patzak et al.[108] The latter found three new phases: the reddish-violet Ti_2O_3 sta-

bilized by Al, the light-gray P- and Al-stabilized Ti_3O_5, and dark-gray calcia-alumina silicate glass of anorthitic composition. The most recent review on the petrography of brown fused alumina, with many photomicrographs of grains and scanning electron microprobe pictures, was presented by Moser.[109]

Due to widely differing temperature gradients, stepwise precipitation of crystals, and variable composition, we can say that there is greater variation in composition between various parts of the pig than from one block to another. Polubelova,[95] in Table XII, presents the compositional variety found between large portions of material from five locations in a brown fused alumina block.

The differences become even more distinct when a block of the average composition of 2.46% TiO_2 and 1.04% SiO_2 (1.6 m in diameter by 1.2 m high) is split in half and samples are taken from a grid with individual squares 10 cm apart. The TiO_2 then varies from 1.25 to 3.17% and the silica from 0.50 to 1.42%. When the melt is accumulated and poured from large continuous furnaces, the composition of the crude in the molds is as varied as in crude made in blocks. The crude is homogeneous in composition only when poured in layers.

When fired in a wheel, brown fused alumina gives the characteristic steely blue color. The only significant colorant is the oxide of titanium, when it is deficient in oxygen and of a general formula TiO_{2-x}. Pure TiO_2 is white; however, when it loses some oxygen its color changes to dark blue until it reaches the oxidation stage of Ti_2O_3, when it becomes dark violet. If further oxygen is lost, it becomes brown and TiO takes on a light bronze metallic color, according to Ehrlich,[110] who investigated color changes in the system Ti-O.

Müller [111] discussed the conditions for obtaining blue wheels after firing, and attributed it to a dispersion of tiny Al_2TiO_5 crystals. This Al_2TiO_5 must be in an oxygen-deficient state. According to Clarke et al.,[112] the second phase in star sapphire is Al_2TiO_5 and this second phase is either white or dark blue, depending on whether aging at 1500°C was done in air or hydrogen.

When roasted, the bluish color of brown fused alumina grains pales with decreasing grain size, indicating that the smaller the grain the easier it is for oxygen to diffuse and oxidize the TiO_{2-x} to colorless TiO_2. Knop[113] observed that darker grains have more TiO_2 and SiO_2 and, further, the standard bluish color is close to the optimum for the $Fe_2O_3 : TiO_2 : SiO_2$ ratio of $1 > 8 < 6$.

Color standardization is done with existing color standards or with the photoelectric reflection meter by determining the reflectance of three colors, e.g., red, green, and blue, as described by Hunter,[114] the so-called tristimulus method.

Patch[115] found that the toughness of brown fused alumina grain is improved by roasting it at high temperatures (>1000°C). In addition, the microhardness for brown grain roasted at 1000°C increases by 27%, according to Wozniak[116] and Yoshikawa.[117] The latter, when quenching different grains, found that grain strength was reduced by about 50% for a quench-temperature difference of 700°C.

The increased toughness of roasted grain is due to the healing of microcracks when they are exposed to high temperatures. Actual tests of grinding wheels with roasted and nonroasted grain showed little or no improvement with roasting, in spite of a 30 to 40% increase in toughness. It appears that the heat treatment of nonroasted grain during the wheel firing operation makes preroasting redundant.

White Fused Alumina

The raw material for white fused alumina is calcined alumina. Its composition, as given in Table VII, has sodium oxide as its main impurity.

Large-scale production was initiated by Jeppson and Saunders.[118] Furnaces are of the block type and shells of different construction are used.[37] Continuous pouring furnaces were developed around 1944 by Ridgway[119] and van der Pyl.[120] The latter furnace had a tapping hole with a withdrawable stopper. The block-type furnaces rarely exceed an energy input of 1500 kW, whereas continuous furnaces reached an input of ≈ 6000 kW, according to Karlin.[92] He also mentioned a furnace with three sections—a bottom, mantle, and cover section.

The melt from continuous furnaces is poured into cast iron molds of 140 kg capacity.[119] In the 1960s, larger molds, first made of steel and then of aluminum metal, were developed[121] for mullite. The same molds

Table XII. Compositional Variety in Different Locations in a Block of Brown Fused Alumina*

Block Location	Composition (%)							
	Al_2O_3	SiO_2	TiO_2	Fe_2O_3	CaO	MgO	Na_2O	C
Top	95.71	0.88	2.63	0.14	0.09	0.13	0.08	0.23
Under the shrinkage cavity	96.15	1.00	3.11	0.17	0.09	0.13	0.11	0.14
Center	95.31	1.06	2.90	0.14	0.09	0.08	0.32	
Side	94.92	0.95	3.27	0.20	0.09	0.12	0.18	0.17
Bottom	94.41	1.33	3.51	0.19	0.10	0.09	0.12	0.15

*According to Polubelova (Ref. 95).

are used successfully for white fused alumina. The water-cooled aluminum mold is especially advantageous as it gives a pig surface free of iron spots. This is difficult to obtain from iron shell molds, even if the latter are coated with an alumina or sand-mold wash.

In white fused alumina production, the main problem is to obtain white blocks or pigs consistently. This problem was investigated quite thoroughly[122–127] and all authors came to the same conclusions, namely that off-white or gray fused alumina is formed due to the presence of impurities like carbon, metallic aluminum, sulfur, and oxides such as Fe_2O_3, SiO_2, and their interaction. To some extent the gray coloration can be removed by roasting at 1100°C and higher. This, however, is not always successful. Wozniak[128] restores the white color by treating gray grains in diluted caustic and sulfuric acid solutions.

There are two patents, by MacZura and Gitzen[129] and Osment et al.,[130] claiming that the whiteness of fused alumina can be improved. The first uses additions of uncalcined alumina, containing crystalline H_2O up to 2.5%. The second, by Osment et al.[130] adds a very small amount of thermoplastic and hydrocarbon resins. Presently, there is a trend to calcine aluminas in fluid beds,[131,132] which means that they will contain increasing amounts of γ-alumina, which is hygroscopic. Thus, additions of uncalcined alumina will no longer be necessary.

The impurity most markedly affecting the abrasive properties of white alumina is sodium oxide. The latter forms, with Al_2O_3, beta alumina of the chemical formula $Na_2O \cdot 11Al_2O_3$. As the Mohs hardness of beta alumina ranges from 6.5 to 7, and is 9 for alpha alumina, the beta content has to be kept within bounds. Ridgway et al.[133] found that a 0.5% Na_2O addition to alumina already containing some Na_2O yields 5 to 7% beta alumina. The Na_2O, due to its volatility, increases the porosity in the white fused alumina, which is desirable for certain applications where a cool cut is required.

In a large pig, the Na_2O concentrates in the top center and Na_2O can be partially removed by discarding the top center section. The Na_2O distribution in a split pig is given in Ref. 125 and is illustrated in Fig. 4. During crushing, the Na_2O-rich portion degrades into smaller sizes, due to its lower hardness. Therefore, a segregation, as evidenced in Table XIII, takes place and the larger grain sizes are richer in alpha alumina.

The beta alumina content in white fused alumina can be determined by the methods given by Jaeger[134] and Podsiadly.[135]

White fused alumina abrasive grain is never roasted, as it does not respond to heat treatment and does not yield a tougher grain, as demonstrated by Patch.[115]

The advantages of caustic and acid solution treatment of grain were explored by Wozniak.[128] Dilute sulfuric acid solution increases the bulk density of 16-grit grain by 9.5% and of 60-grit grain by 10%. In addition, such treatment removes preexistent grayishness in white grain and makes it more lustrous.

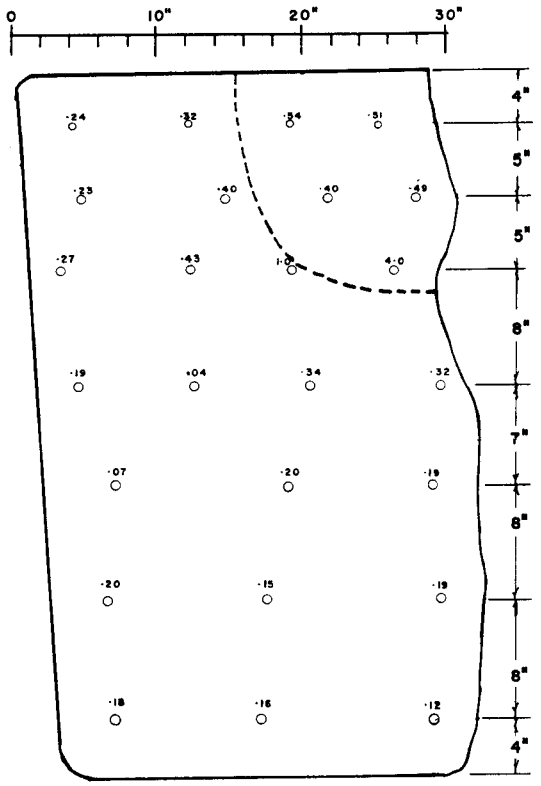

Fig. 4. Na_2O content at different locations in white fused alumina.

Table XIII. Relation Between Size and Na_2O Content in White Fused Alumina

Grit Size	Na_2O Content (%)
Lot I	
14	0.31
24	0.35
46	0.31
120	1.08
Lot II	
24	0.38
46	0.40
120	0.81

A flow sheet for white fused alumina production is given in Fig. 5. A typical block-type furnace consists of a water-cooled Hutchins-type steel pot having an average diameter and height of approximately 1830 mm. The 20 to 25 mm thick steel wall is protected from overheating by water running down its outer surface.

Graphite electrodes (200 to 250 mm in diameter) are used to minimize bath contamination. The pot, resting on a transfer base, remains under the two electrodes until it is filled with molten melt to approximately 150 mm from the top. Then it is guided on tracks to a cooling station for 12 to 16 hours of primary

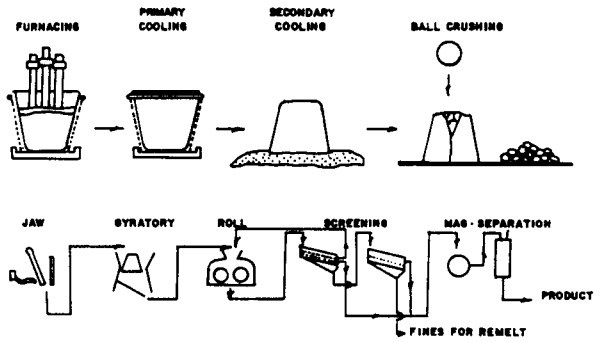

Fig. 5. Simplified flow sheet for white fused alumina abrasive and refractory grain (applicable also for fused mullite, zirconia mullite, and magnesia-alumina spinel).

cooling. During this time, the cooling water flow is maintained on the pot's outer surface to protect the steel from overheating. The secondary cooling period (2 to 3 days) begins when the pig is dumped onto a bed of alumina fines.

The pig, weighing approximately 10 metric tons, is broken by a dropping ball into chunks, smaller than 400 mm, which are fed to a jaw crusher. The material which leaves the jaw crusher flows to a gyratory and/or roll crusher. The product from the roll crusher is sized in a set of screens and then passes over low- and high-intensity magnetic separators. The magnetic treatment has to be very thorough in order to remove all the iron picked up during processing. The sized product is then sent to grinding-wheel and coated-abrasive manufacturing plants.

Alumina Bubbles

In 1928, Horsfield[136] patented a process to produce alumina bubbles, from which insulating bricks were made. This patent was an outgrowth of the Badin process or dry ore process[38] devised to make alumina directly from bauxite, as proposed by Hall.[5] In this process the bauxite was sintered, the sinter was mixed with carbonaceous materials and steel borings, and the blend was fused in a 10 000 kW arc furnace. After the impurities were concentrated in the ferrosilicon, a slag containing around 98.8% Al_2O_3 was formed and dispersed into bubbles by blowing air or steam into the molten slag stream.

The bubbles were collected and leached in diluted sulfuric acid to remove most of the remaining Fe_2O_3, SiO_2, and TiO_2 and to bring the Al_2O_3 content up to 99.7%. The alumina from the bubbles was washed and dried and served as a feed for the electrolytic pots to make aluminum metal. This alumina, however, was not readily soluble in cryolite and the wet Bayer process, with all its complicated technology, became the established process for making smelting-grade alumina.

Girsewald et al.[15] cooled the dispersed bubbles with a water spray shortly after they were blown. If alumina is mixed with SiO_2, B_2O_3, and MgO, multicellular pellets are formed on dispersion. These pellets, according to Benner and Baumann,[137] can be agglomerated into an insulating refractory.

Krug[138] proposed to disperse molten alumina of aluminothermic provenance, crush it, and use it as an abrasive grain. This product is self-sharpening and tough, due to the small crystal size of the alumina.

The fine crystals in the bubbles produced by shock cooling give improved performance for finishing and polishing, when finely crushed bubbles are bonded into an abrasive wheel.[139]

Sandmeyer[140] bonded unbroken alumina bubbles into grinding wheels, either exclusively or mixed with nonporous abrasive grain. This combination provided wheels of open body structure without having to add pore-forming materials. Further, freedom of loading by the ground metal and a highly satisfactory grinding performance are achieved. Fiala[141] dispersed molten alumina through a tungsten screen to obtain bubbles.

A special method of melt discharging through an aspirating nozzle was utilized by Trischuk[142] to make shot-peening spheres from bauxite melts. Broken bubbles making up at least 51%, the remainder being made up of nonporous abrasive grain, were bonded by Tschierf and Hastik[143] into wheels, permitting an open wheel structure, cooler cutting, a reduction in energy expended during grinding, elimination of wheel dressing, and an increased grinding efficiency.

More detailed descriptions on the use of bubbles for abrasive purposes are given by Wozniak,[52] Foot,[144] and Müller and Grau [145] and on their use as insulation by Matsumoto et al.[146]

The composition of fused alumina bubbles is given in Table XIV. The insulating capabilities of bubbles, very early recognized by Horsfield, are still utilized in hot pressurized hydrogen lines, according to Dial.[147] Data on alumina castables, shapes, and bubble bricks are given in Table XV.

Pink, Red, and Ruby Fused Alumina

The coloration of these fused aluminas depends on the amount of chromium oxide admixed to calcined alumina. They are produced in the same manner as fused alumina and, depending on how much chromium oxide they contain, we distinguish:

Pink fused alumina with	0.07 to 0.20% Cr_2O_3
Red fused alumina with	0.20 to 0.70% Cr_2O_3
Ruby fused alumina with	1.50 to 2.50% Cr_2O_3

Pink fused alumina is not much superior to white insofar as performance is concerned. Only the color differs and this can mask the iron staining, which is visible in white wheels.

The introduction of Cr_2O_3 into the corundum, or alpha alumina lattice, causes a much smaller expansion than TiO_2 according to Polubelova[95] for a range from 1 to 5% Cr_2O_3. Rossi and Lawrence[148] gave lattice expansion data for the entire composition range.

Table XIV. Characteristics of Fused Alumina Bubbles

		High Purity	Added SiO_2	Added MgO	Impure
Composition:	Al_2O_3 (in %)	99.65	99.11	98.96	98.66
	Fe_2O_3	0.03	0.05	0.04	0.17
	SiO_2	0.05	0.54	0.02	0.34
	TiO_2	0.01	0.01	0.01	0.47
	CaO	0.08	0.03	0.03	0.10
	MgO	0.04	0.04	0.70	0.08
	Na_2O	0.08	0.15	0.13	0.01
	C	0.09	0.07	0.05	0.17
Bulk density	(kg/m^3)	753–923	432–673	641–753	753–834
	($lb/ft.^3$)	47–58	27–42	40–47	47–52
Color		White	White	White	Cream to brownish
Size	(mesh)	−4	−4	−4	−4
Raw material used		Calcined alumina	Calcined alumina sand	Calcined alumina magnesite	Bauxite coke Fe borings

Table XV. Properties of Refractories Made from Alumina Bubbles

		Insulpure*	Bubble Alumina Brick	Castable
Maximum usable temperature (°C)		1540	1870	1820
Melting point (°C)		1912		
Density	($kg \cdot m^{-3}$)	800	1458	1201
	($lb \cdot ft^{-3}$)		91	75
Porosity	(%)		62	68
Thermal conductivity:				
$g \cdot cal \cdot s^{-1} \cdot cm^{-2} \cdot °C^{-1} \cdot cm$		0.00096	0.00276	0.00162
$Btu \cdot h^{-1} \cdot ft^{-2} \cdot °F^{-1} \cdot in.$		2.8	8	4.7
Modulus of rupture:				
cold	$kg \cdot cm^{-2}$	14	442	21–28
	$lb \cdot in.^{-2}$	200	600	300–400
at 1350°C	$kg \cdot cm^{-2}$		14	21–28
	$lb \cdot in.^{-2}$		200	300–400
Composition:				
Al_2O_3		94.5	98.6	94.6
Fe_2O_3		0.	0.1	0.2
SiO_2		0.3	1.0	0.5
CaO		5.2	0.01	4.2
MgO				0.1
Na_2O			0.05	0.4

*Babcock & Wilcox Refractories, Burlington, ON L7M IL, Canada.

The microhardness increases with increasing Cr_2O_3 content and reaches a peak at 1.25%, as stated by Woźniak and Leźnicka, [149] whereas Goldberg[73] puts this peak at 0.38 wt% Cr. Tests on individual Al_2O_3-Cr_2O_3 grains cutting steel show a 77% smaller abrasion than does white fused alumina.[150]

The vapor pressure of Cr_2O_3[151] is much higher than that of Al_2O_3[87] and, hence, losses of the former can be expected during melting. At the same time, some of the Cr_2O_3 can be reduced to chromium metal with carbon from the graphite electrodes, and minute metallic inclusion can be present. Allowance has to be made for these losses when producing this abrasive crude.

Rosenberg[152] made a 2 to 2.5% Cr_2O_3 addition to alumina and fused the blend in a continuous manner by passing the charge underneath two electrodes, producing a long narrow ingot. Grains with more than 2.5% Cr_2O_3 are not used for abrasive purposes. Higher chromia contents in alumina-chromia are encountered in fused cast refractories.

Monocrystalline Fused Alumina

Monocrystalline fused alumina consists of single crystals formed from a melt containing sulfide. Haglund[153] proposed this approach to make pure alumina, and his method was adopted by Ridgway and Glaze for making abrasive grain. The thus-produced grain excells

in blockiness, has good abrasive and self-sharpening properties, cuts cooler, and requires less power[154] than white fused alumina. The grain is white, grayish-white, or pinkish. Its composition is given in Table I and its main impurity is TiO_2, which ranges between 0.2 and 0.6%.

The monocrystalline material is produced by melting bauxite in an electric furnace together with ferrous sulfide pyrite, iron borings, and coal, according to Ridgway and Glaze.[155] However, because the resulting crystals were too small, Ridgway[156] added a small amount of soda ash, or lime, to obtain larger alpha alumina crystals. A typical charge is calcined bauxite, 74%; iron borings, 15; coke, 6; pyrite, 4; soda ash or lime, 1.

Part of the alumina is reduced and combines with the sulfur from the pyrite to form aluminum sulfide. Soda ash and lime are reduced to sulfides as well, lowering the melting temperature of the alumina. During cooling, alpha alumina crystals larger than 100 grit (≈0.15 mm) crystallize from the sulfide melt. The actual amount of sulfur as Al_2S_3 should be no more than 3%, and no less than 2%, of the total mass. The fused material disintegrates when wetted with water, as the predominant part of the sulfides is either soluble or hydrolyzes, and the freed alumina crystals are collected.

Roschuk[157] produced a highly pure material by a similar method using calcined alumina instead of bauxite and sulfur instead of pyrite.

Jones[158] proposed production of alumina monocrystals from bauxite with fluxes like Na_2O and CaO. The method for making monocrystalline fused alumina is especially suitable for bauxites containing more CaO than the allowable limit, as given on page 394, e.g., Indian bauxite having between 0.5 and 2.0% CaO.

Fused Alumina-Zirconia

Alumina-zirconia abrasives were first experimented with by Saunders and White[159] in 1917. They recognized that additions of zirconia render the abrasive more microcrystalline than previously known in regular fused alumina. The alumina-zirconia product they obtained was well suited for heavy-duty grinding, known as snagging of steel castings. They recommended compositions starting with about 4% and extending to 60% ZrO_2. No practical use was made of this proposal due to two apparent reasons:

1. The higher grinding pressures required for alumina zirconia to become a superior abrasive were not used in 1917.
2. The cost of zirconia was too high at the time to justify the improvements in grinding performance over alumina.

Nothing was heard about zirconia additions until 1945, when Baumann and Wooddell[160] patented the addition of 3% zircon to 97% alumina. The alumina did not necessarily have to be pure, but could have been made by the reduction of bauxite containing from 90 to 98% Al_2O_3. The melt was poured in 100 to 150 mm thick layers, and it possessed a fine-grained dendritic structure, consisting of alpha alumina crystals. The force required to break one of these grains was 18.6 kg, whereas for regular alumina the force was only 12 kg.

Blumenthal[161] made a zirconia-titania crude, which, when crushed and used in the form of a 325-mesh powder in glass grinding, was about 35% better than fused alumina.

In 1956, Polch[162] compared three identically made wheels but incorporated into each a different abrasive grain as follows: fused alumina, stabilized fused zirconia (containing 5% CaO), and baddeleyite. Grinding tests made with those wheels at 9.84 kg/cm^2 (140 psi) pressure and at a speed of 2896 m/min (9500 ft/min) showed that the stabilized zirconia gave the best grinding efficiency as below:

Wheel	Grinding Efficiency
Al_2O_3	1.2
ZrO_2 + 5% CaO	3.47
Baddeleyeite (Natural zirconia mineral around 99% ZrO_2	1.3

The grinding efficiency is defined by the ratio of metal removed (kg/h)-to-wheel wear (cm^3/h or kg/h).

Robie[163] fused a charge of zirconia ore (containing 73% ZrO_2, 12 SiO_2, 3 Fe_2O_3, 1.5 TiO_2) with ilmenite (57 to 59% TiO_2, 31 to 33 Fe_2O_3) and carbon. He obtained an abrasive crude of the following composition: ZrO_2, 57.2%; TiO_2 27.5; Fe_2O_3, 6.85; SiO_2, 2.96; C 0.08.

Wheels were made from five abrasive grains and grinding tests showed the following efficiencies:

Unstabilized zirconia (according to Polch[162])	3.60
Robie's crude	2.93
Fused TiO_2 (according to Blumenthal[161])	2.68
50% of Robie's grain + 50% fused alumina grain	1.73
Fused alumina grain	0.90

In spite of the above success, application of this product remained negligible, mainly due to the higher cost of zirconia-titania crudes and also due to the well-entrenched position of fused alumina.

Kistler and Rue,[164] to keep costs down, fused naturally occurring zircon sand, consisting of about two-thirds ZrO_2 and one-third SiO_2, with alumina to obtain a grain with 53% Al_2O_3, 30 ZrO_2, and 17 SiO_2. Grinding efficiency for wheels made from the above grain improved from 58 to 84% over regular fused alumina.

Foot[165] tested wheels made entirely from fused alumina and zirconia. The grinding efficiency of both kinds was the same. He then made wheels in which 50 vol% each of fused alumina and zirconia grains were mechanically blended. The grinding efficiency exceeded that of the pure component wheels by 13 to 32%.

Toward the end of the 1950s, an increased interest was shown in fusing alumina in the presence of ZrO_2.

Marshall and Roschuk[166] fused calcined alumina and zirconia, containing less than 1% foreign oxides. The composition had 10 to 60 wt% ZrO_2; sodium oxide was limited to 0.10% to restrict the content of beta alumina, which is of inferior hardness. The microstructure of the abrasive grains showed alpha alumina crystals embedded within the eutectic mixture of Al_2O_3 and ZrO_2. The size of the alpha alumina crystals was limited to below 300 μm, and their average was set between 50 and 150 μm. Such small crystals could be obtained only with 11 kg castings.

Cutt[167] assigned to the Carborundum Company the method of making alumina-zirconia crudes from bauxite and zircon sand. The mix fed to the furnace had the following composition: Surinam bauxite, 83.2%; zircon sand, 12.0; petroleum coke, 4.8. This yielded a ZrO_2 content of about 10% in the grain. The melt was poured into 2440 mm diameter steel pans to a thickness of about 10 cm to ensure that the alpha alumina crystals had a dendritic structure.

Dynamit Nobel AG[168] found that the fine porosity in alumina-zirconia is greatly reduced by excluding nitrogen during the pour until after the melt is solidified. One way to prevent nitrogen access is by shrouding the melt stream and mold in carbon dioxide.

Alumina-zirconia abrasive was bettered by introducing a third high-temperature melting oxide as MgO[169] or Cr_2O_3.[170] Brothers et al.[171] added less Cr_2O_3 than did Patchett et al.,[170] along with other oxides, and fused them with alumina and zirconia. This method gave good results.

The traditional molding equipment, capable of holding 150 to 5000 kg, yields alumina-zirconia grain, which has only a marginal advantage over conventional fused alumina. The big improvement is attained only if the cooling rate is greatly increased and the melt is solidified in layers ≤10 mm thick. This is illustrated in Table XVI, where the standard friabilities of alumina-zirconia grains solidified in layers of 100 mm and 5 mm thickness are compared. Only after methods for cooling alumina-zirconia quickly were found did production of the latter became economically rewarding.

The effort to achieve quick cooling of a melt leaving the furnace at a temperature of 1900°C was considerable, as is evident from published patents.

In 1917, the first patent was granted to Kalmus,[172] of the Exolon Company, for a method permitting the formation of fine crystalline fused alumina. His way of cooling the melt is to draw or pour it into a moving mold. The chilling or quick solidification is accomplished by keeping the ratio of the melt mass to the chilling and radiating surface as small as possible. This can also be attained by dividing the molten stream into different rivulets. The chilled fine crystalline alumina was the only satisfactory abrasive for grinding glass for binoculars, range finders, and periscopes during the First World War, according to Milligan.[173]

Hutchins[174] poured a stream of water on the flowing melt stream, or tapped the stream into water flowing at high speed. A porous mass was formed, with alumina crystals of less than 127 μm.

Marshall and Pett[175] poured melt between two rotating water-cooled steel cylinders, where it rapidly solidified into a 2 to 3 mm thick sheet, which can be easily broken.

Another way to quickly chill the molten material, according to Pett and Kinney,[176] is to pour a melt into a bed of prefabricated, 12 to 50 mm lumps of the same composition as the melt. An alumina containing 25% ZrO_2, cooled within the lump interstices, yields alpha alumina crystals smaller than 50 μm.

Richmond,[177] Shurie,[178] and Doutreloux and Ducreux[179] used steel or metal balls instead of lumps to produce finely crystalline material. Müller [180] used ferrosilicon lumps, obtained as a by-product from brown fused alumina production, as a chilling medium for alumina-zirconia melts.

Scott[181] proposed to solidify melt between several metal or graphite plates spaced 12 mm or less apart. Scott[182] also devised a continuous molding machine with many metal plates separated by thin spaces.

Ilmaier and Zeiringer[183] rapidly cooled an alumina-zirconia melt by pouring it into a molten salt melt, consisting of pure or mixed NaCl, $CaCl_2$, $BaCl_2$, and $MgCl_2$. The salt is leached out with water after the main portion of the salt drips off the solidified crude.

Table XVI. Standard Friability of Alumina-Zirconia Abrasive Grain in Relation to Cooling Rate

Nominal ZrO_2 content (%)	10		25		43	
Thickness of solidification layer (mm)	100	5	100	5	100	5
Grit size	14		14		36	
Grain bulk density g · cm^{-3}	2.10	2.10	2.15	2.14	2.10	2.07
Standard friability (%)	15.0	7.5	31	8.2	61.1	30.0
Crystal size:						
40 μm			100	5		
15–40 μm				25		
15 μm				70		

Molten aluminous oxide abrasives, particularly molten mixtures of alumina-zirconia, are cooled rapidly and solidified by pouring them into an agitated molten metal bath with a boiling point above the temperature of the oxide melt, such as molten tin, while being protected from exposure to the atmosphere. The solidified particles float to the top of the metal bath, then are removed as described by Coes.[184]

The bed cooling method, where the melt solidifies within the bed interstices, is limited in height capacity due to the rapid solidification. To counteract the clogging, lumps or metal balls are added continuously as long as melt flows into the bed from the top; the solidified mass of balls and solidified melt is removed from the bottom of the bed. This method[185] uses a vertical cylindrical mold or a rotating horizontal cylinder. The cylinder is inclined slightly to allow the lumps or balls with the solidified melt to be emptied continuously.

In another continuous method proposed by Scott,[186] the melt is poured into a slit formed by two countercurrently and continuously moving metal belts, which are cooled on the cold side by water sprays. The thickness of the solidified two layers is controlled by the belt speed.

Gibson[187] devised a chilling mold with inserted bundles of cylindrical rods, allowing quick retraction and separation of the chilled metal from the solidified alumina-zirconia, making magnetic separation, which is necessary for steel balls, redundant.

The initially successful alumina-zirconia grain containing 10% ZrO_2 was introduced by the Carborundum Company.[37] Later, the 40% zirconia grain was marketed by the Exolon Company. Both grains had too large a crystal structure because they were cooled too slowly during solidification.

A new class of high-efficiency, very fine crystalline abrasive materials, developed by General Abrasive Co. and Norton Co., contained approximately 25% ZrO_2. The optimum crystal size for this grain was an alpha alumina crystal content with at least 70% below 15 μm and none above 50 μm in size. The commercially successful compositions lay in the hypoeutectic region between 25 and 44% zirconia.

The introduction of the Al_2O_3 + 25% ZrO_2 grain in steel conditioning and foundry markets reduced the grinding costs substantially. Due to the introduction of high-speed grinding equipment[188–190] and as a result of longer wheel life, production rates increased up to 300% accompanied by a 60% lower operating cost. The Al_2O_3 + 25% ZrO_2 grain was used in resin-bonded wheels at high machine pressures and it was long thought that the alumina-zirconia was unsuitable for low pressures applied in coated abrasives.

This was soon refuted by Rowse and Watson[191] when they chilled eutectic, or near-eutectic, molten mixtures of Al_2O_3-ZrO_2. Grain from this material has very high strength, with desirable microfractural properties. In coated-abrasive tests, grinding improvements were demonstrated in excess of 100% over prior art standards.[192] Flexible, coated abrasive products from the eutectic material were patented by Rowse and Lakhani.[193]

Kuriakose and Beaudin[194] investigated the microstructure of 25% zirconia and eutectic zirconia-alumina compositions and determined the amount of tetragonal zirconia as a function of the distance from the chilling surface. Eutectic chill-cast compositions show parallel, 10 to 40 μm wide dendrites of alumina-zirconia eutectic cells or colonies. Within the cells, zirconia appears in the form of light-colored, spherical, thin rods in a darker mix of alumina. In compositions containing about 25% zirconia, dendrites of primary alpha alumina are formed in a matrix of alumina-zirconia eutectic composition. In both cases, the structure coarsens with increased distance from the chill.

Gladkov et al.[195] showed that additions of titanium sponge to the finished melt of 70% Al_2O_3 + 30% ZrO_2 preserves from 30 to 70% of metastable tetragonal ZrO_2 on subsequent chilling to room temperature. At the same time, volume changes and cracks in the material are reduced. Iwata[196] showed that a maximum-strength alumina with 30% zirconia is obtained when 3 to 6% TiO_2 is added. He found that in this TiO_2 range the tetragonal zirconia content is between 23 and 33%.

Wozniak[197] found that alumina-zirconia grain contains many tiny pores and fissures, which exert a negative effect on its toughness. If contact with nitrogen from the air is avoided during solidification, the tiny pores and cracks disappear. According to Bockstiegel,[198] the air can be excluded by adding a small amount of reducing agent shortly before pouring the melt. The reducing agent swims on the surface of the melt, and the CO formed prevents contact with nitrogen. Another method of nitrogen contact prevention is to shroud the melt with a CO_2 blanket during pouring and initial solidification. In this way solidified zirconia possesses a 40 to 50% higher toughness.

Alumina-zirconia crude is made from pure raw materials like calcined alumina and zirconia. For economic reasons, the added zirconia used comes from baddeleyite, which is mined in South Africa as a by-product from phosphorite ores.[46] Zirconia also can be obtained from zircon sand by fuming off the SiO_2 with the help of carbon in an arc furnace,[199] via the formation of zirconium carbonitride,[200] and by the plasma process advocated by Wilks et al.[201] The pure raw materials are rather expensive and a satisfactory alumina-zirconia grain can also be made from bauxite, zircon sand, coke, and iron borings.[37]

The thin, chilled plates of crude are crushed in a first step in jaw or impact crushers to process the crude into grain. Thereafter, roll crushing is used, if the grain is for coated applications. In grain production for snagging (25% zirconia-alumina), only the larger grain is used, from 6 to 24 grits. Consequently, from 35 to 50% of the fines have to be returned for remelting. This fact—and the high cost of the raw materials—

makes alumina-zirconia grain an expensive abrasive. Therefore, care has to be taken to use this grain in snagging operations with the most up-to-date grinding equipment capable of sustaining high speeds and high pressures, e.g., 5000 surface meters/min and 650 to 700 kg pressure.

Black Fused Alumina

Melting bauxite without reduction yields a black friable crude. Grain made from it was used in Europe[91] in coated-abrasive manufacture and in the optical industry. It was regarded as being a little poorer than the brown grade for sandpaper and as a good substitute for garnet. The energy required was the same as for white alumina, if calcined bauxite was used as the feed.

Nonconventional Aluminas

In this section will be discussed some unusual approaches on making fused and abrasive aluminas. The older literature was collected by Gitzen[202] and is reproduced here.

Many references relate to methods which have been considered for purification of the melt, or for obtaining the ingot in a more advantageous condition for crushing and sizing. Glezin[203] mentions the addition of 5% TiO_2 to increase abrasive properties and 5% Cr_2O_3 to increase the tenacity.

Baumann and Benner[204] crystallized the alumina with at least one metal of the group Fe_2O_3 and Mn_2O_3 in solid solution, and also in a fused matrix of a manganese, cobalt, or nickel spinel.[205] Benner and Baumann[206] also reported an abrasive containing alumina and a minor amount of monazite.

Schrewelius[207] separated the silicon and silica slag, as an upper layer of the melt, from mixtures of chamotte and a reducing agent. When a member of the sulfur group (selenium) was added, aluminum selenide was formed, which could be broken up by hydrolytic action with water to liberate the corundum grain.[208] Ridgway[209] purified a fused bauxite product by immersion in fused alkali metal cyanide to dissolve a considerable portion of the slagging constituents still clinging to the grain.

Klein[210,211] coated the grain with an alkaline earth-metal sulfate or with cryolite. Yamaguchi and Tanabe[212] synthesized artificial emery by firing powdered bauxite at 1350° to 1550°C, and found a slightly poorer abrasive efficiency than that of the native product.

Klein and Ridout[213] described the properties and applications of 32 Alundum (monocrystalline fused alumina),* a grade of fused alumina (99.6% Al_2O_3), crystallized by cooling the molten bath of bauxite containing a metal sulfide. The sulfide in the solidified mass is water-soluble, releasing the alumina grains of controlled size and rough surface.

*Norton Co., Worcester, MA.

Frost[214] prepared a fused abrasive consisting essentially of about 10 to 50 wt% of fine crystals of titanium carbide dispersed in crystalline alpha alumina. Ueltz[215] sintered (to zero porosity) preformed grains of natural bauxite, characterized by a skin produced by the sintering process. A large proportion of the crystals were randomly oriented in the size range from 5 to 30 μm and composed of alpha alumina and mullite, with glass present as an interstitial component.

A new line of sintered abrasive grains of elongated shape and controlled size was developed from the Ueltz basic patent. Calcined bauxite is ground wet to a fine size in ball or vibratory ball mills using alumina balls. The feed to the ball mill is 20-mesh bauxite, precrushed in roll crushers. The slurry from the ball mill, containing extremely fine particles of bauxite, is fed to centrifuges and the liquid from the centrifuges passes through a filter to collect the last traces of solids.

The cake from centrifuges and filter is dried and pulverized. The pulverized material is mixed with a temporary binder and water to obtain an extrudable mass. The wet mix is extruded from a screw-type extruder, through a die, to form rods of uniform cross section, which are cut into grains of controlled grit size with an average transverse-to-longitudinal dimension ratio of about 1:4 to 1:5. The extruded grain is dried and fed to a rotary kiln, kept at 1400° to 1500°C, where it sinters. After firing, the grain is screened to remove from 5 to 10% fines formed during firing.

The preceding method is used to make grain for snagging wheels,[216] tumbling media, and proppants. Proppants increase the yield of oil wells[217,218] by keeping well fissures open after overburden pressure tends to close them. Lunghofer[219] prepared proppant pellets by the continuous process of fluidized spray granulation.

Another recent development for making abrasive grain without fusion is the use of sol-gel technology, which has been extensively utilized for processing nuclear fuel pellets. The sol of a metal hydroxide—in this case boehmite ($Al_2O_3 \cdot H_2O$ or AlO(OH))—is prepared from an aqueous solution, followed by peptization. Later the sol is transformed into a semi-rigid solid state, such as gel. The gel is dried, crushed, and screened. The sized grain is fired at 1300°C and the nonfired undersize is returned to the aqueous solution in which the original sol raw material is prepared. Zirconium, magnesium, and other compounds can be added to modify the alpha alumina properties.

To make abrasive grain for coated and bonded applications, Leitheiser and Sowman[220] utilized the sol-gel method. This grain outperformed the best alumina-zirconia grains by a factor of 1 to 2. The only drawback of this method is the expensive boehmite—a by-product from the Ziegler process for making primary long-chain alcohols.

McMullen,[221] Amero,[222] and Barks[223] patented methods of sintering bauxite with additions of Cr_2O_3, ZrO_2, and CeO_2 to produce abrasive grains.

Pevzner[224] considered the production of corundum abrasives without using furnaces, but by using heat generated during aluminothermic reduction of some less stable oxide than Al_2O_3. A product containing 95.5% Al_2O_3, 1.24 MnO, 0.95 CaO, 0.56 TiO_2, 1.08 Fe_2O_3, and 0.64 SiO_2 was claimed to be equivalent to brown electrocorundum from bauxite. It could hardly be justified from an economic standpoint for large-scale operation.

Nesin[225] described the process of making crystalline alumina lapping powder from coarsely crystalline Bayer sources by ball milling and elutriation. Polishing grades of Bayer alumina have been described previously (pp. 99). Funabashi[226] stated that aluminum oxide prepared by calcining ammonium alum was the most suitable polishing grade. When calcined at 1250°C, the particle size was 0.1 to 0.2 μm and at 1400°C, 0.4 to 0.6 μm. Ordinary alum, calcined at 1400°C and separated by sedimentation, provides a particle size of 0.7 to 0.8 μm.

Wagner[227] prepared an abrasive with porous grain by decomposing hydrogen peroxide at 60° to 70°C in a moist cake of ground alumina containing a surface-active agent and a manganese compound.

A green alumina-vanadium tetroxide grain,[228] containing about 1.5% V_2O_4, was produced after 1970 for vitrified bonded wheels. This alumina is somewhat harder and is especially useful for grinding hard steels.[229]

A grain useful for inclusion in coated and bonded abrasives contains from 0.42 to 0.84 wt% titanium of the alumina abrasive grain. This is present as a reduced titanium oxide having an average oxidation state lower than that of Ti_2O_3. It also contains up to 0.3 wt% carbon and a gain on ignition from 0.4 to 0.7% is observed before roasting. The grain after roasting in air at 1300°C removes twice as much steel as brown fused alumina when used in abrasive belts.[230]

A new class of a high-hardness and wear-resistant abrasive material was patented by Daire et al.[231] The product is made up of alpha alumina crystals within a eutectic matrix of Al_2O_3-Al_4O_4C or Al_3O_3-Al_2OC.

Abrasive Grain Applications

Abrasive grain is used in (1) loose form, (2) dispersed form glued to a flexible backing (coated abrasive product), or (3) close-packed form held together by an inorganic or organic bond (bonded abrasive product). Each of these groups will be discussed separately.

Loose-Grained Abrasives

Loose abrasives, being unattached to any rigid tool (wheel) or flexible support (belt), have many applications. According to Coes,[232] these applications are divided into three categories: (1) Abrasive is moved by relative motion between the work and a rigid backing; (2) abrasive is moved by relative motion between the work and a soft, or resilient backing; (3) abrasive is moved without a backing. The operations used by these categories are: (1) bed grinding, lapping, and wire sawing†; (2) polishing and buffing; (3) tumbling, vibratory finishing, and pressure blasting.

Lapping is an abrading process for refining and imparting geometrical accuracy to a flat or curved surface. It is done with a "lap" charged with abrasive. Since the lap material is softer than the work material, the loose abrasive can easily embed in it. Together, the lap and the embedded abrasive serve as a grinding tool. Cast iron, steel, brass, copper, lead, babbit, tin, and wood are used as lap materials. The applied abrasive can also be suspended within a pasty material. Lapping, being a precise operation, necessitates accurately sized abrasive. Marslek[233] discussed the charging methods and the preparation of charged laps.

Polishing is the operation which removes scratches or lines from a surface so they are no longer visible with or without magnification. Although polishing can be accomplished in diverse manners, e.g., melting or glazing, by chemical means, or electrolytically, here we will be concerned only with the method involving rubbing a surface with some abrasive grain or powder.

Jacquet[234] described the techniques of surface treatment of metals using files, emery papers, polishing cloths, and powders. Gitzen[202] treated the art of polishing using Bayer alumina trihydrate, gamma and kappa alumina, calcined alumina, and other substances which are nonfused. Their discussion here is therefore unnecessary.

The fused crude is crushed and sized into grain, as already discussed. The choice of equipment to comminute crude is very critical, as it determines the yield in grain of the right size and right shape, without generating an excessive amount of fines. Not only the equipment design, but also the mode of operation of the equipment greatly influences the economy of the process. Therefore, good control of the operating parameters, such as feed rate, size of feed, machine setting and its speed, number of passes through a machine, location of separating screens within the system, and other points, are imperative to obtain the maximum return on expended capital and to achieve minimum operating cost.

To reach these goals, operators can draw heavily on the experience of the mineral processing industry and its handbooks.[40] Since the material comminuted is one of the hardest and toughest known, the abrasive processors have developed many special approaches. Very little of significance has been written about these operations by the abrasive industry. Recently Wozniak[52] gave size distribution curves and bulk densities for different crushing and milling equipment types. If insufficient fine grain for polishing powder use is

†Alumina is never used for wire sawing.

generated in the regular grain-crushing circuit, then additional ball, vibratory ball, and rod mills are necessary.

To define the utility of abrasive grain, it becomes of utmost importance to determine its properties such as: (1) chemical composition, (2) petrographic composition and crystal size, (3) content of metallic inclusions, (4) grain size, (5) grain shape, (6) density (true and bulk), (7) porosity, (8) hardness, (9) mechanical strength (toughness or friability, impact strength), (10) thermal treatment, (11) thermal conductivity, (12) grain surface condition (cleanliness, coating, wettability, surface alkali content), (13) projectability, (14) color, (15) self-sintering, and (16) chemical reactivity. Standards for chemical analysis are provided by the Grinding Wheel Institute.[235] Standard sizing was adopted for abrasive grain as early as 1930, and national[236] and international[237] standards are available.

The finer sizes are classified by water sedimentation methods,[238] hydraulic flotation,[239] or air classification.[240] Dumas[241] described a battery of centrifugal classifiers that produced six fine sizes ranging from 22 to 5 μm.

It was stated[52,242,243] that the mechanical strength of grain depends on its shape. The isometric or blocky grain is the strongest, whereas platy or needle-shaped grain is the weakest. Attempts were made to express the shape on the basis of geometrical models—the cube,[242] sphere,[244] and ellipse[245]—taken as bases. Instead of using the time-consuming method of direct determination of shape factors, a very convenient method is to express the shape of grains by bulk density, for which a standardized method exists.[246]

The first requirement of an abrasive is that it be harder than the material being abraded. The most widely used hardness instrument is the Knoop hardness testing device, which gives the Knoop microhardness value. During actual grinding, abrasive grains are exposed to high temperatures and Westbrook[247] found that the microhardness of Al_2O_3, being about 2100 at room temperature, is only 620 kg/mm^2 at 800°C. At 1400°C, Al_2O_3 is not as hard as ZrO_2—150 and 220 kg/mm^2, respectively, according to Koester and Moak.[248]

A persistent desire exists to determine the pertinent mechanical properties of the abrasive grain in order to make reliable conclusions regarding its subsequent durability during actual abrasive operations. The breakdown resistance of grain against impact, compression, and thrust forces can be summarily represented by toughness, without going into detailed theoretical explanations. Toughness is expressed as the percentage of grains surviving a test. The percentage of grains broken down is called friability, which is determined by a standard method.[101] Impact methods measuring grain breakdown are given by Albrecht et al.[249] and Karpinski and Tervo.[250] Funabashi[251] compared alumina with magnesia and silica for polishing synthetic resins and celluloid.

Buffing consists of imparting a high luster and finish to the surface of the metallic or nonmetallic work piece. This is accomplished by means of a rapidly revolving, soft, flexible wheel onto the face of which a soft, loose abrasive is continuously fed. Frequently, abrasive suspended within a fluid or semifluid is applied. The work piece is held against the wheel, either by hand or by a mounting device. The grain size used for buffing is 180 grit and finer.

Tumbling is done in polygonal, steel rotating barrels, filled with abrasive and a fluid together with the parts to be ground and polished. The objective is to remove burrs, to round corners, and produce a polished surface on small parts which are unsuitable for grinding with bonded or coated abrasive tools. The abrasive can be fused alumina chips or sintered alumina ceramic shapes. Instead of rotation, the mixture of abrasive, media, parts, and water can be subjected to controlled gyratory vibration in horizontal troughs.

The advantages of vibratory finishing over barreling are faster production rates and penetration of shielded areas, as demonstrated by Brandt[252] on jet engine components. The technological details for barrel finishing are given by Fitch,[253] and information on tumbling media, finishing, burnishing, and rustproofing compounds are supplied in an AGA pamphlet.[254] Funabashi and Terada[255] appraised the polishing ability of alumina and mullite barrel-finishing media.

Wills[256–258] discussed the factors governing fine surface quality obtained by grinding and pointed out the necessity for a more scientific classification of surface finish.

Another use for loose abrasives is pressure blasting. Particles of abrasive are propelled by a stream of air and impinge on a work piece. This prepares metal surfaces[259] for painting, electroplating, and enameling. If water is used as the propelling fluid, the method is known as the hydroblast method; it is especially suited for decontamination in nuclear facilities.[260] According to Hashish,[261] abrasive water jets are well adapted for cutting advanced materials like armor plates, besides more conventional materials like concrete, rocks, metals, ceramics, and glass. Baab and Kraner[262] devised a sand-blasting test to determine the relative abrasion resistance of refractory forms.

Vibrating loose abrasive grain in an electroplating bath removes the cathode film continuously, and Eisner[263] reports deposition rates 10 to 50 times faster than in conventional electrodeposition.

Coated Abrasives

Coated abrasives is the general term given to a multitude of products, constructed from a flexible backing, upon which a film of adhesive holds and supports a coating of abrasive grain. The backing may be paper, cloth, vulcanized fiber, or a combination of these materials. Adhesives could be hide glues and

synthetic resins. Different sizes of abrasive grain and coated abrasives types and forms are available. Information may be obtained from the Coated Abrasives Manufacturers Institute.[264] For a comparison between domestic and European coated-grain sizes, see Ref. 265.

Details on coated-abrasives production, application, and uses are well covered in the standard treatise by CAMI[266] and by a booklet of the German affiliate of the Carborundum Company.[267] For the user of coated abrasives, a concise and very handy introduction, with up-to-date information, was presented by Mitchell.[268]

Fused brown and white alumina have replaced natural abrasives in part, but not completely, as garnet is still well entrenched in the market. The fine-grained, eutectic alumina-zirconia grain[191] doubled the amount of removed metal previously attainable by brown fused alumina-coated belts. Sol-gel[220] grain, as produced by the 3M Company, exceeded the performance of fine-grained eutectic alumina-zirconia grain by 100 to 200%.

Long before these two high-performance grains were invented, it was found that surface coating of alumina grain brings two advantages. First, superior adhesion is obtained between the coated grain and the glue backing. Second, the coating toughens the abrasive grain. The application of the frit-iron oxide coating and its composition was given by Walton.[269]

The deficiency of coated abrasives lies in the fact that the grain cannot be utilized completely. Consequently, the smaller the grain the more expensive the supporting structure, if monograin layers are used. However, when multilayer grain structures were tried, the problems increased due to belt stiffness and deeper scratching. A single, densely coated layer glazes over with metal more easily and effective cutting ceases.

The bubble grain[140] was advocated for grinding wheels to obtain a more open structure and allow the swarf to freely disengage itself. The same principle was applied for coated abrasive, by forming small, hollow plastic spheres 0.6 to 2.5 mm in diameter, coating the spheres with fine-grained 120 grit and smaller, and baking them onto flexible backings. These hollow spherical abrasives produced better surface finish at higher production rates, with an increase in grinding performance of 200 to 475% over single-layer-coated abrasives, according to Dziobek and Osterrath,[270] Peters and Lukowski,[271] and Löhmer and Schotten.[272] Helpful information on how to apply coated-abrasive belts for woodworking is available in papers by Stevens,[273] Holland,[274] and Stevens.[275,276]

Amundsen and Lobken[277] described grinding experiments for producing planar surfaces on various metals with various abrasives. A comparison of cut rates for different grit sizes also was given for alumina-zirconia and regular fused alumina. Coated abrasives are prepared in the form of rolls, belts, disks, spiral bands, cartridge rolls, flap wheels, sleeves, and pads.

Bonded Abrasives

Bonded abrasives consist of abrasive grain held in a three-dimensional shape by any of several types of bonding agent. Their size can range from a thin cut-off disk to giant pulpstone wheels mashing logs into pulp for the paper industry. The U.S. Department of Commerce[278] lists 28 standard wheel shapes, of which the majority will fall into eight of the standard categories as follows: (1) straight, (2) cylinder, (3) straight-cup, (4) flairing-cup, (5) dish, (6) saucer, (7) depressed center, and (8) mounted.

In wheel application, the proper wheel must be chosen to obtain the best available accuracy, finish, and burn for the work piece. The choice further depends on wheel size, available power, spindle speed, type of machine, mode of machining (wet or dry), in-feed rate, and head pressure.

The wheel is selected on the basis of kind, size, and shape of abrasive; ratio between abrasive grain and bond (hardness of wheel); reinforcement used; safety considerations; and after-treatment. Each manufacturer marks the wheels according to a standard procedure and Coes[232] and Merritt[279] give the details and illustrations.

The bonding agents fall into seven categories: (1) ceramic (vitrified bond); (2) resin; (3) rubber; (4) shellac; (5) magnesium oxychloride; (6) sodium silicate; and (7) metal, alloy.‡

Testing of the finished wheels was covered by Thomas and Anibal.[280] They also give the ranges of oxides in the vitrified bonds. Moser[109,281] investigated the phase boundaries between grains and ceramic bond.

Vitrified wheels, hones, and rubs are used in tool grinding, cylindrical grinding (center-type and centerless), form grinding, ball grinding, and heavy-duty snagging. Resinoid wheels are used in cut-off and snagging wheels, thread grinding, intaglio stones (engraving finishes), and many others. The same resinoid wheels, cold- or hot-pressed, may be used for grinding red-hot billets at 590° to 970°C. Hot grinding removed 81% more metal, with a decrease in wheel wear of 25%, according to Weymueller.[282] Mueller[283] compared cold and hot grinding performance.

Rubber-bonded wheels[284] are used in cut-off and snagging wheels, where impacts are high. Rubber-bonded wheels provide relatively finer finishes; hence they are suited for finishing ball-bearing races, drill flutes, cutlery, and in centerless grinding.

The magnesium oxychloride bond, or "cold bond," is formed from magnesium oxide and magnesium chloride (20% solution). This bond is especially adapted for the cutlery industry, where no-burn is a precondition.

Shellac-bonded wheels are used for softer abrasive action, as in hemming wheels for cutlery, grind-

‡Used only for diamond and cubic boron nitride.

ing, and in roll grinding. Sodium silicate-bonded wheels also provide a soft abrasive action suitable for hemming wheels. Knife hones may be silicate-bonded.

Buchner[285] described the manufacture of wheels and Miklitsch[286] suggested how the grinding wheel manufacturing process can be integrated and automated.

Foundry cleaning-room grinding operations involve only machines and abrasive wheels used in rough grinding or so-called snagging. Eisaman,[287] Mueller,[288–291] and others[188–190] recommended ways to improve and optimize those operations. Guidelines for big cut-off wheels are given by Avery[292] and cut-off wheels for special steels were discussed by Schittgen.[293] Those of large cross sections were reported by Stiebellehner.[294]

Maslov[295] summarized a thorough mathematical insight on the subjects of how abrasives cut and abrade, the kinetics of the abrasive grain during surface cylindrical and internal grinding, the chip formation, the thermal phenomena during grinding, and the useful life of a wheel. This work was extended by Carnegie Mellon University, under the aegis of Shaw and sponsored by the Grinding Wheel Institute and Abrasive Grain Association. It is documented in the annual reports for the period from 1966 to 1974[296] and can be obtained from the GWI–AGA. A summarized version of grinding research done by Carnegie Mellon, and similar work done in other countries, was collected by Shaw in the form of conference proceedings.[297]

Refractories Made of Bonded Fused Alumina and Alumina-Containing Fused Compositions

These are super-refractories. Generally, they are used where no other materials will perform, or where their use increases capacity or efficiency in addition to allowing higher operating temperatures.

The fused crude poured from the arc furnace is manufactured into grain in the same way as described for brown or white fused alumina. Here sizing is less critical and the size fractions are broader, extending over a series of sizes to form group-graded combinations, e.g., 8/16, 16/35, 35/70 mesh, 4 mesh and finer, 10 mesh and finer, etc.

The judicious selection of proportions of available standard-size fractions gives the producer of bonded refractories the means to achieve maximum bulk density. The physical basis for characterizing the packing of particle beds to achieve maximum density was treated by Dallavalle.[298] As ideal packing is not achieved, the theoretical basis does not yield the desired results. Therefore, triangular graphs—identical to three-component phase diagrams—are constructed from experimentally determined bulk densities of mixtures consisting of three differing size fractions. Any desired density, within the realizable limits, can be found from this type of graph.

Bonded fused alumina is preferred where high bearing loads and resistance to all common slags are required. Various fused aluminas, alone or mixed with calcined or tabular alumina, are bonded with ball clay, kaolin, finely ground or fumed silica, calcium aluminate, and other chemical bonding agents. These blends can be pressed and fired into shapes or made available as monolithic refractories. The utilization of fused alumina and other materials in monolithic refractories was treated in a recent book[299] issued by Plibrico Japan.

Gitzen[300] supplied an exhaustive review on the methods of bonding of mullite and of fused, calcined, and tabular alumina. A more recent example on bonding high-alumina bricks was given by Bakker,[301] who claims a high cold strength, low reheat expansion (<0.8% at 1655°C), and good refractoriness under load by using no more than 0.3% of a lithium compound, such as LiF or Li_2CO_3. Mukhin et al.[302] mixed white fused alumina with wastes from cuttings of bricks or casts and headers from electrocast shapes with high-alumina dust from bag filters and mixed the latter materials with phosphoric acid and aluminum trihydrate to produce insulating refractories.

There are three other fused crudes, containing mainly alumina, which are used in bonded refractories: mullite, zirconia-mullite, and spinel. Their compositions are given in Table II. The essential features of their production are melting, solidification, crushing, and sizing, as shown in the production flow sheet for white fused alumina in Fig. 5. The block furnace in Fig. 5 is nearly always a tilt furnace, which allows continuous production.

The manufacture of fused mullite has been presented in some detail.[303] In addition to sintered mullite, two kinds of fused mullite are available: (1) black mullite, which is now rarely produced, made from calcined bauxite, kaolin, and/or silica sand, and (2) white mullite produced from calcined alumina and silica sand.

White fused mullite grain is bonded into bricks and shapes with special bonds that will also form mullite crystals. However, the bricks and shapes do not have to be fired to higher than cone 16, which gives them improved properties such as thermal shock resistance, accuracy, and ease of cutting. Generally, bonded fused mullite is used due to its outstanding properties such as softening point in excess of 1800°C, excellent load bearing persisting up to the softening point, resistance to acid slags, low coefficient of expansion, resistance against heat shock, and low electrical and thermal conductivity. Its disadvantage is a relatively low resistance to reducing atmospheres, notably hydrogen.

Known applications for bonded mullite are small-base tank crowns, skid rails, delta sections of steel electric furnaces, roofs, burner ports in glass tanks, feeder parts in glass tanks, linings for pouring and vacuum treatment ladles, and kiln furniture, e.g.,

saggers, plates, etc. To obtain more shock-resistant kiln furniture, fused alumina and mullite are mixed to obtain a 90% alumina content.[304] Mullite has been used for pressure casting tubes in the pressure casting of steel.[305] A more suitable material for the latter application, however, proved to be zirconia-mullite.

Zirconia-mullite is made by fusing calcined alumina with zircon sand. The first time zirconia was added to alumina-silica was in fused cast refractories, as proposed by Fulcher and Field[306] in 1939. Characteristic of the latter patent is the rather high Na_2O content (1 to 8%) but which actually is rarely above 1.5%. The findings by Fulcher and Field prompted Partridge and Adams[307] to try a bonded zircon block, which was very resistant to borosilicate glass but unsatisfactory for any glass composition high in alkalis. This deficiency led Busby et al.[308] and Schlotzhauer and Wood[309] to experiment with zirconia-mullite. Their patents are for sintered alumina-zirconia-silica refractories which have been commercially produced by the Charles Taylor Co. after 1960.

Fused zirconia-mullite grain was introduced by the Carborundum Company after 1969 and is known as "Carbomul" or zirconia-mullite. It is used in specialty-product applications where a high resistance to environmental corrosion and a low coefficient of thermal expansion are desired. The composition of the raw materials, alumina and zircon sand, is set close to the mullite ratio, $3Al_2O_3 \cdot 2SiO_2$, so that the microstructure is made up nearly entirely of mullite crystals. These crystals, however, contain tiny globules and streaks of precipitated zirconia within the mullite crystals and on their boundaries. Zirconia-mullite contains less than 1% glassy phase due to its low Na_2O content. Compositions very close to zirconia-mullite are found in alumina-zirconia-silica (AZS) fused cast refractories, yet their crystalline structures are completely different, as they contain no mullite crystals, but are rich in glassy phase (10 to 20%). Mullite is absent because of Na_2O content (0.9 to 1.7%) in AZS fused cast refractories. A recent review by Thomas et al.[310] describes the applications of bonded AZS refractories.

The last composition in this section which finds application in bonded fused refractories is magnesia-alumina spinel. In 1910, Allen[311] patented the fusion of magnesium oxide and bauxite in the presence of a reducing agent to obtain a magnesia-alumina composition below the MgO content in spinel. Tone[312] fused brown fused alumina fines with magnesia and obtained a nearly stoichiometric spinel.

Despite its high melting point, excellent resistance to molten metals, and its high hardness, spinel was never used on a large scale because of its high cost. An attempt was made by Haglund[313] to recover crystalline spinel from melts within the system $MgO \cdot Al_2O_3$ - $2CaO \cdot SiO_2$, a system well-suited for utilizing cheap starting materials like dolomite, olivine, and bauxite. Haglund's proposition was studied by Tyrrell and Pace,[314] who prepared 98% pure spinel at very low cost from self-disintegrating dusting slags after digestion with hydrochloric acid. Even this could not rally much enthusiasm.

Spinel has been successfully fabricated by more conventional ceramic processes such as casting, extrusion, and cold pressing, followed by sintering between 1650° and 1850°C. Well-crystallized dense spinel can be produced only by fusion. The preparation of spinel by electrofusion and casting was described in a patent by the French firm Compagnie de Produits Chimiques et Metallurgiques Alais, Froges et Camarques.[315]

Antonov et al.[316] used Satkins magnesite powder instead of high-grade magnesia to make fused spinel. They made a spinel containing 35.6% MgO, 61.9 Al_2O_3, and 2.7 impurities like SiO_2, Fe_2O_3, and CaO. The material was produced in a 2500 kW arc furnace and the energy consumption ranged from 2500 to 2800 kW • h per metric ton at a material consumption coefficient of 1.06. The spinel grain was bonded and used in an open-hearth furnace roof, showing a 38% longer life than magnesia-chrome bricks. Sintered spinel and periclase-spinel bricks have been successfully applied in the transition and cooling zones of cement kilns, according to Uchikawa et al.[317] and have replaced direct-bonded magnesia-chrome bricks in Japan since 1975. Similarly, 12 to 25% fused spinel is added to periclase-spinel bricks used in rotary cement kilns.[318] Spinel is also an excellent material for lining aluminum remelting furnaces.

Fused Cast Refractories Made from Alumina and Alumina Compositions

Refractories, instead of being produced by bonding and pressing the carefully prepared raw materials and subsequent firing, can also be made by melting the raw materials in an electric arc furnace and pouring the homogeneous liquid into a mold. The latter refractories are known as fused cast, electrocast, or fusion cast. Table III gives compositions and some properties of fused cast refractories containing more than 50% alumina or in which alumina is the largest constituent.

The earliest reference regarding aluminum silicate fusions in the United States was by Jacobs.[319] Kaolin was fused in an arc furnace and some of the SiO_2 was volatilized from the furnace to obtain $Al_2O_3 \cdot SiO_2$. A further step in the art was made by Tone,[320] who added a carbonaceous reducing agent to reduce the silica content of kaolin and obtain a fused composition of 77% Al_2O_3 and 23% SiO_2. Skola[321] mentions even earlier attempts made in Europe by which alumina was electrically fused and poured into a hollow mold.

Malinowski[322] produced fused needlelike mullite crystals in a cupola furnace. The alumina-silica material was heated to the required fusion temperature by blowing air into a bed of coke and lumps of aluminum silicates.

Subsequently, the Bureau of Mines in Seattle, together with the Vitrefax Company[323] in Los Angeles,

investigated the possibility of melting alumina-silica mixes for use as refractories. Thus, the first commercial production of electrothermally fused mullite occurred in Los Angeles in 1920 at the Vitrefax Company plant.

In 1921, Corning Glass Works began investigating "electrocast refractories," the outcome of which was the establishment, in 1928, of the Corhart Refractories Company in Louisville, Kentucky. This plant was well described by Schroeder[324]; it produced, at first, cast shapes in 500 kV • A furnaces which were later increased to 750 kV • A. The cast shapes produced there were called "Corhart Standard."

The biggest difficulty in casting large mullite blocks was eliminating their shrinkage cavities and preventing them from cracking during cooling. The cavities were largely eliminated by suitable risers. Cracking was avoided by special molds devised by Fulcher,[325] which allow very slow cooling.

The Corhart method of manufacture of fused mullite blocks was licensed in the 1930s to Electro-Refractaire in Modane, France. Production in Modane was reported by Skola[321] and Bortaud and Rocco.[326]

The advantages of lining glass tank furnaces with fused cast mullite were a greatly increased furnace life, which reduced the cost per unit of product produced; a reduction in glass defects; and the potential to develop better glass tank furnaces.

The success in producing fused mullite blocks sparked, during the 1930s, the development of blocks melting at even higher temperatures than mullite. The Carborundum Company set up a research program to develop block compositions closer to pure alumina. In the process, the additions of alumina were many and varied, as the patents cited below attest.

Easter[327] patented an alumina block, containing 5 to 8% SiO_2, consisting mainly of alpha alumina crystals, glass, and some mullite crystals. Another patent by Baumann and McMullen[328] proposed a cast block more resistant to sudden temperature changes due to 2 to 10% MgO additions. The microstructure of this type of composition is made up of minute interlocking crystals of magnesia spinel and crystalline alumina and is practically free of glass. Benner and Baumann[329] found that, if a few percent of alkaline oxide is added to an alumina block, corrosion at the melt line is greatly reduced and an alumina with 5% sodium oxide is more resistant to fluoride glasses than any other refractory found. Blau and Baumann[330] recommended a block consisting essentially of sodium beta alumina with an Na_2O content of about 5.2%.

Easter and McMullen[331] melted alumina and chrome ore and discovered that products from this mixture retain the refractory and other characteristics of fused chromite ores but that the defects caused by the associated impurities in the ore are minimized. Typical blends range between 25 and 50 wt% of chromite ore, the remainder being alumina. High chromia content, accompanied by a low silica and magnesia concentration, constitutes the most desirable ores.

Fused cast refractories reduce or eliminate nearly completely seeds and stones in the molten glass. Before their advent, bonded refractories were used.[332] Their main disadvantage was failure through disintegration of the bonding ingredient. This released small particles of the highly refractory constituents which, when entrained in the glassmelt, can never be removed.

With an increasing alumina content, the serious difficulty of forming large shrinkage cavities in the cast refractory block becomes more acute. This is caused by the large difference between the densities of molten alumina and solid alumina. Molten alumina's density ranges from 3.06 to 3.18, depending on the investigator,[58–60] whereas the density for solid alpha alumina is 3.98 $g \cdot cm^{-3}$.

Fulcher[333] suggested that shrinkage problems in making fused cast refractories could be circumvented by the insertion of a solid core into the center of the mold. During the pour this core becomes completely surrounded by the melt cast. Reduction of the cavity, as attempted by Easter and Brownell,[334] consisted of heating the contents of the riser with an auxiliary arc while feeding cullet of the same composition as the melt into the riser. The cullet used was formed from the broken headers of previous castings.

The basic principles of fused cast refractory production, from the standpoint of chemistry and physics, were first published in a book by Litvakovskii.[98] He too described the melting furnaces, the molds, and their cooling patterns in relation to the thickness of the powder insulation. Two newer books are also available, one by Galdina and Tchernina[335] and the second by Popov et al.[336]

A mathematical model of the cooling process of electrocast refractories was presented by Gottardi et al.[337] The finite element method was applied for AZS refractories and was confirmed by comparison with experimental observations.

A production flow sheet for fused cast refractories[338] is given here in the following brief outline for alpha-beta alumina shapes. Raw materials like alumina, soda ash, silica sand, and minor quantities of others are supplied in bulk to storage bins. Proportioning of the furnace feed is accomplished by scales mounted on a traveling deck beneath the storage bins. The properly proportioned charge batches are transferred from the scale hoppers into blenders. Blending is automatically timed and, after a controlled mix period, the individual batches are dumped into mix hoppers which are carried to the furnace platform. The mix is then discharged into the furnace manually with shovels or by gravity over an automatic system. The furnace is identical with a continuously melting fused alumina furnace. As no metal is generated in furnaces making fused cast refractories, no graphite lining is

required for the water-cooled steel shell. The lining for the furnace shell is the congealed layer of the melt itself. After accumulating enough melt to fill the required number of molds, the furnace is discharged and the molds are filled.

The molds for alpha-beta alumina are made of 5 cm thick graphite slabs bolted together with steel rods, with expansion joints to absorb the thermal expansion of the mold. The mold is designed to be readily separated or collapsed, so that it may be removed from the hot casting quickly and smoothly. Since the volume shrinkage is substantial in most fused cast refractories, adequately large risers must be used. For the case described, the riser or header must have a volume of 30% of the total casting volume. Even with this riser, the internal void or pipe is still 5 to 7%. According to Busby,[339] the only completely successful method of eliminating the cavity has been the diamond cut lug (D.C.L.) technique. The block is cast in a "L" shape with the riser at one end, so that the front cavity is left at the end of the shorter limb of the "L." This shorter limb contains the entire shrinkage cavity and is then cut off using a diamond saw.

Pouring into the mold must be done speedily, as slow filling of the mold may cause laminations. The graphite mold is stripped from the casting after 10 minutes to allow the formation of a thin shell sufficient to handle and transport the casting. Immediately after removal of the mold, the casting is surrounded by an annealing bin, where it is completely covered with annealing powder which, in this case, is alumina. Approximately 907 kg (2000 lb) of castings are put into each annealing bin and the castings are separated by a uniform layer of alumina powder. The castings are annealed for 10 days, during which period they cool to approximately 150°C.

To ensure adequate control during production, a 229 mm cube is filled from the furnace stream, along with regularly scheduled production blocks. After cooling, this test block is checked for internal structure, density, and other properties. These samples are necessary, as regular production pieces cannot be inspected until 10 days or longer after pouring.

From the annealing bins, the castings are placed on the cleaning conveyor. The alumina powder is dumped from the annealing bins and is recycled to the annealing powder storage. Some annealing powder sinters to the casting; hence this scale must be removed by pneumatic hammer or sandblast cleaning equipment. To provide close fits between blocks, castings must be dressed with swing frame grinders and aluminum oxide snagging wheels. Electrode holes to close tolerances are drilled with diamond tools.

Each of the cast blocks is then inspected and stored before shipping. Notwithstanding the many compositions developed at Carborundum during the 1930s, only three of the high-alumina products are still on the market (Table III). These are: the alpha-beta alumina (Monofrax M), the beta alumina (Monofrax H), and the chrome-alumina (Monofrax K). Later, in 1964, alpha alumina, in the relatively purest state, was introduced as Monofrax A.

Each of the refractories has its own application field, as outlined below:

Beta alumina is especially adapted for glass tank superstructures and Brown[340] gave an account of its advantages and disadvantages. Its use was recommended in port necks, regenerator mouth hatches, optical glass crowns, feeder entrance covers, and nonglass contact positions beyond the first and second port areas. Frischbutter and Schroeder[341] evaluated the applications of beta alumina. During the emergency between 1941 and 1945, the U.S. Government requested the Carborundum Company to cease all efforts in the fused cast area and direct its attention solely to the production of beta alumina, which was used—and is still in use today—for linings in magnesium-producing cells from molten magnesium chloride.

Alpha-beta alumina is erosion-resistant and is adapted for use in direct contact with all types of molten glass. It can be used throughout the entire melting and refining ends of tanks, according to McMullen and Thompson.[342] Typical uses are in glass tank shadow walls, sodium metasilicate furnace linings, steel reheat furnace skid rails, high-temperature tunnel kiln liners, refiner sidewalls, paver and channels in glass furnaces, and synthesis gas generator linings.

The chrome-alumina as developed at the Carborundum Company by Easter and McMullen[331] originally contained only 9 to 11% Cr_2O_3 and was marketed under the name Monofrax K1. Its modern version was upgraded to a 27% chromia content and is known as Monofrax K3.

The early chromia-alumina cast refractories exhibited a wormy and porous structure throughout the body of the cast. Sandmeyer[343] discovered that, if the chrome ore added is heated to 800°C and held there for 5 hours, a very dense cast results. A 25% Philippine chrome ore and 75% alumina produced a cast with a density of 3.05 $g \cdot cm^{-3}$ without roasting the chrome ore. Conversely, when the chrome ore was roasted the cast density increased to 3.50 $g \cdot cm^{-3}$.

The highly corrosion-resistant material, which solidifies into a solid solution of iron oxide-chromia and alumina crystals interspersed with a complex chrome-aluminous spinel, is finding application in fiberglass tanks, rockwool reverberatory furnace linings, throat facers, and covers in glass furnaces. Without reservation, it can be applied for amber, blue, ruby, emerald, and light-green glasses. In flat and opal glasses, caution has to be exercised. Although iron oxide and chrome oxide are strong coloring agents, they exist in the fused cast material in the form of chrome-spinel crystals with alumina in solid solution. The chrome-spinel crystals are closely interlocked, giving the material superior corrosion resistance.

Sometimes this product is referred to as "the block that has chrome and iron in it, but works well in spite of this."

Where caution on color has to be exercised, the user should be aware that Cr_2O_3 contamination is permissible within the 0.0005 to 0.001% range. Assuming a conservative limit of 0.0005% Cr_2O_3, Brown and Stach[344] determined the allowable proportion of chrome-alumina blocks for a combined amount of chrome-alumina and alpha-beta alumina blocks for a flint glass tank by utilizing the known erosion rate of the chrome alumina and the amount of glass passed through during one campaign.

The purest alumina fused cast blocks marketed by Carborundum Company have been the two alpha alumina varieties designated as Monofrax A1 and A2. Both have alpha alumina crystals surrounded by a second phase. A1 has a high-soda phase, whereas A2 has a modified borate glass phase dispersed throughout the microstructure. The latter phase makes Monofrax A2 much more resistant to high-temperature creep and slag attack. Both varieties show very good resistance to molten alkali carbonate melts and coal ash slags, according to Bonar et al.[345] The basis for the A2 development was stated by LaBar.[346] These cast blocks should be ideally suited in conjunction with Monofrax H (beta alumina) in glass tank superstructures in the doghouse region of the furnace. A2 can complement AZS refractories in this tank area.

As the Carborundum Company has been in the forefront with the development of high-alumina refractories, similarly Corhart was the undisputed leader in the field of fused cast alumina-zirconia-silica for at least 15 years. Corhart's entry into the field was initiated by the patents granted to Field[347] and Fulcher and Field.[306,348] They disclosed a cast refractory made essentially of zirconia, alpha alumina, and small amounts of mullite crystals within a siliceous glassy matrix containing about 20% SiO_2 and the residual zirconia and alumina. The amount of zirconia was greater than 20%, the silica less than 6%, and the alkalies Na_2O and/or K_2O were present in an alkali to alumina ratio of less than 1:19.

At that time the two chief commercial sources of zirconia were the relatively pure zircon sand and zirkite, which contains appreciable amounts of Fe_2O_3, TiO_2, and often 10 to 15% SiO_2. When using zirkite, the refractory tested against soda-lime-silica glasses showed an increasing corrosion resistance with increasing ZrO_2 content. At 60% ZrO_2, however, this increase in resistance ceases, due to an increase in the total content of Fe_2O_3 and TiO_2 to above 6%. As pure zirconia was—and still is—expensive, a low-SiO_2 grade ($\approx$5% SiO_2) was made by melting zircon sand, which contains around 33% SiO_2, with coke in an electric furnace. The widely available and cheap alumina was increased in the compositions as it was found that well-developed alpha alumina crystals are attacked very slowly by magnesium metal. Field[349] was thus led to a high-alumina, low-silica composition containing 45 to 92% Al_2O_3, 1.9 to 40% ZrO_2, and 1.5 to 5% SiO_2.

The ZAC cast refractories, developed from the above patented work by the Corhart Refractories Company by Electro-Refractaire, have been very successful in glass tank furnaces. Their success was best illustrated by Ayçoberry, [350] who gave the life span of single campaigns in glass tank furnaces in relation to the lining material. He reported that, in 1928, a furnace lined with bonded silica-alumina refractories lasted only seven months. In 1939, a furnace started with a complete lining made from Corhart standard blocks (fused alumina-silica) had a life span of 24.6 months. A furnace lined with Corhart ZAC fused cast refractories in 1943 had a duration of 32.2 months. Consequently, the commercial manufacture of alumina-zirconia-silica refractories, done on a limited basis during the Second World War, became soon after a worldwide industry, with plants producing them in France, Hungary, Italy, Germany, Japan, and Russia.

Later, the AZS refractories were modified and improved by additions. Sandmeyer[351] recommended additions of 1.5 to 2.5% alkali oxides and 10 to 0.5% boron trioxide to a 50:50 blend of alumina and zircon sand. Steimke[352] developed the composition: 40 to 60 wt% Al_2O_3, 12 to 22 SiO_2, and 25 to 45 ZrO_2, bonded with a borosilicate glass (0.5 to 1% B_2O_3 but not over 1% Na_2O, K_2O, and/or Li_2O, and substantially free from TiO_2 and Fe_2O_3). Nagashima et al.[353] prepared crack-free castings with mixtures of zircon, alumina, and ores containing rare earth elements. Ono et al.,[354] to obtain more corrosion-proof refractories, eliminated the alkaline earth from the preceding composition.

To reduce cracking in the castings, Alper et al.[355] recommended additions of alkali and/or alkaline earth halides, giving preference to fluorides. The exemplary raw material was CaF_2. The final composition was set within the range 15 to 60% ZrO_2, 1 to 20% SiO_2, 0.5 to 2.5% alkali oxide, and 0.05 to 1.5% halogen. For glass compositions requiring high melting temperatures (1550° to 1650°C and higher), conventional ZAS refractories have an increased tendency to crack and generate stones which cause defects in glass, especially after a temporary shutdown. To correct this, Alper et al.[356] proposed fused cast compositions with a higher ZrO_2 content (62 to 90%).

Cevales[357] reported an improved fused cast refractory after thermally treating castings for about 10 days at 1300° to 1600°C. The latter treatment reduces the glassy phase in the castings so as to increase corrosion resistance. A refined version of AZS fused cast refractories appeared in the early 1960s. The ready-to-pour melt was heated for a required time period by an oxidizing arc. This special technique virtually eliminated metallic impurities and reduced tenfold the carbon content, which significantly reduces refractory outgassing and glass-phase exudation at high temperatures. Grollier-Baron and Gaudin[358] patented the utilization of arcs, somewhat higher in

voltage than used for regular melting. Gutman et al.[359] described the reduction of carbon from the normal 0.1% to 0.03% level with an open arc in Bakor 33, the AZS fused cast refractory made in Russia.

If a Bakor 33 melt is poured into graphite molds placed on a vibratable frame and is vibrated from 3 to 20 minutes, the vibrated 600 by 400 by 250 mm experimental casts show far fewer pores and cavities near the surface, according to Timoshenko et al.[360] The thickness of the densest zone increased from 30 to 50 to 110 to 120 mm and the erosion loss was smaller than for the factory-made nonvibrated shapes.

The cast blocks in large glass tank furnaces use up only the front or dense portion. Once this portion is consumed, the operation becomes risky. Therefore, Didier Werke[361] introduced combination blocks under the name Campral. These blocks, instead of being in one piece, consist of two sections, one a dense, fused cast and more expensive piece and the other made of cheap chamotte. This combination, in which the back was of insulating fireclay and the front of fusion-cast material, was suggested as early as 1928 by Fulcher.[362]

There are other markets for fused cast refractories than their application in glass tanks. Alpha-beta alumina and mullite-alumina are used in skid rails in billet reheat furnaces. AZS products resist abrasion in such diverse fields as coke shutes and hoppers, conveyor skirtboard facings and sinter plant grizzly box facings, ball-mill linings, venturi dust collectors, gas scrubbers, and high-temperature reactors.[363]

The great strides made in developing fusion-cast refractories could not have happened without the information provided by petrographic examination. Microstructural analysis of cast materials and the interfaces between the glass and the refractories from thin and polished sections has been an invaluable tool for determining the behavior of these products in service. Further, the pieces washed away from the refractories could be examined in the glass defects appearing as cords and stones.

The transmitting and reflecting light microscope became the initial tool for microstructural work. In the late 1960s, the scanning electron microscope was made widely available. It identifies even the minutest inclusions if an electron microprobe or an energy dispersive X-ray (EDX) device is attached to it. In one of the first instances, the difference between the mechanical and chemical corrosion processes was observed on fused refractories by Baumann and Turner.[364] Studies on the microstructure of fused cast refractories have been numerous and only a few are quoted here: Baumann,[365,366] Litvakovskii,[98] Clark,[367] Bauer et al.,[368] Clark,[369] Busby,[339] Alper,[370] and Bonar et al.[371]

Developments in glass tank refractories between 1967 and 1977 were thoroughly reviewed in a paper by Busby,[372] in which the fundamental reactions of glass contact corrosion were discussed, with special attention given to flux-line corrosion and upward drilling. Miller[373] reviewed applications of glass tank refractories for the 1980s.

Before ending this section, it should be pointed out that cutting and grinding are inherent parts of the technology of fused cast refractories. Orlov[374] gives the operating data for diamond-wheel-cutting fused alumina, e.g., wheel diameter, diamond particle sizes, cutting speed, feed method, feed advancing speed, and depth of cut per pass.

Economic Considerations

The prevailing economic situation in the fused alumina industry is a rather unstable one. The center of the industry, concentrated around Niagara Falls where cheap electric energy is still available, has operated since 1980 at 40 to 64% capacity. These low capacities are mainly due to a decrease in iron and steel production and to increased imports from Brazil and elsewhere. It also appears that the industry was slow in modernizing and upgrading its furnaces from small inefficient units, with a maximum energy input of 3500 kW, to larger, economically more attractive units of 8000 kW and larger. Further, during its heyday, the industry exported abrasive to countries which today have their own installations, capable of satisfying their own requirements.

The production of more efficient abrasives, like alumina-zirconia, certainly also diminished the demand for high-volume items like brown fused alumina. Even before the introduction of highly efficient abrasives, the industry lacked growth between 1950 and 1970. The two 10-year averages for the latter period do not exceed 181 500 tonnes (200 000 short tons) annually. The growth of the industry in North America can be seen in Fig. 6, which comprises data on the total fused alumina crude production between 1917 and 1985. Data on white and high-alumina crudes are also included for the years the data are available.

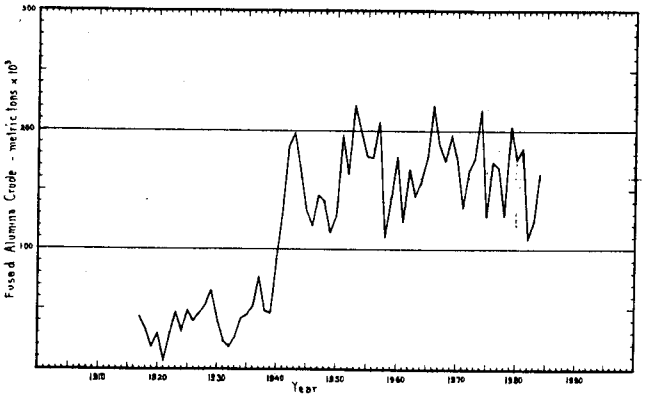

Fig. 6. Annual production of fused alumina crudes in North America.

The fused alumina industry has for a long time tried to expand outside the abrasive field, but has been only partially successful by diverting not more than 5 to 20% into refractory applications. Besides North America, in which Canada is the leading producer in alumina crudes, the following countries produce fused alumina: England, France, Germany, Italy, Austria, Spain, Yugoslavia, Czechoslovakia, Hungary, the U.S.S.R., Sweden, Japan, Brazil, Mexico, and India. The approximate annual total capacities for crude production in tonnes are North America, 250 000; Western Europe, 330 000; the U.S.S.R., 200 000 to 250 000; Eastern Europe without Russia, 110 000 to 120 000; Japan, 120 000; India, 20 000; South America, 60 000 to 70 000. Thus the total world production capacity for all fused alumina crudes is estimated to be between 1 090 000 and 1 160 000 tonnes.

The developments in the fused alumina industry can be gleaned from yearly reports entitled "Abrasives,"[375] which are issued by the U.S. Bureau of Mines, Industrial Minerals Division, and from articles appearing in various journals. *Industrial Minerals* published a succession of articles on fused alumina and fused inorganic materials.[376–380]

References

[1]W. R. Pinkstone, The Abrasive Ages. Livinstone Book, 1974.

[2]I. Wehrlein, "Process for Hardening Aluminous Materials by El. Fusion," Fr. Pat. No. 233 996, November 11, 1893.

[3]F. Hasslacher, "Method of Converting Natural Emery into Iron and Water Free Fused Alumina," Ger. Pat. No. 85 021, November 28, 1894.

[4]C. F. Jacobs, "Process of Manufacturing Abrasive Material," U.S. Pat. No. 659 926, October 16, 1900.

[5]C. M. Hall, "Process of Purifying Bauxite," U.S. Pat. No. 677 207, December 19, 1900; June 25, 1904.

[6]A. C. Higgins, "Electric Furnace," U.S. Pat. No. 775 654, April 4, 1904; November 22, 1904.

[7]M. A. Gaudin, *Com. R.*, **4**, 999 (1837).

[8]F. B. Jacobs, Abrasives and Abrasive Wheels. N. W. Henley, New York, 1919.

[9]W. L. Eardley-Wilmot, Artificial Abrasives and Manufactured Abrasive Products and their Uses, Part IV. Canada Dept. of Mines, Mines Branch, Publ. No. 699, Ottawa, 1929.

[10]M. F. Collie, The Saga of the Abrasive Industry Grinding Wheel Institute and Abrasive Grain Association. Greendale, MA, 1951.

[11]F. B. Jacobs, The Abrasive Handbook. Penton Publishing Co., Cleveland, OH, 1928.

[12]K. B. Lewis and W. F. Schleicher, The Grinding Wheel. Grinding Wheel Institute. Cleveland, OH, 1959.

[13]B. Kleinschmidt, Handbuch der Schleif und Poliertechnik (Handbook of Grinding and Polishing Technology), Vol. I. Edited by H. Cräm. Technischer Verlag, Berlin, 1950.

[14]B. T. Horsfield, "Treatment of Metallic Oxides," U.S. Pat. No. 1 871 792, March 2, 1925; August 16, 1932.

[15]C. von Girsewald, H. Siegens, and M. Marschner, "Disintegrated Alumina," U.S. Pat. No. 1 704 599, May 9, 1926; March 5, 1929.

[16]J. C. McMullen, "Refractory Glass Wool," U.S. Pat. No. 2 557 834, February 23, 1949; June 19, 1951.

[17]C. Z. Carroll-Porczynski, Advanced Materials-Refractory Fibres-Fibrous Metals-Composites. Chemical Publishing Co., New York, 1962.

[18]H. Bederlunger, "Praktische Erfahrungen bei der Herstellung von Tonerde-Schmelzzement" (Practical Experience In Calcium Aluminate Cement Production), *Radex Rundschau*, **2**, 394–400 (1955).

[19]G. R. Pole and D. G. Moore, "Electric Furnace Alumina Cement for High Temperature Concrete," *J. Am. Ceram. Soc.*, **29**, 20–24 (1946).

[20]I. Valeton, Bauxites. Elsevier, Amsterdam, 1972.

[21]S. Patterson, "Bauxite Reserves and Potential Aluminium Resources of the World," U.S. Geological Survey Bulletin 1228, U.S. Government Printing Office, Washington DC, 1967.

[22]H. R. Hose, "Bauxite Mineralogy": in Extractive Metallurgy of Aluminium, Vol. I. Edited by G. Gerard and P. T. Stroup. American Institute of Mining, Metallurgical, and Petroleum Engineers, 1963.

[23]G. J. J. Aleva, "The Bauxites of Guyana Shield as a Source for Refractory Grade Raw Materials," *Interceram.*, **4**, 259–61 (1975).

[24]P. Harben and T. Dickson, "Non-metallurgical Grade Bauxites," *Ind. Mineral.*, **9**, 25–43 (1983).

[25]V. G. Hill, R. J. Robson, and S. Ostojic, "Some Implications of the Changing Bauxite Supply Pattern"; in Light Metals 1982. Edited by J. E. Andersen, The Metallurgical Society of AIME, Warrendale, PA. 1982.

[26]Anon., "Reynolds Guyana—New Source of Calcined Bauxite," *Ind. Mineral.*, **3**, 18–19, 25 (1968).

[27]Anon., "Dania Calcined Bauxite," *Ind. Mineral.*, **5**, 65–67 (1976).

[28]Materials Survey—Bauxite, U.S. Department of the Interior, Bureau of Mines, 1953.

[29]S. S. Kistler, "The German Abrasive Industry" Fiat Final Report No. 370, October 1945, PB 1319. Office of Technical Services, Department of Commerce, Washington, DC.

[30]B. Walker, "Raw Material Economics in Fused Alumina Production"; 9th Midwinter Conference of the Grinding Wheel Inst.-Abrasive Grain Association, Buffalo, NY, February 1966.

[31]C. Burbott, "Electrokorund (Fused Alumina)"; pp. 237–42 in Ulmann's Enzyklopädie der Technischen Chemie, 3d ed, Vol 6. Urban and Schwartenberg, Berlin, 1956.

[32]E. A. Vukolov, A. G. Negovskii, A. E. Jordan, V. I. Malishev, A. A. Mashnitskii, I. A. Klyasktornov, A. B. Raiz, and S. M. Polonskii, "Fusing Electrocorundum from Bauxite Agglomerates," *Energetyka*, **15**, [10] 16–18 (1960).

[33]V. N. Boronenkov, B. A. Kukhtin, M. A. Ryss, G. A. Toporishchev, and T. V. Kotlyarova, "Issledovanie protsessa polutchenya electrokorunda iz agglomerirovannogo boksita" (Investigating the Process of Producing Fused Alumina from Agglomerated Bauxite). *Izv. Vyssh. Zav.-Tchernaya Metallurgiya*, **2**, 11–14 (1959).

[34]D. F. Ball, J. Dartnell, J. Davison, A. Grieve, and R. Wild, Agglomeration of Iron Ores. Heinemann Educational Book Ltd., London, 1973.

[35]K. Meyer, Pelletizing of Iron Ores. Springer-Verlag, New York, 1980.

[36]D. Donis, "Effect of Prior Oxidation of Loose Turnings and Borings in Arc Furnace Melting," *Elect. Furn. Proc. AIME*, **34**, 174–78 (1976).

[37]P. Cichy, "Fused Alumina Production," *Elec. Furn. Proc. AIME*, **29**, 162–75 (1971).

[38]F. D. Frary, J. D. Edwards, and R. B. Mason, The Aluminum Industry, Vol. 1. McGraw-Hill, New York, 1930.

[39]H. Ginsberg and F. W. Wrigge, Tonerde und Aluminium (Alumina and Aluminum), Vol. I. De Gruyter, Berlin, 1964.

[40]W. H. Cundiff, Alumina SME Mineral Processing Handbook, Chap. 19. Edited by N. L. Weiss. Society of Mining Engineers of the AIME, New York, 1985.

[41]J. D. Cooper, "Sand and Gravel"; pp. 1185–99 in Mineral Facts and Problems. Bulletin 650, U.S. Bureau of Mines, 1970.

[42]Anon., "World Chromite Producers," *Ind. Mineral.* **8**, 29–23 (1975).

[43]R. A. Besa and S. D. Dela Cruz, "Masinloc Chromite Operation: Today and the Future," *Ind. Mineral. Refract. Suppl.*, 41–45 (1983).

[44]B. C. Weber, "Baddeleyite of Phalaborwa," *Ber. Dtsch. Keram. Ges.*, **42**, 328–35 (1965).

[45]Anon., "Zircon—Towards Oversupply Again," *Ind. Mineral.*, **4**, 33–34

[46]E. Tauber and R. J. James, "Zircon and its Uses," *J. Austr. Ceram. Soc.*, **7** [2] 27–33 (1971).

[47]B. M. Coope, "Zircon—In Good Shape After a Turbulent Decade," *Ind. Mineral.*, **2**, 19–33 (1983).

[48]Anon., "Magnesite and Sea Magnesia: A Fruitful Rivalry," *Ind. Mineral.*, **12**, 9–44 (1970).

[49]B. M. Coope, "Magnesia Markets—Refractory Contraction and Caustic Stagnation," *Ind. Mineral.*, **8**, 57–87 (1983).

[50]P. J. Bennett and J. E. Castle; pp. 799–807 in Kyanite and Related Minerals, Industrial Minerals and Rocks. 5th ed. American Institute of Mining, Metallurgical, and Petrology Engineers, New York, 1983.

[51]F. Singer and S. S. Singer, Industrial Ceramics. Chemical Publishing Co., Inc., New York, 1963.

[52]K. Wozniak, p. 352 in Materialy scierne-wytwarzanie i wlasności (Abrasive Materials–Production and Properties). Wydawnictwa Naukowo-Techniczne, Warsaw, 1982.

[53]A. I. Beljajev, M. B. Rapoport, and L. A. Firsanova, "Metallurgie des Aluminiums (Aluminum Metallurgy), Vol. II. (German Translation from Russian by G. Schichtel). VEB Verlag Technik, Berlin, 1957.

[54]E. J. Kohlmeyer and S. Lundquist, "Über die Thermische Reduction von Tonerde" (Thermal Reduction of Alumina), *Z. Anorg. Allg. Chem.* **260**, 208–30 (1949).

[55]P. T. Stroup, "Carbothermic Smelting of Aluminum," *Trans. TMS-AIME*, **230**, 356–72 (1964).

[56]L. M. Foster, G. Long, and M. S. Hunter, "Reactions Between Aluminum Oxide and Carbon," *J. Am. Ceram. Soc.*, **39** [1] 1–11 (1956).

[57]H. Ginsberg and V. Sparvald, "Beiträge zur Aluminiumgewinnung durch carbothermische Reduction des Aluminiumoxids unter besonderer Berücksichtigung des Systems Al - C," *Aluminium*, **41**, 181–93 (1965).

[58]C. Paule, "Mass Spectrometric Studies of Al_2O_3 Vaporization Process," *Hi.-Temp. Sci.*, **8**, 257–66 (1976).

[59]S. J. Schneider and C. L. McDaniel, "The Melting Point of Al_2O_3 in Vacuum," *Rev. Haut. Temp. Refract.*, **3**, 351–61 (1966).

[60]E. N. Fomichev, V. P. Bondarenko and V. V. Kandyba, "Enthalpy, Heat of Fusion, and Melting Point of Corundum," *High-Temp.–High-Press.*, **5**, 1–3 (1973).

[61]A. D. Kirshenbaum and J. A. Cahill, "The Density of Liquid Aluminium Oxide," *J. Inorg. Nucl. Chem.*, **14**, 283–87 (1960).

[62]E. E. Shpil'rain, K. A. Yakimowich, and A. F. Tsitsarkin, "Experimental Study of the Density of Liquid Alumina up to 2750°C," *Hi.-Temp.–Hi.-Press.*, **5**, 191–98 (1973).

[63]B. Granier and S. Hertauld, "Méthode de mesure de la densité de réfractaires liquides—Application á l'alumine et á l'oxyde d'yttrium" (Density Measuring Method for Liquid Refractories—Applied to Alumina and Yttria), *Rev. Int. Haut. Temp. Refract. Fr.*, **20**, 61–67 (1983).

[64]M. V. Kamentzev, "Temperatura plavleniya boksita" (Melting Temperature of Bauxites), *Dokl. Akad. Nauk SSSR*, **67** [3] 525–28 (1949).

[65]S. Aramaki and R. Roy, "Revised Phase Diagram for the System Al_2O_3-SiO_2," *J. Am. Ceram. Soc.*, **45** [12] 229–42 (1962).

[66]G. Trömmel, K. H. Obst, K. Konopicky, H. Bauer, and I. Patzak, "Untersuchungen im System SiO_2-Al_2O_3" (Investigating the SiO_2-Al_2O_3 System), *Ber. Dtsch. Keram. Ges.*, **34** [12] 397–402 (1957).

[67]H. Müller-Hess, "Entwicklung und Stand der Untersuchungen über das System Al_2O_3-SiO_2" (Development and Status of Investigations about the System Al_2O_3-SiO_2), *Ber. Dtsch. Keram. Ges.*, **40** [3] (1963).

[68]R. F. Davis and J. A. Pask, "Mullite"; Chap. III in High Temperature Oxides, Part IV. Edited by A. Alper. Academic Press, New York, 1971.

[69]A. M. Alper; p. 339 in Science of Ceramics, Vol. III. Edited by G. H. Stewart. Academic Press, London, 1967.

[70]G. Cevales, Phase Equilibrium Diagram of Alumina Zirconia and Examination of a New Phase, 99% Al_2O_3-1% ZrO_2," *Ber. Dtsch. Keram. Ges.*, **45** [5] 216–19 (1968).

[71]E. N. Bunting, "Phase Equilibrium in the System Cr_2O_3-Al_2O_3," *Natl. Bur. Stand. J. Res.*, **6** [6] 947–49 (1932).

[72]L. Belon and H. Forestier, "Étude du système Al_2O_3-Ti_2O_3 (Study of the Al_2O_3-Ti_2O_3 System), *C. R. Acad. Sc. (Paris)*, **254**, 4282–84 (1964).

[73]D. Goldberg, "Des systémes formés par l'alumine avec quelques oxydes des metaux trivalents et tetravalents, en particulier, l'oxyde de titane" (About Systems Formed by Alumina with Some Tri- and Tetravalent Oxides, Especially with Titania), *Rev. Int. Haut. Temp. Refract.*, **5**, 181–94 (1968).

[74]R. W. Nurse, J. H. Welch, and A. J. Majumdar, "The CaO-Al_2O_3 System in a Moisture-Free Atmosphere," *Trans. Br. Ceram. Soc.*, **64** [9] 416(1965).

[75]A. K. Chatterjee and G. I. Zhmoidin, "The Phase Equilibrium Diagram of the System CaO-Al_2O_3-CaF_2," *J. Mater. Sci.*, **7** [1] 93(1972).

[76]D. M. Roy, R. Roy, and E. F. Osborn, "Fluoride Model Systems: III, The System NaF-BeF_2 and the Polymorphism of Na_2BeF_4 and BeF_2," *J. Am. Ceram. Soc.*, **36** [5] 185–90 (1953).

[77]A. M. Alper, R. N. McNally, P. G. Ribbe, and D. C. Doman, "The System MgO-$MgAl_2O_4$," *J. Am. Ceram. Soc.*, **45** [6] 263–68 (1962).

[78]M. Rolin and P. H. Thanh, "Phase Diagrams of Mixtures not Reacting with Molybdenum," *Rev. Int. Haut. Temp. Réfract.*, **2** [2] 175–85 (1965).

[79]R. C. DeVries and W. L. Roth, "Critical Evaluation of the Literature Data on Beta Al_2O_3 and Related Phases: I, Phase Equilibria and Characterization of Beta Alumina Phases," *J. Am. Ceram. Soc.*, **52** [7] 364–69 (1969).

[80]F. Ya. Galakhov, "Investigating the Al_2O_3 Region of Ternary Al-Si Systems, Communication No. 3, The System TiO_2-Al_2O_3-SiO_2," *Izvest. Akad. Nauk SSSR, Otdel. Khim. Nauk*, 533 (1958).

[81]P. P. Budnikov and A. A. Litvakovskii, "The Al_2O_3-SiO_2-ZrO_2 System," *Dokl. Akad. Nauk. SSSR*, **106**, 267-70 (1956).

[82]G. Cevales, "Neue Untersuchungen im System ZrO_2-Al_2O_3-SiO_2" (New Investigations in the ZrO_2-Al_2O_3-SiO_2 System), *Ber. Dtsch. Keram. Ges.*, **52** [10] 319–21 (1975).

[83]P. P. Budnikov and A. A. Litvakovskii, *Dokl. Akad. Nauk SSSR*, **106**, 258 (1956).

[84]P. G. Herold and W. J. Smothers, "Solid State Equilibrium Relations in the System MgO-Al_2O_3-SiO_2-ZrO_2," *J. Am. Ceram. Soc.*, **37** [8] 351–53 (1954).

[85]A. L. Gentile and W. R. Foster, "Calcium Hexaaluminate and Its Stability in the System CaO-Al_2O_3-SiO_2," *J. Am. Ceram. Soc.*, **46** [2] 74–6 (1963).

[86]I. V. Lavrov, "Issledovanie glinozemnistoi chasti sistemy Na_2O-Al_2O_3-SiO_2" (Investigation of the Alumina Side of the System Na_2O-Al_2O_3-SiO_2), *Akad. Nauk SSSR, Inst. Khim. Silikatov*, 462–70 (1958).

[87]D. R. Stull, and H. Prophet, JANAF Thermochemical Tables, 2nd ed. National Bureau of Standards Reference Data Service-NSRDS-NB537, Supt. of Documents, U.S. Government Printing Office, Washington, DC 1971.

Updates to the above:

1974 Supplement, *J. Phys. Chem. Ref. Data*, **3** [2] 311–480 (1974).

1975 Supplement, *J. Phys. Chem. Ref. Data*, **4** [1] 1–174 (1975).

1978 Supplement, *J. Phys. Chem. Ref. Data*, **7** [3] 795–940 (1978).

1982 Supplement, *J. Phys. Chem. Ref. Data*, **11** [3] 695–940 (1982).

[88]O. Kubaszewski and C. B. Alcock, Metallurgical Thermochemistry, 5th ed. Pergamon, New York, 1979.

[89]G. R. Finlay, "Calculated Energy Requirements of Electric Furnace Products," *Chem. Canada*, **2**, 25–28 (1957).

[90]B. M. Tankelson and M. Zaretskaya, "Investigation of Furnace Lining for Fused Alumina Melting and Proposals for Its Reconstruction," *Ogneupory*, **8**, 39–43 (1980).

[91]J. M. Winter, J. G. Cowan, and E. L. Strasser, "Abrasive Manufacture in Germany," BIOS Final Report 1406, Her Majesty's Stationary Office, London, England; PP 80577, Office of Technical Services, Dept. of Commerce, Washington, DC.

[92]V. V. Karlin, "Development of Fused Alumina Production in the USSR," *Zh. Vses. Khim. O-va*, **24** [6] 609–14 (1979).

[93]A. Altgauzen, "Main Technical Trends in Developing Furnace Constructions in the USSR"; Paper No. 106, VIth Int Congress on Electro-Heat, Brighton 1968, Union Internationale d'Electrothermie.

[94]J. A. Upper, "Pouring Furnace," U.S. Pat. No. 2 579 885, December 4, 1948, December 25, 1951.

[95]A. S. Polubelova, Proizvodstvo abrazivnyh materialov (Production of Abrasive Materials). Mashinostroyenie, Leningrad, 1968.

[96]M. A. Ryss, "Proizvodstvo metallurgitcheskovo elekrokorunda" (Production of Fused Alumina). Mashgiz, Leningrad, 1971.

[97]J. A. Upper, "The Manufacture of Abrasives," *J. Chem. Ed.*, **12**, 676–80 (1949).

[98]A. A. Litvakovskii, "Plavlenye litye ogneupory" (Fused Cast Refractories), Gos. Izd. po Stroit., Arkhitekture i Stroitel'nym Materialam, Moscow 1959. English translation available through National Science Foundation, Washington, DC 1961.

[99]A. W. Dimond and B. Walker, "Putting the X-ray Spectrograph into the Process Control Loop," *ISA J.*, **5**, 2–5 (1957).

[100]A. W. Wilkinson, "Automatic Handling of Bauxite Ore," *Chem. Proc.*, September 1954.

[101]ASA B74.6-1965, "Ball Mill Test for Friability of Abrasive Grain," Sponsor: Grinding Wheel Institute.

[102]H. N. Baumann, "Petrology of Fused Alumina," *Am. Ceram. Soc. Bull.*, **35** [10] 987–90 (1956).

[103]W. D. McKee and E. Aleshin, "Aluminum Oxide-Titanium Oxide Solid Solution," *J. Am. Ceram. Soc.*, **46** [1] 54–58 (1963).

[104]N. G. Schrewelius, "Constitution and Microhardness of Fused Corundum Abrasives," *J. Am. Ceram. Soc.*, **31**, 170–75 (1948).

[105]E. R. Winkler, J. F. Sarver, and I. B. Cutler, "Solid Solution of Titanium Dioxide in Aluminum Oxide," *J. Am. Ceram. Soc.*, **49** [12] 634–37 (1966).

[106]N. E. Filonenko and L. A. Borovkova, "Investigating Fused Alumina with Incident Light," *Ogneupory*, 124–33 (1952).

[107]N. E. Filonenko and I. N. Lavrov, "Petrografia iskustvenniih abrazivov" (Petrography of Artificial Abrasives). Mashgiz, Leningrad, 1958.

[108]I. Patzak, K. Wohlleben, and H. R. Müller, "Studien zu Verunreinigungen in Elektrokorunden" (Investigations about Impurities in Fused Alumina), *Ber. Dtsch. Keram. Ges.*, **46** [2] 51–59; [3] 120–25 (1969).

[109]M. Moser, Microstructures of Ceramics–Structure and Properties of Grinding Tools. Akademiai Kiado, Budapest, 1980.

[110]P. Ehrlich, "Phase Relationships and Magnetic Behaviour in the Titanium-Oxygen System," *Z. Elektrochem.*, **45**, 362–70 (1939).

[111]H. R. Müller, "Blaubrennen von Normal-Korundscheiben" (Firing Regular Fused Alumina Discs Blue), *Ber. Dtsch. Keram. Ges.*, **42** [1] 1–5 (1965).

[112]T. M. Clarke, D. L. Johnson, and M. E. Fine, "Effect of Oxygen Partial Pressure on Precipitation in Titanium Doped Aluminum Oxide," *J. Am. Ceram. Soc.*, **53** [7] 419–20 (1970).

[113]L. Knop, "Badania nad poprawa właściowości elekrokorundu zwyklego" (Investigations into Improving the Properties of Regular Fused Alumina), *Szklo i. Ceram.*, **29**, 77–79 (1978).

[114]R. S. Hunter, "Photoelectric Tristimulus Colorimetry with Three Filters," National Bureau of Standards, Circular C429, Washington, DC, 1942.

[115]J. B. Patch, "Heat Treating Fused Alumina Abrasive Grain," *Ceram. Age*, November 1963.

[116]K. Wozniak, "Wplyw warunkow obróbki cieplnej ziarna ściernego na jego właściwości" (Effect of Heat Treating on the Mechanical Properties of Abrasive Grain), *Szklo i Ceram.*, **27**, 20–22 (1976).

[117]H. Yoshikawa, "Effect of Heat Treatment on Mechanical Properties of Abrasive Grain," CIRP Annual Meeting, 1966.

[118]G. N. Jeppson and L. E. Saunders, "Electric Furnace Product. . .," U.S. Pat. No. 954 808, March 26, 1909; April 12, 1910.

[119]R. R. Ridgway, "Method and Apparatus for Fusing Refractory Materials," U.S. Pat. No. 2 426 649, May 8, 1944; September 2, 1947.

[120]E. van der Pyl, "Furnace Construction for Fusing Refractory Materials and the Like," U.S. Pat. No. 2 426 643, August 11, 1944; September 2, 1947.

[121]P. Cichy, "Electrothermic Production of Mullite," *Elec. Furn. Proc. AIME*, **31**, 136–47 (1973).

[122]L. G. Picyna, V. A. Kvitko, and T. V. Kotliarova, "Diagnostika okrashchennich zeren, prisutstvujushchikh v zerne belogo elektrekorunda proizvodstva CHAZ (Characterization of Colored Grains Present in White Fused Alumina Grains from ChAZ), *Trudy VNIIASh*, **12**, 9–15 (1970).

[123]I. Ya. Rivlin, "Izuchenie tovarnogo vida elektrokorundu belogo (Study of Industrially Produced White Fused Alumina), *Abrazivi i almazi*, **5**, 49–52 (1965).

[124]I. Ya. Rivlin, and K. D. Semashkina, "O vliyanii okisey zheleza i kremniya, soderzhashchikhsya v glinozeme, na cvet elektrokorunda belogo" (About the Influence of Iron Oxides and Silica Contained in Alumina on the Color of White Fused Alumina), *Trudy VNIIASh*, **3**, 18–21 (1966).

[125]P. Cichy, "Difficulties in White Fused Alumina Production"; pp. 111–46 in Light Metals 1978, Vol. 2. Proceedings from the 107th Annual AIME Convention, Denver, CO, 1978.

[126]K. Woźniak and L. Knop, "Wplyw domieszek na zaberwienie electrokorundu szlachetnego" (Effect of Impurities on the Color of White Fused Alumina), *Szklo i Ceram.*, **27**, 181–83 (1976).

[127]K. Woźniak and L. Knop, "Badania nad otrzymywaniem elektrokorundu szlachetnego" (Investigations in the Production of White Fused Alumina), *Przem. Chem.*, **55** [3] 151–54 (1976).

[128]K. Woźniak, "Badania nad wpwem obrobki chemicznej ziarna ściernego na jego wlasności" (Investigations on the Effect of Chemical Treatment of Abrasive Grains), *Szklo i Ceram.*, **29** [1] 9–13 (1978).

[129]G. MacZura and W. H. Gitzen, "Production of Fused Alumina," Can. Pat. No. 815 973, August 22, 1966; June 24, 1969.

[130]H. F. Osment, R. B. Emerson, and R. L. Jones, "Preparation of White Fused Alumina," U.S. Pat. No. 3 409 396, March 30, 1966; November 5, 1968.

[131]E. W. Lussky, "Experience with Operation of the Alcoa Fluid Flash Calciner"; pp 69–80 in Light Metals 1980. Proceedings of the 109th Annual AIME Convention, Edited by C. J. McMinn. February 24–28, 1980, Las Vegas, Nevada.

[132]B. E. Raahauge and J. Nickelsen, "Industrial Prospects and Operational Experience with a 32 MT per day Stationary Alumina Calciner" ibid., pp. 81–102.

[133]R. R. Ridgway, A. A. Klein, and W. J. O'Leary, "The Preparation and Properties of So-called Beta Alumina," *Trans. Electrochem. Soc.* **70**, 71–86 (1936).

[134]G. Jaeger, "Die Bestimmung des Beta-Al_2O_3-Anteiles im Schmelzkorund" (Determination of Beta-Alumina Content in Fused Alumina), *Ber. Dtsch. Keram. Ges.*, **30** [10] 239–41 (1953).

[135]A. Podsiadly, "Ilościowe oznaczanie zawartości fazy beta-Al_2O_3 w elektrokorundzie szlachetnym" (Quantitative Determination of the Beta-Alumina Phase Content in White Fused Alumina), *Szklo i Ceram.*, **31** [5] 171–73 (1981).

[136]B. T. Horsfield, "Refractory Heat Insulating Material and Method of Making the Same," U.S. Pat. No. 1 682 675, December 7, 1925; August 28, 1928.

[137]R. C. Benner and H. N. Baumann, "Cellular Insulating Refractory," U.S. Pat. No. 2 136 096, July 1, 1935; November 8, 1938.

[138]C. Krug, "Verfahren zur Herstellung von Schleifkörnern" (Process for Making Abrasive Grain), Ger. Pat. No. 628 936, April 18, 1936.

[139]R. C. Benner and F. A. Upper, "Abrasive and Method of Making Same," U.S. Pat. No. 2 347 537, June 12, 1941; April 25, 1944.

[140]K. H. Sandmeyer, "Bonded Abrasive Article," U.S. Pat. No. 2 986 455, February 21, 1958; May 30, 1961.

[141]J. Fiala and J. Fialova, "Zpusob výroby kuličkového korundu" (Manner of Producing Alumina Bubbles), Czech. Pat. Nos. 178, 487, January 28, 1977; April 15, 1979.

[142]R. W. Trischuk, "Aluminum Oxide Pressure Blasting Abrasives and Method of Making," U.S. Pat. No. 3 763 603, April 16, 1971; October 9, 1973.

[143]L. Tschierf and F. Hastik, "Schleifkorn und Schleifkorngemisch" (Abrasive Grain and Grain Blend), Ger. Pat. No. 2 349 326, October 1, 1973; April 11, 1974.

[144]D. G. Foot, "Bubble Wheels for Soft Non-Metallics" *Grinding and Finishing*, **1**, 30–31 (1960).

[145]H. R. Müller and G. Grau, "Verwendung von Hohlkugelkorund als Schleifmittel" (Application of Alumina Bubbles as an Abrasive Material), *Ber. Dtsch. Keram. Ges.*, **55** [2] 102–105 (1978).

[146]A. Matsumoto, S. Ito, K. Takaya, and H. Morimoto, "Bubbles as a Refractory," *Taikabutsu*, **34** [298] 29–32 (1982).

[147]R. E. Dial, "High Alumina Refractory Materials for Gas Reforming," *Safety Air Ammonia Plants*, **10**, 29–34 (1968).

[148]L. R. Rossi and W. G. Lawrence, "Elastic Properties of Oxide Solid Solutions: The System Al_2O_3-Cr_2O_3," *J. Am. Ceram. Soc.*, **53** [11] 604–608 (1970).

[149]K. Woźniak and J. Leźnicka, "Badania nad wpywem dodatku Cr_2O_3 na wlasności elektrokorundu" (Investigations On the Effect of Cr_2O_3 Additions On the Properties of Fused Alumina), *Przem. Chem.*, **54** [9] 23–25 (1975).

[150]V. I. Melamed and K. D. Sinjagovskii, "Issledovanie shlifoval 'nykh zeren razlichnykh abrazivnykh materialov na iznos" (Wear Investigations in Different Abrasive Grains), *Trudy VNIIASh*, 1 12–15 (1965).

[151]H. L. Lee, T. Sasamoto, and T. Sata *Yogyo-Kyokai-Shi*, **82**, 603–10 (1974).

[152]J. P. Rosenberg, K. F. Rosenberg, and E. S. Rosenberg, "Abrasives," U.S. Pat. No. 2 768 887, March 19, 1954; October 30, 1956.

[153]T. R. Haglund, "Process for the Treatment of Oxidic Raw Materials," U.S. Pat. No. 1 559 483, August 4, 1922; January 12, 1926.

[154]K. Wozniak and P. Kraszewski, p. 126 in Materialy scierne–wytwarzanie i wlasności (Abrasive Materials–Production and Properties). Wydawnictwa Naukowo-Techniczne, Warsaw, 1982.

[155]R. R. Ridgway and J. B. Glaze, "Aluminous Materials and Process of Preparing Same," U.S. Pat. No. 1 719 131, October 15, 1926; July 2, 1929.

[156]R. R. Ridgway, "Method of Making Crystalline Alumina," U.S. Pat. No. 2 003 867, September 22, 1933; June 4, 1935.

[157]S. J. Roschuk, "Process for Producing Crystalline Alumina," U.S. Pat. No. 3 216 794, October 20, 1961; November 9, 1965.

[158]*(a)*C. M. Jones, "A Method for Producing Alpha-Alumina Crystals from Aluminum Oxide," U.S. Pat. No. 3 615 306, October 12, 1967; October 26, 1971.

(b)"A Method for Producing Alpha-Alumina from Alumina Containing Calcium Oxide," U.S. Pat. No. 3 615 307, October 19, 1967; October 26, 1971.

[159]L. E. Saunders and R. H. White, "Composition Containing Alumina and Zirconia," U.S. Pat. No. 2 240 490, February 12, 1917; September 18, 1917. U.S. Pat. No. 1 240 490, February 12, 1917; September 18, 1917.

[160]H. N. Baumann and C. E. Wooddell, "Aluminous Abrasive Material," U.S. Pat. No. 2 383 035, October 18, 1944; August 21, 1945.

[161]W. B. Blumenthal, "Fused Reduced Titania-Zirconia Product and Method," U.S. Pat. No. 2 653 107, March 30, 1950; September 22, 1953.

[162]F. J. Polch, "Grinding Wheels," U.S. Pat. No. 2 769 699, June 2, 1951; November 6, 1956.

[163]N. P. Robie, "Abrasive Material and Method of Making Same," U.S. Pat. No. 2 877 104, July 5, 1955; March 10, 1959.

[164]S. S. Kistler and C. V. Rue, "Abrasive Articles," U.S. Pat. No. 3 156 545, May 14, 1962; November 10, 1964.

[165]D. G. Foot, "Mixture of Fused Alumina and Fused Zirconia Granules in Bonded Abrasive Articles," U.S. Pat. No. 3 175 894, February 26, 1963; March 30, 1965.

[166]D. W. Marshall and S. J. Roschuk, "Fused Alumina-Zirconia Abrasives," U.S. Pat. No. 3 181 939, January 27, 1961; May 4, 1965.

[167]The Carborundum Co. (J. C. Cutt), "Abrasive Products and Method of Making Same," Br. Pat. No. 993 894, September 8, 1961; June 2, 1965.

[168]Dynamit Nobel AG, "Improvement in or Relating to Zirconium Oxide Aluminum Oxide Abrasive Grain," Br. Pat. No. 1 155 517, December 2, 1966; June 18, 1969.

[169]L. Coes, "Fused Zirconia-Spinel Abrasives and Articles Made Therewith," U.S. Pat. No. 3 498 769, January 16, 1969; March 3, 1970.

[170]J. E. Patchett and A. K. Kuriakose, "Fused Zirconia Chromia Alumina Abrasives," Can. Pat. No. 1 656 605, December 2, 1974; June 19, 1979.

[171]J. A. Brothers, R. C. Doman, and R. N. McNally, "Fused Abrasive Grains Consisting Essentially of Corundum, Zirconia and R_2O_3," U.S. Pat. No. 4 035 162, November 3, 1975; July 12, 1977.

[172]H. T. Kalmus, "Method of Making Abrasive Materials," U.S. Pat. No. 1 226 892, May 7, 1915; May 22, 1917.

[173]L. H. Milligan, "Chemistry-Abrasives-Grinding-Automobiles," *Grits Grinds*, **19** [10] 2–11 (1927).

[174]O. Hutchins, "Aluminous Abrasive Material and Method of Making the Same," U.S. Pat. No. 1 524 134, July 3, 1922; January 27, 1925.

[175]D. W. Marshall and E. A. Pett, "Manufacture of Finely Crystalline Abrasives," U.S. Pat. No. 3 377 660, July 8, 1965; April 16, 1968; U.S. Pat. No. 3 646 713, March 16, 1970; March 7, 1972.

[176]E. A. Pett and G. Kinney, "Abrasive Products and Manufacture Thereof," Br. Pat. No. 1 233 997, April 10, 1968; June 3, 1971.

[177]W. Q. Richmond, "Process for Making Oxide Refractory Material Having Fine Crystal Structure," U.S. Pat. No. 4 415 510, December 12, 1972; November 15, 1983.

[178]J. K. Shurie, "Production of Fused Abrasives," Can. Pat. No. 924 112, February 4, 1971; April 10, 1973.

[179]M. Doutreloux and R. Ducreux, "Process for the Production of Fine Crystalline Abrasive Material," Can. Pat. No. 943 776, March 1, 1971; March 19, 1974.

[180]H. R. Müller, "Schleifmittel mit hoher Kornzähigkeit und Verfahren zu seiner Herstellung" (Abrasives with High Grain Toughness and Method for its Production), Ger. Pat. No. 21 60 705, December 7, 1971; June 14, 1973.

[181]J. J. Scott, "Method of Producing Abrasive Grits," Can. Pat. No. 956 122, December 27, 1971; October 15, 1974.

[182]J. J. Scott, "Progressively or Continuously Cycled Mold for Forming and Discharging a Fine Crystalline Material," U.S. Pat. Apl. B522 038, February 3, 1976.

[183]B. Ilmaier and H. Zeiringer, "Method for Producing Alumina and Alumina-Zirconia Abrasive Material," U.S. Pat. No. 4 059 417, June 10, 1976; November 22, 1977.

[184]L. Coes, "Method of Rapid Cooling Molten Alumina Abrasives," U.S. Pat. No. 4 104 494, October 21, 1977; February 20, 1979.

[185]P. Cichy, "Apparatus for Producing Oxide Refractory Material Having Fine Crystal Structure," U.S. Pat. No. 3 726 621, June 15, 1971; April 10, 1973.

[186]J. J. Scott, "Verfahren und Vorrichtung zum kontinuierlichen Abgusss Geschmolzener Oxide" (Process and Apparatus for Continuously Cast Molten Oxides), Ger. Pat. No. 28 54 680, December 19, 1977; June 28, 1979.

[187]B. Gibson, "Improvements in or Relating to the Solidification of Molten Material," Br. Pat. No. 1 595 196, May 26, 1978; August 12, 1981.

[188]D. G. Bennett, "ZS Alundum a New Conditioning Abrasive," *Grits Grinds*, **60** [5] 327–30 (1969).

[189]Anon., "ZF Alundum—Norton Company's Foundry Grinding Abrasive Proves its Worth," *Grits Grinds*, **61** [1] 3–7 (1970).

[190]W. E. O'Brien, "Substituting Machine Grinders, Using Zirconia Wheels Boosting Speed Helps US Steel Cut Costs, Increase Output," *Abrasive Methods*, April-May, 4–6 (1972).

[191]R. A. Rowse and G. R. Watson, "Zirconia-Alumina Abrasive Grain and Grinding Tools," U.S. Pat No. 3 891 408, August 8, 1973; June 24, 1975.

[192]J. R. Quinan and J. E. Patchett, "Coated Abrasive Material Comprising Alumina-Zirconia Abrasive Compositions," U.S. Pat. No. 3 893 826, August 13, 1973; July 8, 1975.

[193]R. A. Rowse and H. G. Lakhani, "Cut-off Wheels of Fused Alumina-Zirconia Alloy Abrasive Grains," U.S. Pat. No. 3 916 583, May 10, 1974; November 4, 1975.

[194]A. K. Kuriakose and I. J. Beaudin, "Tetragonal Zirconia in Chilled-Cast Alumina-Zirconia," *J. Can. Ceram. Soc.*, **46**, 45–50 (1977).

[195]I. E. Gladkov, N. B. Zhekhanova, A. A. Fotiev, V. V. Viktorov, V. T. Ivashinnikov, and A. S. Zubov, "Vlijanie dobavok okisov titana i kalciya na polimorfizm ZrO_2 pri plavlenii smesi Al_2O_3-ZrO_2 (Effect of TiO_2 and CaO Additions on ZrO_2 Polymorphism During Melting of an Al_2O_3-ZrO_2 Mixture)," *Inst. Khim. Sverdlovsk-Niorganicheskie Materialy*, **21** [3] 435–38 (1985).

[196]A. Iwata, "A Process for the Preparation of Super-heavy Grinding Grains," Jap. Pat. Apl. No. 45-112206, December 14, 1970.

[197]K. Woźniak, "Elektrokorund cyrkonowy" (Fused Alumina-Zirconia), *Szklo i Ceram.*, **29** [8] 272–74 (1978).

[198]G. E. Bockstiegel and P. Hack, "Zirconium Oxide-Aluminum Oxide Abrasives of High Grain Toughness," Ger. Pat. No. 1 571 435, December 2, 1966; December 28, 1972.

[199]D. W. Marshall and J. J. Scott, "Process for the Concentration of Zirconia," U.S. Pat. No. 2 926 993, December 5, 1956; March 1, 1960.

[200]A. J. Hudson and A. C. Haskell, "Electrically Smelted Oxides and Metalloids of Zirconium and Titanium," *Elec. Furn. Proc. AIME*, **16**, 211–18 (1958).

[201]R. H. Wilks, P. Ravinder, C. L. Grant, P. A. Pelton, R. J. Downer, and M. L. Talbot, "Plasma Process for Zirconium Dioxide," *Chem. Eng. Prog.*, **68** [4] 82–83 (1972).

[202]W. H. Gitzen, Alumina as a Ceramic Material. The American Ceramic Society, Columbus, OH, 1970.

[203]B. Glezin, "Perparation of Corundum," *Novosti Tekhniki*, **12**, 31 (1937).

[204]H. N. Baumann and R. C. Benner, "Aluminous Material," U.S. Pat. No. 2 360 841, June 10, 1941; October 24, 1944.

[205]H. N. Baumann and R. C. Benner, "Fused Aluminum Oxide Abrasive Material," U.S. Pat. No. 2 424 645, July 13, 1943; July 29, 1947.

[206]R. C. Benner and H. N. Baumann, "Abrasive," U.S. Pat. No. 2 318 360, May 5, 1941; May 4, 1943.

[207]N. G. Schrewelius, "Abrasive Corundum from Chamotte," Swed. Pat. No. 132 872, May 19, 1947.

[208]N. G. Schrewelius, "Manufacturing Corundum," Swed. Pat. No. 125 868, February 11, 1948.

[209]R. R. Ridgway, "Method of Purifying Crystalline Alumina and an Abrasive Material Made Thereby," U.S. Pat. No. 2 301 706, November 10, 1942.

[210]R. R. Ridgway, "Method of Purifying Crystalline Alumina and an Abrasive Material Made Thereby," U.S. Pat. No. 2 301 706, November 10, 1942.

[211]A. A. Klein, "Abrasive Grain," U.S. Pat. No. 2 301 123, November 3, 1942. U.S. Pat. No. 2 303 284, November 24, 1942.

[212]G. Yamaguchi and H. Tanabe, "Research on Artificial Emery," *J. Ceram. Assoc. Jpn.*, **62** [693] 208–12 (1954).

[213]A. A. Klein and G. T. Ridout, "New Alpha-Alumina Abrasive," *Machinery (London)*, **74** [1893] 145–147 (1949).

[214]L. J. Frost, "Electric Furnace Product," U.S. Pat. No. 2 849 305, August 30, 1954; August 26, 1958.

[215]H. F. G. Ueltz, "Abrasive Grain," U.S. Pat. No. 3 079 243, October 19, 1959; February 26, 1963.

[216]E. E. Howard and J. C. McMullen, "Sintered Abrasives," *Ceram. Age*, August 1963.

[217]P. J. Colpoys and E. A. Neel, "Method of Increasing Permeability in Subsurface Earth Formation," U.S. Pat. No. 3 976 138, October 15, 1975; August 24, 1976.

[218]C. E. Cooke, W. A. Heddes, and W. C. Chard, "Hydraulic Fracturing Method Using Sintered Bauxite Propping Agent," U.S. Pat. No. 4 068 718, October 26, 1976; January 17, 1978.

[219]E. F. Lunghofer, "Process for the Production of Sintered Bauxite Spheres," U.S. Pat. No. 4 440 866, October 28, 1982; April 3, 1984.

[220]M. L. Leitheiser and H. G. Sowman, "Non-fused Aluminum Oxide-Based Abrasive Material," U.S. Pat. No. 4 314 827, May 13, 1980; February 9, 1982.

[221]J. C. McMullen, "Gesintertes Schleifkorn und Verfahren zu seiner Herstellung" (Sintered Abrasive Grain and its Production Process), Ger. Offen. 1 815 911; December 21, 1967; July 24, 1969.

[222]J. J. Amero, "Sintered Alpha-Alumina and Zirconia Abrasive Product and Process," U.S. Pat. No. 3 454 385, August 4, 1965; July 8, 1969.

[223]R. E. Barks, "Sintered Abrasive Containing Ceria, Alumina, Zirconia," U.S. Pat. No. 3 916 585, October 24, 1973; November 3, 1975.

[224]R. L. Pevzner, "Production of Corundum for Abrasives Without the Use of Furnaces," *Dokl. Akad. Nauk SSSR*, **67** [4] 707–709 (1949).

[225]A. Nesin, "Method of Making Crystalline Alumina Lapping Powder," U.S. Pat. No. 3 121 623, March 17, 1961; February 18, 1964.

[226]W. Funabashi, "Study on Abrasives VII," *Nagoya Kogyo Gijutsu Shikensho Hokoku*, **1** [2] 31–35 (1952).

[227]W. Wagner, "Abrasive Material with Porous Grain," Ger. Pat. No. 939 377; June 21, 1956.

[228]R. H. Schleifer, J. E. Price, and H. J. Bowden, "Abrasive Powder of Fused Alumina Containing Vanadium Tetroxide," U.S. Pat. No. 3 792 553, September 28, 1971; February 19, 1974.

[229]Anon., *Abrasive Eng.*, November-December 1971; p. 27.

[230]T. B. Walker, R. J. Seider, and P. Cichy, "Fused Aluminum Oxide Abrasive Grain Containing Reduced Titanium Oxide," U.S. Pat. No. 4 111 668, January 1, 1976; September 5, 1978.

[231]M. Daire, Y. Larrere, and A. Mangin, "High-Hardness Abrasive Product Based on Alumina and Aluminum Oxycarbides and Process for Preparing Same," U.S. Pat. No. 4 341 533, July 3, 1980; July 27, 1982; Fr. Pat. No. 2 460 315, July 5, 1979; January 23, 1981.

[232]L. Coes, Abrasives. Springer-Verlag, New York, 1971.

[233]E. J. Marslek, "Lapping"; paper No. 42 in New Developments in Grinding. Edited by M. C. Shaw. Carnegie Press, Pittsburgh, 1972.

[234]P. A. Jacquet, "Structure of Polished Metallic Surfaces," *Tech. Moderne*, **31** [12] 427–37 (1939).

[235]Standard Methods of Chemical Analysis of Aluminum Oxide Abrasive Grain and Abrasive Crude, American National Standards Institute, B74.14-1971.

[236]Specifications for the Size of Abrasive Grain-Grinding Wheels, Polishing and General Industrial Uses," American National Standards Institute, December 30, 1976, ANSI-B74.12-1976.

[237]Specifications and Publications of the Federation of European Manufacturers of Abrasive Products, FEPA—Federation Europeene des Fabricants de Produits Abrasifs, 39 Rue St. Dominiques, 75, Paris 7, France.

[238]M. A. Eigeles, "Stabilization of Corundum Suspensions in Classification Cones," *Mineral Syr'e*, **114**, 29–38 (1936).

[239]C. Benedicks and P. E. Wretblad, "Granulometric Determination of Fine Abrasive," *Schleif. u. Poliertechnik*, **13** [1] 1–5 (1936).

[240]F. Puppe, "Grinding Electrocorundum," *Schleif. u. Poliertechnik*, **15** [10] 193–97 (1938).

[241]L. P. Dumas, "How More Accurate Sizing Improves Corundum Quality," *Grinding Finishing*, **6** [11] 59–62 (1960).

[242]H. F. G. Ueltz, "The Shape and Friability of Abrasive Grain"; Grinding Wheel Inst.-Abrasive Grain Assoc., Mid-Winter Conference, Philadelphia, PA, 1967.

[243]E. Jankowski and S. Skupinski, Materialy i wyroby ścierne, 2nd ed. (Abrasive Materials and Products). Wydawnictwa Naukowo-Techniczne, Warsaw, 1971.

[244]V. F. Mgeladze, "Ob odnoj kharakteristike izometrichnosti abrazyvnikh zeren" (About One of the Isometric Characteristics of Abrasive Grains), *Trudy VNIIASh*, **1** 25–27 (1965).

[245]V. Rybakov and O. N. Drozdova, "Vliyanie sposoba izmel'chenya abrazyvnikh materialov na formu i fizykomekhanicheskie svojstva poluchenikh zeren" (Effect of the Crushing Method of Abrasive Materials on the Shape and Physico-Mechanical Properties of the Obtained Grains), *Abrazivy*, **4**, 15–28 (1963).

[246]"Bulk Density of Abrasive Grain" American Standards Association, Inc., B74.4-1964.

[247]J. H. Westbrook, "The Temperature Dependence of Hardness of Some Common Oxides," *Rev. Haut Temp. Réfract.*, **3**, 4757 (1966).

[248]R. B. Koester and D. P. Moak, "Hot Hardness of Selected Borides, Oxides and Carbides to 1900°C," *J. Am. Ceram. Soc.*, **50** [6] 290–96 (1967).

[249]H. Albrecht, J. Lukacs, and E. Plötz, "Ü ber eine neue Methode zur Bestimmung der Kornzahigkeit von Schleifkörnern" (About a New Method to Determine the Toughness of Abrasive Grain), *Ber. Dtsch. Keram. Ges.*, **37** [8] 355–61 (1960).

[250]J. M. Karpinski and R. O. Tervo, "Single Impact Testing of Brittle Materials," *SME Trans.*, **229** [6] 126–30 (1964).

[251]W. Funabashi, "Study on Abrasives: XI, Finishing Abrasives for Synthetic Resins and Celluloid," *Nagoya Kogyo Gijutsu Shkensho Hokoku*, **2** [11] 5–8 (1953).

[252]W. E. Brandt, "A New Look at Vibratory Finishing," *Met. Prog.*, **11**, 96–100 (1963).

[253]R. W. Fitch, "Barrel Tumbling: How to Get Best Results," *Product Finishing*, **10**, 2–10 (1957).

[254]"Use of Abrasive Grain in Mass Finishing," Booklet 7, Abrasive Grain Association, 1230 Keith Building, Cleveland, OH 44115.

[255]W. Funabashi and S. Terada, "Melted Media for Barrel Finishing," *Nagoya Kogyo Gijutsu Shikensho Hokoku*, **11** [6] 313–17 (1962).

[256]H. J. Wills, "Securing Fine Surfaces by Grinding," *Machinery (N.Y.)*, **49** [8] 202–204 (1943).

[257]H. J. Wills, "Securing Fine Surfaces by Grinding: III," *Machinery (N.Y.)*, **49** [10] 171–73 (1943).

[258]H. J. Wills, "Securing Fine Surfaces by Grinding: V," *Machinery (N.Y.)*, **50** [1] 172–74 (1944).

[259]S. Spring, Metal Cleaning. Reinhold, New York, 1963.

[260]G. Mosselmans and J. Niehaus, "Auswahl von Abrasiven und Badzusätzen für die Dekontaminierung mittels Schlammstrahlen" (Choice of Abrasive and Fluid Additions during Decontamination with Slurry Blasting) Euratom 4186d, 1968.

[261]M. Hashish, "Cutting with Abrasive Waterjets," *Mech. Eng.*, **3**, 60–69 (1984).

[262]K. A. Baab and H. M. Kraner, "Investigation of Abrasive Resistance of Various Refractories," *J. Am. Ceram. Soc.*, **31** [11] 293–98 (1948).

[263]S. Eisner, "An Ultra High Speed Plating Process Utilizing Small Hard Particles," *Trans. Inst. Metal Finishing*, **51** [1] 13–16 (1973).

[264]Types, Forms and Sizes—Coated Abrasives. 1230 Keith Build., Cleveland, OH 44115-2180.

[265]Anon., "European Coated Grain Size Numbers are Different," *Mach. Tool Blue Book*, **73** [6] 135 (1978).

[266]Coated Abrasives—Modern Tool of Industry 1st ed. McGraw-Hill, New York, 1958. 1982 Reprint by Coated Abrasives Manufacturing Institute, Cleveland, OH.

[267]Carborundum Werke GMBH, Schleifmittel auf Unterlage—Aufbau—Formen—Anwendungen (Coated Abrasives—Structure—Shapes—Uses). Düsseldorf-Reisholz, Federal Republic of Germany, 1972.

[268]W. A. Mitchell, "Selecting the Proper Coated Abrasive Specialty," Abrasive Engineering Society Magazine No. 1 (1986). 1986-87 AES Reference & Buyers Guide.

[269]S. F. Walton, "Surface-Coated Abrasive Grain," U.S. Pat. No. 2 527 044, June 14, 1945; October 24, 1950.

[270]K. Dziobek and H. Osterrath, Verbesserung der Wirthschaftlichkeit beim Bandschleifen von Pressblechen mit Kornhohlkugelschleifbändern (Cost Savings for Belt Grinding of Pressed Metal Sheets with Hollow Spherical Grain Belts). Intergrind, Stockholm, 1976.

[271]W. Peters and H. Lukowski, "Verfahren zur Herstellung von Schleifkörpern auf Unterlage" (Process for the Manufacture of Coated Abrasives) Ger. Pat. No. 24 17 196, April 4, 1974; October 23, 1975.

[272]W. Löhmer and J. Schotten, "Process for the Production of Spherical Bonded Abrasives from Abrasive Grain," U.S. Pat. No. 4 132 533, April 12, 1975; January 2, 1979.

[273]S. F. Stevens, "Coated Abrasives Prove Useful in Prefinishing Hardwood Plywood," *Plywood and Panel Magazine*, March 1978.

[274]C. J. Holland, "Important Consideration in Wide Belt Sanding," *Furniture Methods and Materials*, February 1975.

[275]S. F. Stevens, "Abrasiveness Varies with Particleboard Type," *Forest Industries*, July 1969.

[276]S. F. Stevens, "Care of Belts and Rolls Keys to Good Panel Sanding," *Ind. Woodworking*, November 1966.

[277]S. E. Amundsen and R. C. Lobken, "High Rate Grinding with Coated Abrasive Belts to Produce Planar Surfaces on Various Types of Metals"; 3rd North American Metalworking Research Conference. Edited by M. C. Shaw. Carnegie Press, Pittsburgh, 1975.

[278]"American Standard Specifications for Standard Shapes and Sizes of Grinding Wheels," U.S. America Standards Institute, ASA B74.2-1960, Washington, DC.

[279]R. H. Merritt, "Standard Grinding Wheel Marking System," *Mach. Tool Blue Book*, **73** [6] 116–20 (1978).

[280]D. E. Thomas and R. P. Anibal, "Bonded Abrasives"; pp. 293–312 in Encyclopedia of Industrial Chemical Analysis, Vol. VII. Wiley & Sons, New York, 1968.

[281]M. Moser, "Investigation of the Phase Boundary of Electrocorundum Grains and the Ceramic Bonding in Ceramically Bonded Grinding Tools"; pp. 91–106 in New Developments in Grinding. Edited by M. C. Shaw. Carnegie Press, Pittsburgh, 1972.

[282]C. R. Weymuller, "Hot Cutting and Grinding. . .," *Met. Prog.*, January 1965.

[283]J. Mueller "Grinding Red Hot Billets Doubles Removal Rates," *Steel*, July 27, 1964.

[284]C. von Doenhoff, "Manufacture of Rubber Bonded Abrasives," *Rubber Age*, **10**, 69–71 (1954).

[285]S. Buchner, "Die Herstellung von Schleifmaterialien und Schleif-Scheiben" (Manufacture of Abrasive Materials and Grinding Wheels), *Keram. Z.*, **8** [8] 383–87 (1956).

[286]R. W. Miklitsch, "Unique Handling Integrates Grinding Wheel Processes," *Automation*, March 1964.

[287]G. S. Eisaman, "Grinding Operations in the Cleaning Room," *Foundry*, I, May 1954, 384–89; II, June 1954, 220–35.

[288]J. A. Mueller, "Cost Cutting with Grinding Wheels," *Modern Castings*, **2**, 62–64; **3**, 34–35; **4**, 58–59 (1957).

[289]J. A. Mueller, "Profit in the Cleaning Room Through the Use of Modern High Speed Abrasives," *Modern Castings*, **10**, 102–109 (1967).

[290]J. A. Mueller, "Abrasives in the Cleaning Room: a Means to Generate Profit" *Modern Castings*, I, May 1972, 60–62; II, June 1972, 33–34; III, July 1972, 22–23; IV, August 1972, 38–39; V, September 1972, 55–57.

[291]J. A. Mueller, "How to Design for Abrasive Machining," *Machine Design*, **6**, 83 (1972).

[292]R. Avery, "Big Wheels Cut-off Tough Alloys," *Am. Machinist*, January 10, 1972; pp. 50–51.

[293]W. Schittgen, "Trennschleifen von Stahl unter besonderer Berücksichtigung von Edelstählen" (Steel Cut-off Grinding with Particular Emphasis on Specialty Steels), *Stahl u. Eisen*, **94** [8] 326–35 (1974).

[294]W. Stiebellehner, "Trennen grosser Querschnitte" (Cut-Off of Large Cross Sections), *Werkstatt u. Betrieb*, **104** [11] 827–30 (1971).

[295]E. N. Maslov, Osnovy Teorii Shlifovania Metallov (Fundamentals of Metal Grinding Theory). Gos. Nauch. Tekh. Izd. Mashinostroit. Literatury, Moskov, 1951. Translated into German by H. Behrens, Verlag Technik-Berlin, 1952.

[296]Annual Reports by the Carnegie Institute of Technology for the Abrasive Grain Association entitled "Investigation of Abrasive Grain Characteristics" 1966–73.

[297]M. C. Shaw, "New Developments in Grinding"; Proceedings of the International Grinding Conference, Pittsburgh, April 18–20, 1972. Carnegie Press, Pittsburgh, 1972.

[298]J. M. Dallavalle, Micromeritics—The Technology of Fine Particles. Pitman, New York, 1948.

[299]"Technology of Monolithic Refractories," Plibrico Japan Company Ltd., No 33-7 Shiba 5 chome, Minato-ku, Tokyo, 1984.

[300]W. H. Gitzen, "Clay-bonded Alumina Refractories," pp. 139–41; "Binders for Alumina Refractories," pp. 146–47 in Alumina as a Ceramic Material. The American Ceramic Society, Columbus, OH 1970.

[301]W. T. Bakker, "High Alumina Brick and Method of Making," U.S. Pat. No. 3 591 392, July 1, 1968; July 6, 1971.

[302]A. A. Mukhin, R. S. Milchenko, R. N. Gol'dinova, B. I. Mindin, and B. I. Klochkov, "Using Production Scrap from Alumina Insulating Refractories," *Ogneupory*, **8**, 20–23 (197).

[303]P. Cichy, "Electrothermic Production of Mullite," *Elec. Furn. Proc. AIME*, **31**, 136–47 (1973).

[304]E. P. McNamara, "Alumina and Mullite as Kiln Furniture," *Am. Ceram. Soc. Bull.*, **49** [3] 272–75 (1970).

[305]R. K. Mack, "Pressure Pouring Tube," U.S. Pat. No. 3 529 753, January 13, 1969; September 22, 1970.

[306]G. S. Fulcher and T. E. Field, "Refractory Zirconia Casting," U.S. Pat. No. 2 271 367, October 11, 1939; January 27, 1942.

[307]J. H. Partridge and O. Adams, "Glass Making at 2000°," *J. Soc. Glass Technol.*, **28**, 105–12 (1944).

[308]T. S. Busby, M. Manners, and J. H. Partridge, "Improvements in or Relating to Refractory Materials," Br. Pat. No. 682 961, November 19, 1952.

[309]L. R. Schlotzhauer and K. T. Wood, "Method of Making a Refractory Body and Article Made Thereby," U.S. Pat. No. 2 842 447, September 29, 1955; July 8, 1958.

[310]E. A. Thomas, D. G. Patel, and W. F. Brandt, "Bonded AZS Refractories for Glass Processing," *J. Can. Ceram. Soc.*, **53**, 51–56 (1984).

[311]T. B. Allen, "Composition of Matter Containing Alumina nad Magnesia," U.S. Pat No. 1 001 497, July 28, 1910; August 22, 1911.

[312]F. J. Tone, "Artificial Magnesia Spinel and Process of Manufacture," U.S. Pat. No. 1 448 010, April 5, 1921; March 13, 1923.

[313]T. R. Haglund, "Process for Obtaining Products Containing Spinels," U.S. Pat. No. 2 029 773, May 17, 1933; February 4, 1936.

[314]M. E. Tyrrell and N. A. Pace, "Electric Furnace Synthesis of Spinel in Dusting Slags," U.S. Bureau of Mines Report of Investigations 5833 (1961).

[315]Compagnie de Produits Chimiques et Métallurgiques Alais, Froges et Camarques, "Production of Pure Electrocast Spinel," Fr. Pat. No. 898 463, March 7, 1944.

[316]G. I. Antonov et al., "Making Electrofused Magnesia-Alumina Spinel to Produce High Grade Refractories," *Ogneupory*, 4 41–51 (1972).

[317]H. Uchikawa, H. Hagiwara, M. Shirasawa, and T. Watanabe, "Application of Periclase-Spinel Bricks to Cement Rotary Kilns," *Interceram (Special Issue on Refractories)*, **33**, 40–43 (1984).

[318]P. Bartha, "Direktgebundene Periklasspinellsteine und ihr Einsatz in der Zement Industrie" (Direct Bonded Periclase-Spinel Blocks and Their Application in the Cement Industry), *Zem. Kalk Gips*, **35** [10] 530–36 (1982).

[319]C. B. Jacobs, "Object of Refractory Material and Method of Manufacturing Same," U.S. Pat. No. 711 319, December 26, 1900; December 8, 1902.

[320]F. J. Tone, "Composition of Matter Containing Alumina and Silica," U.S. Pat. No. 906 339, March 17, 1908; December 8, 1908.

[321]V. Škola, "Blocs réfractaires fondu" (Fused Refractory Blocks), *Chimie Industrie*, **29**, 825–29 (1933).

[322]A. Malinowski, "The Malinite Process for the Production of Sillimanite Refractories," *J. Am. Ceram. Soc.*, **23**, 40–68 (1920).

[323]H. M. Kraner, "Some Considerations in the Production of Fused Mullite for Refractories," *J. Am. Ceram. Soc.*, **21**, 360–66 (1938).

[324]T. W. Schroeder, "Electric Furnace Production of High-Heat-Duty Refractories," *Ind. Eng. Chem.*, **23**, 124-26 (1931).

[325]G. S. Fulcher, "Cast Refractory Article and Method of Making the Same," U.S. Pat. No. 1 615 750, July 31, 1925; January 25, 1927.

[326]P. Bortaud and D. Rocco, "Electrocast Refractories," *J. Br. Ceram. Soc.*, **1** [2] 237 (1964).

[327]G. J. Easter, "Furnace Refractory," U.S. Pat. No. 2 017 058, April 17, 1934; October 15, 1935.

[328]H. N. Baumann and C. McMullen, "Refractory Product," U.S. Pat. No. 2 019 208, December 16, 1933; October 29, 1935.

[329]R. C. Benner and H. N. Baumann, "Refractory for Glass Tanks and the Like," U.S. Pat. No. 2 019 209, September 12, 1932; October 29, 1935.

[330]H. H. Blau and H. N. Baumann, "Furnace Lining and Material Therefor," U.S. Pat. No. 2 043 029, April 19, 1934; June 2, 1936.

[331]G. J. Easter and C. McMullen, "Fused Refractory Composition," U.S. Pat. No. 2 063 154, December 18, 1933; December 8, 1936.

[332]J. H. Partridge, Refractory Blocks for Glass Tank Furnaces, The Society of Glass Technology, Sheffield, England, 1935.

[333]G. S. Fulcher, "Refractory Article," U.S. Pat. No. 1 879 676, December 15, 1927; September 27, 1932.

[334]G. J. Easter and K. Brownell, "Refractory and Method of Making It," U.S. Pat. No. 2 154 153, July 21, 1936; April 11, 1939.

[335]N. M. Galsina and L. S. Tchernina, Elektroplavlenye Ogneupory dlya steklovarenyh petchei (Electrofused Refractories for Glass Melting Furnaces). Stroizdat, Moscow, 1975.

[336]O. N. Popov, P. T. Rybalkin, A. S. Sokolov, and S. D. Ivanov, "Proizvodstvo i primenenie plavlenolityh ogneuporov" (Production and Application of Fused Cast Refractories), Metallurgiya, Moscow, 1985; 255 pp.

[337]V. Gottardi, A. Trotta, G. Michelotto and S. Bauer, "A Mathematical Model of Cooling of Electrocast Refractories," *Glass Technol.*, **21** [3] 120–24 (1980).

[338]K. H. Sandmeyer and W. A. Miller, "Electric Arc Fusion Cast Alumina Refractories," *Elec. Furn. Proc. AIME*, **17**, 257–67 (1959).

[339]T. S. Busby, Tank Blocks for Glass Furnaces. Society of Glass Technology, Sheffield, England, 1966.

[340]R. W. Brown, "The Role of Beta Alumina Fused Cast Refractories in Glass Tank Superstructures," *J. Can. Ceram. Soc.*, **31**, 135–44 (1962).

[341]E. F. Frischbutter and W. Schroeder, "Beta Alumina and its Use as an Electrocast Refractory Material," *Silikat Tech.*, **17**, 317–22 (1966).

[342]J. C. McMullen and A. P. Thompson, "Physical Properties of High-Alumina Fused Cast Refractories," *Am. Ceram. Soc. Bull.*, **29** [1] 12–15 (1950).

[343]K. H. Sandmeyer, "Fused Cast Refractory Articles and Method of Making Them," U.S. Pat. No. 2 911 313, November 16, 1956; November 3, 1959.

[344]R. W. Brown and O. R. Stach, "Use and Misuse of Fused Cast High-Alumina Refractories," *Am. Ceram. Soc. Bull.*, **30** [8] 251–57 (1951).

[345]J. A. Bonar, C. B. Clark, and K. H. Sandmeyer, "Interaction of Oxide Refractories with the Environment of High Temperature Reactors," *Am. Ceram. Soc. Bull.*, **59** [4] 473–79 (1980).

[346]R. G. La Bar, "Refractory," Ger. Pat. No. 2 326 419, June 14, 1972; January 4, 1974.

[347]T. E. Field, "Cast Refractory Product," U.S. Pat. No. 2 271 366, October 20, 1939; January 27, 1942.

[348]G. S. Fulcher and T. E. Field, "Refractory Zirconia-Alumina Casting," U.S. Pat. No. 2 271 369, October 24, 1939; January 27, 1942.

[349]T. E. Field, "Alumina Low Silica Refractory," U.S. Pat. No. 2 424 082, April 10, 1945; July 15, 1947.

[350]A. Aycoberry, "Les réfractaires électrofondus," *Memoires Soc. Ing. Civ. France*, **116**, 13–34 (1963).

[351]K. H. Sandmeyer, "Fused Cast Zirconia-Alumina Articles," U.S. Pat. No. 2 903 373, November 30, 1956; September 8, 1959.

[352]F. C. Steimke, "Fused Cast Refractory," U.S. Pat. No. 2 919 994, October 30, 1957; January 15, 1960.

[353]H. Nagashima, E. Miyake, and A. Ito, "Cast ZrO_2-Al_2O_3 Refractories," Jap. Pat. No. 14 348, October 10, 1960; September 18, 1962.

[354]I. Ono, T. Eendo, and K. Onaka, "Zirconia-Alumina Cast Refractories," Jap. Pat. No. 3 896(62), May 30, 1959; June 8, 1962.

[355]A. M. Alper, E. R. Begley, J. W. Londeree, and R. N. McNally, "Fused Cast Refractory and Method of Making," U.S. Pat. No. 3 132 953, July 26, 1961; May 12, 1964.

[356]A. M. Alper, R. M. Lewis, and R. N. McNally, "ZrO_2-Al_2O_3-SiO_2 Fusion Cast Refractory," U.S. Pat. No. 3 632 359, November 29, 1968; January 4, 1972.

[357]G. Cevales, "Thermal Treatment of Electromelted Refractory Materials," U.S. Pat. No. 3 754 950, July 9, 1971; August 28, 1973.

[358]T. Grollier-Baron and J. Gaudin, "Manufacture of Electrically Melted Refractory Products Containing Mineral Oxides," U.S. Pat. No. 3 079 452, July 3, 1959; February 25, 1963.

[359]V. I. Gutman, V. N. Lazorenko, V. A. Lapin, et al. "Reducing the Carbon Content in Baddeleyite-Corundum Products," *Ogneupory*, **6**, 12–14 (1981).

[360]I. V. Timoshenko, G. V. Pavlyukova, A. F. Borisov, I. A. Suslova, and L. L. Chernina, "Use of Vibration to Improve Quality of Electrofused Refractories," *Ogneupory*, **11**, 496–99 (1964).

[361]P. P. Boggum, "Wannesteine zwischen heute und morgen" (Tank blocks of today and tomorrow), *Glastech. Ber.*, **51** [11] 303–306 (1978).

[362]G. S. Fulcher, U.S. Pat. No. 1 868 699.

[363]R. W. Brown and K. H. Sandmeyer, "Applications of Fused Cast Refractories," *Chem. Eng.*, **78** [13] 106–14 (1969).

[364]H. N. Baumann and A. A. Turner, "Use of Cast Alumina Refractories in the Glass Industry," *J. Am. Ceram. Soc.*, **23** [11] 334–38 (1940).

[365]H. N. Baumann, "Petrology of Fused Cast High Alumina Refractories" *Am. Ceram. Soc. Bull.*, **35** [9] 358–60 (1956).

[366]H. N. Baumann, "The Preparation of Petrographic Sections with Bonded Diamond Wheels," *Am. Mineral.*, **42**, 416–21 (1957).

[367]C. B. Clark, "Use of the Petrographic Microscope in Refractory Technology"; pp. 11–25 in Process Mineralogy, Vol. II. Edited by R. D. Hagni. The Metallurgical Society of AIME, 1982.

[368]W. H. Bauer, R. G. LaBar, R. W. Matolka, and D. Reed, "Evaluation of the Fusion Casting Processes for Ceramic Materials"; School of Ceramics, Rutgers, The State University, New Brunswick, New Jersey, 1966.

[369]C. B. Clark, "Petrology of the Reactions of Fused Cast Alumina Refractories with Metals and Slags," *J. Met.*, **18** [9] 1047–54 (1966).

[370]A. M. Alper, "Inter-Relationship of Phase Equilibria, Microstructure and Properties in Fusion Cast Ceramics"; pp. 335–69 in Science of Ceramics, Vol. 3. Edited by G. H. Stewart. Academic Press, New York, 1967.

[371]J. A. Bonar, C. R. Kennedy, and R. B. Swaroop, "Coal Ash Slag Attack and Corrosion of Refractories," *Am. Ceram. Soc. Bull.*, **59** [4] 473–78 (1980).

[372]T. S. Busby, "Progress in Glass Making Refractories," *Glass Technol.*, **20** [4] 117–31 (1979).

[373]W. A. Miller, "Electrofused Refractory Superstructures for Glass Tanks in the Eighties"; Toledo Glass Conference, Spring 1985. Published by Monofrax Inc. Falconer, NY.

[374]I. K. Orloy, "Cutting and Grinding of Fusion Cast Alumina with a Diamond Wheel," *Ogneupory*, **9** [12] 22–26 (1974).

[375]"Abrasives" appearing as a separate chapter in the "Minerals Yearbook" issued by the Bureau of Mines, Industrial Mineral Division, U.S. Department of the Interior, Washington, DC.

[376]Anon., "Abrasives," *Ind. Mineral.*, **7**, 9–24 (1971).

[377]T. Dickson, "Niagara Falls—Power to the Minerals," *Ind. Mineral.*, **2**, 39–43 (1983).

[378]T. Power, "Fused Minerals—the High Purity High Performance Oxides," *Ind. Mineral.*, **7**, 37–57 (1985).

[379]J. Robbins, "The Industrial Minerals of West Germany," *Ind. Mineral.*, **12**, 15–47 (1985).

[380]R. W. Brown and J. A. Bonar, "Special Refractories for the 1980s," *Ind. Mineral.*, Refractories Supplement, 1983.

High-Alumina Refractories for Steelmaking in Europe

Manfred Koltermann
Hoesch Stahl AG
Dortmund, Federal Republic of Germany

In the past 10 years there has been a significant decrease in steel production and a tremendous increase in the use of modern technology for steelmaking in Western Europe. The amount of continuous casting steel has increased from 26.4% in 1977 to 69.7% in 1985. This development has had a remarkable influence on the refractory market. This paper deals with the use of high-alumina materials as a steel-plant refractory. The use of chemically bonded high-alumina refractories may increase in the future. The refractory consumption per ton of crude steel may decrease in Western Europe to values of 10 to 15 kg.

A review of refractories used in the European steel industry was presented at the First International Conference on Refractories 1983 in Tokyo.[1] Several aspects of refractories usage between 1980 and 1990 have been discussed by Spencer.[2] Approximately 60 to 70% of all refractories consumed in Europe are used in the steel industry. The refractories market depends mainly on the tonnage of steel production and the technology of iron- and steelmaking; Homer[3] and Koltermann[4] discussed in some detail the technical and economical aspects of steel-plant refractories. The International Iron and Steel Institute conducted a special study on refractories consumption in the steel industry during 1980 and 1982. The chapters on torpedo ladles, oxygen converters, and continuous casting have been published in part.[5]

Table I shows important trends in steelmaking in Western Europe in the 1970s and 1980s. There has been a significant decrease in steel production and a tremendous increase in the use of modern technology for continuous casting of steel. There were only 2 048 000 tons of open-hearth steel produced in 1985 in Western Europe. In comparison, in Eastern Europe there was a total crude steel production of 198 400 000 tons, including 104 000 000 tons of open-hearth steel in 1985. The amount of continuous casting steel was only 14.3%.

In the past 10 years, the main areas for refractories research and development of new materials were (1) casting of blast furnace runners, (2) high-alumina refractories for torpedo cars, (3) secondary steelmaking and high-quality refractories for steel-plant ladles, (4) continuous casting refractories, and (5) development of chemically bonded products. For refractories, this means a clear tendency to high-quality basic materials, refractories with 50 to 99% Al_2O_3, and high-tech ceramics.

Table I. Crude Steel Production and Continuous Casting Steel in Western Europe

	Crude Steel Production in 10^6 tons	Continuous Casting Production (%)
1977	155.1	26.4
1978	163.5	29.9
1979	173.8	32.1
1980	161.3	39.6
1981	158.9	45.7
1982	144.3	53.6
1983	143.9	60.7
1984	157.1	65.4
1985	159.0	69.7

Classification of Refractories with More than 50% Al_2O_3

There are several classifications in national reports but there is no useful international standard available for the steel industry. The German Iron and Steel Association (VDEh) developed a classification for high-alumina bricks in 1985, giving several laboratory test values and hints for selection of different materials.[6] Nevertheless, the technical development of high-alumina refractories was so fast that this standard does not cover all aspects. This shows the difficulties encountered in developing a meaningful classification system for bricks. Table II gives a proposed classification system which could be useful as a standard for the steel industry. Including information on laboratory test data would greatly upgrade the utility of the system. For characterization of unshaped refractories, a code has been developed which is useful for all refractory products including unshaped high-alumina materials.[7] This coding system is used to identify the composition and properties of unshaped materials. Using 12 digits, information is given on product names, as-delivered condition, bond, and application technique. This system has been successfully used for several years in the German steel industry.

Laboratory Investigation of High-Alumina Refractories and Criteria of Material Suitability

Testing methods in Europe are mainly national standards and PRE recommendations.[8] But there are several tests in use which are not standardized but are very effective for selecting refractory material as re-

Table II. Classification of Refractories with More than 50% Al_2O_3

	Al_2O_3 (%)	Type of Bonding	Typical Additions	Type of Production
Corundum	>90	Ceramic bond	Impregnation with phosphate, tar, pitch, resin	Fired >1600°C
	<90			>1500°
				>1400°
				1000°–1400°
Bauxite	>80	Ceramic-chemical mixed bond	Addition of C	Heat-treated <200°C
	<80			<400°
				<600°
				600°–1000°
Mullite	65–80	Chemical bond-inorganic (phosphate)	Addition of Cr_2O_3	Fusion-cast
	<65			
Sillimanite	55–70	Chemical bond-organic (pitch, resin)	Addition of SiC	
Kyanite	55–70		Addition of ZrO_2, $ZrSiO_4$	
Andalusite	55–65			
	>65			
Fireclay with addition of Al_2O_3	>65			
	>50			
Spinel	>50			

quired for specific plant operating conditions. Especially useful are the refractoriness under load and the creep tests. These methods offer the opportunity to simulate thermomechanical conditions in torpedo cars and steel-plant ladles.[9] To select refractory materials, a test with temperature cycling between 1000° and 1500°C is very useful. A comparison between high-alumina and other refractories is shown in Fig. 1.

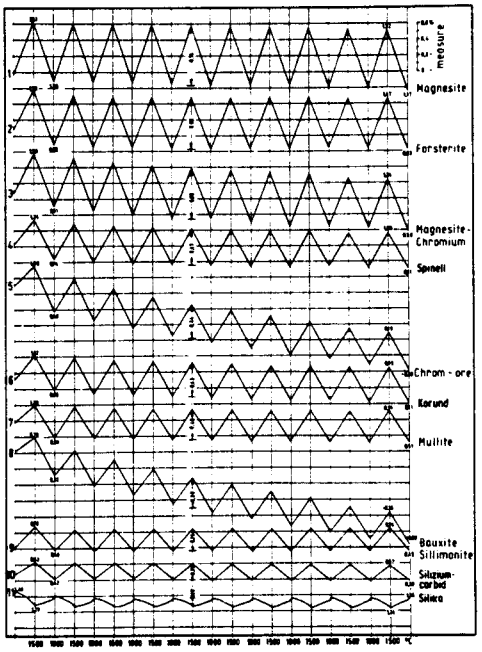

Fig. 1. Creep of refractories under a load of 0.2 N/mm^2 and a temperature cycle of 1000°-1500°-1000°C.

Other useful test methods are hot modulus of rupture and hot crushing strength. Looking at the problems from the viewpoint of the steel industry, the hot crushing strength is more reliable for refractory selection than hot modulus of rupture. Hot crushing strength equipment is shown in Fig. 2.

The slag test is one of the most important tests in relation to the behavior of steel-plant refractories in an industrial furnace. Using the induction furnace shown in Fig. 3, five bricks may be compared in one test.

There are a number of special publications dealing with investigations on high-alumina refractories and

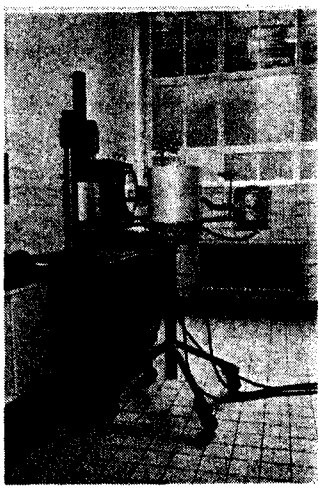

Fig. 2. Hot crushing strength equipment with a three-furnace carousel.

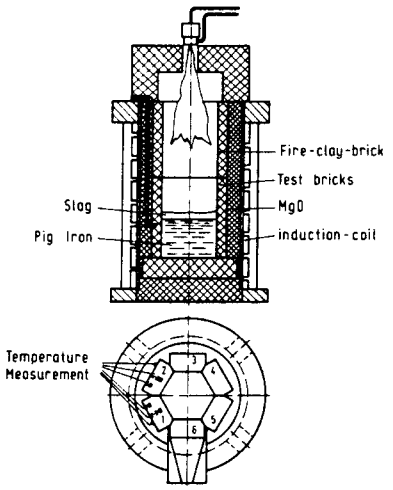

Fig. 3. Induction furnace for testing of refractories against slag attack at 1400° to 1750°C.

giving test results from more than 45 bricks.[10,11] Typical refractory linings and criteria of material suitability are discussed in detail in Ref. 12.

Table III presents typical values of high-alumina bricks for different applications.

High-Alumina Refractories in Blast Furnaces and Torpedo Cars

The rapid development of blast furnace technology in the past 20 years has led to new refractory materials such as Al_2O_3, Al_2O_3-Cr_2O_3, and SiC with different bonding systems.[13] Especially in the area of the bosh and lower stack, a whole range of refractory materials with extremely high slag and abrasion resistance and high thermal conductivity have been used and investigated. Performance results differ greatly, depending on the blast furnace technology, the cooling and lining systems, and the selected refractory material. For blast furnace troughs, the casting and vibration forming methods are being used with an increasing frequency in Western Europe. There are many materials available, mainly with fused alumina as the principal component. The Al_2O_3 content ranges from 50 to 85% and the SiC + C content is usually between 10 and 30%. The different bonding systems are the products of proprietary technology and some look like alchemy. It is very difficult to find a relationship between laboratory testing and plant results.[14,15]

Torpedo car lining techniques have changed considerably since 1970, as shown in Fig. 4. These results are based on plant and laboratory tests, which are

Table III. Typical Test Data for High-Alumina Bricks

	1	2	3	4	5	6	7	8	9	10	11
SiO_2 (%)	4.3	0.8	13.0	7.7	23.0	38.0	0.3	9.0	6.5	0.7	0.7
Al_2O_3	94.8	85.0	81.7	86.5	75.0	60.0	52.0	86.3	57.2	98.0	95.0
TiO_2	0.1	0.1	0.9	3.1	0.1	0.3		0.1	0.1	0.3	0.3
Fe_2O_3	0.2	0.3	1.4	1.7	0.4	0.9	0.3	0.1	0.3	0.1	0.1
CaO	0.2	0.2	0.2	0.2	0.1	0.2	0.6	0.1	0.2	0.4	0.3
MgO	0.1	0.1	0.1	0.2	0.1	0.3	46.0	0.1	0.1	0.1	0.1
Cr_2O_3		12.7									
P_2O_5		0.1	1.9								
Na_2O	0.2	0.3	0.3	0.2	0.2	0.2	0.1	0.2	0.2	0.2	3.5
K_2O	0.1	0.1	0.3	0.2	0.1	0.2	0.1	0.1	0.1	0.2	0.4
C								4.2	7.9		
SiC									24.4		
Bulk density (g/cm^3)	3.30	3.34	2.80	2.96	2.60	2.55	2.92	3.11	2.80	3.40	3.20
Apparent porosity (%)	12	17	17	19	15	15	17	4	11	<1	<1
Cold crushing strength (N/mm^2)	200	120	90	90	100	60	50	240	50	300	300
Hot crushing strength at 1500°C (oxidizing atmosphere) (N/mm^2)	50	50	6	8	15	6	5	18	4	50	30
Hot modulus of rupture at 1500°C (oxidizing atmosphere) (N/mm^2)	14	14	4	5	5	4	4				
Thermal conductivity (W/m • K)											
400°C	3.9	4.1	1.9	1.9	1.9	1.5	4.0		6.8	9.5	2.3
1000°C	3.9	3.3	2.2	2.0	2.1	1.7	3.5		4.8	7.4	3.4

1,2 Blast furnace bricks-fired.
3 Torpedo car brick-corundum; phosphate-bonded and fired.
4 Torpedo car and steel-plant ladle brick—bauxite; fired.
5 Mullite brick; fired.
6 Torpedo car and steel-plant ladle brick—andalusite; fired.
7 Spinel—brick; fired.
8 Slide gate plate—corundum; fired.
9 Torpedo car brick; Al_2O_3-SiC-C brick; resin-bonded.
10 Fusion-cast brick for reheating furnaces; α-corundum.
11 Fusion-cast brick for reheating furnaces; α and β-corundum.

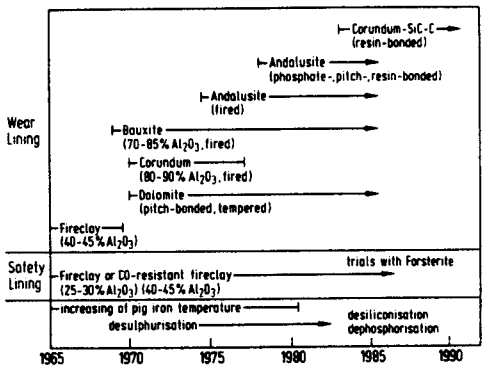

Fig. 4. Development of torpedo car linings in West Germany.

discussed in detail in Ref. 16. A reliable method for selecting a suitable material is the creep test in combination with hot crushing strength and hot modulus of rupture. There is no doubt that bricks with andalusite and corundum as principal components have better creep resistance than bauxite materials with 2 to 4% TiO_2[17] (Fig. 5). Another important property is slag resistance. The slag composition differs greatly, depending on plant conditions such as the $CaO:SiO_2$ ratio and possible metallurgical treatment in the blast furnace trough or torpedo car. As shown in Fig. 6, at $CaO:SiO_2 > 1$ the corundum has less wear than andalusite. For slag with a ratio greater than one and a high alkaline content, the use of a basic lining should be considered. Pitch-bonded, heat-treated dolomite linings have been used for many years in West Germany. Another important factor seems to be the MnO content of the slag. The reaction between MnO and SiO_2—forming Mn_2SiO_4—could increase the degree of wear if the refractory material contains a great deal of SiO_2.

Today, torpedo cars in West Europe are mainly lined with high-alumina refractories such as andalusite and bauxite. There is a tendency to try chemically bonded bricks and to use andalusite enriched with

		1	2	3
SiO_2	%	35.0	8.8	20.8
Al_2O_3	%	62.5	84.5	73.0
TiO_2	%	0.3	3.0	3.0
Bulk density	g/cm³	2.55	2.93	2.60
Cold crushing strength	kp/cm²	950	900	750

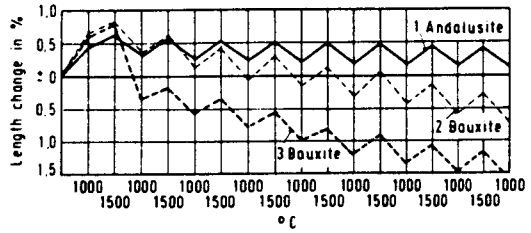

Fig. 5. Creep of andalusite and bauxite bricks under a load of 0.2 N/mm² and a temperature cycle of 1500°-1000°-1500°C.

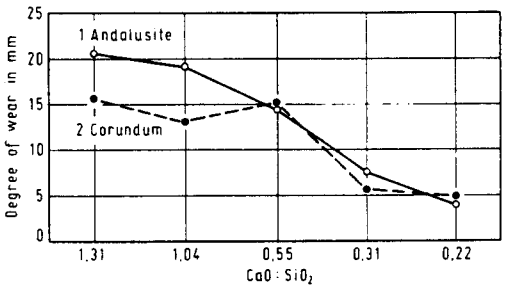

Fig. 6. Resistance of andalusite and corundum bricks against torpedo car slags with different $CaO:SiO_2$ ratios at 1520°C after 4 h in an induction furnace.

corundum up to 70 to 80% Al_2O_3. Increasing desiliconization and dephosphorization in the torpedo car could encourage thinking about zone lining and trials with resin-bonded Al_2O_3-SiC-C bricks.

In the whole blast furnace area—including torpedo cars—the reaction of alumina refractories with alkali is an important topic. (See the review on alkali reactions by Farris and Allen (Ref. 18).) Formation of potassium-containing compounds causes volume expansion and brick disruption; an effective laboratory test method has been described by Havranek.[19]

Steel-Plant Refractories with More than 50% Al_2O_3

The main areas for high-alumina refractories are the steel-plant ladle and the continuous casting plant.

The development of high-performance ladle linings in the years 1975 to 1985 and increasing metallurgical treatment in the ladle led to basic linings. The use of pitch-bonded, heat-treated dolomite bricks in the wall and magnesite-carbon bricks in the slag area is a common technique in West Europe. Ladle linings with basic materials will probably increase in the next 10 years.

Ladle bottoms are a special area where high-alumina refractories such as corundum, bauxite, and andalusite are superior.[20] Even in the bottoms of basic lined ladles there have been successful trials with corundum and andalusite bricks. At some steel plants, lining the bottom with fired and chemically bonded andalusite has been a common practice for many years.[21]

Other areas for high-alumina refractories associated with the ladle operation are the gas-purging systems and the slide-gate systems.[22] Especially in the gas-purging systems, a variety of operating techniques and refractory materials have been used. This is an area for research and development in the 1980s.[23]

Refractory materials for continuous casting have been a main topic for research for many years. Several publications have reviewed development prognosis and plant experience.[24–26] There are different concepts used for refractory lining tundishes, mainly using basic materials. The use of low-cement refractory concretes as tundish backing linings has been reported.[27] Under

special circumstances, lining the tundish with bauxite-based 75% Al_2O_3 could be useful. As magnesite mixes and cold tundish plates have low wear resistance in the impact area of the metal stream, high-alumina impact plates are used in this area.

The monobloc stoppers are made from high-quality corundum-graphite and are isostatically pressed. Properties and behavior of isostatically pressed refractories for the continuous casting process based on alumina-graphite and MgO-graphite composition are discussed in a special publication.[28]

Some data on high-alumina refractories for continuous casting are given in Table IV.

Reheating Furnaces

In comparison to steel plants, reheating furnaces are not a large refractory consumer. But several types of high-alumina refractories are used in these furnaces, such as fusion-cast refractories, bauxite, corundum, and high-alumina cements. (See Ref. 29 for a literature review on types of furnaces and refractory linings for reheating furnaces.)

The development of new fusion-cast refractories is discussed in detail in Ref. 30. The use of stainless steel fibers for reinforcing castables was a research topic for many years.[31] Another interesting topic is the setting time of high-alumina cements by heat evolution.[32] For energy savings, lining techniques using ceramic fibers have increased in the past 10 years. The heat-treating furnaces are one of the very few areas for high-alumina refractories without competition from basic materials.

Future Developments

There will be less tonnage of refractories but a significant increase in high-quality products and special materials. The consumption of refractories per ton of crude steel may decrease in the next 15 years to values between 10 and 15 kg. In West Germany the refractory consumption in the steel industry was (in kg/t of crude steel): 1980, 23.4; 1982, 20.8; 1984, 18.6; 1985, 17.7.

Table IV. Typical Data on High-Alumina Refractories for Continuous Casting

	Submerged Nozzles	Submerged Nozzles, Shrouds, Monobloc Stoppers, Isostatically Pressed
Al_2O_3 (%)	72–75	60–70
C (%)	20–25	25–35
Bulk density (g/cm^3)	2.20	2.35–2.40
Apparent porosity (%)	<24	<18
Thermal conductivity at 1000°C (W/m • K)	1.8	10

The main areas of research and development will be casting materials, special refractories for metallurgical treatment in torpedo cars and steel plant ladles, continuous casting refractories, and energy saving by using special refractories and furnace constructions.

There will be an increasing market for chemically bonded high-alumina materials with added SiC and C. Especially interesting are the resin binders for development of new refractories. Figure 7 shows the hot crushing strength under oxidizing and reducing atmosphere of an Al_2O_3-SiC-C brick. In using these bricks, the temperature, atmosphere, and the quality of the added carbon must be considered in relation to the bond system (see Refs. 33 to 35). Figure 8 shows the importance of these new bricks against slag attack. Compared with other refractory materials, there are remarkable differences in resistance against torpedo car slags with low and high $CaO:SiO_2$ ratios (Fig. 9). Successful operations with chemically bonded high-alumina bricks for lining torpedo cars and the bottoms of steel-plant ladles are described in Refs. 21 and 36. Carbon is becoming more important as a component of refractories with possible additions of metallic Si or Al to prevent oxidation.

Another interesting material for the future is spinel, used successfully for several years for rotary kilns in the cement industry.[37] The so-called spinel bricks are not pure spinel $MgO \cdot Al_2O_3$ but have a chemical composition from 80% MgO to 80% Al_2O_3. With such a range in composition, very different test results are being observed in resistance against slag, temperature shock, and creep behavior. Spinel seems to have potential as a material for special refractories such as sliding-gate plates, continuous casting ceramics, and zone lining in torpedo cars. As in the past 10 years, there will be continued competition between basic and high-alumina refractories in the future. Selecting refractories for specific applications will continue to depend on technology advances in the steel industry and economic factors such as cost of the refractory materials and lining life.

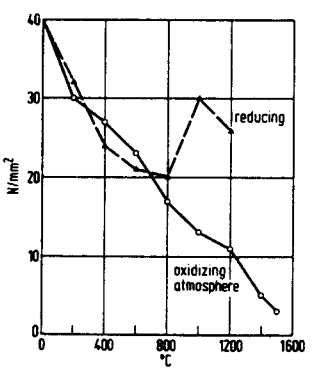

Fig. 7. Hot crushing strength of resin-bonded Al_2O_3-SiC-C.

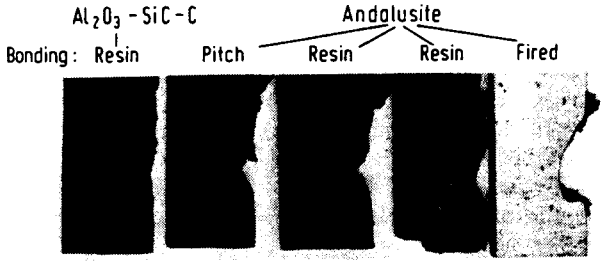

Fig. 8. Slag resistance of high-alumina bricks at 1520°C for 2 h in an induction furnace. Torpedo car slag with $CaO:SiO_2$ ratio of 3:1.

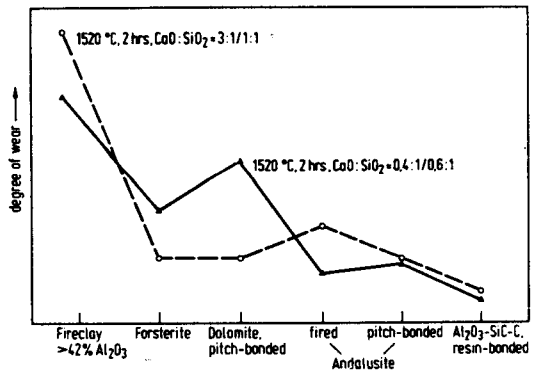

Fig. 9. Slag resistance of different refractories against torpedo car slags at 1520°C.

References

[1]M. Koltermann, "Refractories from the European View Point—Development and Trend of Refractories in the Steel Industry," *Taikabutsu Overseas*, **4** [3] 3–13 (1984).

[2]D. R. F. Spencer, "Refractories in the Eighties," *Refract. J.*, **3**, 12–28 (1979).

[3]D. Homer, "Tonnage Demand for Steel Plant Refractories," *Refract. J.*, **2**, 17–22 (1980).

[4]M. Koltermann, "Economic and Technical Correlations between the Production of Steel, Cement and Refractories from 1920–2000," *Stahl Eisen*, **103**, 917–21 (1983).

[5]"Extracts from the IISI—Report: Refractory Materials for Steelmaking," *Radex–Rundschau*, **1**, 1-/11 (1986).

[6]Stahl-Eisen-Werkstoffblatt 912, Verlag Stahl-Eisen GmbH, 4000 Düsseldorf, FRG.

[7]P. Artelt, "Characterization of Unshaped Refractories by Means of a Code," *Am. Ceram. Soc. Bull.*, **62** [7] 790–92 (1983).

[8]PRE Recommendations for Testing and Classification of Refractories. PRE, Löwenstr. 31, CH-8023, Zürich, Switzerland, 1983.

[9]M. Koltermann, "Andalusite Bricks for Torpedo Ladles," *Steelmaking Proc.*, **62**, 241–45 (1979).

[10]B. Oberfeuer and M. Koltermann, "Investigation and Test Results of Bricks with more than 50% Al_2O_3," *Radex–Rundschau*, **3**, 747-58 (1976).

[11]A. Majdic and G. Routschka, "Investigation of Mullite and Corundum Bricks," *Keram. Z.*, **31** [8] 494–97 (1979).

[12]P. Artelt, "Refractory Linings of Furnaces in the West-German Steel Industry and Criteria of Material Suitability," *Refract. J.*, **3**, 10–22 (1981).

[13]W. Kronert and G. König, "Selection of Refractory Materials for Modern Blast Furnaces," *World Steel Metalworking*, **1**, 15–17 (1979).

[14]B. Clavaud and G. Landman, "High Performance Materials for Blast Furnace Cast House," *Refract. J.*, **4**, 14–21 (1983).

[15]G. Routschka and A. Majdic, "Literature Review about Refractories for Blast Furnace Taphole and Trough Lining," *Keram. Z.*, **34** [9] 468–77 (1982).

[16]M. Koltermann, "Torpedo Ladle Refractories in West-Germany," *Taikabutsu Overseas*, **5** [2] 35–40 (1985).

[17]J. White, "The Chemistry of High Alumina Bauxite Based Refractories with Special Reference to the Effect of TiO_2—a Review," *Trans. J. Br. Ceram. Soc.*, **81**, 109–111 (1982).

[18]R. E. Farris and J. E. Allen, "Aluminous Refractories–Alkali Reactions," *Iron Steel Engineer*, **2**, 67–74 (1973).

[19]P. H. Havranek, "Alkali Attack on Blast Furnace Refractories," *Trans. J. Br. Ceram. Soc.*, **77** [3] 97–99 (1978).

[20]G. P. Carswell, M. P. Crosby and D. R. F. Spencer, "Development of High Performance Ladle Linings," *Refract. J.*, **1**, 9–21 (1980).

[21]"Fired and Chemically bonded Andalusite in Torpedo Cars and in the Bottom of Basic Lined Steel Plant Ladles"; unpublished report, Hoesch Stahl AG, Dortmund 1985/1986.

[22]G. Routschka and A. Majdic, "Refractories for Slide Gate Systems in Steel Plant Ladles—a Literature Review," *Keram. Z.*, **29** [10] 1–11 (1977).

[23]B. Grabner and H. Höffgen, "Application and Wears of Porous Plugs in Secondary Metallurgy," *Radex–Rundschau*, **3**, 581–610 (1985).

[24(a)]M. Oberbach and H. G. Stallmann, "Refractories for Continuous Casting of Steel," *Fachberichte Hüttenpraxis Metallweiterverarbeitung*, **20** [4] 212–21 (1982).

[(b)]E. Lührsen, M. Oberbach, and H. G. Stallmann, "Refractories for Continuous Casting of Steel Requirements: Current State and Developments"; Continuous Casting Symposium 1985, London.

[25]Refractories for Continuous Casting. Verlag Stahleisen, 4000 Düsseldorf, 1982.

[26]Papers presented at the 29th International Refractory Meeting 1986 in Aachen, "Continuous Casting Refractories". Published by the Institut für Gesteinshüttenkunde der RWTH, Aachen.

[27]D. Newbound, "Continuous Casting Tundish Refractories," *Hüttenpraxis Metallweiterverarbeitung*, **23** [10] 796–99 (1985).

[28]O. Krause, G. Mörtl, and C. Weidemüller, "Properties and Behavior of Isostatically Pressed Refractories for the Continuous Casting Process on Alumina-Grafite and MgO-Grafite Basis," *Radex-Rundschau*, **3**, 611–23 (1985).

[29]G. Routschka and A. Majdic, "Refractories for Reheating and Heat-Treating Furnaces—a Literature Review," *Keram. Z.*, **31** [9] 536–44 (1979).

[30]M. Esnoult, A. Krings, and P. Müller, "New Fusion Cast Refractories for Reheating Furnaces," *Stahl Eisen*, **101** [2] 41–49 (1981).

[31]M. Braun and A. Majdic, "Reinforcing Castables with Stainless Steel Fibers," *Interceram*, **29**, 112–18 (1980).

[32]C. H. Fentiman, C. M. George, and R. Montgomery, "Setting Time of High Alumina Cements by Heat Evolution," *J. Inst. Refract. Engineers*, Autumn 1984, pp. 3–5

[33]A. Brown, "The Properties of Ceramic Grafite Bodies," *Refract. J.*, **2**, 7–10 (1983).

[34]C. F. Cooper, "Grafite Containing Refractories," *Refract. J.*, **6**, 11–21 (1980).

[35]P. Haynes and F. T. Palin, "Testing of Carbon Containing Refractories," *Radex–Rundschau*, **2**, 407–16 (1984).

[36]M. Koltermann, "Unfired, Chemically Bonded High Alumina Bricks for Torpedo Cars," *Stahl Eisen*, **101** [19] 33–36 (1981).

[37]P. Bartha, "Chemical and Mineralogical Investigation of New and Used $MgO-Al_2O_3$-Bricks," *Zement-Kalk-Gips*, **28** [2] 96–99 (1985).

Alumina and Aluminous Refractories for Iron- and Steelmaking in Japan

N. Nameishi and T. Matsumura

Harima Ceramic Co., Ltd.
Arai-cho Sinhama 1-3-1
Takasago City, Hyogo Prefecture
Japan

New steelmaking processes used in Japan, such as pretreatment of pig iron, ladle refining, and continuous casting, led to the development of new alumina-based refractories which outperform the classic alumina bricks and monolithic product. The most outstanding group of products emerging from these efforts was those produced from various combinations of alumina, carbon, and silicon carbide. These compositions are being used commercially for production of both bricks and monolithics. Brick usage is decreasing but there has been tremendous growth in monolithics which can be installed by casting. These types of refractories are preferred because they reduce labor, improve the workingplace environment, and lower refractory consumption and cost per ton of steel produced. Concerning alumina-based refractories, ultrahigh-quality shaped refractories, for example, for continuous casting and monolithic refractories, alumina-based refractories which are easy to install, durable, and conserve energy are needed for the future in Japan.

Rapid qualitative and quantitative growth of the Japanese iron and steel industry was stopped by the oil crisis in 1973. Moreover, refractory consumption has been decreasing yearly because of improvements in refractory quality and the development of technologies for using refractories.

In 1985, Japan produced 1 129 100 tons of refractory bricks, which is about 60% of the 1 888 400 tons produced in 1975 (Table I). Meanwhile, production of monolithic refractories is increasing slightly. Examining each kind of brick production shows that clay, silica, and dolomite are decreasing rapidly. Magnesia-carbon is increasing, while high-alumina bricks show no significant change.

Concerning monolithic refractories, the increase in castable materials produced is remarkable. The amount of pig iron and crude steel produced and refractory consumption are decreasing (Fig. 1). While

Table I. Production of Refractories in Japan

	Fiscal Year										
	1975	1976	1977	1978	1979	1980	1981	1982	1983	1984	1985
Brick											
Clay	1,003.0	969.9	839.4	827.2	837.3	829.2	679.3	544.2	484.3	446.5	426.0
High alumina	171.1	167.5	150.3	153.0	163.3	172.8	175.0	162.2	154.7	169.1	160.1
Silica	142.7	77.6	53.1	54.9	54.5	65.6	62.1	43.1	27.8	13.5	20.4
Magnesia-chromite	208.3	245.9	225.0	242.0	247.2	225.6	190.5	159.3	148.9	147.5	136.5
Magnesia-carbon						52.0	65.7	74.0	98.1	118.7	115.6
Dolomite	173.3	166.9	142.2	143.5	133.2	104.4	83.4	65.2	44.9	36.7	32.5
Zircon	67.1	66.3	60.6	69.8	81.5	90.6	96.8	90.2	99.3	109.3	109.3
Silicon carbide	47.9	59.1	49.6	58.3	62.5	53.3	50.7	53.6	49.1	47.7	40.6
Insulation	55.4	53.6	40.6	40.9	43.9	55.2	53.3	39.0	32.2	35.9	33.4
Others	19.9	21.7	21.8	19.1	51.5	44.0	43.9	44.7	43.4	47.7	54.7
Total (brick)	1,888.4	1,828.4	1,587.5	1,608.6	1,675.2	1,692.7	1,500.7	1,275.4	1,182.5	1,172.5	1,129.1
Monolithic											
Castable	242.0	250.7	247.0	262.2	283.5	319.7	340.9	333.1	344.0	360.2	360.3
Plastic	115.2	125.3	111.3	98.3	87.8	84.6	71.3	66.6	69.4	69.1	63.4
Gunning	91.3	112.1	113.1	109.4	123.2	124.7	126.4	130.2	152.7	154.2	152.9
Ramming	147.9	157.0	137.2	143.7	138.5	128.1	109.6	95.5	91.5	95.5	90.2
Sling	56.4	56.0	37.8	29.9	26.0	23.5	14.5	7.6	5.5	2.0	
Patching, coating	97.8	94.7	92.9	90.4	110.1	114.7	121.5	107.0	102.1	108.9	107.0
Mortar	127.6	119.0	103.8	104.3	103.9	111.7	110.3	106.1	111.1	108.0	94.4
Total (monolithic)	878.1	914.8	843.1	838.1	873.0	906.9	894.5	846.0	876.2	897.9	868.2
Total (brick and monolithic)	2,766.5	2,743.2	2,430.5	2,446.7	2,548.2	2, 599.6	2,395.2	2,121.4	2,058.8	2,070.5	1,997.4

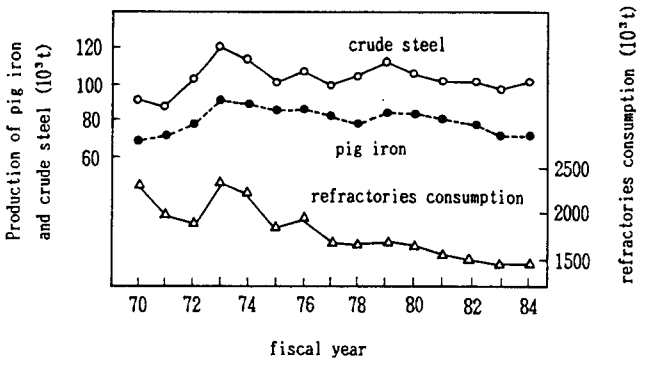

Fig. 1. Production of pig iron and crude steel and refractories consumption.[1]

steel production shows no marked fluctuation, the amount of refractories consumed is decreasing.

Refractory consumption per unit steel production is shown in Fig. 2. Monolithics consumed show little change, while brick consumption is decreasing steadily.

Besides conventional alumina or high-alumina bricks, refractories manufactured from alumina raw materials and carbon or silicon carbide additive have been used in the Japanese steel industry. These kinds of refractory materials have been used frequently, since the adoption of such processes as pig iron pretreatment, ladle refining, vacuum degassing, and continuous casting.

Topics covered in this paper include alumina or high-alumina raw materials, bricks, and monolithic materials manufactured from those raw materials or mixtures with carbon and/or silicon carbide additives, and uses for these products in steelmaking in Japan.

Alumina or High-Alumina Raw Materials

Two kinds of raw materials are available: synthetic and natural. Natural materials, such as alumina shale, bauxite sillimanite, kyanite, and andalusite do not occur in Japan, so they are imported. Synthetic raw materials, including fused alumina, sintered alumina, and sintered mullite are manufactured in Japan and also imported.

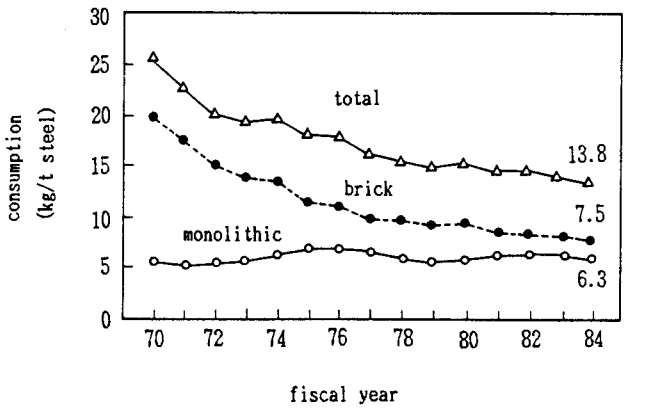

Fig. 2. Refractories consumption by steel industry.[1]

Large amounts of burned alumina shale, which is called "Chinese bauxite" in the western world, is imported. Mineral phases of alumina shale are boehmite, kaolinite, and anatase. Corundum crystals (spherical or columnar, 5 to 200 μm crystal size) and needlelike mullite are present in the burned alumina shale. Properties of burned alumina shale are shown in Table II. As shown in the thermal linear change curve in Fig. 3, alumina shale starts to expand rapidly at 500° to 700°C and shrinks above 1000°C.

Burned bauxite is imported from Guyana and Malaysia. As shown in the thermal linear change curve in Fig. 4, burned bauxite does not shrink like burned alumina shale does and shows excellent volume stability. The porosity change of burned bauxite and burned alumina shale heated at 1650° and 1800°C is shown in Fig. 5. Porosity of burned alumina shale is markedly higher at 1800°C than Guyana bauxite. The reason for this phenomenon is that rutile or aluminum titanate ($Al_2O_3 \cdot TiO_2$) in burned alumina shale reacts with other impurities. This causes the liquid amount to increase and the structure becomes porous.[4]

Properties of the sillimanite group minerals are shown in Table III. None occur in Japan and are imported from abroad. Lapso Buru kyanite produced in Bihar, India, was used formerly, but its quality was decreasing because the mine is nearing exhaustion. Recently, kyanite imports from Georgia, U.S.A., were begun. Sillimanite and andalusite are imported from the Transvaal in South Africa.

Aluminum hydroxide, which is produced by reacting bauxite with caustic soda, is used as the starting material for synthetic alumina raw materials. Alumi-

Table II. Properties of Burned Aluminous Shale*

Grade	Alumina 80	Alumina 85
Chemical composition (wt%)		
L.O.I.	0.10	0.16
SiO_2	6.34	6.50
TiO_2	3.80	4.40
Al_2O_3	88.30	86.98
Fe_2O_3	0.89	0.96
CaO	0.15	0.12
MgO	0.04	0.05
Na_2O	0.06	0.04
K_2O	0.08	0.56
Total	99.76	99.77
Mineral assemblage		
Corundum	5+	5+
Mullite	2	1−
$Al_2O_3 \cdot TiO_2$	1	1−
Rutile	1	1−
Apparent specific gravity	3.53	3.43
Bulk density	3.10	3.04
Apparent porosity (%)	12.3	11.2

*Ref. 2.

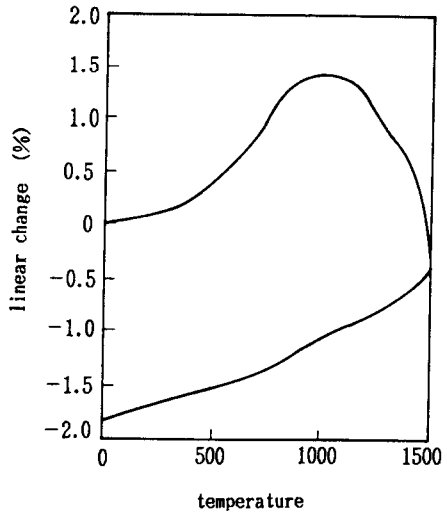

Fig. 3. Thermal linear change of burned aluminous shale.[2]

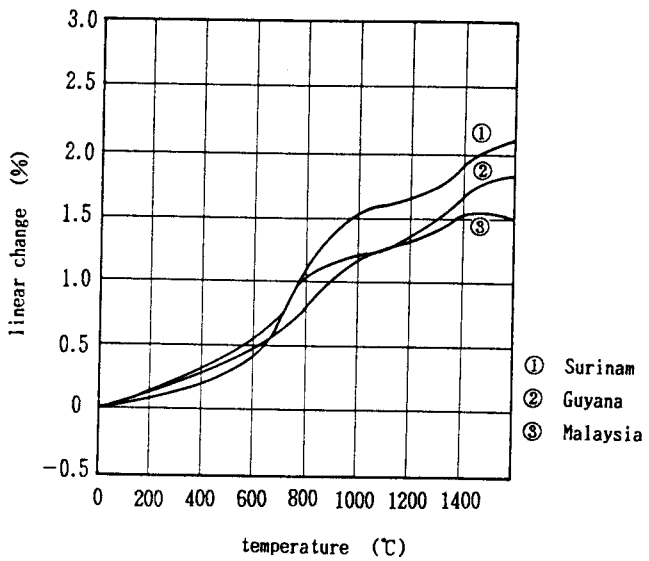

Fig. 4. Thermal linear change of burned bauxite.[3]

num hydroxide is calcined in a rotary kiln or fluidized-bed calcining kiln at >1000°C to obtain calcined aluminas. Properties of the various grades of calcined alumina are shown in Table IV.[5] Samples Nos. 1 and 2 are the most commonly used aluminas produced by the Bayer process. Their molding and sintering characteristics vary, depending on the α-alumina crystal size. Samples Nos. 3 and 4, which are low Na_2O grade, are used for manufacturing electronic ceramics. Because the green bulk density of pressed bodies from sample No. 5 is very high, firing shrinkage is small and dimension accuracy is excellent. Samples 6 and 7 have small crystal sizes and are very reactive. They sinter at relatively low temperatures and are suitable for making high-density and high-strength sintered bodies. They can also be used for manufacturing refractory

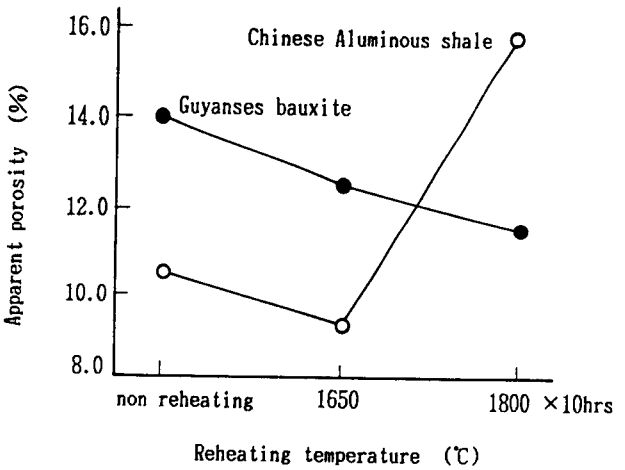

Fig. 5. Porosity change of burned aluminous shale and burned bauxite by heating.[4]

materials. Samples 8 and 9 are high-purity and easily sintered alumina[3] having a purity >99.9%.

A special type of alumina raw material is ρ-alumina. It is called an intermediate alumina, transition alumina, or active alumina. Seven known types of transition aluminas are κ, θ′, δ, γ, ϵ, χ, and ρ. The product with lowest crystalinity is ρ-alumina. Since it can be hydrated, ρ-alumina can be used as a binder for castable refractories instead of alumina cement.[6] The chemical composition of ρ-alumina is shown in Table V.

Sintered alumina is manufactured by the following process. Calcined alumina is mixed with binder, formed into granules for the briquetting machine or vacuum extruder, dried using a band dryer, and burned in a rotary kiln or shaft kiln at 1920° to 1970°C.[7-9] The properties of sintered alumina are shown in Table VI.

Fused alumina is manufactured by melting calcined alumina in an electric furnace. The properties of fused alumina are shown in Table VII.

Synthetic mullite is produced as follows: Aluminum hydroxide is mixed with "Gaerome clay" in a slurry state. Gaerome clay is mainly kaolinite and contains 2 to 5 mm diameter quartz. Water in this slurry is removed by filter-pressing. The filter cake is formed into granules by an Auger machine, dried by a band dryer, and fired in a rotary kiln.[10] The properties of synthetic mullite are shown in Table VIII.

When a sillimanite group mineral is heated, mullite is formed, liberating free SiO_2, which first becomes crystobalite and then is converted to glass above 1600°C. The amount of glass in various products measured by fluoric acid dissolution is shown in Fig. 6.[11]

Blast Furnace Refractories

In Japan, blast furnace refractories have been converted from chamotte bricks to high-alumina, carbon, or carbon-silicon carbide. Lining materials are carbon block for the hearth and carbon-silicon carbide

Table III. Properties of Sillimanite Group Raw Materials

	Sillimanite	Kyanite	Andalusite	
Brand Name		Georgia Kyanite	Macle	Pulsite
Location	Cape Pella South Africa	Georgia, USA	Transvaal South Africa	Transvaal South Africa
Chemical composition				
SiO_2	17.20	43.20	37.34	38.36
TiO_2	2.42	1.48	0.30	0.24
Al_2O_3	77.80	52.53	59.66	59.83
Fe_2O_3	0.94	1.63	1.11	0.60
CaO	0.05	0.12	0.10	0.04
MgO	0.07	0.04	0.12	0.32
Na_2O	0.05	0.05	0.07	0.06
K_2O	0.08	0.15	0.17	0.01
L.O.I.	1.40	0.80	0.52	0.64
Characteristics	Gray-black color, lump corundum-sillimanite	sand, under 35 mesh size	1–10 mm size, cubic	under 5 mm size, columnar

Table IV. Properties of Calcined Alumina*

Aluminas	Calcined Aluminas		Low-Soda Aluminas		High G.D. Alumina	Reactive Aluminas		High-Purity Aluminas	
Items/Sample No.	1	2	3	4	5	6	7	8	9
Chemical composition (%)									
Na_2O	0.3	0.3	0.04	0.02	0.03	0.03	0.03	0.005	0.001
SiO_2	0.01	0.01	0.04	0.05	0.02	0.04	0.02	0.010	0.010
Fe_2O_3	0.01	0.01	0.01	0.01	0.02	0.02	0.02	0.005	0.002
Al_2O_3	99.3	99.6	99.8	99.8	99.8	99.8	99.8	99.9	99.99
Crystal size (μm)	1	1~4	1~2	2~3	0.3~4	0.3	0.3~1.0	0.3	0.3
Average particle size (μm)	35~50	35~50	30~45	30~45	2.5	0.4	0.6	0.4	0.4
Average particle size (μm) After milling	0.5	3.2	1.5	2.3					
Green density† (g/cm^3)	1.90	2.37	2.28	2.33	2.60	2.25	2.37	2.25	2.22
Fired density‡ (g/cm^3)	3.72	3.20	3.80	3.54	3.72	3.91§	3.89§	3.90§	3.90§
Linear shrinkage (%)	20	10	16	13	11	17	15	17	17
Applications	Refractories Whitewares Abrasives		Electronic ceramics (plug. IC-substrate etc.) Wear-resistant parts		Refrac-tories	Electronic ceramics High-strength wear parts		Translucent alumina bodies Ceramic bits	

*Ref. 6.
†No additive. 300 kg/cm^2.
‡No additive, 1700°C–2h.
§No additive, 1600°C–2h.

Table V. Chemical Composition of Commercial ρ-Alumina*

Al_2O_3	94.5
SiO_2	0.02
Fe_2O_3	0.03
Na_2O	0.2
L.O.I.	5.2

*Ref. 6.

Table VI. Properties of Sintered Alumina

		A	B	C
Chemical composition (%)	SiO_2	0.12	0.09	0.12
	Al_2O_3	99.35	99.40	99.40
	Fe_2O_3	0.08	0.04	0.04
	CaO	0.10	0.04	0.01
	MgO	0.19	0.26	0.30
	Na_2O	0.19	0.26	0.30
	K_2O	0.01	0.01	0.01
Apparent density (g/cm^3)		3.82	3.82	3.73
Bulk density (g/cm^3)		3.63	3.69	3.51
Apparent porosity (%)		5.1	3.4	6.0

bricks for the lower shaft. High-alumina bricks are used only for the upper shaft and protection of the hearth carbon block. The properties of alumina bricks and high-alumina bricks are shown in Tables IX and X. Bricks for the stave cooler-type blast furnace require high thermal shock resistance, because those bricks are set-in simultaneously as molten metal is cast to form the stave cooler.

Table VII. Properties of Fused Alumina

		A	B	C
Chemical composition (%)	SiO_2	0.14	0.09	3.74
	Al_2O_3	99.41	99.46	95.93
	Fe_2O_3	0.05	0.07	0.04
	CaO	0.05	0.04	0.05
	MgO	0.01	0.02	0.01
	Na_2O	0.25	0.24	0.16
	K_2O	0.01		
True density (g/cm^3)		3.98	3.99	3.90
Apparent density (g/cm^3)		3.94		3.88
Bulk density (g/cm^3)		3.62		3.75
Apparent porosity (%)		8.0		3.3

Table VIII. Properties of Synthetic Mullite

Chemical composition (%)	SiO_2	27.27	22.32
	TiO_2	0.15	0.29
	Al_2O_3	70.61	76.22
	Fe_2O_3	0.86	0.33
	CaO	0.18	0.05
	MgO	0.16	0.06
	Na_2O	0.34	0.33
	K_2O	0.15	0.10
Apparent density (g/cm^3)		2.89	3.03
Bulk density (g/cm^3)		2.73	2.81
Apparent porosity (%)		5.6	7.2
Mineral detected by X-ray diffraction		Mullite	Mullite α-alumina

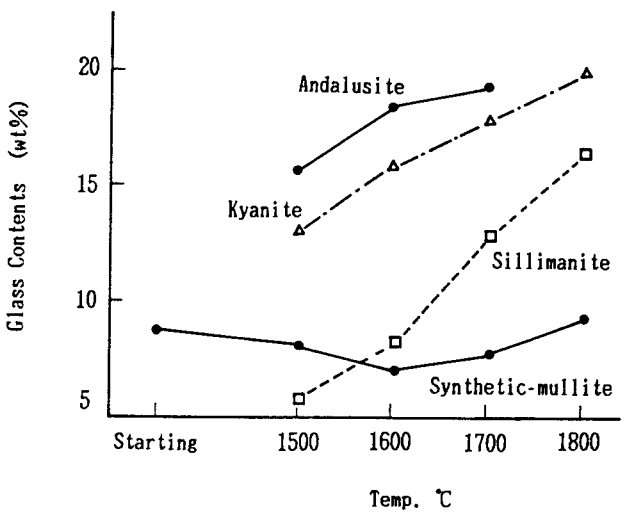

Fig. 6. Relation between glass amount and firing temperature of high alumina raw materials.[11]

Low-porosity and high-corrosion-resistant high-alumina bricks are used for protection of the hearth carbon block. An investigation on used bricks for protecting the hearth showed that pig iron penetrates in a networklike pattern from the hot face to a depth of 100 to 600 mm.

To minimize these occurrences, high-alumina bricks have been developed which have a smaller mean pore radius and fewer pores under 5 μm radius. Pig iron penetration into this type of brick is very small (5 kg/cm^2 pressure). The properties of high-alumina brick for protection of hearth carbon blocks are shown in Table XI.

Refractories for Hot Stoves

Along with high-pressure and high-temperature operation of the blast furnace, wind temperature has been increased from 800° to 1250°C and the dome temperature has now reached 1550°C. Because of such high-temperature operation, silica brick is used for the upper parts of checkers and domes in stoves. High-alumina brick is used under part of the silica brick. The properties of high-alumina bricks for stoves are shown in Table XII.

Trough Materials

Service conditions for troughs are becoming more severe, due to capacity enlargement and high-pressure, high-temperature operations of blast furnaces. To accommodate today's more severe service condition changes, trough materials are changing from mixtures of coke-clay-chamotte to alumina-silicon carbide-carbon. Installation methods are also being shifted from ramming to casting in order to improve the working environment and save labor.

Casting trough mixtures develop enough fluidity during installation by utilizing weak vibrations. To obtain a low-porosity cast body, mixtures are designed to be installed using the lowest possible water addition. Mixtures for casting consist primarily of alumina and silicon carbide. Small amounts of clay and silica flour are added to give the mixture fluidity when water is added.

Fused or sintered alumina are used for trough linings. As shown in Fig. 7, fused alumina shows better corrosion resistance than sintered alumina in an Al_2O_3-SiC-C ramming material.[12] Fused alumina is better due to surface texture differences between fused alumina and sintered alumina.[12]

The relation between slag corrosion wear and SiC content of an Al_2O_3-SiC-C trough lining is shown in Fig. 8.[13] The relation between wear at the slag-metal interface and SiC content is shown in Fig. 9. When the SiC content is >10%, slag corrosion resistance of the trough material improves, while wear at the slag/metal interface increases.

The properties of casting trough materials are shown in Table XIII.[14] Improved materials "B" and "C" use a fine Al_2O_3 powder, which permits use of less water. This results in a higher strength and lower porosity body than conventional type "A."[14]

Refractories for Torpedo Cars

Super-duty chamotte brick was formerly the main product used for torpedo car linings. Because reac tions such as desulfurization by CaC_2 or CaO blowing and desiliconization by addition of Fe oxide or O_2 were carried out in torpedo cars with increasing frequency, lining life became insufficient.

Table IX. Properties of Alumina Bricks for Blast Furnaces

		A	B
Refractoriness (SK)		40	40
Apparent porosity (%)		15.0	13.0
Bulk density (g/cm^2)		3.30	3.13
Crushing strength (kg/cm^2)		900	1500
Thermal expansion at 1000°C (%)		0.73	0.73
Permanent linear change at 1500°C (%)		0	0
Refractoriness under load (2 kg/cm^2 (T_2 °C))		≥1700	≥1700
Chemical composition (%)	Al_2O_3	99.3	92.0
	SiO_2	0.15	6.0
	Fe_2O_3	0.15	0.26
Characteristics		Spalling resistance Alkali resistance Corrosion resistance	Corrosion resistance Low permeability Alkali resistance
Major application		Stave cooler	Lower shaft

Table X. Properties of High-Alumina Bricks for Blast Furnace

		A-1	A-2	B-1	B-2
Refractoriness (SK)		37	38	38	38
Apparent porosity (%)		12.3	13.5	12.8	13.2
Bulk density (g/cm^2)		2.80	2.75	2.55	2.55
Crushing strength (kg/cm^2)		1000	740	1150	1000
Thermal expansion at 1000°C (%)		0.60	0.60	0.60	0.60
Permanent linear change at 1500°C (%)		+0.1	−0.1	0	+0.1
Refractoriness under load (2 kg/cm^2 (T_2 °C))		1620	1630	1650	1650
Chemical composition (%)	Al_2O_3	64.0	64.0	63.0	63.0
	SiO_2	32.05	32.0	33.0	33.0
	Fe_2O_3	1.0	1.0	1.0	1.0
Characteristics		Spalling resistance Erosion resistance	Corrosion resistance Spalling resistance	Corrosion resistance Low porosity	Corrosion resistance Low porosity
Major application		Upper shaft	Large brick for tap hole	Hearth	Large brick for hearth

High-alumina brick was tried, but its durability was unsatisfactory. Finally, resin-bonded unfired Al_2O_3-SiC-C brick was tested, found satisfactory, and is now commonly used for torpedo car linings. Alumina-chromite brick is used in some steel plants for torpedo car linings. High-alumina bricks are being used in the portion where there is no slag or metal contact with brick, such as the roof and metal receiving mouth. The properties of high-alumina brick for torpedo cars are shown in Table XIV.

The relation between corrosion resistance and Al_2O_3 content in Al_2O_3-SiC-C brick with different amounts of SiC is shown in Fig. 10.[15] Carbon is effective in preventing slag penetration and improving thermal shock resistance. Silicon carbide enhances oxidation resistance. The relation between SiC content and oxidation resistance is shown in Fig. 11.[15]

Alumina raw materials for torpedo refractories include fused alumina, sintered alumina, bauxite, and sillimanite, based on the price of brick and its performance in service. The properties of Al_2O_3-SiC-C bricks for lining torpedo cars are shown in Table XV.

Alumina-chromite brick is a burned product consisting of alumina raw material and fine-grained chromite. This brick has excellent corrosion resistance to high-Fe oxide containing desiliconized slag. One defect of this brick is its tendency to cause structural spalling. The properties of alumina-chromite brick are shown in Table XVI.

Table XI. Properties of High-Alumina Bricks for Protection of Blast Furnace Hearth

		Improved		Conventional
		S1	S2	S
Apparent density (g/cm^3)		3.06	3.04	2.96
Bulk density (g/cm^3)		2.66	2.65	2.58
Apparent porosity (%)		13.0	13.1	12.9
Crushing strength (kg/cm^2)		1300	1400	804
Modulus of rupture (kg/cm^2)		220	240	175
Thermal conductivity (kcal/mh • °C)*		1.8	2.4	2.1
Modulus of elasticity (kg/cm^2)		4.2	6.8	4.8
Reheating shrinkage†		0.16	−0.22	−0.23
Wear by pig iron (mm)‡		0.5	0.4	1.2
Wear by slag (mm)‡		2.8	2.7	4.0
Mean pore radius (μm)		0.79	0.97	1.76
Amount ratio of pore over 5 μm (%)		10	5	20
Permeability of pig iron§		Very few	Very few	Penetrate
Refractoriness under load	T_1	1675	1560	1555
	T_2	1730	1690	1615
	T_3	1750+	1750+	1715
Chemical composition (%)	SiO_2	26.13	25.67	33.60
	Al_2O_3	72.95	71.94	63.24
	Fe_2O_3	0.64	0.92	0.98
Thermal shock resistance	Cycle cracks appear	2~3	1	1~2
	Cycle peals off	20+	5~11	9~15

*At 300°C measured by wire method.
†1550°C × 200 h.
‡1550°C × 60 min dip in pig iron and blast furnace slag.
§1550°C × 60 min keep and N_2 gas pressure (5 kg/cm^2).

Table XII. Properties of High-Alumina Bricks for Hot Stoves

	A	B	C	D	E	F	G
Refractoriness (SK)	39	39	38	38	38	37	35
Apparent porosity (%)	18.0	19.0	16.0	20.0	21.0	21.0	21.0
Bulk density (g/cm^3)	2.75	2.80	2.60	2.55	2.50	2.40	2.40
Crushing strength (kg/cm^2)	800	850	800	700	600	600	600
Thermal expansion at 1000°C (%)	0.55	0.55	0.55	0.55	0.58	0.50	0.58
Permanent linear change (1500°C × 2 h (%))	0	0	0	0	0	−0.1	−0.1
Refractories under load (2 kg/cm^2 (T_2 °C))	≥1650	≥1650	≥1610	1640	1620	1590	1520
Creep deformation (%)	0.2	0.2	0	0.2	0.2	0.1	0.2
Temperature (°C) × 50 h	1550	1550	1450	1400	1350	1300	1270
Chemical composition (%)							
SiO_2	15.0	14.5	27.0	27.0	29.0	30.0	42.0
Al_2O_3	83.0	84.0	70.0	71.0	68.0	56.0	55.0
Application	Wall dome checker	Wall checker	Wall checker	Wall checker	Wall checker	Wall checker	Wall checker

Hot-Steel Ladle Linings

There are two trends in the use of ladle lining materials. One is the application of monolithic linings to minimize refractory consumption and installation cost. Another is an increasing reliance on high-grade refractory bricks to minimize lining failures occurring with the widespread use of ladle refining processes.

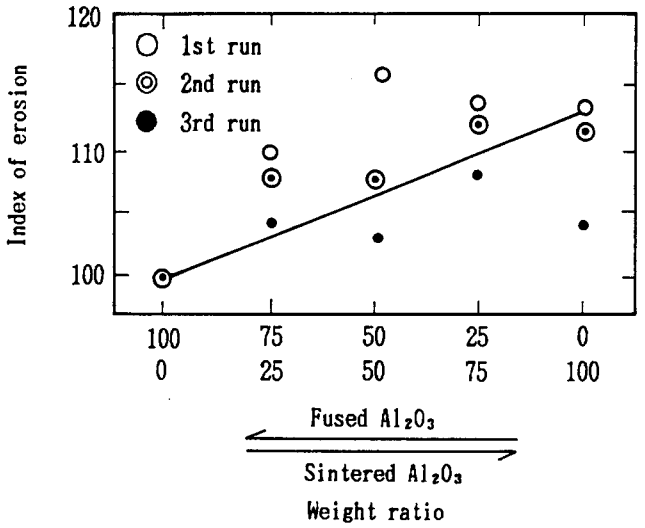

Fig. 7. Erosion test result of trough ramming mixes containing sintered and/or fused alumina.[12]

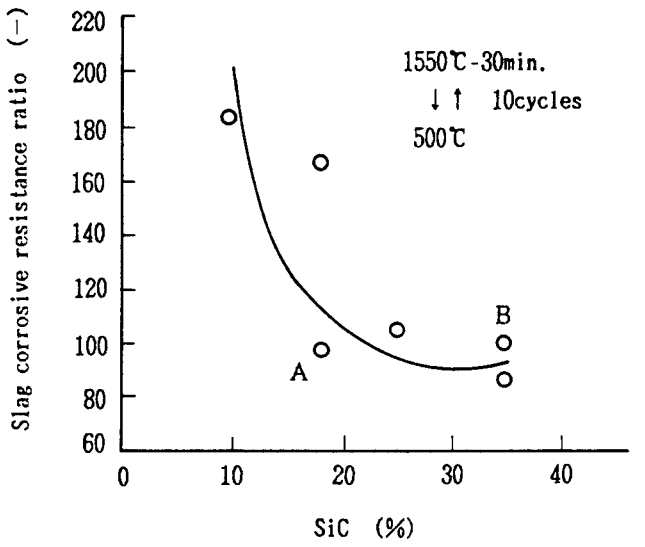

Fig. 8. Effect of SiC content on slag corrosion resistance of trough materials.[13]

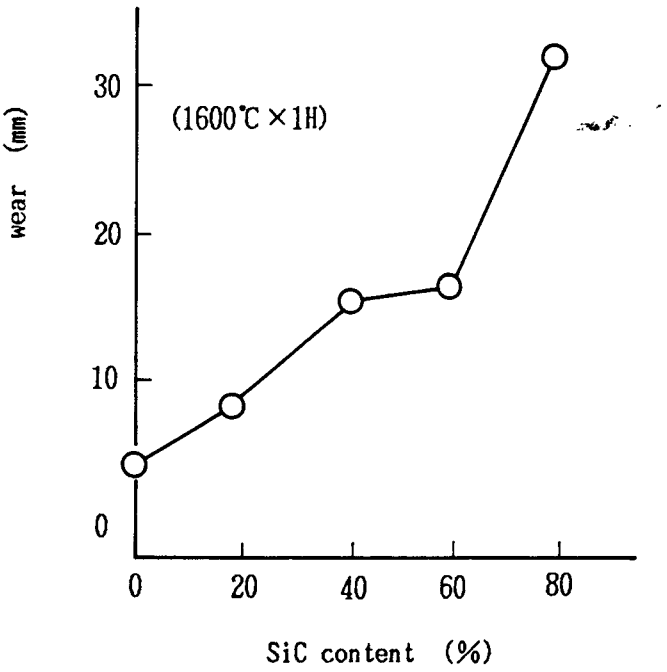

Fig. 9. Relation between SiC content of Al_2O_3-SiC-C trough materials and corrosion slag-metal interface.

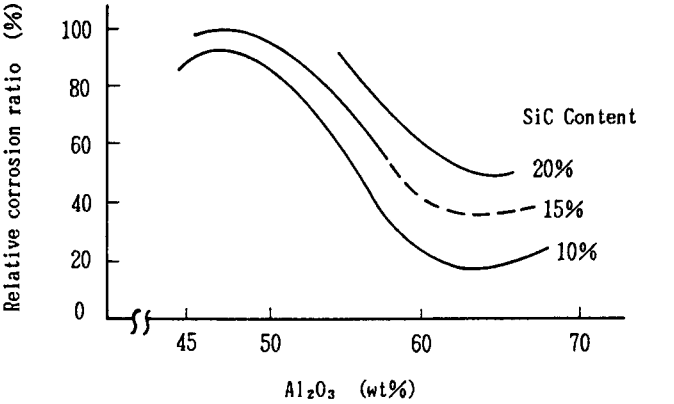

Determined by Rotary Corrosion Method at 1500℃ for 2 Hours Using Mixture of Desulfurization Slag (30%) and Pig Iron (70%)

Fig. 10. Relationship between corrosion resistance and alumina content in alumina-SiC-C bricks with different amounts of SiC.[15]

Formerly, highly siliceous Al_2O_3-SiO_2 or zircon bricks were the most common lining materials for hot-steel ladles, but now these materials are installed as monolithic linings. A defect of highly siliceous or zircon products is their high silica content; silica acts as a source of oxygen or nonmetallic inclusion in steel, causing problems for the production of some kinds of steel.

High-alumina monolithic materials are now being developed to overcome these problems and are approaching commercial use. These products can be installed by slinger, ramming, and casting methods. Casting is the preferred method because of the ease of installation and the possibility of obtaining low-porosity bodies which can be cast with a low water content. The properties of high-alumina casting material are shown in Table XVII. Life of this material on ladles is about 80 heats in 250 tons.

As requirements for ladle lining materials became more demanding, highly siliceous brick gave way first to zircon bricks, then high-alumina brick. Now basic bricks are often used because of severe service conditions such as higher hot-steel temperatures and longer steel-retention times. These adverse conditions are caused by widespread use of vacuum treatment and continuous casting, demands to minimize oxygen and

Table XIII. Properties of Casting Materials for Troughs*

		Conventional Type	Dense and High-Strength Types	
		A	B	C
Chemical composition (%)	Al_2O_3	72.0	80.0	80.5
	SiO_2	5.5	1.5	1.0
	SiC	15.0	15.0	15
	C	1.8	2.0	2.0
	CaO			0.7
Grain size (%)	Max	8	8	8
	>1 mm	57	56	56
	<0.074 mm	26	28	28
Linear change (%)	110°C × 20 h	−0.09	−0.06	0.00
	1400°C × 2 h	+0.02	−0.06	0.00
Apparent porosity (%)	110°C × 20 h	21.5	12.7	11.7
	1400°C × 2 h	24.5	17.8	14.2
Bulk density (g/cm^2)	110°C × 20 h	2.64	3.03	3.06
	1400°C × 2 h	2.56	2.98	3.02
Hot modulus of rupture	at 800°C	46	110	100
	at 1400°C	15	35	43
Additional water (%)		7.0	4.0	4.3

*Ref. 14.

Table XIV. Properties of High-Alumina Bricks for Torpedo Cars

Refractoriness (SK)		38
Apparent porosity (%)		18.0
Bulk density (g/cm^2)		2.55
Crushing strength (kg/cm^2)		1020
Thermal expansion at 1000°C (%)		0.60
Refractoriness under load (2 kg/cm^2 (T_2 °C))		1690
Modulus of rupture (kg/cm^2)	at room temp.	253
	at 1500°C	51
Chemical composition (%)	Al_2O_3	71
	SiO_2	26

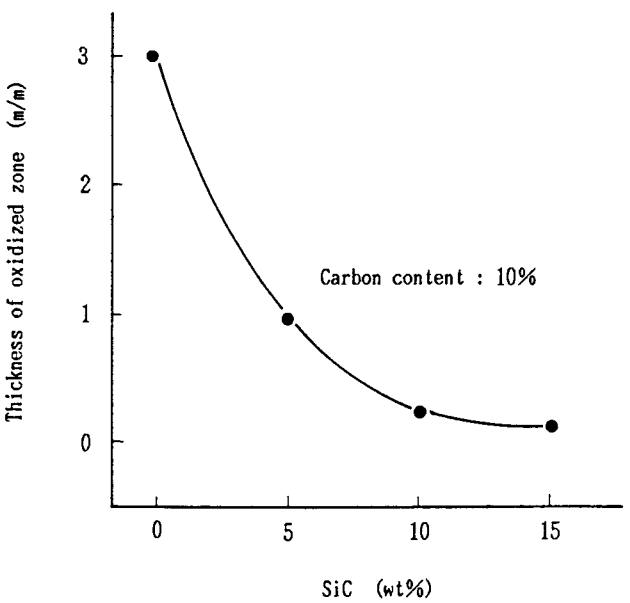

Fig. 11. Relationship between SiC content and oxidation resistance in high alumina-SiC-C brick, after heating at 1400°C for 2 h in air.[15]

nonmetallic inclusions in steel, and extensive use of various ladle refining processes.

Magnesia-carbon brick for the slag line and high-alumina brick for other areas are generally used for ladles in electric arc furnace plants. Phosphate-bonded unburned and burned bricks are used as high-alumina bricks. The properties of high-alumina bricks and VAD ladles are shown in Table XVIII.[16] In one case of a VAD ladle, lining life was 78 to 86 heats for brick "A", 66 to 72 heats for brick "B", and 86 heats for brick "C".

Slide-Gate Plates

Previously, tar-impregnated, burned high-alumina materials were used as slide-gate plates. The problem with this material was the generation of fume, which contaminated air in the steel plant. Alumina-carbon material was developed to solve the pollution problem. This material has excellent durability, so it is mainly used nowadays.

To achieve a balance of corrosion resistance and thermal shock resistance, the carbon content of slide-gate plates today is usually about 10%. The effect of

Table XV. Properties of Al_2O_3-SiC-C Bricks for Torpedo Cars

		A	B
Apparent density		3.17	3.14
Bulk density		2.89	3.00
Apparent porosity (%)		8.9	4.3
Crushing strength (kg/cm^2)		460	368
Modulus of rupture at 1400°C (kg/cm^2)		85	200
Chemical composition (%)	SiO_2	5	4
	Al_2O_3	69	65
	SiC	9	9
	C	13	17

Table XVI. Properties of Alumina-Chromite Bricks

Refractoriness (SK)		39
Apparent porosity (%)		16.0
Bulk density (g/cm^2)		3.10
Crushing strength (kg/cm^2)		1000
Thermal expansion at 1000°C (%)		0.60
Refractoriness under load (2 kg/cm^2 (T_2 °C))		1600
Modulus of rupture (kg/cm^2)	at room temp.	110
	at 1500°C	40
Chemical composition (%)	SiO_2	12
	Al_2O_3	63
	MgO	7
	Cr_2O_3	9

Table XVII. Properties of High-Alumina Casting Material for Steel Ladles

Chemical composition (%)	Al_2O_3	76.7
	SiO_2	9.8
	TiO_2	2.5
	MgO	6.9
Water added (wt%)		6.4
Modulus of rupture (kg/cm^2)	1200°C × 2 h	132
	1500°C × 2 h	158
Linear shrinkage (%)	1200°C × 2 h	−0.20
	1500°C × 2 h	−0.38
Bulk density (kg/cm^2)	after dry	2.85
	1200°C × 2 h	2.82
	1500°C × 2 h	2.86
Porosity (%)	after dry	17.8
	1200°C × 2 h	21.0
	1500°C × 2 h	20.4

carbon content on corrosion and thermal shock resistance is shown in Fig. 12. The properties of alumina-carbon slide-gate plates are shown in Table XIX in comparison with burned alumina material.[17] For commercial use, materials "B-C" and "C-B" showed good results; no crack occurred at the corner of the hole. Material "B-C" is alumina-carbon which has been tar-impregnated and coked, while material "C-B" is burned alumina which has been tar-impregnated and baked. Because of cracks at the corner of the hole and depreciation of the sliding surface, materials "A-C" and "B-C" show bad results.

A quick, simple thermal shock test was used to estimate thermal shock resistance of the above-mentioned materials. Test pieces are cut from plates and tested by a spot spall method in which the specimens are heated intensely in a small area. Plates showing bad practical use results develop cracks in 15 seconds after heating.

Modulus of elasticity at high temperatures, measured by an ultrasonic method, is shown in Fig. 13. Material "A-C", which is alumina carbon but inferior in thermal shock resistance, shows a remarkable increase in modulus of elasticity over 1000°C. Thermal shock fracture resistance parameter R can be calculated by the equation:

$$R = S(1 - \mu)/E \cdot \alpha \quad (1)$$

where S is strength, E the modulus of elasticity, and α the thermal expansion coefficient. Parameter R for each plate in Table XIX at high temperature is shown in Fig. 14. Alumina-carbon materials show excellent thermal shock fracture resistance. Comparing "B-C" (good) in the commercial use result with "A-C" (bad), R of the latter shows a great change.

Corrosion wear of the slide-gate plate used in continuous casting is a problem when calcium is added to steel; Ca in steel reduces SiO_2 in the plates to Si and Ca converts to CaO. Then CaO reacts with Al_2O_3 and SiO_2 in the plates and forms calcium aluminate ($CaO \cdot Al_2O_3$) and gehlenite ($2CaO \cdot Al_2O_3 \cdot SiO_2$)

$$2(Ca) + SiO_2 \rightarrow 2CaO + Si \quad (2)$$

$$nCaO + mAl_2O_3 \rightarrow nCaO \cdot mAl_2O_3 \quad (3)$$

$$2CaO + SiO_2 + Al_2O_3 \rightarrow 2CaO \cdot SiO_2 \cdot Al_2O_3 \quad (4)$$

Similar problems occur in high-manganese steel and high oxygen content steel. In the case of high-manganese steel:

$$\begin{aligned} 2(Mn) + SiO_2 &\rightarrow 2MnO + (Si) \\ MnO + SiO_2 &\rightarrow MnO \cdot SiO_2 \end{aligned} \quad (5)$$

In the case of high-oxygen steel:

$$\begin{aligned} Fe + (O) &\rightarrow FeO \\ FeO + SiO_2 &\rightarrow 2FeO \cdot SiO_2 \end{aligned} \quad (7)$$

Alumina-carbon materials contain SiO_2 because low thermal expansion mullite is added to the raw mixture for producing plates in order to lower the thermal expansion and to improve thermal shock resistance.

This problem is solved by using ZrO_2 instead of SiO_2.[18] Properties of plates with added alumina-zirconia raw material containing 26% ZrO_2 are shown

Table XVIII. Properties of High-Alumina Bricks for VAD Ladles*

Feature of bricks		A Phosphate-Bonded Unburned	B Burned	C Burned
Chemical composition (%)	SiO_2	9.3	10.3	15.7
	Al_2O_3	84.9	85.2	83.0
Apparent density (g/cm^2)		3.54	3.58	3.35
Bulk density (g/cm^2)		3.00	2.90	2.90
Apparent porosity (%)		15.2	19.0	13.4
Crushing strength (kg/cm^2)		720	950	1150
Modulus of rupture (kg/cm^2)	at room temp.	79	147	144
	at 1400°C	71	41	85
Thermal expansion (%)	at 1000°C	0.76	0.62	0.48
	at 1500°C	1.90	1.11	0.87
Permanent linear change 1500°C × 3 h (%)		+0.73	+0.88	+0.04
Modulus of elasticity ($\times 10^4$ kg/cm^2)		45.3	31.5	28.8

*Ref. 16.

in Table XX. The results of a crucible corrosion test are shown in Fig. 15.

The results of thermal shock resistance estimated by Nakayama's radiation and rapid cooling method,[19] in which modulus of rupture of test pieces are measured after rapid cooling over a given temperature difference, are shown in Fig. 16. Plates containing ZrO_2 show better corrosion and thermal shock resistance.

Submerged Nozzle

Fused silica was used initially as a submerged nozzle material but, because of corrosive wear by high-manganese steel and insufficient durability in the many heat uses in continuous casting, alumina-carbon nozzles are now the most commonly used.

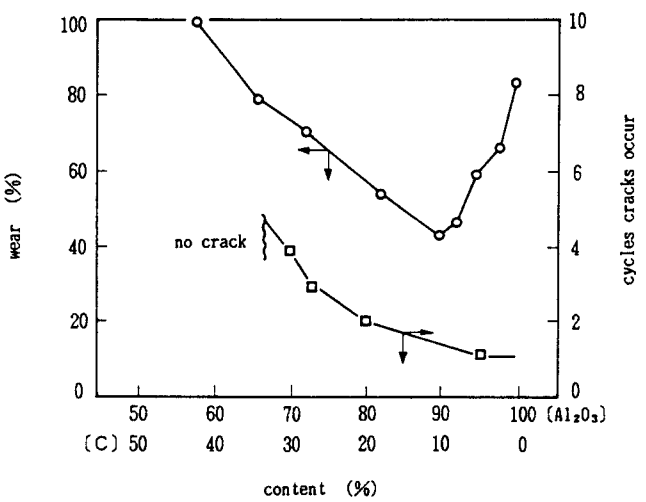

Fig. 12. The effect of carbon content on corrosion and thermal shock resistance of alumina carbon slide gate plate.

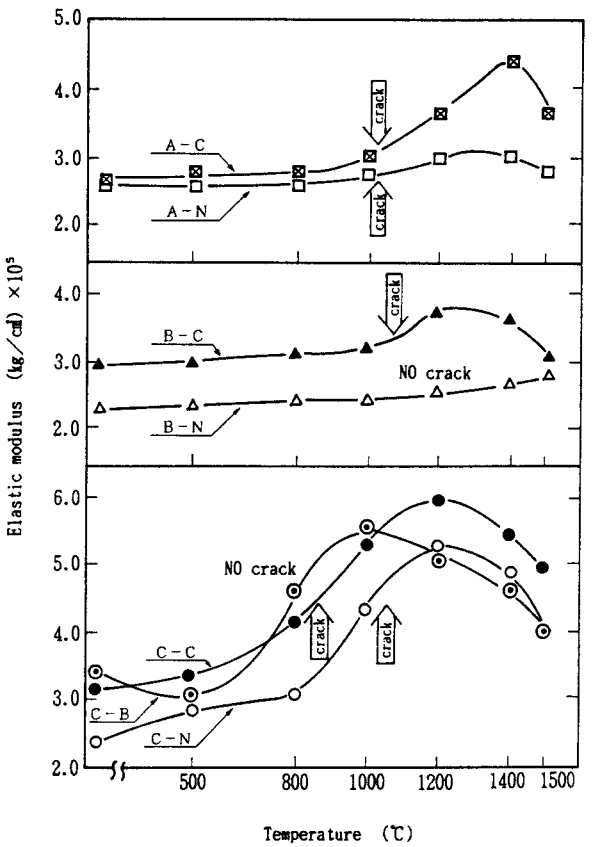

Fig. 13. Relation between elastic modulus of sliding gate plate shown in Table XIX and temperature.[17]

Table XIX. Properties of Alumina and Alumina-Carbon Slide-Gate Plates*

		A		B		C		
		A-N	A-C	B-N	B-C	C-N	C-B	C-C
Apparent density (g/cm^3)		3.20	3.15	3.21	3.10	3.55	3.23	3.54
Bulk density (g/cm^3)		2.68	2.70	2.65	2.74	2.99	3.13	3.09
Apparent porosity (%)		16.5	14.4	17.5	11.7	15.6	3.4	12.1
Crushing strength (kg/cm^2)		1050	1200	1050	1300	1450	2000	1800
Chemical composition (%)	Al_2O_3	74.3		76.0		85.1		
	SiO_2	10.0		9.7		8.3		
	C	9.7	11.5	9.4	12.2		2.9	1.8
	SiC	5.5		4.4				
	Cr_2O_3					3.0		
Type		Al_2O_3-C		Al_2O_3-C		Al_2O_3		
Heat treatment and tar impregnation		None	Coking after tar impregnation	None	Coking after tar impregnation	None	Baking after tar impregnation	Coking after tar impregnation

*Ref. 17.

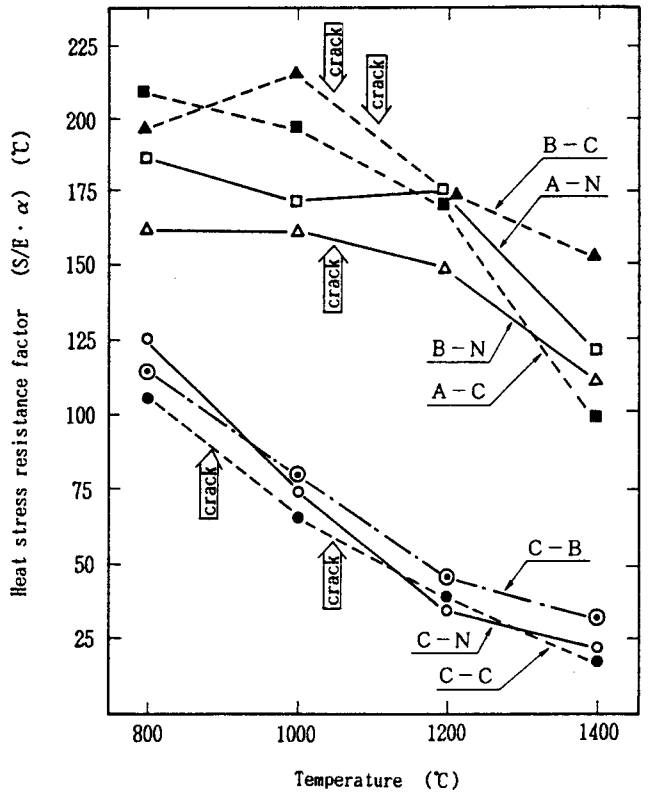

Fig. 14. Relation between thermal stress resistance factor "R" of sliding gate plate shown in Table XIX and temperature.

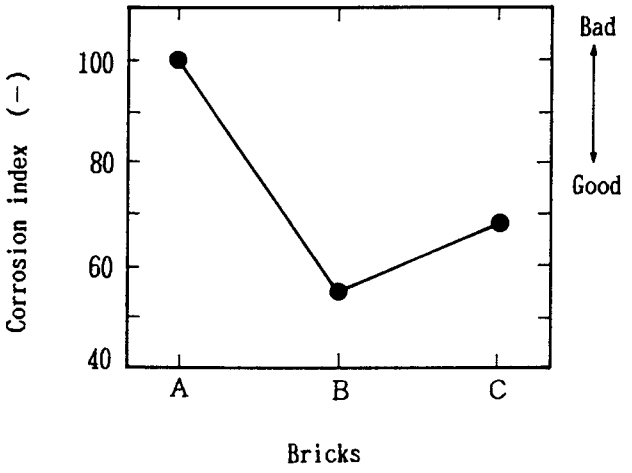

Fig. 15. Result of corrosion test of sliding gate plates shown in Table XX by calcium metal.[18]

The carbon content of alumina-carbon nozzles is high (20 to 40%) in order to provide high thermal shock resistance. In some cases, fused silica is added to a mixture of alumina and carbon to achieve high thermal shock resistance. These compositions generally have lower corrosion resistance than the alumina-carbon body. One approach to solving this problem is improvement of fracture resistance by controlling the carbon bond structure.

Generally, strength and fracture energy depend on the carbon structure remaining after carbonization of the organic binder. A mosaic structure is said to be better than the glassy or flow structure.

Pitch converts to flow structure carbon during carbonization, while phenol resin becomes glassy. When pitch and phenol resin are mixed, a fine mosaic structure appears in the interface. The amounts of both structures can be changed by varying the mixing ratio of pitch and resin, as shown in Fig. 17.[17] The fracture energy was measured for test pieces made by mixing alumina, 30% graphite, pitch, and resin, molding, and firing in a reducing atmosphere. The highest fracture energy is attained when the ratio of fine mosaic structure is at a maximum (Fig. 18[20]).

One of the big problems with nozzles is clogging caused by deposition of alumina in the nozzle pores.

Table XX. Properties of Slide-Gate Plates Containing Alumina-Zirconia Raw Material

		A	B	C
Main grain		Mullite Alumina	Alumina-zirconia Alumina	Alumina-zirconia Alumina
Chemical composition (%)	Al_2O_3	73.5	71.4	71.7
	SiO_2	9.5		
	ZrO_2		9.5	7.6
	SiC	1.5	1.5	5.0
	C	12.5	12.1	12.0
Apparent specific gravity		3.14	3.47	3.36
Bulk density (g/cm^2)		2.18	3.12	3.08
Apparent porosity (%)		10.5	9.9	9.0
Cold crushing strength (kg/cm^2)		1264	1480	1680
Modulus of rupture (kg/cm^2)	at room temp.	209	201	260
	at 1400°C	189	188	200
Thermal expansion (%) at 1500°C		+0.95	+1.10	+1.12

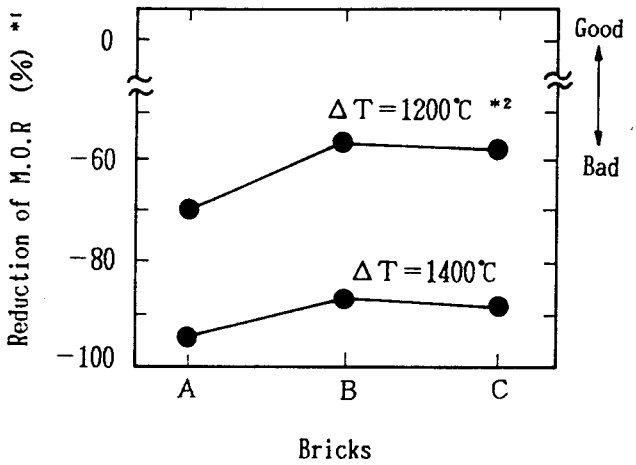

$$*1 \quad \frac{S_2 - S_1}{S_2} \times 100$$

S_1 : M.O.R at room temperature

S_2 : M.O.R at room temperature after thermal shok

$*2 \quad \Delta T = T_2 - T_1$

T_1 : Room temperature

T_2 : Testing temperature

Fig. 16. Reduction of modulus of rupture of sliding gate plates shown in Table XX after thermal shock.[18]

This not only reduces the number of continuous casting heats but also decreases the quality of steel due to large nonmetallic inclusions. To overcome this problem, one method is blowing argon gas from a porous plug set in the side wall of the nozzle (Fig. 19). Another method is blowing argon gas in from the surface from a slit in the side wall (Fig. 20).

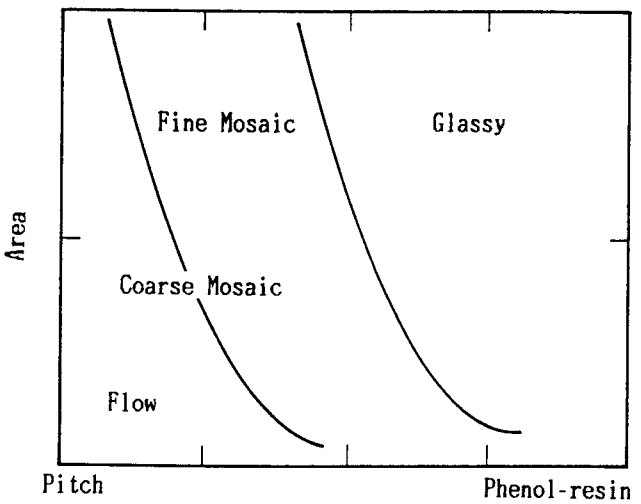

Fig. 17. Ratio of fine mosaic area in relation to the mixing ratio of pitch and phenol resin.[20]

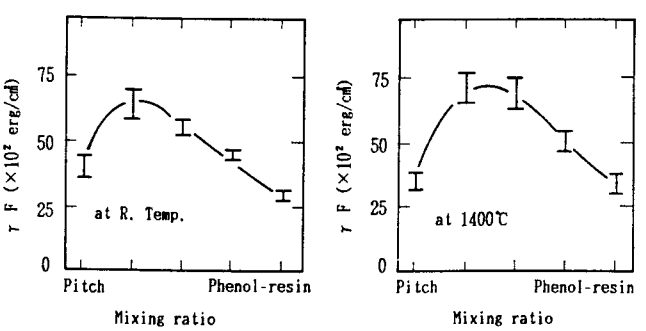

Fig. 18. Relation between fracture energy of alumina-carbon refractories and pitch phenol resin ratio by a work fracture method.[20]

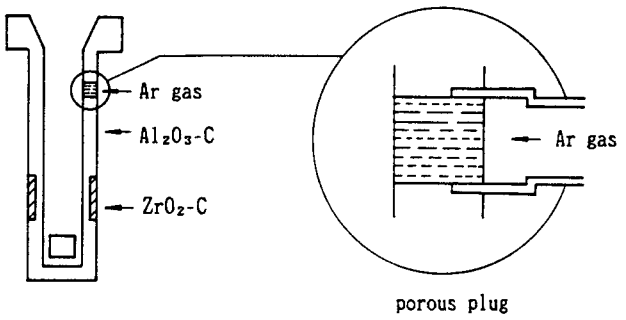

Fig. 19. Argon gas injection method of submerged nozzle by porous plug.[21]

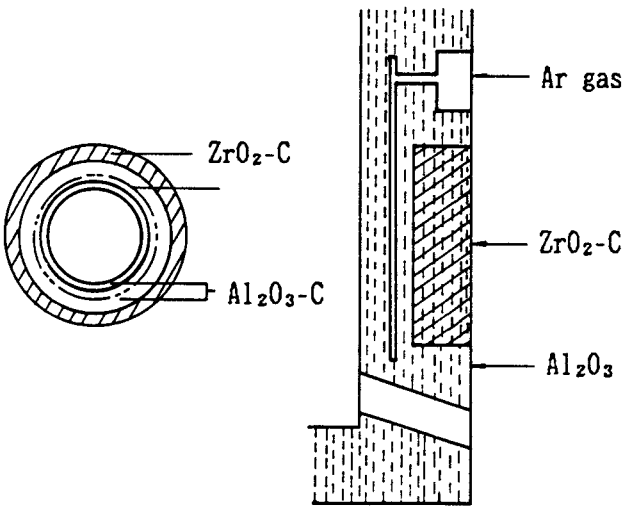

Fig. 20. Argon gas blowing method through slit of submerged nozzle.[22]

Porous Plug

Porous plugs are used to promote the uniformity of the hot-steel temperature and uniform distribution of additives. Porous plugs are practically indispensable for ladle refining.

Porous plugs are manufactured by mixing graded alumina grains with less clay than for the usual brick mixture. This composition is pressed, dried, and burned. The permeability of porous plugs is a function of pore size and porosity of the structure. Increasing pore size and porosity increases permeability. The shape of the alumina grain also affects permeability. Irregularly shaped sintered-alumina grains tend to decrease permeability, while spherical alumina grains increase it.

There is a relation between porosity, pore size, and permeability:

$$\text{(Permeability)} = \text{Constant} \times \text{(Porosity)} \times \text{(Pore size)}^2$$

Experimental data on porous plugs are shown in Fig. 21.[21]

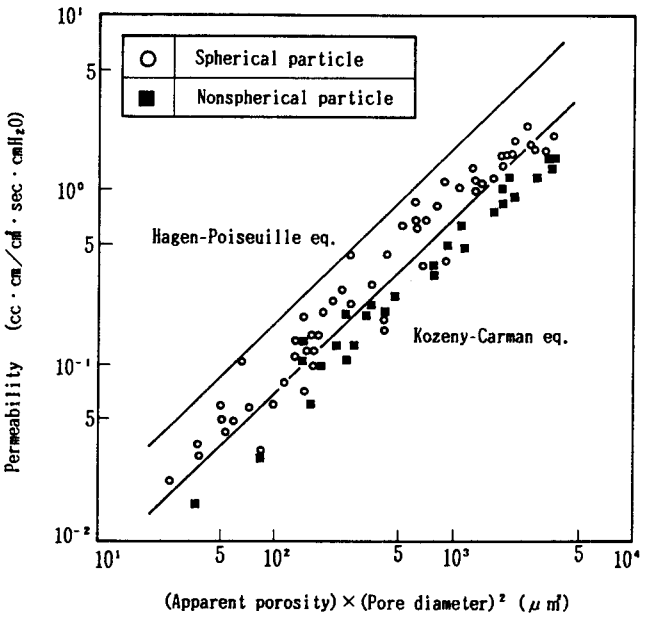

Fig. 21. Influence of apparent porosity and pore diameter on permeability of porous bodies manufactured from spherical on nonspherical particles.[21]

References

[1]Report of Japan Refractories Association, No. 434, 1986.

[2]N. Nameishi, A. Inoue, and T. Kitai, *Taikabutsu*, **31** [1] 48–51 (1979).

[3]Technical Association of Refractories Japan; "Taikabutsu to Sono O-yo".

[4]S. Yoshino, H. Kyoden, K. Ichikawa, and H. Iwado, *Taikabutsu*, **35** [11] 641–51 (1983).

[5]S. Nabeshima and K. Yamada, *Taikabutsu*, **33** [11] 633–36 (1981).

[6]Y. Hongo, *Taikabutsu*, **31** [12] 647–53 (1979).

[7]H. Abe, *Taikabutsu*, **28** [9] 420-21 (1976).

[8]Y. Maeda and K. Tabuchi, *Taikabutsu*, **28** [9] 409–13 (1976).

[9]A. Matsumoto, K. Takaya, and K. Ichikawa, *Taikabutsu*, **28** [9] 414–19 (1976).

[10]Y. Hirata, *Taikabutsu*, **19** [1] 2–4 (1976).

[11]N. Yoshino, K. Ichikawa, and K. Iwase, *Taikabutsu*, **34** [5] 278–82 (1982).

[12]S. Kamei, T. Hosaka, K. Takahasi, and M. Nisimura, *Taikabutsu*, **32** [1] 29–33 (1980).

[13]S. Yoshino and Y. Hamazaki, *Taikabutsu*, **33** [8] 450–53 (1981).

[14]T. Ishibasi, K. Furukawa, K. Suguyama, and N. Yamada, *Taikabutsu*, **36** [8] 467–72 (1984).

[15]N. Nameishi, T. Ishibasi, and T. Kitai, *Taikabutsu Overseas*, **2** [1] 90–97(1982).

[16]K. Kawakami, T. Tanabe, K. Hiragushi, H. Shikano, and M. Hori, *Taikabutsu*, **38** [3] 191–95 (1986).

[17]N. Nameishi, I. Kinosita, M. Goto, and T. Suzuki, *Taikabutsu*, **30** [11] 647–51 (1984).

[18]T. Ishibasi, S. Uto, and M. Goto, *Taikabutsu*, **36** [5] 300–304 (1984).

[19]J. Nakayama, *Ceramics*, **12** [2] 150–55 (1977).

[20]T. Ishibasi, H. Yanagi, and M. Sakaguchi, *Taikabutsu*, **35** [9] 526–29 (1983).

[21]H. Iso, H. Nagai, K. Okawa, and A. Tsuchinari, *Taikabutsu*, **37** [1] 50–56 (1985).

Use of High-Alumina Refractories in the U.S. Steel Industry

D. H. Hubble
U.S. Steel Technical Center
Monroeville, PA 15146

The use of high-alumina refractories in the domestic steel industry is increasing significantly with changes in iron and steel processing such as semicontinuous tapping of blast furnaces; treatment of hot metal before steelmaking; clean-steel practices, including ladle arc reheating and degassing; and the continued conversion to high-quality continuous casting. Several related developments in the refractory industry have also accelerated the use of high-alumina refractories, including the development of oxide-carbon refractories with greatly improved resistance to thermal shock and the development of thixotropic monolithic materials which can be installed rapidly over worn refractory surfaces. High-alumina refractories are now used in almost all phases of the iron, steelmaking, and casting processes in areas where they can technically and economically compete with a variety of other refractory materials (fireclay or other lower-alumina products, basic materials such as magnesite and dolomite, and more expensive materials such as silicon carbide and zirconia). This chapter reviews the use of the various high-alumina materials by process and projects the future directions for use of high-alumina materials in the steel industry.

This chapter reviews the use of alumina-bearing refractories in the U.S. steel industry, including those entirely and partly made from tabular or fused alumina, refractory bauxite, spinel or synthetic mullite, and also those containing some other alumina forms such as calcium aluminate cement or activated aluminas. Most of the various forms of refractories containing alumina will also be described including brick; shapes including tubes, lances, and plates; and monolithic materials installed by casting, vibration, or gunning.

Following an initial generic description of the various factors which are important in the refractory behavior in any steel-plant application, individual applications of high-alumina refractories (HAR) are reviewed by iron and steelmaking process. This review highlights the particular refractory properties important in the specific process, the types of refractories now used and likely to be used in the future, and comments on refractory life and consumption.

Properties Important to Steel-Plant Refractory Behavior

The following properties are required in any steel-plant application to provide safe and cost-effective operation.

Resistance to Thermal Shock and Temperature Gradients and/or Cyclic Temperatures

All steel-plant refractories must withstand some degree of thermal shock (rapid heating or cooling, temperature gradients during use, and/or cyclic temperature behavior from periodic operations). These conditions range widely, as illustrated in Table I for several environments. As shown, the refractories may experience thermal damage due to initial exposure to iron or steel without preheat, cycles during operations, inherent severe gradients on small thicknesses or cross sections, or repeated cooling to ambient conditions.

Table I. Typical Thermal Damage Factors on Steel-Plant Refractories

Application	Typical Refractory Life	Thermal Damage Factors
Blast-furnace lining	Years (3–10)	Slow initial heat up. Severe cycling during unstable operating periods. Occasional cooling to ambient with restarts.
Steel ladle linings, hot-metal ladle linings	Hours (40–1500)	Slow initial heat up with moderate initial shock. Thermal cycling during use. May involve several coolings to ambient to repair or replace components.
Injection lances	Minutes (20–1000)	Severe initial shock. Cooling to ambient between uses.
Slide-gate plates	Minutes (60–240)	Severe initial shock and gradients during use.
Casting shrouds	Minutes (40–500)	Varying degrees of shock on initial use. Very severe gradients during use on thin-wall sections.

Most steel-plant refractories utilize selective grain sizings and unique manufacturing techniques to provide a controlled porosity to improve resistance to thermal damage. Fully dense or fine-grained classic ceramic products do not normally have sufficient resistance to thermal shock for steel-plant use. A variety of other techniques are also used to promote resistance to thermal shock, including controlled heterogeneous microstructures such as oxide-carbon combinations.

Resistance to Metal and Slag Erosion or Corrosion

Most steel-plant refractories must also resist erosion and corrosion by moving metal and slag during iron or steelmaking proper, post- /or preliquid metal treatments, casting to a final shape, or simple transport of the liquid products between process stages. Erosion occurring during violent process reactions, during less-violent stirring or injection, or during liquid transfer are generally resisted by increasing the hot strength of the refractory material while maintaining some degree of its resistance to thermal shock. Hot strength in turn is controlled by final microstructure as developed by the compositions, particle sizings, placement methods (in plant or on use site), and heat treatments used before refractory use.

Slag corrosion must always be considered in the selection of most steel-plant refractories and classic oxide phase diagrams can give an initial broad indication regarding the usefulness of a particular refractory with acid, neutral, or basic slags. In recent years, however, the combination of oxide and nonoxide materials in refractories has become increasingly commonplace.[1,2] Figure 1 illustrates the combination of classic oxide materials with nonoxide materials such as graphite or SiC. The extent of usage of such materials will be apparent in later discussions of alumina-bearing steel-plant refractory materials.

The use of such oxide-nonoxide combinations can appreciably alter the behavior of refractories, essentially by permitting the refractory to restrict the influence of corrosive liquids to the immediate refractory hot face. This is illustrated in Fig. 2, which simplifies the behavior of various refractories as soft, wet, or dry. Classic soft refractories (silica, zircon) soften at operating temperatures and the resulting high-viscosity liquids are actually desirable in preventing penetration and cracking. The viscous hot faces are, however, subject to erosion and corrosion. Classic wet refractories (magnesia-chrome combinations or magnesia refractories) do not form appreciable liquids, but are subject to slag penetrations and structural peeling. Dry refractories (graphite) do not produce liquid or permit penetration, but are subject to oxidation and solubility in steel. As shown, combinations of Al_2O_3, MgO, ZrO_2, and SiC with graphite can behave more like the dry refractory system.

In addition to the liquid effects, graphite can also produce desirable physical effects, as illustrated in Fig. 3 for an Al_2O_3-graphite combination. As shown, the addition of 10 to 25 wt% of relatively coarse graphite can produce a refractory with lower elastic modulus, lower thermal expansion, and higher thermal conductivity. All of these features promote better resistance to thermal shock.

Other Properties

Many other refractory properties are required, but are perhaps more specific to given applications. For example, use in a blast-furnace lining in conjunction with internal or external cooling may require high conductivity (Fig. 4). The result of higher conductivity materials around the copper plate coolers are lower lining temperatures and longer lives. Conversely, other refractory applications can benefit by a low-density (low heat storage) and low-conductivity material such as fibers (Fig. 5).

The special requirements of each environment must also be recognized. In the blast-furnace lining,

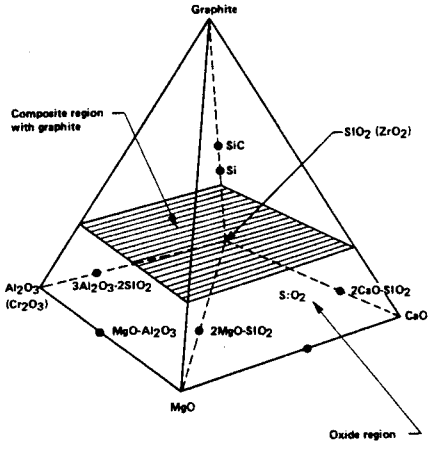

Fig. 1. Oxide-carbon refractory systems.

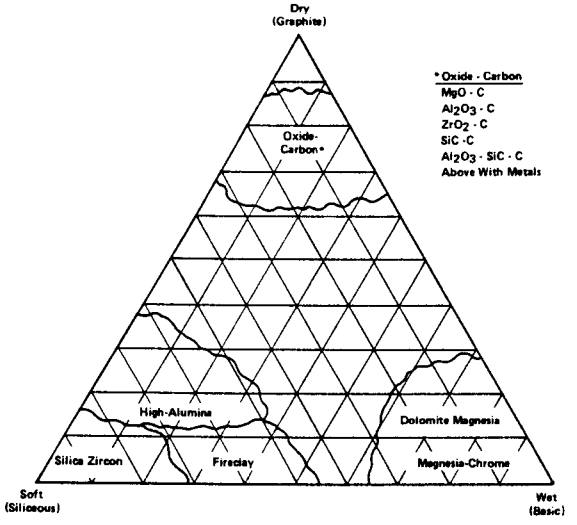

Fig. 2. More modern classification of refractories.

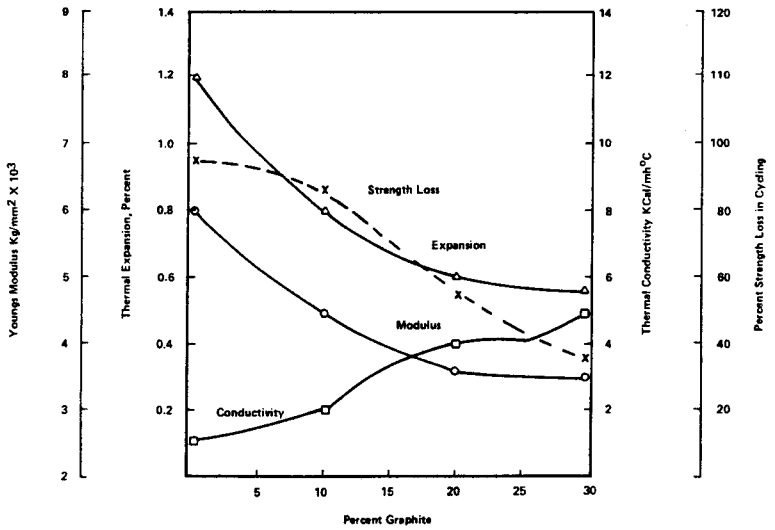

Fig. 3. Effect of graphite content on properties of Al_2O_3-C body.

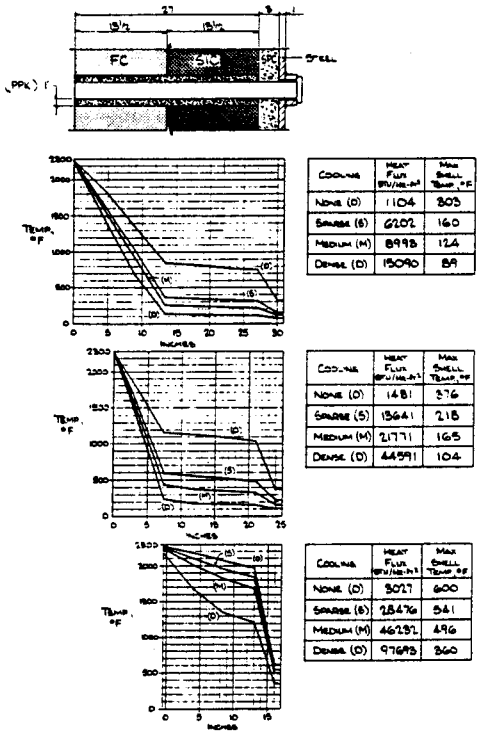

Fig. 4. Temperature profile for lining B as influenced by cooler spacing.

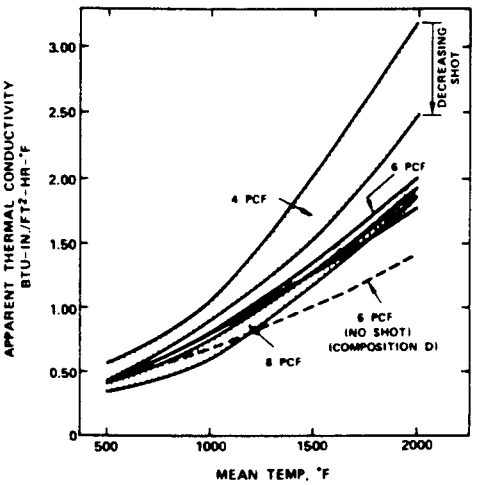

Fig. 5. Thermal conductivity as a function of temperature for various fiber materials.

for example, resistance must be provided to eliminate any free iron in the refractory used as carbon monoxide disintegration can occur as carbon deposits from gas around the iron-rich area. This is illustrated in Fig. 6, which shows a very old furnace lining destroyed by the action of carbon monoxide disintegration back of the lining hot face.

In a more modern context, blast-furnace linings may be subject to alkali attack from recirculating alkali vapor which can deposit in the furnace lining (Fig. 7).

Fig. 6. Classic appearance of used blast-furnace lining subject to localized carbon monoxide disintegration.

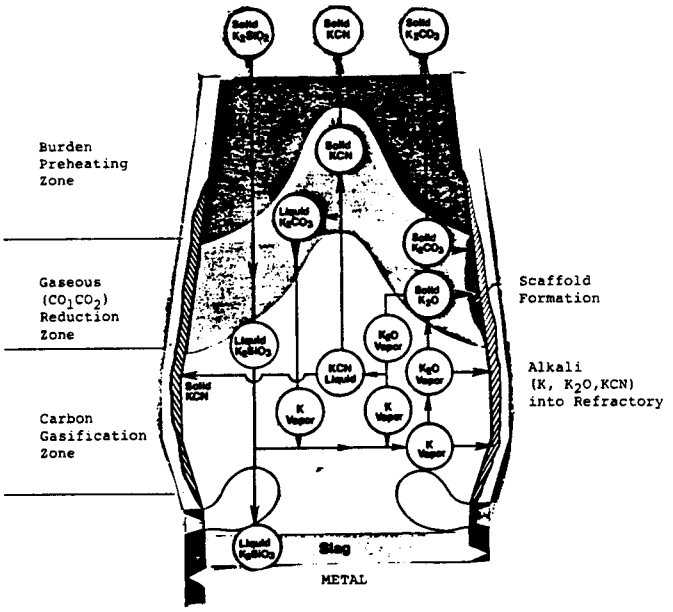

Fig. 7. Simplified flow routes for potassium recirculation in the blast furnace.

Special refractory grades have been developed in an effort to resist this phenomenon.

Such special refractory problems also exist in the steel-casting system. For example, the type and amount of inclusions present in the steel can cause either blockage or erosion of the final refractories used in continuous casting. In the case of solid alumina inclusions, a variety of methods for injecting argon in the tundish-to-mold shroud must be provided to avoid plugging of the system (Fig. 8). Conversely, liquid CaO-Al_2O_3-type inclusions formed when calcium is used to modify the inclusion forms can cause too rapid erosion of the same refractory systems. In this case, special more-basic refractories must be used for added protection (Fig. 9).

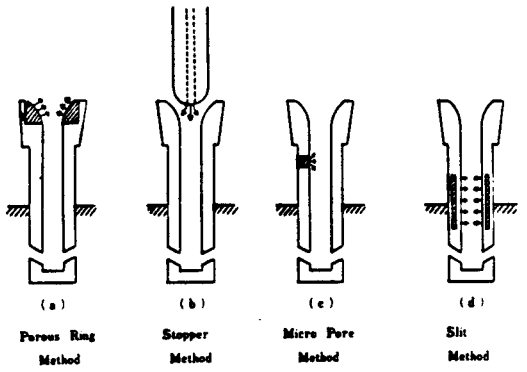

Fig. 8. Inert gas bubbling methods to decrease alumina clogging problems.

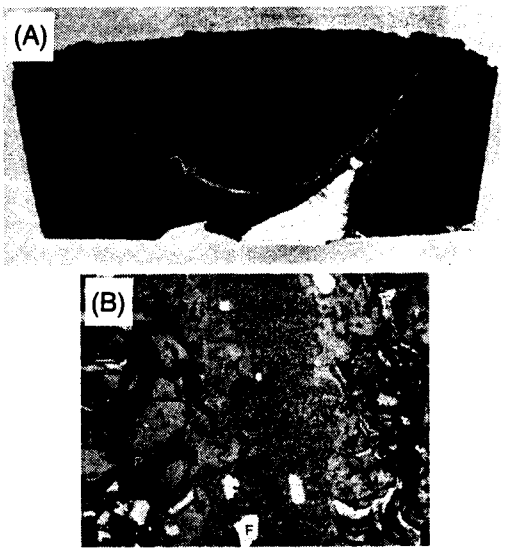

Fig. 9. (*a*) Rod/SEN interface after service with a grade 1010 heat. Note the irregular surface of the Al_2O_3-C stopper rod and the nonmetallics along the interface. The large bright area represents steel. (*b*) Micrograph showing the interface and two refractory materials. Note the elongated calcium aluminate crystals and metallic iron penetrating back into the Al_2O_3-C material, compared to the relatively smooth interface on the MgO-C material.

Applications of High-Alumina Refractories in the Steel Plant

High-alumina refractory products are used extensively in steel-plant applications; Table II is a broad survey of areas of usage, the general types of HAR used, a summary of the particular properties required for the specific application, and the general future direction of usage for the HAR materials. It does not distinguish between refractories made from synthetic aluminas (tabular, fused) and those made from bauxites or mullite. In fact, the products shown may contain both types of materials or be used in conjunction with lower grade alumina-silica materials. More specific compositions will be reviewed as each area of application is discussed. In all cases, however, the HAR must compete with (1) lower cost alumina-silica materials made from fireclay, kyanite, andalusite, bauxitic kaolin, etc.; (2) zircon-based materials; (3) dolomite products; (4) magnesia-chrome and magnesia products having equivalent or somewhat higher costs depending on local economics; and (5) higher priced material with special characteristics such as zirconia or silicon carbide.

It is also apparent from the brief description in Table II that most of the refractory applications involve the use of materials other than the classic fired high-alumina brick. For example, about half of the applications use alumina with graphite, silicon carbide, or impregnated with carbon. Many of the other applications involve either preformed or on-site casting with low-moisture castables.

Table II. Major Areas of High-Alumina Refractory Usage in the Steel Plant

Process Area	Application	Types of High-Alumina Product Used	Desirable Refractory Features	Future U.S. Directions
Blast furnace	1. Furnace lining	90%Al_2O_3, Al_2O_3-Cr_2O_3 brick 60-70% Al_2O_3 brick, often tar-impregnated	Shock and alkali resistance, hot strength	More nonoxide SiC, graphite-type brick.
	2. Stove - hot/air system	Creep-resistance, brick (60–80)	Creep resistance, volume stability	
	3. Cast house (troughs, runners, spouts)	Al_2O_3-SiC-C or high-alumina castables, plastics, ram mixes	Volume stability, metal and slag erosion resistance	Longer life/high-quality Al_2O_3 types.
	4. Hot-metal transfer/treatment (torpedo ladles, mixers, lances, stirrers)	Burned and impregnated high-Al_2O_3 products (70–80) Al_2O_3-SiC-C bricks for metal treatment(s)	Metal and slag erosion resistance Cycle resistance	Increased Al_2O_3-SiC-C types as metal treatment increases.
Steelmaking	1. Runners-EF	Al_2O_3-SiC-C monolithics	Metal and slag resistance	Increased use replacing older material types.
	2. Delta sections, smoke rings-EF	Low-moisture high-alumina castables	Shock resistance	
Ladles	1. Linings	Brick (70–80) Low-moisture castables (70–95)	Thermal shock, metal and slag resistance	Increased castable use. Higher alumina with clean-steel practices.
	2. Pads-blocks	Low-moisture castables preformed		Increased use with clean-steel practices.
	3. Lances	Low-moisture castables preformed	Thermal shock and erosion resistance	Increased use over brick or other materials.
	4. Permeable plugs	Fired shapes	Permeability, resistance to erosion	
Tundish	1. Safety linings	Low-moisture castable	Volume stability	Increased use over brick or other materials.
	2. Covers	Low-moisture castable	Volume stability	
Shrouds	1. Ladle-to-tundish	Al_2O_3-C	Shock resistance, metal and flux erosion resistance	Increased use with decreased fused-silica use.
	2. Tundish-to-mold	Al_2O_3-C		
Slide gates	Ladle and tundish	Fired impregnated Al_2O_3 Al_2O_3-Cr_2O_3 Al_2O_3-C	Shock resistance, metal erosion resistance	Increased use of alumina-carbon types. Repair of plates.
Reheating furnaces	Linings	High-alumina plastics, castables, preformed shapes, fibers	Volume stability, insulating effects	Continued emphasis on energy savings and ease of installation.

Blast-Furnace Applications

Furnace Proper

High-alumina brick have been used in a number of blast-furnace linings in the lower stack and bosh and long campaigns have been reported in both Japan and Europe.[3–5] Tables III and IV show the properties of several types of refractories used in domestic applications, including a 90% alumina brick with a mullite bond having superior density and shock resistance to other high-alumina materials. As shown, the high-alumina has better laboratory properties than the lower alumina materials, but not as good as silicon carbide. Success has also been reported with various Al_2O_3-Cr_2O_3 refractories in Europe.[5] In many actual domestic cases, however, the higher-alumina materials have not significantly outperformed fireclay or 60% alumina brick. The life of any furnace lining is highly dependent on stable furnace operating conditions through the use of proper burden materials, furnace charging and control procedures, and furnace maintenance techniques. These factors are believed to be at least equally important in obtaining long furnace lives for refractory and cooling designs.

The current trend appears to be toward increased cooling in plate or stave forms,[6,7] as illustrated in Fig. 10. With improved cooling, refractories with higher conductivity such as graphite, semigraphite, and/or silicon carbide are being used to obtain planned campaign lives of 8 to 15 years. Figure 11 shows the ultimate cooled design with wet (copper) and dry (graphite) cooling members. Thus the present trend appears to be toward the use of fewer high-alumina materials in blast-furnace linings.

In stoves and the associated hot-blast handling systems, high-alumina refractories in the form of fired

Table III. Typical Properties of USS Blast-Furnace Refractories — Stack

Property	High-duty Fireclay	Special Super-Duty Fireclay	Dense 60% Al_2O_3 Plain	Dense 60% Al_2O_3 TI*	Dense 90% Al_2O_3	SiC	Phosphate-Bonded Burned-75†
Porosity (%)	11–13	7–11	12–16	8–11	15–17	14–16	12–15
Density (g/cm^3)	2.23–2.36	2.40–2.48	2.50–2.60	2.52–2.63	2.88–2.94	2.65–2.68	2.60–2.70
Modulus, kg/cm^2 at room temperature	70–140	190–260	130–160	130–260	160–240	430–570	190–250
815°C	110–140	215–285	130–170	130–180		400–460	285–360
1110°C	140–180	230–290	160–180	160–200	160–200	430–590	
1230°C	70–110	160–200	150–170	170–190		430–570	
1370°C	30–50	70–110	70–110	70–150	160–215	460–640	
Thermal K kcal/m • h, °C	1.2	1.4	1.7		1.3	16.7	2.1
Abrasion, loss (cm^3/min)	2–4	0.2–0.3	0.4–1.0	0.4–1.0	0.4–1.0	0.1–0.2	0.1–0.2
CO resistance	OK	OK	OK	OK	OK	OK	OK
			Ribbon Shock Test				
% Strength loss	60–70	60–70	62–80		20–35	15–20	65–75
MOE loss	9–14	15–18	5–9		3–10	3–8	30–40
			Slag Test BF Slag				
	1.2	1.0	0.8	0.7	0.3	0.2	
			Alkali Test 1093°C, NSC				
% Loss	20–60	16–35	15–40	18–50	0–10	0–20	15–20
Relative cost	1.0	1.1	1.6	1.9	6.2	13.1	3.3

*Tests on tar impregnation in protective atmosphere.
†Stockline only.

Table IV. Test Summary on Blast-Furnace Stack Brick

Brick Type	Resistance to Abrasion: Grit Blast Loss (cm^3/min)	Hot Strength (kg/cm^2) 1100°C	Hot Strength (kg/cm^2) 1300°C	Resistance to Alkali: NSC Test, 1093°C (2000°F) Strength Loss (%)	Remaining Strength (kg/cm^2)	Ribbon Test Strength Loss (%)	Resistance to Shock: Panel FCE Test* 260° to 1371°C (500° to 2500°F) Cracking	Max. Rate, °F/min. ½"	1"	Sonic Change (% loss)	Rating System† Abrasion	Alkali	Shock	Total	Relative Cost	Relative Rating	Relative Relative
High-duty fireclay	2.0–4.0	110–140	30–50	25–50	50–75	60–70	Yes	60	50	70	2	3	4	3.2	1.0	1.00	1.0
Super-duty	0.5–1.5	130–160	32–75	20–35	130–140	55–70					3	3	4	3.4	1.1	1.06	1.0
Hi-fired super-duty	0.2–0.4	215–285	60–75	30–40	100–190	70–90	Yes	55	55	80	5	4	3	3.8	1.3	1.18	1.0
Special super-duty	0.2–0.3	200–290	92–110	16–34	100–200	65–85					5	4	4	4.2	1.6	1.31	1.0
60% alumina	0.4–1.0	150–180	70–110	15–40	160–280	60–80	Yes	60	55	75	4	5	5	4.8	1.6	1.50	1.0
60% alumina TI	0.4–1.0	160–200	60–120	20–50	110–215	60–80					4	5	5	4.8	1.9	1.50	1.0
90% alumina	0.4–1.0	140–210	130–160	0–10	160–180	20–30	No	62	40	8	6	10	10	9.2	5.6	2.88	2.0
SiC	0.1–0.2	380–600	460–520	0–15	380–500	12–20	No	116	100	10	10	10	10	10.0	13.5	3.13	4.0

*Furnace panels with plate coolers at 260°C hot-face temperature immediately exposed to 1371°C by damper movement (stable to unstable condition).
†Rating on 1 to 10 basis — high numbers good. Twenty percent for abrasion, 40 for alkali, and 40 for shock. This rating does not include cooling effects, which would change little, except for some advantages for silicon carbide and more mechanical support for cracked linings with dense cooling.

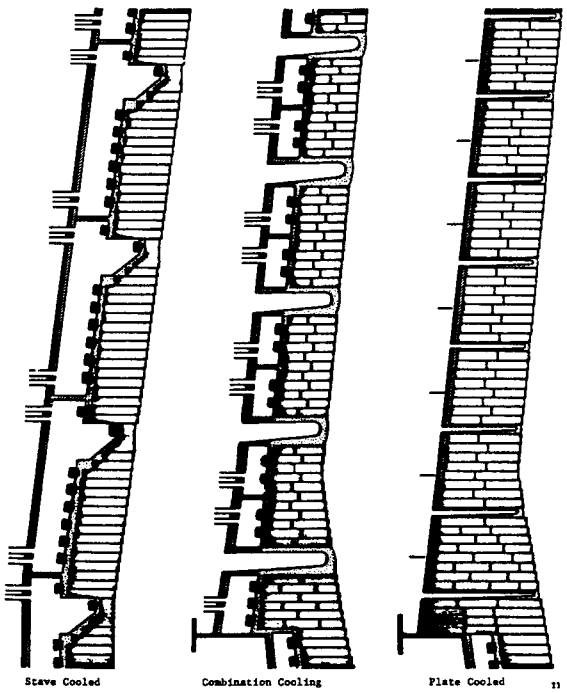

Fig. 10. Various cooling designs used in blast-furnace linings.

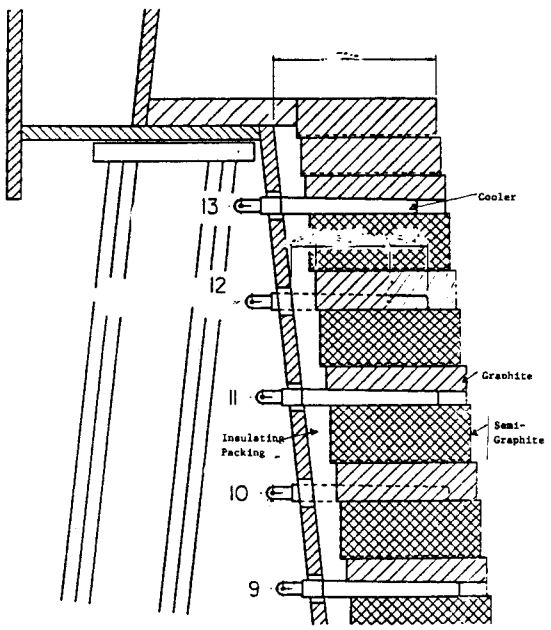

Fig. 11. Use of ultraconductivity materials in a typical bosh construction.

brick and shapes are used extensively. These refractories are, however, mid-alumina products based on andalusites or special bauxites to provide maximum resistance to creep (Fig. 12). These refractories are used in conjunction with silica in the highest temperature zones for maximum resistance to temperature at minimum costs.

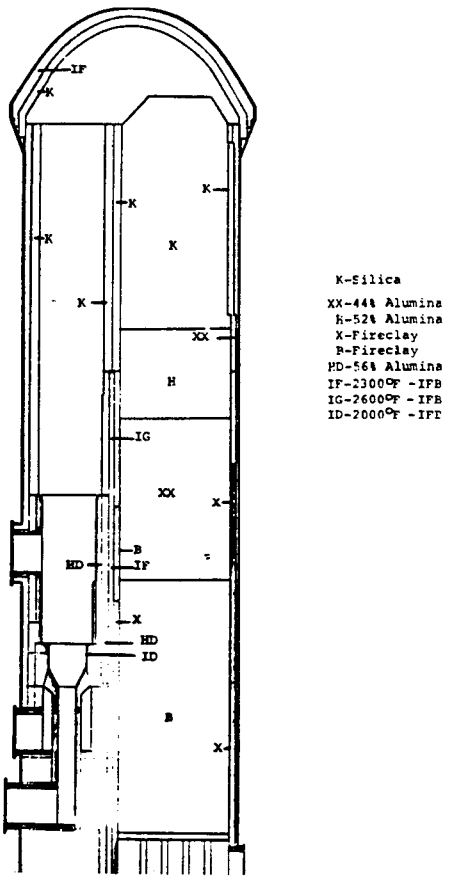

Fig. 12. Location of various types of refractories used in high-temperature stoves.

Cast House

The older low-productivity blast furnaces maintained trough and runner systems periodically with relatively low-cost shovel or rammed materials. These materials and techniques are now largely unsuitable on high-productivity furnaces operating with almost continual tapping through single or multiple tapholes. Changes have also been caused by the use of covered tapping systems for environmental control, and the necessity to minimize exposure of personnel to heat and undesirable fumes during repairs. In the early stages of semicontinuous furnace tapping, the life and cost of the trough-runner refractories represented a significant challenge to the refractory industry. This challenge has been largely met by a series of changes in both the method of applying the refractory materials and the improvement of material properties through the use of various alumina-silicon-carbide, carbon (ASC) materials.

Excellent reviews of the development of installation methods and materials have been presented.[8,9] Figure 13 summarizes the installation developments for both multiple- and single-hole furnaces. (It is necessary to distinguish between these cases as single-

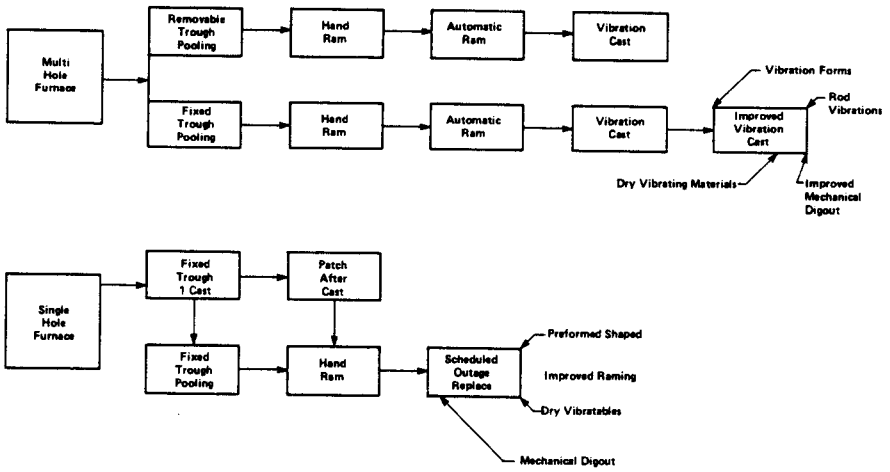

Fig. 13. Changes in trough system maintenance.

hole furnaces can allow only very short installation times without lost production and therefore use different procedures and materials.) As shown, developments for multihole furnaces have progressed to the stage that removable troughs are no longer necessary and large furnaces can operate with periodic patching of the systems using one of several procedures which replace the worn portion of the lining after some period (Fig. 14). These materials and procedures have been developed to a remarkable technical level where bonding is readily obtained between the cast material and the old surface roughened by dig out. The materials used may be low-cement casting materials, low-moisture materials with thixotropic characteristics, or zero-moisture products which are closely grain-sized mixtures heat-bonded by resins or low-temperature fluxes.

Single-taphole furnaces present a different challenge and cannot use low-moisture castables requiring long dry-out times. Present practices involve frequent maintenance by classic ramming techniques with periodic highly concentrated outages using all possible mechanical devices for dig out and replacement using preformed (and predried) refractory sections coupled with dry-vibratable materials.

Table V shows some overall ranges of compositions of currently used ramming, casting, and dry-vibrating materials. The ramming mixes may be used in ram or plastic form. The casting materials include both low-cement, clay, and other binders having desirable flow or thixotropic behavior. The dry-vibrating materials are resin-bonded with other additives to promote density and reduce dusting. As shown, the trough materials used for casting or dry vibration have higher Al_2O_3 contents than the older ram materials. As shown in Table V, the various compositions are all variations of the ASC system made from various grades of alumina, bauxite, and lower grade alumina-silica materials to provide the most economic solutions in zoned trough concepts.

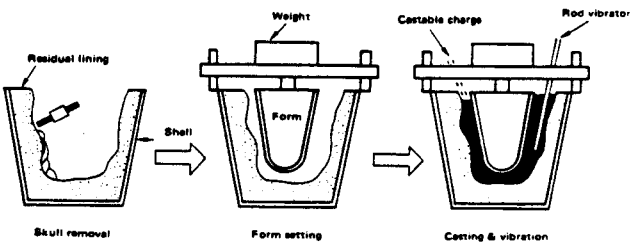

A. Low Moisture Castable

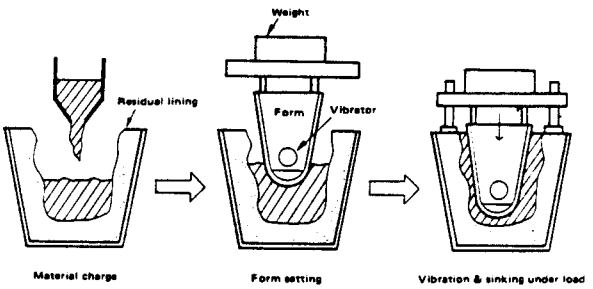

B. Low Moisture Thixotropic Material

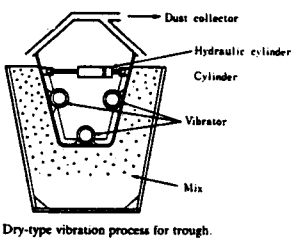

C. Dry Vibratable Material

Fig. 14. Various patching practices for troughs.

The properties of these materials have been extensively studied in a variety of tests and it is generally agreed that improved life is enhanced by improving the shock resistance, volume stability, and resistance of the material to erosion by metal and slag. Current

Table V. Overall Compositions of Current Materials for Trough System

Type	Area of Use	Composition (%)			
		Al_2O_3	SiO_2	SiC	C
Ramming	Trough	45–60	12–30	13–17	5–8
	Trough	73–75	2–4	11–13	3–5
	Runner	28–32	45–60	13–15	4–6
Casting	Trough	73–77	2–6	4–15	2–7
	Trough	58–62	10–11	9–15	8–9
	Runner	20–24	48–53	14–18	4–6
Dry vibration	Trough	70–80	2–5	5–8	3–5

trough total lives on multitaphole furnaces of some 1 to 2 million tons are now common with repairs every 40 to 200 thousand tons. Consumptions at these levels may range from 0.5 to 1.2 kg/ton. These consumption figures have appreciably lower cost when compared to consumption to 2 to 4 kg/ton with older ramming and gunning practices. On single-hole furnaces, consumption figures are significantly higher as gunning and patching are used to postpone the furnace outage for a trough rebuild. The short-term trough rebuilds are very labor-intensive. Various new approaches to preformed shapes are still under development.

Hot-Metal Transfer and Treatment

Hot metal is transferred form the blast furnace to the steelmaking unit in various sized (100- to 300-ton) railway cars (torpedo ladles). In the past 10 to 15 years, an increasing amount of hot-metal pretreatment has been conducted in torpedo ladles and this pretreatment has significantly altered the service conditions and changed the refractory usage.[10–12] Figure 15 illustrates some general paths now used between the blast-furnace runner exit and the steelmaking unit. As shown, hot metal may be simply transferred from torpedo ladles into transfer ladles to the steel furnace, may go through a surge unit (mixer) between the torpedo and transfer ladle, or may go through one or more hot-metal treatments before steelmaking. The most common domestic treatment is desulfurization by injection of materials such as calcium carbide or lime magnesium (Fig. 16). This desulfurization may be accomplished in either the torpedo or transfer ladle, depending on local plant design and costs. Hot metal may also be treated to remove silicon and phosphorus with various mixtures of lime, iron oxide (scale), fluorspar, and soda ash. These treatments are much more common today in Japan where the high price of scrap dictates high hot-metal changes to the steelmaking units. (In the United States and Europe, desiliconization would result in significant added cost because of the reduced ability to melt available low-cost scrap.)

Table VI shows the properties of refractories used in units involved in the various hot-metal handling and treatment practices. As shown, these range from simple fireclay and 60 to 80% alumina brick for the normal ladles used only for transfer to all or partial linings of ASC brick for torpedo ladles (or transfer ladles) used for desulfurization (Fig. 17). The life of torpedo ladles used for desulfurization will depend strongly on the proper design and usage of the unit to control factors such as lance depth, freeboard in the ladle, and slag removal practices following desulfurization. As in the other applications previously described, Al_2O_3-SiC-C refractories owe their superior performance to their excellent resistance to thermal cycling and the absence

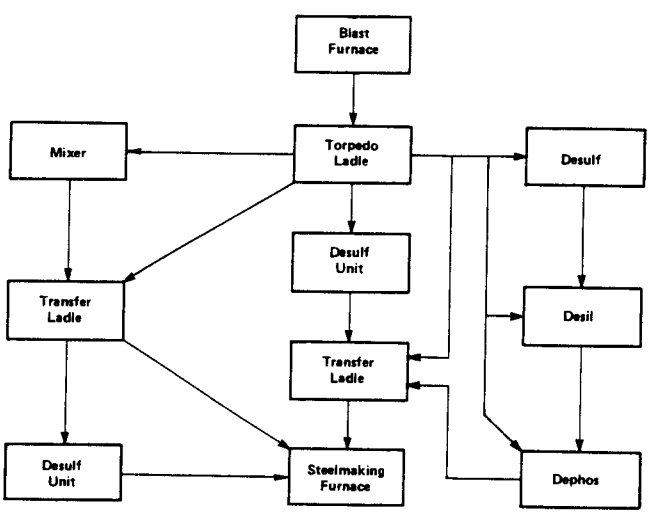

Fig. 15. Various routes for hot-metal handling and treatment between the blast furnace and steelmaking unit.

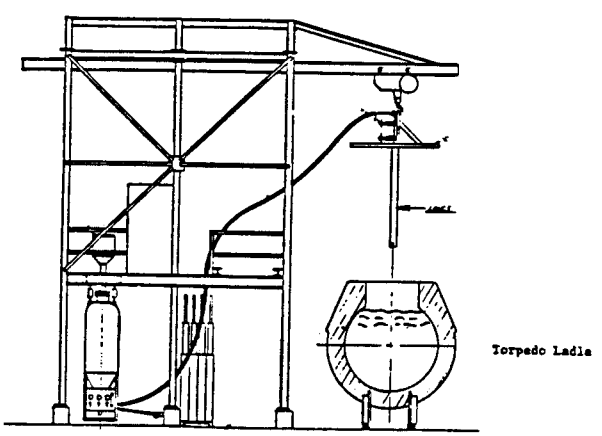

Fig. 16. Injection setup for hot-metal desulfurization by carbide or lime injection.

Table VI. Properties of Refractories Used for Hot-Metal Transfer and Treatment

Brick Type	Composition (%)			Porosity (%)			Modulus °F Rupture (kg/cm²)	Density (g/cm³)	Resistance to Desulfurization Slag	Resistance to Thermal Shock
	Al_2O_3	SiO_2	SiC + C	As-Red'd	Coke	Ignited				
Fireclay	48–50	46–49		12–14			100–180	2.3–2.4	Poor	Poor
60% Al_2O_3	58–62	27–29	0–2*	15–17			130–200	2.4–2.5	Fair	Fair
70% Al_2O_3	67–73		0–2	16–18			100–190	2.5–2.6	Fair	Fair
80% Al_2O_3	78–85		0–2	17–19			130–200	2.7–2.9	Good	Fair
Dolomite†			1–2	3–5	10–12	18–19		2.9–3.0	Good	Fair
Al_2O_3-SiC-C	65–78	2–7	18–25	5–7	12–17	22–26	180–360	2.7–3.2	Excellent	Excellent

*Carbon present if used as tar-impregnated brick.
†60% CaO and 35% MgO.

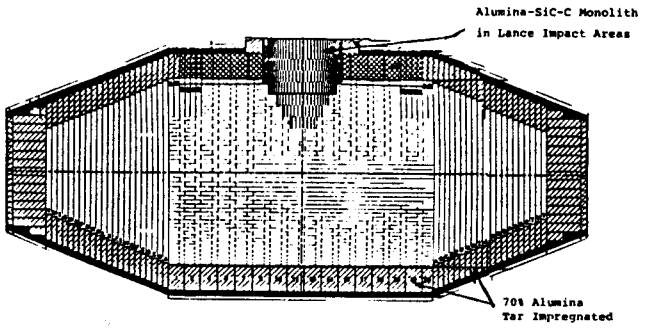

Fig. 17. Zoned torpedo ladle for desulfurization.

of in-depth alteration. In the case of desiliconization or dephosphorization, magnesia-carbon brick use has also been reported. Other changes to torpedo ladles include the use of high-strength insulating materials and covers to reduce temperature losses during transfer and treatment.

Torpedo ladles without pretreatment were used for 100 to 500 thousand tons, depending on the use of gunned patches to extend life. Consumption in those cases ranged from 0.2 to 1.0 kg/ton. With hot-metal desulfurization, lives with conventional material were reduced to 70 to 100 thousand tons and gunning was largely unsuccessful. Full or zoned linings using SiC brick can achieve lives of 100 to 180 thousand tons and consumption rates of 0.5 to 0.8 kg/ton.

Similar benefits can be achieved using ASC brick and monoliths in transfer ladles or mixers when problems with treatment slags are experienced.

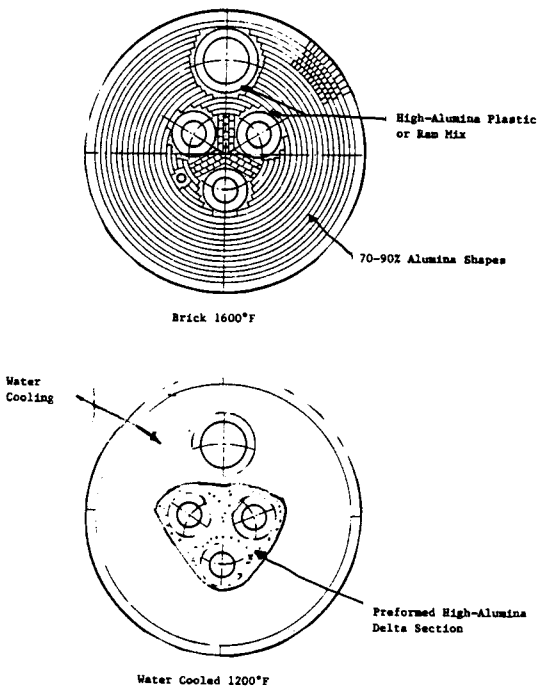

Fig. 18. High-alumina refractories in indicated electric-furnace roofs.

Steelmaking

High-alumina refractories have limited usefulness in the actual steelmaking process (BOP, Q-BOP, electric, open hearth, etc.) because basic refractories (MgO, CaO) have better compatibility with the basic slag used in most of today's production. High-alumina

Table VII. Preformed Shapes Used in Electric-Furnace Applications

Application	Composition (%)			Density (g/cm²)	Type
	Al_2O_3	SiO_2	Other		
Delta section or runners	84–87	1–10	0–4 Cr_2O_3	2.78–3.10	Low-cement castables
Runners	74–80	10–20	8–20 SiC	2.60–2.70	Casting mix
		1–2	85–90 MgO	2.71–2.81	prerammed
				9–10 Carbon	

refractories have historically been used in the roofs of electric furnaces, but modern furnaces with water-cooled sidewalls and roofs require only a minimum of refractory, as illustrated in Fig. 18. High-alumina preformed shapes are also now used extensively in electric-furnace tapping spouts to decrease installation and overall costs in comparison to basic ramming materials. Table VII shows the properties of some of the preformed shapes employed.

Steel Ladles

The evolution to higher quality steel ladle refractories in the past few years is well known[13–16] and has occurred from several changes in steel processing including:

1. The change from ingot to continuous casting which has increased the time and temperature to which the ladle refractories are exposed.
2. Increased quality demands on cast products so that any possibility of contamination by the ladle lining must be eliminated.
3. Increased processing in the ladle (ladle metallurgy) by one or more of a variety of techniques including stirring, alloying, heating, or degassing the steel in the ladle (Fig. 19). This processing not only has required more holding time, but also imposes appreciably more severe conditions on the ladle refractory. For example, Table VIII compares some ladle exposure parameters between an ingot cast product and a product made in one of the more complex ladle metallurgy facilities involving arc reheating and degassing. As shown, many parameters such as time, temperature, slag erosion, etc. are significantly different in this (and other ladle metallurgy routes) than in conventional ingot casting.

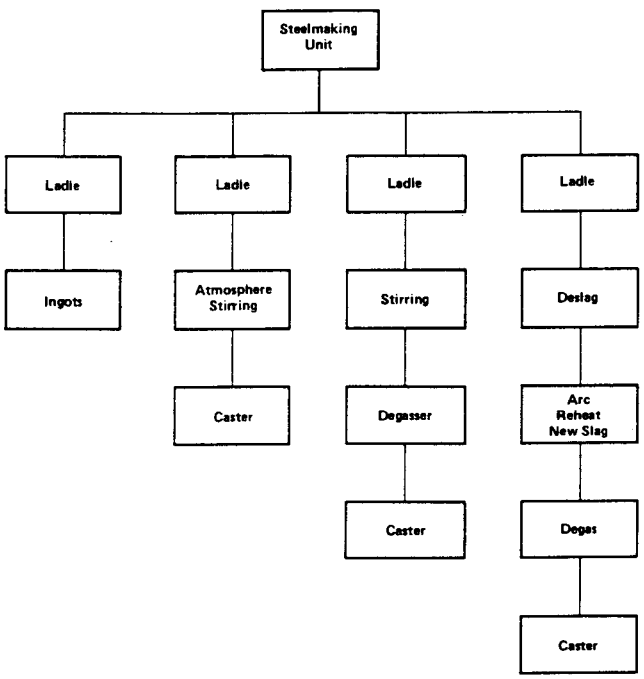

Fig. 19. Various routes for ladle from steelmaking furnace to caster.

Table VIII. Comparison of Ladle Exposure Time for Two Divergent Practices

Stage	Time in Ladle (min) Ingot Cast	Caster Cast	Comments
Tap	10	10	Slag free or less slag on caster heats
Skim and transfer to heating		20	Removal of remaining slag
Heating, slag alloys		60	Contact of artificial superheated slag with refractory
Degas, sample trim, stir		45	Movement of slag/metal
Stir	10		Slag movement
Pour	45		
Cast		90	
Total time	65	225	

A wide variety of materials and processes are being used to economically meet these new ladle conditions. Table IX is a summary of some of the successful lining approaches being used domestically involving zoned linings of high-alumina, zircon, and basic materials installed in either brick form or by casting thixotropic materials. This list is meant only to demonstrate the fairly wide range of possible solutions in high-quality ladles. The exact selection will be highly dependent on local economic, labor, and environmental conditions.

Table IX. Some Examples of High-Quality Ladle Lining Used Domestically

Ladle Type	Shop	Type of Refractory In Slag Line	Barrel	Bottom
Arc reheat	1	MCB	70–85 B	70–85 B or ZB
	2	DBB	70–85 B	70–85 B
	3	DBB	85 C	95 C
Caster	1	DBB	70–80 B	70–80 B
	2	DBB	85–90 B	ZB
	3	DB	DB	DB
	4	DBB	DB	DB
	5	DBB	ZC	ZC
	6	DDB	85 C	95 C
	7	85 C	85 C	85 C
	8	BC	70–85 C	70–85 C

Brick (B)
70–90 B indicates approximate Al_2O_3 content.
MCB indicates magnesia carbon.
DBD indicates direct-bonded periclase-chrome types.
DB indicates resin or burned dolomite.
ZB indicates zircon brick.

Castables (C)
70–95 C indicates approximate Al_2O_3 content.
ZC indicates zircon castable.
BC indicates basic castable.

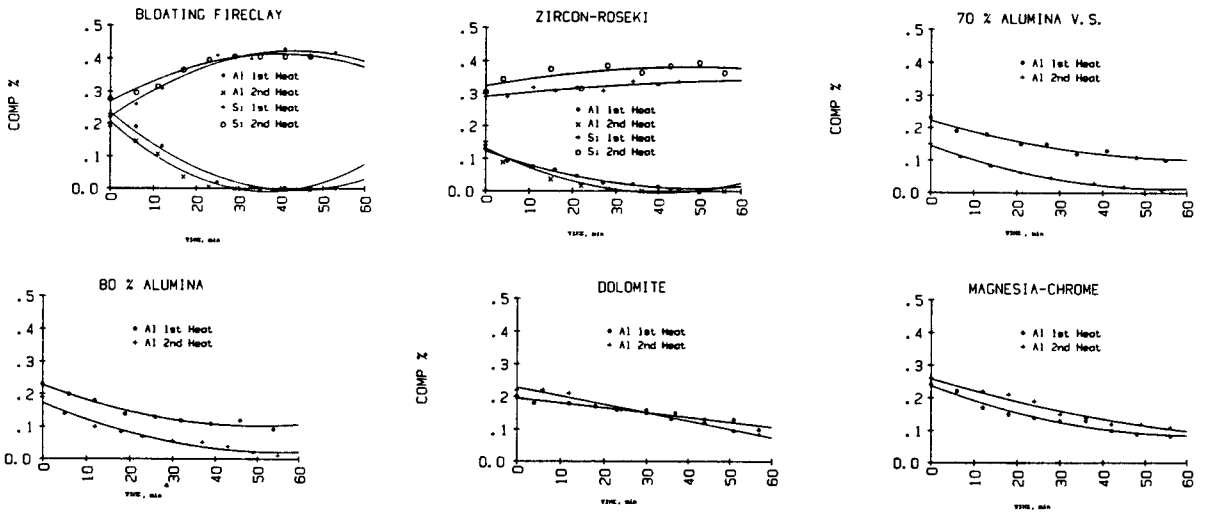

Fig. 20. Aluminum loss and silicon pickup on holding steels in a laboratory furnace.

Some materials such as siliceous fireclay, Rozeki, or sand slug or rammed ladles used in other parts of the world are not listed. It is expected that the future use of such materials in high-quality ladles will be very limited because of possible reaction between the steel and refractory. Figure 20 shows the pickup of silicon and loss of aluminum when holding steel in various ladle linings. Refractories with high silica contents can be reduced by aluminum. In general, it appears that refractories with more than 70% alumina or composed of basic oxide (MgO, CaO) are required for high-quality ladles. There are, however, no significantly apparent advantages in steel cleanliness between good 70% alumina products and purer materials. This is because either the altered refractory hot face or residual ladle or furnace slag become the prime oxygen sources once a lining is used.

As shown in Table IX, the predominant materials for slag lines are basic in nature for the high-quality ladles. The resistance of the basic refractories to basic furnace carryover slags, or to artificial slags such as $CaO\text{-}Al_2O_3$ or mixtures of CaO, $CaO\text{-}Al_2O_3$, and fluorspar, are superior to other materials (Fig. 21). As will be described later, other properties are more important for other areas of the ladle.

Tables X and XI show the properties of the high-alumina brick and castable ladle refractories previously described. The successful high-alumina ladle refractories are characterized by good density, volume stability, and resistance to thermal shock. Figures 22 and 23 are schematics of ladles using high-alumina brick and castable lining, respectively, for parts of the lining.

The exact future of castable linings in the United States is not known. High-alumina or zircon castable materials are used to a greater extent in Japan and Europe than in the United States. The castables used are low-moisture thixotropic materials installed in ladles by vibration around a mold (core) (Fig. 24). After vibration and removal of the core, the cast

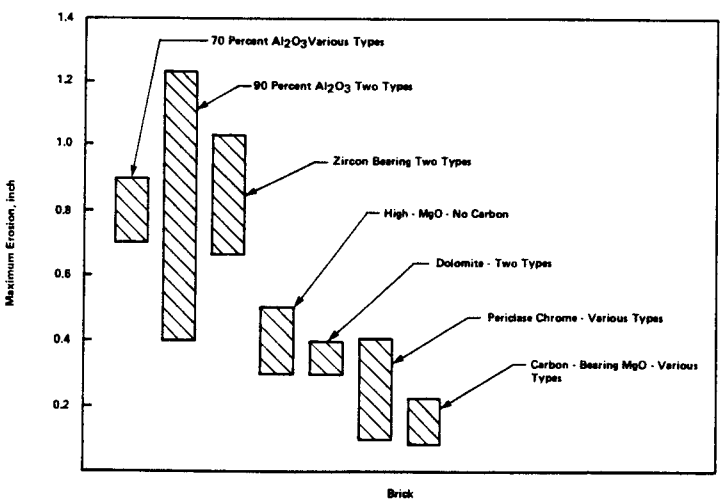

Fig. 21. Range of slag erosion values for various types of brick tests with various basic ladle slags.

Table X. Properties of Indicated High-Alumina Ladle Brick

Brick Type	Composition Al_2O_3	Composition SiO_2	Density (g/cm^3)	Porosity (%)	Reheat Change 1570°C, vol %
			Burned		
70	68–72	26–28	2.50–2.72	15–20	4–12
80	77–82	18–23	2.72–2.85	15–19	4–6
85	83–86	8–11	2.88–2.92	17–19	0–1
90	>88	5–10	2.90–2.97	16–19	0–1
			Unburned		
80–85	78–86	10–18	2.91–2.96	14–17	0–1
90	>87	1–6	2.95–3.13	12–16	0–1

Table XI. Properties of High-Alumina Ladle Castables

Class	Composition Al_2O_3	Composition SiO_2	Composition CaO	Density (g/cm^3)	Porosity (%)	Reheat Change 1570°C (% linear)
70	67–71	28–31	0.4	2.60–2.63	14–16	−0.1
85	80–83	10–12	0.5	2.76–2.80	17–19	+0.2
95	94–96		0.4	2.96–3.05	14–16	+0.0

material must be dried very slowly to avoid problems with entrapped steam in the dense structure. The economics of castable ladles depend strongly on the savings in material consumption associated with repair of the castable material over a worn surface. One of the most important factors of ladle castables is their ability to be mechanically cleaned and have new repair material bind with the roughened surface. Figure 25 shows the relationship between cost and heat life for a typical castable and brick installation. As shown, the castable linings are more expensive per ton of steel contained until near the end of the second casting (original plus one patch). In severe operating cases in which higher quality castables are required, two castable patches may be required to obtain lower costs with castable ladles.

The overall life of steel ladles lined with brick will vary from some 15 to 150 heats, depending on the ladle processing. This is illustrated in Table XII for ladles used in one type of reheating-degassing process. On the longer campaign, bottoms or slag lines may be replaced at one-half to one-third the barrel life. Castable ladle barrels have lives of 40 to 80 heats between patches and castable bottoms are patched

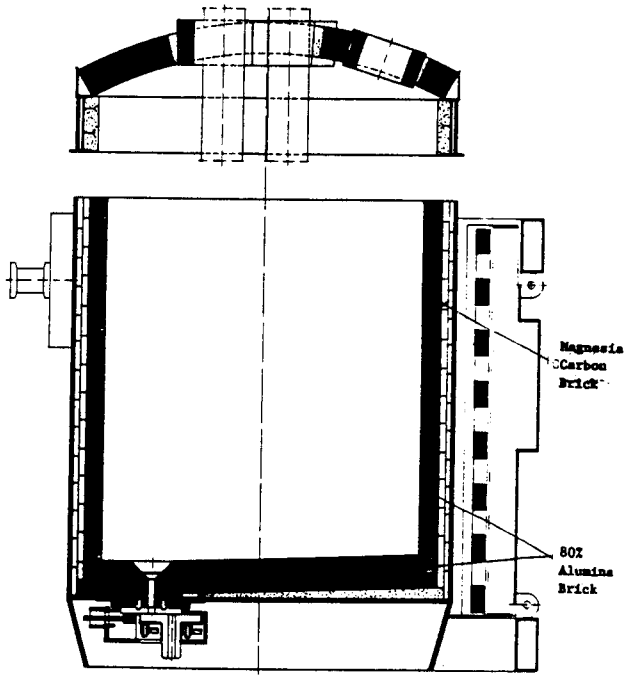

Fig. 22. Lining in a ladle for arc-heating and degassing.

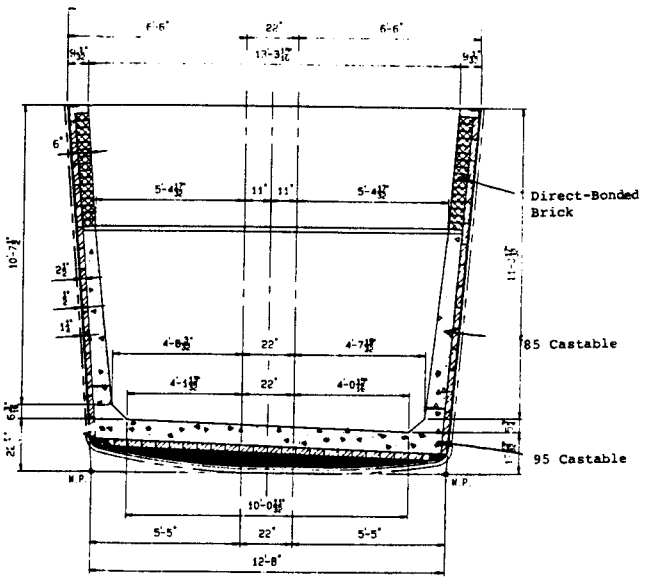

Fig. 23. Lining in a caster ladle using a castable barrel and bottom.

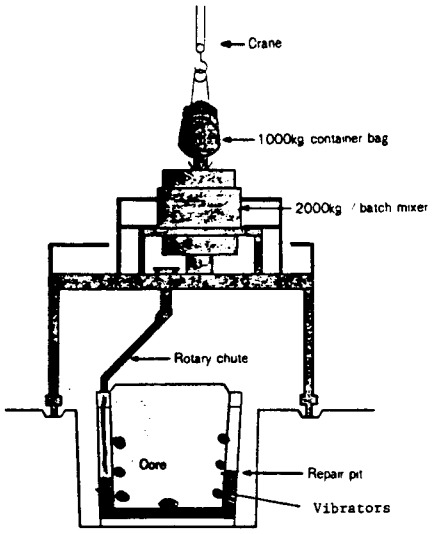

Fig. 24. One method of installing low-moisture castables in steel ladles.

every 30 to 40 heats. It is obviously advantageous to have the different parts of the ladle wear in even multiples. The consumption of high-alumina brick in ladles may range from 1 to 4 kg/ton. High-alumina castable under comparable conditions would wear about 25 to 35% less than brick. The higher quality ladles must be preheated and cycled with much more care than older, less dense, and more shock-resistant materials to avoid excessive ladle heat loss (skulling) and refractory damage.[17,18] Ladle life is strongly dependent on the thermal cycles which occur in a particular shop (delays, use of covers, periodic operations, outages for gate repairs, etc.).

High-alumina refractories are also used in a variety of other ladle areas including:

1. As a monolithic material (plastic, ram mix) between the steel lip ring and lining brick and around pocket (nozzle) blocks, permeable plugs, and pour pads.

2. As preformed castable shapes used as pour pads or pocket blocks (Fig. 26). These are usually 85 to 95% alumina low-moisture castables to provide balanced wear with the less severe ladle areas.

3. In powder-injection lances or stirring lances, as illustrated in Fig. 27. These materials are again very-high-alumina castables which may be enforced with stainless fibers to improve their crack resistance.

4. As permeable or solid stirring plugs (Fig. 28). The degree of permeability in such plugs may be provided by controlled porosity (grain lining, burn-out materials) or by preformed directional voids.

5. As slide-gate components on the ladle. These materials will be described in the following section on steel flow control.

Table XII. Life of Ladles Used in Arc-Reheating and Degassing Process

Heats Reheated (%)	Heats Degassed (%)	Life (Heats)	Patching
100	100	20–30	None
50	0	40–50	BTM/slag line
25	0–25	60–70	BTM/slag line
0	0	90–105	2 BTM

Continuous-Casting Refractories

A wide variety of refractories are used between the steel ladle and continuous casting mold. These refractories serve to (1) provide flow control of the steel streams in conjunction with liquid level control devices, (2) protect the streams from harmful oxidation, and (3) provide for final inclusion modification and control. Figure 29 shows several schematics of ladle-to-mold systems to generally illustrate the various refractory components involved including ladle

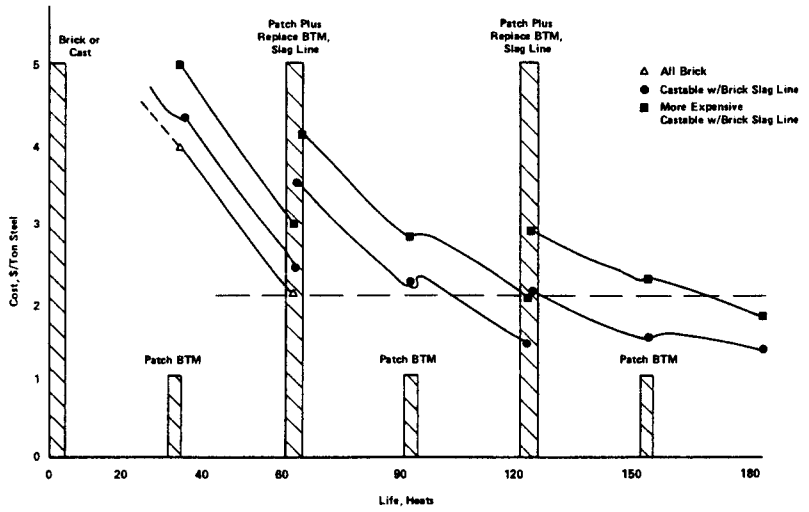

Fig. 25. Typical relation of life/cost for indicated linings.

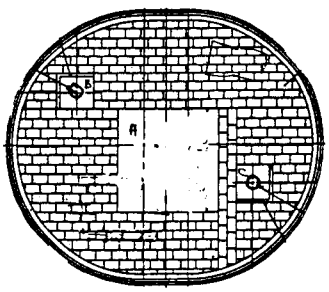

Fig. 26. Brick ladle bottom with preformed block for impact pad (A), nozzle block (B), and permeable plug block (C).

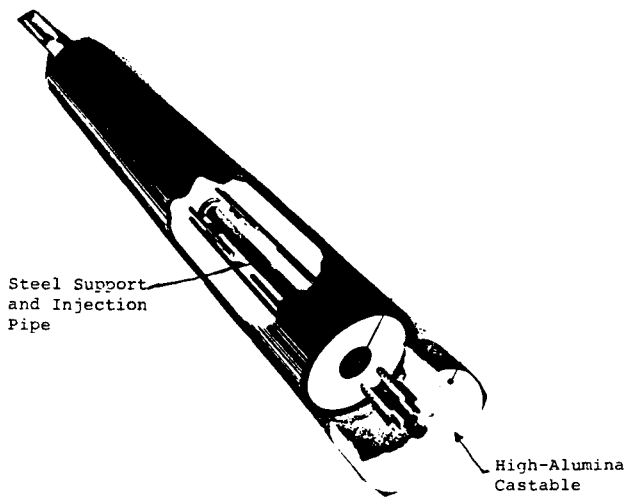

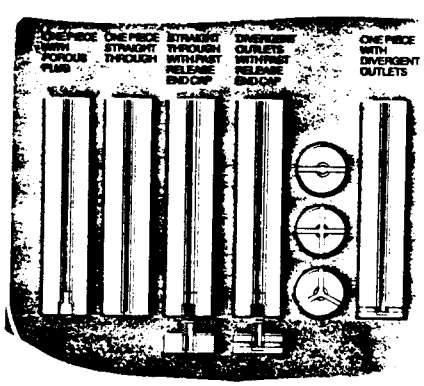

Fig. 27. Some concepts of design of powder-or gas-injection lances for clean-steel processes.

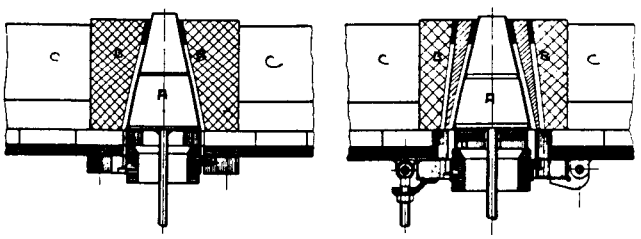

Fig. 28. Typical mounting devices for permeable plugs (A) inside seating blocks (B) in ladle bottom (C).

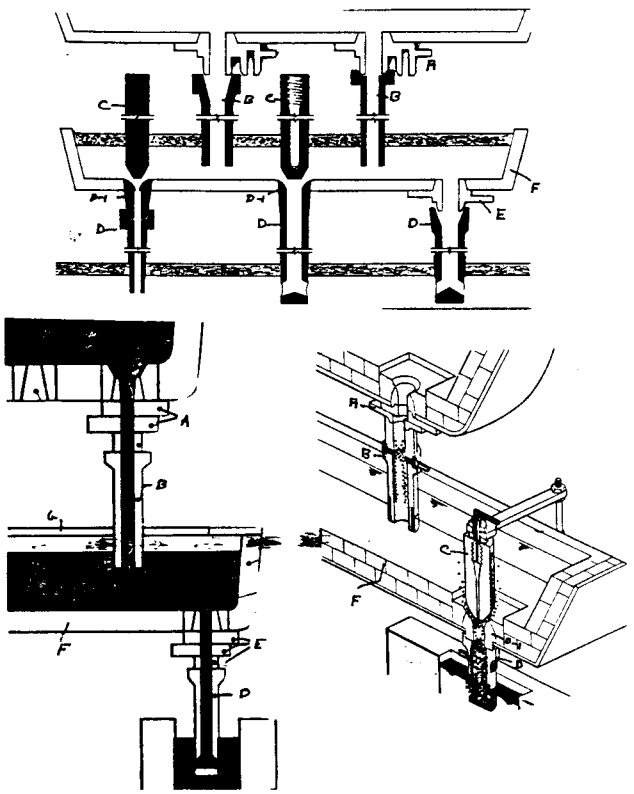

Fig. 29. Typical refractory components in the ladle-to-mold system. A = ladle slide gates, B = ladle-to-tundish shrouds, C = tundish stopper rods, D = tundish-to-mold shrouds with associated nozzles (D-1), E = tundish slide gates, F = tundish linings, and G = tundish covers.

slide gates, ladle-to-tundish shrouds, tundish stopper rods, tundish-to-mold shrouds with associated nozzles, and tundish slide gates. Refractories are also used in the tundish linings and covers and in tundish weirs, dams, and filters.

Although the refractory consumptions in continuous casting are small, refractory costs are high because of the complex nature and high degree of technical development of the refractory materials, and because the life of such materials is relatively short (1 to 20 heats). Refractory life in this system is also often determined by the length of casting sequence for a particular steel grade as it is necessary to provide clean surfaces for steel cleanliness and to permit restart of the system without contamination. As a result, the sequence life of a continuous-cast system may be dictated by product demands and metallurgical considerations. Some refractory components in the system may be changed during a casting sequence, including parts of the gate systems and either of the shrouds if the component life does not match sequence life.

Although there are several wear mechanisms involved in the continuous-casting refractory systems,

Table XIII. Properties of Refractories for Shrouds and Tundish Rods

Type	Area Used	Composition (%) Al_2O_3	SiO_2	C	ZrO_2	MgO	Other	Apparent Porosity(%)	Bulk Density (g/cm^3)
Base	Ladle-to-tundish	50–56	14–18	26–33			0–5	15–18	2.30–2.44
Al_2O_3	shroud, tundish-to-mold shroud, rod for tundish.	42–44	18–24	24–31	0–3		0–2	12–18	2.20–2.35
Fused silica	Ladle-to-tundish shroud, tundish-to-mold shroud.	<0.3	>99					12–17	1.82–1.90
ZrO_2-C	Slag line or nozzle of tundish-to-mold shroud, head of rod.	1–2	5–7	7–10 20–25	75–80 67–74		0–2 0–2	12–16 15–18	3.57–4.18 3.20–3.60
MgO-C	Nozzle of tundish-to-mold shroud, head of rod		0–2 12–16	5–9 10–20		85–92 58–78		15–18 14–17	2.46–2.51 2.25–2.50

they can be broadly summarized as: (1) thermal shock or thermal gradient cracking effects; (2) erosion by steel, inclusions in steel, and tundish or mold slags (fluxes); and (3) buildup of inclusions when casting certain grades which can deposit on refractory surfaces, clog the system, and stop casting. The various refractories and designs used in casting have been developed to resist one or more of these effects.

The properties of various refractories used in the immersed tubes (either type) or stopper systems are shown in Table XIII. Most of the refractories used in these applications contain substantial quantities of carbon (graphite) (5 to 33 wt%). As previously described, graphite is used mainly to impart the degree of thermal shock resistance or resistance to gradient cracking required in these applications.[19–23]

As shown in Table XIII, fused-silica shapes are used in these same applications because the very low thermal expansion of fused silica allows it to survive under several gradient conditions without cracking. The choice of fused-silica or oxide-carbon refractories for these applications depends mainly on the desired component life and the deleterious effect of some steel grades of fused silica (particularly those high in manganese).

The combination of alumina with carbon is used for most of the ladle-to-tundish or tundish-to-mold shrouds and tundish rods. As illustrated in Figs. 30 and 31, however, other oxide compositions may be used to

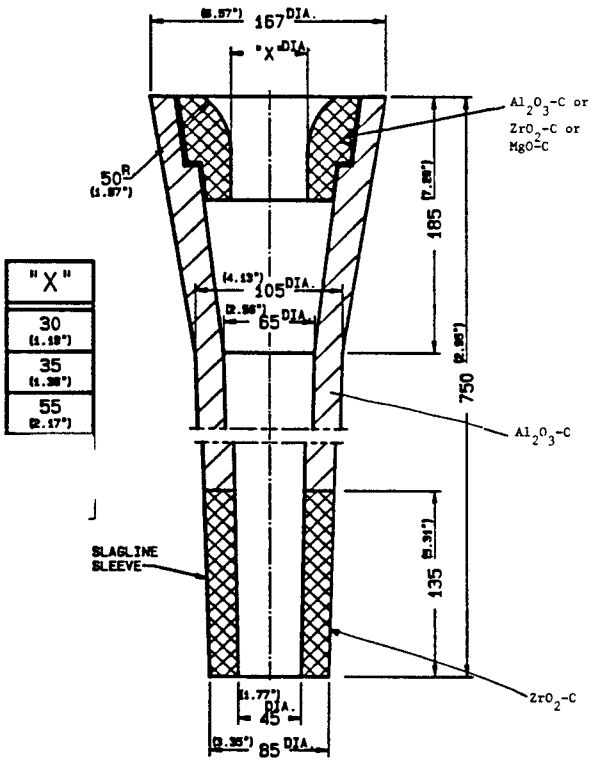

Fig. 30. Typical tundish-to-mold shroud with various nozzles.

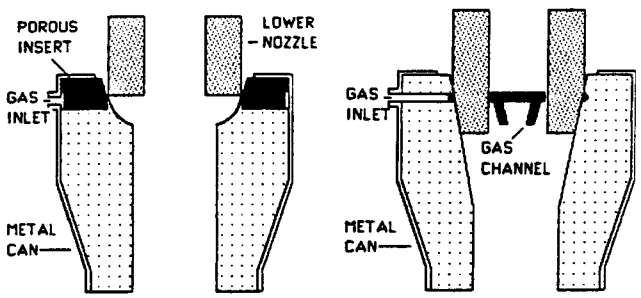

Fig. 31. Example of argon seal between the ladle nozzle and ladle-to-tundish shroud.

impart resistance to erosion-corrosion at the mold-flux slag lines (ZrO_2-C), at the nozzles of tundish-to-mold shrouds (ZrO_2-C, MgO-C), or on the tips of rods (MgO-C, ZrO_2-C). The types of mold fluxes used in continuous casting can vary widely, and can be very corrosive to the outside of the tundish-to-mold shroud. Typical fluxes are low-melting combinations of silicates, oxides, fluorides, and free carbon. Experience has shown that an outside layer or solid bottom of ZrO_2-C refractory is the most resistant to mold-flux corrosion.

Erosion in other parts of the tundish-to-mold shroud or rod head is more complex. This erosion may result from a variety of low-melting liquid inclusions such as $MnO\text{-}Al_2O_3\text{-}SiO_2$ liquids in silicon-killed steels or complex $CaO\text{-}Al_2O_3$ inclusions in calcium-treated aluminum-killed steels. Steels high in oxygen content such as resulfurized, extra-low-carbon, or loaded steels may also be particularly corrosive. Depending on the corrosive liquid inclusion composition, MgO-C, ZrO_2-C, or other special materials may be required in the most corrosive areas, as was illustrated in Figs. 30 and 31. In these cases, improved resistance can also be obtained by increasing the content of refractory oxide (less carbon) and the maximum product density.

The casting of aluminum-killed steels can present severe clogging problems in the various areas of the continuous-casting system. This clogging results due to the formation and deposition of alumina, and the tundish casting systems are designed both to prevent the formation of alumina by minimizing stream oxidation and to prevent buildup in critical areas. For example, the joints between the ladle-to-tundish shroud and ladle nozzle are commonly provided with the best possible seal using compressible gaskets and argon injection to provide an inert atmosphere should aspiration occur, Fig. 32. Argon is also used to prevent buildup in the tundish-to-mold shroud (Fig. 8). There are many systems to supply argon to the critical build-up areas using porous rings and slits. Figure 33 shows recent advanced techniques to supply argon in both the tube body and exit holes of the multiport shroud.

The various complex shroud shapes require very sophisticated manufacturing techniques to provide the multiple compositions and structures. Such shapes are commonly made by isostatic pressing or injection molding. Because the success in casting is fully dependent on consistent refractory performance of the continuous-casting refractories, they are also subject to rigorous nondestructive inspections before use. A considerable effort has also been made by both the manufacturer and user of shrouds to develop methods for preheating, protection from oxidation during preheating, and devices for tube changing without interrupting operations.

Fused-silica tubes do not require preheat, and oxide-carbon tubes with some added fused silica have been developed which may also be used without

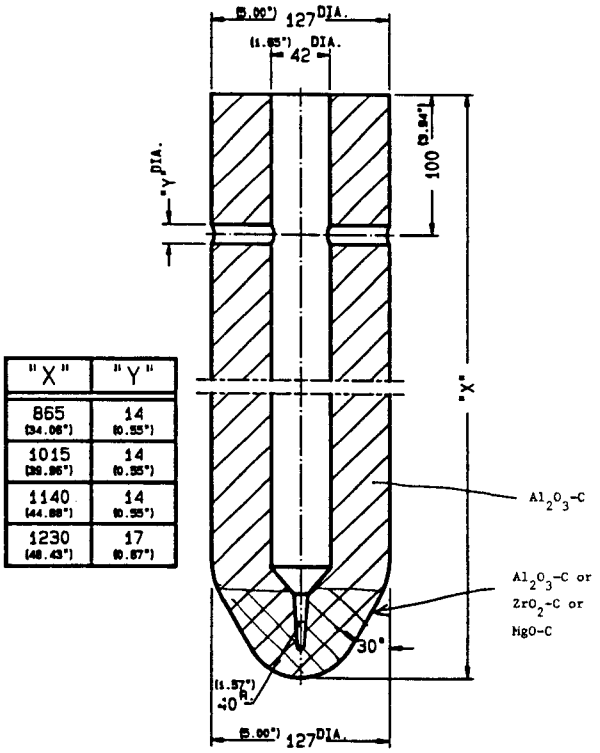

Fig. 32. Typical tundish rod with several types of heads.

preheat. Many systems casting smaller cross sections, however, must use preheat to avoid freezing during caster start-ups.

Ladle and Tundish Gate Systems

Various sliding-gate systems are used to control the flow of steel between the ladle and tundish and tundish and mold.[24] Figure 34 shows the general concepts of sliding-gate systems where moving and fixed pressurized plates are used to control metal flow. The ladle gate system contains several refractory components including the well block, upper nozzle, upper plate, lower plate, and lower nozzle. The upper nozzle and plate are fixed to the ladle bottom below the ladle lining containing the well block. The lower plate and nozzle move back and forth linearly or in a rotating mode. There are a variety of patented gate systems and they differ appreciably in their methods of applying pressure (springs, torque bolts, etc.) in the drive mechanisms (electric, hydraulic) and in the methods of changing plates such as the use of cassettes or hinge mechanisms. Plate designs may also differ (cases or uncased, one surface or reversible, etc.). Figures 35 and 36 show more detail of an actual ladle and tundish gate system.

Tables XIV through XVIII show the properties of various refractories for ladle pocket blocks, nozzles, and gate plates, respectively. Pocket blocks and upper nozzles use high-alumina fired or unburned shapes and higher alumina materials are used to balance block life

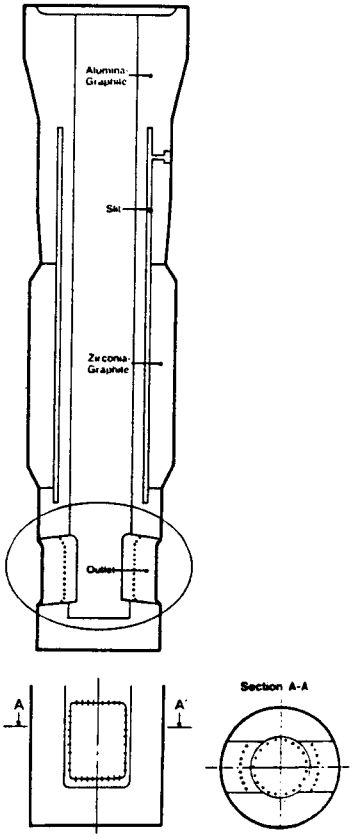

Fig. 33. Example of argon injection in shroud body and parts.

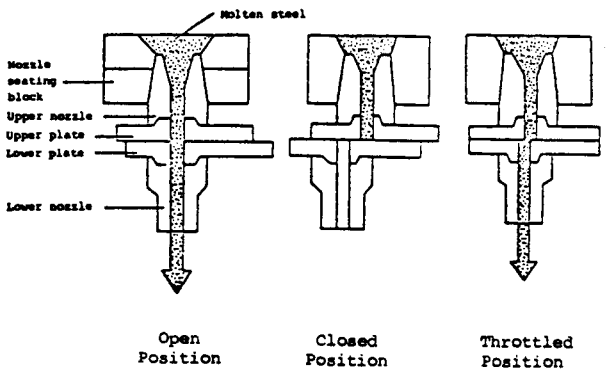

Fig. 34. Different positions of the refractory components in a ladle slide gate.

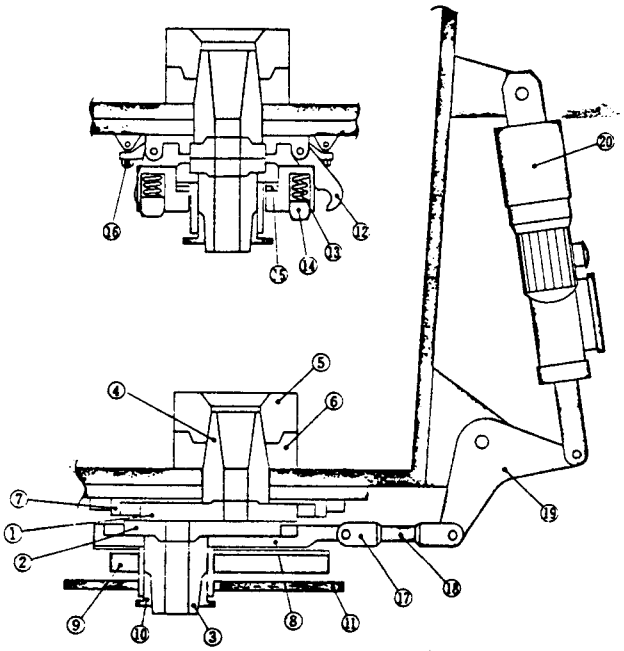

No	Nomenclature	No	Nomenclature	No	Nomenclature
1	Upper plate brick	8	Slide frame	15	Liner
2	Lower plate brick	9	Lower frame	16	Hinge bolt
3	Lower nozzle brick	10	Lower nozzle support ring	17	Fork end
4	Upper nozzle brick	11	Cassette shield	18	Connecting rod
5	Upper nozzle sealing block	12	Hook	19	Arm
6	Lower nozzle sealing block	13	Coil spring	20	Electromotive thruster or Hydraulic cylinder
7	Upper frame	14	Spring compressor		

Fig. 35. Typical ladle with system.

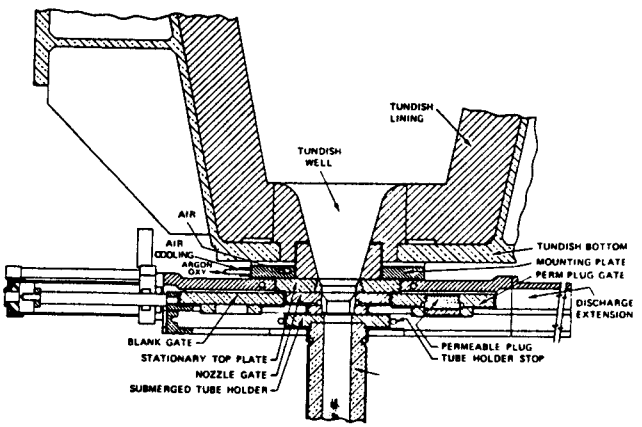

Fig. 36. Tundish valve showing submerged pouring tube in position.

with ladle bottom life. Slide-gate plates were originally developed as fired and tar-impregnated compositions (Table XVII) to develop a balance between thermal shock and erosion resistance. Carefully controlled particle sizing and manufacturing techniques were used to achieve uniform densities and a ground finish for mated sliding surfaces. Basic composition gave better service under certain service conditions such as with calcium-treated or high-oxygen steels. The fired compositions virtually all use tar impregnation to facilitate sliding, prevent metal penetration and adherence to the refractory, and improve the seal between plates to minimize air-oxidation effects. Later developments have involved several types of alumina-carbon compositions (Table XVII). These compositions can produce improved shock and corrosion resistance, very smooth matting surfaces, and an overall improved life. Collector nozzle quality will vary both with steel grade and its design as either a single

Table XIV. Typical Properties of Pocket Blocks

Type	40% Alumina	60%* Alumina	70% Alumina	80%* Alumina	90%† Alumina	99% Alumina	Zircon/ Alumina/ Chrome	Graphite/ Magnesia
Apparent porosity (%)	17	21	20	20	15	18	18	6
Bulk density (g/cm^3)	2.30	2.42	2.60	2.70	3.10	3.20	3.45	2.95
Cold crushing strength (kg/cm^2)	ND‡	600	600	ND	1500	600	850	ND
Thermal expansion (% at 1000°C)	ND	0.46	ND	ND	ND	ND	ND	ND
Major composition (%)								
Al_2O_3	43	60	71	80	90	99	15	
SiO_2		35	24	14	9	1	29	
C					4			5
Cr_2O_3							2	
ZrO_2							51	
P_2O_5		4		4				
MgO								80
Recommended applications	General	General	General	General	Severe	Severe	Severe	Severe

*Available unburned chemically bonded.
†Available unburned resin-bonded.
‡ND = No data available.

Table XV. Typical Properties of Upper Nozzles

Type	70% Alumina	80% Alumina	85% Alumina	90% Alumina	Chrome/ Alumina	Zircon	Resin-Bonded	Manganese
Apparent porosity (%)	21	20	19	18	17	20	7	19
Bulk density (g/cm^3)	2.48	2.60	2.75	2.95	3.05	3.40	3.00	2.91
Cold crushing strength (kg/cm^2)	350	700	900	900	900	700	700	650
Thermal expansion (% at 1000°C)	ND*	0.55	0.55	0.70	0.65	0.40	0.40	0.90
Major composition (%)								
Al_2O_3	70	80	85	90	83	10	90	
SiO_2	26	19	12	6	8	31		1
ZrO_2						55		
C							4	
Cr_2O_3					4			
MgO								95
Recommended applications	Severe nozzle clogging	General	General	General high erosion	High erosion	High erosion	High erosion	

*ND = No data available.

component with the gate plate or an independent (replaceable) system.

Lives in the gate system will vary from one to about 10 heats. Dependability and reproducibility of the gate systems are of vital importance to safe, quality steel production.

Refractories in Tundish Proper

The tundish lining proper may also employ some high-alumina material in the safety or permanent lining or covers (Fig. 37). The actual working lining in most modern tundishes, however, is a thin layer (25 to 50 mm) of preformed board, gunned, or vibrated basic material installed between casting sequences. This "clean" (new) layer allows rapid clean-out of the tundish so that the next casting sequence can start without any residual slag, metal, or other contaminants. In some cases, the relative insulating character of the thin layer also allows start-up with minimum or no tundish preheat. High-alumina coatings or boards with similar densities would also probably function in the same manner, but are more expensive than their basic counterparts. High-alumina or alumina-carbon shapes may also be used in the tundish as weirs, dams, and tundish filters, as generally illustrated in Fig. 38.

Finishing Refractories

Although the demands for refractories in finishing steel (reheat furnaces, annealing furnaces, soaking pits, etc.) are less stringent than those involving metal or slag containment, the applications do represent an important continuing use of high-alumina materials in

Table XVI. Typical Properties of Sliding-Gate Plates—Conventional Type

Type	85% Alumina	90% Alumina	High Alumina, >92% Al_2O_3	Alumina/ Chrome†	MgO
Apparent porosity (%)	16	17	15	16	18
Bulk density (g/cm^3)	2.88	3.00	3.15	2.95	2.91
Cold crushing strength (kg/cm^2)	1700	1500	1500	1500	ND*
Thermal expansion (% at 1000°C)	0.65	0.67	0.78	0.57	ND
MOR 1371°C (2500°F), Pa × 10^5	68	82	82	82	109
Major composition (%)					
Al_2O_3	87	90	95	87	
SiO_2	11	8	3	9	
C‡		2–3	2–3	2–3	2–3
Cr_2O_3				3	
MgO					95
Recommended applications	Mild, general	General	Throttling tundish	General, severe	Low C, billet

*ND - No data available.
†Replaces part of Al_2O_3
‡Carbon from tar-impregnated which may be followed by partial coking.

Table XVII. Properties of Typical Higher Carbon Gate Plates

Property	Alumina-Carbon-A	Alumina-Carbon-B	Alumina-Zirconia Carbon
Composition (%)			
Al_2O_3	89–92	68–75	70–75
SiO_2	4–8	3–6	3–5
C	3–6	10–15	7–12
ZrO_2			6–9
Density (g/cm^3)	3.15–3.20	2.70–2.80	3.00–3.10
Porosity (%)	10–12	11–13	9–11

brick, monolithic, and fiber forms. As in many other applications, high-alumina refractories must, however, compete with lower-cost materials. The continued development of refractory systems which may be readily installed and those which can reduce energy are required.

Overall Use of High-Alumina Refractories

While many current factors make projections of total refractory usage in the U.S. steel industry difficult, projections can be made based on a unit (per ton steel) basis. Table XIX presents estimated unit consumptions for 1990 in a fully integrated plant and a nonintegrated (scrap-oriented electric furnace) plant. These figures were estimated based on projected refractory lives in the various processes and represent mean values of plants which might have highly different consumptions depending on many of the factors previously described, such as the type of ladle metallurgy processes and the length of casting sequence. Slag retarders or fettling materials used in steelmaking are not included in these figures. These projected consumption figures are in reasonable agreement with those reviewed by other authors.[25–31]

Table XVIII. Typical Properties of Collector Nozzle

Type	Fireclay	50% Alumina	60% Alumina	80% Alumina	90% Alumina	Zircon/ Fused Silica	Zircon Alumina
Apparent porosity (%)	17	18	18	19	19	18	20
Bulk density (g/cm^3)	2.25	2.35	2.50	2.65	2.85	3.20	3.15
Cold crushing strength (kg/cm^2)	450	550	600	700	700	600	400
Thermal expansion (% at 1000°C)	0.45	ND*	ND	ND	ND	0.35	0.35
Major composition (%)							
Al_2O_3	25	45	60	78	88	3	14
SiO_2	65	50	35	17	9	40	35
C	4†		4†	4†	4†		
ZrO_2						55	48
Cr_2O_3							
SiC	3‡	14‡	12‡				
Recommended applications	Rimmed steel	Killed steel	Killed steel	General	General severe	General	General

*ND = No data available.
†Component only of unburned, resin-bonded alumina.
‡May replace portion of SiO_2.

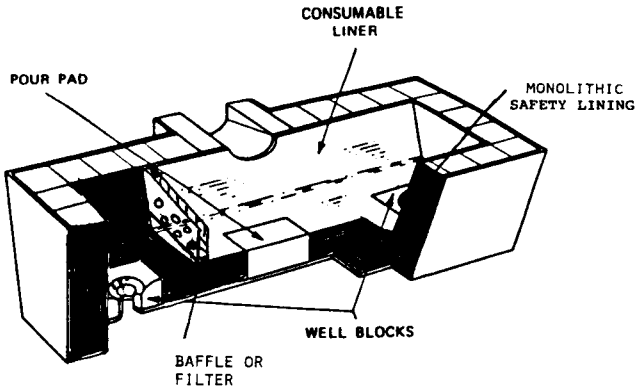

Fig. 37. Consumable liner in tundish for clean-steel practice and to facilitate skull removal.

As shown in Table XIX, refractory unit consumption in a fully integrated plant is similar to that in the nonintegrated plant despite the obvious absence of the coke and ironmaking and treatment processes. This is because of the high refractory consumptions in electric-furnace steelmaking even with the use of water-cooled roofs and wall panels. Reductions in this consumption are expected as improved operating practices are developed. It is important to note, however, that the electric-furnace process would use more basic (and less high-alumina) refractory than the integrated plant.

The nonintegrated plants also may have higher consumptions in some areas (ladle metallurgy, tundish life, etc.). In both of these cases, the assumed processes are the most modern and complex which might either increase or decrease refractory consumptions. (For example, an arc-reheat and all-degassing practice would increase consumption in the ladle, whereas an all-water-cooled electric furnace or a long-casting-sequence caster would decrease consumption in the furnace or tundish.)

Figure 39 shows the downward trend in unit refractory consumption which has occurred from both the significant improvements in refractory technology and the process changes in the past 10 to 20 years. This downward trend is expected to level off in the United States with increased refractory consumption from full adoption of continuous caster and clean-steel practices. Table XX presents a breakdown of the 1990 projected consumption figures by refractory type and form (brick, shape, monolith). Overall, the amount of monolithic refractories projected for the United States is less than for Japan, primarily because the use of fewer castable steel ladles and more board tundish linings are projected to continue in the United States.

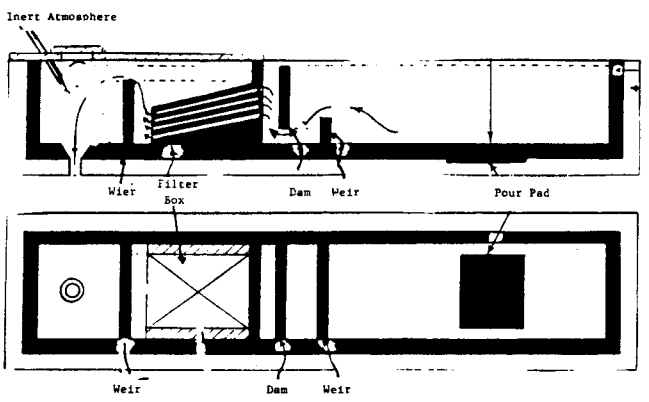

Fig. 38. Use of tundish dams, weirs, and filter box.

Table XIX. Projected U.S. Refractory Usage in Indicated Plant—1990

Area	Consumption (kg/ton) Integrated Plant	Nonintegrated Plant
Coke oven	0.40	
Blast furnace	0.45	
Cast house	2.55	
Hot-metal transfer and treatment	2.25	
Steelmaking	3.05	5–10*
Steel ladles and ladle metallurgy	3.60	4.05
Gates or rods/tubes	0.65	1.05
Tundish	1.25	1.65
Finishing	1.25	1.25
Total	15.45	13–18.00

*Depends on production rate and usage of water-cooled panels and roof.

As shown in Table XX, high-alumina refractories are projected to range from 29 to 50% of the forms used or a weighted average of 38%. On this basis, the projected consumption of high-alumina materials would be some 6 kg/ton for an integrated plant (as previously described this included all high-alumina materials such as bauxite, tabular, fused, synthetic mullite, spinel, calcium-aluminate cement, etc.). The higher quality alumina types (tabular, fused) have a stable future in the more critical refractory components (gates, shrouds) but must continue to compete economically with the lower grade alumina sources and other materials in many other applications.

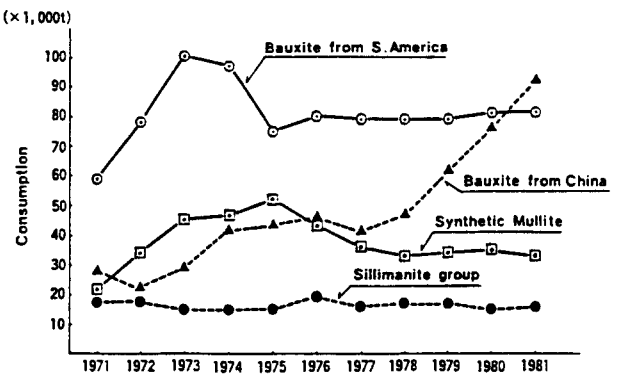

Fig. 39. Transition of consumption for high-alumina raw materials in Japan (Ref. 27) (used by permission) and ladle-to-tundish shroud.

Table XX. Breakdown of Projected 1990 Refractory Usage—Integrated Plant

Refractory Type	Percentage In Indicated Form		
	Brick	Shapes	Monolithic
All	49	15	36
Silica	1	25†	
Fireclay	20		25
High alumina	19	40	30
Al_2O_3-SiC-C	10		20
Burned basic	22		
Magnesia-carbon	25*	2	
Other MgO		23‡	23§
Miscellaneous	3	10	2
Total	100	100	100

*All types including tempered, impregnated, graphite-bearing.
†Mainly fused-silica shrouds.
‡Mainly tundish boards.
§Mainly basic gun mixes.

Table XXI. Breakdown of Projected 1990 Refractory Usage—Nonintegrated Plant

Refractory Type	Percentage In Indicated Form		
	Brick	Shapes	Monolithic
All	41	15	44
Silica		25†	
Fireclay	11		12
High alumina	30	40	21
Al_2O_3-SiC-C		5	
Burned basic	15		
Magnesia-carbon	40*	2	
Other MgO		20‡	65§
Miscellaneous	4	8	2
Total	100	100	100

*Mainly graphite-bearing.
†Mainly fused-silica shrouds.
‡Mainly tundish boards.
§Mainly basic gun materials.

Table XXI shows a breakdown of refractory usage for the nonintegrated plant. In this case, the high-alumina usage ranges from 21 to 45% of the forms used with a weighted average of 28%. On this basis, the consumption of high-alumina materials is some 4 kg/ton. (As previously discussed, more basic materials are used because of the higher relative consumption in the electric furnace proper.)

Further developments are expected in alumina-bearing oxide-carbon refractories to expand their usage, but this expansion may be largely offset by improved component life as this technology is more highly developed. The adoption of labor-saving devices, such as those used in installing ladle or tundish working linings, has been slower in the West than in some other world areas. These adoptions are complicated by labor-management agreements and the shrinking domestic steel market.

Some new demands in iron and steelmaking processes are expected to require new and improved refractories, including those made from high-alumina materials. These new processes include cokeless ironmaking processes and direct-to-size casting processes now under development.

References

[1]Y. Naruse, "Trends of Steelmaking Refractories," *Trans. Iron Steel Inst. Jpn.*, **24** [10] 783–98 (1984).

[2]T. Hayashi et al., "Recent Trends in Refractories Technology of Japan"; pp. 17–29 in IM Refractories Supplement, 1983.

[3]Proceedings Interceram, XXVth International Colloquium of Refractories, Aachen, West Germany, Blast-Furnace Refractories, October 1982.

[4]Ishikawa et al., "Operation Methods and Improved Blast-Furnace Cooling and Lining Techniques for Prolongation of Campaign Life," Nippon Steel Corporation, Aachen Conference, September 1986.

[5]M. Burteaux et al., "Latest Development in Cooling and Refractories of European Blast Furnaces," Aachen Conference, September 1986.

[6]K. Hiragushi, K. Mizutani, and T. Nagai, "A New Approach to Blast-Furnace Stack Linings," *Iron Steel Eng.* **55** [6] 47 (1978).

[7]M. Higuchi, "Life of Large Blast Furnaces," pp. 492–505 in Ironmaking Proceedings, Vol. 37. AIME Publications, Chicago, 1970.

[8]M. Nishi and A. Miyamoto, "Lining Materials and Installation Methods for Blast-Furnace Troughs," *Taikabutsu Overseas*, **6** [1] 26–39 (1981).

[9]H. P. Ruther, "Investigation Into Causes of Wear in the Blast-Furnace Trough System and Measures to Improve the Service Life of the Trough Lining," *Interceram*, Special Issue, 1983.

[10]A. Watanake et al., "Test Results of Refractory Brick for Pig Hot-Metal Pretreatment Vessel," *Taikabutsu Overseas*, **6** [1] 517–18 (1982).

[11]M. Koltermann, "Torpedo Ladle Refractories in West Germany," *Taikabutsu Overseas*, **6** [1] 90–110 (1981).

[12]H. Kyoden et al., "Wear Mechanism of MgO-C Brick for Pretreatment of Hot Metal," *Taikabutsu Overseas*, **5** 13–17 [2] (1985).

[13]R. O. Russell and G. D. Morrow, "Characteristics of Refractories Used in Teeming Ladles, *IISM*, July 1983.

[14]T. Onishi et al., "Improvements of Ladle Refractories in ASGA-SKF Process," 15th Subcommittee Report of Steelmaking Refractories.

[15]J. Stradmann et al., "Dolomite in Secondary Steelmaking Units," U.K. Institute of Refractory Engineers, September 20, 1979.

[16]C. E. Tomazin et al., "The Effect of Ladle Refractories and Practices on Steel Temperature Control," *Steelmaking Proc.*, **69**, 223–30 (1986).

[17]G. Moertz et al., "Vibratable Castables for Ladles and Tundish Linings," *Steelmaking Proc.*, **69**, 215–22 (1986).

[18]L. M. Saunders, "Preheating and Controlling Thermal Cycling of Steel Handling Ladles"; pp. 69–76 in 66th Steelmaking Conference, 1983.

[19]T. M. Bruton, C. F. Cooper, and P. A. Croft, "Microstructures and Performance of Aluminal-Graphite Submerged Pouring Shrouds and Tundish Stoppers," *Am. Ceram. Soc. Bull.*, **60** [7] 709–12, 718 (1981).

[20]G. B. Shaw, "Property Requirements for Submerged Entry Nozzles," Continuous Casting of Steel, Proceedings, International Conference, The Metals Society, IRSID, London, 1977.

[21]C. F. Cooper et al. "The Role of Graphite in the Thermal Shock Resistance of Refractories," *Trans. Br. Ceram. Soc.*, **84** (1985).

[22]G. B. Shaw et al., "New Carbon-Bonded Refractories for the Continuous Casting of Steel," 1986 Steelmaking Proceedings.

[23]B. Brezny et al., "Recent Experiences with Pouring Pit Refractories," *Trans. Br. Ceram. Soc.*, **82** (1983).

[24]K. K. Kappmeyer and J. T. Shaplant, "Flo-Con Sliding Gate Systems for Continuous Casting," *Iron Steel Eng.*, **50** [1] 65–72 (1973).

[25]"Refractory Materials for Steelmaking," International Iron and Steel Institute, Committee on Technology, Brussels, 1985.

[26]P. F. Wieser, "Fundamental Considerations in the Filtration of Steel," *Steelmaking Proc.*, 969–76 (1986).

[27]T. Hayashi et al., "Recent Trends in Refractory Technology in Japan," IM Refractories Supplement, 1983.

[28]"Recent Trends and Outlook for the Refractories Industry in the USA, Japan, and West Germany," *CI News*, Vol. 3 HR 3, September 1983.

[29]P. Schroth, "Refractories for the 1980's—A Look Into the Future"; Minerals in the Refractory Industry, September 12–14, 1982.

[30]R. L. Shultz et al., "Refractories for the Steel Industry—A Diagnosis and Prognosis," ACS Meeting, October 3, 1986.

Petroleum and Petrochemical Applications for Refractories

M. S. Crowley
Amoco Corporation
Naperville, IL 60566

R. E. Fisher
Plibrico Company
Chicago, IL 60614

Refineries and petrochemical plants use a variety of refractory materials, from high-alumina castables to ceramic fiber. The high costs of energy, maintenance, and downtime necessitate a critical selection and application of refractory materials to achieve optimum efficiency. Refining and petrochemical operations, such as fluid catalytic cracking units, naphtha reformers, incinerators, and furnaces subject refractory linings to a variety of aggressive actions, such as erosion, spalling, slagging, and chemical attack. The physical properties of a variety of materials are discussed and units or locations where these properties are needed are outlined. Detailed information is included on selection, installation, curing procedures, and subsequent repair techniques for refractory materials in a variety of applications.

Refractories are construction materials designed to withstand aggressive service conditions at high temperatures. They are generally used as heat-resistant walls, coatings, or linings to protect units from oxidation, corrosion, erosion, and heat damage. The main types include castables, plastic refractories, ceramic fiber, and brick. Each type has advantages and disadvantages related to installation requirements, serviceability, cost, and convenience. For example, refractory concretes that can be cast, gunned, or troweled into place are often the most convenient to use as linings in refinery units, but brick and plastic refractories can sometimes be used to advantage in areas such as incinerators where low porosity and permeability are important.[1-4] Table I lists general types of refractory materials used in refining and petrochemical plants.

Castables

Castable is a general term for refractory concretes composed of an aggregate and a binder. The aggregate usually accounts for 60 to 80% of the volume of the finished product and is generally a prefired mineral product. Broken brick, calcined clay, bloated shale,

Table I. General Types of Refractory Material for C.P.I. Use

	Nominal Density kg/m^3 (lb/ft^3)	Comp. Strength mPa (psi)	Comments
		Castables	
Erosion-resistant	1922–2883 (120–180)	34.5–103.5 (5000–15000)	For cyclones and catalyst lines, need erosion resistance (ASTM C-704) of 10 cm^3 or less.
Dense high strength	1922–2082 (120–130)	20.7–41.4 (3000–6000)	For high-strength vessel and duct lining.
Semiinsulating (one-shot)	1200–1520 (75–95)	6.9–20.7 (1000–3000)	For general vessel, stack, and duct lining.
Insulating	800–1280 (50–80)	3.4–13.8 (500–2000)	For furnace and boiler linings and as a back-up lining.
Chemical-bond mortars	1922–2883 (120–180)	6.9–27.6 (1000–4000)	Both aluminophosphate and silicate-bonded materials are used for patching and rebuilding.
		Plastics	
Chemical bond	1922–2883 (120–180)	6.9–41.4 (1000-6000)	Frequently have good erosion resistance used for patching and rebuilding. Heat sets usually not used because of low temperatures in refining and C.P.I.
		Brick	
Insulating fire (IFB)	480–1280 (30–80)	0.69–6.9 (100–1000)	Used in furnaces and as back-up lining.
Dense firebrick	2080–3200 (130–200)	27.6–82.8 (4000–12000)	Available as working lining in high-abrasion areas.
		Ceramic Fiber	
	64–38.4 (4–24)		Available in blanket, module, and spray-on form.

and expanded volcanic ash are the most commonly used aggregates. Very expensive aggregates, such as silicon carbide or tabular alumina, usually are used only in special applications where severe service conditions preclude the more conventional types. The physical properties of the finished castable are the result of the combined effects of the aggregate and the binder. The aggregate type usually controls the density, the strength, and sometimes the upper temperature limit. The binder and aggregate together control such properties as thermal expansion, firing shrinkage, erosion resistance, and chemical resistance. Castables can be placed by conventional concrete placement techniques such as casting or gunning. Recent technical advances have produced "low-cement" castables which possess improved physical and mechanical properties, especially at high temperatures.

A new concept in castable technology is incorporation of stainless steel fiber into the material.[5,6] The function of the fiber is to (*a*) redistribute the drying and firing stresses so that a network of fine cracks is developed instead of a few large cracks and (*b*) to retain the fractured pieces by bridging the cracks so that all of the lining stays on the wall.

The binder may be a hydraulic type like portland or calcium aluminate cement, or it may be a chemically or thermochemically setting type like the silicates or phosphates. Few heat-setting materials can be used in refineries because of the high temperatures required for setting. Most binders are hydraulic types that use iron-containing calcium aluminate cements. There are also iron-free calcium aluminate cements that are used in ultraformers and other areas where iron would interfere with the process reaction. The hydraulic cements work by reacting with water to form hydrated calcium aluminate phases that set into a rocklike mass.

The chemical binders can be divided into the alkali silicates and the aluminophosphates. The alkali silicates set by polymerizing the silica into a rigid network. The polymerization may be due to dehydration, as in the air-setting types, or to an internal condensation reaction, as in the chemically setting types. The aluminophosphates are thermochemically setting and require a temperature of about 232°C (450°F) to start the reaction:

$$Al_2O_3 + 6H_3PO_4 \rightarrow 2Al(H_2PO_4)_3 + 3H_2O \qquad (1)$$

The final set is completed at about 343°C (650°F) when the aluminophosphate is converted to $AlPO_4$:

$$Al(H_2PO_4)_3 \rightarrow AlPO_4 + 3H_2O + P_2O_5 \qquad (2)$$

Plastic Refractories

Plastic refractories can be thought of as "firebrick before being fired" since they, like brick, are usually composed of a highly calcined clay aggregate with a binder of raw plastic clay. The term "plastic" is used because the material is workable, although very stiff, and usually is placed with an air hammer. The air-setting plastics may incorporate an alkali silicate or some other binder to achieve a hard surface before firing, but the primary bond is usually a true ceramic bond developed in the clays at service temperatures in excess of 982°C (1800°F). Because of the high temperatures required for bond development, most heat-setting plastics can be used in only a limited number of areas in the average refinery—for example, on furnace burner walls, particularly around the burner ports, or in incinerators where temperatures may exceed 1315°C (2400°F). Phosphate-bonded plastics have about the same room-temperature strength as air-setting plastics and develop considerable mechanical strength after drying at 110°C (230°F).

Refractory Brick and Special Shapes

Refractory brick, block, and special shapes are prefired items composed of an aggregate and a binder, often of clay. They are commonly used in furnaces and heaters as roof tile, burner blocks, and floor plates. There are many types of firebrick, but usually only insulating firebrick (IFB) and high-alumina or superduty fireclay brick are used in a refinery or chemical plant. Occasionally, chemical or physical service conditions, such as found in incinerators, call for aluminophosphate or alumina/chrome refractory brick. The possibility of hexavalent chrome compounds in used refractories, especially those exposed to alkalies, can have serious health consequences relative to the safe removal and disposition of such used refractories.

Silicon nitride-bonded silicon carbide has been used in the past as an erosion-resistant liner for slide-valve throats for fluid catalyst cracking units. However, mullite-bonded materials appear to be a better choice for long-term volume stability in regenerator atmospheres since the silicon carbide will slowly oxidize to silica in a high-temperature steam atmosphere with a net volume increase, resulting in disruption of the piece.

Ceramic Fiber Refractories

Ceramic fiber refractories can be used in both modular and fiber wall (wallpaper) designs. Modules are made by a variety of manufacturers[7] and are designed to keep the metal anchor components near the cool side. Most modules are fastened to the shell by welding or bolting an anchor system that retains a folded strip of ceramic fiber blanket. Older modules were made by adhering strips of fiber to a backing plate using high-temperature mortar.

Originally, the modules were 0.93 m^2 (1 ft^2) in area. Recently, new modules of 0.37 m^2 (4 ft^2) (and even larger in some cases) have been used successfully in furnaces. The modules appear to be gaining in popularity because the anchor system is protected from oxidation and fiber shrinkage is accommodated by precompression of the blanket before installation.

Fiber wall is a combination of layers of refractory fiber felt or blanket impaled on pins which have been

welded to the wall. Generally, a layer of low-cost mineral wool block is placed on the pins first to reduce the required thickness of the more expensive ceramic fiber. Fiber wall design is an acceptable approach in lining furnaces and other heat enclosures when the operating conditions are moderate. Temperature limits are 1093°C (2000°F) for most of the materials but several are usable up to 1427°C (2600°F). The higher temperature materials are more expensive than the conventional forms; hence, each job should be engineered with proper materials to ensure optimum results.

The primary advantages of this type of refractory system stem from its construction, i.e., a flexible, low-thermal-mass, easily installed blanket with outstanding insulating value. Correctly installed systems are virtually maintenance-free. Units with new fiber wall construction can be brought on-line quickly without preliminary thermal or hydraulic cure periods. Its primary disadvantage is its inability to resist erosion under high-velocity (15.24 m/s (50 ft/s)) gas movement. In some cases where entrained particulate matter is present, velocities above 3 to 4.5 m/s (10 to 15 ft/s) are considered unacceptable. A second disadvantage is the typical oxidation of the anchor pin and speed clip used to retain the blanket. In some cases, ceramic "cup locks" can be used at the hot face, thus greatly reducing the oxidation of the retaining pin.

A new approach to the "wallpaper" concept is being offered by a number of manufacturers. In this system, a semirigid board of high-temperature ceramic fiber is used as the hot-face material. Ceramic cup locks are used to retain the board in place. Backup material is ceramic-fiber blanket of appropriate density and thermal capability in a design based on a computer program that optimizes overall efficiency. The board is claimed to resist gas velocities of 30 m/s (100 ft/s). Essentially no particles can be in the gas stream if the board is to resist erosion.

Recently, a spray-applied ceramic-fiber system was introduced; it can be used directly over steel, brick, or castable surfaces. It is claimed to have superior refractoriness and excellent adhesion. The binder appears to soak into the fiber spray and develop significant strength. Such a fiber coating has the additional advantage of being a better hot-face insulation than fiber blanket, block, or modules when heat transfer by radiation is the dominate mode. Its higher density reduces the "wide-open spaces" which produce high heat transfer above red heat in modules, block, etc.

Properties of Refractories

Castables make up the bulk of refractories in refineries and chemical plants, so their properties are emphasized here. After firing under service conditions, many of the castables' properties are similar to those of brick or fired-plastic refractory materials. Many of the physical properties of castables are significantly improved by the addition of stainless steel (SS) fibers. In the unfired state, the SS fiber acts like a multitude of small reinforcing bars and significantly improves flexural and compressive strength. During heat-up, the SS fiber expands uniformly as a function of the temperature and the type of alloy. Castables shrink in the 149° to 371°C (300° to 700°F) range because of the collapse of the calcium aluminate hydrate structure. The dual actions of shrinkage of the matrix and expansion of the SS fiber result in all the fibers being disbonded after firing. Thus, when flexural stresses occur, no load is transferred to the fiber so no improvement in flexural strength is observed.

Strength

The strength of a castable, which is determined primarily by the type and amount of aggregate and cement, is often cited as an index of quality. Table I gives the range of expected values for density and strength of the most widely used concretes.

Most refractory concretes are very brittle, and values for their modulus of rupture (MOR) are about 20 to 30% of their cold crushing strengths. The tensile strength is typically about 10% of the compressive strength. Although high compressive strengths are seldom required in most refinery applications, a high value for this property often indicates good erosion resistance. Also, thermal shock resistance is partly related to strength, so the stronger castables have better shock resistance. Low-cement castables are generally less brittle than conventional castables and thus retain more of their strength when exposed to thermal shock. The impact resistance of most refractory concretes follows the flexural strength value. Stainless steel fiber significantly improves the toughness of castables.

The cold crushing strength of a castable refractory is dependent on the quality of the hydraulic bond at temperatures below about 816°C (1500°F). Above this temperature, the strength generally starts increasing as the degree of true ceramic bonding increases. The hydraulic bond is developed in the first few hours after the castable is mixed with water and is the result of the interaction of the cement and the water. Figure 1 shows the temperature increase associated with the cement/water interaction and indicates that both the standard and the high-purity aluminous cements have reacted to form a hydraulic bond within six hours. This bond will start to break down at about 149°C (300°F), and the castable should reach a minimum cold-strength value at 538° to 760°C (1000° to 1400°F). Hot MOR measurements suggest that there is little or no loss of hot strength in this temperature region. In many cases, especially low-cement castables, they actually show an increased strength.

Thermal Conductivity

Figure 2 shows the effect of the mean temperature on the thermal conductivities of a variety of concretes[8]

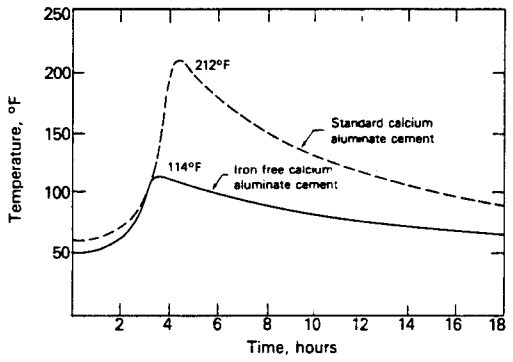

Fig. 1. Temperature increase of gunned sections of refractory concrete.

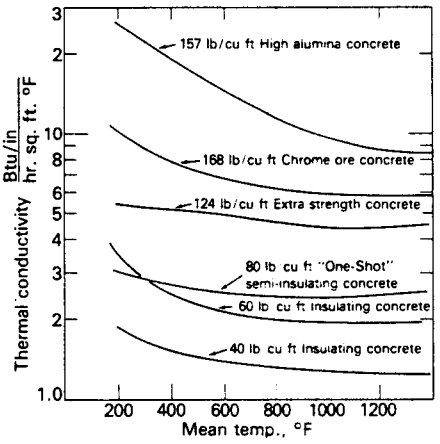

Fig. 2. Thermal conductivities of refractory concretes after 110°C (230°F).

that had been dried at 110°C (230°F). As dehydration of the hydrated cement phases continues with increasing temperature, the density and thermal conductivity decrease. The relationship of density and thermal conductivity is shown in Fig. 3. which plots the results of a large number of runs using a variety of refractory concretes.[9] Low-cement castables usually have higher thermal conductivities than might be expected from their density. This phenomenon is due to their more highly developed crystalline matrix. In general, the curves of Fig. 2 are more useful in refinery applications because they give data on concretes in various stages of dehydration just as we would expect to find them. The curves of Fig. 3 are based on samples that had been prefired on one face to temperatures in excess of 982°C (1800°F).

The effect of high-conductivity gases such as hydrogen on the thermal conductivity of refractories[10] is also shown in Fig. 3. The insulating concretes with a low bulk density (640 to 1280 kg/m^3 (40 to 80 lb/ft^3))—and, consequently, a high ratio of hydrogen-filled pores to solid-phase material—show a 200 to 300% increase over the conductivity in air; but the denser concretes (1920 kg/m^3 (120 lb/ft^3)) with fewer

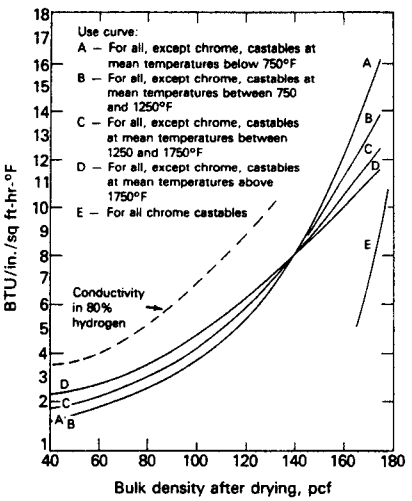

Fig. 3. Curves of thermal conductivity vs dried density for dense refractory, lightweight, and chrome castables. (Data assume that all materials have been fired on one face to 38°C (100°F) below their maximum service temperature, or 1316°C (2400°F), whichever is lower.

pores showed only a 50% increase in the thermal conductivity when tested in a hydrogen atmosphere.

Thermal Expansion

The initial thermal expansion or shrinkage of refractory concrete results from the opposing actions of heat in (*a*) expanding the aggregate and (*b*) dehydrating the hydrated cement phase. Figure 4[11] shows the sine wave curves resulting from heating various mixtures of calcium aluminate cement and water to

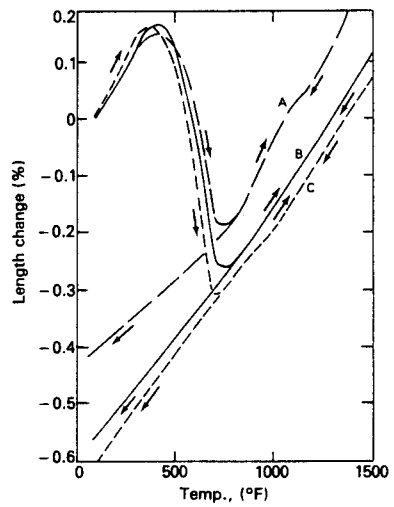

Fig. 4. Initial expansion curves for neat Lumnite with varying water contents (A) 16.7%; (B) 20%; and (C) 25.9% water. Heating rate: 167°C/h (300°F/h) to 538°C (1000°F), and 111°C/h (200°F/h) from 538° to 816°C (1000° to 1500°F).

816°C (1500°F). The sample expands up to about 177°C (350°F), where the hydrated cement starts to lose its water of crystallization. This water loss causes shrinkage, which continues until a "condensed state" is reached at about 399°C (750°F). At this point, the normal thermal expansion resumes and continues with increasing temperatures until the test temperature of 816°C (1500°F) is reached. When cooled, the sample retraces the final part of the expansion curve and continues in an approximately straight line until it reaches room temperature. Subsequent reheating of the sample will cause it to retrace the cooling curve. The thermal expansion value given in most manufacturers' literature is the slope of the reheat curve and does not take the initial expansion characteristics into account. Figure 5 shows the initial expansion curve for pure calcium aluminate cements.

The effect of adding an aggregate to calcium aluminate cement is seen in the thermal expansion curves of Fig. 6. When enough aggregate is added, the cement dehydration effect is reduced to the point where the initial expansion curve does not exhibit any shrinkage, as shown in curve A. Curve B is for the concrete richer in cement than concrete A and illustrates the typical sine wave curve. Figure 7 shows the thermal length changes observed with four common refractory castables. All of the curves show the expansion-contraction-expansion curves typically obtained with a recording dilatometer. Recent reports from the British Ceramic Research Association[12] indicate that wall sections do not behave as dilatometer specimens do when heated. Figure 8 shows the effect on thermal expansion of heating a section of wall on one side. The expansion curve does not have a significant shrinkage in the 177° to 399°C (350° to 750°F) range because the material on either side (i.e., hotter and cooler segments) is strong enough to prevent the dehydration zone from shrinking.

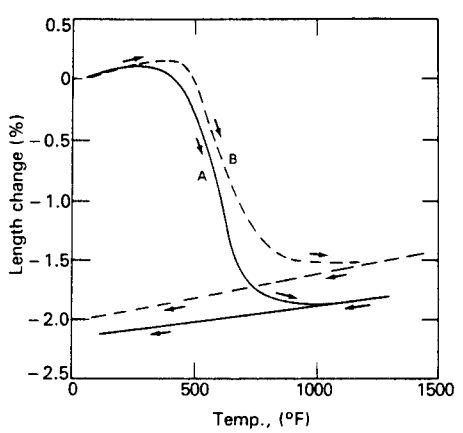

Fig. 5. Effect of heating rates on the initial thermal expansion of neat, pure calcium aluminate cement; (A) 83°C/h (150°F/h); (B) 167°C/h (300°F/h).

In practice, as the lining heats, the hydrated cement structure starts to collapse and shrinkage cracks appear in the hot face. As heating continues,

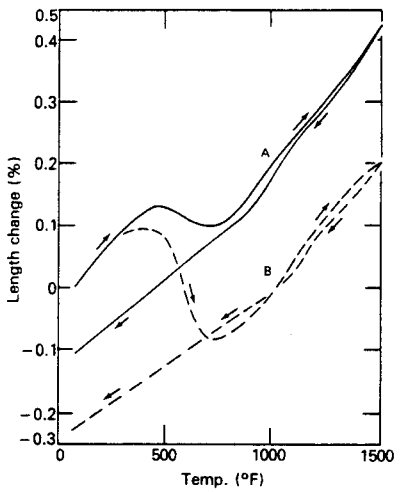

Fig. 6. Initial thermal expansion curves for perlite concretes containing Lumnite cement; (A) 47% cement; (B) 67% cement.

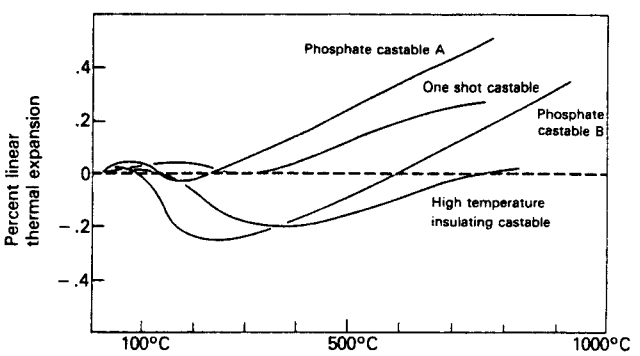

Fig. 7. Initial thermal expansion curves of various materials.

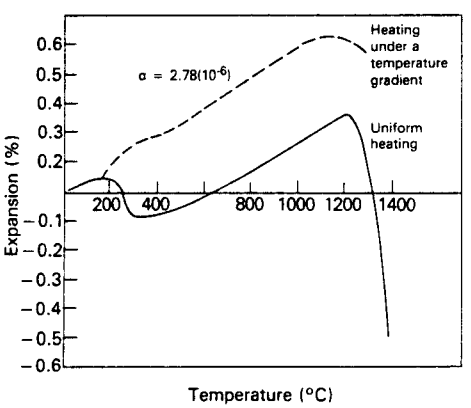

Fig. 8. Comparison of the thermal expansion measured under a temperature gradient with that measured isothermally.

thermal expansion in the midsection of the lining exerts compressive stresses on the hot face and it undergoes enough plastic deformation (i.e., creep) to relieve the stress. Continued heating causes additional expansion and stress adjustment by creep. When cooled, the hot face cracks open up because there is no residual stress to cause them to close. Physical restraint, as a result of anchoring or construction techniques, can exaggerate creep and lead to more extensive and larger cracks in a castable surface. At room temperature, a network of fine cracks with a few medium cracks is seen on the hot face if SS fiber was used in the lining. Without the fibers, a much coarser network of big cracks would be seen in the hot face.

Thermal Spalling

Thermal spalling is the fracture or breakage of refractory material resulting from excessive stresses caused by a sudden temperature change. The stresses arise from unequal rates of expansion and contraction caused by very rapid heating or cooling, but sudden cooling, e.g., cold water sprayed on a hot refractory, is the most common cause.

A laboratory study of the thermal shock resistance of a variety of refractory concretes showed that fused silica-based concretes had the highest resistance to cracking in a 871° to 21°C (1600° to 70°F) water-shock cycle. High-strength phosphate cement-bonded concretes in general had good resistance, but alkali silicate or mixed cement/alkali silicate patching materials did not stand up well. This study, plus previous laboratory work, suggests that areas where the refractory material is subjected to thermal spalling can be repaired most effectively by using fused silica-based materials. Concretes bonded with iron-free calcium aluminate cements were much more shock-resistant than those bonded with calcium aluminate cements containing iron.

Refractory bricks are much more susceptible to thermal shock damage than castables or plastic refractory because of the higher rate of thermal expansion usually associated with the high degree of vitrification often found in high-fired brick. In addition, castables and plastic refractories have greater toughness because of the heterogeneous nature of the bonding and the reduced brittleness. The brick with the greatest resistance to spalling generally will have low average thermal expansion rates and high thermal conductivities to ensure minimum temperature gradients.

The use of SS fiber is often beneficial in areas of severe thermal shock because the fiber tends to act as a crack arrester and thus reduces the depth of the crack. In addition, the fibers bridge the gap between pieces and thus hold the entire section together.

Repeated thermal cycling has the same effect as sudden thermal shocks in breaking up a lining by fracturing and moving segments as a result of thermal expansion.

Erosion Resistance

Erosion is the wearing away of material by the cutting action of entrained particles in a high-velocity stream. The current test (ASTM–C704) uses 1000 g of No. 36-grit silicon carbide to erode a hole in a test sample that is approximately 10 by 10 by 2.5 cm (4 by 4 by 1 in.) or 5 cm (2 in.) thick. The weight loss from the test is converted to a volume loss that is a direct measure of the size of the eroded hole.

Erosion resistance is strongly dependent on the porosity of the material, e.g., fired vs unfired, and only slightly correlates with strength. An unfired phosphate-bonded alumina refractory may have two or three times the erosion resistance of an identical sample that has been fired to 677°C (1250°F) and thus is more porous due to dehydration. Erosion resistance and compressive strength do show a reasonable correlation in the weak to moderate strength category, i.e., 6.9 to 41.4 MPa (1000 to 6000 psi). However, there appears to be little or no correlation of erosion resistance with compressive strengths in the 41.4 to 82.8 MPa (6000 to 12 000 psi) range. Porosity decreases due to factors such as coke and catalyst deposition in FCCU feed lines have resulted in conventional refractories with exceptional erosion resistances.

Aggregate sizing and strength also play a part in developing superior erosion resistance. Very hard grains, e.g., alumina and fused mullite, offer better erosion resistance than calcined clay or expanded shale. Very close sizing of grains that allows low cement levels (6 to 10%) with high strengths has resulted in some hydraulic cement-bonded castables with excellent erosion resistance.

Steam Effects on Refractories

Extended periods of steaming are encountered in start-ups, purging, and in some temperature-control situations. Hydraulic cement-bonded refractories do not appear to be harmed by long periods (six days) of exposure to flowing saturated steam. In fact, test samples showed strength increases of 10 to over 50%, depending on the type of binder and aggregate. It appears that saturated steam is able to penetrate the cement matrix and hydrate any unreacted grains, thus increasing the bonding phase and decreasing the porosity.

Aluminophosphate-bonded refractories, which are used in severe erosion areas or where very severe temperature swings may be encountered, are subject to loss of the bonding phase in flowing saturated steam. Even in cases where the refractory has been fired overnight to 427°C (800°F), heat-setting phosphate-bonded alumina refractories have shown almost a complete loss of strength. Figure 9 shows the effect of 16 hours of flowing steam on two heat-setting and three air-setting aluminophosphate refractories. The flowing steam had little effect on the air-set aluminophosphates but almost destroyed the heat-set materials unless they had been prefired to temperatures

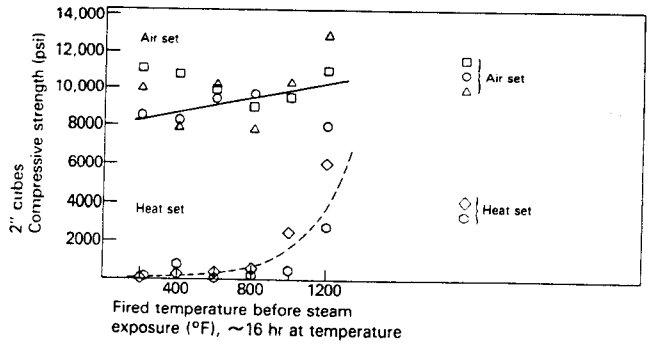

Fig. 9. Effect of prefiring on steam deterioration of aluminophosphates.

above 538°C (1000°F) before the steam exposure. Tests on the air-set materials in flowing steam for six days indicate that, in that length of time, even the air-set refractories start to lose strength and integrity.

Figure 10 plots the compressive strength of two heat-setting aluminophosphates as a function of how long they had been exposed to steam. Prefiring the materials to 204°C (400°F) did not result in a permanent bond and the initial hours in steam caused an almost complete loss of strength. The materials that were prefired to 316°C (600°F) retained approximately one-half their strength after four hours of steaming and showed about 25% of their original strength after 16 hours of steaming. This study suggests that, if heat-setting aluminophosphates are used in a unit, steam exposure should be kept as short as possible, i.e., one shift or less, and preheating before the start of steaming should be as high as possible, preferably above 316°C (600°F). Dry (superheated) steam does not appear to be harmful to phosphate-bonded refractories.

Most alkali silicate-based refractories, e.g., brick mortars, are susceptible to steam attack by dissolution of the bond in the uncured state. Heating to temperatures above 538°C (1000°F) or acid-washing the material results in the precipitation of silica from the sodium silicate bond. The precipitated silica is relatively insoluble in steam atmospheres.

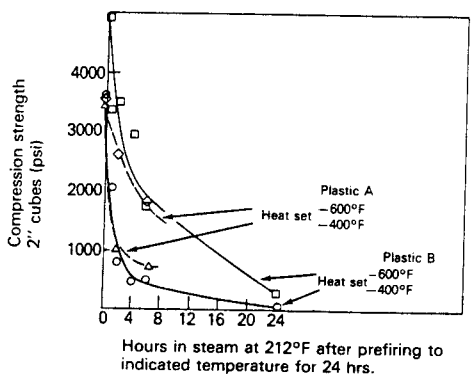

Fig. 10. Effect of steam on strength of aluminophosphate refractories.

Chemical Resistance of Refractories

Refractories are normally selected for use on the basis of their erosion resistance or insulating value. On occasion, however, some chemical resistance may be required. Seal pots will subject the bottom refractories to months of soaking in water that can range from acidic to basic. Condensing flue gases will result in the refractories being attacked by sulfuric acid. Table II shows the effect of various acids and sodium hydroxide on a variety of refractories.

Fired and unfired samples, which averaged in size 1.27 by 2.5 by 5 cm (½ by 1 by 2 in.), were totally immersed in six different acid solutions and one caustic solution for periods of from one day to two weeks. All fired samples were heated to a minimum of 649°C (1200°F) for 16 hours, and unfired samples were air-dried for a minimum of three days. The solutions were held at room temperature and changed three times per week. The results shown in the tables were derived from visual observations only. Loss of strength in apparently good samples was not measured for these tests.

In analyzing the results, it appears that the chemical resistance of the various types of refractories tested are as follows:

1. Phosphate bonds showed fair to poor chemical resistance to both acids and caustic except for acetic.
2. Iron-free calcium aluminate cements showed poor resistance to acids but do well in caustic.
3. Standard calcium aluminate cements showed fair to poor resistance to acids but do well in caustic. Appear good in 1% sulfuric acid.
4. Fired samples of silicates have good resistance to both acids and caustic. Unfired samples do not have good caustic resistance.

Initial Refractory Installations

Design Considerations

The complete design of monolithic refractory vessel and duct linings is beyond the intended scope of this paper, but a simplified method of calculating the approximate temperature gradients, strains, and stresses in single-layer linings is available in the literature.[13] This method is also useful in designing stacks, circular flue ducts, and other installations involving similar refractory linings.

The Department of Energy (DOE) has sponsored several studies on refractory linings for coal gasifier vessels.[14,15] These studies may be consulted for an extensive computer-oriented analysis of the interactions between refractory concrete linings, anchorage, and the shell.

A study of the design strength of refractory concrete linings has been completed that permits calculating the breaking strength of a lining as a function of the thickness and type of concrete, type and spacing of anchorage, and the SS fiber content of the mix.[16] Table III gives the equation and the parameters needed to

Table II. Effect of Acids and Caustic on Refractories (Total Immersion)

	Phosphate bond (air-set)		Phosphate bond (heat-set)	Standard bond calcium aluminate		Iron-free bond calcium aluminate		Alkali Silicate	
	Fired	Unfired	Fired	Fired	Unfired	Fired	Unfired	Fired	Unfired
10% Acetic									
1 Day	1	1	1	2	2	4	2	1	1
5 Days	1	1	1	3	2	5	2	2	1
14 Days	1	1	1	4	3		3	2	1
10% Sod. Hydroxide									
1 Day	1	2	2	1	1	1	1	1	3
5 Days	5	5	5	1	1	1	1	1	5
14 Days				1	1	1	1	1	
10% Nitric									
1 Day	3	5	1	5	5	2	5	1	1
5 Days	5		1			5		1	1
14 Days			1					1	1
10% Phosphoric									
1 Day	3	5	2	3	5	2	5	1	1
5 Days	5		2	5		3		1	1
14 Days			3			4		1	1
10% Hydrochloric									
1 Day	4	4	1	3	5	2	5	1	1
5 Days	5	5	3	5		3		1	1
14 Days			4			5		1	1
10% Sulfuric									
1 Day	5	4	1	2	1	3	2	1	1
5 Days		5	2	3	3	5	3	1	1
14 Days			2	3	4		5	1	1
1% Sulfuric									
1 Day	2	1	1	1	1	1	2	1	1
5 Days	3	2	3	1	1	2	2	1	1
14 Days	4	2	4	1	1	2	2	1	1

1. No apparent attack.
2. Slight attack.
3. Medium attack.
4. Severe attack.
5. Complete destruction.

Table III. Model of Lining Design Strength

Concrete	Anchor	b_0	b_1	b_2	b_3	b_4	b_5
Phos bond	Steer horn	8.98	0.888	−0.142	−0.049	0.0424	0.126
	S Bar*	8.59	0.88	−0.142	0.134	0.0424	0.126
	Twist lock	8.73	0.88	−0.142	0.134	0.0424	0.126
	Chain link	8.35	−0.301	−0.142	0.134	0.0424	0.126
One-shot	Steer horn	6.56	0.888	−0.142	−0.001	0.0424	0.126
	S Bar	7.69	0.888	−0.142	−0.001	0.0424	0.126
	Chain link	7.93	−0.301	−0.142	−0.001	0.0424	0.126
Insulating	Steer horn	5.91	1.683	−0.142	−0.001	0.0424	0.126
	S Bar	6.52	0.888	−0.142	−0.001	0.0424	0.126
	Chain link		6.58	−0.301	−0.010	0.0424	0.126

Ln (load) = b_0 + b_1 (ln thickness) + b_2 (spacing) + b_3 (fiber content) + b_4 (ln thick) (spacing) + b_5 (ln thick) (fiber content)
Example test block No. 8 (one-shot concrete, 4 in. thick, S Bar anchors on 12-in. spacing, 4% SS fiber)
Ln (load) = 7.69 + 0.888 (ln 4) + (−0.142) (12) + (−0.001) (4) + (0.0424) (ln 4) (12) + (0.126) (ln 4) (4)
Ln (load) = 8.6169 calculated load = 5524 lbs.; measure load = 5580 lbs.
*Barrett Mfg. Co., Houston, TX.

calculate the strength of the wall as a function of the design conditions. Usually the thickness is determined by thermal requirements and 3 to 4 wt% SS fiber is used in most mixes. Therefore, the anchor spacing can be calculated for a given design strength.

The design of furnaces, incinerators, and similar "prepackaged" units is usually in the hands of the supplier with, perhaps, an approval of materials by the purchaser. Most proprietary materials will perform satisfactorily in the service for which they were intended, but frequently the manufacturer of prepackaged units wants to install a field-mix material to save money. A widely used refractory field mix for furnaces, stacks, and similar applications is made with 1 part

(vol) calcium aluminate cement, 2 parts expanded shale, and 4 parts expanded vermiculite. Such materials are very weak because of their low cement content and are not recommended for use. The addition of another 50% cement results in a lightweight material with adequate physical properties. A better approach would be to specify ceramic-fiber modules for the lining. Stainless steel sheets can be used in front of the modules if nut blasting is going to be used to keep the tubes clean.

Preparation of Vessels

Most new units are lined in the field because of size and weight limitations in handling the component parts. Occasionally small vessels, components, or pipe sections will be shop-lined to ensure a better job, especially with critical service parts like cyclones. Previously, it had been considered necessary to sandblast the shell to ensure good adherence of the refractory concrete to the steel. The current practice calls for sandblasting only when the vessel interior is exceptionally dirty, oily, or contaminated. It has been shown that sandblasting increases the adherence of refractory concrete to steel at temperatures up to 149° to 204°C (300° to 400°F). However, if the base-metal temperature exceeds 204°C, the differential thermal expansion stress will usually cause the concrete to break loose from the steel.

A tight bond of the concrete to the steel is not needed if the lining is designed so that it is in compression at operating temperatures. If the lining is not held tightly in compression against the shell in areas involving a pressure drop (e.g., grid ledges and fluidized bed zones), gas bypassing between the shell and the lining can cause hot spots on the shell. The presence or absence of a sandblasted surface would make little difference in such a case.

Sandblasting is an effective way to clean dirty or oily surfaces, especially for repair work on old vessels; but it should be remembered that the main bonding mechanism stems from good anchorage rather than adherence of the concrete to the steel. Mechanical cleaning or wire brushing of the surface with solvent wiping of oily areas is often adequate surface preparation for reasonably clean vessels.

Anchorage

Good anchorage is the only way to ensure that the lining remains tight against the shell. Research studies have shown that the most effective type of anchor for 7.6 to 10.2 cm (3 to 4 in.) thick refractory concrete linings is an independent unit that holds effectively, preferably at two different depths in the lining. A new concept in anchoring is the S Bar*, which combines the erosion protection of hexsteel with the independent anchorage of longhorn anchors. The S Bar is used full depth with the top edge flush with the hot face. The metal edge casts a "shadow" of protection for the brittle refractory behind it. Because they are independently welded, the S Bars cannot fail in sheets the way hexsteel does in severe thermal cycle service. Another patented anchor for monolithic refractory construction, the TACKO anchor† has similar advantages of independent welding and can be walked on without bending.

Both the S Bar and "longhorn" anchors have been used extensively to hold vessel linings in place. The S Bar has greater holding power but it is slightly more expensive than the longhorn. In addition, the S Bar can throw a shadow when gunning in confined areas. Therefore, hand packing or the use of longhorns may be required to avoid trapped rebound. When installing S Bars in vessels, the anchors should be aligned vertically rather than horizontally to minimize rebound accumulations on the anchors.

A coating of grease, asphalt, or wax is usually recommended for individual anchors to prevent cracking of the concrete when the lining is heated. The coatings will melt or burn out, leaving enough space to accommodate the thermal expansion of the anchor without decreasing its effective holding power. Table IV lists unit corrosion rates for a variety of alloys in typical CPI atmospheres.

Installation of Refractory Concrete

The primary methods of placing refractory concrete are gunning, casting, and hand packing. Pneumatic gunning is the most common and often the best way of placing refractory concrete. Optimum properties frequently can be obtained because gunning permits the minimum amount of water to be used. In fact, an excess of water in gunning will cause the material to slump and run off of vertical or overhead surfaces, while the same amount of water in a cast section will simply result in a very weak porous material.

One of the most important advances in gunning technology is shown in Fig. 11, which plots the bulk density (after firing to 538°C (1000°F)) of an insulating refractory concrete as a function of predampening water. Most refinery applications use a "dry-type" concrete gun such as the Allentown cement gun, in which the concrete is charged in the dry state and the mixing water is added at the nozzle as the dry material is blown through a hose. Predampening involves adding some of the water to the concrete before it is put in the gun. A mortar mixer or an inclined screw with a series of water jets is often used for predampening. If approximately one-half of the total water required is added beforehand, the rebound loss can be reduced from 25 to below 10%, while the strength and uniformity of the lining are increased. Predampening also decreases dusting and thus permits the nozzleman to see better and control the placement of the concrete with greater accuracy.

*Barrett Mfg. Co., Houston, TX.

†Plibrico Japan, Tokyo.

Table IV. Unit Corrosion Rates of Alloys

Oxidation		Carburization 982°C (1800°F)	Carburization 1093°C (2000°F)	Sulfur 1093°C (2000°F)	Sulfur 816°C (1500°F)	Sulfur and Carburization 816°C (1500°F)	Sulfur and Carburization 982°C (1800°F)	Nitride 538°C (1000°F)	Cl_2	Red	Hydrogen 760°C (1400°F)	Hydrogen 538°C (1000°F)	H_{2S} 538°C (1000°F)	V_{2O5} 982°C (1800°F)
Carbon Steel	538°C (1000°F)										232°C (450°F)			
*430	871°C (1600°F)	Poor	3.1	Poor	2	3.4	16.8	15		2.5	3.2	1.1	2	
*304	1037°C (1900°F)	Poor		25	4	3.9	16	10	316°C (600°F)	2	1.2	1	2	
*446	1204°C (2200°F)	3.5	1.8	1	1	1	1	19		1	15	1	1	1
*310	1149°C (2100°F)	1	1.8	2	1	1.4	1.8		316°C (600°F)	1	1	1	1	
*330	1204°C (2200°F)	4	1	24				1	1	Poor			Poor	
409	704°C (1300°F)	Poor	Poor	Poor	3	4.0	20.0	13		7	3.0	1.1	4	
309	1093°C (2000°F)	6	2	2	1	1.4	3.4	4		1	1.3	1	1	

*Steel fibers available in these alloys.

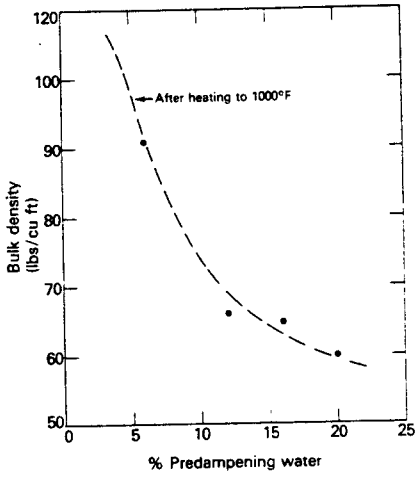

Fig. 11. Effect of predampening on the bulk density of an insulating refractory concrete.

In the past, relatively little casting has been done in refineries and petrochemical plants because of the lower strength and other physical properties usually associated with cast materials, which contain significantly more water than gunned linings. Recently, a new technology called vibration casting has been developed that appears to offer superior results, especially in small-diameter lines. The castables are specifically designed for this method of placement and are critically gap-sized with a low cement content. Very low water contents are used and additives are typically used to promote flow.

Erosion and strength tests on the vibratable castables appear promising. At the present time, no definitive statements or guidelines can be given on the merits of vibration casting. S Bar anchors are not recommended for vibration casting because of the possibility of void formation behind the anchor.

Curing

Curing involves keeping the fresh concrete wet enough to allow time for hydration. Previous practice has been to spray the surface with a light film of water for 24 hours. It was also thought that keeping the concrete cool was necessary in order to develop maximum strength. Recent studies have shown that the best strength is obtained when the concrete is membrane-cured at temperatures above 21°C (70°F), the temperature at which the high-strength hydrated calcium aluminate phase C_3AH_6 starts to form from the cement/water paste. Figure 12 shows the improvement in erosion resistance when various concretes are membrane-cured.

Conventional concrete curing membranes can be used with satisfactory results. Cut-back asphalt coatings have been used, but their inherent messiness on tools and clothes makes them a poor choice for most applications where workmen are liable to bump into them.

In addition to producing better concrete, curing membranes save money by requiring less time to be

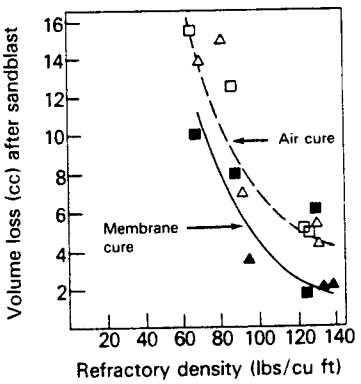

Fig. 12. Effect of air cure vs membrane cure on the erosion resistance of various refractory concretes.

spent on the curing process, allowing more effective inspection of the cured surface and permitting faster close up of units. Once the membrane is applied and the surface has been examined for complete coverage, the scaffolding can be removed and the vessel prepared for service while the concrete is curing.

Most phosphate-bonded aluminas are cured by heating to 343°C (650°F) or higher. Several air-setting phosphate-bonded materials are somewhat unique in that they develop an excellent bond at room temperature and maintain their strength up to their upper temperature limit of 1649°C (3000°F).

The application and curing of refractory concrete in the winter has special problems because of the danger of freezing. Studies have shown that the concrete must be kept above 10°C (50°F) for at least one day in order to develop maximum strength.[17] If fresh concrete is frozen before it has a chance to hydrate, the result will be a weak material with little or no coherence. If the concrete is allowed to membrane-cure at 10°C (50°F) or higher for a day, subsequent freezing cycles will not harm it even if it has not been thoroughly air-dried. Figures 13 and 14 show compressive strength developed with time on cool days.

Heating Rates on Start-Up

A study of the effect of curing temperature on explosive spalling showed that, with explosion-prone cement-bonded castables, hydraulic curing at 21°C (70°F) or higher resulted in a concrete that was not subject to explosive spalling.[18] At 21°C or higher, the cement forms C_3A_6, the high-temperature hydrate, while below 21°C the cement paste forms CAH_{10}, C_2AH_8, and alumina hydrate gel, phases subject to explosive spalling on rapid heating. As seen in Fig. 15, a dense iron-free calcium aluminate-bonded concrete did explode when it was placed in a preheated furnace if the concrete had been cured below 21°C. When the same concrete was cured above 21°C, it did not explode, even when thrust into a furnace at 871°C (1600°F).

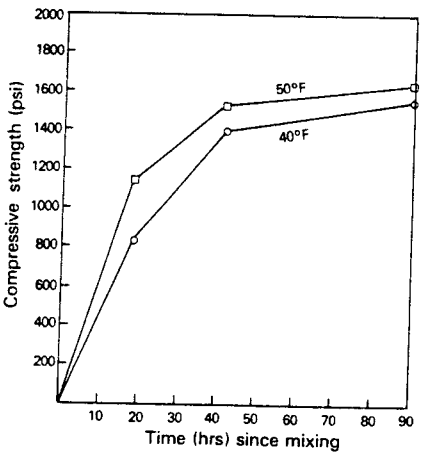

Fig. 13. Compressive strength of insulating refractory concrete from start of mixing.

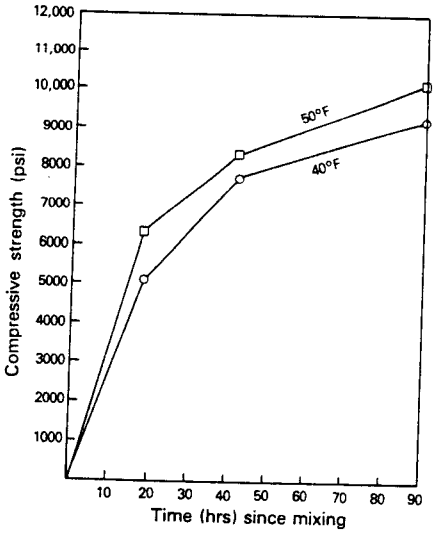

Fig. 14. Compressive strength of dense refractory concrete from start of mixing.

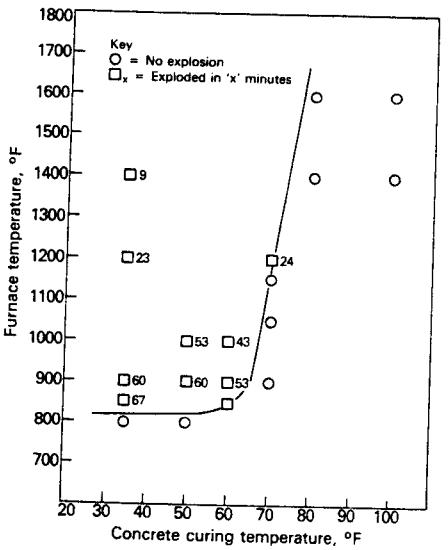

Fig. 15. Explosive tendency of dense concrete "B" made with 7.7% water; 15.24 cm cylinders, 10 cm high (6 in. cylinders, 4 in. high).

This study underscores the need to cure refractory concretes at 21°C or higher if at all possible. The phosphate-bonded alumina concretes are not subject to this phenomenon and can be heated safely at 38° to 93°C/h (100° to 200°F/h). Standard calcium aluminate cement-bonded refractory concretes are usually not as sensitive as iron-free calcium aluminate cement-based materials and can generally be heated at 38° to 93°C/h without danger of spalling. Low-cement castables, especially in thick sections, may require slower heating because of their permeability and porosity.

Currently, several firms specialize in dryouts for new or repaired linings. They have been used successfully in a number of units.

Selection of Refractories for Refinery Units

Table V summarizes guidelines for selecting refractories intended for specific refinery units. In virtually all cases, stainless steel fiber should be added to the hot-face material to improve coherence and to control drying and firing shrinkage.

Fluid Catalyst Cracking Units (Fig. 16)

The FCCUs with their associated cyclones, transfer lines, heat exchangers, and furnaces are the largest single users of refractories. The regenerator vessels, and sometimes the reactors, are lined with 10 to 15 cm (4 to 6 in.) of refractory concrete which must withstand oxidizing (regenerator) or reducing (reactor) conditions at 538° to 760°C (1000° to 1400°F). The moving catalyst bed produces mild erosion, and mechanical or thermal spalling is frequently encountered.

Since the lining must protect the shell from oxidation and corrosion as well as from excessive temperatures, monolithic refractories—i.e., those having no joints, such as gunned or cast refractory concrete—are preferred. Our experience has shown that one-shot linings of a semiinsulating refractory concrete on independent anchors are better and more economical than two-component linings of insulating concrete covered by an inch of dense concrete held in hexagonal steel grating. Most of the semiinsulating concretes are used for this purpose and are composed of calcium aluminate cement and lightweight aggregate. Portland cements are not desirable because of their poor refractoriness and instability in cyclic heating service.

Cyclones and catalyst transfer lines usually are subjected to extreme erosion from fluidized catalyst at temperatures of 316° to 760°C (600° to 1400°F). In

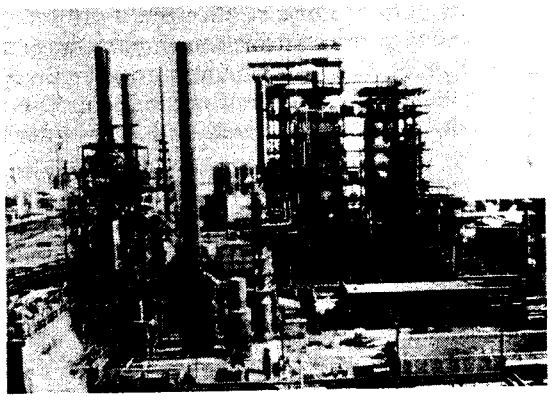

Fig. 16. Fluid catalytic cracking unit.

cyclones, the catalyst is in a dilute phase but is moving at speeds of 37.5 m/s (125 ft/s) or faster. The cyclone lining usually consists of an inch of special erosion-resistant, heat-setting or hydraulic refractory castable held in S Bar anchors or hexsteel grating. It is very important that these linings be installed and cured in accordance with the refractory manufacturer's directions.

The transfer lines are subjected to heavy loadings of catalyst at velocities of 7.5 to 30 m/s (25 to 100 ft/s). This type of service calls for refractory castable or ramming mixes with an erosion resistance nearly as high as that of cyclone linings.

Slide valves in the transfer lines and standpipes are subject to severe erosion but must maintain their original thickness so they can control the catalyst flow. Prefired tilelike inserts of mullite or high-fired alumina have worked well as erosion-resistant inserts. Care

Table V. Selection of Refractories for Refinery Usage

Unit	Conditions	Refractory Type
FCCU vessels	538°–760°C (1000°–1400°F), mild erosion, oxidizing or reducing atmospheres	One-shot lining on independent anchors.
Cyclones, catalyst transfer lines and slide valves	538°–760°C (1000°–1400°F), extreme erosion	Special erosion-resistant castables (consult refractory manufacturer).
Naphtha reformers	538°C (1000°F), low-to-moderate erosion, high-hydrogen atmospheres	Insulating concrete (low iron) protected by a stainless steel shroud or a layer of dense low-iron concrete.
Other H_2 -producing units	1093°–1649°C (2000°–3000°F), high-hydrogen atmospheres	Super-duty brick or castable of low silica content (consult refractory manufacturer).
Process furnaces, stills, and boilers	982°–1316°C (1800°–2400°F), oxidizing atmospheres, some mechanical or thermal spalling	Side walls and roof may be of insulating or one-shot concrete or of insulating firebrick; burner and flame-impingement walls may be of super-duty plastic, brick, or high-strength refractory concrete; floors may be of dense castable or fire-clay brick.
Stacks and breechings	316°–816°C (600°–1500°F), mild erosion, some mechanical or thermal spalling	One-shot linings; areas subject to erosion or thermal spalling can be faced with an aluminophosphate-based refractory.
Incinerators and dutch	1093°–1538°C (2000°–2800°F), ash attack, mechanical	Super-duty brick, plastic.

must be exercised in designing the slide valve because of thermal expansion differentials; therefore, collaboration with the refractory manufacturer and the valve designer is strongly recommended. Phosphate-bonded aluminas have been used successfully in slide valves, as have some very low cement castables.

Plug valves have more tolerance for thermal expansion differentials and are frequently lined with a phosphate-bonded alumina refractory held in S Bars or hexsteel anchorage.

Naphtha Reforming Units (Fig. 17)

Since operating conditions in naphtha reforming units include a hydrogen-rich atmosphere at temperatures of 538°C (1000°F), special care is required in designing the liner because of the increased thermal conductivity of hydrogen-saturated refractories. These units may require low-iron refractory concretes to guard against catalyst poisoning. The linings usually consist of 7.5 to 15 cm (3 to 6 in.) of low-iron insulating concrete protected by a stainless steel shroud or by a layer of dense low-iron concrete. Anchorage may be of the S Bar or longhorn type with two levels to retain the insulating and dense layers independently. Buried S Bars should be coated on the top edge to allow for expansion. Stainless steel fiber (3 to 4 wt%) should be added to the dense hot-face layer to improve coherence and control shrinkage cracks.

Hydrogen Synthesis Units

Hydrogen synthesis units and ammonia plant reformers operate at temperatures of 1093° to 1371°C (2000° to 2500°F) and thus require refractories of very low silica content. At temperatures above 1204°C (2200°F), silica, either in the cristobalite or tridymite form or as a silicate, e.g., aluminosilicate, zirconium silicate, magnesium silicate, may react with hydrogen according to the following reaction:

$$H_2 + SiO_2 = H_2O + SiO \qquad (3)$$

The product SiO is a gas which can be carried downstream from the reaction by the process stream. When the temperature drops below 1204°C, the SiO will disproportionate to produce crystalline silica, usually in the cristobalite structure, and silicon.[20,21] Extraction of silica weakens the refractory and may lead to lining failure; in addition, redeposition of silica will lead to heat-exchanger fouling and product contamination. Present practice calls for the use of special high-alumina castables in areas where high-temperature hydrogen attack is a possibility. High-pressure steam is also capable of extracting silica and phosphates from refractory materials at temperatures above 871°C (1600°F); therefore, phosphate-bonded aluminas should not be used in units with a continuous steam atmosphere.

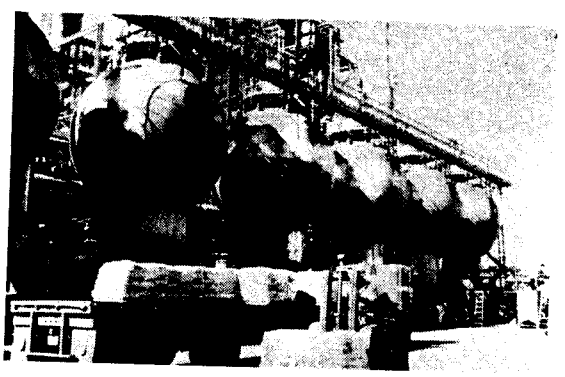

Fig. 17. Naphtha reformer unit.

Some hydrogen synthesis units use steam reforming to generate large quantities of CO. At temperatures of 427° to 649°C (800° to 1200°F), atmospheres containing upward of 30% CO will react with iron-containing refractories and cause layers of carbon to deposit around each iron site. This process results in what is known as carbon monoxide disintegration. Refractories to be used in such service must either be of a low-iron type or be treated with an inhibitor by the manufacturer to make them resistant to CO disintegration. Caution must be observed in selecting CO-resistant refractories as some inhibitors do not have a permanent effect.

Process Furnaces

Recent improvements in ceramic-fiber module designs make them an optimum choice for many process furnaces.[7] The simplest installation is done with an unlined furnace where the shell attachment system can be laid out on bare walls. Table VI lists the current module systems now available and the manufacturers. The increased use of heavy fuels with high sulfur contents has led to the development of a number of combined wallpaper plus module systems. In most of these systems, anchors are welded to the shell, a corrosion-barrier coating is applied to the shell, blankets of fiber are impaled on the anchors, a metal foil barrier is impaled on the anchors, and a module is fastened to the anchor. The blanket next to the shell is usually of lower quality than the module fiber and the metal foil, typically of very thin stainless steel, acts as a barrier to stop corrosive gases from reaching the shell.

Modules are available which can be glued onto the existing refractory lining. Wallpaper systems in which ceramic-fiber blankets are cemented and/or pinned to the refractory wall are also available. A recent development is sprayable ceramic fiber with a binder that toughens the fiber and bonds it to the wall.

Many of the furnaces now in use are lined with refractory castables or insulating firebrick. Thermal shock and temperature cycling are the primary agents of attack. Mechanical movement, nut blasting, and similar forces also contribute to deterioration. Floors are usually made of dense refractory concrete or firebrick to resist foot traffic and mechanical impact during turnarounds.

Table VI. Ceramic Fiber Module Systems

Name	Manufacturer	Comments
Z blok	Manville Products Co.	Available in 929 cm^2 and 3716 cm^2 (1 sq. ft. and 4 sq. ft.) units. Can be used with foil barrier.
Nip and tuck lance and lock	CE Refractories	Available in simple modules and combined with blanket and foil barrier.
Saber bloc	Babcock & Wilcox	Can be used with blanket and foil barrier.
CFB module	Carborundum	Can be used with blanket and foil barrier.
Inswool module	AP Green	Can be used with blanket and foil barrier.
Pyro block	Babcock & Wilcox	Available in 929 cm^2 and 1858 cm^2 (1 sq. ft. and 2 sq. ft.) units.
Octa comb	G. P. Reintjes Co.	Octagonal form.
Monster module	Industrial Furnace Services, Inc.	Single module covers entire wall.

Stacks and Breechings

Stacks and breechings for most types of chemical plant and refinery units have similar service problems: heat resistance, corrosion, erosion, and spalling. The temperatures range from 204° to 816°C (400° to 1500°F) and the flue gas may contain catalyst, sulfur oxides, hydrogen sulfide, or carbon monoxide. Water or steam may be injected into the gas stream to control temperature.

If conditions are mild, e.g., temperatures below 538°C and little or no erosion, insulating or semiinsulating refractory concrete on independent anchors makes a serviceable lining. More-erosive conditions may require the use of dense high-strength refractory castable. It has been shown that two-component linings may be unstable in ducts subject to 6.9 to 13.8 kPa (1 to 2 psi) pressure fluctuations because the hexagonal steel mesh can flex with the pressure change and fail by fatigue in a short time.[23]

Water impingement can be destructive to refractory brick or concrete at high temperatures where waste solutions or quenching water are injected. A target zone of iron-free calcium aluminate cement/fused silica castable or a phosphate-bonded alumina will help to resist the thermal shock and also reduce the wear due to erosion. At this time, almost no refractory will withstand repeated cycling from hot flue gases to water sprays.

High-sulfur fuels generate sulfuric and sulfurous acids in the cooler zones of stacks and breechings where the temperature drops below the dew point (149° to 177°C (300° to 350°F)). These acids attack many conventional refractory castables based on calcium aluminate cement. The alkali silicate- and some calcium aluminate-based materials are moderately acid-resistant and will withstand the condensing flue gas vapors. For many furnace stack linings, densely applied semiinsulating refractory concrete is satisfactory. A number of coatings that can be used to reduce corrosion of stacks are currently available.

Incinerators (Fig. 18)

Incinerators may operate at as high as 1538°C (2800°F) and are particularly susceptible to slag and fly-ash attack because they often burn waste products. Problems involved with fluids containing alkalis and transition metals can be expected. Additionally, because of their higher temperature, incinerators may experience trouble using a fuel that operates trouble-free in a process furnace.

Thermal shock can be a problem if water is injected to control temperatures or if the burner unit is allowed to go on and off several times a day with periods of cooling in between. Such a condition may exist at the start-up of a new unit when other operational difficulties may cause the feed line to be interrupted frequently. Phosphate-bonded alumina-type castables or plastics are apt to be the best materials for this type of cyclic service.

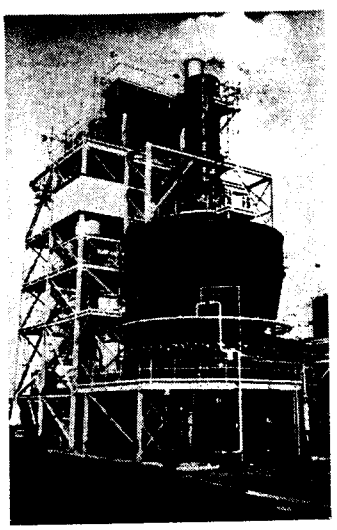

Fig. 18. Fluid bed incinerator.

Phosphate-bonded materials are not a good choice for areas that will undergo extensive steaming. The calcium aluminate cement-bonded refractories rated at 1649°C (3000°F) have proved to be the most effective in these areas. High-temperature stainless steel fiber, e.g., type 330 or 446, will help to control shrinkage cracks that develop on drying and firing. They will also improve coherence of the material even though the fibers near the hot face are apt to melt or oxidize and be absorbed into the matrix.

Inspection Techniques

Because of their complexity, FCCUs are among the most difficult units to inspect for refractory damage. The regenerator lining is the largest single item and typically requires some patching at every turnaround. Spalling of areas due to hot-face compressive stresses, mechanical or thermal expansion of metal components, laminations due to poor installation practices, and thermal cycling is the most common problem. Erosion from the fluidized bed is usually not a factor. The regenerator lining is inspected visually, usually from a distance of 61 to 91 cm (2 to 3 ft.), and spalled areas where the anchors are exposed are critically examined. If 2.5 cm (1 in.) or more of the anchor is visible, the lining is approximately half-thickness (typically 10 cm (4 in.) linings have 7.5 cm (3 in.) anchors) and should be replaced. A small chipping hammer is useful in determining if areas are loose or firmly bonded. All loose segments should be removed.

The reactor lining usually becomes coke-filled and undergoes very little deterioration. Inspection is a matter of examining the lining for thin spots or areas of mechanical damage. Reactor linings are repaired in the same manner as regenerator linings.

Cyclones undergo severe erosion and must be carefully examined for evidence of wear. A sandblast is often used to remove old patch material. The standard rule is to look for the clench if a hexsteel lining had been installed. The clench is in the middle third of the 1.9 cm (¾ in.) high mesh and, if it is visible, indicates that over one-third of the lining is gone and the area should be replaced. When S Bars are used as anchorage, the center opening, which is also in the middle of the lining, serves as a similar guide for replacement, i.e., a gap in the top edge of the S indicates that over one-half of the curved retaining arms have been worn away and the lining should be replaced. Any loose or severely oxidized anchorage must be replaced to keep it from falling down a dip leg and plugging the trickle valve. Areas in which the anchorage is full depth and the refractory is worn down can be repaired by chipping out the old material and installing new full-depth refractory. Areas that should be critically examined include the lower cones and "dust bins" in both the primary and secondary cyclones, the inside and outside of the gas outlet tubes in the primary and secondary units, and the inlet ducts. The outside surfaces should be examined for cracks in welded seams, holes, and similar defects which could contribute to erosion problems inside the cyclone.

Catalyst transfer lines and distribution units, e.g., "cobra heads," must be completely traversed to determine if any of the erosion-resistant or insulating layers are missing. Hot spots noted on the outside of the lines may not be obvious on the inside near the hot spot because the problem may be gas entering the lining upstream and traveling between lining layers before it comes close to the shell to create the hot spot. Such defects can be hard to spot if the entry point is a significant distance from the external evidence. Severe wear in lines, particularly the spent cat return lines, will have the same appearance as cyclones, i.e., hexsteel clench holes or S Bar tab holes will be visible and indicate that the lining should be replaced. The feed risers usually become coke-filled and exhibit relatively little erosion due to their extreme hardness.

The plenum chamber and overhead lines are usually lined with one-shot or erosion-resistant refractory on independent anchors. Spalling is the usual problem encountered in inspection but erosion may be severe in some areas such as bends and near slide valves. Water sprays to control flue-gas temperatures will produce severe spalling due to thermal shock.

Frequently, cracks and minor spalling are seen at the 3 o'clock and 9 o'clock positions as one looks down the axis of a horizontal duct. These cracks arise when the circular duct is heated and the shrinkage of the concrete during dehydration allows the duct to flatten into an oval cross section. Subsequent thermal cycling tends to cause spalling at the pinch points. These areas should be inspected carefully to ensure that any loss is limited to the surface and does not significantly reduce the lining thickness. The use of stainless steel fiber greatly reduces such surface losses.

Seal pots represent a particularly difficult service environment for refractories, which can change from soaking wet to 760°C (1400°F) in a few minutes. The reverse change also takes place in a few minutes. Inspection generally consists of determining how much of the existing lining is still usable. Typically, the area above the water line is in good shape and the soaked area must be completely replaced. Corrosion of the bottom steel plate is often a problem because of the acidic nature of the water as it absorbs gases from the flue. Shock-resistant fused silica-based castables should have the best chance of resisting seal pot cycling.

Furnaces generally encounter thermal cycling and occasional thermal shock. Spalling, anchor failure, and slag development may be found if the furnace was overfired or the burners were poorly adjusted. The use of nut blasting to clean tubes for improved heat transfer may result in severe erosion of the walls unless a metal blast shield is used. The key element in inspecting furnaces, as with most refractory linings, is determining the mode of failure. Poor anchorage and

mechanical movement due to differential thermal expansion between the shell and the refractory often are the prime reasons for loss of wall sections.

New linings of refractory concrete can be inspected using techniques that yield quantitative results. Moderately thick linings, i.e., over 5 cm (2 in.), can be tested nondestructively using a Schmidt hammer. This instrument replaces the ball peen hammer and gives a numerical value that can be converted to compressive strength. It is difficult to use the Schmidt hammer on thin linings because of the influence of the anchorage and base plate.[24]

Erosion-resistant linings can be evaluated in the field or in the vendor's shop using a field erosion tester.[25] This test unit is particularly useful in evaluating linings that have been prefired. The depth of the hole eroded by 100 g of SiC can be equated with the result that would be obtained from an ASTM C–704 erosion unit. Since the hole is usually less than 0.25 cm (0.1 in.) deep, no subsequent repairs are needed and the test can be considered nondestructive. If additional data are required, samples of the lining can be cut out and sent to a laboratory for further analysis.

Refractory Repair Procedures

Most of the patching materials, like other refractories, are designed for the steel industry and assume that operating temperatures will be 1093° to 1649°C (2000° to 3000°F). Because of this, many materials which perform well in steel mills show up rather poorly in CPI service where temperatures of 538° to 760°C (1000° to 1400°F) are more common, and erosion resistance, rather than refractoriness, may be the critical factor. Bond strength and volume stability, in addition to erosion resistance, are important characteristics of a good patching material.

FCCU Regenerators and Reactors

One-Shot Linings: Failures in this type of lining are most often due to spalling, i.e., shelling-off of large thin slices of lining.

There are a number of causes for these failures, such as:

1. Poor installation techniques, e.g., overwatering, resulting in shrinkage cracks which become filled with catalyst and cause pinching as the lining cools. Laminations due to poor gunning techniques are a frequent cause of failure.
2. Overthickness, which causes excessive compressive stress in the hot face because of thermal expansion.
3. Mechanical strains induced by pipes or beams going through the lining. Both thermal expansion and mechanical movement can be involved in this type of failure.

In addition, such causes as excessive vibration, catalyst rat-holing or bypassing, mechanical impact, and mechanical failure of associated parts can damage a lining.

The recommended repair technique is to remove the defective area (i.e., where less than one-half the original thickness remains) back to where the surrounding lining is essentially full thickness. The existing anchorage should be checked and additional anchors added as needed. The patch should be made by gunning-in a one-shot material with 3 to 4% stainless steel fiber to full depth. The surrounding lining should be predampened to reduce the tendency to draw water from the fresh patch material. It is desirable but not essential that the patch material be the same as the original material. Similar densities and strength of the original and patch refractories will help to even out shell temperatures and hot-face stresses.

Cyclones

Repair methods in cyclones are dependent on the type of anchorage and the amount of wear. Many of the older cyclones have hexsteel grid anchorage, usually with a phosphate-bonded alumina refractory. The usual guideline for inspection is full-depth replacement if the clinch, located in the middle third of the hexsteel strand, is visible. If the clinch is not visible, at least two-thirds of the original thickness is left and will probably last for another run. Full-depth replacement calls for removal of the existing lining and installation of new anchorage. S Bars have worked well in patch areas since they will fit easily into any size or configuration desired to fill the space. In cases where the anchorage, either hexsteel or S Bars, is essentially full-depth and the refractory has been eroded between the metal edges, replacement of the refractory only is the logical answer. Typically, air-setting or heat-setting phosphate-bonded high-alumina refractories are the most effective patch materials. The old material can usually be removed rapidly with small pneumatic hammers.

Catalyst Transfer Lines

Catalyst transfer lines have service conditions similar to cyclones in that severe erosion by moving catalyst is encountered. The catalyst loading may be 12 to 48 kg/m^3 (5 to 30 lb/ft^3) while the velocity varies from 30 to 240 m/s (10 to 80 ft/s). The wear pattern is a combination of erosion and abrasion.

Hot spots usually arise because part of the process stream starts flowing next to the shell. This can happen if the anchorage fails, the refractory erodes away, or the process stream bypasses the lining and flows between it and the shell. Anchor failure can frequently be traced to welding problems or poor spacing and orientation. Proper metallurgy and anchor layout should eliminate these problems. Excessive erosion of the refractory indicates either poor selection and installation of material or unusually severe conditions, e.g., at catalyst pick-up junctions. The field erosion tester can be used to determine if the remaining lining is as erosion-resistant as it should be according to established data.

Bypassing of the liner by hot catalyst streams is a more complex problem since it may involve two-component linings of insulating refractory concrete protected by dense erosion-resistant concrete. The process stream can enter at field joints or other breaks in the dense layer and erode out the softer insulating layer in a relatively short time. It is also possible that bypassing can occur with single-component systems if the anchorage permits the lining to separate from the shell.

Past unfavorable experiences with two-component systems has led to a preference for a single thick layer (≈10 cm (≈4 in.)) of an erosion-resistant material. The thickness and type of material will be dependent on the service conditions and the metallurgy of the shell.

Figure 19 shows the effect of an air blast on carbon steel and stainless steel plates that are being heated on one side with a torch while the back side is cooled with air. The test, simulating a hot spot on a line or duct, was designed to measure the hot-face temperature when an air blast was used to cool the outside face to an acceptable level. The carbon steel cools much faster and to a lower temperature than the stainless steel plate under similar conditions because carbon steel has three times the thermal conductivity of stainless steel.

While an air blast can be used to cool both the hot and cold sides, provisions should be made to repair the lining at the first opportunity. In places where an air or steam quench isn't practical, boxes have been welded to the outside and pumped full of mortar to provide a second lining.

Stacks and Flue Ducts

The main service problems in stacks and flue ducts are erosion and mechanical spalling. Erosion is frequently encountered in areas of changing diameter or direction, e.g., control valves, pressure drop plates, elbows. The use of a more erosion-resistant material is usually the most efficient way to prevent excessive wear. Eroded areas should be replaced with full-depth refractory concrete with good erosion resistance.

Mechanical spalling due to differential expansion of metal and concrete components, duct movement, and similar actions has led to failures at a variety of locations. Steel fiber reinforcement and good anchorage combined with selection of the right refractory should eliminate most spalling problems.

In areas where some erosion is evident but full-depth replacement isn't needed, the surface can be toughened with several heavy coats of sodium silicate. Grooves can be filled in with a layer of alkalisilicate mortar to give added resistance.

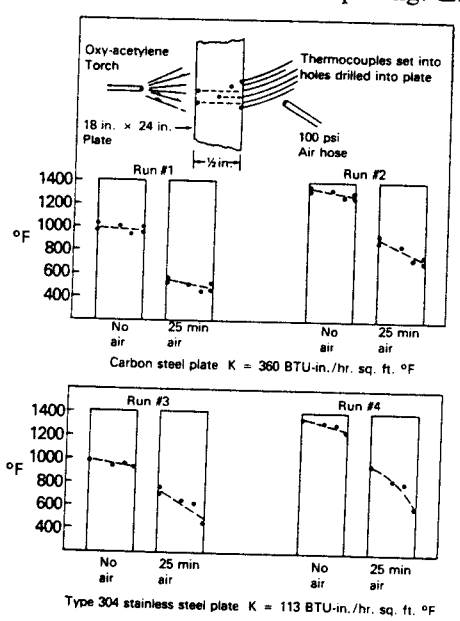

Fig. 19. Temperature profiles in plates heated on one side with a torch, while the back side is cooled with an air blast.

Naphtha Reformers

The usual problems involve hot spots on the shell caused by process gas flowing behind the lining. Any failure of the shroud-to-head weld will result in an immediate hot spot at the weld junction. After repairing the weld, the refractory patch should be replaced in the same design as the surrounding lining.

Erosion is usually not a problem in naphtha reformers because the catalyst is in a fixed bed. However, the frequent regeneration produces thermal expansion and contraction stresses which can lead to excessive cracking. Materials to be used should have a low iron content and SS fiber should be incorporated in the hot-face layer to resist excessive fracturing and loss of fragments.

Furnaces

Brick Walls: The failure of brick walls can be due to many causes—spalling, mechanical pinching, explosion, to name a few. If the failure is only a surface problem, e.g., spalling, several applications of sodium silicate-based mortar may be adequate to restore the original thickness and to reduce further damage. Such materials can be slap-troweled or applied by pneumatic gun. The manufacturer's instructions for repair work should be followed.

Nut blasting to improve heat-transfer efficiency of the tubes has resulted in extensive refractory deterioration of furnace walls of IFB. While thin overlays of alkali-silicate mortar will usually buy some extra life, a more effective answer is to hang SS plates behind the tubes to act as deflectors. Fiber module-lined furnaces with SS deflector plates have been very successful.

If the failure is a major structural one, the wall can be rebuilt in brick but it will probably be much cheaper if a form can be used and hydraulic cement-bonded castable can be used to rebuild the wall. Anchorage and/or reinforcement for a monolithic wall must be considered very carefully because of the fluxing action of hot iron on refractory materials. If the wall is non-load-bearing, there may be no need for anchorage or reinforcement. The use of pilasters or similar stabi-

lizing elements is strongly recommended to improve the integrity of the wall.

Ceramic fiber module walls are apt to be damaged by mechanical impact, especially during turnarounds. Replacement of the defective modules is usually easy if they are accessible. If the modules are behind tubes, special techniques may be required. Most module manufacturers have developed techniques for such replacements.

Monolithic Walls: Furnace walls of castable refractory or plastic refractory usually can be repaired by installation of a new section of castable or plastic refractory. Plastic material can be used if the old material is cut back to the shell, suitable anchorage is installed, and the new material is carefully installed under skilled supervision. There are many areas, e.g., burner block sections and firebox end walls, where plastic refractory material is a better choice than castable refractory because it can be applied overhead easily without forms.

Castable refractories based on hydraulic binders can be used in either the cast or the gun-applied technique. Overhead arches or furnace roofs usually are shielded by tubes, making pneumatic application impossible, so casting from above is often the most practical way to repair such areas. Wall repairs usually can be gun-applied, although forms could be used and the repairs cast in place. It is important, in dealing with castables, to be sure that the anchorage is adequate, because the new material will not bond chemically to the old one. In general, the defective material is cut back to the shell, new anchorage is installed if needed, and the surrounding material is prewet before application of the new material.

A few of the old LHV furnace walls (1 Lumnite:[‡] 2 haydite: 4 vermiculite) which have deteriorated because of thermal shock and cycling have been repaired by "gluing" a layer of ceramic-fiber blanket to the surface. It is necessary to brush away any loose material from the wall and use a strong coherent blanket. Several mortars have been developed by the fiber manufacturers especially for this type of application. Metal pin anchors may be used in addition to the mortar to ensure retention of the blanket on the refractory wall.

One manufacturer has developed a new gun-applied fiber lining for use on existing brick or castable refractory linings. It is necessary to have a sound base before this new lining can be applied.

[‡]Lumnite Products Corp., Salamanca, NY.

References

[1]E. Ruh, Refractories for the Chemical Process Industries. The Materials Technology Institute of the Chemical Process Industries, Inc. Columbus, OH, 1984.

[2]D. E. Becker and D. L. Edwards, "Refractory Castables"; NPRA paper MC84-6, February 14, 17, 1984.

[3]M. S. Crowley, "Refractory Applications in Refining and Petrochemical Operations"; American Concrete Institute Symposium, San Diego, CA, March 17, 1977.

[4]Technology of Monolithic Refractories. Plibrico Japan Company, Ltd. 1984.

[5]J. R. Peterson and F. H. Vaughan, "Metal Fiber Reinforced Refractory for Petroleum Refinery Applications"; Corrosion 80 NACE, March 3–7, 1980, Chicago, IL.

[6]M. S. Crowley, "Steel Fibers in Refractory Applications"; NPRA paper MC81-5, February 17–20, 1981.

[7]M. S. Crowley, "New Developments in Refractory Linings"; NPRA paper MC-83-9, February 8–11, 1983.

[8]E. Ruh and A. L. Renkey, "Thermal Conductivity of Refractory Castables," *J. Am. Ceram. Soc.*, **46** [2] 89–92 (1963).

[9]R. W. Wallace and G. H. Criss, "Thermal Conductivity of Castable Refractories and Its Relationship to Bulk Density," *Am. Ceram. Soc. Bull.*, **46** [4] 431 (1967).

[10]M. S. Crowley, "The Effect of High Conductivity Gases on the Thermal Conductivity of Refractory Concrete Linings"; paper No. 64 PET 31, ASME Petroleum Mechanical Engineering Conference, Los Angeles, CA, 1964.

[11]M. S. Crowley, "Initial Thermal Expansion Characteristics of Insulating Refractory Concretes," *Am. Ceram. Soc. Bull.*, **35** [12] 465–68 (1956).

[12]F. T. Palin and G. C. Padgett, "Thermomechanical Behaviour of Refractory Castable Linings," The British Ceramic Research Association, Tech. Note 320, March 1981.

[13]J. F. Wygant and M. S. Crowley, "Designing Monolithic Refractory Vessel Linings," *Am. Ceram. Soc. Bull.*, **43** [3] 173–82 (1964).

[14]O. Buyukozturk and Tsi-Min Tseng, "Thermomechanical Behavior of Refractory Concrete Linings," *J. Am. Ceramic Soc.*, **65** [6] 301–307 (1982).

[15]"Improvements in the Mechanical Reliability of Monolithic Refractory Linings for Coal Gasification Process Vessels," Babcock & Wilcox Company Report LRC 5258, September 1981.

[16]M. S. Crowley, "Equation Helps Select Refractory Anchor System," *Oil Gas J.*, **80** [35] 122–25 (1982).

[17]M. S. Crowley and R. C. Johnson, "Guidelines for Installing Refractory Concrete Linings in Cold Weather," *Am. Ceram. Soc. Bull.*, **51** [2] 171–75 (1972).

[18]M. S. Crowley and R. C. Johnson, "Guidelines for Installing and Drying Refractory Concrete Linings in Petroleum and Petrochemical Units," *Am. Ceram. Soc. Bull.*, **51** [3] 226–30 (1972).

[19]D. L. Hipps and J. J. Brown, "Internal Pressure Measurements for Control of Explosive Spalling in Refractory Castables," *Am. Ceram. Soc. Bull.*, **63** [7] 905–10 (1984).

[20]M. S. Crowley, "Hydrogen Silica Reactions in Refractories," *Am. Ceram. Soc. Bull.*, **46** [7] 679–82 (1967).

[21]M. S. Crowley, "Hydrogen Silica Reactions in Refractories, Part II," *Am. Ceram. Soc. Bull.*, **49** [5] 520–27 (1970).

[22]"Investigation of Carbon Monoxide Desentegration of Refractories in Coal Gasifiers," J. J. Brown Jr., Dept. of Materials Engineering, Virginia Polytechnic Institute, Blacksburg, VA, July, 1984.

[23]M. S. Crowley, "Failure Mechanism of Two-Component Linings in a Flue Gas Duct," *Am. Ceram. Soc. Bull.*, **47** [5] 481–83 (1968).

[24]M. S. Crowley, "Inspection and Repair of Refractory Concrete Linings in Refinery Units," *Chem. Eng. Prog.*, **68** [8] 48–51 (1970).

[25]M. S. Crowley, R. A. Gormley, and F. E. Linck, "Field Testing of Erosion-Resistant Refractories," *Am. Ceram. Soc. Bull.*, **63** [4] 638–29 (1984).

Refractories Used for Aluminum Processing

G. Edward Graddy, Jr. and Douglas A. Weirauch, Jr.
Aluminum Company of America
Alcoa Center, PA 15069

Many different materials have been used to contain molten aluminum alloys. They have ranged from cast iron and clays in the early days of the industry to high-technology ceramics for the specialized alloys that are produced today. The trend to aluminum alloys which have more stringent impurity specifications and are more corrosive in the molten state is expected to continue, making the selection of appropriate containment materials more challenging. Emphases are placed on corrosion test methodology and a review of evaluated materials. The evolution of refractory technology as it pertains to molten aluminum containment is presented, with some predictions about its future. Aluminum oxide and materials based on it are expected to continue to play a major role.

Worldwide production of aluminum in 1985 was slightly over 15 million metric tons,[1] trailing only iron and steel. The unique combination of properties found in aluminum makes it useful for applications as diverse as aircraft, beverage cans, and electrical transmission lines. Aluminum production therefore represents one of the major manufacturing industries in the world. Because high temperatures are involved, it is a large consumer of refractory products.

The industrial process for smelting aluminum was only 100 years old at this writing, yet it is fairly complex. Figure 1 outlines the steps involved in processing bauxite (an alumina-rich ore) into aluminum metal ingots.[2] Several high-temperature processes are involved in producing aluminum, and many of them require the use of sophisticated refractory products.

Refractory Usage in the Aluminum Industry

History and Overview

Refractories used in the manufacture of nonferrous metals represented less than 8% of all refractories sold in 1985.[3] Refractories for aluminum represented slightly over one-half of this amount. Although the percentage of total refractory sales was relatively small, they often played a critical role in determining the final properties of the aluminum alloys. For these reasons, much of the refractory development work has been conducted by the aluminum producers.

Many types of refractories have been used in the various processes involved in aluminum production. Historically, they have been selected from readily available materials or those developed for steel and other applications which were then adapted for use in aluminum processes. As the level of sophistication of the aluminum products increased, however, the tolerable levels of impurities in the products decreased, and refractories designed for specific applications became necessary. These impurities often influenced or controlled the properties of the final aluminum product.

The protective nature of the oxide of aluminum (Al_2O_3, commonly known as alumina) has long been known. It protects aluminum products from most common types of corrosion. It also protects the metal in the molten state from oxidation, provided a thin, continuous surface skin is formed. The thermodynamic stability, high-temperature resistance, and good

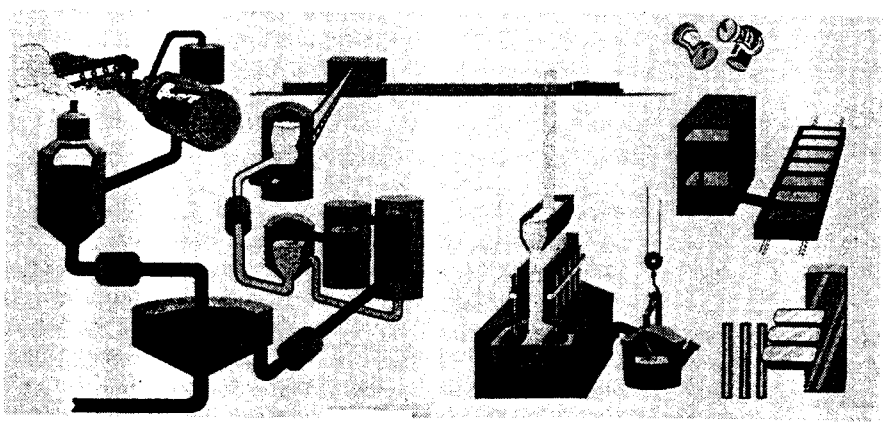

Fig. 1. Processing steps in producing aluminum metal ingots from bauxite. (Artwork by Pierre Mion, © National Geographic Society. Used by permission.)

formability also make this material a prime candidate for use as a containment material or refractory in many aluminum processes.

Of the refractory applications in the production of aluminum, those involving direct contact with the molten metal are the most demanding of the final product. For this reason, the screening and selection of refractory materials usually involve molten-metal contact.

Applications

Alumina Production: As shown in Fig. 1, the first steps in producing aluminum involve refining bauxite through a process of chemical digestion, precipitation, and ultimately calcination in order to produce aluminum oxide. Temperatures of about 1000°C are required during calcination, and residual impurities can greatly affect the suitability of the alumina for aluminum production and other applications.

Flash calciners or rotary kilns are used to calcine the Bayer-process aluminum hydroxide, yielding "smelting-grade" alumina. The linings of these furnaces are important in determining the final properties of the alumina as well as the economic feasibility of the process. In addition to high-temperature stability; high-temperature strength, abrasion resistance, and low contamination potential are important requirements for these lining materials.

Smelting: In the smelting operation, electrolytic cells produce molten aluminum from smelting-grade alumina in a molten-fluoride salt bath. These cells are designed to allow a frozen crust of salt to act as the containment material. Important properties of the materials which contain the salt include structural integrity at about 980°C, high thermal conductivity, and resistance to high-temperature vapors containing fluorides and sodium. The linings of these cells are typically composed of various forms of carbon, although dense tabular alumina aggregate has been found to provide a good patch material when holes or leaks develop in the cell.[4] This patching allows the life of a cell to be extended. Dense tabular alumina can be used since its rate of solution is much less than that of the high-surface-area smelting-grade alumina dissolved in the process.

Another use of alumina refractories in the smelting operation involves the lining of crucibles used to siphon metal from the Hall cells and transport it to either the ingot or "pigging" operation. Since the metal typically emerges from the cells at about 960°C, a noncontaminating, high-temperature refractory is required. Materials suitable for the containment of molten aluminum are used for this purpose.

Ingot: The ingot plant represents the most critical use of refractories in the aluminum industry. The properties of temperature stability and corrosion resistance of the containment materials used in ingot manufacture are particularly important as they often determine the final chemistry and, therefore, properties of the final product.

The most severe application involves the containment of the aluminum alloy during melting, alloying, and gas purging. It is during these processes that the greatest potential exists for contamination of the alloy and destruction of the refractory materials.

A typical ingot plant configuration consists of melting and holding furnaces. Melting furnaces are used to melt pig ingots, scrap, and/or metal from the Hall cells ("pot metal"). Holding furnaces are used to do final alloying, remove impurities through a gas-bubbling process, and provide metal of uniform temperature to the casting operation. Metal from the holding furnace is typically transported via troughs to metal-treatment and filtration operations before being cast into ingots in a semicontinuous operation.

Test Methods

Numerous test methods have been used to select refractories for use in aluminum applications. As mentioned earlier, most of these tests have dealt with problems associated with direct contact by molten metal. A brief discussion of test methods and a summary of historical results follows.

In 1927, Thews[5] published results of tests of aluminum containment materials and concluded that graphite crucibles were preferable to iron pots for the containment of aluminum. Performance was enhanced when a coating of "aluminum bronze" was applied to the graphite. He also stated that highly refractory crucibles such as "magnesia-alumina or circon dioxide* crucibles" had not been sufficiently developed for practical use by the aluminum industry. Thews went on to point out the strong affinity of aluminum for iron and silicon, as well as its tendency to dissolve silica from clays.

In 1940, Burrows[6] published the results of an evaluation of refractory materials for the containment of aluminum. Commercially available refractories were immersed in aluminum at 760°C (1400°F) for 35 days, followed by measurement of weight change and visual examination. He concluded that density played an important role in refractory performance, and found that "chrome brick" had the lowest weight changes, followed by magnesite, silicon carbide, and fused alumina. Fireclay and silica materials were found to be the poorest performers.

Work published in Japan in 1941 and 1942[7,8] considered the Cr_2O_3-MgO-Al_2O_3, MgO, Al_2O_3, MgO-Al_2O_3, Cr_2O_3, and Cr_2O_3-MgO families systems for the containment of aluminum. Test crucibles were fabricated from these bodies, filled with aluminum and a cryolite-sodium chloride mixture, and held for five hours at 900° and 1300°C, followed by sectioning and visual examination. Materials containing Cr_2O_3 and possessing low porosity exhibited the best corrosion

*What Thews meant by "circon dioxide" is unclear. It could have referred to zircon ($ZrSiO_4$) or zirconia (ZrO_2).

resistance, although all the candidates stood up well against molten aluminum.

Brondyke,[9] in 1953, published the results of a study involving alumina-silica refractories. In this study he introduced an evaluation technique which involved forming a cup of defined dimensions from a candidate refractory material. Molten alloys were poured into the cup, and the assembly was held in a furnace for a desired time and temperature. He demonstrated that SiO_2 is reduced by aluminum, regardless of the refractory mineral composition and the source or type of fireclay. Degradation occurred by the following reaction:

$$4Al + 3SiO_2 \rightarrow 2Al_2O_3 + 3Si \quad (1)$$

Although various alloys and temperatures were investigated, most of the work was conducted at 760°C for 72 hours with 24S[†] alloy. The test method was adopted by the industry as a useful screening technique, and his results were significant in providing supporting evidence for the use of high-alumina refractories in the containment of molten aluminum.

Work published by McDonald et al.[10] dealt with the selection of plastic refractories for molten aluminum contact. These materials were defined as blends of ground fireclay materials and an aggregate material suitable for ramming into a monolithic lining. They showed that the resistance of the refractory was inversely related to its uncalcined clay content and highly dependent on its firing history. Metakaolin (unstable above 982°C (1800°F)) formed a protective layer over the aggregate. High-alumina, low-clay-containing materials were found to perform best above 982°C.

In 1959, Stock and Dolph[11] published the results of evaluations using Brondyke's cup test with 7075 alloy[‡] at 927°C (1700°F). Under these conditions, they found that magnesite-chrome, chrome-magnesite, and experimental high-alumina bricks performed well in the tests. They promoted the use of a high-alumina castable material.

Also in 1959, Brown and Landback[12] recommended the use of ceramic-bonded and silicon nitride-bonded silicon carbide brick, as well as electrically fusion-cast alumina refractories for processes involving molten aluminum. The potential for degradation of ceramic-bonded silicon carbide was discussed, as was the poor thermal shock resistance of the fusion-cast material. Nevertheless, positive experiences with each of these materials were presented.

Schweinsberg and Dolph[13] pointed out the advantages of 99% alumina refractories for applications where extreme metal purity was paramount. They also discussed 85% alumina bricks with "special" bonding which exhibited exceptional results in immersion tests. They suggested that 35 to 50 million pounds of melted aluminum represented satisfactory furnace life.

In an assessment of the state-of-the-art,[14] Bloch reviewed the appropriate thermodynamic data, the existing refractory practice in both smelting and ingot production, and the refractory developments of 1961. He cited the excellent service in holding furnaces of fusion-cast refractories containing >98% alumina. Service trials revealed an improvement of 500 times in the stability of 90% alumina brick when a borate glass was used as a bonding agent. He discussed the use of nitride-bonded silicon carbide refractories for smelting applications and suggested the nitrides of silicon, boron, aluminum, titanium, and zirconium as well as the borides of titanium and zirconium for aluminum applications.

The work of Lindsay et al.[15] involved the immersion of laboratory-prepared samples in aluminum alloys of various magnesium contents at 760° to 825°C for 48 hours. They found that magnesia and magnesium-aluminate spinel refractories were unaffected in all cases. High-alumina samples reacted to form MgO or $MgAl_2O_4$ at alloy concentrations of 2.4 and 7.7% Mg.

A paper by Pardee[16] in 1966 described a test in which samples were immersed in 7075 alloy at 760°C (1400°F) for 15 days of total exposure. During the test, samples were removed from the melt at 24-hour intervals and placed into a 538°C (1000°F) furnace to determine spalling characteristics. Several additives were incorporated into refractories of 80 to 90% alumina for the study. A 90% alumina material with a clay bond and boron glass additive[§] was found to have maximum resistance to attack by aluminum as well as thermal and mechanical shock resistance. He also showed the economics of using this material, and indicated how improvements in furnace design and operation were possible as a result of proper refractory selection and use.

A paper by Hess and Caprio[17] discussed the use of the cup test and B immersion test[18] to evaluate commercial refractories. The B immersion test consisted of preheating a refractory specimen to 540°, suspending it in 7075 alloy at 760° for 22 hours, followed by removal, cleaning, and placement in a furnace at 540°C for 2 hours. This cycle is repeated six times, followed by slow cooling, sectioning, and examination of the condition of the specimen. Phosphate-bonded alumina and frit-bonded alumina materials were found to have promise for critical areas of melting furnaces, as were nitride-bonded silicon carbide products for the charging areas of remelt furnaces.

Siegwart[19] conducted refractory tests similar to the aforementioned cup test. These results were combined with those of a test wherein compacts of powdered aluminum and powdered refractories were cofired. He concluded that either the aluminum-refractory interface temperature must be kept below 800°C (to prevent refractory attack) or a nonwettable refractory surface must be provided.

[†]Alloy 24S contains 4.3% Cu, 1.5% Mg, and 0.6% Mn.
[‡]Alloy 7075 contains 5.6% Zn, 2.5% Mg, 1.6% Cu, and 0.23% Cr.
[§]Lo-Sil Super, Kaiser Aluminum and Chemical Corp., Oakland, CA.

Judd[20] and then Judd and Nelson[21] reported results of immersion tests using 7075 alloy at different temperatures and times ranging to five days. They found evidence of reaction between MgO and the aluminum-magnesium alloy to form $MgAl_2O_4$ and attributed it to oxidation of aluminum followed by reaction with MgO. No evidence of reaction between $MgAl_2O_4$ and the alloy was seen, although densification, again attributed to aluminum oxidation and subsequent solution into the spinel, was suggested. They recommended that magnesium-aluminate spinel be pursued as a containment material for alloys of this type. They also indicated that future studies should emphasize the physical aspects of metal penetration as well as chemical reactivity.

A paper by Steinke and Stett[22] gave results of immersion and modified cup tests with 6061¶ and 7075 alloys. They pointed out that different refractories should be used, depending on the anticipated service conditions. An 88% alumina brick performed excellently in the tests, but was expensive and lost strength about 870°C (1600°F). An 80% alumina ramming mix was cheaper and felt to be adequate for most applications and a 94% alumina castable was felt to be good for general use. A phosphate-bonded 85% alumina brick was seen as the best choice for situations involving severe mechanical abuse.

In 1979, LaBar[23] discussed the use of large blocks of phosphate-bonded, high-alumina refractory for melting- and holding-furnace construction. Major advantages in construction and alloy change-over were cited through the use of these preformed shapes, and good refractory life was anticipated with blocks of this type.

DeLiso and Hammersmith[24] presented the test methods used by Alcoa to select refractories for aluminum contact and gave some insight to materials offering the most promise for good service. Candidate refractories were first required to pass a cup test and a B immersion test. Next, a small-scale furnace lined with test refractories was run for 43 days with 5182 alloy** at 927°C and the materials were carefully autopsied. A calcium-aluminate, cement-bonded, tabular alumina castable composition was found to perform best in the reported run. A mullite-based block performed almost as well. Phosphate-bonded 85% alumina materials performed poorly under the conditions of the test.

Bray[25] conducted work which indicated that hazardous hexavalent chromium compounds can form at aluminum-making temperatures when chrome-containing materials are mixed with calcium-aluminate cements. This information caused at least one major aluminum producer to eliminate refractories of this type from its operations.

A rotating cylinder technique has been used by the authors[26] to screen materials for use in situations where molten metal flow is anticipated (e.g., induction melters, molten-metal pump systems, etc.). Experiments have confirmed that refractory attack is not limited by mass transport in the alloy. Rather, the degradation proceeds by a complex process involving oxide film destruction, wetting, capillary penetration, and chemical reaction.[27]

Alumina-Based Refractory Usage

Refractory practice in the aluminum industry varies greatly. Some things can be said about the general trends and the apparent future of refractory use, however. It is clear that no one refractory material provides the solution to all aluminum needs. Judicious selection of refractories for well-defined conditions is the key to a successful campaign. The drive to tighten alloy specifications and develop more-corrosive alloys has made this job more difficult. The most critical refractory applications still involve containment of molten alloys with minimal contamination. Furnace-limiting applications in conventional furnaces involve refractory materials used in the hearths of melting furnaces and the materials used at and just above the metal line.

Nitride-bonded silicon carbide has gained much acceptance for use in high wear areas such as melting furnace hearths and appears to have applications in other areas. Alumina-bearing materials are still widely used and undoubtedly will continue to play a major role due to their lower cost and flexibility.

Monolithic construction through the use of large blocks and the application of gunnable plastic refractories has expanded the role of alumina-bearing raw materials in the future of the aluminum industry. The advantages of monolithic construction and ease of repair are expected to lead to an increase in its use.

The use of special additives to create refractory surfaces not easily wet by aluminum has allowed the effective usage of materials known to be thermodynamically unstable in contact with aluminum alloys (e.g., Ref. 28). This includes such aggregate materials as mullite, bauxite, and other aluminosilicates. For highly corrosive magnesium-containing alloys, however, even tabular alumina has been shown to be unstable. Finding suitable, effective additives with reasonable life has been more difficult for these applications. It appears that magnesium-aluminate spinel products may provide an answer to the problem of magnesium-containing alloys. On the other hand, the authors' experience indicates that spinel products are unstable in alloys where magnesium is not present. Therefore, spinel products are not a universal solution to alloy containment needs.

Currently, alumina-bearing refractories are used for the containment of most molten aluminum alloys. Aggregate materials range from mullites to refractory-grade bauxites to tabular aluminas. Bonding systems vary widely from aluminum phosphates to calcium aluminates to self-bonded products. The forms also

¶Alloy 6061 contains 1.0% Mg, 0.6% Si, 0.28% Mn and 0.2% Cr.
**Alloy 5182 contains 4.5% Mg and 0.35% Mn.

vary, including brick; ramming mixes; castables; and precast, prefired large blocks.

Future of Alumina-Based Refractories in the Aluminum Industry

The aluminum industry is currently being driven to produce metals with tighter impurity requirements and more exotic compositions. This, in turn, makes the task of containment much more difficult. Lithium-containing alloys developed for aerospace applications present a particularly serious challenge to the refractory industry due to their highly corrosive nature and low surface tension. The trend to even more exotic alloys and tighter alloy specifications is expected to continue, making development of better refractory materials designed for specific applications essential.

Another trend which is expected to continue involves the concept of monolithic construction. "Seamless" furnaces offer the potential for minimizing problems often encountered with joints, as well as the possibility of minimizing furnace downtime. Plastic gunning mixes using bauxite or other alumina-bearing raw materials presently offer the greatest potential to produce a "seamless" furnace lining.

Furnaces that circulate molten metal and involve melting in a "heat bay" offer relief from some of the problems present in conventional furnaces. A uniformly heated chamber avoids the problems associated with high-temperature excursions. Problems associated with circulating metal and the frequently used salt flux covers present different challenges. Molten salts are often used to minimize oxidation problems associated with melting aluminum scrap.

The use of induction melting is also expected to escalate. It offers the potential of a "cleaner" system, run at lower temperatures, combined with the advantage of a closed metal vessel. The closed vessel protects easily oxidized and highly volatile alloying elements. Refractory "plumbing" is also needed for these systems.

Because of the widely varied refractory selection techniques employed by aluminum producers, the need for better, more definitive tests which are recognized by the refractory community is foreseen. Work to develop such tests is underway by ASTM Committee C-8.

Alumina-based refractories undoubtedly will play a role in the future of the aluminum industry. There is a good chance, however, that they will be used in many different forms, depending on the alloy of interest. Magnesium-aluminate spinel appears to have particularly great promise for the containment of magnesium-containing aluminum alloys.

References

[1]Aluminum Statistical Review for 1985, The Aluminum Association, Inc., Washington, D. C., 1986.

[2]T. Y. Canby, "Aluminum, The Magic Metal," *Natl. Geographic*, **8**, 186–211 (1978).

[3]U.S. Department of Commerce, Bureau of the Census, Current Industrial Report on Refractories, Summary for 1985; issued 1986 July.

[4]G. C. Efird, "Repairing Electrolytic Cells," U.S. Pat. No. 3 766 025, 1972.

[5]E. R. Thews, "Melting Pot and Crucible Furnaces in the Aluminum Industry," *Met. Ind.*, December 30, 597–99, (1927).

[6]H. O. Burrows, "Effect of Aluminum on Various Refractory Brick," *J. Am. Ceram. Soc.*, **23** [4] 125–33 (1940).

[7]S. Suzuki and Y. Fujita, "Refractory Materials for Light Metal Metallurgy, Research on Light Metal Use Refractories—Part 1," *J. Jpn. Ceram. Assoc.*, **49** [584] 466–73 (1941).

[8]S. Suzuki and Y. Fujita, "Refractory Materials for Light Metal Metallurgy, Research on Light Metal Use Refractories—Part 2," *J. Jpn. Ceram. Assoc.*, **50** [585] 15–20 (1942).

[9]K. J. Brondyke, "Effect of Molten Aluminum on Alumina-Silica Refractories," *J. Am. Ceram. Soc.*, **36** [5] 171–74 (1953).

[10]H. A. McDonald, J. E. Dore, and W. S. Peterson, "How Molten Aluminum Affects Plastic Refractories," *J. Met.*, **1**, 35–37 (1958).

[11]D. F. Stock and J. L. Dolph, "Refractories for Aluminum Furnaces," *J. Am. Ceram. Soc.*, **38** [7] 356–60 (1959).

[12]R. W. Brown and C. R. Landback, "Applications of Special Refractories in the Aluminum Industry," *J. Am. Ceram. Soc.*, **38** [7] 352–55 (1959).

[13]C. H. Schweinsberg and J. L. Dolph, "Aluminum Furnace Refractories," *Modern Castings*, **40** [2] 81–86 (1961).

[14]E. A. Bloch, "New Refractories for Aluminum Smelting Pots and Remelt Furnaces," *Erzmetall.*, **14** [8] 400–409 (1961).

[15]J. G. Lindsay, W. T. Bakker, and E. W. Dewing, "Chemical Resistance of Refractories to Al and Al-Mg Alloys," *J. Am. Ceram. Soc.*, **47** [2] 90–94 (1964).

[16]R. E. Pardee, "Refractories and Furnace Design for Primary Aluminum Melting Furnaces," *J. Met.* **94**, 56–60 (1966).

[17]P. D. Hess and M. J. Caprio, "Refractories for Aluminum Melting Operations"; Fourth Annual Refractories Symposium, St. Louis, MO, March 22, 1968.

[18]H. A. McDonald, "Procedures for Evaluating Refractories for Aluminum Melting," AIME Meeting, New York, February 17–20, 1958.

[19]R. I. Siegwart, "Experience with Refractory Materials in Small Aluminum Furnaces," *Trans. J. Br. Ceram. Soc.*, **73** [7] 213–18 (1973).

[20]M. S. Judd, "Reactivity of Molten Aluminum in Contact with Magnesium Aluminate and Magnesium Oxide Refractories"; M. S. Thesis, University of Illinois, Urbana, 1974.

[21]M. S. Judd and J. A. Nelson, "Interaction of Molten Aluminum and Magnesium Oxide Refractories," *J. Am. Ceram. Soc.*, **55** [7] 643–44 (1976).

[22]T. D. Steinke and M. A. Stett, "Refractories for Aluminum Melting Furnaces"; pp. 257–70 in *Light Metals 1977*, Vol. 2. Edited by T. M. S. Higbie. American Institute of Mechanical Engineers, New York, 1977.

[23]R. G. LaBar, "Large Refractory Block for Aluminum Melting Furnaces"; Fifteenth Annual St. Louis Refractories Symposium, St. Louis, MO, April 06, 1979.

[24]E. M. DeLiso and V. L. Hammersmith, "Testing Refractories for Molten Aluminum Contact," *Am. Ceram. Soc. Bull.*, **62** [7] 804–808 (1983).

[25]D. J. Bray, "Toxicity of Chromium Compounds Formed in Refractories," *Am. Ceram. Soc. Bull.*, **64** [7] 1012–16 (1985).

[26]G. E. Graddy and D. A. Weirauch, "Use of a Rotating Cylinder Method to Select Refractories for Molten Aluminum Applications"; presented at The American Ceramic Society Pacific Coast Regional Meeting, Seattle, WA, October 22, 1986.

[27]D. A. Weirauch and G. E. Graddy, "Wetting and Corrosion in the Al-Mg-Si-O System," International Symposium on Refractories, Winnipeg, Manitoba, Canada, August 23–26, 1987.

[28]R. G. LaBar, "Corrosion Resistant Castable Refractory Mix," U.S. Pat. No. 4 088 502, 1978.

The Use of Alumina in Refractories for Melting Glass

Everett A. Thomas
Didier Taylor Refractories Corp.
Cincinnati, OH 45244

The evolution of the glassmelting process from clay pot origin to continuous drawing of some 600 tons of glass per day has been totally dependent on availability of improved refractories based on alumina. The areas of most concern during this evolution have been the melter glass contact refractory and the condensate zone in the regenerator. Fusion-cast, bonded, and monolithic refractories now provide the glass industry with the capability to operate efficiently for six- to eight-year campaigns.

Commercial glasses cover a wide range in composition, physical properties, and refractory corrosion characteristics. To meet the melting requirements of these glasses from both an economic and environmental aspect, a wide selection of refractories has been developed over the past 60 to 70 years. This worldwide program has been synonymous with and dependent on the development and availability of high-purity alumina raw materials.

Refractories for glassmelting are derived mainly from five elemental oxides—alumina, silica, zirconia, magnesia, and chrome. Alumina, as such, finds little direct application but, when combined with appropriate oxides to form mullite, beta alumina, solid solutions, and/or mixed phases, it is an essential ingredient and contributes significantly to the melting process. The exception here is with silica and zircon refractories where the presence of alumina must be kept very minimal for high-performance standards.

Evolution of Refractories and the Glassmelting Process

Prior to the nineteenth century, glasses were melted and refined in crude handmade clay pots that were heated in simple fire boxes constructed of natural fire-resistant rock. The idea of a tank or some means of continuous melting was first patented by R. and R. Russel in England in 1769 and 12 patents covering various designs were issued prior to 1870.[1] Friedrick and Wilhelm Siemens[2] of Dresden, Germany were granted a British patent in 1861 for improvements in furnaces, i.e., the arrangement of four regenerators on a tank. The Siemens tank serves as a basic design for the modern continuous glass tank, as illustrated in Fig. 1. Some 40 glass furnaces[1] were in operation in England by 1872, one of which was of the Siemens regenerative design.

These early furnaces were constructed of firestone (sandstone), a sedimentary rock of 80 to 90% silica, with the exception of the flux-line area where hand-molded shapes in siliceous fireclay were found to be more suitable. Furnace life with such construction seldom exceeded six months for melting soda-lime-type glasses for bottles and flatware. In 1917, Davidson[3] reported that sandstone was preferred for blocks below the glass level as it wore smoothly, whereas fireclay blocks were considered to be better at the glass level. Currie[4] describes a tank that was built in 1908 and rebuilt in 1913. The top course of fireclay blocks had to be renewed each year and the

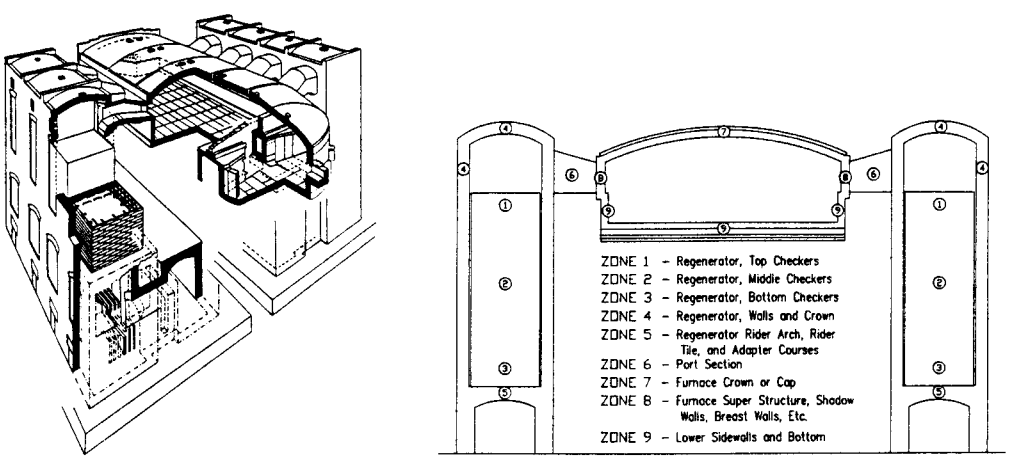

Fig. 1. Typical regenerative furnace for melting glass.

second course below about every two years. Sandstone blocks in the bottom and lower courses corroded at the rate of about one inch per year. Glass-surface temperature was probably in the range of 1300° to 1400°C.

Early fireclay flux blocks were made from plastic siliceous clays by the handmolding process and contained numerous voids and laminations. The ramming process, using pneumatic hand tools, was later adopted. This method allowed for blocks of higher alumina content (lower clay and more nonplastic) to be formed. The S. and G. process[5] developed by Scheidhauer and Giessing used over 90% prefired clay or aluminous grain with a deflocculated clay bond. The pneumatic ramming process for tank blocks has essentially been replaced by slip casting and machine stamping. Slip-cast blocks are formed in plaster-lined molds using a heavy deflocculated slip containing about 17% water that is vacuum treated prior to casting. These blocks require a slow drying process and undergo some 3 to 4% total shrinkage on firing. Stamped blocks are formed in rigid molds under pressure from impact of a massive weight that may undergo some 100 drops for a 30.5 cm- (12 in.-) thick cross section. The mix may be similar to that used in the S. and G. process, containing about 5% moisture and undergoing less than 1% total shrinkage on firing. Typical properties of tank blocks made by various manufacturing techniques are given in Table I.

Clay flux blocks formed by casting, ramming, or stamping were used extensively for melter sidewalls in continuous melting tanks up to about 1960, being gradually replaced by more corrosion-resistant fusion-cast blocks. Corhart Standard,[6] having a fused mullite structure, was introduced in 1928 by Corhart Refractories Company of Louisville, Kentucky. These blocks were first used as a top course at the flux line and gradually replaced clay blocks in the lower sidewall.

Table I. Properties of Clay Tank Blocks Made by Various Manufacturing Techniques

	"S & G" Mix	Casting	Stiff Mud
Grog (wt%)	92.2	71.0	67.5
Bonding clay (wt%)	7.8	29.0	33.0
Water content (%)	5.0	17.0	18.0
Method of molding	Stamping	Casting	Beating
Drying period (days)	1	27	27
Burning period (days)	12	12	12
Total time of manufacture	13	39	39
Drying shrinkage (%)	0.1	3.1	3.3
Total shrinkage (%)	0.2	3.8	6.5
Inflection (mm)	1.0	7.5	6.0
Bulk sp. g.	2.03	1.85	1.90
Total porosity (%)	18.0	26.4	24.0
Crushing strength ($kg \cdot cm^2$)	707	147	220

Ref. 1.

About 1923, a natural igneous rock was found in India having a molar composition of $Al_2O_3 \cdot SiO_2$. This rock, imported into England under the name *sillimanite,* was found to offer some potential advantages over clay and siliceous refractories in glassmelting furnaces. The so-called sillimanite rock that later was identified as kyanite was brought into the United States in 1924 by the Charles Taylor Sons Company, Cincinnati, Ohio and soon became widely accepted as an improved raw material for making super refractories to upgrade the silica upper structure and for the forehearth glass contact area of the furnace.

The use of Corhart Standard flux block for the melter sidewall and sillimanite-type brick and shapes for ports, breast wall, and upper regenerator area allowed for an increase in both furnace output and campaign life from 1930 through 1950.

Just prior to World War II, further development in fusion-cast melts led to trial tests of blocks made from alumina-zirconia-silica (AZS), alumina-chrome, and soda-alumina compositions but these new refractories were not fully accepted until about 1950. The use of such special blocks, together with the introduction of fused alpha-beta alumina blocks for the refiner area; bonded zircon brick for melter bottom paving over clay flux, and to supplement silica as a buffer course against alumina-bearing refractory in the upper structure; basic brick for checkers and regenerator construction; and bonded AZS for hot repair made furnace campaigns of four to five years a reality by 1965.

Further developments in casting techniques to reduce the void structure of fusion-cast blocks, the introduction of oxidized AZS and its use in superstructures, together with improved direct-bonded basic brick, mullite, and sintered AZS now provide for furnace production rates below 2787 cm^2 (3 ft^2) per ton per 24 hours and campaigns of 6 to 8 years of continuous service. In European countries, the production rate is expressed as specific pull-tons/m^2/24 h. Figure 2 shows the evolution of specific pull and temperature for container furnaces from 1920 to 1985. Data up to 1971 were supplied by Garstang[7] and projected to 1985

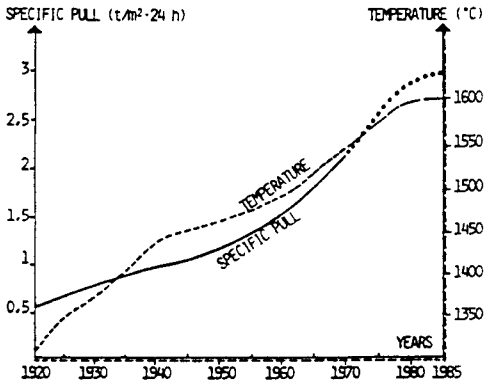

Fig. 2. Evaluation of specific pull and temperature for hollow glass furnaces (Ref. 8). (Used by permission.)

by Moreau et al.[8] Melting temperatures have gradually increased from about 1300° to 1600°C over this period to allow for more tonnage output per melting area. This has been made feasible only through improved quality of glass contact and upper structure refractories.

Corrosion Factors in Melting

The life of a glassmelting furnace is limited by the safe conditions of the refractory enclosure and the thermal efficiency of the operation. Busby[9] states, "The two most important areas of corrosion to be considered are those at the glass-refractory interface and in the regenerator."

Glass Contact Corrosion

Solution of refractory below the glass level is a diffusion-controlled process—the rate being temperature-dependent. A diffusion barrier, which may be a viscous glass barrier or combination of refractory and viscous glass, is formed at the interface of all refractory-glass systems. Any disturbance of this barrier leads to increased rates of attack such as is evident at the flux line and where upward drilling may be active. Corrosion below the flux line may be affected by density currents that form as a result of refractory corrosion and convection flow within the furnace. For soda-lime glass, the interfacial glass formed on alumina-bearing refractory is heavier than the host glass; thus, there is a tendency for downward flow that tends to protect the lower refractory surface. In high-lead glass the reverse situation may occur, resulting in upward flow and more corrosion below the flux line.

Busby[9] states that "At the flux line the glass is pulled up into the meniscus above the general glass level by surface tension forces and the increased rate of attack at this point is caused by the stirring action brought about by a surface tension gradient." Busby further states that "Upward drilling occurs in the presence of gas bubbles and a development of the stirring action around the periphery of contact causes an increased rate of solution." In effect, the turbulent action of the bubble removes the diffusion barrier and exposes a new refractory surface to further corrosion.

Upward drilling attack may be very evident in the throat (a submerged channel that connects the melter and refiner) and at all horizontal joints. In early furnace construction, several courses of block were used to build up the melter sidewalls but it soon became evident that the horizontal joint was a point of weakness due to upward drilling corrosion. As larger blocks became available, the use of horizontal joints was eliminated or confined to the lower course where temperature and corrosion activity are less apparent. Many furnaces now utilize fusion-cast sidewall blocks 25.4 cm (10 in.) thick and up to 1.83 m (72 in.) high. This allows for continuous backup insulation to reduce heat loss, starting at a point about 15 cm (6 in.) down from the top to allow for air cooling of the flux line.

Based on a study of corrosion mechanism by Hrma,[10] Busby[11] in a review states that "The surface tension of glass melts varies only slightly with temperature but depends strongly upon composition." Dietzel,[12] in a study of surface tension forces, states, "There is a decrease in surface tension when silica is replaced by the aggressive fluxes potash, boric oxide, lead oxide, soda and fluorine and an increase when replaced by the polyvalent metal oxides alumina, magnesia or lime, the rise with alumina being very marked." Busby[11] further states, "If the interface between a melt and a gas or an immiscible liquid is exposed to considerable variation in concentration, such as those found at the interface between a melt and a refractory, then surface forces will arise and induce flow which may be very vigorous, causing enhanced dissolution of the refractory." For an AZS refractory in a soda-lime glass, the solution rate of the refractory may vary considerably on an individual basis, silica having the greater corrosion rate followed by alumina and then zirconia. Petrographic examination of such an interface usually shows a concentration layer of zirconia grains held in place by a viscous glass matrix. As silica and alumina diffuse into the solvent glass, the viscosity of the glass matrix is maintained by further solution from the base refractory. Alumina serves a prime function in this process as it greatly contributes to the viscosity of the matrix glass in the soda-lime glass system.

Tress,[13] in a study of distinctive contour corrosion on aluminous-silica refractory in various molten glasses, states that "An increase of alumina at the expense of the corrosive fluxes raises viscosity and lessens chemical attack on the refractory. Consequently, the viscous film of solution which slowly forms at the refractory face gives some protection against the solvent glass." In other glass systems it may be less effective. For example, sodium borate has a strong affinity for alumina so that, in borosilicate glasses, silica may contribute more than alumina to maintaining a viscous glass interface.

The kinetics of corrosion of refractory in a CaO-Al_2O_3-SiO_2 slag was investigated by Reed and Barrett,[14] who showed that the solution rate of alumina was controlled at first by a chemical process but that this quickly changed—in a matter of minutes—to a diffusion-controlled process as a reaction-product layer built up at the interface.

Upward drilling and flux-line corrosion were studied by Loffler[15] and by Jebsen-Marwedel.[16] Their conclusion, as expressed by Busby,[17] is that "Flow is induced at the flux line and in upward drilling and brought about by interfacial energy conditions. The mechanism was envisaged as alkali from the glass reacting with the refractory and forming a silica-rich

glass layer. Between this layer and the refractory block the solution process produced an alumina-rich reaction layer and increased surface tension led to a continuous movement. No stationary condition can be achieved because of the constant solution of Al_2O_3." In effect, this may be referred to as the process of selective solution of alumina-silica in an AZS refractory whereby silica is first taken into solution, followed by alumina, and finally the more inert zirconia phase.

Corrosion tests conducted by the writer on sintered compositions of the AZS system in soda-lime glass have indicated that optimum corrosion resistance is obtained when 40 to 60 wt% alumina is present. The same may not hold true for fusion-cast compositions but economics of raw material sources favor this range. Fusion-cast AZS refractories containing over 41% zirconia have not proved to be practical for most commercial glasses.

Worldwide, some 80% of all glass melted is of the soda-lime type, being used mainly for flatware, containers, tableware, and lighting. This represents well over 500 container furnaces melting some 100 to 300 tons per day, over 150 flat-glass furnaces melting 300 to 600 tons per day, and several hundred furnaces melting less than 100 tons for container, tableware, and lighting usage. Today, this tonnage of glass is wholly dependent on the use of fusion-cast AZS sidewall blocks for its containment during the melting process.

Borosilicate, lead, and TV glasses make up some 10% of the worldwide demand. These glasses are also totally dependent on the use of fusion-cast AZS. Insulation wool glass and fiberglass represent the balance of commercial glass being melted on a continuous basis. These glasses are more corrosive and require the use of chrome-bearing refractory for the melting process. Fused alumina-chrome, sintered alumina-chrome, and fused alumina-chrome-zirconia-silica (ACZS) find extensive use in melting insulation wool glass. Fiberglass of "E" composition is totally dependent on the use of sintered, dense chrome for the sidewall glass contact area.

Sodium silicate, used in many industrial processes and detergents, is a water-soluble glass produced by thermal reaction of soda ash and silica. The ratio of soda to silica may vary from 1:1 to 1:3.2 based on the end use. An optimum glass contact refractory sidewall is not as critical since the glass quality requirements are much less stringent than for the above commercial glasses. Furnaces are often run for short campaigns of two to three months and then shut down for necessary repairs. Corrosion-wise, fused alpha-beta alumina and 90% alumina firebrick are favored for the 1:1 to 1:2 ratio glasses and fused AZS for the higher-silica melts. However, clay flux block and firebrick continue to be used extensively in view of economics and the thermal cycling of the process.

Regenerator

The regenerator extracts waste heat from the combustion gases and returns it to the melter as preheated air for further combustion. The efficiency of a regenerator decreases with age, mainly as a result of plugging of flues or corrosion and loss in volume of the checker packing.

Early regenerators were of fireclay brick construction and became more and more susceptible to corrosion as melting temperatures and production rates increased. The regenerator crown and upper walls were subject to slagging by batch dust carryover and alkali vapors, resulting in rundown and plugging of the top checkers. The lower part was corroded away by condensates in the waste gases. Condensates prevalent in this area will depend on the type of glass being melted. For soda-lime glass, the condensate is mainly sodium sulfate. For lead glasses, it may contain sodium and potassium sulfate as well as lead compounds. For borosilicate glasses, the condensate is mainly sodium borate and, to a lesser extent, sodium sulfate. Such condensates[18] are very corrosive on fireclay brick, resulting in more or less complete loss of the checker setting after one to two years of service.

The use of high burned firebrick made from kaolin has been preferred over superduty grades for both upper structure and checker packing. Mullite brick based on Indian kyanite (1930–1950) and from bauxite clays from Alabama (1950–1970) found extensive use in the upper walls and crown to resist slagging attack but they eventually contributed to checker plugging by nepheline reaction and continual peeling away of the reaction zone. Such brick were found to have better resistance to subsidence than the superduty grades and thus could support more insulation without slumping.

Basic brick based on natural magnesite, periclase grain, and various grades of chrome-magnesite or magnesite-chrome significantly helped to extend regenerator life and to improve operating efficiency but have had to be constantly improved in quality and bonding phases to meet the changing conditions of the industry.

Busby[9] states that "Reactions in the regenerator are very temperature dependent and confined to two principal areas:

1. Top of the chamber and first few courses of packing.
2. The middle zone of the packing where condensate attack may occur."

Temperatures in the top chamber may range from 1450° to 1650°C on the target wall. Firing with oil in preference to natural gas further contributes to the reaction problem by the presence of fuel oil ash—mainly based on sulfur, vanadium, and nickel.

Unburned magnesite and conventional fired magnesite are subject to reaction by silica batch dust, resulting in expansion and cracking due to the forma-

tion of forsterite (magnesium silicate). Busby[9] states that the "... calcium silicate bond in such brick is subject to conversion to calcium sulfate at temperatures below 1400°C in the presence of sodium sulfate forming a low melting point fluid in the bond phase." Direct bonding between the periclase grains or use of direct-bonded magnesite-chrome is thus preferred to conventional silicate bond for severe upper chamber service.

In the condensate zone area, basic brick are subject to attack by alkali sulfates and SO_3 gas. Busby[9] has shown in laboratory tests that the formation of magnesium sulfate occurs at about 1100°C and that the conversion by sodium sulfate is more rapid in the presence of SO_3 gas. Likewise, the presence of vanadium pentoxide from fuel and arsenic from the glass batch will decrease the peak conversion temperature by some 100°C. Materials that have shown good resistance to sulfate attack in the above test are magnesite-chrome, fused AZS, and forsterite brick made from olivine.

Weichert[19] states that "Waste gases from both natural gas and fuel oil firing contain Na_2O and SO_3. An excess of Na_2O is found in natural gas fired furnaces and an excess of SO_3 in oil fired furnaces. Na_2O is released by the dissolution of the soda contained in the batch. SO_2 is formed in the gas fired furnace through dissolution of refining agents containing sulfates. In oil fired furnaces, SO_2 is formed by the burning of the oil. Below 1000°C, SO_2 is transformed into SO_3 by the catalytic effect of V_2O_5 that may run as high as 200 ppm in the oil."

Based on some 10 to 15 years of evaluation in soda-lime furnaces, Weichert offers the following concepts for checker layers in the middle chamber area[19]:

1. Furnaces fired with natural gas
   a. Forsterite-bonded magnesia brick.
   b. Calcium silicate-bonded magnesia.
   c. Forsterite brick with magnesium-alumina spinel additive.
2. Furnaces fired with oil
   a. Forsterite brick with MA spinel additive.
   b. Forsterite-bonded magnesia brick.
   c. Magnesia-chrome brick.
   d. Chrome-magnesia brick.

Weichert further states that "Longer service life and increased melting temperatures have led to higher loading of the regenerator chamber. There has been an increase in use of heavy oil with high sulfur content—especially in foreign countries where natural gas is not available. The result is that the checker brick in the middle checker area have been more heavily subjected to Na_2O, SO_3, and Na_2SO_4. In some cases the admission of sulfates was so intense that the flues became clogged with sulfates to such an extent that they had to be regularly melted free. The forsterite bricks used in these instances were thermomechanically overloaded by the melting free process and they spalled.

"Mixed firings have become more and more prevalent. Oil and gas are used depending on their pricing and their availability on the fuel market. As a result, there are strongly varying corrosion loads for the brick in the middle checker area. Furthermore the changing of fuels and the varying of service conditions may lead to movement of the alkali sulfate condensate zone into other parts of the checkers and cause failure."

Weichert further states that "The use of chrome-magnesia brick for the difficult service conditions in the middle checker area is completely justifiable in many cases. The chrome ore in such brick is corroded in an oxidizing atmosphere in the presence of alkalies. The wear on the chrome ore is slow, as it is believed that the corrosion occurs via the vapor (phase) and the vapor pressure of Cr_2O_3 at the prevalent temperature is low. Thereby sexivalent chrome is formed from the trivalent chrome of the chrome ore. The compounds of the sexivalent chrome and the alkalies are called alkali chromates. Although the combinations of the trivalent chrome in the original brick are not toxic, the alkali chromates so formed are classified as highly toxic compounds. For example, the inhalation of chromate dust can lead to tumors in the breathing passages and watery chromate solutions can cause severe skin injury."

Weichert further states that "The waste disposal problems connected with chrome-ore-containing bricks have already resulted in many glass works, particularly in the Federal Republic of Germany, refusing to install these bricks in their furnaces. The waste disposal law promulgated on January 5, 1977 forbids the disposal of chrome-magnesia waste brick on normal garbage dumps. The possible formation of chromates during service makes their disposal on special dumps necessary. As is widely known in the glass industry, the disposal costs can run as high as DM 500 per ton of waste brick."

Weichert[19] reports that crucible tests conducted with chrome-ore-containing bricks at 900° and 1000°C using Na_2CO_3 and Na_2SO_4 as slagging agents will show evidence of chromate formation after only five hours of testing.

The problem with use and disposal of chrome-ore-containing brick from glass furnace regenerators has become a major issue in all Western countries. Many states in the United States now have restrictions on disposal, making it necessary to consider alternate materials for the checker chamber.

In 1974, Busby[9] reported that fused cast AZS was very resistant to the alkali sulfate and SO_3 environment in the condensate zone; however, the high cost of using fused AZS brick shapes in the zone made this approach very prohibitive. Moreau et al.[8] report that the fused, cast AZS cruciform shape was introduced in 1977. The shape has a cross-section thickness of 40 mm and is designed to form vertical flues of 140 × 140 mm, as opposed to much larger flues and cross sections for the more conventional brick setting. This new

design, together with the material's low rate of aging, provides for improved regenerator efficiency and continued efficiency throughout a campaign. By 1985, some 360 installations and test settings were reported to be in service. It is further reported that the useful life of a regenerator packing has now doubled as compared to the classical brick settings.

It has been observed that, after a campaign, the top courses of the fused AZS cruciform settings may need to be replaced due to various degrees of cracking. This is mainly the result of stresses from formation of nepheline due to alkali reaction and thermal fatigue. Fused AZS top checkers are now being replaced with fused alumina based on the molar composition $Na_2O \cdot 4MgO \cdot 15Al_2O_3$. In 1978, Cheetham[20] reported use of the integrated checker system to overcome many of the problems that exist when using standard shaped bricks. The I.C. system uses an I shape to form vertical 15 cm (6 in.) square flues. This provides for more mass or heat storage, excellent stability, and no flat surfaces for batch dust or condensate buildup. The I.C. modules can be produced in a range of qualities to meet the conditions present throughout the vertical setting.

Scheiblechner[21] reported that the first installation of chimney-block checkerwork was made in 1979 and that 25 installations were operating successfully at the time of his presentation in 1983. Chimney blocks have been supplied with square passage widths of 108, 140, and 160 mm. The trend is toward smaller passage sizes for better operating efficiency. Like the I.C. modules, chimney-block shapes can be produced in a range of materials for specific conditions. Where environmental restrictions do not permit use of chromite-containing brick, the sulfate area is packed with magnesite brick of special bonding additives such as alumina spinel. In comparison to conventional brick settings, the author states that chimney blocks offer the following advantages[21]:

"1. Fuel savings due to greater specific surface and higher efficiency.
2. Maximum stability resulting in longer life.
3. Rapid, simple, and safe installation.
4. Versatility in that they are independent of brands and packing systems.
5. High economy."

Robyn et al.[22] performed thermal fatigue tests to simulate conditions for both the upper layers and the condensate zone. For the upper zone, samples were impregnated with a mixture of 75% V_2O_5 and 25% Na_2SO_4 and subsequently exposed to thermal fatigue between 1300° and 1500°C for one week. The results of the vanadium simulated test show that the fused alumina cruciform checkers undergo less attack and transformation than high-purity magnesia brick. The high-purity magnesia brick reacted in various degrees, depending on the nature and calcining of the raw material and the firing of the brick. Alumina-spinel bricks were found to be unsuited for the upper layer in high-vanadium fuel fired furnaces.

The simulated test for the condensate zone was performed in a double-pass regenerator where temperatures ranged from 1100° to 450°C. Sodium sulfate and sodium bisulfate were injected into the flame during the 15-minute heating cycle and then preheated air was blown through the setting in the reverse direction for 15 minutes. The test was run for one month. Robyn et al.[22] state that "Three types of alteration have to be taken into account for the sulfate zone:

1. Sulfate attack.
2. Damage caused by thermal cycling.
3. Alkali attack which is a transition from the sulfate attack at higher temperatures (around 1000°C)."

The test results showed that fused AZS, chrome, magnesia-chrome, and alumina-spinel brick all have good resistance to the test conditions. It was concluded that alumina-spinel could be a good substitute for chrome-containing refractories in the sulfate zone.

Robyn et al.[22] further conclude that "The energy problem has led to improvements in the regenerator with creation of new types of checkers such as the cruciform and the chimney block setting. The economics of the new types must now be seen in terms of

1. Optimal quality–cost selection.
2. Longer lasting efficient heat recovery.
3. Longer carefree operation due to reduced sulfate plugging.
4. High probability for recuperation for a second campaign due to less destruction."

The references cited point out the on-going refractory problems that the glass industry has had to face up to in its effort to improve on regenerative melting efficiency. The use of electric melting is one approach to completely eliminate the regenerator and associated condensate corrosion problems related to the melting of glasses containing fluorine, lead, and boron. Electric melting is very efficient but the high cost of power in some geographic areas must be offset by potential savings in batch losses, environmental control, and construction costs of the regenerator. Several cold-top electric furnaces are operating economically on soda-lime glass for containers but the main emphasis has been for melting insulation wool glass. Davis[23] showed that essentially all of the glass batch volatiles such as SO_2, F_2, B_2O_3, and lead vapors can be entrapped in the batch crust and "mush" layer of the cold-top furnace and eventually recycled back to the glassmelt.

Another approach is direct firing and use of a metallic recuperator to maintain an efficient firing system. Textile fiberglass is melted exclusively by the recuperative direct firing process. Stark[24] points out that 25 to 30% fuel savings can be realized and the payback for installation of a recuperator on a direct-fired fiberglass furnace is less than three years.

Classification

Refractories are derived from many raw-material sources. In most cases the raw-material source must be beneficiated and calcined or sintered to obtain a processed grain suitable for end use. Table II relates processed grain with source and the manufactured end product such as fused AZS, bonded mullite, or alumina-chrome.

Refractories used in glass furnace construction may be classified into three general groups based on degree of heat treatment, namely: fusion-cast, bonded-sintered, and monolithic.

Table II. Refractory Raw Materials—Source and Use

Processed Grain	Source	Brick Use
Quartzite	Quartzite rock	Silica
Fused silica	Quartz sand	Fused silica
Calcined clay	Flint clay Kaolin	Firebrick and clay flux
Bayer alumina	Bauxite	Fused AZS Fused chrome-alumina Boned AZS Fused alumina Dense alumina Fortified mullite MA spinel magnesia
Tabular alumina	Bayer alumina	Bonded AZS Fortified mullite High alumina Alumina-chrome
Calcined kyanite	Kyanite rock	Bonded mullite
Andalusite	Andalusite ore	Bonded mullite
Sintered mullite	Kaolin and Bayer alumina	Bonded mullite
Sintered mullite	Bauxitic clay	Bonded mullite
Fused mullite	Bauxite	Bonded mullite
	Quartz and Bayer alumina	Bonded mullite
Calcined bauxite	Bauxite or diaspore	Fused mullite
Zircon	Beach sand	Fused AZS Bonded AZS Zircon
Olivine	Olivine rock	Forsterite
Periclase	Magnesite rock	Magnesite
	Seawater	Magnesite-chrome
Chrome	Chrome ore	Chrome Chrome-magnesite Fused chrome-alumina Fused chrome-spinel
Chromic oxide	Chrome ore	Dense chrome Alumina-chrome Fused chrome-spinel Fused ACZS
MA spinel	Periclase and Bayer alumina	MA spinel-magnesia

Fusion-Cast Refractories

Fusion-cast refractories are produced by melting and casting a molten magma from an electric arc furnace into sand or graphite molds. The blocks must be slowly cooled and annealed to prevent major cracking. Location of casting voids may be partially controlled by tilt casting or casting headers and cutting away an excess part of the block. Several types of fusion-cast blocks are of interest in glassmelting.

The fusion-cast process, according to Humphrey,[6] dates back to early patents granted to Jacobs in 1902 and Tone in 1908. The first trial brick were cast by Fulcher of Corning Glass Works in 1922 and a test block was installed in a glass furnace the same year. Commercial production of Corhart Standard, a fused-mullite block, was started in 1928 in Louisville, Kentucky. Licensee arrangements were granted to L'Electre Refractaire Company of France in 1929 and to Asahi Glass Company of Japan in 1930.

The transition to the fused AZS composition was a progressive change as some zircon addition to the mullite composition was considered necessary to reduce cooling cracks. This led to the development of Corhart Zed, containing about 20% ZrO_2, in the 1940s and higher zirconia-bearing blocks in the 1950s. Up to this time, the cast block contained some carbon which contributed to seed and blister defects in the glass when such blocks were used in the refiner or drawing end of a furnace. The fully oxidized fusion-cast process was developed by L'Electro Refractaire Company in France in 1960 to 1962 and was considered a major innovation as it permitted fused AZS to be used more extensively throughout the furnace. An oxidized process was soon adopted by other manufacturers.

The production of Corhart Standard was discontinued in the early 1960s but similar compositions may still be available in eastern Europe and China. The worldwide production of fused AZS is shown in Table III. This extensive list is an indication of the wide acceptance of fused AZS refractories for glassmelting.

Other fusion-cast compositions have been developed over the years, starting with a chrome-alumina block produced by Carborundum Company in the 1930s for use in the metallurgical field and followed by Monofrax H (beta alumina) for use in magnesium reduction cells. Following World War II, Monofrax H and the alpha-beta version "Monofrax M" became available to the glass industry. Over the past 20 years, improvements have been made in fused chrome-alumina and modified compositions containing Cr_2O_3 have been developed for specific application in glassmelting. Both Monofrax H and Monofrax M are produced in France under the name Jargal by license agreement with L'Electro Refractaire (now known as SEPR) and in Japan and India.

Further comments on the various types of fusion-cast refractories are as follows:

1. Fused alumina-silica is formed from calcined bauxite or diaspore. It contains a coarse crystalline

Table III. Fused AZS Brands

ZrO_2 (%)	Brand	Country
32-33	Electrofrax S3	India
	Bakor 33	U.S.S.R.
	Zircosit 30	Hungary
	KLB 303	Czechoslovakia
	Zac 1681	France
	Monofrax S3	U.S.
	Unicor 501	U.S.
	Criterion I*	U.S.
	Zetacor AT2	Italy
	Monofrax S3	Japan
	Zirconite ZB 1681	Japan
36	Electrofrax S4	India
	Monofrax S4	U.S.
	Zetacor A	Italy
	FC101*	U.S.
	Unicor 37	U.S.
41-42	Bakor 41	U.S.S.R.
	Electrofrax S5	India
	Zircosit 40	Hungary
	Zac 1711	France
	Monofrax S5	U.S.
	Monofrax SF	Japan
	Unicor I	U.S.
	Zirconite ZB 1711	Japan
	Criterion II*	U.S.
45	Bakor 45	U.S.S.R.
50	Bakor 50	U.S.S.R.

*Discontinued brands.

mass of mullite needles embedded in a glassy matrix. Although formerly used extensively as melter sidewall blocks, production and use are now confined mainly to eastern Europe and China.

2. Fused AZS is formed from Bayer alumina and zircon. The structure contains a corundum-zirconia eutectic phase with segregated nodular zirconia and primary dendritic zirconia in a glassy matrix. It is used for glass contact sidewall blocks, throat construction, and bottom paving and may be used in the refiner and for forehearth channels. For upper structures, the main applications are the Tuck stone course, port and port jambs, backwall, and breast-wall construction. Melter crowns may be used on furnaces melting special glasses that exhibit high attack on silica. In the regenerator, it is now being used extensively for checker packing.

3. Fused alumina is formed from Bayer alumina with controlled amounts of soda to form either alpha, alpha-beta, or the beta structure. The alpha type finds very limited use as glass contact with special glasses. The alpha-beta intergrowth structure has very low seed and blister potential and is used extensively for glass contact in the refiner, working end, and forehearth. Corrosion resistance[17] in soda-lime glass is considered equivalent to fused AZS (32%) up to about 1300°C.

The beta form has a coarse friable structure with no glassy phase. It is used extensively in the melter upper structure for port, port jamb, and breast-wall construction. It is subject to conversion to the alpha form in the presence of silica batch dust, resulting in some degree of surface shelling, but its relative freedom of exudation glass makes its use preferable in some furnaces. It may also be used for forehearth cover blocks on special glasses.

4. Fused chrome-alumina is formed from chrome ore and Bayer alumina. It contains an intergrowth of iron-chrome and alumina in solid solution and an enveloping spinel phase of magnesia-chrome-alumina with minimal glassy phase. It has high corrosion resistance in soda-lime glass for use in critical areas but can be a potential source of discoloration. It is used extensively for melter sidewall, paving, and forehearth construction on alkaline borosilicate glasses for insulation wool.

5. Fused chrome-spinel is formed from chrome ore and chromic oxide. It contains a spinel phase in an R_2O_3-glass matrix. Use is mainly as glass contact in melting "E" textile glass.

6. Fused alumina-chrome-zirconia-silica is formed from Bayer alumina, zircon, and chromic oxide. It contains a solid solution of chrome-alumina and zirconia in a glassy matrix and has high corrosion resistance in soda-lime and alkaline borosilicate glasses. It finds application in critical areas in melting soda-lime glass and is used extensively for melter sidewall, paving, and forehearth construction for insulation wool glass.

Table IV. Composition of Fusion-Cast Refractories

	Alumina-Silica	AZS	ACZS	Fused Alumina			Chrome-Alumina	Chrome-Spinel
				Alpha	Alpha-Beta	Beta		
Al_2O_3 (%)	74	45–51	28–37.5	99.3	95	94.5	60	4.7
ZrO_2 (%)	1	32–41	20–28					
SiO_2 (%)	19	10–16	10–15	0.1	1.0	0.1	1.8	1.3
Cr_2O_3 (%)			28–30				27	79.7
Alkali and others (%)	6	1–1.6	1–1.5	0.6	4.0	5.4	10.5	
Bulk density								
kg • dm^3	2.88	3.44–4.00	4.00	3.52	3.14	2.80	3.44	4.08
(lb/ft^3)	180	215–250	250	220	196	175	215	255

Typical compositions of fusion-cast blocks are given in Table IV.

Bonded, Sintered Refractories

Bonded refractories cover a wide range in composition from acidic to basic, from dense fine-grained homogeneous to coarse grog heterogeneous structures, and from highly insulating materials of low k factor to those having high thermal conductivity. Heat-treatment temperatures may range from chemically cured in the case of unburned basic brick to highly sintered AZS and alpha alumina shapes. Table V gives information on the composition of various bonded refractories used in glassmelting.

Silica (SiO_2): The manufacture of silica brick[25] in the United States dates back to about 1866 at a Diamond Fire Brick Works plant in Akron, Ohio. The production of silica in England was about 1820, according to Chester.[26]

Although silica is a very acid refractory for consideration in an alkaline environment that usually exists with glassmelting, it has been used extensively for melter and refiner upper structures since the conception of continuous melting. Silica brick and shapes are formed by conventional pressing, impact pressing, pneumatic ramming, and handmolding from graded mixtures of crushed quartzite or ganister with an addition of lime. For optimum performance, the alumina content must be limited to about 0.5%.

Trends toward higher furnace output and melting temperature now limit the use of silica almost exclusively to the melter crown in large production furnaces. The refiner and working end of furnaces melting soda-lime glass will continue to use silica for many years in view of its low cost and excellent performance.

In recent years, the use of fused quartz grain has become of interest in making silica brick shapes to resist thermal shock during the hot patching of silica crowns and for expendable shapes for use in the forehearth or drawing end.

Zircon ($ZrSiO_4$): Zircon is acidic and thus very compatible with silica and highly siliceous glasses. The potential for zircon refractories was first recognized in melting the low-expansion borosilicate-type glasses and a need developed with the industrial growth of these glasses in the early 1950s. This was prior to the development of the oxidized AZS fusion-cast block which later replaced zircon as a glass contact refractory in the refiner and forehearth area for these glasses. During this same period, the development and demand for "E" fiberglass created a market for dense zircon glass contact blocks which later was gradually replaced by dense chrome. (The corrosion resistance of dense chrome was found to be about 10 times better than dense zircon in "E" glass; thus, service life of the melter could be extended by a factor of 10 without need for extensive water cooling.)

Zircon brick offer good resistance to the sodium borate vapor environment that is present throughout the furnace in melting borosilicate glasses. Zircon is thus used extensively in the upper structure on these glasses.

Alkali reaction with zircon refractory results in surface alteration to form a zirconia interface, which

Table V. Typical Composition of Bonded Refractories

	Silica	Clay	Mullite	AZS	Zircon	Alumina	Chromic Oxide	Alumina-Chrome
Al_2O_3 (%)	0.2–0.8	25–50	60–76	55–70	0.5	90–99		67–86
SiO_2 (%)	95–97	45–70	38–20	10–20	33	0.1–8.5		1.5–2.5
ZrO_2 (%)				20–30	65			
Cr_2O_3 (%)							95–98	9.8–29.5
Others (%)	1.0–2.0	3–5	1–4	0.2–0.3	1.5	0.5–2.0	2–5	1–2
CaO (%)	1.8–3.0							
Bulk density								
kg • dm^3	1.66–1.95	2.08–2.24	2.32–2.72	3.04–3.28	3.36–4.32	2.96–3.36	4.24–4.48	3.09–3.30
(lb/ft^3)	104–122	130–140	145–170	190–205	210–270	185–210	265–280	193–206

	Magnesite	MA Spinel-Magnesite	Forsterite	Magnesite-Chrome	Chrome
MgO (%)	90–98	45–93	47–55	42–81	15–20
Cr_2O_3 (%)				10–30	28–38
SiO_2 (%)	1–8.5	1–2	30–40	3–6	3–6
Al_2O_3 (%)		5–50	1–10	5–20	15–35
Fe_2O_3 (%)			7–10	3–10	10–18
Others (%)	1–3	1–2	1–3	2	1–2
Bulk density					
kg • dm^3	2.88–3.04	2.88–3.20	2.72	3.04–3.12	3.25
(lb/ft^3)	180–190	180–200	170	190–195	203

offers excellent corrosion resistance if not disturbed by the glass flow. This allows zircon brick to be used effectively as paving and subpaving in bottom construction on moderately pulled soda-lime glass.

Zircon also serves as a buffer course to reduce joint reaction between silica- and alumina-bearing refractory in the melter upper structure.

Zircon is found in nature as granular zircon, an associated mineral of beach sand which is commercially mined in Florida, Australia, and Africa. The beneficiated zircon sand is processed to yield various grades of milled zircon used in the manufacture of dense zircon block, zircon brick, and monolithics. Dense zircon is formed by slip casting and isostatic pressing. Zircon brick and shapes are formed by conventional pressing, pneumatic ramming, and casting. The alumina content of zircon, like silica, must be limited to about 0.5% for optimum service.

Fireclay and Clay Flux

Clay refractories have gradually been replaced throughout the glass contact area in most continuous melting furnaces. A few furnaces melting flat glass may still continue to use clay flux block for the melter bottom but this is now the exception. Clay brick and block continue to serve a function as backup media, both along the melter sidewall and in bottom construction, to conserve heat. An effective intermediate or subpaving layer (preferably a seal layer) must be used under the top paving to protect the clay from glass seepage and corrosion on highly insulated construction.

Clay brick have essentially been replaced by mullite and/or basic in the regenerator area but clay will continue to be used in the lower regenerator and stack area where temperatures below 800°C may prevail.

Furnaces melting soda-lime glass for float production of flat glass use clay flux block to contain the molten tin bath. These are complex shapes that must be bolted in place to resist the buoyant effect of the molten tin. Blocks in the hot bay area that receives glass from the furnace may need to be replaced after one campaign of six to eight years. Blocks in the colder bays can effectively serve two or three campaigns.

Clay firebrick ranging from first quality to superduty grades are made from selected blends of flint clay, calcined fireclay, or kaolin and raw clay and formed on conventional presses. Firing temperatures may range from PCE of cone 10 to cone 18 for the superduty quality. Clay flux blocks are formed by either slip casting or stamping. The alumina content is controlled by selected natural alumina-silica raw materials.

Day tanks and some continuous tanks used for handforming of glass will continue to depend on use of clay flux block for furnace construction.

Mullite ($3Al_2O_3$-$2SiO_2$): Mullite refractories make up a select group in the alumina-silica system. Superduty brick, due to high firing, may contain a substantial amount of mullite crystalline phase (40 to 60%) but the glassy matrix present contributes to slagging and subsidence under high stress conditions. The discovery and availability of Indian kyanite rock as a source of mullite grain made a significant contribution to progress in upgrading glassmelting furnaces. From 1930 to 1960, mullite brick and shapes replaced silica in the more vulnerable areas of the upper structure while furnaces were being pushed for higher yield and service life.

The development[27] in the 1950s of sintered and fused mullite based on bauxitic raw materials and high-purity grain, dependent on Bayer alumina, gradually replaced the Indian kyanite sources which were becoming limited in both supply and quality.

Mullite shapes are used exclusively for the upper structure in the drawing end on soda-lime glass. This includes the roof area on the forehearth for container, tableware, and lighting ware production and the suspended roof over the tin bath on float glass. Mullite is used as a backup course to suspend AZS veneer on the end wall over the charging bay and as a suspended cover in the waist area connecting the refiner and working zone of the float-glass furnace.

Applications for mullite in furnaces melting sodium silicate and special glasses may include melter crowns, port and breast-wall construction, and the regenerator. For furnaces melting "E" glass, mullite is considered standard construction for the melter crown, breast walls, and the complete refiner-forehearth upper structure.

In the production of container, tableware, and lighting ware, expendable shapes including feeder spouts, tubes, plungers, orifice rings, and stirrers are required to control the flow of glass to the forming machine. These shapes are formed by casting procedures using mullite or blends of mullite and tabular alumina grain as may be specified. Special calcined alumina may also be used in the matrix or bond phase. In this application, high purity of the grain is essential to prevent formation of seed and blister defects. Busby[9] showed that traces of iron impurity present as Fe_2O_3 in the refractory grain or structure can be a source of oxygen seed when the ferric iron is reduced to the ferrous state by the glassmelt.

Andalusite from the Transvaal province in South Africa also is an excellent source for mullite grain as it can be used without precalcination. Andalusite has excellent resistance to slag penetration and attack, especially by alkalies. This is due to its dense, homogeneous, single-crystal structure. Andalusite grain that became available in the 1950s and 1960s was contaminated with an iron-alumina-silicate intergrowth and thus of little interest in glassmelting application. Current sources of grain, after some beneficiation, now have application in brick and shapes for melter upper structure and in the regenerator chamber.

Bonded AZS (Alumina-Zirconia-Silica): Thomas et al.[28] reviewed the development of bonded AZS refractories. Commercial refractories first became available in 1961 and found wide acceptance for hot repair work in the melter. Composition and structure have been modified over the years to improve on properties for specific applications. The range of bonded AZS refractories produced, worldwide, is shown in Table VI. Raw materials used in processing may include calcined alumina, tabular alumina, mullite grain, fused AZS grain, and zircon, depending on desired structure and intended use. Brick and shapes may be formed by conventional pressing, stamping, and casting procedures.

Bonded AZS combines excellent corrosion resistance, thermal spalling resistance, hot load strength, uniform density, ease of cutting, and relatively low thermal conductivity into one refractory.

Applications include melter bottom paving in soda-lime glass for containers, flat glass, tableware, and lighting ware. Upper structure applications in such furnaces range from suspended walls over the batch feeder, port and breast-wall construction to shadow or front-wall areas. A relatively new use[29] is a backup protection layer over fused AZS prior to installation of insulation media to effectively reduce the high heat loss[30] through the melter sidewall. The bonded AZS course serves as a built-in overcoat starting just below the flux line. Bonded or fused AZS patch blocks may later be applied at the flux line as required.

In the forehearth area, bonded AZS channels are used on soda-lime, fluoride-opal, and lead glass giving a service life equivalent to that of fusion-cast shapes. Expendable shapes offer two to three times the service life over mullite for use on long shop runs. This also includes expendable shapes for TV glasses.

Bonded AZS is used extensively in the melter upper structure on special glasses including insulation wool, fluoride-opal, lead, and borosilicate glasses. This may include melter crowns, breast walls, end walls, and refiner upper structures, where corrosive volatiles may prevail.

In borosilicate glass, the use of bonded AZS for checker brick in the sodium borate condensate zone has been effective in balancing out regenerator life and as a support for silica or mullite top checkers.

In melting sodium silicate glass, bonded AZS has been very effective in the regenerator target wall of one furnace and for top checkers in other furnaces. Krings[31] reports that "The only satisfactory results

Table VI. Bonded AZS Refractories

	ZrO_2 %	Al_2O_3 %	SiO_2 %	Others %	Bulk Density kg/dm^3 (lb/ft^3)	App Por %	MOR N/mm^2 (psi)	Forming
Germany	6	70	23	0.3	2.70 (169)	14	16.2 (2300)	P
Germany	10	84.5	5	0.5	3.10 (194)	18.5	14.0 (2000)	P
U.S./ Germany	11	73	15	1.0	2.90 (181)	18	18.3 (2600)	C
Japan	12	81.2	5.9	0.9	3.17 (198)	18.5	21.1 (3000)	P
England	12.7	76.9	9.5	0.5	3.33 (208)	22		C
U.S.	16.1	55.7	26.8	1.4	2.80 (175)	10	24.6 (3500)	P
Germany	18	68	11	3	2.94 (184)	19	20.4 (2900)	P
U.S.	18	69.3	12.2	0.5	3.09 (193)	16	11.4 (1620)	P
Japan	18.7	72.2	8.7	0.4	3.18 (199)	15	21.1 (3000)	P
Australia	19.3	67.8	12.5	0.4	3.07 (192)	15	7.0 (1000)	
U.S./ Germany	19.5	70	10.2	0.3	3.17 (198)	17	14.0 (2000)	P/C
Australia	19.6	70	10	0.4	3.15 (197)	13	14.0 (2000)	P
U.S.	19.8	63.5	16.3	0.4	2.94 (184)	19	15.4 (2200)	P
Japan	20	70	9.8	0.2	3.15 (197)	16	21.1 (3000)	C
U.S.	20	68	11	1.0	3.15 (197)	21	21.1 (3000)	C
U.S.	20	67.6	11.9	0.5	2.88 (180)	22	12.0 (1700)	C
U.S.	21.5	64.5	13	1.0	3.02 (189)	18	28.2 (4000)	C
U.S.	26	59	14.5	0.5	3.25 (203)	12	31.6 (4500)	P
U.S.	27.8	55.6	16.2	0.4	2.82 (176)	21.5	10.5 (1500)	C
U.S.	28.5	57.4	12.9	1.2	3.17 (198)	14.3	47.8 (6800)	C
Japan	31	47	17	2	3.49 (218)	3	59.8 (8500)	
France	32.5	50	15.5	2	3.34 (209)	0.5	77.5 (11000)	P
France	33	50	16	1	3.09 (193)	18	14.0 (2000)	
Germany	33	47			3.55 (222)	1.0	40.8 (5800)	IP
U.S.	36	42.8	19.6	1.6	3.20 (200)	13	91.5 (13000)	C
U.S.	42.3	34.4	22.9	0.4	3.06 (191)	21	16.2 (2300)	C
Japan	47	28	22	2	3.10 (194)	23	9.8 (1400)	C

P: pressed, C: cast, IP: isostatically pressed.
*Ref. 28. (Used by permission.)

with top checkers were those obtained with zircon-mullite containing 17% ZrO_2. A 5 mm thick reaction layer is formed on the surface that erodes away at the rate of 5 mm per year. It does not fault or shift like a shell and therefore does not protrude and block passages as was experienced with bonded AZS containing fused AZS grain and high-grade mullite brick. High burned magnesite and magnesite-chrome crumbled away due to formation of forsterite by silicic acid attack."

Bonded AZS brick serve as built up sidewalls in day tanks melting fluoride-opal and soda-lime glass. Service life may range from 12 to 18 months.

Bonded Alumina-Chrome (Al_2O_3-Cr_2O_3): Bonded alumina-chrome containing 10 and 16% Cr_2O_3 was developed during the late 1960s primarily for metallurgical applications. In 1976, Thomas and Manigault[32] reported on corrosion test results in sodium borate flux, borosilicate, and soda-lime glasses. As a result of this test work, field trials were conducted in the United States and Europe in selective furnaces melting insulation wool and soda-lime and borosilicate glasses. The results of some of these furnace applications were reported in 1986 by Thomas and Patel[33] and Boggum et al.[34]

Tirlocq and Dramais[35] evaluated the corrosion resistance of reaction-sintered alumina-chrome containing 9% Cr_2O_3 in a $Na_2CO_3/Na_2B_4O_7$ fused bath at 1200°C and found that it compared favorably with 41% fused AZS.

Bonded alumina-chrome may be formed from tabular alumina, calcined alumina, and chromic oxide with the Cr_2O_3 ranging from about 10 to 30%. The matrix consists of an alumina-chromic oxide solid solution which has excellent chemical resistance to alkaline attack, mechanical strength, and creep resistance at high temperatures. Brick and shapes are formed by conventional pressing, stamping, and casting procedures.

Applications for bonded alumina-chrome containing 10 and 16% Cr_2O_3 in green soda-lime glass include melter bottom paving, sidewall blocks, and patch or overcoat blocks. Bottom protection layers serve to reduce tramp metal penetration and bottom failure.

Applications for 16 and 30% bonded alumina-chrome in glasses containing alkaline borates such as insulation wool glass are melter sidewall blocks in electric and fuel-fired furnaces, patch and overcoat blocks, bottom paving, forehearth channel construction, and port and stack construction in direct recuperative fired furnaces.

Bonded Alumina (Al_2O_3): Alumina brick and shapes containing 90% and higher Al_2O_3 find very limited application in glassmelting furnaces. Slip-cast and isostatically pressed dense alumina shapes and crucibles containing over 99% Al_2O_3 find some application as a glass contact refractory in melting special glasses, mainly of optical quality. In this melting system, the glass-refractory interface remains very finite, showing a sharp demarcation between glass and refractory to provide for a minimum defect source. Finely ground calcined aluminas are required in the processing of slip-cast and isostatically formed shapes.

Brick shapes of 90% Al_2O_3, formed by conventional pressing, are used in furnaces melting sodium silicate glass. Such brick are preferred for use at the flux line in sidewall construction. In such cases, the lower sidewall may be of clay flux or fused AZS block and the flux line frequently repaired with 90% alumina brick.

Brick and shapes of 90 to 99% Al_2O_3 are required in melting calcia-alumina-silica glasses used in lighting systems. These glasses require a melting temperature of 1732° to 1760°C (3150° to 3200°F). The alumina brick shapes are used for the complete upper structure of the melting furnace while dense zircon blocks may be used for the glass contact area. Brick and shapes of 90 to 99% Al_2O_3 are based mainly on tabular alumina utilizing some calcined alumina in the matrix phase.

Expandable shapes of 90 to 95% Al_2O_3 find limited application in some forehearth shops for production of container and tableware. The main concern here is a prime need for expandable shapes that will give initial seed-free glass in the subject shop. Frequently, a mullite or AZS expandable will be prone to form an oxygen seed streak that may take several hours to clear up. The redox level of the subject glass (oxidized state) is believed to be a factor in such a situation. Expandable shapes of 90 to 95% Al_2O_3 are formed by casting, and utilize tabular alumina and calcined alumina in the matrix phase.

Basic Refractories: The use of basic brick in glass-melting is confined mainly to the regenerator. For the checker pack, materials having high specific gravity, specific heat, and thermal conductivity are preferred to provide good thermal capacity. This favors the use of magnesia and dense periclase grain for the brick structure. Other factors to be considered in the selection are resistance to solids from batch carryover, alkaline volatiles, condensates, temperature profile, and oxidation-reduction cycling.

Early furnaces utilized various grades of fireclay with preference to superduty and kaolin grades for better service. The transition from clay to mullite to basic has been dictated by the demand for higher performance and campaign life. Basic brick have undergone many changes over the past 30 years in an attempt to meet higher performance standards and operating conditions imposed by the use of oil firing in some geographic areas. This situation has now culminated due to restrictions imposed on the disposal of chrome-bearing brick from the regenerator system.

The use of fused AZS cruciform checker packing is one approach which may prove to be economically acceptable by demonstrating longer life and high operation efficiency levels. This has been countered by

introduction of the chimney block shape setting and use of MA spinel, spinel-magnesia, or spinel-bonded forsterite for the condensate zone.

High burned magnesite is the most economical selection for the crown and upper walls but may need to be supplemented with fusion-cast block in the target-wall area. In furnaces having problems with high silica (silicic acid) carryover, the use of mullite based on andalusite may be an alternative, with bonded AZS being used in the target-wall area. For the lower walls, in the condensate area, several choices exist based on use of MA spinel or olivine grain with spinel bonds.

The trend in refractory usage in the regenerator now points in the direction of alumina-bearing products, namely, fused AZS, fused beta alumina-magnesia, fused MA spinel, periclase-MA spinel, and forsterite with MA-spinel bond.

Special Oxides and Metals: In melting special glasses which must meet very stringent specifications, conventional bonded and fusion-cast refractories may have limitations so that the use of special oxides and refractory metals can be justified. Of this group, chromic oxide, tin oxide, zirconia, alumina, platinum, and molybdenum have been of major interest.

Dense chrome shapes are made from refined chromic oxide by slip casting and isostatic pressing. The main application has been as melter glass contact refractory in direct-fired furnaces melting "E" textile fiber. Dense chrome has excellent corrosion resistance but is subject to volatilization above the flux line and is vulnerable to cracking from thermal stress. A porous chrome is used for backup of joints on insulated construction.

Fused zirconia refractory shapes of 90% plus are available for melting special glasses.

Tin oxide exhibits excellent corrosion resistance and low electrical resistivity. It is used mainly as electrode blocks in the melting of lead glasses where molybdenum cannot be used. Shapes are formed by slip casting and isostatic pressing.

Platinum is used extensively as sheathing over mullite shapes to form throat, skimmer, stirrer, plunger, and orifice blocks used in melting "E" glass and special optical glasses.

Molybdenum is used as electrodes in electric melting and boosting of fuel-fired furnaces melting soda-lime glass. Molybdenum metal tubes are used to convey special glasses from the melter to the drawing position to prevent the loss of volatiles. The metal has excellent corrosion resistance but is subject to oxidation and must be sealed from air contact.

Monolithic Refractories

Monolithic refractories serve three basic functions in glassmelting furnaces, namely, (1) original construction, (2) cold furnace repair, and (3) maintenance and hot repair.

Original Construction: Mortars available for construction cover the general range of refractories being used. With the exception of silica mortar for silica brick and zircon mortar for zircon brick, alumina-bearing mortars may be widely used both below and above the flux line.

Alumina mortars based on tabular alumina grain and calcined alumina have been used extensively with fused AZS paving and upper structure blocks. Sidewall blocks are usually trued enough on the mating faces so that joints are dry to provide for expansion on heatup. The back faces of these blocks may receive a plaster coat of an AZS mortar prior to installation of bonded AZS continuous backup and insulation.

Alumina-zirconia-silica mortars based on tabular alumina, calcined alumina, and zircon are used with bonded AZS paving and upper structure. Such mortars have demonstrated better glass corrosion resistance than alumina mortars in soda-lime glass at temperatures of 1205° to 1371°C (2200° to 2500°F).[29]

In 1980, Jeanvoine and Guigonis[36] described the use of a bedding mortar and joint mortar based on fused AZS grain to provide for improved joint sealing of fused AZS paving, a problem that over the years has limited the effective use of fused AZS paving in glass bottom construction. The improved corrosion resistance of the fused AZS grain mortar over a conventional alumina mortar is illustrated in a bottom joint test after five days in soda-lime glass at 1450°C.

Alumina-chrome mortars based on tabular alumina and chromic oxide have demonstrated corrosion resistance superior to that of AZS mortars in soda-lime glass.[29] Unfortunately, these mortars contribute a green coloration to the glass but are used extensively with alumina-chrome brick in insulation wool glasses.

Alumina-zirconia-silica mortars have found extensive use with mullite and superduty brick in upper structure and regenerator construction where a sodium borate vapor environment is present. The AZS mortar extends brick life by reducing joint wear—a problem evident with use of fireclay and mullite mortars.

A tamped monolithic course has been used in melter bottom construction for some 30 years. Zircon tamps are used as a seal course under the paving or subpaving layer to reduce glass penetration into the clay and insulation support structure in soda-lime glass. The zircon tamp, ranging from 2.5 to 7.6 cm (1 to 3 in.) in thickness, also very effectively encapsulates tramp metal and thus reduces bottom failure from metal-drilling activity.

In Europe, the practice has been to use an AZS tamp rather than zircon under the paving. Such AZS tamps may contain tabular alumina, calcined alumina, and zircon. Jeanvoine and Guigonis[36] offer an improved solution consisting of an AZS castable, based on fused AZS grain, that is vibrated in place to form a concrete sublayer that may range in thickness from 35 to 80 mm.

Furnaces melting insulation wool glasses may use an alumina-chrome tamp sublayer under the paving course. This has helped to reduce glass penetration and corrosion of the clay substructure.

Cold Furnace Repair: During interim repairs it may be necessary to completely replace a bottom structure using a tamp or cast monolithic as described above. If the melter is being repaired for a one- or two-year run, a monolithic tamp of zircon or AZS may be used only to patch areas showing some wear or metal-drilling activity.

Sidewall blocks showing excessive wear and cracking may be patched with an appropriate monolithic. Fused AZS blocks in soda-lime glass may be patched with an AZS patch. Fused chrome-alumina blocks in an insulation wool glass may be patched with an alumina-chrome plastic. Melter sidewalls in sodium silicate furnaces may be veneered with a high-alumina castable based on tabular alumina and calcium aluminate cement. Such veneer-patched areas usually give better service than the original brick, clay flux, or fused AZS block structure.

Maintenance and Hot Repair: Glassmelting furnaces are inspected frequently to detect for high-wear areas that may appear as hot spots. If the hot spot can be patched from outside, a zircon patch is often used. This may involve sealing of joints in the upper structure with a caulking gun or applying the patch directly over the distressed arch or block to build up a layer and seal off the flame. Holes in silica crowns are usually patched with a mix prepared from fused silica grain and sodium silicate that is tamped or poured into the distress cavity.

A new technique has been developed recently for repairing distress areas within the melter upper structures. Annett et al.[37] and Deschepper and Robyn[38] describe the use of a ceramic welding process to build up the hot face that may show distress from corrosion, joint reaction, or spalling. A water-cooled lance is used to project a thermite reacting mixture to the surface to be restored. The metallic powder, either silicon or aluminum, ignites on contact with the hot face and a temperature above 2200°C develops, melting the refractory powder and bonding it to the repair zone substrate.

For repairing a silica refractory surface, a mixture of vitreous silica and 5% silicon would be applied. For a mullite surface, a mixture of mullite grain, alumina, and silicon metal may be used. For a fused AZS surface, the mix may contain baddeleyite, zircon, alumina, and either silicon or aluminum to form an AZS patch. The authors state that "Based upon experience and research, one can expect to increase the production life of a furnace by some 50% depending upon the furnace dimensions and whether or not the repair process is used systematically to maintain the refractory structure."

Conclusion

Alumina in combination with silica, zirconia, magnesia, and/or chrome serves a vital function in refractories for glassmelting. The industry is almost totally dependent on fused AZS sidewall blocks for containing the glass during the melting process. The exception is the use of dense chrome for melting "E" textile glass, the use of platinum for melting and working special glasses, and fused chrome-alumina or bonded alumina-chrome in melting the corrosive insulation wool glass. The melter bottom is maintained with fused AZS and bonded AZS supplemented with zircon or AZS monolithics.

For the refining and drawing end of the furnace, fused alpha-beta alumina and fused AZS equally serve this area.

In the melter upper structure, fused AZS and bonded AZS have almost totally replaced silica except for the melter crown on medium and large spans.

Alumina in combination with silica in the form of mullite is the standard upper structure material for the forehearth or drawing end of soda-lime and "E" textile glass.

The use of chrome-bearing refractory in the regenerator is now being limited due to disposal regulations. Alumina in the form of fused AZS and magnesia-alumina spinel is a viable substitute in the condensate zone for soda-lime glass. Table VII shows typical refractory usage in the melter, refiner, and forehearth area for various glasses, ranging from the more acidic compositions on the left to more basic on the right.

References

[1] T. S. Busby; p. 1 in Tank Blocks for Glass Furnaces. Society for Glass Technology, Sheffield, UK, 1966.

[2] G. Stein, "History of the Tank Furnace"; p. 190 in Glass Melting Tank Furnaces. Society for Glass Technology, Sheffield, UK, 1958.

[3] J. H. Davidson, *J. Soc. Glass Technol.*, **1**, 126T (1917).

[4] J. Currie, *J. Soc. Glass Technol.*, **6**, 125T (1922).

[5] T. S. Busby, p. 20 in Tank Blocks for Glass Furnaces. Society for Glass Technology, Sheffield, UK, 1966.

[6] E. E. Humphrey, "History of the Fused Cast Refractory Industry," *Am. Ceram Soc. Bull.*, **56** [7] 661–62 (1977).

[7] A. Garstang, *Glass Technol.*, **12** [1] 1–7 (1971).

[8] R. Moreau, P. Bony, and A. Krings, "Evolution of the Performance and Profitability of Hollow Glass Furnaces During the Last 25 Years," *Interceram, Special Issue*, **35**, 48–49 (1986).

[9] T. S. Busby, "Laboratory Testing and the Prediction of Refractory Wear"; pp. 20-30 in Tenth International Congress on Glass, Kyoto, 1974.

[10] P. Hrma, *Glass Technol.*, **23** [3] 151 (1982).

[11] T. S. Busby, "Progress in Refractory Usage in the Glass Industry," *Glass Technol.*, **28** [1] 30–37 (1987).

[12] A. Dietzel, *Sprechsaal*, **82** (1942).

[13] H. J. Tress, "Some Distinctive Contours Worn on Alumina-Silica Refractory Faces by Different Molten Glasses: Surface Tension and the Mechanism of Refractory Attack," *J. Soc. Glass Technol.*, **38**, 89–100 (1954).

[14] L. Reed and L. R. Barrett, *Trans. Br. Ceram Soc.*, **63**, 509–34 (1964).

[15] J. Loffler, *Glastech. Ber.*, **38**, 398–405 (1965).

[16] H. Jebson-Marwedel, *Glastech. Ber.*, **39** [9] 399–402 (1966).

Table VII. Refractory Usage vs Glass Composition

	Sodium Phosphate	"E" Textile	Neutral Borosilicate	Semineutral	Insulation Wool
		← Acidic			
SiO_2 (%)		54	80	74	60–64
Al_2O_3 (%)		15	2	2.5	3–4
B_2O_3 (%)		8	12	8–10	5–6
CaO•MgO (%)		22	1.5	2	11–13
$Na_2O \cdot K_2O$ (%)	33–37%	0.5	4.5	8–10	14–15
PbO (%)					
F_2 (%)		0.5			
P_2O_5 (%)	63–67				
Melter					
Sidewall	Zircon	Chrome	AZS	AZS	Cr-Al Al-Cr
Bottom	Zircon	Chrome-zircon	Zircon-AZS	Zircon-AZS	Cr-Al Al-Cr
Crown	$60Al_2O_3$	Mullite-silica	Silica	Silica-AZS	Mullite AZS
Upper structure	$60Al_2O_3$	Mullite-zircon	Silica-zircon	AZS zircon	AZS
Checker			Silica-AZS	Mullite-AZS	
Refiner					
Sidewall		Chrome	AZS	AZS	Cr-Al
Upper structure		Mullite	Silica	Silica	AZS
Forehearth					
Channel		Chrome/zircon	AZS/zircon	AZS	Al-Cr
Upper structure		Mullite	Zircon	AZS	Zircon

	Fluoride-Opal	Soda-Lime	Sodium Silicate		30% Lead
		Basic →			
SiO_2 (%)	71.2	72	65	75	56
Al_2O_3 (%)	7.3	1.0			1.3
B_2O_3 (%)					0.6
CaO•MgO (%)	4.8	14			
$Na_2O \cdot K_2O$ (%)	14.2	13	35	25	11.9
PbO (%)					29
F_2 (%)	4.2				
Melter					
Sidewall	AZS	AZS	FA-A	AZS-clay	AZS
Bottom	AZS-zircon	AZS-zircon	A	AZS-clay	AZS
Crown	Silica-AZS	Silica	Mullite		Silica
Upper structure	AZS	AZS-FA	Mullite-AZS		AZS
Checker	Basic	Basic	Basic		Basic
Refiner					
Sidewall	AZS	FA/AZS			AZS
Bottom	AZS	AZS			AZS
Upper structure	Silica	Silica			Zircon
Forehearth					
Channel	AZS	FA/AZS			FA/AZS
Upper structure	Mullite	Mullite			Mullite

Cr-Al = Fused chrome-alumina.
Al-Cr = Bonded alumina-chrome.
AZS = Fused or bonded AZS.
FA = Fused alumina.
A = Bonded alumina.

[17] T. S. Busby, "Progress of Glass Making Refractories," *Glass Technol.*, **20** [4] 117–31 (1979).

[18] E. A. Thomas and H. D. Prior, "Application des Refractaires de Zircon et de Zirmul dans les Superstructures de Fours a Bassin de Verrerie," *Verres Refract.*, **5**, 385–90 (1967).

[19] T. Weichert, "Soda-Lime Glass Furnace: Basic Refractory Checker Bricks in the Condensation Zone of Alkali Sulfates—Lining and Service Requirements," *Interceram, Special Issue*, **35**, 10–13 (1986).

[20] S. E. Cheetham, "A New Concept in Glass Tank Chequer Construction"; pp. 91–101 in 39th Annual Conference on Glass Problems, November 15–16, 1978, Columbus, OH.

[21] G. P. Scheiblechner, "Chimney-Type Checker-Block Packing and Latest Developments in Checkerwork Design"; pp. 34–48 in 44th Annual Conference on Glass Problems. November 15–16, 1983, Urbana-Champaign, IL.

[22] P. Robyn, G. Soumoy, and G. Decelles, "Laboratory Simulative Testing of Checker Bricks Leading to Economic and Efficient Regenerators," *Interceram Special Issue*, **35**, 31–34 (1986).

[23] R. E. Davis, "Why the Cold Top Electric Furnace is a Nonpolluter," *Glass Ind.*, **5**, 18–21 (1987).

[24] T. E. Stark, "Recuperators in Insulation-Glass Unit Melters"; pp. 43–53 in 43rd Conference on Glass Problems, November 10–11, 1982, Columbus, OH.

[25] F. H. Norton, p. 19 in Refractories. McGraw-Hill, New York, 1931.

[26] J. H. Chester, p. 93 in Steel Plant Refractories. Society for Glass Technology, Sheffield, 1957.

[27] E. A. Thomas and K. W. Smith. "Synthetic Mullite as a Ceramic Raw Material," *AIME Trans. (Mining)*, **223**, 210–14 (1962).

[28] E. A. Thomas, D. G. Patel, and W. F. Brandt, "Bonded AZS Refractories for Glass Processing," *J. Can. Ceram. Soc.*, **53**, 51–56 (1984).

[29] E. A. Thomas and W. A. Underwood, "Backup Insulation Practice for AZS Refractories," *J. Can. Ceram. Soc.*, **54**, 43–47 (1985).

[30] E. A. Thomas, W. F. Brandt, and D. G. Patel, "Glass Furnace Insulation Practice," *Glass Ind.*, **62** [8] 12–16 (1981).

[31] H. Krings, "Durability of Various Refractory Materials in the Upper Layers of Regenerator Checkers in High Pull Sodium Silicate Furnaces," *Interceram Special Issue*, **35**, 29–30 (1986).

[32] E. A. Thomas, and E. L. Manigault, "Evalution of Bonded Alumina-Chrome Refractories in Boro-Silicate and Soda-Lime Glasses," *J. Can. Ceram. Soc.* **45**, 21–25 (1976).

[33] E. A. Thomas & D. G. Patel, "The Application of Bonded Alumina-Chrome Refractories in the Glass Industry," *Interceram Special Issue*, **35**, 50–53 (1986).

[34] P. Boggum, B. Schmalenbach, and K. Schulte, "Chrome-Corundum-Bricks—Application Examples in the European Glass Industry," *Interceram Special Issue*, **35**, 53–56 (1986).

[35] J. Tirlocq and R. Dramais, "Reaction Sintering of Mixed Oxides and Their Application in the Glass Industry," *Interceram Special Issue*, **35**, 68–69 (1986).

[36] P. Jeanvoine and J. Guigonis, "Improvements in Wear Resistance of Glass Furnace Bottoms," *Glass Int.*, **9** (1980).

[37] K. Annett, R. Plumat, and R. Deschepper, "Repair of Glass Furnaces by Ceramic Welding Techniques," *J. Can. Ceram. Soc.*, **50**, 34–38 (1981).

[38] P. Deschepper and P. Robyn, "Application of the Ceramic Welding Process to Maintenance and Repair of Glass Furnaces," *Interceram Special Issue*, **35**, 70–72 (1986).

Refractories Used for Investment Casting of High-Temperature Alloys

Manuel Guerra, Jr.*
Howmet Corporation
Technical Center
Whitehall, MI 49461

Alumina refractories play a key role in contemporary precision investment casting. As one of the main constituents in shell molds for high-temperature alloys, alumina is favored because of its chemical inertness and high-temperature capability. This chapter summarizes the principal physical and chemical characteristics of alumina in relation to the requirements for its use in both the slurry and stucco components of typical shell molds. Particular attention is given to factors affecting slurry stability and shell strength. Other applications for alumina in investment casting, including crucibles, alloy filters, and mold insulating wrap, are briefly reviewed. The current trend to increasing process temperatures, dictated by advances in directional solidification technology, points to expanded use of alumina refractories in the investment casting of high-temperature alloys.

Refractories play an important role in the quality and final cost of investment casting. In such casting, refractories are primarily used to make the shell molds into which molten metal is poured; therefore, this overview will focus on the shell-making portion of investment casting. Alumina refractories are highlighted because of their chemical inertness and high-temperature capability, properties which are highly desirable during the casting process.

To understand why certain refractory materials are preferred, it will be necessary to review the investment casting process and ceramic shell making. To present an overview of these concepts, this chapter contains five sections. "Investment Casting" outlines the investment casting process and describes ceramic shell making. Next, "Shell Composition and Requirements" lists typical shell components and selection criteria. The third section, "Physical Properties of Shell," describes the shell system and some of its important properties. "Production Practice and Problems" discusses some of the considerations in shell making and potential problems. The final section, "Future Trends in Shell Technology," mentions some possible directions of shell-making technology.

Investment Casting

The History of Investment Casting

The investment-casting process, often referred to as the "lost wax" process, is thousands of years old. The Shang Dynasty in China (1766–1122 B.C.) used the lost wax method to cast fine jewelry, metal images, and sculptures from a wax replica of the article being produced.

In the early 1940s, U.S. involvement in World War II created the need for internal engine components that were both durable and capable of higher temperatures. The aircraft industry investigated the investment-casting process (then confined to medical and dental use) as a means of producing high-temperature metal castings. Austenal Laboratories, now a division of Howmet Turbine Components Corporation, was experienced in the use of investment casting for dental prostheses and surgical instruments. Working with General Electric Company, Austenal Laboratories investigated the investment casting of several alloy compositions (including one of their own, cobalt-based Vitallium) for aircraft engine supercharger testing. They discovered that a variation of Vitallium was successful for this high-temperature airfoil application. Investment casting also yielded the close dimensional control these precision components required. By the end of World War II, over 35 million supercharger turbine blades had been cast in Vitallium and its variations.[1]

The postwar period saw the development of alloys with much improved high-temperature strength and fatigue properties needed for gas turbine engine components. Because few of these new alloys could be forged at high temperatures, a new family of cast superalloys was created. With these successes, investment casting became a significant factor in the production of high-temperature, turbine engine components.

The Investment-Casting Process

The investment-casting process consists of three distinct steps: (1) making an initial pattern (an exact replica of the article to be produced); (2) building a refractory "shell" (mold) around the pattern and removing the original pattern, usually by heat; and (3) pouring molten alloy of the desired composition into the shell. After the metal has solidified, other operations involve shell removal, finishing, and heat treating, but the actual casting process is accomplished in these three steps.

*Currently with Remet Chemical Corp., Utica, NY.

Step One: Making the Pattern: Pattern making is a critical step in investment casting because surface flaws in the initial pattern will manifest themselves as defects in the final casting. Historically, pattern materials have been waxes, thus the term "lost wax." Although wax is still the predominant pattern material, thermoplastics are occasionally used.

A typical pattern wax is blended from natural and synthetic waxes and resin. Fillers are often added to the pattern wax to minimize shrinkage during solidification. The wax composition is formulated to provide dimensional stability, strength, and desirable injection characteristics. The wax must resist warping or bending, as well as possess low thermal expansion near room temperature. Maintaining the proper wax properties helps ensure that the final metal shape will be an exact replica of the wax pattern.

Most wax patterns are made by injecting molten wax into a precision metal die. For parts that require internal passages, the wax is injected around a ceramic core body. These cores, used extensively in investment casting, will be removed after casting, leaving a hollow passageway used primarily for air-cooling the airfoil.

Wax is also used to make the "runners" or "gating" to which the patterns are attached. The gating becomes the feeding system for the molten alloy to reach the pattern cavity during the casting process. When the wax patterns are joined by gating to form "clusters," the wax assembly is ready for the second step of the casting process, creating the refractory shell.

Step Two: Building the Refractory Shell: The finished wax assembly is encased in a ceramic mold material known as the "investment." Two methods of mold manufacture are commonly used. In the flask-molding method, the wax assembly is set into a flask (container) and ceramic slurry is poured around the pattern. This technique generally uses a chemical setting ceramic mixture (gypsum, for example), and the resulting mold is in the shape of a solid cylinder or block. Solid or block molds are primarily used today for investment casting of light metals such as aluminum or magnesium.

The second method of mold manufacture uses a ceramic shell built in several stages around the wax assembly. First, a handle is attached, and the wax assembly is dipped into a slurry of refractory ceramic (Fig. 1), usually tabular alumina or zircon for the first dip; tabular alumina is chemically inert to many of the molten metals used in investment casting. Excess slurry is allowed to drain off and the assembly then is covered with "stucco," a graded ceramic sand. The stucco has been selected on the basis of part configuration, thermal expansion, and temperature resistance (refractoriness). The stuccoed part is allowed to dry (or it also can be set chemically), and the process is

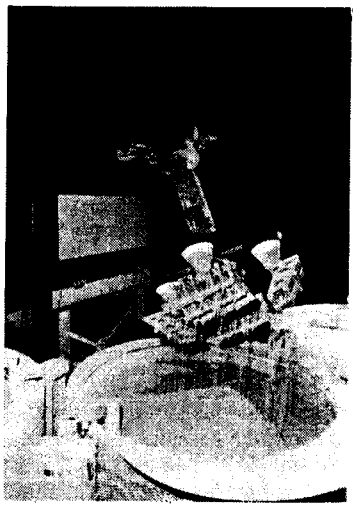

Fig. 1. Automated dipping of four wax assemblies into a typical first-dip, refractory ceramic slurry.

repeated until a shell of sufficient thickness is built up around the original wax assembly, normally five to ten coats.

The size of the stucco used to sand the first dip (also called the facecoat or prime coat) is commonly 90 or 120 mesh, U.S. Standard sieves. For subsequent dips (normally called backup dips), coarser stuccos are selected so that the shell thickness builds up more rapidly. Tabular alumina is commonly used for backup stucco because it undergoes little or no shrinkage after firing at normal investment-casting temperatures, ensuring that the dimensional integrity of the shell will be maintained.

The mold must be thoroughly dry before the pattern is removed, or the mold may rupture due to the large volume expansion of any residual moisture. Pattern removal, most often referred to as "dewax," is usually accomplished by inserting the mold into a steam autoclave or a high-temperature furnace (flash firing). Alternatively, other methods can be used to remove the pattern, such as hot oil, molten wax, or microwave heating. After dewax, the inside of the mold will be hollow, except when ceramic cores are used (Fig. 2). If flash firing has not been used, the shells are normally fired immediately after dewaxing to burn off any residual wax and other organics. After the organic materials have been burned out, the mold is ready to accept metal.

Step Three: Metal Casting: The last step is the casting operation. To produce components for the aerospace industry, alloys are melted and cast in either air or vacuum. Vacuum casting replaced air casting for most aerospace applications with the advent of reactive element (e.g., Al, Cr, Hf, Ti, Zr, etc.) additions to the cobalt- and nickel-based alloy formulations. Most of the alloys used today for turbine components are known as "superalloys." These superalloys are superior to traditional steel alloys because of their high

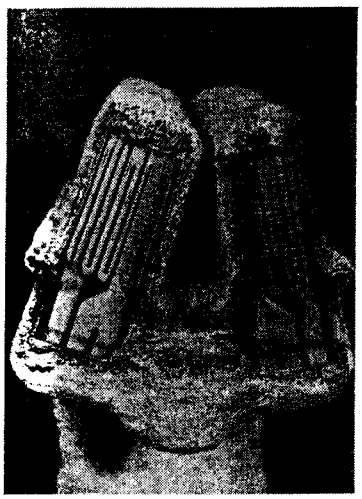

Fig. 2. Cutaway view of a shell mold for an air-cooled turbine blade.

strength, dimensional stability, oxidation and sulfidation resistance. and temperature capability. Outside the aerospace industry, however, air melting and casting still predominate due to the relative nonreactivity of the alloys being cast.

Molds are preheated just prior to casting to aid the flow of the molten metal into thin cross sections. Normal preheat temperatures range from 816° to 1093°C (1500° to 2000°F). Metal is normally cast statically, with or without vacuum assist, and the molds are cooled in air or under a protective atmosphere. Centrifugal casting is also used, but only in those cases where added force is needed to fill out the mold properly.

There are three types of castings produced for turbine components: equiaxed, directionally solidified, and single-crystal (Fig. 3). Equiaxed refers to conventional metal castings that have randomly oriented equiaxed grains (crystals). Directionally solidified (D.S.) components have the grains oriented in one preferred direction, while the single-crystal (S.C.) casting is comprised of a single grain. Directionally solidified and single-crystal castings have replaced many of the equiaxed grain parts in modern gas turbine engines because their improved creep resistance and thermal fatigue life allow higher turbine inlet temperatures for greater engine efficiency.

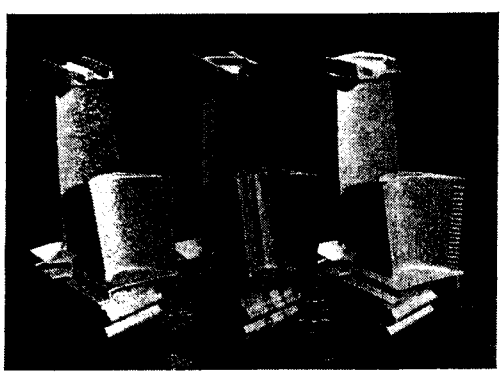

Fig. 3. Examples of cast parts from three investment-casting processes (left to right- equiaxed, directionally solidified, and single-crystal), acid-etched to reveal the respective grain structures.

Shell Components and Composition

All investment-casting shells are formed from two basic components: the slurry and the stucco. Individual shell ingredients help to establish overall shell quality and properties. The composition of the shell is important because minor changes in component composition can result in significant variations in the quality of the casting.

Slurry Composition

A typical slurry is composed of three ingredients: (1) a silica binder, (2) a refractory flour, and (3) a surfactant (wetting agent). Other ingredients are added at the discretion of the individual foundry. Latex may be added to increase green strength and/or decrease hot strength; metal fibers may be added to improve both green and hot strength; and various antifoaming agents may be added to control excessive foaming during slurry agitation.

The first ingredient of slurry, the silica binder, is either colloidal silica or ethyl silicate. Colloidal silica is an aqueous suspension of discrete, submicrometer, amorphous silica particles. Colloidal silica for investment casting generally is purchased and used at 30 wt% silica concentration. The colloid is stabilized to retard gellation by adding sodium hydroxide, which imparts a negative charge to the individual silica particles. Enough sodium hydroxide is added to raise the pH of the colloidal silica to a level greater than 9.0; this product is most stable between pH 8.5 and 10.0.[2]

Ethyl silicate binders contain chains of polymerized silica in an organic solvent. This type of binder typically sets more quickly than colloidal silica binders. It also can be set by chemical means, such as by exposure to gaseous ammonia, which significantly accelerates the shell-making process.

The silica binders used in investment casting have specific surface areas greater than 100 times that of the refractory grains used in the slurry. When mixed, the binder becomes uniformly distributed around each refractory particle and bonding occurs between grains through the silica binder.

The slurry refractories for the investment casting of high-temperature alloys are usually alumina, zircon (zirconium silicate), or silica (either fused silica or quartz). Zirconia and various aluminosilicates are also used for special applications. The criteria necessary for selecting a slurry refractory are chemical inertness,

low thermal expansion, ultimate temperature resistance, availability, and cost.

A special refractory flour is often added to the facecoat slurry to control the grain size of equiaxed castings. Referred to as "nucleating agents" or "inoculants," cobalt oxide (CoO) or cobalt aluminate ($CoAl_2O_4$) is added to the facecoat slurry in small percentages, thus promoting a very fine grain size in the alloy. This smaller grain improves the low and intermediate temperature strength of the casting.

A surfactant usually is added to the facecoat slurry to ensure the wetting of the wax pattern. The surfactant used should not cause foaming nor react with either the other slurry ingredients or the wax. This additive is not required with ethyl silicate slurry systems because the alcohol in the binder acts as the wetting agent.

Slurry Requirements

To produce an acceptable quality shell, several requirements must be met during shell making. The silica-binder phase of a facecoat slurry must be stable when applied to a wax pattern to ensure good surface quality after firing. The type of slurry binder used (acidic or basic) is also important; it should not react with the wax formulation. Backup dip slurries must exhibit the same stability as facecoat slurries or shell strength will be adversely affected. Additionally, the backup slurries must be stable in relation to previously applied shell layers.

If one or more of the slurry components reacts with the silica binder, dipcoat gellation may occur. (The composition and particle size of the refractory flour have the most influence on slurry stability and rheological properties.) Microgellation is an ongoing process once the refractory has been added to the binder. By carefully controlling the slurry components, massive gellation is retarded and acceptable slurry life can be achieved in production. Slurry life normally is several months, but certain systems, such as the tabular alumina/ethyl silicate slurry system, have a life expectancy of only a few weeks. Since alumina flour refractories are basic and also can have relatively high surface activity, the addition of an acidic ethyl silicate binder may affect the useful life of the slurry.

The high temperatures involved in casting gas turbine components inherently remove the organic ingredients in investment-cast shells, leaving only the silica binder and the refractory flour. The purity of the starting flour is therefore very critical. The iron and alkali contents are of major concern because of potential mold/metal reactions. Tabular alumina or zircon are used extensively as slurry materials (especially as the facecoat) because of their purity and inertness to most molten superalloys. Aluminosilicates having high mullite contents are also used, but not so frequently for facecoat applications because of their higher iron and titanium contents.

Stucco Composition and Requirements

During shell building, the particle size of the stucco progresses from fine to coarse as successive layers are applied. In selecting a stucco composition, the following criteria must be met: stability at high temperatures, thermal expansion, density, availability, and cost. For the first dip, inertness to molten alloy is also a major concern.

The stucco serves several functions in the shell-building process. First, it is important in controlling the rate at which the dipcoat dries. (By covering the wet first-dip coat with stucco, the rate of evaporation is reduced significantly.) If the liquid in the applied slurry is allowed to evaporate too quickly, dipcoat cracking may occur. Reducing cracking on the first dip is especially important. If some of the first dip subsequently spalled during further processing, it could result in a shell inclusion, or it might establish a mold/metal reaction site. The latter would happen only if the backup slurries (or stuccos) were reactive with the casting alloy.

The stucco size determines the rate of shell build. If a very coarse stucco is used, the thickness of the shell increases rapidly. It is advantageous to use the largest stucco size that will not seriously degrade shell strength, as the time necessary to make a shell of adequate thickness can be reduced. Some foundries use slurries having a predetermined percentage of stucco added, which increases shell thickness more rapidly. This practice, however, generally decreases overall shell strength because less slurry is picked up, thereby increasing the porosity of the shell. Last, the stucco also provides a rough surface to aid adherence of each successive dip during the shell-building process.

Fused alumina is the most common stucco for sanding the first dip because of its characteristically high purity and low porosity. A low level of porosity is necessary to prevent the stucco from absorbing too much of the liquid in the facecoat, causing a shell defect known as "stucco penetration." This defect manifests itself as "positive metal" on the resultant casting, causing excess rework. Virtually all the refractories previously mentioned as components in slurries can be used as stuccos, with the exception of silica (quartz), which has a relatively high thermal expansion. Quartz can be successfully used as a slurry refractory, but materials with a lower thermal expansion are normally used as the accompanying stucco to lower the overall thermal expansion of the shell.

The most commonly used stucco materials are aluminosilicates and tabular alumina. Various grades of aluminosilicates are used, depending on the high-temperature requirements. High-silica stuccos containing vitreous silica can lower shell strength at high casting temperatures because some of the silica may be present in the liquid phase. A high-purity material such as tabular alumina does not tend to react with other shell ingredients. It is therefore more desirable

for high-temperature applications as, for example, in the directionally solidified and single-crystal casting processes. However, another factor that must be considered is that tabular alumina has a higher density than any of the aluminosilicates and will therefore result in a heavier shell. This can be a significant factor when dipping large shells, as care must be exercised to ensure that the shell-handling equipment is capable of accommodating this additional weight.

Physical Properties of Shell

The major requirement of any investment-casting shell is that it contain the molten metal during casting. However, there are other considerations in selecting shell materials. For example, silica binders (colloidal silica and ethyl silicate) are used almost exclusively in shell because they usually yield very stable slurries and provide strong binding, but they are limited to temperatures below 1593°C (2900°F). The refractories, like the binder, strongly influence shell properties and must be carefully selected. The four main concerns when designing a shell system are thermal expansion, thermal conductivity, refractoriness, and strength of the overall shell.

Thermal Expansion

The thermal expansion of shells can generally be determined from the rule of mixtures. This can be done because in most cases the slurry and stucco contribute equally on a weight basis, which makes the calculations rather straightforward. A comparison of the thermal expansions of commonly used ceramic materials (Table I) indicates that fused silica has the least expansion, while quartz has the greatest. Alumina has a moderately high thermal expansion but, like zircon, fused SiO_2, and the aluminosilicates, its expansion is linear. Linear expansion is very important, as this will minimize shell failure (cracking) during flash firing. On the other hand, during heating very pure quartz undergoes a displacive transformation from alpha to beta quartz at 573°C (1063°F), with an accompanying large increase in volume.[4] Since the quartz used in shells is not always pure, shells made with quartz must therefore be fired slowly through the 510° to 620°C (950° to 1150°F) temperature range. Obviously, a shell made with a significant quartz content cannot be flash-fired. A quartz shell also cannot be cooled to room temperature once it has been heated beyond this transformation temperature, as the strength of the shell will be degraded so much that it could not hold metal.

Table I.* Mean Thermal Expansion Coefficients for Ceramics Used in Investment Casting.

Material	Linear Expansion Coefficient 0°–1000°C (in./in.°C × 10^6)
Alumina	8.8
Mullite	5.3
Zircon	4.2
ZrO_2 (stabilized)	10.0
Fused SiO_2	0.5
SiO_2 (quartz)	9.0–14.0

*Ref. 3. (Used by permission.)

The overall thermal expansion of the shell system is very important in another respect. When the wax patterns are designed, the expansion (or contraction) of the shell at the desired casting temperature must be taken into account for dimensional control of the casting. Retooling a wax die is usually expensive and, unless the overall thermal expansion of the shell remains constant, refractory components of a significantly different composition cannot be introduced into a shell system.

Thermal Conductivity

Thermal conductivity can be approximated by using the rule of mixtures. However, the calculated values may not truly reflect the actual thermal conductivity because the shell more closely resembles a composite, layered structure than a homogeneous substance (Fig. 4). The thermal conductivity of alumina, while much lower than that of metals, is relatively high when compared to the other refractories used for investment casting. The higher conductivity of alumina promotes rapid cooling during solidification and can yield a finer alloy grain size, thus improving low- and intermediate-temperature mechanical properties.

Conversely, control of the solidification rate is necessary both for casting integrity (avoiding microshrinkage porosity) and for development of the optimum microstructure. To achieve this control, insulation is wrapped around part or all of the mold before casting, thus regulating the rate of heat extraction. The insulation material is a low-density blanket composed of fibrous aluminosilicate.

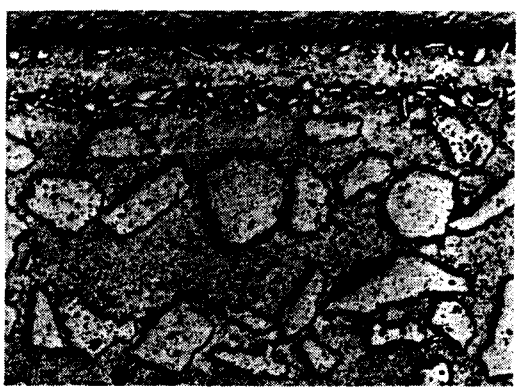

Fig. 4. Optical photomicrograph of cross section of a typical investment-cast shell mold. Note the layered structure of the shell and the progression from fine to coarse stucco. Depth from front to back represents approximately 0.3 cm, with four dips and four stuccos shown.

Refractoriness

Refractoriness, manifested as the ability of the shell to withstand the thermal stresses placed on it during the casting process, is probably the most important of all the shell characteristics. Of all the materials commonly used for investment-casting shells, alumina is considered to be the best choice for high-temperature applications. Even though zircon has a higher melting point than alumina (Table II), it begins to dissociate at temperatures over 1650°C (3000°F); subsequently, its ultimate temperature capability is lower.

Normally, any of the refractories listed in Table II can be used successfully for most applications. The shell temperatures required in casting D.S. and single-crystal parts, however, are much greater. The shell must remain dimensionally stable at temperatures above 1370°C (2500°F) for up to several hours in this type of casting. Tabular alumina is the most preferred shell-refractory material because of its low sintering rate at normal shell temperatures.

Shell Strength

Shell strength is of great concern in investment casting. "Just enough" strength to contain the molten metal is desired but "too much" can be deleterious. For this reason, the "hot strength" (strength of the shell at the desired temperature) must be known. Based on this information, the strength of the shell can be adjusted accordingly.

A casting defect known as "hot tearing" has occasionally been associated with excessively high shell strength. Hot tearing of the alloy may occur during "freezing" because of impeded contraction of the solidifying shape. Hot tearing is normally attributed to alloy segregation, excessive mold cooling rates, or part of or gating configuration (geometry).

Shell strength is monitored in both the green and fired conditions. Green strength is influenced predominately by the binder and the particle size of the refractory flour; the flour composition does not seem to influence green strength. Green strength is mainly an indicator of resistance of the shell to cracking during pattern removal. A dried ceramic shell has very little elasticity, and during the dewaxing process the wax undergoes significantly greater expansion than the shell. If the shell is not strong enough to withstand this stress before the wax is molten, cracking will occur. Small cracks may be repaired by application of a ceramic "mud" patching material (usually an aluminosilicate mortarlike material), but severe cracking causes the shells to be scrapped.

The fired strength of any particular system is a function of both flour and binder type, firing time, and temperature. Depending on the system, the higher the firing temperature the stronger the shell becomes but, above a certain temperature, shell strength decreases. Because of its higher melting temperature and chemical inertness, a high-alumina shell system has greater strength at very high temperatures (>1315°C or 2400°F) than most other shell systems.

In theory, a shell system composed of all-alumina refractories would seem to be a good choice for directionally solidified and single-crystal casting. However, in actual practice, an all-alumina shell may be too strong (possibly inducing hot tears in the casting) as well as very difficult to remove after casting. Alumina is essentially inert to the common chemical shell-removal solutions used in investment casting (such as boiling KOH). Other solutions which would be effective at dissolving alumina could attack the casting surface, causing intergranular attack (IGA) on non-single-crystal castings, and interdendritic attack (IDA) on single-crystal castings. Too strong a shell also causes problems for normal mechanical removal techniques, especially for single-crystal castings, as sufficient plastic deformation may be induced in the casting to cause localized recrystallization during heat treatment.

Table II.* Melting Points of Commonly Used Ceramics for Investment Casting

Material	Melting Point (°C)
Alumina	2054 (Ref. 5)
Mullite	1828 (Ref. 5)
Zircon	2550 (Ref. 6)
Silica	1726 (Ref. 5)

*Refs. 5 and 6.

Production Practice and Problems

Raw Material and Slurry Testing

Quality assurance for mold materials in production begins with the preparation of procurement specifications which combine the published technical data for the various shell components with preferred ranges for material characteristics based on actual foundry experience. All incoming raw materials are sampled and tested for conformance to these specifications. Most of the materials for shell use are controlled primarily for particle size and chemistry.

Because the particle size of the refractory flours is critical, it is necessary to control both particle size and distribution. Particle-size analysis has been aided by advances in laboratory instrumentation; instruments based on sedimentation and on laser light scattering have been found to be especially useful. Slurry properties are routinely monitored during use, and replenishment and adjustments (for pH and viscosity, for example) are made when appropriate. Facecoat slurries are usually checked more frequently than the later dips.

Slurry Stability

Because of the critical nature of the first dip slurry, its long-term stability must be maintained. The pH of a slurry is of particular importance, being a good

indicator of the stability of the binder phase. If the pH changes rapidly, then binder gellation is probably occurring (usually resulting in slurry control problems and reduced slurry life).

Problems with slurry control and slurry life are not uncommon in investment casting. Moreover, slurry problems may not manifest themselves until after metal has been poured into a mold, at which time it may be too late to save those particular castings. The key to slurry control is regular monitoring of the slurry chemistry, with particular emphasis on slurry colloidal silica content and pH.

The colloidal silica/tabular alumina system is particularly difficult to control. The most apparent problem is slurry instability, which ultimately leads to shorter than normal life. The destabilizing mechanism in this system may be the leaching of residual elements from the tabular alumina (such as boron, magnesium, and calcium) in the slurry. If high enough concentrations are leached, the colloidal silica binder may coagulate (gel).[7] This destabilization not only causes short slurry life but may also lead to shell spalling. If the spalled ceramic inclusions are not removed from the mold before casting, they could cause casting defects. Shell inclusions act as crack-initiation sites and could cause premature failure of a casting in service.

Shell Integrity

Shell inclusions are an indicator of poor shell integrity. Conversely, high shell integrity is evident when few or no shell pieces are found and when the shell appears to be crack-free after the dewaxing and firing processes. Investment-casting plants normally have a "shell inspection" department which checks and repairs shells before casting. Shells with significant shell defects are scrapped, while those that show few defects can be blown out with air or washed with water to remove shell fragments.

Shell inclusions can be caused by premature binder gellation or by insufficient binder content in the slurry. If there is not enough binder to coat all the flour particles, particle-to-particle bonding will not be optimal. In addition, overall shell strength will be compromised by a lower binder content, leading to an increase in shell cracking. The optimum ratio of binder-to-flour to produce shells with sufficient strength has been studied extensively.[8] Changing the particle size of the flour can affect this ratio.

The proper binder-to-flour ratio must be maintained, even though the flours used for facecoat and backup slurries may have different particle sizes (because of their different requirements). To ensure a good surface finish on the casting, the particle size of the facecoat flour must be very fine (<200 mesh screen size). An even finer flour can be used, but caution must be exercised because greater surface activity is associated with the increased surface area, potentially resulting in binder gellation.

The backup slurry may use a coarser flour. The principal requirement here is for the refractory particles to be held in suspension, maintaining the proper binder-to-refractory ratio to yield good strength. Particle sizes for backup slurries can range from −100 to −325 mesh, depending on the application. For example, when high shell permeability is desirable to help prevent the entrapment of gas, a coarser flour can be used to create greater shell porosity.

Casting

Shell permeability is of greater concern in air casting than in vacuum casting; however, many shell problems are common to both processes. Casting imposes significant thermal and mechanical stresses on the mold. If these stresses are too great, the mold may rupture, causing molten metal to run out. If leakage occurs, the cast part may not possess enough alloy to be filled completely and will be scrapped. On the other hand, if the mold is too thick, its excessive strength can produce hot tears in the resulting casting.

Tabular alumina is used extensively as the facecoat refractory in aerospace investment casting because of its resistance to mold/metal reaction. Some of the most widely used superalloys are reactive with silica and, because there is very little silica in the typical high-purity aluminas (>99.5% alumina) used in the facecoat, the reaction is minimal. (The silica binder will react with these alloys, but the binder portion of the facecoat is small enough that this is generally not a problem.)

Refractories Used For Casting

Alumina refractories are not only used extensively in shell making but are also widely used in the investment-casting foundry. Molten metal is poured through different types of alumina filters to remove nonmetallic inclusions from either the melt crucible or the master-melt refractories. One example is the commonly used reticulated (foam) filter. This type of filter has a large, open network which enables the alumina (which has only moderate thermal shock resistance) to withstand the thermal stresses induced when pouring super-heated molten metal through it. Alumina balls are sometimes used to filter metal, as are cone (basket-type) filters made of mullite.

Alumina crucibles are used for melting many superalloy compositions. Other crucible refractories used in the investment foundry are zirconia, fused silica, and magnesium oxide. Alumina and zirconia are preferred because of their compatibility with the more reactive investment-cast superalloys.

Shell Removal

Shell strength and composition must be balanced to allow easy removal of the shell materials after casting. Air-operated "knockout" hammers are often used to remove shell from castings that will not be damaged by the induced stresses. However, pieces of residual shell may remain after the knockout opera-

tion. Boiling KOH or NaOH is ideal for removing the shell when there are enough leachable constituents; however, this is rarely the case. With non-silica-based refractories, such as alumina, the silica binder is dissolved, thus softening the rest of the shell. The castings are then cleaned with particulate fused alumina (typically 70 mesh) to remove the residual shell and any oxide scale. Fused alumina is used extensively as a blasting medium to remove the shell from the castings because of its high hardness and shape (sharp cutting edges).

Future Trends in Shell Technology

As the mold temperatures used in the casting process for directionally solidified and single-crystal castings increase, shell refractoriness must also be improved. Therefore, more alumina flour and stucco will probably be incorporated into these shell systems. Improved methods for removing this higher-alumina shell will also be required. One method that may be effective is high-pressure water blast.

The silica binder now used in shell making will have to be replaced for higher temperature applications. A colloidal alumina binder has been developed; however, a shell mold using this binder cannot be dewaxed by normal methods or fired at traditional temperatures. Subsequently, the higher temperature advantage of this binder has not yet been realized. Additional binders are available (i.e., colloidal yttria, zirconia, etc.) but their use is limited (mostly because of their low percent solids concentration). Additionally, advanced sol-gel systems are being investigated as binders.

Increasingly larger castings will be produced in the future, with a single casting replacing fabricated shapes comprising numerous smaller castings and forged and machined parts. Castings that were considered large (>20 inches in diameter) only 10 to 15 years ago are now referred to as medium-sized; castings larger than 36 inches in diameter are now commonplace (Fig. 5). The ever-increasing size of these castings creates problems with holding dimensional tolerances both in wax and in shell. These castings will require a shell system that is not only stronger but also more resistant to high-temperature creep.

Ceramic cores used to form the passages that cannot be made easily by the slurry dipping process are currently silica-based, but alumina cores are being developed for higher temperature applications. Correspondingly, those alloys that are highly reactive with silica would also benefit from such cores. A rapid removal method for these cores has commercial interest.

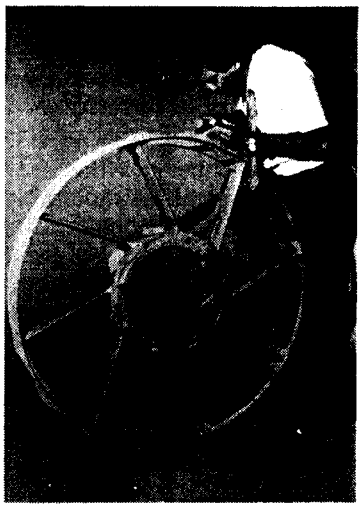

Fig. 5. Fifty-in. (diameter) investment-cast turbine rear frame of nickel-based superalloy. This single part replaced an eight-component fabricated assembly.

Statistical process control (SPC) will be more widely implemented in future shell making, dictated by increasingly stringent part requirements. Computer modeling will take a more important role in casting-process development, supplanting the empirical approach that has been employed historically. Modeling will require collection of extensive physical and thermal data for the shell as a system (as distinct from the individual components of the shell).

Refractories will continue to play a very important role in the investment-casting process in the years ahead. Alumina refractories will have a key place since many of the alloys commonly used today (and in the future) could not be as successfully or economically cast against other types of refractories.

References

[1]R. Thielemann, "The Extra Flask," *J. Met.*, **5**, 21–23 (1981).

[2]Du Pont Industrial Chemicals Department, "Properties, Uses, Storage and Handling of Ludox Colloidal Silica," A–85845, June 1973; p. 2.

[3]W. D. Kingery; pp. 594–95 in Introduction to Ceramics, 2d ed. Wiley & Sons, New York, 1976.

[4]Ibid, p. 87.

[5]Ibid, p. 305.

[6]CRC Handbook, 64th ed. Edited by Robert Weast. CRC Press, Boca Raton, Florida, 1983-1984; p. B-158.

[7]R. K. Iler; pp. 372–84 in The Chemistry of Silica. Wiley & Sons, New York, 1979.

[8]R. L. Rusher, "Strength Factors of Ceramic Shell Molds, Parts I and II," *AFS Cast Metals Res. J.*, **10** [4] (1974); **11** [1] (1975).

Alumina in Monolithic Refractories

Leonard P. Krietz and Robert E. Fisher
Plibrico Company
Chicago, IL 60614

Monolithic refractories are materials which are gaining in acceptance and application. Most of these materials utilize alumina and/or alumina-containing raw materials. The role of aluminous raw materials as aggregate, filler, and binder in refractory castables, gunning mixes, and plastic and ramming mixes is discussed.

Refractory monolithics are materials which have been gaining greater acceptance as the preferred refractories in many applications. By their nature, monolithic refractories are better suited for complex lining configurations and are in many cases easier and quicker to install than refractory brick. Alumina and alumina-containing raw materials are used in most of the monolithic materials manufactured today.

Refractory monolithics are manufactured in either dry or moist form, depending on the type of material and/or bond system used. Various types of refractory monolithics are listed in Table I. In 1986, monolithic refractories comprised 50% of total U.S. refractory production, up from 40% in 1983.[1] Those monolithics containing alumina, or alumina-containing raw materials, make up 60 to 70% of this total.

While some technical aspects of alumina-containing raw materials will be discussed, it is not the specific purpose of this chapter to cover the technology of these products. This information can be obtained from other texts and sources, some of which are listed in the references.[2–5]

History and Development

Development of the family of monolithic refractories began in 1914 when the first commercial plastic refractory was produced.[2] This material was similar in composition to high-duty firebrick, being composed of crushed firebrick and raw fireclay. Castable refractories developed with the introduction of calcium aluminate cement, which was first applied to refractory concrete in the 1920s, initially as field mixes. An early patent on a refractory concrete was issued in 1926.[6] By the late 1920s, bagged preblended refractory castables were being offered.

As these materials grew in acceptance and application, other aggregates and fillers were used to increase service limits and to provide specific physical properties. Alumina-containing aggregates such as bauxite, calcined fireclay, calcined kaolin, kyanite, sillimanite, and fused and tabular aluminas were used to create a wide range of compositions.

Table I. Refractory Monolithics

Castables	Gunning Mixes	Plastics	Ramming Mixes
Dense	Dense	Ramming	Moist
Insulating	Insulating	Gunning	Dry (vibrating)

Binders were also improved. The bond choices in plastic refractories were expanded from the original clay bond to include other bonding agents, such as aluminum phosphate, as well as air-bonding agents (both organic and inorganic). Calcium aluminate cement was also developed to include not only the original low-purity compositions, but high-purity calcium aluminates capable of 1820°C service limits with pure alumina aggregate.

Monolithic Refractory Compositions

All monolithic refractory types are generally based on a mixture of aggregate and filler raw materials, though naturally in different proportions and grain sizings. Binder choice is dictated by the type of monolithic produced. Refractory castables and gunning mixes are generally based on calcium aluminate cement and are manufactured as dry materials with water (for cement hydration) added at the installation site. Plastics and ramming mixes are manufactured with moisture levels from zero (dry vibratable mixes) up to 10% (or more in certain cases). Plastics generally contain more moisture than ramming mixes. Aggregate grains of plastics are also coarser than those of ramming mixes. Binder choice is wider with plastics and ramming mixes, with bond systems covering a wide spectrum from organic to inorganic bonds.

General classifications for both castables and plastics have been developed by ASTM Committee C-8 on Refractories. Tables II and III list these classifications. As can be seen, refractory plastics are classified mainly by alumina content.

Aggregates

The aggregate used in refractory monolithics generally comprises between 50 and 80% of the total composition. Since monolithics are not heated until they have been installed, the aggregates used are usually calcined to high temperatures for maximum volume stability and to crystallize the mineralogy of the aggregate. In monolithics based on alumina-

Table II. ASTM Plastic Refractory Classification C-673

Class	PCE	Alumina Content (%)
High duty	31	NR
Super duty	32½	NR
60% alumina	35	57.6–62.5
70% alumina	36	67.6–72.5
80% alumina	37	77.6–82.5
85% alumina	NR	82.6–87.5
90% alumina	NR	87.6–92.5
95% alumina	NR	92.6–97.5
100% alumina	NR	>97.5

containing raw materials, service temperature generally (but not always) increases with increasing alumina content. Table IV lists the common alumina-containing aggregates used in monolithics, and their service limits.

Modifying Additives and Fillers

The modifying additives and fillers used in refractory monolithics cover a wide range of materials which are used to modify the chemistry or mineralogy or physical characteristics of the final product. Alumina and alumina-containing raw materials, some of which are used in this capacity, are listed in Table V. These materials are generally fine grain sized (<35 m) and can include powdered milled materials, which are also present in the composition as coarse aggregate.

Of the materials listed in Table V, calcined alumina is used quite extensively, as is kyanite. Low-soda calcined alumina is essential for good storage characteristics of phosphate-bonded plastics. It also acts to raise the alumina content of the refractory, fortify the

Table III. ASTM Castable Specifications C-401

Class	Shrinkage <1.5% When Fired at °C (°F)	Maximum Bulk Density after Drying kg/m³ (pcf)
	Dense	
A	1093 (2000)	
B	1260 (2300)	
C	1371 (2500)	
D	1482 (2700)	
E	1593 (2900)	
F	1704 (3100)	
G	1760 (3200)	

Normal strenth — > 2070 Pa (300 psi) MOR after drying.
High strength — > 4140 Pa (600 psi) MOR after drying.

Class	Shrinkage< 1.5% When Fired at °C (°F)	Maximum Bulk Density after Drying kg/m³ (pcf)
	Insulating	
N	927 (1700)	880 (55)
O	1038 (1900)	1040 (65)
P	1149 (2100)	1200 (75)
Q	1260 (2300)	1440 (90)
R	1371 (2500)	1520 (95)
S	1482 (2700)	1520 (95)
T	1593 (2900)	1600 (100)
U	1649 (3000)	1680 (105)
V	1760 (3200)	1680 (105)

Table IV. Alumina-Containing Refractory Aggregates Used in Monolithics

Raw Material	Avg. Al_2O_3 (%)	Service Limit (°C)
Alumina	100	1870
Fused white	100	1870
Tabular	100	1870
Bubble	100	1870
Fused brown	96	1760
Calcined bauxite		
Guyanese (gibbsite)	75–90	1760
Chinese (diaspore)	75–90	1760
Mullite		
Fused	72	1760
Sintered	72	1760
Bauxitic kaolins	60–70	1760
Kaolins	44–48	1650
Flint clay	40–45	1600
Pyrophyllite	20–25	1425

matrix, and increase the service limit. Kyanite is used most extensively to help compensate for the shrinkage of monolithic materials. Kyanite undergoes a mineral conversion to mullite and silica at approximately 1325° to 1410°C, with a corresponding volume expansion. When properly used in a monolithic refractory composition, this can overcome most of the shrinkage due to clay sintering encountered in this temperature range.

Bond Agents

There are various bond agents based on aluminum-containing compounds used in monolithic refractories. Different agents are utilized in plastics and castables.

Plastic Refractory Bonding Agents

There are more bonding systems available for various classes of plastic refractories and ramming mixes than the castables. The most basic (and the first monolithic refractory bonding agent used in 1914) is clay. Clays impart plasticity to the plastic formulations. They also provide low-temperature (though weak) bonding and contribute to high-temperature ceramic bond formation. Various types of clays are used in formulations, at levels from 1 to 25%. Table VI lists some of the common clays used. Clay selection is

Table V. Alumina-Containing Modifying Additives and Fillers Used in Monolithics

Alumina
Fused white
Tabular
Fused brown
Calcined
Reactive
Sillimanite Group Minerals
Sillimanite
Andalusite
Kyanite
Fireclays

Table VI. Bonding Clays Used in Plastic Refractories

Clay Type	% Alumina
Plastic fireclay	25–40
Ball clays	25–35
Kaolins (raw)	30–45
Bentonites	
Sodium	20–25
Calcium	12–18

also dependent on the other bond systems used in the refractory plastic or ramming mix.

Various air-bonding agents are also used in refractory plastics. Air-bonding agents act in conjunction with clay bonds and contribute added low-temperature strength. While many are organic, some are based on alumina compounds. One example is aluminum sulfate [$Al_2(SO_4)_3$ $18H_2O$] (more commonly known as alum), which has been used for years as an air-bonding agent. Alum produces a gel phase on hydration and, when dispersed in the plastic refractory matrix, hardens on drying. The dehydrated gel phase is stable to much higher temperatures than when organic bonding agents are used. A major drawback of alum as a bonding agent is the fact that it decomposes above 760°C and releases SO_x fumes. Therefore, proper ventilation must be used on bake-out of plastic refractories containing this bond agent. Other alumina-based bond agents which have been used include aluminum hydroxychloride and alumina sol.

One of the most important refractory plastic and ramming mix bond systems is the phosphate bond. While many phosphates have been used, the one used most extensively in refractory plastics is aluminum phosphate [$2Al(H_2PO_4)_3$]. It is produced by reacting aluminum hydroxide and phosphoric acid according to the following reaction:

$$3H_3PO_4 + Al(OH_3) \rightarrow Al(H_2PO_4)_3 + 3H_2O \quad (1)$$

When heated, aluminum phosphate goes through many phase changes[7–9] which will not be discussed here. However, aluminum phosphate-bonded plastics normally exhibit high hot strength and abrasion resistance when fired between 350° and 1200°C. While aluminum phosphate-bonded materials are strong when dried between 100° and 250°C, the bond in this temperature range is hygroscopic and can be severely affected by steam or storage in humid conditions.

Castable Refractories

Refractory castables are usually bonded by calcium aluminate cements. These cements are produced by heating bauxite or alumina with limestone in a fusion or sintering process. There are many commercial brands of calcium aluminate cement available, but they all can be classified into three groups—low, intermediate, or high purity. The purity level (amount of Al_2O_3, SiO_2, Fe_2O_3, and CaO) affects the cementitious compounds present and the service limit of the cement. Table VII categorizes the three classifications of calcium aluminate cements by chemistry and maximum useful service limits. This is a broad classification and should be used only as a guide.

Table VII. Types of Calcium Aluminate Cement

	Low Purity	Intermediate Purity	High Purity
Chemistry (%)			
Al_2O_3	36–47	48–62	70–80
SiO_2	3–9	3–9	0.0–0.5
Fe_2O_3	7–16	1–3	0.1–0.2
CaO	35–42	26–39	18–26
Maximum service temperature (°C)	1370	1540	1820

Generally—but not always—the service limit of a castable will indicate the type of calcium aluminate cement it contains. Certain low-temperature applications require materials made with high-purity cement. For example, in furnace atmospheres where large amounts of carbon monoxide are present, high-purity calcium aluminate cements with low iron content are required. The amount of cement used in a castable can vary from 50% (in lightweight castables) to as low as 1% in ultralow-cement castables. Conventional castables will contain between 10 and 35% cement, low-cement castables 4 to 10%, and ultralow-cement castables 1 to 4%.

In recent years, various cement-free castables have been developed for specialized steel mill applications. One bonding agent used in these materials is fine powdered aluminum metal, which hydrates on water addition to form a gel bond phase.

Physical Properties

The percentage of alumina in refractory monolithics has certain fairly predictable effects on physical properties, but refractory monolithics are complex formulations in which the aggregate, additives, fillers, and binders all interact and influence physical properties. Mineralogy of the components and the resultant final mineralogy of the monolithic refractory compo-

Table VIII. Alumina Content vs Service Limit of Refractory Monolithics

Al_2O_3 (%)	Service Limit (°C)
Plastics	
40-50	1540–1600
60	1650–1760
80	1700–1800
90	1800–1900
Castables	
40–50 (Low-purity cement bond)	1260–1370
40–50 (High-purity cement bond)	1500–1650
70 (High-purity cement bond)	1650–1700
80 (High-purity cement bond)	1700–1760
95 (High-purity cement bond)	1820–1870

Table IX. Effect of Aggregate Type on Hot MOR of 85% Alumina Phosphate-Bonded Plastic Refractory

Aggregate Base	Tabular Alumina/Kaolin	Bauxite
Density (kg/m^3)	2720	2690
Hot MOR (MPa)		
815°C	11.0	14.0
1090°C	3.5	5.1
1370°C	2.4	4.3

sition has more influence on physical characteristics than the percentage of one of the oxides present.

As alumina content of a monolithic increases, in most cases the refractory's service limit and PCE will increase. Higher alumina refractories thus are used in higher temperature applications. Table VIII lists the alumina content of various plastic and castables along with their service limits. Density will also increase with increased alumina content due to the increased density of aggregates and fillers with higher alumina contents.

Strength of monolithics is naturally controlled to a major extent by the bond system present. Figure 1 illustrates this characteristic by comparing the hot modulus of rupture (MOR) of various 45 to 50% alumina monolithics using different bonding agents. Mechanical strength is also affected to a greater degree by the specific mineralogy of a monolithic composition than solely by the amount of alumina present. Table IX illustrates this by comparing two 85% alumina plastics, one using tabular alumina and kaolin aggregates and the other based on bauxite.

Alumina content also affects the thermal expansion coefficient of monolithic refractories. As alumina increases, the thermal expansion coefficient increases, as illustrated in Table X.

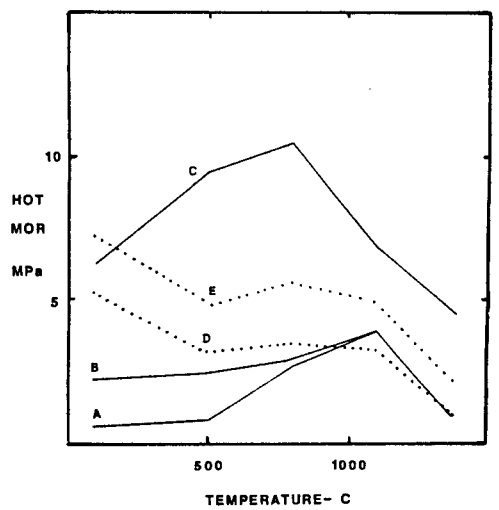

Fig. 1. Hot MOR of 40–50% alumina monolithic refractories. (A) clay-bond plastic; (B) air-bond plastic; (C) phosphate-bond plastic; (D) low-purity CA cement-bond castable; (E) high-purity CA cement-bond castable.

Table X. Alumina Content vs Thermal Expansion of Refractory Monolithics

Al_2O_3 (%)	Coefficient of Thermal Expansion ($\times 10^{-6}$/°C)
Plastics	
45	5.7
70	7.1
90	8.0
Castables	
40–50	6.0
70	7.0
95	8.5

Finally, alumina content in a monolithic refractory also has a direct effect on thermal conductivity. While increased density partially contributes to this effect, so does the increased quantity of crystalline alumina present. To illustrate this, Fig. 2 plots the effect of alumina content on the thermal conductivity of refractory plastics.

Summary

Monolithics containing aluminous raw materials have been used in virtually every application where alumina-containing refractory brick have been used. They include applications in steel mills, petrochemical complexes, aluminum plants, cement plants, foundries, boilers, and incinerators, to name a few. In recent years, due to new developments in monolithic refractories (such as the low, ultralow, and cement-free castables, improved castable gunning mixes, gunnable plastic refractories, and dry vibratable mixes) applications have increased, as has service performance. Monolithic refractories appear to be increasing in sophistication or application. Many efforts are underway to improve the quality of the current raw materials used and to develop new ones for future high-

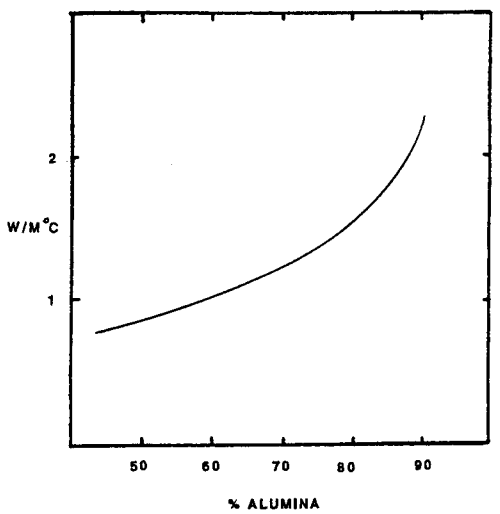

Fig. 2. Thermal conductivity vs alumina content for plastic refractories.

technology refractory monolithics. Alumina and alumina-containing raw materials will continue to be the basic building blocks for most of this class of refractory products.

References

[1]U.S. Department of Commerce Bureau of Census, "Current Industrial Reports—Refractories," Rept. Nos. MQ32C(86-1), MQ32C(86-2), MQ32C(86-3), and MQ32C(86-4).

[2]"Technology of Monolithic Refractories," Plibrico Japan Company, Ltd., Tokyo, Japan, 1984.

[3]Refractory Concrete, American Concrete Institute Publica tion ACI 547 R-79, Detroit, MI, 1983.

[4]T. D. Robson, High Alumina Cements and Concretes. Wile & Sons, New York, 1962.

[5]A. Petzold and M. Rohrs, Concrete for High Temperature Maclare & Sons, London, 1970.

[6]T. D. Robson, High Alumina Cements and Concretes. Wile & Sons, New York, 1962; p. 263.

[7]W. D. Kingery, "Fundamental Study of Phosphate Bondin in Refractories," *J. Am. Ceram. Soc.*, **33** [8] 239–47 (1950).

[8]M. J. O'Hara, J. J. Duga, and H. D. Sheets. "Studies i Phosphate Bonding," *Am. Ceram. Soc. Bull.*, **51** [7] 590–95 (1972)

[9]J. E. Cassidy, "Phosphate Bonding Then and Now," *Am Ceram. Soc. Bull.*, **56** [7] 640–43 (1977).

Space Vehicle Thermal Protection

Daniel B. Leiser
NASA Ames Research Center
Moffett Field, CA 94035

The materials which became a part of the thermal protection system (TPS) used on the space shuttle met some very ambitious goals. These goals are reviewed. The applications of alumina in the TPS used on the exterior of the orbiters are described. The increased future use of alumina both in flexible and rigid insulations and in the high-temperature gap fillers used between blocks of insulation (tiles) on future space vehicles is discussed.

Space vehicles which enter a planetary atmosphere (i.e., earth) like the space shuttle orbiter, shown in Fig. 1, require a thermal protection system (TPS) to protect them from aerodynamic heating. This heating is generated at the surface of an entering object due to the combination of compression and surface friction of the atmospheric gas. The vehicle's configuration and entry trajectory, in combination with the type of thermal protection system used, define the temperature distribution on the vehicle. Figure 2 illustrates "predicted" maximum temperature isotherms on the space shuttle for a typical trajectory. The space shuttle features a TPS system based on the use of surface materials with a high-temperature capability in combination with an underlying thermal insulation to inhibit the conduction of heat to the interior of the vehicle. The heat developed from the aerodynamic heating process is thereby radiated back into space by virtue of the high surface temperature. The leading edges of wings and the nose cap are the highest temperature regions. Due to the wide variation of these temperatures, the TPS selected for the space shuttle was composed of many different materials.[1] Some of the materials and their locations on the shuttle are shown in Fig. 3. Illustrated are the high-temperature reusable surface insulation tiles (HRSI), gap fillers, low-temperature reusable surface insulation tiles (LRSI), reinforced carbon/carbon (RCC) (a structural material), felt (flexible) reusable surface insulation (FRSI), and advanced flexible reusable surface insulation (AFRSI) applied in lower temperature areas. Each material's temperature capability, durability, and

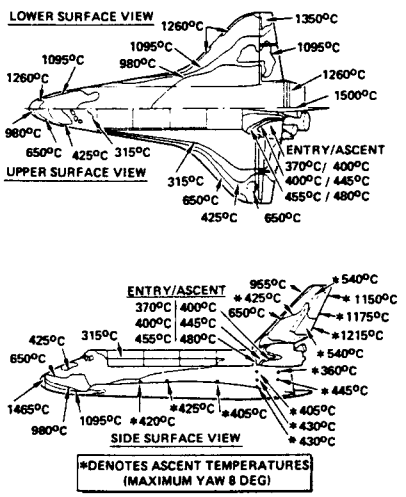

Fig. 2. Orbiter isotherms for a typical trajectory (Ref. 1).

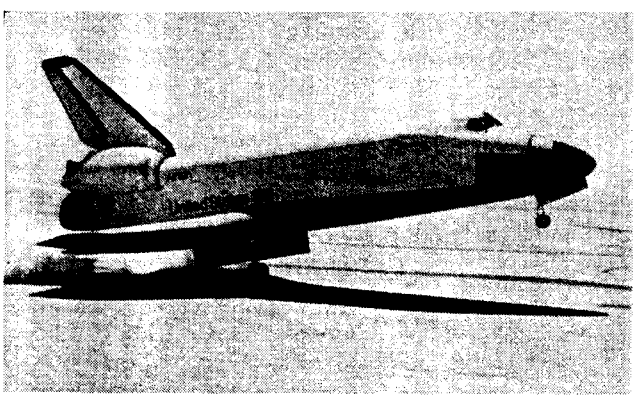

Fig. 1. Shuttle

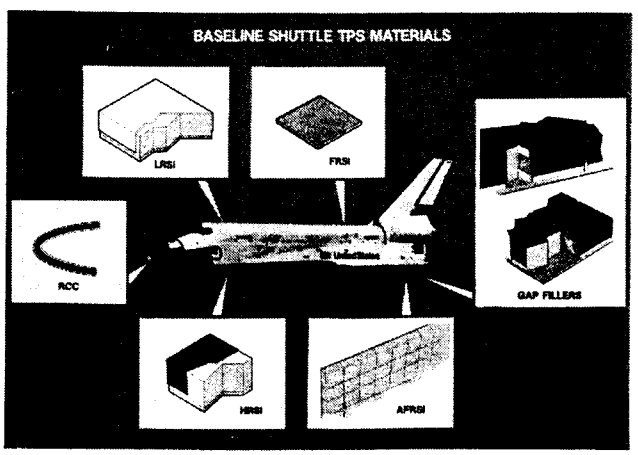

Fig. 3. Baseline shuttle TPS materials.

weight determined the extent of its application on the vehicle. Alumina-containing insulation materials were considered in the higher temperature areas where they would be most advantageous. In those areas the shuttle performance requirements (e.g., cost, rapid turnaround, etc.) dictated the design goals of the TPS materials. The goals were:

1. Maximize the payload capability of the vehicle by minimizing the insulation's thermal conductivity and density as much as possible, thereby reducing TPS weight.
2. Maximize the insulation's temperature capability to increase the flight envelope of the vehicle.
3. Maximize the insulation's thermal shock resistance by minimizing its thermal expansion coefficient in order to support, without failure, the expected rapid temperature changes and large thermal gradients achieved during reentry.
4. Maximize the insulation's mechanical strength to increase its durability and resistance to thermal shock.
5. Maximize the insulation's resistance to its environment including sea water, rain, and humidity.

Background

When the shuttle was in the design stage (in the early 1970s), several new materials were produced[2,3] to meet the ambitious goals described above. Two types of low-density insulation, aluminosilicate (mullite) and silica, produced by three manufacturers,[4–9] were evaluated. Each material was produced using different processes, additives, and binder systems. Extensive testing of the three candidate materials was done to evaluate their performance in a convectively heated environment which simulated the actual reentry.[10] Thermal shock/stress was the most common mode of failure for the insulations tested in the simulated flight heating environment. The final insulation was chosen because of its low weight and resistance to thermal stress failure resulting from its low thermal expansion coefficient, thermal conductivity, and density, 0.14 g/cm^3 (9 lb/ft^3), relative to the other candidate materials. It was composed of silica fibers* (1 to 3 μm) bonded together with a colloidal silica binder.

The properties of the initially chosen material, called LI-900, were adequate for most of the high-temperature locations, although there were areas where additional mechanical strength and temperature capability were desirable. Another silica insulation having equivalent thermal shock resistance was developed for those limited areas. It was produced by a different process without a binder and contained silicon carbide powder to act as both an opacifier and an emittance agent. It was produced at a higher density, 0.35 g/cm^3 (22 lb/ft^3). This material, designated LI-2200, and the original silica material made up the majority of the high-temperature heat shield on the first two orbiters, Columbia and Challenger. The material was applied to the vehicle in the form of 15 by 15 cm (6 in. by 6 in.) tiles with variable thicknesses, which were coated with borosilicate glass coatings[11,12] to give them the correct optical properties and to improve their handleability. The successful flight of the first reusable Space reentry vehicle, the orbiter Columbia in April 1981, proved the viability of this ceramic TPS concept. Subsequent flights of the orbiters have demonstrated that the TPS is reusable. It has performed beyond expectations in actual use.

Current Applications of Alumina Chemicals

The limited temperature capability and toughness of the LI-900 and LI-2200 provided the impetus for many studies into improved materials. Those studies resulted in the development of a new family of materials with variable compositions, densities, and properties. Several versions exhibit improved mechanical and thermal properties relative to silica while maintaining similar thermal shock resistance. Others had properties that were midway between silica and the "old" aluminosilicates evaluated in the early 1970s. Several compositions had both the desired increased temperature capability and the required thermal shock resistance. These materials utilized aluminoborosilicate (62% Al_2O_3-24% SiO_2-14% B_2O_3) fibers in combination with the silica fibers used previously to produce a "composite" insulation material. The new family of materials was referred to as fibrous refractory composite insulation (FRCI).[13,14] It was produced by the process shown schematically in Fig. 4. The blown silica fiber* (1 to 3 μm) was mixed in a V blender with a drawn (11 μm) aluminoborosilicate fiber† (cut into 0.32 cm (⅛ in.) lengths to facilitate mixing). The fibrous slurry was molded into a billet in a vacuum press and the billet was then dried, fired, and machined into finished tiles. One version of the composite insulation family, FRCI-12 0.19 g/cm^3 (12 lb/ft^3) containing 22 wt% of the aluminoborosilicate fiber (12% alumina), was eventually scaled up from a laboratory material to one having mass production capability. It was eventually selected for use on the third and fourth orbiters, Discovery and Atlantis, due to its lower weight per unit area, greater toughness, and similar temperature capability relative to the LI-2200 it replaced.

Another application of alumina in Space vehicle protection is illustrated by the two types of "gap fillers" currently used to seal the gaps between insulation tiles (shown schematically in Fig. 3). Both are different varieties of a composite material. They restrict the flow of hot gases in the gaps between tiles, preventing over-temperature of the vehicle's structure during entry. One consists of a pad made from a woven aluminoborosilicate (same fiber as used in FRCI) cloth

*Of type manufactured by Johns-Manville Corp., Manville, NJ.

†Of type manufactured by 3M Co., Minneapolis, MN.

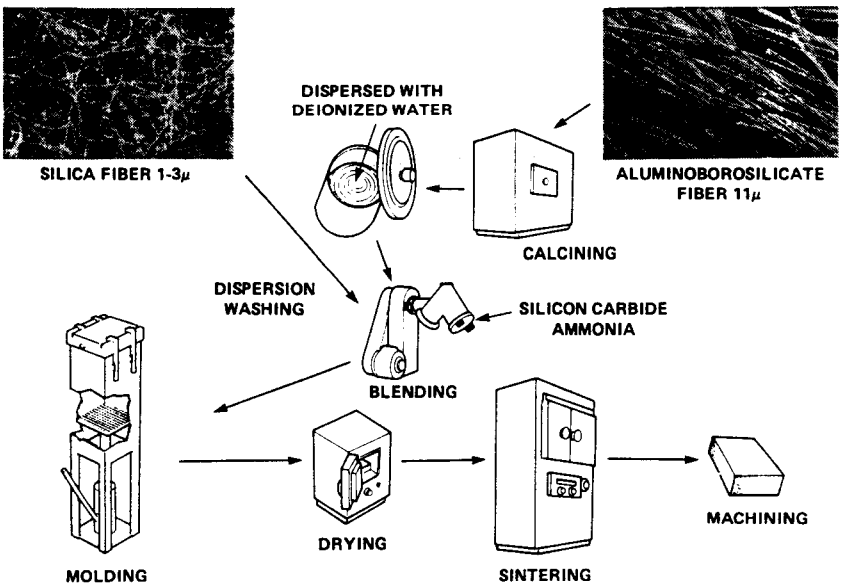

Fig. 4. FRCI process (Ref. 14).

filled with bulk alumina fibers[‡] (2 to 4 μm).[15] The cloth is sewn together with a refractory thread into the form of a pillow which holds the bulk alumina fibers. The filler pad is installed in the tile gaps using a Velcro[§] strip fastened to the base of the pad that engages with another Velcro strip attached under the heat-shield tiles. The bulk alumina fiber is used as the filler due to its dimensional stability at the high temperatures possible within the gaps. This dimensional stability prevents the opening of the gap at high temperature due to filler shrinkage, thereby eliminating a potential overtemperature exposure of the insulation tiles on either side of the gap. The other type of filler is composed of a strip or multiple strips of woven aluminoborosilicate[‡] cloth. The cloth serves as the skeleton of the filler into which is impregnated a high-emittance composition comprised of a mixture of (*a*) a silicone rubber that can be cured at room temperature (initial temporary plasticizer), (*b*) a borosilicate glass (permanent protection for the emittance pigment), and (*c*) a high-emittance pigment.[16,17] The cloth strip is inserted into an existing gap and fastened with room-temperature vulcanizing silicone rubber. The thickness of the filler can be adjusted to any size gap by bonding together multiple strips of the impregnated cloth with the standard silicone rubber. This makes it possible to accomplish a retrofit repair of any existing gaps that are too wide.

Future Applications of Alumina Chemicals

The goals established for the heat-shield materials used on the first shuttle orbiters also apply to any advanced reentry vehicle proposed for future use. The requirement that it weigh as little as possible will still be a primary concern. Higher temperature capability insulation materials than those currently used on the space shuttle will also be desirable because the TPS temperatures on most of the exterior of advanced vehicles will necessarily be driven higher to improve the overall vehicle performance and flight capabilities. One improvement provided by the higher temperature capability materials is the opening up of the flight envelope of future space vehicles, some of which are illustrated in Fig. 5. Figure 5 shows artists' drawings of three proposed reentry vehicles, including an aeroassisted space transfer vehicle (ASTV), national aerospace plane (NASP), and a transatmospheric vehicle (TAV).

Many multicomposition insulation materials have resulted from the research completed since the development of FRCI in 1979. Some have promise for use on future space vehicles.[18–20] One of the processes developed to make these materials is shown in Fig. 6.

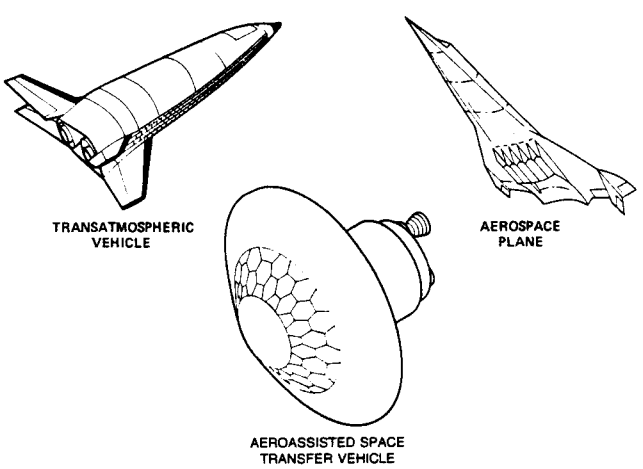

Fig. 5. Advanced space vehicles.

[‡]Of type manufactured by ICI U.S. Inc., Wilmington, DE.
[§]Velcro USA, Inc., Manchester, OH.

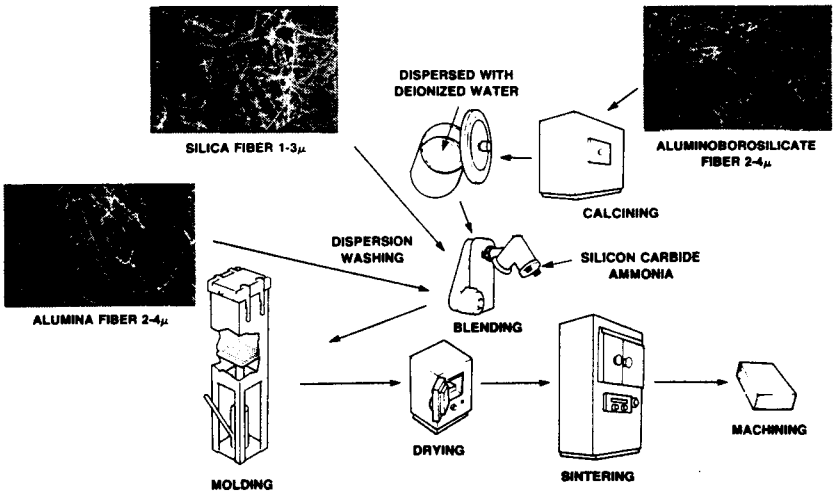

Fig. 6. AETB process (Ref. 14).

It shows the process for producing an alumina-enhanced thermal barrier (AETB). Other materials of this type are now commercially available, including high thermal performance (HTP) insulation materials showing similar characteristics.[20] These ultralow-density materials are available in a wide range of compositions, configurations, and densities which can be tailored to meet a specific application. The process shown in Fig. 6 is very similar to the one used to make FRCI, with the exception of introducing bulk alumina fibers[¶] into the composite and utilizing a blown smaller diameter (2 to 4 μm) aluminoborosilicate fiber. The result is a more homogeneous, dimensionally stable insulation. All of the insulations being developed for higher temperature applications use a higher concentration of alumina in some form.

An indication of the relative performance and improvement of these materials can be seen in Fig. 7, which shows both the tensile strength and dimensional stability of AETB and FRCI as a function of composition after 90 minutes at 1480°C (2700°F). The characteristics of one specific type of AETB material 0.19 g/cm^3 (12 lb/ft^3) are shown in Fig. 7. Each insulation contained a constant amount (10 wt%) of the (2 to 4 μm) aluminoborosilicate fiber. The effect of increasing the amount of refractory (alumina plus aluminoborosilicate) fiber in the insulation is shown in the figure by the substantial improvement in dimensional stability (less shrinkage) after the 90-minute isothermal exposure. At the same time, a drop in the tensile strength was observed. This plot shows that these new materials do have a higher temperature capability than the current shuttle materials: LI-900, FRCI-12, and LI-2200.

Lack of dimensional stability at high temperatures for the current shuttle materials limits the flight capabilities of the vehicle. One problem with materials

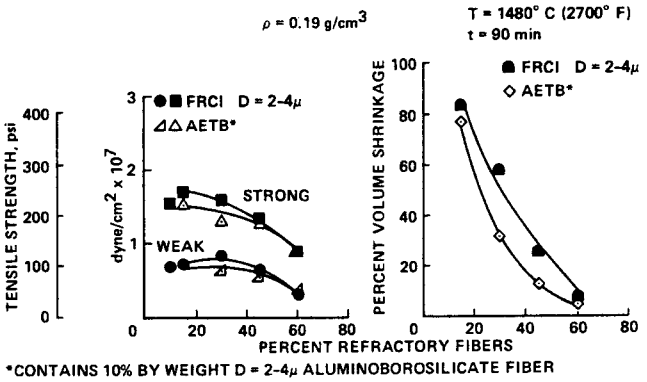

Fig. 7. High-temperature isothermal dimensional stability and tensile strength of FRCI and AETB as a function of refractory-fiber content (Ref. 18).

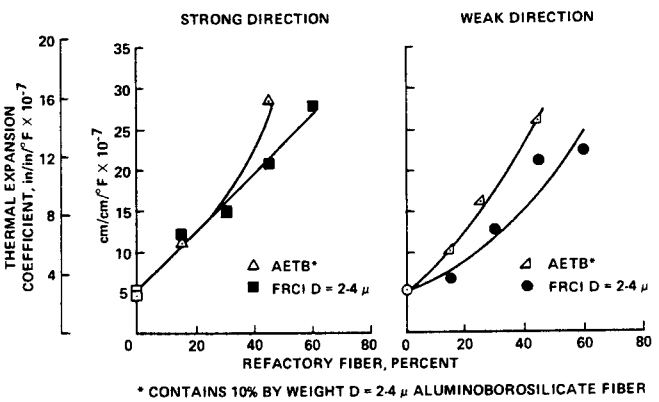

Fig. 8. Thermal expansion coefficient of FRCI and AETB as a function of refractory-fiber content (Ref. 18).

having higher concentrations of alumina is illustrated in Fig. 8, which shows the effect of alumina concentration on the thermal expansion coefficient in both the strong direction (perpendicular to the molding direction) and weak direction (parallel to the molding

[¶]Of type manufactured by ICI U.S. Inc., Wilmington, DE.

direction). The thermal expansion coefficient has a major influence on the material's thermal shock resistance along with its modulus of elasticity and tensile strength.

The relative thermal shock resistance is inversely proportional to both the elastic modulus and the expansion coefficient and directly proportional to the tensile strength. The increase in expansion coefficient as more alumina is added (Fig. 8), along with the decreasing tensile strength (Fig. 7), represent a significant problem relative to the insulation's performance in aerodynamic heating environments. In 1972, the candidate aluminosilicate (mullite type) insulation materials were eliminated from consideration for shuttle use because testing in a convective heating environment demonstrated a lack of adequate thermal shock resistance. The large thermal gradients which caused test failures are characteristic of the actual environment in which these materials must survive on both the shuttle and any future entry vehicle.

Another potential problem is the expected increase in the relative thermal conductivity of higher alumina content insulations. The data available and the predictions made using a thermal conductivity model[21,22] indicate that the amount of increase to be expected is a direct function of the alumina content and could be large enough to increase the weight of the heat shield for future vehicles. That weight is a problem because minimizing heat-shield weight is one of the primary goals in maximizing payload capability of the vehicle.

Another potential application of alumina-containing heat-shield material is in higher temperature flexible ceramic insulations (blankets). The first version of these new materials was composed of a silica cloth (outer face sheet), an S-glass cloth (inner face sheet), and a silica fiber batting (interior) sewn together with a quartz yarn sewing thread.[23,24] This quilted blanket was flown successfully on the second orbiter, Challenger, as a replacement for most of the low-temperature reusable insulation tiles on the top of the orbiter, where temperatures are below 760°C (1400°F). It was designated as advanced flexible reusable surface insulation (AFRSI). It is now used on all orbiters for about 40% of the surface area. Other potential applications of alumina in the general category of flexible ceramic insulation would be in the replacement of components of AFRSI.[25] In particular, the silica outer face sheet could be replaced by a woven aluminoborosilicate cloth which has a potentially higher temperature capability (980°C (1800°F)). The silica-fiber batting may also be replaced by an aluminoborosilicate or alumina-fiber batting with the same temperature capability. These new AFRSI materials may be used in limited areas where flexibility is particularly important on future vehicles.

Another type of flexible insulation material is also being developed which is more tailorable to the thermal performance requirements of future space vehicles and eliminates the potential limitations observed in AFRSI[26] due to the presence of sewing threads. This material uses a three-dimensional integrally woven structure filled with an insulative filler. The three-dimensional woven structures are currently made from commercially available ceramic yarns in a variety of complex weave constructions for structural applications. This concept for flexible TPS is designated as tailorable advanced blanket insulation (TABI). It has been produced using both an aluminoborosilicate-fiber construction and an aluminoborosilicate-fiber batting. It has the potential for higher temperature applications than AFRSI.

Summary

The future applications of alumina in thermal protection systems are many and varied. Alumina will be used to a greater extent in rigid insulation materials like AETB and HTP and in versions yet to be developed. In gap fillers its use will continue as both the filler in pads and as a component of the filler cloth. The need for more-refractory thermal protection systems will necessarily drive the ultralow-density materials' producer toward alumina since it represents the best means, at present, of reaching the desired goals.

Acknowledgments

The author gratefully acknowledges Wendell Love and Howard Goldstein for their helpful discussions and review of this manuscript.

References

[1]L. J. Korb, C. A. Morant, R. M. Calland, and C. S. Thatcher, "The Shuttle Orbiter Thermal Protection System," *Am. Ceram. Soc. Bull.*, **60** [11] 1188-93 (1981).

[2]J. D. Buckley, G. Strouhal, and J. J. Gangler, "Early Development of Ceramic Fiber Insulation for the Space Shuttle," *Am. Ceram. Soc. Bull.*, **60** [11] 1196–1200 (1981).

[3]W. Schramm, "HRSI and LRSI-the Early Years," *Am. Ceram. Soc. Bull.*, **60** [11] 1194–95 (1981).

[4]R. M. Beasley, Y. D. Izu, et al., "Fabrication and Improvement of LMSC's All-Silica RSI," Tech. Rept. No. NASA TMX-2719, November 1972.

[5]S. Musikant, F. P. Magin III, and J. J. Gebhardt, "Development of REI Mullite (Reusable External Insulation) for Application to the Space Shuttle"; pp. 413–45 in National SAMPE Technical Conference on Space Shuttle Materials, Vol. 3. SAMPE, Azusa, Calif., 1971.

[6]R. A. Tanzilli, S. M. Musikant, P. N. Bolinger, and J. P. Brazel, "Optimization of REI-Mullite Physical Properties," NASA TM X-2719, 1972; pp. 227–60.

[7]J. J. Gebhardt and P. D. Gorsuch, "Processing of Rigidized REI-Mullite Insulative Composites," Tech. Rept. No NASA TMX 2719, 1973; pp. 17–61.

[8]E. L. Rusert and H. Christensen, "HCF-External Thermal Insulation for Space Shuttle Thermal Protection System"; pp. 403–13 in National SAMPE Technical Conference on Space Shuttle Materials, Vol. 3. SAMPE, Azusa, Calif., 1971.

[9]P. P. Plank, A. Feldman, et al., "MAR-SI, Martin Surface Insulation," NASA TM X-2719, 1972; pp. 107–54.

[10]D. A. Stewart, "Cyclic Arc Plasma Tests of RSI Materials Using a Preheater," NASA TM X-2919, 1972; pp. 559–90.

[11]H. E. Goldstein, D. B. Leiser, and V. W. Katvala, "Reaction Cured Glass and Glass Coatings," U.S. Pat. No. 4 093 771, 1978.

[12]H. E. Goldstein, D. B. Leiser, and V. W. Katvala; pp. 623–34 in Reaction Cured Borosilicate Glass Coating for Low density Fibrous Silica Insulation, Borate Glasses: Structure, Properties, Applications. Plenum, New York, 1978.

[13]D. B. Leiser, H. E. Goldstein, and M. Smith, "Fibrous Refractory Composite Insulation," U.S. Pat. No. 4 148 962, 1979.

[14]D. B. Leiser, M. Smith, and H. E. Goldstein, "Development in Fibrous Refractory Composite Insulation," *Am. Ceram. Soc. Bull.*, **60** [11] 1201–1204 (1981).

[15]L. J. Korb, C. A. Morant, R. M. Calland, and C. S. Thatcher, "The Shuttle Orbiter Thermal Protection System," *Am. Ceram. Soc. Bull.*, **60** [11] 1192 (1981).

[16]D. B. Leiser, D. A. Stewart, C. A. Estrella, M. Smith, and H. E. Goldstein, "Adjustable High Emittance Gap Fillers," U.S. Pat. No. 4 308 309, 1981.

[17]D. B. Leiser, D. A. Stewart, M. Smith, C. Estrella, and H. E. Goldstein, "Heat Shield Gap Filler," NASA Tech Brief, Summer 1984; p. 570.

[18]D. B. Leiser, M. Smith, and D. A. Stewart, "Options for Improving Rigidized Ceramic Heatshields," *Ceram. Eng. Sci. Proc.*, **6** [7–8] 757–68 (1985).

[19]D. B. Leiser, M. Smith, and D. A. Stewart, "Effect of Fiber Size and Composition on Mechanical and Thermal Properties of Low Density Ceramic Composite Insulation Materials," NASA CP 2357, 1984; pp. 231–44.

[20]J. F. Creedon, Y. D. Izu, and W. H. Wheeler, "Advanced Ceramic Composite Insulation: Keeping Cool at 2,900°F," *Mater. Eng.*, **101** [5] 57–60 (1985).

[21]D. A. Stewart and D. B. Leiser, "Characterization of the Thermal Conductivity for Fibrous Refractory Composite Insulations," *Ceram. Eng. Sci. Proc.*, **6** [7–8] 769–92 (1985).

[22]D. A. Stewart, D. B. Leiser, P. Kolodziej, and M. Smith, "Thermal Response of Integral Multicomponent Composite Thermal Protection Systems," AIAA 20th Thermophysics Conference. Virginia, 1985.

[23]H. E. Goldstein, D. B. Leiser, P. M. Sawko, H. K. Larson, C. Estrella, and M. Smith, "Insulation Blankets for High-Temperature Use," NASA Tech Brief, Winter 1985; pp. 107–108.

[24]Paul M. Sawko, "Advances in TPS and Structures for Space Transportation Systems," NASA CP 2315, 1983; pp. 179–82.

[25]Paul M. Sawko, "Advances in TPS and Structures for Space Transportation Systems," NASA CP 2315, 1983; pp. 183–86.

[26]Paul M. Sawko, "Advances in TPS and Structures for Space Transportation Systems," NASA CP 2315, 1983; pp. 187–91.

SECTION V

Industrial Hygiene *and* Toxicology *of* Alumina Chemicals

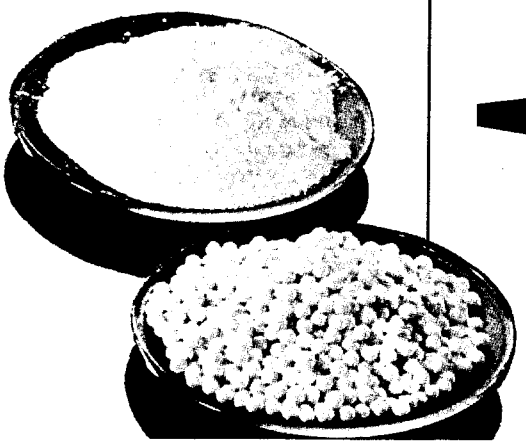

The Aluminas and Health

Bertram D. Dinman
Graduate School of Public Health
University of Pittsburgh
Pittsburgh, PA 15261

Since most sites of absorption from the gastrointestinal tract exist at a near-neutral pH range, aluminas usually are poorly absorbed after oral ingestion. However, under appropriate conditions, inhalation of fine particulate forms may potentially present a relatively more significant site of absorption and/or local damage. Nevertheless, numerous studies of occupational exposures to aluminas in aluminum refining, smelting, and the pottery industry repeatedly indicate that all the aluminas per se are essentially inert in the lungs. But, because several experimental studies in animals have indicated that specific aluminas may produce lung damage, there have been some continuing health concerns. A critical examination of these data indicates that there had been inconsistent physical characterization and identification of these aluminas; this reflects in part earlier confusion among physical scientists revolving about the identification of the "gamma" aluminas. The other factors contributing to this confusion stem from the use of differing types of experimental models which hold differing implications. When a catalytically active, ultrafine (0.02 to 0.04 μm) alumina, probably the low-temperature range eta transitional Al2O3 (identified erroneously as gamma Al2O3) is administered *directly* into the lungs of animals, it produces severe fibrosis. Similarly, when extremely fine (0.02 μm), gelatinous boehmite particulate possessing no catalytic activity is administered directly into lungs of animals, it too causes slightly less serious lung damage than does the similar size low-temperature (eta?) transitional Al2O3. When alpha Al2O3 ground to submicrometer size is placed in the lung, it produces a mild degree of lung fibrosis. Finally, when well-crystallized boehmite (γ-AlOOH) with a small surface area is administered similarly, it is inert in the lung. It would appear in the direct lung insufflation experimental model that lung damage is a function of (1) surface area and surface thermodynamic instability and (2) catalytic reactivity associated with the transitional aluminas. But it is also apparent that the confusion regarding the implications of the "gamma" designation has contributed to doubts regarding alumina's bioreactivity. By contrast, it has now become apparent that when a catalytically active chi transitional form is administered to animals by inhalation no pulmonary damage occurs. Further, when massive doses of gamma transitional alumina were administered by inhalation, a nonspecific response occurred characteristic of such large doses; however, this differed qualitatively from the nonreversible, more serious fibronodular pathology associated with the intratracheal insufflation studies. Finally, on the basis of specific human exposures to transitional aluminas produced as catalysts or adsorbents, to mixtures of higher temperature transitional aluminas increasingly used in modern smelters, and on the basis of exposure to alpha aluminas used in potteries, it appears that this full range of aluminas has little—if any—bioreactivity. Ultimately, evaluation of the human toxicity potential of environmental agents must consider both the experimental model systems and their limitations and human experience with similar agents. When considered in this fashion, it would appear that concerns revolving about alumina's pulmonary damage potentials are misplaced, since human exposure and models which more directly reflect such exposures do not result in the consequences seen with animal models associated with the artificial loading conditions.

For the aluminas to precipitate human health effects, some mode of entry into the body's internal environment is required. Consistent with their extremely low water solubility in the near-neutral pH range, aluminas usually are minimally absorbed from the essentially aqueous intestinal contents. For much the same reasons, they are effectively blocked from absorption through the skin. It is only as a fine particulate (i.e., less than 5 μm diameter) suspended in air that aluminas may possibly gain ready entry in amounts of interest into the body via the lungs. And, as such biological effects are dose-dependent (i.e., dose or concentration × time), theoretically very large quantities over a short period of time might produce immediate or acute effects, while small amounts over protracted periods could induce chronic tissue responses.

In actuality, workplace conditions usually produce long-term exposures to relatively small amounts of dust. Large doses are not usually tolerated for more than a short burstlike exposure, given the simple physical irritancy of a heavy dose of any fine particulate; by contrast, small doses are generally physically accepted since they produce few perceptible immediate effects. Accordingly, occupational exposures usually are long term; if excessive over many years, they may lead to both increased body uptake and functional lung alteration.[1]

Effects of Aluminas on the Lungs

Occupational exposures consisting solely of the aluminas unmixed with other elements or compounds have been unusual; accordingly, it is difficult to ascertain from the scientific literature what specifically may result from exposure to aluminas encountered in the workplace. For example, since the major industrial use of aluminas occurs in aluminum smelting, these sites of exposure have been studied for health effects from the earliest days of the industry. As early as 1910 and 1913, studies concerned with health effects were reported in Germany; they resulted in negative find-

ings. However, the presence of hydrofluoric acid in the smelting environment complicated interpretation of the meaning of such exposures since, as a strong irritant, it could by itself produce lung changes. Despite this confounding issue, studies repeated in 1933 produced similar outcomes.[2] In the early 1920s, as sandstone was being replaced in abrasive grinding by aluminum oxide and silicon carbide, health studies were undertaken by Macklin and Middleton[3]; once more, no deleterious impact on the lungs was seen. In contrast to studies in smelters, although these were relatively simpler exposures, there remained still unanswered questions regarding aluminum's effects since silicon carbide exposures existed concomitantly.

Because of the problem of silicosis that had existed in the pottery trade since its inception in Great Britain in the 1720s, substitutes for silica necessary to support unfired porcelain bisque were sought for many years.[4] A material which was nonfusible, nonreactive, and nonadherent to green china was required to provide a bedding for first firings of china bisque. Discussions between the manager of Royal Doulton potteries and the chief chemist of British Aluminum Company led to a proposal for alumina substitution. Accordingly, since there did not appear to be any evidence indicating that alumina presented any respiratory health risk, in August of 1928 Royal Doulton potteries made a complete changeover from flint to alumina. An alumina-china-clay mixture first used, however, did not prove successful for bulk firing: it appeared that the ware was not being held sufficiently straight. The smelter chemist suggested they use another alumina calcined to 1600°C, instead of that previously used, which had been fired to 1200°C.

However, it was observed that alumina, being lighter than flint, tended to become airborne; accordingly, even dustier atmospheres obtained in these potteries, consisting of particle sizes in the dangerous respirable range (i.e., <5 to 10 μm diameter). In view of these observations, the British Home Office intervened regarding the question of lung hazard to pottery workers. As a result, the matter was referred to the British Medical Research Council for investigation.

On the basis of these concerns, the Industrial Pulmonary Diseases Committee of the Medical Research Council was asked to do a study of workers in aluminum reduction operations at Kinlochleven and Lochaber, Scotland. In these pot lines, alumina dust exposures occurred which were comparable to those existing among china bisque workers. Sickness absence among workers was investigated; similarly, clinical and X-ray examinations of workers exposed to dust, and investigation of the dust clouds themselves, were also undertaken. These studies concluded that there was no substantial difference in the pattern of the sickness incidence, and that the X-ray examinations of a sample of 50 workers demonstrated neither adverse effects on the lung nor evidence of pneumoconiosis.[5] It was concluded that this substitution, which had been extensively carried out in the pottery industry, was both safe and successful in eliminating the scourge of silicosis.

Experimental Studies of Alumina Exposures

Simultaneously with these activities, in the mid-1930s interest in the prevention of silicosis by inhalation of powdered metallic aluminum was sparked by the report of Denny et al.[6] Quite independently, Leroy Gardner and coworkers[7] at the Saranac Laboratory also were attempting to neutralize the pathogenic effect of silica by coating it with colloidal aluminum hydroxide. Gardner and coworkers, as well as Denny et al., working with colloidal alumina supplied by Dr. Francis Frary of the Aluminum Company of America, studied the effects of inhalation of this material on the lungs of guinea pigs.

Among the numerous aluminas studied by Gardner et al.[7] was one designated as "HX1010" (Table I), specially prepared in the Aluminum Company's laboratory from sodium aluminate; it was reported to have maximum chemical reactivity with silica. Although Gardner et al. reported that it appeared to be a largely amorphous, gelatinous alumina with an X-ray diffraction (XRD) pattern showing some boehmite and a small amount of calcite, examination of the XRD patterns indicates that this alumina actually was gelatinous boehmite. In addition to this material's apparent effectiveness against the deleterious effects of quartz, it appeared to be nonreactive in the lungs after being inhaled for many months by rats.

In addition to treatments with gelatinous boehmite, the Saranac group also studied the effect of an $Al(OH)_3$, designated C-730, derived from gibbsite. This trihydroxide was heated or "activated" sufficiently to produce what the authors believed to be a "gamma" alumina. Given the inadequate knowledge base and the inclusivity of the "gamma" designation extant prior to 1950, it presently appears that their "activation" resulted in formation of the chi transitional form; this observation was not apparent until now.

The Gardner et al.[7] inhalation studies found that this chi transitional form is essentially inert in the lungs. In view of subsequent events, it is important to note that these inhalation studies of (1) large surface area gelatinous boehmite and (2) catalytically active eta transitional alumina failed to show evidence of a pathogenic effect on the lungs.

Until the early 1940s, aluminum and its oxides had been generally considered biologically inert. That aluminum in all of its forms was indeed inert was suddenly open to serious doubt following German experiences in World War II with powdered metallic flake produced for pyrotechnic purposes. As a result of these reports, concerns regarding the use of aluminas in the pottery industry once more were stimulated in

Table I. Identity, Physical Constants, Administration, and Response to Alumina Species Studies, 1944–1961

Investigator	Agent: Investigator Designation	Agent: Identity 1987	Agent: Crystalline Packing Arrangment	Route of Admin.	Particle Size (μm)	Surface Area m^2/g	Crystallinity	Catalytic Activity	Response
Gardner et al. (Ref. 9)	"Activated" C-730	Chi (?) transitional	γ	Inhalation	?	250–?	Low	+	"No harmful effects"
	HX1010	Gelatinous boehmite	γ	Inhalation	0.02	250–350	Low	–	"No harmful effects"
King et al. (Ref. 10)	"γ-AlOOH HX1010"	Gelatinous boehmite	γ	Intratracheal insufflation	0.02–0.04	300	Low	–	Fibrosis +3/5†
Stacy et al. (Ref. 11)	"γ-AlOOH HX1010"	Gelatinous boehmite	γ	Intratracheal insufflation	0.02–0.04	300	Low	–	Fibrosis +3/5‡
	"HX1010" heated to 850°C to gamma	Eta (?) transitional	γ	Intratracheal insufflation	0.02–0.04	100–?	Low	+	Fibrosis +5/5‡
	γ-AlOOH Cera hydrate®	Boehmite	γ	Intratracheal insufflation	3	0.6*	High	–	0 Fibrosis‡
	HX1010 heated to 1200°C	Alpha	α	Intratracheal insufflation	0.1–0.8†	3*	High	–	Fibrosis +1/5‡
Klosterkötter (Ref. 12)	γ-Al_2O_3	Gamma transitional	γ	Inhalation	0.005–0.04	95–105	Low	+	Alveolar proteinosis
	γ-Al_2O_3	Gamma transitional	γ	Intratracheal insufflation	0.005–0.04	95–105	Low	+	Fibrosis +3/5‡

* = Calculated.
† = Estimated by review of authors' photomicrographs.
‡ = System of fibrosis grading, King et al. (Ref. 10).

Great Britain. In response to these questions, the Silicosis Medical Board of Great Britain reexamined smelter workers from the same Scottish smelters studied in 1936.[5] Thus, in 1948[8] a second study indicated that no smelter worker had died of respiratory disease and that the previous conclusions seemed valid.

Despite continuing concerns and confusion regarding the facts surrounding these German cases with severe pulmonary damage, repeated surveys in Great Britain amply reconfirmed that not a single case of a pneumoconiosis had occurred among workers exposed to alumina dust in smelters or potteries.[9] Finally, in 1961 this question was once more investigated in pottery manufacturers and the British Aluminum Company; again, despite significant alumina dust exposures its innocuousness was fully confirmed.[4] While no definitive data are available as regards which specific alumina was in use in the Scottish smelters, one could reasonably surmise that it was largely α-Al_2O_3, as was clearly indicated in Meiklejohn's[4] review of alumina use in the potteries.

Because of continued interest at mid-century in the possibility of prevention and prophylaxis of silicosis by inhalation of aluminas, laboratory studies of the effects of alumina on the lungs were being pursued in Great Britain. In view of the foregoing data, medical researchers were perplexed by a report from Professor E. J. King's laboratory[10] in 1955 that found severe pulmonary damage ensued on *injection* of the same gelatinous boehmite, γ-AlOOH (HX1010), which previously had been believed innocuous by Gardner et al.[7] (Table I).

It is extremely important to note here that the studies in King's laboratories consisted of injection of 50 mg of these aluminas *directly into the lungs via intratracheal insufflation*. It is presently believed that such doses delivered to the lungs by this approach are unphysiologic and consequently artifactual, reminiscent of megadose experiments in carcinogenesis studies. To observers of that time, however, it appeared that this same alumina, gelatinous boehmite, HX1010, previously believed harmless by Gardner et al.[7] was now producing severe damage. Once more, dormant concerns were reawakened.

Fortunately, the British experiments were extremely well documented. This alumina, HX1010, was characterized by broadened XRD bands, indicating a boehmitic form with poor crystalline order. Surface area was reported as approximately 300 m2/g; the material consisted of poorly resolved laths 20 to 40 nm long and 5 to 10 nm wide. From their descriptions and the XRD pattern, it appears in retrospect that King and his coworkers were studying gelatinous boehmite, which they identified as "gamma AlOOH." The impact of this material on the lungs of rats was quite severe when administered by direct intratracheal

insufflation; a fatal fibrosis of the lung ensued in most of these animals. This new information was indeed alarming, in view of the widespread use of aluminas in the pottery industry.

These findings stimulated further studies by Stacy et al.[11] Again, intratracheal administration of the same extremely fine (i.e., 0.02 μm) HX1010, gelatinous boehmite (γ-AlOOH), produced moderately severe fibronodular lung damage. This gelatinous boehmite was heated to 850°C and thermally dehydroxylated to what the authors believed was "gamma Al_2O_3." Although Stumpf et al.[12] had demonstrated in 1950 that this so-called "gamma" thermal dehydration production actually consists of three specific transitional aluminas, viz. eta, chi, and gamma, common usage imprecisely has referred to these three different forms collectively as "gamma." In actuality, as later shown by Lippens[13] and confirmed by Abrahams and Low,[14] heating this "HX1010" gelatinous boehmite to 850°C probably would have produced largely the eta transitional form. When this extremely small particulate (0.02 μm), which was probably eta transitional form, was administered intratracheally, even more severe fibronodular damage to the lungs ensued (Table I).

A third alumina, a highly crystalline, large particle size (3 μm) boehmite ("γ-AlOOH, Cera hydrate*") was also administered by intratracheal insufflation; it was totally inert in the lung. Finally, HX1010 was heated to 1200°C to form alpha aluminum oxide; after grinding to reduce particle size to ". . .less than one micra," intratracheal insufflation of this alpha form produced minimal fibronodular change in the lungs.

All of these designations, size specifications, physical characteristics, and experimental results are summarized in Table I.

Critical review of these experiments sheds considerable light on our understanding of the biological effects of the aluminas, insofar as they result from direct lung insufflation of aluminas. Although Stacy and coworkers[11] attempted to relate solubility to fibrogenic potential, they probably were also correlating surface area and crystalline order with fibrosis (Fig. 1). The fibrogenicity of several of these different "gamma" forms was marked, although unfortunately these biomedical researchers did not realize that the designation "gamma" was applied on the basis of two different concepts. That is, the alumina identified as "gamma Al_2O_3" (in actuality probably the eta form) represented a transitional alumina; the gelatinous boehmite, i.e., their "gamma AlOOH, HX1010," was designated "gamma" because of its boehmitic, cubic crystalline lattice packing arrangement. Oblivious to this confusion, the biomedical literature has fixated—but in an indecisive fashion—on the "gamma" form of alumina as being hazardous. In addition, for reasons that still are not clear, insufficient attention was paid to the Stacy et al. finding that another "gamma" AlOOH (i.e., boehmite, which they referred to as Cera hydrate) produced absolutely *no* fibrosis. Regardless of these errors and inconsistencies, since that time "gamma alumina" has been regarded in the biomedical literature as possibly possessing serious damage potentials for the lungs.

A major factor bearing on interpretation of these experimental alumina effects relates to how these materials were administered to test animals. In review-

*Cerac, Inc., Milwaukee, WI.

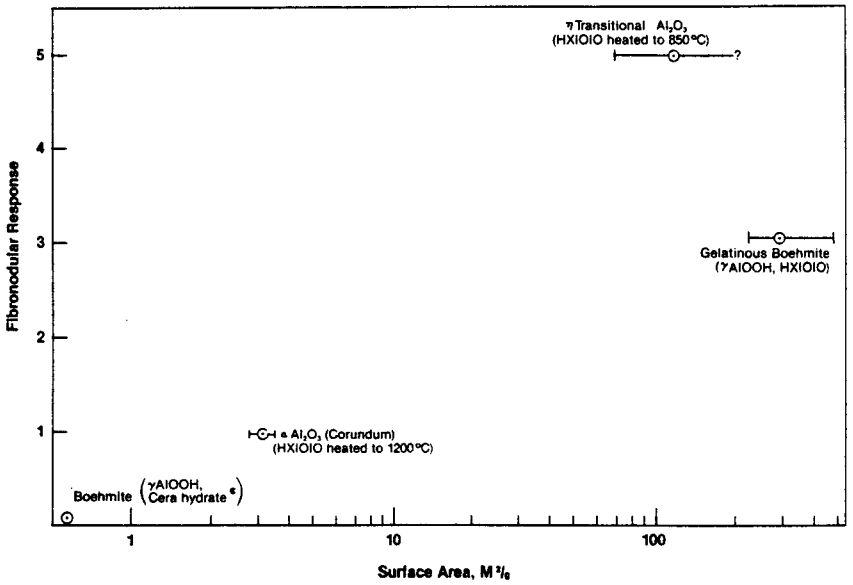

Fig. 1. Relationship between surface area and pulmonary fibrosis for several aluminas, as reported by Stacy et al. (Ref. 11).

ing the three studies (Table I), it is noteworthy that aluminas were introduced by *inhalation* into the lung in Gardner's studies[7]; this was quite different from the King groups'[10,11] intratracheal *insufflation*. It has since been pointed out by numerous other investigators that intratracheal insufflation of the lungs represents an unphysiologic, artifactually burdened methodology for the study of dust effects on the lung. In large part, this method's artifactual nature stems from the large, localized dose delivered to the lungs which quantitatively exceeds that which could possibly be carried by inhalation; such megadoses also overwhelm normal lung clearance mechanisms and are, hence, most unphysiologic.

This situation was further complicated by another misreading of the important 1960 study of Klosterkötter.[15] In this experiment, a gamma transitional alumina believed similar to Stacy's was administered to animals by inhalation. In contrast to the aluminas studied by Stacy et al.,[11] this was probably a true gamma transition form, reportedly produced by hydrolysis of aluminum chloride in the vapor phase. Although the effects of this inhalation exposure on the lungs were marked, the fibronodular damage seen by King et al. and Stacy et al. did *not* occur here; rather, a severe but *reversible* change in the lung, now known as alveolar proteinosis, was induced by these exposures. (Unfortunately, at that time a consensus regarding the meaning of this response had not been established; presently, it is believed that this lung reaction represents a nonspecific response to any *heavy* dosing with a wide variety of mineral dusts both pathogenic and nonpathogenic.) Consistent with this concept, it should be noted that the dose here was exceedingly high, i.e., 33 g/m^3 daily for 285 days. Nevertheless, the net result of this experiment was to reinforce a belief that gamma alumina had a serious—though inconsistent—effect on the lungs by inhalation.

In spite of the confusions and inconsistencies surrounding these various results, "gamma" aluminas until today have been suspected as posing an occupational hazard to the lungs. Although Klosterkötter commented that the concentrations used in his studies were intolerable to accidentally exposed laboratory attendants and hence unacceptable in occupational settings,[15] this reservation has essentially been disregarded. Thus, the matter rested for many years, and gamma alumina accordingly has continued to be treated with some concern, e.g., in standard-setting processes as recently as 1986.[16] Clearly, the biomedical literature has not appreciated that the "gamma" designation may be applied to a specific, individual thermally induced transitional form as well as to a number of different aluminas which simply have a common cuboidal lattice packing arrangement. Finally, the fact that Stacy et al.[11] probably studied the eta transitional form, and that Gardner et al.[7] studied the chi transitional form has not been discerned until this discussion.

Experimental Induction of Lung Damage by the Aluminas: A Physical-Chemical, Biological Interpretation

A full understanding of the effects of environmental agents on health requires careful synthesis of *both* experimental studies of animals and clinical evaluation following inadvertent or occupational exposures to man. Because the experimental approach is constrained to use animal models, extrapolation from such artificial systems to issues of human health and well-being is fraught with problems. Nevertheless, other advantages may accrue from the use of such experimental models; e.g., the sequential or stepwise mode of response can be delineated by serial examination of events and chemical and physiologic mechanisms can be elucidated within the model's constraints. Usually such animal studies begin with large doses to determine if the experimental system is responsive; large doses are often necessitated since repeated, long-term, low-dose exposure conditions occurring in humans poses an economic hurdle to the researcher. In sum, while biological mechanisms and processes can be defined in these model systems, their applicability to the human condition must be approached with caution.

This situation applies to the studies of King et al.[10] and Stacy et al.[11]; despite these limitations, their studies were both useful and unique because they rather carefully characterized the specific nature of the aluminas investigated. Accordingly, their data provide interesting models for scrutiny—insofar as their model's limitations are recognized. Ultimately, any mechanisms such models may propose must be considered within the light of human exposures and what these have revealed.

The Stacy et al. and King et al. studies both dosed animals by direct insufflation of various aluminas via the trachea into the lungs. The doses involved, i.e., 50 mg per treatment, were massive compared to what may possibly be inhaled at any one breath. Further, such large amounts disabled the normal mechanisms for cleansing the lungs of foreign dusts. In the presence of these effects, the meaning of these experiments for human exposure conditions should be regarded with reservations.

Within such constraints, careful analysis of the Gardner et al., King et al., Stacy et al., and Klosterkötter studies reveals a consistent relationship between the physical character of the aluminas and their effects on the lung in a peculiar experimental model. It is clear from examination of Table I and Fig. 1 that particle size—or more particularly, surface area—and catalytic activity apparently are related to biological reactivity of the aluminas directly injected into the lungs.

The basis of bioreactivity of what was probably the eta transitional form administered by intratracheal insufflation derives from its physical-chemical reactiv-

ity, at least in this large dose range. In the course of heating the aluminas, on thermal decomposition there is first diffusion of protons to react with OH^- ions to form H_2O. This leads to a loss of up to 30% of the mass of the aluminum trihydroxide, about 15% when AlOOH is decomposed. As the outer shape of the particle does not change, the result is an increasing porosity and surface area. The loss of the 2 OH as H_2O leaves behind one oxygen and an exposed Al^+ ion; given its electron deficiency, the Al^+ behaves as a Lewis acid site. Additionally, since some hydroxyl groups are retained during thermal decomposition of $Al(OH)_3$, such OH^- ions may act as proton donors, i.e., Brönsted acids. It is presently believed that Lewis and Brönsted acid sites account for these aluminas' catalytic activity.[17] Further, "defect" structures resulting from dehydration (especially the triplet vacancies) provide the opportunity of unusual exposure of aluminum ions in underlying layers which also constitute strong acid sites.[18]

Given this enhanced reactivity potential, the biological impact of the catalytically active transitional forms might be predicted. However, since gelatinous boehmite shows no similar catalytic activity, its apparent bioreactivity following intratracheal insufflation is not explicable on a similar basis.

It is proposed that the extremely large surface area (i.e., 250 to 350 m^2/g) of gelatinous boehmite is responsible for its activity in the King et al.-Stacy et al. model. As total surface area per unit mass increases, thermodynamic stability decreases as surface free energy increases.[19]

The contribution of large surface area and resulting thermodynamic instability in determining biological activity is highlighted by a minimal fibrogenic reactivity of α-Al_2O_3, as compared with the nonreactivity of boehmite administered by Stacy et al.[11] as "gamma AlOOH Cera hydrate." In their studies, Stacy et al. ground the corundum so that its particle size ranged between 0.1 and 0.7 μm, with a calculated surface area of 3 m^2/g. By contrast, the unmilled boehmite demonstrated a mean particle diameter of 3 μm with a nominal surface area of 0.6 m^2/g. If one arrays lung fibrosis activity versus surface area, an association is apparent between these two parameters, with what was probably the eta transitional alumina being the exception (Fig. 1). However, given that form's catalytic activity in addition to its relatively large surface area (i.e., 100 to 350 m^2/g), an incrementally enhanced lung bioreactivity beyond that which might be produced by increased surface area should not be unexpected.

Although such proposed physical interactions with lung tissue might be reasonable under the conditions of the foregoing experiments, experimental exposure to the aluminas by a route more analogous to human experience (i.e., by inhalation) does not appear to be associated with such responses.

Clearly, Gardner et al.[7] exposed animals to the large surface area gelatinous boehmite (i.e., "gamma AlOOH HX1010") and to a catalytically active chi transitional alumina. Neither exposure produced a severe, specific fibronodular response similar to that seen by King et al.[10] and Stacy and coworkers11 when similar aluminas were administered by intratracheal insufflation. In addition, Klosterkötter's [15] exposure by inhalation to a gamma transitional form resulted simply in nonspecific, reversible lung changes characteristic of overloading with any of a wide range of unrelated mineral dusts; this was *not* the fibronodular response seen by King et al. or Stacy et al.

Occupational Studies of Alumina Exposures

A case might be made that British occupational exposure experience in the pottery industry and aluminum smelting contradicts and negates the animal experimental findings in Great Britain. But it should also be noted that these studies of smelters prior to 1965–75 have largely represented exposures to alpha aluminas or the higher fired aluminas used in the pottery industry; accordingly, the British workplace studies probably do not present exposures to the low-temperature transition forms or to the large-surface-area gelatinous boehmite.

One could also attempt to at least partially resolve this issue of the biohazard of the catalytically active transitional aluminas by investigation of exposures in alumina chemical refineries producing "activated" aluminas, i.e., the eta, chi, and gamma transitional forms. Certainly, if these most reactive of aluminas are not associated with health risks, some comfort could be afforded as regards the transitional forms. Such studies had not been performed until 1985 when, for the first time, the respiratory status of workers in a chemical alumina refinery was reported.[1] In that investigation, 1109 potentially exposed workers handling a full range of nonsmelting-type chemical-grade aluminas between 1959 and 1982 were tested. Approximately 3% of the production at this refinery consisted of the transitional forms gamma, chi, and eta, there being 10 000 to 12 000 tons produced annually.

A roentgenographic search for lung alterations yielded minimal evidence of structural change.[20] There was a tendency for an increased prevalence of small irregular opacities in the chest radiographs among a few of the most exposed workers. But in contrast to the severe fibronodular changes seen with intratracheal insufflations of aluminas in animals, seldom did the radiographic category exceed this minimal 1/0—or at the most 1/1—classification. Smoking was more clearly related to the presence of irregular opacities; this association was much stronger than that seen as a result of exposure to dust. No significant increased prevalence of rounded opacities was noted in this group of workers. Similar findings have been described in other occupations exposed to mixed dusts, e.g., among workers exposed to iron dust in found-

ries,[21] in employees exposed to man-made fibers,[22] and among coal miners.[23] In summary, these observations cannot support the hypothesis that an increased frequency of irregular opacities is specific to alumina exposures, either transitional or other forms.

Nevertheless, one cannot consider any excessive dust exposure to be harmless to the lung's functional integrity. In the 1985 report from this same refinery, Townsend and coworkers[1] demonstrated that excessive dust loading with the aluminas may produce a nonspecific industrial bronchitis. This study indicated that those individuals most highly exposed to the aluminas (greater than 100 mg/m^3-year exposure for more than 20 years) had a 2.21- to 4.05-fold excess of workers with an abnormal forced expiratory volume at 1 second, abnormal being defined as a value below 80% of the predicted figure. However, smoking clearly appeared to have a far more deleterious effect on ventilatory capacity.

In summary, these reports by Townsend et al.[1,20] represent the only definitive investigation dealing with alumina exposures to these potentially most biologically active of the aluminas, i.e., the lower temperature eta, chi, and gamma transitional forms unmixed with other dusts or lung irritants. Unfortunately, because of the economic realities of the alumina refining industry, these specific aluminas are not commonly produced in facilities wherein exposure to other aluminas does not occur. However, in view of the higher levels of exposures experienced here in the past, if the transitional or other aluminas found to be so active in animals were also dangerous for man, one should have had some indication of this occupational hazard.

Clearly, with reasonable engineering controls and work practices, these catalytic and chemical-grade alumina exposures do not seem to present an important health risk. Doses sufficient to cause alveolar proteinosis in experimental animals by inhalation apparently do not occur under these workplace conditions. Thus, while a minimal, essentially asymptomatic chronic bronchitis was seen by Townsend et al.,[1] doses as large as occurred in Klosterkötter's study[15] probably did not occur. This conclusion is further supported by the observation that the lung alterations seen at that refinery are qualitatively and quantitatively quite different from those produced in Klosterkötter's experiment. Furthermore, protective mechanisms that ordinarily sweep the lungs clear of dusts continue to be active under the comparatively minor dusting of occupational exposures.

Technologic changes in aluminum smelting since the 1950s have led to changes in the character of the aluminas utilized. Because of energy savings associated with flash and fluid bed calcination in refineries, in reduction-cell operational efficiencies, and the absorptive requirements for effluent cleaning with process alumina, there has been a shift from the more highly fired alpha aluminum oxide (corundum), to the lower temperature gamma, kappa, delta, and theta transitional forms. These forms have a larger surface area than alpha. In addition, because of the gamma form in these newer smelting aluminas, these aluminas may also possess a minor degree of catalytic activity. Thus, more recent smelter population studies could represent populations at some slightly greater risk of exposure to the potentially biologically reactive transitional form of alumina. However, the most recent studies of aluminum smelter populations neither demonstrate convincing evidence of pulmonary fibrosis nor nodularity,[24] nor any excess of mortality attributable to pneumoconiosis.[25]

Indeed the most serious—though only slightly differing—reports indicative of pneumoconiosis were reported from Italian smelters.[26] However, those investigators did not stratify smokers and nonsmokers in regard to the frequency of X-ray opacities, as was done in the Arkansas studies where smokers showed a slight increase in frequency of occurrence of small X-ray opacities. In any studies of population at risk of pulmonary disorders, stratification for smoking status must be undertaken to differentiate from the far more serious effects of smoking. Further, the series of workers studied in this Italian smelter was one-tenth the size of the Arkansas report.

In summary, although critical analysis of experimental evidence suggests some possible mechanisms of biological action occurring in one peculiar model, human experience with the aluminas strongly suggests that they are not associated with significant specific pulmonary hazards under conditions of occupational inhalation exposure. Until evidence is accrued to the contrary, it appears that considering either transition aluminas, i.e., gamma, eta, chi, or gelatinous, high surface area boehmite (γ-AlOOH) as a subspecies of special concern is unwarranted as regards occupational exposures. While this position can be held with a reasonable degree of assurance, grossly excessive occupational exposure to any alumina—like any excess—should be avoided.

Other Health Considerations

Might the aluminas represent a possible source of increased aluminum body burden, with possible serious health aspects, particularly as regards the putative connection with various neurologic disorders, such as Alzheimer's disease and amyotrophic lateral sclerosis? At present, an important association of these conditions with aluminum is speculative; however, aluminum is not believed to cause these conditions. Certainly, given the aluminas' low solubility in aqueous milieus at the neutral pH region and the competition for absorption with calcium or phosphate, the potential for significant incremental whole body loadings via the gastrointestinal or pulmonary portal of entry is relatively improbable. Although a relatively small increase in blood aluminum concentrations has been demonstrated in workers in smelters,[27] the expo-

sure potential for body uptake of more soluble aluminum compounds used as food additives[28] or as antacid medication is several orders of magnitude greater. Finally, if there were to be any association with the neurologic disorders, the aluminas per se would simply act as still another possible source of aluminum ion. But as aluminum oxides or hydroxides, on the basis of present knowledge, they cannot be proposed as having any specific or significant role in connection with these conditions.

Appendix

Uses and Implications of Material Safety Data Sheets for Aluminas

A review of Material Safety Data Sheets (MSDS) (Figs. A1 to A5) indicates the contents provided by these documents. Their purpose is self-evident: These forms provide information regarding physical and chemical data of materials or mixtures entering commerce, plus their health and safety hazards. These concise compendia are also designed to assist in the safe handling of materials under conditions of normal usage, as well as under emergency situations. They also cross-reference pertinent Department of Transportation regulations in addition to general scientific references which may be pursued for additional information.

Under provisions of the Occupational Safety and Health Act (OSHAct) Regulations (CFR 1910.1200) regarding employee hazard communication, and Title III of the Superfund Amendment and Reauthorization Act of 1986, i.e., "The Emergency Planning and Community Right-to-Know Act of 1986," such MSDS are to be made available to a broad range of interested parties. Under the provisions of the OSHAct, MSDS are to be made available to all employees and their representatives on request. Proposed Environmental Protection Agency regulations promulgated under the Emergency Planning and Community Right-to-Know Act indicate that MSDS, in addition to other information, must be available by October 1987 to local emergency planning committees, state emergency response commissions, and local fire departments. In addition, any member of the public must be permitted access to this information under the aegis of such groups.

Additionally, there are diverse implications as regards tort liability exposure potentially incurred as a result of inappropriate or inadequate usage and applications of this information. Given these diverse legal and regulatory requirements, the implications underlying the design and completion of these MSDS merit some further discussion.

In actuality, prior to promulgation of these regulatory requirements, many producers of commercial chemicals had developed MSDS for customer use with the intent of minimizing tort liability exposure by meeting the adequate warning test. However, with passage of worker right-to-know regulations, this regulatory requirement to provide MSDS has been imposed on all employers who may either produce, purchase, or otherwise use industrial chemicals. Accordingly, the provision of MSDS has become a normal part of sales activities.

However, with the almost explosive growth in the number of MSDS presently in circulation, it has become apparent that various producers and purveyors of aluminas—as well as other materials—have provided MSDS containing inconsistent or contradictory information. It is useful to understand the cause of these variations and the implications of these inconsistencies.

The cause of content variability among current MSDS stems from several factors. Some producers or repackagers frequently do not have access to knowledgeable sources adequate to produce or generate appropriate MSDS. In such cases, MSDS will be copied from other MSDS provided by other producers in the industry, often without regard for their adequacy or pertinence. The knowledgeability of some producers without professional resources in areas of toxicology, fire and safety, medical management, etc., inevitably will result in MSDS with highly variable contents. Where there is inadequate or superficial evaluation of the adequacy of such sources of information as are used, the MSDS may be essentially inadequate or, at the other extreme, raise undue alarm and restrictions of use and application of chemicals. Still another factor impacting on the breadth and contents of the MSDS reflects the impact of legal consultation. Depending on inclinations of legal counsel, the MSDS may be very general and nondescript or, at the other extreme, highly restrictive as regards details and limitations of usage.

There is growing concern that such variations enhance the ability of the plaintiff's bar to make a case that due warning has not been provided, if producers should be held to the strictest test of warning.

Given the current level of tort liability activity, legal actions undertaken for those who believe they have been damaged or hurt inevitably leads to a review of MSDS produced by defendant parties and other MSDS extant. Counsel will attempt to find MSDS which differ, e.g., provide more stringent protective requirements or report more serious consequences than originally described in MSDS of a defendant provider. Such divergent contents could be taken as prima facie evidence that due warning was not provided in the MSDS provided by a defendant. Clearly, the ability to "whip-saw" a defendant will be enhanced by inconsistencies between MSDS dealing with the same material. It should be apparent that these inconsistencies can be very deleterious to the industry; this clearly suggests that the involved industrial sectors and associations should attempt to coordinate and make MSDS consistent within that industry for materials in question.

Common Name	Hydrated Alumina, Bayer	Phone No. 412-553-4001	Date 1985-02-01	Revised 1985-11-01

Hazardous Material (as Defined in 29 CFR 1910.1200)

☐ Flammable ☐ Explosive ☐ Organic Peroxide ☐ Irritant ☐ Ingestion ☐ Other Health Hazard (See Sec. VI)
☐ Combustible ☐ Reactive ☐ Pyrophoric ☐ Sensitizer ☐ Inhalation
☐ Oxidizer ☐ Water Reactive ☐ Compressed Gas ☐ Corrosive ☐ Absorption ■ OSHA or ACGIH Limit

SECTION I. Material Description

Chemical Name & Formula: Hydrated Alumina; $Al_2O_3 \cdot 3H_2O$
Other Designation: Alcoa Hydrated Alumina, C-30 fall, C-230, C-330, C-430, C-433, C-530, H-710-B, PCA-B-SD, C-730, OF-2000.
CAS No.: Hydrated Alumina (14762-49-3)
Manufacturer: Alcoa

SECTION II. Ingredients

	% Typical
Al_2O_3	65.0
*SiO_2	0.02
*Fe_2O_3	0.03
*Na_2O	0.30
Loss on ignition	34.5

*Expressed as oxide equivalent

Occupational Exposure Limits

ACGIH TLVs (1985-86)
Alumina Dust:
Total Fraction - 10 mg/m³ (TWA)
- 20 mg/m³ (STEL)
Respirable Fraction - 5 mg/m³ (TWA)

SECTION III. Physical Data

Physical Form: Crystalline powder
Boiling Temperature: NA
Freeze-Melt Temperature: 3700°F (2035°C)
Vapor Pressure: NA
Evaporation Rate: NA
Specific Gravity: 2.4
Density: See above, right
Water Solubility: Insoluble; soluble in concentrated acids & alkalies
pH: 8.5 (20% solution)
Color: Off-white
Odor: None

DENSITY: (H-710-B, PCA-B-SD)
Loose bulk: 8-22 lb/ft³; Packed bulk: 16-44 lb/ft³
(C-30, C-230, C-330, C-430, C-433)
Loose bulk: 43-90 lb/ft³; Packed bulk: 60-100 lb/ft³

SECTION IV. Fire and Explosion Data

Flashpoint	NA	Auto-ignition Temp.	NA	Flammability Limits in Air	NA	Lower:	Upper:

Product is non-flammable.
Not an explosion hazard.

SECTION V. Reactivity Data

With air: None
With water: None
With heat: When exposed to fire or heat, hydrated alumina loses its water of crystallization, beginning at 392°F (200°C).
With strong oxidizers: None
Non-corrosive.

Section VI. Health Hazard Information (See Section II for exposure limits.)

Low health risk by inhalation. Treat as a nuisance dust as specified by the American Conference of Governmental Industrial Hygienists (ACGIH).

According to AIHA Hygiene Guide:
Toxicity by ingestion: None expected.
Skin & Eyes: Not an irritant.

Section VII. Spill, Leak & Disposal Procedures

Use any cleanup procedures; avoid dusting. Collect in containers or bags. If reuse or recycling is not possible, material may be disposed at a sanitary landfill.

RCRA Hazardous Waste No. Not Federally Regulated

Section VIII. Special Protection Information

Use with adequate ventilation to meet the exposure limits as listed in Section II. Where the exposure limit is or may be exceeded, use NIOSH approved respiratory protection. The selection of the appropriate respirator (dust respirator, etc.) should be based on the actual or potential airborne contaminants and their concentrations present.

Section IX. Special Precautions & Comments

Chemical substance components have been reported to the EPA Office of Toxic Substances in accordance with the requirements of the Toxic Substances Control Act (Title 40 CFR Part 710).

D.O.T. Shipping Name, Hazard Class, I.D. No. (if applicable) Not Regulated

Section X. References

American Industrial Hygiene Assoc. (AIHA) Hygienic Guide Series (Revised June 1978).

Information herein is given in good faith as authoritative and valid; however, no warranty, express or implied, can be made.

Fig. A1

Chemicals Division
Material Safety Data Sheet

ALCOA Aluminum Company of America
1501 Alcoa Building, Pittsburgh, PA 15219

No. 501C

Common Name	Alcoa Activated Alumina, H-51 & H-151	Phone No. 412-553-4001	Date 1985-03-19	Revised 1985-09-09

Hazardous Material (as Defined in 29 CFR 1910.1200)

☐ Flammable ☐ Explosive ☐ Organic Peroxide ☐ Irritant ☐ Ingestion ☐ Other Health Hazard (See Sec. VI)
☐ Combustible ☐ Reactive ☐ Pyrophoric ☐ Sensitizer ☐ Inhalation
☐ Oxidizer ☐ Water Reactive ☐ Compressed Gas ☐ Corrosive ☐ Absorption ■ OSHA or ACGIH Limit

SECTION I. Material Description

Chemical Name & Formula: Alumina Hydrate; $Al_2O_3 \cdot xH_2O$
Other Designation: Activated Alumina H-51, H-151
CAS No. Al_2O_3 (1333-84-2)
Manufacturer: Alcoa

SECTION II. Ingredients

	% Typical
Al_2O_3	88
$Na_2O \cdot Al_2O_3 \cdot 2SiO_2$	4
Fe_2O_3	.03
Loss on ignition (water)	6

Occupational Exposure Limits

ACGIH TLVs (1984)
Alumina Dust:
Total Fraction - 10 mg/m³ (TWA)
- 20 mg/m³ (STEL)
Respirable Fraction - 5 mg/m³ (TWA)

SECTION III. Physical Data

Physical Form: 1/8" and 1/4" balls, crushed granular 8-14, 14-28, 20-80, -325 mesh
Boiling Temperature: NA
Freeze-Melt Temperature: 3700°F (2038°C)
Vapor Pressure: NA
Evaporation Rate: NA
Specific Gravity: 3.2
Density: Loose bulk: 44 - 52 lb/ft³
Water Solubility: Insoluble; soluble in concentrated acids and alkalies
pH: ~10 (20% slurry solution)
Color: Off-white
Odor: None

SECTION IV. Fire and Explosion Data

Flashpoint	NA	Auto-ignition Temp.	NA	Flammability Limits in Air	NA	Lower:	Upper:

Product is non-flammable.
Not an explosion hazard.

SECTION V. Reactivity Data

With water: Generates heat
With air: None
With heat: None
With strong oxidizers: None
Non-corrosive.

F35-14720

Section VI. Health Hazard Information (See Section II for exposure limits.)

The dessicant properties of Alcoa Activated Alumina may cause irritation to the eyes and upper respiratory tract.

Alumina is a low health risk by inhalation. Alumina should be treated as a nuisance dust, as specified by the American Conference of Governmental Industrial Hygienists (ACGIH).

According to AIHA Hygiene Guide, alumina:
Toxicity by ingestion: None expected.
Skin and eyes: Not an irritant.

Section VII. Spill, Leak & Disposal Procedures

Clean up using dry procedures; avoid dusting.
Waste may be considered as inert material, suitable for landfill.

RCRA Hazardous Waste No. Not Federally Regulated

Section VIII. Special Protection Information

Use with adequate ventilation to meet the exposure limits as listed in Section II. Where the exposure limit is or may be exceeded, use NIOSH approved respiratory protection. The selection of the appropriate respirator (dust respirator, etc.) should be based on the actual or potential airborne contaminants and their concentrations present.

Section IX. Special Precautions & Comments

Chemical substance components have been reported to the EPA Office of Toxic Substances in accordance with the requirements of the Toxic Substances Control Act (Title 40 CFR Part 710).

D.O.T. Shipping Name, Hazard Class, I.D. No. (if applicable) Not Regulated

Section X. References

American Industrial Hygiene Association (AIHA) Hygienic Guide Series (Revised June 1978).

F35-14720

Information herein is given in good faith as authoritative and valid; however, no warranty, express or implied, can be made.

Fig. A2

Chemicals Division

Material Safety Data Sheet

ALCOA — Aluminum Company of America, 1501 Alcoa Building, Pittsburgh, PA 15219 — No. 1518

Common Name	Phone No.	Date	Revised
Calcined Alumina	412-553-4001	1981-01-23	1985-10-31

Hazardous Material (as Defined in 29 CFR 1910.1200)

☐ Flammable ☐ Explosive ☐ Organic Peroxide ☐ Irritant — Acute Toxicity: ☐ Ingestion ☐ Other Health Hazard (See Sec. VI)
☐ Combustible ☐ Reactive ☐ Pyrophoric ☐ Sensitizer ☐ Inhalation
☐ Oxidizer ☐ Water Reactive ☐ Compressed Gas ☐ Corrosive ☐ Absorption ■ OSHA or ACGIH Limit

SECTION I. Material Description

Chemical Name & Formula: Aluminum Oxide, Al_2O_3

Other Designation: Alcoa Calcined Aluminas - A1% A-grades, OF-2000, Reale-, ground, unground, and superground special catalytic, mixed phase coarse, mixed phase fines, abrasive grade alumina, and PCT.

CAS No.: Alumina (1344-28-1)

Manufacturer: Alcoa

SECTION II. Ingredients *Expressed as oxide equivalent

	% Typical
Al_2O_3	98.6 - 99.7
*SiO_2	0.01 - 0.12
*Fe_2O_3	0.01 - 0.05
*Na_2O	0.04 - 0.50
Total H_2O	0.3 - 1.0

NOTE: A-5 and A-2-4 - less than 0.14F
A-10 and mixed phase - less than 0.15% B_2O_3
A-1% less than 0.05% B_2O_3

Occupational Exposure Limits

ACGIH TLVs (1985-86)
Alumina Dust:
Total Fraction - 10 mg/m³ (TWA)
- 20 mg/m³ (STEL)
Respirable Fraction - 5 mg/m³ (TWA)

SECTION III. Physical Data

Physical Form: Crystalline powder
Boiling Temperature: NA
Freeze-Melt Temperature: 3727°F (2053°C)
Vapor Pressure: NA
Evaporation Rate: NA
Specific Gravity: 3.6 - 3.9
Density: 48 - 63 lb/ft³ (loose bulk)
Water Solubility: Insoluble; very slightly soluble in acid alkalies; insoluble in organic solvents
pH: Not determined
Color: White
Odor: None

SECTION IV. Fire and Explosion Data

Flashpoint	Auto-ignition Temp.	Flammability Limits in Air	Lower	Upper
NA	NA	NA		

Product is non-flammable.
Not an explosion hazard.

SECTION V. Reactivity Data

With air: None
With water: None
With heat: None
With strong oxidizers: None
Non-corrosive.

F35-13201

Section VI. Health Hazard Information (See Section II for exposure limits.)

Low health risk by inhalation. Treat as a nuisance dust as specified by the American Conference of Governmental Industrial Hygienists (ACGIH).

According to AIHA Hygiene Guide:
Toxicity by Ingestion: None expected.
Skin & Eyes: Not an irritant.

Section VII. Spill, Leak & Disposal Procedures

Use dry cleanup procedures; avoid dusting. Collect in containers or bags. If reuse or recycling is not possible, material may be disposed of at a sanitary landfill.

RCRA Hazardous Waste No. Not Federally Regulated

Section VIII. Special Protection Information

Use with adequate ventilation to meet the exposure limits as listed in Section II. Where the exposure limit is or may be exceeded, use NIOSH approved respiratory protection. The selection of the appropriate respirator (dust respirator, etc.) should be based on the actual or potential airborne contaminants and their concentrations present.

Section IX. Special Precautions & Comments

Chemical substance components have been reported to the EPA Office of Toxic Substances in accordance with the requirements of the Toxic Substances Control Act (Title 40 CFR Part 710).

D.O.T. Shipping Name, Hazard Class, I.D. No. (if applicable) Not Regulated

Section X. References

American Industrial Hygiene Assoc. (AIHA) Hygienic Guide Series (Revised June 1978).

Fig. A3

Chemicals Division

Material Safety Data Sheet

ALCOA — Aluminum Company of America, 1501 Alcoa Building, Pittsburgh, PA 15219 — No. 1548

Common Name	Phone No.	Date	Revised
Tabular Alumina	412-553-4001	1985-01-28	1985-11-01

Hazardous Material (as Defined in 29 CFR 1910.1200)

☐ Flammable ☐ Explosive ☐ Organic Peroxide ☐ Irritant — Acute Toxicity: ☐ Ingestion ☐ Other Health Hazard (See Sec. VI)
☐ Combustible ☐ Reactive ☐ Pyrophoric ☐ Sensitizer ☐ Inhalation
☐ Oxidizer ☐ Water Reactive ☐ Compressed Gas ☐ Corrosive ☐ Absorption ■ OSHA or ACGIH Limit

SECTION I. Material Description

Chemical Name & Formula: Aluminum Oxide; Al_2O_3

Other Designation: Alcoa Tabular Alumina - T-60, T-61, T-64 (all mesh sizes including Tabalox), T-160, T-162, Tabular Alumina Fines (TAF), OF-2000

CAS No.: Alumina (1344-28-1)

Manufacturer: Alcoa

SECTION II. Ingredients

	% Typical
Al_2O_3	99.5+
*SiO_2	0.04-0.06
*Fe_2O_3	0.06
*Na_2O	0.10-0.30
*CaO	0.03

*Expressed as oxide equivalent

Occupational Exposure Limits

ACGIH TLVs (1985-86)
Alumina Dust:
Total Fraction - 10 mg/m³ (TWA)
- 20 mg/m³ (STEL)
Respirable Fraction - 5 mg/m³ (TWA)

SECTION III. Physical Data

Physical Form: Crystalline powder, granules, or balls
Boiling Temperature: NA
Freeze-Melt Temperature: 3727°F (2053°C)
Vapor Pressure: NA
Evaporation Rate: NA
Specific Gravity: 3.9
Density: Loose bulk: 125 - 140 lb/ft³
Water Solubility: Insoluble; very slightly soluble in acids & alkalies; insoluble in organic solvents
pH: Not determined
Color: White
Odor: None

SECTION IV. Fire and Explosion Data

Flashpoint	Auto-ignition Temp:	Flammability Limits in Air	Lower	Upper
NA	NA	NA		

Product is non-flammable.
Not an explosion hazard.
No hazardous products formed when exposed to heat or fire.

SECTION V. Reactivity Data

With air: None
With water: None
With heat: None
With strong oxidizers: None
Non-corrosive.

F35-13202

Section VI. Health Hazard Information (See Section II for exposure limits.)

Low health risk by inhalation. Treat as a nuisance dust as specified by the American Conference of Governmental Industrial Hygienists (ACGIH).

According to AIHA Hygiene Guide:
Toxicity by Ingestion: None expected.
Skin & Eyes: Not an irritant.

Section VII. Spill, Leak & Disposal Procedures

Use dry cleanup procedures; avoid dusting. Collect in containers or bags. If reuse or recycling is not possible, material may be disposed of at a sanitary landfill.

RCRA Hazardous Waste No. Not Federally Regulated

Section VIII. Special Protection Information

Use with adequate ventilation to meet the exposure limits as listed in Section II. Where the exposure limit is or may be exceeded, use NIOSH approved respiratory protection. The selection of the appropriate respirator (dust respirator, etc.) should be based on the actual or potential airborne contaminants and their concentrations present.

Section IX. Special Precautions & Comments

Chemical substance components have been reported to the EPA Office of Toxic Substances in accordance with the requirements of the Toxic Substances Control Act (Title 40 CFR Part 710).

D.O.T. Shipping Name, Hazard Class, I.D. No. (if applicable) Not Regulated

Section X. References

American Industrial Hygiene Assoc. (AIHA) Hygienic Guide Series (Revised June 1978).

Fig. A4

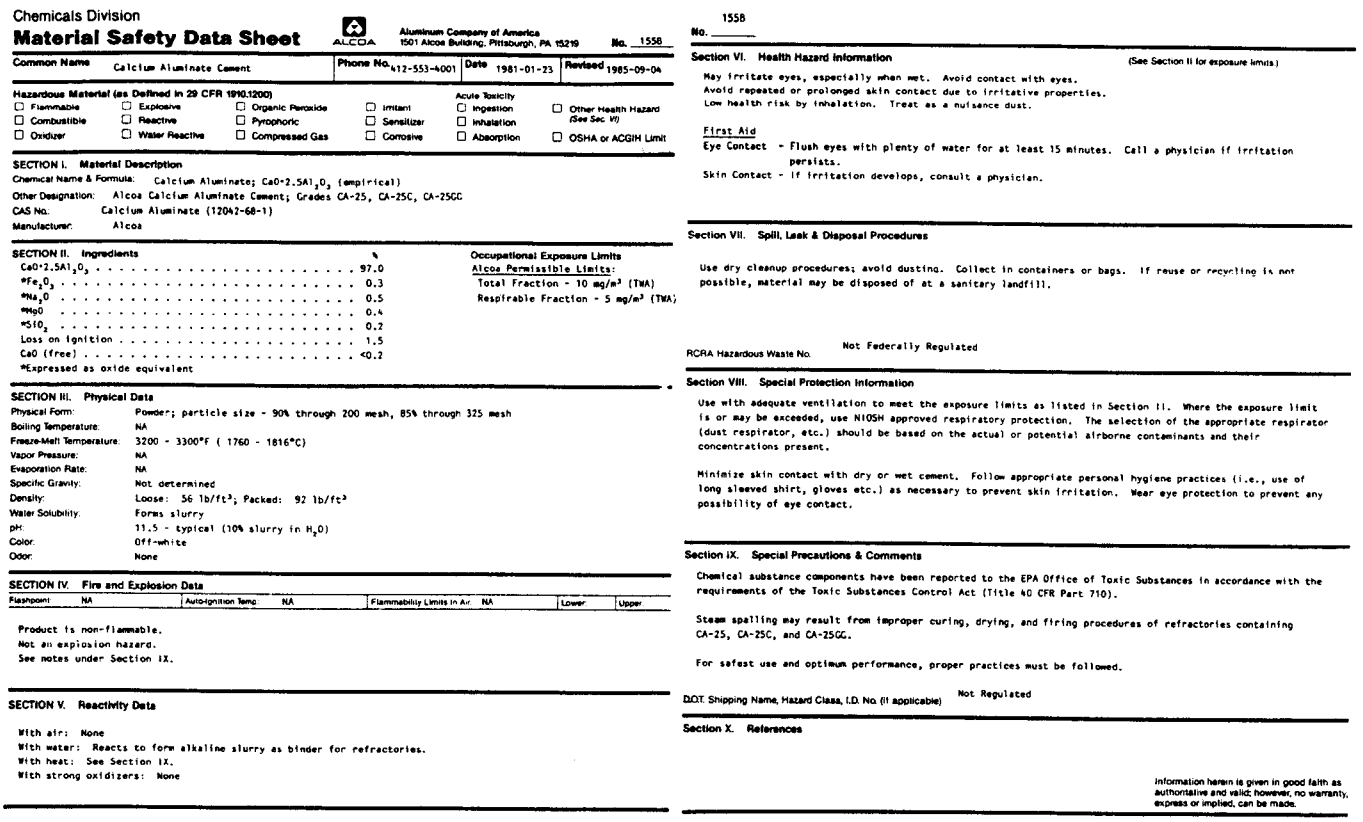

Chemicals Division

Material Safety Data Sheet

ALCOA — Aluminum Company of America, 1501 Alcoa Building, Pittsburgh, PA 15219 — No. 1558

Common Name	Phone No.	Date	Revised
Calcium Aluminate Cement	412-553-4001	1981-01-23	1985-09-04

Hazardous Material (as Defined in 29 CFR 1910.1200)

☐ Flammable ☐ Combustible ☐ Oxidizer ☐ Explosive ☐ Reactive ☐ Water Reactive ☐ Organic Peroxide ☐ Pyrophoric ☐ Compressed Gas ☐ Irritant ☐ Sensitizer ☐ Corrosive

Acute Toxicity: ☐ Ingestion ☐ Inhalation ☐ Absorption

☐ Other Health Hazard (See Sec VI) ☐ OSHA or ACGIH Limit

SECTION I. Material Description

Chemical Name & Formula: Calcium Aluminate; $CaO \cdot 2.5Al_2O_3$ (empirical)

Other Designation: Alcoa Calcium Aluminate Cement; Grades CA-25, CA-25C, CA-25CG

CAS No: Calcium Aluminate (12042-68-1)

Manufacturer: Alcoa

SECTION II. Ingredients

	%
$CaO \cdot 2.5Al_2O_3$	97.0
*Fe_2O_3	0.3
*Na_2O	0.5
*MgO	0.4
*SiO_2	0.2
Loss on ignition	1.5
CaO (free)	<0.2

*Expressed as oxide equivalent

Occupational Exposure Limits

Alcoa Permissible Limits:

Total Fraction - 10 mg/m³ (TWA)

Respirable Fraction - 5 mg/m³ (TWA)

SECTION III. Physical Data

Physical Form:	Powder; particle size - 90% through 200 mesh, 85% through 325 mesh
Boiling Temperature:	NA
Freeze-Melt Temperature:	3200 - 3300°F (1760 - 1816°C)
Vapor Pressure:	NA
Evaporation Rate:	NA
Specific Gravity:	Not determined
Density:	Loose: 56 lb/ft³; Packed: 92 lb/ft³
Water Solubility:	Forms slurry
pH:	11.5 - typical (10% slurry in H_2O)
Color:	Off-white
Odor:	None

SECTION IV. Fire and Explosion Data

Flashpoint	Auto-Ignition Temp.	Flammability Limits in Air	Lower	Upper
NA	NA	NA		

Product is non-flammable.

Not an explosion hazard.

See notes under Section IX.

SECTION V. Reactivity Data

With air: None

With water: Reacts to form alkaline slurry as binder for refractories.

With heat: See Section IX.

With strong oxidizers: None

No. 1558

Section VI. Health Hazard Information (See Section II for exposure limits)

May irritate eyes, especially when wet. Avoid contact with eyes.

Avoid repeated or prolonged skin contact due to irritative properties.

Low health risk by inhalation. Treat as a nuisance dust.

First Aid

Eye Contact - Flush eyes with plenty of water for at least 15 minutes. Call a physician if irritation persists.

Skin Contact - If irritation develops, consult a physician.

Section VII. Spill, Leak & Disposal Procedures

Use dry cleanup procedures; avoid dusting. Collect in containers or bags. If reuse or recycling is not possible, material may be disposed of at a sanitary landfill.

RCRA Hazardous Waste No. Not Federally Regulated

Section VIII. Special Protection Information

Use with adequate ventilation to meet the exposure limits as listed in Section II. Where the exposure limit is or may be exceeded, use NIOSH approved respiratory protection. The selection of the appropriate respirator (dust respirator, etc.) should be based on the actual or potential airborne contaminants and their concentrations present.

Minimize skin contact with dry or wet cement. Follow appropriate personal hygiene practices (i.e., use of long sleeved shirt, gloves etc.) as necessary to prevent skin irritation. Wear eye protection to prevent any possibility of eye contact.

Section IX. Special Precautions & Comments

Chemical substance components have been reported to the EPA Office of Toxic Substances in accordance with the requirements of the Toxic Substances Control Act (Title 40 CFR Part 710).

Steam spalling may result from improper curing, drying, and firing procedures of refractories containing CA-25, CA-25C, and CA-25CG.

For safest use and optimum performance, proper practices must be followed.

D.O.T. Shipping Name, Hazard Class, I.D. No. (if applicable) Not Regulated

Section X. References

Information herein is given in good faith as authoritative and valid; however, no warranty, express or implied, can be made.

Fig. A5

References

[1]M. C. Townsend, P. E. Enterline, N. B. Sussman, et al., *Am. Rev. Resp. Dis.*, **132**, 1174 (1985).

[2]F. Koelsch, E. Lederer, and L. Kaestele, *Arch. Gewerbepathol. Gewerbehyg.*, **5**, 108 (1933).

[3]E. L. Macklin and E. L. Middleton, Report of the Grinding and Cleaning of Castings. Her Majesty's Stationery Office, London, 1923.

[4]A. Meiklejohn, *Br. J. Ind. Med.*, **20**, 255 (1963).

[5]C. L. Sutherland, A. Meiklejohn, and F. N. R. Price, *J. Indust. Hyg. Toxicol.*, **19**, 312 (1937).

[6]J. J. Denny, W. D. Robson, and D. A. Irwin, *Can. Med. Assn. J.*, **37**, 1 (1937).

[7]L. U. Gardner, M. Dworski, and A. B. Delahant, *J. Ind. Hyg. Toxicol.*, **26**, 211 (1944).

[8]A. Meiklejohn and W. W. Jones, *J. Ind. Hyg. Toxicol.*, **30**, 160 (1948).

[9]A. Meiklejohn and E. Posner, *Br. J. Ind. Med.*, **14**, 229 (1957).

[10]E. J. King, C. V. Harrison, G. P. Mohanty, and G. Nagelschmidt, *J. Path. Bact.*, **69**, 81 (1955).

[11]B. D. Stacy, E. J. King, C. V. Harrison, et al., *J. Path. Bact.*, **77**, 417 (1959).

[12]H. C. Stumpf, A. S. Russell, J. W. Newsome, et al., *Ind. Eng. Chem.*, **42**, 1398 (1950).

[13]B. C. Lippens, Ph.D. Thesis. University of Delft, 1961.

[14]L. Abrahams and M. J. D. Lowe, *Ind. Eng. Chem. Product R&D*, **8**, 38 (1969).

[15]W. Klosterkötter, *Arch. Ind. Health*, **21**, 458 (1960).

[16]American Conference of Governmental Industrial Hygienists. Aluminum oxide; p. 21 in Documentation of Threshold Limit Values, 5th ed. American Conference of Governmental Industrial Hygienists, Cincinnati, Ohio; 1986.

[17]H. Knozinger and P. Ratnasamy, *Catal. Rev.–Sci. Eng.*, **17**, 31 (1978).

[18]L. K. Hudson, C. Misra, and K. Wefers; p. 557 in Ullmann's Encyclopedia of Industrial Chemistry, 5th ed. Edited by W. Gerhartz. VCH Verlagsgesellschaft (A1), Weinheim, West Germany; 1985.

[19]A. B. Thompson, *Contrib. Mineral. Petrol.*, **48**, 123 (1974).

[20]M. C. Townsend, N. B. Sussman, P. E. Enterline, W. K. C. Morgan, H. D. Belk, and B. D. Dinman; *Am. Rev. Resp. Dis.*

[21]B. Saia, *Med. Lav.*, **66**, 603 (1975).

[22]H. Weill, J. M. Hughes, Y. Y. Hammad, et al., *Am. Rev. Resp. Dis.*, **128**, 104 (1983).

[23]H. E. Amandus, N. L. Lapp, G. Jacobson, et al., *Br. J. Ind. Med.*, **33**, 13 (1976).

[24]M. Chen-Yeung, R. Wong, L. MacLean, et al., *Am. Rev. Resp. Dis.*, **127**, 465 (1983).

[25]G. S. Gibbs, *J. Occ. Med.*, **27**, 761 (1985).

[26]B. Saia, S. Cortese, G. Piazza, A. Camposampietro, and E. Clonfero, *Med. Lav.*, **72**, 323 (1981).

[27]C. Schlatter, A. Steinegger, U. Rickenbacher, C. Hans, and A. Lengeyl, *Sozial u Praventivmed.*, **31**, 125 (1986).

[28]J. L. Greger, *Food Technol.*, **39**, 73 (1985).

SECTION VI

Long-Range Future Technology The Role *of* Alumina Chemicals

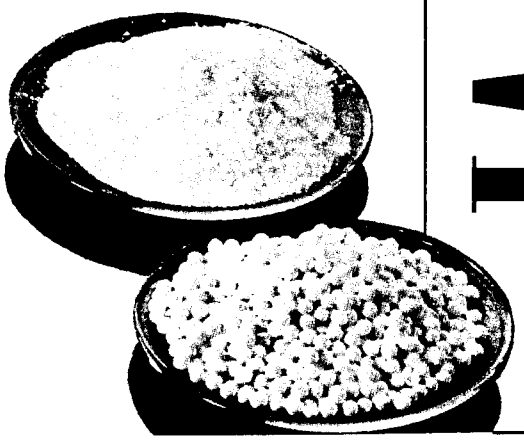

The Future of Alumina Chemicals in Europe

Paul Rothenbuehler and Yvon Lazennec
Alcoa International
Lausanne, Switzerland

L. D. Hart
Litle Rock, AR 72213

The future of the alumina chemicals industry in Europe is examined. New technologies, products, and markets expected in the next decade are discussed. Strategies are outlined for promoting future growth and profitability.

The future of alumina chemicals in Europe, and in other regions of the world, will continue to be highly dependent on the value of the U.S. dollar and on a variety of other economic forces. For many years, production of alumina chemicals in the United States led all other regions of the world. In 1979, production in North America peaked at over 920 000 metric tons compared with 770 000 metric tons in Europe. During the early 1980s, markets for the products declined sharply in the United States because of a severe recession and a strong dollar. These events, coupled with an expansion of the European markets, resulted, in 1982, in North American production falling behind Europe for the first time. In 1987, production in Europe, projected at almost 930 000 metric tons, continues to lead North America, projected at about 590 000 metric tons, by a considerable margin. (Refer to data in chapters comprising Sections I and VI of this book).

European producers of alumina chemicals face a challenging future. Growth of the worldwide alumina chemicals industry has slowed as markets for existing products have matured. Technology advances are needed to establish new products and new markets, but this requires time and substantial investments in research and development programs. Competition will be keen and require improved production efficiencies and cost reductions. Given this kind of business environment and the available resources, the following strategies should be employed to keep the European alumina chemicals industry growing and profitable.

Technical Orientation in Europe

As we approach the year 2000, the trend toward more rigid control over physical and chemical properties for all types of alumina products should be intensified. Producers should work more closely with customers to ensure that exacting specifications for these products are met. Fully implemented statistical process control (SPC) and total quality control (TQC) programs will be required to achieve the degree of control and uniformity of products sought by customers.

Demand for "ready to use," granulated ceramic powders with high thermal reactivity and low shrinkage will increase. Specialty firms will emerge to produce such products. Customers for these products will specify basic materials and their own additives to enhance compaction and sinterability. High-purity alumina powders with fine, monosized crystals are needed for producing high-strength ceramic parts with controlled microstructures for a variety of applications in advanced ceramics.

In the field of refractories, efforts to develop new or improved alumina-based raw materials will be continued in the 1990s and beyond. These products are required to meet the ever-increasing severity of service conditions in the steel and other industries utilizing refractories. The prime objective in these development programs has been and will continue to be reducing refractory costs per unit of production. This will be achieved by developing materials which provide longer and more predictable service life. New refractory aggregate products currently being investigated are: spinel; brown tabular; and a series of three tabular-based products with additions of CaO, SiO2, and ZrO2, respectively. (See chapter on "Tabular Alumina" in Section III of this book.) Performance of these products in the laboratory and later in actual service will require years of testing to determine. Work also should be continued on improving control of aggregate particle size.

Markets

No radical changes in the basic product lines or markets for alumina chemicals are expected in the next decade in Europe. Hydrates; activated, calcined, reactive, and tabular aluminas; and calcium aluminate cement will continue to be the major product classes produced from the Bayer process. No supply problems in the major product lines are anticipated for some years to come.

Major markets for the Bayer products will continue to be refractories, traditional and advanced ceramics, abrasives, glass, catalysts, and desiccants. The refractories industry will continue to be the dominant market segment, consuming well over 50% of alumina chemicals produced in Europe. Little change is expected in the future distribution of the other markets for these products. Growth of the major markets from Bayer process alumina chemicals is not expected to

exceed the growth in GNP for several years. Somewhat higher than GNP growth is anticipated in the production of ultrahigh-purity aluminas from non-Bayer sources for use in advanced ceramics.

The future of advanced ceramics is as promising in Europe as it is in other regions of the world. Structural, electronic, optical, and biomedical ceramic products have the highest probability for success. Ceramic membranes for separation processes, car engine parts, IC substrates, wear-resistant ceramics, cutting tools, catalyst substrates, and human body replacement parts represent potentially large markets for alumina and competitive materials such as carbides, nitrides, and plastics, to name a few. Much research and development work over considerable time is required before proper choices of materials for all the various applications can be made. Final selection of materials will be based primarily on performance and cost of the end-products.

Summary and Conclusions

The European alumina chemicals industry will continue to grow at a moderate rate and remain profitable in the next decade. Competition will be keen and some of the marginal producers may find it necessary to withdraw from the market. Cost-reduction programs will be aggressively pursued by all the remaining producers.

Producers and customers will work together cooperatively to fully implement SPC and TQC programs for controlling the physical and chemical properties of all products. This will ensure that rigid control and uniformity of products sought by customers will be achieved and maintained.

Demand for "ready to use" granulated ceramic powders with high thermal reactivity and low shrinkage will increase. Specialty firms will emerge to produce these products to conform to customer specifications.

New and improved alumina-based refractory aggregates with additions of metal oxides will continue to be investigated. These products are aimed at prolonging service life so that refractory costs per unit of production in a given application are reduced. Increasing severity of service conditions in the steel and other industries requires that these ongoing development programs continuously provide new commercial raw materials.

No radical changes in basic product lines or markets for Bayer alumina chemicals are expected in the next decade in Europe. Growth of markets for Bayer alumina chemicals is not expected to exceed growth of the GNP. Higher than GNP growth is anticipated for ultrahigh-purity aluminas from non-Bayer sources. A number of advanced ceramics products having high probability for success and large market potential could emerge from research and development work on these materials.

Long-Range Future Trends: The Role of Alumina Chemicals—The Japanese Viewpoint

Hiroaki Yanagida
University of Tokyo
Department of Industrial Chemistry
Faculty of Engineering
Tokyo, Japan

Alumina chemicals have been widely used for many years in a broad range of applications. As we approach the year 2000, changes are likely to occur in the production and use of these versatile materials, leading in turn to reorganization of industrial systems and changes in our cultural background. The ceramics industry is one of the most important fields of application for alumina chemicals. Four areas of potential change in alumina ceramics are discussed. It is expected that alumina will continue to play a leading role as a high-technology ceramic material for many years to come.

Alumina chemicals have many uses; one of the most interesting and economically important is its use in ceramics. Alumina has been—and will continue to be—a "champion of ceramics."[1] Most of the ceramic technologies used today originated with alumina. As new materials have been developed, new methods of manufacture and new social attitudes have also developed—from Stone Age man's discovery of the uses of sharpened stone to our present "high-tech" age and all that it implies.

So it is that we have now entered the "information age." This new era started about 25 years ago with the advent of alumina substrates. At about the same time, the precision machining industry began with the birth of alumina cutting tools.

Today, fine ceramics (advanced ceramics) technology is being used to significantly improve the fabrication, properties, and performance of alumina ceramics.[2]

And what about tomorrow? How will alumina be used in the future? Advanced ceramics will continue to support high-technology systems such as computers, communications, information, transportation, energy, precision machining, defense, and biotechnology/life sciences. Advanced ceramics have enabled the development of high-performance materials and novel functions, which has led to the introduction of many technological fields that were unknown a few years ago.

Aluminas for General Use in Ceramics

In the future, aluminas will be widely available in all forms, including powders, single crystals, sintered shapes, porous bodies, thin films, fibers, and as constituents for composite materials. The performance of these products in a broad spectrum of applications will depend greatly on rigid control of their physical and chemical properties.

Powders, in particular, will be in great demand as the starting materials for fabricated shapes. The chemical composition and crystalline structure of these raw materials must be precisely controlled. Powders must be ultrapure and comprised of very fine, monosized, spherical particles. A new technology for handling very fine powders should be developed. New methods for precision handling of alumina-powder slurries must become prime research priorities for manufacturers.

In the future, greater control will be required over the size and shape of prefabricated alumina ceramics specified by the design engineer. New technology should be developed for fabricating products with excellent surface finish and precise size and shape without the need for costly sizing and surface finishing operations after sintering. In porous aluminas, control of pore size and its distribution must be effected. The thickness of films and the diameter of fibers must be precisely controlled during manufacture to meet design specifications.

Alumina As a Key Material for Integrated Circuits

Alumina powders that sinter at as low a temperature as possible are needed for production of prime-quality multilayer substrates for ultralarge-scale integrated circuits. Simple yet precise systems for locating pores and controlling pore size must be developed.

Impurities along grain boundaries must be minimized so that phonon propagation is not disturbed and thermal conductivity is not diminished. These problems do not exist with single crystals. Crystal-growth techniques should be developed for controlling film shape.

Another promising material for manufacture of substrates for integrated circuits is aluminum nitride, which has a high thermal conductivity, making it an excellent material for this application. Until very recently, it was difficult to obtain pure aluminum nitride

powders and sintered shapes. Eliminating oxygen as an impurity affecting phonon scattering has been another difficult problem to overcome. There is now evidence indicating that adding yttria or calcia to aluminum nitride not only acts as a sintering aid but also eliminates oxygen.[3]

Bioceramics Made of Alumina

Biotechnology is now closely related to advanced ceramics technology. Polycrystalline alumina will continue to be used successfully as an artificial bone implant material for body joints and other parts. Tooth implants made of single-crystal alumina will become more common in the future. Immobilized enzyme supports made of porous alumina were proposed in the past and are currently being reinvestigated. A highly controlled pore size is required to capture the specialized enzyme and produce a selective enzyme reaction.

Alumina Ceramics for Mechanical Applications

For many years, alumina has been a leading candidate material for producing ceramics used in mechanical applications. Although nonoxide ceramics such as silicon nitride or silicon carbide have excellent mechanical properties, more expertise is required on design, fabrication, and successful use of these materials for mechanical applications. Furthermore, these materials are still very expensive. Thus, for some time to come alumina ceramics will probably continue to dominate the field of candidate materials for mechanical applications.

Conclusion

Novel materials are the key to new industries and new cultures. As mankind enters the "knowledgeware age," it is clear that alumina will continue to play a prominent role as a high-technology ceramic material with great potential for use in new devices and new engineering systems. Thus, aluminas are—and will remain—at the core of novel technologies.

References

[1]H. Yanagida, Fine Ceramics—Science of Magic Ceramics. Kodansha-Bluebooks, B517. Kodansha Ltd., Tokyo, 1982.

[2]H. Yanagida, "Industrial and Cultural Revolution Through High-Tech Ceramics," *Adv. Ceram. Mater.*, **2** [1] 31–33, 38 (1987).

[3]H. Yanagida and K. Yamayoshi, "Creation of Novel Functions Through Multiphase Reactions," *Kagaku Kogyo*, **40** [10] 820–23 (1986).

The Future Role of Alumina In Ceramics Technology

Michael J. Cima and H. Kent Bowen
Ceramics Processing Research Laboratory
Materials Processing Center
Massachusetts Institute of Technology
Cambridge, MA 02139

Predicting future applications and markets for advanced ceramics is difficult because of the tendency to optimize product specifications and because of imponderables such as the right technology at the right time. Nevertheless, because of the large data and production-experience bases for alumina, alumina alloys, and alumina composites, these materials can give insight into future scenarios. In the past, alumina and alumina-based ceramics were prototypes in the lab and on the production floor for new applications and technical systems. Examples abound, including the alumina-based integrated circuit package, single-crystal ceramic developments (Czochralski, CVD, etc.), and whisker-toughened composites. Perhaps the most speculative prediction for the future is the development of flexible manufacturing systems for alumina-based products. If this technology evolves it will bring with it a critical breakthrough for wide-scale use of ceramics. Such flexible systems could greatly reduce the problems of cost, quality, reliability, and time-to-market that have reduced the broader impact of ceramic materials in commerce.

If ceramics are to fulfill their promise as important technical materials and have a broad economic impact, industry must (1) produce ceramics with physical properties matched to applications and (2) create new processes for fabricating reliable devices to meet these applications. Research over the past several decades has shown that these two endeavors are nowhere more intimately linked within manufacturing than in ceramics processing. It seems that some of the most difficult challenges posed by the structure-property-processing paradigm of materials science and engineering[1] concern the cost-effective fabrication of sound ceramic parts. Ceramics processing is difficult because the requirements for producing the desired microstructure are frequently at odds with the methods required to produce a part with a specific shape and precise macroscopic dimensions. Many applications for which ceramics are being considered require a degree of microscopic homogeneity that rivals that needed in microelectronics, particularly when maximum defect size is compared to the device volume.

Alumina has and will continue to have a major role at the forefront of understanding the unique relationships between structure and properties at one end and applications and processing on the other.[2,3] This is because contemporary processing research can build on an already large alumina knowledge base, so alumina is often used as the prototype for both functional and structural applications.

For example, Coble's work on alumina powders revolutionized the paradigms of processing ceramic powders by establishing that control of densification and grain growth can lead to theoretical densities. This has led to thousands of similar studies on other ceramics. The early work of Verneuil on sapphire growth using flame heating methods and later work at Union Carbide on Czochralski growth techniques led to large-scale production of synthesized single crystals. This work, along with the hydrothermal synthesis of quartz, expanded the horizons for commercial single-crystal ceramics. Furthermore, alumina served as the prime example of CVD single-crystal growth,[4] floating-zone crystal growth,[5] Bridgeman growth to very large diameters,[6] and the revolutionary edge-defined film-fed growth technique for forming shapes developed by Tyco Labs.[7] The recently invented Lanxide process for making ceramic articles starting from molten aluminum is just one further example, as is the alumina matrix-SiC whisker composite.

Alumina as a Ceramic Material

Many features of alumina indicate an increasing role for it in high-performance ceramics. For example, research has shown that many of the physical properties of alumina can be manipulated through the elimination of impurities or the addition of other elements and phases. Furthermore, recently developed chemical synthesis routes have resulted in high purity and particle-size control.

Recent work on the effect of impurities in alumina has shown that silica, which is commonly found in ceramics of mineralogical origin, is detrimental to alumina microstructural control and performance, Indeed, the effect of silica contamination on the sintering behavior and corrosion rate of alumina is well documented.[8,9] McRae et al. and Higgins have found that high-density alumina samples with overall purities greater than 99.7% but different silica contents display significantly different reactivities toward alkali metal vapors. Furthermore, the modulus of rupture decreased 75% when specimens containing 0.25 wt% silica were exposed to potassium vapor at 870°C, while those containing only 0.025 wt% did not change in flexural strength.[8]

Calcium contamination in alumina is also thought to degrade the mechanical properties of alumina.[10] It has been found that an overall calcium content of 5 ppm results in calcium concentrations greater than 1 at.% (as determined by Auger analysis) at the grain boundaries.[11] Segregation of larger cations to the grain boundary is thought to decrease the grain-boundary fracture stress. Cook and Schrott also observed a transition from predominantly intergranular fractures to transgranular fractures when calcium contamination was reduced to very low levels.

While the elimination of specific impurities has been known to improve alumina's performance, the careful addition of dopants can tailor the material for a particular application or improve its mechanical properties. For example, more and more applications are being considered for alumina as its fracture toughness is steadily increased by incorporating fine dispersions of zirconia. Also, magnesium oxide has long been known to control grain growth in Al_2O_3, though the addition of more than is soluble in the alumina matrix degrades the performance of Al_2O_3 cutting tools.[3] Chemical techniques that ensure the homogeneous distribution of small amounts of dopants within ceramic powders have been proposed[12]; thus excess magnesia may no longer be needed to maintain reproducibility. Finally, solution hardening of Al_2O_3 by Cr_2O_3 additions is now regularly practiced in the commercial alumina industry.[13]

High-performance products based on the close control of alumina's chemical composition are only now becoming commercial, but will prove that basic research in physical ceramics over the past 25 years has paid off.

Alumina as a Material for Innovation

Because of the large amounts of physical-property data for alumina, alumina-based ceramics may be the first to be fabricated from a truly flexible manufacturing system, and therefore demonstrate new innovations in ceramic device production. Such a system would allow shape, configuration, composition, and microstructure to be designed into the component to meet end-use needs and would be flexible across many compositions and shapes. The establishment of principles to make the manufacturing process more flexible is a critical step for broadening the industrial use of ceramics.

The identification of ceramics with useful physical properties has been very successful and has resulted in a multitude of materials for which there are potential applications. Unfortunately, the development of large-scale processing techniques for these materials has not kept pace and the necessary fabrication research programs are expensive and specific to each material and application. There have been recent advances in the body of knowledge concerning the microstructural changes that occur during firing, but the scientific base for powder processing, or the operations performed between particle synthesis and firing, is very small.

Advanced ceramic powder-processing techniques are derived in part from applying sophisticated concepts in fields such as colloid chemistry and polymer science to familiar processes such as slip-casting. Such efforts are directed toward improving the applicability and usefulness of new processing techniques or widening the applicability of existing techniques. Alternatively, radical new processes for forming and firing are being developed to circumvent problems such as defects and dimensional control that are common to conventional processing methods.

All of these innovations are based on knowledge of the physical and chemical properties of the ceramic in question. Properties such as the dispersion characteristics of the ceramic starting powder and the stability of the microstructure to contaminants during firing make up the foundation of new process design. Because alumina is by far the most studied of ceramic materials and has been the subject of countless symposia and reviews, it offers the critical knowledge base for processing innovation.

Research has shown that many microstructural features observed in sintered ceramic articles are dictated by the microstructure of the green ceramic, which must be carefully controlled to get the best sintered bodies. Many investigators have proposed that a controlled microstructure can be attained by consolidating and forming while the particles are in a "colloidal state," a technique called colloidal processing.[14,15]

Colloidal processing is most frequently associated with wet-processing ceramics, in which the interactions between particles are controlled by the addition of chemical dispersing agents. Though the technique has received a great deal of attention recently, it can certainly be argued that, used in this sense, it is not a new idea. Surface-charge control through pH adjustment has long been an important tool for processing clay bodies.[16] Much of modern mineral-dressing technology is based on careful understanding of oxide surface chemistry and has provided insights into the processing of commercial ceramic powders.

Alumina was among the first powders to be investigated in the context of dispersion chemistry applied to ceramics-processing technology. Studies in both aqueous and organic media have been important in the development of systems for making tape-cast products or in the classification of submicrometer alumina particles on a large scale.[17] Furthermore, alumina and silica were used in early demonstrations of surface-charge control using colloidal processing.[18] Because of the materials' different isoelectric points at solution pH values between 2 and 9, the particles have opposite charge and therefore associate with each other as they are consolidated.

Recently, a technique was demonstrated for dispersing small amounts of zirconia particles in an

alumina matrix.[19] Rather than depending on differences in surface charge, this method relies on the rapid flocculation of both types of particles from a dispersed state in a solution that contains a small amount of poly(vinyl alcohol) (PVA). The solution is flocculated by adding a nonsolvent for PVA (e.g., acetone). A viscous second liquid phase rich in PVA forms rapidly and drags the particles into it. Processing by this "coacervation" method improved the modulus of rupture and Weibull modulus in alumina-zirconia composites. Presumably this technique provided a more intimate mixture of zirconia within the alumina matrix.

As in the past, alumina will be the prototype for other ceramic materials because it offers the critical knowledge base for processing innovation. Furthermore, by joining the extensive powder-processing science we already have with physical-property and component-design studies and the eventual work expected on manufacturing equipment and systems, the processing revolution can be extended to a manufacturing revolution.

Conclusions

Regardless of whether progress in ceramics is made in the form of single crystals, films or coatings, composites, or polycrystalline bulk materials, alumina is most often the reference material for progress and innovation. It is likely that alumina will be the first material for which advanced processing methods are introduced on a commercial scale. Because of its continuing, unique position in history and its unique inherent properties, including its natural abundance, alumina could become an even more important commercial material in the future.

References

[1]H. K. Bowen, "Ceramics as Engineering Materials: Structure-Property-Processing," *Mater. Res. Soc. Sym. Proc.*, **24**, 1–11 (1984).

[2]W. Gitzen, ed., Alumina as a Ceramic Material. The American Ceramic Society, Columbus, OH, 1970.

[3]E. Dörre and H. Hübner, Alumina: Processing, Properties, Applications. Springer-Verlag, Berlin, 1984.

[4]H. Hobbs and W. D. Kingery, research done 1967–70 at Lexington Laboratories, Cambridge, MA.

[5]J. S. Haggerty, "Production of Fibers by a Floating-Zone Fiber-Drawing Technique," Final Report Contract NAS 3–14328 for the National Aeronautics and Space Administration, NASA Lewis Research Center, Cleveland, OH, May 1972.

[6]F. Schmid and D. J. Viechnicki, "New Approach to High-Temperature Crystal Growth from the Melt," *Solid State Technol.*, **16** [9] 45–48 (1973).

[7]H. E. Labelle Jr., "EFG, the Invention and Application to Sapphire Growth," *J. Cryst. Growth*, **50** [1] 8–17 (1980).

[8]R. C. McRae, L. Reed, J. Toth, and R. Lindberg, "Compatibility of Alumina and Beryllia Ceramics with Potassium Vapor," *Am. Ceram. Soc. Bull.*, **47** [5] 484–88 (1968).

[9]J. K. Higgins, "Reaction of Alumina with Caesium Vapor," *Trans. Br. Ceram. Soc.*, **65**, 643 (1968).

[10]R. S. Jupp, D. F. Stein, and D. W. Smith, "Observations on the Effect of Calcium Segregation on the Fracture Behavior of Polycrystalline Alumina," *J. Mater. Sci.*, **15**, 96–102 (1980).

[11]R. F. Cook and A. G. Schrott, "Calcium Segregation to Grain Boundaries in Alumina," *J. Am. Ceram. Soc.*, **71** [1] 50–58 (1988).

[12]R. R. Landham, M. V. Parish, H. K. Bowen, and P. D. Calvert, "Organotitanate Dispersants for $BaTiO_3$ and Al_2O_3," *J. Mater. Sci.*, **22**, 1677–81 (1987).

[13]B. B. Ghate, W. C. Smith, C. H. Kim, D. P. H. Hasselman, and G. E. Kane, "Effect of Chromia Alloying on Machining Performance of Alumina Ceramic Cutting Tools," *Am. Ceram. Soc. Bull.*, **54** [2] 210–15 (1975).

[14]H. K. Bowen, "Basic Research Needs on High-Temperature Ceramics for Energy Applications," *Mater. Sci. Eng.*, **44**, 1–56 (1980).

[15]F. F. Lange et al., "Processing-Related Fracture Origins: I, II, III," *J. Am. Ceram. Soc.*, **65** [6] 396–408 (1983).

[16]G. W. Brindley, "Ion Exchange in Clay Minerals"; pp. 7–22 in Ceramic Fabrication Processes. Edited by W. D. Kingery. MIT Press, Cambridge, MA, 1958.

[17]P. Nahass, R. L. Pober, and H. K. Bowen, "Semi-Continuous Classification of Ceramic Powders"; unpublished work, 1988.

[18]P. E. Debely, E. A. Barringer, and H. K. Bowen, "Preparation and Sintering Behavior of Fine-Grained Al_2O_3-SiO_2 Composites," *J. Am. Ceram. Soc.*, **68** [3] C-76–C-78 (1985).

[19]W. C. Moffatt, P. Cortesi, P. White, and H. K. Bowen, "Alternative Processing Technologies for Alumina-Zirconia Composites"; in High Tech Ceramics. Edited by P. Vincenzini, Elsevier Amsterdam, 1987.

Long-Range Technology—The Role of Alumina Chemicals as Seen from the Japanese Viewpoint

Soichi Kazama
Showa Aluminum Industries K. K.
Research and Development Department,
Yokohama Works
8 Ebisu-cho, Kanagawa-ku
Yokohama, Kanawagawa, Japan

Having extremely well-balanced physical and chemical characteristics, alumina finds a wide range of applications, from electronics parts to flocculants for water treatment and abrasives for toothpaste, all of which are important in our daily lives. We have no doubt that alumina chemicals will continue to contribute to the development of mankind in the future. In the field of fine ceramics, in particular, alumina is bound to perform a leading role and its application is expected to increase dramatically with the anticipated increase in demand for composite-oxide Sialon, beta alumina for batteries, bioceramics such as dental implants and artificial joints, and alumina-fiber-reinforced metal. Alumina manufacturers will energetically promote their R&D and market development programs with a view to expanding their activities to creation of new materials and downstream businesses taking advantage of their technical expertise, without confining themselves to alumina production.

The production of chemical alumina in Japan increased from 355 000 tonnes in 1975 to 630 000 in 1985. In other words, the average annual growth rate of chemical alumina production here during the 10-year period was 5.9%, which compares favorably to the corresponding growth rate of 3.3% achieved by the free world in general during the corresponding period.[1,2] Japan is expected to have a chemical alumina market of 800 000 tonnes/year minimum in the first 10-year period of the 21st century.

Now, let us review the background of this comparatively high growth of chemical alumina production in Japan.

First of all, the high growth rate is attributable to manufacturers' research efforts to find new applications and their efforts to develop markets for them. Some of the examples[3]:

1. Development of a market for synthetic zeolite as a chemical to absorb and remove Ca^{2+} and Mg^{2+} cations from washing water.
2. Development of chemicals such as polyaluminum chloride (PAC) for purification of city water and treatment of industrial waste water.
3. Development of super-fine, high-purity alumina that is suitable for application to magnetic tapes to impart an appropriate polishing strength.
4. Development of low alpha ray-type alumina.

Of course, the Japanese chemical alumina industry has benefited significantly from the products developed principally in the United States, such as flame retardants, pigments for paper coating, and activated alumina. But what encouraged them to commit their resources to development of applications for water treatment were environment and pollution problems peculiar to the geography of Japan.

On the other hand, the Japanese alumina manufacturers had to retain their chemical businesses to survive after the dramatic decrease in the domestic demand for smelter-grade alumina, caused by the two successive "oil crises." The resultant increase in the cost of energy caused Japanese aluminum smelters to suffer irreparable damage. Power costs in Japan are the highest in the world and likely to remain so for many years. Thus, it has become imperative for Japanese alumina manufacturers to develop a demand for non-smelter-grade alumina in their efforts to find ways for survival.

Also, Japanese alumina manufacturers have been exerting their utmost efforts in changing their mode of production from smelter-grade alumina only to production of a variety of grades, each in a small quantity, of chemical alumina. This has also contributed to expansion of the market.

Such efforts were necessary to meet the extremely severe requirements of their customers in the electroceramics field to stabilize product quality. For example, low-soda alumina for electronics parts, such as IC substrates and packages, is mostly produced using a tunnel kiln. Alumina produced with a rotary kiln plays only a minor role, insofar as the electronics grade is concerned.

Why a tunnel kiln? The process is more complex and the cost is higher than for a rotary kiln. There is, however, a good reason. For the electronics-grade alumina, an extremely severe linear shrinkage tolerance ($\pm 0.15\%$) in sintering is required. Unless such a requirement is met, the customers will not accept the material.

Showa Aluminum Industries has established a technology to meet such a requirement and the prod-

uct thereof is accepted by its customers without any concern on their part. It is expected that the quality requirements of the customers will become more and more severe in the future.

Another factor that cannot be overlooked is the care taken by Japanese alumina manufacturers in rendering technical services to their customers. Close technical contacts with customers often lead to development of new products or improvement of existing products.

The chemical alumina manufacturers' policy of meeting their customers' requirements to the highest possible extent has lead to a situation in which they must provide each of their customers with a unique product having specifications different from the others because each of the customers has different process and product specifications. Thus, in Japan, chemical alumina has come to be produced in more grades than anywhere else. This ensures that customers will receive products meeting their specifications in their required amounts at their required time.

This situation conflicts with the basics of Bayer-process alumina production. The process has been designed essentially for mass production of smelter-grade alumina and is not very suitable for a variety of grades, each in a small quantity. Hence, changes in equipment and processing are constantly being made to satisfy customer needs for specialty products.

Future of Chemical Alumina Technology

Development of Alumina-Related Technology

Japanese alumina manufacturers will undoubtedly continue to compete with one another, aiming at development of specialty aluminas having higher added values. They agree that the most promising market for such specialty aluminas will be structural and functional materials of fine ceramics for the electronics industry.

Let us consider alumina as a material for the IC substrate, in comparison with other materials.[4–7]

In the backdrop of improvements in complexity and functional speed of IC, various new requirements for the quality of IC substrates have emerged, including: (1) higher electrical conductivity, (2) a thermal expansion coefficient close to that of single crystals of silicon or gallium arsenide, (3) outstanding high-frequency property (lower inductivity), and (4) high thermal conductivity. To meet these requirements, studies were made of materials like silicon carbide and aluminum nitrides. In fact, these materials are partly superior to alumina-based materials.

In the case of the SiC-based material, for example, Hitachi, Ltd. has developed a technology for manufacturing an IC substrate by sintering SiC powder containing less than 1% of BeO. Although it substantially satisfies the requirements of (2) and (4) above, the product cannot be considered a complete one because its inductivity is as high as five times that of alumina ceramics and four times that of silicon single crystal.

The thermal conductivity of AlN is about one-half of that of SiC, although it is superior to that of alumina ceramics. AlN has a thermal expansion coefficient slightly higher than that of silicon single crystal and its inductivity is just about the same as that of alumina ceramics. Although its compatibility with metal is not as good as that of alumina ceramics, it is valued as a unique material. Successful development of AlN in the future depends on improvement of its dimensional stability and cost reduction.

Since many companies are vying with each other to develop various materials, it is expected that a number of high-performance materials will be developed and commercialized in the early years of the 2000s. Still, many people agree that few materials match alumina ceramics in cost, physical strength, and compatibility with other materials, such as solder used in assembling IC. For this reason, it is believed that alumina ceramics IC substrates will occupy a major portion of the market, especially in the field of hybrid IC.

Alumina manufacturers must improve product quality to maintain and improve their competitive position with other ceramics materials. For example, the chemical alumina manufacturers must develop a process which enables them to manufacture a voidless alumina ceramic that has few abnormally grown grains and can be sintered at as low a temperature as possible.

Some of the important factors[8] of such a process are: (1) purity control, (2) design of particle size and shape of the ultimate crystal and control of their uniformity, and (3) minimization of chippings in pulverization of the secondary crystals (agglomerated particles).

Already various studies have been made on these factors and, in consequence, a far better quality alumina than those produced several years ago has been placed on market. The alumina manufacturers still face the challenge of manufacturing even better quality products.

It will be necessary for chemical alumina manufacturers to further analyze the impacts of the changes in physical properties of alumina powder on production of alumina ceramics. Data obtained from such analyses should contribute most significantly to development of chemical aluminas having new characteristics and various outstanding ceramic properties.

From the viewpoint of overcoming the defects of alumina, composites of materials would be another way to go. A combination of alumina and zirconia is one composite that falls in this category and Sialon is another.

For development of alumina which is most suitable for ceramics, chemical alumina manufacturers should first determine the ideal characteristics of the material and then try to realize such characteristics

through improvement of the manufacturing process. Any chemical alumina manufacturer who is confined to the limitations of the existing Bayer process is not likely to achieve anything significant.

Bayer Process

A reference was made in the previous section to limitations of the Bayer process. We should not, however, forget some unique features of the Bayer-process components.

The precipitation (crystallization) unit, for example, is based on a unique philosophy of precipitating solids from a supersaturated solution. It would be easier for engineers of an alumina plant than anybody else to conceive the idea of using such a philosophy for formation of submicrometer particles, purification by means of recrystallization, and preparation of various sols and gels. Alumina plant engineers should take full advantage of their knowledge and experience in crystallization to new products.

The same thing applies to the separation/filtration unit. Showa Aluminum Industries already have proven technology for separation of particles up to 100 μm from submicrometer particles. It also has highly sophisticated know-how for drying, blending, and conveying such powder in different ways, depending on its characteristics.

Thus, the technical expertise of chemical alumina manufacturers should be of great help to them in exploring ideas for new products and shortening the time required for commercialization of such products.

Interesting Technology

Alumina Fiber: In the past 10 years, active efforts have been made to develop alumina fibers to effectively utilize the outstanding features of alumina.

Conventionally, alumina fiber meant short ceramic fibers of low alumina content. It was principally used as a furnace lining material but, as the service temperatures of the lining material became higher and technology for composites progressed, strong interest arose for high alumina content fibers.[9,10]

At present, commercially available alumina fiber is mostly short fiber, which is comparatively cheap. Research and market development are under way for continuous fiber and whiskers.

Alumina fiber is broken down into two categories by crystal phases, namely, α-Al_2O_3 and δ- or γ-Al_2O_3. Alumina fiber of α-Al_2O_3 is characterized by high thermal stability and high Young's modulus. Fiber of δ- and γ-Al_2O_3, on the other hand, has extremely fine crystal particles and a glasslike appearance. It also has a high tensile strength.

Characteristics of alumina fiber are as follows:

1. Stability under high temperature: Alumina fiber has an outstanding ratio of physical strength retention under an oxidation atmosphere. Figure 1 is a comparison of E. I du Pont de Nemour's "Fiber-FP", alpha alumina fiber, and other fibers.[11]

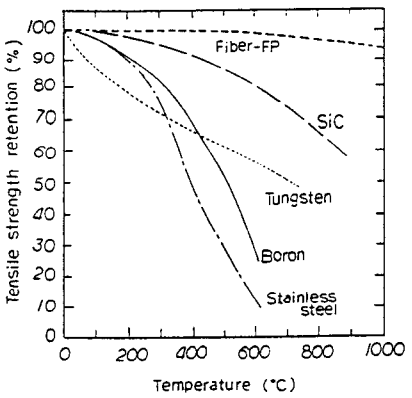

Fig. 1. Relation between fiber strength retention and temperature.

2. It is high in modulus. This characteristic is especially conspicuous in the above mentioned Fiber-FP.

3. Continuous fiber-reinforced metal has an extremely high compressive strength.

Alumina fiber meets requirements for applications such as furnace material,[12] FRP, FRM, and FRC. In this paper, the author will limit his discussions to FRM.

Various FRMs have been trial-manufactured using various fibers, such as boron, silicon carbide, carbon, and alumina. Active efforts are being made by various research organizations for development of FRM as a next-generation material.

Except for some limited examples of its application as advanced composite materials, more development time is needed before FRM will have stable markets. The price of fiber itself is still high and practical methods for fabricating composites have not been fully established.

Now, let us take a brief look at the present situation on development of aluminum-based FRM.

Short fiber: FRM has rarely been commercialized as a low-cost compound material. Toyota has, however, commercially adopted an aluminum matrix composite reinforced with short high-alumina fiber to the topland of its engine piston. This takes advantage of the composite's wear-resistant properties at high temperatures.

Figure 2 shows the results of a wear test[13] (comparative value) versus AC-8A (aluminum alloy). Since car parts must be mass-produced and pistons are used under extremely severe conditions, it must be said that commercial adoption of FRM by Toyota is quite significant.

Continuous fiber: Insofar as FRM is concerned, it is expected that those produced with continuous fiber will find principal applications. They are, however, still in the development stage and only a few have been commercialized. It is, however, reported that Toyota has trial-manufactured connecting rods using FRM produced with du Pont's Fiber-FP and is using

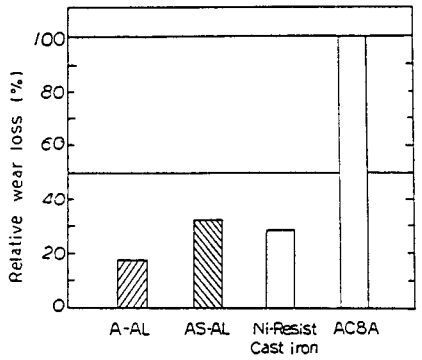

Fig. 2. Total wear loss of piston and piston ring under endurance test on diesel engines. (A-AL alumina short fiber/AL(AC8A); (AS-AL alumina-silica short fiber/AL(AC8A); AC8A aluminum alloy (AA standard A332).

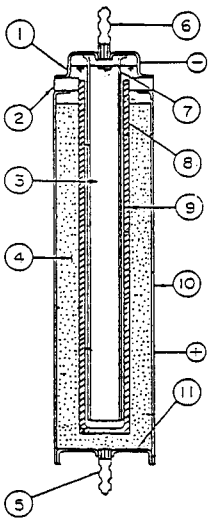

Fig. 3. Schematic of the outer sulfur-type sodium sulfur battery: 1, upper cap; 2, α-alumina insulator; 3, sodium; 4, sulfur/sodium polysulfide + carbon felt mixture (sulfur electrode); 5, inert gas insert tube; 6, sodium insert tube; 7, current collector; 8, solid electrolyte tube (β- or β″-alumina); 9, wisk; 10, metal container; 11, lower cap.

them on a trial basis. Such FRM is claimed to have stability under high temperature,[14] a characteristic of continuous alumina fiber.

Outstanding features of alumina fiber appear most conspicuously in continuous fiber. Further difficulty is expected in commercialization of this material because of the complexity of the fabrication process (sophisticated technology is believed to be required for even distribution of fiber in metal) and high cost.

We expect, however, that cost will be significantly reduced once the problems for mass production are resolved. The technology, therefore, will have far-reaching results on various industrial fields.

Beta Alumina: Of the various types of alumina, beta alumina[15] (Na_2O-Al_2O_3 system) is known as a solid electrolyte having a high ionic conductivity. Because of its unique electrical characteristics, beta alumina is expected to be used in Na/S storage batteries for load leveling in power storage systems and as a secondary battery for electric cars.

The Na/S battery features the use of beta alumina as a solid electrolyte and Na and S as reaction-active materials. It enables a high energy density to be obtained and its energy conversion efficiency is extremely higher (80% minimum) than that of other secondary batteries.

The electrode reaction mechanism for charging and discharging the Na/S battery is considered to be as follows:

$$x\mathrm{Na} + y\mathrm{S} \underset{\text{Charge}}{\overset{\text{Discharge}}{\rightleftharpoons}} \mathrm{Na}x\mathrm{S}y$$

A schematic of the construction of the Na/S battery[16] is shown in Fig. 3.

The characteristics required of the sintered electrolyte tube of beta alumina for the Na/S battery are: (1) high density and no permeability, (2) high mechanical strength (170 to 240 MN/m^2 • min), (3) high ionic conductivity (3 to 15 Ω • cm at 300°C), (4) fine particle size (3 to 5 μm) and even particle-size distribution, and (5) resistance against deterioration.

The fabrication process for beta alumina is largely broken down, as in the case of ceramics-grade alumina, into three stages: calcination, molding, and sintering. An important point in the sintering stage is how to minimize dispersion of Na.

For commercial use of beta alumina in the Na/S battery, it is generally believed that it must give the battery a service life of more than 10 years. It is, therefore, necessary to develop a sintered electrolyte tube which does not deteriorate easily.

Needless to say, the Na/S battery must successfully compete with other power storage systems, such as pumping-up power generation and fuel cells.

For more information on the Na/S battery see the chapter on "Alumina Usage in Electric Power Generation and Storage"; pp. 309–14.

Bioceramics: Alumina is most widely used for production of ceramic dental implants. It can be polycrystalline sintered alumina, which is obtained by sintering alumina powder, or single crystal produced by various means such as the Czochrolaski method. Since artificial dental roots are implanted into the maxilla, sufficient consideration must be given to rejection symptoms and foreign-body response.[17,18] Requirements for artificial dental implants are: (1) nontoxicity, (2) adequate physical properties that do not deteriorate for a long time, and (3) biocompatibility with the organism (it would be better if it could form an integral body with the organism).

Metallic material is not desirable since it corrodes in the human body and releases metallic ions or, by

way of abrasion, metal powder. Polycrystalline sintered alumina is excellent in that it has good affinity for bone and that it is neither toxic nor subject to degradation.

On the other hand, Kyocera has developed single-crystal alumina (or sapphire) for dental implants. This new material has been attracting the attention of concerned persons the world over because it is claimed to have mechanical strength higher than that of polycrystalline alumina, to lend itself to delicate workmanship, and to have good affinity for organisms. Kyocera's single-crystal alumina for dental application will be available in screw and blade types. Thus the appropriate type can be used in each case of implant. Since Japanese people's maxillas are generally smaller than those of Caucasians, dental implants for them must be smaller. Single-crystal alumina having a high physical strength is, therefore, considered most advantageous. Kyocera's product has already been applied to more than 1000 clinical cases on a trial basis.

Sintered tricalcium phosphate has been tested for dental application. Its solubility is, however, reported to be higher than that of other materials and its mechanical strength lower. Also, a study is now under way for the development of sintered hydroxyapatite.[18] It is claimed to have such a good affinity with organisms that, once it is implanted, it is covered by new live bone in a short time.

Artificial joints are proving to be of great help to those who had their joints damaged by traffic accidents or illnesses such as bone tumors. Polycrystalline alumina ceramics have been used successfully for coxal and scapular joints. Generally, alumina ceramics are used for artificial joints and alumina ceramics and sintered hydroxyapatite for dental implants.

Downstream Businesses

It is probable that, in the future, some of the companies specializing in the production and supply of alumina will integrate forward and become ceramics manufacturers. Extremely careful judgments are, however, required to actually implement such a plan.

It is believed that no one can be successful in such a plan unless:

1. He has developed a technology which enables him to manufacture a product which is identical to those already in the market at a price substantially lower than that of his competitors.
2. He has developed a technology which enables him to supply a product, performance of which is far superior to those already on the market, at a price equal to or less than that of his competitors.

Any attempt by an alumina manufacturer to go downstream would be assured of failure if his technical and cost advantage over the existing manufacturers is marginal. In such a case, he would be competing with his customers head on and would lose his alumina business with them.

In this respect, Japanese alumina manufacturers are considered to be in a unique position. In this country, the alumina manufacturing operations were launched about 50 years ago by multiline chemical companies engaged in versatile businesses such as coal chemical, petrochemical, fertilizers, metals, gases, and various chemicals. Each of the Japanese chemical alumina manufacturers has, therefore, access to the proprietary technology of its parent company and its affiliates.

Recently, for example, development of a technology for manufacturing complex shaped ceramic parts by injection molding was studied[19]; this technology had been developed for processing plastics. Such a new technology has been put to partial commercial use.

It would, therefore, be reasonable to consider that an alumina manufacturer like Showa Aluminum Industries, whose parent company is engaged in petrochemical businesses, should have certain advantages. It would be most interesting for such a company to consider possibilities of combining its own technology for alumina calcination and sintering with the technology of its family companies.

Conclusion

In approximately a quarter of a century, the Japanese chemical alumina market had grown to 630 000 tonnes/year (in terms of Al_2O_3) by 1985. This remarkable growth is, of course, mainly attributable to the outstanding features of alumina as a basic material. However, alumina manufacturers' great efforts are also considered to have contributed greatly. In the early stages of the chemical alumina business they established the need for processes to produce many grades, each in a small quantity, to meet customers' requirements promptly. Furthermore, the high quality of their products has always been ensured by their thoroughgoing quality control programs.

Further increase in demand and improvements in quality, together with development of new applications, are expected to expand the alumina market in Japan in the year 2000 to more than 800 000 tonnes per year. Especially promising to alumina manufacturers are the fine ceramics products. Because of its well-balanced characteristics, low price, and easy-to-handle features, alumina is expected to maintain its superiority over competitive materials, such as nonoxides, for fine ceramics. Pursuit of ideal physical properties of alumina suitable for fine ceramics and studies on combining alumina with other materials will become increasingly important.

Alumina manufacturers will develop entirely new materials and launch fabrication businesses, such as production of ceramics, taking advantage of the technology they have accumulated for years. Alumina, indeed, has a promising future.

References

[1]A. Nagai; data presented to "Refractory/Ceramics Technology Seminar" of July 29, 1982, co-sponsored by Chugoku/Shikoku Branch, The Ceramic Society of Japan and the Technical Association of Refractories, Japan.

[2]K. Hayashi (reporter), "Chemical Alumina," *Nikkei Sangyo Shimbun*, June 16, 1986.

[3]M. Kanehara, "New Uses of Alumina," *Light Met.*, **33** [4] 221–29 (1983).

[4]N. Kuramoto, "Translucent AIN Ceramics," FC Report, Vol. 3, No. 12, 14–16, 1985–12, Japan Fine Ceramics Association (JFCA).

[5]K. Kajima and Y. Tajima, "Recent Research and Development of Silicon Carbide," FC Report, Vol. 1, No. 12, 20–26, 1983–12, JFCA.

[6]M. Ura and O. Asai, "Development and Application of Sintered SiC Having High Thermal Conductivity and Electric Insulation Capability," FC Report, Vol. No. 4, 5–13, 1983–4, JFCA.

[7]M. Ura, "Materials for Ceramic Substrate Having High Thermal Conductivity," *Kogyo Zairyo*, **34** [4] 98–106 (1986).

[8]S. Kazama and Y. Oda, "Alumina for Ceramics and Its Latest Developments," *Taikabutsu*, **36** [322] 47–57 (1984).

[9]H. Nagai, "Compound High-Strength Fiber for New Generation Rapidly Development and Commercialization," *Nikkei New Materials*, March 17, 1986; pp. 40–56.

[10]K. Okamura, "Ceramics Fiber as Structural Material," *Ceramics*, **19** [3] 172–81 (1984).

[11]A. K. Dhingra "What Are Fibers Doing in Metal Castings?," *Chemtech.*, **11** [10] 600–608 (1981).

[12]Y. Maruyama and G. Kurihara, "Durability of Alumina Fiber; Its Quality After Two Years of Use in Heating Furnace," *Taikabutsu*, **36** [7] 28–32 (1984).

[13]T. Donomoto, "Ceramic Fiber Alloy for High Performance Diesel Pistons," *Jidosha Gijutsu*, **37** [8] 884–89 (1983).

[14]Shimokawa, Yokoi, Konda, "Materials for Cars and Requirements for Weight Reducing: Present Situation and Trend," *Jidosha Gijutsu*, **33** [8] 645–00 (1979).

[15]"Research on Electrode and Electrolytes for the Ford Sodium-Sulfur Battery," Ford Motor Co., Semiannual Report (June 30–December 31, 1976), Contract No. NSF-C805, January 1977.

[16]H. Kawamoto, "Estimation of the Current Density at a Solid Electrolyte, Tube Surface in a Sodium-Sulfur Battery," *Denki Kagaku*, **53** [2] 98–103 (1985).

[17]H. Aoki, "Medicine, Medical Chemistry," Introduction to Ceramic Materials and Technologies, 1,029-35, Committee for Compilation of Ceramics Material Technology.

[18]A. Makishima and H. Aoki, "Actuals of Organisms Related Ceramics"; pp. 43–70 in Bioceramics, Ceramic Science Series No. 7. Gihodo Shuppan, 1984.

[19]Y. Arakida, "Injection Molding of Fine Ceramics," FC Report, Vol. 4, No. 2, 16–21, 1986–2, JFCA.

Present Situation and Future Technology of Alumina Chemicals in Japan

K. Yamada
Sumitomo Chemical Co., Ltd.
Tsukuba Research Laboratory
Tsukuba-Shi, Japan

The present situation for aluminum hydroxide and alumina is described. Future products and technologies are suggested by the explanation of properties of current alumina chemicals. It is very important to develop economic processes in which the purity, particle size, and particle shape of products can be controlled over a wide range.

In Japan, the demand for alumina for aluminum smelting has been dramatically reduced since the oil shortage of 1974. Japanese alumina manufacturers are trying to expand alumina chemical production by developing or improving aluminum hydroxide (gibbsite) for aluminum salts or plastic fillers and alumina for ceramics. This paper presents the present situation of aluminum hydroxide and alumina products and future products in Japan.

Aluminum Hydroxide

Aluminum hydroxide is used for raw materials for aluminum salts, plastic fillers, glasses, and so on. In these applications, improved properties such as purity, particle size, and particle shape are desired. Points to be improved will be described here. The Bayer process for manufacturing aluminum hydroxide will still be used in the future due to economics. Table I shows the various properties of commercial grade aluminum hydroxides.

Raw Materials for Aluminum Salts

Important properties of aluminum hydroxide used for raw materials for aluminum sulfate, basic aluminum chloride, sodium aluminate, and zeolite are the chemical purity and reactivity with chemicals.

Purity: Generally, the chemical impurity level of commercial aluminum hydroxide is satisfactory. However, some aluminum hydroxides cause coloring problems in resulting salts because of a high organic carbon or iron-impurity level.

These impurity levels depend on the kind of bauxite and digestion conditions. The iron level can be controlled by adjusting digestion conditions or applying adsorption or coprecipitation technology.[1,2]

It is difficult to lower the organic carbon level of aluminum hydroxide. Many technologies have been proposed[3-6] and commercialized for organic carbon removal from Bayer liquor. However, much more economical and efficient technologies should be developed.

Reactivity: Aluminum hydroxides having different primary and secondary crystal sizes are shown in Fig. 1. An ideal aluminum hydroxide for aluminum salts should be highly reactive with raw material chemicals (e.g., HCl, H_2SO_4, NaOH) and easily handled.

Yamada et al.[7] reported that the reaction rate of aluminum hydroxide with HCl was as shown by Eq. (1). The rate constant k increased with a decrease in primary crystal size and was not affected by the secondary crystal size.

$$-dw/dt = k \cdot w^{2/3} \quad (1)$$

where w is weight of $Al(OH)_3$ and t is time.

This result suggests that aluminum hydroxide with a smaller primary crystal size and larger secondary crystal size is preferable.

In commercially available aluminum hydroxide, the minimum primary crystal size is about 3 μm, with the secondary crystal size higher than 50 μm. A technology to produce a primary crystal size of less than 1 μm should be developed by controlling precipitation conditions.

Table I. Properties of Aluminum Hydroxide

Powder	A	B	C	D	E	F
Impurity (%)						
Fe_2O_3	0.02	0.02	0.01	0.01	0.01	0.01
SiO_2	0.01	0.01	<0.01	0.01	0.01	0.01
Na_2O	0.30	0.35	0.20	0.05	0.17	0.15
Mean particle size (μm)	0.5	1.0	8	10	70	85

Commercial names (Sumitomo Chemical Co.); A (C-3005), B (C-301), C (CW-308), D (CL-310), E (C-12S), F (C-12C).

Filler

Aluminum hydroxide is used as a filler for plastics, rubbers, and papers, because of its flame retardance and better appearance. Recently, the demand for synthetic marble and epoxy compounds for IC substrates has been increasing.

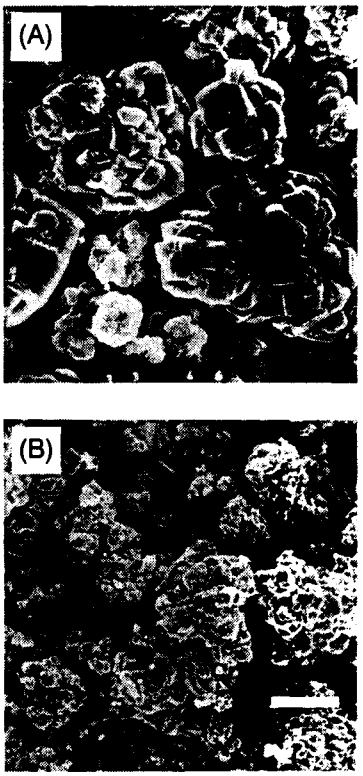

Fig. 1. Scanning electron micrographs of aluminum hydroxides for aluminum salts (*a*) sample F; (*b*) sample E.

Purity: The purity of aluminum hydroxide filler affects the color, electrical resistivity, dehydration temperature, and so on. For synthetic marble, control of whiteness and transparency is required.

Figure 2 shows the effect of organic carbon content on the whiteness of aluminum hydroxide. It is clear that the organic carbon level of aluminum hydroxide for synthetic marble should be very low (<0.01%). Such an aluminum hydroxide can be produced only by an expensive process (e.g., use of a special bauxite in a liquor burning process). A more economical process should be developed.

Na_2O in aluminum hydroxide reduces electrical resistivity. The maximum level of Na_2O for an epoxy compound is 0.1%. High thermal stability of epoxy compounds for electronic parts or polyethylene compounds for cable covers is required. The thermal stability is determined by the dehydration temperature of aluminum hydroxide.

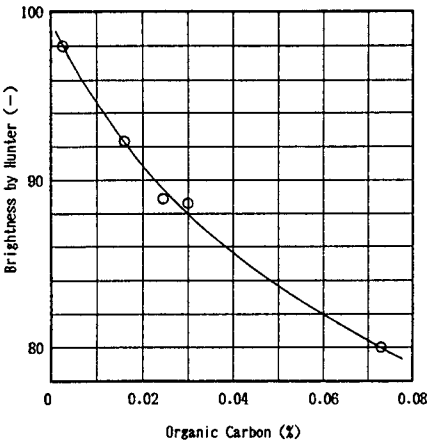

Fig. 2. Effect of organic carbon in aluminum hydroxide on the color of synthetic marble.

The dehydration temperature is affected by the Na_2O content of aluminum hydroxide, that is, 210°C at an Na_2O content of 0.3% and 225°C at an Na_2O content of 0.1%. Methods for raising the dehydration temperature to higher than 250°C are being investigated.

Particle Size and Shape: The mean particle sizes of aluminum hydroxides for fillers are controlled within 1 to 80 μm, as shown in Fig. 3. Recently, 0.5 μm powder for a rubber filler has been developed and used. Finer powders will be developed in the future. As a filler, the particle-size distribution and particle shape are important properties. They affect the rheological properties of the mixture of aluminum hydroxide and plastics. Technologies to produce aluminum hydroxide with a narrow particle-size distribution at any particle size should be developed.

When aluminum hydroxide particles crystallize from sodium aluminate solution, they usually occur as platelets (Fig. 4(*a*)). Sometimes, pillar-type crystals

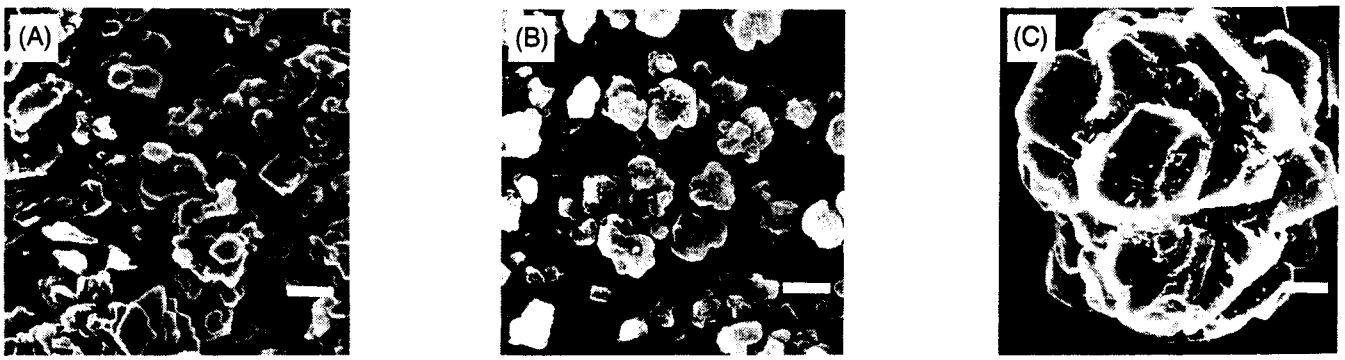

Fig. 3. Scanning electron micrographs of aluminum hydroxides for fillers (bars = (*a*) 0.5 μm; (*b*), (*c*) 10 μm).

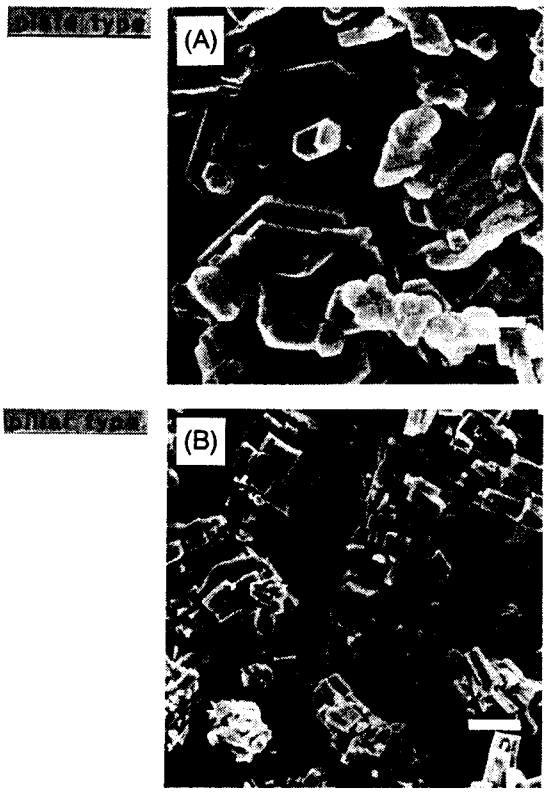

Fig. 4. Shapes of aluminum hydroxides: (*a*) plate type; bar = 0.5μm; (*b*) pillar type; bar = 20μm.

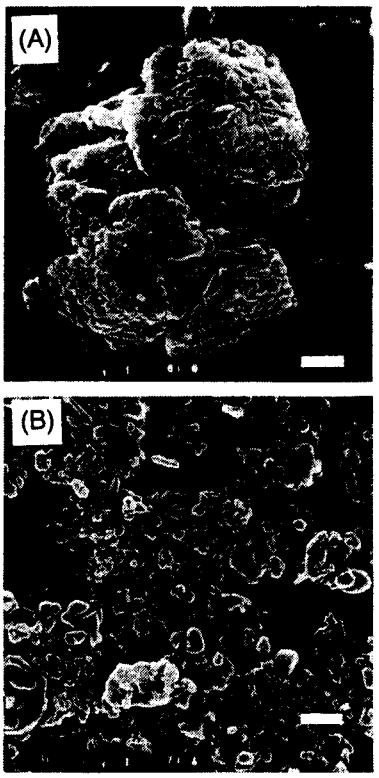

Fig. 5. Scanning electron micrographs of low-soda aluminas (sample G); (*a*) agglomerated; (*b*) deagglomerated. (Bar = 2 μm).

(Fig. 4(*b*)) are required. The crystallization method to control both the crystal shape and particle size is very important, but has not yet been established industrially.

Alumina

Alumina has excellent chemical and physical properties, and is economically produced. Therefore, it is widely used as a ceramic raw material.

Manufacturing Process

The Bayer process is used to produce more than 99% of the available alumina. The alumina purity from that process is usually 99.7%. A purer alumina, such as low-soda or high-purity alumina (≥4*N*) can be produced by controlling precipitation or calcination conditions in the Bayer process. For the production of high-purity alumina, hydrolysis of aluminum alkoxide, thermal decomposition of ammonium alum, and aluminum arc in water processes are being applied industrially.[8,9] The first two processes will be improved to produce better grades of alumina in the future.

Alumina Grade

Aluminas as ceramic grades are commercially available with a purity of 99.6 to 99.999% (5*N*) and an ultimate α crystal size of 0.2 to 5 μm. Tables II and III

Table II. Properties of Low-Soda Alumina

Powder	G	H	I	J	K
Impurity (%)					
Fe_2O_3	0.01	0.01	0.03	0.02	0.01
SiO_2	0.04	0.05	0.03	0.02	0.02
NaO_2	0.04	0.03	0.02	0.03	0.03
Particle size (μm)*	1.7	2.4	4.2	2.9	0.6
Ultimate crystal size (μm)	1–2	2–3	3–5	0.3–4	0.3
Green density (g/cm^3)†	2.29	2.35	2.32	2.60	2.23
Commercial name‡	ALM-41	ALM-43	ACLM-27	AL-31	AES-12

*By Sedigraph.
†At CIP 500 kg/cm$_2$.
‡Sumitomo Chemical Co.

Table III. Properties of High-Purity Alumina

Process	Hydrolysis of Aluminum Alkoxide			Thermal Decomposition of Ammonium Alum	
Powder	L*	M*	N*	O†	P†
Crystal form	α-Al_2O_3	α-Al_2O_3	α-Al_2O_3	α-Al_2O_3	α + transition Al_2O_3
Purity (%)	>99.99	>99.99	>99.99	99.99	99.99
Impurity (ppm)					
Si	<40	<40	<40	40	40
Na	<10	<10	<10	50	50
Mg	<10	<10	<10	5	5
Ca	< 5	< 5	< 5	10	10
Fe	<20	<20	<20	25	25
Ga	< 5	< 5	< 5	15	15
Cr	< 5	< 5	< 5	10	10
Particle size (11 μm)‡	0.58	0.42	0.23	0.52	0.54
S.A., BET (m^2/g)	4–6	5–10	9–15	6	30
G.D (g/cm^3)§	2.30	2.25	1.95	1.87	1.60

*Sumitomo Chemical Co., L (AKP-20), M (AKP-30), N (AKP-50).
†Baikowshi Co., O (CR-6), P (CR-30).
‡By CP-50.
§At CIP 1000 kg/cm^2.

show the properties of low-soda and high-purity aluminas.

The alumina from the Bayer process is composed of agglomerated particles maintaining the shape of aluminum hydroxide, as shown in Fig. 5(*a*). The alumina powder for ceramics is usually used as milled particles to an ultimate crystal size as shown in Fig. 5(*b*).

Powder with a rapid milling rate is preferable. A common low-soda alumina has an ultimate crystal size >1 μm and a reactive grade <1 μm, as shown in Fig. 6. High-purity aluminas are usually submicrometer powders and the particle shape of the alumina produced by the hydrolysis of aluminum alkoxide is uniformly fine.

For future grades, complex powders such as Al_2O_3-ZrO_2 and Al_2O_3-MgO will be developed by a coprecipitation process. Regarding a pure alumina powder, future improvement will be explained below.

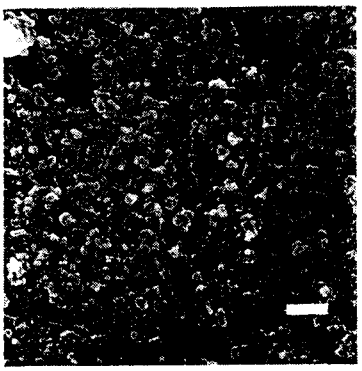

Fig. 6. Scanning electron micrograph of reactive alumina (sample K); bar = 2 μm.

Properties

Purity: The highest purity of commercial alumina is 5*N*. This level is satisfactory for ceramic applications. The aluminum alkoxide process to produce such high-purity powder will be further rationalized.

A low-soda alumina contains 0.3 to 1.0 ppm uranium, which radiates an α ray and causes a soft error[10] in computer memory. Recently, a low-α-radiation alumina (<0.01 $Ci/cm^2 \cdot h$, U< 0.1 ppm) was developed. However, a lower radiation alumina (<0.001 $Ci/cm^2 \cdot h$, U< 0.01 ppm) is required. For the production of such alumina, a special ion-exchange technology will be developed.

Size and Shape of Particle: As a dispersed powder, the 0.2 μm alumina shown in Fig. 7 is commercially available. Transition aluminas are composed of very fine particles (smaller than 100 nm (1000 Å), as shown in Fig. 8. However, these particles agglomerate strongly and are not preferable for ceramic applications. As an ideal powder, a spherical, monosized, fine alumina will be developed, as already reported for SiO_2 and ZrO_2 powders.[11,12]

The 0.3 μm high-purity alumina shown in Fig. 7 is a nearly monosized powder. However, further improvement on the shape and size should be done. Large particles (>1 μm) are of various shapes and sizes, as shown in Fig. 5. We recently developed a spherical powder, as shown in Fig. 9. Such development work will be performed in many laboratories.

Green Density: A green body with a high green density is suitable for the production of a large sintered body with a precise dimension. Usually, an alumina green body has a green density of 50 to 60% of theoretical. When various particle-size powders are

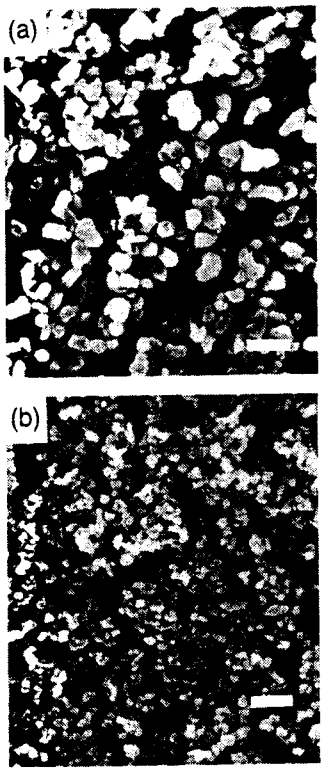

Fig. 7. Scanning electron micrographs of high-purity aluminas (samples L (*a*); N (*b*): bar = 1 μm).

mixed, to obtain the highest packed density, and dispersed well, a high green density (>80% of theoretical) can be obtained. For that purpose, various monosized powders, as explained above, should be developed. The present commercial aluminas give a green density of 73% of theoretical.[13]

Fired Density: When the particle size of alumina decreases, its surface energy relating to the driving force of sintering increases and therefore the sintering rate increases. Figure 10 shows fired densities of

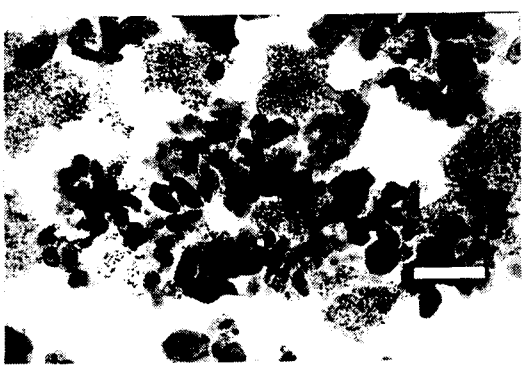

Fig. 8. Transmission electron micrograph of high-purity alumina containing transition phase (sample P). (Bar = 0.5 μm.)

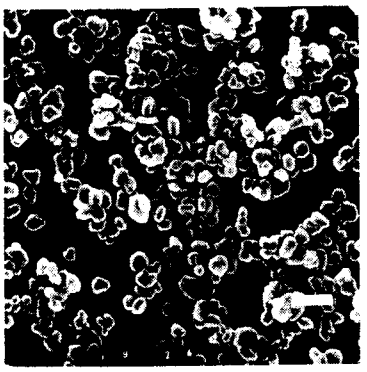

Fig. 9. Scanning electron micrograph of spherical alumina (bar = 2 μm).

various-size aluminas as a function of temperature. At the same temperature, a smaller powder gives a higher fired density.

Various submicrometer aluminas have been developed to achieve high fired density bodies. It is difficult to predict the sintering behavior of these products knowing only the mean particle size. This is because the alumina particles are a mixture of various shapes and sizes and the sintering process is complex.

Hamano et al.[14] reported that high-purity aluminas whose advertised properties were similar showed different sintering behaviors. This difference was caused by differences in particle uniformity in each of the powders. The effect of particle uniformity is shown below.

The spherical uniform low-soda alumina shown in Fig. 9 was compared with the usual low-soda alumina shown in Fig. 5. The particle-size distributions of these aluminas at a mean size of 1 μm are shown in Fig. 11. It is clear from the figure that the particle-size distribution of the newly developed alumina is very narrow. The particle sizes of these aluminas were changed, maintaining the sharpness of the particle-size distribution, and their fired densities were measured.

As shown in Fig. 12, the spherical uniform powder gives a high fired density. The 1 μm powder (2 m^2/g) had a fired density of 3.8 at 1600°C, although the usual

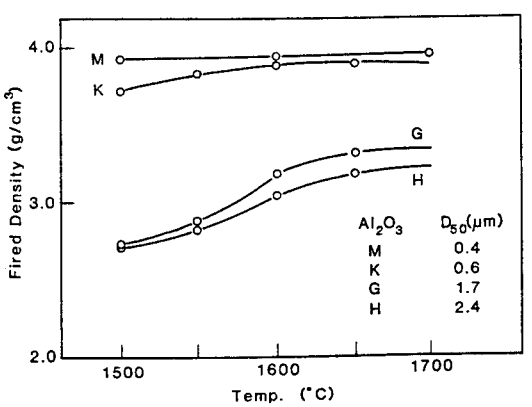

Fig. 10. Effect of particle size on fired density.

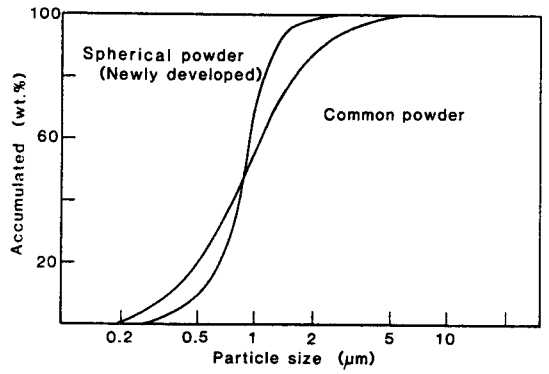

Fig. 11. Particle-size distributions of aluminas.

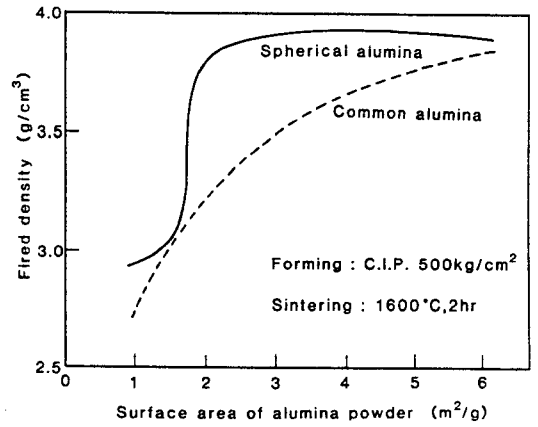

Fig. 12. Fired density vs alumina surface area curves.

powder had only a 3.2 fired density. Economical processes should be developed for the production of such spherical powder.

Kumagai and Messing[15] reported technology for obtaining a microstructure with high fired density by using boehmite sol to which α-Al_2O_3 seed was added. When this technology is combined with a tape-casting or extruding process, it can be used to produce high-performance ceramics economically. This seems to be a very attractive process for the future.

Microstructure of Sintered Body: Alumina sintered bodies are mainly used for electronic materials, machine parts, and optical materials. For these materials the mechanical strength, translucency, and electrical breakdown strength are important properties and are closely related to the microstructure of the sintered body.[16] The mechanical strength of ceramics can be expressed as:

$$\sigma_f = \frac{K_{Ic}}{Y\sqrt{c}} \tag{2}$$

where σ_f is strength, K_{Ic} fracture toughness, Y a geometric constant, and c length of the defect. Generally, the K_{Ic} value is approximately constant for alumina sintered bodies. Therefore the ceramic strength is determined by the defect size.

The defect size is affected by the existence of pores, exaggerated grain growth, other materials, and surface defects. In practice, contamination by other materials and the occurrence of surface defects are often observed with ceramics. However, these phenomena are independent of the properties of the alumina powder.

The remains of pores or exaggerated grain growth are associated with the properties of the alumina powder. When sintering proceeds homogeneously, maintaining a uniform microstructure, the number and size of pores can be decreased and exaggerated grain growth can be avoided. Such a sintering process makes strong, high-electrical-breakdown, translucent ceramics. To produce these ceramics, a high-purity, monosized, fine, spherical alumina is required.

Figure 13 shows the microstructures of sintered bodies produced by different purity and particle-size distribution aluminas. It can be seen that the microstructure becomes more uniform as the alumina powder becomes purer and the particle-size distribution becomes narrower.

Conclusions

The present situation for aluminum hydroxide and alumina was explained and future products and technologies were suggested.

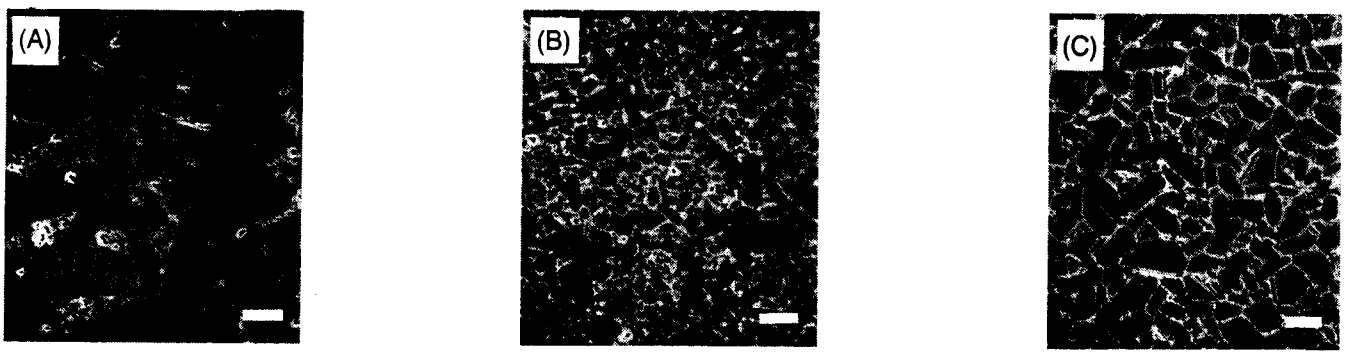

Fig. 13. Microstructures of sintered body (1650°C, 2 h). Al_2O_3 purity (%) (*a*) 99.88; (*b*) 99.93; (*c*) 99.99. Particle size (μm) (*a*) 0.6; (*b*) 0.4; (*c*) 0.2. Sharpness of P.S.D. ($\sqrt{D75/D25}$) (*a*) 1.41; (*b*) 1.40; (*c*) 1.16. Bar = 10 μm.

Important technologies to be developed are: (1) production of high-purity powders, (2) production of dispersed and monosized powders, (3) control of particle size and shape, (4) characterization of powders, and (5) accumulation of application data.

References

[1]K. Yamada et al., "Removal of Iron Compounds from the Bayer Liquor"; Proceedings of the 103rd AIME Annual Meeting, p. 713–23, Dallas, 1974.

[2]ALCOA, U.S. Pat. No. 3 607 140 (1971).

[3]Kaiser Co., U.S. Pat No. 3 120 996 (1964).

[4]J. Deabriges et al., "Purification of Bayer Liquor by Barium Salts"; paper presented at the 106th AIME Annual meeting, New York, 1977.

[5]K. Yamada et al., "Oxidation of Organic Substances in the Bayer process"; paper presented at the 110th AIME Annual Meeting, Chicago, 1971.

[6]Showa Aluminum Industries K.K., U.S. Pat. No. 4 280 987 (1981).

[7]K. Yamada et al., "Reactivities of Aluminum Hydroxide with Acids and Caustic Soda"; paper presented at the 115th AIME Annual Meeting, New Orleans, February, 1986.

[8]K. Yamada, *Ceramics (Jap.)*, **17**, 810–16 (1982).

[9]S. Horikiri, *FC Report*, **3** [7] 9–17 (1985).

[10]S. Okamoto, *Kagaku Kogyo*, **7**, 61–65 (1980).

[11]K. S. Mazdianski, "Powder Synthesis from Metal-Organic Precursors," *Ceramurgia Int.*, **8** [1] 42–56 (1982).

[12]B. Fegley et al., *Am. Ceram. Soc. Bull.*, **64** [8] 1115–19 (1985).

[13]I. A. Aksay; pp. 339–47 in Advances in Materials Characterization, II. Edited by R. L. Snyder et al. Plenum, New York, 1985.

[14]K. Hamano et al., *Yogyo-Kyokai-Shi*, **94**, 70–76 (1985).

[15]M. Kugagai and G. L. Messing, *J. Am. Ceram. Soc.*, **68** [9] 500–505 (1985).

[16]M. Mitomo and Y. Bando, *Kino Zairyo*, **6**, 52–61 (1985).

[17]K. Miyauchi and G. Toda, *Ceramics (Jap.)*, **12**, 13–23 (1977).

[18]M. Yoshimura and H. K. Bowen, *J. Am. Ceram. Soc.*, **64** [7] 404–10 (1981).

A View of the Future for Alumina Chemicals

J. P. Starr
Alcoa Separations Technology Division
Warrendale, PA 15086-7527

Market and technical trends are changing for alumina chemicals as demand matures and customer concentration shifts. Major opportunities lie in specialty-niche markets. Cost control and production efficiencies will be critical to build competitive advantage.

Alumina chemicals are one of the highest volume inorganic chemical products in the world. Buoyed by low production costs offered by the enormous economies of scale of the Bayer process, which also serves as the base of raw-material supply for the production of primary aluminum metal, alumina chemicals have been utilized in a wide variety of markets for over 75 years. Worldwide consumption now totals over 2 000 000 metric tons and represents an annual market of over $500 million dollars.

The reason that this market has developed is based not only on low costs but on the number of variations that the product can take. As the initial product from the Bayer process, aluminum trihydroxide, it is a fairly soft, off-white powder that is used as a mild abrasive in toothpastes, as a raw material in the production of industrial chemicals like aluminum sulfate and sodium aluminate, and as a filler in plastic compounds. Here, the primary advantage of the product is that, although it is a dry powder, it contains almost 35% chemically combined water by weight. This water releases around 200°C, or below the decomposition temperature of most plastics. The endotherm of this release acts to retard the onset of the plastic's burning.

Driving the chemically combined water off the aluminum trihydroxide itself also leads to the rest of the range of products in the family. If the water is only partially removed (through controlled heating at around 400°C), the resultant material has an extremely high surface area. These products, called activated aluminas, are used in desiccants and catalyst applications. Further heating at over 1000°C drives off the remainder of the water and creates white, inert powders that are known as calcined aluminas. These products are used in the refractory and abrasives industries.

Other products in the alumina chemicals line include high-refractory calcium aluminate cement, which is made by combining calcined aluminas and lime at high temperatures, and tabular alumina which is produced by controlled heating of calcined aluminas near the melting point. Both of these products find their main application in the refractory industry, where their chemical resistance and excellent thermal stability offer long life in tough service areas.

The Golden Age

The development of this line of products and the application data to support their penetration of major markets was the result of extensive research and development efforts by the producers. Giulini Chemie (acquired by Alcoa in 1982) and Martinswërke in Germany; Pechiney in France; Showa Aluminum and Sumitomo in Japan; Alcan in Canada; and Kaiser, Reynolds, and Alcoa in the United States all had a role in the development of new products. The unquestioned early leader in product development was Alcoa. Interestingly, an overwhelming percentage of the products that now sell extensively throughout the world were developed at one place—Alcoa's East St. Louis, Illinois, research center.

In East St. Louis, Alcoa assembled an extremely talented group of scientists and engineers beginning in the mid-1920s. From this time until its ultimate closure in the mid-1970s, East St. Louis (ESL) was a hotbed of creative activity. Among the developments that emerged from ESL were the first activated aluminas, the first alumina gels, primary work on catalysis applications, calcium aluminate cements, reactive calcined aluminas, and tabular alumina. Tabular, for example, was first developed as a replacement material for clay bodies in spark plugs for aircraft engines. While tabular represented a very substantial breakthrough in spark plug reliability over clay, it was ultimately replaced by new, more thermally reactive calcined aluminas. Tabular then found a very substantial application niche in refractories, particularly flow-control slide gates for the steel industry and in castable refractories in combination with calcium aluminate cement.

The technology roots of a high percentage of the alumina chemical products and processes in use today can be traced back to work originally performed in East St. Louis. If one also examines the history of alumina chemicals, it is quite easy to see the impact of this golden period of technology in U.S. and world markets. From the initial uses in the early 1910s, the use of alumina chemicals grew slowly until the early 1950s, reaching only about 50 000 MT of demand in the United States. As the impact of Alcoa's new

product developments began to take hold, market growth accelerated, reaching a peak in 1979. Growth rates averaged considerably in excess of GNP throughout this period, primarily fueled by the new applications emerging for hydrates, calcines, cement, and tabular.

A Market Shift

Since 1979, there has been a noticeable shift in a number of the dynamics of the market. First, there has been a dramatic contraction in the North American market. This occurred for several reasons. First was the severe recession in the United States in the early 1980s, accompanied by the rising dollar, which led to large reductions in output in many manufacturing segments of the U.S. economy. Particularly hard hit were the steel and foundry industries, which are the largest single market area for alumina chemicals. At the same time, there was a decided maturation of many of the other major market arenas. Water treatment had become saturated, catalysts were in a downturn, and the large markets for flame retardants in the carpet industry had greatly shrunk as customers had learned how to use cheaper clays as extenders. Also impacting growth rates was the fact that neither Alcoa nor any of the other producers could recapture a creative spark in R&D like that which existed at East St. Louis.

While the U.S. market was contracting, stronger refractory product demand, supported by steel industry modernization programs coupled with additional volume and aided by very competitive exchange rates, kept the European markets expanding. From 1979 through 1985, European suppliers also captured many export markets in Africa, the East Bloc, and South America that had previously been supplied by North American producers. As can be seen in Fig. 1, the result of this evolution was that, in 1982, the European market actually exceeded the North American market for the first time.

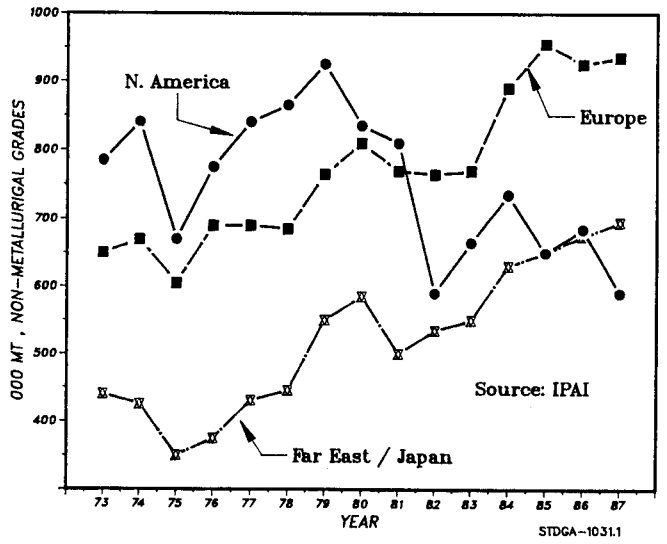

Fig. 1. Alumina chemical production by region.

The Far East markets also continued to grow through this period. A strong steel market in Japan and Korea and expansion in water-treatment markets in several of the developing countries sparked demand. Also helping market growth were the introduction of many new locally produced high end-products like tabular, reactive calcines, ultrafine hydrates, and alumina cements. Previously, these products had been imported from the United States at very high prices and major users had been reluctant to commit to large uses. As was the case in Europe, these dynamics combined to edge the total Far East market past the North American market by 1985.

The Future

As we approach the end of the 1980s, it has become obvious that worldwide growth for alumina chemicals has slowed. In many cases, markets for existing products have become mature. Major suppliers have also significantly scaled back R&D expenditures. While it is expected that demand in some areas (particularly in less developed countries as their standard of living and per capita income rises) will increase, growth is unlikely to exceed GNP in the industrialized countries. The heyday of high growth and sales of high volumes of commodity-type products has quite probably seen its peak.

What then does the future hold for alumina chemicals? What will be the likely strategies for success for suppliers? What changes are anticipated in business approaches?

Production Changes

One interesting fact in the history of alumina chemicals is that specialty chemical products production capability has historically been centered at the older, smaller Bayer refineries. All around the world—at Alcoa's Arkansas Operations, Kaiser's Baton Rouge facility, British Alcan's Burntisland Works, Alusuisse's Martinswërke, VAW's Schwandorf facility, Alcoa's Ludwigshafen Plant, Showa's Yokohama Works, and at Sumitomo, the alumina chemical facilities have typically been supplied from the smaller, older refineries.

For years, these smaller refineries, most of which were 500 000 MT/year capacity or smaller, survived in spite of higher base alumina costs (when compared to the large 1 000 000 MT megacomplexes like those in Australia) by being able to custom-tailor their feedstock supplies for high-quality chemical production. This custom production was necessary because the large refineries could not easily alter their singular focus on smelter-grade alumina (SGA) production.

Today, these dynamics are beginning to change. First, technology has emerged that has improved the basic quality of smelter-grade production. Impurity levels in SGA are being reduced and additions of flash

calcination equipment and improved rotary kilns have improved firing control. This has made it somewhat easier for SGA facilities to generate chemical-quality feedstock. Even more important, however, has been the advent of technology that allows many chemical products to be made from more generic feedstocks. Kaiser Chemicals in Baton Rouge, for example, was the first alumina chemical facility to close its own refining operation and rely totally on externally supplied alumina. Alcoa recently announced that it will supply its Ludwigshafen, West Germany, chemical plant from external sources (a move that was anticipated as early as 1982 when Alcoa first acquired the chemical facilities). Alcoa has also been supplying its tabular and calcium aluminate cement facilities from numerous sources since the late 1960s.

As the future unfolds, it is highly likely that other producers in the United States, Europe, and Japan will take advantage of the lower feedstock costs offered by the economies of scale of the large Bayer refineries. The effort required to accomplish this change is expected to be significant at each of the major producers, however, due to staff dislocations, difficulties with refining waste lake closures, and the need to develop special process technology. Those that accomplish the transition will undoubtedly have an advantage over their competitors and may well rule the economic roost in what may become a highly competitive future.

Also likely to continue to expand in the future is the role of specialty-niche market suppliers. These small, highly focused competitors originally emerged to pursue service segments of the marketplace that the large integrated producers found difficult to handle. The first company in this field, Solem Industries of Atlanta, Georgia, was formed in the mid-1970s to pursue a new market for fine and ultrafine hydrated alumina powders in plastic compounds. Solem developed specialized milling and sizing technology along with an outstanding service network and ultimately captured a large market share from the major producers who did not adapt as easily to the changing demands in the marketplace. Solem has continued to grow and today they are the largest supplier of fire-retardant aluminas in the world. As a result, they are also one of the largest customers for base hydrated alumina.

Another company which has focused on a different market segment is Aluchem of Cincinnati, Ohio. Aluchem has concentrated on supplying ceramic and refractory products and has been successful in carving a second or third supplier position in calcines and tabular in particular.

It is likely that other specialty suppliers may emerge in the United States, Europe, or the Far East, especially as production technology changes to lessen the advantages which had been offered in the past by the dedicated refinery operations.

In addition to the technology advances needed to be able to adapt to feedstock changes, alumina chemical producers will be faced with the need to create new products to open or expand markets. This will be a particularly difficult task, because no longer are large new markets available by the addition of a new or altered phase of the basic alumina product.

The attractive markets that are likely to emerge may require technology which links an alumina product with another material. Opportunities that come to mind here are in the area of hydrated alumina fire retardants, where additives are needed that would improve the processibility of the dry powder hydrate into plastic formulations (silanes have been used to some extent but more dramatic breakthroughs are needed to open the potentially huge market). Also needed are technologies which would elevate the hydrate's decomposition point which is currently too low to allow hydrate to be incorporated effectively into many thermoplastic compounds. The ability to more economically produce uniform micrometer-sized hydrate particles for incorporation into plastic compounds would also help expand markets.

In the large-volume refractory markets, the greatest technology impacts would come from creating products which are more resistant to thermal shock and chemical attack. Here again, the prime technology need to create new demand is not likely to be accomplished through improvements in alumina products alone. Evolution of the refractory system into which the product is incorporated will be critically important.

The same will be true in ceramic markets. Outside of spark plugs, china, and abrasives, ceramic markets do not consume large volumes of alumina products. While the high-technology, fine ceramic markets like electronics and structurals hold much promise for the future, they are unlikely to demand large volumes. They do offer the potential for high profit margins if alumina's properties can be improved to compete with some of the exotic ceramic raw materials like silicon carbide or zirconia.

Market Trends

If a conclusion can be drawn from the earlier comments, it is that the alumina chemicals industry is a large, worldwide business that has substantially matured. While there are numerous new product opportunities that still exist, the current competitive environment is one that, by necessity, focuses on production efficiencies and cost reductions rather than new-product development. Even in some of the most attractive new-product areas there is severe competition and it is likely that only the strong companies or the resourceful entrepreneurs will be able to maintain enough competitive advantage to generate strong profitability. In the last few years, for example, several major producers have dropped out. Alumina Italia curtailed operations in 1982 and Reynolds Metals did the same in 1984. Several independent producers have also been acquired by large concerns, for example, Giulini Chemie by Alcoa and Baco by Alcan in 1982.

One or more Japanese producers are likely to be reduced within the next few years.

This smaller base of competitors will vie for a market that should be steady, if unspectacular. Refractories, which are driven primarily by the steel industry, currently account for over 50% of the total worldwide market demand for alumina chemicals. Worldwide growth in steel consumption is primarily in the newly developing countries and it is expected that alumina chemical demand in these regions will increase as the sophistication of the industries in these countries increases.

A bright spot for the future may be the reemergence of a worldwide focus on end-use performance. In refractories, in particular, tabular alumina and calcium aluminate cement represent products that can improve mill utilization and reliability. In the past, where the prime focus of a steel company refractory purchaser was to purchase the lowest cost material as measured by dollars/ton refractory cost, tabular and other premium alumina products often lost out. With new total quality control (TQC) and statistical process control (SPC) methods being used more frequently throughout the industry, it is highly likely that the premium products like tabular alumina and calcium aluminate cement, which can result in a lower refractory cost per ton of steel produced, will be selected more often.

Hydrated alumina may also find greater application in fire retardants. Here the unique nonsmoking, nonhazardous properties of hydrated alumina may win over other fire-retardant possibilities—especially if the product's performance can be extended as mentioned earlier.

Summary

The 1980s have been the toughest period in the history of alumina chemicals. Markets in the United States have shrunk dramatically and worldwide growth has slowed.

Through these rough times, the industry has proved to be amazingly resilient and adaptable. Producers have moved aggressively to chase opportunities in the newly developing corners of the world, to reduce their production costs, and to explore those new application areas which offer the greatest potential. These tough changes have positioned the best in the industry well. The strong companies now have their cost and quality positions well under control, have developed much more extensive worldwide market coverage, and have focused their development efforts on the most attractive future markets.

This combined position should mean that alumina chemicals will remain a strong, vibrant worldwide product line. More and more, high-technology products in the refractory industry, fire retardants, and ceramics will continue to be identified and linked closely with alumina. Because of this high quality and low cost compared to competitive alternatives, alumina chemicals should remain strong and secure by providing strong value in end-use applications.

Appendix A

Alumina Refinery Production by Country, 1973, 1974 (000 tonnes per year)

Region/Country	1973	1974
Nonmetallurgical Grades		
North America		
Canada	80	100
United States	705	741
Total	785	841
Latin America		
Brazil	20	20
Guyana	0	0
Jamaica	0	0
Suriname	18	15
Venezuela	0	0
Total	38	35
Europe		
France	250	250
Germany (Federal Republic)	304	330
Greece	0	0
Ireland	0	0
Italy	0	0
Norway	0	0
Spain	0	0
Turkey	0	0
United Kingdom	97	95
Yugoslavia	0	0
Total	651	675
Africa		
Guinea	0	0
Asia		
India	0	0
Japan	444	430
Taiwan	0	0
Total	444	430
Oceania		
Australia	0	0
Total Market Economies	1918	1981

Appendix B

Alumina Refinery Production by Country, 1975–1984 (000 tonnes per year)

Region/Country	1975	1976	1977	1978	1979	1980	1981	1982	1983	1984
	Nonmetallurgical Grades									
North America										
Canada	80	50	98	100	125	133	125	125	120	120
United States	590	727	740	763	800	700	689	464	549	617
Total	670	777	838	863	925	833	814	589	669	737
Latin America										
Brazil	40	50	50	50	52	47	52	50	47	80
Guyana	0	0	0	0	0	0	0	0	0	0
Jamaica	0	0	0	0	0	0	0	0	0	0
Suriname	23	16	48	55	60	50	50	26	22	30
Venezuela	0	0	0	0	0	0	0	0	0	0
Total	63	66	98	105	112	97	102	76	69	110
Europe										
France	250	200	220	220	230	240	240	240	275	280
Germany (Federal Republic)	278	398	375	377	448	466	440	439	400	449
Greece	0	0	0	0	0	0	0	0	0	0
Ireland	0	0	0	0	0	0	0	0	0	0
Italy	0	0	0	0	0	0	0	0	0	0
Norway	0	0	0	0	0	0	0	0	0	0
Spain	0	0	0	0	0	0	0	0	0	0
Turkey	0	0	0	0	0	0	0	0	0	0
United Kingdom	83	96	99	94	88	102	90	88	94	106
Yugoslavia	0	0	0	0	0	0	0	0	0	50
Total	611	694	694	691	766	808	770	767	769	885
Africa										
Guinea	0	0	0	0	0	0	0	0	0	0
Asia										
India	0	1	20	1	1	36	13	0	1	2
Japan	355	377	418	444	551	549	488	537	550	628
Taiwan	0	0	0	0	0	0	0	0	0	0
Total	355	378	438	445	552	585	501	537	551	630
Oceania										
Austrailia	0	50	50	50	50	50	50	50	50	50
Total Market Economies	1699	1965	2118	2154	2405	2373	2237	2019	2108	2412

Appendix C

Alumina Refinery Production by Country, 1985-1988 Q1 (Production in 000 tonnes per period)

Region/Country	Annual			1986				1987				1988
	1985 Year	1986 Year	1987 Year	Q1*	Q2	Q3	Q4	Q1	Q2	Q3	Q4	Q1
				Nonmetallurgical Grades								
North America												
Canada	120	120	120	30	30	30	30	25	30	30	30	30
United States	527	562	469	133	170	131	128	115	117	118	118	116
Total	647	682	590	163	200	161	158	140	147	149	149	145
Latin America												
Brazil	106	135	150	30	30	40	35	37	37	38	38	37
Guyana	0	0	0	0	0	0	0	0	0	0	0	0
Jamaica	0	0	0	0	0	0	0	0	0	0	0	0
Suriname	29	29	20	6	8	12	3	2	2	8	8	7
Venezuela	0	0	0	0	0	0	0	0	0	0	0	0
Total	135	164	170	36	38	52	38	39	40	45	45	44
Europe												
France	300	275	300	70	75	60	70	70	75	76	76	74
Germany (Federal Republic)	454	445	471	117	118	99	111	96	126	130	120	120
Greece	0	0	0	0	0	0	0	0	0	0	0	0
Ireland	0	0	0	0	0	0	0	0	0	0	0	0
Italy	30	28	0	7	7	7	7	7	0	0	0	0
Spain	15	16	0	4	4	4	4	4	4	4	4	4
Turkey	0	0	0	0	0	0	0	0	0	0	0	0
United Kingdom	108	108	107	27	27	27	27	26	27	27	27	26
Yugoslavia	50	50	50	13	13	13	13	13	12	12	13	13
Total	957	922	928	238	244	210	232	220	243	249	239	236
Africa												
Guinea	0	0	0	0	0	0	0	0	0	0	0	0
Asia												
India	12	23	32	14	1	6	2	2	10	10	10	10
Japan	637	582	590	147	142	142	151	142	148	150	150	147
Taiwan	0	0	0	0	0	0	0	0	0	0	0	0
Total	649	605	622	161	143	148	153	144	158	160	160	157
Oceania												
Australia	0	66	75	17	20	15	14	17	17	20	20	20
Total Market	2388	2439	2384	615	645	586	595	560	606	623	613	603

*Quarter.

SECTION VII

Glossary

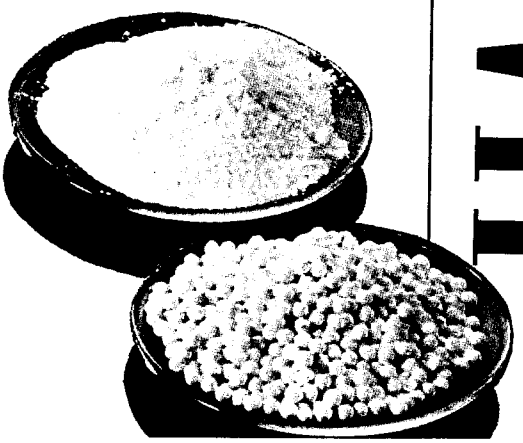

A Glossary of Terms Most Frequently Used in Alumina Technology*

S. C. Carniglia and Burton J. Beadle

This glossary contains nearly 550 terms frequently used in the field of aluminas and their major applications. Insofar as possible, the definitions are given in familiar rather than technical language. Because technical definitions cannot be entirely avoided, extensive use is made of *cross-referencing*: words in **boldface** will be found listed as terms in the glossary and themselves defined so as to make their meaning clear. Thus this addendum should be useful both to lay persons and to professional engineers and scientists not necessarily familiar with all of the areas of technology encompassed by these versatile products.

This is a working glossary, sufficient for most usage and basic understanding, but not represented as an official glossary of any given discipline or technology. It is not to be used for forensic purposes. While the editors have attempted to present accurate information, neither they nor Kaiser Aluminum & Chemical Corporation can assume any liability for the results of use of this information by others.

Table I. Common Units and Conversion Factors

A. Prefixes with Any Unit

pico	= trillionth, 10^{-12}	tera	= trillion, 10^{12}
nano	= billionth, 10^{-9}	giga	= billion, 10^{9}
micro	= millionth, 10^{-6}	mega	= million, 10^{6}
milli	= thousandth, 10^{-3}	kilo	= thousand, 10^{3}
centi	= hundredth, 10^{-2}	hecto	= hundred, 10^{2}
deci	= tenth, 10^{-1}	deka	= ten, 10

B. Mass or Weight

Grams (g)	Kilograms (kg)	Avoir. (oz)	Avoir. (lb)	Tons (short)
1	0.001	0.0353	0.0022	1.1×10^{-6}
1000	1	35.27	2.205	0.0011
28.35	0.0284	1	0.0625	0.00003
453.6	0.4536	16	1	0.0005
0.91×10^{6}	907.2	32 000	2000	1

C. Length

Centimeters (cm)	Meters (m)	Inches (in.)	Feet (ft)	Yards (yd)
1	0.01	0.3937	0.0328	0.0109
100	1	39.37	3.280	1.094
2.540	0.0254	1	0.0833	0.0278
30.48	0.3048	12	1	0.3333
91.44	0.9144	36	3	1

D. Area

cm^2	m^2	in^2	ft^2	yd^2
1	0.0001	0.1550	0.0011	0.0001
10 000	1	1550	10.76	1.196
6.452	0.0006	1	0.0069	0.0008
929.0	0.0929	144	1	0.1111
8361	0.8361	1296	9	1

E. Volume

cm^2, mL	Liters, L	m^3	$in.^3$	ft^3	qt (liq)	gal (U.S.)
1	0.001	10^{-6}	0.0610	0.00004	0.0011	0.0003
1000	1	0.001	61.02	0.0353	1.057	0.2642
10^6	1000	1	61 023	35.31	1057	264.2
16.39	0.0164	0.00002	1	0.0006	0.0173	0.0043
28 317	28.32	0.0283	1728	1	29.92	7.483
946.3	0.9463	0.0009	57.75	0.0334	1	0.25
3785	3.785	0.0038	231.0	0.1337	4	1

F. Stress or Pressure

Pascals (Pa)	g/cm^2	kg/m^2	psi	atm	mm Hg
98.069	1	10	0.0142	0.00097	0.7356
9.807	0.1	1	0.0014	0.00010	0.0736
6 894.7	70.30	703.0	1	0.0680	51.71
101 325	1033	10 332	14.70	1	760.0
133.32	1.3595	13.595	0.0193	0.0013	1
1×10^6	10 197	101 969	145.0	9.869	7 501

G. Density

lb/ft^3 (pcf)	= 62.43 × density in g/cm^3
g/cm^3	= 0.01602 × density in lb/ft^3
lb/gal	= 8.345 × density in g/cm^3 or g/mL
g/cm^3	= 0.1198 × density in lb/gal
Density of water at 4 °C	= 1.000 g/cm^3 or g/mL
Wt. of 1 gal water	= 8.33 lb (at room temperature)
Wt. of 1 gal X	= 8.33 lb × specific gravity of X
Wt. of 1 ft^3 water	= 62.4 lb (at room temperature)
Wt. of 1 ft^3 X	= 62.4 lb × specific gravity of X

H. Temperature

°F	= 9/5 × Temp. in °C + 32
°C	= 5/9 × (Temp. in °F − 32)
°Rankin (absolute)	= Temp. in °F + 459.7
kelvin (absolute)	= Temp. in °C + 273.2

I. Force— 1 newton (N) = 10^5 dynes = 101.969 gf = 0.2248 lbf

J. Energy— 1 joule (J) = 1 watt·sec = 0.2387 cal = 0.000948 Btu

Table II. Tyler and U.S. Standard Sieve Sizes

Tyler Mesh	Opening in	Opening mm	Opening μm	U.S. No.
	0.500	12.70		1/2-in
	0.375	9.52		3/8-in
	0.250	6.35		3
4	0.185	4.76		4
5	0.156	4.00		5
6	0.131	3.36		6
7	0.110	2.83		7
8	0.093	2.38		8
9	0.078	2.00		10
10	0.065	1.68		12
12	0.055	1.41		14
14	0.046	1.19		16
16	0.039	1.00		18
20	0.0328	0.84		20
24	0.0276	0.71		25
28	0.0232	0.59		30
32	0.0195		500	35
35	0.0164		420	40
42	0.0138		350	45
48	0.0116		297	50
60	0.0097		250	60
65	0.0082		210	70
80	0.0069		177	80
100	0.0058		149	100
115	0.0049		125	120
150	0.0041		105	140
170	0.0035		88	170
200	0.0029		74	200
250	0.0024		62	230
270	0.0021		53	270
325	0.0017		44	325
400	0.0015		37	400

Table III. Common Chemical Elements in the Technology of Alumina

Element	Symbol	Atomic Wt.
Aluminum	Al	26.97
Barium	Ba	137.36
Boron	B	10.82
Calcium	Ca	40.08
Carbon	C	12.01
Chlorine	Cl	35.46
Fluorine	F	19.00
Hydrogen	H	1.01
Iron	Fe	55.84
Lithium	Li	6.94
Magnesium	Mg	24.32
Nitrogen	N	14.01
Oxygen	O	16.00
Phosphorus	P	30.98
Potassium	K	39.10
Silicon	Si	28.06
Sodium	Na	23.00
Sulfur	S	32.06
Titanium	Ti	47.90
Zirconium	Zr	91.22

Table IV. Other Elements Less Frequently Encountered*

Element	Symbol
Antimony	Sb
Argon	A,Ar
Arsenic	As
Beryllium	Be
Bismuth	Bi
Bromine	Br
Cadmium	Cd
Cerium	Ce
Chromium	Cr
Cobalt	Co
Copper	Cu
Gallium	Ga
Gold	Au
Hafnium	Hf
Helium	He
Indium	In
Iodine	I
Iridium	Ir
Lanthanum	La
Lead	Pb
Manganese	Mn
Mercury	Hg
Molybdenum	Mo
Neon	Ne
Nickel	Ni
Palladium	Pd
Platinum	Pt
Rhodium	Rh
Selenium	Se
Silver	Ag
Strontium	Sr
Tantalum	Ta
Thorium	Th
Tin	Sn
Tungsten	W
Uranium	U
Vanadium	V
Yttrium	Y
Zinc	Zn

*For atomic weights of these elements, any chemical or chemical engineering handbook or reference volume should be consulted.

Use of the Tables of Chemical Elements, Symbols, and Atomic Weights

One **atom** of an **element** is represented by its **symbol**. A **formula** is used similarly to represent each **substance** (either **compound** or **free element**) by its ultimate chemical particle: either one **molecule**, or (especially in crystals) the simplest convenient **repeat unit**. Thus, "Al" stands either for 1 **atom** of the **element** aluminum, or as the formula for the **repeat unit** (also 1 **atom**) of the **substance** aluminum metal. "O" and "S" stand for 1 **atom** each

of the **elements** oxygen and sulfur; formulas "O_2" and "S_8" stand for 1 **molecule** each of the **substances** oxygen gas and elemental sulfur, and "$Al_2(SO_4)_3$" = "$Al_2S_3O_{12}$" stands for 1 **repeat unit** of the **substance (compound)**, aluminum sulfate. Subscripts in the formula give the number of atoms of each element in the molecule or repeat unit. Sometimes cofficients are used, as: "$3Al_2O_3 \cdot 2SiO_2$ = "$Al_6Si_2O_{13}$" (mullite), or "$Al_2O_3 \cdot 3H_2O$" = $2 \times$ "$Al(OH)_3$" (alumina trihydrate, gibbsite). The ratios of numbers of atoms present in molecules or repeat units are largely determined by nature.

Atoms of each element occur in nature with a fixed average mass or weight (see Table III). The unit in which this is expressed is very small: 1 **atomic wt. unit** = 1.66×10^{-24} **gram**. But atomic weights with chemical formulas make possible the calculation of **weight relationships** in substances, as well as among substances in chemical **reactions**. For example, "$NaAl(OH)_2CO_3$" = "$H_2NaAlCO_5$" (dawsonite) has a **formula weight** of 144.0, comprised of 2.0 awu hydrogen, 23.0 awu sodium, 27.0 awu aluminum, 12.0 awu carbon, and 80.0 awu oxygen. The wt% of each element in dawsonite follows easily. Or, double the formula and rewrite as "$Na_2O \cdot Al_2O_3 \cdot 2H_2O \cdot CO_2$," whose **formula weight** of 288.0 is comprised of 62.0 parts Na_2O, 102.(parts Al_2O_3, 36.0 parts H_2O, and 88.0 parts CO_2. Th equivalent "Al_2O_3" in dawsonite is $102.0 \times 100/288.0$ = 35.42 wt%. Or, combine the relative weights of H_2O anc CO_2 to give the **loss on ignition** (decomposible volatil components): **LOI** = $(36.0 + 88.0) \times 100/288.0 = 43.$ wt%.

Define 1 **gram-atom** as 6.022×10^{23} **atoms**, and 1 **mol** as 6.022×10^{23} **molecules** or **repeat units**. If 1 atom (o molecule, etc.) of some substance weighs X awu = $X \times 1.66 \times 10^{-24}$ grams, then 6.022×10^{23} atom (molecules, etc.) will weigh $6.022 \times 10^{23} \times X$ awu = $X \times 6.002 \times 10^{23} \times 1.66 \times 10^{-24}$ grams = **precisely X grams**. Thus one **gram-atom** weighs in **grams** what one **atom** weighs in **awu**, and one **mole** weighs in **grams** what one **molecule** or **repeat unit** weighs in awu. The chemical **symbol** may then equally represent 1 **gram-atom** of an **element**, and the **formula** may equally represent 1 **mole** of a **substance**. Using the same table of numerical atomic weights, all calculations like those above are performed identically but the amounts are in larger and more familiar units, namely grams. If lbs or tons are wanted, the **lb-atom** and **lb-mole** or **ton-atom** and **ton-mole** are available as well. It's only a matter of scale.

Glossary

Abrasion Wearing down or wearing away of a massive solid by rubbing or friction; often deliberate. See also *Erosion, Attrition.*

Abrasive A granular or particulate solid used with mechanical action to abrade or remove another material, e.g., by grinding, lapping, honing, or polishing. *Grain* or *grit size, hardness, and toughness* are important.

Absorption The taking up of a liquid or gas by *capillary, osmotic,* or solvent action. See also *Sorption, Adsorption, Chemisorption, Physisorption.*

Acid, Acidic A proton (H^+) donor or electron-pair acceptor in *neutralization reactions*; opposite of *bases.* Examples: binary compounds of hydrogen with most nonmetallic elements, and most simple oxides and/or hydroxy compounds of *nonmetals* or *metalloids*; others by analogy. See also *pH.*

Acid Insols The weight percentage of undissolved solids remaining when commercial *alumina trihydrate* is dissolved in hot 1:1 aqueous *sulfuric acid* according to a fixed procedure. In general, a like residue from other acid treatments.

Acid Refractories *Refractories* which are reactive toward (i.e., *corroded* by) *basic melts, slags,* and *fluxes*, and resistant to *acidic* melts, slags, and fluxes. Examples are *silica* and relatively high-silica-containing refractories, including those of *mullite* and *clay-alumina* mixtures.

Acid Site On a solid surface, e.g., a local atomic configuration that is *acidic* in behavior. The density and acid strengths of such sites are important in *chemisorption* and numerous *catalytic reactions.*

Activation A process of developing optimum chemical or surface *reactivity* in a solid material, usually by appropriate heating. See also *Calcination.*

Active Alumina, Activated Alumina Any of several synthetic high-surface-area *transition-alumina* products made by proprietary *activation* processes; available in various convenient forms and modifications. Chi/rho/eta alumina.

Additive A substance distributed in another material in relatively small amounts to improve desirable *properties* or suppress undesirable ones.

Adobe A hand-formed lump of a wet particulate solid (e.g., alumina), made as a stand-in for machine-formed material for testing purposes.

Adsorption The taking up of a liquid or gas or of a dissolved substance, only one to a few *molecular* layers in thickness, on a solid surface; held there by molecular forces. Often subdivided into *chemisorption* and *physisorption.* See also *Absorption, Sorption, Sorbate, Desiccant.*

Agglomerate The clustering together of a few to many fine *particles* or *crystals* into a larger solid mass; also, the resultant assemblage of fine particles or crystals, which may itself be a *particle,* or larger.

Aggregate The hard, dense, coarse granular material such as sand, gravel, *periclase,* or *tabular alumina,* etc. with which a cementing or bonding material is mixed to form a *mortar,* concrete, *brick, block,* or other strong *heterogeneous* mass by setting, *curing,* or *firing.*

Alpha Alumina The highest-temperature, hardest, most chemically stable, and inert *crystalline* form of *alumina,* Al_2O_3; found in nature as "corundum," or made synthetically by intense heating of *alumina hydrates* or other aluminas, usually to temperatures from 900 °C to even above the melting point (2050 °C).

Alum The hydrated double sulfate *salt* of aluminum with a *univalent* metal or *radical*, e.g., sodium, potassium, or ammonium. Also, commonly used to refer to *aluminum sulfate*, $Al_2(SO_4)_3 \cdot xH_2O$; but, correctly, alum is $MAl(SO_4)_2 \cdot 12H_2O$.

Alumina Aluminum oxide, Al_2O_3, in any of its many forms. As a general term, includes the lower-temperature *transition-alumina* forms (containing perceptible hydroxide as well as oxide *anions*) and may even include *alumina hydrates* and a few related *compounds* such as *dawsonite.* See also *Alpha Alumina, Beta Alumina.*

Alumina Hydrates See *Aluminum Hydroxide, Alumina Trihydrate, Gibbsite*; also, *Alumina Monohydrate, Boehmite.* A general term most often used for the trihydrate.

Alumina Monohydrate The oxyhydroxide of aluminum, AlO(OH), also written $Al_2O_3 \cdot H_2O$, in any of several forms. Occurs in nature as a constituent of *bauxite*; also made synthetically by any of several aqueous reactions or by *hydrolysis* of certain aluminum-*organic compounds.* See *Boehmite, Pseudoboehmite, Gel Alumina, Substrate Alumina*; also *Diaspore.*

Alumina Trihydrate The true hydroxide of aluminum, $Al(OH)_3$, also written $Al_2O_3 \cdot 3H_2O$, in any of several crystalline forms. Occurs in nature as a constituent of *bauxite*; also made synthetically by the *Bayer process.* See *Gibbsite, Bayer Hydrate, Bayerite, Nordstrandite.*

Aluminate The negative *ion* (*anion*) or *radical* of aluminum, usually written AlO_2^-, made by dissolving *alumina hydrate* in aqueous *base* or *caustic.* See also *Sodium Aluminate.* Similarly, the anion contained in numerous other *compounds,* e.g., *spinel, clays,* and other minerals.

Aluminum A bluish-silver metallic *element,* used alone or as the major component of many useful alloys; noted for its light weight, good electrical and thermal conductivity, ductility (when pure), high reflectivity, and resistance to air oxidation (due to an adherent, protective, transparent oxide skin—see also *Anodized Aluminum*). Occurs in nature only in chemical combination, as in *bauxite, clays,* etc.; manufactured as metal almost exclusively by the *Hall process*, i.e., *electrolysis* of a molten mixture of *alumina* with fluorides of aluminum, sodium, and other elements.

Aluminum Fluoride AlF_3, a *crystalline* compound used to *flux* (lower the melting point of) *alumina* in the *Hall process* for aluminum manufacture; and, admixed in small quantities with *gibbsite* as a *mineralizer* in mak-

ing certain *calcined* aluminas. See also *Cryolite.*

Aluminum Hydroxide Properly, aluminum trihydroxide or *alumina trihydrates*; loosely, a general term for any of the *alumina hydrates.*

Aluminum Hydroxychloride, Aluminum Chlorhydroxide A precipitated, *gel*-derived mixed *compound* of aluminum, of variable OH and Cl content; used chiefly in pharmaceuticals or personal products. See *Gel Alumina.*

Aluminum Salts A general term for aluminum *compounds* usually made by treating *alumina trihydrate, bauxite,* or *clays,* or aluminum metal, with an *acid.*

Aluminum Sulfate A colorless or white *crystalline salt,* $Al_2(SO_4)_3$, soluble in water, made by treating *bauxite, clay,* or *alumina trihydrate* (for iron-free product) with *sulfuric acid.* The salt crystallizes as the 18-*hydrate*; some of this water is commonly removed by heating.

Amorphous Lacking a detectable *crystallinity*; liquid-like (i.e., disordered) in its structure, though solid in appearance. A loose term, dependent on the tools used and dimensions allowed in identifying the regular ordering of *atoms.* See also *Glassy.* Often, lacking discrete *X-ray diffraction* peaks.

Amphoteric Under different circumstances, capable of acting either as an *acid* or a *base* in *neutralization reactions.*

Anatase A particular *crystalline* form of titanium dioxide, TiO_2, differing from *rutile.* Useful in *ceramic, catalytic,* and pigment applications.

Andalusite An aluminum silicate mineral, Al_2SiO_5, of a particular *crystalline* form. See also *Kyanite, Sillimanite.*

Angle of Repose The angle that a loose pile of rocky, nodular, granular, crystalline, or powdered solid material makes with the horizontal when the sloping upper layer is just at the point of sliding.

Angstrom A unit of length: one-tenth *nanometer* ($1\text{Å} = 0.1\text{ nm} = 10^{-10}$ m). About equal to the diameter of a single *atom* of hydrogen.

Anion A negatively charged *atom* or *radical* (chemically bonded cluster of atoms). Attracted to the *anode* in *electrochemical* systems, hence the name. See *Ion.*

Anisotropic, Anisotropy Of a given *crystal* or *grain*, or of a massive solid object; having different values of one or more properties in different characteristic directions.

Annealing A heat-treating process used to relieve undesirable stresses, e.g., in *glass*; or to adjust the *crystal* size or state of distribution of alloying or minor components of a solid, e.g., in aluminum alloys, also in *ceramics.*

Anode the positive (*electron*-deficient) *electrode* in an *electrochemical* circuit. Attracts negative charges (usually *ions*) from a surrounding medium.

Anodized Aluminum Aluminum or its alloys on which a protective oxidic skin has been developed by special *electrochemical* processes, resulting in exceptional resistance to weathering *corrosion.*

Apparent Density, Apparent Porosity, Apparent Specific Gravity See under each parent term.

Apparent Volume The volume of a quantity of solid material or of a solid object, measured in such manner as to include its *closed porosity* but to exclude its *open* or *connected porosity,* and also excluding the intergranular *packing space* in unconsolidated or bulk materials. See under *Density.*

Atom The ultimate (i.e., smallest) *particle* of which each chemical *element* is composed. Atoms are in turn subdivisible, but in so doing lose their chemical identity. See Tables III and IV.

Attrition The act of wearing or chipping away of a formed, granular, or particulate solid by rubbing and impact, usually between pieces of like material; ordinarily undesirable. See also *Abrasion, Erosion.*

Attrition Loss The weight percentage of *fines* produced when a sample of solid material is subjected to *attrition* in a standardized test. The mode and severity of attrition (by air jet, shaking, etc.) and the size definition of "fines" are ordinarily mated to anticipated use conditions.

Avogadro's Number The number of atomic weight units in 1 g, hence number of *atoms* in a *gram-atom,* etc.: 6.022×10^{23}. See Table III.

Balling The *agglomeration* of particles into large spheroidal masses during high-temperature rotary *calcining,* usually due to melting of a minor constituent or *sintering* of a major one. Also, see *Nodulizing*; *Clinker.*

Ball Mill A cylindrical or conical shell rotating on a near-horizontal axis and charged with balls of a *grinding medium* substantially harder and larger than the material to be ground. Used for fine *grinding* as opposed to *crushing.*

Base, Basic A proton (H^+) acceptor or electron-pair donor in *neutralization reactions*; opposite of *acids.* Examples: the oxides or hydroxides of Li, Na, K, Mg, Ca, Ba, and other strongly *metallic elements*; other compounds of like or similar behavior. See also *pH.*

Basic Refractories *Refractories* which are reactive toward (i.e., *corroded* by) *acidic melts, slags,* and *fluxes,* and resistant to *basic* melts, slags, and fluxes. Examples are compositions high in *magnesia* (*periclase*) and/or *lime,* often in conjunction with lesser amounts of other oxides, and with carbon.

Basic Site On a solid surface, e.g., a local atomic configuration that is *basic* in behavior. The density and strengths of such sites are important in *chemisorption* and some *catalytic reactions.*

Bauxite A mineral or ore containing one or more *alumina hydrates* in conjunction with other oxidic *compounds* of aluminum, silicon, iron, etc. The principal source of synthetic *aluminas, aluminum,* and other derivatives via the *Bayer process.*

Bayer Hydrate *Gibbsite,* a particular *crystalline* form of *alumina trihydrate,* $Al(OH)_3$; the primary product of the *Bayer Process.*

Bayer Process The near-universal commercial process for producing *alumina* (and hence *aluminum*) from *bauxite*. Consists of digestion in hot *caustic* to yield a solution of *sodium aluminate*; separation of undissolved solid wastes ("red mud"); and precipitation of *gibbsite*, $Al(OH)_3$, from the liquor by *seeding* and cooling, followed by filtration and washing.

Bayerite *Alumina trihydrate* of a different *crystalline* form from *gibbsite*; rare. Not related to the *Bayer process.*

Bead A small, usually narrowly sized, spheroidal form of solid material such as a *catalyst, substrate, proppant, desiccant, ion-exchange* medium, etc.

Bed Support A layer (e.g., 3"–6" thick) of *inert* material such as *tabular alumina* spheres, placed on the bottom screen of a tower and underlying a stationary bed of somewhat finer formed *desiccant* or *catalyst*, in industrial processing.

BET (Brunauer-Emmett-Teller) An instrumental method for determining *surface area* of a solid sample, measuring monomolecular nitrogen gas *adsorption* at the temperature of liquid nitrogen (−210 °C). Some other *sorbates* are also used.

Beta Alumina Properly, not an *alumina* but one of a family of alkali metal poly*aluminates*, e.g., $Na_2O{\cdot}11Al_2O_3$. Often a minor impurity in *fused alumina*; also, a synthetic *ceramic* material.

Birefringence Having two different values of the *refractive index* for light of the same wavelength but dependent on orientation of the plane of polarization of the light relative to the medium. Gives double images or, with broad-spectrum light, color effects.

Blind Porosity See *Closed Porosity.*

Boehmite The commonest *crystalline* form of *alumina monohydrate*, AlO(OH). A constituent of *bauxite*; also, an important synthetic: the major component of commercial *gel*-derived *alumina*, also called *substrate alumina*. See also *Gamma Alumina,* a derivative. *Pseudoboehmite* is ultrafine-crystalline.

BOF Basic oxygen furnace, used extensively in steelmaking. A major consumer of *basic refractories.*

Boiling Point ("Normal") The temperature at which a liquid and its *vapor* at 1 atmosphere pressure are at *equilibrium*; hence, approximately, the temperature at which the liquid will boil on application of heat.

Bond An adhesive or cementing or fusible fine *matrix* material that joins *abrasive grains* to a backing or that joins *refractory aggregate* or *cement particles* to one another, imparting strength to the assemblage after *curing* or *firing*. See also *Sinter.* In chemistry, the very high attractive force that holds *atoms* together in a *molecule, crystal,* or *radical.*

Borax One of the several *hydrated* sodium borate *compounds*; formula $Na_2B_4O_7{\cdot}10H_2O$.

Boric Acid Common formula H_3BO_3, derived from sodium borate, related to *boric oxide* by *dehydration.* Used in some *ceramic* and *refractory* manufacture, most often as a chemical *bonding* agent or for *vitrification.*

Boric Oxide Formula B_2O_3, derived from *boric acid* by heating; a component of some important *glass* formulations.

Bound Chemically combined including *chemisorbed*; sometimes also, physically *bound*, as in *physisorption.*

Bound Water See *Water.*

Brain Coral The characteristic surface *morphology* of certain *calcined aluminas* as seen under magnification. So named because of the similarity to a natural marine coral skeleton of this name.

Brick, Block In *refractories*, an individual rectangular or other shaped solid masonry unit of prescribed dimensions, composition, structure, density, etc., for the intended duty.

Brittle Fracturing under load or stress with little if any *plastic* deformation (i.e., permanent change in shape). Characteristic of the majority of *ceramic* materials at temperatures well below incipient melting

Bulk Density See *Density.*

Bulk Specific Gravity See *Specific Gravity.*

Bulk Volume The volume of the container occupied by a quantity of unconsolidated solid material in the form of *particles, grains, agglomerates, nodules*, pellets, etc. Must be given other descriptors, as "loose," "packed," and the manner of packing. See also *Nominal Volume.* As applied to massive *consolidated* materials or objects, the *bulk volume* and the *nominal volume* are the same. See *Density.*

Burn To heat particulate material, *grain, aggregate, refractory bricks,* or *ceramic ware* in a furnace or *kiln*, sufficient to cause desired chemical, structural, or crystalline changes in the material though below the *melting point* of the major component. To *fire,* to *calcine,* or *sinter*; usually, more intense than to dry or to *activate.*

Calcine, Calcination *Firing* or heating a granular or particulate solid at less than *fusion temperature,* but sufficient to remove most of its chemically combined volatile matter (e.g., H_2O, CO_2) and otherwise to develop the desired *properties* for use. Also importantly, the product of such a process, e.g., "calcine" - "calcined alumina," available in numerous modifications for numerous uses. See *Burn;* also *Degree of Calcination.*

Calcium Aluminate Cement A *hydraulic cement* used to form the *bond* in certain *refractories,* notably of high *alumina* composition. The *cured* product is often called a refractory "concrete"; it does not require *firing* prior to installation or service.

Capillary Action The phenomenon of intrusion of a liquid into interconnected small *voids, pores,* and channels in a solid, resulting from *interfacial tension.*

Castable Any of the family of *monolithic refractories* which can be cast in place, deriving interim preservice strength by drying or *curing* of a cementitious *bond.* See *Casting*; also, *Ramming Mix.*

Casting A process of pouring a molten or otherwise *fluid* material or mixture into or on shaped molds, surfaces, or rolls and allowing it to solidify by freezing

(cooling) or by drying or *curing*. See also *Slip Casting*.

Catalyst A chemically active agent which functions to increase the rate of some chemical *reaction* without itself being appreciably consumed or altered. Often such agents are solids (*heterogeneous* catalysts), distributed as very thin layers over the immense surface area of a suitable porous solid *substrate*.

Catalyst Carrier See *Substrate*.

Catalytic Of a chemical *reaction*, being (usefully) increased in rate by presence of a *catalyst*. Of a material or substance, having the property of a catalyst for some given reaction.

Cathode The negative (*electron*-rich) *electrode* in an *electrochemical* circuit. Attracts positive charges (usually *ions*) from a surrounding medium.

Cation A positively charged *atom* or *radical* (chemically bonded cluster of atoms). Attracted to the *cathode* in *electrochemical* systems, hence the name. See *Ion*.

Caustic Usually, caustic soda or sodium hydroxide, NaOH, and most often applied to aqueous solutions thereof. Also refers to the chemically *basic* or alkaline quality of this material.

Caustic Insols, Caustic Sed The volume percentage of undissolved solids remaining when commercial *alumina trihydrate* is dissolved in hot *caustic* solution and *centrifuged* according to a fixed procedure.

Cellulosic Any of a number of fibrous *organic* materials made from the cell walls of plants or woods; materials such as paper or cloth constructed of such fibers; and chemical derivatives or partial degradation products of cellulose retaining the carbohydrate *molecular* structure but not necessarily fibrous form. They have a host of uses related to chemical and *ceramic* technology.

Celsius (also Centigrade, °C) A *temperature* scale on which the *freezing point* of pure water is 0°C and the normal *boiling point* of pure water is 100°C; extended uniformly above and below these points. See also *Fahrenheit, Kelvin*. See Table I.

Centrifuge A circular vessel or array of vessels whirled at high speed; used to separate a more dense material from a lesser, at least one of which is a liquid.

Ceramic, Ceramics Any of a broad class of *inorganic, nonmetallic* materials or products which are subjected to temperatures above about 540°C or 1000°F in either manufacture or use; by incorporation, many others of similar constitution or characteristics which are not necessarily so heated.

Ceramic Fiber A *ceramic* material in fibrous or filamentary form, whether *glassy, polycrystalline,* or single *crystal* in structure; made by, e.g., blowing, spinning, drawing, whisker growth, etc. Useful as *fillers* or reinforcement, as fabrics and insulating felts, in optics, etc.

Cermet A *composite* material or article comprised of a *ceramic* and a *metal,* interdistributed in any of various geometrical forms but intimately bonded together.

Chemical, Chemical Product Any substance, material, or mixture, in whatever form, whose usefulness derives from its chemical *reaction* or interaction with another or, less frequently (e.g., in explosives), within itself.

Chemical Properties Those intrinsic characteristics of any substance, material, mixture, or article made therefrom which relate to its chemical interactions, *reactions,* or changes; either internal, on contact with others, or with components of its environment. Loosely, includes the chemical analysis or composition itself, often with emphasis on *impurity* content.

Chemisorption The taking up of a liquid or gas or of a dissolved substance, only one *molecular* layer in thickness, wherein a new chemical *compound* or *bond* is formed between the sorbent surface atoms and those of the *sorbate*. Reversible with difficulty. See also *Adsorption, Absorption, Sorption, Physisorption*.

China *Vitreous, translucent* white *porcelain ware* for domestic and ornamental use, as distinguished from industrial *whitewares* and other less-fine domestic *ceramic wares*. Usually *glazed,* esp. for decorative purposes.

Chrome Ore An ore comprised principally of $FeCr_2O_4$, used, e.g., in formulating industrial *refractories*. See also *Chromia*.

Chromia, Chromic Oxide Formula Cr_2O_3, a *compound* having many properties and derivatives similar to those of *alpha alumina*, with which it also forms solid *solutions*. Reacts with, e.g., MgO to form a refractory chrome *spinel*.

Clarification The process of slowly settling suspended solid particles to the bottom of a body of relatively quiescent liquid, in a settling tank or "clarifier" usually operated continuously, for the purpose of separation of the *phases*.

Classifier A device used to segregate or separate otherwise-like solid *particles* into two or more groups according to some characteristic such as size, or by magnetic or electrostatic properties. See *Screen*; also *Separator*.

Claus Catalyst An *active alumina* or modified alumina *catalyst,* available in spherical form in various sizings, used to promote the *Claus reaction*. By extension, similar catalysts for the destruction of carbonyl sulfide (COS) and/or carbon disulfide (CS_2), often accompanying H_2S in refinery gas streams.

Claus Reaction The *reaction* of H_2S with SO_2 to form elemental sulfur; employed on a large scale to destroy by-product hydrogen sulfide in natural gas plants and petroleum refineries. Applicable as well to the processing of other fossil fuels (shale oil, coal, etc.). A *catalytic* reaction.

Clay Any of a broad class of natural mineral *agglomerates* of very fine, usually platelike *particles* of hydrous compositions including combined *alumina* and *silica*. Often *plastic* when wetted, somewhat cementitious on *drying,* and *vitrified* when *fired*. Used in making numerous *ceramics* and some *refractories*.

Clay-Alumina Refractories *Refractories* mainly comprised of various *clays,* bauxite clays, *bauxite,* and/or

synthetic *alumina,* selectively or together in prescribed proportions. In order of increasing Al_2O_3 and decreasing SiO_2 content, these range from *acidic* to near-*neutral* and generally increase in refractoriness.

Clinker A stony *agglomerate, vitrified* or *fused* together in the operation of a *kiln* or furnace; usually a product or by-product of some desired *reaction,* as in *portland* or *calcium aluminate cement* manufacture, coal combustion, or *calcining.*

Closed Porosity The volume fraction of all *pores* within a solid mass that are closed off by surrounding dense solid, hence inaccessible to each other and to the external surface; thus not detectible by gas or liquid penetration. See also *Porosity, Connected Porosity.*

Colloid A relatively stable suspension of some material within a *fluid* host, the dimensions of the former usually being about 1 μm or less. Fogs, smokes, foams, emulsions, *sols,* and *gels* are examples.

Colloid Mill High-shear *mill* designed to grind *particles* down to *colloidal* size, i.e., to the order of 1 μm or less.

Comminution The act or process of reduction of *particle* size, usually but not necessarily by *grinding* or *milling.*

Compaction The act of forcing particulate or granular material together (*consolidation*) under pressure or impact to yield a relatively dense mass or formed object. Usually followed by *drying, curing,* or *firing* in *refractory, ceramic,* and powder-metallurgical manufacture.

Composite A *heterogeneous* material, body, or article comprised intimately of two or more widely different material classes: metal-*ceramic, ceramic-organic, glass-crystalline,* etc.; ordinarily combined for some *synergistic* effect on performance. Components may be layered, fibrous, particulate, etc.

Compound In chemistry, a *substance* of relatively fixed composition and *properties,* whose ultimate structural unit (*molecule,* or *repeat unit*) is comprised of *atoms* of two or more different *elements.* The number of atoms of each kind in this ultimate unit is determined by natural laws and is part of the identification of the *compound.* See Tables III and IV, *Valence.*

Conductivity (thermal, electrical) The ability of a material to conduct or transmit heat or electric current, measured by standard means.

Connected Porosity The volume fraction of all *pores, voids,* and channels within a solid mass that are interconnected with each other and communicate with the external surface; thus measurable by gas or liquid penetration. See also *Porosity, Closed Porosity.*

Consolidated In solids comprised of *particles, agglomerates,* granular materials, etc., the condition in which these smaller units are substantially bonded together to form a *monolithic* shaped mass of some strength, though still perhaps porous. Term borrowed from the field of geology.

Contact Angle Angle formed at the edge of a liquid on a solid surface, the resultant of the several *interfacial tensions* at work. Low angles characterize "wetting," high or negative angles increasingly "nonwetting."

Contamination Undesirable *impurities,* foreign or tramp material distributed in or on a *chemical* or material of commerce.

Conversion The change of one material or *substance* into another (chemical), or of one *crystalline* form or *phase* into another (physical); or of one product into another by virtue of one or a combination of the above.

Converter A vessel (usually a furnace) employed to conduct a material *conversion* in industry. In aluminas, applied to the *shaft kiln* for firing *tabular alumina.* The definition used in electrical engineering does not apply here.

Converter Discharge The *tabular-alumina* kiln-run product (without size selection). See *Select Converter Discharge.*

Cord A stringy or ropy region in glass, differing in composition, hence *refractive index* and other properties from the bulk; results from incomplete homogenization of the melt. See also *Seed, Stone.*

Cordierite A mineral silicate of aluminum, magnesium, and iron, $(Mg,Fe)_2Al_4Si_5O_{18}$; used in manufacture of ceramic industrial *whitewares.*

Corrosion The eating away of the surface layers of a material by an external chemical agent, e.g., of iron by moist air or of *refractories* by *melts, slags,* and *fluxes.* See also *Stress Corrosion.*

Corundum See *Alpha Alumina.*

Cracking In petroleum refining and similar *organic* chemical operations, any of a number of high-temperature processes, usually employing a *catalyst,* used to break larger *molecules* down into smaller ones, thus higher-boiling liquids down to lower-boiling or "lighter" ones.

Creep Relatively slow, *plastic* or microplastic and hence substantially permanent deformation occurring when a solid object is subjected to a mechanical load. In *brittle* materials, creep is seen at high temperatures.

Critical Stress The *stress* (or load) at which catastrophic fracture occurs. See *Fracture, Fracture Strength.*

Crush Strength The linear compressive force or load required to crush (fracture) a brittle material in the form of *grain,* spheroids, etc., in a prescribed test procedure; either on individual entities or in bulk.

Crusher A mechanical device used to break down large lumps or rocks of material into a range of predominantly coarse sizes, preparatory to use or to further *comminution* by *grinding.* Crushers are of various types; jaw, roll, cone, gyratory, vibratory, etc.

Cryolite The *compound* Na_3AlF_6; used as a *flux,* expecially in aluminum smelting.

Crystal That form or *particle* or piece of a substance in which its *atoms* are distributed in one specific orderly geometrical array, called *lattice,* essentially throughout. Crystals exhibit characteristic optical and other *properties* and growth or cleavage planes, in characteristic orientations. See *Diffraction.*

Crystalline That form of a *substance* which is comprised predominantly of (one or more) *crystals,* as opposed to *glassy* or *amorphous* solids and liquids.

Crystallite A small or tiny *crystal;* or each individual crys-

talline domain in a *polycrystalline* solid mass, differing from its neighbors at least in orientation. See *Grain.*

Crystallization The progressive process in which *crystals* are first *nucleated* (started) then grown in size within a host *medium* which supplies their *atoms.* The host may be gas, liquid, glass, or of another crystalline form.

Curing The progressive chemical process of hardening and strengthening a cement, including its bonding to adjacent surfaces; or of cross-linking of polymers to form a massive three-dimensional network.

Cyclone A cylindrical-conical vessel, entered tangentially by a gas stream such that the internal gas path is circular at high velocity. Used to separate entrained particulate solids from gases by centrifugal action.

Dawsonite Sodium aluminum hydroxycarbonate, $NaAl(OH)_2CO_3$, crystallized as a needlelike *hydrate* by carbonating a *sodium aluminate* solution with CO_2.

Degradation A successive stepwise process of *converting* a more complex substance to a simpler, usually by heating. In aluminas, the stepwise conversion of an *alumina hydrate* through a chain of *transition-alumina phases* to *alpha.*

Degree of Calcination "Light-burn" to "medium-burn" to "hard-burn" or "dead-burn." Other more detailed measures are used for degree of *conversion* of a material by heating: e.g., in calcined aluminas, *LOI* or *crystal* or *morphology* analysis. See also *Burn, Calcine.*

Dehydration Removal of water, especially water of *hydration* or chemically *bound water.*

Density Without modifier, the weight of an object or material divided by the volume it occupies (its external volume), hence its weight per unit volume; ordinarily expressed either in grams per cubic centimeter (g/cc or g/cm^3) or in pounds per cubic foot (lb/ft^3 or pcf). The weight of an object or material is readily determined. However, in materials handling and usage several characteristic "volumes" and their corresponding *void* fractions have to be recognized; each "volume" gives rise to a different characteristic *density*:

Theoretical Density ("True" Density) Computed from the *theoretical volume* of the solid as measured, for example, by X-ray *diffraction.* This characteristic volume contains no *pores* or *voids.* Use of the word "true" is discouraged.

Apparent Density Computed from the *apparent volume,* which is the *theoretical volume* plus the volume of *closed pores* only; measured, for example, by determining the *nominal* or *envelope volume* and subtracting from it the *water absorption* or *mercury porosity (approximating the connected* or *open pore volume).* For *nodules,* pellets, and *extrudates* used as *desiccants* and *catalysts,* the *apparent density* is also called the *skeletal density.*

Particle Density Computed from the *nominal* or *envelope volume.* This characteristic volume includes the *theoretical volume* plus that of all internal *pores,* both *closed* and *open.* It can be measured, e.g., by *pycnometer* after wax-coating the particles or object.

Bulk Density Computed from the *bulk volume* of an unconsolidated solid. This is the overall volume (viz., volume of container) occupied, now including also the interparticle *packing space.* The manner of filling (e.g., "loose," "packed," "tap," "tamped," or "vibrated," and details) must be specified as well. For a *consolidated* solid, the *bulk volume* and *nominal volume* are the same, and the *bulk density* computed therefrom accounts for the *total porosity.* Consolidated materials may require further process descriptors prefixed to *density* as well, e.g., "green," "dried," "cured," "fired."

Desiccant A material used to dry another or to dry the atmosphere, by virtue of its ability to sorb water, e.g., *active alumina, zeolite, silica gel,* etc. See *Sorption, Adsorption, Drying.*

Desorption The reversal of any of the processes of *sorption:* the removal or reevaporation of a sorbed substance. See *Adsorption, Absorption, Chemisorption.*

Devitrify To convert, partially or completely, from a *glassy* to a *crystalline* state; usually by controlled heating. See *Crystallization,* also *Vitreous.*

Dew Point The temperature at which air or other gas containing a given concentration of water vapor is or would become saturated, i.e., in *equilibrium* with liquid water. See *Humidity.* Also used for other condensibles than water.

Diaspore A particular *crystalline* form of *alumina monohydrate,* AlO(OH), occurring as a mineral usually bonded by *clay.* See also *Boehmite.*

Die A rigid case with shaped aperture, through which a *plastic* material is forced or extruded to form and densify it. See *Extrusion.* Also, a *mold.*

Dielectric A nonconductor of direct electric current, an insulator material; also, one which exhibits the phenomenon of polarization (internal molecular reorientation under an electric field), useful in capacitors, hence in electronics.

Dielectric Strength A measure of the ability of a *dielectric* (insulator) to withstand a potential difference across it without electric discharge.

Differential Thermal Analysis (DTA) An instrumental method of tracing the temperature of a sample while its container is heated at a constant rate; discloses *endothermic* and *exothermic* processes occurring in the sample, e.g., decomposition, *phase* changes, combustion, etc. See also *Thermogravimetric Analysis.*

Diffraction (X-ray or electron) An optical phenomenon and instrumental method whereby *crystals* can be identified and their atomic arrays and dimensions accurately determined; also provides the *theoretical density of each crystalline substance,* and can estimate the size of crystals up to a few hundred *angstroms.*

Diffusion The relatively slow movement of one or more kinds of *atoms, molecules,* or *ions* through a host material, in consequence of concentration or temperature

gradients. Also, especially of a gas, through the *connected porosity* of a solid; see also *Permeation, Knudsen Diffusion.*

Digestion The process of soaking a material in hot water or a hot aqueous reagent, to *leach* or dissolve or otherwise *convert* a component of the material; usually in a closed vessel and may be at elevated pressure.

Dilatant, Dilatency Of *colloidal* suspensions, the *property* of increasing in *viscosity* (i.e., stiffness) under increasing pressure or shearing force or speed. (Also means volume increase under shear.) See also *Thixotropic.*

Dolime, Doloma A mixture of *magnesia* (MgO) and *lime* (CaO), resulting from *calcination* of *dolomite.* Used in *basic refractories* and *periclase* manufacture.

Dolomite A mineral comprised principally of the double carbonate, $MgCO_3 \cdot CaCO_3$; see also *Dolime*, above. "Dolomitic limestone" consists of intermixed dolomite and *limestone,* in various proportions.

DPH, Diamond Pyramid Hardness (also, Vickers Hardness) A hardness scale in terms of the depth of indent made by a specified pyramidal diamond point under a specified steady load. See *Hardness.*

Dry Pressing A *ceramic* or *refractory* forming process in which the solid material, relatively dry (usually not over about 10% added water), is forced into a *mold* under high pressure; followed by *drying, curing,* or *firing.*

Dryer A device for *drying* a material or product by evaporation of water, usually by modest heating with forced ventilation, sometimes by use of vacuum. See also *Desiccant.*

Drying Removal of the *free water* from a moist material or product, insofar as practicable without other physical or chemical change; as opposed to *dehydration, curing, activation, calcination, conversion.*

Drying Agent See *Desiccant.*

Ductile Capable of considerable *plastic* deformation without fracture, especially at temperatures well below that of incipient melting. See also *Brittle.*

Elastic Characterized by recoverable (and nearly linearly related) deformation with applied load or *stress.*

Elastic Modulus A constant relating *stress* to *strain* in an *elastic* material: *Young's modulus* relates to tension and compression, the *shear modulus* to shear and hence also to torsion. Each is temperature-dependent.

Electrochemical Reaction A *reaction* caused by passage of an electric current through a *medium* which contains mobile *ions* (as in *electrolysis*); or, a spontaneous reaction made to cause current to flow in a conductor external to this medium (as in a *galvanic cell*). In either event, electrical connection is made to the external portion of the circuit via a pair of *electrodes.* See also *Electrolyte.*

Electrode One of a pair of conductors introduced into an *electrochemical* cell, between which the *ions* in the intervening *medium* flow in opposite directions and on whose surfaces *reactions* occur (when appropriate external connection is made). In dc operation, one electrode or "pole" is positively charged, the other negatively. See *Electrochemical Reaction, Anode, Cathode, Electrolyte.* Alternatively, such conductors separated by a gap across which an arc or spark is made to occur.

Electrolysis In an appropriate cell, an *electrochemical reaction* induced by an impressed electric current. Actually a pair of such reactions, one (*oxidation*) occurring at the *anode* and the other (*reduction*) at the *cathode,* in many cases usefully kept separate by barriers or otherwise.

Electrolyte The mobile-*ion*-containing *medium* (ionic conductor) in an *electrochemical* cell. Most often, an aqueous solution or a molten mass or "bath" of *inorganic compound(s)*; more rarely, a solid ionic conductor. By extension, any such "ionic" material system whether used electrochemically or not.

Electron The ultimate particle and (negative) unit of electric charge. A component part of all *atoms* and *ions.* Roughly one electron per atom is mobile in *metals,* their coherent motion (flow) accounting for electric current.

Electrostatic Precipitator (ESP) A device used to separate very fine solid *particles* from an entraining gas, by inducing a charge on the particles and collecting them by attraction on a surface of opposite charge.

Element In chemistry, any of some 90+ fundamental natural species of which all stable matter is comprised, either singly (i.e., as the *free* or uncombined element) or in chemical combinations with one another in *compounds.* Every *element* is identified by the unique constitution of its ultimate particle, or *atom,* which in turn determines its *properties* and in part those of its compounds. See Tables III and IV, also *Valence.*

Enamel, Porcelain Enamel In *ceramics*, a *glaze* applied to a metal rather than a ceramic underbody, and specially formulated for this purpose.

Endothermic In chemical or physical changes, one which absorbs energy or heat and thus tends to cool the *medium* in which it occurs. See also *Exothermic.*

Energy The ability to do "work" by virtue of moving mass (kinetic), or stored heat, or a particular chemical or physical state, etc.; quantitatively measurable and accountable by, e.g., calorimetry, etc.

Envelope Volume See *Nominal Volume.*

Equant Of *crystals, crystallites*, or *grains,* being of roughly equal dimensions in the several different directions. Opposed to elongate or fibrous or platelet in shape. See *Morphology.*

Equilibrium State of affairs existing when the rate of some dynamic *reaction,* physical process, etc., is exactly equaled by that of its reverse. Nature tends to approach and maintain this state when possible, in contained systems.

Erosion The process of grinding or wearing away of a massive solid surface by rubbing or friction, generally by impact of *particles* of some other material. Usually undesirable. See also *Abrasion, Attrition, Corrosion.*

Evaporator An apparatus for driving off excess liquid (from a liquid rather than solid source); usually by

means of heating, sometimes in conjunction with partial vacuum.

Exothermic In chemical or physical changes, one which liberates energy or heat and thus tends to raise the temperature of the *medium* in which it occurs. See also *Endothermic.*

Extender A substance added in appreciable quantity to a product, especially as a diluent, *filler*, or modifier; in proper usage, primarily for economic rather than performance reasons. See also *Additive.*

Extrudate The product of *extrusion*; any cylindrical, prismatic, or pellet-shaped material so made. A useful form of a solid *catalyst* or catalyst *substrate*, for example; also, elsewhere in *ceramics.*

Extrusion The process of forcing a *plastic* material or mixture through the opening(s) of a *die* at relatively high pressure. The material may thus be *compacted* (as in *ceramic* forming), and emerges in elongate cylindrical or ribbon (or wire, etc.) form having the cross section of the die opening. Ordinarily followed by *drying, curing, activating,* or *firing.*

Fahrenheit (°F) A *temperature* scale on which the *freezing point* of pure water is 32° and the normal *boiling point* of pure water is 212°; extended uniformly above and below these points. See also *Centigrade, Rankine.* See Table I.

Fatigue Stepwise or gradual reduction in *strength* of a material when subjected to repeated or cyclic mechanical or thermal *stresses* somewhat below that causing *fracture.* Results from gradual growth of *flaws.*

FCC (Fluid Cracking Catalyst) A *bead* form of *catalyst* used to accelerate *cracking* of hydrocarbons in refinery and similar operations, in which the catalyst is maintained as a *fluid bed* instead of stationary.

Feldspar A family of anhydrous minerals comprised of *alumina, silica*, and oxides principally of Na, K, and/or Ca in chemical combination: $(Ca, Na_2, K_2)O \cdot Al_2O_3 \cdot (2, 4, 6)SiO_2$. Alteration products occur in some *clays.* Useful in *ceramic* and *glass* manufacture.

Filler Generally a fine particulate solid, admixed in significant quantities into a product to provide bulk, color, opacity, dimensional stability, or other desired *properties,* or simply as an *extender.* See also *Additive.*

Filter A porous membrane, sheet, plate, or bed of particles, with openings sized for a particular duty, used to effect the mechanical separation of a suspended solid from a gas, liquid, or slurry. Of many types: gravity, pressure or vacuum; stationary (e.g., plate-and-frame, bed), or moving as in rotary, belt, etc.

Filter Cake The still-wet material collected on a *filter*, the excess liquid having passed through. That liquid is the "filtrate."

Fines A loose term used for a fraction of a particulate or granular solid; the finer sizings of a distribution; or, finer than some specified diameter or size; or finer than desired or specified for a given product; etc. Criteria must be understood in the particular usage, though "passing through 325-mesh *screen*" is common.

Finish See *Surface Finish.*

Fire See *Burn*; generally more intense than to *calcine.* To *sinter* products or *wares* in a furnace or *kiln.*

Fire Retardant, Flame Retardant A chemical diluent, *filler*, coating, or treatment used to retard or inhibit the start or initial spread of flame in a combustible material. Examples: *alumina trihydrate,* sodium borate, ammonium phosphate, numerous chloro and bromo *organics.*

Fix In dyeing, to render the color permanent by chemically attaching the dye molecules to the host, often by means of an agent called a *mordant,* such as *aluminum sulfate.* In general, to render insoluble in water by chemical alteration.

Flaw In the mechanics of solids, a general term for a discontinuity from which a crack can propagate under mechanical or thermal *stress.* (Other definitions in other contexts are evident.) See *Fracture; Weibull Statistics.*

Floury In particulate solids, exhibiting a fine powdery texture and a high or large *angle of repose*; also dusty, easily airborne.

Fluid A gas, liquid, or slurry or even particulate solid material readily pourable under its own weight. Opposed to viscous, stiff, thick, or rigid. See also *Plastic.*

Fluid Bed, Fluidized Bed A bed of particulate or granular solid that is lifted and diluted by an upflow of gas or liquid so that the mixture is *fluid* and turbulent.

Flux One or more substances added to a mineral or material mixture to lower the melting temperature so that the mass more readily liquefies and coalesces; often as well, to lower the *viscosity* of such a *melt.* Used e.g., in slagging of molten metals, in welding, and in glassmaking.

Formula Chemist's quantitative representation of a *substance* (*compound* or *free element*). See also *Molecule, Repeat Unit.* See Tables III and IV.

Fracture (Brittle Fracture) Under mechanical or thermal *stress*, existing *flaws* in a body may or may not grow as small cracks (see, e.g., *Fatigue, Stress Corrosion,* also *Weibull Statistics*). Differential crack growth consumes energy, derived from relaxation of stored *elastic strain energy.* If the former exceeds the latter, crack growth, if any, is stable. But under a certain combination of *critical stress* and crack size, the energy relation reverses and the most severe (i.e., largest) flaw or crack then existing in the region of highest local stress propagates catastrophically: this is identified as "fracture" or "failure." See *Strength, Toughness.*

Fracture Strength The mechanical load (properly described as *stress*) at which *fracture* occurs. Depends on numerous material and specimen properties, history, and method of loading: compressive, tensile, bending, torsion, etc. Usually variable in brittle materials: see, e.g., *Weibull Statistics.* Is also typically dependent on temperature.

Fracture Toughness A measure of the energy consumed during differential extension of *flaws* or crack(s), determined at the *critical stress.* Affects the energy bal-

ance described for *fracture*, as well as, e.g., resistance to *fatigue*. Expressed by different numbers depending on test methods of loading a crack tip: K_{Ic} for tension, K_{IIc} for shear, K_{IIIc} for torsion. Others apply to *ductile* materials.

Free Uncombined chemically, e.g., a *free element* is that uncombined elemental *substance*. Also, e.g., "free moisture" or *free water* is water present in a material by *absorption* or *occlusion* as opposed to water of *hydration* or otherwise chemically combined; often determined by a specific procedure for a given material and use. See *Element*; see also *Water*.

Freezing Point See *Melting Point*; also *Fusion*.

Friable Easily crumbled or pulverized (reduced to powder).

Frit Any *glassy* material cooled and then ground to powder. Used mainly in compounding *glazes* or *enamels*; also lightly repacked and *sintered* to make a porous medium or *filter*.

Fuse-Cast Poured into *molds* in the liquid state, then allowed to freeze or solidify by cooling. Applicable to some refractories and glasses, for example.

Fused Alumina *Alpha alumina* made ordinarily by arc-melting and refreezing; crushed and sized, for example, in *abrasive* and *refractory aggregate* manufacture.

Fusion The process of melting; the *transition* or *conversion* from a *crystalline* solid state to the liquid state. "Freezing" is precisely the reverse.

Fusion Point, Fusion Temperature See *Melting Point*.

Galvanic Cell A cell or system in which a spontaneous *oxidation-reduction reaction* occurs, the resulting flow of *electrons* being conducted in an external part of the circuit. See *Electrochemical Reaction*. In galvanic *corrosion* (of metals), the cells are minute, identified with surface inclusions.

Gamma Alumina A particular *crystalline transition alumina*, derived thermally from *boehmite* and hence a major component of lightly *calcined gel alumina*. See also *Substrate Alumina*.

Gel A *colloidal* state comprised of interdispersed solid and liquid, in which the solid particles or ligaments are themselves interconnected or interlaced in three dimensions. See also *Sols*.

Gel Alumina Any of a family of porous, high-surface-area *aluminas* and modified aluminas composed substantially of *pseudoboehmite* or *boehmite*, or derived from them by further processing; available in various convenient forms. See also *Substrate Alumina*.

Gibbsite A particular *crystalline* form of *alumina trihydrate*; occurs in *bauxite* but is most notable as the primary product of the *Bayer process*, hence the synthetic raw material from which *aluminum* and most *aluminas* of commerce are in turn derived. See *Bayer Hydrate*; also *Reduction-Grade Ore*.

Glass, Glassy A state of matter that is *amorphous* or disordered like a liquid in structure, hence capable of continuous composition variation and lacking a true *melting point*, but softening gradually with increasing temperature. *Glasses* of commerce are mainly complex silicates in chemical combination with numerous other oxidic substances; made by melting the source materials together, forming in various ways while *fluid*, and allowing to cool. See *Vitreous*; also *Polymer*.

Glaze In *ceramics*, a mineral or chemical mixture usually applied as a fine suspension to the surface of a body, then dried and *fired* to produce a bonded, *vitreous* coating. Used for color, decoration, or sealing. See also *Enamel, Glass*.

Grain As a subdivision of uncompacted solid materials, i.e., "granular," an irregular piece ranging in diameter from perhaps a centimeter or two to considerably less than a millimeter, with both limits depending on the usage. In *refractories*, refers to each individual piece or to a quantity of either loose or *consolidated aggregate*. In *ceramic* and metallic microstructures, a *grain* is a single *crystallite* of the multitude comprising a *polycrystalline* material, these either self-*bonded* or bonded by some intergranular *phase*.

Grain Growth In *polycrystalline* materials, a diffusion-controlled, thermally activated phenomenon in which the larger *grains* grow still larger while the smallest ones usually diminish or disappear. See *Recrystallization*.

Grain Size, Grain-Size Distribution Measures of the characteristic *grain* or *crystallite* dimensions (usually, diameters) in a compact *polycrystalline* solid; or of their populations by size increments from minimum to maximum. Usually determined by microscopy. See also *Particle-Size Distribution*.

Gram A metric unit of weight, about 1/30 of an avoirdupois ounce. See Table I; also, *S.I. Units*.

Gram-Atom See Use of Tables of Chemical Elements.

Graphite A *crystalline* form of elemental carbon, its stablest and most refractory form; each crystal consisting of macro*molecular* sheetlike layers of atoms stacked in parallel packets. Made by extremely high-temperature heating of *polymeric organic* materials like coke and pitch, in the absence of air. Carbons and graphites are major or minor constituents of numerous *refractories* as well as *electrodes* and many other articles.

Green Jargon for a highly unfinished, young, still wet, impure, or crude material in a complex process, as a "green" formed *ceramic* or *refractory*, "green" *liquor*, "green" *acid*, etc. Dignified through usage in numerous technologies.

Grindability The relative ease of reducing the *particle size* of a solid to some desired end-point by *grinding*; often stated as the amount of energy required, or the time required in a particular piece of equipment.

Grinding As opposed to *crushing*, the size reduction or *comminution* of solids into relatively small particles by mechanical means; generally, to diameters of the order of 1–2 mm and less. See *Mill, Milling*. Alternatively, a means of material removal used in shaping or finishing parts: see *Abrasion, Abrasive*.

Grinding Aid An *additive* to a *grinding* system which pro-

motes more efficient size reduction, usually by subtle alteration of the surface *properties* of the material being ground.

Grinding Media Hard objects tumbled or propelled in a grinder or *mill* to conduct *grinding* action, such as balls, rods, or grains. See, e.g., *Ball Mill.*

Grit Sized or size-classified *abrasive* material. See *Abrasion.*

Grog In *ceramics* and *refractories, fired* material that is recrushed or ground for incorporation in a mix with *green* materials; used to reduce the firing shrinkage of the mix, or as a form of *aggregate.*

Grout A thin, pourable *mortar slurry,* used for filling-in joints or spaces between masonry units and hardenable or *fired* to become part of the structure.

Gunning The process of forcibly spraying or throwing of fluid cement, concrete, or *refractory* mixtures onto a surface to build up a *monolithic* layer or body.

Gunning Mix A *mix* particularly compounded or developed for efficient *gunning.*

Hall Process The commercial *electrolysis* process for manufacturing *aluminum* metal.

Hammer Mill A machine for *grinding* or pulverizing solids, in which free-swinging hammers are rotated at high speed within a stationary cylindrical grating. See *Milling, Mill.*

Hardness Resistance of a solid material to indenting, also to *abrasion*; a measure of the cohesive forces between its *atoms.* See *Mohs, Rockwell, DPH, Knoop,* for measurement methods.

HDS (Hydrodesulfurization) See *Hydrotreating.*

Heat A form of *energy,* representing the energy of motion of the *atoms* of matter (as opposed to nuclear, chemical, and radiant energy). The intensity of heat in a body is its *temperature.*

Hertz The *S.I. unit* of frequency, namely 1 cycle per second.

Heterogeneous Of a body of material or matter, comprised of more than one *phase* (solid, liquid, and gas) separated by boundaries; similarly of a solid, comprised of more than one chemical, *crystalline,* and/or *glassy* species, separated by boundaries. See *Homogeneous*; also *Composite.*

Homogeneous Of a body of material or matter, alike throughout; hence, comprised of only one chemical composition and *phase,* without internal boundaries. (Homogeneous *polycrystalline* materials contain orientational boundaries only.)

Hot Face The working face or side of a *refractory* lining, in contact with the heated material (charge, slag, gases) within a vessel.

Hot Zone In a furnace or *kiln,* that portion or region in which the heated material reaches its highest temperature.

Humate One or a family of *compounds* of humic acids (from "humus," the *organic* portion of soil), dark in color; found, e.g., in *bauxite,* hence a potential contaminant of *gibbsite.*

Humidity Dampness or water-vapor content of air or other gas. See *Relative Humidity, Dew Point.*

Hydrate A *crystal* or chemical *substance* containing chemically combined *water,* in (nearly) fixed proportions relative to its other constituents.

Hydrated Alumina See *Alumina Hydrate.*

Hydration The act or process of taking up water chemically, as opposed to *adsorption* or *absorption.* Forming a *hydrate.*

Hydraulic, Hydrostatic Force, pressure, or motion delivered by or through a liquid. *Hydraulic cement* is one made workable, and *cured,* by the action of water.

Hydrolysis A kind of *acid-base* reaction with water which combines only its hydrogen (H^+) or hydroxide *ion* (OH^-), releasing the other one (hence changing the *pH*); infrequently, both at once.

Hydrotreating In petroleum refining and similar *organic* chemical operations, the process of treating with hydrogen gas at high temperatures and pressures to effect desired chemical changes; usually employing a *catalyst.* Examples: *hydrodesulfurization (HDS),* hydrodenitrification (HDN), hydrocracking. See also *Cracking.*

Hygroscopic The ability or tendency to take up moisture, usually from the air but hence from other moist materials as well. See, e.g., *Desiccant.*

Immiscible Of two *phases,* the inability to dissolve in one another to form a single *solution*; mutually insoluble. May occur in a limited range of ratios of the two, or at any ratio.

Impact Strength The force or energy of a blow (given by a fixed procedure) required to cause fracture, as opposed to *fracture strength* under a gradually increasing applied force.

Impurity, Impurities In a *chemical* or material, minor constituent(s) or component(s) not included deliberately; usually to some degree or above some level, undesirable. See also *Contaminant.*

Index of Refraction See *Refractive Index.*

Inert Unreactive, stable, or indifferent to the presence of other materials; a relative term, usually applying under some limited set of circumstances or application. See also *Reaction, Reactivity.*

Inorganic Of chemical *substances* or mixtures, comprised other than of most *compounds* of carbon. See *Organic,* including limited exceptions.

Insoluble, Insolubles Not appreciably dissolved in water or some other specified reagent or solvent (e.g., *acid, caustic, organics,* etc.). A relative term of *impurities,* usually determined by a fixed procedure: see *Acid Insols, Caustic Insols.* See also *Leach.*

Insulating Refractories Highly porous (including fibrous) *refractories* used to efficiently contain or retard the passage of heat; often, behind or outside the working refractory which contacts the heated material.

Interfacial Tension A measure of the adhesive forces between two *phases* (gas-solid, gas-liquid, liquid-solid, liquid-liquid) in contact. Usually determined by measuring the *energy* or *work* required to extend the area of contact by a unit amount. See also *Surface Tension, Contact Angle.*

Investment Casting A special *casting* process in which the *mold* is itself cast around the original form which can be removed by melting (e.g., wax). Filling the mold thus reproduces the original form.

Ion A charged particle of *atomic* or *molecular* dimensions that contains one, two, three, etc., *electrons* above or below the neutral complement. See *Anion, Cation.* May be mobile, as e.g., in aqueous *solutions* or *melts,* or identifiable within chemical *compounds.* See also *Radical,* and *Valence.*

Ion Exchange A chemical process involving intimate contact of a solid and a liquid (e.g., aqueous solution), whereby *ions* on the surface of the former are exchanged for other ions contained in the latter. Used for water softening and other selective chemical processes.

Iron The metallic element; or, more loosely, applied to *substances* containing combined iron and often to such substances as *impurities.*

Isostatic A type of *ceramic* or powder-metallurgical forming or *compaction* process in which the *mold* is flexible and pressure is applied *hydrostatically* or *pneumatically* from all sides.

Isotropic Having the same value of a given property measured in any direction, or (sometimes) in all directions perpendicular to each other.

Joule The *S.I. unit* of *work* or *energy.* See Table I.

Kaolin A fine, usually white *clay* material containing principally kaolinite, $Al_2Si_2O_5(OH)_4$; used in *ceramics* and *refractories.* Related minerals contained include nacrite and dickite, of the same formula.

Kelvin (K) An "absolute" *temperature* scale whose degree (interval) is the same as that of *Celsius* but whose zero is at the vanishing point of translational molecular motion such that *heat* energy can no longer flow. See Table I; also *Rankine,* and *S.I. Units.*

Kiln An oven, furnace, or heated enclosure used for heating loose solids or formed solid objects as in *calcining, firing,* or *burning.* Of numerous types, e.g., rotary, shaft, fluid-bed, tray or hearth, tunnel, etc.

Kiln Furniture Various supports, shapes, or boxes (*saggers*) used to hold or contain *ceramic ware* during *firing.* Generally themselves of ceramic material (*alumina,* etc.), much more heat-resistant than the material to be fired.

Knoop Hardness A "micro" *hardness* scale and instrumental measurement method: the depth of indent made by a rhombohedral diamond point of specified dimensions, when pressed into a surface under specified load. Used especially for materials harder than quartz.

Knudsen Diffusion *Diffusion* of a gas through very small *pores* or channels in a solid, wherein intermolecular collisions in the gas phase are far less frequent than collisions with the walls. Also can occur in larger cavities under reduced gas pressure. Characteristic diffusion rates differ markedly from those of "ordinary" diffusion.

Kyanite A light bluish-colored claylike but anhydrous material, Al_2SiO_5; used in making *ceramics* and *glasses.*

Ladle In iron- and steelmaking and in foundaries, a vessel used to convey molten metal from a furnace to another processing unit or to a *mold*-filling station.

Lattice The regular, repeated geometrical array of *atoms, ions,* or *molecules* (chemically bonded clusters of atoms) in a *crystal.* See *Repeat Unit.*

Leach To subject a particulate or porous solid to the action of water or other liquid or reagent, to remove one or more components soluble in the latter. The resulting *solution* is called the "leachate."

Leachable Soda The percentage of sodium, in any form but expressed as Na_2O, that can be *leached* from a material by hot water using a fixed procedure.

Lime Calcium oxide, CaO; a refractory but moderately water-soluble and *caustic* substance usually obtained by *calcining limestone,* seashells, coral, or other forms of $CaCO_3$. Also called quicklime, burnt lime. *Dolime* contains about equimolar CaO, MgO. As-is or *slaked* (*hydrated* to Ca $(OH)_2$), lime has many used in materials, *refractories,* cements, *chemicals,* and chemical treatments.

Limestone A mineral rock or deposit consisting chiefly of calcium carbonate, $CaCO_3$. "Dolomitic limestone" contains some $MgCO_3$. See also *Dolomite.*

Liquor Any chemical process *solution,* usually containing a fairly high concentration of solute (dissolved substance).

Liter A metric unit of volume. See Table I.

Loss on Ignition (LOI) The fractional or percentage weight loss of a material on heating in air from an initial defined state (usually, dried) to a specified temperature such as 1000°C, and holding there for a specified period such as 1 hour. Fixed procedures are designed, usually, such that *LOI* represents the loss of combined H_2O, CO_2, certain other volatile *inorganics,* and combustible *organic* matter.

Macropore Volume The volume fraction of a porous solid comprised of all *connected pores* or openings larger than a designated equivalent size, determined arbitrarily. In some *alumina* products, this limit is set at a diameter of 350 *angstroms*; in some, at 700 Å.

Magnesia Magnesium oxide, MgO: *calcined,* or hard-*burned* as *periclase.* Loosely, applied also to the *hydrate,* $Mg(OH)_2$. Made synthetically from seawater or brines, also (impure) from *magnesite.* Used in *basic refractories,* as a *filler* in rubbers, and elsewhere.

Magnesite A mineral consisting chiefly of magnesium carbonate, $MgCO_3$; a source of "magnesite" as opposed to "periclase" *basic refractories.* The latter, made from synthetic MgO, are usually somewhat lower in silica and/or iron (typical contaminants of magnesite ores). See *Magnesia*; also *Dolomite, Dolime.*

Malleable Especially of metals, capable of being formed or deformed *plastically* under hammer blows, as in forging.

Mass Transfer Zone In a process conducted in a *fluid* moving through a porous solid bed (e.g., *desiccant* or *absorber*), that part of the bed at any instant in which

the reaction is in progress. Upstream of this zone the bed is saturated, while downstream of it the active agent in the fluid has been exhausted.

Matrix In a *polycrystalline* and especially *heterogeneous* mass, e.g., igneous rocks and in *refractories*, the material between large *crystals* or *grains* of the major component(s), which bonds them together. May itself be *crystalline* or *vitreous*.

Mechanical Properties Those characteristics of a material that relate force, load, or stress to deformation, flow, and/or fracture; e.g., elastic modulus, brittleness, ductility, malleability, yield stress, "toughness," creep, viscosity, various expressions of "strength," etc.

Medium, Media A quantity of material contained in some volume or location, generally for the purpose of reacting or doing some other useful thing, e.g., a *grinding* or *hydraulic* agent; or the host, solvent, or reagent within which some change or *reaction* is conducted. See also *Grinding Media*.

Melt To pass from a solid or rigid state to the liquid state; to *fuse*. Also, a quantity or batch or mass of liquid (sometimes also called a "bath") contained in a vessel or otherwise localized.

Melting Point The temperature (or very narrow range) at which a specified *crystalline* solid *converts* to a liquid and the reverse, or at which a specified solid and its liquid are at *equilibrium*. See *Fusion Point, Freezing Point*.

Mercury Immersion A manner of measurement of the *nominal* or *envelope volume* of a solid, for purposes of determining the *total porosity* when the *true* or *theoretical volume* is known. See also *Density*.

Mercury Porosity The volume fraction of *connected pores, voids,* and channels in a material as determined using mercury intrusion at high pressures. See *Porosimeter*.

Mesh, Mesh Size The opening(s) or size of opening(s) in a designated *sieve* or *screen,* hence the approximate diameter of particles below which they will pass through and above which they will be retained on the screen. "Mesh sizes" are given as number of wires per inch of standard screen construction, e.g., Tyler or U.S.; these are translated by tables into equivalent particle diameters in inches, millimeters (mm), or micrometers (μm or μ). See Table II.

Metal Class of *elements* exhibiting when *free*: metallic luster, relatively high electronic and thermal conductivity, and the ability to form simple positive *ions* by *reaction* with common *oxidizing agents*. Also alloys and some *compounds* comprised exclusively of metallic elements. (Sometimes also, hydrogen.) See also *Nonmetal*.

Metalloid Class of *elements* chemically intermediate between *metals* and *nonmetals*. Commonly taken to include boron, carbon, and silicon; arsenic and selenium may be included by some, or else classed as *metals*.

Metastable Of a material, not truly stable with respect to some *transition, conversion,* or *reaction,* but stabilized kinetically either by rapid cooling or by some *molecular* characteristics as, for example, by the extremely high *viscosity* of *polymers*. *Transition aluminas* and cooled *glasses* are examples.

Meter (m) The basic metric unit of length. See Table I; also *S.I. Units*.

Micrometer, Micron (μm, μ) One-thousandth of a millimeter or one-millionth (i.e., 10^{-6}) *meter*. See Table I.

Micropore Volume The volume fraction of a porous solid comprised of all *connected pores* or openings smaller than a designated equivalent size, determined arbitrarily. In some *alumina* products, this limit is set at a diameter of 120 *angstroms*. See also *Knudsen Diffusion*.

Mil An English measure of thickness or diameter: 0.001 inch. A common designation of wire size, also of thin metal or *ceramic* sheets.

Mill A *grinding* machine or grinder, used for size reduction (*comminution*) of solids below "crushed" sizes, though overlapping. Of various mechanical types: *ball* or *pebble mills*, rod mills, roll mills, *hammer* mills, plate or disk mills, jet mills, etc. See *Colloid Mill*; also *Crusher*.

Milling The act or process of *grinding* to reduce the size of particulates, usually finer than by *crushing*. Often conducted dry, sometimes wet. See *Mill*.

Mineralizer A processing *additive* that promotes either the *recrystallization* or the partial *fusion* or *sintering* of certain mineral or *ceramic* materials, often thus facilitating the desired *conversion* at a lower temperature.

Miscible Of two *phases*, the ability of each to dissolve in the other. May occur in a limited range of ratios of the two, or in any ratio.

Mix A formulated batch or ratio of different materials, usually sized, prepared as feed to a *refractory, ceramic, glass*, or other forming or manufacturing process, or fed into a *reaction* vessel. May be dry, wet, or even a *slurry* or suspension.

Modulus of Elasticity See *Elastic Modulus*.

Modulus of Rupture The strength of a brittle material as measured by a specified bending test performed on a bar or rod. Usually relatable to the *tensile strength*. See *Fracture, Fracture Strength*.

Mohs Hardness A *hardness* scale originally developed for minerals; ranging from 1, that of talc, to 10, that of diamond, the hardest known substance. Determined by the ability of one substance to scratch another. The modified *Mohs scale*:

1. Talc
2. Gypsum
3. Calcite
4. Fluorite
5. Apatite
6. Orthoclase feldspar
7. Fused silica
8. Quartz

9a. Garnet
9b. Topaz
9c. Fused zirconia

9d. Fused alumina, corundum
9e. Silicon carbide
9f. Boron carbide
10. Diamond

In the original scale, quartz was 7, garnet 8, corundum 9, and diamond 10, the others above 6 omitted.

Mold A shaped cavity in which a fluid or malleable material is given form, as by *casting, ramming,* or *tamping*. Also sometimes, a *die.*

Mole See Use of Tables of Chemical Elements. Also called "mol."

Molecular Sieve One of a family of *zeolite* minerals or other (often synthetic) *crystalline* materials characterized by connected voids in the crystal lattice that are of molecular dimensions; hence having size-selective *adsorptive, catalytic,* and other surface properties. See also *Ion Exchange.*

Molecule The smallest unit of which a *substance* (*compound* or *free element*) may be comprised, retaining its chemical identity. Contains one or more *atoms* of one or more kinds. See also *Repeat Unit.* See Use of Table of Chemical Elements; also *Valence.*

Monolith, Monolithic An object comprised entirely of one massive piece (although *polycrystalline* or even *heterogeneous*), as opposed to being built up of preformed units as in laid masonry. Formed, for example by *casting, gunning, extrusion, dry pressing, ramming, tamping,* etc. Also, the honeycomb form of automotive exhaust *catalyst* cartridge.

Mordant In dyeing, an agent used to attach the dye molecules to the base material (textile, etc.) by chemical action, rendering the assemblage resistant to *leaching* or washing. See *Fix.*

Morphology The characteristic shape, form, or surface texture or contours of the *crystals, grains,* or *particles* of (or in) a material, generally on a microscopic scale. Less commonly, the specific crystal *lattice* itself (e.g., as in "polymorph," one of two or more crystal forms of the same *substance*).

Mortar A *slurried plastic* mixture of cementitious material and *filler* or fine *aggregate*, applied to the surfaces of masonry units to provide firm and relatively impervious joints, e.g., in the erection of *refractory* linings and structures.

MSA (Mine Safety Appliances) A particular instrumental method of determining the *subsieve particle-size distribution* of a solid by sedimentation or settling in a liquid medium, using *centrifuges* at different speeds for specified durations.

Muffle An enclosure within a furnace, protecting the *ware* from direct impingement of the flame or stream or combustion products; used to achieve a more uniform *hot zone.*

Mullite A mineral or synthetic *compound* of *alumina* and *silica*, $3Al_2O_3 \cdot 2SiO_2$; used or created by *firing* as a constitutent of *refractories,* as either *aggregate* or *matrix.* Also a constitutent of *porcelain, china,* etc.

Nanometer One billionth (i.e., 10^{-9}) *meter.* As an *S.I. unit*, preferred over the *angstrom* (10^{-10} m) for the representation of atomic and molecular dimensions and of the wavelengths of "hard" electromagnetic radiation (e.g., *X rays*). "Optical" wavelengths (uv, visible, and ir) may equally be represented in *micrometers.*

Neutral Refractories *Refractories* that are about equally resistant to chemical attack by *acidic* or *basic slags, melts,* or *fluxes. Alumina, alumina-chrome, spinel, zirconia,* carbon, *graphite*, and silicon carbide are examples of near-neutral materials.

Neutralization In chemistry, the *reaction* of an *acid* and a *base* to form a *salt.* Originally $HY + XOH = H_2O + XY$; now much broader, including many nonaqueous systems and analogous reactions.

Newton The *S.I. unit* of force. See Table I.

Nodule A rounded or spheroidal mass or *agglomerate* of solid material; a useful form for *desiccants, scavengers, catalysts, substrates, bed supports,* and other purposes. Available in specified sizes.

Nodulizer A machine, usually containing a rotating pan, used to *agglomerate* fine particles into *nodules.*

Nominal Approximate or typical or represented by (a dimension, composition, etc.), as opposed to actual or accurate.

Nominal Volume* For any single *particle, agglomerate, grain, nodule,* pellet, piece, or any formed and *consolidated* body of a solid, the exterior or geometric volume it occupies (as though it were shrink-wrapped in an infinitely thin film and measured, e.g., by displacement in a liquid). Also called *Envelope Volume.* See *Density.*

Nonmetal Class of *elements* comprised of bromine, chlorine, fluorine, iodine, nitrogen, oxygen, phosphorous, and sulfur. The "noble gases" (argon, helium, neon, etc.) are usually included. Hydrogen is often included, though in *inorganic compounds* it behaves most often like a *metal.* See also *Metal, Metalloid*; and see *Nonmetallic.*

Nonmetallic As to *elements,* synonymous with *nonmetal.* As to *compounds,* those which are not *electronic* conductors of electricity; hence all but the intermetallic compounds and a few metal borides, carbides, hydrides, nitrides, and silicides. See also *Semiconductor.*

Nordstrandite A particular *crystalline* form of *alumina trihydrate*; rare.

Nucleation The first step in the process of *crystallization,* in which the characteristic atomic arrangement is first established in a submicroscopic (molecular-sized) zone, cluster, or *particle.* Loosely, also sometimes applied to *agglomeration.* See *Nucleus,* also *Seed.*

Nucleus A (usually minute) central or original core or region about which more or other material may be clustered, deposited (as in *crystallization*), or *agglomer-*

*In ASTM nomenclature, this is called *Bulk Volume.* However, the risk of confusion with that of consolidated bulk solids is so great that "nominal" or "envelope" volume is greatly preferred and hence used in this glossary. For *consolidated* solids, the *nominal* and *bulk volumes* are identical. In loose particulate or granular solids the *bulk volume* includes the *nominal volume* plus the *packing space* or interstitial volume.

ated. See also *Seed.* In *atoms,* such a core comprised of protons and neutrons fixing the atomic number (hence, *elemental* identity) and weight, surrounded at much larger distance by *electrons.*

Occlude, Occlusion To gather in and retain one material within an enveloping mass of another, often in the process of creation, forming, or growth of the latter as may occur in coprecipitation or rapid *crystallization.*

Onionskin A spheroidal texture of an *agglomerate,* often evidenced by shell-like fragments, resulting from slight nonuniformities in rolling or *nodulizing* or from shrinkage effects when such an agglomerate is *fired.*

Opaque, Opacity, Opacifier Nontransparent and non-*translucent*; absorbing and/or reflecting rather than transmitting light or radiation. An agent incorporated into a *glaze* or *enamel* to impart this quality, usually as *crystallites* in a *vitreous* medium, is called an *opacifier.*

Open Porosity See *Connected Porosity.*

Optical As *properties* or characteristics, having to do with radiation or the interactions of matter with radiation; especially of visible wavelengths but not necessarily so restricted.

Organic Of *compounds* or mixtures thereof, the class comprised of most of the compounds of carbon. The exceptions are generally taken to include the carbides of *metals* and *metalloids*; certain solid interlayer or "edge" compounds of carbon or graphite; and CO, CO_2, and the derivative carbonates and bicarbonates (e.g., M_2CO_3, $MHCO_3$). In fact, CO, CO_2, COS, and CS_2 may be regarded as *organic* or *inorganic*, depending on the chemical context. Similarly, *elemental* carbon may sometimes be regarded as *organic* in respect to its origins, but *inorganic* as a structural material.

Osmosis, Osmotic The selective passage of a *molecular* or *ionic* component of a fluid through a semipermeable membrane or film.

Ovenware Heat-resistant *pottery* or *ceramic ware* used for baking and serving food.

Oxalate A *salt* or other *compound*, derivative of oxalic acid, $H_2C_2O_4$; *organic* in origin, present with *humates* in *bauxite* and some other *hydrated* or hydrous minerals as a decomposition product of celluloses, starches, and sugars.

Oxidation A type of chemical *reaction* characterized by the removal of *electrons* from, hence a positive change in *valence* of, some contained *atom.* Often caused by oxygen of the air, hence the name. See also *Reduction.*

Oxidize To form an oxide from the *elements*, or otherwise in general to cause *oxidation.* See also *Reduce.*

Oxidizing Agent or Condition An agent, or presence of an agent, e.g., in *firing,* that causes *oxidation.* Examples are oxygen (O_2); chlorine (Cl_2); nitrogen oxides; or nitric acid; even CO_2 when hot; etc. See also *Reducing Agent.*

Packing Fraction In an unconsolidated or bulk solid comprised of *particles, grains, agglomerates, nodules,* pellets, etc., that fraction of the overall volume which is occupied by the smaller units. See also *Packing Space, Nominal Volume, Density.*

Packing Space Sometimes called *Interstitial Volume.* In an unconsolidated or bulk solid, the unoccupied space or volume lying between the smaller units of which it is comprised, but not the void volume (*porosity*) within these units themselves. See also *Packing Fraction, Density.*

Pallet A portable platform, capable of being moved by forklift, truck, crane, etc., used for storage and transport of stacked objects or packaged (e.g., bagged) materials.

Particle In solid materials, a convenient, identifiable unit of subdivision present; ordinarily applied to loose or unconsolidated materials or to suspensions. May be a *crystallite* or *crystal,* a ground or milled fragment, a *grain* or other small *agglomerate*, etc.

Particle Density See *Density.*

Particle Size The size or size range (usually, equivalent diameter) of a given or typical *particle*, expressed either as *nanometers, micrometers,* millimeters, etc., or as *mesh* or *sieve* size. The *ultimate particle size,* the finest ordinarily achievable by *grinding* a *polycrystalline* material, sometimes equates to the size of its *crystallites.*

Particle-Size Distribution The population of *particles* of a loose or suspended material for each size increment between the minimum and maximum size present; expressed either by increment or cumulatively, usually by weight fraction or weight percent. Especially important to the *bulk density,* and to the density achievable by *compaction.*

Pascal The *S.I. unit* of *stress* or pressure. See Table I.

Pebble Mill See *Ball Mill.*

Peptize To disperse a particulate solid in a liquid, producing a *sol*, the process or procedure often including de-*agglomeration* and/or chemical stabilization of the *sol.*

Periclase Highly *crystalline,* hard-*burned magnesia,* MgO, ordinarily synthetic and of higher purity than burned *magnesite*; used extensively in *basic refractories.*

Periodic Kiln A *kiln* which is loaded, closed, fired, cooled, opened, and unloaded to complete a cycle; opposed to a "continuous" kiln which is fed and discharged continuously or semicontinuously while constantly kept hot.

Permeability The quality, of a porous solid or film, of permitting a gas or liquid to pass into it or (more often) through it. See also *Diffusion.*

pH An instrumental measure of acidity or alkalinity of water and aqueous *solutions*: the negative logarithm of the concentration of *free* hydrogen ion, H^+. At room temperature, pH = 7 is neutral; values below 7 are increasingly *acidic*; and values above 7 are increasingly alkaline or *basic.*

Phase Any *homogeneous* volume of gas, liquid (including *glass*), or specific *crystalline* solid, including its constant or fixed chemical identity. In a multiphase system,

the total of each one of these present, regardless of its own subdivision or distribution in the system, is one *phase*.

Physical Properties Those characteristics of any *substance,* material, or mixture which describe its nonchemical interactions with gravity (e.g., weight, density), heat, radiation (e.g., color, transmission, refraction), magnetism, electricity or electric fields, changes of state (e.g., melting, boiling), etc.; and often by inclusion, the *mechanical properties*. Thus, all *properties* except *chemical* and nuclear properties.

Physisorption A subtype of *adsorption* in which the bonding of *sorbate* to the surface is weak ("physical") and the *sorbate* is not chemically altered; hence, easily reversed. See *Chemisorption*.

Plastic, Plasticity Of a solid or particulate solid *mix*, the quality of readily deforming or flowing under applied force or pressure while remaining rigid under its own weight; hence *ductile* or capable of *extrusion, ramming, tamping*, or even trowelling. Alternatively, a loose term for an *organic polymer* material. See also *Creep*.

Plasticizer A processing *additive* which, by lubricity, imparts *plasticity* or workability to a material or *mix* that is otherwise difficult to deform.

Platelet A minute flat *particle* such as a *tabular alumina crystal* or typical *clay* particle. See *Morphology*.

Pneumatic Employing forced or compressed air or gas to transmit force, pressure, or motion.

Polish To make smooth, often lustrous, by a mechanical process such as rubbing or friction, often using the finest *abrasives*. See *Surface Finish*.

Polycrystalline Comprised of many *crystals* or *crystallites,* intimately bonded together. May be *homogeneous* (one *substance*) or *heterogeneous* (two or more different crystal types or compositions).

Polymer A large, even a macro *molecule,* containing a repeated atomic array or pattern. Occurs in *inorganic* systems as in *silica,* polysilicates, polyphosphates, polyaluminates, etc., as well as *organics*. Polymers impart high *viscosity* to liquids, hence are always present in *glasses* (which do not adopt the molecular or atomic ordering of *crystals* on cooling).

Polymorph In *crystals*, one of two or more geometrical forms of the same composition, i.e., its atoms occupying one of two or more different *lattices*.

Porcelain A hard, fine-*grained,* high-fired, *vitreous* (hence often *translucent*) *ceramic* body; used as table and ornamental *wares*, industrial *whitewares* (e.g., insulators), and chemical wares.

Pore A small opening, *void*, interstice, or also channel within a *consolidated* solid mass or *agglomerate*; usually larger than atomic or molecular dimensions. See also *Porosity*.

Pore Size The characteristic or equivalent dimensions or range of same (e.g., diameter) of a *pore* or family of pores in a material; usually measured indirectly by differential liquid (e.g., Hg) intrusion or cryogenic gas *adsorption*-desorption; or, microscopically on a section.

Pore-Size Distribution The specific *pore volume* of all measurable *pores* in each of a set of equivalent diameter increments from the smallest to the largest present in a material; expressed either by increment or cumulatively. Most commonly measured by mercury intrusion at successively higher pressures. See *Connected Porosity, Porosity*.

Pore Volume, Specific Pore Volume The *porosity* of a solid, otherwise subclassified, when expressed as cc/g or cm^3/g or similarly.

Pore Volume Fraction The *porosity* of a solid, otherwise subclassified, when expressed as cm^3/cm^3 or correspondingly in percent by volume.

Porosity Has meaning only for a *consolidated* form of solid, whether that be a *particle, agglomerate, grain,* formed object such as *nodule*, pellet, or larger *monolithic* mass or object. Any such single unit has a *nominal volume*, sometimes also called the *envelope volume*. Given that characteristic volume for reference, the *porosity* is the volume (hence, volume fraction) of *pores* contained in the solid within it. Since pores can be described in various specific ways, there is an equal number of corresponding expressions of *porosity:*

Macroporosity See *Macropore Volume*.
Microporosity See *Micropore Volume*.
By Size Increment See *Pore Size, Pore-Size Distribution*.
Connected or Open Porosity Also called *Apparent Porosity*.
Closed or Blind Porosity.
Total Porosity The sum of *Connected* plus *Closed Porosity*.

Porosity may also be expressed as determined by a given instrument or techniques, as, e.g.:
Mercury Porosity which approximates *Connected Porosity*.
Water Absorption which also approximates *Connected Porosity*.

To eliminate the problem of determining *nominal volume* and also for engineering convenience, *porosity* with any of the above modifiers is often determined and expressed in cubic centimeters per gram (cc/g or cm^3/g) instead of volume fraction. *Porosity* should not be confused with the *interstitial volume* or *packing space* between particles of an unconsolidated solid.

Portland Cement A *hydraulic* cement of impure and variable calcium aluminum silicate composition; made by *sintering* mixtures of *limestone* and *clay* followed by fine *grinding* or *milling*. Used in construction, not in refractories.

Potash Potassium carbonate (K_2CO_3), oxide (K_2O), hydroxide (KOH), or any of several potassium *salts* (e.g., KCl, K_2SO_4). Derived from mineral sources; used in *glass, pottery,* and *glazes*; agriculture; and *chemicals*.

Pottery The art, craft, materials, or products of the potter; *fired* earthenware or clayware domestic and art products as opposed to *porcelain* and *stoneware* on the

one hand and to industrial clay products, brick, and tile on the other.

Precipitator An industrial vessel, reactor, or apparatus in which a chemical or physical precipitation process (formation of a solid *phase*) is carried out in a liquid *medium*. Less commonly, a solid-gas *separator*.

Precritical (Subcritical) Crack Growth Growth in size of one or more cracks in a body, resulting from applied or thermal or residual internal *stress*, but not resulting in catastropic *fracture*. See *Fracture*, also *Fatigue* and *Stress Corrosion*.

Property A characteristic of a *substance*, material, or mixture that is ordinarily independent of whatever object it may happen to comprise, e.g., a characteristic of *alumina* as opposed to that of an alumina crucible. Expressed quantitatively, as measured in a specific way.

Proppant A hard, high-strength material in sandlike or *bead* form and narrowly sized, used with hydraulic fluids in oil and gas wells while fracturing subterranean rock formations, forced into the fractures to keep them from collapsing again. Increases the flow and total capacity of the well.

Pseudoboehmite An extremely fine-*crystalline* (perhaps 1 to 5 nm) *boehmite*, AlO(OH), precipitated as an indefinitely hydrous *agglomerate* by aqueous *acid-base* neutralizations involving aluminum or aluminate *salts*. Variable deliberately by choice of reagents and reaction and aging conditions. See *Gel Alumina, Substrate Alumina*.

Pug-Mill Not a *mill* as ordinarily defined, but a mechanical mixing device consisting of one or more rotating shafts bearing arms or blades, within a drum or trough.

Pycnometer An instrument comprised of a vessel of calibrated volume, such that it can be filled (and weighed) with a given liquid alone, then with the same liquid plus a weighed quantity of a denser solid material (and weighed again). The displaced volume of liquid is calculated; this is the *nominal* or *envelope volume* of the solid if the liquid does not penetrate its *connected porosity*, or its *apparent volume* if the liquid does fill all connected pores.

Pyrometry The measurement of high *temperatures* or time-temperature accumulations in a furnace or *kiln*, either by optical radiation instruments or by standardized "pyrometric cones" contrived to bend in accordance with the firing requirements of *ceramic* materials and *wares*; or by thermocouple, etc.

Quartz One of several *crystalline* forms of *silica*, SiO_2; others include cristobalite and tridymite. All occur as minerals, also synthetic. Fused silica, one of the most refractory of all industrial and optical *glasses*, is none of these and should not be misnamed as "quartz."

Quench In processing, to cool rapidly from a heated state to retain certain high-temperature properties or structural features at low temperatures where they are not stable but "frozen in" by reduced molecular motion. See *Metastable*. Alternatively, to put out, squelch, extinguish.

Quicklime See *Lime*.

Radical In *inorganic* chemistry, most commonly an *ion* comprised of a cluster of two or more kinds of *atoms*, e.g., AlO_2^- or Co_3^{3-}. A "free radical," on the other hand, is electrically uncharged.

Ram A mechanically driven plunger, piston, or head thereof, used for pressure or impact forming or *compaction* of a material or *mix*, prior to *drying, curing, firing*, or usage. *Tamping* may be a manual *ramming* operation.

Ramming Mix A dryish, semi-*plastic mix*, usually in *refractories*, formulated to be installed as a *monolithic* mass by *ramming*, impacting, or *tamping*.

Rankine (°R) An "absolute" *temperature* scale whose degree (interval) is the same as that of *Fahrenheit* but whose zero is the same as that of *kelvin*. See Table I.

Reaction A chemical change, i.e., one in which one or more chemical *substances* (reagents) are consumed and one or more new ones appear (as chemical products). Differentiated from "physical" changes, in which substances describable by chemical formulas persist but are changed in *crystalline* form, state (solid, liquid, gas), concentration, etc.

Reactivity The susceptibility of a material to chemical change or action, often by virtue of its state of subdivision, *surface area, metastable* form, composition, etc. See e.g., *Active Alumina, Substrate Alumina, Transition Alumina, Calcine, Degree of Calcination*. The opposite of inertness: see *Inert*.

Reactor An industrial vessel or device, in or by which any chemical *reaction* is conducted.

Recrystallization A process, usually physical, by which one *crystal* species is grown at the expense of another or at the expense of others of the same *substance* but smaller in size. See *Crystallization, Grain Growth*; also *Mineralizer*.

Reduce, Reduction To cause or conduct a chemical *reaction* characterized by addition of *electrons* to, hence a negative change in *valence* of, some contained *atom*. The opposite and complement of *oxidation*.

Reducing Agent or Condition An agent, or presence of an agent, e.g. in *firing*, that causes *reduction*. Prominent industrial process examples are hydrogen (H_2), carbon (C), carbon monoxide (CO), and methane (CH_4) or other hydrocarbons. See also *Oxidizing Agent*.

Reduction-Grade Ore (RGO) or Alumina A particular grade of *calcined alumina* developed especially for most effective use as feed in the manufacture of *aluminum* metal by the *Hall* electrolysis process.

Reflectance An instrumental measure of the fraction of incident light that is reflected by the surface(s) of a material, as opposed to that absorbed and/or transmitted. A complex matter, requiring detailed specification of the sample preparation and the conditions of measurement. For *aluminas*, an arbitrary scale is sometimes adopted for whiteness, brightness, or reflectance, using "100" for that of finely ground reagent-grade MgO.

Refractive Index *Refraction* is the phenomenon of directional change of light (or other electromagnetic) rays

on passing from one medium into another. The *refractive index* of every liquid or solid *substance* or other *homogeneous* medium is a measure of this phenomenon when the second medium is air or vacuum; it is the inverse velocity of light (etc.) in that medium relative to that in air. It is a function of wavelength, often of direction (see *Birefringence, Anistropy)* and of temperature.

Refractory, Refractories "High-temperature-resistant"; hence, a large family of industrial lining and construction materials that are high melting and *corrosion-erosion*-resistant when used as linings or walls of furnaces, *kilns, reactors*, and other vessels for the containment or processing of other materials (most often molten) at high temperature.

Regeneration A process, conducted periodically or cyclically, of restoring an active agent such as a *desiccant, scavenger,* or *catalyst* substantially to its initial condition after it has been reversibly altered by performance of its function or by contamination or "poisoning."

Relative Humidity The water-vapor content per volume of air or other gas, divided by the saturation level at the same temperature and pressure, i.e., by the content that would be in *equilibrium* with liquid water. See also *Dew Point.*

Repeat Unit For *substances* (*free elements* and *compounds*) that are not in fact comprised of *molecules*, the simplest convenient grouping of whole numbers of *atoms* that represents the composition, hence can be described by a chemical *formula*. In *crystals*, for example, the *repeat unit* is extended repetitively in three dimensions in the form of the *lattice*. See Tables III and IV.

Rheology Any or all of the *mechanical properties* of *fluid* or semifluid or *plastic* mixes of particulate solids with liquids.

Rockwell Hardness A *hardness* scale and instrumental method originally developed for metals, consisting of pressing or driving a small diamond cone into the surface and measuring the required driving force.

Rotap A laboratory apparatus for shaking a material on a graded succession of *sieves* to determine the *particle-size distribution* by selected *mesh* or *sieve sizes.*

Rotary (drier, calciner, kiln) An inclined cylindrical tube, heated externally or more often internally, which rotates about its axis while feed material enters the elevated end and the processed product exits the other. Imparts a rolling or overturning motion to the bed.

Rutile A particular *crystalline* form of titanium dioxide, TiO_2; useful as a pigment and as an *additive* or component in some *ceramic, glass,* and *glaze* manufacture. See *Opacifier,* also *Mineralizer.* See also *Anatase.*

Sagger A fired *ceramic* container used to hold *ware* during firing in a *kiln*, often also to protect the ware from direct flame impingement.

Salt In *inorganic* chemistry, any *compound* of a metallic *element, cation,* or *radical* (other than H) combined with a nonmetallic element, *anion*, or radical (other than OH or simple O). See also *Acid, Base.*

Sandy Of a particulate material, resembling fine sand in its state of subdivision and *angle of repose,* hence of free-flowing, nondusting quality. As in *calcined aluminas*, contrasted with *floury.*

Sanitary Ware *Porcelain enameled* metal or else *ceramic ware* such as sinks, lavatories, and bathtubs. Impermeable at least at the surface.

Scale, Scaling The formation of a layer of *agglomerated* or *sintered* solid material on the working surfaces of a reaction vessel, container, precipitator, drier, calciner, kiln, etc., whereas the processed material is intended to remain *fluid* or suspended. The layer of material so formed.

Scanning Electron Microscope (SEM) A high-power magnifying and imaging instrument using an accelerated electron beam as an optical device, and containing circuitry which causes the beam to traverse or scan an area of sample in the same manner as does an oscilloscope or TV tube. May utilize reflected (SEM) or transmitted (TEM) electron optics.

Scavenger An active agent, frequently a porous solid as, for example, *active alumina*, utilized to remove specific chemical *contaminants* (e.g., fluorides) from industrial waste streams or in water treatment.

Screen A wire mesh with specific sized openings for grading or separating various sizes of particulate or granular solids, or to "scalp" large *agglomerates*, rocks, and coarse tramp material. See *Mesh,* also *Sieve.*

Second The *S.I. unit* of time: an international standard.

Sedigraph An instrument for determining the *particle-size distribution* of a particulate solid, making use of a physical relation between rate of settling ("sedimentation") in a liquid and the particle size.

Seed Small *particles* or *agglomerates, crystals,* or *crystallites* introduced in large numbers into a vessel to serve as nuclei or centers for further growth of material on their surfaces. See *Crystallization, Agglomeration, Nucleation.* Alternately, in *glass*, a small bubble (manufacturing defect); see also *Cord, Stone.*

Select(ed) Converter Discharge (SCD) A *nodulized tabular alumina* product with most chips and spalls removed; or, size-classified.

Semiconductor An otherwise nonconductor of electricity, promoted to limited electronic conduction either thermally or by alloying or "doping" according to certain principles of metallurgical chemistry or physics.

Separator A device for removing particulate solids from an entraining gas stream or of selectively removing one solid component; as for example a *cyclone, electrostatic precipitator,* magnetic or electrostatic separator, or *classifier.*

Setting Time Of a cement or concrete or similar *plastic* mix, the time required from placement or forming until the material becomes suitably hard or rigid. See also *Working Time.*

Settling Tank See *Clarification.*

Shaft Kiln A direct-fired stationary cylindrical *kiln* on a vertical axis, whose charge or bed is continuously fed from above and discharged through a gate below, mov-

ing slowly downward by gravity. Capable of extremely high firing temperatures, to above 2000°C or 3630°F in some cases.

Shear Modulus See *Elastic Modulus.*

Shrinkage The fractional reduction in dimensions or volume of a material or object when subjected to *drying, calcining,* or *firing* (*sintering*).

S.I. (Système Internationale) Units The recommended set of "metric" units of measurement, now widely promulgated in tables and handbooks. Those in commonest use are shown here in Table I: the *meter* (*m*), *gram or kilogram* (*g* or *kg*), *second* (*s*), *newton* ($N = kg \cdot m/s^2$), *pascal* ($Pa = N/m^2$), *joule* ($J = N \cdot m$), *watt* ($W = J/s$), and temperature in *kelvins* (*K*) or in *degrees Celsius* (°*C*). See also decimal fractions and multiples given in the table.

Sieve A standard wire *mesh* or *screen,* especially when used in graded sets to determine the *mesh size* or *particle-size distribution* of particulate and granular solids. See also *Subsieve.* See Table I.

Sieve Analysis The *particle-size distribution* of a particulate or granular solid or sample thereof, when determined by passage through and retention on a graded set of *sieves.* See Table I.

Silica Silicon dioxide, SiO_2, in any of its *crystalline* or *glassy* forms. See also *Quartz,* one member of the family.

Silica Gel A precipitated *colloidal* mass or *gel* of indefinitely *hydrated silica*; also, the dried or *activated* product of same. Useful as *desiccant, scavenger,* and *catalyst substrate.*

Sillimanite An anhydrous aluminum silicate mineral, Al_2SiO_5, *polymorphous* with *kyanite* and *andalusite.* For uses, see *Kyanite.*

Sinter To densify, *crystallize,* bond together, and/or stabilize a particulate material, *agglomerate,* or product by heating or *firing* close to but below the *melting point.* Often involves *melting* of minor components or constitutents, and/or chemical *reaction.* Also, the product of such firing. See also *Clinker.*

Size, Sizing Apart from the common reference to dimensions, a material used in papermaking to fill or coat the fibers, add body, and inhibit the penetration of liquids. Also, similar materials used in textiles.

Skeletal Density See *Density.*

Slag A mixture of oxides formed and lying over a charge of molten metal; generally containing deliberate *additives* and *fluxes,* used to control its chemical composition and ensure melting and coalescence to form a protective layer.

Slake To cause to undergo initial *reaction* with water (i.e., *hydration*), as applied to a *hydraulic cement* or *lime* or other similar anhydrous materials.

Slip A *slurry* or suspension of fine *clay* or other *ceramic* powders in water, having the consistency of cream; used in *slip casting* or as a cement or *glaze* preparation.

Slip Casting The *ceramic* forming process consisting of filling or coating a porous *mold* with a *slip,* allowing to dry, and removing for subsequent *firing.*

Slurry Any pourable suspension of a high content of insoluble particulate solids in a liquid medium, most often water.

Soda Sodium carbonate (Na_2CO_3) or bicarbonate ($NaHCO_3$) or hydroxide (*caustic soda,* NaOH); or, any contained or combined form of sodium in a material, including as *impurity,* expressed as the equivalent Na_2O. See also *Leachable Soda.*

Sol-Gel Process An important *ceramic* process operation in which a *sol* is converted to a *gel* by partial evaporation of the liquid *phase* and/or by neutralizing the electric charges on particles which cause them to repel each other. The *gel* is usually further processed (e.g., formed, dried, fired).

Solution A *homogeneous* or single-*phase,* variable-composition mixture of one *substance* (solute) in another (solvent), in which the former is dispersed as separated *molecules, ions,* or *atoms.* The solvent or the solution may be solid, liquid, or gas.

Sorbate In any process of *sorption,* the species in the fluid medium which enters preferentially into the solid and adheres to its surfaces. See *Adsorption.*

Sorption In general, the taking up of some substance (sorbate) into or on the surface of another (sorbent), without specification of the type of process. See *Absorption, Adsorption, Chemisorption, Physisorption.*

Spall To break off chips, slabs, shells, or fragments from a more massive solid piece or article, usually by rapid temperature change. Also, the smaller fragment resulting from such action. See also *Onionskin.*

Specific Prefix to many *properties,* as *specific heat* = heat capacity, *specific resistance* = resistivity, *specific conductance* = conductivity; *specific volume, specific surface,* etc. Refers to the given property expressed per unit weight or per unit volume of a material and/or otherwise for some reference conditions. Used for concise numerical tabulations of properties or coefficients, such that dimensions, etc., can be reintroduced in engineering equations to derive statements of behavior in many and varied real situations.

Specific Gravity (sp. g.) The ratio of the *density* of any material to the *density* of pure water at 4°C, i.e., the maximum density of water; infrequently, to the density of water at the same temperature as the material. Both densities must be expressed in the same units, hence the *sp. g.* is dimensionless. Subject to all the modifiers of the term "density" in use for solid materials, and having the same meaning, hence:

Apparent Specific Gravity is obtained from the *Apparent Density*

Bulk Specific Gravity is obtained from the *Bulk Density*

Particle or Grain-Specific Gravity is obtained from the *Particle Density*

Theoretical Specific Gravity is obtained from the *Theoretical Density.*

Specific Volume The volume per unit weight (e.g., per gram or pound) of any material; the inverse of *densi-*

ty. Subject to all the modifiers of the term "volume" in use for solid materials, as: *Apparent Volume, Bulk Volume, Nominal Volume, Theoretical Volume.*

Spinel Any of a group of *compounds* of the same *crystal* type and general formula as magnesium aluminate, $MgAl_2O_4$ or $MgO \cdot Al_2O_3$. That compound itself, which is refractory and chemically near-neutral. See *Spinel Refractories.*

Spinel Refractories *Refractory* materials containing an *aggregate* of *spinel*; or, alternatively, "spinel-bonded" refractories comprised of *periclase* or *alumina aggregate* with a spinel *bond* or *matrix.*

Spray Dryer A large vessel into which a *slurry* is sprayed through orifices in a stationary or revolving head and thrown as droplets into a stream of heated air which dries them. The dried droplets are typically tiny *agglomerates*, often in hollow bead form, hence free-flowing.

Standard, Standardized Of a reagent or material, or an analytical or instrumental measurement method or procedure, one which is fixed, specified, or established, often calibrated, so as to produce reliable results that are sensibly the same wherever used or employed.

Standard Practices Method(s), Manual A set of standard or standardized analytical and test methods and procedures, adopted and catalogued by a given laboratory.

Stone In *glass*, a foreign object, typically non*vitreous.* See *Cord, Seed.*

Stoneware A *vitreous* or semivitreous fine-textured *ceramic* body or *ware,* made primarily from various moderate-firing *clays.*

Strength For *brittle* materials, see *Fracture Strength.*

Stress Restoring force of a body (or local part of it) when strained, i.e., deformed. Expressed in units of force/area, e.g., *pascals.*

Stress Corrosion *Corrosion* at the tip of a *flaw* or crack, enhanced by a local state of *stress*, resulting in *precritical crack growth* or *fracture.*

Subcritical Crack Growth See *Precritical Crack Growth.*

Subsieve Size In particulate solids, those sizes passing through a 325 mesh or 400 mesh *screen* or *sieve* and hence of diameters less than 44 or 37 μm. Sizes in this fine range are measured, classified, or analyzed by sedimentation methods and importantly by various types of "particle counters" based on other properties of suspensions. See *Particle-Size Distribution*; also *Sieve Analysis.*

Substance A chemical entity (*free element* or *compound,* and *crystal* or other form of same) describable by a fixed *formula* giving the composition by relative numbers of *atoms.* Opposed to *solution, mixture,* etc., which are not of narrowly fixed composition. See Use of Tables of Chemical Elements; also *Valence.*

Substrate A body, board, or layer of material, on which some other active or useful material(s) or component(s) may be deposited or laid, as, for example, in electronic circuitry laid on an *alumina ceramic* board. In *catalysts*, the formed, porous, high-surface-area *carrier* on which the catalytic agent is widely and thinly distributed for reasons of performance and economy.

Substrate Alumina *Alumina* especially for use as *substrate* in the second definition given above; and, particularly, such an alumina originating as *gel alumina,* hence as *pseudoboehmite* or *boehmite.* After forming, *catalyst* application, and *activating* or *calcining,* likely to be *gamma* or other *transition alumina.* Other useful substrates of alumina may be made from *active alumina* or still other forms. See also *Nodules* and *Extrudates* as to geometrical shapes.

Sulfuric Acid Formula H_2SO_4; a relatively inexpensive, nonvolatile *acid* of great industrial usefulness and large commercial tonnage.

Surface Of solids, the external boundary; or, alternatively, the total of external and all internal surfaces bounding *pores, voids,* channels, crevices, cracks, etc.

Surface Activity, Acidity, Basicity The extent and degree of *adsorptivity* or *reactivity* (*acidity, basicity,* etc.) of a given area of accessible solid *surface*, resulting from chemical modification and crystalline or other imperfections thereon. *Aluminas* are capable of extensive tailoring of these properties. See also *Acid Site, Basic Site.*

Surface Area The area, per unit weight of a granular or powdered or formed porous solid, of all external plus internal *surfaces* that are accessible to a penetrating gas or liquid. See *Connected Porosity*, also *BET.*

Surface Finish Degree of roughness or of surface damage left by a finishing operation (grinding, polishing, etc.). Apart from obvious importances, may control the severity of surface *flaws.*

Surface Tension A measure of the cohesive forces among surface *molecules*, etc. Generally represented by *energy* per unit surface area, sometimes by force per unit edge length. See *Interfacial Tension.*

Symbol Chemist's quantitative representation of (one *atom* of) a free or combined *element.* See Use of Tables of Chemical Elements.

Synergism, Synergistic A quality of mutual reinforcement of some *property* by two components or agents, such that the property of some mixture of the two is more favorable than the linear combination or weighted average between them. Also can be extended to three or more components. Often exhibited, for example, by aluminas in combination with additives, modifiers, or promoters.

Tabular From "table": platelike or *platelet* in *crystal morphology* or habit.

Tabular Alumina High-fired, dense *alpha alumina*, whose relatively large *crystals* or *grains* are predominantly of *tabular* or *platelet morphology.*

Talc, Talcite A *hydrated* mineral of predominantly magnesium silicate composition, $Mg_3Si_4O_{10}(OH)_2$ or related, whose layered *crystals* have a slippery or soapy quality.

Tamp To form or *compact* a *ceramic* mixture or a particulate solid by tamping or repeated impact, usually

performed manually. See also *Ramming.*

Temperature A measure of the intensity of *molecular* and/or *atomic* kinetic activity or energy (see *Heat*), such that this energy flows spontaneously from any body at a higher temperature to any other at a lower temperature in communication with it. See *Celsius, Kelvin, Fahrenheit, Rankine.* See Table I.

Tensile Strength The maximum load or stress borne by unit cross section of a solid material at fracture, when pulled apart in tension. See *Fracture.*

Theoretical Of a material *property* such as density, strength, etc., the calculated value for a perfect or ideal model of the material.

Theoretical Density, Specific Gravity See *Density, Specific Gravity.*

Theoretical Volume Of a quantity of a solid material, the volume it would occupy if all *voids* were removed and the material were at 100% of its *true* or *theoretical density.* See *Diffraction* as a means of measuring.

Thermal Conductivity A measure of the ability to transmit *heat* through a mass of given material, expressed as heat flux per unit of *temperature* gradient, either at a given base temperature or by a temperature-dependent equation.

Thermal Expansion (Coefficient of) The linear or volume expansion of a given material per degree rise in *temperature,* expressed at an arbitrary base temperature or as a more complicated equation applicable to a wide range of temperatures.

Thermal Shock A large and rapid *temperature* change, resulting in large temperature differences within or across a body. See *Thermal Stress.*

Thermal Stress Internal stresses developed within a body by virtue of *temperature* gradients or differences and accompanying *thermal expansion* or contraction effects. Can result in fatigue, fracture, or *spalling* in brittle materials.

Thermogravimetric Analysis (TGA) An instrumental method of continuously recording the weight of a material sample (exposed to controlled atmosphere or vacuum) while its *temperature* is gradually raised and recorded. Gives evidence of evaporation and of *reactions* (e.g., combustion, decomposition) producing volatile products. See also *Differential Thermal Analysis.*

Thixotropic, Thixotropy Of *colloidal* suspensions, the *property* of decreasing in *viscosity* (i.e., of becoming more *fluid*) under increasing shearing force or speed. See also *Dilatant.*

Torr A unit of pressure, namely that of a column of mercury 1 mm high (i.e., mm Hg). See Table I.

Total Porosity See *Porosity.*

Toughness See *Fracture Toughness.*

Transition A physical change from one *crystalline* form to another or a change of state (solid, liquid, gas), in any direction.

Transition Aluminas A family (several series) of *metastable crystalline aluminas* containing minor but detectable OH^- as well as O^{2-} *ions.* Produced more or less sequentially by gradual heating of the different *alumina trihydrates* and *monohydrates*; also in some cases synthesized by other processes. Examples are *active alumina, substrate alumina,* and the light-burned *calcines*

Translucent Transmitting some incident light, but no clear images due to scattering within the material.

Tub A wide, low, circular vessel; a rotating pan for *nodulizing.*

Tunnel Kiln A direct-fired (less often, indirect-heated continuous *kiln* in the form of a stationary tube or tunnel, through which cars containing *ceramic* or *refractory wares* are pushed as a train. Usually "zoned" for controlled heating and cooling rates and for soaking at the maximum temperature.

Valence (Oxidation State, Formal Charge) One or more + or − integers giving the difference between the number of *electrons* on an *atom* in its *free* state and that in a *combined* state. Since in *compounds* these add up to zero and in *radicals* to the *ionic* charge, chemical *formulas* are determined. Examples: given Mg[+2] Cr[+3 or +6], O[−2], Mg_xO_y is MgO, Cr_xO_y is Cr_2O_3 or CrO_3, $Mg_xCr_yO_z$ is $MgCr_2O_4$ or $MgCrO_4$ or $MgCr_2O_7$; $Cr_xO_y^-$ is CrO_2^-, $Cr_xO_y^{2-}$ is CrO_4^{2-} or $Cr_2O_7^{2-}$ etc. This is somewhat simplified, e.g., not all species whose formulas can be written actually exist.

Vapor Same as gas; to be precise, a condensible gas.

Viscosity A measure of the resistance of a *fluid* (liquid or gas) or semifluid material to motion in shear, viz. one layer across another; determined by specified instrumental methods.

Vitreous Partially or completely comprised of a *glass*; often containing solid *particles* distributed therein.

Vitrify To render *vitreous*, generally by heating; usually, achieving enough *glassy phase* to render impermeable.

Void Any empty (or, gas-filled) space in a solid material: see *Packing Space, Pore, Porosity.* A *void* in a liquid is called a bubble.

Volatile A relative term expressing the tendency to form *vapor*, e.g., at room temperature or in some other temperature domain.

Volatilize To vaporize, convert to the *vapor* or gas state including to boil; applied also to a component, including as a result of decomposition or other chemical change. To sublime (pass from solid to gas without intervening liquid).

Volume See under modifier: *Apparent Volume, Bulk Volume, Nominal Volume, Theoretical Volume,* and others. See also *Density, Specific Volume.*

Ware Formed or shaped or manufactured articles (*ceramic* or otherwise), of utility derived from design as well as material. Also, broad classes of body and/or surface coating compositions or materials of which ceramic articles are comprised.

Water H_2O. Described in quantitative analytical terms suited to its presence as a solvent, host, medium, diluent, lubricant, plasticizer, constituent, sorbate, component (physical or chemical), etc., by a host of specified procedures meaningful respectively to the

many pertinent systems, uses, and circumstances. These measures and their methods must be clearly understood in relation to the materials, processes, and technologies to which they relate. Following are classifications of water as a *component* of a solid:

Combined Water That fraction or percentage composed of H_2O that is chemically combined as part of one or more *compounds* present; see *Hydrate.*

Free Water That fraction or percentage composed of H_2O that is present as "moisture," "dampness," or "wetness": i.e., *absorbed* and *occluded.*

Bound Water Especially in high-surface-area materials, that fraction or percentage composed of H_2O that is *adsorbed* (subdivided as *physisorbed* or *chemisorbed*) on the surface. *Chemisorbed* and *combined water* as defined here may, however, be quite difficult to distinguish; and indeed the distinction between *adsorbed* and *absorbed* water may not be sharp either. Hence, often, a resort to arbitrary analytical methods.

Water Absorption The amount of liquid water absorbed by a *consolidated* (though porous) solid under a fixed test procedure; commonly expressed as weight percent of the dry material. Can be converted arithmetically to cm^3/g or to vol% as a measure of *porosity.*

Watt (W) The *S.I. unit* of power: one *joule* per second.

Weibull Statistics A mathematical system describing the distribution of severity of *flaws* in a material, hence the distribution of its measured *fracture strengths* when *precritical crack growth* is absent.

Whitewares A broad class of fired *ceramic* products or bodies that include *china, porcelain, stoneware,* earthenware, pottery, and tile; often but not necessarily white; usually relatively fine-textured, and usually to some degree *vitreous* but often permeable unless *glazed.*

Work The equivalent of *energy,* but often restricted to mechanical forms such as force × distance, pressure × volume.

Working Time In a *plastic,* especially cementitious *mix,* the time elapsed from mixing the ingredients until the desired plastic or forming qualities have degraded by progressive aging, curing, etc., such as to lead to inferior forming or placement.

X ray Radiant energy falling within a band of wavelengths or frequencies, or energy quanta, corresponding to any of numerous electronic transitions within excited *atoms.* Shorter in wavelengths and more penetrating than uv; ionizes matter. Useful in numerous instrumental and analytical methods including *diffraction* and various kinds of spectrometry.

Young's Modulus See *Elastic Modulus.*

Yttria Yttrium oxide, Y_2O_3; used as a chemical modifier of some *aluminas,* other oxides, etc.

Zeolite(s) Any of a large family of mineral or synthetic *hydrated crystalline* alkali metal aluminosilicates, having the properties of *molecular sieves.*

Zirconia Zirconium oxide, ZrO_2, in any of several *crystal* forms. Used as a structural *ceramic,* "oxygen sensor" in analyzing combustion gases, *refractory* material, *catalyst,* or *substrate, ceramic* modifier, etc.

Contributors

WATE T. BAKKER *Alumina Usage in Electric Power Generation and Storage*

Bakker is Technical Area Manager, Materials Support Program, at the Electric Power Research Institute (EPRI) in Palo Alto, CA. Before joining the Institute in 1979, Mr. Bakker spent four years as Chief of the Materials Branch of the Fossil Energy Department at the Department of Energy in Washington, DC. From 1966 to 1975, he was a Research Associate for General Refractories Company, Baltimore, MD. From 1961 to 1966, Bakker worked as a Research Chemist for the Aluminum Company of Canada, based in Arvida, Quebec. Prior to this, he was a Geophysicist with the Royal Dutch Shell Company, The Hague, Netherlands. Mr. Bakker received a Professional Engineer's degree (M.S. with Ph.D. course completion) from the Delft Technical University, Netherlands. His areas of specialty were mineralogy, geophysics, and geology. The author of numerous publications, primarily on the subjects of refractories, ceramics, and gasification, Mr. Bakker also holds nine patents. He is a Fellow of the American Ceramic Society and has held numerous offices in ACerS, including that of Chairman of the Refractories Division. In 1985, he received the Allen W. Allen Award for his paper "Refractory Practice in Slagging Gasifiers."

LUKE M. BAUMGARDNER *World Production and Economics of Alumina Chemicals*

Mr. Baumgardner serves in the Washington, DC, office of the Bureau of Mines as the Bauxite and Alumina Commodity Specialist, a position he has held since 1980. He is responsible for the collection and reporting of worldwide data on production, consumption, capacity, and trade in these commodities. Prior to this position, he worked as a Geologist with a mineral consulting firm; as an Exploration Manager directing bauxite exploration programs in Australia, Brazil, and Southeast Asia; and as a Marine Geologist carrying out research in the Atlantic and Pacific Oceans and the Caribbean, Mediterranean, and Black Seas. Mr. Baumgardner received a B.S. degree in Geology from the University of Wisconsin in 1951.

BURTON J. BEADLE *Co-author, A Glossary of Terms Most Frequently Used in Alumina Technology*

Mr. Beadle retired from Kaiser Aluminum and Chemical Corporation in 1983 as the Technical Service Manager of Hydrated, Calcined, and Tabular Aluminas. He had been with Kaiser since 1953, working as a Bayer Plant Process Control Engineer; area Technical Superintendent in the areas of Digestion, Precipitation, and Calcination; and Production Area Superintendent and Production Manager in the Chemical Division Special Products Plants. Prior to his employment at Kaiser, Beadle worked at Cities Service Refining Corporation as a Chemical Engineer in Pilot Plant Research, in Process Control, and as a Technical Superintendent in the Topping and Catalytic Cracking Units. Mr. Beadle received a B.S. degree in Chemical Engineering from the University of Southwestern Louisiana in 1943.

ROBERT J. BEALS *Dinnerware Manufacture and Use in the United States*

Dr. Beals joined the Department of Ceramic Engineering of the University of Illinois in 1947 as a Research Assistant. He resigned in 1962 as Associate Professor of Ceramic Engineering to join the Argonne National Laboratory as Associate Ceramist. In 1969, he became Technical Director of the Chas. Taylor Sons Co., Cincinnati, OH; and in 1971, he became Director, Research and Development, of the Hall China Company, where he now works. He is the author of approximately 30 technical papers and holds one patent. Beals received a B.S. degree in Chemical Engineering in 1947, an M.S. degree in Ceramic Engineering in 1950, and a Ph.D. in Ceramic Engineering in 1955, all from the University of Illinois at Champaign-Urbana. Dr. Beals is a Fellow of the American Ceramic Society, where he has served on the Board of Trustees and as Treasurer, President-Elect, and President. He is active in the National Institute of Ceramic Engineers and the Ceramic Educational Council, he was initiated into the Keramos Fraternity at the University of Illinois and has served as its National President, and he is a member of Sigma Xi. Dr. Beals represents the National Institute of Ceramic Engineers on the Engineering Accreditation Commission of the Accreditation Board for Engineering and Technology.

ALAN BLEIER *Colloidal Properties of Alumina*

Bleier joined the Structural Ceramics Group at Oak Ridge National Laboratory in 1983 after serving on the faculty in the Department of Materials Science and Engineering at the Massachusetts Institute of Technology. Prior to that position, he was a Research Chemist in mineral beneficiation at Union Carbide Corporation. He earned his Ph.D. in Physical Chemistry from Clarkson University in 1976. His research interests focus on fundamental and generic principles of ceramic processing, especially surface thermodynamics of oxide powder dispersibility, adsorption of polyelectrolytes, and control of composite ceramic suspensions that contain more than one type of powder. Bleier has authored over 30 scientific papers, has served as Program Chair for the Symposium on Structures in Concentrated Colloidal Suspensions at the 58th Colloid and Surface Science Symposium of the American Chemical Society, Chairman for the P&G Fellowship Committee for the Division of Colloid and Surface Chemistry of the American Chemical Society, and serves in various editorial roles for the American Ceramic Society.

JOHN W. BORETOS *Alumina as a Biomedical Material*

Boretos is a Physical Scientist and Senior Materials Engineer with the Biomedical Engineering Branch of the National Institutes of Health, Bethesda, MD. Over the past 25 years, he has provided direct and consultative materials support to medical research in areas such as devices for extracorporeal circulation of blood, vascular and valvular prostheses, maxillofacial and dental prostheses, and electronic and neurosurgical implants. He is the author of the book *Concise Guide to Biomedical Polymers,* editor of the book *Contemporary Biomaterials, Materials and Host Response, Clinical Applications, New Technology, and Legal Aspects,* and he is a contributing author to many other books. He holds several materials and medical device patents and has published extensively on his work related to biomaterials.

H. KENT BOWEN *Co-author, The Future Role of Alumina in Ceramics Technology*

Dr. Bowen is the Ford Professor of Engineering at the Massachusetts Institute of Technology. He is also Director of

MIT's Manufacturing Systems Engineering and Management Program and the Ceramics Processing Research Laboratory. Professor Bowen received a B.S. degree in Ceramic Engineering in 1967 from the University of Utah and a Ph.D. from MIT in 1971. His research has focused on ceramic materials and materials processing, which has led to well over 100 published papers and co-authorship of the key textbook in the field. He has received many awards in recognition of his contributions to the literature and leadership in his field, and he was selected by *R&D* magazine as the 1986 Scientist of the Year.

RICHARD C. BRADT *Co-author, Mechanical Properties of Alumina*

Dr. Bradt is the Dean of the Mackay School of Mines, University of Nevada-Reno. Prior to this, he was at the University of Washington, serving as their first Chairman of the Materials Science and Engineering Department and then as the Kyocera Professor of Ceramic Engineering. Dr. Bradt came to the University of Washington from the Pennsylvania State University, where he was the Head of the Department of Materials Science and Engineering, which included programs in Ceramic Engineering, Metallurgy, Polymer Science, and Fuel Science. Bradt received a B.S. in Metallurgy from MIT in 1960 and an M.S. (1965) and Ph.D. (1967) in Materials Engineering from Rensselaer Polytechnic Institute, NY. An active educator and researcher both in the U.S. and Japan, Dr. Bradt has edited or co-edited a dozen volumes of conference proceedings, co-authored two undergraduate texts, and published nearly 200 technical papers. His research interests include thermal expansion; thermal shock damage; fracture of structural technical ceramics, glasses, carbons, and commercial refractory materials; and the processing of materials. His contributions to the study of the mechanical behavior of glasses and ceramics were recognized in 1980 by the receipt of the Richard M. Fulrath Award from the American Ceramic Society. Bradt is a Fellow of the American Ceramic Society, has served ACerS as a Vice-President and as a Trustee, and is active in the Refractories Division.

WARREN S. BRIGGS *Pelleted Catalyst Systems*

At present, Dr. Briggs is an Independent Consultant. From 1957-1986, he was employed by W.R. Grace and Company, Davison Chemical Division, where he held various positions including Group Leader, Research Supervisor, Director of Research, Technical Director, Technical Services Director, and General Manager. Prior to Grace, Briggs worked at Houdry Process Corporation as a Research Chemist. Dr. Briggs received a B.S. in 1948 from Juniata College, Huntingdon, PA, and a Ph.D. in 1955 from Northwestern University. He holds 35 patents and has authored eight papers and one chapter on Applied Industrial Catalysis.

THOMAS J. CARBONE *Production Processes, Properties, and Applications for Calcined and High-Purity Aluminas*

Since 1984, Mr. Carbone has been Market Manager of the Industrial Chemical Division of Alcoa, which includes the ceramics, refractory, and abrasives markets. He is responsible for pricing and strategic planning for existing alumina products and for new product development. Carbone's previous positions with Alcoa include working in various R&D positions at the Alcoa Technical Center. Prior to coming to Alcoa, he worked as a Development Engineer at Union Carbide and served as Commercial Development Representative and Research Engineer at PPG. Mr. Carbone holds B.S. and M.S. degrees in Ceramic Engineering from Alfred University.

STEPHEN C. CARNIGLIA *Co-author, A Glossary of Terms Most Frequently Used in Alumina Technology*

Dr. Carniglia retired from Kaiser Aluminum and Chemical Corporation as the Manager, Chemicals R&D. He had been employed at Kaiser since 1970, first working as a Senior Scientist, Refractories R&D, before moving to Section Head, Chemicals R&D. He also spent 14 years at Rockwell International Corporation as Group Leader and Project Manager of Nuclear and Aerospace Materials R&D. He headed the Chemistry Department at the College of Marin, CA, and continues to be a Guest Lecturer/Professor/Consultant in his retirement. Carniglia received a B.S. (1943), an M.S. (1945), and a Ph.D. (1954) in Chemistry, all from the University of California at Berkeley. He is the author of approximately 36 research papers and publications in chemistry, materials science, refractories, and catalysis. He is a member of Phi Beta Kappa, Sigma Xi, Keramos, and the Catalysis Society. He is a Life Member and Fellow of the American Ceramic Society, and in 1974, he received their Ross Coffin Purdy Award.

PAWEL CICHY *Fused Alumina—Pure and Alloyed—as an Abrasive and Refractory Material*

Cichy studied technical chemistry at three European universities and completed his education with a degree in Chemical Engineering in London, England. He spent one year in organic synthesis research and pilot plant development at the British Celanese, Spondon, England. After working briefly in an analytical laboratory in Toronto, Canada, he was employed as a Group Leader in alumina and bauxite reduction research in Arvida, Quebec, at the Aluminum Laboratories Ltd. for ten years. The next 26 years were spent with The Carborundum Co., Niagara Falls, NY, as a Research Specialist and Principal Engineer in electrothermics and research and development of high temperature compounds. Cichy has written eight publications and holds 12 U.S. and numerous foreign patents. He is presently self-employed as a consultant.

MICHAEL CIMA *Co-author, The Future Role of Alumina in Ceramics Technology*

Dr. Cima is the IBM Assistant Professor of Materials Science and Engineering at the Massachusetts Institute of Technology. He earned a B.S. in Chemistry in 1982 and a Ph.D. in Chemical Engineering in 1986, both from the University of California at Berkeley. His general research interest is in applying chemical principles to the area of ceramics processing and powder synthesis. Dr. Cima has begun work to investigate the chemical and transport phenomena involved in solvent and binder removal from ceramic greenware. He is a member of the Electrochemical Society and the Materials Research Society.

C.N. COCHRAN *Co-author, Gallium*

At Alcoa Laboratories since 1947, Mr. Cochran has managed and conducted research on catalysis and gas sorption with aluminas, aluminum purification, oxidation of aluminum, gas in aluminum, fluxes for joining of aluminum, composites, gallium arsenide, aluminum nitride, modeling of chemical processes, use of aluminum in transportation, energy in the aluminum industry, technology forecasting, aluminum in

batteries, and aluminum smelting processes. He obtained a B.S. in Chemistry from Westminster College, New Wilmington, PA, in 1945 and an M.S. in Physical Chemistry from the Ohio State University in 1947. He has published 37 papers and holds a dozen patents.

LAWRENCE P. COOK *Phase Equilibria of Alumina*

Cook joined the staff of the National Institute of Standards and Technology (formerly the National Bureau of Standards) in 1974, where he has continued since then to work in the areas of ceramic processing and phase equilibria. Dr. Cook has numerous publications in these areas. He served as Director of the Phase Diagrams for Ceramists Data Center during the initial stages of its expansion and the development of the joint NIST/ACerS phase equilibria program. He has served as co-editor of Phase Diagrams for Ceramists and is the chief editor of Volume VI in this series. Dr. Cook's general areas of interest include thermodynamics, crystal chemistry, and phase equilibria; kinetics of high temperature transformations; and interfacial phenomena. He completed his formal education in Geology at three universities: A.B., Princeton, 1966; M.A., University of Texas at Austin, 1969; Ph.D., Harvard University, 1975. Dr. Cook was the recipient of the Department of Commerce Bronze Metal Award; he is a member of the Mineralogical Society of America and the American Ceramic Society.

MICHAEL S. CROWLEY *Co-author, Petroleum and Petrochemical Applications for Refractories*

Dr. Crowley has been Senior Research Associate at Amoco Corporation since 1959; he is responsible for materials selection, research, and evaluation in the areas of refractories, fireproofing, insulation, concrete, plastics, rubber, and other nonmetals and the design of refractory linings and field inspection of installation and repair. Crowley received a B.S. in Ceramic Engineering from Iowa State University in 1953. He worked as a Research Engineer at the Standard Oil Company (Indiana) from 1953-1955, when he became API Fellow at the Pennsylvania State University. He earned a Ph.D. in Geochemistry from Penn State in 1959. A registered Professional Engineer in Illinois, California, and Texas, Dr. Crowley is a Fellow of the American Ceramic Society and a member of the National Institute of Ceramic Engineers, Keramos, ASTM, Sigma Xi, and NSPE. He served as chairman of the Refractories, Metal Properties Council Task Force on Materials of Construction for Coal Gasification, 1972-1977.

BERTRAM D. DINMAN *The Aluminas and Health*

Dr. Dinman is Clinical Professor of Occupational Medicine at the Graduate School of Public Health of the University of Pittsburgh. He received an M.D. from Temple University in 1951 and a Sc.D. in Industrial and Environmental Health from the University of Cincinnati in 1957. Dr. Dinman was on the faculty of the Ohio State University College of Medicine from 1957 until 1965, then Professor and Director of the Institute of Environmental and Industrial Health at the University of Michigan School of Public Health until 1973. He then became Alcoa's Medical Director; in 1977, he was named General Manager, Health and Safety Services, and in 1978 he was elected Vice President, Health and Safety. Dr. Dinman is a Fellow and Past President of the American Academy of Occupational Medicine and a Fellow and Past Vice President of the American College of Preventive Medicine. He is a Fellow of the American Occupational Medical Association and a member of the American Industrial Hygiene Association, American Medical Association, and Society of Toxicology. An author of over 100 scientific and medical papers, Dinman has received merit awards from the Industrial Medical Association and the American Academy of Occupational Medicine, and he was the American Academy of Occupational Medicine's 1982 Gehrmann Lecturer.

JUDITH C. DOWNING
Co-author, Production Processes, Properties, and Applications for Activated and Catalytic Aluminas
Co-author, Claus Catalysts and Alumina Catalyst Materials and Their Application

Downing is currently the Marketing Manager for the Petrochemicals/Catalyst Division of the Alcoa Separations Technology Division. She has over eleven years of service and experience in development engineering, sales, and technical service in the Claus catalyst and alumina catalyst materials markets. Downing earned a B.S. degree in Engineering from Virginia Polytechnical Institute and State University. She has co-authored papers and conducted seminars on the deactivation mechanism and activity maintenance of Claus catalyst.

GREG FISHER *Alumina as a Composite Material*

Fisher is currently with the Chemical Abstracts Division of the American Chemical Society. Prior to his association with ACS, he served as Director of Technical Services at the American Ceramic Society. In this role, he authored more than 15 technical and business review articles which have been extensively cited by the ceramics community, including articles dealing with the state of the art in ceramic composites, heat engine ceramics, and the current market position of advanced ceramics. Fisher received a B.S. in Physics and a B.A. in Philosophy from Rutgers University in 1974 and an M.S. in Ceramics Science and Engineering from Rutgers in 1981. Upon earning his M.S., he joined Cahners Publishing Co. as Senior Editor of *Ceramic Industry*, an industrial ceramic trade publication, where he traveled extensively to report on the industrial practices being used in the modern ceramic industry, and he authored more than 50 reports on ceramic processing and editorials on the position of the ceramics community.

ROBERT E. FISHER *Co-author, Petroleum and Petrochemical Applications for Refractories*
Co-author, Alumina in Monolithic Refractories

Fisher has been employed at the Plibrico Company since 1973, where he has held various positions and is now Managing Director of Plibrico USA operations. He received a B.S. in Chemistry from Grinnell College in 1961 and an M.S. in Metallurgical Engineering from the Illinois Institute of Technology in 1964. Mr. Fisher has published a dozen papers, is the editor of two volumes of symposium proceedings, holds seven patents, and is active in giving professional lectures and oral presentations. He holds memberships in the American Ceramic Society, ASTM, the British Ceramic Society, and the American Concrete Institute. He has been an active member of ACerS's Refractories Division, having served on the Division's Executive, Editorial Review, and Awards Committees. He has also been a member of ASTM C-8 on Refractories and ACI Committee 547 on Refractory Concretes.

HUBERT L. FLEMING *Co-author, Selective Adsorption Processes*
Author, Water-Treatment Products and Processes

Fleming is Technical Manager of the Separations Technology Division of Alcoa. He is generally responsible for the technical capability of the Division, including all technical activities of the various domestic and international research efforts. Dr. Fleming received his B.S. in Chemistry and Applied Mathematics at Alderson-Broaddus College and his M.S. and Ph.D. in Chemical Engineering at Cornell University. He is active in research in the area of interfacial phenomena in separations, is an Adjunct Professor at numerous universities, and serves on various national and international scientific committees, including the NATO Task Force on Adsorption and AIChE Task Force on Education in Separations. He has published extensively and holds several patents on the synthesis and use of adsorbents, catalysts, and membranes.

KENNETH P. GOODBOY
Co-author, Production Processes, Properties, and Applications for Activated and Catalytic Aluminas
Co-author, Selective Adsorption Processes
Co-author, Claus Catalysts and Alumina Catalyst Materials and Their Application

Goodboy is the Director of Strategic Planning and Technology at Alcoa's Separations Technology Division in Pittsburgh, PA. He has been with Alcoa for over 17 years in various research, finance, technical, and marketing assignments. Goodboy earned a B.S. in Chemical Engineering from the University of Missouri-Rolla and is a member of the American Institute of Chemical Engineers.

G. EDWARD GRADDY, JR. *Co-author, Refractories Used for Aluminum Processing*

Graddy is Technical Supervisor of Ceramics and Refractories in the Ceramics Division of Alcoa. He received B.S. and M.S. degrees in Ceramic Engineering from the University of Illinois in 1976 and 1977, respectively. Before joining Alcoa in 1979, he worked as a Glass Technologist for Owens/Corning Fiberglass Corporation. Mr. Graddy is currently involved with issues pertaining to containment of processes related to aluminum production and glass technology.

MANUEL GUERRA, JR. *Refractories Used for Investment Casting of High-Temperature Alloys*

Guerra is currently Development Supervisor at Remet Corporation. Formerly, he was with Howmet Turbine Components Corporation at their Technical Center in Whitehall, MI. He received his B.S degree in Ceramic Engineering from the University of Illinois at Urbana-Champaign in 1978. Mr. Guerra has extensive experience in the precision investment casting industry. His major areas of endeavor have been in ceramic shell molds and on mold/metal reactions. His main interests include slurry rheology, high temperature mold systems, and high strength mold systems.

RICHARD A. HABER *Co-author, Advanced Ceramics Involving Alumina*

Haber earned his B.S., M.S., and Ph.D. degrees in Ceramic Engineering from Rutgers University, where he is now an Assistant Professor. Dr. Haber is a member of the American Chemical Society, American Vacuum Society, and the American Ceramic Society. His interests include pressure casting of alumina ceramics, alumina-glass composites, and mechanical and tribological properties of ceramic materials.

LEROY DAVID HART *History of Alumina Chemicals*
Co-author, The Future of Alumina Chemicals in Europe

Mr. Hart operates Hart Associates, an engineering consulting firm that specializes in projects associated with industrial applications for alumina chemical products. Hart established this company shortly after his retirement from Alcoa, where he had been employed since 1948, serving as Special Technical Consultant for the Worldwide Chemicals Division; Technical and Quality Assurance Manager for Alcoa's Arkansas Operations; Manager of the Alumina and Chemicals Division; and Manager of the Chemicals Division. He earned his B.S. degree in 1948 and his M.S. degree in 1958, both in Chemical Engineering from Washington University, St. Louis, MO. Hart's broad research and development experience in the fields of chemical engineering, ceramic engineering, and chemistry includes laboratory, pilot plant, and plant investigations pertaining to the production and use of alumina, fluorides, ceramic aluminas, fillers, fibers, sorbents, desiccants, catalysts, refractories, monoliths, high temperature cements, and other chemical and ceramic products. Mr. Hart holds nine patents and has published 24 technical papers. He is a past Vice-President and Fellow of the American Ceramic Society, a Fellow of the American Institute of Chemical Engineers, and is the recipient of the T.J. Planje-St. Louis Refractories and the Samuel Geijsbeek Awards. He has also conceived and helped to establish a National Registry of Retired Professional People within the American Ceramic Society.

DAVID H. HUBBLE *Use of High-Alumina Refractories in the U.S. Steel Industry*

Hubble is a 1957 graduate of Virginia Polytechnic Institute with degrees in Ceramic and Metallurgical Engineering. Mr. Hubble has been with U.S. Steel since 1957, and he is currently Chief Research Consultant in refractories at the Technical Center, Monroeville, PA. During his career, Hubble has been involved in the testing, development, and practical application of refractories for all phases of iron and steelmaking. In particular, such efforts have been concentrated on refractories for open hearths, basic oxygen steelmaking, steel ladles, and continuous casting. He has been part of start-up and troubleshooting teams in all the USS plants and on several international projects. His professional activities include Chairman of the Refractories Division of the American Ceramic Society, Chairman of the AISI Committee on Refractories, and Chairman of ASTM Subcommittees on Refractory Testing.

ROBERT H. INSLEY *Electrical Properties of Alumina Ceramics*

Mr. Insley retired from Champion Spark Plug Co. in 1987, having served in various capacities there since 1952, including Director of Research and Development, Assistant Director of Research and Development, Manager of Ceramic Research, Senior Research Engineer, and Petrographer. He received his M.S. from the Pennsylvania State University in 1952. He is a member of the American Ceramic Society, the National Institute of Ce-

ramic Engineers, Deutsche Keramische Gesellschaft, the British Ceramic Society, and the Society of Sigma Xi. He served as Vice-President of the American Ceramic Society from 1979-1980. In 1964, Insley and Barczak were given the Ross Coffin Purdy Award for outstanding contribution to the ceramic technical literature for their paper on "Thermal Conditioning of Polycrystalline Alumina Ceramics." Other recognitions include Fellow, the American Ceramic Society and the Engineering Society of Detroit and Fellow and Award of Merit, ASTM.

SOICHI KAZAMA *Long-Range Technology—The Role of Alumina Chemicals as Seen from the Japanese Viewpoint*

Kazama is General Manager of Research and Development of the Yokohama Works, Showa Aluminum Industries K.K. He joined Showa Denko K.K. in 1962 and was assigned to the Yokohama Works, where he was engaged in research on alumina production technology. He has spent over 20 years in research and development of alumina chemical products. Kazama is a graduate of the Applied Chemistry Section, National University of Niigata, 1962.

LISA A. KETRON *Alumina in Coatings*

Ketron is employed by International Pressure Service, Inc. Previously, she was the Technical Editor of the American Ceramic Society. She earned a B.S. in Biochemistry in 1977 and an M.S. in Ceramic Engineering in 1985, both from the Ohio State University. Prior to earning her Master's Degree, she worked as a certified medical technologist at the OSU Hospitals Clinical Chemistry Laboratory. She is a member of the American Ceramic Society, Sigma Delta Epsilon, Keramos, and the Society of Women Engineers.

TOIVO KODAS *Co-author, Alumina Powder Production by Aerosol Processes*

Kodas is a Professor at the Center for Micro-Engineered Ceramics at the University of New Mexico. Prior to this, he was a Visiting Scientist at IBM Research, San Jose, CA. He received a Ph.D. in Chemical Engineering from the University of California at Los Angeles in 1986. He is author or co-author of over 15 technical papers in the fields of powder production by aerosol methods, chemical vapor deposition, and laser-induced deposition processes. He has also worked and consulted for Alcoa on methods for alumina powder production by aerosol processes.

MANFRED KOLTERMANN *High-Alumina Refractories for Steelmaking in Europe*

Dr. Koltermann is head of the Refractory Materials Laboratory of the Hoesch Stahl AG Dortmund, a position he has held since 1968. He received a degree in Mineralogy from Humboldt University, Berlin, in 1957 and a Dr.-Ing. in Ceramic Engineering from Technical University Clausthal in 1961. He spent the next four years as a Research Assistant and Lecturer at the Technical University Clausthal, and one year on a Thyssen Foundation Fellowship at U.S. universities, primarily the University of California at Berkeley. Koltermann has remained active in education, serving as Guest Lecturer for Applied Mineralogy and Refractory Technology at the Universities of Kiel and Göttingen from 1970-1985, and organizing continuing education seminars in refractory technology for iron and steel engineers. Professionally, he has served as the Chairman of the BOF-Refractories Committee of West European producers and users of refractories (SIPRE) and as Chairman of the Refractory Materials Committee of the German Iron and Steel Association (VDEh). His primary research interests, which are covered in approximately 60 publications, are high alumina refractories, basic materials, refractory raw materials, testing methods, torpedo car and steel plant ladle linings, chemically bonded refractories, and Forsterite and Andalusite as a refractory material.

JOSEPH E. KOPANDA *Co-author, Production Processes, Properties, and Applications for Calcium Aluminate Cements*

Mr. Kopanda was Senior Technical Specialist at Alcoa; he had 36 years of experience at Alcoa and Universal Atlas Cement Division of U.S. Steel in performing research and development and providing technical guidance to manufacturers, marketing personnel, and customers in all phases of calcium aluminate and portland cement technology. Mr. Kopanda's involvement was from raw material selection for cement production to product performance behavior in concrete environments. Kopanda received a B.A. in Chemistry in 1949 from Illinois Benedictine College. He co-authored eight papers and three patents on cement and refractory technology, participated in many seminars on related topics, and contributed to professional committee published reports. He was a Fellow of the American Society for Testing and Materials and the recipient of their Award of Merit and Editorial Excellence. He was also a Fellow of the American Ceramic Society, and he held memberships in the American Concrete Insitute, the National Institute of Ceramic Engineers, the Pennyslvania Ceramic Association, and Sigma Xi Scientific Research Society.

LEONARD P. KRIETZ *Co-author, Alumina in Monolithic Refractories*

Krietz is Technical Director at Plibrico Company, USA, where he has been employed since 1976. Previous positions with Plibrico have included Research Engineer, Senior Research Engineer, Research Manager, and Technical Manager. Prior to employment with Plibrico, Krietz worked at Corhart Refractories as Developmental Engineer from 1973 to 1975. He received a B.S. in Ceramic Science from Rutgers Unviersity in 1973. He is a member of the American Ceramic Society, the American Foundry Society, ASTM Committee C-8, and The Refractories Institute-Technical Advisory Committee. His areas of interest include fracture and thermal shock behavior of monolithic refractories, low and ultra low cement castable systems, and phosphate bonding systems.

IRWIN M. LACHMAN *Monolithic Catalyst Systems*

Lachman is a Senior Research Associate in Corning Incorporated's Research and Development Laboratories, Ceramic Research Department. He received a B.S. degree in Ceramic Engineering from Rutgers Unviersity and M.S. and Ph.D. degrees in Ceramic Engineering from the Ohio State University. He holds 17 U.S. patents covering thermal shock-resistant ceramics, refractories, and glass-ceramics. Prior to joining Corning Incorporated he was with Sandia Laboratories and served in the U.S.A.F. at Wright Air Development Center.

YVON LAZENNEC *Co-author, The Future of Alumina Chemicals in Europe*

Lazennec is the Director of the Industrial Ceramic Department of S.C.T./Ceraver, a subsidiary of Alcoa. He also spent 10 years as the Head of the Ceramic Division of Laboratoires de Marcoussis, the Central Research Laboratory of C.G.E. Group. Lazennec holds degrees in Ceramic Engineering and Management from Ecole Nationale Superieure de Ceramique Industrielle and Paris University.

DANIEL LEISER *Space Vehicle Thermal Protection*

Dr. Leiser is a Research Scientist at NASA Ames Research Center, Moffett Field, CA. He received a B.S. in 1966 and a Ph.D. in 1971 in Ceramic Engineering from the University of Washington. He was a National Research Council Postdoctoral Research Associate studying the response of ceramic insulation materials to aeroconvective heating environments. Prior to joining NASA in 1979, he worked for Stanford University as a Research Associate on both developing coatings and insulations capable of use in aeroconvective heating environments. At NASA, he has been working on the development of higher temperature insulation materials and coatings for potential use initially on the space shuttle and subsequently on advanced space vehicles. For his contributions to the development of the thermal protection systems used on the current orbiters, he received five Group Achievement Awards from various organizations within NASA. In addition, he received the Medal for Exceptional Engineering Achievement from NASA. He has authored and co-authored over 35 papers and holds 5 U.S. and several foreign patents. He has served as the General Chairman of the 33rd Pacific Coast Regional Meeting of the American Ceramic Society and as the Chairman of the Northern California Section of ACerS. Dr. Leiser is currently a member of the Engineering Ceramics Division of ACerS and the National Insitute of Ceramic Engineers.

RONALD H. LESTER *Alumina in Electrical Porcelain*

Lester graduated with a B.S. and an M.S. from Virginia Polytechnic Institute and has held various managerial positions in research and development, quality control, and manufacturing for General Electric, Ohio Brass, and Lapp Insulator. He is currently Manager of Ford City Operations for Eljer Plumbingware Division of Household International. He is a registered Professional Engineer, the author of "Quality Control for Profit," and has made numerous contributions to literature on management science, electrical insulation, and quality assurance.

JOHN F. MACDOWELL *Alumina in Glasses and Glass-Ceramics*

MacDowell received a B.S. in 1958 and an M.S. in Geology/Mineralogy in 1959, both from the University of Michigan. He joined Corning Incorporated in 1959 as a scientist working for Dr. S.D. Stookey, the noted inventor of glass-ceramics. He was promoted to Senior Scientist in 1961 and to Manager of the Glass-Ceramic Research Department in 1964. During this time, he developed nepheline glass-ceramics for use in the Centura® and Pyroceram® lines of strong dinnerware. He also made major technical contributions to the development of Corelle® lightweight laminated tableware. Mr. MacDowell became Director of Chemical Research in 1966, which included glass, glass-ceramics, ceramics, and composite materials research departments. During his 12 years as Materials Research Director, several major technologies that began in his research group were developed and commercialized: Corelle® dinnerware, Photogray Extra® high performance photochromics for eyeglass use, Emcon® extruded cordierite ceramic substrate now used for auto exhaust catalysis, Visions® transparent glass-ceramic cookware, and optical waveguides for telecommunications. In 1982, MacDowell was named Corning Research Fellow in recognition of his excellent track record and for his ability to generate new research projects of high potential impact to Corning. He holds 20 U.S. patents and has published numerous articles on glass and glass-ceramics in technical journals and books. He is a Fellow of the American Ceramic Society, was Chairman of the Glass Division's Program Committee, and has served on the Society's Publications Committee.

GEORGE MACZURA
Production Processes, Properties, and Applications for Tabular Alumina Refractory Aggregates
Co-author, Production Processes, Properties, and Applications for Calcium Aluminate Cements

Mr. MacZura's career has been spent with Alcoa working on CA cement, phosphate bonding, and calcined and tabular alumina developments relating to refractories, ceramic, and abrasive applications. Beginning as a Research Engineer at their East St. Louis Laboratory, he spent 34 years in Research and Development. George is currently Technical Service Manager-Refractories for Alcoa Industrial Chemicals Division at their Chemicals Sales Office in Pittsburgh. He consults and directs refractories technical programs associated with customer technical-related projects and new products. MacZura holds a number of patents and has authored numerous technical papers. He received his B.S. degree in Ceramic Engineering from the University of Missouri-Rolla in 1952 and an honorary Professional Degree of Ceramic Engineering from UMR in 1972. He is a member of Keramos, Tau Beta Pi, Sigma Xi, the National Institute of Ceramic Engineers, ASTM C-8 Committee on Refractories, ACI Committee 547 on Refractory Concrete, and Materials Review Board for nuclear waste forms. He has been a member of the American Ceramic Society since 1948, became a Fellow in 1969, and has served as the Refractories Division Chairman and Trustee. In 1980, MacZura received the St. Louis Refractories Award and the University of Missouri-Rolla American Ceramic Society Student Branch/Keramos/Ceramic Department Distinguished Alumnus Award.

T. MATSUMURA *Co-author, Alumina and Aluminous Refractories for Iron and Steelmaking in Japan*

Matsumura is General Manager in the Refractory Research Office, Research and Development Department, at Harima Refractories Co., Ltd. He earned his B.S. in Applied Chemistry from Himeji Institute of Technology. His current work involves the development of new refractories for the steel industry.

LARRY L. MUSSELMAN
Production Processes, Properties, and Applications for Aluminum-Containing Hydroxides;
Alumina Chemicals as Additives for Paper, Dentrifices, Paints, Coatings, Rubbers, and Plastics with Emphasis on Fire-Retardant Products

Musselman is currently Director-Technology and Operations, AMAX Technical Center. He held positions of Technical Manager-Hydrated and Industrial Chemicals, Technical Service Manager, Senior Scientist, Senior Research Engineer, and Staff

Engineer with Alcoa over the previous 12 years. He has done work in areas of heat transfer, fluid flow, process engineering, plastics product design economics and manufacture, materials testing, and fire retardancy of plastics. He holds patents having to do with plastics components in bearing applications, particulate color, surface treatments, and fire retardants. He has over 30 technical publications and presentations to his credit, and he has presented many applications seminars involving thermoplastic, thermoset, and elastomeric polymers internationally. A graduate of Akron University with B.S. and M.S. degrees in Chemical Engineering (minor in polymer science), he was a scholar at Akron, chosen for Sigma Tau Engineering Honorary Fraternity, Sigma Xi, and Who's Who in the World. He is a member of SPE, ASME, ASTM, a past member of the Board of Directors of CAM/ASME, and the Technical Advisory Committee to the Ohio Legislature, as well as various technical committees of SPI, CMI, FRCA, and the associations noted above.

N. NAMEISHI *Co-author, Alumina and Aluminous Refractories for Iron and Steelmaking in Japan*

Dr. Nameishi is Managing Director at Harima Refractories Co., Ltd., Takasago City, Japan. He received his B.S. in 1949 and Ph.D. in 1970 in Mineralogy, both from Kyusyu University. He has been working on the development and production of refractories for the steel industry. He is now in charge of research and development, technology, and production.

ALAN PEARSON *Co-author, Gallium*

Pearson is currently a Technical Consultant in the Ceramics Division of Alcoa Laboratories. He received B.S. and M.S. degrees in Chemical Engineering from Washington University, St. Louis, MO, in 1959 and 1968, respectively. He joined Alcoa Laboratories in 1962 after serving in the U.S. Army Ordnance Corps. During his career at Alcoa, he has worked on a wide variety of projects involving manufacture and uses of alumina chemicals, gallium, and related products. Pearson holds seven patents and is a registered Professional Engineer.

PAUL ROTHENBUEHLER *Co-author, The Future of Alumina Chemicals in Europe*

Rothenbuehler earned a B.S. degree from Paris University as a Refractory Specialist. After extensive experience in the foundry industry, he joined Alcoa in 1972 as an Application Engineer and in 1980 become Technical Service Manager in charge of application and product development for the European region. In association with Alcoa's interregional activities and presently located in Lausanne, Switzerland, Rothenbuehler is actively pursuing new opportunities in new alumina refractory aggregates.

BERNARD SCHWARTZ *Electronic Ceramics*

Dr. Schwartz is a Senior Engineer with the IBM Corporation, where since 1984 he has been at the Research Laboratories in Yorktown Heights, NY. In his 24 years at IBM, Schwartz developed ferrite recording heads and memory cores, multilayer modules, substrate and photomask technology, gas panels, chip joining, and advanced packaging. His industrial experience has also included one year as Manager of the Beryllia Laboratory at MIT, two years as Manager of the Sylvania Electric Products Ceramics Laboratory, one year as Manager of the Burroughs Corporation Ferrite Laboratory, three years as Senior Research Engineer at the International Resistance Company (now TRW), four years as Manager of Component Development at RCA for the Microelectronics Department, and one year at the RCA Labs at Princeton. Dr. Schwartz received his B.S., *cum laude,* from Alfred University in 1948 and an Sc.D. in Ceramics from the Massachusetts Institute of Technology in 1951. He also attended Brown University from 1943-1944, where he studied mathematics and physics, and he attended U.S. Air Force schools, where he studied radar and electronics.

WILLIAM D. SCOTT *Co-author, Mechanical Properties of Alumina*

Scott is Professor of Ceramic Engineering in the Department of Materials Science and Engineering at the University of Washington, Seattle. He earned his B.S. in Ceramic Engineering from the University of Illinois in 1954. After two years in the U.S. Army, he entered the University of California at Berkeley and received an M.S. degree in 1959 and a Ph.D. in 1961. He was a visiting scientist at the University of Leeds, England, for two years and a Research Fellow at C.N.R.S., Laboratoire de Physique des Materiaux, Paris (Bellevue), for one year. Dr. Scott has been a member of the faculty of the University of Washington since 1965. His research interests include optical and electron microscopy and the relation of processing and microstructure to mechanical properties of materials.

RUSSELL D. SMITH *Refractory Ceramic Fiber*

Mr. Smith is Technical Manager in the Fibers Division of The Carborundum Company, where he has worked since 1977. From 1973-1977, he served as Research Engineer, Inorganic Chemicals Research, at Dow Chemical. Smith received both his B.S. and M.S. degrees in Ceramic Engineering from the University of Missouri-Rolla. He received an Alcoa Fellowship; was J.B. Arthur Scholar; belongs to Tau Beta Pi, Phi Kappa Phi, and Keramos; and has appeared in Who's Who in American Colleges and Who's Who in Technology. He is a member of the American Ceramic Society and the National Institute of Ceramic Engineers. Smith has authored five publications covering refractory ceramic fiber, refractory ceramic fiber applications, and mechanical properties of refractories. He holds eight U.S. patents covering refractory ceramic fiber, refractory ceramic fiber applications, and refractory raw materials.

AJAY SOOD *Co-author, Alumina Powder Production by Aerosol Processes*

Dr. Sood is a Ph.D. Chemical Engineer with over 12 years of experience as a technical specialist/project leader in process engineering and new materials development with major petrochemical, specialty chemical, and pollution control companies. He has provided technical leadership in the areas of advanced ceramics, separations technology, and catalyst development. In ceramics, his expertise is in the development of new synthesis routes for preparation of advanced ceramic powders; chemical reactor modelling, design, and scale-up; process design and development; and characterization of dispersion, forming, and sintering behaviors for ceramic powders. He has developed novel materials for removing contaminants from petrochemicals and hazardous heavy metal ions from waste water. He has also successfully executed a catalyst development, evaluation, and scale-up program for an innovative synthesis gas-to-diesel conversion process. He has published 28 articles and has seven patent applications pending. He is a member of the American Ceramic Society, the American Institute of Chemical Engineers, the American Chemical Society, and the American Association for Aerosol Research.

JOHN P. STARR *A View of the Future for Alumina Chemicals*

Starr is General Manager-Separations Technology Division of Alcoa. Mr. Starr joined Alcoa as a Chemical Engineer at the Arkansas Operations. He served in several plant engineering assignments there before being named as Application Engineer in the Chemicals Divsion in Pittsburgh in 1976. He became Manager of Primary Products Applications Engineering in 1977. In 1979, he was named Manager of Chemical Sales and Marketing for Alcoa's European Region, based in Lausanne, Switzerland. He was promoted to Marketing Manager-Chemicals Division in 1983, and named to his present position in 1985. He received a B.S. degree in Chemical Engineering from the University of Arkansas in 1971. Starr is a member of the American Ceramic Society and the American Institute of Chemical Engineers.

EVERETT A. THOMAS *The Use of Alumina in Refractories for Melting Glass*

Thomas is a consultant with Industrial Technical Services, Didier Taylor Refractories Corporation. He has held several positions at Didier Taylor, including Director, Glass Industry Technical Services; Director of Research; and Manager of Research, Glass Industry. He received a B.S. in Ceramic Engineering from Alfred University and performed a year of graduate study at Alfred on an Orton Fellowship. Mr. Thomas is a Fellow of the American Ceramic Society and the Canadian Ceramic Society, and he also holds memberships in Keramos, the Ceramic Educational Council, the National Institute of Ceramic Engineers, Engineering Society of Cincinnati, Society of Glass Technology, and the British Ceramic Association. He served as Chairman from 1973-1979 for ASTM C-8 Subcommittee .04.06 Glass Contact Refractories, and he served on the International Commission on Glass, Subcommittee XI, Glass Contact Refractories. Mr. Thomas has authored or co-authored over 20 technical papers and he holds four patents.

JOHN B. WACHTMAN *Co-author, Advanced Ceramics Involving Alumina*

Dr. Wachtman is the Director of the Center for Ceramics Research and Robert B. Sosman Professor of Ceramics at Rutgers University. He received a B.S. in 1948 and an M.S. in 1949, both from Carnegie Institute of Technology, and a Ph.D. in 1961 from the University of Maryland; all of his degrees are in Physics. Prior to taking his current position in 1983, Wachtman was Director of the Center for Materials Science at the National Bureau of Standards (now the National Institute of Standards and Technology). He received the Department of Commerce Silver Medal Award in 1960 and Gold Medal Award in 1971. In 1975, he was presented the Samuel Stratton Award by NBS for "accomplishments in advancing the theory and extending the applications of inorganic materials."He was elected a member of the National Academy of Engineering in 1976. A Fellow and Past President of the American Ceramic Society, he is a past Chair and past Trustee of the Basic Science Division. Dr. Wachtman also holds memberships in the Engineering Ceramics Division and the National Institute of Ceramic Engineers. He is Past President of the Federation of Materials Societies and has represented ACerS on the FMS Board of Trustees. He has served as Chair of the ACerS Publications Committee and has been a member of various other committees. In 1987, he received the FMS National Materials Advancement Award.

KARL WEFERS *Nomenclature, Preparation, and Properties of Aluminum Oxides, Oxide Hydroxides, and Trihydroxides*

Wefers has been with Alcoa Laboratories in Alcoa Center, PA, since 1967. Prior to that, he was employed by Leichtmetall Forschungsinstitut, VAW, Bonn, West Germany. Dr. Wefers earned a Sc.D. in Crystallography from Friedrich-Wilhelms Universität, Bonn, in 1958.

DOUGLAS A. WEIRAUCH, JR. *Co-author, Refractories Used for Aluminum Processing*

Weirauch is a Staff Scientist in the Ceramics Division at Alcoa Laboratories in Pennsylvania. He received a B.S. degree with a double major in Mathematics and Geology from the University of Wisconsin at Platteville in 1972. An M.S. in Geosciences was granted him by the University of Wisconsin-Milwaukee in 1974, and in 1979, he received a Ph.D. in Geochemistry from the Pennyslvania State University. Prior to joining Alcoa Laboratories, he worked as a raw material technologist and glass scientist at the Technical Center of Owens/Corning Fiberglass, Granville, OH. Dr. Weirauch's current research interests include the control of interfacial reactions, the kinetics of liquid-solid interactions, the controlled crystallization of glasses, and the prediction of glass properties.

R. DALE WOOSLEY *Activated Alumina Desiccants*

Mr. Woosley joined Alcoa in 1954 as a Chemist at the Bauxite, AR, Operations and later became Assistant Chief Chemist there. In 1967, he transferred to Alcoa Laboratories in East St. Louis, IL, and headed a section in the development of adsorbent and catalytic aluminas. Since 1977, he has directed technical services activities for desiccants and presently is a Technical Service Manager for Desiccants in Houston, TX. Also included in this current assignment are development projects at the Vidalia, LA, Operations. A native of Arkansas, Woosley received a B.S. degree in Chemistry from Hendrix College in 1949. He is a member of the American Chemical Society, the American Institute of Chemical Engineers, and the American Society of Heating, Refrigerating, and Air Conditioning Engineers.

KOICHI YAMADA *Present Situation and Future Technology of Alumina Chemicals in Japan*

Yamada is Senior Research Associate in the Ehime Research Laboratory, Sumitomo Chemical Co., Japan. He earned a B.S. in Electrochemistry from Yokohama National University in 1962 and a Ph.D. in Industrial Chemistry from Tokyo University in 1982. He joined Sumitomo Chemical Co. in 1962. Yamada's work involves the fabrication and characterization of alumina chemicals and raw materials powders for ceramics.

HIROAKI YANAGIDA *Long Range Future Trends: The Role of Alumina Chemicals—The Japanese Viewpoint*

Dr. Yanagida is Professor and Chair of Ceramic Materials in the Department of Industrial Chemistry, University of Tokyo, where he has taught since 1963. He was recently appointed director of the Research Center for Advanced Science and Technology at the University. Yanagida received a B.S. in Engineering in 1958, an M.S. in Engineering in 1960, and a Ph.D. in Engineering in 1963, all from the University of Tokyo. His major interest is the correlation between crystal chemistry and electrical properties of ceramic materials. Dr. Yanagida has authored or co-authored over 200 papers and has authored or edited nearly 20 books. He received Distinguished Young Researcher and Distinguished Scholar Awards from the Ceramic Society of Japan and the Chemical Society of Japan; he is also a Fellow of the American Ceramic Society.

Author Index

Subject Index